

Second Edition

Fire Retardancy of Polymeric Materials

Fire
ohēñ Lume
Sunog zjarri
Ild אש Feuer
TEINE آتش Fuego

Edited by

Charles A. Wilkie • Alexander B. Morgan

 CRC Press
Taylor & Francis Group

Second Edition

Fire Retardancy of Polymeric Materials

Second Edition

Fire Retardancy of Polymeric Materials

Edited by

Charles A. Wilkie • Alexander B. Morgan



CRC Press

Taylor & Francis Group

Boca Raton London New York

CRC Press is an imprint of the
Taylor & Francis Group, an **informa** business

CRC Press
Taylor & Francis Group
6000 Broken Sound Parkway NW, Suite 300
Boca Raton, FL 33487-2742

© 2010 by Taylor and Francis Group, LLC
CRC Press is an imprint of Taylor & Francis Group, an Informa business

No claim to original U.S. Government works

Printed in the United States of America on acid-free paper
10 9 8 7 6 5 4 3 2 1

International Standard Book Number: 978-1-4200-8399-6 (Hardback)

This book contains information obtained from authentic and highly regarded sources. Reasonable efforts have been made to publish reliable data and information, but the author and publisher cannot assume responsibility for the validity of all materials or the consequences of their use. The authors and publishers have attempted to trace the copyright holders of all material reproduced in this publication and apologize to copyright holders if permission to publish in this form has not been obtained. If any copyright material has not been acknowledged please write and let us know so we may rectify in any future reprint.

Except as permitted under U.S. Copyright Law, no part of this book may be reprinted, reproduced, transmitted, or utilized in any form by any electronic, mechanical, or other means, now known or hereafter invented, including photocopying, microfilming, and recording, or in any information storage or retrieval system, without written permission from the publishers.

For permission to photocopy or use material electronically from this work, please access www.copyright.com (<http://www.copyright.com/>) or contact the Copyright Clearance Center, Inc. (CCC), 222 Rosewood Drive, Danvers, MA 01923, 978-750-8400. CCC is a not-for-profit organization that provides licenses and registration for a variety of users. For organizations that have been granted a photocopy license by the CCC, a separate system of payment has been arranged.

Trademark Notice: Product or corporate names may be trademarks or registered trademarks, and are used only for identification and explanation without intent to infringe.

Library of Congress Cataloging-in-Publication Data

Fire retardancy of polymeric materials / edited by Charles A. Wilkie and Alexander B. Morgan. -- 2nd ed.

p. cm.

Includes bibliographical references and index.

ISBN 978-1-4200-8399-6

1. Polymers--Fire testing. 2. Polymers--Fires and fire prevention. 3. Fire resistant plastics. I. Wilkie, C. A. (Charles A.) II. Morgan, Alexander B. III. Title.

TH9446.5.P65F56 2010
668.9--dc22

2009020827

Visit the Taylor & Francis Web site at
<http://www.taylorandfrancis.com>

and the CRC Press Web site at
<http://www.crcpress.com>

Contents

Preface.....	ix
Contributors	xi
Chapter 1 An Introduction to Polymeric Flame Retardancy, Its Role in Materials Science, and the Current State of the Field.....	1
<i>Alexander B. Morgan and Charles A. Wilkie</i>	
Chapter 2 Polymer Degradation and the Matching of FR Chemistry to Degradation	15
<i>Dennis Price and A. Richard Horrocks</i>	
Chapter 3 Physical Parameters Affecting Fire Growth	43
<i>Jose L. Torero and Guillermo Rein</i>	
Chapter 4 Halogen-Containing Flame Retardants	75
<i>Sergio Bocchini and Giovanni Camino</i>	
Chapter 5 Phosphorus-Based Flame Retardants.....	107
<i>Paul Joseph and John R. Ebdon</i>	
Chapter 6 Intumescence-Based Fire Retardants.....	129
<i>Serge Bourbigot and Sophie Duquesne</i>	
Chapter 7 Fire-Retardant Fillers	163
<i>Peter Hornsby</i>	
Chapter 8 Recent Developments in Silicon-Based Flame Retardants	187
<i>Walid H. Awad</i>	
Chapter 9 Boron-Based Flame Retardants and Flame Retardancy	207
<i>Kelvin K. Shen, Saied H. Kochesfahani, and Frederic Jouffret</i>	
Chapter 10 Char Formation and Characterization.....	239
<i>Sophie Duquesne and Serge Bourbigot</i>	
Chapter 11 Polymer Nanocomposites.....	261
<i>David D. Jiang</i>	

Chapter 12	Multicomponent FR Systems: Polymer Nanocomposites Combined with Additional Materials.....	301
	<i>J.-M. Lopez-Cuesta and F. Laoutid</i>	
Chapter 13	Design of Interlayers for Fire-Retarded Polymeric Systems.....	329
	<i>György Marosi, Botond B. Marosfői, Brigitta Bodzay, Tamás Igricz, and György Bertalan</i>	
Chapter 14	Fundamentals of Fire Testing and What Tests Measure	349
	<i>Marc Janssens</i>	
Chapter 15	Uses of Fire Tests in Materials Flammability Development.....	387
	<i>Bernhard Schartel</i>	
Chapter 16	High Throughput Techniques for Fire Resistant Materials Development	421
	<i>Rick D. Davis, Richard E. Lyon, Michael T. Takemori, and Naomi Eidelman</i>	
Chapter 17	Fire Toxicity and Its Assessment.....	453
	<i>Anna A. Stec and T. Richard Hull</i>	
Chapter 18	Modeling Thermal Degradation of Polymers by Population Balance Methods	479
	<i>J. E. J. Staggs</i>	
Chapter 19	Micro- to Mesoscale Testing and Modeling for Nanocomposite Polymers in Fires.....	509
	<i>Michael A. Delichatsios and Jianping Zhang</i>	
Chapter 20	Full-Scale Fire Modeling	551
	<i>Chris Lautenberger and Simo Hostikka</i>	
Chapter 21	Regulations, Codes, and Standards Relevant to Fire Issues in the United States	587
	<i>Marcelo M. Hirschler</i>	
Chapter 22	Changing Chemical Regulations and Demands.....	671
	<i>Susan D. Landry</i>	
Chapter 23	Flame Retardant Design for Fiber-Reinforced Materials	703
	<i>Michael G. Stevens and Alexander B. Morgan</i>	

Chapter 24 Flame Retardancy Design for Textiles	725
<i>Baljinder K. Kandola</i>	
Chapter 25 FR Design for Foam Materials.....	763
<i>Michele Modesti and Alessandra Lorenzetti</i>	
Chapter 26 Material Design for Fire Safety in Wire and Cable Applications.....	783
<i>Jeffrey M. Cogen, Thomas S. Lin, and Paul D. Whaley</i>	
Index	809

Preface

The second edition of *Fire Retardancy of Polymeric Materials* is very different in layout from the first edition, and is more than just an update of the first edition. Rather, it is a more comprehensive version of the book, covering more fire-retardant chemistry, regulations, fire-safety engineering, fire phenomena, and all the other ancillary issues related to this applied field of materials science. Indeed, this edition reflects the strong multidisciplinary approach of material flame retardancy today.

When the first edition was published in 2000, it was the first comprehensive book on fire retardancy that had been published since the 1970s. Since then, the number of books on polymeric flame retardancy has increased greatly, with as many as one to two books being published every year. Some of the books specialize on just one class of polymeric materials, or cover only flame-retardant chemistry, and the first edition of this book seemed to have coincided with an increase in flame-retardant research in the late 1990s and early 2000s. The factors that have influenced this increase in research are discussed in Chapter 1, but the purpose of this preface is to reflect the recent developments and to introduce the second edition to both new and experienced researchers in this field. While the book is primarily aimed at a scientific audience (academic, government, and industrial researchers), it will be of value to those who have never encountered this field of research and who wish to either enter it or at least learn more about this field that gets more and more press (both good and bad) all the time.

This book is a mix of “how-to” directions and a distillation of technical knowledge. While we have tried to make this book as comprehensive as possible and build upon what was published in the first edition, not everything could be included. Therefore, beginners should use this book as a guide on where to start and on where to go to learn more. You will not be able to learn everything just by reading this book—some experimentation and experience in this field is necessary. For experienced hands, this book promises to be an excellent one-stop reference guide. For those of you reading this book hoping to find a quick answer to solving a specific material flame-retardancy problem, you may find answers, but as you read this book you will realize that there is no real quick answer to material fire safety and material flammability. This field of applied material science is one of the most challenging in science today, as one must not only provide protection against fire for a polymeric material but one must also consider all other property issues (cost, mechanical and thermal performance) while simultaneously addressing increasing regulations that deal with the composition of matter and life-cycle issues (recycling, end-of-life disposal, etc.). Therefore, you will not get a quick answer, but you will find all the guidance you need to come up with your own answer, which will be unique to your system even if it does borrow from a wealth of previous knowledge. We hope that you will find this book useful as you develop new fire-safe materials, and for those of you who are already experts, we hope you will find this book a great source of information all in one handy book.

We would like to thank all those who helped make this book possible, especially the authors of the individual chapters who have taken time out of their busy lives to pass on their knowledge to the readers. We also wish to thank the reviewers who gratefully gave so much of their time to review each chapter, as well as those at Taylor & Francis who helped convert the book from a series of digital files into a hardcover book. Finally, we would like to thank our wives, Julie Ann Morgan and Nancy Wilkie, for their tireless support, editing skills, and putting up with us talking on and on about how great it is to be able to burn things every day and make it boring by talking about the science of it.

Alexander B. Morgan
Charles A. Wilkie

Contributors

Walid H. Awad

Department of Chemistry and Fire Retardant
Research Facility
Marquette University
Milwaukee, Wisconsin

György Bertalan

Department of Organic Chemistry
and Technology
Budapest University of Technology
and Economics
Budapest, Hungary

Sergio Bocchini

Department of Materials Science
and Chemical Engineering
Polytechnic University of Turin
Alessandria, Italy

Brigitta Bodzay

Department of Organic Chemistry
and Technology
Budapest University of Technology
and Economics
Budapest, Hungary

Serge Bourbigot

Laboratoire de Structure et Propriétés
de l'Etat Solide
National Graduate School of Engineering
Chemistry of Lille
Villeneuve d'Ascq, France

Giovanni Camino

Department of Materials Science
and Chemical Engineering
Polytechnic University of Turin
Alessandria, Italy

Jeffrey M. Cogen

The Dow Chemical Company
Piscataway, New Jersey

Rick D. Davis

Building and Fire Research Laboratory
National Institute of Standards and
Technology
Gaithersburg, Maryland

Michael A. Delichatsios

Fire Safety Engineering Research
and Technology Centre
University of Ulster
Newtownabbey, Northern Ireland
United Kingdom

Sophie Duquesne

Laboratoire de Structure et Propriétés
de l'Etat Solide
National Graduate School of Engineering
Chemistry of Lille
Villeneuve d'Ascq, France

John R. Ebdon

Department of Chemistry
University of Sheffield
Sheffield, United Kingdom

Naomi Eidelman

Paffenbarger Research Center
National Institute of Standards and
Technology
Gaithersburg, Maryland

Marcelo M. Hirschler

GBH International
Mill Valley, California

Peter Hornsby

School of Mechanical and Aerospace
Engineering
Queen's University
Belfast, Northern Ireland, United Kingdom

A. Richard Horrocks

Centre for Materials Research and Innovation
University of Bolton
Bolton, United Kingdom

Simo Hostikka

VTT Technical Research Centre
of Finland
Espoo, Finland

T. Richard Hull

Centre for Fire and Hazard Science
University of Central Lancashire
Preston, United Kingdom

Tamás Igricz

Department of Organic Chemistry
and Technology
Budapest University of Technology
and Economics
Budapest, Hungary

Marc Janssens

Fire Technology Department
Southwest Research Institute
San Antonio, Texas

David D. Jiang

Organic Technology
Corning Incorporated
Corning, New York

Paul Joseph

School of the Built Environment and the Built
Environment Research Institute
University of Ulster
Newtownabbey, Northern Ireland
United Kingdom

Frederic Jouffret

Rio Tinto Minerals
Denver, Colorado

Baljinder K. Kandola

Centre for Materials Research and Innovation
University of Bolton
Bolton, United Kingdom

Saied H. Kochesfahani

Rio Tinto Minerals
Denver, Colorado

Susan D. Landry

Albemarle Corporation
Baton Rouge, Louisiana

F. Laoutid

Materia Nova ASBL
Mons, Belgium

Chris Lautenberger

Department of Mechanical Engineering
University of California, Berkeley
Berkeley, California

Thomas S. Lin

The Dow Chemical Company
Piscataway, New Jersey

J.-M. Lopez-Cuesta

Centre des Matériaux de Grande Diffusion
Alès School of Mines
Alès, France

Alessandra Lorenzetti

Department of Chemical Process Engineering
Padova University
Padova, Italy

Richard E. Lyon

William J. Hughes Technical Center
Federal Aviation Administration
Atlantic City, New Jersey

Botond B. Marosfői

Department of Organic Chemistry
and Technology
Budapest University of Technology
and Economics
Budapest, Hungary

György Marosi

Department of Organic Chemistry
and Technology
Budapest University of Technology
and Economics
Budapest, Hungary

Michele Modesti

Department of Chemical Process Engineering
Padova University
Padova, Italy

Alexander B. Morgan

Multiscale Composites and Polymers Division
University of Dayton Research Institute
Dayton, Ohio

Dennis Price

Centre for Materials Research and Innovation
University of Bolton
Bolton, United Kingdom

Guillermo Rein

School of Engineering
University of Edinburgh
Edinburgh, United Kingdom

Bernhard Schartel

BAM Federal Institute for Materials
Research and Testing
Berlin, Germany

Kelvin K. Shen

Rio Tinto Minerals
Huntington Beach, California

J. E. J. Staggs

Energy Resources Research Institute
University of Leeds
Leeds, United Kingdom

Anna A. Stec

Centre for Fire and Hazard Science
University of Central Lancashire
Preston, United Kingdom

Michael G. Stevens

Ashland Inc.
Covington, Kentucky

Michael T. Takemori

Global Research
General Electric Company
Niskayuna, New York

Jose L. Torero

School of Engineering
University of Edinburgh
Edinburgh, United Kingdom

Paul D. Whaley

The Dow Chemical Company
Piscataway, New Jersey

Charles A. Wilkie

Department of Chemistry and Fire Retardant
Research Facility
Marquette University
Milwaukee, Wisconsin

Jianping Zhang

Fire Safety Engineering Research
and Technology Centre
University of Ulster
Newtownabbey, Northern Ireland
United Kingdom

1 An Introduction to Polymeric Flame Retardancy, Its Role in Materials Science, and the Current State of the Field

Alexander B. Morgan and Charles A. Wilkie

CONTENTS

1.1	Fire and Society	1
1.2	Definitions of Flame Retardancy	2
1.2.1	Flame Retardancy	2
1.2.2	Fire Risk Scenario	2
1.2.3	Flame Retardant.....	2
1.2.4	Combustibility.....	3
1.2.5	Thermal Degradation/Decomposition	3
1.3	Protection from Fire: Modern versus Historical Viewpoints.....	3
1.4	Changing Perceptions, Regulations, and Customer Demands.....	6
1.5	Flame-Retardant Chemistries	8
1.6	Flame-Retardant Research.....	9
1.7	The Future of Flame-Retardant Science and Polymeric Material Fire Safety	10
	References.....	13

1.1 FIRE AND SOCIETY

In 2006, there was \$11.3 billion in property loss, 16,400 people injured, and 3,334 people killed by fire, just in the United States.¹ While worldwide statistics on fire loss are not available,² it can be guaranteed that fire losses occurred in just about every country on the planet last year and either increased or stayed constant when compared to previous years. Statistics, though, are just numbers, and do not really tell the whole story even though they attempt to. Most people are not swayed by numbers that try to tell them something, but humanity does react to stimuli, and one of those stimuli is an innate fear of fire, and with good reason. Fire is a unique destructive force of nature; what it touches cannot easily be repaired, rebuilt, or restored to its original form. Scientifically, fire is a thermo-oxidative decomposition of a material, which means it converts carbon and other combustible materials into CO₂ and water. In layman's terms, fire consumes what it touches and leaves behind nothing but ashes. Fire is fatal to almost all life on the planet (except for a few plants that germinate after fire has destroyed forest and underbrush) and is something that all of us know to avoid since we know it will burn and maim us, and if we cannot escape, it will kill us. But in modern society, fire is something we use to make life easier. It is a universal energy source for converting matter into heat energy, which is either used directly or is used to drive other devices that do work for us. It is not that modern society has lost its fear of fire, but instead we have grown accustomed

to controlled fire, where we ignite the flame and control its use. Uncontrolled fire activates our instinctual fear mechanism but until we see it, we really do not think about it. Only those who have encountered accidental fires in their lifetime become acutely aware of fire dangers and hazards—the rest of us tend to not think about it until it appears. So, at first glance we might say that humanity has conquered fire except for the occasional outbreak, but when we return to the statistics we see that this is not the case. Fire can be prevented in most cases, and yet we still have catastrophic fire losses that result in the loss of wealth, possessions, livelihood, and life. It is for these reasons that there are scientists and engineers who not only study fire, but seek to provide passive fire protection for daily life so that we, as a society, will not have to worry about fire, and should an accidental fire begin, it can be rapidly extinguished before it grows. If you are reading this book, a lot of this may be very obvious to you, but it is not obvious to everyone for many of the reasons described earlier. Yes, we all know fire is there, but what many people do not realize is the great potential for fire all around us. It is due to this potential that flame retardancy exists.

1.2 DEFINITIONS OF FLAME RETARDANCY

Before one begins to read a book about flame retardancy, there are some terms that need to be defined for both inexperienced and experienced readers, since one will see many terms throughout the book that at first glance look similar, but have a very different meaning when studying flame retardancy of materials. First of all, the terminology of “fire retardancy” and “flame retardancy” are used more or less interchangeably. There is some perception that flame retardancy involves a lower risk than fire retardancy; in this volume both these terms are used and mean the same thing.

1.2.1 FLAME RETARDANCY

This means that something has been done to a material so that when exposed to a flame, either the material will retard the growth and propagation of that flame, or it will retard (slow) the growth and propagation of any flames that may come from the material once it has been ignited. Fire retardant does not mean that the material will not burn, but rather that it will be harder to burn. In some cases, the flame-retardant material may self-extinguish after being ignited if the external flame is removed, but in other cases the flame-retardant approach assumes the material will stay lit once ignited, and will instead just burn slowly. What is required of a flame-retardant material (self-extinguishment or slow burn rate) is dictated by the specific regulatory test under which the material is rated/sold, which in turn is governed by fire risk scenarios.

1.2.2 FIRE RISK SCENARIO

A fire risk scenario is a study and risk assessment of the potential of the material to become ignited, or to contribute to fire growth in a particular situation. The fire risk scenario, once identified, helps to determine how a material will be fire retarded or made fire safe to resist that particular fire risk scenario, or at least not contribute negatively to fire growth. Fire risk scenarios are highly varied, and their relationship to regulatory tests is not always straightforward. For more details on this, the reader is encouraged to peruse Chapters 3, 14, 15, and 21.

1.2.3 FLAME RETARDANT

This term is used for any additives that allow a polymer to retard a flame, or for any polymer that shows the ability to slow fire growth when ignited. It does not mean noncombustible or ignition resistant—these are very different terms and should not be used to describe a flame-retardant material. A material that is truly noncombustible or ignition resistant either cannot be combusted (no thermo-oxidative decomposition can occur) or cannot be ignited with a particular size

flame/heat source. Here, things sometimes get confusing: A material could be flame retarded so that under a test that measures aspects of ignition or combustibility, the material is measured/assessed to be noncombustible/ignition resistant, but under another set of conditions it burns with ease. Of final note, the term “flame retardant” is often abbreviated as “FR,” such that flame-retardant additives are described as “FR additives” or sometimes just as “FRs.” A flame-retardant plastic, though, may be listed as “FR plastic” or “FR resin” or described simply as an “FR material.” When reading, look at how the author uses the term because one may use an FR additive to make a FR polymer.

1.2.4 COMBUSTIBILITY

Combustibility is defined by a series of conditions, as is the ability to resist ignition. It can be said that all carbon-based materials can be combusted (converted to CO_2 and H_2O) with enough heat and oxygen, but it may be hard to do so under some conditions, so a particular test may define certain carbon-based materials as noncombustible. Only inorganics (glasses, ceramics) and metals in their highest oxidation state would be noncombustible using the definition of thermo-oxidative decomposition. Again, Chapters 3, 14, 15, and 21 address aspects of these definitions, but the reader is encouraged to understand that fire retardant does not always mean noncombustible.

1.2.5 THERMAL DEGRADATION/DECOMPOSITION

Another set of definitions with which one should be aware is the difference between thermal degradation and thermal decomposition, because they are not exactly the same thing. *Thermal degradation* means that under heat exposure, some property of the material has degraded or become less than what it was before exposure to heat.

Thermal decomposition, on the other hand, means that the material has decomposed from its component parts upon exposure to heat, and for polymeric materials, this means that bonds have been broken, causing the polymer to depolymerize and break up into potential fuel molecules. It is important to remember that polymer decomposition is a free-radical process under fire conditions, and the chemical reactions of bond cleavage and the subsequent pyrolysis of smaller molecular weight fragments from the polymer can be quite complex. A synopsis of these chemical pathways is discussed in more detail throughout the book, with primary emphasis in Chapters 2, 4 through 6, 8 through 10, 12, 13, 17 through 19. Indeed, understanding how a polymer decomposes is essential to understanding its flammability behavior and how to flame retard it.

1.3 PROTECTION FROM FIRE: MODERN VERSUS HISTORICAL VIEWPOINTS

The need to protect materials against fire has been a scientific undertaking for a very long time. The use of flame-retardant additives for polymeric materials is, of course, a more recent thing, with modern synthetic polymeric materials having been invented in the early twentieth century. The earliest fire retardants for synthetic polymers were halogen based, based on the discovery of halogenated hydrocarbons and waxes that effectively flame retarded Army tents. New chemistries followed shortly thereafter, but each of these chemistries was created in response to a particular need to flame retard an object. It began with tents, but as more and more polymers moved into daily life, fire-safety engineers and insurance companies found a need to push for additional fire safety. It is worth mentioning again that this field of research is regulation driven, and many of the fire-safety regulations in effect today began in the early twentieth century when insurance companies, tired of paying on losses due to fire, began to push for greater fire safety. Eventually fire-safety advocates took over pushing fire safety from the insurance companies, but this early start in the insurance industry is why so many fire-safety standards were created by organizations like Underwriters Laboratories (UL) and Factory Mutual (FM); commercial products today are certified by these organizations before they can be sold in the United States. Later the U.S. federal government added

its own regulations for particular fire-safety needs, as did U.S. state governments and other organizations worldwide. There is no one universal fire standard worldwide, which is why fire risk scenarios set the fire test that a material must pass, and, in turn, why a particular flame-retardant system is designed to pass that test. This is important to understand because no one system will pass all fire tests, and, in general, today one designs a system to meet a particular test, not to be flame retardant against all fire situations. Since the intensity of a flame will vary from situation to situation, it is almost impossible to create a universal flame-retardant system; instead, industry and others design flame-retardant polymeric materials try to pass the test that is related to a specific fire risk scenario. This approach, though, runs into trouble with the “reactive” approach of providing fire safety for a material.

The way that new fire-safety regulations have come into being is from a reaction or response to a particular problem. There are many examples to choose from here, but we will focus on three: plastics in cars, polyurethane foam, and polymers for electronics.

For automobiles in the United States in the 1970s, there was not only a strong concern over the high number of fires in automobile crashes, but also over how the plastics in the interior of the car would respond to small ignition sources (cigarette ashes). A fire standard, Federal Motor Vehicle Safety Standard 302 (FMVSS 302), was created to assess the potential for flame spread in an automobile. At the time, the standard did its job, but as there is an ever-increasing demand for fuel efficiency in cars and a desire to use new materials in automobile construction, the amount of plastics in a car crept up from 10 kg in a 1970s car to 90–100 kg in a modern 1990s–2000s car.³ The FMVSS 302 test, which is a very simple test to pass, really just assesses how well a flame will spread once a car interior material is ignited, and almost any plastic today will pass the test. This presents a problem in that a historical standard, which worked for its time, has not kept up with modern changes, so that now the primary fire risk in a collision is not just from the fuel tank rupturing and leading to fire, but the fact that there is about 90–100 kg of solid fuel inside the automotive compartment where the passengers are located. Indeed, studies have shown that modern cars do much worse in fires than their older counterparts,^{4–6} but the standard has remained unchanged since only recently has this concern begun to be voiced. It will likely again take catastrophic fire losses for people to react and demand a change in fire safety, but there is hope that regulators will listen to history and be proactive, rather than reactive, to the problem. If a change in fire-safety performance for automotive plastics is enacted, then there will be a huge demand for flame-retardant products in cars. Of course, with the advent of electrical and alternative energy cars, the fire risk scenario may change again, so that one only needs flame-retardant materials around batteries and fuel cells as the fuel pool fire scenario disappears in future cars that no longer use the internal combustion engine. How the standard will change and what it will look like in the future remains to be seen, but change is needed.

The flammability issues of polyurethane foam have been well understood for some time now, but the approaches to fire safety with this highly flammable material have been varied. In the United States, the fire risk scenario was identified as people smoking in bed, and the solution at the time was to educate the public about smoke detectors, as well as to make sure the fabrics used could resist a smoldering ember source, like that from a cigarette. In the United Kingdom, though, the problem was tackled at the polyurethane level, and required high levels of flame retardancy to pass a very strict fire test, the Crib V test.⁷ This test, named for the class V wooden “crib” fire source, is still the strictest in the world for fire safety of polyurethane foam used in furniture or bedding, and as such, the United Kingdom has practically no fire losses due to furniture or bedding ignition. While the smoking problem has been addressed in the United States, the polyurethane foam is still very flammable. Recent state regulations, like California Technical Bulletin 117 (TB 117), have sought to address this by using a stricter fire test which in turn causes manufacturers selling in California to provide a more fire safe (flame retardant) product. By default, as most manufacturers wish to sell a global or U.S.-wide product, many polyurethane foam products are meeting TB 117, which as a whole improves the fire safety of all U.S. homes because polyurethane foam has been identified as

the number-one fuel load in household fires.⁸ Further, in the United States there have been several major programs at the U.S. National Institute of Standards and Technology (NIST) to study and improve the flammability performance of polyurethane foam.^{9,10} This work, along with industry recognition to improve their products, has led to significant progress in addressing the flammability issues of polyurethane foam. So, while progress has been made in this area (again, a reaction to a problem) in the United States, there may be other changes on the way which again change the nature of the fire risk for a polyurethane-containing product. More and more synthetic fabrics are being used, especially those based on polyolefins, which are well known to be highly flammable. So, if the polyurethane foam is flame retardant but the fabric is not, what then? Or, as some manufacturers are requesting, what if a performance-based standard was in place, where one tests the entire bed or piece of furniture to ensure low heat release rather than passing a regulatory pass/fail test? In this case, the use of protective fabrics that char and protect the underlying polyurethane foam may provide the same level of fire protection as flame retarding the foam. Therefore, the field of flame retardancy for polyurethane foam is in flux. Much research on flame retarding the foam is underway, and yet other market forces and indecision about performance-based versus measurement-based fire-safety standards make one wonder if improvements in the fire safety of polyurethane foam will occur in countries other than the United Kingdom. Polyurethane foam represents an example of a new material far superior to those of old (straw/hay/animal fiber) for use in bedding and furniture, and yet its use still causes struggle for those promoting fire safety. No one would ever propose getting rid of it, and yet its fire risk still is largely unaddressed throughout most of the world.

Polymers for electronics are the class of materials in use today that has perhaps led to the most change in flame retardancy. Certainly electronics technology has changed the most in the past 50+ years, and as it has changed, so has plastic usage. Originally, plastic components were a minor part of electronics, only used in some circuit boards and internal wiring and parts of keyboards. Today, they are a part of almost every component on a computer (laptop or desktop) as well as most modern electrical equipment and electronic appliances. As electrical short circuits (failures) can be possible ignition sources, it is very important to flame retard the polymer if the plastic is anywhere near a power supply or electrical component that can give off heat when it fails (capacitors, heat sinks, etc.). Again, the insurance industry helped to create the early regulations and fire testing standards to protect electrical and electronic equipment, and the best example of this, still in use today, is the UL-94 test.¹¹ This test exposes a small plastic specimen, in either a vertical or horizontal configuration, to a small calibrated Bunsen burner flame (25–125 mm in height) for short 10 s ignitions, and the time to extinguishment is recorded. The time to self-extinguishment determines the rating of the material, with higher ratings (V-0 or 5-V) being typically used for electronic equipment. This test originated in the early days of electronic equipment in the U.S. home, specifically the 1950s, where many U.S. homes had a television set in the living room. The UL-94 V test (V for vertical test) was designed to mimic the television (TV) set on wheels, which was often moved over the 1950s style carpet for typical American family gatherings. If the television set caught fire, flaming drips could fall from the TV set and ignite the carpet underneath. Since then, parts of the carpet have become flame retardant, and more importantly, the design of the television set has changed. Flat screen TVs can be mounted on walls, ceilings, or many other surfaces, and therefore if the power supply ignites and the polymer drips, where would it go? The flame spread may be much less if the plastic sticks to a painted wall (gypsum wallboard, plaster), but could be much worse if the wall is wooden. With other electronic equipment becoming so ubiquitous in the home, now the question arises about not only internal ignition (electrical failure inside the equipment) but also external ignition. There are increasing concerns about small flame sources igniting electrical equipment from the outside,¹² especially in Europe.^{13–15} So when a candle flame touches a non-flame-retardant plastic on the outside of an electrical equipment item, what will happen? The answer is very complex, and it depends upon the level of flame retardant in the plastic exposed to the candle-like flame. If the plastic is UL-94 rated V-1 or better, nothing will happen, as the flame will go out; but if the plastic has a lower flame-retardant rating, the flame can spread rapidly, and in some cases can lead

to very large fires. Extensive studies done by many laboratories have shown that a small candle-like flame can ignite a non-flame-retardant plastic casing for a TV set or printer that can easily lead to room flashover.¹⁶ The U.S. NIST had a program called “Flammability Measures of Electronic Equipment” that studied several commercial plastics at both bench scale and large scale, and they found that parts made from UL-94 V-1 or better plastics would not ignite with a small candle-like flame.^{17–19} However, if a non-flame-retardant keyboard was put under a computer monitor case, and the keyboard was ignited, the heat release from the burning keyboard would overwhelm even the higher-rated flame-retardant plastics. Therefore, the fire risk scenario of electronics is continuing to change as new technology enters the marketplace and the regulations are not keeping pace. Keeping materials with a UL-94 V rating in place appears to be a reasonable place to start, but many changes in how these items are mounted on walls or used in homes may result again in regulators reacting to change rather than being proactive in fire-safety performance.

None of these scenarios described earlier are easy to address in a proactive manner. If regulators kept products from entering into use until they could determine all possible fire risk scenarios, many products might never come to the marketplace. Practically speaking, no regulator can envision all possible fire risk scenarios for a material. Some things cannot be envisioned until they are used by the consumers, and therefore some regulation changes must be reactive rather than proactive. Still, regulators and consumers need to be aware that fire risk never goes away, and so one should not be surprised when changes in technology lead to changes in consumer use, which either defeats the fire protection in place for that material or makes the fire protection irrelevant for the ways the material is used. Perhaps, now more than at any other time in human history, the rapid changes in technology require all of us to be flexible not just about how we use a material, but also how we think about that material from a fire-safety perspective and a total life cycle view.

1.4 CHANGING PERCEPTIONS, REGULATIONS, AND CUSTOMER DEMANDS

Just as changes in technology result in new fire risk scenarios, societal changes can affect flame retardancy and fire safety as well. Some of the biggest changes in flame-retardant materials have come from changes in waste disposal and recycling of materials that have reached the end of their usefulness. The best example of this is how the European Union (EU) disposes of its waste and the laws it enacted to deal with the waste. In the EU, landfills are not typically permitted because land in Europe is at a premium, with almost all existing land either used for agriculture or for living space and industry. So, waste is incinerated rather than sent to a landfill. Early on in this process, it was found, in some cases, that the brominated flame retardants in flame-retardant plastics would produce brominated dioxin compounds. When this was discovered, some EU states pushed to have these compounds removed from use in plastics, which led to a decade long legal struggle between EU governments, environmental nongovernmental organizations (NGOs), fire-safety regulators, and the makers of brominated flame retardants. Much of this story and the current state of these regulations are described later in Chapter 22, but to summarize, the change in a non-fire-related activity has led to changes in how flame retardants are used and which ones are perceived to be safe. More importantly, it has led to a discussion on fire safety in general and whether fire-safety/flame retardancy is still an acceptable environmental policy.

The environmental impact of waste disposal and of chemical use in Europe has led to three legislative actions that, in today’s global economy, greatly affect flame-retardant use and research. These actions go by the acronyms of RoHS (Reduction of Hazardous Substances), WEEE (Waste Electrical and Electronic Equipment), and REACH (Registration, Evaluation, Authorisation, and Restriction of Chemical substances). These actions are discussed in detail in Chapter 22, but need to be mentioned here as they are clear examples of how changing regulations affect flame-retardant use, selection, and new fire-safety developments. The first one, RoHS, refers to how new items are manufactured, and specifically bans chemicals and elements of environmental and toxicological concern in Europe. One fall-out item of RoHS is the move from a lead-based solder on circuit

boards to a non-lead-based solder. The new solders (usually tin based) are higher melting, and as such, require epoxy circuit boards of higher thermal stability. This has led to the some deselection of brominated flame-retardant epoxies simply because the C-Br bond on tetrabromobisphenol A is not thermally stable enough to survive exposure to the higher melting point solder. The organobromine bonds break down upon exposure to this solder, which degrades circuit board performance. So, the selection of a material which at first glance has nothing to do with FR performance has led to a new paradigm in flame-retardant research: Higher thermal stability of the polymer itself to withstand high-temperature solder while maintaining flame-retardant performance.

WEEE has had a direct affect on flame-retardant use, because flame retardants are used in almost all electrical and electronic equipment to prevent fires from short circuits. This directive lays down rules for disposal and recycling of all electrical and electronic equipment that goes back to the previous incinerator discussion. For flame retardants, this directive affects how the plastic parts, cable jackets, and enclosures are flame retarded. If the plastic cannot be reground and recycled, it must go to the incinerator, in which case it cannot form toxic by-products during incineration. This has led to the rapid deselection of brominated FR additives in European plastics that are used in electronics, or the complete removal of FR additives from plastics used in electronics in Europe. This led, in turn, to increases in electrical fires in Europe, and now customers and fire-safety experts demand low environmental impact and fire safety. However, the existing nonhalogen flame-retardant solutions brought in to replace bromine have their own balance-of-property issues, and so research continues to develop materials that can meet WEEE objectives.

Of all the new regulations affecting flame-retardant research, REACH is likely to have the greatest impact on any new flame-retardant solution created to address RoHS and WEEE regulations. As this regulation affects all new and existing chemicals in the EU, all flame-retardant additives (each of which is a chemical compound) in use, or proposed for future use, must go through extensive testing and certification before they can be used. If they do not pass this battery of tests, then they are banned from future use, which means there would be fewer solutions available for fire safety. Therefore, REACH affects not only current flame-retardant additive use, but also research to develop new flame-retardant additives. Why spend any time and effort on the development of a new flame-retardant solution if it has no chance of passing REACH? This makes it more difficult for the flame-retardant researcher to figure out which chemical compounds to synthesize and test if they do not pay attention to potential environmental impact and toxicology first. Therefore, REACH may add yet another scientific discipline to flame-retardant research—toxicology and environmental science. So one can ask—why did these regulations come into being in the EU and not everywhere at once? To understand this, one must again look at the life cycle (creation, use, and disposal) of plastics.

Plastics that contain flame-retardant additives have one of three fates at the end of their life cycle. The first is to put the material into a landfill, the second is to incinerate it to recover energy from the material, and the third is to regrind, recycle, and reprocess the plastic for later use. All three approaches have their advantages and disadvantages, but overall, incineration and recycling are preferred. Within those two approaches though, the perception exists that flame retardants do not belong due to the pollution they cause during incineration or the pollution caused by recycling the plastic that may cause the additive to leach out of the plastic. There are data both for and against these perceptions of flame retardants in plastics, but the environmental NGOs have been winning public opinion that it is better environmental policy to leave the flame retardants out completely. This argument, though, only holds true if that non-flame-retardant plastic does not catch fire. Several studies have shown that the amount of pollution that enters the environment when a plastic catches fire is far greater than the pollution used in the creation and disposal of a flame-retardant plastic.^{20–24} This is because when a non-flame-retardant plastic catches fire, it tends to give off so much heat that it ignites other nearby objects, and those objects in turn quickly cause the heat release in the room to escalate, leading to major fire losses, large amounts of toxic emissions, and in some cases, loss of life. So, one has to make a decision—is it more acceptable to lose life and property to fire for the

potential long-term benefit of the environment, or is it more acceptable to save lives and deal with potential pollution issues when the plastics are not dealt with correctly at the end of their lifetime? The answer to this question is complex and both sides of the argument have made impassioned pleas for their side. It is possible to have both fire safety and good environmental policy, but it requires an understanding of the following:

1. Passive fire protection (flame retardants in plastics) is an important societal benefit.
2. Passive fire protection can be developed in a way that is environmentally friendly and is easily recycled.
3. Both sides will need to set aside their preconceived notions about the other and be willing to work together.

Humanity is, by nature, emotional, and emotions on both sides of this issue make progress difficult for new fire safe materials, whether in response to new fire risk scenarios or in response to non-fire-related issues. This last point should make it clear that flame retardancy of plastics is not a simple scientific issue, but one that must take into consideration societal, emotional, and non-fire-related issues to make an acceptable new flame-retardant material in the twenty-first century.

Along with the changes in the perceptions of flame retardants, there are changes in fire-safety requirements as well. Many of the changes were discussed in Section 1.3, and they are covered in detail in Chapter 21, but one of the changes is a move from pass/fail testing to performance-based testing. Performance-based testing allows for more freedom in how an item is constructed or assembled to meet fire-safety needs. This tends to be a final article testing rather than testing of a specific flame-retardant material, and therefore modeling becomes quite important in performance-based methodology. These modeling approaches are discussed in Chapter 20, and modeling allows regulators and fire-safety engineers to see how a construction performs in a particular fire scenario. While this approach yields high flexibility for the fire-safety engineer, it can make things difficult for the scientist trying to flame retard a material for an application. With no guidance on what the flame-retardant test should be for a particular component of the final article, the flame-retardant materials scientist will need to understand fire-safety engineering and these new models to better design their materials. It is likely that the change in performance-based codes, along with changes in environmental standards, will yield all sorts of new flame-retardant materials used in new and very creative ways. However, this change indicates that the burden of flame retarding the polymeric material may fall upon the final item/assembly producer, and no longer on the resin companies that compound flame retardants into plastics before they sell it. All of this is uncharted territory, and the correct path for polymeric fire-retardant materials remains to be seen. It is likely, though, that there are multiple paths forward where new engineering approaches and flame-retardant chemistry will coexist to produce new fire-safe and environmentally friendly polymeric materials.

1.5 FLAME-RETARDANT CHEMISTRIES

With this background, one begins to see why this field is so complex and that there is no simple answer to flame retardancy of polymers. This complexity is also why there are so many flame-retardant chemistries to choose from because many flame-retardant chemistries are tailored to a specific polymer for a specific test (see Chapters 22 through 26). However, there are some broad categories of flame retardants in use today, including halogenated compounds (Chapter 4), phosphorus-based compounds (Chapter 5), intumescent protective systems (Chapter 6), mineral fillers (Chapter 7), silicon and inorganic oxides (Chapter 8), boron chemistry (Chapter 9), polymer nanocomposite systems (Chapters 10 and 11), and interfacial systems composed of multiple components to generate flame-retardant effects (Chapter 12). For many of the reasons described in Section 1.7, halogenated flame-retardant chemistry is not as greatly researched in academic

circles as it once was, although it continues to be a robust field of flame-retardant chemistry, especially among the industrial manufacturers who produce these compounds. Non-halogenated flame-retardant systems have grown by leaps and bounds in the open literature as well as in the patent literature, again for the reasons described previously.

Within each of these chemical approaches to flame retardancy, one will find a variety of chemical structures and compounds that yield specific effects of flame retardancy under specific conditions. Some compounds are fairly universal and reduce heat release under all conditions (halogen, phosphorus, and mineral fillers), while others have unique activation conditions and protective schemes that can be very robust, but are limited to a small number of polymers with which they can be used (intumescent, inorganic compounds, and nanocomposites). Some materials by themselves enhance the flame retardancy of other compounds (boron, inorganic oxides, and nanocomposites), while others not only enhance a wide range of flame retardants, but also bring multifunctional performance to a material. Polymer nanocomposite technology fits this last category in that the nanocomposite brings enhanced mechanical, thermal, and sometimes electrical properties while also reducing the heat/fuel release of that specific polymer.²⁵⁻²⁹ Normally, flame-retardant chemistry has involved the addition of a particular material only for the enhancement of flammability performance to the material, so the promise of bringing something in for flame retardancy and thermal, mechanical, and other properties has led to an explosion in new materials science research for nanocomposites in general, and it certainly has been a boon to flame-retardant research as well. The field of flame-retardant polymer nanocomposites will only continue to expand as the realization grows that the nanocomposite brings enhanced properties to the final system and, in many cases, serves as a superior system to the traditional flame-retardant materials in use today. However, not all material choices will require nanocomposite technology to be successful in the future, especially when one considers the current cost of some nanoparticle sources (such as, carbon nanotubes). It is important to remember, again, that this field of research is driven by regulations, both fire and nonfire related, and with that the research sometimes is reactive to the regulations rather than proactive. Flame-retardant chemistry is much more varied now than it has ever been, and it will continue to grow as chemists look for new alternatives to existing flame-retardant systems.

1.6 FLAME-RETARDANT RESEARCH

Research into the flame retardancy of polymeric materials, and indeed the fire safety of all materials in use today (wood, steel, glass, plastics, etc.), is truly a worldwide field of materials science study. Research is done in academia, government, and industry on every continent in the world today, and each group has its own areas of emphasis and expertise. Industrial work focuses largely on the development of new materials for sale that meet the regulations, and as such, is not broadly shown in the scientific literature and is almost completely limited to the patent literature. Therefore, it is hard to determine which companies are leading the way in new flame-retardant material research other than by looking at their offerings of flame-retardant products. Obviously, the main flame-retardant additive manufacturers (e.g., ICL, Albemarle, Clariant, and Chemtura) conduct the greatest amount of new flame-retardant chemical research, but it is not unheard of for the end-users of these additives to conduct their own flame-retardant chemical research. So, in published research of access to everyone, most of the conducted research focuses on fire-safety engineering more than new flame-retardant chemistry, but still, the work is related as the new fire safety engineering research leads to new regulations that the flame-retardant chemistry has to meet.

Some of the preeminent fire-safety and flame-retardant research organizations worldwide are listed in the following text. The list is by no means comprehensive, and focuses on the organizations that are known to publish often in the fields of flame-retardant research or fire-safety engineering. This list includes links to the organizations to learn more about the range of services and research they offer.

- National Institute of Standards and Technology-Building and Fire Research Laboratory (NIST-BFRL): <http://www.bfrl.nist.gov/>
- Underwriters Laboratories (UL): <http://www.ul.com/>
- FM Global (Factory Mutual): <http://www.fmglobal.com/>
- Southwest Research Institute (SwRI) Fire Technology Division: <http://www.swri.org/4org/d01/fire/home.htm>
- Federal Institute for Materials Research and Testing (Germany – BAM): <http://www.bam.de/>
- SP Technical Research Institute of Sweden: <http://www.sp.se/en/areas/fireprotection/Sidor/default.aspx>
- Bolton Institute Centre for Materials Research and Innovation <http://www.bolton.ac.uk/CMRI/>
- State Key Laboratory of Fire Science, Hefei, China <http://fire.ustc.edu.cn/>
- Commonwealth Scientific and Industrial Research Organization (CSIRO) Fire Safety & Control Division: <http://www.csiro.au/science/FireSafety.html>
- The Centre for Engineering of Plastic Materials, Polytechnic of Torino, Sede de Allessandria, http://www.cdcmp.it/englishversion/ricerca_eng.html

1.7 THE FUTURE OF FLAME-RETARDANT SCIENCE AND POLYMERIC MATERIAL FIRE SAFETY

With all the changes underway for flame-retardant technology, sustainability requirements for polymeric materials, and ever-changing fire risk scenarios, it can be quite hard to predict what the future of flame retardancy will be, but there are some trends and information that allow us to make some suggestions about the future. So, our predictions for the future are the following:

- Multifunctional fire safe materials
- Combinations of additives (or reactives), rather than use of a single FR additive
- Less use of flame-retardant additives and more use of reactive flame retardants and inherently nonflammable polymers
- More use of engineering solutions to meet performance-based standards
- More emphasis on heat release measurements from polymeric materials and total fire-safety assessments
- Development of new fire behavior prediction tools and small-scale screening/testing tools

Multifunctional materials are materials that have more than one enhanced property, allowing those materials to simplify the construction of devices. This means that a multifunctional polymeric material could replace a metal or ceramic in some applications, because the multifunctional material now has properties similar to the metal or ceramic, allowing for weight and density savings in some devices and complex constructions. Polymer nanocomposite technology has been at the forefront of producing multifunctional materials, as the nanoparticles often bring more than one property enhancement to a polymer. For example, carbon nanotubes/nanofibers bring enhancements in electrical conductivity to nonconductive plastics, allowing them to replace metals in some applications. Many polymeric nanocomposites show enhanced flammability performance as well, so as nanocomposites are used more, the lowered flammability of those materials will be gained as well. Today, many materials do require multiple property enhancements, such as high mechanical strength, ability to be colored, antioxidant/UV resistance, flame retardancy, and the ever-demanded low cost. Obviously, flame retardancy will just be one of many on a long list of requirements, but balancing that flame retardancy with other properties will continue to be a challenge, as it is today. However, the producer of these materials may be able to justify higher cost if the material is truly multifunctional and can replace other materials in device construction. Polymer nanocomposite technology is more expensive today (for good reason) and it will not be used in all applications—only

where it makes sense to do so. Therefore, the flame-retardant researcher should focus on flame retardancy that will fit into a multifunctional material where something else in the system is lowering flammability, allowing less flame-retardant additive to be used. This involves paying attention to how the multifunctional material will be used as well as focusing on what the potential fire risks will be and whether flame retardancy will be needed at all in the material.

The general situation at the moment is that only a single FR additive is used; this may include a synergist, as with halogen synergized with antimony oxide. The future is likely to bring combinations of additives in which one has certain advantageous effects, but also disadvantages, and another additive overcomes the disadvantages of the first. Nanocomposites are very likely to be used in this way with the nanocomposite formation offering some advantage, and this may be not only in fire retardancy but also in some of the multifunctional realms mentioned earlier, with other materials accomplishing other needs (Chapter 12). Or instead, the combinations may address more than one aspect of a fire risk scenario, with one additive being used to address flame spread/heat release while another addresses smoke/toxic gas release.

With all the demand to prevent the accidental release of flame-retardant additives into the environment, one must begin to completely reconsider the approach of using flame-retardant additives. Certainly, putting an additive into a plastic is one of the cheapest ways of providing flame retardancy, but since the additive is not bound to the plastic, it can be released. Therefore, a better approach may be to consider flame retardants which either co-polymerize with the polymer monomers during the polymer production process or react onto the polymer backbone during the melt compounding process. The advantage of this approach is that the additive cannot leach out of the plastic and into the environment over time—it is part of the polymer, and as long as the polymer is disposed of properly, the flame-retardant additive no longer presents an environmental concern. Further, when this type of flame-retardant plastic is recycled, the flame-retardant additive stays with the polymer and can be used again. Another solution to the use of the additive problem is to use inherently flame-retardant polymers; specifically polymers with a low heat release. No carbon-based polymer is flame resistant, but there are many commercial polymers today that are inherently flame retardant and are difficult to burn.

The disadvantage of using these inherently flame-retardant polymers or flame retardants, which become part of the polymer is that they are much more expensive today than the additives that can be simply added to the plastic. The demands for the better sustainability of plastics could be met with technology available today, but the costs prevent them from being implemented. However, these ever-increasing demands will eventually lead to the use of these materials, and therefore the future emphasis will be on finding cheaper feedstocks for these reactive flame retardants and inherently flame-retardant polymers, or finding new flame-retardant chemistry that can be made from less expensive chemical feedstocks. Some of this new technology is likely to come from the revolution in bio-based chemistry and plant-based polymers, but the wide diversity of organic chemical structures suggests that finding new flame-retardant polymers and co-reactive flame retardants is a wide and unexplored area for future research work.

Performance-based codes and standards were created to allow for more creativity to address a fire risk need, rather than to force a particular solution for all situations. With this slowly developing trend, more and more engineering solutions are being implemented to address fire risk scenarios. An engineering solution can best be described as using a design to thwart ignition and fire growth rather than using flame-retardant additives. This solution can include removing the possible ignition source (e.g., a power supply) from flammable plastic, or encasing the flammable fuel in a nonflammable shield. For the former example, power supplies for inkjet printers and laptop computers are outside the main electronic device. For the latter example, more manufacturers of beds are using inherently low-flammable fabrics as “wraps” for polyurethane foam so that the beds can meet some of the new strict fire-safety codes. Engineering solutions are already in place today in the form of sprinkler systems, intumescent coatings for steel, and flame arrestors on engines and fuel pumps. As the complexity of flame-retardant codes and regulations increases,

it is highly likely that there will be more uses of engineering solutions to meet fire-safety needs. These engineering solutions will be unique to each product and, like flame-retardant chemistry today, there will be no one solution for all applications.

The changes in fire-safety regulations, especially with an emphasis on performance-based fire standards, suggest a major change is coming as to how the flame-retardant researcher measures flame retardancy and develops new fire safe materials. Simply getting a UL-94 V-0 result may not be enough for future systems, and so the researcher may need to work with fire-safety engineers to see how their material performs not just in bench-scale fire tests, but also in full-scale performance-based fire tests. This will involve more scientific fire testing, such as cone calorimeter heat release testing, as well as assessments on smoke and toxic gas release from fires. Further, the flame-retardant researcher may also need to be involved in the product design from start to finish to ensure the final product meets the performance-based code. This change involves a different way of thinking about flame retardancy when considering performance-based fire codes. Rather than just looking at a series of pass/fail tests to dictate which materials can be used in an application, the researcher and engineer have more freedom to design the system however they want—provided it meets a level of fire-safety performance. So now the researcher must think about the fire risk scenario and use materials that meet the fire risk in that specific design, not just provide materials that pass a test. This goes back to the comment that what is a flame retardant for one application may not be appropriate for another application, and more importantly, what shows a pass result in one test in one polymer may not be equal in fire performance to another polymer which passes, or does not pass, that same test. Flame retardancy today is tailored to pass a specific test, not to be universal, and this trend will continue under performance-based codes, but now will require greater awareness of the inherent heat release and flammability characteristics of that material. Perhaps, more than the other changes mentioned earlier, the coming of performance-based fire standards will be the most challenging for flame-retardant materials researchers to deal with. With that said, the flame-retardant researcher will need to become more multidisciplinary, and will need to learn to speak the language of fire-safety engineering while maintaining high levels of proficiency in flame-retardant chemistry and polymer thermal decomposition science to design the new flame-retardant materials for the twenty-first century.

One example of the fusing of disciplines to design new flame-retardant materials is the growing need for small-scale flame-retardant testing and fire behavior prediction tools. Researchers in the area of high-throughput research and combinatorial chemistry are just now starting to tackle the needs of flame-retardant research, and it is made clear in Chapter 16 that there have been some great advances, but much still needs to be done. Modeling efforts are also ongoing to better understand how different materials affect fire risk scenarios, and to predict fire-retardant behavior; these involve the disciplines of chemistry, materials science, physics, and computer science. Some of this is covered in Chapters 18 through 20, but the ability to correlate the results of a small-scale fire test to a large-scale fire test is an ongoing need that continues to elude many fire-safety researchers. As the regulatory tests all address very specific fire risk scenarios and very specific flammability behavior (both chemical and physical), it is not surprising that there are no universal models for this type of prediction. Still, correlations between small-scale and large-scale tests will continue to be an area of future research, difficult though it may be.

The field of polymeric flame retardancy is undergoing a great deal of change, reacting to new requirements, fire risk scenarios, and other requirements for polymeric materials. Those who pay attention to these coming changes, as well as being aware of the current technology available to flame retardancy, should be able to develop new materials in response to these changes, as well as come up with new innovations in flame retardancy. Fire will not just go away as our society advances, and it is very likely that we will see more, not fewer, polymers in use throughout society worldwide. With this increase it seems that there will be more need, not less, for those of us who practice this field of science. At the moment, in some countries the level of flame-retardant research funding is quite low (United States) while in other countries the funding is higher (EU, Asia),

but perhaps still not high enough to keep up with the changes. Since polymeric materials will only be used more in modern society, it falls upon fire scientists and fire-safety engineers to educate the public that these materials are inherently flammable unless they are made flame retardant. Ideally, we would like to have the fire protection in place before catastrophic fires occur, but we have to keep in mind that there are many demands on the few resources that society has at the moment, and if we want those resources, we will have to voice the need for it. Until then, it is up to those of us who practice in this field to keep guard over the potential for fire in plastics, and be willing to lend a hand when society asks for our help.

REFERENCES

1. 2006 Fire Statistics—National Fire Prevention Association <http://www.nfpa.org/categoryList.asp?categoryID=951&URL=Research%20%26%20Reports/Fire%20statistics>
2. Some statistics are available, but only for selected countries. Please see http://www.genevaassociation.org/Affiliated_Organizations/WFSC.aspx
3. Digges, K. H., Gann, R. G., Grayson, S. J., Hirschler, M. M., Lyon, R. E., Purser, D. A., Quintiere, J. G., Stephenson, R. R., and Tewarson, A. Human survivability in motor vehicle fires. *Fire Mater.* 2008, 32, 249–258.
4. Ahrens, M. *U.S. Vehicle Fire Trends and Patterns*. National Fire Protection Association: Quincy, MA, 2005.
5. U.S.F.A. *Highway Vehicle Fires. Topical Fire Research Series*, Vol. 2, No. 4. U.S. Fire Administration, Emmitsburg, MD, March 2002.
6. Friedman, K., Holloway, E., and Kenney, T. Impact induced fires and fuel leakage: Analysis of FARS and state data files (1978–2001). *Society of Automotive Engineers World Congress*, Detroit, MI, 11–14 April 2005. Paper 200501-1421.
7. BS5852, Methods of test for assessment of the ignitability of upholstered seating by smoldering and flaming ignition sources, British Standards Institution, London, United Kingdom, 2006.
8. Hirschler, M. M. Polyurethane foam and fire safety. *Polym. Adv. Technol.* 2008, 19, 521–529.
9. Ohlemiller, T. and Shields, J. Aspects of the fire behavior of thermoplastic materials, *NIST Technical Note* 1493, January, 2008.
10. Zammarano, M., Kramer, R. H., Harris, Jr. R., Ohlemiller, T. J., Shields, J. R., Rahatekar, S. S., Lacerda, S., and Gilman, J. W. Flammability reduction of flexible polyurethane foams via carbon nanofiber network formation. *Polym. Adv. Technol.* 2008, 19, 588–595.
11. UL-94: Test for Flammability of Plastic Materials for Parts in Devices and Applications [Includes ASTM D635-98 (UL-94 HB), ASTM D3801-96 (UL-94 V), ASTM D4804-98 (UL-94 VTM), ASTM D5048-97 (UL-94 5V), ASTM D4986-98 (UL-94 HBF)].
12. Hall, J. R. Fires involving appliance housings: Is there a clear and present danger? *Fire Technol.* 2002, 38, 179–198.
13. Hoffmann, J. M., Hoffmann, D. J., Kroll, E. C., and Kroll, M. J. Full scale burn tests of television sets and electronic appliances. *Fire Technol.* 2003, 39, 207–224.
14. Simonson, M., Andersson, P., and Bliss, D. Fire performance of selected IT-equipment. *Fire Technol.* 2004, 40, 27–37.
15. Hong, S., Yang, J., Anh, S., Mun, Y., and Lee, G. Flame retardancy performance of various UL94 classified materials exposed to external ignition sources. *Fire Mater.* 2004, 28, 25–31.
16. Babrauskas, V. and Simonson, M. Fire behaviour of plastic parts in electrical appliances: Standards versus required fire safety objectives. *Fire Mater.* 2007, 31, 83–96. Cite papers from Fire and Materials conferences and other TV set fire papers.
17. Morgan, A. B. and Bundy, M. Cone calorimeter analysis of UL-94 V-rated plastics. *Fire Mater.* 2007, 31, 257–283.
18. Bundy, M. and Ohlemiller, T. Full scale flammability measures for electronic equipment. *NIST Technical Note* 1461 August 2004, U.S. Department of Commerce.
19. Bundy, M. and Ohlemiller, T. Bench-scale flammability measures for electronic equipment. *NISTIR (National Institute of Standards and Technology Internal Report) 7031* July 2003, U.S. Department of Commerce.
20. Simonson, M., Blomqvist, P., Boldizar, A., Möller, K., Rosell, L., Tullin, C., Stripple, H., and Sundqvist, J. O. Fire-LCA model: TV case study. SP Report 2000:13 ISBN 91-7848-811-7 Printed in 2000.

21. Blomqvist, P., Rosell, L., and Simonson, M. Emissions from fires Part I: Fire retarded and non-fire retarded TV-sets. *Fire Technol.* 2004, 40, 39–58.
22. Blomqvist, P., Rosell, L., and Simonson, M. Emissions from Fires Part II: Fire Retarded and non-fire retarded TV-sets. *Fire Technol.* 2004, 40, 59–73.
23. Simonson, M., Andersson, P., and van den Berg, M. Cost benefit analysis model for fire safety and deca BDE case study. *Proceedings of Fire and Materials 2007 Conference*, January 29–31, 2007, San Francisco, CA. Interscience Communications.
24. Blomqvist, P., Persson, B., and Simonson, M.T. Fire emissions of organics into the atmosphere. *Fire Technol.* 2007, 43, 213–231.
25. Alexander B. M. and Charles A. W. (Eds.), *Flame Retardant Polymer Nanocomposites*, John Wiley & Sons, Hoboken, NJ, 2007. ISBN 978-0-471-73426-0.
26. Morgan, A. B. Flame retarded polymer layered silicate nanocomposites: A review of commercial and open literature systems. *Polym. Adv. Technol.* 2006, 17, 206–217.
27. Ray, S. S. and Okamoto, M. Polymer/layered silicate nanocomposites: A review from preparation to processing. *Prog. Polym. Sci.* 2003, 28, 1539–1641.
28. Okada, A. and Usuki, A. Twenty years of polymer-clay nanocomposites. *Macromol. Mater. Eng.* 2007, 291, 1449–1476.
29. Utracki, L. A., Seppehr, M., and Boccaleri, E. Synthetic, layered nanoparticles for polymeric nanocomposites (PNCs). *Polym. Adv. Technol.* 2007, 18, 1–37.

2 Polymer Degradation and the Matching of FR Chemistry to Degradation

Dennis Price and A. Richard Horrocks

CONTENTS

2.1	Thermal Degradation of Polymers.....	15
2.2	Oxidative Degradation	19
2.3	Degradation of Individual Polymer Types	19
2.3.1	Thermoplastics.....	20
2.3.1.1	Polyolefins	20
2.3.1.2	Aliphatic Polyamides	20
2.3.1.3	Polyesters.....	21
2.3.1.4	Polyacrylonitrile	21
2.3.1.5	Polystyrene	22
2.3.1.6	Poly(vinyl chloride)	23
2.3.1.7	Ethylene/Vinyl Acetate Copolymers	23
2.3.2	Foams.....	23
2.3.3	Thermosets.....	25
2.3.3.1	Polyester Resins.....	25
2.3.3.2	Vinyl Ester Resins	26
2.3.3.3	Epoxy Resins	26
2.3.3.4	Phenolic Resins	27
2.3.3.5	Maleimide and Polyimide Resins.....	28
2.3.4	Natural Polymers	28
2.3.4.1	Cellulose.....	28
2.3.4.2	Protein Polymers	28
2.3.5	High Temperature-Resistant Polymers	30
2.4	Polymer Fire.....	31
2.5	Polymer Combustion Cycle.....	32
2.6	Flame Retardance	32
2.7	Relevance of Polymer Stabilization to Flame-Retardant Processes	34
2.8	Alternative Polymer Degradation Processes, (e.g., Photochemical, Plasma, Irradiation), and Their Potential Influence on Flame-Retardant Behavior	36
	References.....	38

2.1 THERMAL DEGRADATION OF POLYMERS

In fires, the polymeric materials are consumed by the flaming combustion which is a gas-phase process. Thus, the polymer must degrade to yield volatile combustible species to fuel the conflagration. To begin, this chapter first considers the various processes by which pure polymer systems degrade.

Then, the influences by which the presence of oxygen can affect these processes are discussed. The different structures of the various polymer types influence the end consequence of any decomposition, and this may affect the resistance, if any, to combustion. At this point, the polymer combustion cycle will be described.

Pure polymeric materials get degraded via one or more of the following simple processes:

- End-chain scission—individual monomer units successively cleaved from the chain end
- Random chain scission—scissions occur at random locations along the polymer chain
- Chain stripping—atoms or groups not part of the polymer backbone are cleaved off
- Cross-linking—bonds created between the polymer chains

Table 2.1 collates various examples of each of these processes and the decomposition polymers obtained.¹

Degradation is also influenced by the chemical structure of the polymer, i.e., straight chain, branched chain, or cross-linked. In addition, synthetic polymers fall into three physical types, each of which will decompose in a different manner when heated. These are: thermoplastics, which will soften and melt before decomposing; thermosetting (cross-linked) which do not melt and decompose yielding char and evolving volatiles; and elastomers which are rubber-like materials. On the other hand, the pure polymers are degraded by some kinetic process. Madorsky² defined their relative thermal stability in terms of the temperature, T_h , at which their half-life equaled 30 min (see examples given in Table 2.2). From the T_h values, the effects of the various chemical structures on the thermal stability of these pure polymers can be deduced (see Table 2.3). The Madorsky approach has the advantage of providing a simple method for comparing the thermal stabilities of a range of polymers by determining the temperature at which a polymer has lost half of its initial weight in 30 min. However, it should be appreciated that it is based on the simplified assumption of a single first-order decomposition reaction, which is not always valid. Thus, the fundamental information concerning the decomposition should not be deduced from the T_h values determined.

TABLE 2.1
Typical Decomposition Products for Each Generalized Mechanism of Polymer Decomposition

Mechanism	Examples of Polymer	Typical Products
Random chain scission	Polyethylene	Alkanes, alkenes, very little monomer
	Polypropylene	Alkanes, alkenes, very little monomer
	Polystyrene	Styrene monomer, dimer, and trimer
	More generally	Monomers and oligomers
End-chain scission	Polymethylmethacrylate	90%–100% monomer
	Polytetrafluoroethylene	90%–100% monomer
	More generally	Monomer
Chain stripping	Poly (vinyl chloride)	Hydrogen chloride, aromatic hydrocarbons, and char
	Polyvinyl alcohol	Water and char
	General	Small molecules and char
Cross-linking	Polyacrylonitrile, poly(oxy- <i>m</i> -xylene)	Char (and HCN), char
	General	Much char, few volatile products

Source: Adapted from Cullis, C.F. and Hirschler, M.M., *The Combustion of Organic Polymers*, Oxford University Press, Oxford, U.K., 1981, 117.

TABLE 2.2
Relative Thermal Stability of Selected
Polymers Based on the Temperature
at Which Their Half-Life T_h Is 30 min

Polymer	T_h (°C)
Polymethylmethacrylate A (molecular wt. 1.5×10^5)	283
Polymethylmethacrylate B (molecular wt. 1.5×10^6)	327
Poly α -styrene	287
Polyisoprene	323
Polymethylacrylate	328
Polyethylene oxide	345
Polyisobutylene	348
Polystyrene	364
Polypropylene	387
Polydivinyl benzene	399
Polyethylene	406
Polymethylene	415
Polytetrafluoroethylene	509

Source: Adapted from Madorsky, S.L., *Thermal Degradation of Polymers*, Wiley, New York, 1964.

TABLE 2.3
Factors Which Affect the Thermal Stability of Polymers

Polymer	Effect on Thermal Stability	Examples	T_h (°C)
Chain branching	Weakens	Polymethylene	415
		Polyethylene	406
		Polypropylene	387
		Polyisobutylene	348
Double bonds in polymer backbone	Weakens	Polypropylene	387
Aromatic ring in polymer backbone	Strengthens	Polyisoprene	323
		Polybenzyl	430
High molecular weight	Strengthens	Polystyrene	364
		PMMA B	327
Cross-linking	Strengthens	PMMA A	283
		Polydivinyl benzene	399
Oxygen in the polymer backbone	Weakens	Polystyrene	364
		Polymethylene	415
		Polyethylene oxide	345
		Polyoxymethylene	<200

Source: Adapted from Madorsky, S.L., *Thermal Degradation of Polymers*, Wiley, New York, 1964.

However, the intrinsic thermal degradation characteristics of any polymer may be influenced by impurity species present, as polymers are rarely pure in the true chemical sense. Such impurities may include one or more of the following:

- Impurities already present in monomeric feeds of the polymerization plants, although it may be generally stated that monomer purity is recognized as a critical variable by commercial polymer producers
- Polymerization initiation or catalyst residues present in both addition and condensation polymers
- Products of degradation generated during polymerization and processing, often of a thermally derived origin. These may include products of thermal oxidation (see below)
- Contaminants introduced during processing including atmospheric oxygen and metallic ions released from the processing plant equipment

These factors tend to be specific to each polymer type and its related polymerization history, and will be referred to in the following sections when discussing individual polymer degradation behavior, if relevant. It is sufficient to state at this point that the consequences of these impurities is usually that of promoting the overall degradation, and may give rise to the slow thermal degradation and related deterioration in the polymer properties often experienced when in use, and exposed to service temperatures well below their normal rapid degradation temperatures as defined by T_h mentioned earlier. In many cases, when exposing a polymer to its maximum service temperature, its effective lifetime is determined by the length of the induction period for these low-temperature degradation reactions to promote sufficient loss in properties, as to render it useless for its intended purpose. Such induction times may be quantified in terms of times to embrittlement, to lose 50% of the tensile strength or to change its character (e.g., color) by a specified magnitude. Often, aging at temperatures above the service life temperature but below the polymer melting point, for example, enables an “apparent” activation energy to be determined based on the assumed Arrhenius law behavior, from which service lives may be predicted.^{3,4} As the decomposition process is complex, consisting of a series of simultaneous and possibly consecutive reactions, it should be stressed that such “apparent” activation energies determined in this manner are oversimplified values, because they are composite values. Thus, these “apparent” activation energies do not provide any fundamental information concerning the individual reactions that contribute to the overall complex decomposition process. Thermogravimetric analysis has been widely used to investigate polymer decompositions.^{5,6} Such studies often indicate that the decomposition is a multistep process, where the chemistry of the decomposition changes as the temperature is raised. To gain an insight into the chemistry occurring, evolved gas analysis techniques such as FTIR⁷ and mass spectrometry (MS)⁸ are coupled to the TGA instrument. The microscale calorimetry technique developed by Lyon and Walters⁹ combines the ability to study the pyrolysis of polymers in an inert gas flow followed by complete combustion of the evolved volatile gases. Oxygen depletion¹⁰ is used to measure the heat of combustion, which can be related to the flammability of the material under investigation. The technique provides a method of evaluating both the thermal behavior and the flammability of the polymer materials in milligrams.^{11,12} Solid-state NMR¹³ and selective isotopic labeling¹⁴ provide even more detailed insight into the degradation chemistry. Most research has been carried out on single polymers. Sometimes, the behavior of polymer mixtures is of interest. The distribution kinetics of a binary polymer mixture decomposition has been investigated by applying distribution kinetic theory, based on molecular weight distributions.¹⁵ Attempts have been made to apply quantum chemistry and molecular simulation techniques to determine the mechanisms and rates of polymer degradations.¹⁶ It is hoped that this work will lead to methods for predicting material flammability and the development of strategies to improve fire resistance.

In addition to the challenges posed by the presence of impurity, polymeric materials are rarely used in the “pure” or even stabilized state, but are normally compounded with various compounds

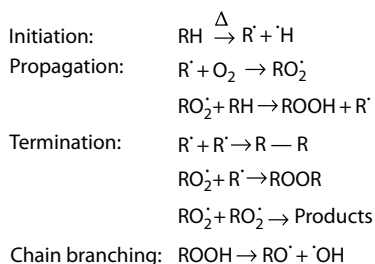
designed to enhance their properties, for example, flexibility, mechanical strength, color, stability, fire resistance, so that they can be deemed “fit for purpose.” For example, stabilizing additives are usually included during the processing stages of any polymer, and because of the complexity and often interrelated nature of secondary reactions, such stabilizers may be required to minimize thermal degradation and oxidation in a concerted manner (see the subsequent paragraph).

This chapter and the subsequent chapters in the book are focused on the fire resistance aspect of modern-day polymeric materials, plastics, and textiles as they are more commonly referred to.

2.2 OXIDATIVE DEGRADATION

Polymer degradation is almost always faster in the presence of oxygen or air due to the accelerating reactions between oxygen- and carbon-centered radicals ($\text{RO}\cdot$) released from the initial degradation products. These interactions with oxygen result in an increase in the concentration of polymer alkyl radicals ($\text{R}\cdot$), leading to higher levels of scission and cross-linked products. Also, fragmentation reactions of oxygen-centered radicals yield new oxidation products with structures not found under an inert atmosphere. These radicals can proceed to undergo abstraction, fragmentation, and combination reactions, both with the original polymer and other products from the decomposition. Such reactions can affect the polymer during processing, particularly, if the temperature required is high, and also its performance during its end-use. For example, photooxidation reactions cause deterioration in the mechanical and physical properties of low-density polyethylene (LDPE) during the early stages of exposure. Antioxidants can be added to the plastic formulation to inhibit such effects. Antioxidants function by interfering with the radical reactions leading to polymer oxidation and degradation.

To understand these reactions, the so-called Bolland and Gee reaction scheme^{17,18} and its subsequent developments has been applied to explain the chain reaction characteristics of both thermal and photooxidation of polyolefins. The scheme (Scheme 2.1) has been found to be a useful model for many other polymers comprising significant aliphatic character, such as aliphatic polyamides and polyesters and certain polyvinyls including poly(vinyl chloride) (PVC).



SCHEME 2.1 The general Bolland and Gee mechanism for the oxidation of polymers, RH.

2.3 DEGRADATION OF INDIVIDUAL POLYMER TYPES

When polymers are subjected to heat, generally, the weakest bonds will break first and these determine the overall character of the subsequent degradation pathways defined in Section 2.1 above and exemplified in Table 2.1. As flammability is associated with the availability and ease of oxidation of volatile degradation products, it is the degradation pathways that form volatiles that are of importance in the first instance. However, as cross-linking reactions give rise to eventual char formation and thus, may minimize volatile formation, these reactions are essential in determining the potential of a polymer to be rendered flame retardant by condensed phase flame retardants that may favor cross-linking. In the following discussion, these reactions will be emphasized only within the overall context of the complex degradation processes that most polymers exhibit when thermally degraded.

2.3.1 THERMOPLASTICS

2.3.1.1 Polyolefins

For both polyethylene and its many copolymeric variants and polypropylene, the main thermal degradative routes follow initial random chain scission. These reactions are only slightly affected by the differences in the physical structure such as crystallinity, but are influenced by the presence of impurities. However, it is largely true that while these may influence the processibility and long-term stability of respective polyolefins, they may have little or no effect on the flammability.

In the case of polypropylene, pyrolysis is dominated by initial chain scissions, usually at either the carbon–carbon bond adjacent to the labile tertiary hydrogen atom in the repeat group, $-\text{CH}_2-\text{CH}(\text{CH}_3)-$. Research has shown that heating the polymer, including waste polypropylene, generates a mixture of quite clean hydrocarbon fuels^{19,20} and other valuable products such as lubricants.^{21,22} This fuel-forming tendency explains the high flammability of polypropylene, and the difficulty of generating high levels of flame-retardant properties while maintaining optimum polymer properties.

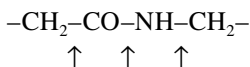
When heated under nonisothermal conditions, the maximum volatile product evolution temperature was 425°C for isotactic PP, yielding volatile products comprising dienes, alkanes, and alkenes. Furthermore, the hydrogen content of pyrolysis products obtained by flash pyrolysis at 520°C indicates the magnitude of the flammability problem in term of its fuel-forming potential.²³ The flammability of volatiles is further enhanced by the abundance of unsaturated less-volatile fuel fragments that behave as secondary fuel sources and which decompose further.²⁴

The complete absence of cross-linking reactions prevents potential char-forming reactions being favored in the presence of conventional condensed-phase flame retardants, and hence, the most effective flame retardants for polyolefins are usually bromine-based so that flame inhibition in the vapor phase is effected or intumescent-based, where char-promotion arises from the flame retardant itself.

2.3.1.2 Aliphatic Polyamides

The examples of PA 6 and 6.6 illustrate the challenges that these polymers create. The classical research into the thermal degradation occurred during the 1950–1970 period, and extensive reviews of this work include those by Kohan²⁵ and Peters and Still.²⁶ Essentially, for all linear, aliphatic polyamides, thermal degradation is influenced by two major factors:

- (i) The strength of the weakest chain bonds around the amide group:



with bond cleavages occurring at the arrowed positions, and preferential cleavage is suggested to occur at the $-\text{NH}-\text{CH}_2-$ bond.^{27,28} These occur randomly and give rise to the gaseous products, NH_3 , CO , and CO_2 , low molecular weight fragments, and subsequent degradation products from these latter compounds. Among the simple gases, only CO is flammable, but the volatiles generated from the smaller polymer chain fragments provide the major fuel components. The earliest PA 6.6 pyrolysis work published showed the products to comprise cyclopentanone, its derivatives, and various hydrocarbons, and this was supported by later work,²⁵ although the former was unique to PA 6.6 and not PA 6. Thermal decomposition of nylon 6 involves the depolymerization to its monomer, caprolactam, which is not only faster at higher temperatures, but is volatile.

Thermal lability of aliphatic polyamides, in general, is influenced by the potential for ring-formation during chain degradation, and this is particularly the case with PA 6.6, in which the adipate repeat unit enables the formation of a six-membered intermediate along the polymer chains with eventual formation of cyclopentanone and its derivatives.²⁹

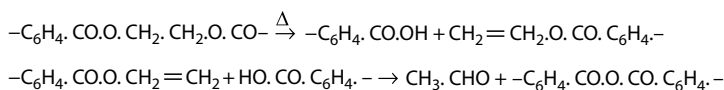
- (ii) The tendency of certain aliphatic polyamides to form three-dimensional structures leading to gel formation. PA 6.6 is particularly prone to this and explains why melt extrusion processes often require more interruptions, because of potential gel blockages than in the case with nylon 6, for example. PA 6.6 gels typically after 6 h at 305°C, while PA 6 may be heated for up to 10 days at 281°C before it gels.²⁵ While gel formation mechanisms are not well understood, in nylon 6.6, the formation of cyclopentanone derivatives and their subsequent reaction products are believed to be involved.

It is thus apparent that the overall flammability of the simple polyamides is determined by their relative propensities to shrink and melt away from an ignition source in the first instance, followed by the nature of the volatiles formed, and if ammonia and CO₂ are significantly present, it will have a reduced fuel value. Any flame retardant strategy may thus address this volatile formation or perhaps more interestingly accelerate gel formation, which could lead to a significant char-forming character. Unfortunately, to date, few successful flame retardants have been successfully commercialized for PA 6 and 6.6, partly because of the reactivity of the polyamide melts to bromine-containing retardants and also owing to the adverse effects of phosphorus-containing species on the molecular weight of melts during processing. Levchik and Weil³⁰ reviewed this whole area and showed that certain melamine salts in particular show promise.

2.3.1.3 Polyesters

The principal linear polyester is poly(ethylene terephthalate) (PET), and hence, this will be the chosen exemplar. Studies of its thermal degradative behavior mirror those of the aliphatic polyamides mentioned earlier. The basic research work was undertaken during the commercial development of PET during the 1950s and 1960s.²⁶ While some cross-linking tendency has been identified,³¹ the random chain scission dominates the thermal degradation with the major product being acetaldehyde, formed at temperatures up to 290°C along with smaller amounts of CO, CO₂, and ethane, and very small amounts of other fuels such as methane and benzene.²⁷

A simplified version of the primary stage appears as shown in Scheme 2.2, in which it can be observed that acetaldehyde is formed as the major initial flammable volatile.



SCHEME 2.2 Initial stage of thermal degradation of PET.

Action of further heat causes polymerization of the vinyl ends, coupled with loss of CO and CO₂ as the anhydride links undergo further scission.

It is evident that any flame retardant must counteract the effect of or reduce the amount of the acetaldehyde formed. While the actions of bromine- and phosphorus-containing species have achieved varying degrees of success, no successful flame retardant to date has managed to confer a significant char-forming character to the degradation mechanism, and this is perhaps an indication of the challenges involved with effectively flame-retarding linear polyesters in general.

2.3.1.4 Polyacrylonitrile

Most commercial polymers comprising acrylonitrile (AN) are copolymeric and those containing the highest levels of AN monomer, usually 85 wt% or more, are used in fiber end-uses including carbon fibers, where they are major precursors. As a consequence of their importance as carbon fiber precursors, most of the researches on the thermal degradative and oxidative processes associated with AN copolymers have focused on this area and took place over the 1960–1980 period.^{26,32,33}

It is generally accepted that the pyrolysis of AN-containing copolymers of this type are dominated by the behavior of the AN monomeric unit itself, and that this undergoes a cyclization reaction accompanied by an intense exotherm either in an inert atmosphere or in the presence of oxygen.³⁴ This gives rise to a so-called ladder structure as opposed to the random chain scission of chains into potential volatile product formation. In carbon fiber production, this cyclization is closely controlled by heating in an oxygenated atmosphere to produce the so-called oxidized acrylic fibers that have acceptable fiber properties in their own right.³⁵ Furthermore, as they are highly carbonized, these fibers have a high inherent fire resistance with limiting oxygen index (LOI) values of 50–55 vol%. Subsequent heating in an inert atmosphere converts these fibers into carbon fibers having an essentially graphitic structure.

In parallel, however, has been the exploitation of fiber-forming acrylic copolymers in the textile area, where they produce fabrics having similar levels of flammability as cotton with similar LOI values of about 18 vol%. This high level of flammability at first sight appears to be at odds with the cross-linking carbonizing reactions observed in carbon fiber production. However, work in our own laboratories³⁶ showed that the pyrolysis mechanism is both temperature and heating-rate dependent. Under the slow heating conditions and temperatures up to 400°C associated with carbon fiber production, the cyclization and cross-linking reactions prevail, whereas under the high heating rates and temperatures above 400°C associated with burning, volatilization and fuel-forming reactions predominate.

Therefore, it becomes evident that to flame retard polymers containing high levels of AN, this tendency to volatilize at high heating rates must be overcome. In commercial terms, this has proved to be impossible to date, and the only successful AN-containing, fiber-forming polymer is the group of modacrylics, containing between 35 and 85 wt% AN, with the other comonomers being halogen-containing species such as vinyl chloride or vinylidene chloride. These release chlorine atoms into the flame on heating and hence, act as vapor-phase flame retardants. However, at the experimental level, we have also shown that the volatilization reactions may be suppressed in favor of char formation, if ammonium polyphosphate (APP) and similar flame retardants are introduced, but to date, these have not been commercialized.³⁷

2.3.1.5 Polystyrene

Polystyrene (PS) is well known for a multitude of general purpose applications. Derivatives with superior properties for particular applications, in particular, AN–butadiene–styrene (ABS) and rubber-modified, high-impact polystyrene (HIPS) are used to replace PS or used in conjunction with it. General purpose polystyrene has been shown to degrade at 280°C.³⁸ The decomposition is initiated by main chain scission at a head-to-tail unit present in the polymer, due to polymerization termination by radical coupling. The resulting macroradicals readily unzip to expel styrene monomer. A more thermally stable form of PS can be produced via nitroxyl-mediated polymerization of styrene monomer, followed by removal of the nitrosyl-end groups by a reductive technique.³⁹ Untreated PS decomposes above 300°C mainly producing styrene monomer plus lesser amounts of the dimer, trimer, and tetramer, all of which are highly flammable; as a consequence, the LOI value for PS is 19.0 vol%. The mechanism is dominated by chain scission, depolymerization, intramolecular hydrogen transfer, and bimolecular termination.^{1,40} The main products are styrene monomer and its oligomers along with benzene and toluene. As would be expected from the aromatic nature of the PS structure, the principle flame retardant mechanism occurs in the condensed phase facilitating char formation. Postpolymerization modification to flame retard PS is easily achieved via electrophilic aromatic substitution of suitable flame retardant groups onto the phenyl rings. Successful methods include boronation,⁴¹ silylation,⁴² and phosphorylation.⁴³ PS, ABS, and HIPS are more often flame retarded using additives that are cost effective and easy to process. Various halogenated-flame retardant/antimony III oxide (ATO) combinations which evolve flame inhibitors under fire conditions are often used.

2.3.1.6 Poly(vinyl chloride)

Loss of the flame inhibitor HCl, via autocatalytic chain stripping, occurs from about 100°C. Thus, PVC has its own “in-built” fire retardant, and hence, PVC initially had extensive use in hazardous situations such as coal mines. This reaction yields other products that can be involved in other reactions such as cross-linking.⁴⁴ The conjugated double bonds resulting from the loss of HCl give rise to aromatic structures, for example, benzene, that burn producing significant quantities of hazardous smoke. Extensive studies have been undertaken to identify efficient smoke suppression systems for PVC, in particular, those by Starnes⁴⁵ and Carty and White.⁴⁶ Alternatively, the polyene structures can continue to undergo cross-linking to produce much less flammable char.

2.3.1.7 Ethylene/Vinyl Acetate Copolymers

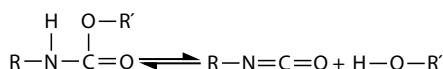
Ethylene/vinyl acetate (EVA) is a widely used material, particularly, as a low cost, zero-halogen sheathing material in the electric cable industry. EVA is known to form a protective layer that can inhibit combustion.⁴⁷ TGA/FTIR studies by Maurin et al.⁷ showed that heating of EVA composites resulted in a two-step decomposition over the ranges of 360°C–450°C and 450°C–550°C. The first step is due to the evolution of acetic acid, and the second is a mixture of 1-butene, CO₂, ethylene, methane, and CO. A recent study¹³ of the mechanism and kinetics of polyvinyl alcohol (PVA) and EVA degradations has shown that the deacetylation process leaves a highly unsaturated polyene-type residue. The deacetylation of PVA is autocatalytic, but upon incorporation of ethylene entities into the polymer backbone, this autocatalysis disappears. Between 400°C and 500°C, the polyene will degrade further by chain scission reactions in inert conditions or aromatize in an oxidative environment into char, and eventually produce CO₂ above 500°C. Under inert conditions, deacetylation is endothermic, but in the presence of oxygen, large exothermic effects are found for each degradation step. This indicates the occurrence of additional oxidation reactions during deacetylation, an important reorganization of the polyene structure prior to char formation and oxidation of the latter to CO₂.

2.3.2 FOAMS

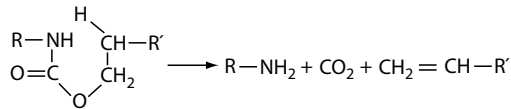
Thermal degradation of foams is not different from that of the solid polymer, except in that the foam structure imparts superior thermal insulation properties, so that the decomposition of the foam will be slower than that of the solid polymer. Almost every plastic can be produced with a foam structure, but only a few are commercially significant. Of these flexible and rigid polyurethane (PU) foams, those which have urethane links in the polymer chain are the most important. The thermal decomposition products of PU will depend on its composition that can be chemically complex due to the wide range of starting materials and combinations, which can be used to produce them and their required properties. Basically, these involve the reaction between isocyanates, such as toluene 2,4- and 2,6-diisocyanate (TDI) or diphenylmethane 4,3-diisocyanate (MDI), and polyols. If the requirement is for greater heat stability and reduced brittleness, then MDI is favored over TDI.

Urethane linkages tend to dissociate above about 200°C. Fabris⁴⁸ indicated that urethanes from many isocyanates and primary and secondary alcohols begin to decompose at 150°C–200°C proceeding at a measurable rate above this range. Urethane bonds decompose by the following three mechanisms:

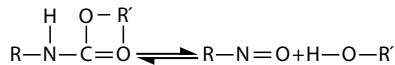
1. Reversal to the original isocyanate and alcohol:



2. Formation of the primary amine, olefin, and CO₂ through the intermediate state of a six-membered ring:

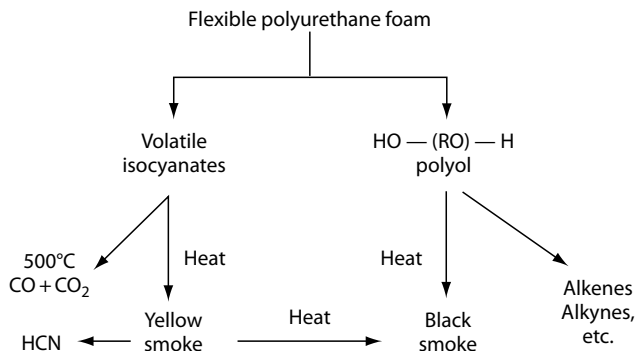


3. Formation of the secondary amine and CO₂ through the intermediate state of a four-membered ring:

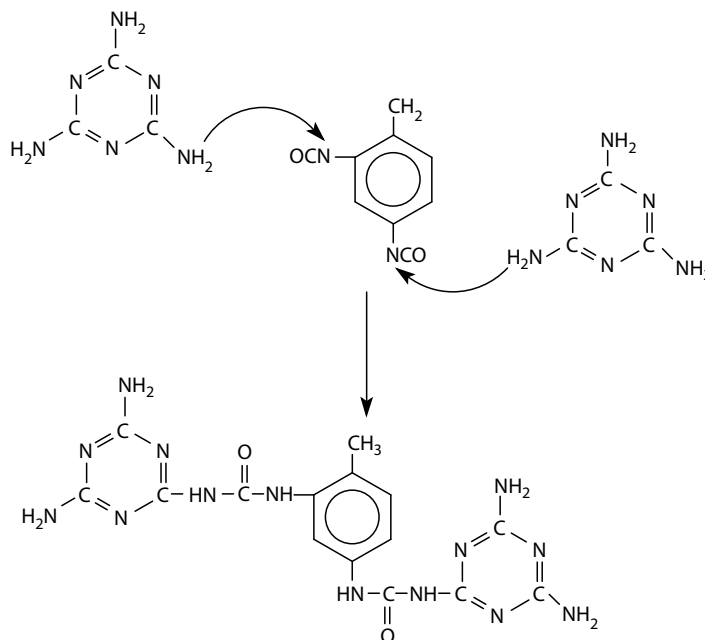


Wooley⁴⁹ used gas chromatography (GC)/MS to investigate the thermal decomposition of commercial TDI-based flexible foams under nitrogen. The degradations began with urethane bond scissions at 200°C–300°C, to yield relatively nonvolatile polyol components and nitrogen-rich volatiles. The latter were termed “yellow smoke” and appeared to be polymerized or condensed forms of TDI with some free TDI. At higher temperatures, further degradation of the polyol residue occurs to yield small organic species. Scheme 2.3 describes the mechanism outlined earlier.

The major application of PU foam is for upholstered furniture. Because of their large surface area and high air permeability, PU foams are highly flammable. As a consequence, it is essential that flame retarded PU foam be used in upholstered furniture.⁵⁰ Chlorinated phosphate esters are widely used to flame retard PU foams. These have the disadvantage that they can increase smoke formation. An additive that can effectively trap the volatile isocyanate evolved during the thermal decomposition of the foam can lead to a reduction in the smoke and toxic gas yields. A common example is melamine. Price et al.⁵¹ studied the reduction of smoke due to the presence of melamine in PU foams. Overall, the interaction between melamine and the released isocyanate fraction arising from the decomposition of PU foam is considered as the main reason for the smoke suppression of melamine. Although no reaction is believed to occur between melamine and TDI during the manufacture of PU foam at processing temperatures around 100°C, at higher temperatures, interaction may occur. The melamine –NH₂ group is very reactive toward an isocyanate (–NCO) group. Thus, the reaction shown in Scheme 2.4 would be expected to occur when temperature is over 250°C. The polymeric structure so formed would reduce the amount of aromatic smoke precursors volatilized, thus reducing the smoke released. This type of structure would degrade to char that will protect the remaining foam.



SCHEME 2.3 Thermal degradation of flexible PU foam.⁴⁹ (From Wooley, W. D., *Brit. Polym. J.*, 4, 27, 1972. With permission.)



SCHEME 2.4 Melamine–isocyanate interaction above 250°C.⁵¹ (From Price, D. et al., *Fire Mater.*, 26, 201, 2002.)

TABLE 2.4
Thermoset Resins Used
in Composites

Resin Type	LOI (vol%)
Polyester	20–22
Vinyl ester	20–23
Epoxy	23
Phenolic	25
Polyaromatic melamine	30
Bismaleimide	35

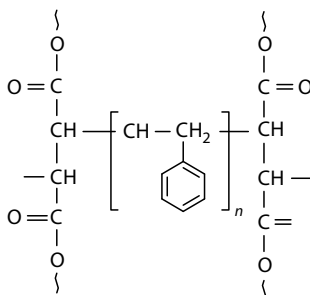
2.3.3 THERMOSETS

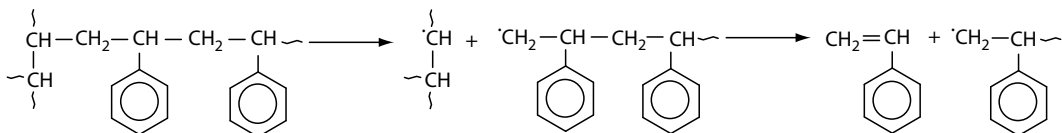
Thermoset resins covers an extremely wide range, including phenol formaldehyde polymers, aminopolymers, PUs, epoxies, and thermoset polyesters, which include the alkyd and unsaturated vinyl ester resins. Of special interest at the present time are those that comprise the resin component of fiber-reinforced composites that are finding increasing use in commercial and defense sectors, where fire resistance is of paramount importance. Typical resins used are those listed in Table 2.4 along with typical, respective LOI values in descending order of increased inherent fire resistance.

Their general thermal stability and flame retardancy have been recently reviewed.⁵²

2.3.3.1 Polyester Resins

Polyesters are probably the most commonly used polymeric resin materials, and consist of a relatively low molecular weight unsaturated polyester chain dissolved in styrene, which on curing forms cross-links across unsaturated sites in the polyester. The typical formula for a resin is





SCHEME 2.5 Initial chain scissions in polyester.⁵³ (From Levchik, S.V., *Thermosetting polymers*, in *Plastics Flammability Handbook*, Troitzsch, J. (ed.), Hanser, Munich, 2004, pp. 83–98.)

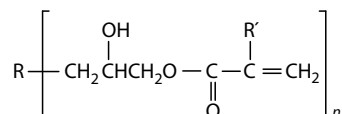
Most polyesters start to decompose above 250°C, whereas, the main step of weight loss occurs between 300°C and 400°C.⁵³ During thermal decomposition, PS cross-links start to decompose first and styrene is volatilized according to Scheme 2.5.

The linear polyester portion undergoes scission similar to thermoplastic polyesters, undergoing decarboxylation, decarboxylation, or splitting off of methylacetylene.

Because of the ease of formation of these flammable pyrolysis products, polyesters have LOI values of 20–22 vol% (see Table 2.4), and hence, burn readily and because of the styrene content, give heavy soot formation. As these resins are cured at room temperature, bromine-containing flame retardants, which would decompose in melt-processed, thermoplastic polymers, may be effectively used.

2.3.3.2 Vinyl Ester Resins

These are mainly derived from the reaction of an epoxy resin, for example, bisphenol A diglycidyl ether, with acrylic or methacrylic acid. Their general formula is:



where

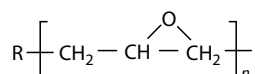
R is any aliphatic or aromatic residue

R' is typically either H or CH₃

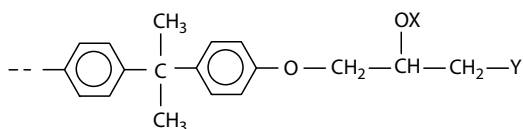
Similar to unsaturated polyesters, they are copolymerized with diluents such as styrene using similar free-radical initiators. They differ from polyesters in that the unsaturation is at the end of the molecule and not along the polymer chains. Their burning behavior falls between that of polyester and epoxy resins (LOI = 20–23 vol%, Table 2.4).

2.3.3.3 Epoxy Resins

These resins, extensively used in the aerospace industry, consist of an epoxy resin component, often based on epichlorohydrin and a curing agent, and comprise the following epoxy or glycidyl group:



where R is any aliphatic or aromatic residue. This group will react typically with phenolic –OH groups and bisphenol-A type resins to yield the following general structure:



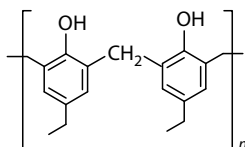
where X can be H, and Y depends on the structure of the curing agent. This yields a relatively thermally stable structure with the weakest bonds at the ether linkage, $-O-$.

During early stages of thermal degradation, the reactions are mainly nonchain-scission type, whereas at higher temperatures, chain scissions occur.⁵⁴ The most important nonscission reactions occurring in these resins are the competing dehydration and dehydrogenation reactions associated with secondary alcohol groups in the cured resin structures. The main products are methane, CO_2 , formaldehyde, and hydrogen.

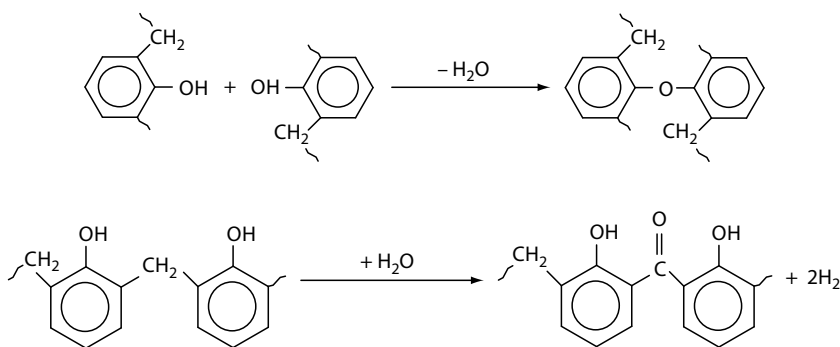
During chain scission reactions, the aliphatic segments break down into methane and ethylene (and possibly propylene), acetone, acetaldehyde, and methane (and probably CO and formaldehyde), all of which are flammable. From the aromatic segments of the polymer, phenol is liberated. For phthalic anhydride—cured resins, phthalic anhydride is regenerated together with CO and CO_2 , benzene, toluene, *o*- and *p*-cresols, and higher phenols. However, the flammable volatiles outlined earlier are produced only in relatively small quantities, and this, coupled with their cross-linked and related char-forming character, ensures that epoxy resins are less combustible than polyester resins with higher LOI values in the range of 22–23 vol%.

2.3.3.4 Phenolic Resins

Reaction of phenol with less than equimolar proportions of formaldehyde under acidic conditions gives the so-called novolac resins containing aromatic phenol units linked predominantly by methylene bridges. These are thermally stable and can be cured by cross-linking with formaldehyde donors such as hexamethylenetetramine. However, the most widely used phenolic resins for composites are resoles manufactured by reacting phenol with a greater than equimolar amount of formaldehyde under alkaline conditions. Resoles are essentially hydroxymethyl functional phenols or polynuclear phenols with the following general formula:



Phenolics have LOI values of about 25 vol%, and this high level of inherent flame resistance is associated with the general thermal stability and often indicates that no further flame retarding is necessary to create composites having required performance levels. During heating, water is generated chemically during the first step of thermal degradation, primarily because of phenol–phenol condensation by reactions of the type shown in Scheme 2.6. This is followed by the oxidation



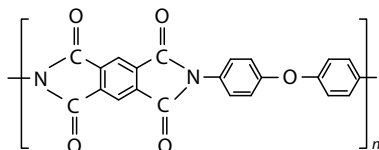
SCHEME 2.6 Condensation formation of methylene groups and their subsequent oxidation.⁵³ (From Levchik, S.V., *Thermosetting polymers*, in *Plastics Flammability Handbook*, Troitzsch, J. (ed.), Hanser, Munich, 2004, pp. 83–98.)

of methylene groups by the released water to carbonyl linkages,⁵³ which then decompose further, releasing CO, CO₂, and other volatile products, ultimately yielding char.

In the case of highly cross-linked material, water is not released until above 400°C, and decomposition starts above 500°C as confirmed using differential thermal analysis (DTA).⁵⁵ The amount of char depends on the structure of phenol, initial cross-links, and tendency to cross-link during decomposition. The main decomposition products may include methane, acetone, CO, propanol, and propane.

2.3.3.5 Maleimide and Polyimide Resins

Their chemistry is often complex with a general formula for polyimide resins represented by



The aromatic structure of polyimides, in particular, ensures that they are thermally resistant, and hence, characterized by high char formation on pyrolysis, low flammability (LOI > 30 vol%), and low smoke production.

2.3.4 NATURAL POLYMERS

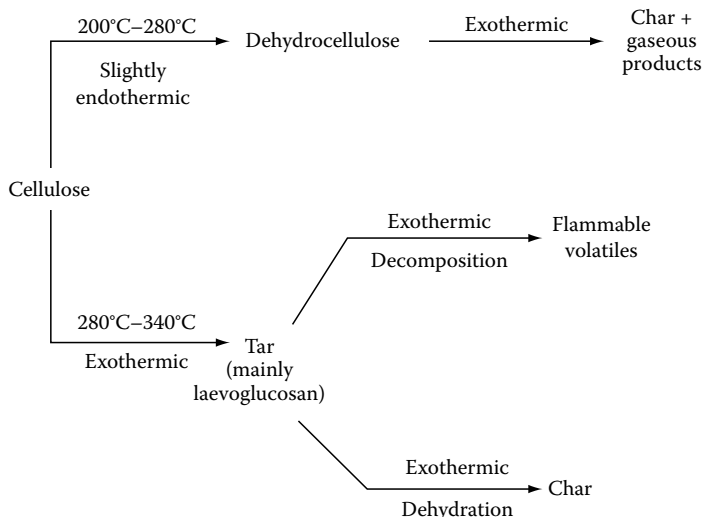
2.3.4.1 Cellulose

Cellulose, either as the major component of wood or as the major textile fiber cotton, is frequently involved in fires. Thermal degradation of cellulose results in the evolution of highly combustible volatiles that will be consumed in a flame if ignited. Flame-retardant treatments affect this degradation process either by reducing the extent of volatile escape in favor of less flammable residue formation or evolve flame inhibitors such as Br• or Cl• species. Cellulose consists of long, linear chains of β-1,4-D(+)-glucopyranose units linked by 1,4-glycosidic bonds. The cellulose molecule is not planar but has a screw axis, with each cellulose unit being at right angles to the previous one. Free rotation about the C–O–C link does not occur due to the steric effects in the solid state. The degradation of wood will not be discussed here, because in addition to cellulose, wood and plant cells contain hemicellulose and lignin that further complicate the degradation process. Because of its wide usage in the textile and other industries, as a source of alternative fuels, the pyrolytic decomposition of cellulose has been extensively studied.⁵⁶ While other more detailed mechanisms have appeared in the literature,^{57,58} the basic processes proposed are all in line with that first suggested by Bradbury et al.,⁵⁹ who suggested a precursor step in which an “activated” cellulose species, Cellulose*, is produced, which then undergoes further reaction depending on the temperature regime, as presented in Scheme 2.7.

While there is controversy as to whether or not this Cellulose* species exists, experimental evidence for the Cellulose* species was obtained by Price et al.,⁶⁰ who suggested that it could be a free radical in nature. At lower temperatures, oxygen plays a dominant role in cellulose degradation, and pyrolysis is faster in an oxidative atmosphere than in an inert one.⁶¹ Oxygen catalyzes the formation of both volatiles and char-promoting reactions.⁶² At higher temperatures, the degradation products are little affected.⁶¹

2.3.4.2 Protein Polymers

Proteins or poly(α-amino acids) feature the amide link common to the polyamides and may, in fact, be considered to be α-carbon substituted polyamide-2 variants. Thus, their potential thermal degradation behavior might be expected to be similar to that of the aliphatic polyamides defined earlier.



SCHEME 2.7 Basic scheme for cellulose degradation process; with reference to Bradbury et al.⁵⁹ (From Bradbury, A.G.W. et al., *J. Appl. Polym. Sci.*, 22, 497, 1978.)

However, the α -substituents or R groups are often quite reactive because of their functionalities, and hence, these will significantly influence, if not determine, the thermal degradation behavior and potential flammability.

Commercial protein polymers were first developed during the early twentieth century, a prime example being casein from milk. On reaction with formaldehyde, this gives a polymer that has been much used as a synthetic horn or tortoiseshell material, and still has some commercial presence in milk-producing countries like New Zealand. However, the most important protein polymers that require flame retardation are those associated with textiles with silk and wool as the principle examples. On the other hand, the aesthetics of silk define its commercial importance and the effect that most proprietary flame-retardant treatments have on this fiber precludes it from being used in fire-resistant textiles, and there has been recent commercial interest in its use in executive jet aircraft interior décor in which, as with normal commercial airliners, stringent fire standards are demanded. We have published studies in this area to demonstrate the flame-retardant challenges that needs to be overcome.⁶³ Silk comprises 16 α -amino acids of which glycine (R = H), alanine (R = CH₃), and serine (R = CH₂OH) are the major comonomers present. When heated, silk starts to decompose above 250°C and forms a char. This charring characteristic is probably largely influenced by the dehydrating and cross-linking tendency of the hydroxyl group within the serine—CH₂OH α -substituent. Charring can be increased by application of phosphorus-containing species as might be expected, given this assumed chemistry.⁶⁴ The natural fiber LOI value is 22–23 vol% reflecting this higher char-forming tendency, than the simple aliphatic polyamides which have LOI values of about 21 vol%.

Wool fibers and fabrics, however, have significantly greater commercial applications in products such as protective clothing and contract upholstery, where high levels of fire-resistant performance are demanded. Wool, while also comprising a large number (18) of α -amino acids, some of which are common with silk, is uniquely identified by the presence of sulfur-containing α -substituents, of which cystine (R = —CH₂—S—S—CH₂—) comprises nearly 10 wt% of the whole fiber and provides cross-links between adjacent polypeptide chains. This high sulfur content (3–4 wt%) coupled with the high nitrogen content (15–16 wt%) present in both chain and side groups contributes to the inherently low flammability of wool. The fiber also contains about 15 wt% of adsorbed moisture under

normal atmospheric conditions and LOI values lie in the 25–26 vol% range. When wool is heated, it starts to give off its adsorbed moisture at 100°C and above, and then starts to thermally degrade rapidly above 200°C, giving off gases that include H₂S, following the cleavage of disulfide bonds above 230°C⁶⁵ alongside char formation.⁶⁶ The relatively nonflammable volatiles coupled with char formation are encouraged by cross-linking and dehydrating tendencies of the α -substituents present. The overall action of these is to give a relatively high ignition temperature of 570°C–600°C and low flame temperature of about 680°C. The cystine disulfide link is particularly interesting here, as it has highly reducing properties and hence, encourages subsequent oxidation by oxygen during the pyrolysis/combustion process. Preoxidation of the cystine to cysteic acid (R = CH₂·SO₃H) residues actually improves flame retardancy.

2.3.5 HIGH TEMPERATURE-RESISTANT POLYMERS

These tend to be highly aromatic in character with rigid polymer-chain backbones to yield polymers having very high second-order transition values, absence of achievable melting transitions, and decomposition temperatures rarely below 400°C. It is generally the case that the lower the aliphatic content, the lower is the hydrogen to carbon ratio, and hence, the lower is the flammability of any polymer. Aromatic chain polymers generally have H/C ratios less than 1, and hence, their ability to generate volatile and flammable degradation species at temperatures below 500°C or so, is very limited. Consequently, they have LOI values generally above 30 vol% and are generally deemed to be sufficiently flame resistant for the applications for which they are selected.

Table 2.5 illustrates a selection of the more common high temperature, aromatic-structured polymers used for producing heat and flame resistant, high-performance fibers, and their related thermal transitions and LOI values.⁶⁷

These polymers may be compared with the more detailed discussion of thermal degradation pathways for phenol–formaldehyde resins described in Section 2.3.3 earlier, which explains the

TABLE 2.5
Thermal Transitions and LOI Values for Selected Aromatic,
High Temperature-Resistant Fiber-Forming Polymers

Fiber Genus	Second Order Temperature (°C)	Melting Temperature (°C)	Onset of Decomposition (°C)	LOI (vol%)
Phenol formaldehyde: Novoloid	NA	NA	>150	30–34
<i>m</i> -Aramid	275	375–430 (decomposition)	425	28–31
<i>p</i> -Aramid	340	560 (decomposition)	>590	29–31
Copolymeric <i>p</i> -aramid	—	—	500	25
Arimid (P84)	315	—	450	36–38
Aramid–arimid	<315	—	380	32
Semicarbon	NA	NA	NA	55
Polybenzimidazole (PBI)	>400	NA	450/air; 1000/inert	>41
Polybenzoxazole (PBO)	—	—	650; >700/inert	68

Source: Adapted from Horrocks, A.R. et al., Thermally resistant fibers, in *High Performance Fibers*, Hearle, J.W.S. (ed.), Woodhead Publishing, Cambridge, U.K., 2001, 289–324.

Note: NA = not applicable; (decomposition) = with decomposition.

reasons for the generally low flammabilities in such highly aromatic structures, in more detail. This same polymer in its novoloid form is commercially available as a fiber with properties defined in Table 2.5.

Addition of flame retardant species to these polymers is rarely undertaken, as not only are they intractable during processing, but also the added value in terms of improved fire resistance is usually difficult to observe. The high costs of these polymers also negate the use of additional additives, unless a real benefit is to be achieved.

2.4 POLYMER FIRE

Figure 2.1 is a schematic cross-section of a polymer fire indicating the important reaction zones.

The flame is fuelled by combustible pyrolysis products escaping from the polymer surface owing to heat being conducted from the flame in contact with the polymer surface and also that radiated from the flame. The latter is the significant cause of flame spread and this process is modeled by the cone calorimeter.⁶⁸ The oxygen required to sustain the flame combustion diffuses in from the air environment. Various solid particles escape from the flame as smoke that is accompanied by gaseous species, some of which can be toxic.⁶⁹ The significant polymer degradation reactions occur within a millimeter or so of the interface between the flame and the solid polymer. Here, the temperature is high enough for condensed-phase degradation reactions to occur. These involve the polymer and any additive systems included in the polymer formulations. Volatile species formed escape into the flame, while heavier species remain to undergo further reaction and may eventually degrade leaving a char. This is where the significant condensed-phase chemistry occurs. Experimental studies of this region have been undertaken by Price⁷⁰ and Marosi et al.⁷¹

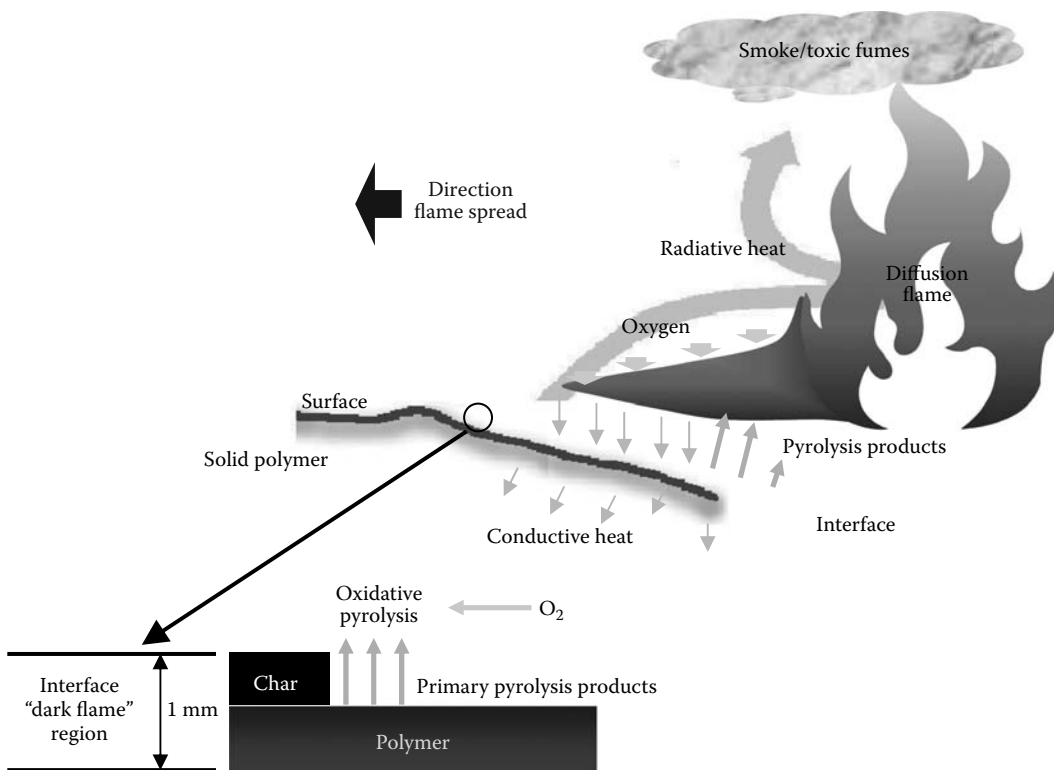


FIGURE 2.1 (See color insert following page 530.) Schematic representation of a burning polymer.

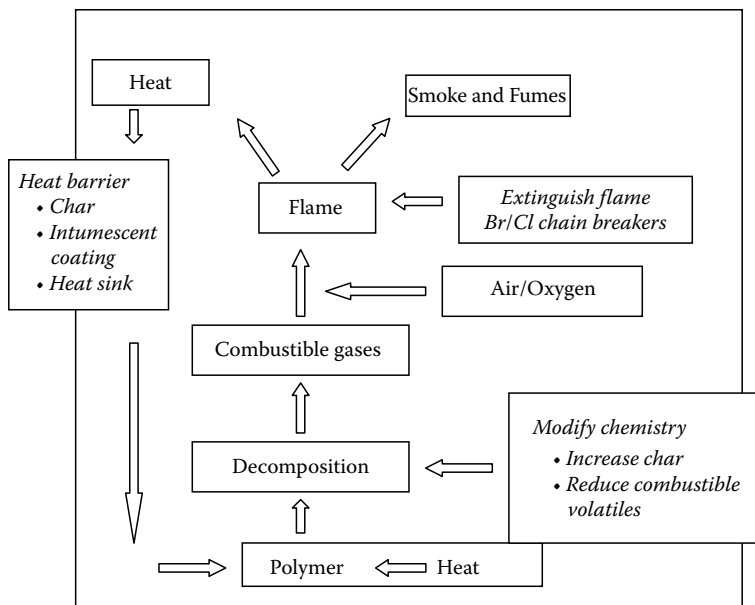


FIGURE 2.2 Schematic representation of the polymer combustion cycle; main approaches to flame retardancy are shown in italics.

2.5 POLYMER COMBUSTION CYCLE

An account of the polymer combustion cycle is simplified by reference to the schematic representation given in Figure 2.2. For a polymer material to undergo flaming combustion, it must first degrade to evolve combustible volatiles that escape and mix with an oxidative atmosphere. If the temperature is above the ignition temperature or a suitable ignition source, such as a spark, is present, then this mixture will ignite. The flames will yield gaseous products, some of which may be toxic, smoke, fumes, as well as heat. Some of the heat will be conducted or radiated back to the original polymer to cause further degradation. If this heat is sufficiently intense, then a combustion cycle will be established as indicated schematically in Figure 2.2.

This scheme may now be used to understand how different flame-retardant strategies may be designed and adopted to break the combustion cycle. For a given polymer, the strategy to be adopted will be largely dictated by its particular thermal degradative chemistry, which has been briefly reviewed in Section 2.3 earlier, for all the significant polymer types.

2.6 FLAME RETARDANCE

Most plastics and textiles are organic and thus, vulnerable in a fire situation. A major concern of their manufacturers is, therefore, to render their products resistant to ignition or, if they are ignited, to burn less efficiently, so that their rate of heat release is significantly reduced. The approach to achieving this is termed “flame retardance.” Unless the polymer is inherently flame retarded, the various approaches indicated in Figure 2.2 can be used to reduce the fire threat of such materials. One method is to prevent access of oxygen to the flame, and another is to introduce flame inhibitors such as halogen atoms, Cl•, and particularly, Br• or phosphorus into the flame. This can be accomplished by including additives in the material’s formulation, which release these flame inhibitors if the material is exposed to temperatures approaching the ignition temperature. An alternative approach is to introduce suitable chemical groups into the polymer structure, the so called “reactive flame retardants,” which provide the same effect. The combustion can also be halted by reducing

the heat flow back to the polymer, thus preventing further degradation. This can be achieved by the introduction of a heat sink such as aluminum oxide trihydrate ($\text{Al}(\text{OH})_3$) or magnesium hydroxide ($\text{Mg}(\text{OH})_2$), which decompose with a large endothermicity. Formation of a heat barrier, for example, either a char or intumescent barrier as a result of exposure of the material to a fire, is another successful method. Finally, there exists the option to modify the polymer degradation chemistry, so that the amount of flammables released is below the level required to fuel the flames, while at the same time, increasing the less combustible char formation. The char has the beneficial effect of forming a barrier between the polymer surface and the flame. It is during these latter condensed-phase processes, polymer degradation plays a significant role in flame retardant action. This chapter is focused on such processes.

As mentioned in Section 2.3.5 earlier, some polymers can be said to be inherently flame retarded. Bourbigot and Duquesne⁷² recently classified such polymers as having a continuous operating temperature range from 180°C to 300°C or above, together with a decomposition temperature above 350°C. Such polymers can have high thermal stability due to their high aromatic and low hydrogen contents, for example, polyarylates and polycarbonates, phenolic resins and aromatic polyesters, polyethers, and polyamides. Others, like PVC, decompose to evolve flame inhibitors such as HCl from PVC, or release sufficient quantities of nitrogen or similar heteroatoms, for example, polyamides and aminoresins, to blanket out any flames at high temperature. Poly(aryl ketone)s and ether ketones have above-average thermal and thermooxidative stability at high temperature, which will result in resistance to fire.

Few conventional synthetic polymers, however, are inherently resistant to heat and fire. The traditional method of rendering them fire retarded is to include a flame retarded additive in the formulation during polymer processing. The choice of fire retardant depends on whether the fire retardant is required to predominately function in the gas phase, for example, alumina trihydrate (ATH), magnesium hydroxide ($\text{Mg}(\text{OH})_2$), halogen/ATO systems, or the condensed phase via char formation enhancement, for example, ammonium polyphosphate (APP). In addition, the chosen additive must be stable at the polymer-processing temperature while being compatible with the polymer itself. In addition, cost is another significant factor, for example, ATH-containing plastic sheathing used as insulation for low-cost electrical wiring. Gas-phase retardants function by releasing species that either blanket out the flames with noncombustible gases such as water from ATH, or halogen flame inhibitors from the halogen/ATO-type systems. The incorporation of additives, however, does have several disadvantages. The additive is often required in high loadings to be effective (typically 10–60 wt%) which may result in adverse changes to the physical and mechanical properties of the polymer, rendering the polymer unsuitable for a particular end use. The alternative reactive fire-retardant approach is to incorporate the fire retardant species, via copolymerization or some other chemical modification, to produce what is essentially an inherently fire-retarded polymer.⁷³ The relatively low load required to achieve sufficient fire retardance, and careful selection of the comonomer, can keep detrimental changes to the physical and mechanical properties at an acceptable level. Also, as it is chemically incorporated into the polymer, the fire retardant will not be easily lost from the polymer. Thus, one of the major problems associated with additive systems is eliminated.

Because of the advantages and despite their higher costs, in the recent years, there has been a growing interest in the reactive approach to produce high-value, high-performance fire-retarded polymers. Because of the environmental pressures to reduce/eliminate the use of halogen-containing systems, much interest has focused on phosphorus as the fire-retardant moiety incorporated in the polymer chain. One example is the work by Ebdon et al., who synthesized⁷⁴ and studied the flammability and decomposition behavior^{75–77} of poly(methyl methacrylate) and PS polymers copolymerized with a range of phosphorus-containing comonomers. Typical comonomers were diethyl(acryloyloxymethyl)phosphonate (DEAMP), diethyl(methacryloyloxymethyl)phosphonate (DEMMP), diethyl(acryloyloxyethyl)phosphate (DEAEP), and diethyl(methacryloyloxyethyl)phosphate (DEMEP). Their structures are given in Figure 2.3.

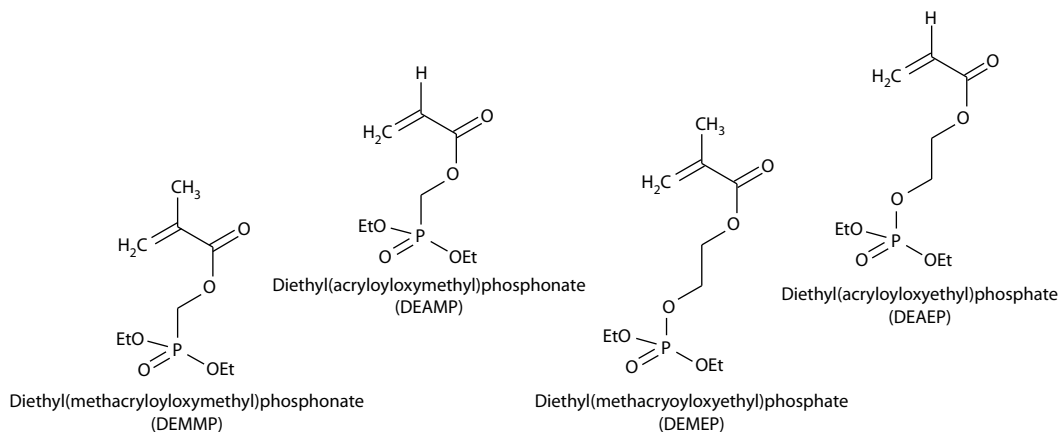


FIGURE 2.3 Structures of comonomers used for reactive fire retardant studies of Price et al.^{75–77} (From Price, D. et al., *Polym. Adv. Technol.*, 19(6), 710, 2008.)

The fire-retardant mechanisms identified for the various phosphorus moieties in these polymethylmethacrylate (PMMA) and PS copolymers investigated can be summarized as follows:

- Vapor-phase fire-retardant action assumed for gas-phase phosphorus species released from all polymers.
- The rate of volatile production was reduced for phosphorus-containing copolymers when compared with that of the corresponding additive system.⁷⁷
- The normal unzipping process of PMMA decomposition was obstructed in the case of the acrylate copolymers, thus reducing the evolution of the flammable methylmethacrylate (MMA) monomer.
- Condensed-phase cross-linking occurred as the copolymer-containing phosphorus decomposed, facilitating char formation and reducing flammable volatile evolution.
- Interference with the H-transfer reactions occurred during PS decomposition for acrylate copolymers.

Other work in this area has been reported in recent years. Of particular note is that of Lyon, which has also been involved in synthesizing inherently flame-retardant materials to improve the fire resistance of aircraft interiors.^{11,12}

2.7 RELEVANCE OF POLYMER STABILIZATION TO FLAME-RETARDANT PROCESSES

It might be assumed that, as condensed-phase flame retardants function by modifying the normal thermal degradation processes of polymers, they would also function as thermal stabilizers and that thermal antioxidant stabilizers would show flame-retardant properties. However, these statements are rarely the case, and to understand why, it is necessary to compare the mechanistic aspects of flame retardance as discussed earlier with those of thermal degradation and thermal oxidation as well, briefly alluded earlier, and in the case of the latter, the Bolland and Gee mechanism,¹⁷ in Scheme 2.1.

Cursory comparison of the character and behavior of flame retardants and thermal stabilizers including antioxidants yields the following:

- Flame retardants are generally present at concentrations of greater than 10 wt% to be effective, and relate to effective elemental concentrations in the case of phosphorus of the order of 2–4 wt% and in the case of bromine 5–10 wt% with respect to the polymer
- Thermal and photoantioxidants are often present and effective at concentrations of the order of 0.5–1.0 wt%

- Flame retardants at low concentrations (≤ 1 wt%) are seldom, if ever, known to function as thermal stabilizers
- Antioxidants, when introduced at high concentrations (which would be very expensive given their relatively high costs), are not reported to be flame retardant.

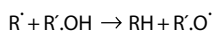
There is only perhaps one significant case where low concentrations of an antioxidant shows flame-retardant behavior, in the case of certain hindered amine stabilizers (HAS) that at the normally used concentrations (≤ 1 wt%), offer low levels of flame retardancy in polypropylene and show synergy with bromine-containing flame retardants.^{78–80}

Before returning to this example, it is pertinent to review the mechanisms by which thermal antioxidant stabilizers work. As thermal stability is determined inherently by the lability of the bonds present within a polymer, the only means of developing thermal stabilization is to offer means of scavenging or rendering inert impurities present, which might otherwise sensitize degradation. Thus, for example, in PVC where release of HCl sensitizes further degradation, the presence of a basic additive, such as metal carboxylates and even calcium carbonate, have thermal stabilizing properties. Similarly, the presence of radical scavengers such as hindered phenols may interact and terminate impurity-generated radicals that might otherwise promote eventual chain-scission mechanisms as shown in Scheme 2.1.

Most thermal stabilizers fall into one of the two groups; they function either as antioxidants or in some other manner, such as buffers, to remove excess acidity as exemplified by the PVC example mentioned earlier. In the case of antioxidants, these are often characterized according to their means of operation^{3,81–83}:

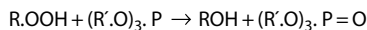
1. “Primary” antioxidants, also termed as chain-breaking antioxidants, interfere with the chain reaction in Scheme 2.1, by trapping radicals or labile hydrogen atom donors. These are exemplified by hindered phenols and alkylarylamines. Scheme 2.8 schematically demonstrates the scavenging activity of a typical hindered phenol.
2. “Secondary” antioxidants or hydroperoxide decomposers (see Scheme 2.1) are typified by organosulfur species having reducing properties such as sulfides and thioethers. Tertiary phosphites also fall into this category (see Scheme 2.9).
3. Photoantioxidants are typified by the class of HAS which although were developed for photostabilization of polyolefins, also possess thermal antioxidant properties. They are generally assumed to function as “primary” antioxidants in that they scavenge radicals and in particular, peroxy radicals.
4. Metal ions and particularly heavy metal ions tend to sensitize peroxy radical formation, and hence, the presence of metal scavenging or chelating species can offset this effect. This form of stabilization is particularly important for polymers in which metal-containing polymerization catalyst residues are present, such as polyolefins. While simple additives like calcium stearate may be used, more sophisticated ones based on bifunctional chelating species also are available commercially.
5. Some redox systems have been developed for certain polymers. The copper/iodine system is well established for polyamide thermal stabilization, and in spite of introducing a heavy metal ion into the polymer, works well in an oxygen-free environment.^{83,84}

Very often, antioxidants are used in combinations to ensure maximum activity and typically, a commercial additive system may comprise both a primary and secondary antioxidant species, although

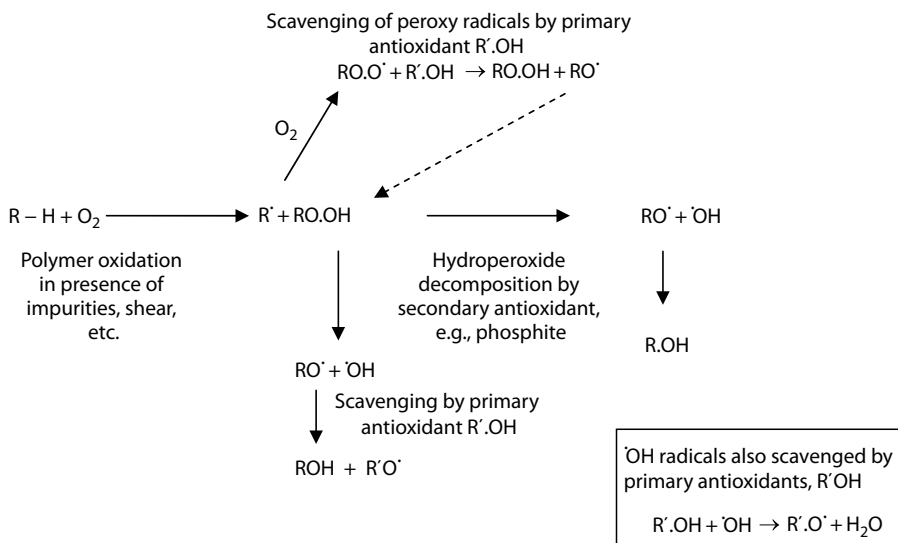


SCHEME 2.8 Stabilizing activity of chain-breaking, primary antioxidants.

the total concentration remains ≤ 1 wt%. Scheme 2.10 schematically shows how a combination of primary and secondary antioxidants functions in a polyolefin matrix.⁸² Some metal-chelate scavengers may also be based on a tertiary phenolic structure, thereby introducing two antioxidant properties into the same molecule.



SCHEME 2.9 Stabilizing activity of hydroperoxide-decomposing secondary antioxidants.



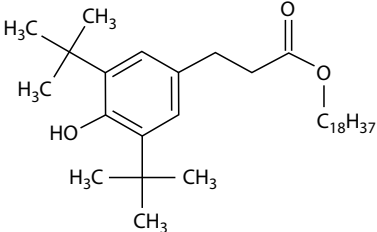
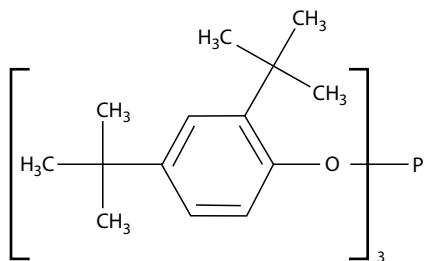
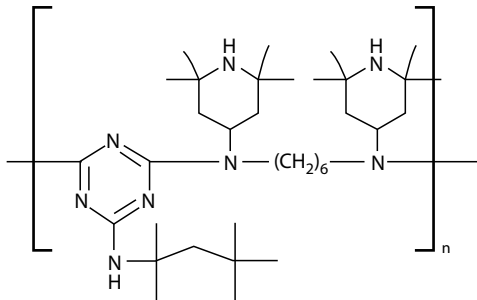
SCHEME 2.10 Combined stabilizing activity of primary and secondary antioxidants.

Table 2.6 provides typical examples of each of these antioxidants from which it may be seen that they bear little resemblance to the flame-retardant molecular structures described in the remaining parts of this book. However, notwithstanding this observation, it was briefly mentioned earlier that a recently developed HAS-based system, commercialized as NOR116 by Ciba, is marketed as both a photoantioxidant and a flame retardant for polypropylene.⁷⁹ While very little, if any, literature is available to explain its flame-retardant activity, it is worth noting that research into the burning behavior by Stuetz et al.^{85,86} 30 years ago suggested that the burning process of polypropylene involves an oxidative pyrolytic step as a prerequisite for fuel formation, and hence, it is possible that the introduction of a HAS photoantioxidant will interfere with this stage, thus promoting a flame-retardant effect. Furthermore, there is also a synergy observed between NOR116 and bromine-containing flame retardants like decabromodiphenyl ether,⁷⁸ for example, in which bromine radical formation and reaction determine the flame-retardant behavior. It is possible that the radical-interacting character of the HAS may have a beneficial effect on the effectiveness of the Br• radicals in terminating the chemical chain reactions of the flame.

2.8 ALTERNATIVE POLYMER DEGRADATION PROCESSES, (E.G., PHOTOCHEMICAL, PLASMA, IRRADIATION), AND THEIR POTENTIAL INFLUENCE ON FLAME-RETARDANT BEHAVIOR

In the previous section, comparison was made between the nature and means of operation of antioxidants (including some photoantioxidants), which are introduced into the polymers to improve either the processing or long-term stability, and flame retardants that may interact with and modify the thermal degradation process as well as the ensuing flame chemistry. It is evident that while there are considerable differences between the chemistries of flame retardancy and thermal (and photo-) stabilization, there are similarities in that the polymer degradation pathways, while being specific for each polymer, are driven by the thermal energy and involve the same thermal degradation pathways.

TABLE 2.6
Examples of Primary, Secondary, and Hindered Amine Antioxidants Marketed by Ciba for Use with Polypropylene

Type	Commercial Name (Ciba)	Chemical Formula
Primary (radical scavenger)	Irganox 1076	Octadecyl 3,5-di(<i>tert</i> -butyl-4-hydroxyhydrocinnamate
		
Secondary (hydroperoxide decomposer)	Irgafos 168	Tris(2,4-di- <i>tert</i> -butylphenyl)phosphite
		
HAS (combined light and heat)	Chimassorb 944	
		
HAS with flame retardant properties	Flamstab NOR116	The reaction product of 2,4-bis[(1-cyclohexyloxy-2,2,6,6-piperidin-4-yl) butylamino]-6-chloro-s-triazine with <i>N,N'</i> -bis(3-aminopropyl)ethylenediamine [CAS Reg. No. 191680-81-6]

A major difference is, of course, the rates of heating, which during normal polymer processing and long-term exposures during service are generally low while in a fire, are large. The effect of rate of heating was noted for the acrylic copolymers mentioned earlier, in which low rates favor carbonization (and char-forming), whereas high rates favor volatilization.³⁶

As most polymer degradation processes tend to lead to chain scission, cross-linking, or both, it might be assumed that flammability would be influenced by the degradation history of any given polymer. cursory analysis of the literature shows that little if anything has been published on the effects of aging or degradation on the resulting polymer flammability. This is not to be confused with the loss of flame retardants during service life by leaching, cleaning, or other process. Generally,

however, the influence of polymer history of nonretarded polymers does not appear to be an important issue, as during the service life of a polymer, only a minority of polymer chains require to be broken before the polymer becomes unserviceable in terms of reduced tensile, impact, or other significant property. In fact, most degradation processes comprising external agencies involve attack of polymer chains in the amorphous regions in the first instance. In highly crystalline polymers like polyethylene, polypropylene, and aliphatic polyamides, for example, these comprise less than 50 wt% of the total polymer and often much less, and hence, the majority of the polymer molecules present are nondegraded even when the overall polymer serviceability has reduced. Furthermore, it is generally noted that during the weathering of linear crystalline polymers, where the degrading agencies are a complex combination of heat, light, water, and possibly air-polluting species, crystallinity increases following internal relaxation of polymer chains after scission reactions have occurred. For example, weathering of linear LDPE increases its degree of crystallinity from just less than 40% to over 55% during a 12-month period.⁸⁷ In the other even more highly crystalline polymers like polypropylene (>70%), this means that nominally degraded polymer actually comprises a higher proportion of pure polymer in the crystalline phase, with products of degradation concentrated in the minor amorphous phase. The effects of this concentrated, but minor zone of degradation appear to have little effect on the overall flammability, although research in this area would be welcome. This would be especially relevant to the generally amorphous polymers such as the thermosets, PS, and copolymers like EVA and ABS.

Conversely, degrading treatments that may modify a polymer surface in a manner that enables a subsequent or simultaneous modification to be undertaken may reduce polymer flammability. Such modifications could be seen to be potential flame-retardant processes. Surface graft copolymerization of an activated underlying polymer surface comes to mind here, which comprises, for example, activation during surface chemical grafting,⁸⁸ radiation,⁸⁹ preirradiation,^{90,91} and plasma⁹² treatments. This area may be considered to be an important and emerging means of conferring flame retardancy in a more sophisticated and both environmentally and cost-effective manner, than the traditional use of bulk flame retardants for a number of polymers. The current state of developments here, along with the recent interest in depositing nanoparticulates onto the polymer surfaces, with a view of improving the overall flame retardancy, also needs to be mentioned and have been recently reviewed by us with an emphasis on the textile substrates.⁹³

REFERENCES

1. C.F. Cullis and M.M. Hirschler, *The Combustion of Organic Polymers*, Oxford University Press, Oxford, 1981, p. 117.
2. S.L. Madorsky, *Thermal Degradation of Polymers*, Wiley, New York, 1964.
3. J. Verdu, X. Colin, B. Fayolle, and L. Audouin, Methodology of lifetime prediction in polymer aging. *J. Testing Eval.*, 35(3), 289–296 (2007).
4. S. Halim Hamid and I. Hussain, Lifetime prediction of plastics. In *Handbook of Polymer Degradation*, 2nd edn., S.S. Halim Hamid (ed.), Dekker, New York, pp. 699–726, (2000).
5. Plastics-Thermogravimetry(TG) of polymers—General principles, BS EN ISO 11358:1997; BS 2782-1: Method 127A:1997.
6. Plastics-Thermogravimetry(TG) of polymers—Part 2: Determination of activation energy, BS ISO 11358-2:2005.
7. M.B. Maurin, L.W. Dittert, and A.A. Hussain, Thermogravimetric analysis of ethylene-ethyl acetate copolymers with FTIR analysis of the pyrolysis products. *Thermochim. Acta*, 186, 97–102 (1991).
8. A.C. Draye, O. Persenaire, J. Brozzek, J. Roda, T. Kosek, and Ph. Dubois, Thermogravimetric analysis of poly(ϵ -caprolactam) and poly[(ϵ -caprolactam)-*co*-(ϵ -caprolactone)] polymers. *Polymer*, 42, 8325–8332 (2001).
9. R.E. Lyon and R.N. Walters, Combustion flow calorimetry. *J. Anal. Appl. Pyrolysis*, 71, 27–46 (2004).
10. C. Huggett, Estimation of rate of heat release by means of oxygen consumption measurements. *Fire Mater.*, 4, 61–65, (1980).

11. R.N. Walters and R.E. Lyon, Flammability of polymer composites, *SAMPE 2007*, Baltimore, MD, June 3–7, 2007.
12. R.E. Lyon, R.N. Walters, M. Beach, and F.P. Schall, Flammability screening of plastics containing flame retardant additives, *ADDITIVES 2007, 16th International Conference*, San Antonio, TX, 2007.
13. B. Rimez, H. Rahier, G. Van Assche, T. Artoos, M. Biesemans, and B. Van Mele, The thermal degradation of poly(vinyl acetate) and poly(ethylene-co-vinyl acetate), Part I: Experimental study of the degradation mechanism, *Polym. Degrad. Stab.*, 93, 800–810 (2008).
14. R. Bernstein, S.M. Thornberg, R.A. Assink, A.N. Irwin, J.M. Hochrein, J.R. Brown, D.K. Derzon, S.B. Klamo, and R.L. Clough, The origins of volatile oxidation products in the thermal degradation of polypropylene, identified by selective isotopic labeling. *Polym. Degrad. Stab.*, 92, 2076–2094 (2007).
15. G. Madras and B.J. McCoy, Distribution kinetics for polymer mixture degradation. *Ind. Eng. Chem. Res.*, 32, 352–357 (1999).
16. S.I. Stoliarov, P.R. Westmoreland, H. Zhang, R.E. Lyon, and M.R. Nyden, Molecular modeling of the thermal decomposition of polymers. In *Fire and Polymers IV, Materials and Concepts for Hazard Prevention*, C.A. Wilkie and G.L. Nelson (eds.), American Chemical Society, Washington, DC; *ACS Symp. Series 922*, 306–319 (2006).
17. J.L. Bolland and G. Gee, Trans. A review of the role of basic iron(III) oxide acting as a char forming/smoke suppressing/flame retarding additive in halogenated polymers and halogenated polymer blends. *Faraday Soc.*, 42, 236 (1946).
18. A.J. Chirinos-Padrón, Aspects of polymer stabilisation. In *Handbook of Polymer Degradation*, S. Halim Hamid, M.B. Amin, and A.G. Maadhah (eds.), Dekker, New York, 1992, Chapter 8, pp. 261–303.
19. L. Ballice, Classification of volatile products evolved during temperature-programmed co-pyrolysis of low-density polyethylene (LDPE) with polypropylene (PP). *Fuel*, 81(9), 1233–1240 (2002).
20. L. Ballice and R. Reimerta, Classification of volatile products from the temperature-programmed pyrolysis of polypropylene (PP), atactic-polypropylene (APP) and thermogravimetrically derived kinetics of pyrolysis. *Chem. Eng. Process.*, 41(4), 289–296 (2002).
21. W. Ding, J. Liang, and L.L. Anderson, Thermal and catalytic degradation of high-density polyethylene and commingled post-consumer plastic waste. *Fuel Process. Technol.*, 51, 47 (1997).
22. R. Ochoa, H.V. Woert, W.H. Lee, R. Subramanian, E. Kugler, and P.C. Eklund, Catalytic degradation of medium density polyethylene over silica-alumina supports. *Fuel Process. Technol.*, 49, 119 (1996).
23. N.K. Jha, A.C. Misra, and P. Bajai, Flame-retardant additives for polypropylene. *J. Macromol. Sci. Chem.*, 24(1), 69–116 (1984).
24. E.M. Pearce, Y.P. Khanna, and D. Raucher, In *Thermal Characterization of Polymeric Materials*, E. Turi (ed.), Academic Press, London, 1981, Chap. 8.
25. M.I. Kohan, *Nylon Plastics*, John Wiley & Sons, New York, 1973, p. 46ff.
26. R.H. Peters and R.H. Still, In *Applied Fiber Science*, F. Happey (ed.), Academic Press, London, 1979, pp. 321–427.
27. S. Straus and L.A. Wall, *J. Chem. Natl. Bur. Std.*, 60, 39 (1958); 63A, 269 (1959).
28. B.Kamerbeek, G.H. Kroes, and W. Grolle, In *Thermal Degradation of Polymers*, SCI Monograph No. 13, London, pp. 357–391, 1961.
29. I. Goodman, The thermal degradation of 66 nylon, *J. Polym. Sci.*, 13, 175 (1955).
30. S. Levchik and E. Weil, Combustion and fire retardancy of aliphatic nylons. *Polym. Int.*, 49, 1033–1076 (2000).
31. H. Sobue and J. Kajiura, Kogyo Kagaku Zasshi. *J. Chem. Soc. Jpn., Ind. Chem. Sect.*, 62, 1766 (1969).
32. N. Grassie, The pyrolysis of acrylonitrile homopolymers and copolymers. In *Developments in Polymer Degradation*, N. Grassie (ed.), Vol. 1, Applied Science Publishers, London, 1977, pp. 137–169.
33. G. Henrici-Olive and S. Olive, Chemistry of carbon fiber formation from polyacrylonitrile. *Adv. Polym. Sci.*, 51, 1–60 (1983).
34. R.C. Houtz, “Orlon” acrylic fiber: Chemistry and properties. *Textile Res. J.*, 20, 786–801 (1950).
35. J. Vosburgh, The heat treatment of Orlon acrylic fibre to render it fireproof. *Textile Res. J.*, 30, 882 (1960).
36. A.R. Horrocks, J. Zhang, and M.E. Hall, Flammability of polyacrylonitrile and its copolymers. II. Thermal behaviour and its mechanism of degradation. *Polym. Int.*, 33, 303–314 (1994).
37. J. Zhang, A.R. Horrocks, and M.E. Hall, Flammability of polyacrylonitrile and its copolymers. III. The flame retardant mechanism of ammonium polyphosphate. *Fire Mater.*, 18, 307–312 (1994).
38. B.A. Howell, The utilisation of TG/GC/MS in the establishment of the mechanism of polystyrene degradation. *J. Thermal Anal. Cal.*, 89, 393–398 (2007).

39. B.A. Howell, Y. Cui, K. Chaiwong, and H. Zaho, Polymerization as a means of stabilization for polystyrene. *J. Vinyl Addit. Technol.*, 12, 198–203 (2006).
40. M.M. Hirschler, Chemical aspects of thermal decomposition of polymeric materials. In *The Fire Retardancy of Polymers*, A.F. Grand and C.A. Wilkie (eds.), CRC Press, Boca Raton, FL, 2000, Chapter 2, pp. 28–79.
41. P. Armitage, J.R. Ebdon, B.J. Hunt, M.S. Jones, and F.G. Thorpe, Chemical modification of polymers to improve flame retardance. I. The influence of boron-containing groups. *Polym. Degrad. Stab.*, 54, 387–393 (1996).
42. J.R. Ebdon, B.J. Hunt, M.S. Jones, and F.G. Thorpe, Chemical modification of polymers to improve flame retardance. II. The influence of silicon-containing groups, *Polym. Degrad. Stab.*, 54, 395–400 (1996).
43. Y.L. Liu, G.H. Hsiue, Y.S. Chiu, R.U. Jeng, and C. Ma, Synthesis and flame retardant properties of phosphorus-containing polymers based on poly(4-hydroxystyrene). *J. Appl. Polym. Sci.*, 59, 1619–1625 (1996).
44. V.H. Tran, Polaron mechanism in the thermal degradation and stabilisation of poly(vinyl chloride). *J. Macromol. Sci. Rev. Macromol. Chem. Phys.*, C38, 1 (1998).
45. R.D. Pike, W.H. Starnes Jr., J.P. Jeng, S.W. Bryant, P. Kourtesis, C.W. Adams, S.D. Bunge, Y.M. Kang, A.S. Kim, J.A. Macko, and C.P.O'Brian, Low valent metals as reductive crosslinking agents: A new strategy for smoke suppression of poly(vinyl chloride). In *Chemistry and Technology of Polymer Additives*, S. Al-Malaika, A. Golovoy, and C.A. Wilkie (eds.), Blackwell Science, Oxford, 1999, Chapter 11.
46. P. Carty and S. White, A review of the role of basic iron(III) oxide acting as a char forming/smoke suppressing/flame retarding additive in halogenated polymers and halogenated polymer blends. *Polym. Compos.*, 6, 33 (1998).
47. T.R. Hull, D. Price, Y. Liu, C.L. Wills, and J. Brady, An investigation into the decomposition and burning behavior of ethylene-vinyl acetate copolymer nanocomposite materials. *Polym. Degrad. Stab.*, 82, 365–371 (2003).
48. J.H. Fabris, Novel poly(urethane-amide)s from polyurethane prepolymer and reactive polyamide. Preparation and Properties. *Adv. Urethane Sci. Technol.*, 4, 89–111 (1976).
49. W.D. Wooley, Nitrogen-containing products from the thermal decomposition of flexible polyurethane foams. *Brit. Polym. J.*, 4, 27–43 (1972).
50. *Consumer Protection Act (1987), the Furniture and Furnishings (Fire) (Safety) Regulations, 1988*, SI1324 (1988), London, HMSO, 1988.
51. D. Price, Y. Liu, G.J. Milnes, T.R. Hull, B.K. Kandola, and A.R. Horrocks, An investigation into the mechanism of flame retardancy and smoke suppression by melamine in flexible polyurethane foam. *Fire Mater.*, 26, 201–206 (2002).
52. A.R. Horrocks and B.K. Kandola, Flammability and fire resistance of composites. In *Design and Manufacture of Textile Composites*, A.C. Long (ed.), Woodhead Publishing, Cambridge, U.K., 2005, pp. 330–363.
53. S.V. Levchik, Thermosetting polymers. In *Plastics Flammability Handbook*, Troitzsch J. (ed.), Hanser, Munich, 2004, pp. 83–98.
54. D.P. Bishop and D.A. Smith, Combined pyrolysis and radiochemical gas chromatography for studying the thermal degradation of epoxy resins and polyimides. I. The degradation of epoxy resins in nitrogen between 400° and 700°C. *J. Appl. Polym. Sci.*, 14, 205 (1970).
55. B.K. Kandola, A.R. Horrocks, P. Myler, and D. Blair, Thermal characterisation of thermoset matrix polymers. In *Fire and Polymers*, G.L. Nelson and C.A. Wilkie (eds.), ACS Symposium Series No. 797, Washington, D.C., 2001, pp. 344–360.
56. A.R. Horrocks, D. Price, B.K. Kandola, and G.V. Coleman, Flame-retardant treatments of cellulose and their influence on the mechanism of cellulose pyrolysis. *J. Mol. Sci., Rev. Macromol. Chem. Phys.*, C36 (4), 721–794 (1996).
57. D. Price, A.R. Horrocks, M. Akalin, and A.A. Farooq, Influence of flame retardants on the mechanism of pyrolysis of cotton (cellulose) fabrics in air. *J. Anal. Appl. Pyrolysis*, 40–41, 511–524 (1997).
58. A.A. Farooq, D. Price, G.J. Milnes, and A.R. Horrocks, Use of GC analysis of volatile products to investigate the mechanisms underlying the influence of flame retardants on the pyrolysis of cellulose in air. *Polym. Degrad. Stab.*, 33, 155–170 (1991).
59. A.G.W. Bradbury, Y. Sakai, and F. Shafizadeh, A kinetic model for pyrolysis of cellulose. *J. Appl. Polym. Sci.*, 22, 497 (1978).
60. D. Price, G.V. Coleman, and A.R. Horrocks, Use of cyclic differential scanning calorimetry. *J. Thermal Anal.*, 40, 649 (1993).

61. F. Shafizadeh and A.G.W. Bradbury, Thermal degradation of cellulose in air and nitrogen at low temperatures. *J. Appl. Polym. Sci.*, 23, 1431 (1979).
62. C. Fairbridge, R.A. Ross, and S.P. Sood, A kinetic surface study of the thermal decomposition of cellulose powder in inert and oxidizing atmospheres. *J. Appl. Polym. Sci.*, 22, 497 (1978); also A.R. Horrocks, D. Davies, and M. Greenhalgh, The use of DTA to study spontaneous combustion of cellulose. *Fire Mater.*, 9, 57 (1985).
63. B.K. Kandola, A.R. Horrocks, K. Padmore, J. Dalton, and T. Owen, Comparison of cone and OSU calorimetric techniques to assess behavior of fabrics used for aircraft interior. *Fire Mater.*, 30 (4), 241–256 (2006).
64. J.-P. Guan and G.-Q. Chen, Flame retardancy finish with an organophosphorus retardant on silk fabrics. *Fire Mater.*, 30 (6), 415–424 (2006).
65. E. Menefee and G. Yee, Thermally-induced structural changes in wool. *Textiles Res. J.*, 35, 801 (1965).
66. L. Benisek, Flame retardance of protein fibers. In *Flame Retardant Polymeric Materials*, Vol. 1, M. Lewin et al. (ed.), Plenum, New York, 1975, p. 137.
67. A.R. Horrocks, H. Eichhorn, H. Schwaenke, N. Saville, and C. Thomas, Thermally resistant fibers. In *High Performance Fibers*, J.W.S. Hearle (ed.), Woodhead Publishing, Cambridge, U.K., 2001, pp. 289–324.
68. ISO DIS 5660: Fire Test—Reaction to Fire—Rate of Heat Release from Building Products: 1990: STD. BSI DD 246-ENGL 1999: Recommendations for use of the Cone Calorimeter.
69. T.R. Hull, Challenges in fire testing: Reaction to fire tests and assessment of fire toxicity. In *Advances in Fire Retardant Materials*, D. Price and A.R. Horrocks (eds.) Woodhead Publishing Ltd., Cambridge, U.K., 2008, Chap. 11, pp. 255–290.
70. D. Price, F. Gao, G.J. Milnes, B. Eling, C.I. Lindsay, and T.P. McGrail, Laser pyrolysis/time-of-flight mass spectrometry studies pertinent to the behavior of flame-retarded polymers in real fire situations. *Polym. Degrad. Stab.*, 64, 403–410 (1999).
71. A. Szabo, B. Marosfoi, P. Anna, and Gy. Marosi, Complex micro-analysis assisted design of fire retardant nanocomposites—Contribution to the nano-mechanism, to be published in *Flame Retardancy of Polymers: New Strategies and Mechanisms*, T.R. Hull and B.K. Kandola (eds.), The Royal Society of Chemistry, Cambridge, U.K., 2009, pp. 74–91.
72. S. Bourbigot and S. Duquesne, Fire retardant polymers: Recent developments and opportunities. *J. Mater. Chem.*, 17, 2283–2300 (2007).
73. D. Price, K. Pyrah, T.R. Hull, G.J. Milnes, J.R. Ebdon, B.J. Hunt, P. Joseph, and C.S. Konkel, Flame retarding poly(methyl methacrylate) with phosphorus-containing compounds: Comparison of an additive with a reactive approach. *Polym. Degrad. Stab.*, 74, 441–447 (2001).
74. J.R. Ebdon, D. Price, B.J. Hunt, P. Joseph, F. Gao, G.J. Milnes, and K.L. Cunliffe, Flame retardance in some polystyrenes and poly(methyl methacrylate)s with covalently bound phosphorus-containing groups: Initial screening experiments and some laser pyrolysis mechanistic studies. *Polym. Degrad. Stab.*, 69, 267–277 (2000).
75. D. Price, L.K. Cunliffe, K.J. Bullett (formerly Pyrah), T.R. Hull, G.J. Milnes, J.R. Ebdon, B.J. Hunt, and P. Joseph, Thermal behavior of covalently bonded phosphonate flame retarded poly(methyl methacrylate) systems. *Polym. Adv. Technol.*, 19 (6), 710–723 (2008) and previous references therein.
76. K.J. Bullett (formerly Pyrah), Flame retarding acrylic and styrenic polymers by modification with phosphorus-containing compounds, PhD thesis, University of Salford, 2002.
77. L.K. Cunliffe, Decomposition studies of fire retardant action of phosphorus compounds in poly(methyl methacrylate), polystyrene and their copolymers PhD thesis, University of Salford, Salford, U.K., 2005.
78. N. Kaprinidis, P. Shields, and G. Leslie, Antimony free flame retardant systems containing Flamestab NOR 116 for polypropylene modelling. In *Flame Retardants 2002*, Interscience Communications, London, 2002, pp. 107–111.
79. S. Zhang and A.R. Horrocks, A review of flame retardant polypropylene fibers. *Prog. Polym. Sci.*, 28, 1517–1538 (2003).
80. N. Kaprinidis and N. Lelli, Flame retardant compositions, Ciba, U.S. Patent 7109260, 19 September 2006 and related patents.
81. F.L. Gugumus, Polymer stabilization—From single stabilizers to complex systems. In *Handbook of Polymer Degradation*, 2nd edn., S. Halim Hamid (ed.), Dekker, New York, 2000, pp. 1–38.
82. J. Malík and C. Kröhnke, Polymer stabilization: Present status and possible future trends. *C.R. Chim.*, 9, 1330–1337 (2006).
83. M.I. Kohan, *Nylon Plastics*, John Wiley & Sons, New York, 1973, p. 426.
84. G.S. Stamatoff (to E.I. DuPont de Nemours and Co.), U.S. Patent 2705277, March 29, 1955.

85. D.E. Stuetz, A.H. DiEdwardo, F. Zitomer, and B.P. Barnes, Polymer combustion. *J. Polym. Sci., Polym. Chem. Edn.*, 13, 585–621 (1975).
86. D.E. Stuetz, A.H. DiEdwardo, F. Zitomer, and B.P. Barnes, Polymer flammability, Parts I and II. *J. Polym. Sci., Polym. Chem. Edn.*, 18, 967–986 and 987–998 (1980).
87. F.S. Qureshi, M.B. Amin, A.G. Maadhah, and S.H. Hamid, Weather-induced degradation of linear low density polyethylene: Mechanical properties. *Polym. Plast. Tech. Eng.*, 28 (7 & 8), 649–662 (1989).
88. W.-Y. Chiang and C.-H. Hu, The improvements in flame retardance and mechanical properties of polypropylene/FR blends by acrylic acid graft copolymerization. *Eur. Polym. J.*, 32 (3), 385–390 (1996).
89. K. Friese and F. Tannert, Radiation-induced grafting of chlorinated PVC for preparation of plastic foams. *Radiat. Phys. Chem.*, 55 (1), 47–54 (1999).
90. J. Wang, S. Zhang, L. Xie, and C. Wen, Approaches to the flame retardancy of polymers. I. Electron-beam pre-irradiation and grafting of acrylic monomers onto EVA copolymers. *J. Fire Sci.*, 15 (1), 68–85 (1997).
91. S. Zhang, J. Wang, Y. Ding, S. Wu, L. Xie, and C. Wen, The electron-beam (EB) irradiation and grafting of acrylic monomers onto EPDM copolymer. *Chin. Sci. Bull.*, 45 (4), 322–325 (2000).
92. L. Shi and J. Wang, Approach to the flame retardancy of EVA copolymer by plasma treatment. *J. Beijing Inst. Technol. (English Edn.)*, 6 (4), 313–320 (1997).
93. A.R. Horrocks, Flame retardant resistant textile coatings and laminates. In *Advanced Fire Retardant Materials*, A.R. Horrocks and D. Price (eds.), Woodhead Publishing, Cambridge, U.K., 2008, Chapter 7.

3 Physical Parameters Affecting Fire Growth

Jose L. Torero and Guillermo Rein

CONTENTS

3.1	Fire Safety	44
3.1.1	Objectives of Fire Safety.....	44
3.1.2	Basic Definition of Fire Growth	45
3.2	Fundamentals of Combustion	46
3.2.1	Reactive Gaseous Mixtures	46
3.2.2	Premixed and Diffusion Flames.....	47
3.2.3	Burning of Condensed Fuels.....	47
3.3	Fundamentals of Fire Dynamics.....	48
3.3.1	Open Fires.....	48
3.3.2	Compartment Fires	49
3.3.3	Fire Modeling	49
3.4	Material Parameters Controlling the Ignition of Solid Fuels.....	51
3.4.1	Spontaneous Ignition	51
3.4.2	Induced Ignition	52
3.4.2.1	Pyrolysis Time.....	53
3.5	Material Parameters Controlling Flame Spread	57
3.5.1	Definition	57
3.5.2	Classification.....	58
3.5.3	Opposed Flame Spread.....	59
3.5.4	Co-Current Flame Spread.....	62
3.5.5	Propagation of a Smoldering Front.....	62
3.5.5.1	Opposed Smoldering	65
3.5.5.2	Forward Smoldering.....	66
3.5.5.3	Physical Parameters Controlling Smoldering	66
3.6	Mass Burning Rate: Energy Release Rate	67
3.6.1	Definition	67
3.6.2	Heat Release Rate	67
3.6.3	Energy Balance at the Material Surface.....	68
3.6.4	The Mass Transfer Number	69
3.7	Material Parameters Controlling Extinction.....	70
	Nomenclature.....	71
	Greeks	72
	References.....	72

3.1 FIRE SAFETY

3.1.1 OBJECTIVES OF FIRE SAFETY

As fire represents a threat to life, property, and the environment, there is a need to control its impact in such a way that life is fully protected, and damage to property and the environment are minimized. Fire safety is the means by which infrastructure is designed in a manner such that these goals are achieved.

The schematic presented in Figure 3.1 represents the possible sequence of events during a fire in a building. The safety objectives for a building can be quantified in terms of the different characteristic times of the events. It follows that the time needed to evacuate a particular compartment, $t_{e,i}$, is required to be much smaller than the time needed to reach untenable conditions in that compartment, $t_{f,i}$. The characteristic values of $t_{e,i}$ and $t_{f,i}$ can be established for different levels of containment, that is, room of origin ($i = 1$), floor ($i = 2$), and building ($i = n$). Furthermore, it is necessary for the time to evacuate the building to be much smaller than the time when structural integrity starts to be compromised (t_s).

In summary,

$$\begin{aligned} \forall i, \quad i = 1 \text{ to } n; \quad t_{e,i} \ll t_{f,i} \\ \forall i, \quad i = 1 \text{ to } n; \quad t_{e,i} \ll t_s \end{aligned} \tag{3.1}$$

It could be added to these objectives that full structural collapse is an undesirable event, irrespective of how long the fire lasts, and therefore,

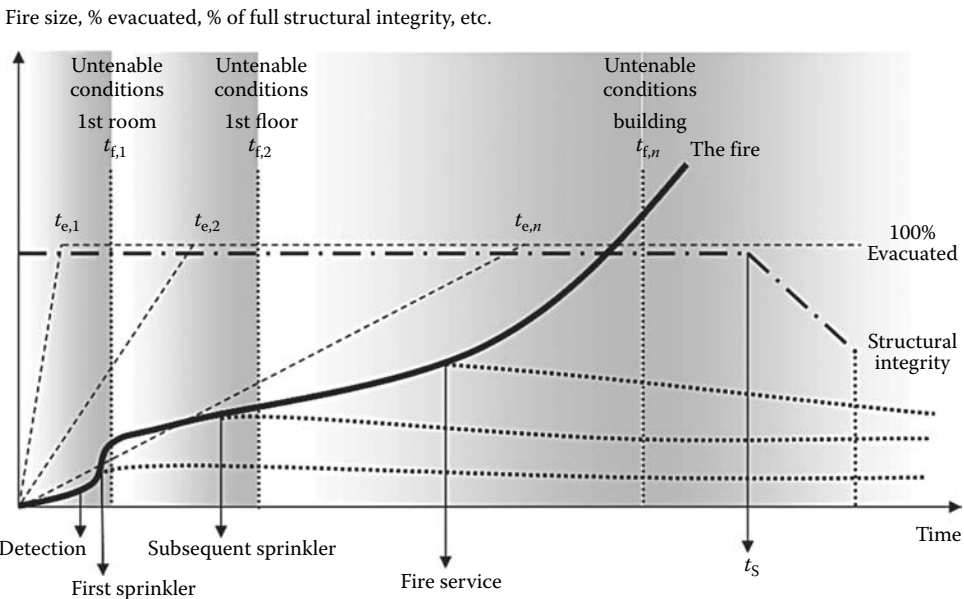


FIGURE 3.1 Schematic of the sequence of events following the onset of a fire in a multi-storey building. The solid line corresponds to the “fire size,” and the dotted lines to the possible outcome of the different forms of intervention (sprinkler activation, fire service). The units of fire size could be defined as HRR, area of fire, or any other means to quantify the magnitude of the event. The units of fire size could be defined as HRR, area of fire, or any other means to quantify the magnitude of the event. The dashed lines are the percentage of people evacuated from the room, floor, and building, respectively, with the ultimate goal of 100% represented by a horizontal dashed line. The dashed and dotted line corresponds to the percentage of the full structural integrity of the building.

$$t_s \rightarrow \infty \quad (3.2)$$

Although these generalized criteria for safety times are a simplified statement, they describe well the main objectives of a fire safety strategy.

When designing for fire safety, a number of strategies are put in place, aiming at achieving these objectives. These include those factors that are intended to increase t_s and $t_{e,i}$, such as active (e.g., sprinklers, or the intervention of the fire service) and passive systems (e.g., fire proofing or compartmentation). As shown in Figure 3.1 (the dotted lines branching off below the fire curve), success of these strategies can result in control or suppression of the fire. Passive protection such as thermal insulation of the structural elements becomes a part of the design, with the purpose of increasing t_s . Finally, but most importantly, evacuation protocols and routes are designed to reduce $t_{e,i}$ at all stages of the building evacuation. It is important to note that the safe operation of the fire service within these times should also be included in the design.

Figure 3.1 makes clear that fire safety is the superposition of three different types of events occurring simultaneously. Two of these events, egress and structural behavior, are reactive events, while the rate of fire growth is the driving process. The structure will be designed and it will respond to the fire. Some passive fire protection systems (detection, alarm) are designed and implemented to warn about the fire, and others are designed to affect the rate of growth (suppression). People within a building are located according to the general use of the premises, but will change their behavior in response to the fire. Occupants will mostly have a passive role, while fire fighters will have an active role attempting to control the growth of the fire.

Building design and fire-fighter intervention procedures are defined on the basis of one or more fire growth scenarios. In the case of prescriptive design (codes and standards), the fire growth scenarios are implicit, while in the case of performance-based design (engineering based methods), they are explicitly defined and are referred to as “design fires.” Prescriptive design rules use knowledge on fire dynamics and empirical data to bound the fire growth for the specific conditions of the implied scenarios. Fire safety systems are designed to operate within these bounds and are deemed adequate for a range of buildings. However, given that there are unavoidable and significant differences between the buildings, there is a risk of extrapolating codes and standards outside its range of applicability. Therefore, to know the extent of the extrapolation of prescriptive solutions requires understanding the parameters that govern and bound the fire growth scenario. In the case of performance-based design, knowledge on fire dynamics is used to predict fire growth under the particular conditions of the building. Thus, the link between fire safety objective and understanding of the physical parameters controlling fire growth is important and explicit.

3.1.2 BASIC DEFINITION OF FIRE GROWTH

While Figure 3.1 implies that there is a single variable to quantify fire growth, the reality is that there are many different variables. The variable or variables of interest depend on the objective of the system under design.

At the core of a fire, there exists a flame or a reaction front that is effectively a combustion process, and thus, is governed by the mechanisms and variables controlling combustion [1]. The interaction between the fire and the environment determines the behavior of the flame and nature of the combustion processes. This is commonly referred to as fire dynamics. An extensive introduction to the topic is provided by Drysdale [2].

As indicated by Drysdale [2], fire dynamics involves a compendium of different subprocesses that start with the initiation of a fire and end with its extinction. The onset of the combustion process, i.e., ignition, in a fire is a complex process that implies not only the initiation of an exothermic reaction, but also a degradation process that provides the fuel feeding the fire. In a fire, it is common to have different materials involved and given the nature of the fire growth, many could be involved

simultaneously, and others, sequentially. The sequence of ignitions of items in an enclosure will affect the nature of the combustion processes. Thus, ignition mechanisms set the dynamics of the fire and are also affected by the fire itself, creating a feedback loop.

Once a material is ignited, the flame propagates over the condensed fuels by transferring sufficient heat to the fuel until a subsequent ignition occurs. This process is commonly referred to as flame spread and is described in detail by Fernandez-Pello [3], and is covered in Section 3.5 of this chapter. Flame spread defines the surface area of the flammable material that delivers the gaseous fuel to the combustion process. The quantity of fuel produced per unit area is the mass burning rate. The mass burning rate multiplied by the surface area determines the total amount of fuel produced. If the total amount of fuel produced is multiplied by the effective heat of combustion (energy produced by combustion per unit mass of fuel burnt), it yields the heat release rate (HRR). The HRR is generally considered as the single most important variable to describe fire growth [4]. Given the nature of the environment, the oxygen supply might not be enough to consume all the fuel, thus, in many cases, combustion is incomplete and therefore, the heat of combustion is not a material property, but a function of the interactions between the environment and the fire. In these cases, it is usually deemed appropriate to calculate the HRR as the energy produced per unit mass of oxygen consumed, multiplied by the available oxygen supply. This is covered in more detail in Section 3.6.

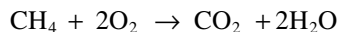
A fire can end when it is extinguished or when oxygen or fuel supplies are depleted (oxygen starvation and burnout, respectively). In all the cases, extinction of the combustion process is brought by interactions of the fuel and oxygen supply, and the energy balance that permits the combustion reaction to remain self-sustained [5–7]. Suppression agents affect a fire by reducing the fuel and oxygen supply or by removing heat (i.e., disturbing the fire triangle). At each stage of fire growth, it is more or less feasible to affect these three variables. Thus, the effectiveness of a suppression system is dictated by its capability to affect the targeted variables at the moment of deployment.

This chapter describes all the abovementioned processes in more detail, extracting at each stage, the main material properties and physical parameters that affect fire growth and how they relate to the fire safety.

3.2 FUNDAMENTALS OF COMBUSTION

3.2.1 REACTIVE GASEOUS MIXTURES

A flame is the thin sheet where a gas-phase combustion reaction is taking place, resulting in gases at high temperature. These gases could be hot enough to radiate their own light, and thus be visible to the naked eye. An exothermic reaction is the essential chemical phenomena driving the combustion, and involves the exchange of atoms between two reactants brought together, a fuel and oxidizer (typically, the oxygen in air). It results in the release of heat and species products. In general, the process can involve millions of elementary chemical reactions, but the overall process can be represented by a reduced set of lumped pathways. For example, for methane, the overall combustion reaction for ideal and stoichiometric conditions can be simplified to



A reaction is said to be stoichiometric when the fuel and oxygen consume each other completely, forming carbon dioxide (CO_2) and water (H_2O) under ideal conditions. The equivalence ratio is the parameter relating a mixture proportion to stoichiometry. It is defined as the ratio of fuel-to-oxygen amounts times the stoichiometric ratio of oxygen-to-fuel amounts. If there is an excess of fuel, then the mixture is called fuel-rich or rich, and the equivalence ratio is greater than 1, and if there is an excess of oxygen, then it is called fuel-lean or lean and the equivalence ratio is less than 1.

Not all mixtures of reactants lead to combustion. There is a limiting amount of fuel per amount of oxygen, above which the reaction does not take place. This is called the upper flammability

limit (for methane/air mixtures this is 15% at atmospheric conditions). Likewise, there is a limiting amount of fuel per amount of oxygen, below which the reaction does not take place. This is called the lower flammability limit (for methane/air mixtures this is 5% at atmospheric conditions). The tabulated values of these limits for different gaseous fuels can be found in [1,2].

The net heat that is liberated in the overall combustion reaction is called heat of combustion, and is equal to the heat released by the exothermic reactions minus the heat absorbed by the endothermic reactions. The heat of combustion is partially stored in the combustion product as sensible energy, thus increasing their temperature, and partially lost to the environment. The maximum temperature that the combustion products can ever reach is given for the ideal conditions of no heat losses or adiabatic combustion. This is called adiabatic temperature and it sets the theoretical maximum limit for the temperature of a flame (for methane/air mixtures this is 1950°C at atmospheric conditions). The tabulated values of adiabatic temperature for different gaseous fuels can be found in [1,2].

3.2.2 PREMIXED AND DIFFUSION FLAMES

There are two basic flame structures depending on the mixing process of the gaseous reactants; premixed and diffusion (or non-premixed) flames. In premixed flames, fuel and oxygen are premixed before combustion. The process in a gasoline engine is a good example. The traveling of a freely premixed flame can be characterized by its flame speed, which is a function of the fuel, equivalence ratio, pressure, and thermal properties of the reactants (for stoichiometric methane/air mixtures, this is 36 cm/s). The tabulated values of flame speed for different gaseous fuels can be found in [1]. The flame speed, together with the heat of combustion and the adiabatic flame temperature, are the most fundamental properties of premixed flammable mixtures. If the speed at which the reactants arrive to the reaction front is lower than the flame speed, then the reaction-zone location is unstable and the flame is said to blow off. Premixed flames are easier to study and control under laboratory conditions, and thus, are preferred for research purposes. This has led to the largest body of combustion knowledge to be on premixed flames, especially in laminar flows.

In diffusion flames, fuel and oxygen are initially separated and mixed at the flame location during the combustion process. Most combustion systems of technological interest, like diesel engines, gas burners, and accidental fires, are diffusion flames. The distinctive characteristic of a diffusion flame is that the burning rate is determined by the rate at which the fuel and the oxygen are brought together. Thus, the chemistry can be assumed infinitely fast and the reaction be approximated by a one-step overall reaction (as the methane example presented earlier). The mixing is controlled at a small-scale through molecular and turbulent diffusion (quantified by a variable called scalar dissipation rate [1]), and at a large-scale, through the flow conditions around the flame (convective transport). There is a two-way coupling between the flame and the flow, as the heat released induces buoyancy motion of combustion products and thus, affects the flow environment. Thus, flames that are larger than approximately 30 cm are turbulent, and in most cases of technological interest, the flame is turbulent.

3.2.3 BURNING OF CONDENSED FUELS

The fuel can be in the form of a gaseous jet or a condensed medium (either solid or liquid). Diffusion flames do not have a fundamental characteristic property that can be measured, such as flame speed. The equivalence ratio of the flame is not uniquely defined, but covers a wide range of values in the spatial locations around the flame zone. The overall ratio of fuel-and-oxygen-flow over the stoichiometric ratio of fuel-and-oxygen-flow to the reaction zone, are used for the classification of diffusion flames as overventilated or underventilated. Overventilated flames have enough oxygen supply to burn all the available gaseous fuel. Underventilated flames do not have enough oxygen supply to burn all the gaseous fuel.

The process via which a flame is started is called ignition. There are two types of ignition for gaseous mixtures: “induced ignition” via a hot spot, spark, or a small pilot flame, and

“spontaneous ignition” via exothermic chemical processes inherent to the mixture at particular conditions and where no external source is involved. The necessary condition for a thermal ignition is that the rate of energy release should be greater than the rate of the energy loss (dissipation). Ignition conditions are discussed in more detail in Section 3.4. The process via which a flame is terminated is called extinction. A flame can be extinguished by quenching (excessive removal of heat by the presence of a solid) or can be blown out (excessive removal of heat via convective flow). Both the extinction mechanisms can be explained in terms of the dimensionless parameter, Damköhler number (Da). This is defined as the ratio of a characteristic reaction time over a characteristic mixing time (or residence time). Large values of Da lead to extinction of the flame. Extinction conditions are discussed in more detail in Section 3.7.

When a condense-phase fuel, either liquid or solid, is burning, a diffusion flame is established at some distance on top of the free surface of the fuel. The gaseous fuel supply feeding the flame is produced by evaporation, gasification, and pyrolysis of the condensed fuel. Pyrolysis is the chemical decomposition of the organic materials by heating, and does not involve oxygen reactions. In solids, it leads to charring of the fuel which is the chemical process of degradation and incomplete combustion resulting in char as a solid residue. The gaseous fuel produced this way is then transported away from the surface into the air towards the flame, as the oxygen is transported from the surroundings to the burning front. At the diffusion flame, the chemical process can be assumed to be infinitely fast and thus, the burning rate of condense fuels is determined by heat and mass transfer rates alone. The rate at which the condensed fuel is converted into gaseous form is generally determined by the rate of heat transfer from the flame to the fuel surface. This heat is in turn conducted into the condensed fuel, and drives the process of evaporation or pyrolysis.

Before a flame is established, the ignition of the condensed fuel takes place. For the case of induced ignition with a pilot, the process has two conditions that are of interests and are generally considered as material properties of the condensed fuels. Upon heating from initial ambient temperature, the material produces gaseous fuels that are transported away and mixed with air, thus creating a spatial distribution of different fuel concentrations. The first point of interest is reached when the temperature of the material is high enough to produce a flammable gaseous mixture that reaches the location of the pilot. Subsequently, the mixture ignites and a flame propagates rapidly over the surface of the fuel consuming the gaseous fuel like a flash. This is termed as the flash point, and is quantified by the temperature of the fuel when the flash is observed in a standard test (flash-point temperature). The temperature of the condensed material keeps increasing, and as the supply of the gaseous fuel is large enough, a stable flame is anchored over the surface. This is termed as the fire point and is quantified by the temperature of the fuel when the stable flame is observed in a standard test (fire-point temperature). In some fuels, the flash point and the fire point are identical as measured in the test.

3.3 FUNDAMENTALS OF FIRE DYNAMICS

3.3.1 OPEN FIRES

Accidental fires, the main objective of fire dynamics, mostly involve condensed fuels and thus, are driven by diffusion flames. The single most important variable to describe and quantify fire is the HRR, which is the rate of the thermal energy liberated at the combustion process. After ignition of the condensed fuel, if flame spread occurs, then the surface area of the burning fuel will increase in time, and also ignition of other fuel packages might take place. The evolution in time of the HRR is related to the global fire growth from flame spread to burn out and extinction. In the early stages, the HRR typically follows a t^2 law in time with different strengths/speeds for different fire scenario. During the burn-out phase, it follows an exponential decay in time.

The rate of productions of bulk combustion products (CO , CO_2 , soot, and smoke in general) is proportional to the HRR, as both of them are originated by the reaction rate at the total burning

surface of the fuel. The hot smoke emitted from a fire will rise up due to buoyancy, forming the plume. As the plume rises, it entrains air from the surroundings, in turn feeding the fire with oxygen. Also, the diameter and mass flow rate of the plume increase with elevation as a result of air entrainment. Air entrainment has the effect of increasing the mass flow of gas in the plume, but also dilutes smoke concentration and lowers the smoke temperature.

The heating mechanisms from an open fire are the radiation from the flames that transport energy in rays going in all directions originated at the fire, but is of relatively short range, and the heat convection of the hot smoke can travel significant distances. Heat transfer by conduction is important only very close to the flame rim on the surface of the fuel.

3.3.2 COMPARTMENT FIRES

When the fire is located inside an enclosure bound by a ceiling and walls, the fire dynamics differ from those of an open fire. The products of combustion, together with the air entrained by the fire, flow up, until they reach the ceiling. Upon reaching the ceiling, a ceiling jet is formed and smoke spreads concentrically from the fire axis. The smoke accumulates between the ceiling and the upper parts of the walls, eventually building a hot layer. The enclosure is then divided into two distinct horizontal layers filling the space. The hot products of combustion occupy the upper layer, while the cooler gas, mostly ambient air, occupies the lower layer. The hot gases can also flow through openings, and smoke and fire can spread to other compartments of the buildings.

Similar to the classification of diffusion flames, the overall flows of fuel and oxygen are used to classify fuel-controlled and ventilation-controlled compartment fires. Fuel-controlled fires have enough oxygen supply from the opening to the compartment, to burn all the available gaseous fuel. The size and evolution of the fire is then governed by the amount and configuration of the fuel load in the compartment. Ventilation-controlled fires do not have enough oxygen supply to burn all the gaseous fuel, and the combustion reaction is incomplete. The size and evolution of the fire is then governed by the amount and configuration of the area of openings in the compartment. This leaves a significant fraction of unburnt gaseous fuel in the smoke. This fuel-rich smoke could burn once it reaches a fresh supply of oxygen at the compartment openings, resulting in external flaming from doors in corridors or windows on the façade of the building. Also, as the fire heating of window covers can lead to their breakage, the total area of the openings in the compartment would increase and hence, the fire size will also increase.

As a fuel-controlled fire grows in size and involves more fuel surface area and more fuel packages, it can reach a condition where the entire fuel load in the compartment burns at once. When this condition takes place as a transition suddenly, it is termed as flashover. The transition from fuel-controlled to ventilation-controlled conditions usually takes place at flashover event.

The other fate of interest for compartment fires is vitiation. When some smoke instead of pure air is entrained into the flame, the combustion reaction is incomplete, releasing less heat, and the flame could be locally extinguished. If the smoke layer keeps growing and the vitiation continues, then the fire could be extinguished by this process. Alternatively, the fire could be extinguished by consumption of most of the oxygen in the compartment volume. Oxygen starvation and vitiation are possible in compartments with very small openings relative to the fire load.

3.3.3 FIRE MODELING

Computer fire modeling was first developed as a research tool in the 1970s, after the surge of computer resources. It reached its first applications to real fire engineering problems in the late 1980s, and now is widely used in many aspects of fire science and engineering. Its current applications range from forensic investigations, risk assessments, life safety, smoke movement and detection, sprinkler performance, structural behavior, and design of fire safety. Modeling is among the fastest developing areas in fire-safety science. However, its ability to reproduce fire phenomena lags experimental understanding by about 10 years.

There are three main approaches to model compartment fires [2,3]. The simplest is to use the basic expressions and experimental correlations of the thermochemical and fluid processes occurring to produce an analytical model of the fire development. Analytical fire models are fast to set up and easy to use, because of the few mechanisms involved [2]; however, the results are only correct in the order of magnitude, because coupling of the different fire phenomena is difficult in these models. Nevertheless, they can serve as a baseline for more sophisticated computer modeling.

Of a more complete approach are the zone models [3], which consider two (or more) distinct horizontal layers filling the compartment, each of which is assumed to be spatially uniform in temperature, pressure, and species concentrations, as determined by simplified transient conservation equations for mass, species, and energy. The hot gases tend to form an upper layer and the ambient air stays in the lower layers. A fire in the enclosure is treated as a pump of mass and energy from the lower layer to the upper layer. As energy and mass are pumped into the upper layer, its volume increases, causing the interface between the layers to move toward the floor. Mass transfer between the compartments can also occur by means of vents such as doorways and windows. Heat transfer in the model occurs due to conduction to the various surfaces in the room. In addition, heat transfer can be included by radiative exchange between the upper and lower layers, and between the layers and the surfaces of the room.

Zone models are in general computer-based, such as FIRST and CFAST, but can also be set up and solved by hand (i.e., using pen and paper). In a modern desktop computer, the computational time for the solution is in the order of seconds. Their main advantage is that this small computer-time allows for extensive parametric studies. As they take into account more coupled physical mechanisms, they have the potential to give better results than the analytical models. The primary inputs to zone models are the geometry of the compartments, including all vents and windows, and the primary fire, in terms of the HRR, fire area, and the yields of products. The most important limitations of zone models are that the radiation is elementary, there is no significant horizontal layer growth, the enclosure has to be simple and nearly of uniform cross-section, and the plume-entrainment mechanism applies only to simple scenarios.

The most complete approach is computational fluid dynamics (CFD) [3] (also called field modeling), which numerically solves the transient conservation equations of mass, momentum, energy, and species for the motion of a gas. It divides the three-dimensional space into small rectangular volumes. Within each volume, the gas variables are assumed to be uniform, but change with time. For momentum conservation, CFD solves the Navier–Stokes equations using Reynolds-averaged Navier–Stokes equations (RANS) or large eddy simulations (LES) to account for turbulence. For the combustion reactions, CFD can use mixture fraction or flamelet models assuming infinitely fast chemistry, or more complex chemical models. Heat transfer to the solid surfaces and convection within the fluid are taken into account. In addition, the radiative transport equation for an absorbing/emitting and scattering medium can also be solved. Examples of field models are JASMINE, SOFIE, and FDS.

The major advantage of CFD is that it gives spatial variation and temporal evolution of the fire variables, and visual information about the complex fire development. They require a more significant setup effort and longer computational time, in the order of hours or days on a modern desktop PC. These models consider the most important fire mechanisms in more detail, with the immediate advantage that its range of applicability widens, although it also implies an increase in the number of fundamental parameters required, and therefore, further calibration and validation is needed. With the ever-increasing computer power available, it can be expected that the field models will become more important in fire modeling.

However, current CFD cannot provide good predictions of HRR evolution (i.e., fire growth) in real complex enclosures/scenarios. Fire modeling is not yet able to predict the HRR, and research efforts need to be tailored toward this issue. However, fire environments for fire safety design can still be calculated using CFD, if the HRR is an input data to the design process. This is because, current CFD tools provide good predictions of the effects of a fire (e.g., temperature field, smoke movements, etc.) once the HRR is provided.

Every model, as an approximate representation of an actual phenomenon, has limitations that constrain its use and narrow its range of applicability. Generally, a more complete model contains fewer simplifications that imply more freedom and fewer limitations. However, fewer simplifications imply the need to know a larger number of fundamental parameters, to be extracted, in general, from experiments, which in fire science, often are associated to significant uncertainties. There has to be a consideration also toward whether the model has been validated for the particular circumstances of interest.

3.4 MATERIAL PARAMETERS CONTROLLING THE IGNITION OF SOLID FUELS

3.4.1 SPONTANEOUS IGNITION

Spontaneous ignition of a fuel results from the self-heating of the material induced by a chemical reaction that produces more heat than the heat that can be locally lost. Detailed analysis of this process can be found in Bowes [8] or Kanury [9]. The general requirement for spontaneous ignition to occur is that both fuel and oxygen are present in sufficient quantities at the same location. Thus, a porous media or a material that can self-oxidize become a requirement. The solution requires the resolution of mass, heat, and momentum conservation equations within a porous media that include all chemical heat sources and sinks. A simple way of looking at the phenomenon is to assume that the porous media is a solid through which heat is gained and lost only through convection and conduction. The transient energy equation for a three-dimensional Cartesian control volume takes the following form:

$$\rho C \left(\frac{\partial T}{\partial t} + \vec{u} \cdot \nabla T \right) = \Delta H \frac{\dot{\omega}_O'''}{\phi} - \nabla \cdot (-k \nabla T) \quad (3.3)$$

where the reaction rate is given by $\dot{\omega}_O''' = AY_O^{n-j} Y_F^j e^{-E/RT}$ and in this particular case, A , E , and R . For simplicity, the reaction has been represented by a single step, but in most cases, the reaction term will be described by the summation of multiple chemical reactions. The flow could be described by Darcy's law:

$$\vec{u} = -\frac{K}{\mu} (\nabla P - \rho \vec{g}) \quad (3.4)$$

If Equation 3.3 is rearranged, then we get

$$\underbrace{\rho C \left(\frac{\partial T}{\partial t} \right)}_{\text{Change}} = \underbrace{\Delta H \frac{\dot{\omega}_O'''}{\phi}}_{\text{Generation}} - \underbrace{\left[\rho C (\vec{u} \cdot \nabla T) + \nabla \cdot (-k \nabla T) \right]}_{\text{Losses}} \quad (3.5)$$

The appropriate boundary conditions need to be included before a solution can be achieved. The solution to this problem remains complex, therefore, simplifications are necessary.

The first approach was developed by Semenov, who treated the system as a lumped control volume V which results in the following equation:

$$\underbrace{V \rho C \left(\frac{\partial T}{\partial t} \right)}_{\text{Change}} = \underbrace{V \Delta H \frac{\dot{\omega}_O'''}{\phi}}_{\text{Generation}} - \underbrace{A h_T (T - T_0)}_{\text{Losses}} \quad (3.6)$$

where

h_T is the total heat-transfer coefficient

A is the area for heat transfer

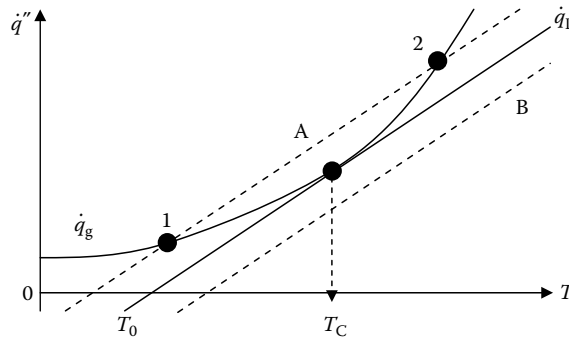


FIGURE 3.2 Schematic of the conditions leading to spontaneous ignition. The horizontal axis is the system temperature, and the vertical axis is the rate of heat generation/loss.

The analysis leads to two eigenvalues, the ignition temperature (T_C) and the critical ambient temperature that will lead to spontaneous ignition (T_0). These are found by making generation and loss terms and their derivatives equal. This is illustrated in Figure 3.2, where the curve is the generation term (\dot{q}_g) and the line is the heat loss term (\dot{q}_L). T_0 is the minimum ambient temperature that will lead to heat generation being always greater than heat losses. The dotted line to the right of T_0 shows that if the ambient temperature increases, the condition of generation being greater than the losses is maintained. However, the dotted line to the left of T_0 shows that if the ambient temperature decreases, then the losses line intercept the heat generation at two points. Once point (1) is reached, stable thermal equilibrium will be attained. Point (2) is an unstable equilibrium.

A more elaborated approach is that of Frank–Kamenetski who relaxed the assumption of homogeneous solid temperature allowing conduction within the solid. A similar eigenvalue analysis will lead again to a critical ignition temperature (T_C) and the ambient temperature required for ignition to occur (T_0). Nevertheless, the ambient temperature, given that conduction of heat from the core to ambient is allowed, becomes a function of the volume of the solid, and hence, for each T_0 , a critical volume, V_C is obtained.

At a fundamental level, the process of spontaneous ignition depends strongly on the thermal properties (ρ , k , C) and the reaction constants, and weakly, on the viscosity (μ) and permeability (K). The final parameter is the eigenvalue of the problem corresponding to the ignition temperature, T_C . The critical ambient temperature, T_0 , and the critical volume V_C are truly not physical parameters controlling spontaneous ignition, but the result of the mathematical analysis.

3.4.2 INDUCED IGNITION

The mechanisms leading to gas-phase ignition from a solid fuel sample can be described as follows. The solid fuel sample is considered initially at ambient temperature, T_∞ . After suddenly imposing an incident heat flux (\dot{q}_i''), the temperature of the solid fuel sample rises until the surface reaches the pyrolysis temperature, T_p . The time required for the fuel surface to attain T_p will be referred to as the pyrolysis time, Δt_p . After attaining T_p , the vapor (pyrolyzate) leaves the surface, is diffused and convected outward, mixes with the ambient oxygen, and creates a flammable mixture near the solid surface. This period will be referred here as the mixing time, Δt_m . The flow and geometrical characteristics determine the mixing time. If the mixture temperature is increased, then the combustion reaction may become strong enough to overcome the heat losses to the solid and

the ambient, thus becoming self-sustained, at which point flaming ignition will occur. This period corresponds to the induction time, Δt_i .

Extending the analysis proposed by Fernandez-Pello [3], the ignition delay time Δt_{ig} is given by

$$\Delta t_{ig} = \Delta t_p + \Delta t_m + \Delta t_i \tag{3.7}$$

Under ideal conditions, introducing a strong pilot reduces the induction time Δt_i making it negligible when compared with Δt_p and Δt_m . Here, we will focus on the piloted ignition as opposed to the auto-ignition, where the absence of a pilot requires the heating of the gas-phase mixture. For assessment of the physical variables controlling ignition, piloted ignition is preferred to spontaneous ignition, because it reduces the uncertainty associated with the mass and heat-transfer processes required to bring the mixture to ignition temperature.

A strong pilot ensures a minimal induction time (Δt_i), but owing to the effect that scale has on the flow, the relative importance of the mixing time Δt_m sometimes needs to be evaluated [11], thus, the ignition delay time could be presented as

$$\Delta t_{ig} = \Delta t_p + \Delta t_m \tag{3.8}$$

Mixing is commonly considered to be a fast process when compared with heating of the solid fuel sample; therefore, the fuel and oxygen mixture becomes flammable almost immediately after pyrolysis starts. Pyrolysis temperatures and times are thus commonly referred to as ignition temperature (T_{ig}) and ignition delay time (Δt_{ig}) [10], and Equation 3.7 finally simplifies to

$$\Delta t_{ig} = \Delta t_p \tag{3.9}$$

and T_{ig} can be defined as T_p . Although such a definition is not physically correct, it can be very useful in some practical applications, as it provides a reference parameter that could serve to characterize ignition. In the case of liquids, the ignition temperature, T_{ig} , is referred to as the flash-point temperature.

3.4.2.1 Pyrolysis Time

The energy balance at the surface of the fuel sample under radiative heating is shown in Figure 3.3 and given by Equation 3.10:

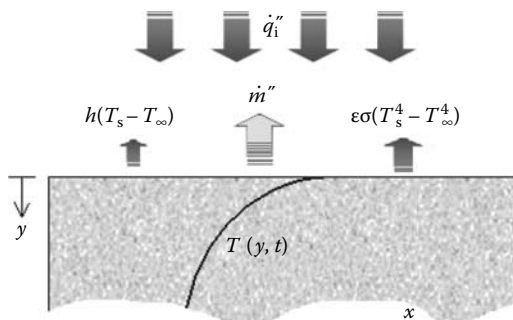


FIGURE 3.3 Energy flows at the surface of the solid fuel sample.

$$\dot{q}_s''(0,t) = a\dot{q}_i'' - \varepsilon\sigma(T^4(0,t) - T_\infty^4) - h_c(T(0,t) - T_\infty) \quad (3.10)$$

where

\dot{q}_s'' is the net heat flux at the surface of the solid fuel sample

a is the absorptivity of the solid fuel sample

ε is the emissivity of the solid fuel sample

σ is the Stefan–Boltzmann constant

$T(0,t)$ is the surface temperature at time t

h_c is the convective heat-transfer coefficient

T_∞ is the ambient temperature

The classical analysis corresponding to the ignition process assumes a linear approximation for the surface re-radiation. The radiative term is then defined as

$$\varepsilon\sigma(T^4(0,t) - T_\infty^4) = h_r(T(0,t) - T_\infty) \quad (3.11)$$

This simplification allows an analytical solution of the one-dimensional heat conduction energy equation. By substituting Equation 3.11 into Equation 3.10, and assuming that the total heat-transfer coefficient (h_T) is equal to the sum of the convective heat-transfer coefficient (h_c) and the radiative heat-transfer coefficient (h_r), the following expression (Equation 3.12) defines the net heat flux (\dot{q}_s'') at the surface of the solid fuel sample.

$$\dot{q}_s''(0,t) = a\dot{q}_i'' - h_T(T(0,t) - T_\infty) \quad (3.12)$$

A series of assumptions are regularly made to provide a solution to the heating problem arising from Equation 3.12. If the heat flux is applied on only one face, then the heating problem can be treated in one dimension. Most materials relevant to fire can be assumed to be thermally thick and can be simplified to a semi-infinite solid, and the material remains inert until the pyrolysis time (t_p). This allows the elimination of reactive and convective terms and to solve the energy equation in one dimension. The differential formulation governing energy equation is then given by

Boundary Conditions:

$$\begin{aligned} \frac{\partial^2 T}{\partial x^2} &= \frac{1}{\alpha} \frac{\partial T}{\partial t} & x = 0, \quad -k \frac{\partial T}{\partial x} &= \dot{q}_s''(0,t) \\ & & t = 0 & \\ & & x \rightarrow \infty & \quad T = T_\infty \end{aligned} \quad (3.13)$$

where α is the thermal diffusivity ($k/\rho C$). The change of variable $\theta = (T - T_\infty)$ produces the following differential equation:

B.C.

$$\frac{\partial^2 \theta}{\partial x^2} = \frac{1}{\alpha} \frac{\partial \theta}{\partial t} \quad x = 0, \quad -k \frac{\partial \theta}{\partial x} = \dot{q}_s''(0, t)$$

$$t = 0 \quad \theta = 0$$

$$x \rightarrow \infty$$
(3.14)

This can be solved (e.g., by means of a Laplace transformation) to provide a general solution for the temperature distribution in the sample as a function of the location (x) and time (t):

$$T - T_\infty = \frac{a\dot{q}_i''}{h_T} \left[\operatorname{erfc}\left(\frac{x}{\sqrt{4\alpha t}}\right) - e^{\left(\frac{h_T}{k}\right)x + \left(\frac{h_T^2}{k\rho C}\right)t} \operatorname{erfc}\left(\frac{h_T}{\sqrt{k\rho C}}\sqrt{t} + \frac{x}{\sqrt{4\alpha t}}\right) \right]$$
(3.15)

To obtain the surface temperature (T_s), x is set to 0 and $T_s = T(0, t)$. Therefore, Equation 3.15 simplifies to

$$T_s = T_\infty + \frac{a\dot{q}_i''}{h_T} \left[1 - e^{\left(\frac{h_T^2}{k\rho C}\right)t} \operatorname{erfc}\left(\frac{h_T}{\sqrt{k\rho C}}\sqrt{t}\right) \right]$$
(3.16)

Details of this resolution can be found in any heat-transfer book [12]. Figure 3.4 presents a typical set of data that show the evolution of the surface temperature as a function of time. The peaks indicate the moment of ignition.

From Equation 3.16,

$$\bar{T} = \frac{a\dot{q}_i''}{h_T}$$
(3.17)

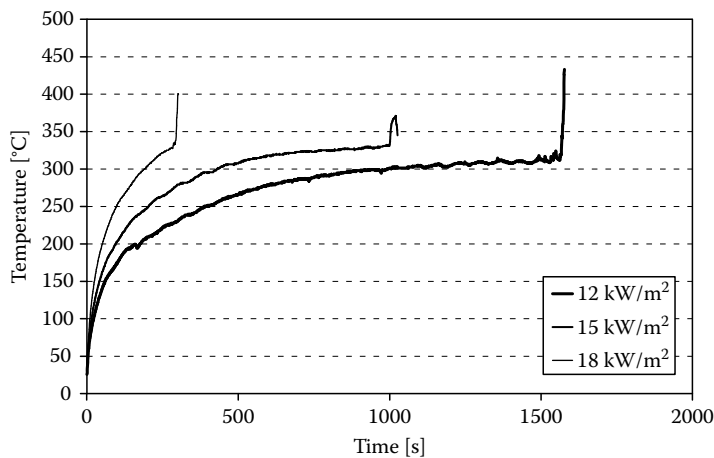


FIGURE 3.4 Characteristic surface temperature histories (thermocouple at the center of ignition test specimen) for several heat fluxes. The material used is PMMA.

can be defined as a characteristic temperature and

$$t_c = \frac{k\rho C}{h_T^2} \quad (3.18)$$

can be defined as a characteristic time. Equations 3.17 and 3.18 establish the physical parameters governing the piloted ignition, and these are the absorptivity a , the thermal inertia $k\rho C$, while the heat flux and total heat-transfer coefficient represent the environmental variables.

Equation 3.16 is the general solution to the surface temperature at all levels of incident heat flux. To obtain the pyrolysis time t_p , the surface temperature T_s is substituted by T_p , and Equation 3.16 can be rewritten as

$$T_p = T_\infty + \bar{T} \left[1 - e^{-\frac{t_p}{t_c}} \operatorname{erfc} \left(\left(\frac{t_p}{t_c} \right)^{\frac{1}{2}} \right) \right] \quad (3.19)$$

where T_p is the final physical parameter to define ignition.

To avoid the complex form of the error function, simplified solutions have been proposed in the literature [10]. To solve for the ignition delay time ($t_p \approx t_{ig}$), a first-order Taylor series expansion of Equation 3.19 is conducted. The range of validity of this expansion is limited, and thus, cannot be used over a large range of incident heat fluxes. Therefore, the domain has to be divided at least into two.

The first domain corresponds to high-incident heat fluxes, where the pyrolysis temperature (T_p) is attained very fast, thus $t_p \ll t_c$. Application of the first-order Taylor Series expansion to Equation 3.13 around $t_p/t_c \rightarrow 0$ yields the following formulation for the pyrolysis time (t_p):

$$\frac{1}{\sqrt{t_p}} = \frac{2}{\sqrt{\pi}} \frac{a}{\sqrt{k\rho C}} \frac{\dot{q}_i''}{(T_p - T_\infty)} \quad (3.20)$$

As can be seen from Equation 3.20, the short-time solution for the pyrolysis time, t_p , is independent of the total heat-transfer coefficient term, $h_T = (h_r + h_c)$. Thus, the pyrolysis time t_p is only a function of the energy absorbed $a\dot{q}_i''$ due to radiation from the radiant panel and the properties (k , ρ , C_p) of the solid fuel sample.

For low-incident heat fluxes where $t_p \gg t_c$, the Taylor series expansion is made around $t_p/t_c \rightarrow \infty$, where the first-order approximation yields

$$\frac{1}{\sqrt{t_p}} = \frac{\sqrt{\pi h_T}}{\sqrt{k\rho C}} \left[1 - \frac{h_T(T_p - T_\infty)}{a\dot{q}_i''} \right] \quad (3.21)$$

Solving Equations 3.20 and 3.21 for the pyrolysis time t_p will yield a theoretical value for the time at which the solid fuel sample begins to pyrolyze and produce fuel vapors. The use of the appropriate simplified solution will allow the evaluation of the pyrolysis time t_p over the entire domain of the imposed incident heat fluxes.

Figure 3.5 shows $t_{ig}^{-0.5}$. This representation of the data corresponds to the dependencies established in Equations 3.20 and 3.21. The dotted line corresponds to Equation 3.21, while the full line corresponds to Equation 3.20.

Equations 3.20 and 3.21 are used to extract the ignition temperature and the product, $k\rho C$. A typical set of data are presented in Table 3.1.

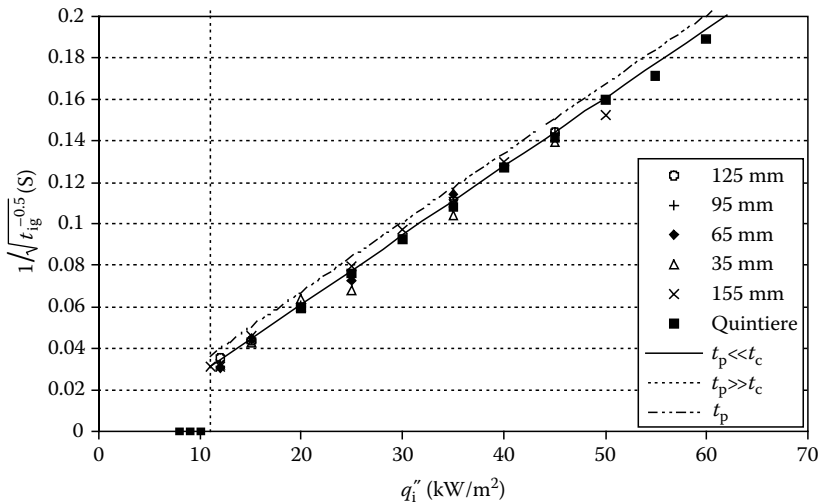


FIGURE 3.5 Ignition delay time ($t_{ig}^{-0.5}$) for different external heat fluxes. The material for the tests is PMMA.

TABLE 3.1
Ignition Data from ASTM E-1321 per Quintiere

Material	T_{ig} [°C]	$k\rho C$ [(kW/m ² K) ² s]
Wood fiber board	355	0.46
Wood hardboard	365	0.88
Plywood	390	0.54
PMMA	380	1.00
Flexible foam plastic	390	0.32
Rigid foam plastic	435	0.03
Acrylic carpet	300	0.42
Wallpaper on plasterboard	412	0.57
Asphalt shingle	378	0.70
Glass-reinforced plastic	390	0.32

Source: Quintiere, J.G., *Principles of Fire Behavior*, Delmar Publishers, New York, 1998.

3.5 MATERIAL PARAMETERS CONTROLLING FLAME SPREAD

3.5.1 DEFINITION

One of the most clearly defined fire-safety issues is that of flame propagation. When a heat source is in contact with a combustible material (liquid or solid), ignition might occur. Once the fuel is ignited, the flame propagates or spreads across its surface, establishing a diffusion flame over the fuel. The flame transfers heat to the surface and the combustible material vaporizes providing the necessary gaseous fuel to sustain the flame. Once the flame has propagated throughout the fuel, the diffusion flame releases heat that is partially used to vaporize the fuel that, in its turn, feeds the flame.

The characteristics of the flame propagation process are determined by the fuel, oxygen-flow structure, and orientation. If the fuel is vertical or a forced flow is imposed parallel to its surface, then a boundary layer is formed. If the fuel is horizontal and the oxygen is quiescent, a pool fire will

develop. If the fuel is inclined or a flow nonparallel to the surface is imposed, then a complex mixed-flow problem will arise.

3.5.2 CLASSIFICATION

Different types of flame spread can be grouped into two main categories, based on the relative direction of the propagating flame to the gas oxygen flow:

- Flame spread in gas flows moving in the opposite direction of the flame propagation (opposed flame spread)
- Flame spread in gas flows moving in the same direction as that of the flame propagation (concurrent flame spread)

In the first case, as shown in Figure 3.6, the flame front is usually distinctive and well behaved, and the flame propagates rather slowly, because the heat transfer from the flame to the unburned fuel is hindered by the opposing gas flow. In the second case, shown in Figure 3.7, the gas flow drives the diffusion flame ahead of the pyrolysis region and largely enhances the heat transfer from the flame to the fuel. Therefore, concurrent flame spread propagates much more rapidly than other cases, and it is known as the most dangerous type of flame spread.

Extensive studies have been conducted both analytically and experimentally to study the opposed and concurrent flame spread [14,15]. One frequently used approach is to isolate the effects

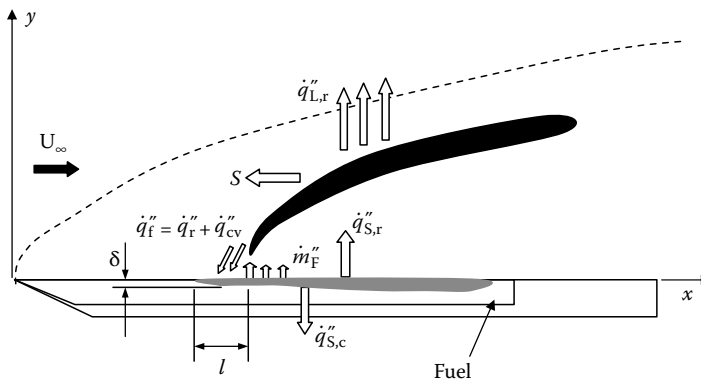


FIGURE 3.6 Schematic of opposed flow flame spread.

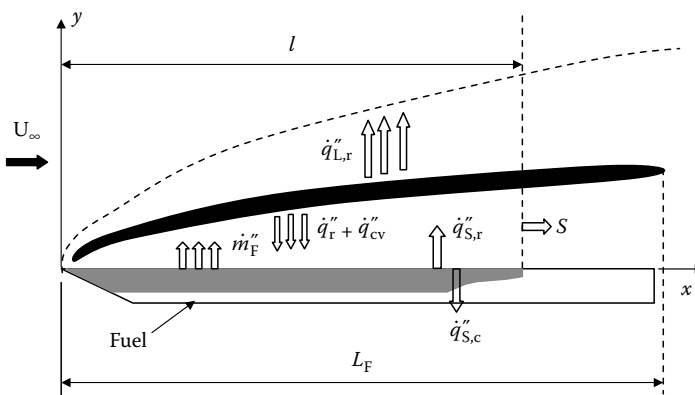


FIGURE 3.7 Schematic of concurrent flow flame spread.

of individual parameters and concentrate on the influence of one parameter at a time for the sake of simplicity. Among the most frequently studied is the effect of gas flow velocity [16], external radiation [10], oxygen concentration [17], buoyancy [18], and fuel sample dimension [19]. A relation to determine the flame spread rate can be obtained from a simple energy balance at the fuel surface:

$$\rho S \Delta h \delta = \dot{q}_f'' l \tag{3.22}$$

where

- ρ is the fuel density
- S is the flame spread rate
- δ is the thickness of the pyrolysis layer
- l is the length of the pyrolysis region exposed to heat flux
- \dot{q}_f'' is the energy per unit area, per unit time transferred across the surface
- Δh is the critical enthalpy increase per unit mass of the fuel needed for ignition to occur

3.5.3 OPPOSED FLAME SPREAD

There are many mechanisms involved in the propagation of a flame through a condensed fuel [13]. The problem is extremely complicated; therefore, the simplest case will be used here, namely, the opposed-flow flame spread. The tip of the flame controls the opposed-flow flame spread and all the transport mechanisms involved are presented in Figure 3.8.

There are three independent sources of heat that will lead to the spread of a flame and that will define the boundary condition:

1. Heat transfer from the flame through the gas: \dot{q}_g''
2. Heat transfer through the solid: \dot{q}_s''
3. Any external heat contribution: \dot{q}_e''

The external heat transfer can be independently controlled, and hence, will not be addressed here. Heat transfer through the solid is given by the following expression:

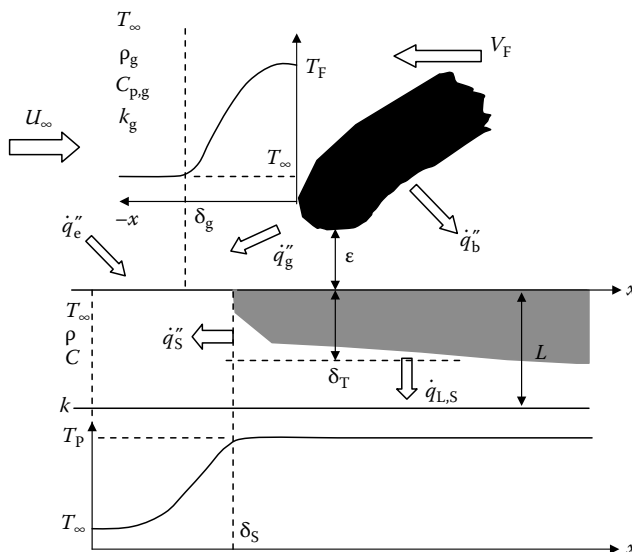


FIGURE 3.8 Schematic of the leading edge of the flame.

$$\dot{q}_s'' \approx k \frac{(T_P - T_\infty)}{\delta_s} \quad (3.23)$$

Heat transfer through the gas phase has been observed to be mainly due to conduction; therefore, radiation is generally neglected. The following expression gives an estimate of the heat flux from the flame to the surface and how that heat is transferred inward into the material:

$$\dot{q}_g'' \approx k_g \frac{(T_F - T_P)}{\varepsilon} \approx k \frac{(T_P - T_\infty)}{\delta_T} \quad (3.24)$$

Estimation of the relative importance of both these parameters was presented in [15]. It can be seen that for thin fuels, the heat transferred through the gas is dominant, while for thick materials, it is the opposite.

The abovementioned results correspond to Poly (methyl) Methacrylate (PMMA) under downward burning conditions, and are not general to all the materials or configurations. In most cases, heat transfer through the gas phase will be dominant for most conditions, mainly because the fire grows as the contribution from the flame radiation increases, enhancing the relative importance of the gas-phase heat transfer. A number of papers summarizing different results can be found in the work by Fernandez-Pello and Hirano [15].

As can be seen in Figure 3.9, only ~50% of the total available energy \dot{q}_T'' is used to heat up the solid, while the rest is lost from the surface either through convection or re-radiation to the environment. As for ignition, both the heat loss terms have generally been simplified to a total heat-transfer coefficient:

$$\dot{q}_L'' = h_T(T_P - T_\infty) \quad (3.25)$$

As observed earlier, the material thickness plays a significant role in the rate of flame spread, either through the mode of heat transfer or through the losses that can occur through the solid. Materials are generally defined as thermally thin, where $\delta_T \approx L$ or thermally thick, where $\delta_T \ll L$. The thermal thickness δ_T needs to be carefully defined, and generally, is given by

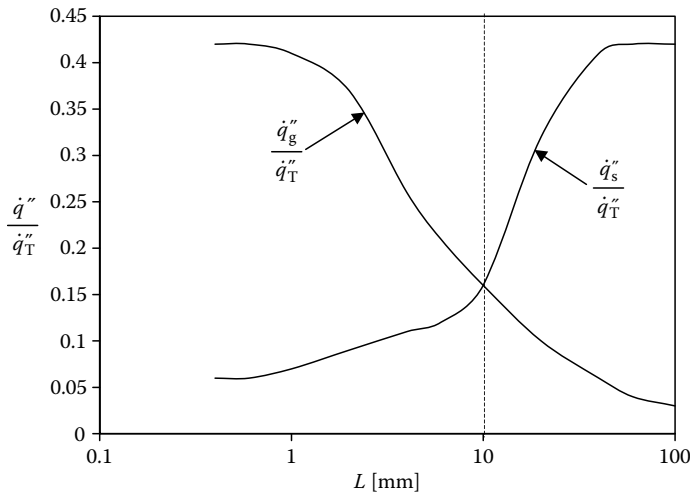


FIGURE 3.9 Relative magnitude of different modes of heat transfer. (Adapted from Fernandez-Pello, A.C. and Hirano, T., *Combust. Sci. Technol.*, 32, 1, 1983.)

$$\delta_T = \sqrt{\alpha t_C} \quad (3.26)$$

where the characteristic time is defined as

$$t_C = \frac{\delta_S}{S} \quad (3.27)$$

Assuming that all the energy used for the propagation comes through conduction in the gas phase, Equation 3.22 can be rewritten as

$$\rho C S (T_P - T_\infty) \delta_T = \dot{q}_g'' \delta_S \quad (3.28)$$

And, therefore,

$$S = \frac{\dot{q}_g'' \delta_S}{\rho C (T_P - T_\infty) \delta_T} \quad (3.29)$$

For thermally thick materials, δ_T can be extracted from Equation 3.24:

$$\delta_T = \frac{k(T_P - T_\infty)}{\dot{q}_g''}$$

and for thermally thin materials,

$$\delta_T = L$$

Thus, the following expressions for the propagation velocity can be obtained for a thermally thick solid:

$$S = \frac{(\dot{q}_g'')^2 \delta_S}{k \rho C (T_P - T_\infty)^2} \quad (3.30)$$

At this point, two different pathways can be followed. The first approach takes all the unknowns and brings them together into “global properties” that are evaluated experimentally. This is the approach followed by Quintiere [10].

Flame spread parameter: $\phi = (\dot{q}_g'')^2 \delta_S$

Thermal Inertia: $k\rho C$

which gives the following expression for the flame spread velocity:

$$S = \frac{\phi}{k \rho C (T_P - T_\infty)^2} \quad (3.31)$$

where the pyrolysis temperature T_P and the thermal inertia $k\rho C$ were described in the ignition section.

An alternate approach is to evaluate the unknown terms of Equation 3.30, $(\delta_S, \dot{q}_g'')^2$. Several expressions can be found in the literature, where the original solutions were presented by DeRis [16] and Tarifa et al. [20]. The following expression was obtained from the work by Fernandez-Pello [21]:

$$S = c \frac{k_g \rho_g C_{p,g} (T_F - T_p)^2 (U_\infty Lx)^{1/2}}{k \rho C (T_p - T_\infty)^2} \quad (3.32)$$

Equation 3.32 provides an expression for the flame spread velocity based only on the parameters of the problem and on the experimental conditions, but still relies on the presence of an unknown constant that needs to be determined experimentally.

In a similar manner, the flame spread velocity can be obtained for thermally thin materials:

$$S = \frac{q_g'' \delta_s}{\rho_g C_{p,g} (T_p - T_\infty) L} \quad (3.33)$$

where similar global parameters can be extracted or the solution can be represented in terms of the properties and experimental parameters with the supplement of an empirical constant. The following expression was provided by Fernandez-Pello [21]:

$$S = c \frac{(k_g \rho_g C_{p,g})^{1/2} (T_F - T_p)^2}{\rho C L (T_p - T_\infty)} \quad (3.34)$$

It is important to note that the physical parameters controlling opposed flame spread are the same as those controlling ignition, with the added parameter associated with the flame heat flux. Depending on the approach to be followed, the flame input can be either defined by the flame temperature, T_F or by q_g'' .

3.5.4 CO-CURRENT FLAME SPREAD

The analysis of co-current flame spread is very similar to that of opposed flame spread. However, it is further complicated because the flame covers the fuel; thus, the flame length is a further parameter that needs to be analyzed. The flame length can be represented empirically as being proportional to the pyrolysis length or can be calculated using boundary layer theory and the assumption of infinitely fast gas-phase chemistry [22]. Despite the added complexity, co-current flame spread is controlled by the same physical parameters as ignition or opposed flame spread.

3.5.5 PROPAGATION OF A SMOLDERING FRONT

Smoldering is characterized by an exothermic heterogeneous combustion reaction that occurs on the surface of a solid fuel and the interior of the porous combustible materials. The heat released during the heterogeneous oxidation of the solid is transferred toward the unreacted material by conduction, convection, and radiation, supporting the propagation of the smolder reaction. The oxygen, in turn, is transported to the reaction zone by diffusion and convection. These transport mechanisms not only influence the rate at which the smolder reaction propagates, but also the limiting factors of the smolder process, that is, ignition and extinction (lower bounds), and transition to flaming (upper bound). The propagation of the smolder reaction is, therefore, a complexly coupled phenomenon involving processes related to the transport of heat and mass in a porous media, together with surface pyrolysis and combustion reactions [1,23].

The main difference between smolder and any of the other combustion processes is that oxidation does not occur in the gas but on the solid phase. Fuels that sustain smolder consist, in general terms, of an aggregate and permeable medium formed by particulates, grains, fibers, or a porous matrix (Figure 3.10). These aggregate fuel elements facilitate the surface reaction with oxygen by providing

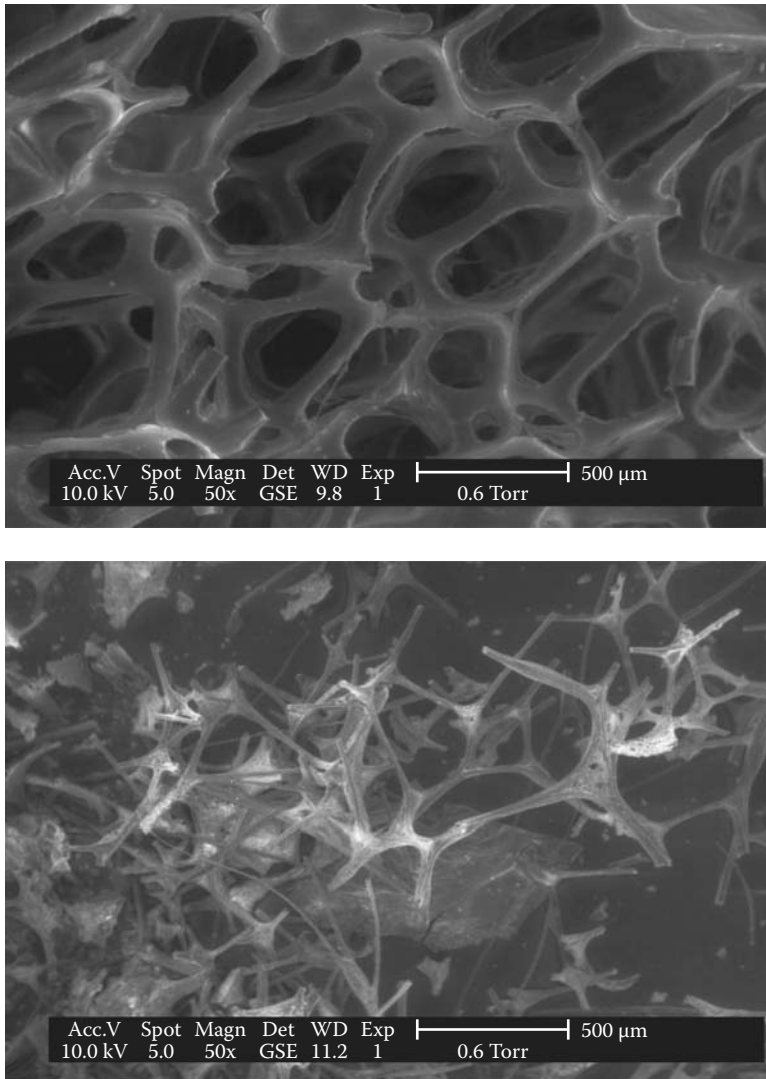


FIGURE 3.10 Scanning electron microscopy imaging of the porous matrix of polyurethane foam. Virgin foam (top) and smoldered char (bottom).

a large surface area per unit volume. They also act as thermal insulation and reduce heat loss, but, at the same time, permit oxygen transport to the reaction sites by convection and diffusion.

As the reaction propagates, the oxygen inside the porous matrix is completely consumed leaving residual char. Figure 3.11 shows a picture of smoldered polyurethane foam. The foam was ignited at the top of the sample and the reaction was allowed to propagate downward leaving a black char behind.

A smoldering reaction is not always established when heat is applied to a porous fuel susceptible to smolder. Actually, the conditions for the onset of smoldering are in some cases (i.e., polyurethane foam) very restrictive. The following possible pathways have been established as viable when heating a fuel susceptible to smolder.

The first step of the degradation process, as shown in Figure 3.12, corresponds to the different magnitudes of the net heat flux imposed onto the material. A typical ignition plot is presented in Figure 3.13 for polyurethane foam. If the net heat flux is weak (i.e., for polyurethane foam $<6 \text{ kW/m}^2$

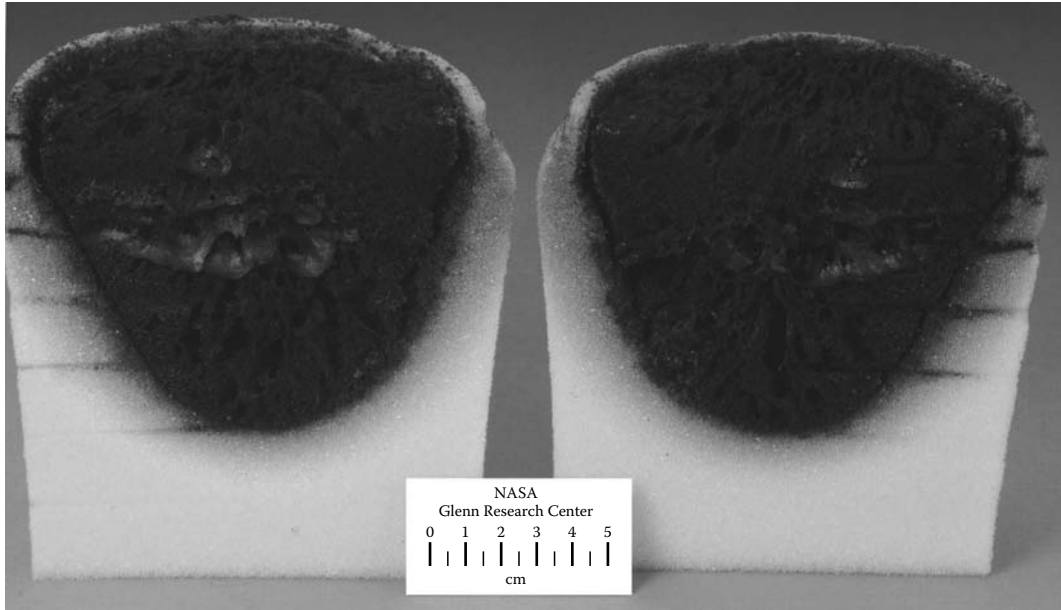


FIGURE 3.11 (See color insert following page 530.) Photograph of a polyurethane foam sample through which a smolder reaction has propagated. (Photo courtesy of NASA.)

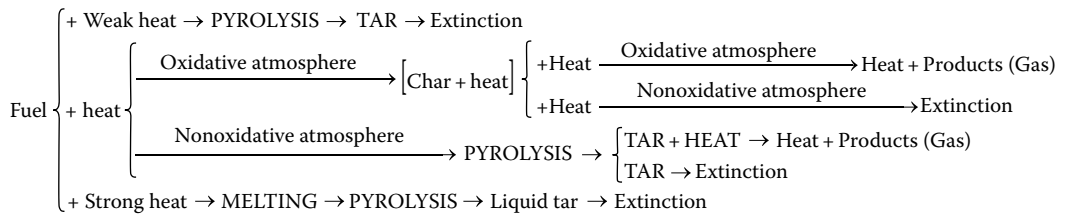


FIGURE 3.12 Possible reaction pathways for a smolder reaction.

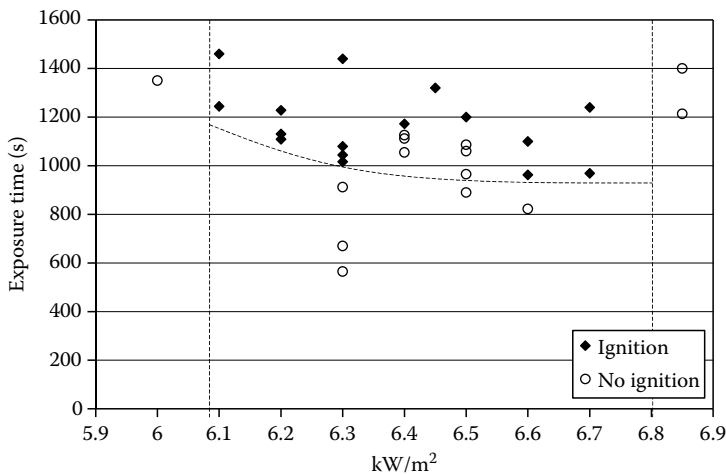


FIGURE 3.13 Ignition characteristics of polyurethane foam as a function of an external heat flux. (Extracted from Anderson, M. et al., *Fire Safety J.*, 35, 131, 2000.)

(Figure 3.13)), Figure 3.12 shows that the fuel is degraded via pyrolysis. Nonetheless, a degraded material is formed. This material is generally of a liquid form and is commonly referred to as tar. If the net heat flux is very strong (i.e., for polyurethane foam $>7 \text{ kW/m}^2$ (Figure 3.13)), then a similar process is observed where a liquid tar remains as the product of the degradation. Both degradation branches are endothermic and once the external heat source is withdrawn extinction follows. The main difference between the two branches seems to be that the amount of heat determines the fraction of tar that will be evaporated, thus, the production of airborne aerosols.

Smoldering of the material occurs only when the heat flux imposed on the material is in between the two limits described earlier. In the presence of an oxidative atmosphere, an exothermic surface reaction (smolder) will lead to the release of heat and gaseous products and the formation of a residual char. Char is a solid matrix that generally conserves the structure of the original fuel. The char has high carbon content and is combustible. The char can further react in the presence of oxygen if its temperature is high enough. Reaction temperatures of char have been observed to be higher than the temperatures observed during direct smolder of the fuel. The final products are in most cases in gaseous form and particulate (smoke), but some fuels lead to a residual noncombustible ash. If all the oxygen is consumed by the smolder reaction, then the char will not react and will subsequently cool down.

Even under the appropriate heating conditions, if sufficient oxygen is not available, then the decomposition chemistry will privilege the endothermic pyrolysis of the fuel. This will again lead to the formation of tar and the consequent extinction. Attempts to identify the exothermic and endothermic degradation processes have been made by means of thermogravimetric analysis (TGA) and differential scanning calorimetry (DSC) [25]. These methods can provide important and insightful information about the smolder mechanism, and can be used as input parameters in complex smoldering propagation models [26].

Once the smolder reaction has been initiated, the reaction front propagates across the porous matrix. When studying smolder propagation, it is very common to use simplified scenarios. A frequent approach is that of treating the smolder front as a flame spread problem and classifying the smolder reaction into two main groups: opposed and forward propagation. These are defined according to the direction in which the fuel and oxygen enter the reaction zone (Figure 3.14).

3.5.5.1 Opposed Smoldering

In opposed (or reverse) smolder, the reaction front propagates in a direction opposite to the oxygen flow. This configuration is also referred to as co-current, or premixed-flame-like smolder, because with the coordinate system anchored at the reaction zone, fuel and oxygen enter the reaction zone from the same direction, albeit with different velocities. In forward smolder, the smolder reaction front moves in the same direction as the oxygen flow. This configuration is also referred to as counter-current or diffusion-flame-like smolder, because the fuel and the oxygen enter the reaction zone from opposite directions. Processes involved in the transport of heat and mass include radiation (heat), convection (natural and forced), and diffusion. In the presence of gravity, buoyancy interferes with both forced convection and diffusion, and consequently, with the transport processes controlling smoldering. In opposed smolder propagation, the heat released by the heterogeneous oxidation (smolder) reaction is transferred ahead of the reaction by conduction and radiation, heating the unreacted fuel and the incoming oxygen. The resulting increase of the virgin fuel temperature leads to the onset of the smolder reaction, and consequently, gives way to its propagation through the fuel. The combustion process is generally oxygen deficient, and the propagating reaction leaves behind a char that contains a significant amount of unburnt fuel. The rate of smolder propagation is basically dictated by a balance between the rate of heat released by the reaction and the energy required to heat the solid fuel and gaseous oxygen to the smolder reaction temperature. Increasing the oxygen flow rate increases the rates of fuel oxidation and heat release, and consequently, the rate of smolder propagation, until it reaches a point at which the rate of heat losses to the incoming oxygen overwhelm the heat released at the reaction, and extinction occurs.

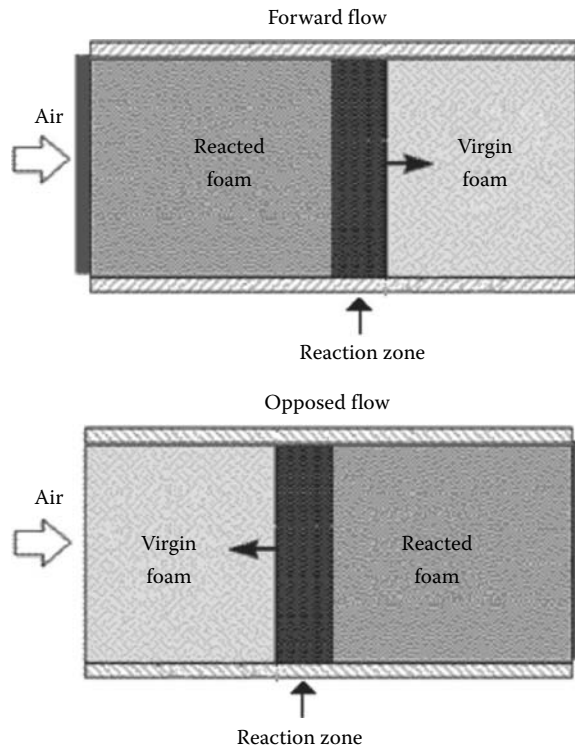


FIGURE 3.14 Schematic of forward and opposed flow smolder.

3.5.5.2 Forward Smoldering

Also known as countercurrent smolder, in this case, the smolder wave travels in the direction of the flow. In forward smolder propagation, oxygen reaches the reaction zone after passing through the hot char left behind by the propagating reaction, and the hot post-combustion gases flow through the virgin fuel ahead of the reaction, preheating it. Thus, increasing the oxygen flow rate increases the oxygen supply to the reaction zone, which enhances the reaction, and increases fuel preheating, which also tends to enhance the reaction. However, post-combustion gases will also tend to dilute the oxygen contained inside the fuel pores and thus, lower the oxygen concentration ahead of the reaction. Furthermore, oxidation of the char may deplete the oxygen in the gas flowing ahead of the reaction. As explained earlier, under these conditions, the fuel may undergo an endothermic, thermal decomposition reaction ahead of the oxidation reaction. These two reactions may propagate at different velocities depending on the oxygen flow and fuel characteristics. Another important process that may occur in forward smolder is the transition from the heterogeneous surface reaction to a gas-phase homogeneous reaction (flaming). This transition process may occur as the oxygen flow rate is increased, and may be caused by the acceleration of the smolder reaction (due to fuel preheating) or by vigorous oxidation of the char (due to the increased oxygen supply).

3.5.2.3 Physical Parameters Controlling Smoldering

Smolder propagation is generally treated as a flame spread problem, thus, a similar thermal analysis to the one presented in Section 3.5.5.1 is conducted for both opposed and concurrent smoldering. Many expressions for a smoldering propagation velocity can be found in the literature. Here, we will use only the one presented by Torero et al. for illustration [27]:

$$S = \frac{\rho_g [\Delta H_{O_2} Y_{O_2} - C_{pg}(T_s - T_i)]}{(1 - \phi)\rho C(T_s - T_i)} U \quad (3.35)$$

where the physical parameters affecting the smolder propagation velocity are the heat of the reaction per unit oxygen mass consumed ΔH_{O_2} , the void fraction ϕ , the smoldering temperature T_s , the density ρ , and the specific heat C . All other parameters of Equation 3.35 are environmental variables such as the ambient density ρ_g , ambient oxygen concentration Y_{O_2} , specific heat C_{pg} , and temperature T_i . The term U corresponds to the air flow velocity through the porous material and U is quantified using expressions of the form of Equation 3.4.

3.6 MASS BURNING RATE: ENERGY RELEASE RATE

3.6.1 DEFINITION

Once a flame is ignited and spreads over a surface, the area under the flames undergoes degradation supported by the energy released by the flame. The production of fuel is known as the burning rate. The fuel emerging from the surface will react at the flame, releasing energy, and this is called the HRR. A brief summary of the different components of the mass burning and HRRs, and their association to the physical material parameters will be presented here. Details on how to evaluate the burning rate are given by Drysdale [2] and Quintiere [13], and on the energy release rate and its estimation by Babrauskas and Grayson [4].

3.6.2 HEAT RELEASE RATE

The energy release rate is the amount of energy produced by the flame per unit time. Its simplest form is given by Equation 3.36:

$$\dot{Q} = A \Delta H_{C,F} \dot{m}_F'' \quad (3.36)$$

where

A is the area

$\Delta H_{C,F}$ is the heat of combustion per unit mass of fuel burnt

\dot{m}_F'' is the mass of the fuel produced at the surface (mass burning rate)

An alternate way to express the energy release rate is by means of the heat of combustion per unit mass of oxygen consumed \dot{m}_O

$$\dot{Q} = \Delta H_{C,O} \dot{m}_O \quad (3.37)$$

where $\Delta H_{C,O}$ is the heat of combustion per unit mass of oxygen consumed (a constant value of 13.1 MJ/kg is generally used for most materials relevant to fire [4]). It must be noted that the mass of oxygen consumed (\dot{m}_O) is not expressed per unit area, this is because the area through which the oxygen reaches the flame is difficult to determine. Equations 3.1 and 3.2 are equivalent, and the one to be used depends mostly on practical issues related to the quantification of the different values.

The total energy released by the flame can be divided into different parts that are transferred by different modes of heat transfer or toward different directions:

$$\dot{Q} = \dot{Q}_C + \dot{Q}_R + \dot{Q}_H + \dot{Q}_F \quad (3.38)$$

\dot{Q}_C is the energy that is convected toward the plume above the flame. Natural convection will drive the hot products (and consequently, the energy) above the flame.

\dot{Q}_R is the energy that is radiated away from the flame toward external targets. The fraction of the energy radiated is generally given by a radiative fraction χ which is generally taken as approximately 30%, $\chi \approx 0.3$ [3] and thus, $\dot{Q}_R \approx \chi \dot{Q}$.

\dot{Q}_H is the energy that remains within the control volume of the flame. Once the flames have attained steady-state conditions, \dot{Q}_H tends toward zero. The gas-phase transient tends to be very short and thus, is neglected for most fire analyses.

\dot{Q}_F is the energy transmitted by the flame toward the surface of the fuel. This energy includes convection, conduction, and radiation. Convection and conduction will be positive inputs toward the fuel, but convection will vary depending on the temperature of the gases over the material at a specific location within the surface.

3.6.3 ENERGY BALANCE AT THE MATERIAL SURFACE

Conducting an energy balance per unit area allows a closer analysis of the fuel surface. This implies the assumption that the energy is distributed homogeneously across the surface. This assumption is justifiable for most of the surface area of the fuel. The energy input to the surface is given by

$$\dot{Q} = A\dot{q}'' \quad (3.39)$$

The energy necessary to vaporize a unit mass of fuel varies depending on the nature of the gasification process. Most liquid fuels (light hydrocarbons) undergo gasification without any chemical decomposition. The energy necessary for the phase change of a unit mass of fuel is called the latent heat of vaporization, (ΔH_V). For most solids and liquids formed by heavier hydrocarbons, the decomposition process implies a chemical breakdown of the molecules. This process is generally endothermic and the energy necessary to gasify a unit mass of fuel is called the heat of pyrolysis, (ΔH_P). For the purposes of this analysis, the distinctions in the decomposition pathway are not relevant; however, the endothermicity of the process is important, and therefore, a generic heat of gasification will be used (ΔH_G). The energy necessary to vaporize a unit mass of fuel per unit is thus given by

$$\dot{q}_V'' = \Delta H_G \dot{m}_{F,G}'' \quad (3.40)$$

where $\dot{m}_{F,G}''$ is the mass of fuel generated per unit surface area.

As indicated in Figure 3.3, the heat feedback (\dot{q}_c'') is used for vaporization (\dot{q}_V'') and to compensate for in-depth conduction (\dot{q}_C'') and heat losses (\dot{q}_L''). The heat lost from the fuel surface includes convection and re-radiation, and can be described by any of the following formulations:

$$\dot{q}_L'' = \dot{q}_{CV}'' + \dot{q}_{S,R}'' = h_C(T_P - T_\infty) + \epsilon\sigma(T_P^4 - T_\infty^4) = h_C(T_P - T_\infty) + h_R(T_P - T_\infty) \quad (3.41)$$

As it was done for ignition and flame spread, it is a common practice to simplify this term to a simple linearized total heat-transfer coefficient

$$\dot{q}_L'' = h_T(T_P - T_\infty) \quad (3.42)$$

Finally, in-depth conduction is given by the temperature gradient at the surface

$$\dot{q}_C'' = -k \left. \frac{\partial T}{\partial x} \right|_{x=0} \quad (3.43)$$

This term varies significantly with the nature of the fuel. Liquid fuels are characterized by the presence of recirculation currents induced by buoyancy. These currents homogenize the temperature distributions, reducing in-depth conduction. Nevertheless, convective motion transfers heat to the interior of the pool leading to an additional term of in-depth convection. Convective heat transfer in polymer melts has a similar behavior and could potentially have an important effect on burning rates; nevertheless, the impact of polymer melt rheology on the flammability of materials is still a matter of great controversy.

Assuming that in-depth heat transfer is only by conduction, the energy balance at the surface is then given by

$$a\dot{q}_e'' = \dot{q}_V'' + \dot{q}_C'' + \dot{q}_L'' \quad (3.44)$$

For convenience, the right-hand side of the equation is generally presented in a different form:

$$a\dot{q}_e'' = \Delta H_G \dot{m}_{F,G}'' + \left(\frac{\dot{q}_C'' + \dot{q}_L''}{\dot{m}_{F,G}''} \right) \dot{m}_{F,G}'' = (\Delta H_G + Q_L) \dot{m}_{F,G}'' \quad (3.45)$$

where Q_L represents the total heat not used to vaporize the fuel normalized per unit mass of fuel generated. In other words, of the total heat available, a fraction goes to gasification (ΔH_G) and the rest goes away to the solid or the gas (Q_L). Assuming the absorptivity to be unity ($a = 1$), the mass of fuel generated is given by

$$\dot{m}_{F,G}'' = \frac{\dot{q}_e''}{(\Delta H_G + Q_L)} \quad (3.46)$$

3.6.4 THE MASS TRANSFER NUMBER

From Equation 3.39, the HRR per unit area is given by the following expression:

$$\dot{q}_g'' = \frac{\dot{Q}}{A} = \Delta H_{C,F} \dot{m}_{F,B}'' \quad (3.47)$$

where $\dot{m}_{F,B}''$ is the mass of the fuel burnt. As shown earlier, the energy generated can be divided into the energy fed back to the fuel (\dot{q}_e''), the energy necessary to heat the gases that subsequently will be lost due to convection

$$\dot{q}_{L,C}'' = \frac{\dot{Q}_C}{A} = (\dot{m}_{F,B}'' + \dot{m}_{O,B}'') C_{pg} (T_F - T_\infty) \quad (3.48)$$

and the energy lost due to radiation which can be given by the radiative fraction χ

$$\dot{q}_{L,r}'' = \frac{\dot{Q}_R}{A} = \chi \Delta H_{C,F} \dot{m}_{F,B}'' \quad (3.49)$$

Therefore, an energy balance in the gas phase is given by

$$\dot{q}_g'' = \Delta H_{C,F} \dot{m}_{F,B}'' = \chi \Delta H_{C,F} \dot{m}_{F,B}'' + (\dot{m}_{F,B}'' + \dot{m}_{O,B}'') C_{pg} (T_F - T_\infty) + \dot{q}_e'' \quad (3.50)$$

As diffusion flames are expected to burn at stoichiometric conditions then

$$\frac{\dot{m}''_{O,B}}{\dot{m}''_{F,B}} = \Theta$$

where Θ is the stoichiometric coefficient. By substituting the abovementioned expression in Equation 3.50 and rearranging an expression for the energy feedback per unit area, we can obtain

$$\dot{q}''_e = (1 - \chi)\Delta H_{C,F} \dot{m}''_{F,B} + \dot{m}''_{F,B}(1 + \phi)C_{pg}(T_F - T_\infty) \quad (3.51)$$

And substitution into Equation 3.50 leads to a phenomenological definition of the mass transfer number:

$$B = \frac{\dot{m}''_{F,G}}{\dot{m}''_{F,B}} = \frac{(1 - \chi)\Delta H_{C,F} + (1 + \phi)C_{pg}(T_F - T_\infty)}{\Delta H_G + Q_L} \quad (3.52)$$

As can be noted, the mass transfer number represents the mass of fuel generated per unit mass of fuel burnt, and is the additional physical parameter that controls the burning rate.

Although there are many definitions of the mass transfer number, they are mostly generated for specific conditions such as droplet burning or boundary layer burning. All retain the same physical concept, which is the capability of the flame to self-sustain by generating more fuel. If $B > 1$, then the flame will produce more fuel than that necessary to sustain burning.

As observed from Equation 3.52, the B number has several unknown or difficult to determine parameters, the first of them being the losses (Q_L). As the losses depend on the particular conditions and could evolve in time [7], there is a tendency to neglect them when tabulating values for the B number. This is appropriate as a reference value, but loses quantitative meaning when it is used to calculate the mass burning rate. A set of idealized values commonly reported in the literature is presented in Table 3.2. In most cases, the B number will be presented for liquid fuels; it is not so common to have these values derived for solid materials. This is because, the B number is considered to be representative of the steady mass burning rate where, in the case of liquids, Q_L will tend to be zero. In the case of solids, there is recognition that the role of Q_L will be more important and remain relevant throughout the entire sample burning.

3.7 MATERIAL PARAMETERS CONTROLLING EXTINCTION

Suppression is probably one of the most complex processes associated with fire. Extinction of fires implies the understanding of heat and mass transfer in the solid and gas phase, as well as the concept of chemical inhibition of the combustion reactions. Only a brief summary of the different material parameters controlling extinction will be presented here.

Extinction can be ultimately defined as the reduction of the combustion reaction rates below a critical threshold that

TABLE 3.2
Examples of the “ B Number”
for Different Liquids

Fuel	B Number
<i>n</i> -Pentane	8.1
<i>n</i> -Hexane	6.7
<i>n</i> -Heptane	5.8
<i>n</i> -Octane	5.2
<i>n</i> -Decane	4.3
Benzene	6.1
Toluene	6.1
Xylene	5.8
Methanol	2.7
Ethanol	3.3
Acetone	5.1
Kerosene	3.9
Diesel oil	3.9

Source: Drysdale, D., *An Introduction to Fire Dynamics*, 2nd edn., John Wiley & Sons, Chichester, U.K., 1998.

do not permit a self-sustained reaction. This is ultimately achieved in the gas phase and is the result of a negative energy balance at the flame that will lead to the local reduction of the flame temperature. A detailed analysis of the energy equation leads to the definition of two-dimensional groups:

$$\text{First Damköhler number: } Da_1 = \frac{\tau_{\text{Residence}}}{\tau_{\text{Conduction}}} \quad (3.53)$$

$$\text{Second Damköhler number: } Da_{II} = \frac{\tau_{\text{Residence}}}{\tau_{\text{Chemical}}} \quad (3.54)$$

The first Damköhler number quantifies the ratio between the heat transferred from the flame (conduction time) and the energy required to heat the reactants to the ignition temperature (residence time). Extinction will occur when heat cannot be transferred fast enough. Equation 3.53 is written in terms of the ratio between conduction and convection (residence time), but in a more general form, could include all forms of heat transfer like gas-phase radiation. The second Damköhler number indicates if the reaction has sufficient time to proceed. In general, extinction is attained when either of the Damköhler groups is reduced below unity.

Other criteria can be used to establish the extinction condition and that are partially equivalent to the critical Damköhler number. Such criteria are a critical mass transfer numbers (B_{cr}) [21,32], critical mass flux of fuel [2,6,28] or critical temperatures (T_{cr}) [2,5,29–31]. The critical mass transfer number has a direct influence over the flame temperature, and thus, represents the link between the condensed phase (i.e., production of fuel) and the chemical time. The critical mass flux operates under the same principle, but assumes a consistent heat input. Combustion reactions generally have high activation energy, therefore, the reaction can be assumed to abruptly cease when the temperature reaches a critical value (T_{cr}).

A different way to look at extinction is by reducing the oxygen concentration and thus, increasing the characteristic chemical time. This will result in a decrease of the second Damköhler number. This mechanism of extinction is analyzed in a standardized manner by the limiting oxygen index (LOI) [32].

NOMENCLATURE

A	Area
A_i	Pre-exponential factor
a	Radiative absorptivity
C	Specific heat
Da	Damköhler number
E_i	Activation energy
\vec{g}	Gravity acceleration
h	Heat-transfer coefficient
ΔH	Heat of reaction
k	Thermal conductivity
\dot{m}''	Mass flow
P	Pressure
\dot{q}''	Heat flux
\dot{Q}	Heat release rate
R	Universal gas constant
S	Spread
T	Temperature
t	Time
\vec{u}	Velocity vector

U	Gas velocity
V	Volume
x	Spatial location
Y	Species concentration

GREEKS

α	Thermal diffusivity
ε	Emissivity
σ	Stephan–Boltzmann constant
ρ	Density
ϕ	Porosity
$\dot{\omega}''$	Reaction rate
μ	Viscosity
θ	Nondimensional temperature
Θ	Stoichiometric coefficient
χ	Flame radiative fraction

REFERENCES

1. Williams, F.A., *Combustion Theory*, second edition, The Benjamin/Cummings Publishing Company, Inc., San Francisco, CA, 1985.
2. Drysdale, D., *An Introduction to Fire Dynamics*, second edition, John Wiley & Sons, Chichester, U.K., 1998.
3. Cox G. (Ed.), *Combustion Fundamentals of Fire*, Academic Press, London, 1995.
4. Babrauskas, V. and Grayson, S.J. (Eds.), *Heat Release in Fires*, Elsevier Applied Science, London, 1992.
5. Quintiere, J.G. and Rangwala, A.S., A theory for flame extinction based on flame temperature, *Fire and Materials*, 28 (5), 387–402, September/October, 2004.
6. Beyler, C., A unified model of fire suppression, *Journal of Fire Protection Engineering*, 4 (1), 5–16, 1992.
7. Torero, J.L., Vietoris, T., Legros, G., and Joulain, P., Estimation of a total mass transfer number from stand-off distance of a spreading flame, *Combustion Science and Technology*, 174 (11–12), 187–203, 2002.
8. Bows. P.C., *Self-Heating: Evaluating and Controlling the Hazards*, Elsevier, Amsterdam, 1984.
9. Kanury, A.M., *Introduction to Combustion Phenomena*, *Combustion Science and Technology*, Volume 2, Gordon and Breach Publishers, New Jersey, 1984.
10. Quintere, J.G., A simplified theory for generalizing results from a radiant panel flame spread apparatus, *Journal of Fire and Materials*, 5, 85, 1974.
11. Long, R.T., Torero, J.L., Quintiere, J.G., and Fernandez-Pello, A.C., Scale and transport considerations on piloted ignition of PMMA, *Fire Safety Science*, 6, 567–578, 1999.
12. Carslaw, H.S. and Jaeger, J.C., *Conduction of Heat in Solids*, second edition, Oxford University Press, Oxford, 1963, pp. 70–76.
13. Quintiere, J.G., *Principles of Fire Behavior*, Delmar Publishers, New York, 1998.
14. Williams, F.A., Mechanisms of fire spread, *Proceedings of the Combustion Institute*, 16, 1281, 1976.
15. Fernandez-Pello, A.C. and Hirano, T., Controlling mechanisms of flame spread, *Combustion Science and Technology*, 32, 1, 1983.
16. De Ris, J.N., Spread of a laminar diffusion flame, *Proceedings of the Combustion Institute*, 12, 241, 1969.
17. Fernandez-Pello, A.C., Ray, S.R., and Glassman, I., flame spread in opposed forced flow: The effect of ambient oxygen concentration, *Proceedings of the Combustion Institute*, 8, 579, 1980.
18. Altenkirch, R.A., Eichorn, R., and Rizvi, A.R., Buoyancy effects on flame spreading down thermally thin fuels, *Combustion and Flame*, 37, 71, 1980.
19. Perrins, L.E. and Pettet, K., Measurements of flame spread velocities, *Journal of Fire and Materials*, 5, 85, 1974.

20. Tarifa, C.S., Perez del Notario, P., and Munoz Torralbo, A., *Proceedings of the Combustion Institute* 12, 229–240, 1969.
21. Fernandez-Pello, A.C., *Combustion Fundamentals on Fire: The Solid Phase*, Academic Press, London, 1995, pp. 31–100.
22. Pagni, P.J. and Shih, T.M., Excess pyrolyzate, *Proceedings of the Combustion Institute*, 16, 1329, 1978.
23. Ohlemiller, T.J., Modeling of smoldering combustion propagation, *Progress in Energy and Combustion Science*, 11, 277–310, 1986.
24. Anderson, M., Sleight, R., and Torero, J.L., Downward smolder of polyurethane foam: Ignition signatures, *Fire Safety Journal*, 35, 131–148, 2000.
25. Bilbao, R., Mastral, J.F., Ceamanos, J., and Aldea, M.E., Kinetics of the thermal decomposition of polyurethane foams in nitrogen and air atmospheres, *Journal of Analytical and Applied Pyrolysis*, 37 (1), 69–82, 1996.
26. Rein, G., Lautenberger, C., Fernandez-Pello, A.C., Torero, J.L., and Urban, D.L., Smoldering combustion of polyurethane foam: Using genetic algorithms to derive its kinetics, *Combustion and Flame*, 146 (1–2), 95–108, 2006.
27. Torero, J.L., Kitano, M., and Fernandez-Pello, A.C., Opposed flow smoldering of polyurethane foam, *Combustion Science and Technology*, 91 (1–3), 95–117, 1993.
28. Rasbash, D.J., Drysdale, D.D., and Deepak, D., Critical heat and mass transfer at pilot ignition and extinction of a material, *Fire Safety Journal*, 10, 1–10, 1986.
29. Williams, F.A., A review of flame extinction, *Fire Safety Journal*, 3, 163–175, 1981.
30. Quintiere, J.G., *Fundamentals of Fire Phenomena*, John Wiley & Sons, Chichester, U.K., 2006.
31. Thomson, H.E., Drysdale, D.D., and Beyler, C.L., An experimental evaluation of critical surface temperature as a criterion for piloted ignition of solid fuels, *Fire Safety Journal*, 13, 185–196, 1988.
32. ASTM-D2863-06a Standard Test Method for Measuring the Minimum Oxygen Concentration to Support Candle-Like Combustion of Plastics (Oxygen Index), American Society for Testing and Materials, Philadelphia, 2003.

4 Halogen-Containing Flame Retardants

Sergio Bocchini and Giovanni Camino

CONTENTS

4.1	Introduction.....	75
4.2	Mechanism of Gas-Phase Action of Halogen Compounds.....	77
4.3	Gas-Phase Mechanism: Synergistic Effect Based on Halogen–Antimony Compounds	79
4.4	Mechanism of Action of Halogenated Compounds in the Condensed Phase.....	82
4.5	Mechanism of Condensed Phase Action of Synergistic Systems Based on Halogen–Metal Compounds	86
4.6	Main Application of Halogenated Flame Retardants by Families of Polymers	87
4.6.1	Styrenic Homopolymer and Copolymers.....	88
4.6.2	Aromatic Polyesters	88
4.6.3	Polycarbonate.....	89
4.6.4	Polyamides	89
4.6.5	Polyolefins.....	89
4.6.6	Poly(vinyl chloride).....	90
4.6.7	Thermosetting Resins	90
4.6.8	Polyurethanes.....	90
4.6.9	Textiles	91
4.7	Environmental Concerns.....	91
4.8	Conclusions and Future Trends	95
	Appendix A.....	96
	References.....	102

4.1 INTRODUCTION

Organic polymer materials may originate or propagate fire because they decompose under the action of heat-evolving combustible products. The complex overall burning process can be schematically represented, as shown in Figure 4.1. Combustion begins when the heat from the ignition source leads to volatile combustion products whose concentration is within the flammability limits and at a temperature above the ignition temperature. The combustion, which is a radical chain thermal oxidation process producing heat and light, proceeds then as long as the heat supplied to the polymer is sufficient to sustain its thermal degradation at a rate exceeding that required to feed the flame. Otherwise, the flame extinguishes. When the heat supply from the ignition source is discontinued or is negligible, a self-sustaining process occurs, if the above heat requirements are satisfied by thermal oxidation taking place either in the gas phase (flame), in the condensed phase, or in both phases. Although the scheme in Figure 4.1 is of general applicability, some steps, such as charring or thermal oxidation in the condensed phase, might not take place depending on the type of polymer and the burning conditions.

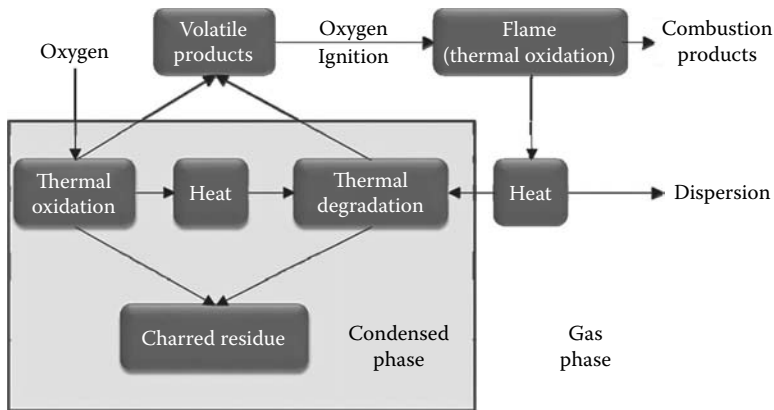


FIGURE 4.1 Self-sustained polymer combustion cycle.

The purpose of fire-retardant systems is to reduce the heat supplied to the polymer below the critical level for flame stability. This can be achieved by modifying (generally decreasing) the rate of chemical or physical processes taking place in one or more of the steps of the burning process.

The most effective, generally applicable commercial fire-retardant systems presently available are based on halogen-containing compounds. Their mechanism of action is related to the scission of the carbon–halogen bond. The order of stability for this bond in halogen compounds, derived from Table 4.1, is $F > Cl > Br > I$. The thermal stability of iodine compounds is below that required to stand polymer processing, whereas fluorine compounds are too stable to be generally useful. Some fluorine compounds have however been used as a component in a synergistic mixture.¹

Typically a brominated or chlorinated organic compound is added to the polymer or, in suitable cases, halogenated structures are introduced into the polymer chain by copolymerization to prepare fire-retardant polymer materials. Metal compounds, such as antimony trioxide, which do

TABLE 4.1
Bond Energies for Carbon–Halogen Bonds

Bond	Bond Energy (kJ/mol)	Temperature at Which Degradation Begins (°C)
C _{aliph} –F	443–450	>500
C _{arom} –Cl	419	>500
C _{aliph} –Cl	339–352	370–380
C _{benzilic} –Br	214	150
C _{aliph} –Br	285–293	290
C _{arom} –Br	335	360
C _{aliph} –I	222–235	180
C _{aliph} –C _{aliph}	330–370	400
C _{aliph} –H	390–436	>500
C _{aliph} –H	469	>500

Source: Van Krevelen, D.W., *Properties of Polymers: Their Correlation with Chemical Structure; Their Numerical Estimation and Prediction from Additive Group Contributions*, Elsevier, New York, 1997; Mita, I., *Aspects of Degradation and Stabilisation of Polymers*, Jellinek, H.H.G., Ed., Elsevier, New York, 1978, 247–294.

not, by themselves, impart significant fire-retardant properties to polymers can strongly enhance the fire-retardant effectiveness of halogenated compounds (synergistic effect). On heating, these fire retardants evolve volatile metal halides which are well-known flame inhibitors of much greater effectiveness as compared to hydrogen halides evolved in the absence of the metal compound. The detailed mechanism of the reactions which produce the volatile flame inhibitors are, however, not fully understood although these systems have been used for several decades.

These systems are of great importance in spite of the current cautious attitude, which will be discussed below, toward the use of halogen-based systems. Recent mechanistic results show that the active species formed by halogen compounds in the condensed phase may play a fundamental role in the fire-retardant mechanism, which could be reproduced using halogen-free moieties.

Some basic concepts of the mechanism of action of halogen-containing fire-retardant systems are reported below including reactions of halogen products in the vapor and in the condensed phase, thermal decomposition of halogen-containing compounds, and the interaction of polymers with halogen-containing fire retardants and with metal compounds.

4.2 MECHANISM OF GAS-PHASE ACTION OF HALOGEN COMPOUNDS

The purpose of this section is to consider the molecular-level mechanistic aspects of the gas-phase fire-retardancy action of halogen-based compounds. Often fire-extinguishing agents are evaluated from their addition to flames to achieve flame suppression. The action is attributed to the ability of the added substance to trap radicals propagating thermal oxidation in the flame. From literature data, which compare halogenated compounds as fire-extinguishing agents for *n*-heptane–air flame, expressed as minimum volume percentage (vol.%) to snuff out a flame,² the molar ranking of halogens in terms of fire-extinguishing effectiveness in halogenated molecules is



It has been shown that oxygen is consumed in hydrocarbon flames in the branching reaction³



and the highly exothermic oxidation of CO to CO₂ is carried out by hydroxyl radicals:



The mechanism of action of an effective fire retardant acting in the vapor phase should inhibit one or both reactions (Equation 4.2 and Equation 4.3) because they have a paramount effect on the increase of the overall rate of thermal oxidation process occurring in the flame. Indeed, the reaction represented by Equation 4.2 increases radical concentration while reaction represented by Equation 4.3 increases the temperature. From a mass spectrometry study of species sampled in low-pressure flame,⁴ it is evident that the introduction of halogen species into a premixed CH₄/O₂ flame leads to the production of the hydrogen halide, HX, early in the flame. It was also observed that the production of H₂ is enhanced. This provides evidence for removal of H atoms from the flame and the predominant reaction is considered to be



This is a fast reaction under flame conditions and it effectively competes with the chain-branching reaction (Equation 4.2) in the preflame region.⁵ Moreover, the observed degree of inhibition is greater than that which would be predicted considering the above reaction to reach equilibrium.

The mechanism by which halogen radical is removed from the system has been established, it is represented by⁶



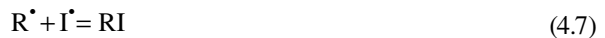
in which RH represents the combustible gas or volatile moieties from polymer thermal degradation. Reaction (Equation 4.5) accounts for the high efficiency of flame inhibition by halogen species because it regenerates the flame inhibitor HX which is not consumed and acts thus in a catalytic mode.

Note that this inhibition mechanism readily accounts for the noninhibiting properties of fluorides, since the high stability of HF provides an excessively high activation energy barrier for a reaction with H atoms to take place. The much lower effectiveness of chloride as compared with bromide inhibitors is probably due to the HCl reaction being very close to thermo-neutral, hence it is likely that the reaction can also proceed in the back direction to generate H atoms.

The scavenging effect of halogen radicals were also used to justify iodine action:



But in this case, the weakness of the HI bond means that HI is not readily formed by attack of RH groups, instead the presence of R^{\bullet} radicals can lead to combination with iodine atom through the reaction (Equation 4.7):⁷



which explains the low effectiveness of iodine compounds as flame inhibitors.

Trapping of OH^{\bullet} radicals is also performed by HX:⁸⁻¹¹



In time-resolved studies on the low-pressure explosive combustion of styrene–oxygen mixtures, Petrella¹² observed that the production of OH was delayed in the presence of HBr. The general understanding with regard to the action of halogens on OH in flames remains somewhat unsettled. Some of the apparent difficulties may be related to the use of different flames for inhibition studies. In particular, Wilson et al.⁴ have obtained indirect evidence for an increase in the maximum OH level in low-pressure lean CH_4 – O_2 flames containing HBr. However, using 1 atm lean propane fueled flames, indirect evidence was provided¹³ for a reduction in the maximum OH concentration in the presence of HBr. Nevertheless in the higher temperature reaction zone region of the flame, reactions involving H, OH, and O are known to be balanced and a pseudo-equilibrium exists between these species. Hence under these conditions, arguments as to whether OH, O, or H are the inhibited species are not particularly critical, as a reduction of any of these radicals would serve to inhibit chain branching.

An interesting alternative theory has been proposed which attempts to explain the action of halogens in purely physical terms.¹⁴⁻¹⁶ The proponents of the physical theory of the flame-retardant activity of halogenated additives compare the halogen activity to that of inert gases, CO_2 , and water.¹⁷ Reexamination of flammability limits for halocarbons shows that over 70 wt% halogen is needed in a compound to prevent flame propagation and that indeed only the total amount of halogen and not its nature is important. The peak flammability limit “ k ” of halocarbon–fuel mixtures, defined as minimum quantity of halogen to snuff out the flame, is a constant given by the relation

$$k = \frac{\text{wt.halogen}}{\text{wt.halocarbon} + \text{wt.fuel}} \times 100 = 69.8 \pm 3.5 \text{ wt\%} \quad (4.9)$$

where

wt.halogen is the weight of halogen present in the flame

wt.halocarbon is the weight of the halogenated compound

wt.fuel is the weight of the organic compound that feeds the flame

Furthermore, the relative effectiveness of the various halogens is directly proportional to the ratio of their atomic weights, namely

$$F:Cl:Br:I \quad 1:1.9:4.2:6.7 \quad (4.10)$$

The role of the halogens is therefore simply to increase the total mass of material which must be vaporized per unit time without an equivalent increase in heat flux from the flame fuel.¹⁸ However, these physical processes can be important only when the polymers are overwhelmingly converted to gaseous fuels.¹⁹

Thus there appears to be no contradiction between the radical trap theory and the physical theory with regard to halogen; halogens can strongly inhibit the ignition of polymers but will probably not be very efficient in preventing combustion when the external heat flux is large enough to vaporize most of the polymer.¹⁸ Both approaches complement each other; it is difficult to determine in a general way the relative contribution of each of the two modes of activity. This will usually depend on the structure and properties of the polymer and of the flame retardant as well as on the conditions and parameters of the flame and, finally, on the size of samples.

4.3 GAS-PHASE MECHANISM: SYNERGISTIC EFFECT BASED ON HALOGEN-ANTIMONY COMPOUNDS

The flame-retardant properties of halogen compounds are often considerably enhanced when they are used in conjunction with antimony oxides which used alone have no effect on fire retardancy. This is a typical case of synergism, that is a larger effect of combination of polymer additives than that expected from individual contribution. Among practicing fire-retardancy researchers, achieving synergism is one of the most desirable goals because it allows the utilization of flame-retardant additives at lower concentrations than predicted on the basis of separate additives performances. Antimony oxide-halogen combination represents one of the most important synergistic fire-retardant combinations. The ability of antimony to enhance the effectiveness of halogen-based flame retardants was first demonstrated for cellulosic fabrics treated with chlorinated paraffins and antimony trioxide;^{20,21} the synergism has also been shown in polyester resins,²²⁻²⁴ polystyrene resins,²⁵ and polyolefins.²⁶ The use of antimony compounds in conjunction with halogenated flame retardants is also documented for polyurethanes, polyacrylonitrile, and polyamides.^{20,27}

The first studies made on the effect of antimony oxides and various chlorinated compounds^{20,21} on the flammability of cotton demonstrated that the flame retardance imparted increased with the ease of elimination of hydrogen halide from the chlorinated additive. Therefore, the active species inhibiting combustion was thought to be antimony oxychloride liberated within the polymer during heating; most experiments were thus carried out at an atomic ratio of antimony chloride of 1:1. Attempts to determine the optimum ratio led to the discovery that higher chlorine levels improved the efficiency of additives up to atomic ratios of about 1:2.²⁰ The discrepancies were attributed to incomplete volatilization of hydrogen chloride. Coppick et al. found for chlorinated alkane an optimal atomic ratio of about 1:3.²¹

The literature contains numerous speculations as to the mechanism. Some involve a condensed phase mechanism, as, for example, in the case of cellulose in which it is suggested the formation *in situ* of antimony chloride which may react with cellulose to alter the course of thermal decomposition and/or form a "heavy vapor tending to extinguish the flame."²⁸ Some involve a physical gas-phase mechanism such as formation in the flame of nonvolatile, antimony-containing solid or

liquid particles whose surface provides a site for dissipation of energy with resulting modification of the flame chemistry (e.g., formation of HO_2 rather than HO). Also, gas-phase chemical mechanisms have been proposed based either on the oxygen-inhibiting effect of the heavy vapors of antimony chloride or oxychloride in addition to the physical inhibition of the oxidation chain reaction (wall effect) and chemical inhibition by chlorine²⁹ or based on formation of an antimony oxygen halogen intermediate compound which increases the presence of halogen radicals with resulting interference in the free radical mechanism of the flame propagation.²⁵

It is known that much of the antimony is vaporized during burning³⁰ or char formation.²⁸ The ignition behavior of polyester resins inhibited by antimony halogen systems has been considered to indicate the likelihood of gas-phase inhibition.^{23,24}

An indication of whether a fire-retardant additive acts in the gas phase by inhibiting the radical chain reactions which occur in the flame (flame poisoning) or in the condensed phase, can be obtained by carrying out oxygen index measurements using nitrous oxide instead of oxygen as the oxidizer. If a fire-retardant additive acts by flame poisoning, its effectiveness in the nitrous oxide atmosphere would be negligible compared to that in the oxygen atmosphere. This criterion for distinguishing between flame poisoning and condensed phase mechanism of fire retardancy is supported by the finding that in oxygen flames fed by hydrocarbons or hydrogen, oxygen is mainly consumed in the branching reaction (Equation 4.2) while nitrous oxide is mostly consumed in the nonbranching reaction:³¹



The greatest inhibition effect in the gaseous phase is due to partial indirect suppression of the branching step (Equation 4.2). Hence, N_2O flames would be less susceptible to poisoning because reaction (Equation 4.11) is a nonbranching reaction.

The observation³⁰ that Sb_2O_3 inhibits the burning of chlorinated polyethylene in air, but not in nitrous oxide, suggests inhibition of gas phase reactions specific to the fuel-oxidizer system. The same results are obtained with a ternary system polypropylene/chloroparaffin/antimony trioxide;³² comparison between the oxygen and nitrous oxide index (Figure 4.2) indicates that the Sb-Cl "synergism" depends on a flame poisoning effect, in fact there is no variation of nitrous oxide index as

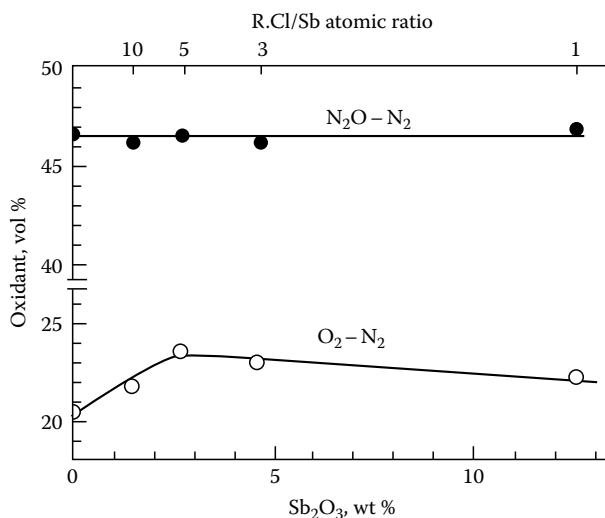


FIGURE 4.2 Oxygen and nitrous oxide index of polypropylene-chloroparaffin mixtures, 95-5 wt%, with added antimony trioxide. (From Costa, L. et al., *Polym. Degrad. Stabil.*, 14(2), 116, 1986. With permission.)

a function of antimony trioxide addition whereas in the same range of Cl/Sb ratio, the oxygen index increases to a maximum followed by a decrease in fire retardancy at ratios lower than 3.

On the other hand, some involvement of antimony in decomposition of the solid phase is indicated by the fact that char formation may be enhanced in antimony-containing systems.^{27,33}

The synergistic action clearly involves interaction of Sb_2O_3 with either the halogenated compound or a decomposition product of the halogenated material, presumably HX, in fact optimum conditions for retardancy depend on the ratio of antimony to chlorine and on the ease of decomposition of the halogenated species.²⁷

Studies on antimony oxides/fire-retardant compounds containing chlorine/bromine confirm formation of gaseous species containing antimony and halides. It is believed that first some hydrogen halide is released from the halogen compound due to interaction with antimony trioxide or with polymer. The HX reacts with Sb_2O_3 producing SbX_3 .^{9,34-37} Although it is clear that the final product of halogenated additives/antimony reaction is antimony trihalide, which is volatile at the temperature of the burning polymer, different mechanisms have been proposed for its formation. Literature data^{36,38,39} favor the formation of SbX_3 through intermediate oxyhalides as compared to direct complete halogenations,³⁷ for example, in the case of Sb_2O_3 reacting with chlorinated or brominated compounds (Figure 4.3).

It can be seen that chemical halogenation of Sb_2O_3 leads to progressively halogen-rich oxyhalides up to the trihalide while the oxyhalides undergo thermal disproportionation with evolution of the trihalide and formation of the halogen-poorer oxyhalide. Therefore, the mechanism of the process depends on the temperature and on the interplay between thermal stability and chemical reactivity of the oxyhalides. Evidence for catalysis of the dehalogenation of halogenated compounds by metal oxyhalides or halides acting as Lewis acids, has been reported in the literature.³⁵

In the case of chlorinated additives, independent of whether or not they release HCl on heating, $\text{Sb}_4\text{O}_5\text{Cl}_2$ was the dominant oxychloride found in conditions close to those of polymer burning, although $\text{Sb}_8\text{O}_{11}\text{Cl}_2$ was expected to be the most stable oxychloride under these conditions.^{40,41} This was explained assuming that $\text{Sb}_8\text{O}_{11}\text{Cl}_2$ is formed first but does not accumulate because it is a highly reactive dechlorinating agent and gives $\text{Sb}_4\text{O}_5\text{Cl}_2$. This last would give SbCl_3 at a relatively lower rate either through thermal disproportionation or direct complete chlorination. $\text{Sb}_4\text{O}_5\text{Cl}_2$ and $\text{Sb}_8\text{O}_{11}\text{Cl}_2$ might also undergo chlorination to SbOCl which then rapidly disproportionates. It is not possible to demonstrate whether SbOCl is an intermediate in the process because of its high thermal instability under these conditions.

In the case of brominated additives the process is less studied, for decabromodiphenyl oxide, a widely used brominated fire-retardant additive, $\text{Sb}_8\text{O}_{11}\text{Br}_2$ is the dominant oxybromide, whereas $\text{Sb}_4\text{O}_5\text{Br}_2$ was not detected in measurable amounts. It was assumed that, if this last is formed by bromination of $\text{Sb}_8\text{O}_{11}\text{Br}_2$, it eliminates SbBr_3 relatively rapidly either by thermal disproportionation or by chemical reaction with decabromodiphenyl oxide.⁴²

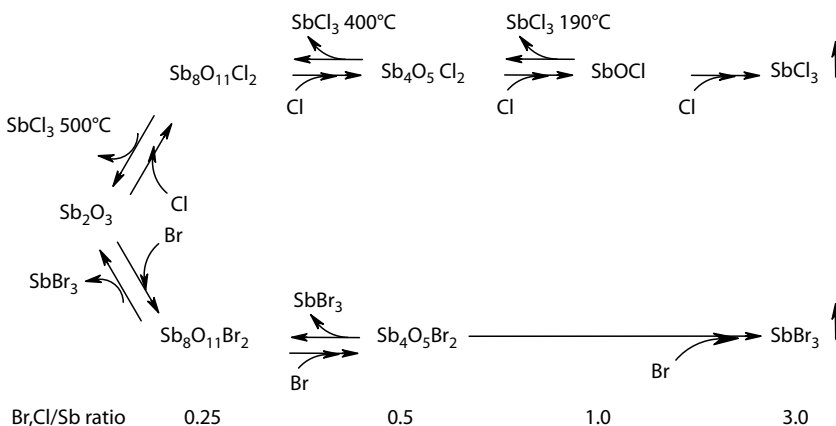


FIGURE 4.3 Reaction scheme occurring between antimony oxide and halogen compounds.

The role of antimony halides as flame-retardant species in the gaseous phase is well established: when SbX_3 ($X = \text{chlorine or bromine}$) is introduced into premixed methane–oxygen flames, atomic antimony and antimony monoxide are found in the flame.⁴³ Sb_2O_3 was shown by mass spectrometry to be present only in the preflame zone and no antimony–halogen species could be detected in the flame itself.

The proposed sequence of reactions taking place in the flame includes the following steps, where X^\bullet is a halogen atom:



Antimony halides are believed to have two functions in the flame. The first is to provide a ready source of hydrogen halide early on and the second is to produce a “mist” of fine particles of solid SbO in the middle of the flame region. The function of SbO as an inhibitor independent of the presence of halogen species is verified by the effect on fire retardancy of triphenylantimony in the absence of halogen compounds.⁴⁴ Triphenylantimony is an efficient flame retardant for epoxy resins, even in the absence of halogen.⁴⁴ This can be explained in terms of the low volatility but ready oxidizability of triphenylantimony so that it forms particles of antimony oxides in the gaseous phase. It is supposed by Hastie⁴³ that antimony monoxide is sufficiently stable in the flame to catalyze the recombination of H , O , and OH via the formation of transient species (Equation 4.15 through 4.19) such as SbOH analogous to what suggested to explain the catalytic effect of other oxides such as SnO .⁴⁵

The evidence for the action of halogen and halogen antimony compounds in the gaseous phase is well established; however halogen-containing flame-retardant systems are often twofold systems providing radical action inhibition in the gaseous phase and, at the same time inhibition in the condensed phase as will be seen in the next section.

4.4 MECHANISM OF ACTION OF HALOGENATED COMPOUNDS IN THE CONDENSED PHASE

Measurement of the oxygen and nitrous oxide index of chlorinated polyethylene^{26,30} suggests that, for this polymer, the flame-retardant influence of chlorine primarily takes place in the condensed phases. This suggestion is confirmed by the fact that the addition of quite large amounts of gaseous chlorine or hydrogen chloride to the nitrogen/oxygen atmosphere above burning polyethylene does not affect the oxygen index.

The studies of fire-retardant action of halogenated compounds in the condensed phase were performed mostly on mixtures of chloroparaffin with vinyl polymers such as polyethylene,

TABLE 4.2
Oxygen Indices of Polyethylene, Polypropylene, and Polystyrene and Their Mixtures with 30 wt% Chloroparaffin before and after Elimination of 50 wt% of Total Chlorine

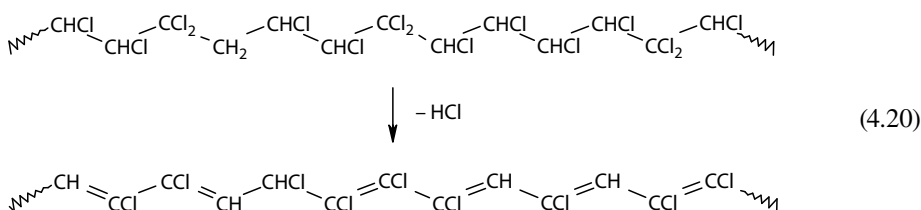
Sample	Oxygen Index	
	Original	Dehydrochlorinated
Polyethylene	18	—
Polyethylene/chloroparaffin	22	22
Polypropylene	18	—
Polypropylene /chloroparaffin	28	22
Polystyrene	18.5	—
Polystyrene /chloroparaffin	24	24

Source: Camino, G., *Developments in Polymer Degradation*, Vol. 7, Grassie, N., Ed., Elsevier Applied Sciences, London, U.K., 1987, Table 2, p. 230. With permission.

polypropylene, and polystyrene.³⁵ The comparison of the oxygen index measured on chloroparaffin-polymer mixtures before and after HCl elimination by preliminary heat treatment (Table 4.2) demonstrates that chemical flame inhibition by HCl evolved from chloroparaffin appears to contribute to the fire retardation of polypropylene (PP) but not of polyethylene (PE) and polystyrene (PS).

The oxygen index increase was suggested to be due to a condensed phase mechanism and explained by taking into account the mechanism of thermal degradation of chloroparaffin and the interaction with the polymers.

The thermal degradation of chloroparaffin occurs in two main steps. The first takes place below 400°C and consists of an endothermic HCl elimination, a chain elimination of HCl (Equation 4.20). For example, in the case of a 70% Cl containing chloroparaffin:⁴⁶



The second step, between 400°C and 800°C is exothermic. In this step, elimination of HCl takes place from the polyene at a lower rate since chlorine atoms linked to unsaturated carbon atoms are involved which gives a more thermally stable bond than chlorine-saturated carbon of the original chloroparaffin. Intermolecular addition, responsible for the exothermic effect, takes place between double bonds leading to cross-linked products⁴⁶ and possibly to aromatization.

The curves of isothermal weight loss at 260°C for chloroparaffin/polymer mixtures show that the polymers are thermally destabilized by the presence of chloroparaffin, the destabilization increases in the sequence polyethylene, polypropylene, and polystyrene; chain scission is induced in polypropylene and polystyrene whereas cross-linking is promoted in polyethylene, as shown in Table 4.3.³⁵ At the same time, the rate of elimination of HCl from chloroparaffin is decreased by the presence of the three polymers.

Finally, the chloroparaffin modifies the composition of volatile products. In the case of polyethylene, the main effect is to increase the ratio of saturated to unsaturated hydrocarbons.⁴⁷ A similar effect is observed for polypropylene in which an important reduction of the overall amount of the lighter

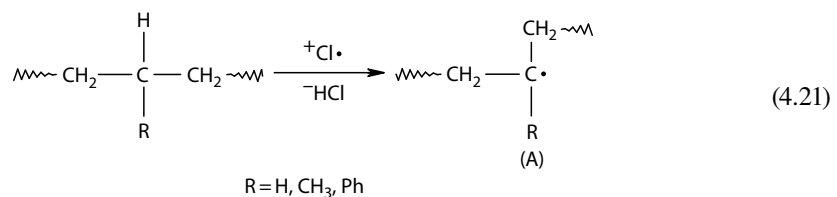
TABLE 4.3
Molecular Weight after Treatment under Nitrogen
Flow at 260°C

Polymer	Original	M_v	
		After Treatment	
		Control	Mixture with 30 wt % of Chloroparaffin
Polyethylene	138,000	112,000	Crosslinked
Polypropylene	285,000	99,000	12,000
Polystyrene	137,000	109,000	1,700

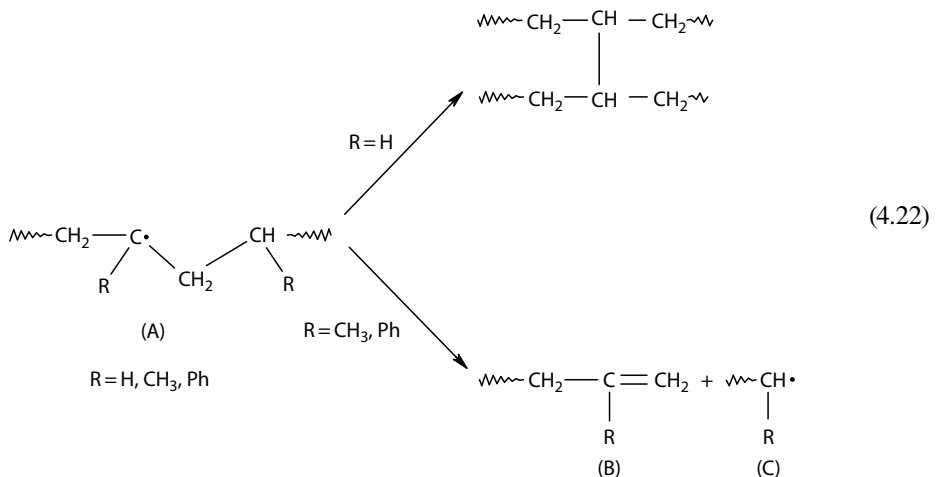
Source: Camino, G., *Developments in Polymer Degradation*, Vol. 7, Grassie, N., Ed., Elsevier Applied Sciences, London, U.K., 1987, Table 2, p. 243. With permission.

hydrocarbons ($C_n > C_9$), in favor of longer oligomeric or chain fragments ($C_n > C_9$) was also detected.³¹ In polystyrene, the presence of chloroparaffin induces a decrease in the yield of styrene and an increase in that of oligomeric products.^{48,49} Chloroparaffin also induces a noticeable increase in the yields of toluene, ethylbenzene, and several other fragments evolved in small amounts by pure polystyrene.

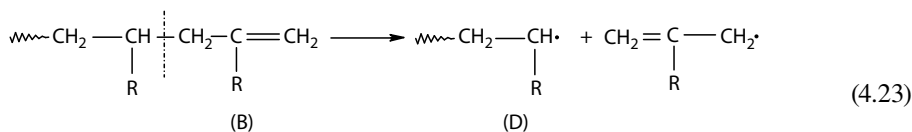
The thermal degradation behavior of the mixtures can be explained by the assumption that in chloroparaffin-polymer blends, chlorine radicals that propagate the dehydrochlorination in the chloroparaffin domains can migrate in the polymer phase where they abstract hydrogen atoms from the polymer backbone:



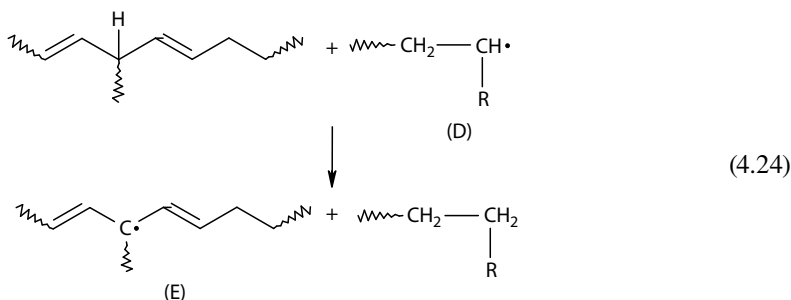
Further reactions of the resulting macroradicals (A) depend on the substituent R:



When the substituent R stabilizes radicals as in (A) and (C), chain scission is more likely than termination by coupling. Radicals (C) then propagate the depolymerization process with volatilization of polypropylene and polystyrene at a temperature at which these polymers would not give significant amounts of volatile products when heated alone. Moreover, unsaturated chain ends such as (B) would also initiate the volatilization process because of the thermal instability of carbon-carbon bonds in β position to a double bond (Equation 4.23).



The dehydrochlorination rate of chloroparaffin is lowered by elimination of chlorine radical chain carrier of chloroparaffin dehydrochlorination through the hydrogen abstraction process. The larger ratio of saturated to unsaturated hydrocarbons is explained on the basis of interaction between the degrading polymer and the cross-linked polyene formed by chloroparaffin. For example, reactive allylic hydrogen atoms can react with the volatile hydrocarbons diffusing through the degrading mixture or with the radical propagating the volatilization process (Equation 4.24) increasing the hydrogen-carbon ratio in the polymers and their degradation products.



The resulting radical (E) is stabilized by the polyene sequence and may terminate by coupling. After evolution of part of the hydrogen chlorine from the chloroparaffin, the terminating effect of reaction (Equation 4.24) can compensate for the initial destabilization; this indeed happens in the case of polystyrene with the reduction of the relative rate of volatilization in the mixture as the degradation proceeds.⁵¹ Moreover, because of reaction (Equation 4.24), the lifetime of radical (D) is reduced and so reactions such as depolymerization by β -scission will be reduced; thus further volatilization of the polymer will lead to a larger fraction of longer and saturated chain fragments instead of monomer produced by depolymerization.

The fire-retardant action of chloroparaffin through the condensed phase mechanism agrees with the expected somewhat lower flammability of the products evolved by thermal degradation of polyethylene, polypropylene, and polystyrene in combination with chloroparaffin as compared to those evolved from the polymer heated alone. The chain fragments produced in larger amount are less flammable than the hydrocarbons of low molecular weight whose yield is correspondingly reduced. For example, for the polystyrene degradation products, styrene and ethyl benzene have oxygen indices of 14.4 and 14.7, respectively, whereas that of diphenyl methane is 16.4.⁴⁸ Furthermore, polystyrene also benefits from the reduction of pyrolysis rate attributed to interaction with the polyene. Thus the polyene accumulating on the surface of the burning polystyrene could reduce the rate of products of degradation of polystyrene to the flame.

Concluding, the destabilization of the above polymers by chloroparaffin should be beneficial in terms of fire retardance because it induces the formation of fuel at the temperature at which HCl is evolved. Thus, the occurrence of a polymer additive interaction in the condensed phase

may simply optimize the gas phase retardant action of HCl. However, the composition of the volatile products of degradation of the polymers is modified, giving a mixture likely to be less flammable than that obtained from the pure polymers. Moreover, preventive elimination of the HCl released did not affect the oxygen index of polyethylene and polystyrene while it decreased the oxygen index of polypropylene.³⁵ It is possible to conclude that chemical inhibition of the flame by HCl evolved from chloroparaffin should contribute to the fire retardation in polypropylene, whereas in polyethylene and polystyrene the reduced flammability is the direct result of the chloroparaffin–polymer interaction in the condensed phase which overwhelms the contribution of flame poisoning by HCl.

4.5 MECHANISM OF CONDENSED PHASE ACTION OF SYNERGISTIC SYSTEMS BASED ON HALOGEN–METAL COMPOUNDS

The mechanism of fire-retardant action of synergistic halogen–metal fire retardant systems is not yet completely understood in spite of their wide use. In particular, besides the well-known flame inhibition activity of volatile metal halide resulting from halogen–metal compounds reaction in the degrading polymer, condensed phase reactions of halogen derivatives with the polymer have also been suggested to contribute to fire retardance.^{35,50} Interaction of chloroparaffin with antimony^{32,51,52} and bismuth^{32,51,53} were extensively studied, and the studies were extended to other metal salts⁵⁴ in order to understand the mechanism of chloroparaffin/metal systems condensed phase action in polypropylene.

The comparison between oxygen and nitrous oxide index (Figure 4.2) of a ternary system polypropylene/chloroparaffin/antimony trioxide indicates that the Sb–Cl “synergism” depends on a flame poisoning effect.³² For the ternary system polypropylene/chloroparaffin/bismuth carbonate (Figure 4.4), a maximum in both the oxygen and nitrous oxide indices is present at the same Cl/Sb ratio in both oxidant atmospheres, which indicates that the Bi–chlorine synergism must depend essentially on a condensed phase effect. The mixture at which maximum of oxygen index is observed is also that at which polypropylene pyrolyzes at the lowest rate.³² Furthermore, the oxygen index increase produced by direct addition of the potential flame poison BiCl_3 to polypropylene is

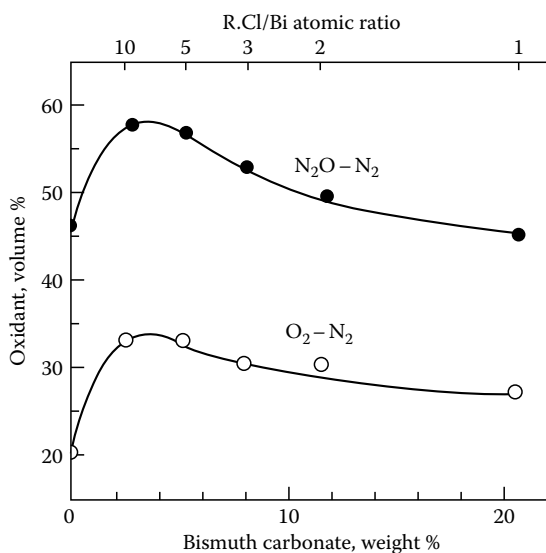
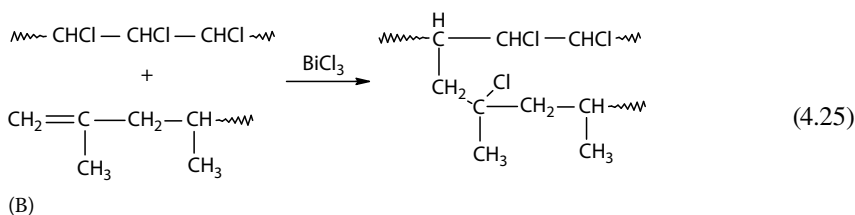


FIGURE 4.4 Oxygen and nitrous oxide index of polypropylene–chloroparaffin mixtures, 95–5 wt%, with added bismuth carbonate. (From Costa, L. et al., *Polym. Degrad. Stabil.*, 14(2), 117, 1986.)

1 order of magnitude smaller than that obtained for the ternary system.⁵¹ Addition of BiCl₃ or BiOCl to polypropylene/chloroparaffin mixtures gives similar results as for the addition of bismuth carbonate.⁵¹

Thus the flame poisoning activity of BiCl₃ evolved is overwhelmed by condensed phase effects. This is in agreement with the fact that the flame poisoning activity of BiCl₃ is only slightly better than that of HCl⁵⁵ and would not account for the large “synergistic” effect observed upon addition of bismuth carbonate. Further evidence of the condensed phase mechanism is shown by the higher effectiveness of bismuth carbonate compared to antimony oxide in the polypropylene/chloroparaffin ternary mixture,³⁵ which is in contrast with the higher efficiency of SbCl₃ respect to BiCl₃ in flame inhibition.⁵⁵

The condensed phase mechanism was explained taking into account the decrease of the pyrolysis rate of polypropylene; BiCl₃ could catalyze the condensation between chloroparaffin and polypropylene by addition to chain end double bonds (Equation 4.25) formed either in reaction (Equation 4.22) or in chain scission occurring during volatilization of polypropylene:³¹



The above reaction (Equation 4.25) would reduce the rate of volatilization of polypropylene by reducing the concentration of unsaturated chain ends which act as initiating structures.⁵⁶ As an alternative or in addition, a stabilization mechanism based on the reported formation of metallic bismuth can be proposed.^{53,57} Stabilization of polypropylene by metal compounds is in agreement with activity of several metal compounds as radical catalyst/inhibitor depending on metal concentration and/or temperature of the system.⁵⁸

Reduction of bismuth compounds could take place by reaction with polymer radicals propagating the depolymerization of polypropylene, either by electron transfer or ligand transfer which are typical redox reactions between alkyl radicals and metal compounds:⁵⁹



Successive repetition of reactions (Equation 4.26 or Equation 4.27) lead to formation of Bi⁰. These redox reactions act as termination steps for polymer degradation. Radical terminations by metal compounds through redox reaction are well known.^{35,58}

Further catalytic terminating activity may be displayed by the finely divided metallic bismuth within polypropylene by the so-called wall-effect in which radicals recombine at the active surface of the metal.

The results obtained with bismuth carbonate were extended to other metals which increase the oxygen index of PP, with a study of their interaction with polypropylene/chloroparaffin mixtures, which is reported in the work of Costa et al.⁵⁴

4.6 MAIN APPLICATION OF HALOGENATED FLAME RETARDANTS BY FAMILIES OF POLYMERS

The names, structures, and physical properties of the most important halogen-containing fire-retardant chemicals are reported in Appendix A. This comprehensive list includes the chemical name, the

common trade names, the chemical structure, the halogen content (percentage by weight), the melting or softening temperature range, and the polymer families with which they are used.

4.6.1 STYRENIC HOMOPOLYMER AND COPOLYMERS

Halogen fire retardants are used in two members of this family: polystyrene homopolymer foams and styrenic copolymers, including high-impact polystyrene (HIPS) and acrylonitrile–butadiene–styrene (ABS). Foams used in the building industry for thermal insulation and for decorative profiles (extrusion-foamed polystyrene XPS) and polystyrene foam (expanded polystyrene) used in the packaging of electronic goods generally need to be fire retarded. Hexabromocyclododecane is the most commonly used halogen-containing flame retardant for these applications; the mechanism of fire-retardant action is due to a combination of chain scission that causes molecular weight reduction and helps cool the flame by enhanced dripping and flame poisoning.⁶⁰ As alternatives, tribromophenyl allyl ether and the bisallylether of tetrabromobisphenol A introduced by copolymerization are also used. The main properties of these compounds are summarized in Appendix A. Antimony trioxide is not used as a synergist in fire-retarded polystyrene foam. The loading of the fire retardant is typically between 0.8 and 4 wt %. The higher loadings are necessary to counteract the replacement of low-flammability chlorofluorocarbon foaming agents with the much more flammable olefins (e.g., cyclopentane/*n*-pentane).

The traditional halogen fire retardants used in styrenic copolymers are decabromodiphenyl ether and octabromodiphenyl ether, tetrabromobisphenol A, bis(tribromophenoxy) ethane, ethylene bis-tetrabromophthalimide, and chlorinated paraffins. Actually the octabromodiphenyl ether has been banned on precautionary principles, as will be explained below. The fire-retardant capabilities of the more effective halogen-containing compounds are in line with the quantity of halogen in the final polymer blend, with consideration for the use of synergists. Thus, the practical utility of these flame-retardant compounds (once the issue of degradation temperature is resolved) is often based on their ability to be blended into the polymer and to not substantially affect the physical properties of the polymers.

New fire retardants not related to the chemistry of diphenyl ethers have been developed for more environmentally friendly applications.^{61,62} Among these newer compounds available for use in styrenic copolymers are a proprietary compound, brominated trimethylphenyl indan, brominated epoxy oligomers, and tris(tribromophenyl) cyanurate.

4.6.2 AROMATIC POLYESTERS

Polymeric fire retardants, such as poly(pentabromobenzyl acrylate) or the phenoxy-terminated carbonate oligomer of tetrabromobisphenol A, may be used in PBT at bromine contents as low as 5%–6% to produce short total after-flame times. Commercial products generally contain between 7% and 10% bromine in order to provide a safety factor and to maintain the UL 94 rating after several recycling steps. Glass-reinforced flame-retarded PBT also contains brominated fire-retardant additives. Increasing the loading of poly(pentabromobenzyl acrylate) in a glass-reinforced PBT has been shown to increase the oxygen index, but also to improve certain mechanical and impact properties for the resin, compared to the lower loading of FR. This is attributed to the efficient coupling effect of the FR additive between glass fibers and the polymeric matrix.⁶³

High-molecular-weight brominated epoxy polymers are used in both non-reinforced and glass-reinforced PBT. They are used in conjunction with a UV stabilizer and a UV screener in order to provide light stability. Poly(ethylene terephthalate) is usually made fire retardant by the addition of brominated polystyrene, which has the necessary thermal stability to withstand processing temperatures that may exceed 300°C. Some compounders are using sodium antimonate as a synergist because it is believed that antimony trioxide contributes to the thermal decomposition of PET during processing.

4.6.3 POLYCARBONATE

The most widely used halogen flame retardant for polycarbonate is tetrabromobisphenol A that is copolymerized into the polycarbonate resin in the 3–5 wt% concentration range.

Phenoxy-terminated carbonated oligomers of tetrabromobisphenol A and brominated epoxy oligomers were also developed which could be added to the polymerized PC in a compounding step. An occasionally overlooked problem with the use of halogen fire retardants for polycarbonate is that the use of antimony oxide, a common synergist with halogen FR systems, is not an option as it will degrade the PC molecular weight.⁶⁴

4.6.4 POLYAMIDES

Decabromodiphenyl ether continues to be a popular fire-retardant additive for polyamide 6, its cost, high bromine content, and good thermal stability make it an attractive product. In Europe and the United States, most of its applications have been replaced by brominated polystyrene in order to address environmental issues. Brominated polystyrene is less expensive than the other polymeric fire retardants and has very good thermal stability. Moreover, it contributes to good electrical tracking index. On the other hand, it has lower efficacy as a fire retardant.

Poly(pentabromobenzyl acrylate), another polymeric fire retardant, is particularly suitable for use with polyamides whether or not they contain fiber reinforcement. Its advantages over other fire-retardant additives result from a combination of its polymeric nature, high bromine content, and thermal stability.

High-molecular-weight brominated epoxy polymers are efficient fire retardants for nylons, which offer the following advantages: high thermal stability and thermal aging, excellent processability, nonblooming, high UV stability, and low corrosivity. It is important to mention that only brominated epoxies with negligible epoxy content are suitable for nylon applications, in order to avoid adverse reactions between epoxies moieties and amine groups in nylon.

The Diels–Alder adduct of hexachlorocyclopentadiene and 1,5-cyclooctadiene is the only chlorinated fire retardant that can be used in nylons. Several published reports^{61,65,66} have referred to the possibility of replacing antimony trioxide, totally or partially, by another synergist such as iron oxide, zinc borate, or zinc oxide. Unlike brominated polystyrene, the chemical structure of dodecachloropentacyclooctadeca-7,15-diene fits the ignition temperature of nylons. This results in a high limiting oxygen index (LOI) value of 38, achieved in glass-reinforced nylon 6.

Brominated indan in nylon 6,6 results in a high oxygen index value. A further increase can be achieved by combination with surface-treated magnesium hydroxide.⁶³

4.6.5 POLYOLEFINS

Polypropylene has few fire-retarded applications, because of the difficulty to reach the high performances required for applications. The high fire-retardant loading required tend to increase brittleness and decrease mechanical properties.⁶¹

As already seen in Section 4.3, the primary action of halogen fire-retardant action for polypropylene is in the gaseous phase, thus the fire-retardant additives for polypropylene are often based on aliphatic bromine compounds in order to develop bromine at its low ignition temperature.

To improve the fire retardancy of polypropylene, beyond the UL 94 V-2 level, it is necessary to use blends of aromatic bromine fire retardants with antimony trioxide as a synergist. The usual loading is between 35% and 40% fire retardant; however, the additional cost may prohibit commercialization. Moreover, the presence of aromatic bromine increases the photooxidation of polypropylene^{67–69} inactivating hindered amines. To reduce the cost without losing in efficacy the combination of brominated flame-retardant/antimony trioxide system with magnesium hydroxide

has been proposed⁷⁰ to provide a balance of properties at optimal cost. A typical loading might be 15% brominated flame retardant, 5 wt% antimony oxide, and 20 wt% magnesium hydroxide. When magnesium hydroxide is used alone, a concentration of at least 60 wt% is necessary, affecting the impact and elongation properties of the polymer system.

Tris(tribromoneopentyl) phosphate combines bromine and phosphorus in the same molecule; it has been successfully incorporated into polypropylene. Studies have dealt with the question of synergism between bromine and phosphorus present in the same molecule.^{71,72} Fire-retardant efficiency without the need for antimony oxide opens the door for this product in the field of PP fibers and textiles.

Decabromodiphenyl ether is also used for polyethylene wire and cable applications included at a level of 20–24 wt%. Chlorinated paraffin with a loading of about 25 wt% is also used.

4.6.6 POLY(VINYL CHLORIDE)

Liquid chlorinated paraffins are the main halogen-containing fire-retardant additives used for poly(vinyl chloride) often in combination with a phosphate ester. In this case, the chlorinated paraffins have the secondary function of plasticizers. The thermal degradation mechanism of chlorinated paraffins is similar to that of poly(vinyl chloride), so in this case poly(vinyl chloride) stabilizers have also the secondary function to stabilize chlorinated paraffins.

For more demanding applications, tetrabromophthalate ester is a thermally stable liquid fire-retardant additive with a bromine content of approximately 45 wt%. Decabromodiphenyl ether is used for foamed soft PVC for thermal insulation even if diphenyl ether-free systems have been developed because of environmental concerns.

4.6.7 THERMOSETTING RESINS

In the case of thermosetting resins the fire retardant is usually copolymerized with the resin.

Tetrabromobisphenol A is used in epoxy resins especially for glass fiber reinforced used in printed circuit board. Nonreactive compounds such as tetrabromophthalate ester, bis(tribromophenoxy) ethane, and decabromodiphenyl ether are also used. The use of synergists, such as antimony oxide, reduces the quantity of brominated flame retardant necessary but decreases the electrical properties required.

Phenolic resins have a low flammability by themselves due to the high aromatic content which leads to a high char formation on thermal degradation. However, end-capped brominated epoxy resins are used when necessary. Decabromodiphenyl ether in combination with antimony oxide is also used.

The main reactive flame-retardant compounds used in unsaturated polyesters are tetrabromophthalic anhydride, dibromoneopentyl glycol, bis(2-hydroxyethyl) ether of tetrabromobisphenol A, and chlorendic anhydride. Tetrachlorophthalic anhydride is also used.

Additive flame-retardant compounds include brominated epoxy resins, chlorinated hydrocarbons, decabromodiphenyl ether, and pentabromodiphenyl ether. Where transparency is not important, antimony oxide can be used as a synergist to reduce the amount of halogen required.

4.6.8 POLYURETHANES

Rigid and flexible polyurethane foams often utilize fire-retardant chemicals. For flexible foams, pentabromodiphenyl ether (now banned in Europe) is used, particularly to avoid the problem of scorch (yellowing of the inside of the block foam), which is most prevalent in hot, humid conditions. Tribromoneopentyl alcohol, which reacts into the urethane polymer, is also used. Brominated

flame-retardant compounds for rigid foams are primarily of the reactive type. These include a mixed tetrabromophthalate ester of diethylene and propylene glycol, polyether polyol made from brominated diol and epichlorhydrin, and dibromoneopentyl glycol and tribromoneopentyl alcohol. All these flame-retardant products are reactive with the isocyanate group and, hence, are incorporated into the polymer chain.

4.6.9 TEXTILES

There are three primary methods for controlling the flammability of textile products. These include the following: incorporation of the fire retardant into the fiber during production, wet treatment of the fabric after production, or back-coating the fabric.

Fiber modification is applicable to synthetic fibers only. The basic polymer could be modified during manufacture by the use of reactive bromine-based monomers. More commonly, however, treatment is performed during extrusion of the fiber with either reactive or melt-blendable fire-retardant compounds. The fire retardant must be sufficiently stable to withstand the extrusion conditions and be compatible with other additives (e.g., hindered amines are used as UV stabilizers). A halogen–phosphorus-containing retardant,⁷³ tris(tribromoneopentyl) phosphate,³⁹ $(\text{CH}_2\text{BrC}(\text{CH}_2\text{Br})_2\text{O})_3\text{PO}$ is designed for incorporation into fiber-grade polypropylenes. This molecule has a high bromine content (70 wt%), which coupled with a 3 wt% phosphorus level ensures that it can be reasonably efficient as a flame retardant at low concentrations. It may be melt blended with polypropylene and is stable at normal extrusion temperatures. FR-372 is claimed to have minimal effect on extrusion behavior and resulting fibre properties at levels of 3–5 wt% sufficient to yield levels of flame retardancy sufficient for carpets, contract upholstery, office partitions, curtains and drapes, and wall coverings; moreover it has an excellent UV stability and it is compatible with HALS stabilizers.

The only halogen-based product used in wet treatment of fabrics is ammonium bromide. Although effective due to its high bromine content (80 wt%), its high solubility prevents its use as a durable treatment.

Back-coating is the major area where bromine-based flame-retardant compounds are used for textiles. This technique is applied primarily in applications such as upholstery and wall coverings. The system would comprise an FR additive with a latex binder, the latter often based on acrylic or ethylene vinylacetate. Use of vinylidene chloride-modified acrylics reduce the amount of fire-retardant additive required.

4.7 ENVIRONMENTAL CONCERNS

A campaign of national and international environmental and consumers agencies against the use of halogen-based fire retardants, which is due to growing concern for possible side effects of these compounds when they perform the fire-retardant action, has been ongoing for about two decades. Indeed, halogen-based fire retardants are very effective in reducing fire risk, i.e., the probability of occurrence of a fire, but they show a high fire hazard, that is, the probability of producing toxic, corrosive, obscuring smokes while performing the fire-retardant action or when involved in a fully developed fire, beyond flashover, when the fire can no longer be extinguished.

Indeed, radical trapping in the gas phase performed by HX is bound to increase production of CO which would otherwise be oxidized by OH radicals. Furthermore, restriction of oxidation increases the amount of nonoxidized products which may condense into droplets or particles when they leave the flame, increasing the optical density of the smoke. Finally HX and metal halides are highly corrosive. The ensuing threat to people, structures, and goods involved in the fire may discourage the use of these fire retardants in spite of their high effectiveness and versatility which

is far ahead of any other system developed so far. Moreover, the environmental impact of halogenated fire retardants during their entire life cycle, including end of life disposal, has been of growing concern since planetary contamination by bioaccumulation of synthetic halogenated compounds such as polychlorobiphenyls (PCBs) and 1,3,7,8-tetrachlorodibenzodioxine (Dioxine) and benzofuranes have been discovered.

PCBs ($C_{12}H_{10-n}Cl_n$), which have been widely used as fire retardants before their very high toxicity was discovered in the 1960s,⁷⁴ are a class of organic compounds with 1–10 chlorine atoms attached to biphenyl (Figure 4.5).

PCBs, originally called “chlorinated diphenyls,” were commercially produced as complex mixtures containing multiple congeners at different degrees of chlorination. In the United States, commercial production of PCBs started in 1929. Manufacturing levels increased in response to the electrical industry’s need for a “safer” (than flammable mineral oil) cooling and insulating fluid for industrial transformers and capacitors.

The toxicity associated with polychlorinated hydrocarbons, including polychlorinated naphthalenes were recognized very early due to a variety of industrial accidents.⁷⁵ However, the first evidences of bioaccumulation and toxicity on animals was noted in 1966 when emaciated seabird corpses with very high PCB body burdens washed up on beaches.⁷⁴ Concern over the toxicity and persistence (chemical stability) of PCBs in the environment led the United States Congress to ban their domestic production in 1977, although some use continues in closed systems such as capacitors and transformers. PCBs are persistent organic pollutants and despite the production ban in the 1970s, they still persist in the environment and remain a focus of attention.⁷⁶ Their use as fire retardants was discontinued when their toxicity was discovered.

Unfortunately in an unwise decision, PCBs as fire retardants were replaced by chemically analogous polybrominated biphenyls (PBBs) without any prior toxicity evaluation. PBBs have a structure similar to PCBs (Figure 4.6), their use as flame-retardant additives for plastics begins in the 1970s as mixture of many different congeners. In 1973, several thousand pounds of PBB-based fire retardant were accidentally mixed with livestock feed that was distributed to farms in West Central Michigan, United States.⁷⁷ Some 1.5 million chickens, 30,000 cattle, 5,900 pigs, and 1,470 sheep then consumed this feed, and became contaminated with PBBs before the error was discovered in April 1974. Approximately 85% of the Michigan population received some exposure to PBBs because dairy product marketing involves mixing milk from many farms. This episode permitted the study of the effects of PBBs on animals and humans, evaluating the toxicity of these fire-retardant additives. Michigan dairy farmers exposed to PBBs had significant immune system abnormalities including reduced numbers of circulating blood lymphocytes, increases in lymphocytes with no detectable surface markers, and reduced functional response to specific test antigens.⁷⁸ The production was discontinued in United States (1974), United Kingdom (1977), and Germany (1985).

PBBs were substituted with “safer” polybromo diphenyl (or biphenyl) ethers (or oxides) (PBDPEs or PBBPEs or PBDPO or PBBPOs) (Figure 4.7) this time after a very thorough toxicity

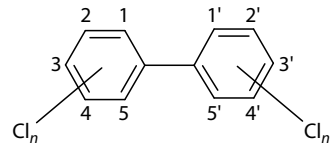


FIGURE 4.5 Chemical structure of PCBs. Position and substitution isomers (209) are collectively termed “congeners.”

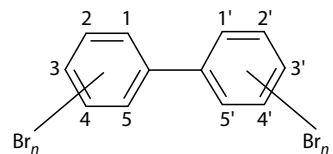


FIGURE 4.6 Chemical structure of PBBs.

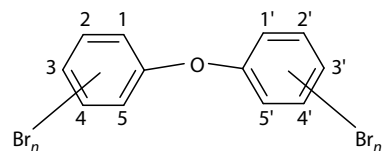


FIGURE 4.7 Chemical structure of PBDPEs (or PBBPEs or PBDPOs or PBBPOs).

study which assessed that PBDEs are biodegradable owing to replacement of the biphenyl link of bioaccumulating PCBs and PBBs with the ether bond.

Nowadays the main concern on brominated aromatic flame retardants such as PBDPE is due to an industrial accident known as “Seveso disaster” that focused the public attention for the first time on very high toxicity of “dioxins.” In 1976, due to accidental reaction run out, an aerosol cloud containing sodium hydroxide, ethylene glycol, sodium trichlorophenate, and somewhere between a few hundred grams and up to a few kilograms of 2,3,7,8-tetrachlorodibenzo-*p*-dioxin (TCDD) was released over an 18 km² area. Also in this case, there are a number of studies reporting on the short- and long-term effects of dioxin on the population.⁷⁹

Super toxic halogenated dibenzofurans and dibenzodioxins can be formed from halogenated aromatic fire retardants such as PCBs, PBBs, and PBDPEs on heating under various laboratory conditions.⁸⁰ In the late 1980s, many pyrolysis experiments on brominated flame retardants and flame-retardant systems were performed and the breakdown products measured. Flame retardants and intermediates tested included PBBs, PBDEs, 2,4,6-tribromophenol, pentabromophenol, tetrabromobisphenol A, and tetrabromophthalic anhydride.^{81–85} Pyrolysis of the flame retardants alone, as well as in combination with polymer mixtures, was investigated.^{86–88} Pyrolysis indicates the tendency of these flame retardants to form halogenated dibenzofurans and dibenzodioxins, although the results are generally not comparable to actual fire situations. On the other hand, the products of pyrolysis and of thermal oxidation can vary very widely depending on conditions of heating. Indeed supertoxic production can be restricted below acceptable limits, for example, in controlled incineration of waste of polymer materials fire retarded with halogenated fire retardants whereas the same cannot be assured in fires in which conditions are uncontrolled and extremely variable. This topic is well reviewed by Lomakin and Zaikov.⁸⁹

Toxicity and environmental concerns led to submission of a proposal to European Union to ban the use of PBDPE in 1989 (111-4301-89-EN Draft). The proposal was rejected on the basis of recommendations issued by a thorough debate between scientists, regulators, producers, and users of fire retardants, stating that banning would involve an unacceptable fire risk since alternatives were not available to replace halogen-based fire retardants with comparable effectiveness. Ever since, fire-retardant research has been mostly devoted to the development of nonhalogenated replacements for the halogen fire retardants.

Over the years directives on usage/waste and recycling on halogenated flame retardants were more and more restrictive with the accumulation of evidences on their environmental effects.⁸⁹ In February 2003, the Restriction of Hazardous Substances Directive or RoHS was adopted by the European Union. This directive is on the restriction of the use of certain hazardous substances in electrical and electronic equipments.⁹⁰ The RoHS directive took effect on 1 July 2006, and is required to be enforced and become law in each member state. This directive restricts the use of six hazardous materials, included brominated flame retardants, in the manufacture of various types of electronic and electrical equipment. It is closely linked with the Waste Electrical and Electronic Equipment Directive (WEEE) 2002/96/EC which sets collection, recycling, and recovery targets for electrical goods and is part of a legislative initiative to solve the problem of huge amounts of toxic e-waste.⁹¹ The RoHS restricts the use of PBBs and PBDPEs. The maximum concentrations allowed are 0.1 wt % of homogeneous material. The WEEE directive imposes separated collection of polymer materials fire retarded with brominated aromatics unless the size is below 10 cm² for printed circuits.

Besides the actions taken by the EU regulating bodies, an independent industrially supported thorough risk assessment has been planned and is still under execution on commercial halogenated fire retardants to assess their toxicity and environmental impact.

While PBBs have not been used for many years, as a consequence of the results of the EU Risk Assessments, the PBDPEs penta and octabromodiphenyl ether have been banned, while decabromodiphenyl ether (DBDPE) was shown to necessitate no risk reduction measures. Thus, following

the positive outcome of the Risk Assessment, in a Commission Decision published on 15 October 2005, the EU has exempted DBDPE from the RoHS Directive.

The EU Commission has made a clarification concerning DBDPE authorization; in a nonlegal binding letter of 21 June 2006, the EU Commission has written to Member States confirming that DBDPE is exempted from the RoHS ban on PBDPEs in electrical and electronic equipment sold in Europe if the impurities content in terms of other PBDPEs is <0.1%. This could be an issue because commercial DBDPE may contain up to 3% of nona-BDE. Industry and users have reacted to indicate that the Commission's interpretation is not relevant because the EU Risk Assessment of DBDPE, at the basis of the exemption decision, already took into account the presence of PBDPEs impurities. As such, the interpretation question remains open within the Commission, which is currently examining the issue of DBDPE exemption from RoHS.

On the basis of RoHS, practically all PBDPE were banned, however article 6 of the RoHS requires the European Commission (EC) to carry out a review of the RoHS directive and to consider any changes that are needed. The review started in 2005 and all aspects of the directive have been considered. There have been stakeholder consultations and studies by consultants into several aspects of RoHS. The Commission published its proposals on 3 December 2008. The main changes are as follows.

Unlike in the original RoHS Directive, the European Commission now has to take into account the aims of the Lisbon strategy so that development of an environmental strategy also considers growth and employment. Another fundamental change is that RoHS substance restrictions would be imposed only if there is an unacceptable risk to human health and the environment, whereas previously it was based only on the precautionary principle.

The RoHS procedure has now combined with European Union Registration, Evaluation, Authorisation and restriction of Chemicals (REACH), which is a new European Union Regulation (EC/2006/1907 of 18 December 2006). Four additional substances are listed that will be assessed as a priority, among these substances is hexabromocyclododecane, a brominated flame retardant widely used in expanded polystyrene for which no alternatives have been found so far. REACH addresses the production and use of chemical substances and their potential impacts on both human health and the environment; it has been described as the most complex legislation in the Union's history and the most important in the last 20 years. It is the strictest law to date regulating chemical substances and will impact industries throughout the world. REACH entered into force in June 2007, with a phased implementation over the next decade.

The aims of the proposed new regulations are to improve the protection of human health and the environment while maintaining the competitiveness and enhancing the innovative capability of the EU chemicals industry. REACH would furthermore give greater responsibility to industry to manage the risks from chemicals and to provide safety information on the substances. This information would be passed down the chain of production.

The brominated flame retardants were one of the first categories investigated by REACH and at the end of 2008 the registration was practically complete. The results of REACH for the main halogenated flame retardants are summarized in Table 4.4.

In contrast to RoHS, the REACH regulation has the tendency to avoid general banning of chemicals by class at which they belong but to carry a risk assessment program, it is in fact true that a complete reconsideration in polymer flame retardants in the direction of ecologically friendly systems, on the other hand flame retardants such as DBDPE are extremely effective and have important role in saving lives, preventing or reducing the spreading of fire. An equilibrium should be so found balancing flame-retardant benefits and environmental and human risks.

Mechanistic studies described above show that halogenated fire-retardant systems can act by a condensed phase mechanism that in some cases could be induced by a halogen-free compound.

TABLE 4.4
REACH Status for the Main Halogenated Flame Retardants

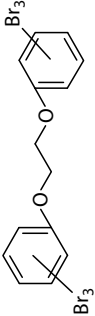
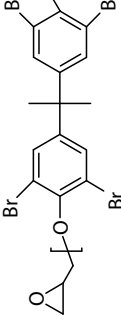
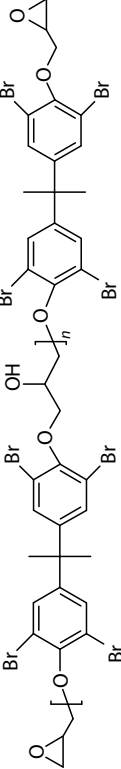
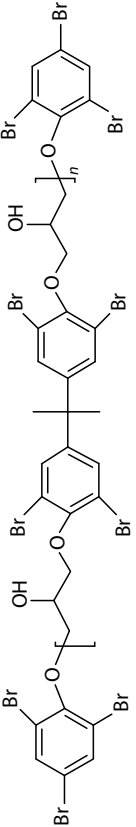
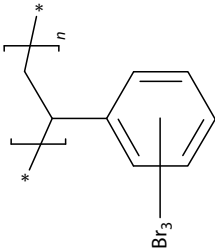
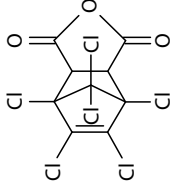
Molecule	Status
Pentabromodiphenyl ether	The risk assessments was unfavorable
Octabromodiphenyl ether	The risk assessment indicates some risks. Production was stopped on the basis of precautionary principles.
Decabromodiphenyl ether	Risk assessment closed. No restrictions due to the lack of risks identified for the use of this substance.
Hexabromocyclododecane	Review of RoSH published on 10 December 2008 will impose a review with REACH directive
Short chain chlorinated paraffin	The risk assessment for short chain (C ₁₀ –C ₁₃) chloroparaffins (SCCPs) was completed with the conclusion that the use of SCCPs in metal working and leather processing poses a risk to the aquatic environment. As a consequence, risk reduction measures have been implemented (EU Directive 2002/45). No significant risks to human health were identified. In all applications where they are used as flame retardants, no risk of secondary poisoning through accumulation in the environment or the food chain was found. Further studies of SCCPs have been specified by EU Regulation 642/2005: emissions and biodegradation in marine environment.
Medium-long-chain chlorinated paraffin	The EU Risk Assessment (Part I—Environment was completed in 2005) identifies a risk of accumulation in the food chain, and suggests risk reduction measures for all applications. Part II—Human Health are under evaluation
Tetrabromobisphenol A	EU human health risk assessment, completed on May 2005, concluded that TBBPA presents no risk to human health. Therefore TBBPA is not subject to any classification for health. TBBPA is classified in the EU as an R50/53 substance for the environment: “toxic to aquatic organisms” and “may cause long-term adverse effects in the aquatic environment.” Hazard can be managed by appropriate product stewardship measures. In epoxies: full integration into the epoxy resin ensures that the final product, no longer contains free TBBPA.

4.8 CONCLUSIONS AND FUTURE TRENDS

Halogen-based flame retardants have served a great need for effective flame retardancy for several years. Due to relatively recent environmental concerns, there is a continuing trend toward the development of nonhalogenated materials to replace these systems. While this has been underway for quite some time, it does not appear that nonhalogenated materials will be available in the near future. Hence it appears that there is still a need for these materials to prevent fires.

APPENDIX A

Halogenated Flame Retardants: Properties and Typical Use

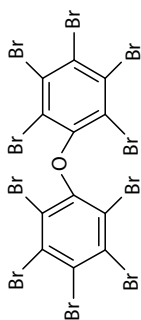
Chemical Name (Trade Name)	Structure	Physical Properties	Halogen Content (wt%)	Typical Use
Ammonium bromide (DSB FR-11)		Sublimation 452°C	81.6 (Br)	Textile
Bis(tribromophenoxy)ethane (GLCC FF-680)		Melting point, 223°C–228°C	70 (Br)	ABS
Brominated epoxy oligomers (DSB F-2000 series; DIC Pratherm®)		Softening range, 105°C–158°C	49-54 (Br)	ABS, PBT, HIPS, PA
Modified brominated epoxy oligomers (DSB F-3020)		Softening range, 113°C–127°C	56 (Br)	ABS, PBT, HIPS, Textile
Brominated polystyrene (PyroChek® 68PB)		Softening range, 113°C–127°C	67 (Br)	PBT, PET, PA
Chlorenic Anhydride (HET Acid)		Melting point, 235°C–239°C	54.7 (Cl)	UPE

Chlorinated Paraffins

Liquid, mixture
Melting point,
304°C–309°C

40-70 (Cl)
83 (Br)

PVC
HIPS, PBT, PE,
PP

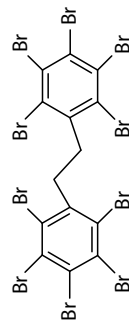


Decabromo-biphenylethane
(Saytex® S-8010)

Melting point,
385°C–389°C

82 (Br)

HIPS, PBT, PE,
PP

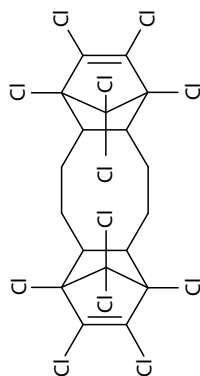


Dodecachloro pentacyclo
octadeca-7,15-diene
(Dechlorane Plus®)

Melting point, 350°C

65 (Cl)

PA, PBT

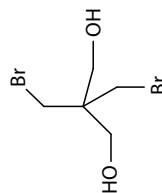


Dibromopentyl glycol
(DSB FR-522)

Melting point,
109°C–110°C
Boiling point, 134°C
(1 mmHg)

61 (Br)

PUR, UPE

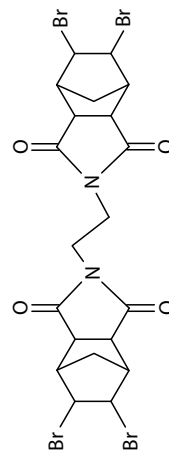


Ethylene-bis(5,6-dibromo-
norbornane-2,3-
dicarboximide) (Saytex®
BN-451)

Melting point, 294°C

45 (Br)

PP

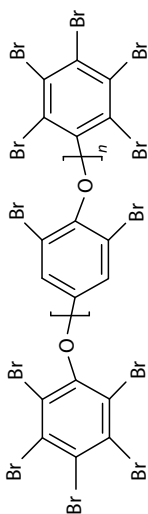


(continued)

Halogenated Flame Retardants: Properties and Typical Use (continued)

Chemical Name (Trade Name)	Structure	Physical Properties	Halogen Content (wt%)	Typical Use
Ethylene- <i>bis</i> (tetrabromonaphthalimide) (Saytex® BT-93)		Melting point, 450°C	67 (Br)	HIPS, PBT, PE, PP
Halogenated polyetherpolyols (IXOL® B350)		Mixture, liquid	32 (Br) (Cl) 1.1 (P)	PUR
Hexabromo-cyclododecane (Saytex® HP-900; GLCC CD-75P; DSB FR-1206)		Melting point, 175°C–195°C (mixture)	74.7 (Br)	PS foam, PP, Textile
Octabromo diphenyl ether (DSB FR-1208; GLCC DE-79)		Melting point, 70°C–150°C	79 (Br)	ABS
Octabromotrimethyl phenyl indane (DSB FR-1808)		Melting point, 230°C–250°C	73 (Br)	HIPS, ABS, PA
Pentabromodiphenyl ether (DSB FR-1208; GLCC DE-79)		Mixture, melting point <30°C	70.8 (Br)	PUR, Textile

Poly(dibromophenylene ether) (GLCC PO-64P)

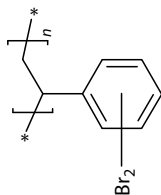


Melting point,
210°C–240°C

62 (Br)

PA

Poly(dibromostyrene) (GLCC PDBS-80)

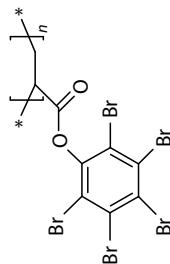


Softening range,
210°C–230°C

59 (Br)

PBT, PET, PA

Poly(pentabromo benzyl acrylate) (DSB FR-1025)

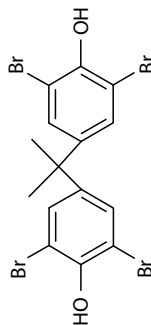


Melting point,
190°C–210°C

70 (Br)

PBT

Tetrabromo-*bis*phenol-A (Saytex® CP-2000; GLCC BA-59; DSB FR-1524)

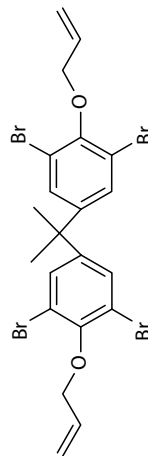


Melting point,
179°C–181°C

58.5 (Br)

Epoxy resins,
ABS

Tetrabromo-*bis*phenol-A *bis*(allyl ether) (GLCC BE-51)

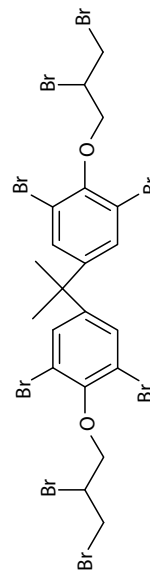


Melting point,
115°C–120°C

51.2 (Br)

PS

Tetrabromo-*bis*phenol-A *bis*(2,3-dibromopropyl ether) (Saytex® HP-800; GLCC PE-68; DSB FG-3100)



Melting point,
90°C–100°C

68 (Br)

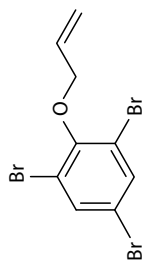
PP

(continued)

Halogenated Flame Retardants: Properties and Typical Use (continued)

Chemical Name (Trade Name)	Structure	Physical Properties	Halogen Content (wt%)	Typical Use
Tetrabromo- <i>bis</i> phenol-A carbonate oligomer phenoxy terminated (GLCC BC 52 & 58)		Melting point, 210°C–230°C and 230°C–260°C	51 & 58 (Br)	PBT
Tetrabromophthalate diol (Saytex® RB-79; GLCC PHT4-DIOL)		Mixture liquid	46 (Br)	PUR
Tetrabromophthalic anhydride (Saytex® RB-49; GLCC PHT4)		Melting point, 270–276°C	68.2 (Br)	UPE
Tetradecabromo-diphenoxybenzene (Saytex® S-120)		Melting point, >350°C (decomposition)	81 (Br)	PET, PA, PBT
Tribromoneopentyl alcohol (DSB FR-513)		Melting point, 65°C	73.8 (Br)	PUR

Tribromophenol allyl ether
(GLCC PHE-65)

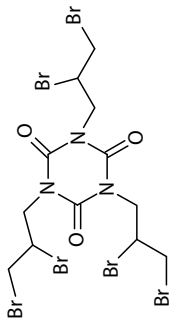


Melting point, 74°C

64.2 (Br)

PS

Tris(2,3-dibromoPropyl
isocyanurate) (TAIC 6B)

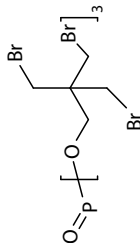


Melting point, 107°C

65 (Br)

PP

Tris(tribromoneopentyl)
phosphate (CR-900;
FG-3100; DKS SR-720;
DSB FR-720)

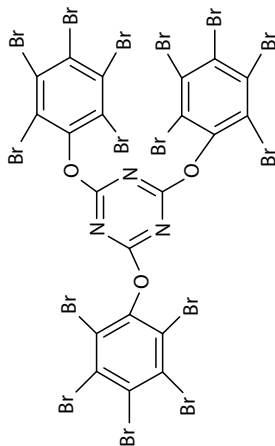


Melting point, 181°C

70 (Br) 3 (P)

PP

Tris(tribromophenyl)
cyanurate (DKS SR-245;
DSB FR-245)



Melting point, 230°C

67 (Br)

HIPS, ABS

Source: Georlette, P. et al. *Fire Retardancy of Polymeric Materials*, Grand, A.F. and Wilkie, C.A., Eds., Marcel Dekker Inc., New York, 2000, Tables 2-6, 257-269.

Note: ABS, acrylonitrile/butadiene/styrene; EPS, expandable polystyrene; HIPS, high-impact polystyrene; PA, polyamide; PBT, poly(butylene)terephthalate; PC, polycarbonate; PE, polyethylene; PET, poly(ethylene)terephthalate; PP, polypropylene; PUR, polyurethane; PVC, polyvinylchloride; UPE, unsaturated polyester; Textile, textile application.

REFERENCES

1. Roma, P.; Camino, G.; Luda, M. P.; Mechanistic studies on fire retardant action of fluorinated additives in ABS, *Fire and Material*, 1997, 21(4), 199–204.
2. Lyons, J. W.; *The Chemistry and Uses of Fire-Retardants*, 1970, 16. New York: Wiley-Interscience.
3. Minkoff, G. I.; Tipper, C. F. H.; *Chemistry of Combustion Reactions*, 1962. London, U.K.: Butterworth.
4. Wilson, W. E.; O'Donovan, J. T.; Fristrom, R. M.; Flame Inhibition by Halogen Compounds, *Twelfth Symposium (International) on Combustion*, The Combustion Institute, Pittsburgh, PA, 1969, 929–942.
5. Fristrom, R. M.; Sawyer, R. F.; *Flame Inhibition Chemistry Advisory Group for Aerospace Research and Development Conference Proceedings, No. 84 on Aircraft Fuels, Lubricants and Fire Safety*, AGARD-CP-84-71, Section 12, North Atlantic Treaty Organization, 1971.
6. Day, M. J.; Stamp, D. V.; Thompson, K.; Dixon-Lewis, G.; Inhibition of hydrogen–air and hydrogen–nitrous oxide flames by halogen compounds, *Thirteenth Symposium (International) on Combustion*, The Combustion Institute, Pittsburgh, PA, 1971, 705–712.
7. Noto, T.; Babushok, V.; Burgess, D. R.; Hamins, A.; Tsang, W.; Miziolek, A.; Effect of halogenated flame inhibitors on C₁–C₂ organic flames, *Twenty-Sixth Symposium (International) on Combustion*, The Combustion Institute, Pittsburgh, PA, 1996, 1377–1383.
8. Rosser, W. A.; Wise, H.; Miller, J.; Mechanism of combustion inhibition by compounds containing halogen, *Seventh Symposium (International) on Combustion*, London, U.K.: Butterworth, 1959, 175–182.
9. Hastie, J. W.; Molecular basis of flame inhibition, *Journal of Research of NBS-A Physics and Chemistry*, 1973, 77A, 733–754.
10. Levy, A.; Droege, J. W.; Tighe, J. J.; Foster, J. F.; The inhibition of lean methane flame, *Eighth Symposium (International) on Combustion (Williams and Wilkins Co.)*, 1962, 524–533.
11. Petrella R. V.; Factors affecting combustion of polystyrene and styrene. In *Flame Retardant Polymeric Materials*, Lewin, M.; Atlas, S. M.; Pearce, E. M., Eds., Vol. 2, New York: Plenum Press, 1978, pp. 159–201.
12. Petrella, R. V.; Studies of the combustion of hydrocarbons by kinetic spectroscopy. II. The explosive combustion of styrene inhibited by halogen compounds, private communication, 1972.
13. Pownall, C.; Simmons, R. F.; Some observation on the near flame limit. *Thirteenth Symposium (International) on Combustion*, The Combustion Institute, Pittsburgh, PA, 1971, 585–592.
14. Larsen, E. R.; Mechanism of flame inhibition. I: The role of halogens, *Journal of Fire and Flammability/Fire Retardant Chemistry*, 1974, 1, 4–12.
15. Larsen, E. R.; Mechanism of flame inhibition II: A new principle of flame suppression, *Journal of Fire and Flammability/Fire Retardant Chemistry*, 1975, 2, 5–20.
16. Larsen, E. R.; Some effects of various unsaturated polyester resin components upon FR-agent efficiency, *Journal of Fire and Flammability/Fire Retardant Chemistry*, 1975, 2, 209–223.
17. Larsen, E. R.; Fire retardants (halogenated). In *Kirk-Othmer Encyclopedia of Chemical Technology (3rd edition)*, Vol. 10, 1980, 373–395.
18. Larsen, E. R.; Ludwing, R. B.; On the mechanism of halogen's flame suppressing properties, *Journal of Fire and Flammability/Fire Retardant Chemistry*, 1979, 10, 69–77.
19. Hindersinn, R. R.; Witschard, G.; The importance of intumescence and char in polymer fire retardance. In *Flame retardancy of Polymeric Materials*, vol. 4, Kuryla, W. C. and Papa, A. J., Eds., Marcell Dekker, New York, 1978, pp. 1–107.
20. Little, R. W.; Metallic oxide-chlorinated: Laboratory impregnations. In *Flameproofing Textile Fabrics*, Little R. W., Eds., New York: Reinhold Publishing Company, 1947, pp. 248–256.
21. Coppick, S.; Metallic oxide-chlorinated: Fundamentals of process. In *Flameproofing Textile Fabrics*, Little R. W., Eds., New York: Reinhold Publishing Company, 1947, pp. 239–248.
22. Nametz, R. C.; Self extinguish polyester resins, *Industrial and Engineering Chemistry*, 1967, 59(5), 99–116.
23. Learmonth, G. S.; Nesbitt, A.; Thwaite, D. C.; Flammability of plastics I. Relation between pyrolysis and burning, *British Polymer Journal*, 1969, 1, 149–153.
24. Learmonth, G. S.; Thwaite, D. C.; Flammability of plastics II. Effect of additives on the flame, *British Polymer Journal*, 1969, 1, 154–160.
25. Lindemann, R. F.; Flame-retardants for polystyrenes, *Journal of Industrial and Engineering Chemistry*, 1969, 61(5), 70–75.
26. Fenimore, C. P.; Martin, F. J.; Flammability of polymers, *Combustion and Flame*, 1966, 10, 135–139.
27. Lyons, J. W.; *The Chemistry and Uses of Fire-Retardants*, New York: Wiley-Interscience, 1970, pp. 209–218.

28. Read, N. J.; Heighway-Bury, E. G.; Flameproofing of textile fabrics with particular reference to the function of antimony compounds, *Journal of the Society of Dyers and Colourists*, 1958, 74(12), 823–829.
29. Thiery, P.; *Fireproofing, Chemistry, Technology and Applications*, English translation by Goundry J. H. Barking: Elsevier, 1970.
30. Fenimore, C. P.; Jones, G. W.; Modes of inhibiting polymer flammability, *Combustion and Flame*, 1966, 10, 295–301.
31. Camino, G.; Costa, L.; Trossarelli, L.; Thermal degradation of polymer-fire retardant mixtures: Part III—Degradation products of polypropylene-chlorinated paraffin mixtures, *Polymer Degradation and Stability*, 1982, 4(2), 133–144.
32. Costa, L.; Camino, G.; Luda, M. P.; Effect of the metal on the mechanism of fire retardance in chloroparaffin-metal compound-polypropylene mixtures, *Polymer Degradation and Stability*, 1986, 14(2), 113–123.
33. Hindersinn, R. R.; Wagner, G. M.; Fire Retardancy. In *Encyclopedia of Polymer Science and Technology*, Vol. 7, New York: Interscience, 1967, pp. 1–57.
34. Hastie J. W.; McBee, C. L.; Mechanistic studies of triphenylphosphine oxide poly(ethyltereftalate) and related flame retardant systems NBS Final report NBSIR, 1975, pp. 75–742.
35. Camino, G.; Mechanism of fire retardancy in chloroparaffin-polymer mixtures. In *Developments in Polymer Degradation*, Vol. 7, Grassie, N., Ed., London, U.K.: Elsevier Applied Sciences, 1987, pp. 221–269.
36. Camino, G.; Fire retardant polymeric. In *Atmospheric Oxidation and Antioxidants*, Chapter 10, Vol. II, Scott, G., Ed., Amsterdam: Elsevier, 1993, pp. 461–493.
37. Lum, R. M.; Antimony oxide-PVC synergism: Laser pyrolysis studies of the interaction mechanism, *Journal of Polymer Science: Polymer Chemistry Edition*, 1977, 15(2), 489–497.
38. Pitts, J. J.; Scott, P. H.; Powell D. G.; Thermal decomposition of antimony oxychloride and mode in flame retardancy, *Journal of Cellular Plastics*, 1970, 6(1), 35–37.
39. Camino, G.; Costa, L.; Luda, M. P.; Overview of fire retardant mechanism, *Polymer Degradation and Stability*, 1991, 33(2), 131–154.
40. Costa, L.; Goberti, P.; Paganetto, G.; Camino, G.; Sgarzi, P.; Thermal behaviour of chlorine-antimony fire-retardant systems, *Polymer Degradation and Stability*, 1990, 30(1), 13–28.
41. Costa, L.; Paganetto, G.; Bertelli, G.; Camino, G.; Thermal decomposition of antimony oxyhalides I. Oxychlorides, *Journal of Thermal Analysis*, 1990, 36(3), 1141–1153.
42. Bertelli, G.; Costa, L.; Fenza, S.; Marchetti, E.; Camino, G.; Locatelli, R.; Thermal behavior of bromine-metal fire retardant systems, *Polymer Degradation and Stability*, 1988, 20(3–4), 295–314.
43. Hastie, J. W.; Mass spectrometric studies of flame inhibition: Analysis of antimony trihalides in flames, *Combustion and Flame*, 1973, 21, 49–54.
44. Martin, F. J.; Price, K. R.; Flammability of epoxy resins, *Journal of Applied Polymer Science*, 1968, 12(1), 143–158.
45. Bulewicz, E. M.; Padley, P. J.; Photometric observations on the behaviour of tin in premixed $H_2 + O_2 + N_2$ flames, *Transactions of the Faraday Society*, 1971, 67, 2337–2347.
46. Camino, G.; Costa, L.; Thermal degradation of a highly chlorinated paraffin used as a fire retardant additive for polymers, *Polymer Degradation and Stability*, 1980, 2(1), 23–33.
47. Costa, L.; Camino, G.; Thermal degradation of polymer-fire retardant mixtures: Part V—Polyethylene-chloroparaffin mixtures, *Polymer Degradation and Stability*, 1985, 12(2), 105–116.
48. Costa, L.; Camino, G.; Thermal degradation of polymer-fire retardant mixtures: Part VII—Products of degradation and mechanism of fire retardance in polystyrene-chloroparaffin mixtures, *Polymer Degradation and Stability*, 1985, 12(4), 287–296.
49. Costa, L.; Camino, G.; Trossarelli, L.; A Study of the thermal degradation of polystyrene-chloroalkane mixture by thermogravimetry-high resolution gas chromatography, *Journal of Analytical and Applied Pyrolysis*, 1985, 8, 15–24.
50. Pitts, J. J.; Antimony-halogen synergistic reactions in fire retardants, *Journal of Fire and Flammability*, 1972, 33, 51–84.
51. Costa, L.; Camino, G.; Luda, M. P.; Mechanism of condensed phase action in fire retardant bismuth compound-chloroparaffin-polypropylene mixtures: Part I—The role of bismuth trichloride and oxychloride, *Polymer Degradation and Stability*, 1986, 14(2), 159–164.
52. Bagdanova, V. V.; Fedeev, S. S.; Lesnikovic, A. I.; Klimovtsova, I. A.; Sviridov, V. V.; The formation of antimony oxychloride in flame retardant mixtures and its influence on flame retardant efficiency, *Polymer Degradation and Stability*, 1985, 11, 205–210.

53. Costa, L.; Camino, G.; Luda, M. P.; Mechanism of condensed phase action in fire retardant bismuth compound-chloroparaffin-polypropylene mixtures: Part II—The thermal degradation behavior, *Polymer Degradation and Stability*, 1986, 14(2), 165–177.
54. Costa, L.; Luda, M. P.; Trossarelli, L.; Mechanism of condensed phase action in flame retardants. Synergistic systems based on halogen-metal compounds, *Polymer Degradation and Stability*, 2000, 68(1), 67–74.
55. Learmonth, G. S.; Thwaite, D. G.; Flammability of plastics: IV. An apparatus for investigating the quenching action of metal halides and other materials on premixed flames, *British Polymer Journal*, 1970, 2, 249–253.
56. Camino, G.; Costa, L.; Trossarelli, L.; Thermal degradation of polymer-fire retardant mixtures—Part II: Mechanism of interaction in polypropylene-chlorinated paraffin mixtures, *Polymer Degradation and Stability*, 1982, 4(1), 39–49.
57. Ballistreri, A.; Foti, S.; Montaudo, G.; Pappalardo, S.; Scamporrino, E.; Thermal decomposition of flame retardants: Mixtures of chlorinated polymers with Sb_2O_3 and $(BiO)_2CO_3$, *Journal of Polymer Science: Polymer Chemistry Edition*, 1979, 17(8), 2469–2475.
58. Laver H. S.; Chapter 5. The influence of metal chelates on the oxidation of polymers. In *Developments in Polymer Stabilization*, Vol. 1, Scott, G., Ed., London, U.K.: Applied Science Publisher, 1979, pp. 167–197.
59. Nonhebel, D. C.; Tedder, J. M.; Walton, J. C.; *Radicals*, Cambridge University Press, Cambridge, 1979, 316 pp.
60. Kaspersma, J.; Doumen, C.; Munro, S.; Prins, A. M.; Fire retardant mechanism of aliphatic bromine compounds in polystyrene and polypropylene, *Polymer Degradation and Stability*, 2002, 77(2), 325–331.
61. Smith, R.; Georlette, P.; Finberg, I.; Reznick, G.; Development of environmental friendly multifunctional flame retardants for commodity and engineering plastics. *Polymer Degradation and Stability*, 1996, 54(2–3), 167–173.
62. Finberg, I.; Utevski, L.; Kallos, M.; Brominated indan as highly compatible systems. Styrenic plastics. IMEC 8, 1997, 19.
63. Reznick, G.; Bar Yaakov, Y.; Utevskaa, L.; Georlette, P.; Lopez Cuesta, J. M.; Optimization of flame retarded thermoplastics for engineering applications. In *Proceedings of "Flame Retardants '98*, London, U.K.: Interscience Communications, 1998, pp. 125–137.
64. Innes, J.; Innes, A.; Flame retardants for polycarbonate—New and classical solutions, *Plastics, Additives and Compounding*, 2006, 8(1), 26–29.
65. Markezich, R. L.; Use of alternate synergists with a chlorinated flame retardant in nylon. In *FRCA Meeting*, Lancaster, PA: Fire retardant chemical association, 1987.
66. Markezich, R. L.; New flame retardant HIPS, ABS and nylon formulations. In *Proceedings of "Flame Retardants Conference '92"*, 1992, pp. 187–197.
67. Sinturel, C.; Philippart, J. L.; Lemaire, J.; Gardette, J.; Photooxidation of fire retarded polypropylene. I. Photoageing in accelerated conditions, *European Polymer Journal*, 1999, 35(10), 1773–1781.
68. Sinturel, C.; Lemaire, J.; Gardette, J. L.; Photooxidation of fire retarded polypropylene: II. Photooxidation mechanism, *European Polymer Journal*, 1999, 35(10), 1783–1790.
69. Sinturel, C.; Lemaire, J.; Gardette, J. L.; Photooxidation of fire retarded polypropylene: III. Mechanism of HAS inactivation, *European Polymer Journal*, 2000, 36(7), 1431–1443.
70. Montezin, F.; Lopez-Cuesta, J. M.; Crespy, A.; Georlette, P.; Flame retardant and mechanical properties of a copolymer PP/PE containing brominated compounds/antimony trioxide blends and magnesium hydroxide or talc, *Fire and Materials*, 1997, 21(6), 245–252.
71. Green, J.; Phosphorous-bromine flame retardant synergy in engineering thermoplastics. In: *Advances in Organobromine Chemistry II proceedings, ORGABROM '93*, Amsterdam: Elsevier. 1995, pp. 341–354.
72. Squires, G. E.; Flame retardant polypropylene - A new approach that enhances form, function and processing. In *Proceedings of "Flame Retardants Conference '99"*, 1996, pp. 107–114.
73. Buszard, D. L.; Inherently flame retardant polypropylene fibres. In *Proceedings of Conference Textile Flammability: Current and Future Issues*, March 30–31, Textile Institute, Manchester, 1999.
74. Jensen, S.; Report of a new chemical hazard, *New Scientist*, 1966, 32, 612.
75. Drinker, C. K.; Warren, M. F.; Bennet G. A.; The problem of possible systemic effects from certain chlorinated hydrocarbons, *Journal of Industrial Hygiene and Toxicology*, 1937, 19(7), 283–311.
76. Final report of the subcommittee on health effects of PCBs and PBBs. *Environmental Health Perspectives*, 1978, 24, 133–198.

77. Carter, L. J.; Michigan's PBB incident: Chemical mix-up leads to disaster, *Science*, 1976, 192(4236), 240–243.
78. Fries, G. F.; The PBB episode in Michigan: An overall appraisal, *Critical Reviews in Toxicology*, 1985, 16(2), 105–156.
79. Bertazzi, P. A.; Long-term effects of chemical disasters. Lessons and results from Seveso, *The Science of the Total Environment*, 1991, 106(1–2), 5–20.
80. Buser, H. R.; Brominated and brominated/chlorinated dibenzodioxins and dibenzofurans: Potential environmental contaminants, *Chemosphere*, 1987, 16(8–9), 1873–1876.
81. *IPCS Environmental Health Criteria 140: Polychlorinated Biphenyls and Terphenyls*, 2nd edition, Geneva: World Health Organization, International Programme on Chemical Safety, 1992.
82. *IPCS Environmental Health Criteria 152: Polybrominated Biphenyls*, Geneva: World Health Organization, International Programme on Chemical Safety, 1994.
83. *IPCS Environmental Health Criteria 172: Tetrabromobisphenol-A and Derivatives*, Geneva: World Health Organization, International Programme on Chemical Safety, 1995.
84. *IPCS Environmental Health Criteria 205: Polybrominated Diphenyl-p-dioxins and Dibenzofurans*, Geneva: World Health Organization, International Programme on Chemical Safety, 1996.
85. Addink, R.; Olie, K.; Mechanism of formation and destruction of polychlorinated dibenzo-p-dioxins and dibenzofurans in heterogeneous systems, *Environmental Science & Technology*, 1995, 29(6), 1425–1435.
86. Ahling, B.; Lindskog, A.; Emission of chlorinated organic substances from combustion. In *Chlorinated Dioxins and Related Compounds, Impact on the Environment*. Hutzinger, O.; Safe, S., Eds., New York: Pergamon Press, 1982, pp. 462–472.
87. Behrooz, G. S.; Altwicker, E. R.; Rapid formation of polychlorinated dioxins/furans during the heterogeneous combustion of 1,2-dichlorobenzene and 2,4-dichlorophenol, *Chemosphere*, 1996, 32(1), 133–144.
88. Blumenstock, M.; Zimmermann, R.; Schraumm, L. W.; Kaune, A.; Henkelmann, B.; Kettrup, A.; Presence of polychlorinated dibenzo-p-dioxins (PCDD), dibenzofurans (PCDFs), biphenyls (PCB), chlorinated benzenes (PCBz) and polycyclic aromatic hydrocarbons (PAH) under various combustion conditions in a post combustion chamber, *Organohalogen Compounds*, 1998, 36, 59–63.
89. Lomakin, S. M.; Zaikov, G. E.; Polyhalogenated flame retardants and dioxins, *Journal of Environmental Protection and Ecology*, 2003, 4(1), 95–119.
90. Directive 2002/95/EC.
91. Castrovinci, A.; Lavaselli, M.; Camino, G.; Recycling and disposal of flame retarded materials. In *Advances in Fire Retardant Materials*. Horrocks, A. R.; Price, D., Eds., Boca Raton, FL: CRC, 2008, pp. 213–232.
92. Costa, L.; Camino, G.; Luda, M. P., Effect of the metal on the mechanism of fire retardance in chloroparaffin-metal compound-polypropylene mixtures, *Polymer Degradation and Stability*, 1986, 14(2), 116.
93. Costa, L.; Camino, G.; Luda, M. P., Effect of the metal on the mechanism of fire retardance in chloroparaffin-metal compound-polypropylene mixtures, *Polymer Degradation and Stability*, 1986, 14(2), 117.
94. Van Krevelen, D. W.; *Properties of Polymers: Their Correlation with Chemical Structure; Their Numerical Estimation and Prediction from Additive Group Contributions*. New York: Elsevier, 1997.
95. Mita, I.; Effect of structure on degradation and stability of polymers. In *Aspects of Degradation and Stabilisation of Polymers*, Jellinek, H. H. G., Ed., New York: Elsevier, 1978, 247–294.
96. Camino, G.; Mechanism of fire retardancy in chloroparaffin-polymer mixtures. In *Developments in Polymer Degradation*, Vol. 7, Grassie, N., Ed., London, U.K.: Elsevier Applied Sciences, 1987, Table 6, p. 230.
97. Camino, G.; Mechanism of fire retardancy in chloroparaffin-polymer mixtures. In *Developments in Polymer Degradation*, Vol. 7, Grassie, N., Ed., London, U.K.: Elsevier Applied Sciences, 1987, Table 7, p. 243.

5 Phosphorus-Based Flame Retardants

Paul Joseph and John R. Ebdon

CONTENTS

5.1	Background.....	107
5.2	Elemental Phosphorus and Its Compounds	108
5.3	Phosphorus-Based Inorganic Additive Flame Retardants.....	109
5.3.1	Red Phosphorus	109
5.3.2	Ammonium Phosphates.....	110
5.4	Organophosphorus Additive Flame Retardants	110
5.4.1	Phosphates and Phosphonates.....	110
5.4.2	Halogenated Phosphates and Phosphonates	111
5.4.3	Dimeric, Oligomeric, and Cyclic Phosphates and Phosphonates	111
5.4.4	Phosphine Oxides	113
5.5	Reactive Flame Retardants	113
5.6	Step-Reaction Polymers.....	114
5.6.1	Polyesters and Polycarbonates	114
5.6.2	Polyamides.....	114
5.7	Chain-Reaction Polymers	115
5.7.1	Acrylics.....	115
5.7.2	Polystyrene.....	116
5.7.3	Polyolefins.....	116
5.8	Thermosets	116
5.8.1	Epoxy Resins	117
5.8.2	Polyurethanes.....	117
5.8.3	Unsaturated Polyesters.....	118
5.9	Surface Grafting	118
5.10	Mechanisms of Flame Retardance: General Considerations.....	119
5.10.1	Mechanisms of Flame Retardance by Phosphorus Compounds	119
5.11	Concluding Remarks and Future Trends	123
	References.....	123

5.1 BACKGROUND

Elemental phosphorus and its various compounds have been used to flame retard a wide variety of polymer-based materials for several decades. Environmental considerations, especially concerning the use of halogen-based systems, have paved the way, in recent years, for the increased use of phosphorus-based flame retardants as alternatives to the halogen-containing compounds. Furthermore, this has generated active research in identifying novel flame retardants based on phosphorus, as well as synergistic combinations with compounds of other flame-retardant elements (such as nitrogen and the halogens) and with several inorganic nanofillers (e.g., phyllosilicates and carbon nanotubes).^{1,2} This research on halogen alternatives has resulted, especially in recent years,

in a wealth of literature (including patents) and in the market acceptance of several phosphorus-based flame retardants.³

Although phosphorus compounds can be highly effective flame retardants, they are not effective in some major classes of polymers such as styrenic resins and polyolefins.⁴ Furthermore, the basic mode of the intervention of phosphorus compounds, regardless of the phase in which they are active, is to suppress the efficiency of combustion reactions that are mostly radical in nature occurring in the gas phase. This invariably involves the less oxidation of a carbonaceous substrate to carbon dioxide, and thus leads to the production of more soot/smoke and to a comparatively higher value of the CO/CO₂ ratio.⁵ Needless to say, the increased smoke production and toxic vapors (mainly CO) are a major concern, especially in real fire scenarios, where materials passively protected with phosphorus flame retardants are involved. However, from an ignitability point of view, albeit only a low-level indicator of the overall flammability hazard associated with a material, the use of phosphorus-containing flame retardants has proved to be of great value in that they generally increase the ignition resistance of materials very significantly.⁶

The structure–toxicity relationships of organophosphorus compounds have been extensively studied and are relatively well understood.⁷ Generally, phosphorus-containing flame retardants, as a class, exhibit only low to moderate toxicity, as gauged by their Lethal Dose-LD-values. However, there are exceptions to the aforementioned norm. These include the neurotoxicity of tricresylphosphate (mainly owing to the presence of the *o*-isomer) and the mutagenic/carcinogenic effects of tris(2,3-dibromopropyl) phosphate, a flame retardant used for polyester fabric in the 1970s. The main effect of phosphorus fire retardants on the overall combustion toxicity of materials seems to stem from the increased yields of toxic gases such as CO and, in some instances, HCN. However, the results from various studies proved inconclusive owing to the variables involved in these experiments, such as the fuel–air ratios, burning configurations, equipment design, heat input, and the particular toxicity criterion in question.⁸

5.2 ELEMENTAL PHOSPHORUS AND ITS COMPOUNDS

Phosphorus, which exists in various singly bonded allotropic forms, has vital biological functions and was first isolated from human urine. This element can be also volatilized from phosphate rock by heating with sand and coke. With an electronic configuration [Ne]3s²3p³, phosphorus, like nitrogen, can complete its octet by forming three σ bonds, to give compounds such as PX₃, which can use the lone pair of electrons to act as the Lewis bases. Unlike nitrogen, however, but like silicon, phosphorus can also expand its octet. Predictably, phosphorus is slightly smaller than silicon and is slightly more electronegative. The strengths of the P–H and Si–H bonds are about the same, with phosphorus having the closer approach but forming an almost nonpolar bond, but the P–P bond is weaker than Si–Si, and phosphorus forms somewhat weaker σ bonds than silicon to carbon, oxygen, fluorine, and chlorine.⁹

There are several solid forms of phosphorus, all containing single bonds. The low melting, white allotrope, which is soluble in carbon disulfide, is very toxic and reactive. The other major allotrope, red phosphorus, formed by heating the white form in the absence of air, is denser, harder, and is less toxic and less reactive. Heating the white form at high pressures forms the more stable black form. Phosphorus can form a great variety of binary compounds with almost all elements, often by direct action. In addition, phosphorus may form a number of different binary compounds with a given element (e.g., with Ni). It also forms a series of hydrides, P_{*n*}H_{*n*+2}, of which the first member, PH₃, is stable. Phosphorus forms about 12 possible halides, and also some mixed derivatives. All are hydrolyzed to the corresponding oxoacids. When two hydroxyl groups are attached to phosphorus, the particular oxoacid formed is phosphoric acid, H₃PO₄. A lower hydroxylated species, H₃PO₂, is a moderately strong monobasic acid. Two or more OPOH groups in oxoacids may be joined together, often through –P–O–P– links, to form polyphosphorus acids; species with chains containing up to 17 links are known, together with highly polymerized “meta” phosphoric acid.

Phosphorus also forms a wide variety of compounds in which it is joined to nitrogen. P–N bonds are short and strong, and many of these compounds are quite stable. There is a great tendency to form chains and rings, some of which are planar. For example, in $(\text{NPCl}_2)_x$, which can exist as a planar six-membered cyclic trimer, all P–N distances are very similar, suggesting the presence of electron delocalization. In the case of the phosphazene unit ($-\text{N}=\text{P}-$), which is isoelectronic with the silicone unit ($-\text{O}-\text{Si}-$), a range of phosphazene polymers resemble the silicones, as they are water repellent, flexible, and stable to heat and solvents. There are also a vast number of compounds in which phosphorus is bound to carbon, since it can replace both nitrogen atoms and CH groups. The resulting compounds are collectively termed organophosphorus compounds. These include several classes such as aliphatic and aromatic phosphines, phosphine oxides, phosphites, phosphates, phosphinites, phosphinates, phosphonate esters, phosphonium salts, and so on.¹⁰ Several of the aforementioned classes of compounds have been very successfully used both as additives and as reactive flame retardants for a wide variety of polymer-based systems.

5.3 PHOSPHORUS-BASED INORGANIC ADDITIVE FLAME RETARDANTS

Phosphorus-containing flame retardants include red phosphorus, inorganic phosphates, organophosphorus compounds, and chlorophosphorus compounds.¹¹ From a practical point of view, adequate flame retardancy is achieved either by the mechanical blending of a flame-retardant compound with the polymeric substrate (i.e., by introducing an additive) or by the chemical incorporation of the flame retardant into the polymer molecule by simple copolymerization or by chemical modification of the preformed polymer, that is, using a reactive component. Currently, synthetic polymers are usually made more flame retardant by adding additives. Such additives often have to be used at high loadings to achieve a significant effect, for example, 30% by weight or more, which occasionally can have a more detrimental effect on the physical and mechanical properties of polymers than that produced by reactive flame retardants. Nevertheless, additives are more generally used as they are usually cheaper and more widely applicable.^{12,13}

It is a common practice, especially from a commercial point of view, to use a combination of flame retardants for polymeric materials. In many cases, these flame-retardant mixtures can give an enhanced performance at low cost and possibly at a lower overall loading. The synergistic effects of phosphorus-nitrogen and phosphorus-halogen are well-documented.^{14,15} Certain inorganic phosphorus compounds (especially the ammonium salts of phosphoric acid oligomers) have been extensively used as components in intumescent systems.¹⁶ In recent years, there has been an intense research interest in the effects of nanoscopic inorganics (such as clays) in polymeric systems containing phosphorus compounds, both as additives and as reactives.¹⁷

5.3.1 RED PHOSPHORUS

The red allotropic form of phosphorus is relatively nontoxic and, unlike white phosphorus, is not spontaneously flammable. Red phosphorus is, however, easily ignited. It is a polymeric form of phosphorus, thermally stable up to *ca.* 450°C. In its finally divided form, it has proved to be a powerful flame-retardant additive.¹⁸ Elemental red phosphorus is a highly efficient flame retardant, especially for oxygen-containing polymers such as polycarbonates and poly(ethylene terephthalate). Red phosphorus is particularly useful in glass-filled polyamide 6,6, where high processing temperature (about 280°C) excludes the use of most phosphorus compounds.¹⁹ In addition, coated red phosphorus is used to flame retard nylon electrical parts, mainly in Europe and Asia.²⁰

Red phosphorus will react with atmospheric moisture to form toxic phosphine gas and will ignite readily in air. As a result, the commercial product is often encapsulated in an appropriate polymer matrix. Suitable stabilization and encapsulation have led to commercial concentrates containing 50% red phosphorus. Handling hazards and the color of the final flame-retardant products may be a deterrent for wider use.

5.3.2 AMMONIUM PHOSPHATES

Ammonium phosphates were first recommended for flame retarding theater curtains by Gay-Lussac in 1821. Mono- and diammonium phosphates, or mixtures of the two, are widely used to impart flame resistance to a wide variety of cellulosic materials such as paper, cotton, and wood.²¹ These salts have proven to be highly efficient at relatively low costs of application. They are also very effective in preventing afterglow. However, flame-retardant formulations based on these salts are generally nondurable, because they are water soluble and, therefore, are easily susceptible to leaching out from the material matrix.

Ammonium polyphosphates, on the other hand, are relatively water insoluble, nonmelting solids with very high phosphorus contents (up to about 30%). There are several crystalline forms and the commercial products differ in molecular weights, particle sizes, solubilities, and so on. They are also widely used as components of intumescent paints and mastics where they function as the acid catalyst (i.e., by producing phosphoric acid upon decomposition). They are used in paints with pentaerythritol (or with a derivative of pentaerythritol) as the carbonific component and melamine as the spumific compound.²² In addition, the intumescent formulations typically contain resinous binders, pigments, and other fillers. These systems are highly efficient in flame-retarding hydroxylated polymers.

A series of compounded flame retardants, based on finally divided insoluble ammonium phosphate together with char-forming nitrogenous resins, has been developed for thermoplastics.²³ These compounds are particularly useful as intumescent flame-retardant additives for polyolefins, ethylene-vinyl acetate, and urethane elastomers. The char-forming resin can be, for example, an ethyleneurea-formaldehyde condensation polymer, a hydroxyethyl isocyanurate, or a piperazine-triazine resin. Commercial leach-resistant flame-retardant treatments for wood have also been developed based on a reaction product of phosphoric acid with urea-formaldehyde and dicyandiamide resins.

5.4 ORGANOPHOSPHORUS ADDITIVE FLAME RETARDANTS

5.4.1 PHOSPHATES AND PHOSPHONATES

There are several classes of amine phosphates commercially available to flame retard a wide variety of polymeric substrates, both natural and synthetic.²⁴ A classic example is the three variations of melamine phosphate: melamine orthophosphate, dimelamine orthophosphate, and melamine pyrophosphate. Of these, the pyrophosphate is the least soluble and the most thermally stable. Melamine orthophosphate is converted to the pyrophosphate upon heating, with the loss of water. All the aforementioned variations are available as finally divided solids, are used commercially in coatings, and have utility in a wide variety of thermoplastics and thermosets (mostly presented in the patent literature).

Phosphate esters (alkyl or aryl, or mixed) of phosphoric acid constitute an important family of organophosphorus flame retardants.²⁵ Triethylphosphate, a colorless liquid boiling between 209°C and 218°C, and containing 17 wt % phosphorus, has been used commercially as an additive for polyester resins/laminates and in cellulosics. In polyester resins, it functions as a viscosity depressant as well as a flame retardant. Trioctylphosphate is employed as a speciality flame-retardant plasticizer for vinyl composites where low temperature flexibility is critical. It can be also included in blends, along with general purpose plasticizers, such as phthalate esters, to improve low temperature flexibility.

Aryl phosphates were introduced into commercial use early in the twentieth century for flammable plastics such as cellulose nitrate and later for cellulose acetate.²⁶ In vinyls (plasticized), aryl phosphates are frequently used with phthalate plasticizers. Their principal applications are in wire and cable insulation, connectors, automotive interiors, vinyl moisture barriers, plastic greenhouses, furniture upholstery, and vinyl forms. Triaryl phosphates are also used, on a large scale, as flame-retardant hydraulic fluids, lubricants, and lubricant additives. Smaller amounts are used as nonflammable dispersing media for peroxide catalysts. Blends of triaryl phosphates and pentabromodiphenyl oxide are extensively used as flame-retardant additives for flexible urethane foams. It has been also

used as a flame-retardant additive for engineering thermoplastics such as polyphenylene oxide, high impact polystyrene, and ABS-polycarbonate blends.

Mixed esters, such as isopropylphenyl diphenyl phosphate and *tert*-butylphenyl diphenyl phosphate, are also widely used as both plasticizers/flame retardants for engineering thermoplastics and hydraulic fluids.¹¹ These esters generally show slightly less flame-retardant efficacy, when compared to triaryl counterparts; however, they have the added advantage of lower smoke production when burned. Some novel oligomeric phosphate flame retardants (based on tetraphenyl resorcinol diphosphate) are also employed to flame retard polyphenylene oxide blends, thermoplastic polyesters, polyamides, vinyls, and polycarbonates.

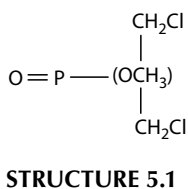
Dimethyl methylphosphonate, a water soluble liquid (boiling point: 185°C), made by the Arbuzov rearrangement of trimethyl phosphite, has a phosphorus content of 25 wt %, the highest possible for an alkyl phosphonate ester.²⁷ Applications of dimethyl methylphosphonate include the use as a viscosity depressant and as a flame retardant in alumina trihydrate-filled polyester resins, and as a flame suppressant for halogenated polyesters. It is also used in flame-retardant rigid polyurethane foams, and as a component in blends with triarylphosphates to make flame-retardant plasticizer for synthetic rubber and cellulotics. Diethyl ethylphosphonate, a higher member of this family of alkyl phosphonates, has a higher boiling point and is believed to be less susceptible to undesirable interactions with halogenated aliphatic components, such as blowing agents, or with amine catalysts.

5.4.2 HALOGENATED PHOSPHATES AND PHOSPHONATES

In this important class of additives, the halogen contributes to some extent to the flame retardancy although this contribution is offset by the lower phosphorus content. The halogens generally reduce vapor pressure and water solubility, thus aiding retention of these additives. Thus, more efficient and effective blending/manufacturing processes involved usually lead to a favorable economics of polymer flame retardation.²⁶

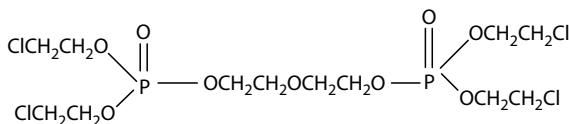
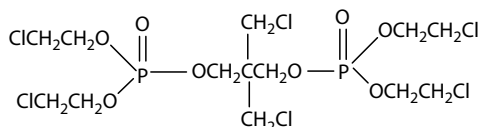
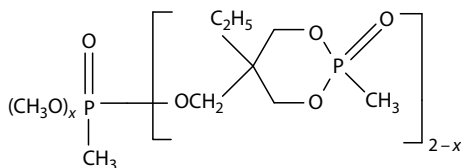
Tris(2-chloroethyl)phosphate, tri(1-chloroethyl)phosphate, 1,3-dichloro-2-propanol phosphate, bis(2-chloroethyl) 2-chloroethylphosphonate are the cardinal members of this class of flame retardants, and are quite compatible with polymers containing polar groups. These compounds have different viscosities, solubilities, hydrolytic stabilities, and boiling points. Their flame-retardant efficacies generally depend on the structural features as well as on the phosphorus–halogen ratios. Tris(2-chloroethyl)phosphate is widely used in rigid polyurethane and polyisocyanurate foams, most classes of thermosets, cast acrylics, and in wood-resin composites. Tri(1-chloroethyl)phosphate, owing to the presence of a branched alkyl group, has lower reactivity to water and bases than the 2-chloroethyl homologue. It is a preferred additive for rigid urethane foams where good storage stability in the isocyanate or the polyol-catalyst mixture is required.²⁵

1,3-Dichloro-2-propanol phosphate (Structure 5.1) has, compared to the mono-halogenated phosphates, high boiling point, much lower water solubility, and enhanced stability toward the amine catalyst used in the foam manufacture. Therefore, it is the leading additive for flexible polyurethane foams, and can be added to the isocyanate or the polyol–catalyst mixture. This halogenated phosphate is also useful as a flame retardant in styrene–butadiene and acrylic lattices for textile back coating and the binding of nonwovens. Bis(2-chloroethyl) 2-chloroethylphosphonate, commercially available as a mixture of isomers, is not as stable as the corresponding phosphate; however, it is widely used as a flame-retardant additive for rigid urethane foams, adhesives, and coatings.



5.4.3 DIMERIC, OLIGOMERIC, AND CYCLIC PHOSPHATES AND PHOSPHONATES

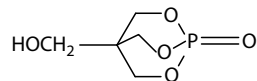
Dimeric phosphates include several compounds among which three different 2-chloroethyl diphosphates have proved to be of commercial significance.²⁵ Generally, they have very low volatilities and reasonably good thermal stabilities, and thus are useful in those open cell (flexible) foams where there are

**STRUCTURE 5.2****STRUCTURE 5.3****STRUCTURE 5.4**

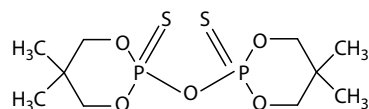
requirements for improved resistance to dry and humid aging. The commercially available variants include tetrakis(2-chloroethyl) ethylenediphosphate and tetrakis(2-chloroethyl) ethyleneoxyethylenediphosphate (Structure 5.2). A third member of the family (Structure 5.3), having additional pendant chloromethylene groups in the bridging segment of the diphosphate, was introduced into the market later on, has enhanced hydrolytic stability, and is useful in many types of flexible foams, as well as in adhesives and in epoxy- or phenolic-based laminates.

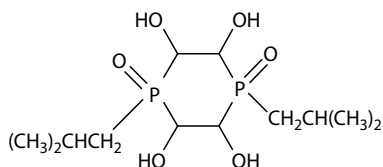
Pentaerythritol phosphate has an excellent char-forming ability owing to the presence of the pentaerythritol structure. The bis-melamine salt of the bis acid phosphate of pentaerythritol is also available commercially. This is a high melting solid that acts as an intumescent flame-retardant additive for polyolefins. Synergistic combinations with ammonium polyphosphates have also been developed primarily for urethane elastomers. Self-condensation of tris(2-chloroethyl) phosphate produces oligomeric 2-chloroethylphosphate. It has a low volatility, and is useful in resin-impregnated air filters, in flexible urethane foams and in other structural foams.¹¹

Cyclic oligomeric phosphonates with the varying degrees of structural complexity (Structure 5.4) are also available in the market.²⁵ They are widely used as flame-retardant finishes for polyester fabrics. After the phosphonate is applied from an aqueous solution, the fabric is heated to swell and soften the fibers, thus allowing the phosphonate to be absorbed and strongly held. It is also a useful retardant in polyester resins, polyurethanes, polycarbonates, polyamide-6, and in textile back coatings. A bicyclic pentaerythritol phosphate has been more recently introduced into the market for use in thermosets as well as for polyolefins (preferably, in combination with melamine or ammonium polyphosphate) (Structure 5.5). Cyclic neopentyl thiophosphoric anhydride

**STRUCTURE 5.5**

(Structure 5.6), a solid additive, is used to flame retard viscose rayon, especially in Europe. In spite of the anhydride structure, it is remarkably stable, surviving addition to the highly alkaline viscose, the acidic coagulating bath, and also resisting the multiple launderings of the rayon fabric.

**STRUCTURE 5.6**



STRUCTURE 5.7

5.4.4 PHOSPHINE OXIDES

Phosphine oxides have hydrolytically stable P–C bonds, whereas the P–O–C bond of phosphate esters hydrolyzes readily.²⁶ They also generally have higher phosphorus contents than the corresponding aromatic phosphate esters and, therefore, are more effective flame retardants. Triphenylphosphine oxide is disclosed in many patents as a flame retardant, and may find some limited usage as such a vapor-phase flame inhibitor. A phosphine oxide (Structure 5.7), incorporating hydroxyl groups, has been proposed as a flame retardant for use in polypropylene (PP). In spite of its high hydroxyl content, it is a relatively stable, high melting solid additive.

5.5 REACTIVE FLAME RETARDANTS

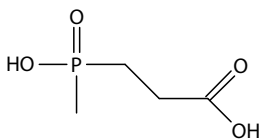
Reactive flame retardants, that is, those that are covalently attached to polymer chains, offer several advantages over those that are merely additives. For example, reactive flame retardants are inherently immobile within the polymer matrix and therefore will not be susceptible to loss during service through migration to the polymer surface (blooming) or solvent leaching. Reactive flame retardants incorporated at the time of the synthesis of the polymer also can be homogeneously dispersed throughout the polymer at the molecular level and because of this may be required at lower concentrations than comparable additives to give a desired level of flame retardance. The lower levels of incorporation of flame-retardant groups may bring with it an added advantage that the overall properties of the polymer (chemical, physical, and mechanical) are less likely to be adversely affected when compared with those of the nonflame retarded counterpart. Moreover, reactive flame retardants are prevented from forming a separate phase within the polymer matrix; this is particularly important in uses of polymers as fibers in which a heterogeneous phase structure is likely to bring with it problems during fiber spinning and reductions in the modulus of the resultant fibers.

However, the reactive incorporation of flame-retarding groups can also bring problems, not least the relative difficulty and expense of reactively modifying polymers for which commercially well-established methods for manufacturing the unmodified variants already exist. Furthermore, the extensive reactive modification of a partly crystalline polymer is likely to lead to a significant loss of crystallinity, whereas if an additive is introduced to a partly crystalline polymer, it will most probably end up in the amorphous phase and have little impact upon crystallinity (although it may plasticize the amorphous regions). Moreover, in general, the reactive modification of chain reaction polymers is less readily accomplished than for step reaction polymers, unless the reactive modification is applied after the manufacture of the primary chain, for example, through a post-polymerization grafting reaction. Grafting reactions may also be useful for covalently attaching flame-retardant groups to the surfaces of polymer-based plastics moldings, films, and fibers, where they will be particularly effective at the point of first impingement of any flame.

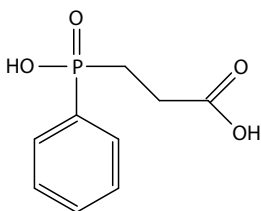
5.6 STEP-REACTION POLYMERS

5.6.1 POLYESTERS AND POLYCARBONATES

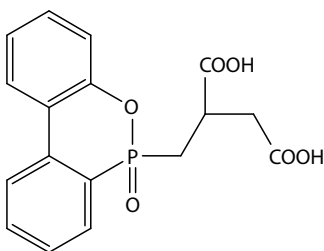
The most commercially important linear polyester is poly(ethylene terephthalate) (PET), used extensively as a fiber and as a film. A P-containing comonomer can be introduced into PET either as a diacidic component (or its diester derivative) or as a diol. In commercial practice, the former strategy has been preferred. Thus, flame retardancy has been achieved in commercial PET fibers by incorporation of 2-carboxyethyl(methyl)phosphinic acid (Structure 5.8), 2-carboxyethyl(phenyl) phosphinic acid (Structure 5.9), or their cyclic anhydrides. PETs based on the former are marketed under the trade name Trevira CS. It has been suggested that fibers containing either Structure 5.8 or Structure 5.9 might be further improved by the additional incorporation of aromatic dicarboxylic acid monomers to act as charring agents.²⁸ Another commercially utilized P-containing



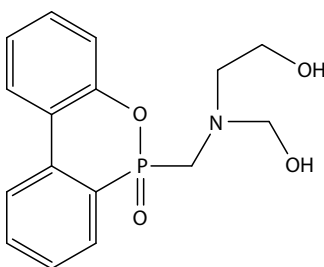
STRUCTURE 5.8



STRUCTURE 5.9



STRUCTURE 5.10



STRUCTURE 5.11

comonomer is the 9,10-dihydro-9-oxa-10-phosphaphenanthrenyl-10-oxide (DOPO) adduct of itaconic acid²⁹ (Structure 5.10). Filament fibers and fabrics based on PET copolymers containing this flame-retardant comonomer are commercially available from Toyobo under the trade name, HEIM, and have LOIs (limiting oxygen index) of up to 28.

It has been reported that the effectiveness of copolymerized DOPO-type monomers can be further improved if the alcohol-amine derivatives of DOPO, for example, Structure 5.11, are used rather than similar structures not containing nitrogen.³⁰ Of the FR fibers based on P-containing comonomers, it has been found that those based on Structure 5.10 are more hydrolytically stable, presumably because the P-containing group is in a cyclic structure and also should the hydrolysis of the P-O bond occur, it will not lead automatically to a marked reduction in molecular weight.³¹ All the P-modified PETs appear to be subject to both the vapor- and condensed-phase mechanisms of flame retardance, with the former predominating.^{32,33}

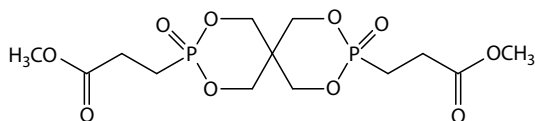
Other reactive P-containing comonomers reported to improve flame retardance in PET include aliphatic and alicyclic (spiro) bisphosphonates³⁴ such as Structure 5.12.

Poly(butylene terephthalate) (PBT) and poly(ethylene-2,6-naphthenate) (PEN) can be reactively flame retarded with the same types of reagent³⁵ as are used for PET, for example, Structure 5.10.

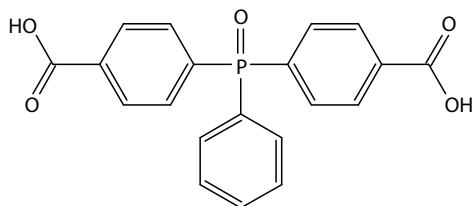
There have been some reports also of polycarbonates reactively modified with P-containing groups. For example, a novel P-containing copolycarbonate was prepared via the melt polycondensation of diphenyl carbonate, bisphenol A, and 2-(6-oxo-6H-dibenz[c,e][1,2]oxaphosphorin-6-yl)-1,4-benzenediol. This polycarbonate exhibited significantly a better flame retardancy, a higher char yield, a higher degradation temperature, and a better thermal stability than conventional bisphenol A polycarbonate.³⁶

5.6.2 POLYAMIDES

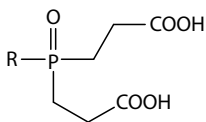
Reactive strategies, that is, chemical modifications, appear not to have been explored to a large extent as a route to improved flame retardance in aliphatic polyamides, probably because the chemical



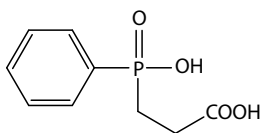
STRUCTURE 5.12



STRUCTURE 5.13



STRUCTURE 5.14



STRUCTURE 5.15

modification of aliphatic polyamides disrupts intermolecular hydrogen bonding and hence crystallinity, thus reducing melting points. Thus, although the reactive incorporation of bis(4-carboxyphenyl)phenylphosphine oxide (Structure 5.13) at up to 20 mol% into polyamide-6,6 gives flame-retardant polymers that are still partly crystalline, at 30 mol% incorporation, all crystallinity is lost.³⁷ Similar results have been observed with incorporated diphenylmethylphosphine oxide groups.³⁸

Aromatic polyamides modified with phosphine oxide groups have been synthesized also by condensation of bis(4-carboxyphenyl)phenylphosphine oxide but with various aromatic diamines.^{39,40}

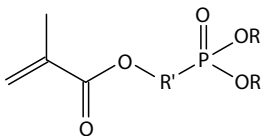
As yet, it is not clear that there has been any successful commercial production of flame-retarded polyamides incorporating P-containing reactives, although both Monsanto and Solutia have patented P-containing diacids (Structures 5.14 and 5.15, respectively) designed to replace some of the adipic acid in the manufacture of flame-retardant polyamide-6,6 for fibers.^{41,42}

5.7 CHAIN-REACTION POLYMERS

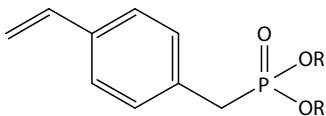
The most obvious way of reactively flame retarding a chain-reaction polymer is by incorporating a P-containing comonomer during polymerization. However, there have been no reports, to date, of significant commercial progress on this front, although a variety of chain reaction polymers have been reactively modified with P-containing groups on the laboratory scale and have been shown to be significantly flame retarded when compared with their unmodified counterparts. Some of these are discussed in the following text.

5.7.1 ACRYLICS

A variety of P-containing acrylates, methacrylates (Structure 5.16), and styrene derivatives (Structure 5.17) have been synthesized and copolymerized using free-radical initiators with methyl methacrylate (MMA)^{43–45} and acrylonitrile (AN).^{46,47} Copolymers of MMA with diethyl(methacryloyloxy)methyl phosphonate (DEMMP, Structure 5.16 with R = C₂H₅ and R' = CH₂), for example, have higher LOIs, the lower rates of heat release, the lower overall heats of combustion, and give a V0 rating in a UL94 protocol.⁴⁴ Other P-containing comonomers give similar improvements. Moreover,



STRUCTURE 5.16



STRUCTURE 5.17

these copolymers have transparencies comparable with that of poly(methyl methacrylate) (PMMA), are hydrolytically reasonably stable and have the physical and mechanical properties not significantly inferior to those of PMMA. Studies of the thermal degradation and combustion of some of these reactively modified PMMAs indicate that flame retardance involves both the vapor- and condensed-phase activity, with the latter leading to significant char production. Char production probably involves transesterification reactions and interchain cyclizations catalyzed by phosphonic acid groups liberated during combustion. The reactive route to flame retardance has been shown also to offer significant advantages over routes using analogous P-containing additives, in that additives tend to plasticize PMMA significantly and to give rise only to vapor-phase modes of flame retardance.^{5,27,43,45}

The incorporation of P-containing comonomers such as diethyl-*p*-vinylbenzene phosphonate (Structure 5.17 with R = C₂H₅) and acrylate and methacrylate phosphates and phosphonates (Structure 5.16) into polyacrylonitrile (PAN) also greatly increases char production during combustion. In this case, the P-containing comonomer appears to act by initiating the intramolecular cyclization of C≡N groups along the PAN chain leading to the well-known precursor structure to a graphitic char.^{46,47}

5.7.2 POLYSTYRENE

Monomers such as Structures 5.16 and 5.17 copolymerize, free radically, as readily with styrene as they do with MMA and give rise to products that are also significantly flame retarded. Flame retardance here too involves both the vapor- and condensed-phase action, with the condensed-phase activity leading to a significant char. In this case, char production is probably initiated by the Friedel–Crafts type condensation of phenyl groups, catalyzed by phosphorus acids liberated during combustion.^{43,48,49}

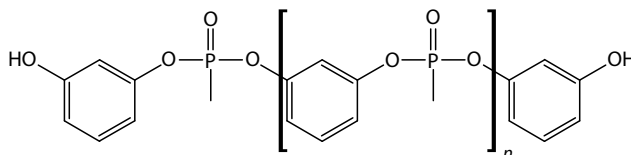
5.7.3 POLYOLEFINS

The reactive modification of polyolefins via copolymerization with P-containing monomers is not straightforward given the stringent conditions that pertain during the polymerization of olefin monomers, especially using organometallic coordination catalysts. However, both polyethylene (PE) and PP can be chemically modified after polymerization so as to introduce P-containing side groups. For example, PE has been oxidatively phosphorylated to give a polymer containing about 5 wt % P in –P(O)(OCH₃)₂ side groups. This polymer has an LOI significantly greater than that of unmodified PE but unfortunately the crystallinity is greatly reduced leading to the inferior physical and mechanical properties.⁵⁰

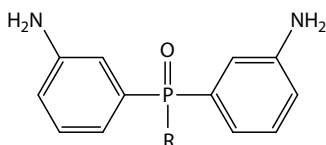
PP is commercially modified by radical grafting with maleic anhydride to give maleated PPs used as compatibilizers for additives such as nanoclays. Similar strategies can be used to graft P-containing monomers to PPs. These copolymers, when blended with virgin PP, also allow compatibilization with nanoclays but in addition work synergistically with the clays to improve flame retardance.⁵¹

5.8 THERMOSETS

In thermosetting systems, the reactive flame retardant can be incorporated either in one or more of the principal chain-forming components, or in the cross-linking agent. Both strategies have been employed with P-containing flame retardants in a variety of thermosets.



STRUCTURE 5.18



STRUCTURE 5.19

5.8.1 EPOXY RESINS

The major developments in reactive phosphorus-based flame retardants for epoxy resins to 2005 have been well reviewed.⁵² It will suffice here, therefore, to outline just the major developments and to highlight the most recent work.

Since the P–H bond (like N–H, O–H, and S–H) can add across an epoxy group with consequent ring-opening, hydrogen phosphonates or phosphinates can readily be incorporated covalently into epoxy resins. This reaction is currently widely used to incorporate DOPO (see Section 5.6.1) into epoxies destined for electronic applications.^{53–56} Reacting DOPO first with reagents such as *p*-benzoquinone or naphthaquinone gives (after mild reduction) diphenolic derivatives (e.g., DOPO-HQ) that can be incorporated in an epoxy resin through a conventional chain-extension process with no net loss of functionality.⁵⁷ The itaconic derivative of DOPO (Structure 5.10) used in the manufacture of flame-retardant polyesters can be cured also into epoxies^{58,59} as can dicyanate ester,⁶⁰ tris(4-aminophenyl) methyl,⁶¹ succinic anhydride,⁶² epoxy silane,⁶³ and oligomeric tricyanurate derivatives.⁶⁴

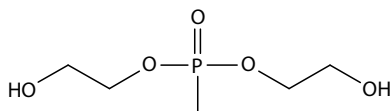
The major commercial alternative to DOPO and its derivatives for reactively flame retarding epoxy resins, especially for electronic applications, is an oligo(1,3-phenylene methylphosphonate) (Structure 5.18) marketed by Supresta under the tradename Fyrol PMP. Fyrol PMP has a functionality higher than that of DOPO and can be used either as a hardener (curing agent) or be precondensed with an epoxy.

Amino and functional aromatic phosphates, phosphonates, and phosphine oxides have also been used as reactive components to impart flame retardancy to cured epoxy resins. Phosphine oxides are particularly hydrolytically stable and several studies have been reported, for example, of the curing of epoxy resins with bis(aminophenyl) alkyl and aryl phosphine oxides^{65–67} (Structure 5.19). The relative performances of epoxies cured with aromatic diamine hardeners containing phosphine oxide, phosphinate, phosphonate, or phosphate units have recently been assessed.⁶⁸ Aromatic phosphine oxides have been functionalized also with maleimide and hydroxyl groups for use as epoxy resin hardeners.^{69,70}

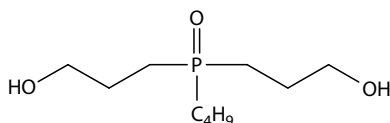
5.8.2 POLYURETHANES

Organophosphorus compounds, monomeric and oligomeric, additive and reactive, have a history of exploration, development, and use as flame retardants and anti-scorch agents in polyurethanes (PUs) dating back to the 1960s. This history, together with the pertinent details of mechanisms of the thermal degradation and combustion of polyurethanes has recently been comprehensively reviewed.^{71,72} It will thus suffice here merely to highlight the more important strategies that have been suggested and employed for reactively flame-retarding PUs with reactive organophosphorus compounds.

A common approach with segmented PUs has been to incorporate a P-containing group (phosphate, phosphonate, phosphine oxide, or phosphazene) into a diol which is then chain-extended with a diisocyanate (e.g., Structures, 5.20 and 5.21).^{73,74} In one such study,⁷⁵ phosphonate was found to be a more effective flame retardant than phosphate at the same phosphorus concentration, and in



STRUCTURE 5.20



STRUCTURE 5.21

another,⁷⁶ in-chain phosphorus to be more effective than phosphorus in a side chain. UV curable PUs containing reactively incorporated phosphorus have been synthesized from acrylate-ended species.⁷⁷ P-containing species can also be incorporated in PUs in curing. For example, P-containing aziridines have been suggested as curing agents for carboxylated PU aqueous dispersions used as surface coatings.^{78–80}

Some of the most critical applications of PUs are as foams for which flammability can be particularly high owing to their high surface areas and, in the case of flexible foams, their open-cell structures. Commercially, such foams are still flame retarded mainly with organophosphorus additives, albeit sometimes of high molecular weight. The use of high molecular weight additives is particularly important for foams used in automotive applications where the use of more volatile, low molecular weight, additives can lead to the excessive fogging of glass surfaces. Reactive organophosphorus flame retardants such as P-containing diols (e.g., Structure 5.20) have clear potential here.

5.8.3 UNSATURATED POLYESTERS

Clearly, P-containing unsaturated polyesters can readily be synthesized using many of the same P-containing diols and diacids used for constructing P-containing saturated polyesters and polyurethanes. However, such reagents have not found commercial favor for use in unsaturated polyester resins, either as components of the main polyester chain or as components of the cross-linking vinyl monomer system. This has been ascribed to the general poor hydrolytic stability of aliphatic polyesters based on P-containing diols and diacids, and on the poor free-radical copolymerizability of readily available P-containing cross-linking monomers, such as vinyl phosphonates.⁸¹ Nevertheless, there are a number of P-containing acrylates, methacrylates, and styrenes now available, at least on a laboratory scale (e.g., Structures 5.16 and 5.17), that copolymerize more readily than vinyl phosphonates, so this is an area that might repay further work.

5.9 SURFACE GRAFTING

Given that pyrolysis, ignition, and combustion affects first the surface of a polymeric material, it is sensible to ask whether or not flame-retardant treatments might optimally be applied to the surfaces of materials, especially in cases in which the surface to volume ratios are high, for example, films, fibers, and textiles. A number of interesting studies have been reported in this regard in which, for example, radical graft copolymerizations have been used to attach P-containing monomer units to the surfaces of cotton fabrics to impart flame retardancy.^{82,83} Cotton surfaces have also been grafted with P-containing monomers by plasma polymerization as have the surfaces of PAN fabrics.^{84,85}

5.10 MECHANISMS OF FLAME RETARDANCE: GENERAL CONSIDERATIONS

When subjected to a sufficient length of time to an external heat source, organic polymeric materials undergo thermal degradation, generating various products in varying concentrations over different temperature ranges. The chemical steps leading to the formation of volatiles may be homolytic or heterolytic, that is, be radical or ionic.¹² The three overall processes implicated in the thermal degradation of most thermoplastic polymers are as follows:

1. Random chain cleavage followed by chain unzipping is characterized by high monomer yields and a slow decrease in the molecular weight of the polymer, for example, exhibited by PMMA, poly(α -methyl styrene), polystyrene polytetrafluoroethylene.
2. Random chain cleavage followed by further chain scission is characterized by very low monomer yields among the degradation products and a rapid drop in molecular weight, for example, exhibited by PE, PP, poly(methyl acrylate), and polychlorotrifluoroethylene.
3. An intra-chain chemical reaction is followed by a cross-linking reaction and the formation of a carbonaceous residue, or a random chain cleavage. This generates a relatively high yield of volatiles from the intra-chain reaction, but produces little monomer, and produces, no, or only a very slight, reduction in molecular weight during the initial stages of degradation, for example, exhibited by poly(vinyl chloride), poly(vinyl alcohol), and PAN.

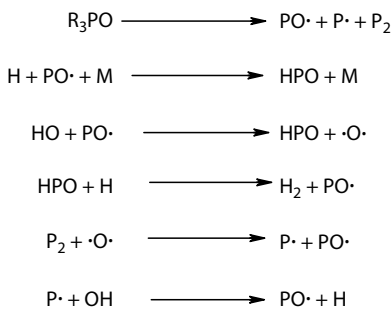
In some cases, several of these processes occur simultaneously, depending on the sample size, the heating rate, the pyrolysis temperature, the environment, and the presence of any additives. Although polymer degradation schemes can be greatly altered by the presence of comonomers, side-chain substituents, and other chemical constituent factors, the ultimate thermal stability is determined by the relative strengths of the main-chain bonds. Many additives and comonomers employed as flame retardants are thermally labile and as a result the thermal stability of the polymer system is reduced. In order to reduce the observed effects of the flame-retardant additives on the thermal stability of the polymeric materials, more thermally stable and hence inherently flame-resistant polymers are of increasing interest.

Thermosets, on the other hand, owing to their highly cross-linked three-dimensional nature, have a much lesser propensity to thermally degrade (especially at lower temperatures) to yield flammable volatiles. The rupture of bonds does not initially generate combustible gases, and carbonization is usually promoted. Ladder polymers, in which the main chains are bonded together at each repeat unit by a cross-link, show similar behavior. Polymers with relatively strong main-chain bonds and/or with aromatic and heterocyclic structural units are also inherently thermally stable.⁸⁶ There are several classes of polymers, such as polyphenylenes, poly(*p*-phenylene oxide)s, polybenzimidazoles, and polybenzamides, which have relatively high thermal decomposition temperatures coupled to low levels of fuel production on degradation.

The ability to form char is related to the flammability of a polymer. The higher the amount of residual char after combustion, the lower the amount of combustible material available to perpetuate the flame and the greater is the degree of flame retardance of the material.⁸⁷ Therefore, one of the ways to achieve high degrees of flame retardancy or noncombustibility of a polymeric material is to increase the amount of char produced on combustion. This is illustrated by the fact that aromatic polymers, for example, polycarbonate and poly(phenylene oxide), have lower flammabilities than purely aliphatic polymers. The greater thermal stability of cross-linked and aromatic structures in thermosets gives rise to a greater degree of condensation into an aromatic char, and therefore only relatively low levels of flammable gases are available to feed the flame.

5.10.1 MECHANISMS OF FLAME RETARDANCE BY PHOSPHORUS COMPOUNDS

Phosphorus-containing fire retardants can be active in the condensed phase or in the vapor phase, or in both phases.⁸⁸ The relative predominance of the different mechanisms actually operating in a



SCHEME 5.1 Elementary steps involved in vapor-phase flame retardation by triphenylphosphine oxide and triphenyl phosphate (**M** is a third body species).

particular system depends on the structural features of the base polymer as well as on the chemical environment of the phosphorus, that is, whether phosphorus is in the elemental state or, if present as a compound, the valency and the nature of the chemical moieties surrounding the P atom. Physical and chemical actions have also been implicated in both phases. These could involve flame inhibition, heat loss owing to melt flow, surface protection by phosphorus-containing acids, acid catalyzed char accumulation, char enhancement, and the protection of char from oxidation. Flame-retardant mechanisms can also be influenced by the presence of other additives, for example, the synergistic combinations of co-additives such as compounds of nitrogen or halogens.

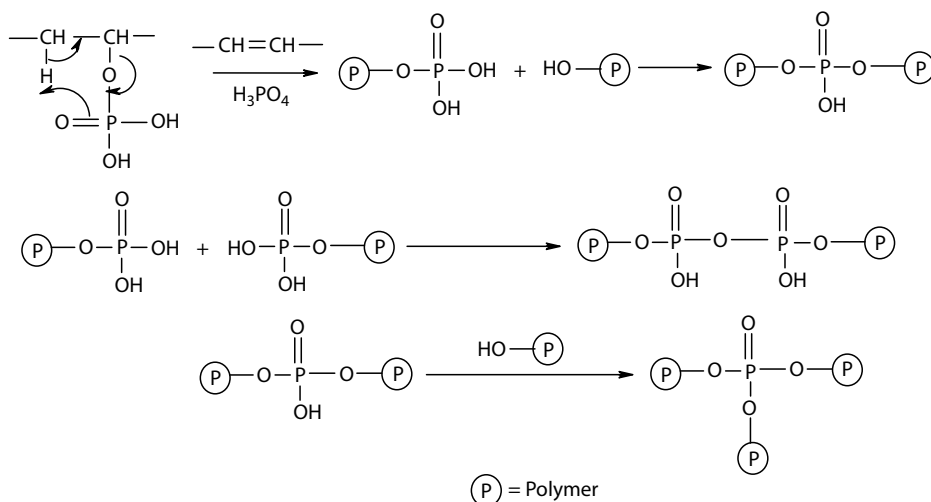
A predominantly vapor-phase mechanism of flame retardation has been proposed for flame retardants based on triphenylphosphine oxide and triphenyl phosphate has been proposed (Scheme 5.1).

The salient features of these reactions are the promotion of hydrogen recombination and the scavenging of oxygen radicals by molecular phosphorus. This in turn will reduce the number of effective flame propagating radical species below the level at which the flame can be sustained.²⁶

A classical and thoroughly investigated example, which amply illustrates the condensed-phase activity of phosphorus flame retardant, is the flame retardation of cellulosic substrates with phosphoric acid and/or its organic/inorganic esters.⁸⁹ In the presence of phosphoric acid and/or its organic and inorganic esters, or compounds having P–O–C bonds, the phosphorylation of cellulose occurs predominantly at the C-6 hydroxyls. This in turn alters the degradation pathway of cellulose at the C-6 hydroxyls, where instead of the depolymerization reactions, the dehydration of the cellulose substrate occurs, thus, leading to enhanced char production. Similar explanations can be given for P–N synergism in cellulose. The polar nature of P–N bond, as compared with P–C and P–O bonds, would result in the enhanced rates of phosphorylation at the cellulose hydroxyls. Thus, the formation of P–N bonds in situ increases the reactivity of the phosphorus compound toward the cellulose hydroxyls, leading to a reduction in volatiles and a corresponding increase in char formation.

Another mode of action in which phosphorus is important as a char promoter is in intumescent fire-retardant paints and mastics.⁹⁰ These typically have a phosphorus compound, such as ammonium phosphate; a char forming polyol, such as pentaerythritol; a blowing agent, such as melamine; and a binder. On decomposition, the phosphorus compound provides the phosphorylating agent that in turn reacts with the pentaerythritol to form polyol phosphates, which then break down to char through a series of elimination steps. The spumific agent will endothermally decompose to form gaseous products that will expand the char already formed.

Phosphorylated poly(vinyl alcohol) and ethylene-vinyl alcohol polymers were found to be significantly flame retarded as compared to their unmodified parent polymers.⁵⁰ The flame retardance in these systems is shown to arise primarily from a condensed-phase mechanism involving dehydration, cross-linking, and char formation (Scheme 5.2). The authors have also reported that phosphorylation of PE, achieved through the reaction of molecular oxygen with a solution of the polymer in PCl_3 , resulted in significant improvements in the flame retardance. However, the higher degrees of



SCHEME 5.2 Formation of phosphorus anhydride cross-links in phosphorylated poly(vinyl alcohol).

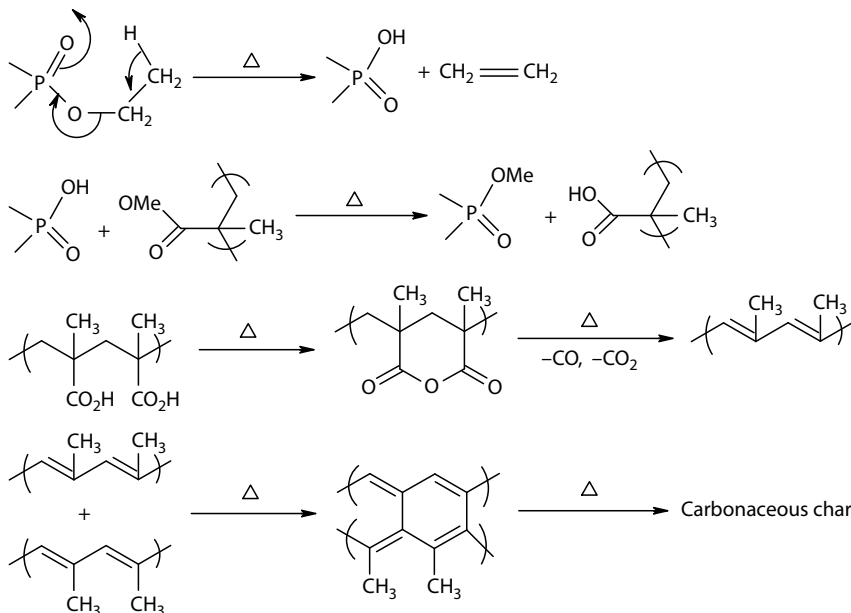
phosphonylation of PE (above 10 mol% or above) resulted in reduced crystallinity and, as a consequence, its physical and mechanical properties were substantially impaired. The flame retardance of the modified PE is believed to arise, at least in part, through a vapor-phase mechanism.

A systematic exploration of the effects of incorporating various phosphorus-containing comonomer units on the flame retardance, particularly of polystyrene and PMMA, has been reported.⁶ It is found that the introduction of phosphorus, irrespective of its chemical environment within the comonomer unit, increases flame retardance to a significant degree and also leads to enhanced production of char. Phosphorus retention in the char residues of the modified systems was also found to be significant, suggesting a predominant element of condensed-phase activity of the phosphorus-containing groups. In addition, copolymers of acrylamide with phosphorus-containing comonomers appear to display considerable nitrogen–phosphorus synergism.⁹¹

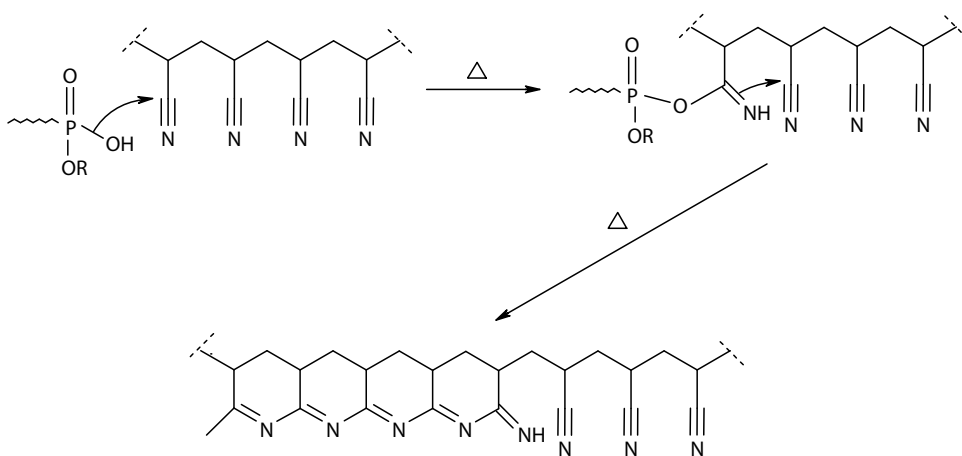
The mechanistic studies of thermal degradation and flame retardance in some copolymers of MMA containing pendant phosphonate ester groups were performed using analyses of the gaseous products of degradation and through the spectroscopic examinations of solid residues.⁴³ Flame retardance in these systems is believed to occur by a combination of vapor-phase processes and condensed-phase activity, that is, char formation. The condensed-phase mechanism is believed to involve the generation of phosphonic acid species and their subsequent reactions with the MMA units to give methacrylic anhydride units, which then decarboxylate en route to forming char (Scheme 5.3).

Condensed-phase activity of phosphorus-containing covalently bound groups is also reported for chemically modified PAN polymers.^{47,92} It is shown that, in these systems, the intramolecular cyclization of the pendant nitrile groups is greatly favored, which in turn decreases the production of combustible volatiles including the monomer in the initial stages of the thermal degradation of the copolymer. The mechanistic pathway involves the thermal cracking of the pendant phosphorus groups to produce phosphorus acid species. These species later acts as nucleophilic centers, aiding the cyclization processes (Scheme 5.4). Thus, the condensed-phase activity of the modifying groups in PAN, in enhancing the extent of intramolecular cyclization, leads to increased production of char.

The predominant mode of action of phosphorus-containing flame retardants (both additives and reactives), when present in thermoplastics or thermosets, is considered to be in the condensed phase. Generally, as with cellulose, flammable gas generation is reduced and char formation is promoted. In some cases, the char cohesiveness is also enhanced. The retention of phosphorus in the chars in



SCHEME 5.3 Suggested mechanism for char formation in methacrylate/phosphonate ester copolymer.



SCHEME 5.4 Cyclization of polyacrylonitrile initiated by a nucleophilic phosphorus-containing species.

these systems is also generally high. Furthermore, vapor-phase inhibitory mechanisms alone cannot account for the very high flame-retardant efficiencies observed, even in polymers with nominal char formation tendency.⁴⁸ For example, in polystyrenes, phosphorus compounds can affect the burning behavior by altering the gas generation rate.⁴⁹

The mechanistic details of flame-retardant synergism in phosphorus-halogen have not been as well studied when compared with phosphorus–nitrogen systems.¹⁵ In the case of halogen-containing organophosphorus fire retardants, the formation of phosphorus halides and oxyhalides is implicated. Other proposed mechanisms involve nominal condensed-phase activity of halogens coupled to an enhanced vapor-phase activity for the phosphorus in the presence of the halogen compounds. In the absence of any clearly established mechanistic pathways, it is sensible to assume that halogens and phosphorus will generally act more or less independently of each other when they are present together.

Physical effects such as those involving an increased heat capacity, the heat of vaporization, and an endothermic dissociation in the vapor phase, may make a nominal, but recognizable, contribution to the overall efficacies of various phosphorus-based flame-retardant systems.³ These types of mode of actions, especially in the vapor phase, become more important in the case of readily volatile additives. An example is the case of tris(dichloroisopropyl) phosphate, which is used to flame retard flexible urethane foam. Phosphorus acid species, particularly phosphoric acid and its oligomers, can form a protective layer over a decomposing polymer matrix; this essentially acts as an oxygen-excluding physical barrier, thus protecting the underlying unburnt polymer.

5.11 CONCLUDING REMARKS AND FUTURE TRENDS

It has been seen that a wide variety of phosphorus compounds have been explored, both as additives and reactive components, for the flame retardation of a wide range of polymers, both thermoplastics and thermosets. As yet, however, the commercial exploitation of phosphorus-based flame-retardant systems is still somewhat in its infancy, with halogen-containing flame retardants still dominating the market. Mostly this is a consequence of the generally higher cost of phosphorus-based materials, especially organophosphorus compounds, and the lower flame-retardant efficiency of many. As environmental pressures to reduce the use of halogenated organic flame retardants increase, as they almost certainly will, it is likely that the commercial exploitation of phosphorus-containing alternatives will increase, bringing with it economies of scale and reduced costs. In the interim period, the use of phosphorus compounds in combination with established halogenated flame retardants is likely to increase, leading at least to some reductions in the overall use of the latter.

The use of phosphorus-based flame retardants in combination with other, better established, flame retardants is most effective in situations in which the combination proves synergistic. However, as yet our understanding of such synergistic effects is far from complete and more fundamental work is required in this area: Work in which the gaseous and solid products of combustion, with and without the presence of flame retardants, are carefully analyzed. Such analyses can now be undertaken more readily than in the past, owing to the relatively recent development of techniques such as gas-phase FT-infrared spectroscopy and laser-pyrolysis time-of-flight mass spectrometry for the identification of volatiles, and solid-state NMR spectroscopy and x-ray photoelectron spectroscopy for the analysis of chars.

Perhaps the most exciting developments, however, are likely to be in the increasing use of various nanoscopic additives, such as nanoclays and carbon nanotubes, in combination with both halogenated and phosphorus-containing flame retardants. Moreover, we are likely to see increased emphasis on the topical treatments of polymeric materials with flame-retardant chemicals. Such treatments, involving conventional chemical or physical processes, are already well-established in the textile arena, but will be augmented by more technologically advanced processes, such as those involving plasma polymerizations. Surface treatments in which a flame-retardant barrier layer is laid down by plasma polymerization could be particularly effective for polymeric materials having high surface-to-volume ratios, such as fibers and films.

REFERENCES

1. Gilman, J. W., Flammability and thermal stability studies of polymer layered-silicate (clay) nanocomposites, *Appl. Clay Sci.*, 1999, 15, 31–49.
2. Moniruzzaman, M. and Winey, K. I., Polymer nanocomposites containing carbon nanotubes, *Macromolecules*, 2006, 39, 5194–5204.
3. Levchik, S. V. and Weil, E. D., A review of recent progress in phosphorus-based flame retardants, *J. Fire Sci.*, 2006, 24, 345–364.
4. Lewin, M. and Weil, E. D., Mechanisms and modes of action in flame retardancy of polymers, in *Fire Retardant Materials*, Horrocks, A. R. and Price, D. (Eds.), 2000, Woodhead Publishing Limited, Cambridge, U.K., pp. 31–68.

5. Price, D., Bullett, K. J., Cunliffe, L. K., Hull, T. R., Milnes, G. J., Ebdon, J. R., Hunt, B. J., and Joseph, P., Cone calorimetry studies of polymer systems flame retarded by chemically bonded phosphorus, *Polym. Degrad. Stab.*, 2005, 88, 74–79.
6. Ebdon, J. R., Price, D., Hunt, B. J., Joseph, P., Gao, F. G., Milnes, G. J., and Cunliffe, L. K., Flame retardance in some polystyrenes and poly(methyl methacrylate)s with covalently bound phosphorus-containing groups: Initial screening experiments and some laser pyrolysis mechanistic studies, *Polym. Degrad. Stab.*, 2000, 69, 267–277.
7. Muir, D. C. G., Anthropogenic compounds, in *Handbook of Environmental Chemistry*, Vol. 3, Hutzinger, O. (Ed.), 1984, Springer-Verlag, Berlin, Germany, pp. 41–66.
8. Hasegawa, H. K., *Characterisation and Toxicity of Smoke*, Publication STP 1082, 1990, American Association for Testing and Materials, Philadelphia, PA.
9. Rossotti, H., *Diverse Atoms: Profiles of the Chemical Elements*, 1998, Oxford University Press, Oxford, U.K.
10. Greenwood, N. N. and Earnshaw, A., *Chemistry of Elements*, 1984, Pergamon Press, Oxford, U.K., pp. 546–636.
11. Green, J., A review of phosphorus containing flame retardants, *J. Fire Sci.*, 1996, 13, 353–366.
12. Joseph, P. and Ebdon, J. R., Recent developments in flame-retarding thermoplastics and thermosets, in *Fire Retardant Materials*, Horrocks, A. R. and Price, D. (Eds.), 2000, Woodhead Publishing Limited, Cambridge, U.K., pp. 220–263.
13. Ebdon, J. R., Hunt, B. J., Joseph, P., and Konkel, C. S., Flame-retarding thermoplastics: Additive versus reactive approach, in *Speciality Polymer Additives: Principles and Applications*, Al-Malaika, S., Golvoy, A., and Wilkie, C. A. (Eds.), 2001, Blackwell Science, Oxford, U.K., pp. 231–257.
14. Kannan, P. and Kishore, K., Novel flame retardant polyphosphoramidate esters, *Polymer*, 1992, 33, 412–422.
15. Green, J., A phosphorus-bromine flame-retardant for engineering thermoplastics: A review, *J. Fire Sci.*, 1994, 12, 38–408.
16. Troitzsch, J. H., Methods for the fire protection of plastics and coatings by flame-retardant and intumescent systems, *Progr. Org. Coatings*, 1983, 11, 41–69.
17. Kandola, B. K., Nanocomposites, in *Fire Retardant Materials*, Horrocks, A. R. and Price, D. (Eds.), 2000, Woodhead Publishing Limited, Cambridge, U.K., pp. 204–219.
18. Weil, E. D., Formulations and modes of action of red phosphorus, *Proceedings of the Conference on Recent Advances in Flame Retardancy of Polymeric Materials*, Business Communication Corporation, Stamford, CT, 2000.
19. Levchik, S. V., Levchik, G. F., Balanovich, A. I., Camino, G., and Costa, L., Mechanistic study of combustion performance and thermal decomposition behaviour of Nylon 6 with added halogen-free fire retardants, *Polym. Degrad. Stab.*, 1996, 54, 217–222.
20. Weil, E. D., Recent developments in phosphorus flame retardants, *Proceedings of 3rd Beijing International Symposium on Flame Retardants and Flame Retardant Materials*, 1999, Beijing, China, pp. 177–183.
21. Horrocks, A. R., Flame retarding finishing for textiles, *Revs. Prog. Colouration*, 1986, 16, 62–101.
22. Caze, C., Devaux, E., Testard, G., and Reix, T., New intumescent systems: An answer to the flame retardant challenges in the textile industry, in *Fire Retardancy of Polymers: The Use of Intumescence*, Le Bras, M., Camino, G., Bourbigot, S., and Delobel, R. (Eds.), 1998, Royal Society of Chemistry, London, pp. 363–375.
23. Scharf, D., *Fire Retardant Engineering Polymers and Alloys*, Fire Retardant Chemicals Association, 1989, Lancaster, U.K., pp. 183–202.
24. Nelson, G. (Ed.), *Fire and Polymers*, American Chemical Society Symposium Series: 425, 1990, Washington.
25. Weil, E. D., Flame retardants: Phosphorus compounds, in *Kirk-Othmer Encyclopedia of Chemical Technology*, 4th edn., Howe-Grant, M. (Ed.), Vol. 10, 1993, Wiley-Interscience, New York, pp. 976–979.
26. Green, J., Phosphorus-containing flame retardants, in *Fire Retardancy of Polymeric Materials*, Grand, A. F. and Wilkie, C. A. (Eds.), 2000, Marcel Dekker, New York, pp. 147–170.
27. Price, D., Pyrah, K., Hull, T. R., Milnes, G. J., Ebdon, J. R., Hunt, B. J., and Joseph, P., Flame retardance of poly(methyl methacrylate) modified with phosphorus-containing compounds, *Polym. Degrad. Stab.*, 2002, 77, 227–233.
28. Asrar, J., Berger, P. A., and Hurlbut, J., Synthesis and characterization of a fire-retardant polyester: Copolymers of ethylene terephthalate and 2-carboxyethyl(phenylphosphinic) acid, *J. Polym. Sci., Polym. Chem. Edit.*, 1999, 37, 3119–3128.
29. Endo, S., Kashihara, T., Osako, A., Shizuki, T., and Ikegami, T., (Toyo Boseki Kabushiki Kaisha), Phosphorus-containing compounds, U.S. Patent, 1978: 4 127 590.

30. Kim, Y. C., (Kolon Industries, Inc.), Phosphorus-containing nitrogen compounds as flame retardants and synthetic resins containing them, U.S. Patent, 1988: 4 742 088.
31. Sato, M., Endo, S., Araki, Y., Matsuoka, G., Gyobu, S., and Takeuchi, H., The flame-retardant polyester fiber: Improvement of hydrolysis resistance, *J. Appl. Polym. Sci.*, 2000, 78, 1134–1138.
32. Day, M., Suprunchuk, T., and Wiles, D. M., Combustion and pyrolysis of poly(ethylene terephthalate) II. Study of the gas-phase inhibition reactions of flame retardant systems, *J. Appl. Polym. Sci.*, 1981, 26, 3085–3098.
33. Chang, S. J. and Chang, F. C., Synthesis and characterization of copolyesters containing the phosphorus linking pendent groups, *J. Appl. Polym. Sci.*, 1999, 72, 109–122.
34. Murayama, K. and Kashiwara, T., (Toyo Boseki Kabushiki Kaisha), Flame resistant polyesters, U.S. Patent, 1978: 4 086 208.
35. Wang, C. S. and Lin, C. H., Synthesis and properties of phosphorus-containing PEN and PBN copolyesters, *Polymer*, 1999, 40, 747–757.
36. Wang, C. S. and Shieh, J. Y., Synthesis and flame retardancy of phosphorus containing polycarbonate, *J. Polym. Res. (Taiwan)*, 1999, 6, 149–154.
37. Wan, I. Y., McGrath, J. E., and Kashiwagi, T., Triarylphosphine oxide containing nylon-6,6 copolymers, *ACS Symp. Ser.*, 1995, 599, 29–40.
38. Wan, I. Y. and McGrath, J. E., Synthesis and characterization of diphenylmethylphosphine oxide containing nylon-6,6 copolymers, *Abstracts of Papers of the American Chemical Society*, 1995, 209(2), 119.
39. Delaviz, Y., Gungor, A., McGrath, J. E., and Gibson, H. W., Soluble phosphine oxide containing aromatic polyamides, *Polymer*, 1993, 34, 210–213.
40. Zhang, Y. H., Tebby, J. C., and Wheeler, J. W., Polyamides incorporating phosphine oxide groups. 1. Wholly aromatic polymers, *J. Polym. Sci., Part A, Polym. Chem.*, 1996, 34, 1561–1566.
41. Pickett, Jr., O. A. and Stoddard, J. W., Phosphorus-containing copolyamides and fibers thereof, U.S. Patent, 1977: 4 032 517.
42. Asrar, J., (Solutia Inc.), Polymer-bound non-halogen fire resistant compositions, U.S. Patent, 1988: 5 750 603.
43. Ebdon, J. R., Hunt, B. J., Joseph, P., Konkel, C. S., Price, D., Pyrah, K., Hull, T. R., Milnes, G. J., Hill, S. B., Lindsay, C. I., McCluskey, J., and Robinson, I., Thermal degradation and flame retardance in copolymers of methyl methacrylate with diethyl(methacryloyloxymethyl)phosphonate, *Polym. Degrad. Stab.*, 2000, 70, 425–436.
44. Price, D., Pyrah, K., Hull, T. R., Milnes, G. J., Ebdon, J. R., Hunt, B. J., Joseph, P., and Konkel, C. S., Flame retarding poly(methyl methacrylate) with phosphorus-containing compounds: Comparison of an additive with a reactive approach, *Polym. Degrad. Stab.*, 2001, 74, 441–447.
45. Price, D., Pyrah, K., Hull, T. R., Milnes, G. J., Wooley, W. D., Ebdon, J. R., Hunt, B. J., and Konkel, C. S., Ignition temperatures and pyrolysis of a flame-retardant methyl methacrylate copolymer containing diethyl(methacryloyloxymethyl)-phosphonate units, *Polym. Int.*, 2000, 49, 1164–1168.
46. Crook, V. L., Flame retardant acrylonitrile copolymers, Ph.D. Diss., 2004, University of Sheffield, Sheffield, U.K.
47. Wyman, P., Crook, V., Ebdon, J., Hunt, B., and Joseph, P., Flame-retarding effects of dialkyl-p-vinylbenzyl phosphonates in copolymers with acrylonitrile, *Polym. Int.*, 2006, 55, 764–771.
48. Price, D., Cunliffe, L. K., Bullett, K. J., Hull, T. R., Milnes, G. J., Ebdon, J. R., Hunt, B. J., and Joseph, P., Thermal behaviour of covalently bonded phosphate and phosphonate flame retardant polystyrene systems, *Polym. Degrad. Stab.*, 2007, 92, 1101–1114.
49. Price, D., Cunliffe, L. K., Bullett, K. J., Milnes, G. J., Ebdon, J. R., Hunt, B. J., and Joseph, P., Thermal behaviour of covalently bonded phosphonate flame-retarded poly(methyl methacrylate) systems, *Polym. Adv. Technol.*, 2008, 19, 710–723.
50. Banks, M., Ebdon, J. R., and Johnson, M., Influence of covalently bound phosphorus-containing groups on the flammability of poly(vinyl alcohol), poly(ethylene-co-vinyl alcohol) and low-density polyethylene, *Polymer*, 1993, 34, 4547–4556.
51. Kandola, B. K., Smart, G., Horrocks, A. R., Joseph, P., Zhang, S., Hull, T. R., Ebdon, J., Hunt, B., and Cook, A., Effect of different compatibilisers on nanoclay dispersion, thermal stability, and burning behavior of polypropylene-nanoclay blends, *J. Appl. Polym. Sci.*, 2008, 108, 816–824.
52. Levchik, S., Piotrowski, A., Weil, E., and Yao, Q., New developments in flame retardancy of epoxy resins, *Polym. Degrad. Stab.*, 2005, 88, 57–62.
53. Wang, C. S. and Lin, C. H., Synthesis and properties of phosphorus containing epoxy resins by novel method, *J. Polym. Sci., Polym. Chem.*, 1999, 37, 3903–3909.

54. Wang, C. S. and Lin, C. H., (National Science Council, Taiwan), Epoxy resin rendered flame retardant by reaction with 9,10-dihydro-9-oxa-10-phosphaphenanthrene-10-oxide, U.S. Patent, 2001: 6 291 627.
55. Lin, C. H. and Wang, C. S., Novel phosphorus-containing epoxy resins part I: Synthesis and properties, *Polymer*, 2001, 42, 1869–1878.
56. Lin, C. H. and Wang, C. S., Halogen-free FR-4 printed circuit board, *ACS Polym. Prepr.*, 2002, 43(2), 908–909.
57. Wang, C. S. and Lee, M. C., Synthesis and properties of epoxy resins containing 2-(6-oxid-6H-dibenz(c,e)(1,2) oxaphosphorin-6-yl) 1,4-benzenediol (II), *Polymer*, 2000, 41, 3631–3638.
58. Lin, C. H., Wu, C. Y., and Wang, C. S., Synthesis and properties of phosphorus-containing advanced epoxy resins II, *J. Appl. Polym. Sci.*, 2000, 78, 228–235.
59. Hörold, S. and Kleiner, H. J., (Clariant GmbH), Phosphorus-containing dicarboxylic reaction product of epoxy resins and phosphorus acid (anhydride) with hardener, U.S. Patent, 1999: 5 959 043.
60. Lin, C. H., Synthesis of novel phosphorus-containing cyanate esters and their curing reaction with epoxy resin, *Polymer*, 2004, 45, 7911–7926.
61. Lin, C. H., Cai, S. X., and Lin, C. H., Flame-retardant epoxy resins with high glass-transition temperatures. II. Using a novel hexafunctional curing agent: 9,10-dihydro-9-oxa-10-phosphaphenanthrene 10-yl-tris(4-aminophenyl) methane, *J. Polym. Sci., Part A: Polym. Chem.*, 2005, 43, 5971–5986.
62. Cho, C. S., Fu, S. C., Chen, L. W., and Wu, T. R., Aryl phosphinate anhydride curing for flame retardant epoxy networks, *Polym. Int.*, 1998, 47, 203–209.
63. Hou, M., Liu, W., Su, Q., and Liu, Y., Studies on the thermal properties and flame retardancy of epoxy resins modified with polysiloxane containing organophosphorus and epoxide groups, *Polym. J. (Japan)*, 2007, 39, 696–702.
64. Perez, R. M., Sandler, J. K. W., Altstaedt, V., Hoffmann, T., Pospiech, D., Artner, J., Ciesielski, M., Doering, M., Balabanovich, A. I., and Schartel, B., Effective halogen-free flame retardancy for a mono-component polyfunctional epoxy using an oligomeric organophosphorus compound, *J. Mater. Sci.*, 2006, 41, 8347–8351.
65. Levchik, S. V., Camino, G., Luda, M. P., Costa, L., Muller, G., and Costes, B., Epoxy resins cured with aminophenylmethylphosphine oxide I: Combustion performance, *Polym. Adv. Technol.*, 1996, 7, 823–830.
66. Shau, M. D. and Wang, T. S., Synthesis, structure, reactivity, and thermal properties of new cyclic phosphine oxide epoxy resins cured by diamines, *J. Polym. Sci., Polym. Chem.*, 1996, 34, 387–398.
67. Levchik, S. V., Camino, G., Luda, M. P., Costa, L., Muller, G., and Costes, B., Epoxy resins cured with aminophenylmethylphosphine oxide: Mechanism of thermal decomposition, *Polym. Degrad. Stab.*, 1998, 60, 169–183.
68. Perez, R. M., Sandler, J. K. W., Altstaedt, V., Hoffmann, T., Pospiech, D., Artner, J., Ciesielski, M., Doering, M., Balabanovich, A. I., Knoll, U., Braun, U., and Schartel, B., Novel phosphorus-containing hardeners with tailored chemical structures for epoxy resins: Synthesis and cured resin properties, *J. Appl. Polym. Sci.*, 2007, 105, 2744–2759.
69. Jeng, R. J., Lo, G. S., Chen, C. P., Liu, Y. L., Hsiue, G. H., and Su, W. C., Enhanced thermal properties and flame retardancy from a thermosetting blend of a phosphorus-containing bismaleimide and epoxy resins, *Polym. Adv. Technol.*, 2003, 14, 147–156.
70. Ren, H., Sun, J., Wu, B., and Zhou, Q., Synthesis and properties of a phosphorus-containing flame retardant epoxy resin based on bisphenoxy(3-hydroxy) phenyl phosphine oxide, *Polym. Degrad. Stab.*, 2007, 92, 956–961.
71. Levchik, S. V. and Weil, E. D., Thermal decomposition, combustion and fire-retardancy of polyurethanes: A review of the recent literature, *Polym. Int.*, 2004, 53, 1585–1610.
72. Weil, E. D. and Levchik, S. V., Commercial flame retardancy of polyurethanes, *J. Fire Sci.*, 2004, 22, 183–210.
73. Witte, A. and Krieger, W., (Clariant GmbH), Halogen-free, pentane-blown, flame-retardant rigid polyurethane foam and a process for its production, U.S. Patent, 2001: 6 593 385.
74. Lee, F. T., Green, J., and Gibilisco, R. D., Recent developments using phosphorus-containing diol as a reactive combustion modifier for rigid polyurethane foams 3, *J. Fire Sci.*, 1984, 2, 439–453.
75. Yanchuk, N. I., Fireproof phosphorus-containing polyurethanes, *Khim. Technol. (Kiev)*, 1981, (1), 56–58.
76. Wang, T. L., Cho, Y. L., and Kuo, P. L., Flame-retarding materials II. Synthesis and flame-retarding properties of phosphorus-on-pendent and phosphorus-on-skeleton polyols and the corresponding polyurethanes, *J. Appl. Polym. Sci.*, 2001, 82, 343–357.

77. Huang, W. K., Chen, K. J., Yeh, J. T., and Chen, K. N., Curing and combustion properties of a PU-coating system with UV-reactive phosphazene, *J. Appl. Polym. Sci.*, 2002, 85, 1980–1991.
78. Shao, C. H., Huang, J. J., Chen, G. N., Yeh, J. T., and Chen, K. N., Thermal and combustion behaviors of aqueous-based polyurethane system with phosphorus and nitrogen containing curing agent, *Polym. Degrad. Stab.*, 1999, 65, 359–371.
79. Wang, T. Z. and Chen, K. N., Introduction of covalently bonded phosphorus into aqueous-based polyurethane system via postcuring reaction, *J. Appl. Polym. Sci.*, 1999, 74, 2499–2509.
80. Huang, W. K., Yeh, J. T., Chen, K. J., and Chen, K. N., Flame retardation improvement of aqueous-based polyurethane with aziridinyl phosphazene curing system, *J. Appl. Polym. Sci.*, 2001, 79, 662–673.
81. Weil, E. D. and Levchik, S. V., Commercial flame retardancy of unsaturated polyester and vinyl resins: Review, *J. Fire Sci.*, 2004, 22, 293–303.
82. Abdel-Mohdy, F. A., Graft copolymerization of nitrogen- and phosphorus-containing monomers onto cellulose for flame-retardant finishing of cotton textiles, *J. Appl. Polym. Sci.*, 2003, 89, 2573–2578.
83. Kaur, I., Sharma, V., and Sharma, R., Development of flame retardant cotton fabric through grafting and post-grafting reactions, *Indian J. Fibre Textile Res.*, 2007, 32, 312–318.
84. Tsafack, M. J. and Levalois-Grutzmacher, J. L., Plasma-induced graft-polymerization of flame retardant monomers onto PAN fabrics, *Surf. Coat. Technol.*, 2006, 200, 3503–3510.
85. Tsafack, M. J. and Levalois-Grutzmacher, J., Flame retardancy of cotton textiles by plasma-induced graft-polymerization (PIGP), *Surf. Coat. Technol.*, 2006, 201, 2599–2610.
86. Arnold Jr., C., Stability of high temperature polymers, *J. Polym. Sci., Macromol. Revs.*, 1979, 14, 265–378.
87. Martel, B., Charring process in thermoplastic polymers: Effect of condensed phase oxidation on the formation of chars in pure polymers, *J. Appl. Polym. Sci.*, 1988, 35, 1213–1226.
88. Ebdon, J. R. and Jones, M. S., Flame retardants: An overview, in *Polymeric Materials Encyclopaedia*, Salamone, J. C. (Ed.), 1995, CRC Press, Boca Raton, FL, 2397–2411.
89. Kandola, B., Horrocks, A. R., Price, D., and Coleman, G., Flame retardant treatment of cellulose and their influence on the mechanism of cellulose pyrolysis, *Revs. Macromol. Chem. Phys.*, 1996, C36, 721–794.
90. Le Bras, M., Camino, G., Bourbigot, S., and Delobel, R. (Eds.), *Fire Retardancy of Polymers: The Use of Intumescence*, 1998, Royal Society of Chemistry, London.
91. Banks, M., Ebdon, J. R., and Johnson, M., The flame-retardant effect of diethylvinyl phosphonate in copolymers with styrene, methyl methacrylate, acrylonitrile and acrylamide, *Polymer*, 1994, 35, 3470–3473.
92. Ebdon, J. R., Hunt, B. J., Joseph, P., and Wilkie, T. K., Flame retardance of polyacrylonitriles covalently modified with phosphorus and nitrogen-containing groups, in *Fire Retardancy of Polymers: New Strategies and Mechanisms*, Hull, T. R. and Kandola, B. K. (Eds.), 2009, Royal Society of Chemistry, Cambridge, U.K., pp. 331–340.

6 Intumescence-Based Fire Retardants

Serge Bourbigot and Sophie Duquesne

CONTENTS

6.1	Introduction	129
6.2	Fundamentals of Intumescence	130
6.3	Intumescent on the Market	133
6.4	Reaction to Fire of Intumescent Materials	135
6.4.1	Intumescent Organic Polymer	135
6.4.1.1	Organic-Based Systems	135
6.4.1.2	Inorganic-Based Systems	140
6.4.2	Intumescent Textile	141
6.4.3	Intumescent Inorganic Polymer	144
6.4.4	Synergy in Intumescent	144
6.5	Resistance to Fire of Intumescent Coating	148
6.5.1	Evaluation of the Resistance to Fire	148
6.5.2	Small-Scale Test and Measurement of Intumescence	151
6.5.3	Recent Developments	155
6.6	Conclusion and Future Trends	158
	References	158

6.1 INTRODUCTION

The word “intumescence” comes from Latin “intumescere” which means “to swell up.” It well describes the behavior of an intumescent material. When heated beyond a critical temperature, the material begins to swell and then to expand. The result of this process is a foamed cellular charred layer on the surface which protects the underlying material from the action of the heat flux or the flame.^{1,2} While the word “intumescence” is not mentioned, the first described application in the patent literature appeared in 1938.³ The typical formulation combined diammonium phosphate (or sulfate), dicyandiamide, and formaldehyde, and was applied on wood to protect it against inflammation and burning. We may think that intumescence is a relative older concept, since the first comprehensive paper was published in the early 1970s,¹ but a brief review of the literature shows that intumescence is still largely employed to make flame-retardant (FR) polymers or FR paints and that some recent developments are very promising.⁴ This concept of intumescence appears then as an attractive topic as demonstrated by the number of papers or patents dealing with this subject which has been studied since the 1970s (Figure 6.1).

This chapter is organized in four parts. In Sections 6.2 and 6.3, intumescence is briefly reviewed to provide the reader the basic understanding on the mechanisms of action by intumescence and then the main intumescent products available on the market associated with their typical field of application are surveyed. Reaction of intumescent polymers and textiles to fire, i.e., the contribution

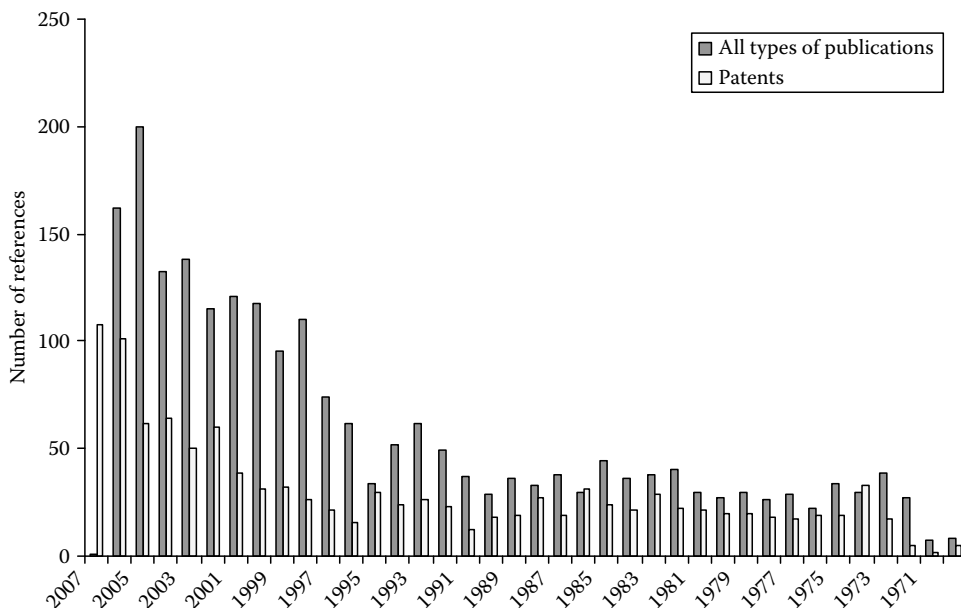


FIGURE 6.1 Number of references dealing with intumescence. (From Chemical Abstract Plus.)

of the material to fire growth, is examined in Section 6.4. The latest developments of flame retardants (FRs) as well as synergists are considered, and the mechanism of action is discussed based on published work and on our own experience. Section 6.5 is devoted to the resistance to fire of materials using intumescent paint or coating. Resistance to fire is defined as the ability of materials to resist the passage of fire and/or gaseous products of combustion, and the capability to meet specified performance criteria to those ends. A short description of the normalized tests is given. The need for the development of a “small test” is explained and the correlation with small/large-scale tests is shown. The mechanism of action is discussed taking into account the chemical, physical, and thermal aspects.

6.2 FUNDAMENTALS OF INTUMESCENCE

Flame-retarding polymers or textiles by intumescence are essentially a special case of a condensed-phase mechanism.^{5–9} Intumescent systems interrupt the self-sustained combustion of the polymer at its earliest stage, i.e., the thermal degradation with the evolution of gaseous fuels. The intumescence process results from a combination of charring and foaming at the surface of the burning polymer. The resulting foamed cellular charred layer, whose density decreases as a function of temperature, protects the underlying material from the action of the heat flux or of the flame (Figure 6.2). Thus, the charred layer acts as a physical barrier that slows down heat and mass transfer between gas and condensed phase.

After the fundamentals were first expressed by Vandersall,¹ it was the pioneering comprehensive work of Camino which permitted the development of intumescence in polymers.^{5,10} Typically the ingredients of intumescence are composed of an inorganic acid or a material yielding acidic species upon heating, a char former, and a component that decomposes at the right temperature and at the right time to enable the blowing of the system. Typical examples of components used in intumescent systems are reported in Table 6.1.

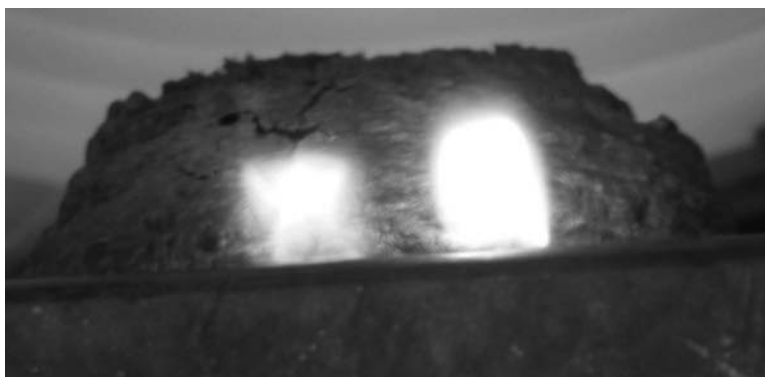


FIGURE 6.2 (See color insert following page 530.) Intumescent poly lactide (PLA) during a cone calorimeter experiment. Note the small flames on the side of the intumescent “cake” showing how the intumescent coating smothers the fire.

TABLE 6.1
Examples of Components of Intumescent Systems

<p>(a) Acid source</p> <p><i>Inorganic acid source</i></p> <p>Phosphoric</p> <p>Sulfuric</p> <p>Boric</p> <p><i>Ammonium salts</i></p> <p>Phosphates, polyphosphates</p> <p>Borates, polyborates</p> <p>Sulfates</p> <p>Halides</p> <p><i>Phosphates of amine or amide</i></p> <p>Products of reaction of urea or guanidyl urea with phosphoric acids</p> <p>Melamine phosphate</p> <p>Product of reaction of ammonia with P_2O_5</p> <p><i>Organophosphorus compounds</i></p> <p>Tricresyl phosphate</p> <p>Alkyl phosphates</p> <p>Haloalkyl phosphates</p>	<p>(b) Carbonization agent</p> <p>Starch</p> <p>Dextrins</p> <p>Sorbitol, mannitol</p> <p>Pentaerythritol, monomer, dimer, trimer</p> <p>Phenol-formaldehyde resins</p> <p>Methylol melamine</p> <p>Char former polymers (PA-6, PA-6/clay nanocomposite PU, PC, ...)</p> <p>(c) Blowing agents</p> <p>Urea</p> <p>Urea-formaldehyde resins</p> <p>Dicyandiamide</p> <p>Melamine</p>
---	---

The following sequences of events take place in the development of the intumescent phenomena:

1. Inorganic acid is released typically between 150°C and 250°C depending on its source and other components.
2. The acid esterifies the carbon-rich components at temperatures slightly above the acid release temperature.
3. The mixture of materials melt prior or during esterification.
4. The ester decomposes via dehydration resulting in the formation of a carbon-inorganic residue.

5. Released gases from the above reactions and degradation products (in particular those resulting from the decomposition of the blowing agent) cause the carbonizing material to foam.
6. As the reaction nears completion, gelation and finally solidification occurs. This solid is in the form of multicellular foam.

A typical example of an intumescent system is polypropylene (PP) containing ammonium polyphosphate (APP)/pentaerythritol (PER) (intumescent additives: ammonium polyphosphate (APP: $(\text{NH}_4\text{PO}_3)_n$, $n = 700$)/PER = 3/1 (wt/wt)) or an intumescent commercial additive (Exolit AP750 of Clariant (APP with an aromatic ester of tris(2-hydroxyethyl)-isocyanurate).¹¹ The evaluation of the fireproofing performance shows that the formulation containing AP750 has better performance than that with APP/PER (LOI of 38 vol % vs. 32 vol %), but that in the two cases a V-0 rating is achieved in the UL-94 test. These results are confirmed by cone calorimetry exhibiting the formation of an intumescent protective char for the two systems but more efficient for the formulation containing AP750.¹²

The main mode of action of an intumescent coating is to limit heat transfer from the flame to the underlying material. Temperature profiles have been measured using thermocouples embedded in plaques that are 2 cm thick during a cone calorimeter experiment on the formulations described above. It was shown that the temperature is reduced in the case of the PP-AP750 system in comparison with PP-APP/PER. As an example at $t = 1600$ s, the temperature (depending on the distance) in the case of PP-APP/PER lies between 200°C and 350°C, and in the case of PP-AP750 between 200°C and 250°C. It is noteworthy that the temperatures of PP-AP750 are always below the temperature (about 310°C measured by TGA) where the degradation rate of PP is maximum. In the case of PP-APP/PER, the temperature reaches 310°C at about 900 s and the degradation rate can increase rapidly. Using this experimental protocol, it is demonstrated that the intumescent system really acts as an insulative coating.

In the case of PP-APP/PER, the reaction of the acidic species (APP and its degradation products, orthophosphates, and phosphoric acid) with the char former agent (PER) takes place in the first stage ($T < 280^\circ\text{C}$) with formation of esters mixtures. The carbonization process then takes place at about 280°C (mainly via a free radical process).¹³ In a second step, the blowing agent decomposes to yield gaseous products (i.e., evolved ammonia from the decomposition of APP) which cause the char to swell ($280^\circ\text{C} \leq T \leq 350^\circ\text{C}$). The intumescent material then decomposes at higher temperatures and loses its foamed character at about 430°C. Concurrently, the heat conductivity of the char decreases between 280°C and 430°C and the insulating quality of the underlying material is enhanced.¹⁴ In addition to this, it is obvious that the inorganic acid (in our example APP) must be available for the dehydration action with the char former (PER) at a temperature below that at which the degradation of the polymeric materials begins. Then the formation of the effective char must occur via a semiliquid phase (high viscous material) which coincides with gas formation and expansion of the surface (here we can compare the expansion of the char to a “bubble-gum” effect). This action must occur before the solidification of the liquid charring melt. Gases released from the degradation of the intumescent material and/or of the polymeric material to be protected have to be trapped and have to be diffused slowly in the highly viscous molten material in order to create a layer with the morphological properties of interest. Thus it is essential to examine carefully the dynamic viscoelastic properties of the intumescent shield, since control of the melt rheology is necessary to obtain a multicellular and highly expanded structure.¹⁵ Moreover, the mechanical integrity of the char is a crucial parameter because it has to resist external stress.

In short, an intumescent formulation has to be optimized in terms of physical (char strength, expansion, viscosity, ...) and chemical (thermal stability, reactivity) properties in order to form an effective protective char that will be able to protect its host polymer (reaction to fire) or a substrate like steel or wood (resistance to fire).¹⁶

6.3 INTUMESCENTS ON THE MARKET

According to a recent report from the Swiss science and business consultancy firm Acon AG, the worldwide market for halogen-free FRs is set to increase strongly from US\$1.62 billion in 2005 to \$2.72 billion in 2010, representing a global compound annual growth rate of about 11%.¹⁷ In addition to this, in western Europe, the United States, and Japan, public consciousness of potential hazardous halogenated products, industrial end-user initiatives, and environmental legislation are together driving the market trend toward halogen-free products, which is an opportunity for a growing demand of intumescent products. These last products are phosphorus-based compounds which are expected, along with mineral FRs, to show the fastest growth.¹⁸ This study also reports that nanotechnology will play a key role in improving fire-retardant performance and reducing production costs. It makes sense because the benefit of combining nanoparticles with conventional FRs is known.¹⁹ Some advantages include the decrease of the total loading, the increase of the mechanical properties, the multifunctionality, and the strong increase of the flame retardancy.^{4,19-21} It is also mentioned in this same study that among the new developments in the field of flame retardancy, one of the most important technological trends include intumescent substances and we can expect major developments in the near future as nanotechnology does for coatings what it has already done for cables and wires (usually a combination of metal hydroxides with organoclay).²²

The world's plastic consumption grew from 86 Mio. tons in 1990 to 230 Mio. tons in 2005. The forecast for 2010 is 295 Mio. tons, which is an average annual growth of around 5.5%. This growth and the various forecasts for FRs ranging between 3% and 5% show good expectations for the demand of FRs, particularly halogen-free compounds including phosphorus compounds which are the main ingredients in intumescent formulations. Figure 6.3a shows the consumption of phosphorus compounds compared to the other FRs. It is relatively low (9%) compared to metal hydroxides, but this is easily understandable because of the quantity needed to make FR polymers with metal hydroxides (usually 60 wt %) compared to phosphorus-based compounds (20–25 wt %). On the other hand, phosphorus-based compounds are the second largest in terms of sales value, showing their strong interest for the industry (Figure 6.3b).

Typically, a phosphorus-based FR is designed to develop its activity just before the start of the decomposition of the specific polymer for which it is used. They offer a partial gas-phase contribution to the flame extinguishing effect, which is comparable to bromine- or chlorine-containing FRs.

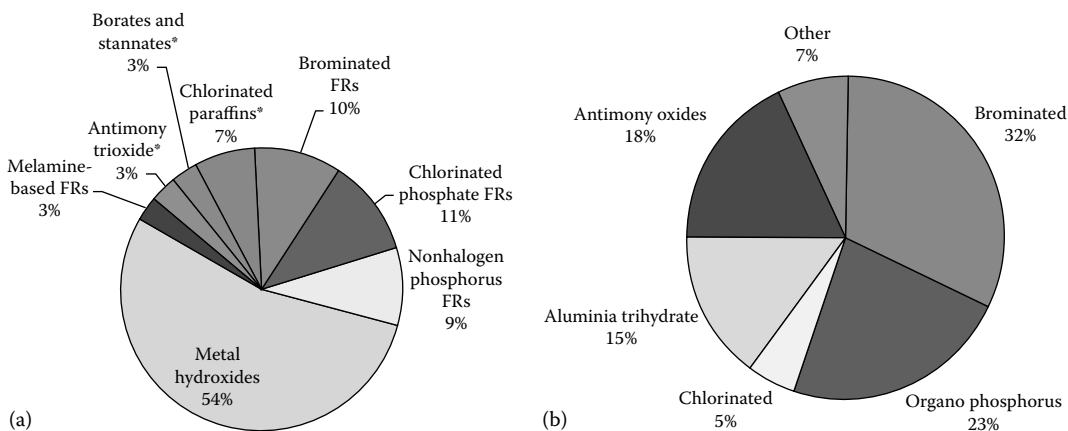


FIGURE 6.3 (a) Industry estimate for total consumption of flame retardants in Europe in 2006 (total = 465,000 metric tons). (b) Flame retardants distributed by type and by sales value in 2004 (total = 2.9 billion USD).

However, the main feature is char-forming activity like intumescence. The phosphorus-based FRs can be used in numerous polymers and resins such as polyamides, polyesters, polyolefins, epoxy, and styrenics. The main area of application for the compounded materials is injection-molded electrical and electronic (E&E) parts. Besides the electrical market, a very important market is FR fabrics for public buildings and public transportation seating. Compounds other than those of phosphorus can be used in intumescent systems (see Table 6.1), but they are not widely employed, except for boron-based compounds for nondurable textile applications and in intumescent coating for fire protection, and also expandable graphite for applications including intumescent seals, foams, and strips. Table 6.2 gathers (it is not our intention to make an exhaustive list) intumescent compounds as typical examples of products available on the market. It shows that four main groups of additives are available and used industrially: phosphate, phosphinate, borate, and expandable graphite.

TABLE 6.2
Examples of Intumescent Compounds Available on the Market

Type	Brandname	Supplier	Examples of Application
Ammonium polyphosphate ^a	AP420 series	Clariant (Germany)	Intumescent gelcoats (epoxy, UP, or PUR based)
Coated ammonium polyphosphate ^b	AP760 series		FR polyolefins for E&E and building/transportation applications
Aluminum phosphinate salt	OP1230/1240 series		FR high performance polyamides and polyesters for E&E applications
Aluminum phosphinate salt + melamine polyphosphate ^c	OP1310 series		FR polyamides for E&E applications
Zinc phosphinate salt	OP950		Polyester for textile applications
Ammonium polyphosphate ^a (crystal forms I and II)	FR CROS480 series	Budenheim (Germany)	FR for PU, EP
Melamine phosphate	Budit 310 series (310–312)		Unsaturated polyester resins, particularly for the SMC process
Melamine borate	Budit 313		In combination with melamine phosphate for phenolic resin bound nonwoven based on cotton fibers
Encapsulated ammonium polyphosphate ^b	Budit 3000 series		FR polyolefins for E&E and building/transportation applications
Melamine polyphosphate	Melapur 200	Ciba (Switzerland)	PA66/glass fibers, epoxies, synergistic blends with other flame retardants
Ammonium polyphosphate ^a	Antiblaze MC	Albemarle (the United States)	Used in the formulation of intumescent paints, coatings, sealants, and mastics
Phosphorus/nitrogen-based intumescent FR	Rheogard 1000 and 2000 series	Chemtura (the United States)	PP for applications in appliances, conduit, transportation, and battery casings
Expandable graphite	Expandable graphite	Inca (Sweden)	Intumescent coating, intumescent seal, intumescent strips, and firestop collars
Expandable graphite	GrafGuard	GrafTech (the United States)	FR additive in plastics (processing up to 200°C), foams, putties, and coatings

^a Typical acid source (dehydrating agent) used in numerous intumescent formulations.

^b This product contains all intumescent ingredients, i.e., acid source, char former, blowing agent, and a synergist.

^c In some specific grade, zinc borate is added as synergist and processing aid.

6.4 REACTION TO FIRE OF INTUMESCENT MATERIALS

This section focuses on the recent developments in the field of the intumescent polymers and textiles. For former reviews, the reader should read for example, the basics written by Vandersall,¹ and the reviews of Delobel and Camino²⁴ for polymers, and of Horrocks for textiles.²⁵ Note that an exhaustive review on commercial FR polyolefins including intumescent came out very recently and provides the latest development on the market.²⁶ The section is organized in four parts concerning the latest work on intumescent polymers using appropriate additives, intumescent textiles using additives in the fibers or the surface treatment on fabrics (Sections 6.4.1 and 6.4.2). The third part (Section 6.4.3) is devoted to intumescent inorganic polymer because this topic is rarely reviewed in the literature, and the last part of this section (Section 6.4.4) considers the aspects of synergy in the intumescent systems.

6.4.1 INTUMESCENT ORGANIC POLYMER

6.4.1.1 Organic-Based Systems

In the 1980s, intumescent systems (APP-based formulations) were used to flame retard polymers, in particular, thermoplastics.^{27–29} However, such systems present some drawbacks (water solubility, migration of the additives throughout the polymer) that can be prevented by synthesizing novel phosphorus- and/or nitrogen-containing systems. The last 25 years have seen the improvement of the intumescent concept applied to polymers in terms of performance, processability, and durability. A rapid survey of the recent literature shows that numerous new intumescent compounds have been synthesized. Basic concepts are used combining in a single molecule the three main ingredients of intumescence, i.e., the acid source, the char former, and the blowing agent (see the pioneering paper of Halpern).²⁹ Novel strategies based on “mineral intumescence” also appear in the literature, which is discussed below.

The use of polyols such as pentaerythritol, mannitol, or sorbitol as “classical” char formers in intumescent formulations for thermoplastics is associated with migration and water solubility problems. Moreover, these additives are often not compatible with the polymeric matrix and the mechanical properties of the formulations are then very poor. Those problems can be solved (at least partially) by the synthesis of additives that concentrate the three intumescent FR elements in one material, as suggested by the pioneering work of Halpern.²⁹ b-MAP (4) (melamine salt of 3,9-dihydroxy-2,4,8,10-tetraoxa-3,9-diphosphaspiro[5,5]-undecane-3,9-dioxide) and Melabis (5) (melamine salt of bis(1-oxo-2,6,7-trioxa-1-phosphabicyclo[2.2.2]octan-4-ylmethanol)phosphate) were synthesized from pentaerythritol (2), melamine (3), and phosphoryl trichloride (1) (Figure 6.4). They were found to be more effective to fire retard PP than standard halogen-antimony FR.

Based on this work and searching for an environmentally friendly process, Fontaine et al.³⁰ suggested the synthesis of PEPA (1-oxo-4-hydroxymethyl-2,6,7-trioxa-1-phosphabicyclo[2.2.2]octane) and bis(PEPA)phosphate-melamine salt derivatives prepared by a novel and safe protocol (one step–one pot process). These new salts were incorporated in PP and exhibit high fire performance via an intumescence mechanism (LOI of 32 vol % and V-0 rating in the UL-94 on bars of 3.2 mm thick). Recently, Liu and Wang proposed to use the catalytic action of phosphotungstic acid³¹ in the synthesis of melamine salts of pentaerythritol phosphate (called MPP in their paper but it is the same molecule as b-MAP) in order to solve the problems of conventional preparation methods (the use of POCl₃; the high temperature of the reaction and thus the high energy consumption) (Figure 6.5). It was shown that the acid catalysis can enhance the conversion degree of the reaction and decrease the reaction temperature while keeping a satisfactory conversion, thus greatly controlling the energy consumption in the preparation process of MPP (or b-MAP). The results also indicated that as compared to the noncatalyzed MPP, the catalyzed MPP FR system remarkably improved the FR properties reinforcing and stabilizing the char layer, while maintaining acceptable mechanical properties.

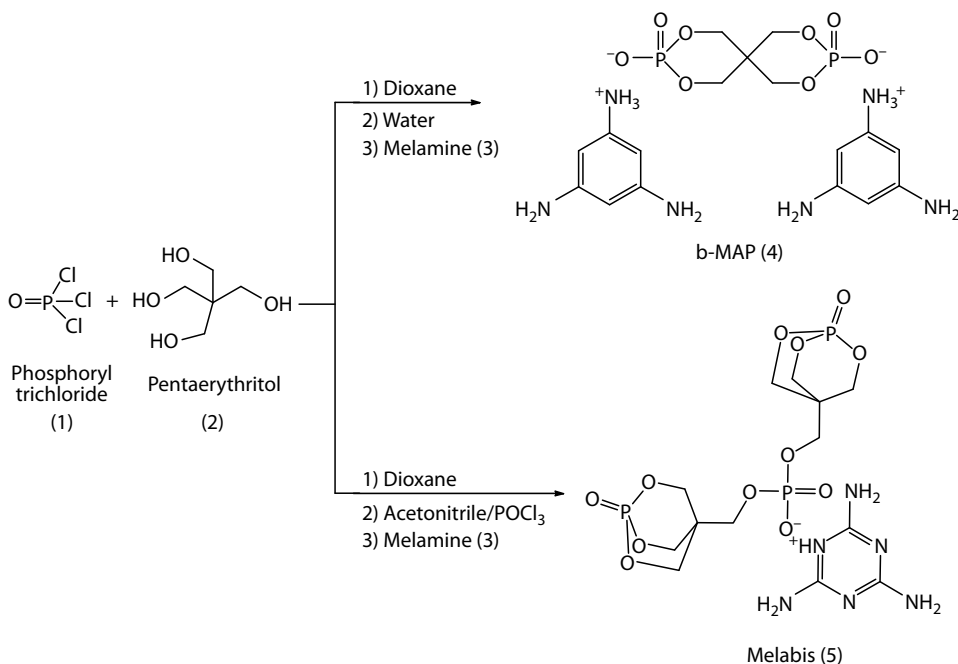


FIGURE 6.4 Melabis and b-MAP synthesis.

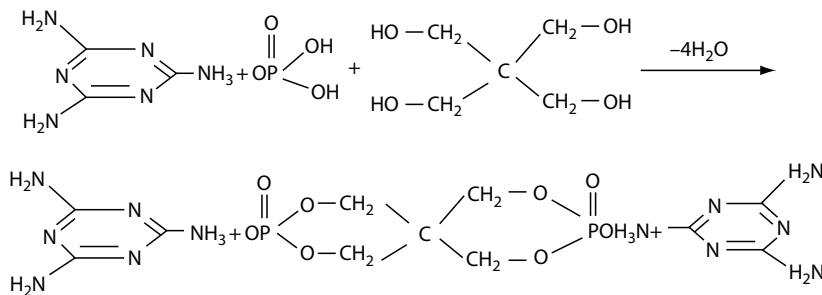


FIGURE 6.5 Synthesis of melamine salts of pentaerythritol phosphate (MPP or b-MAP). (From Liu, Y. and Wang, Q., *Polym. Deg. Stab.*, 91, 2513, 2006.)

It is worth noting that MPP salt can be prepared directly by reactive extrusion in a twin screw extruder and so, via a continuous process.^{32,33} The mixture of the reactants, melamine phosphate (MP) and PER, are extruded with a small amount of PP carrier resin. This method is promising because it simplifies the preparation process and should increase the yield of production compared with a batch reactor. Nevertheless, the authors mention some disadvantages such as high degree of foaming when processing temperature is too high and low conversion degree when the residence time is short and/or the temperature is too low. Based on their experience with the preparation of catalyzed-MPP, they used a silicotungstic acid³⁴ in their reactive extrusion process. They found that this solid catalyst permits the preparation of catalyzed-MPP without the aforementioned disadvantages and as a bonus, the presence of silicotungstic acid acts as a synergist in PP-based formulations. They also investigated the influence of the molar ratio MP:PER on the flame retardancy of PP, and they recommended the ratio of 2 (mol/mol) to obtain the product with the most efficient structure (structure shown in the Figure 6.5).³⁵ Finally, they applied their approach in polyamide-6 reinforced by glass fibers (GFs) without PER but with a solid acid containing sulfur encapsulated in thermoplastic

polyurethane (TPU).³⁶ This approach provides an effective approach to prepare intumescent PA-6 with UL94–1.6 mm V-0 rating and acceptable mechanical properties.

Other authors also suggested the synthesis of organic compound “3 in 1” containing the three main ingredients of intumescence. Wang et al. reported³⁷ the synthesis of a novel intumescent FR, poly(2,2-dimethylpropylene spirocyclic pentaerythritol bisphosphonate) to yield PET with both excellent flame retardancy and antidripping properties. A novel phosphorus–nitrogen containing intumescent FR was prepared via the reaction of a caged bicyclic phosphorus (PEPA) compound and 4,4-diamino diphenyl methane (DDM) in two steps (Figure 6.6).³⁸ Incorporated in poly(1,4-butylene terephthalate) (PBT) and in combination with TPU as additional char former, the intumescent PBT exhibits V-0 rating in the UL-94 test (3.2 mm) and an enhanced thermal stability. It is suggested that P–N bonds detected in the charred structure might play a role in its efficiency.

To avoid dissolution or extraction of the FR, FR oligomer can be used instead of monomer. Using this approach, Ma et al.³⁹ reported the synthesis of phosphate–polyester copolymers from spirocyclic pentaerythritol di(phosphate acid monochloride)s. It was shown that LOI of the copolymer increases with increasing phosphate content to reach a maximum of 30 vol %.

As the polyol-based char formers needs to be substituted, Li and Xu⁴⁰ reported the synthesis of a novel char former for intumescent system based on triazines and their derivatives. It is a macromolecular triazine derivative containing hydroxyethylamino, triazine rings and ethylenediamino groups (Figure 6.7). They showed that the new char former in an intumescent formulation containing APP

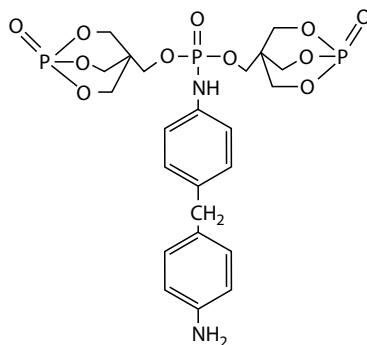


FIGURE 6.6 Phosphorus–nitrogen intumescent flame retardant. (From Gao, F. et al., *Polym. Deg. Stab.*, 91, 1295, 2006.)

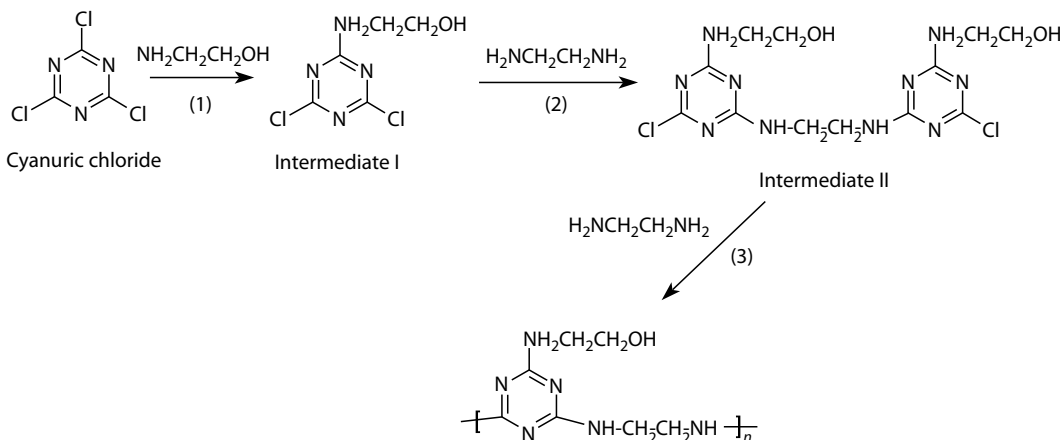


FIGURE 6.7 Synthesis of macromolecular triazines derivatives as char former for intumescent systems. (From Li, B. and Xu, M., *Polym. Deg. Stab.*, 91, 1380, 2006.)

and a zeolite as synergist can achieve low flammability at only 18 wt % loading in PP (LOI of 30 vol % and V-0 rating (3.2 mm) in the UL-94 test). No tentative mechanism is suggested, but we suspect that it should be close to that we described in a previous paper.¹⁹

A novel carbonization agent (so-called by the author) was also synthesized and characterized by Xie et al. (Figure 6.8).⁴¹ It was evaluated in polyethylene (PE) combined with a mixture of APP and MP at 30 wt % total loading. It only achieves a V2 rating (3.2 mm) in the UL-94 test. Using novel metal chelates acting as catalyst, they showed promotion of charring to yield a more efficient coating. At the same total loading and with only 1 wt % metal chelates, a V0 rating (3.2 mm) is achieved in the UL-94.

The same authors applied the same strategy synthesizing a compound containing phosphorus and nitrogen as acid source combined with metal chelates in polyvinyl alcohol (PVA).⁴² It is an ammonium salt of 2-hydroxyl-5,5-dimethyl-2,2-oxo-1,3,2-dioxaphosphorinane (PNOH) (Figure 6.9). APP and PNOH acting as acid sources and blowing agents were incorporated in PVA acting as a carbonization agent, and combined with metal chelates acting as a catalyst promoting charring. All formulations exhibit V0 rating (3.2 mm) in the UL94 test, and LOI is higher than 30 vol % at total loading as low as 15 wt %.

Phosphinate salts available on the market as OP series (see Table 6.2) are FRs designed for polyamides and polyesters. The incorporation of OP1311 (23 wt % loading) in PA-6 permits one to achieve a V-0 rating (3.2 mm) and to reach a LOI of 29 vol %.²⁰ Figure 6.10 shows superficial carbonization of the samples with a limited expansion.⁴³ In this particular case, we may not really talk about intumescence.

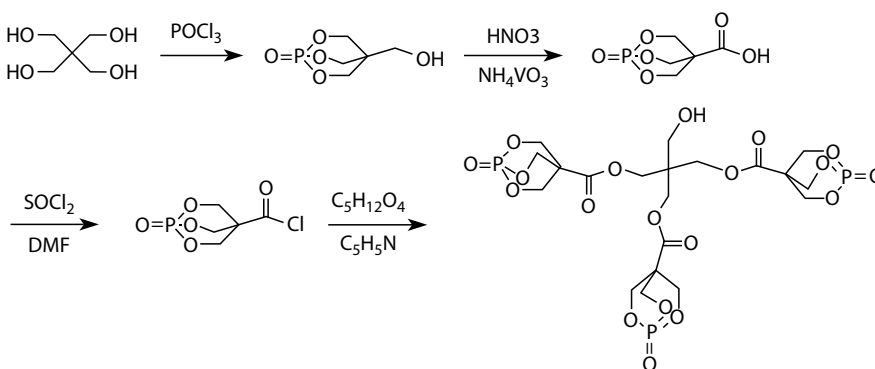


FIGURE 6.8 Synthesis of a phosphorus-containing char former. (From Xie, F. et al., *Macromol. Mater. Eng.*, 291, 247, 2006.)

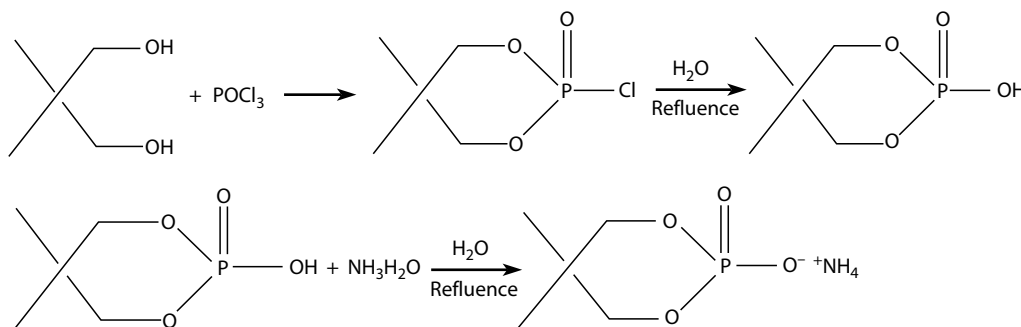


FIGURE 6.9 Synthesis of a phosphorus-containing char former. (From Wang, D.L. et al., *Polym. Deg. Stab.*, 92, 1555, 2007.)

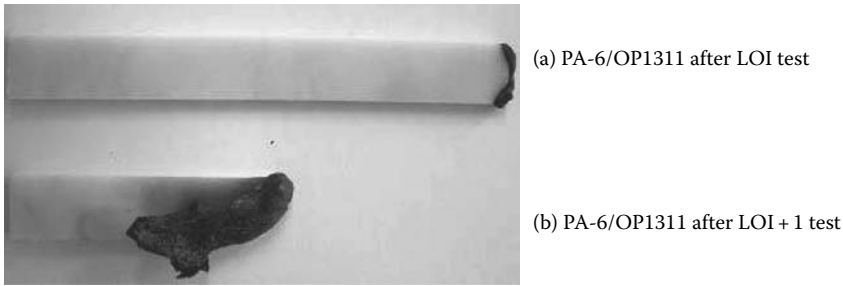
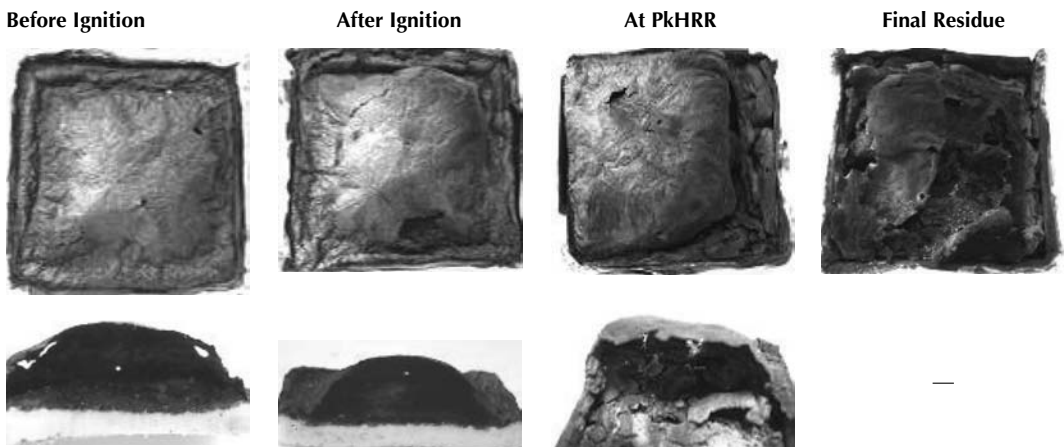


FIGURE 6.10 Samples of PA-6/OP1311 after LOI test.

Mass loss calorimetry confirms the good FR performance of OP1311 in PA-6 (not shown) and an intumescent phenomenon can be observed during this test. Peak of heat release rate (P_kHRR) of PA-6/OP1311 is decreased by 60% but the time to ignition is not improved. Before the ignition of the formulation PA-6/OP1311, charring and formation of a large single bubble is observed at the surface of the material (Table 6.3). Cracks appear in the bubble at the P_kHRR and the final residue only exhibits a noncohesive charred structure containing large holes. Undegraded polymer on the bottom is detected before and after the ignition and at longer times all materials turn entirely into char.

Braun et al.⁴⁴ investigated the flame retardancy of polyamide-6,6 (PA-66) reinforced by GFs containing melamine polyphosphate (MPP; brand name Melapur 200) and aluminum phosphinate salt (AlPi; brand name OPI230). They found HB classification for PA66/GF and PA66/GF-MP and LOI of 22 and 29 vol % respectively. Although PA66/GF-AlPi achieved only a HB classification in UL 94 test, the LOI was increased impressively (38 vol %). They assigned this “apparent” discrepancy between improvement in LOI and UL 94 to a different residue performance in the two test geometries. In the LOI test the vertically positioned residue/char on top of the specimen remained during the test, whereas in the UL 94 test the residue fell off and exposed the untreated polymeric material directly to the flame. They showed the benefit of combining AlPi with MP since in this case, a V0

TABLE 6.3 (See last page of color insert before page 531.)
Combustion Residues of PA-6/OP1311 from the Cone Calorimeter Obtained at Different Characteristic Times



rating is achieved and an acceptable LOI of 28 vol % was measured. Cone calorimetry confirms the good performance of the formulations (see full details in Ref. 44).

The zinc phosphinate salt (OP950) is also a candidate for flame-retarding polyesters and in particular, polyethylene terephthalate (PET). The incorporation of OP950 in PET permits the LOI values to reach 29 and 35 vol % at 10 and 20 wt % loading, respectively.²¹ An intumescent layer is developed on the top of the material in the case of the filled polymer (note here that no blowing agent is incorporated in the polymer and we suspect that the evolving degrading product of PET might play the role of a blowing agent). Cone calorimetry confirms this performance. Virgin PET exhibits a PkHRR of 750kW/m² associated to time to ignition of 75 s. The incorporation of OP950 in PET decreases the PkHRR by 30% (500kW/m²) associated with a large increase of the time to ignition (125 s vs. 75 s). The formation of an intumescent coating with a slight expansion at the surface of the polymer is observed, but cracks appear rapidly leading to a sharp PkHRR. Braun et al.⁴⁵ also showed the efficiency of aluminum phosphinate in polyester (PBT) reinforced by GF. At 20 wt % loading in FR, the LOI reaches 43 vol % in PBT/GF-AlPi formulation associated with a V0 rating in the UL-94 test. No significant effect is observed using melamine cyanurate (MC) in the formulation.

6.4.1.2 Inorganic-Based Systems

The organic intumescent systems represent a large part of the studies dealing with intumescence but the processing of intumescent mineral systems is even older.⁴⁶ However it is rarely discussed in the literature. Mineral intumescent systems are based on alkali silicates. The swelling of the material upon heating or on contact with a flame is due to an endothermic process and is associated with the emission of water vapor that is ionically hydrated in the silicate system.⁴⁷ The solid foam formed is rigid and consists of hydrated silica. The structure remains solid until it reaches its glass-softening point. Since only water vapor is released, toxic fumes that may be released from organic-based systems are eliminated. But intumescent alkali have serious limitations, in particular they are sensitive to carbon dioxide and water, which are present in the atmosphere, causing the silicate coating to gradually lose its intumescence, to become brittle, and to lose its adhesion.

Hermansson et al.⁴⁸ showed that incorporation of chalk filler and silicone can greatly improve the FR properties of ethylene-butyl acrylate (EBA) formulations. A filling of 30 wt % of chalk filler and 5 wt % silicone was employed. Compared to the pure polymer, an increase of LOI from 18 to 30 vol %, and a decrease in the PkHRR from 1300 to 330kW/m² were measured. The improvements were assigned to an intumescent process. The suggested mechanism is as follows:⁴⁹ (1) Ester pyrolysis occurs when degradation starts at 300°C producing carboxylate ions on the copolymer backbone, (2) volatile degradation products of EBA copolymer lead to foaming of the melt, which is stabilized by the formation of carboxylate ions, and (3) calcium ions from the chalk (Figure 6.11). Other copolymers (EBA blended with PP and poly(ethylene-*co*-methacrylic acid) (EMAA)) have

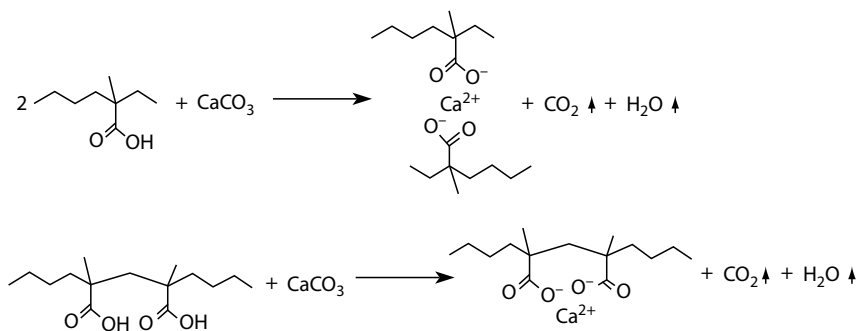


FIGURE 6.11 Reaction scheme for the calcium salt formation in EBA copolymer containing chalk. (From Krämer, R.H. et al., *Polym. Deg. Stab.*, 92, 1899, 2007.)

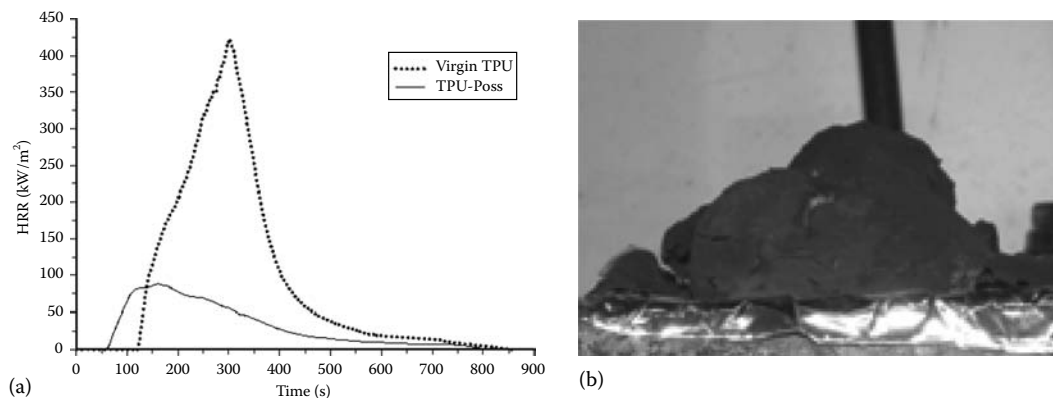


FIGURE 6.12 (See color insert following page 530.) HRR as a function of time of pure TPU and TPU/FQ-POSS composite (external heat flux = 35 kW/m²) (a) and intumescent char residue at the end of the cone experiment (b).

been investigated by Krämer et al.⁵⁰ and they found that EMAA formulation has the most effective intumescent process with a low HRR and good char stability.

Polyhedral silsesquioxanes (POSS) are not known as intumescent FRs but as nanoparticles for making polymer nanocomposites. POSS can provide low flammability to polymer via a mechanism in the condensed phase.⁵¹ In previous work,⁵¹ it was shown that the incorporation of POSS in TPU used as coating on woven PET fabrics permitted 50% reduction in PkHRR. The suggested mechanism is char formation at the surface of the material which can act as an insulative barrier. Recently it was reported²⁰ that the incorporation of 10 wt % FQ-POSS (Poly(vinylsilsesquioxane) with the brand name Fire Quench from Hybrid Plastics, the United States) in TPU (in bulk polymer) permits an 80% decrease in the PkHRR (Figure 6.12a) without any significant enhancement of LOI (22 vs. 23 vol %) and UL-94 (V-2 at 3.2 mm in the two cases). It is noteworthy that the dispersion of FQ-POSS is at the microscale and not at the nanoscale. Visually, the mechanism of protection occurs via an intumescent phenomenon (Figure 6.12b) and it is believed that the mechanism consists of the following steps: (1) charring of TPU and POSS taking place at similar temperatures with the formation of a “viscous” paste, (2) expansion of a ceramified char (char reinforced by a silicon network) from the evolution of the degraded products and partial sublimation of POSS, and (3) strong reduction of heat transfer to the substrate (measured experimentally) by the formation of the intumescent layer.⁵²

Expandable graphite represents another class of inorganic intumescent systems. Expandable graphite is a graphite intercalation compound (GIC), which appears in the literature in 1841.⁵³ It is a layered crystal consisting of sheets of carbon atoms tightly bound to each other. Chemicals (such as sulfuric acid) may be inserted between the carbon layers. Upon heating EG expands and generates a voluminous insulative layer, thus providing fire performance of interest to the polymeric matrix. EG has been used advantageously in PU coatings to develop fire protective coating for polymeric substrates.⁵⁴ Examples will be given in the following in the case of inorganic polymer and in Section 6.5.

6.4.2 INTUMESCENT TEXTILE

In this part, we will distinguish between natural and synthetic fibers because different methods are usually involved to provide flame retardancy by intumescence for the two classes. A few papers report recent development and performance of intumescent textiles. Very often the authors describe the mechanism of action of their materials as “mechanism via charring enhancement” or something similar. Nevertheless based on the chemical nature of the flame retardant used and by the described

mechanism, we can sometimes suspect an intumescent behavior. In the following we will only review the latest developments done in the field of intumescent textiles (see Ref. 25 for the former developments).

Horrocks et al.⁵⁵ (and references therein) have undertaken considerable work on intumescent applied to textile structures, in particular substantive fiber treatments for cellulose. Based on the work of Halpern²⁹ on cyclic organophosphorus molecules, they developed a phosphorylation process for cotton fibers achieving intumescent cotton fabric with considerable durability. Char enhancement is as high as 60 wt % compared to pure cotton, which is associated with very low flammability. Coating (or back-coating) on fabric is another way to provide flame retardancy to cotton. Horrocks' group⁵⁶ used intumescent back-coatings based on APP as the main FR combined with metal ions as synergist. Metal ions promote thermal degradation of APP at lower temperatures than in their absence, and this enables FR activity to commence at lower temperatures in the polymer matrix thereby enhancing FR efficiency. Giraud et al.⁵⁷⁻⁶⁰ developed the concept of microcapsules of ammonium phosphate embedded in PU and polyurea shells to make an intrinsic intumescent system compatible in normal PU coating for textiles. The advantage of this concept is to reduce the water solubility of the phosphate and to produce textile back-coatings with good durability. The flame-retarding behavior of these coated cotton fabrics was evaluated with the cone calorimeter and it was shown that they exhibit a significant FR effect. Development of intumescent char at the surface of the fabric was observed, confirming the expected mechanism.

Within the area of natural fibers, wool has the highest inherent nonflammability. It exhibits a relatively high LOI of about 25 vol % and low flame temperature of about 680°C.²⁵ The inherent FR activity of the fiber can be associated with char-forming reactions which may be enhanced by a number of flame retardants. Based on their fundamental work to enhance char formation, Horrocks and Davies offer intumescent formulations based on MP to flame-retarded wool.⁶¹ From TGA and SEM characterization, they proposed a comprehensive model on the mechanism of protection via an intumescent process, which involves the formation of cross-linked char by P-N and P-O bonds resistant to oxidation. More recently, they used spirocyclic pentaerythritol phosphoryl chloride (SPDPC) phosphorylated wool to achieve intumescent wool which exhibits large char expansion and good flame retardancy.⁶²

Polyester fibers are the main synthetic fibers used in the industrial manufacturing sector and can be found in several areas of application. Several FRs have also been designed for polyester extrusion (bisphenol-S-oligomer derivatives from Toyobo, cyclic phosphonates (Antiblaze CU and 1010) from Albemarle, or phosphinate salts such as OP950, from Clariant). According to our previous work on PET,²¹ phosphinate salts provide flame retardancy to PET via an intumescent process but it is never clearly discussed in the literature when it is applied to textile. In the recent published literature, Chen et al.⁶³ proposed the use of a novel antidripping flame retardant, poly(2-hydroxy propylene spirocyclic pentaerythritol bisphosphonate) (PPPBP) (Figure 6.13) to impart flame retardancy and dripping resistance to PET fabrics. Flammability of PET fabrics treated with PPPBP

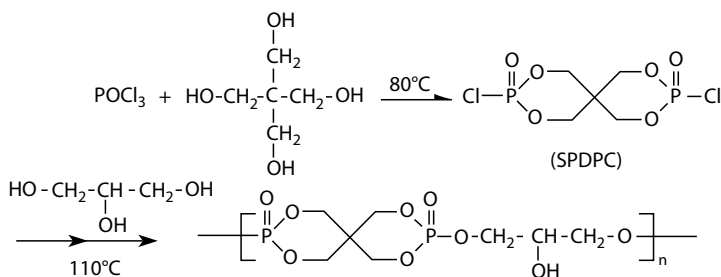


FIGURE 6.13 Synthesis scheme of poly(2-hydroxy propylene spirocyclic pentaerythritol bisphosphonate) or PPPBP. (From Chen, D.Q. et al., *Polym. Deg. Stab.*, 88, 349, 2005.)

was investigated by the vertical burning test which showed a significant enhancement of the flame retardancy (producing a nonignitable fabric) and either a significant reduction of melt dripping at low levels or an absence of dripping at higher levels of PPPBP.

The same authors investigated in detail the mechanism of flame retardancy of their FR PET fabrics.⁶⁴ They showed that it is a condensed-phase mechanism via char promotion (Figure 6.14) in which PPPBP produces phosphoric or polyphosphoric acid during thermo-decomposition leading to the formation of phosphorus-containing complexes at higher temperatures. They suggest that the high yields of char are protected from thermo-oxidation by the presence of phosphoric acid contained in the charred residue and because of the high thermal stability of C=C groups in the char. In their paper, the authors do not report any intumescent behavior, but we suspect because of the type of the compound used and according to the mechanism described that an intumescent process should be involved.

Concurrently, a new halogen-free FR master batch for polyester has been developed in our laboratories which at only 5 wt % incorporation enables PET to obtain classification according to several standards such as the NF P 92 501 or NF P 92 503 (M classification), FMVSS 302 or BS 5852 (Crib 5).⁶⁵ In this case, an intumescent behavior is observed but its mechanism of formation should be investigated.

Like polyester, polyamides are synthetic fibers made from semicrystalline polymers which find use in a variety of applications in textiles almost similar to those of polyester. A recent work of Horrocks et al.⁵⁵ has investigated the effect of adding selected intumescent FRs based on APP, MP,

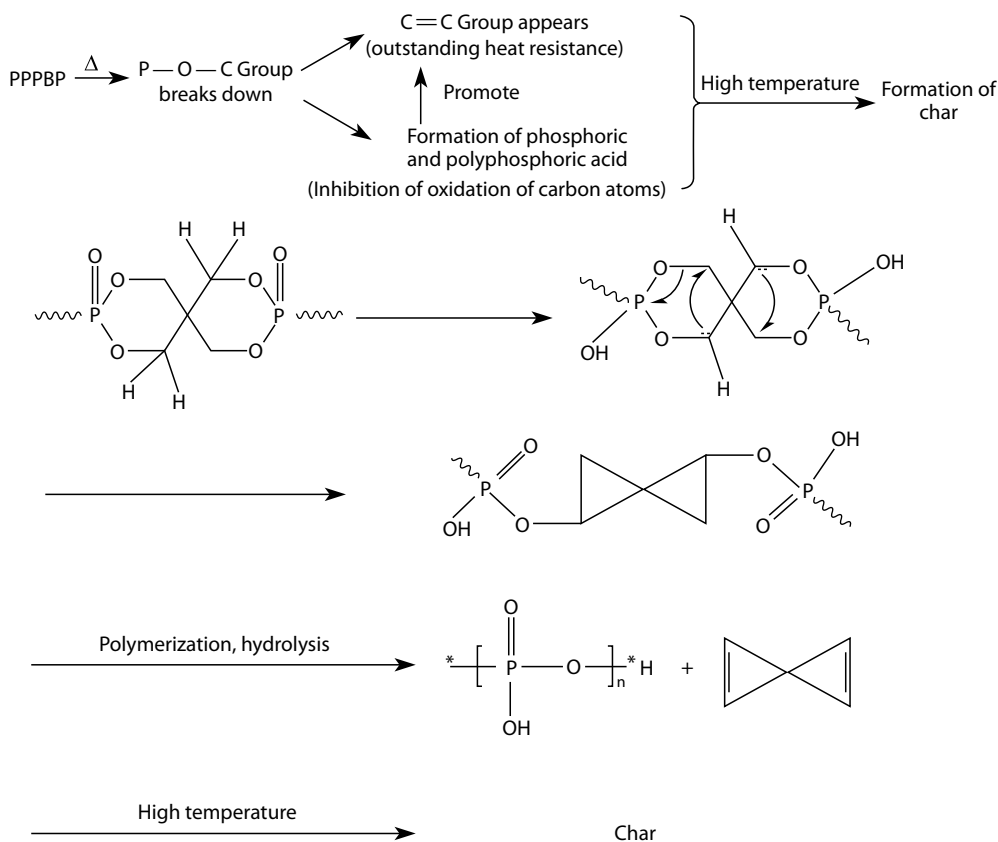


FIGURE 6.14 Flame retardancy mechanism of FR PET fabrics treated with PPPBP. (From Liu, W. et al., *Polym. Deg. Stab.*, 92, 1046, 2007.)

pentaerythritol phosphate, cyclic phosphonate, and similar formulations into polyamide 6 and 6.6 in the presence and absence of nanoclay. They found that in polyamide 6.6 all of the systems containing the nanoclay demonstrated significant synergistic behavior except for MP because of the agglomeration of the clay.

PP is presently one of the fastest-growing fibers for technical end uses where high tensile strength coupled with low cost are essential features. While PP fibers may be treated with FR finishes and back-coatings (intumescent or not) in textile form with varying and limited success,^{66–68} the ideal FR solution for achieving fibers with good overall performance demands that the property is inherent within the fiber. Presently, the use of phosphorus-based, halogen-free FRs in PP fibers is prevented by the need to have at least 15–20 wt % additive. Since the latter are char-promoting while all halogen-based systems are essentially non-char-forming in PP, the way forward for a halogen-free, char-forming FR conferring acceptable levels of retardancy at low additive levels, 10 wt %, will require either completely new FR chemistry or the development of a suitably synergistic combination. Based on this, Zhang and Horrocks⁶⁶ report that the flammability of PP is reduced by the addition of small amounts of clay in conjunction with a conventional phosphorus-containing FR and a hindered amine. The authors suspect P–N synergy and the LOI value for the best formulation is 22 vol % compared to 19 vol % for neat PP, with only 6 wt % total loading.

6.4.3 INTUMESCENT INORGANIC POLYMER

As far as we know, only a few papers report on the fire behavior of intumescent inorganic polymers. A possible explanation is that inorganic polymers are inherently FR and are used “as is.” The particular case of inorganic–organic polymers is either they are already flame retardant or they are used in applications which do not require high level of flame retardancy. The only published work devoted to intumescent inorganic polymer concerns polyphosphazene, and will be discussed below.

While polyphosphazene exhibits some level of flame retardancy, its performance is not enough to fulfill the requirements of the FAA for aircraft interiors. In order to make ultra fire resistant elastomers, the use of expandable graphite was investigated.⁶⁹ The expandable graphite is an intumescent additive constituted by chemicals trapped between the graphite layers. The expansion can be more than 100 times its original thickness, resulting in a nonburnable, insulating layer. In a cone calorimeter experiment, the addition of the expandable graphite to polyurethane reduces its HRR to a level approximating that of the pure polyphosphazene rubber. The addition of the expandable graphite to the polyphosphazene rubber reduces its HRR to a level approximating that of the fire resistant engineering plastics or of thermoset resins currently used in aircraft interiors (<100 kW/m²). The post fire test photos (not shown) show that the PU rubber is completely consumed in the fire test. In contrast, the polyphosphazene leaves a char residue equal to 35% of the original weight. The PU and polyphosphazene formulated with the expandable graphite leave a light friable char on the order of 20–50 times the original sample volume. The expanded graphite char insulates the underlying polymer from burning. The high thermal efficiency of the expanded char results in a peak HRR that is five and seven times lower than that for the virgin polyphosphazene and PU polymers, respectively.

6.4.4 SYNERGY IN INTUMESCENTS

Several interesting developments have occurred recently that involved unexpected “catalytic” effects in various intumescent systems. Performance in terms of LOI, UL-94, or cone calorimetry was enhanced dramatically by adding a small amount of an additional compound leading to a synergistic effect. In the following, we will use the definition of synergy as “a synergistic effect occurs when the combined effects of two chemicals are much greater than the sum of the effects of each agent give alone.”

Work done in our laboratory showed that adding small amounts of minerals such as zeolites,^{70,71} natural clays,⁷² and zinc borates^{30,73} in intumescent systems, the FR performance can be drastically enhanced. Concurrently, Levchik et al. proposed the use of small amounts of talc and manganese dioxide combined with APP in PA-6 to promote charring and to enhance insulative properties of the intumescent coating leading to a significant improvement of the flammability performance.^{74,75} Another recent approach using borosiloxane elastomer in PP allows also one to obtain a very large synergistic effect in intumescent systems.^{76,77} Large synergistic effects are observed when incorporating nanofillers in intumescent formulation, and most of the recent works on synergy are devoted to this. In this section, we will then focus on this aspect.

The presence of a nanofiller can modify the chemical (reactivity of the nanofiller vs. the ingredients of the intumescent system) and physical (expansion, char strength, and thermophysical properties) behavior of the intumescent char when exposed to a flame or heat flux leading to enhanced performance. In a recent paper, Lewin describes this phenomenon as a catalytic effect.⁷⁸ It is noteworthy that the catalyst (the nanofiller) is a crucial ingredient (reactant) in the development of intumescence forming additional species stabilizing the structure and modifying the rheological behavior. The nanofiller is incorporated at an amount as low as 1 wt % (sometimes less as in the case of the incorporation of nanoparticles of copper at an amount as low as 0.1 wt % in epoxy resin containing APP⁷⁹), and it permits the formation of active species selecting chemical reactions in the condensed phase and yielding char with the dynamic properties of interest.

Many papers were published in the 1990s on intumescent PP because intumescent systems are well adapted to their processing temperature and are efficient.⁵⁻⁷ More recently, Marosi et al.⁸⁰ combine an APP-based intumescent system in PP with organomodified montmorillonite (OMMT) and borosiloxane elastomer. The addition of a small amount of OMMT (1 wt %) in the formulation permits the achievement of a V-0 rating in UL-94, but the jump of LOI is only two points. The authors also developed a novel approach using borosiloxane as a carrier of flame retardant and ceramic precursor. The combination of OMMT with borosiloxane increases LOI by eight points compared to the reference and a V-0 rating is still achieved. These beneficial effects are confirmed by cone calorimetry. They explain the improvement of flame retardancy by the increase of viscosity in the conditions of fire, permitting the V-0 rating (addition of OMMT). The possible role of the nanofiller in controlling the activity of flame retardants is also suggested; the flame retardant might promote the exfoliation of the clay at the earliest stage of the degradation and provides the first protective barrier (concept of the expandable nanocomposite).⁸¹ A similar explanation is reported with the borosiloxane. Here the main benefit of borosiloxane is to make a relatively "flexible" char compared to a fragile charred structure. It is claimed that borosiloxane-coated OMMT acts as a carrier of OMMT and delivers OMMT at the surface of the char creating additional protection. No evidence of reaction between APP and/or borosiloxane and/or OMMT is detected on samples heat treated at 250°C and 300°C. According to our previous work on intumescent systems containing zeolite as synergist,⁸² phosphosilicate is only formed above 350°C and this is a possible reason why it was not detected by Marosi et al. Our understanding is that borosiloxane should act as a carrier, and also in the same way as zeolite forms phosphosilicate and probably borophosphate.⁸³ The formation of those compounds might enhance the efficiency of the intumescent structure.

Tang et al.^{84,85} also examined the incorporation of MMT in intumescent PP with a compatibilizer (hexadecyltrimethylammonium bromide) which is usually used as surfactant for making OMMT. Evidence of making a nanocomposite is shown with and without the intumescent system. Cone calorimetry shows a large improvement in the flammability properties when using OMMT. The results are similar to what we showed above. They postulated a mechanism of action suggesting the formation of an aluminophosphate structure but no evidence was given.

Wilkie et al. prepared polyvinylester (PVE) nanocomposites using different OMMT and POSS.⁸⁶ As expected, significant reduction in PkHRR was observed. The goal was to strongly reduce the flammability of PVE. With the nanocomposite approach, the reduction was not enough for military applications on ships. They added phosphorus-containing FRs like tricresylphosphate (TCP) and

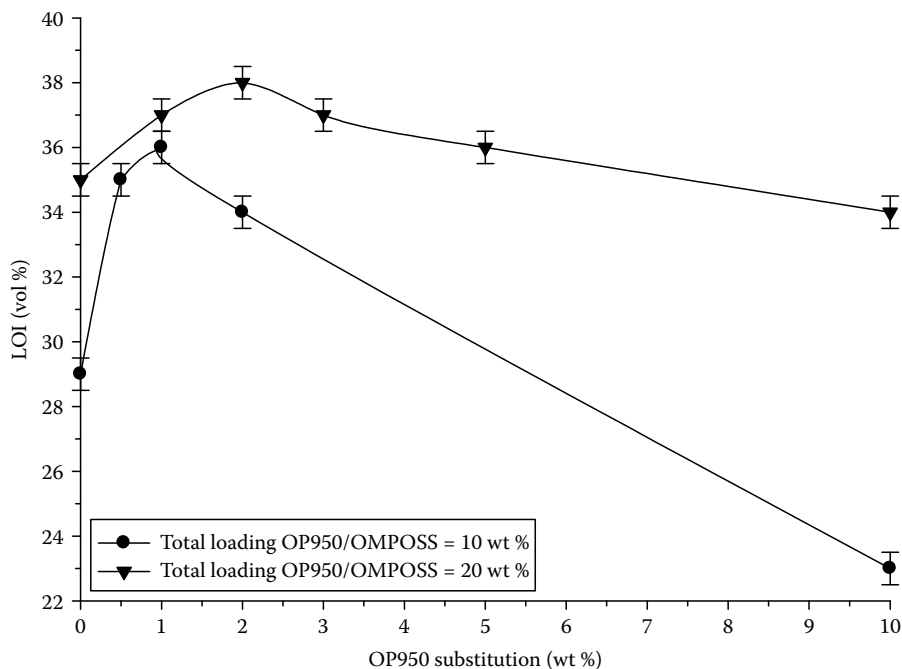


FIGURE 6.15 LOI as a function of OP950 substitution by OMPOSS in formulations containing 10 or 20 wt % additives.

resorcinol diphosphate (RDP) selected using high throughput techniques.⁸⁷ It is not mentioned in the paper if the samples exhibit an intumescent behavior, but according to the chemical nature of PVE and TG results suggesting a condensed-phase mechanism, we may assume that there is formation of charred protective materials in the conditions of fire. Synergy between the phosphorous-containing fire retardants and PVE nanocomposites (OMMT and POSS) is shown through cone calorimetry by reductions in the peak HRR, total heat release, and mass loss rate; there is no improvement in the time to ignition. With this resin, the type of clay used showed different effects on the flammability of the nanocomposites formed. In this study, no mechanism of action is postulated but we may assume that interactions should take place between the synergist (OMMT or POSS) and the phosphate enhancing the properties of the char.

As shown above, the combination of POSS with phosphates provides promising synergistic effects. In a recent work,²¹ it was reported that the combination of POSS with a novel zinc phosphinate salt (OP950 from Clariant) in PET leads to a large synergistic effect. The incorporation of OP950 in PET permits the LOI values to reach 29% and 35% at 10 and 20 wt % loading, respectively. Large synergistic effects are observed when substituting a small amount of OP950 by OMPOSS (Figure 6.15): LOI jumps from 29% to 36% at 10 wt % loading and from 35% to 38% at 20 wt % loading.

Figure 6.16 shows that an intumescent coating is developed on the top of the material in the case of the filled polymers. It is noteworthy that the char is more expanded when using POSS, which suggests that it is the reason why the formulation containing POSS is more efficient than that without POSS.

Cone calorimeter data (Figure 6.17) confirm the advantage of using POSS in PET/OP950 formulations. In the case of the formulation without POSS, the formation of an intumescent coating with a slight expansion at the surface of the polymer is observed, but cracks appear rapidly leading to a sharp PkHRR. The combination of POSS with OP950 reinforces the intumescent char and the expansion is higher permitting a better reduction of the heat transfer between the top and the substrate. HRR curve is spread out over time and PkHRR is decreased by 70% compared to virgin PET.

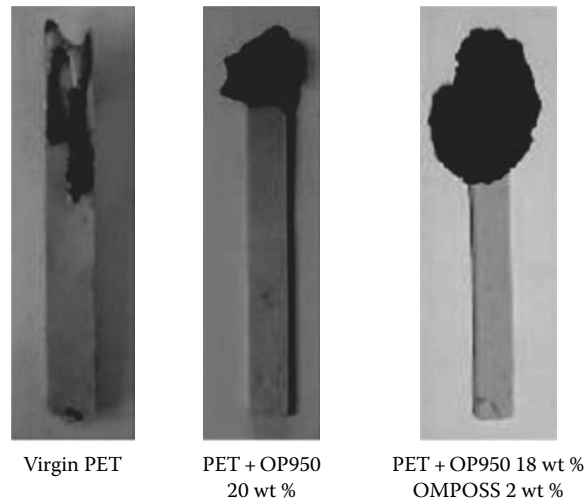


FIGURE 6.16 Burnt barrels in the conditions of LOI (LOI = 1) of PET, PET/OP950, and PET/OP950-OMPOSS.

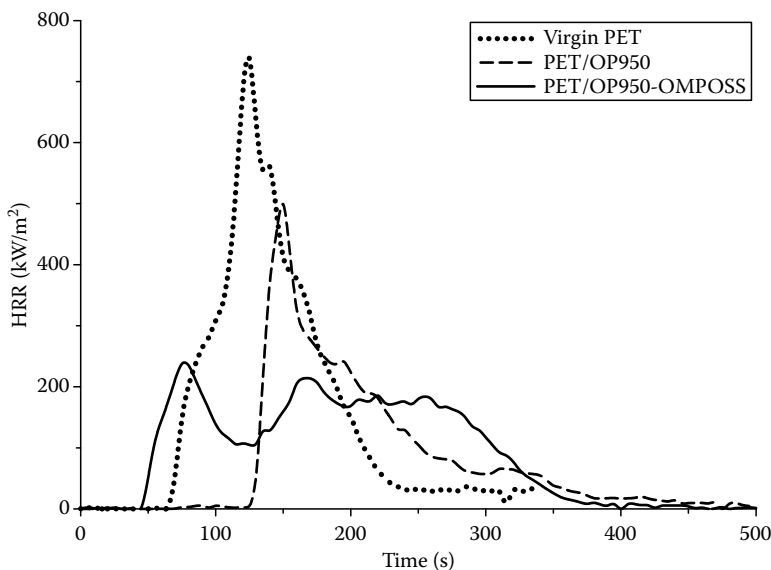


FIGURE 6.17 HRR curves as a function of time of PET, PET/OP950, and PET/OP950-OMPOSS (total loading = 20 wt %; substituting of 2 wt % OP950 by OMPOSS; external heat flux = 35 kW/m²).

Note that the time to ignition is significantly shortened (45 s vs. 75 s). In this particular example, we can note that the incorporation of nanoparticles in intumescent formulations seems to act as “char reinforcer” and “char expander.”

Based on those results and previous work,¹⁹ we may suggest that the chemistry of the system OP950/OMPOSS (see complete description of the degradation of the system in Ref. [88]) does not explain the role of the nanofiller in the improvement of the performance since no specific interaction between the ingredients were detected. Considering the physical aspect, the results suggest that high char strength is required to get the best performance associated with a reasonable expansion. The expansion is related to the formation of an expanded foamed material with the role of limiting heat transfer.

6.5 RESISTANCE TO FIRE OF INTUMESCENT COATING

Intumescent coatings have had a large increase in use, as a method of passive fire protection, over the past few years. Their main purpose is to protect construction materials such as steel and wood, in case of fire. Intumescent coatings are passive fire protections that swell when subjected to high temperatures. They must resist fire and avoid its passage and/or that of gaseous products of combustion. The intumescent coating acts as thermal barrier limiting heat transfer from the heat source to the substrate. The ultimate goal is to keep the integrity and the functionality of the substrate as long as possible. That is why the main parameters taken into account to measure the resistance to fire of a material is the “curve temperature versus time” and the determination of a “time to failure” (time to reach a given temperature, temperature depending on the specifications). In this part, evaluation of the resistance to fire of materials is presented and discussed in Section 6.5.1. Section 6.5.2 is devoted to the development of small-scale tests and to recent protocols developed to measure key parameters of intumescence. Recent results on the performance of intumescence coating is reviewed and discussed in Section 6.5.3.

6.5.1 EVALUATION OF THE RESISTANCE TO FIRE

The protection of metallic materials against fire has become a very important issue in the construction and petrochemical industries, as well as in the marine and military fields. Structural steel loses a significant part of its load-carrying ability when its temperature exceeds 500°C. Prevention of the structural collapse of a building is crucial to ensure the safe evacuation of people from the building, and it is a prime requirement of building regulations in many countries. Intumescent coatings are designed to perform under severe conditions and to maintain the integrity of the steel for 1–3 h when the temperature of the surroundings is in excess of 1100°C.

Several means exist for the protection of steel. These are called “passive fireproofing materials,” which means insulating systems designed to decrease the heat transfer from a fire to the structure being protected. Structural systems can be made fire resistant by increasing the member sizes (structural overdesign), by encasing the structural element in an insulating material of low thermal conductivity (panels, blankets), or by protecting the entire assembly or system with an insulating membrane (mineral or organic resin-based coatings). The type of protection best suited for a particular structure depends primarily on the type of material used in its construction, as each material behaves differently at elevated temperatures. In most cases passive fire protection materials are used in conjunction with foam generation and inert gas suppression, and other “active” systems such as water sprays, and sprinklers and deluge.

The need for these passive fireproofing materials arises from at least one of the following:

- Fire risk assessment carried out by both public and private bodies
- Enforcement of fire safety codes resulting from risk assessment
- The absence of active systems or unavoidable delays in their activation
- Requirements for personnel protection (safe areas, evacuation, etc.)
- Protection of assets

The human and economic costs of fire damage can be significantly reduced if not eliminated by the use of a suitable passive fire protection system.

The key parameters to be considered for structural protection include the usual fire protection standards and the specific authorities governing fire regulations; the nature, the location, and the critical temperature of the substrate protected are also essential parameters. Finally, the conditions that the protection is required to resist during its service life have also to be considered.

Required levels of protection are normally specified in terms of time and temperature on the basis of one or more criteria, which may include statutory requirements, design considerations, and

insurance cost implications. It can vary from a few minutes to several hours, but it usually takes the form of 15 min increments. The duration is established by a time rating which is determined by testing in accordance with an approved standard. Some of the more commonly specified test standards are listed below in Table 6.4.

The standards depend on the kind of fire the material should resist. There are three main categories of fires: the cellulosic or wood fire, the hydrocarbon fire, and the jet fire. However a number of different fire test curves have been proposed (Figure 6.18).^{89,90}

The cellulosic fire curve (ASTM E119) simulates the rate of temperature increase observed in a residential or commercial building fire where the main sources of combustion fuel are cellulosic in nature, such as wood, paper, furniture, and common building materials.⁹¹ The fire curve is characterized by a relatively slow temperature rise to around 927°C after 60 min. There has been some

TABLE 6.4
Usual Test Standards Established by Different Countries

Standard	Country	Description	References
ASTM E-119 (equivalent UL 263)	The United States	Cellulosic or wood fire, used since 1903	[92]
BS 476 Part 8 and Parts 20–22 (1987)	The United Kingdom	Cellulosic or wood fire (similar to ASTM E-119)	[93]
ISO 834 (standard time/temperature curve)	International	Cellulosic or wood fire (similar to ASTM E-119)	[94]
DIN 4102	Germany	Cellulosic or wood fire (similar to ASTM E-119)	[95]
BS 476 (Part 20, Appendix D)	The United Kingdom	Hydrocarbon fire	[96]
ISO 834 (hydrocarbon time/temperature curve)	International	Hydrocarbon fire; developed in the early 1970s	[94]
UL 1709	The United States	Hydrocarbon fire; developed in the early 1970s	[97]

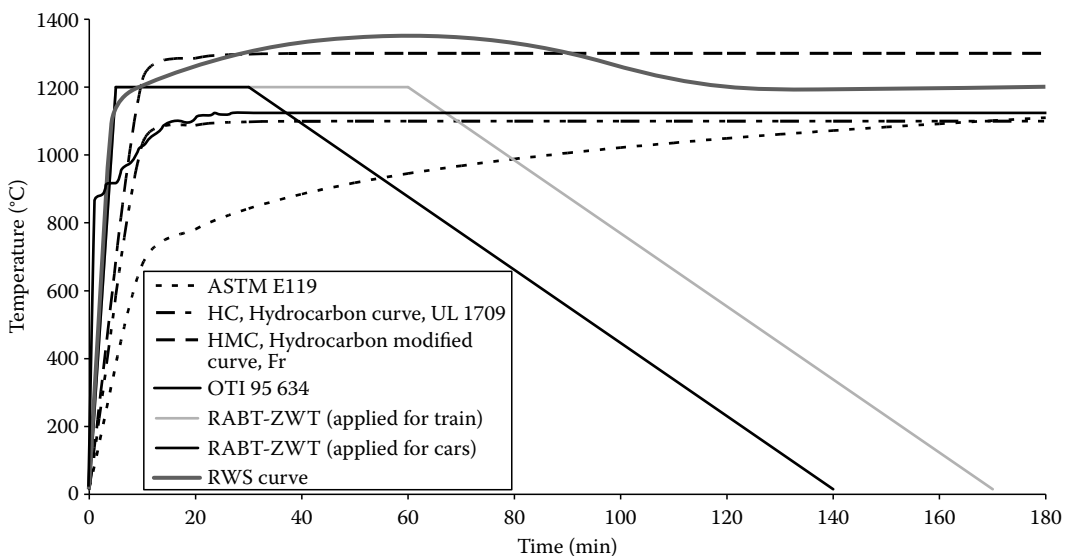


FIGURE 6.18 Standard fire test curves.

discussion recently about the usefulness and applicability of ASTM E-119, given its age, as an indicator of how well it mimics, or predicts the performance of modern steel structures in a fire. In the development of new fireproofing products, this test method is currently used primarily to evaluate the relative performance of fireproofing on full-scale standard sizes and shapes of structural steel under controlled conditions. Although this fire curve is still used, it is noteworthy that the burning rates for certain materials e.g., petrol gas, chemicals, etc., are well in excess of the rate at which, for instance, timber burns. As such, there was a need for an alternative fire test for the evaluation of structures and materials used within the petrochemical industry, and therefore the hydrocarbon test curve was developed.

The hydrocarbon test curve should duplicate or be indicative of the rapid temperature rise seen when a hydrocarbon fuel such as oil or natural gas burns: The temperature rises rapidly to 900°C within 4 min and significantly higher overall temperatures are reached (between 1100°C and 1200°C). This hydrocarbon fire test curve, developed by the Mobil Oil Company in the early 1970s and adopted by a number of organizations and, in particular, Underwriters laboratories (UL 1709 “Rapid Temperature Rise”),⁹⁷ U.K. Department Of Energy, BSI, ISO, and the Norwegian Petroleum Directorate is now a common test method for high-risk environments such as petrochemical complexes and offshore platforms.

Derived from the above-mentioned hydrocarbon curve, the French regulators asked for a modified version, the so-called hydrocarbon modified curve (HCM). The maximum temperature of the HCM curve is 1300°C instead of the 1100°C standard HC curve. However, the temperature gradient in the first few minutes of the HCM fire is as severe as all hydrocarbon-based fires. This test has been developed to consider jet fire scenarios in which leaking high-pressure hydrocarbon gases ignite to produce intense, erosive jet flames that can reach speeds of 150 m per second. A standard jet fire test, denominated OTI 95 634, has been developed jointly by the U.K. Health and Safety Executive and the Norwegian Petroleum Directorate for use predominantly on offshore installations.^{98–100} The test impinges the high-speed stream of ignited propane fuel onto a substrate coated with the product.^{101,102} The propane is delivered at a rate of 0.3–20 kg/s, depending on the test site setup and can consume up to one ton of fuel per minute.

The RABT (Richtlinien für die Ausstattung und den Betrieb von strassen Tunnels) curves were developed in Germany as a result of a series of test programs such as the Eureka project FIRETUN.¹⁰³ In the RABT curve, the temperature rise is very rapid up to 1200°C within 5 min, faster than the HC curve which rises only to 1150°C in 10 min. The duration of the 1200°C exposure is shorter than other curves with the temperature drop off starting to occur at 30 min. This test curve can be adapted to meet specific requirements. In testing to this exposure, the heat rise is very rapid, but is only held for a period of 30 min: It is similar to the sort of temperature rise that would be expected from a simple truck fire, but with a cooling down period of 110 min. If required, for specific types of exposure, the heating period can be extended to 60 min or more, but the 110 min cooling period would still be applied.

The RWS (Rijks Water Staat) curve¹⁰⁴ was developed by the Ministry of Transport in the Netherlands. This curve is based on the assumption that in a worst-case scenario, a fuel, oil, or petrol tanker fire with a fire load of 300 MW could occur, lasting up to 120 min. The RWS curve was based on the results of testing carried out by TNO Centre for Fire Research in the Netherlands in 1979. The difference between the RWS and the HC curve is that the latter is based on the temperatures that are expected from a fire occurring within a relatively open space, where some dissipation of the heat occurs, whereas the RWS curve is based on temperature found in a fire occurring in an enclosed area, such as a tunnel, where there is little or no chance of heat dissipating into the surrounding atmosphere. The RWS curve simulates the initial rapid growth of a fire using a petroleum tanker as the source, and the gradual drop in temperatures to be expected as the fuel load is burnt off.

The standards listed above are the most commonly used standards. However, national authorities governing fire regulations can play a significant role and add more specific standards for

applications within each country. These authorities may be independent certifying authorities or a government body, such as the Health and Safety Executive in the United Kingdom. Regulations are also produced by professional associations and private organizations. In the civil construction field the requirement for fire protection is manifest in building codes and regulations.

Intumescent materials are classified as either thick or thin film intumescent coatings. Intumescent thick films are usually based on epoxy, vinyl, or other elastomeric resins and contain agents that intumesce when exposed to heat. They are available as solvent-free systems that allow application of up to 8–10 mm per coat. These films are particularly efficient in the case of hydrocarbon and jet fires. They are hard and durable and can provide excellent protection against corrosion. This is due to their very high adhesion to the substrate and resistance to impact, abrasion, and vibration damage. High tensile and compressive strengths can be obtained and weather resistance is excellent. However, they are relatively expensive and skilled operators must carry out the application under carefully controlled conditions. Additionally, these coatings have more stringent surface preparation requirements than cementitious materials, and smoke produced in fires makes them unsuitable for certain applications, such as enclosed living areas.

Thin film intumescent coatings were introduced as early as the 1930s and are used for protection from cellulosic-type fires. They are generally available as solvent- or water-based systems, and applied by spray or brush-roller in thin film coats up to 3 mm thick. They typically use thermoplastic acrylic or poly(vinyl acetate) resin, and they respond rapidly and intumesce quickly when exposed to a cellulosic type fire environment. One hour protection can be achieved with between 1 and 3 mm of product. Thin film intumescent coatings are often referred to as “fire retardant paints” rather than “fireproofing” materials due to their inferior fire resistance compared to thick film intumescent coatings. Many of them are unsuitable for exterior without topcoat, and the test ratings are limited to cellulosic fires only. Advantages of these products include their availability in a wide range of colors, price, and ease of application. They are mostly used inside buildings because of their poor durability.

6.5.2 SMALL-SCALE TEST AND MEASUREMENT OF INTUMESCENCE

Resistance to fire of intumescent coating is typically measured by a curve, “temperature as a function of time,” and requires large-scale equipment (see above). Those tests are very expensive and time consuming. The development of a small-scale laboratory test using an external heat flux should be then investigated. As far as we know, only one paper reports this type of approach suggesting a reliable, repeatable, and fast small-scale test¹⁰⁵ and this is discussed in the following.

The basic idea for making a small-scale test was to build a setup permitting one to measure the temperature on the backside of a given substrate (typically steel or wood) when a coated sample is exposed to a heat flux. The heat source chosen is a heat radiator and provides a radiative heat flux. This source is stable and can be easily calibrated. Square plates of $5 \times 5 \text{ cm}^2$ of typical thickness lying between 2 and 10 mm are put on a holder. A black coating of known emissivity and heat resistant is applied on the backside of the plate. The constant emissivity of the backside of the plate allows accurate measurement of the surface temperature of the plate using an infrared pyrometer. The infrared pyrometer is positioned at a constant distance from the steel plate and the beam is pointed on the center of the plate. The temperature on the nonheated face of the plate is detected and the time/temperature curve is registered. The test is shown in Figure 6.19. This small-scale test is very stable and repeatable. The reference curve is the time/temperature curve obtained for a virgin steel plate black coated on its nonheated face. The whole system is placed into a box in order to avoid the effect of the fume cupboard: The aim is to reduce and to control the convective and chimney effects.

Industrial furnace tests, according to UL-1709 standard, have been carried out in a 1.5 m^3 furnace (Figure 6.20) for further comparison with the heat radiator test. Different intumescent formulations have been examined: The first type comprised three basic intumescent (ingredients include APP, PER, and melamine) epoxy resins (IF1, IF2, and IF3) whose performance is compared to a reference commercial intumescent epoxy resin (IF4).

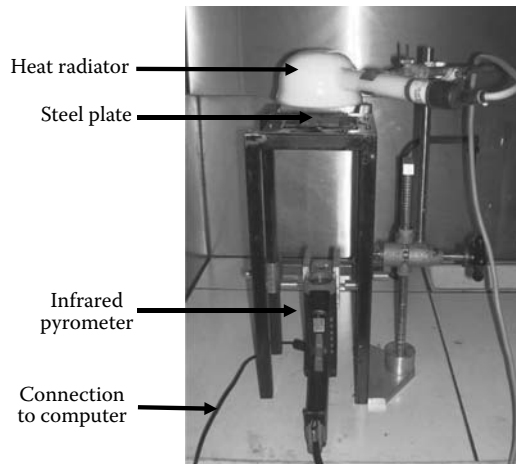


FIGURE 6.19 Presentation of the small-scale test.

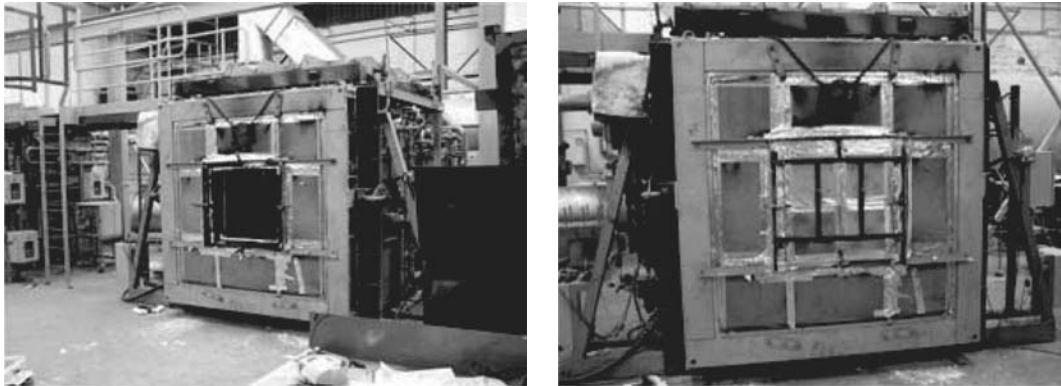


FIGURE 6.20 Industrial furnace.

Heat radiator and UL-1709 tests are compared in Figure 6.21a and b, respectively. The time/temperature curves carried out in the industrial furnace are shown up to 400°C (taken as failure temperature). The materials exhibit very different behavior: The most efficient coating is IF4 (time of failure of about 40 min) while the worst is IF1 (time of failure of 10 min). During the heat radiator test, there is an important increase of temperature at the beginning of the test (from 0 to 5 min) in all cases, but after 8 min the temperature reaches a steady state. For this test, the best performance is obtained when the temperature increases slowly during initial heating ($t < 5$ min) and when the lowest temperature is reached at the end of the test ($t > 8$ min). According to these observations, the curves can be well distinguished. The best formulation is still IF4 with a temperature of about 320°C reached at 20 min, and the worst one is still IF1, which reaches about 400°C at 20 min.

The ranking of results obtained after 20 min in the heat radiator test and at 400°C in the furnace tests agree well with each other. So the heat radiator test appears to be a very interesting tool to carry out an initial assessment of whether a coating might perform well in a HC fire. Another interesting facet of the heat radiator test is that it is possible to look at the expansion of the resulting formed char. Based on this last comment, an experimental protocol permitting the measurement of the expansion of the coating in the dynamic mode or heat gradient through the intumescent coating should be added to the test.

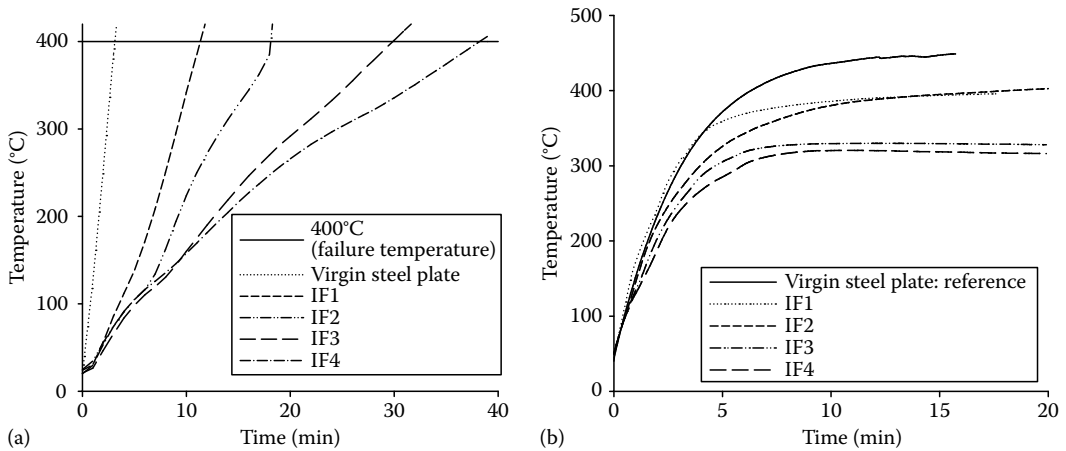


FIGURE 6.21 (a) Industrial furnace and (b) heat radiator test on five intumescent formulations.

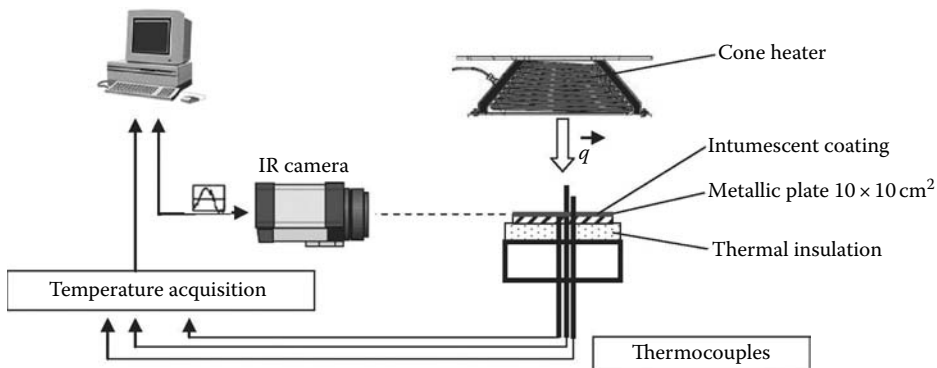


FIGURE 6.22 Experimental setup for measuring the swelling during a cone experiment using infrared camera.

The cone calorimeter used in this investigation was discussed above and it permits one to reproduce a fire scenario. Using an infrared camera, an experimental setup was designed to film a cone calorimeter experiment, as shown in Figure 6.22.¹⁰⁶

The advantage of the infrared camera is to obtain clear images for image analysis. Typical infrared images at the beginning of the experiment and at the maximum of expansion of the intumescent coating are shown on Figure 6.23. Note here that intumescent coating is applied on a steel plate.

Using image analysis in dynamic conditions (from a movie), swelling of the intumescent can be measured and quantified (see the arrow on Figure 6.23b). In this approach, it is assumed during calculation on images that the expansion is homogeneous and occurs in one dimension. Typical curve exhibits a sigmoidal shape showing first a rapid development of intumescence and second a pseudo-steady state at longer times (Figure 6.24). The benefit of this approach is to obtain a quantitative phenomenological model which might be included in further modeling.

One of the primary roles of intumescence is to create a thermal barrier at the surface of the material. Heat gradients can be measured using thermocouples located at the coating—air interface beyond the surface of the coating and at the coating—substrate interface (Figure 6.25).¹⁰⁶ The thermocouple located beyond the surface of the coating permits one to obtain temperature measurement in intumescent layers close to the surface when the intumescent structure is developed. In this experimental setup, it is necessary to assume that additional heat gradients because of the thermocouples are negligible.

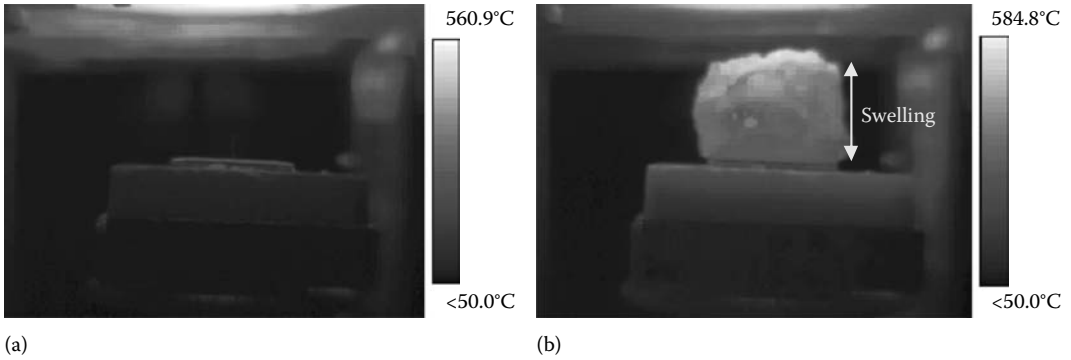


FIGURE 6.23 (See color insert following page 530.) IR images of an intumescent coating on steel plate upon heating at $t = 0$ s (a) and at the maximum of expansion (b).

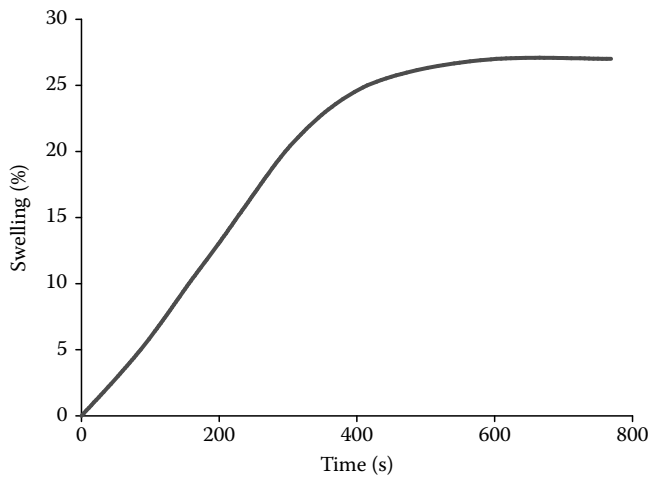


FIGURE 6.24 Typical relative expansion as a function of time of an intumescent coating on a steel plate during a cone calorimeter experiment (external heat flux = 35 kW/m^2).

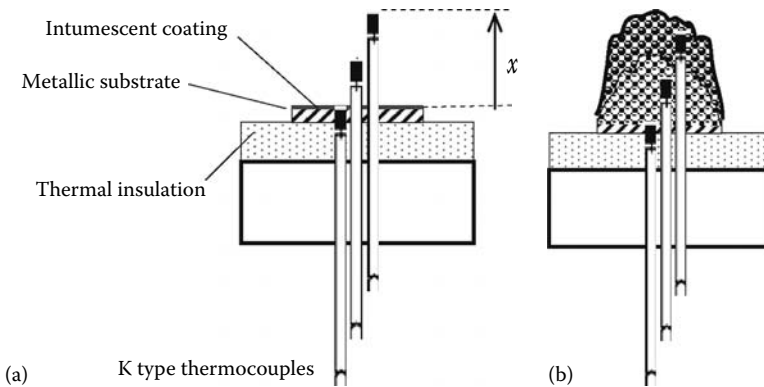


FIGURE 6.25 Experimental setup for measuring heat gradient in an intumescent coating for a cone calorimeter experiment at the beginning of the experiment (a) and at the steady state (b).

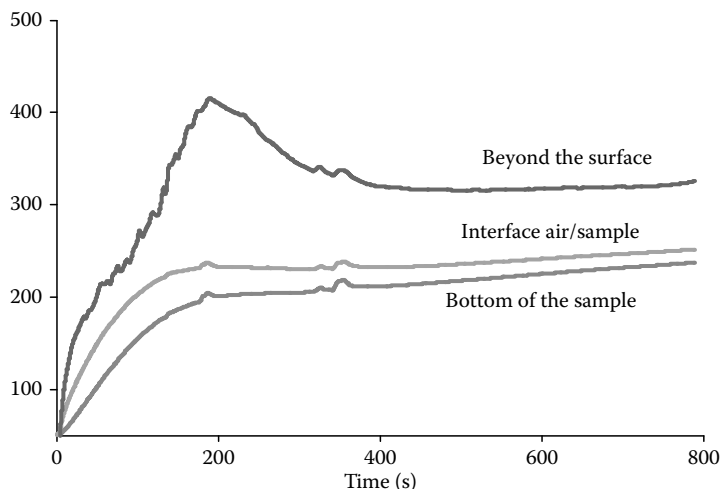


FIGURE 6.26 Temperature as a function of time in an intumescent coating during a cone calorimeter experiment (external heat flux = 35 kW/m^2).

In typical experiments (further examples will be discussed in the third section), the temperature measured by the thermocouple located beyond the surface (higher temperatures in Figure 6.26) rises rapidly because it is not in the expanded char, but the temperature decreases when intumescence reaches the thermocouple indicating the time for the intumescence to reach a certain location (note it is well correlated with expansion measured by IR camera). A steady state is observed at longer times. Comparing the three temperatures, a large heat gradient (about 150°C) can be observed demonstrating the efficiency of the intumescent coating as a heat barrier.

6.5.3 RECENT DEVELOPMENTS

Few recent scientific papers are devoted to resistance to fire using intumescent coating, but a growing market for this application exists. A rapid survey of the literature shows that the formulations used are always based on the well-known trio APP/PER-Melamine. Nevertheless a lot of work remains to be done to understand and to quantify the mechanisms of intumescence acting as protective heat barrier.

A comparison in temperature development, foaming ratios, and rheological behavior was performed by Andersson et al.¹⁰⁷ between formulations containing PER, di-PER, and tri-PER. A simulated fire test developed by the authors (the coated face is upside down and exposed to a Bunsen burner, and an infrared pyrometer records the temperature on the backside), in which the temperature increases during intumescence was studied, showed that the formulations containing PER were considerably more efficient in maintaining a low temperature throughout the process. A more rapid temperature development was displayed using di- and tri-PER as char former. Rheometer tests indicate that PER formulations enter the intumescent process at a lower temperature and stays in it for a longer time than the di- and tri-PER formulations. No explanation is given why PER is more efficient than the others. It might be because of the higher reactivity of PER to APP (reaction of esterification between APP and PER occurs at 190°C) occurring at lower temperature permitting a faster development of the intumescent coating.

The use of synergists (micro- and nanoparticles) was also investigated in intumescent coatings. The most recent work conducted is based on the studies done in intumescent bulk polymer (see reaction to fire part). Li et al.¹⁰⁸ suggested combining EG and/or molybdenum disilicide (MoSi_2) in an intumescent system based on APP/PER-melamine. The results show that incorporating the

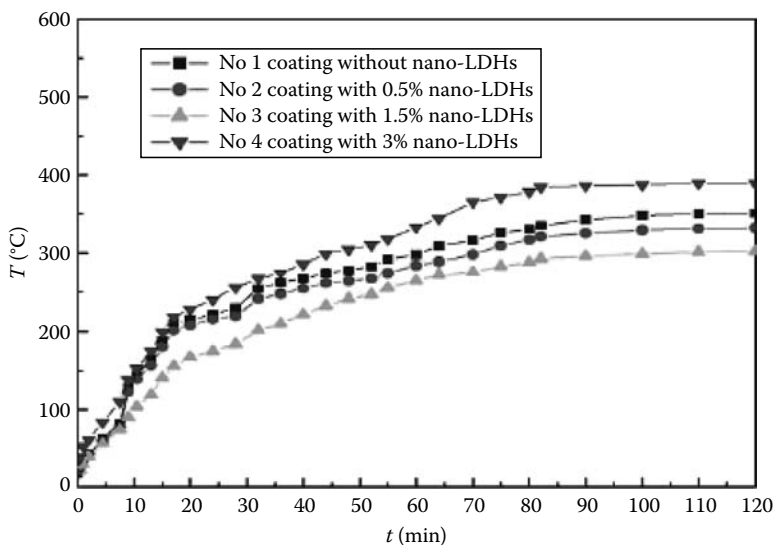


FIGURE 6.27 Temperature curves as a function of time of intumescent coating containing different amount of OLDH. (From Wang, Z. et al., *Prog. Org. Coating*, 53, 29, 2005. With permission.)

synergists, the time to failure (time required to reach 500°C, in this case) is prolonged (heat insulation test similar as that described in the previous paragraph) and the char formation rate is enhanced. The largest improvement is achieved combining the two synergists MoSi_2 and EG in an appropriate ratio. The suggested mechanism of action is revealed using scanning electron microscopy (SEM) images and thermogravimetry showing that the synergistic effect is obtained through a ceramic-like layer produced by MoSi_2 covered on the surface of an “open-cellular” structural char and a better resistance to the thermo-oxidation.

Wang et al.¹⁰⁹ used organomodified layered double hydroxide (OLDH) as a nanofiller combined with an intumescent system in acrylate resin. The intumescent paints were evaluated on steel plate measuring the temperature on the backside of the plate as a function of time while increasing the temperature (standard ISO-834) (Figure 6.27). Upon the incorporation of 1.5% OLDH, the fire resistant time (time to reach 300°C) jumps to 100 min compared to 60 min without OLDH (virgin coating). It is also noteworthy that the thickness of char layer of the formulation with 1.5% OLDH is similar to that of the formulation without clay. This confirms our results suggesting that the highest expansion is not necessary to obtain the best performance. The improvement of the performance is partially explained by the char strength and the specific heat of char layer.

The morphology of char layer exhibits interesting features (Figure 6.28). Close holes can be distinguished in the two pictures but the diameters of holes of the char containing OLDH are much smaller (10–30 μm) than those of the char without OLDH. Wang suggests that small holes reinforce the char strength and avoid the formation of cracks at the surface of the char. Indeed, the formation of close cells in the char structure, evenly dispersed as in foam, reduces heat transfer, and increases the efficiency of the char. When the cells are too big, char strength is reduced and cracks can appear. The postulated mechanism is that OLDH catalyses the esterification between the phosphate and the char former (polyol) but no evidence of this is given.

The same group¹¹⁰ also investigated the use of nanoclay in intumescent acrylic coatings. TEM shows a reasonable dispersion of the nanoclay in the coating, suggesting the formation of a nanocomposite. The FR efficiency of the intumescent nanocomposite coating is improved by augmenting the intumescent formulation with 1.5 wt % nanoclay. However, at 3 wt % substitution nanoclay produces a negative effect on the fire performance of the coating. An interesting feature of the intumescent coating is that the incorporation of 1.5 wt % nanoclay leads to the lowest thermal conductivity

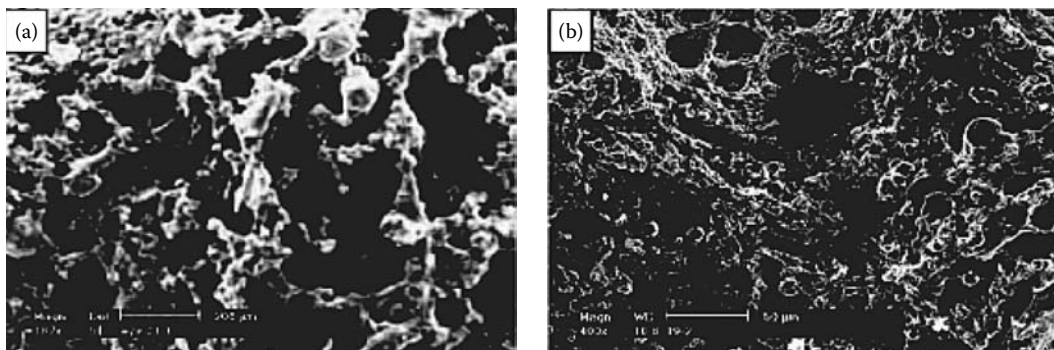


FIGURE 6.28 SEM image of inner surface of char layer of the formulation without OLDH (a) and with 1.5 wt % OLDH (b). (From Wang, Z. et al., *Prog. Org. Coating*, 53, 29, 2005. With permission.)

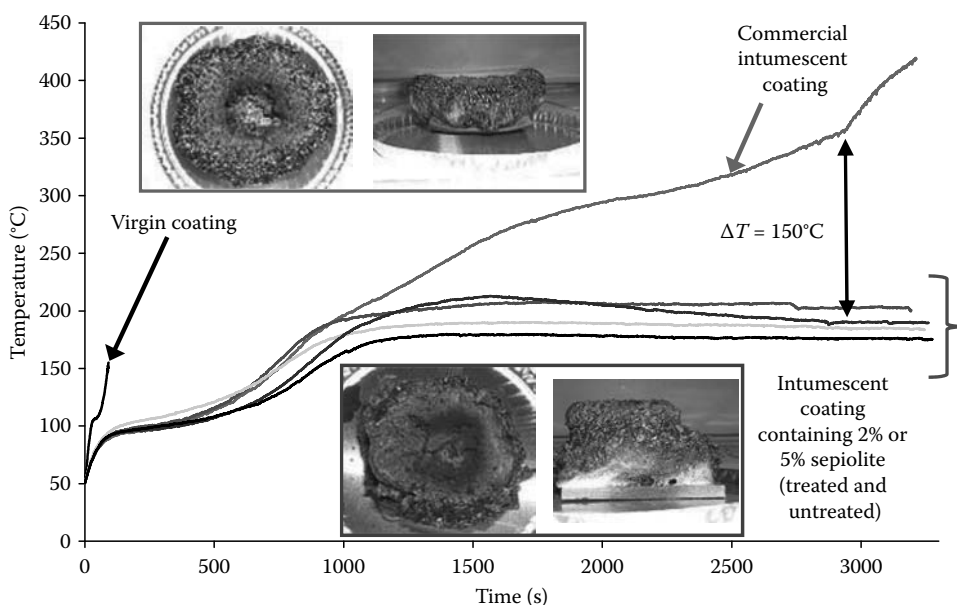


FIGURE 6.29 (See color insert following page 530.) Temperature as a function of time of the backside of wooden plate protected by an intumescent coating containing sepiolite or not.

(measured between 20°C and 1000°C) while it is the highest at 3 wt %. This might explain at least partially the enhancement of the performance. The authors also suggest the formation of a ceramic-like structure at the surface of the intumescent coating, but no evidence is given. According to our previous work,⁷⁴ we may suggest that nanoclay should react with APP contained in the formulation to yield aluminophosphate stabilizing the intumescent coating.

Using the heat radiator test presented in the previous section, an intumescent clear coat containing or not containing sepiolite (2 or 5 wt % loading) was applied on a wooden plate. In this particular case, the considerable benefit of incorporating additional nanofiller (sepiolite) in the formulation is shown (Figure 6.29). The incorporation of sepiolite permits the formation of an intumescent shield strongly limiting heat transfer between the top of the coating and the backside of the wooden plate (difference of 150°C at 3000s between the coatings with and without sepiolite). Besides, the intumescent coating containing the sepiolite permits the preservation of the integrity of the wooden

plate beyond 3000 s while for the coating without sepiolite a dramatic increase of temperature is observed, which is assigned to the degradation of wood which is no longer protected due to the lack of cohesiveness of the coating without sepiolite compared to that with sepiolite. This is probably the explanation for the performance of the coating containing sepiolite.

6.6 CONCLUSION AND FUTURE TRENDS

In this chapter, we have discussed recent developments of intumescent flame-retarded materials in terms of reaction and resistance to fire. Research work in intumescence is very active. New molecules (commercial molecules and new concepts) have appeared. Nanocomposites are a relatively new technology in the field of flame retardancy. This technology gives the best results combined with conventional FRs and leads to synergistic effects with intumescent systems. Very promising developments in the synergy aspects are then expected and efforts should be continued in this way.

The quick overview of the mechanisms of action reveals that the formation of an expanded charred insulative layer acting as thermal shield is involved. The mechanism of action is not completely elucidated, especially the role of the synergist. Reaction may take place between the nano-filler and some ingredients of the intumescent formulation (e.g., the phosphate) in order to thermally stabilize the charred structure. Only physical interactions are observed (e.g., action of POSS with phosphinate), and these interactions permit the reinforcement of the char strength and avoid the formation of cracks. The development rate and the quality of this layer are therefore of the primary importance and research work should be focused on this.

REFERENCES

1. Vandersall, H.L. 1971. Intumescent coating systems, their development and chemistry. *J. Fire Flammability* 2:97–140.
2. Bourbigot, S., Le Bras, M., Duquesne S., and Rochery, M. 2004. Recent advances for intumescent polymers. *Macromol Mater. Eng.* 289:499–511.
3. Tramm, H., Clar, C., Kühnel, P., and Schuff, W. 1938. U.S. 2,106,938, assigned to Ruhrchemie Aktiengesellschaft.
4. Bourbigot, S. and Duquesne, S. 2007. Fire retardant polymers: Recent developments and opportunities. *J. Mater. Chem.* 17:2283–2300.
5. Camino, G., Costa, L., and Trossarelli, L. 1985. Study of the mechanism of intumescence in fire retardant polymers: Part V—Mechanism of formation of gaseous products in the thermal degradation of ammonium polyphosphate. *Polym. Deg. Stab.* 12:203–211.
6. Delobel, R., Le Bras, M., Ouassou, N., and Alistiqsa, F. 1990. Thermal behaviors of ammonium polyphosphate-pentaerythritol and ammonium pyrophosphate-pentaerythritol intumescent additives in polypropylene formulations. *J. Fire Sci.* 8:85–92.
7. Bourbigot, S., Le Bras, M., and Delobel, R. 1995. Fire degradation of an intumescent flame retardant polypropylene. *J. Fire Sci.* 13:3–9.
8. Kandola, B.K., Horrocks, A.R., Myler, P., and Blair, D. 2002. The effect of intumescent on the burning behaviour of polyester-resin-containing composites. *Composites, Part A: Appl. Sci. Manufacturing* 33A(6):805–817.
9. Zhang S. and Horrocks, A.R. 2003. Substantive intumescence from phosphorylated 1,3-propanediol derivatives substituted on to cellulose. *J. Appl. Polym. Sci.* 90(12):3165–3172.
10. Camino, G., Costa L., and Trossarelli, L. 1984. Study of the mechanism of intumescence in fire retardant polymers: Part II—Mechanism of action in polypropylene-ammonium polyphosphate-pentaerythritol mixtures. *Polym. Deg. Stab.* 7(1):25–31.
11. Jenewein, E. and Pirig, W.D. 1996. European patent EP 0 735 119 A1 assigned to Hoechst A.G.
12. Morice, L., Bourbigot, S., and Leroy, J.M. 1997. Heat transfer study of polypropylene-based intumescent systems during combustion. *J. Fire Sci.*, 15:358–374.
13. Le Bras, M., Bourbigot, S., Delporte, C., Siat C., and Le Tallec, Y. 1996. New intumescent formulations of fire retardant polypropylene: Discussion about the free radicals mechanism of the formation of the carbonaceous protective material during the thermo-oxidative treatment of the additives. *Fire Mater.* 20:191–203.

14. Bourbigot, S., Duquesne S., and Leroy, J.-M. 1999. Modeling of heat transfer study of polypropylene-based intumescent systems during combustion. *J. Fire Sci.* 17:1–15.
15. Jimenez, M., Duquesne S., and Bourbigot S. 2006. Characterization of the performance of an intumescent fire protective coating. *Surf. Coatings Technol.* 201:979–987.
16. Jimenez, M., Duquesne S., and Bourbigot S. 2006. Multiscale experimental approach for developing high-performance intumescent coating. *Ind. Chem. Eng.* 45:4500–4508.
17. *Additives for Polymers*, December 10, 2006.
18. <http://www.freedoniagroup.com/brochure/22xx/2277smwe.pdf>
19. Bourbigot, S. and Duquesne, S. 2007. In *Polymer Nanocomposite Flammability*, C.A. Wilkie and A.B. Morgan (Eds.), pp. 131–162. Hoboken, NJ: John Wiley & Sons.
20. Bourbigot, S., Duquesne, S., Fontaine, G., Bellayer, S., Turf, T., and Samyn, F. 2008. Characterization and reaction to fire of polymer nanocomposites with and without conventional flame retardants. *Mol. Cryst. Liq. Cryst.* 486:325–339.
21. Vannier, A., Duquesne, S., Bourbigot, S., Castrovinci, A., Camino, G., and Delobel, R. 2008. The use of POSS as synergist in intumescent recycled PET. *Polym. Deg. Stab.* 93:818–826.
22. Beyer, G. 2005. Flame retardancy of nanocomposites from research to technical products. *J. Fire Sci.* 23:75–87.
23. EFRA Update No 63, December 2007.
24. Camino, G. and Delobel, R. 2000. In *Fire Retardancy of Polymeric Materials*, A.F. Grand and C.A. Wilkie (Eds.), pp. 217–243. New York: Marcel Dekker.
25. Horrocks, A.R. 2001. In *Fire Retardant Materials*, A.R. Horrocks and D. Price (Eds.), Chapter 5, pp. 128–181. Cambridge, U.K.: Woodhead Publishing Ltd.
26. Weil, E. and Levchik, S. 2008. Flame retardants in commercial use or development for polyolefins. *J. Fire Sci.* 26:5–43.
27. Brady, G., Moberly, C.W., Norell J.R., and Walters, H.C. 1977. Intumescence: A novel effective approach to flame retarding polypropylene. *J. Fire Retardant Chem.* 4:150–164.
28. Montaudo, G., Scamporrino, E., and Vitalini, D. 1983. Intumescent flame retardants for polymers. II. The polypropylene-ammonium polyphosphate-polyurea system. *J. Polym. Sci., Polym. Chem. Ed.* 21:3361–3371.
29. Halpern, Y., Mather, M., and Niswander, R.H. 1984. Fire retardancy of thermoplastic materials by intumescence. *Ind. Org. Chem. Prod. Res. Dev.* 23:233–238.
30. Fontaine, G., Bourbigot, S., and Duquesne, S. 2008. Neutralized flame retardant phosphorus agent: Facile synthesis, reaction to fire in PP and synergy with zinc borate. *Polym. Deg. Stab.* 93:68–76.
31. Liu, Y. and Wang, Q. 2006. Catalytic action of phospho-tungstic acid in the synthesis of melamine salts of pentaerythritol phosphate and their synergistic effects in flame retarded polypropylene. *Polym. Deg. Stab.* 91:2513–2519.
32. Chen, Y.H., Liu, Y., Wang, Q., Yin, H., Nico, A., and Kierkels, R. 2003. Performance of intumescent flame retardant master batch synthesized through twin-screw reactively extruding technology: Effect of component ratio. *Polym. Deg. Stab.* 81:215–224.
33. Wang, Q., Chen, Y.H., Liu, Y., Yin, H., Nico, A., and Kierkels, R. 2004. Performance of an intumescent-flame-retardant master batch synthesized by twin-screw reactive extrusion: Effect of the polypropylene carrier resin. *Polym. Int.* 53:439–448.
34. Liu, Y. and Wang, Q. 2008. Reactive extrusion to synthesize intumescent flame retardant with a solid acid as catalyst and the flame retardancy of the products in polypropylene. *J. Appl. Polym. Sci.* 107:14–20.
35. Chen, Y.H. and Wang, Q. 2007. Reaction of melamine phosphate with pentaerythritol and its products for flame retardation of polypropylene. *Polym. Adv. Technol.* 18:587–600.
36. Wang, Z.Y., Feng, Z.Q., Liu, Y., and Wang, Q. 2007. Flame retarding glass fibers reinforced polyamide 6 by melamine polyphosphate/polyurethane-encapsulated solid acid. *J. Appl. Polym. Sci.* 105:3317–3322.
37. Wang, D.Y., Ge, X.G., Wang, Y.Z., Wang, C., Qu, M.H., and Zhou, Q. 2006. A novel phosphorus-containing poly(ethylene terephthalate) nanocomposite with both flame retardancy and anti-dripping effects. *Macromol. Mater. Eng.* 291:638–645.
38. Gao, F., Tong, L., and Fang, Z. 2006. Effect of a novel phosphorous-nitrogen containing intumescent flame retardant on the fire retardancy and the thermal behaviour of poly(butylene terephthalate). *Polym. Deg. Stab.* 91:1295–1299.
39. Ma, Z., Zhao, W., Liu Y., and Shi, J. 1997. Synthesis and properties of intumescent, phosphorus-containing, flame-retardant polyesters. *J. Appl. Polym. Sci.* 63:1511–1515.
40. Li, B. and Xu, M. 2006. Effect of a novel charring-foaming agent on flame retardancy and thermal degradation of intumescent flame retardant polypropylene. *Polym. Deg. Stab.* 91:1380–1386.

41. Xie, F., Wang, Y.Z., Yang, B., and Liu, Y. 2006. A novel intumescent flame-retardant polyethylene system. *Macromol. Mater. Eng.* 291:247–253.
42. Wang, D.L., Liu, Y., Wang, D.Y., Zhao, C.X., Mou, Y.R., and Wang, Y.Z. 2007. A novel intumescent flame-retardant system containing metal chelates for polyvinyl alcohol. *Polym. Deg. Stab.* 92:1555–1564.
43. Samyn, F. 2007. Compréhension des procédés d'ignifugation du polyamide-6—Apport des nanocomposites aux systèmes retardateurs de flamme phosphorés. PhD dissertation, Lille University, Lille, France.
44. Braun, U., ScharTEL, B., Fichera, M.A., and Jaeger, C. 2007. Flame retardancy mechanisms of aluminium phosphinate in combination with melamine polyphosphate and zinc borate in glass-fibre reinforced polyamide 6,6. *Polym. Deg. Stab.* 92:1528–1545.
45. Braun, U. and ScharTEL, B. 2008. Flame retardancy mechanisms of aluminium phosphinate in combination with melamine cyanurate in glass-fibre-reinforced poly(1,4-butylene terephthalate). *Macromol. Mater. Eng.* 293:206–217.
46. Arthur, W. 1912. Making intumescent alkali silicate, U.S. 1041565.
47. Langille, K., Nguyen D., and Veinot, D.E. Inorganic intumescent coatings for improved fire protection of GRP. *Fire Technol.* 35:99–110.
48. Hermansson, A., Hjertberg, T., and Sultan, B.-A. 2003. The flame retardant mechanism of polyolefins modified with chalk and silicone elastomer. *Fire Mater.* 27:51–70.
49. Lundgren, A., Hjertberg, T., and Sultan, B.-A. 2007. Influence of the structure of acrylate groups on the flame retardant behavior of ethylene acrylate copolymers modified with chalk and silicone elastomer. *J. Fire Sci.* 25:287–319.
50. Krämer, R.H., Blomqvist, P., Hees, P.V., and Gedde, U.W. 2007. On the intumescence of ethylene-acrylate copolymers blended with chalk and silicone. *Polym. Deg. Stab.* 92:1899–1910.
51. Bourbigot, S., Le Bras, M., Flambard, X., Rochery, M., Devaux, E., and Lichtenhan, J.D. 2005. In *Fire Retardancy of Polymers: New Applications of Mineral Fillers*, M. Le Bras, M. Wilkie, C.A. Bourbigot, S. Duquesne, and C. Jama (Eds.), pp. 189–201. Cambridge, U.K.: The Royal Society of Chemistry.
52. Bourbigot, S., Turf, T., Bellayer, S., and Duquesne, S., 2009. Polyhedral oligomeric silsesquioxane as flame retardant for thermoplastic polyurethane. *Polym. Deg. Stab.* 94:1230–1237.
53. Schafhautl, P.J. 1841. *Praktische Chemie.* 21:155–168.
54. Duquesne, S., Le Bras, M., Bourbigot, S., Delobel, R., Vezin, H., Camino, G., Eling, B., Lindsay C., and Roels, T. 2003. Expandable graphite: A fire retardant additive for polyurethane coating. *Fire Mater.* 27:103–117.
55. Horrocks, A.R., Kandola, B.K., Davies, P.J., Zhang, S., and Padbury, S.A. 2005. Developments in flame retardant textiles: A review. Analyse des Porphyrins von Kreuznach im Nahethale, *Polym. Deg. Stab.* 88:3–12.
56. Davies, P.J., Horrocks, A.R., and Alderson, A. 2005. The sensitisation of thermal decomposition of ammonium polyphosphate by selected metal ions and their potential for improved cotton fabric flame retardancy. *Polym. Deg. Stab.* 88:114–122.
57. Giraud, S., Bourbigot, S., Rochery, M., Vroman, I., Tighzert, L., and Delobel, R. 2002. Microencapsulation of phosphate—Application to flame retarded cotton. *Polym. Deg. Stab.* 77:285–297.
58. Giraud, S., Bourbigot, S., Rochery, M., Vroman, I., Tighzert, L., Delobel, R., and Poutch, F. 2005. Flame retarded polyurea with encapsulated ammonium phosphate for textile coating. *Polym. Deg. Stab.* 88:106–113.
59. Saihi, D., Vroman, I., Giraud, S., and Bourbigot, S. 2005. Microencapsulation of ammonium phosphate with a polyurethane shell—Part I: Coacervation technique. *React. Funct. Polym.* 64:127–138.
60. Saihi, D., Vroman, I., Giraud, S., and Bourbigot, S. 2006. Microencapsulation of ammonium phosphate with a polyurethane shell—Part II: Interfacial polymerization technique. *React. Funct. Polym.* 66:1118–1125.
61. Horrocks A.R. and Davies, P.J. 2000. Char formation in flame-retarded wool fibres. Part 1. Effect of intumescent on thermogravimetric behaviour. *Fire Mater.* 24:151–157.
62. Horrocks, A.R. and Zhang, S. 2004. Char formation in polyamides (nylons 6 and 6.6) and wool keratin phosphorylated by polyol phosphoryl chlorides. *Textile Res. J.* 74:433–441.
63. Chen, D.Q., Wang, Y.Z., Hu, X.P., Wang, D.Y., Qu, M.H., and Yang, B. 2005. Flame-retardant and anti-dripping effects of a novel char-forming flame retardant for the treatment of poly(ethylene terephthalate) fabrics. *Polym. Deg. Stab.* 88:349–356.
64. Liu, W., Chen, D.Q., Wang, Y.Z., Wang, D.Y., and Qu, M.H. 2007. Char-forming mechanism of a novel polymeric flame retardant with char agent. *Polym. Deg. Stab.* 92:1046–1052.
65. Almeras, X., Vannier, A., Vandendaele, P., Duquesne, S., Bourbigot, S., Delobel, R., Ortiz, M., Gupta, G., and Pivotto, E. 2008. New halogen free masterbatch for PET fibers. *Chem. Fibers Inter.* 58:178–181.

66. Zhang, S. and Horrocks, A.R. 2003. A review of flame retardant polypropylene fibres. *Prog. Polym. Sci.* 28:1517–1538.
67. Horrocks, A.R. 2003. Flame-retardant finishes and finishing, chemical testing of textiles, D.H. Heywood (Ed.), pp. 214–250. Bradford, U.K.: Society of Dyers and Colourists.
68. Drevelle, C. 2005. Conception et développement de systèmes retardateurs de flamme pour fibres synthétiques. PhD dissertation, Lille University, Lille, France.
69. Lyon, R.E., Speitel, L., Walters N., and Crowley, S. 2003. Fire-resistant elastomers. *Fire Mater.* 27:195–208.
70. Bourbigot, S., Le Bras, M., Delobel, R., Bréant, P., and Trémillon, J.-M. 1996. 4A Zeolite synergistic agent in new flame retardant intumescent formulations of polyethylenic polymers—Study of the constituent monomers. *Polym. Deg. Stab.* 54:275–283.
71. Bourbigot, S., Le Bras, M., Trémillon, J.-M., Bréant, P., and Delobel, R. 1996. Zeolites: New synergistic agents for intumescent thermoplastic formulations—Criteria for the choice of the zeolite. *Fire Mater.* 20:145–158.
72. Le Bras, M. and Bourbigot, S. 1996. Mineral fillers in intumescent fire retardant formulations—Criteria for the choice of a natural clay, filler for the ammonium polyphosphate/pentaerythritol. *Fire Mater.* 20:39–49.
73. Samyn, F., Bourbigot, S., Duquesne, S., and Delobel, R. 2007. Effect of zinc borate on the thermal degradation of ammonium polyphosphate. *Thermochim. Acta* 456:134–144.
74. Levchik, S.V., Camino, G., Costa, L., and Levchik, G.F. 1995. Mechanism of action of phosphorus-based flame retardants in nylon 6. I. Ammonium polyphosphate. *Fire Mater.* 19:1–10.
75. Levchik, S.V., Levchik, G.F., Camino, G., and Costa, L. 1996. Lesnikovich, A.I. Mechanism of action of phosphorus-based flame retardants in nylon 6. III. Ammonium polyphosphate/manganese dioxide. *Fire Mater.* 20:183–190.
76. Marosi, Gy., Bertalan, Gy., Anna, P., Ravadits, I., Bourbigot, S., Le Bras, M., and Delobel, R. 2000. In *Recent Advances in Flame Retardancy of Polymeric Materials XI*, M. Lewin (Ed.), pp. 115–128. Norwalk, CT: BCC.
77. Anna, P., Marosi, Gy., Csantos, I., Bourbigot, S., Le Bras, M., and Delobel, R. 2002. Intumescent flame retardant systems of modified rheology. *Polym. Deg. Stab.* 77:243–251.
78. Lewin, M. 2005. Unsolved problems and unanswered questions in flame retardance of polymers. *Polym. Deg. Stab.* 88:13–19.
79. Antonov, A., Yablokova, M., Costa, L., Balabanovich, A., Levchik, G., and Levchik, S. 2000. The effect of nanometals on the flammability and thermooxidative degradation of polymer materials. *Mol. Cryst. Liquid Cryst.* 353:203–210.
80. Marosi, G., Marton, A., Szep, A., Csontos, I., Keszei, S., Zimonyi, E., Toth, A., Almeras X., and Le Bras, M. 2003. Fire retardancy effect of migration in polypropylene nanocomposites induced by modified interlayer. *Polym. Deg. Stab.* 82:379–385.
81. Marosi, G., Keszei, S., Marton, A., Szep, A., Le Bras, M., Delobel, R., and Hornsby, P. Flame retardant mechanisms facilitating safety in transportation. In *Fire Retardancy of Polymers: New Applications of Mineral Fillers*, M. Le Bras, C.A. Wilkie, S. Bourbigot, S. Duquesne, and C. Jama (Eds.), pp. 347–360. Cambridge, U.K.: The Royal Society of Chemistry.
82. Bourbigot, S., Le Bras, M., Delobel, R., Décessain R., and Amoureux, J.P. 1996. Synergistic effect of zeolite in an intumescent process—Study of the carbonaceous structures using solid state NMR. *J. Chem. Soc., Faraday Trans.* 92:149–161.
83. Jimenez, M., Duquesne, S., and Bourbigot, S. 2006. Intumescent fire protective coating: Toward a better understanding of their mechanism of action. *Thermochim. Acta* 449:16–26.
84. Tang, Y., Hu, Y., Wang, Y.S., Gui, Z., Chen Z., and Fan, W. 2003. Intumescent flame retardant-montmorillonite synergism in polypropylene-layered silicate nanocomposites. *Polym. Inter.* 52:1396–1400.
85. Tang, Y., Hu, Y., Li, B., Liu, L., Wang, Z., Chen, Z., and Fan, W. 2004. Polypropylene/montmorillonite nanocomposites and intumescent, flame-retardant montmorillonite synergism in polypropylene nanocomposites. *J. Polym. Sci. A Polym. Chem.* 42:6163–6173.
86. Chigwada, G., Jash, P., Jiang D.D., and Wilkie, C.A. 2005. Fire retardancy of vinyl ester nanocomposites: Synergy with phosphorus-based fire retardants. *Polym. Deg. Stab.* 89:85–100.
87. Gilman, J.W., Bourbigot, S., Schields, J.R., Nyden M., Kashiwagi, T., Davis R.D., VanderHart D.L., Demory, W., Wilkie C.A., Morgan, A.B., Harris, J., and Lyon R.E. 2003. High throughput methods for polymer nanocomposites research: Extrusion, NMR characterization and flammability property screening. *J. Mater. Sci.* 38:4451–4460.

88. Vannier, A. 2008. Procédés d'ignifugation du poly(éthylène téréphtalate)—Application au textile. PhD dissertation, Lille University, Lille, France.
89. Promat Tunnel Fire Protection, <http://www.promat-tunnel.com/idprt004.htm>
90. Rockwool, fire safe insulation, A guide to risk and changes in the legislation <http://www.rockwool.com/graphics/RW-GB-implementation/brochures/Fire-Protection.pdf>
91. ASTM. Standard test methods for fire tests of building construction and materials, ASTM E-119, American Society for Testing and Materials, West Conshohocken, PA.
92. BSI Test methods and criteria for the fire resistance of elements of building construction, BS 476: Part 8, 1972, British Standard Institute, London.
93. BS 476: Part 20–22, 1987, British standard Institute, London, <http://www.firetherm.com/frames2.htm?jargonpage.htm~home>
94. ISO Fire resistance tests, elements of building construction, ISO 834, 1999, International Organisation for Standardization.
95. DIN Brandverhalten von Baustoffen und Bauteilen, DIN 4102, 1998, Deutsches Institut für Normung.
96. BSI Test methods and criteria for the fire resistance of elements of building construction, BS 476: part 20, Appendix D, 1987, British Standard Institute, London.
97. UL Rapid rise fire tests of protection materials for structural steel, UL 1709, 1994, Underwriter Laboratories.
98. HSE Offshore Technology Report OTI 95634, Jet fire resistance test of passive fire protection materials, 1996.
99. Norsok Standard, Piping and Equipment Insulation, 2005.
100. http://www.standard.no/pronorm-3/data/f/0/10/28/4_10704_0/R-004d1r3.pdf
101. Buckland I., Characterisation of passive fire protection materials against jet fire impingement, DIN TD5/005, 2003.
102. <http://www.hse.gov.uk/foi/internalops/hid/din/505.pdf>
103. Eureka-Project EU 499: FIRETUN, Fires in transport tunnels, Report of Full Scale Tests. Ed.: Studiengesellschaft Strahlanwendung e.V., Düsseldorf, 1995.
104. RWS Curve, SP Swedish national testing and research Institute http://www.sp.se/fire/Eng/Resistance/RWS_curve.htm
105. Jimenez, M., Duquesne, S., and Bourbigot, S. 2006. High throughput fire testing for intumescent coating. *Ind. Eng. Chem. Res.* 45:7475–7481.
106. Paul, Y., 2009. Master Thesis, Conservatoire des Arts et Métiers, Lille.
107. Andersson, A., Landmark, S., and Maurer, F.H.J. 2007. Evaluation and characterization of ammonium polyphosphate-pentaerythritol-based systems for intumescent coatings. *J. Appl. Polym. Sci.* 104:748–753.
108. Li, G., Liang, G., He, T., Yang, Q., and Song, X. 2007. Effects of EG and MoSi₂ on thermal degradation of intumescent coating. *Polym. Deg. Stab.* 92:569–579.
109. Wang, Z., Han, E., and Ke, W. 2005. Influence of nano-LDHs on char formation and fire-resistant properties of flame-retardant coating. *Prog. Org. Coating.* 53:29–37.
110. Wang, Z., Han, E., and Ke, W. 2007. Fire-resistant effect of nanoclay on intumescent nanocomposite coatings. *J. Appl. Polym. Sci.*, 103:1681–1689.
111. Pagella, C., Samyn, F., and Bourbigot, S. 2008. Laboratory scale testing of nanocomposite intumescent coating. Paper presented at 19th BCC Conference—Recent Advances in Flame Retardancy of Polymeric Materials, Stamford, CT, USA.

7 Fire-Retardant Fillers

Peter Hornsby

CONTENTS

7.1	Introduction.....	163
7.2	Fire-Retardant Filler Types.....	164
7.2.1	Aluminum Hydroxide.....	164
7.2.2	Magnesium Hydroxide.....	166
7.2.3	Basic Magnesium Carbonates.....	166
7.2.4	Boehmite.....	167
7.2.5	Calcium Sulfate Dihydrate (Gypsum).....	167
7.2.6	Hydrotalcite.....	167
7.3	Scope of Application.....	167
7.4	Flame-Retardant Mechanism.....	168
7.4.1	Thermal Effects from Filler.....	169
7.4.2	Filler–Polymer Interactions.....	171
7.4.3	Vapor-Phase Action.....	173
7.5	Smoke Suppression.....	173
7.6	Enhancing the Efficiency of Fire-Retardant Fillers.....	174
7.6.1	Synergism.....	175
7.6.2	Multicomponent Structures.....	178
7.6.3	Nanosize Fire-Retardant Fillers.....	179
7.7	Conclusions.....	181
	References.....	182

7.1 INTRODUCTION

On a mass basis, inorganic hydroxides represent more than 50% of flame retardants sold globally. This results from their low cost, relative to antimony-halogen systems and phosphorus-containing fire retardants, their low toxicity, and minimal corrosivity. In addition to their flame-retardant action, they can also contribute to reduced smoke emission during polymer combustion, in isolation, or in combination with other flame-retardant types. Aluminium hydroxide (ATH) is by far the largest-selling inorganic hydroxide used as a fire retardant and is used in a wide range of elastomers, thermoplastics, and thermosetting resins processed at temperatures below 200°C. Due to the higher thermal stability of magnesium hydroxide (in excess of 300°C), it can be used in polymers processed at higher temperatures, including polypropylene (PP) and engineering thermoplastics, in addition to many elastomers. Both these hydroxides are available in a number of forms that can critically determine their suitability as fire retardants and general acceptability in polymer parts.

There are also a number of other hydroxides and hydroxycarbonates, which are increasingly being used as alternatives to halogen- and phosphorus-containing fire-retardant additives, since they are perceived to have less adverse impact on the environment.

A major drawback to the industrial use of fire-retardant fillers is the high addition levels needed in most polymers to confer adequate fire retardancy. This can detrimentally influence processability and melt rheology, and, when used in load-bearing situations, the presence of the filler generally

results in a deterioration in the strength and toughness of the composite. Both these limitations can be ameliorated by judicious formulation using surface treatments.

In this chapter, an overview is presented of the principal fire-retardant filler types, including details of their origin, characteristics, and application. Consideration will then be given to their mechanism of action both as flame retardants and as smoke suppressants, and to means for potentially increasing their efficiency using synergists and nanoscale variants.

7.2 FIRE-RETARDANT FILLER TYPES

The presence of particulate fillers in polymers can strongly influence their combustion characteristics, including flammability resistance, and the extent and the nature of smoke and toxic gas emission products. This may simply result from the dilution of the combustible fuel source, slowing down the diffusion rate of oxygen and flammable pyrolysis products, or in some instances, such as with polyamides, reducing the tendency of the polymer to drip. Additionally, the inclusion of filler may change the heat capacity, thermal conductivity, and emissivity of the polymer, causing increased rates of heat transfer or greater thermal reflectivity, which can also slow the rate of burning.

Hence, fillers cannot be classed as totally inert in terms of their effect on polymer combustion; however, metal hydroxides, hydrates, and carbonates can confer additional flame retardancy and smoke suppressing qualities. This results from the endothermic decomposition of the filler, which cools the solid or condensed phase, and the release of gases (water and/or carbon dioxide), thereby diluting and cooling flammable combustion products in the vapor phase. The inorganic residue remaining after filler decomposition may also be highly significant in providing a thermally insulating barrier between the underlying polymer substrate and external heat source, in addition to contributing to overall smoke suppression. Further details and examples of this mechanism are discussed later.

The following properties are ideally required for the successful commercial use of a fire-retardant filler:¹

1. A significant endothermic decomposition in the temperature range 100°C–300°C, with release of at least 25% by weight of water and/or carbon dioxide, depending on the polymer, its mechanism of decomposition, and inherent resistance to combustion
2. Ready availability and low cost
3. Low toxicity
4. Available with small particle sizes, with defined morphology and ideally low surface area and capable of being used at high filler loadings
5. Low levels of solubility, extractable salts, and of potentially detrimental impurities (such as those causing premature polymer degradation)
6. Colorless

Hydroxides, hydroxy carbonates, and hydrates of aluminum, calcium, and magnesium that potentially meet these requirements are shown in Table 7.1, together with relevant thermal properties and gaseous products evolved on decomposition. However, of those in commercial use, aluminum hydroxide makes up about 90% of the market by tonnage, with magnesium hydroxide and basic magnesium carbonate products being used in niche applications.

There are several different ways of producing these fillers resulting in various forms differing in particle size, surface area, purity, and morphology, which can have a profound influence on their performance as fire retardants. An overview of their principal methods of production is considered in the following text.

7.2.1 ALUMINUM HYDROXIDE

Aluminum hydroxide ($\text{Al}(\text{OH})_3$), also known as alumina trihydrate or ATH, is produced using the Bayer process from the mineral bauxite (a crude form of aluminum hydroxide containing 40%–70%

TABLE 7.1
Current and Potential Fire-Retardant Fillers

Candidate Material (Common Names and Formula)	Approximate Onset of Decomposition (°C)	Approximate Enthalpy of Decomposition (kJ/g × 10 ³)	Volatile Content (%w/w)		
			Total	H ₂ O	CO ₂
Nesquehonite MgCO ₃ · 3H ₂ O	70–100	1750	71	39	32
Alumina trihydrate, aluminum hydroxide Al(OH) ₃	180–200	1300	34.5	34.5	0
Basic magnesium carbonate, hydromagnesite 4MgCO ₃ · Mg(OH) ₂ · 4H ₂ O	220–240	1300	57	19	38
Sodium dawsonite NaAl(OH) ₂ CO ₃	240–260	Not available	43	12.5	30.5
Magnesium hydroxide Mg(OH) ₂	300–320	1450	31	31	0
Magnesium carbonate subhydrate MgO · CO _{2(0.96)} H ₂ O _(0.30)	340–350	Not available	56	9	47
Calcium hydroxide Ca(OH) ₂	430–450	1150	24	24	0
Boehmite AlO(OH)	340–350	560	15	15	0
Magnesium phosphate octahydrate Mg ₃ (PO ₄) ₂ · 8H ₂ O	140–150	Not available	35.5	35.5	0
Calcium sulfate dihydrate, gypsum CaSO ₄ · 2H ₂ O	60–130	Not available	21	21	0

Source: Reprinted in part from Rotheron, R.N., *Particulate Filled Polymer Composites*, 2nd edn., Rapra Technology Ltd., Shawbury, U.K., 2003, Chapter 6. With permission.

aluminum-containing minerals, principally gibbsite and boehmite). This involves dissolution with sodium hydroxide to form a solution of sodium aluminate, followed by controlled precipitation. Its low cost is due to the ability to link the production of fire-retardant grades to that of the same material produced on a major scale as an intermediate for the manufacture of alumina.

Ground Bayer hydrate represents the largest volume of ATH sold as a flame retardant in particle size ranges from 1.5 to 35 μm, sometimes classified to give a narrower particle size distribution. Although these are low in cost they have platy, irregular particles, not ideally suited for many applications. The second largest segment of the market is ATH precipitated from purified sodium aluminate, using conditions that give the control of shape and size and remove the need for milling. Median particle size typically ranges from 0.25 to 3 μm.

Aluminum hydroxide is available in a wide range of sizes and shapes and with different surface treatments. Grades with specially tailored particle size distributions are available for applications

requiring very high loadings. When appropriately surface treated, the effects on mechanical properties of using high filler loadings can be reduced, and adverse viscosity increases can be minimized with suitable formulation additions and appropriate mixing techniques to optimize dispersion.

By reacting aluminum hydroxide with oxalic acid, basic aluminum oxalate can be produced, which is thermally stable to 330°C, losing 51% of its mass on decomposition at temperatures above 450°C. It is reported to have a flame-retarding and smoke-suppressing action similar to ATH, but because of its increased thermal stability, it can be used in polyamides and thermoplastic polyesters. However, unlike magnesium hydroxide, in these polymers it does not cause hydrolytic degradation.²

7.2.2 MAGNESIUM HYDROXIDE

This is the second most widely used fire-retardant filler. It is more expensive than aluminum hydroxide, but has a higher decomposition temperature (about 300°C), making it more suitable for use in thermoplastic applications where elevated processing temperatures are encountered.

There are a number of different origins for this product.³ First, there is a limited use of milled natural product (known as brucite), which is impure, less thermally stable than refined magnesium hydroxide and, depending on purity, is generally colored. This is suitable for some applications, where low cost is a requirement and color, and thermal stability are not critical.

Second, there is material precipitated with lime from seawater and brines with high magnesium content. The magnesium is precipitated as the hydroxide using slaked lime or dolomite. Seawater is pretreated with sulfuric acid to remove bicarbonate salts. The precipitate is washed, filtered, and dried. The products tend to comprise small aggregates of crystallites yielding high surface areas.

Concentrated magnesium chloride brine solution can also be used as the source of magnesium and through the Aman process, the solution is hydrolyzed to produce a mixture of magnesium hydroxide, hydrogen chloride, and soluble alkaline salts. The hydroxide produced is then filtered, washed, and dried.

Serpentinite or magnesium hydroxysilicate, $[\text{Mg}_3(\text{Si}_2\text{O}_5)(\text{OH})_4]$, can also be leached with hydrochloric acid to convert the magnesium into the chloride. This magnesium chloride is then hydrolyzed to magnesium oxide and hydrochloric acid and the magnesium oxide formed hydrolyzed to form the hydroxide. By this means, particles with low surface area and defined platy morphology can be produced.

Many variations of these processes exist with the aim of controlling particle surface area, shape, and purity; these characteristics define the fire retarding performance of magnesium hydroxide fillers, especially in more demanding applications where processability and good mechanical properties are also important considerations. In more recent developments, nanosize magnesium hydroxide variants have also been produced.

A more recent innovation has been the development of nickel-doped forms of magnesium hydroxide, which are claimed to have superior fire-retardant properties.⁴

7.2.3 BASIC MAGNESIUM CARBONATES

These products are related to the mineral hydromagnesite, $[4\text{MgCO}_3 \cdot \text{Mg}(\text{OH})_2 \cdot 4\text{H}_2\text{O}]$, which is a mixture of magnesium carbonate and magnesium hydroxide. This decomposes over a range of temperatures, starting at about 220°C and with a total weight loss of 57%. In principle, they should be excellent fire retardants for many polymers, including some thermoplastics, but due to their unsuitable morphology and relatively high price, market acceptance has been limited.

There are natural forms of hydromagnesite found in Greece, but these are mixed with varying amounts of other minerals, notably huntite (a calcium magnesium carbonate stable to 450°C), which is less effective and has a platy morphology that can affect processing.⁵ The huntite content can be up to 50% w/w. Products approximating to the hydromagnesite composition can also be precipitated

from solutions of magnesium salts and this process has been used and is mainly sold for smoke suppressing applications, where it is effective at lower levels than those needed for fire retardancy.

7.2.4 BOEHMITE

Boehmite is, in effect, partly decomposed aluminum hydroxide, where two-thirds of the water has been removed. Although it has been promoted as a fire retardant in its own right, but because of the relatively low water content, does not seem to be very effective for this purpose. However, it does seem to have some potential in mixtures with other fire-retardant fillers and this is where it is now being targeted.⁶

7.2.5 CALCIUM SULFATE DIHYDRATE (GYPSUM)

This is a low cost material with limited fire-retardant properties. It has a low onset of decomposition (under 100°C), but it is reported to find some use as a fire retardant in unsaturated polyester resins.⁷

7.2.6 HYDROTALCITE

These are a series of magnesium aluminum hydroxycarbonates with varying magnesium to aluminum ratios between 1.5 and 3.0 g-atoms of magnesium to 1 g-atom of aluminum. They have layers of magnesium hydroxide interspersed with aluminum cations and carbonate anions. They show similar flame-retardant activity and thermal stability to ATH, but their higher cost currently limits their potential use.

7.3 SCOPE OF APPLICATION

There is widespread application of ATH in elastomers, thermosetting resins, and thermoplastics, its use being generally limited to polymers processed or cured below 200°C. This ranges from styrene-butadiene rubber latex for carpet backing, flame-retardant rubber-insulated cable, conveyor belting roofing and hoses, to flame-retardant unsaturated polyester resins in a wide range of molded products using sheet and dough molding compounds.⁸ ATH is also used in epoxy and phenolic resins, especially in electrical and construction applications, and in cross-linked acrylic resins, for example, in countertops, sinks, and bathroom panels. In thermoplastics, applications for ATH have been found in rigid and plasticized PVC, high, low, and linear low density polyethylene, ethylene-propylene rubber, ethylene-propylene-diene cross-linked rubbers, ethylene-ethyl acrylate copolymers, and ethylene-vinyl acetate (EVA) copolymers.⁹⁻¹² A major use is in low smoke, halogen-free wire, cable, and conduit applications, where there has been significant commercial activity.¹³⁻¹⁷ Although it is claimed that ATH can also be used in PP, the limited thermal stability of this filler generally necessitates special compounding and processing measures, which has inhibited its large-scale application in this polymer.¹⁸

The greater thermal stability of MH to temperatures in excess of 300°C permits its use (or potential use) in polymers such as PP, polyamides, acrylonitrile-butadiene-styrene terpolymer (ABS), modified-poly(phenylene oxide), and aliphatic polyketones, in addition to certain elastomers, where increased thermal stability is a requirement. Major end uses are in wire and cable, appliance housings, and electrical components. A particularly important consideration in engineering components, is the effect of the filler on mechanical properties, and, as is the case with ATH, a variety of surface-treated grades are available to suit the physical demands of intended applications. However, use in thermoplastic polyesters is restricted by its tendency to hydrolyze and degrade the polymer during melt processing. Unlike ATH, in unsaturated polyester resins, MH acts as chain extender adversely affecting resin rheology. Although this effect can be ameliorated by using maleic acid coated grades of MH filler, there are long-term issues concerning the stability of these systems.^{19,20}

Hydromagnesite (usually found in combination with huntite) has intermediate thermal stability, decomposing between 220°C and 240°C.^{21,22} Mixtures of these minerals are used in wire and cable applications, due to their higher thermal resistance than ATH and lower cost compared to MH. They have also been considered for use in ethylene–propylene copolymers²³ and poly(vinyl chloride) (PVC) formulations, where reduced smoke and acid gas emission are requirements.²⁴

7.4 FLAME-RETARDANT MECHANISM

As indicated earlier, a major drawback of using fire-retardant fillers, in relation to alternative flame retardants, including phosphorus-based intumescent and halogen-containing formulations, is their inefficiency, requiring significant addition levels in order to achieve acceptable combustion resistance. Typically filler levels required are between 40% and 60% by weight (Figure 7.1), but lower levels may be acceptable in combination with more effective alternative fire retardants or where the purpose of their inclusion in a formulation is principally to aid smoke suppression.

It is difficult to generalize on the mechanism of fire retardancy in polymers modified with hydrated fillers, since additive levels required are very dependent on polymer type, and, in particular, on their decomposition mechanism. For example, with PP, 60% by weight would be required to achieve an oxygen index in excess of 26%. In polyamide 6 (PA-6) at the same addition level, an oxygen index of nearly 70% can be achieved.²⁵ However, the testing mode can also influence the required filler loading. In order to satisfy UL94 test requirements in terms of dripping during combustion, polyamides, like PP, require significant filler levels despite their high oxygen index, since this raises the viscosity of the decomposing polymer, inhibiting its tendency to drip.²⁶

Furthermore, the effect of hydrated fillers on polymer fire retardancy will depend not only on the nature of the filler, including its particle characteristics (size, shape, and purity) and decomposition behavior, but also on the degradation mechanism of the polymer, together with any filler/polymer interactions that might occur, influencing thermal stability of the polymer and possible char formation.

Contributory effects, which combine to determine the overall mechanism of fire retardancy in polymers are discussed in the following text.

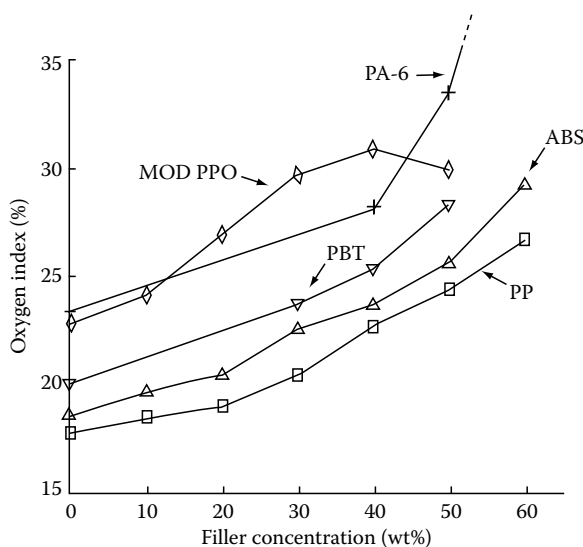


FIGURE 7.1 The influence of magnesium hydroxide filler loading on the oxygen index of selected thermoplastics. (From Hornsby, P.R., *Fire Mater.*, 18, 269, 1994. With permission.)

7.4.1 THERMAL EFFECTS FROM FILLER

This represents the key aspect of polymer fire retardancy using hydrated fillers, and involves energy changes that occur on the decomposition of the filler, related heat capacity effects, which influence the degradation profile of the polymer and thermal barrier formation resulting from the residue remaining from degraded filler.

Differential scanning calorimetry (DSC) and thermogravimetric analysis (TGA) have been widely applied to study the thermal decomposition and the endothermic breakdown of hydrated mineral fillers.²⁷ As shown in Figure 7.2, and mentioned earlier, there are large differences in decomposition temperature with different filler types. Different grades of the same filler type may also behave very differently in terms of the decomposition temperature and the magnitude of the decomposition endotherm.²⁸ Furthermore, the rate of degradation of different grades of magnesium hydroxide may vary, depending on filler morphology and surface area.²⁹ A further complication results from the observation that filler decomposition kinetics can be influenced by the procedure adopted during thermal analysis.²⁷ For example, differences have been observed depending on the sample size, the rate of heating, the rate of inert gas flow rate, and the extent of sample pan closure.

The endothermic decomposition of aluminum hydroxide has been extensively studied giving an enthalpy for the complete decomposition of about 1300 kJ/kg. As with magnesium hydroxide, thermal breakdown depends very much on heating rates and on the ability of gaseous decomposition products to escape from the system. Isothermal studies show that decomposition starts about 200°C. ATH is reported to be less thermally stable as the particle size increases,³ with precipitated grades being significantly more stable than those produced by grinding.³⁰

Although, the decomposition of aluminum hydroxide to oxide is usually written as one step, it can proceed through an intermediate mono-hydroxide [boehmite, $\text{AlO}(\text{OH})$], which often has a much higher stability than the hydroxide, decomposing at about 450°C and, if present, can reduce fire-retardant effectiveness. In addition, several so-called transition aluminas are formed upon heating of hydroxides, depending on the applied temperature.³¹ Boehmite formation can occur when the

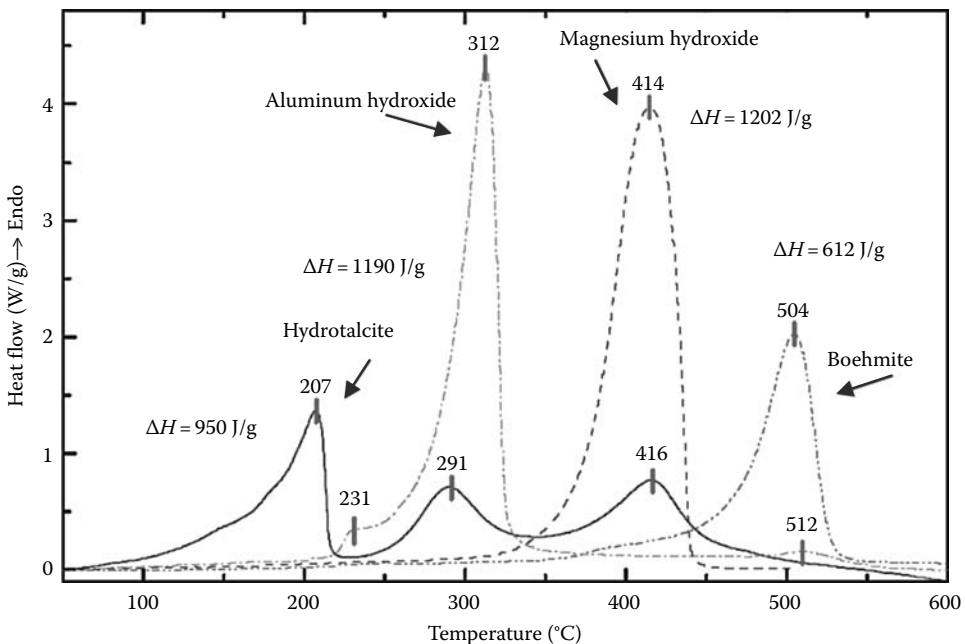


FIGURE 7.2 (See color insert following page 530.) Endothermic decomposition of hydrated fillers. (From Camino, G. et al., *Polym. Deg. Stab.*, 74, 457, 2001. With permission.)

escape of water is hindered. Early in the decomposition process the alumina produced is very reactive, readily combining with water vapor to rehydrate to ATH. In larger particles, water escaping nearer the center of the particle has a larger diffusion path, giving more time to react with alumina formed near the surface of the decomposing particle. During this process boehmite or pseudo-boehmite is formed as a partial decomposition product. In relation to the effects of particle size on thermal stability, it has been shown that there is a greater transition from gibbsite to pseudo-boehmite, as the particle size increases.⁹ Both boehmites and pseudo-boehmites are quite often produced by a hydrothermal treatment of a gibbsite suspension.

The heat capacity of these fillers and, in particular, their strong endotherm can strongly influence the input of heat required for polymer decomposition and release of combustible volatiles.²⁵ Based on the oxygen index test, this effect has been modeled using a heat balance approach that can be applied to the whole combustion process.¹ Apart from very fine fillers, there is a good fit between model and experimental data. From this approach, it can be shown that at sufficiently high filler levels, hydrated fillers can also reduce the mass burning rate by inhibiting the rates of heat transfer from the flame to the underlying matrix, causing the flame to extinguish due to fuel starvation.³² Hence, reductions in applied heat flux or increased surface heat losses will lead to a decrease in the mass burning rate of the polymer. This effect has been reported for PP/aluminum hydroxide composites.³³

There is evidence to show that the particle size of the filler also plays a significant role in flammability resistance. For example, below a certain particle size (about 1–2 μm), in many tests, including oxygen index, aluminum hydroxide shows enhanced fire-retarding performance,³⁴ which may be associated with the rate of filler decomposition and/or with the formation of a more stable ash. However, it has been found that the particle size effect is absent, or less evident, in the cone calorimeter test.³⁵ Similarly, particle size reduction has been shown to enhance fire retardancy in magnesium hydroxide-filled PP; in this case, samples were characterized by the UL94 test.³⁶ This raises the question as to whether further reductions in particle size to the nanoscale will lead to an additional increase in flammability performance, and perhaps enable filler overall levels to be significantly reduced. This aspect is considered in a later section.

Forced combustion studies provide a practical method for quantifying this thermal insulating effect and enabling the measurement of rates of heat transfer through a fire-retardant polymer composition exposed to an externally applied ignition source. During the thermal breakdown of PP, magnesium and aluminum hydroxides decompose to their respective oxides, which together with any carbonaceous char produced, provide an effective thermal barrier, reducing heat transmission to the underlying substrate (Figure 7.3).³⁷ Similar behavior has been demonstrated with other polymer types, including modified-polyphenylene oxide (PPO), poly(butylene terephthalate) (PBT), and ABS terpolymer.³⁸

In magnesium hydroxide-filled PP compounds, the oxide/char residue formed during combustion has a morphology similar in form to the parent hydroxide.³⁹ In this regard, hexagonal platelets show preferred alignment and in some cases overlap, in contrast to aggregated structures derived from hydroxide particles comprising an association of small crystallites. There is some evidence from oxygen index tests of increased crystal growth and that the coherency of the association between oxide particles contributes to the stability of the decomposition residue observed from combustion products, which may partially account for reported differences in performance observed between different grades of the same filler.¹ It is possible that partial sintering between oxide particles will also occur. In this regard, the strength of agglomerates containing magnesium hydroxide pseudo-morphs has been estimated as 50 MPa, arising from physiochemical association between magnesium oxide and water.⁴⁰

The high filler loadings required using hydrated fillers create a significant dilution effect resulting from the presence of the filler, thereby reducing the amount of combustible polymer available. With magnesium hydroxide, the presence of 60% by the weight of filler is equivalent to around 35% by the volume reduction of polymer. However, not all so-called inert fillers appear to act in the same

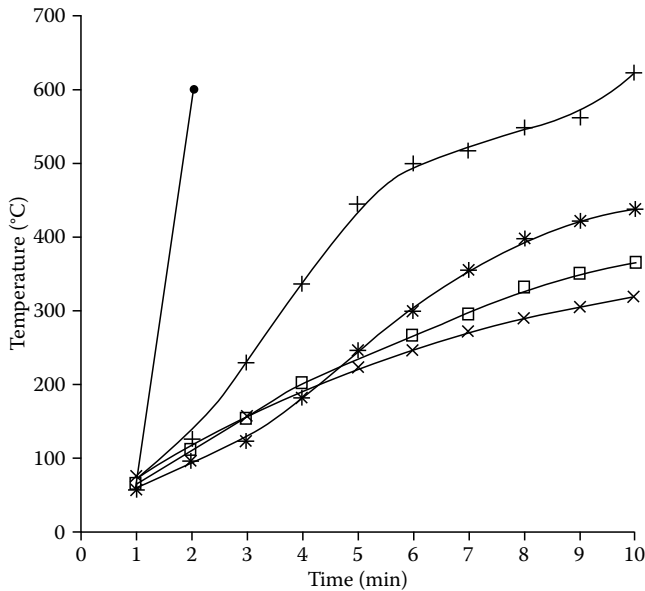


FIGURE 7.3 Temperature profiles for polypropylene compounds containing increasing loadings of magnesium oxide filler. (From Hornsby, P.R. and Watson, C.L., *Plast. Rubber Process. Appl.*, 11, 45, 1989. With permission.)

way as matrix diluents. With PP compositions containing different grades of magnesium hydroxide, magnesium oxide, and glass beads, values of heat release rate (HRR) were determined by cone calorimetry.³⁹ It was found in all cases that rates of heat release were significantly reduced, after allowing for the volume dilution of each of these fillers, but not to the same extent. Unexpectedly, magnesium oxide was far more effective than the glass beads in suppressing HRR, even though both are considered inert fillers. This suggests that even with thermally stable fillers showing no endothermic transition, other factors have a role in influencing fire retardancy, such as particle geometry, surface chemistry, chemical interactions between the filler and the polymer, and possibly thermal conductivity.

7.4.2 FILLER-POLYMER INTERACTIONS

The changes in thermal degradation profile often observed in thermoplastics in the presence of many fillers can also be a significant factor affecting the action of fire-retardant fillers. TGA and DSC provide insights concerning the nature of filler/polymer interactions, together with their relative decomposition temperatures, especially when used in combination with evolved gas analysis (EGA) and online FTIR techniques. In studies with polyamides, it was shown that on decomposition, magnesium hydroxide promotes the degradation of PA-6 and polyamide 66 (PA-66), which can be attributed to the hydrolysis of the polymer resulting from water release from the filler.⁴¹ Water, carbon monoxide, carbon dioxide, ammonia, and various hydrocarbon fragments were shown to be evolved gases detected by mass spectrometry from the degradation of both filled and unfilled PA compositions. It was evident that there was much greater overlap in thermal decomposition between PA-6 and magnesium hydroxide, than with PA-66, where the polymer decomposed before the filler (Figure 7.4). This resulted in significantly improved fire retardancy in PA-6 relative to PA-66.

Filler-polymer interactions have also been observed in EVA copolymer yielding differences in fire retarding effectiveness between ATH and MH.⁴² In EVA with 30% vinyl acetate content, magnesium hydroxide had an oxygen index of 46%, whereas aluminum hydroxide gave a value of

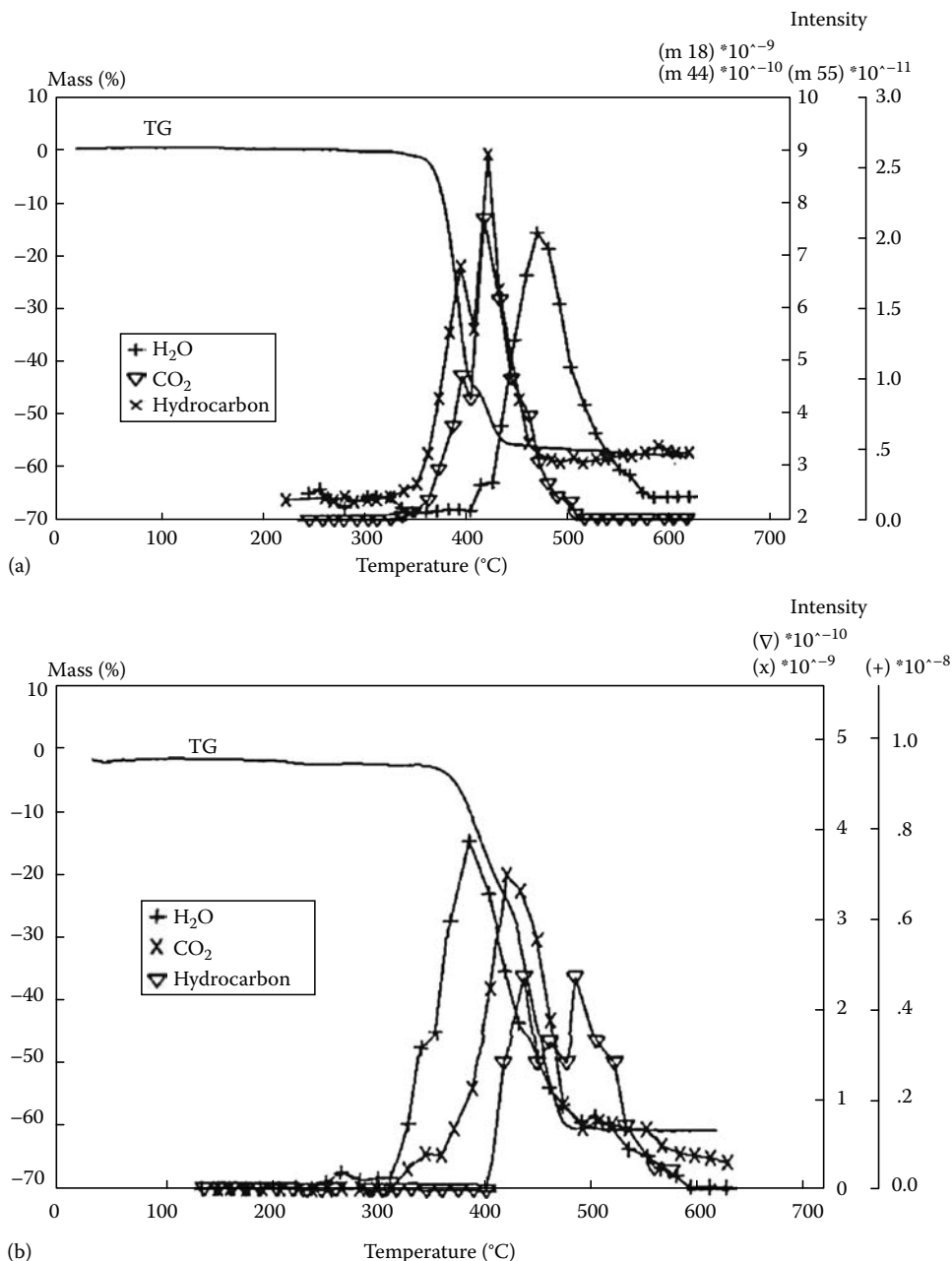


FIGURE 7.4 FTIR EGA profiles for water, carbon dioxide, and hydrocarbon in (a) magnesium hydroxide/PA-6,6 (top) and (b) magnesium hydroxide/PA-6 compounds. (From Hornsby, P.R. et al., *Polym. Deg. Stab.*, 51, 235, 1996. With permission.)

only 37%. From nonisothermal TGA, it was proposed that in this polymer, water release is delayed from aluminum hydroxide, whereas it is accelerated from magnesium hydroxide, arising from the reaction of acetic acid, evolved from the polymer, and this filler. This example again highlights the importance of relative decomposition temperatures of the filler and the polymer. Cone calorimetry data, however, may lead to a different conclusion regarding the effectiveness between ATH and MH in these types of compounds.⁴³ In EVA with 19% vinyl acetate content and a filler loading of 60 wt %

of ATH or MH grades with a similar particle size distribution and specific BET surface area, the peak heat release rate (PHRR) measured at 35 kW/m² was significantly lower (121 kW/m²) for ATH than for MH (200 kW/m²).

The tendency of polymers, such as polyamides, to drip during combustion can be inhibited by the presence of hydrated fillers. In this connection, the physical influence of the filler on melt rheology of the decomposing polymer is of significance. Although this is difficult to measure during polymer combustion, it has been shown using parallel plate rheometry, that different magnesium hydroxide filler variants influence the rheological behavior of thermally decomposing polyamides in different ways and hence their resistance to dripping.⁴⁴ In this study, plate-like filler particles give the greatest increase in viscosity.⁴⁵

7.4.3 VAPOR-PHASE ACTION

Although the fire retarding mechanism of hydrated fillers is generally considered to depend primarily on reactions in the condensed phase through the decomposition endotherm and heat capacity effect from the oxide residue, the heat capacity of the evolved gases and the resulting cooling in the vapor phase can also have a significant effect. For aluminum hydroxide, it has been estimated that the endotherm contributes about 51% of the effect, the oxide residue about 19% and the evolved gases about 30%.^{1,46} In addition, there will be a dilution of volatiles emitted on polymer degradation.²⁵

7.5 SMOKE SUPPRESSION

While being more efficient than hydrated fillers in preventing flame ignition, in the event of a fire halogenated and phosphorus-containing fire retardants can actually increase toxic smoke evolution and hence the potential for fatalities. In contrast, hydrated fillers exert a strong smoke suppressing effect and are frequently chosen for this purpose in situations, such as cables used in underground railways or in ships, where legislation or specific demands of the application require it. Although there are many reports of the use of hydrated fillers as smoke suppressants, little detailed work has been undertaken on the mechanism.

By way of an early example, the effect of calcium carbonate, ATH, and MH fillers on smoke production from styrene butadiene (SBR) foams has been reported.⁴⁷ It was evident that all the fillers reduced soot formation relative to unfilled foam with the hydrated fillers being more effective than the calcium carbonate, which was considered to act merely as matrix diluent. ATH and MH were found to give enhanced char formation with the promotion of solid-state cross-linking as opposed to pyrolytic degradation. An afterglow effect, occurring after the extinction of the flame, was noted with MH and attributed to the slow combustion of carbon residues.

Many other reports have demonstrated the smoke suppressing tendencies of hydrated fillers in various polymers including ethylene-propylene-diene elastomers,⁴⁸ PP,³⁸ polystyrene,⁴⁹ modified polyphenylene oxide, polybutylene terephthalate, and ABS.³⁷ In addition to suppressing smoke generation, a delay in the onset of smoke evolution is also achievable.²⁵ Figure 7.5 illustrates smoke reductions obtained in PP.

The analysis of smoke and soot formation from polymers during combustion has been extensively studied,^{50,51} however, less is understood on how hydrated fillers influence this mechanism. It is likely that smoke reduction results from the deposition of carbon onto the high surface area oxide surface, produced on the decomposition of the filler.³⁸ The volatilization of carbonaceous residue as carbon oxides then occurs, reducing obscuration effects from the smoke.

It is well known that freshly formed oxides have high surface areas and in addition, can be catalytically active,⁵² thereby promoting both carbon deposition and subsequent oxidation processes.⁵³ The reduced combustion rate arising from the effects of the fire-retardant filler also contributes to lowering the rate of smoke evolution and, by improving oxygen to fuel ratios, further limits levels of smoke density.¹

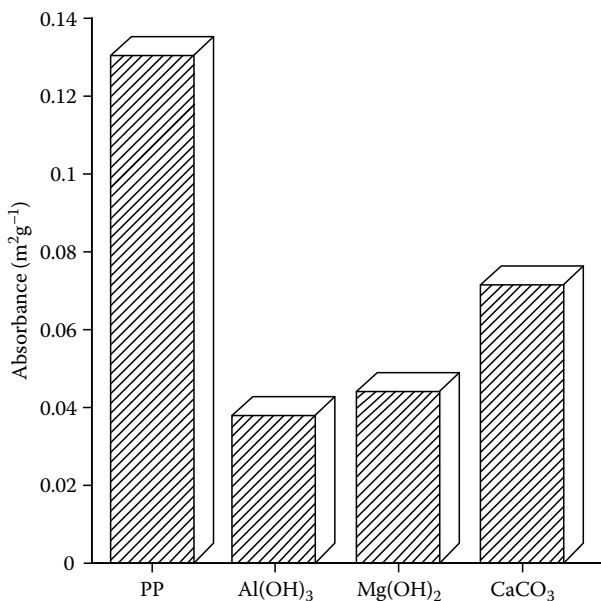


FIGURE 7.5 Smoke emission from selected polypropylene compounds filled with 50 wt % of filler. Tests undertaken according to UITP E4. (From Hornsby, P.R. and Watson, C.L., *Plast. Rubber Process. Appl.*, 11, 45, 1989. With permission.)

In this context, the role of evolved water from hydroxide decomposition is of interest, since water is also known to oxidize carbon. However, comparing smoke yields from PP compounds containing magnesium hydroxide and magnesium oxide, little difference was seen in levels of smoke emitted.³⁸ There were also similar CO emissions from burning ABS containing oxide and hydrated forms of magnesium, suggesting that water has a limited effect on the smoke suppression mechanism.³⁷ This observation is supported by the fact that the so-called water-gas oxidation reaction occurs at temperatures and pressures well in excess of those normally found at the burning surface of a polymer.⁵⁴

Other aspects of fire-retardant performance include the effect of the additives on the interrelationship between smoke and afterglow or incandescence. The oxidation of trapped carbonaceous species on the oxide surface is the likely cause of afterglow commonly observed with fire-retardant fillers.^{55,56} In studies using EVA copolymer oxidation, self-ignition and incandescence were monitored as a function of temperature and filler loading. Both ATH and MH were found to increase the self-ignition temperature, but to decrease the incandescence temperature of the EVA copolymer. Using TGA, in these systems it was concluded that the solid-state afterglow effects observed were due to the oxidation of carbonaceous residues.

7.6 ENHANCING THE EFFICIENCY OF FIRE-RETARDANT FILLERS

As discussed previously, hydrated fillers have many attributes, including their low toxicity and smoke suppressing character; however, their use is restricted by their relative inefficiency as fire retardants. A significant challenge, therefore, is to develop more effective means of using them to reduce the necessary filler loadings and thereby minimize their impact on processability and physical properties of the host polymer. The use of processing additives and/or filler surface treatments are well-established routes for minimizing these adverse effects,⁵⁷ which are beyond the scope of this chapter.

Alternative means for improving fire retarding and mechanical performance of the composites are considered in the following text, which include the use of co-additives which act in a synergistic manner with the hydrated filler, multicomponent structures formed during processing, where the fire retardant is only located when it is most needed in the part (generally at the surface) and fillers with significantly reduced particle size (at the nanoscale).

7.6.1 SYNERGISM

There are many reported examples of synergists used in combination with hydrated fillers. Examples are given in Table 7.2; however, this list is not exhaustive. In many of these cases, although beneficial effects are observed, the mechanisms of interaction are not clear or there are other reasons, such as cost, which limit their use industrially.

TABLE 7.2
Examples of Synergists for Metal Hydroxides

Co-Additives	Hydrated Filler(s)	Polymer(s)	Effect(s)
Antimony trioxide/zinc borate	ATH	PVC (flexible)	Reduced overall filler level/ lower smoke
Borate compounds (zinc borate/calcium borate)	ATH	EVA	Enhanced flammability resistance at low co-additive additions Increased char promotion
MH/ATH combinations	ATH	PVC	Reduced flammability Wider range of endotherm and water release
	MH		Enhanced oxide thermal barrier(?)
Molybdenum compounds (molybdenum oxide/ molybdate salts)	ATH	PVC	Reduced flammability and smoke emission Increased char promotion
	MH		Reduced overall filler levels
Red phosphorus	ATH	—	Suppression of phosphine formation by metal hydroxide Colored formulations
	MH		Low co-additive additions
Silicon-containing compounds (organosilicones)	ATH	Polyolefins	Enhanced flammability resistance/reduced smoke
	MH		Improved processibility and physical properties Handling issues
Polyacrylonitrile fibers	ATH	Polyolefins	Char promotion
	MH		Reduced filler levels Can be pigmented
Transition metal oxides (nickel oxide/cobalt oxide)	ATH	Polyolefins	Reduced overall filler levels
	MH		Color limitations Possible adverse toxicity effects

(continued)

TABLE 7.2 (continued)
Examples of Synergists for Metal Hydroxides

Co-Additives	Hydrated Filler(s)	Polymer(s)	Effect(s)
Metal nitrates (copper nitrate/iron nitrate)	ATH	EVA	Enhanced flammability resistance with low co-additive additions
Melamine	ATH MH	PP	Improved fire retardancy Reduced afterglow
Tin compounds (zinc stannate/zinc hydroxystannate)	ATH MH	PVC Cl-rubbers EVA	Enhanced flammability resistance/reduced smoke especially with ZH/ ZHS-coated filler variants
Nanoclays	ATH MH	EVA	Lower heat release rates/ increased time to ignition/ increased char promotion/ reduced smoke emission Used in combination with tin compounds

Combinations of MH and ATH can give improved performance when used together, due to the increased range of endothermic reaction (180°C–400°C) and the release of water in the vapor phase.^{58,59} The different metal oxides produced on dehydration may also contribute to this effect.

ATH and red phosphorus (3%–5%) have also been used in synergistic mixtures to increase fire retardancy and enable lower filler loadings.⁶⁰

The addition of melamine and novolac (~1%) to PP/MH mixtures has been found to reduce the burning time and give a UL94 V-0 rating at lower filler levels (30%–50%) as opposed to a more usual value of around 60%, allowing the formulation to be mechanically more flexible. The novolac causes a structurally stabilizing effect above the melting point of PP. Thermal evidence suggests that a novolac magnesite gel may be formed.⁶¹

Metal hydroxides in combination with various silicon-containing compounds have been used to reduce the amount of additive required to achieve a required level of flame retardancy in a variety of polymeric materials, including polyolefins.^{62,63} Systems that have been used contain a combination of reactive silicone polymers, a linear silicone fluid or gum, and a silicone resin, which is soluble in the fluid, in addition to a metal soap, in particular magnesium stearate. However, there is little insight given into how these formulations work.

It has been shown that the required loading levels of metal hydroxides to flame retard polyolefins can be reduced by the addition of transition metal oxides as synergistic agents. For example, a combination of 47.6% MH modified with nickel oxide in PP gave a UL94 V-0 flammability rating, which would require ~55% of unmodified MH.⁴ These systems, however, can only be used where the color of the product is not important.

The addition of metal nitrates to improve the flame retardancy of metal hydroxides and EVA has been reported.⁶⁴ Synergistic behavior was observed by an addition of 2% of copper nitrate to EVA containing only 33% ATH, in which the oxygen index was raised from 19.9% to 30.0%.

The flammability properties of an intumescent fire retardant PP formulation with added MH has been investigated.⁶⁵ The results show that the intumescent flame-retardant ammonium polyphosphate-filled PP has superior flammability properties but gives higher CO and smoke evolution. The addition of MH was found to reduce smoke density and CO emissions, in addition to giving superior fire resistance. PP filled with ammonium polyphosphate, pentaerythritol, and melamine has given improved flammability performance, without reducing its mechanical properties.

TABLE 7.3
Effect of ZHS- and ZS-Coated Fillers on Flammability of PVC
 Cone Calorimeter Data (@50kW/m² Irradiance) for Flexible PVC Samples

Sample	TTI	Peak RHR	Av. RHR, 3 min	FPI	Av. SEA	SP
Control	16	290	232	0.06	963	279
20 phr ATH	22	173	153	0.13	769	133
30 phr ATH	31	173	133	0.18	622	108
40 phr ATH	78	120	98	0.65	186	22
50 phr ATH	43	104	80	0.41	192	20
20 phr ZHS-coated ATH	23	146	122	0.16	350	51
30 phr ZHS-coated ATH	32	118	102	0.27	368	43
40 phr ZHS-coated ATH	51	95	77	0.54	287	27
50 phr ZHS-coated ATH	47	96	79	0.49	284	27
20 phr MH	16	195	164	0.08	475	93
30 phr MH	11	208	161	0.05	398	83
40 phr MH	27	214	161	0.13	379	81
50 phr MH	21	203	156	0.10	309	63
20 phr ZHS-coated MH	17	167	142	0.10	311	52
30 phr ZHS-coated MH	30	161	127	0.19	316	51
40 phr ZHS-coated MH	36	164	106	0.22	254	42
50 phr ZHS-coated MH	42	162	109	0.26	195	32

Source: From Cusack, P.A. and Hornsby, P.R., *J. Vinyl Additive Technol.*, 5, 21, 1999. With permission.

Note: FPI, fire performance index (m² s/kW); RHR, rate of heat release (kW/m²); SEA, smoke extinction area (m²/kg); SP, smoke parameter (MW/kg); TTI, time to ignition (s).

In halogen-containing polymers, zinc hydroxystannate (ZHS)- or zinc stannate-coated hydrated fillers can give significantly improved flame resistance and lower smoke emission compared with uncoated fillers (Table 7.3).^{66,67} The efficiency of the coated fillers was found to be superior to simple admixtures of these components, reflecting improved dispersion and possible synergism in these systems. The detailed characterization of the nature of the ZHS coating using X-ray photoelectron spectroscopy has revealed the level of coverage and interaction between the coating and the supporting substrate surfaces.⁶⁸

The addition of silane cross-linkable PE copolymer to PE/metallic hydroxide systems can significantly improve the flame-retardant properties of these materials allowing lower filler levels to be used.⁶⁹

The combination of melamine with hydrated mineral fillers can improve the fire retardancy behavior of PP, eliminating at the same time the afterglow phenomenon associated with these fillers used in isolation.⁷⁰ Similarly in EVA copolymer, antimony trioxide used in combination with metal hydroxides has been reported to reduce incandescence.⁵⁶ Chlorinated and brominated flame retardants are sometimes used in combination with metal hydroxides to provide a balance of enhanced fire-retardant efficiency, lower smoke evolution, and lower overall filler levels. For example, in polyolefin wire and cable formulations, magnesium hydroxide in combination with chlorinated additives was reported to show synergism and reduced smoke emission.⁷¹

A natural mineral filler containing mainly huntite and hydromagnesite, has been used, together with a blend of antimony trioxide and decabromodiphenyl oxide to reduce the flammability of an ethylene-propylene copolymer.⁷²

The addition of very small amounts of fine carbon fibers⁷³ or polyacrylonitrile fibers⁷⁴ can reduce the level of inorganic hydroxide required to achieve UL94 V-0 flammability ratings in polyolefin compounds. These secondary additives are thought to function as char promoters.


The addition of low levels (~3%) of zinc borate to metal hydroxides can give synergistic effects.⁷⁵ For example, in an EVA/MH formulation, LOI was found to increase from 39% to 43%, together with a significant reduction in HRR. The solid-state carbon NMR of the residues showed that polymer fragments were in the char layer. It was suggested that zinc borate slows the degradation of the polymer, creating a vitreous protective physical barrier to combustion.

7.6.2 MULTICOMPONENT STRUCTURES

In most parts modified with flame retardants, a uniform distribution of additive is created throughout the polymer. However, commercially available processing technologies can enable structuring within the component in order to control the location, type, and amount of fire retardant, and achieve maximum effect without unduly compromising mechanical properties. This can be undertaken using co-extrusion, co-injection molding, and potentially, bicomponent fiber spinning processes. In principle, different fire retardants may be combined, fire-retardant levels may be graded, and/or reinforcing additives may be judiciously introduced all within the same part.⁷⁶

Using this concept, it has been shown by cone calorimetry that over a 3 min combustion period, 3 and 6 mm thick laminated structures, made with different fire-retardant skin and unfilled core combinations can give similar resistance to ignition and comparable HRR and smoke extinction area (SEA) results to fully fire-retardant compositions (Table 7.4). Mechanical properties, in particular impact strength, were also found to be greatly enhanced by this approach, since less fire-retardant filler is present in the material. Whereas this approach has been demonstrated to be effective with hydrated fillers, it is applicable to all fire-retardant types.

TABLE 7.4
Cone Calorimetry Results for Multicomponent Structures (Magnesium Hydroxide in Polypropylene)

					
	PP	All FR	Sandwich (1 mm FR Skin)	Sandwich (2 mm FR Skin)	Multilayer (3FR + 2PP)
Time to ignition (s)	50	86	78	80	87
<i>Average during 3 min period</i>					
Heat release rate (kW/m ²)	273	118	111	96	105
Specific extinction area (m ² /kg)	386	126	172	106	98
Carbon monoxide yield (kg/kg)	0.017	0.005	0.006	0.003	0
Carbon dioxide yield (kg/kg)	1.6	1.5	1.3	1.5	1.5

Note: FR—40% PP + 60% Mg(OH)₂. Heat flux—35 kW/m².

7.6.3 NANOSIZE FIRE-RETARDANT FILLERS

There is currently widespread interest in the use of nanoparticulate fillers as modifiers for polymers due to the significant increases in performance achievable with only small levels of additive (typically up to 5% by weight). In this connection, there are many publications demonstrating the large increase in mechanical properties, reduced gas and vapor transmission, and decreased flammability, which can be obtained under certain preparation and test conditions. In terms of fire retardancy, much of this work considers silicate layer nanoparticles and polyhedral oligomeric silsesquioxanes (POSS), which in the context of this chapter are not classed as fire-retardant fillers as they do not undergo endothermic decomposition. However, with the aim of reducing filler loadings, there is an increasing interest in the development of hydrated nanofillers, for potential use as fire retardants.

In this regard, a number of reports consider the synthesis and the application of magnesium hydroxide nanoparticles as flame retardants in polymers.⁷⁷⁻⁷⁹ Magnesium hydroxide nanoparticles with different morphological structures of needle-, lamellar- and rod-like nanocrystals have been synthesized by solution precipitation reactions of magnesium chloride in the presence of water-soluble polymer dispersants.⁸⁰ The size and the morphologies of the magnesium hydroxide nanocrystals were controlled by the reaction conditions, in particular temperature, alkaline solution injection rate, and reactant concentration. Needle-like morphologies were produced having dimensions of $10 \times 100\text{nm}$,² the lamellar particles were made around 50 nm in diameter and an estimated 10 nm in thickness, with rod-like particles formed being 4 μm in length and 95 nm in diameter. The thermal analysis of the lamellar crystals gave a pronounced weight loss between 250°C and 396°C with a corresponding endothermic peak near 354°C ascribed to the decomposition of magnesium hydroxide. The overall weight loss for the MH was 30.1%. A comparison of LOI and tensile strength (TS) data for EVA/MH composites using three different types of MH, nano-sized filler, and micron-sized filler, showed that tensile strength for the larger particles decreased with increasing filler level, whereas values for the nano-MH/EVA composite increased. LOI results for the nano-MH were also superior, especially at high filler levels. The enhancement in fire retardancy seen using these nanoscale fillers was attributed to a more compact char structure creating more effective gas barrier properties.⁸¹ However, it should be noted that in this work high nano-MH filler levels were still required to achieve reasonable resistance to ignition, in common with more conventional MH fillers.

Nanotubes of magnesium hydroxide have been synthesized by a solvothermal reaction from basic magnesium chloride and ethylenediamine solvent.⁸² These were reported to have diameters of 80–150 nm, a wall thickness of 30–50 nm, and lengths of 5–10 μm . However, their use as polymer fire retardants was not considered.

Nano-magnesium hydroxide and three forms of micro-magnesium hydroxide filler (all commercially available in China) were mixed with EPDM rubber and the mechanical properties and fire resistance of these composites determined.⁸³ The particle size of the micro-MH used was around 2.5 μm and the nano-MH had a hexagonal sheet-like structure with dimensions of 100 nm width by <50 nm thick. Thermal analysis on the fillers showed that the nano-filler had a lower decomposition temperature and a larger endotherm. The LOI of these composites were very similar, although it was noted that the nano-filled material showed less tendency to drip and gave a more coherent char residue. The HRR from the nanocomposite was substantially lower than the micro-filled systems (259 relative to 329–346 kW/m²) and the time to ignition increased from 81–89 s to 95 s. It should be noted, however, that filler levels for all the composites was again high with test samples containing between 60 and 100 phr of additive.

A further study considered the use of nano-magnesium hydroxide on the mechanical and the flame-retarding properties of PP.⁸⁴ The nanofiller was synthesized from MgCl₂ and poly(ethylene glycol) solution by an in situ technique yielding a particle size of 25 nm. Substantial improvements in mechanical properties were obtained by the addition of only small amounts of nano-magnesium hydroxide. For example, the addition of 12 wt % of filler gave a 433% increase in Young's modulus

and a 35% improvement in flame retardancy (expressed as a burning rate). However, no comparison was given with conventional micron-sized magnesium hydroxide filler.

Nano-magnesium hydroxide particles have been made by a phase transfer reaction with a mean particle size of about 10 nm and a core-shell structure comprising a magnesium hydroxide inner region surrounded by an alkyl chain.⁸⁵ This filler was combined in EVA at a 5 wt % loading and its fire properties compared with conventional 1 μm sized filler at addition levels of 5, 30, and 60 wt %. It was shown that the peak HRR of the EVA/n-MH composite was reduced by 60% compared to pure EVA even though only 5 wt % of n-MH was present. The n-MH also causes a significant reduction in smoke (specific extinction area), although, LOI was not significantly affected. It was evident that the n-MH significantly outperformed μ -MH at equivalent filler loadings.

Magnesium–aluminum layered double hydroxides (LDH) are also increasingly being studied. The use of hydrotalcite as a filler in polymer compounds is of particular interest because of its layered structure and high ion-exchange capacity. It is a form of hydrated magnesium–aluminum (Mg–Al) hydroxycarbonate with lamellar structure and general formula $\text{Mg}_6\text{Al}_2(\text{OH})_{16}\text{CO}_3 \cdot 4\text{H}_2\text{O}$. The structure can potentially be chemically modified to allow the intercalation of polymer chains and subsequent exfoliation into nano-platelets in a similar manner to silicate layer nanofillers, for example, based on montmorillonite.

The DSC of hydrotalcite shows three peaks at 207°C, 291°C, and 416°C with corresponding decomposition enthalpies of 356 J/g associated with the first peak and 594 J/g from the second and third peak.⁸⁶ The weight loss begins at a very low temperature (50°C), which is attributed to water loss, but overall its thermal behavior in terms of heat absorption capacity and mass loss is comparable with that of magnesium and aluminum hydroxide and, therefore might be expected to confer similar fire-retarding properties to polymers. In this regard, additions of only 30% by the weight of hydrotalcite to unplasticized PVC gave an LOI value of 29 and UL94 V-0 rating.⁸⁷ However, it should be noted that in this study the initial hydrotalcite particles, made by chemical co-precipitation, were found to be very coarse with an average size of around 200 μm . This dimension was reduced substantially after treatment with a titanate coupling agent and by shearing with the polymer on a two-roll mill.

A comparison has also been given of the fire-retarding performance in the EVA of a commercially available hydrotalcite, with median particle size of 2.26 μm and surface area 17 m^2/g , and aluminum and magnesium hydroxides with similar particle sizes.⁸⁶ It was demonstrated that the most significant flame retardancy effect in terms of slowest HRR, lowest evolved gas temperature, and longest ignition time, was in EVA filled with 50 wt % hydrotalcite. This was attributed to the wide temperature range (200°C to 500°C) for water loss and associated heat absorption, a delay in deacetylation of the EVA due to interlayer water loss at about 207°C and a possible intercalation of acetate anions in the layer structure.

It has also been reported that the interlayer spacing in hydrotalcite particles can be increased by intercalation with organic molecules, such as citric acid.⁸⁸ Results were given for linear burning rates from a UL-94 horizontal burn test comparing nano- and micro-hydrotalcite modified epoxy resin. At 5 wt % addition level the microcomposite gave a reduction in burn rate of unmodified epoxy resin from around 22 to 18 mm/min. With the apparent nanocomposite variant, also at 5 wt %, the burn rate was less than 5 mm/min.

At an optimum addition level of only 1.5 wt %, nano-size magnesium–aluminum LDHs have been shown to enhance char formation and fire-resisting properties in flame-retarding coatings, based on an intumescent formulation of ammonium polyphosphate, pentaerythritol, and melamine.⁸⁹ The coating material comprised a mixture of acrylate resin, melamine formaldehyde resin, and silicone resin with titanium dioxide and solvent. It was reported that the nano-LDH could catalyze the esterification reaction between ammonium polyphosphate and pentaerythritol greatly increasing carbon content and char cross-link density.

SiO_2 -coated nano-LDH particles have been prepared by a sol–gel process with a film thickness of about 5 nm through the formation of Mg–O–Si and Al–O–Si bonds.⁹⁰ Thermal analysis showed

that both coated and uncoated nano-LDH particles showed three stages of mass loss between 40°C and 700°C. The uncoated material gave two endothermic peaks at 244°C and 430°C with corresponding heat absorption capacities of 412 and 336 J/g respectively. However, the coated nano-LDH exhibited only one endothermic peak at 243°C with a heat absorption capacity of 221 J/g. The influence of these fillers as polymer flame retardants was not reported.

As discussed earlier boehmite, $\text{AlO}(\text{OH})$, is a partly decomposed aluminum hydroxide in which two-thirds of the water is removed. It has been shown to undergo endothermic decomposition, commencing around 400°C, which is considerably higher than the temperature of breakdown of aluminum hydroxide. Results from this study yielded a heat absorption of 612 J/g relative to 1190 J/g for ATH.⁸⁶ With a high theoretical residue of 85% it could potentially act in the condensed state by the formation of an insulating layer, but is not considered to have high fire-retarding qualities. In this study, the boehmite had a median particle size of 0.6 μm and surface area of 17 m^2/g .

Colloidal boehmite nanorods have been included in a PA-6 matrix to yield a homogeneous dispersion by in situ polymerization.⁹¹ At weight fractions up to 9%, improvements in the Young's modulus of the composite and changes in the crystalline morphology of the PA-6 matrix were observed, although fire properties were not reported.

Some potentially relevant work concerns the attachment of magnesium hydroxide nanoparticles onto multiwall carbon nanotubes (MWCNTs).⁹² These were prepared from water-in-oil emulsions specifically for conversion into MgO to functionalize and preserve the mechanical and the electrical properties of the CNTs, although not for fire-retardant purposes. However, although more speculative, this work may be of interest as it has been reported that combinations of MWCNT and micron-sized particles of ATH in EVA function as very efficient fire retardants through enhanced char formation and coherency.⁹³

A method for synthesizing nano-aluminum hydroxide with an ATH core and alkyl hydrocarbon chain shell structure has been described.⁹⁴ In the resulting composites prepared using EVA, mechanical properties of the nanofilled material were almost the same as a conventional 1 μm sized ATH variant; however, the HRR of the former composition was markedly lower. In this work 10 phr of filler was used.

Magnesium hydroxide sulfate hydrate (MHSH) whiskers have been used with and without microencapsulated red phosphorus synergist as fire retardants in low density polyethylene.⁹⁵ The MHSH whiskers were shown to degrade endothermically with the release of water in a two-step process with time derivative (DTG) peaks at 301°C and 411°C. The additive was shown to be an effective fire retardant and smoke suppressant but only at high filler levels. For example, to achieve a UL-94 V-0 rating required 60% by weight loading, similar to that for magnesium hydroxide. However, these fibers appear to have length dimensions in the micron range, which combined with their relatively inefficient fire retarding efficiency, makes their useful application unlikely.

7.7 CONCLUSIONS

Aluminum and magnesium hydroxides are the principal fire-retardant fillers used in polymers, the former being by far the most important; commercially they find a large number of applications in thermoplastics, elastomers, and thermosets. Many variants of these fillers exist, however, differing in particle size, surface area, and morphology, which can have a strong influence on their cost and fire-retarding efficiency. They also function as effective smoke suppressants due to the presence of high surface area oxides generated on filler decomposition.

Their fire-retardant mechanism is predominantly due to condensed phase action involving a combination of endothermic decomposition, water release, and oxide residue formation.

The high filler levels generally required relative to most alternative fire retardants, can be reduced by various synergists, using two-component polymer processing technologies, and potentially by using nanoscale variants of these fillers, although reports describing this approach are conflicting.

REFERENCES

1. Rotheron, R., Effects of particulate fillers on flame retardant properties of composites, in *Particulate-Filled Polymer Composites*, 2nd edn., Rotheron, R.N. (Ed.), Rapra Technology Ltd., Shawbury, U.K., 2003, Chapter 6, p. 271.
2. Stinson, J.M. and Horn, W.E. Flame retardant performance of a modified aluminum hydroxide with increased thermal stability, *Proceedings from Society of Plastics Engineers 52nd Annual Technical Conference (ANTEC'94)*, Part 3, Newtown, CT, U.S.A, May 1–5, 1994, pp. 2829–2833.
3. Hancock, M. and Rotheron, R.N., Chapter 2 Principal types of particulate fillers, in *Particulate Filled Polymer Composites*, 2nd edn., Rotheron, R.N. (Ed.), Rapra Technology, Shawbury, U.K., 2003, pp. 88–90.
4. Imahasi, T., Okada, A., and Abe, T., Flame retardant aid, flame retardant and flame-retardant composition, U.S. Patent 5,583,172, December 10, 1996.
5. Doyle, M., Clemens, M., Lees, G., Briggs, C., and Day, R., *Proceedings of Flame Retardants '94*, Interscience, London, U.K., 193, 1994.
6. Sauerwein, R., *Proceedings of Fire and Materials 2001*, Interscience, San Francisco, CA, 395, 2001.
7. Rust, D.A., *Proceedings of Functional Fillers and Reinforcements '99*, Intertech, Atlanta, GA, Paper 22, 1999.
8. Horn, W.E., Inorganic hydroxides and hydroxycarbonates: Their function and use as flame-retardant additives, in *Fire Retardancy of Polymeric Materials*, Grand, A.F. and Wilkie, C.A. (Eds.), Marcel Dekker, Basel, Switzerland, 2000, Chapter 9.
9. Sobolev, I. and Woychesin, E.A., Alumina trihydrate, in *Handbook of Fillers for Plastics*, Katz, H.S. and Milewski, J.V. (Eds.), Van Nostrand Reinhold, New York, 1987, Chapter 16.
10. Kirschbaum, G.S., Aluminum hydroxide for non-halogen compounds-well known- and still ever young, *Proceedings from Flame Retardants '94*, British Plastics Federation, London, Interscience Communication Ltd., London, U.K., 1994, p. 169.
11. Brown, S.C. and Herbert, M.J., New developments in ATH technology and applications, *Proceedings from Flame Retardants '92*, Plastics and Rubber Institute, London, U.K., Elsevier Applied Science, London, U.K., 1992, p. 100.
12. Szablowska, B. and Pelica, J., Fire proofed floor coverings on the basis of polyolefins, in *Proceedings from Flame Retardants '96*, Grayson, S.J. (Ed.), British Plastics Federation, London, Interscience Communications Ltd., London, U.K., 1996, p. 241.
13. Jow, J. and Gomolka, D. (Union Carbide Chemicals), Flame-retardant compositions useful for cable insulating and jacketing, U.S. Patent 5482990A, 1996.
14. Sezaki, E., Akami, M., and Endo, H., Flame-retarded thermoplastic elastomer composition, European Patent 0331358, 1989.
15. Yamamoto, Y. and Tanmachi, M., Thin fire-resistant electrically insulated wire, Japanese Patent 06215644, 1994.
16. Hitachi Cable Ltd., Fire-resistant electrically insulating polyolefin compositions, Japanese Patent 04253748, 1992.
17. Hitachi Cable Ltd., Manufacture of halo-free flame-retardant polyolefin-covered electric wires, Japanese Patent 07122140, 1995.
18. Brown, S.C., Evans, K.A., and Godfrey, E.A., New developments in alumina trihydrate, in *Proceedings from BPF/PRI Conference Flame Retardants '87*, London, U.K., Paper 11 1987.
19. Wan Hanafi, W.Z.A., A study of magnesium hydroxide as a flame retardant and smoke suppressant for unsaturated polyesters, MPhil thesis, Brunel University, London, U.K., July, 1988.
20. Wan Hanafi, W.Z.A. and Hornsby, P.R., Smoke suppression and fire retardancy in unsaturated polyester compositions containing hydrated fillers, *Plast. Rubber Composites Process. Appl.*, 19, 175–184, 1993.
21. Bolger, R., Flame retardant materials, *Industrial Minerals*, 29, January, 1996.
22. Govanucci, K.-L., New huntite site expands possibilities for FR, *Functional Filler News*, 40, 1–2, November 20, 1995.
23. Toure, B., Cuesta, J.-M.L., Benhassaine, A., and Crespy, A., The combined action of Huntite and hydromagnesite for reducing flammability of an ethylene-propylene copolymer, *Int. J. Polym. Anal. Characterisation*, 2, 193, 1996.
24. Briggs, C.C., Bhardwaj, B., and Gilbert, M., Flame retardant PVC cable compounds using huntite-hydromagnesite, Paper 9.51, *Proceedings of 5th BPF International Fillers Conference*, May 19–20, Manchester, U.K., 1992.

25. Hornsby, P.R., The application of magnesium hydroxide as a fire retarding and smoke suppressing additive for polymers, *Fire Mater.*, 18, 269, 1994.
26. Hornsby, P.R., Wang, J., Cosstick, K., Rothon, R.N., Jackson, G., and Wilkinson, G., Mechanism of fire retardancy in polyamides filled with magnesium hydroxide, *Progr. Rubber Plast. Tech.*, 10, No. 3, 204–220, 1994.
27. Rothon, R.N., Effects of particulate filler on flame-retardant properties of composites, in *Particulate Filled Polymer Composites*, Rothon, R.N., (Ed.), Longman, Harlow, U.K., Chapter 6, 1995.
28. Hornsby, P.R. and Watson, C.L., Aspects of the mechanism of fire retardancy and smoke suppression in metal hydroxide filled thermoplastics, *IOP Short Meetings Series No 4*, Institute of Physics, London, U.K., April 1997, p. 17.
29. Hornsby, P.R. and Mthupha, A., Mechanism of fire retardancy in magnesium hydroxide filled polypropylene, *Proceedings from Society of Plastics Engineering Annual Technical Conference (ANTEC '93)*, New Orleans, LA, 1954–1956, May 9–13, 1993.
30. Dando, N.R., Clever, T.R., Pearson, A., Stinson, J.M., Kolok, P.L., and Martin, E.S., Aluminum trihydroxide (ATH) as a filler for polymer composites: Improvements in thermal stability by controlled precipitation, *Proceedings from 50th Annual Technical Conference, Composite Institute*, Society of Plastics Industry Inc., Washington D.C., Session 1-D, 1995, pp. 1–4.
31. Souza, S.P., Souza S.H., and Toledo S.P., Standard transition aluminas. Electron microscopy studies, *Mater. Res.*, 3(4), 104–114, 2000.
32. Tewarson, A., *Flame Retardant Polymeric Materials*, Lewin, M., Atlas, S.M., and Pearse, E.M. (Eds.), Plenum Press, New York, 1982.
33. Spilda, I., Kosik, M., and Blazej, A., The mass burning rate of flame-retarded polypropylene in an oxygen-enriched atmosphere, *J. Appl. Polym. Sci.*, 31, 589, 1986.
34. Hughes, P., Jackson, G.V., and Rothon, R.N., Particle morphology effects on the performance of PMMA filled with aluminum hydroxide in a variety of fire tests, *Makromol. Chem. Makromol. Symp.*, 74, 179, 1993.
35. Herbert, M.J., Aluminum hydroxide for non-halogen compounds, *Proceedings of Flame Retardants '94*, Interscience, London, U.K., 1994, p. 59.
36. Miyata, S., Imahashi, T., and Anabuki, H., Fire-retarding polypropylene with magnesium hydroxide, *J. Appl. Polym. Sci.*, 25, 415, 1980.
37. Hornsby, P.R. and Watson, C.L., A study of the mechanism of flame retardancy and smoke suppression in polymers filled with magnesium hydroxide, *Polym. Deg. Stab.*, 30, 73–87, 1990.
38. Hornsby, P.R. and Watson, C.L., Mechanistic aspects of smoke suppression and fire retardancy in polymers containing magnesium hydroxide filler, *Plast. Rubber Process. Appl.*, 11, 45–51, 1989.
39. Hornsby, P.R. and Mthupha, A., Analysis of fire retardancy in magnesium hydroxide-filled polypropylene composites, *Plast., Rubber Composites Process. Appl.*, 25, 347–355, 1996.
40. Itatani, K., Kiyotaka, K., Koizumi, K., Howell, F.S., Kishioka, A., and Kinoshita, M., Agglomeration of magnesium oxide particles formed by the decomposition of magnesium hydroxide, *J. Mater. Sci.*, 23, 3405, 1988.
41. Hornsby, P.R., Wang, J., Rothon, R., Jackson, G., Wilkinson, G., and Cosstick, K., Thermal decomposition behaviour of polyamide fire retardant compositions containing magnesium hydroxide filler, *Polym. Deg. Stab.*, 51, 235–249, 1996.
42. Rychlý, J., Vesely, K., Gal, E., Kummer, M., Jancar, J., and Rychla, L., Use of thermal methods in the characterization of the high-temperature decomposition and ignition of polyolefins and EVA copolymers filled with $Mg(OH)_2$, $Al(OH)_3$ and $CaCO_3$, *Polym. Deg. Stab.*, 30, 57, 1990.
43. Herbiet, R., Nanocomposites based on boehmite alumina, *Proceedings of the Functional Fillers Conference*, Hamburg, Germany, September 15–17, 2004.
44. Hornsby, P.R., Wang, J., Jackson, G., Rothon, R.N., Wilkinson, G., and Cosstick, K., Analysis of fire retardancy in polyamides modified with magnesium hydroxide filler, *Proceedings from Society of Plastics Engineers Annual Technical Conference (ANTEC '94)*, San Francisco, CA, May 1–5, 1994, pp. 2834–2839.
45. Wang, J., Mechanism of flame retardancy in polyamides containing magnesium hydroxide, Ph.D. thesis, Brunel University, London, U.K., 1994.
46. Case, J.R. and Jackson, G.V., ICI, Runcorn, U.K., Unpublished work.
47. Lawson, D.F., Kay, E.L., and Roberts, D.T., Mechanism of smoke inhibition by hydrated fillers, *Rubber Chem. Technol.*, 48, 124, 1975.
48. Moseman, M. and Ingham, J.D., Smoke properties of highly filled ethylene-propylene-diene terpolymer rubbers, *Rubber Chem. Technol.*, 51, 970, 1978.

49. Hirschler, M.M. and Thevaranjan, T.R., Effects of magnesium oxide/hydroxide on flammability and smoke production tendency of polystyrene, *Eur. Polym. J.*, 21(4), 371, 1985.
50. Lahaye, J., Mechanisms of soot formation, *Polym. Deg. Stab.*, 30, 111–121, 1990.
51. Jagoda, I., Prado, G., and Lahaye, J., An experimental investigation into soot formation and distribution in polymer diffusion flames, *Combust. Flame*, 37, 261, 1980.
52. Krylov, O.V., *Catalysis by Non-Metals*, Academic Press, London, U.K., 1970.
53. McKee, D.W., The catalyzed gasification reactions of carbon in *Chemistry and Physics of Carbon*, Vol. 16, Walker, P.L. and Thrower, P.A. (Eds.), Marcel Dekker, New York, 1981.
54. Walker, P.L., Shelef, M., and Anderson, R.A., Catalysis of carbon gasification, in *Chemistry and Physics of Carbon*, Vol. 4, Walker, P.L. (Ed.), Edward Arnold, London, U.K., 1968.
55. Delfosse, L., Baillet, C., Brault, A., and Brault, D., Combustion of ethylene-vinyl acetate copolymer filled with aluminum and magnesium hydroxides, *Polym. Deg. Stab.*, 23, 337, 1989.
56. Baillet, C. and Delfosse, L., The combustion of polyolefins filled with metallic hydroxides and antimony trioxide, *Polym. Deg. Stab.*, 30, 89–99, 1990.
57. Hornsby, P.R. and Watson, C.L., Interfacial modification of polypropylene composites filled with magnesium hydroxide, *J. Mater. Sci.*, 30, 5347–5355, 1995.
58. Kirschbaum, G.S., Recent developments in ATH and magnesium hydroxides—A challenge to traditional materials, *Proceedings of the 1995 Fall Conference of the Fire Retardant Chemical Association*, Rancho Mirage, CA, Technomic Publishing Co., Lancaster, PA, October 29–November 1, 1995, p. 145.
59. Kirschbaum, G.S., Halogenfreier flammenschutz, *Kunststoffe*, 79(11), 62–64, 1989.
60. Staendeke, H., *Proceedings of the Spring Conference of the Fire Retardant Chemical Association*, Grenelefe, FL, Technomic Publishing Co., Lancaster, PA, March 20–23, 1988, p. 32.
61. Weil, E.D., Lewin, M., and Lin, H.S., Enhanced flame retardancy of polypropylene with magnesium hydroxide, melamine and novolac, *J. Fire Sci.*, 16, 383–404, January, 1998.
62. Chavez, M.J. and Romanesco, D.J., Fire retarded plastics: Computer manipulation and video cone calorimeter data, *Proceedings of the 1995 Fall Conference of the Fire Retardant Chemical Association*, Rancho Mirage, CA, Technomic Publishing Co., Lancaster, PA, October 29–November 1, 1995, p. 169.
63. Huber, M.S., Non-halogenated flame retarded systems for olefins, *Proceedings of the Spring Conference of the Fire Retardant Chemical Association*, New Orleans, LA, Technomic Publishing Co., Lancaster, PA, March 25–28, 1990, p. 237.
64. Zhu, W. and Weil, E.D., A paradoxical flame-retardant effect of nitrates in ATH-filled ethylene-vinyl acetate copolymer, *J. Appl. Polym. Sci.*, 56, 925–933, 1995.
65. Chiu, S.H. and Wang, W.K., Dynamic flame retardancy of polypropylene filled with ammonium polyphosphate, pentaerythritol and melamine additives, *Polymer*, 39, 1951–1955, 1998.
66. Baggaley, R.G., Hornsby, P.R., Yahya, R., Cusack, P.A., and Monk, A.W., The influence of novel zinc hydroxystannate-coated fillers on the fire properties of flexible PVC, *Fire Mater.*, 21, 179, 1997.
67. Cusack, P.A. and Hornsby, P.R., Zinc hydroxystannate/zinc stannate-coated fillers: Novel flame retardants and smoke suppressants for polymeric materials, *J. Vinyl Additive Technol.*, 5, 21–30, 1999.
68. Mohai, M., Tóth, A., Hornsby, P.R., Cusack, P.A., Cross, M., and Marosi, G., XPS analysis of zinc hydroxystannate coated fillers, *Surf. Interface Anal.*, 34, 735–739, 2002.
69. Yeh, J.T., Yang, H.M., and Huang, S.S., Combustion of polyethylene filled with metallic hydroxides and crosslinkable polyethylene, *Polym. Deg. Stab.*, 50, 229–234, 1995.
70. Bertelli, G., Goberti, P., Marchini, R., Camino, G., and Luda, M.P., Combined melamine/mineral fillers as fire retardants for polypropylene, *Proceedings from 6th European Meeting on Fire Retardancy of Polymeric Materials (FRPM '97)*, Lille, France, 1997, p. 34.
71. Markezich, R.L. and Aschbacher, D.G., Chlorinated flame-retardant in combination with other flame retardants, *ACS Symp. Ser.*, 599, 65–75, 1995.
72. Toure, B., Cuesta, J.M.L., Gaudon, P., Benhassaine, A., and Crespy, A., Fire resistance and mechanical properties of a huntite/hydromagnesite/antimony trioxide/decabromodiphenyl oxide filled PP-PE copolymer, *Polym. Deg. Stab.*, 53, 371–379, 1996.
73. Namiye, Y., Kato, Y., Kitano, Y., Kuriso, H., and Yokata, Y., Flame retardant polyolefin compound having low smoking and toxicity, U.S. Patent No. 5,654,356, August 5, 1997.
74. Miyata, S. and Imahasi, T., Fire-retardant resin composition, U.S. Patent No. 5,094,781, March 10, 1992.
75. Carpentier, F., Bourbigot, S., Le Bras, M., Delobel, R., and Foulon, M., Charring of fire retarded ethylene vinyl acetate copolymer—magnesium hydroxide/zinc borate formulations, *Polym. Deg. Stab.*, 69, 83–92, 2000.

76. Hornsby, P.R., Ahmadnia, A., Marosi, G., and Anna, P., Tailoring the fire retardant performance of polymers using multi-component processing technologies, *Proceedings from Society of Plastics Engineers Annual Technical Conference (ANTEC'03)*, Nashville, TN, May 5–8, 2003.
77. Gui, H., et al., Effect of rubbers on the flame retardancy of EVA/ultrafine fully vulcanized powdered rubber/nanomagnesium hydroxide ternary composites, *Polym. Compos.*, 28, 479–483, 2007.
78. Liu, L.-h., Chen, J.-m. Song, Y.-h., Guo, F., and Chen, J.-f., Application of nano-sized magnesium hydroxide flame retardant in flexible PVC, *J. Chem. Eng. Chin. Univ.*, 18, 339–343, 2004.
79. Dalian Fumeida New Materials-Nano-magnesium hydroxide flame retardants <http://www.fmd.cn/doce/indexecp.htm> (2008).
80. Lv, J., Qie, L., and Qu, B., Controlled synthesis of magnesium hydroxide nanoparticles with different morphological structures and related properties in flame retardant ethylene–vinyl acetate blends, *Nanotechnology*, 15, 1576–1581, 2004.
81. Qiu, L., Xie, R., Ding, P., and Qu, B., Preparation and characterization of Mg(OH)₂ nanoparticles and flame retardant property of its nanocomposites with EVA, *Compos. Struct.*, 62, 391–395, 2003.
82. Fan, W., Sun, S., You, L., Cao, G., Song, X., Zhang, W., and Yu, H., Solvothermal synthesis of Mg(OH)₂ nanotubes using Mg₁₀(OH)₁₈Cl₂·5H₂O nanowires as precursors, *J. Mater. Chem.*, 13, 3062–3065, 2003.
83. Zhang, Q., Tian, M., Wu, Y., Lin, G., and Zhang, L., Effect of particle size on the properties of Mg(OH)₂-filled rubber composites, *J. Appl. Polym. Sci.*, 94, 2341–2346, 2004.
84. Mishra, S., Sonawane, S.H., Singh, R., Bendale, A., and Patil, K., Effect of nano-Mg(OH)₂ on the mechanical and flame-retarding properties of polypropylene composites, *J. Appl. Polym. Sci.*, 94, 116–122, 2004.
85. Okobo, N., Okumura, H., Okoshi, M., and Hamada, H., Flame retardancy of EVA/Nano magnesium hydroxide hybrid, *Proceedings from Additives 2004*, Clearwater Beach, FL, March 22–24, 2004.
86. Camino, G., Maffezzoli, A., Braglia, M., De Lazzaro, M., and Zammarano, M., Effect of hydroxides and hydroxycarbonate structure on fire retardant effectiveness and mechanical properties in ethylene-vinyl acetate copolymer, *Polym. Deg. Stab.*, 74(3), 457–464, December, 2001.
87. Wang, X. and Zhang, Q., Effect of hydrotalcite on the thermal stability, mechanical properties, rheology and flame retardance of poly(vinyl chloride), *Polym. Int.*, 53, 698–707, 2004.
88. Torno, O., Nanocomposites based on boehmite alumina, *Proceedings from Conference on Functional Fillers for Plastics*, September 15–17, Intertech, Portland, Maine, U.S.A., Paper 19, 2004.
89. Wang, Z., Han, E., and Ke, W., Influence of nano-LDHs on char formation and fire-resistant properties of flame-retardant coating, *Prog. Org. Coat.*, 53, 29–37, 2005.
90. Zhang, Z., Mei, X., Xu, C., and Qui, F., Study on the coating of nanoscale SiO₂ film on the surface of nanocrystalline Mg–Al layered double hydroxides, *Sci. China, Ser. B: Chem.*, 48(2), 107–114, 2005.
91. Ozdilek, C., Kazimierzak, K., van der Beek, D., and Picken, S.J., Preparation and properties of polyamide-6-boehmite nanocomposites, *Polymer*, 45, 5207–5214, 2004.
92. Sun, J., Gao, L., and Iwasa, M., Noncovalent attachment of oxide nanoparticles onto carbon nanotubes using water-in-oil microemulsions, *Chem. Commun.*, 832–833, 2004.
93. Beyer, G., Nanocomposites—A new class of flame retardants for polymer and cable applications, *Proceedings from Conference on Functional Fillers for Plastics*, September 15–17, Intertech, Portland, Maine, U.S.A., Paper 16, 2004.
94. Okoshi M. and Nishizawa, H., Flame retardancy of nanocomposites, *Fire Mater.*, 28, 423–429, 2004.
95. Lu, H., Hu, Y., Yang, L., Wang, Z., Chen, Z., and Fan, W., Study of the fire performance of magnesium hydroxide sulfate hydrate whisker flame retardant polyethylene, *Macromol. Mater. Eng.*, 289, 984–989, 2004.

8 Recent Developments in Silicon-Based Flame Retardants

Walid H. Awad

CONTENTS

8.1 Introduction	187
8.2 Silicones and Silanes	187
8.3 Polyhedral Oligomeric Silsesquioxane	190
8.4 Silica and Silicate	198
8.5 Conclusion	203
References.....	203

8.1 INTRODUCTION

Silicon is one of the most widely used elements. Many monographs and reviews have been written in the areas of organic, inorganic, organometallic, polymer, and mechanistic silicon chemistry.¹⁻¹¹ A considerable amount of research has shown that the addition of relatively small amounts of silicon compounds to various polymeric materials can significantly improve their flame retardancy. This class of flame-retardant materials was developed in response to the international pressure to develop nonhalogenated flame retardants. Silicon-containing flame retardants are considered to be “environmentally friendly” additives because their use leads to a reduction in the harmful impact on the environment when compared with existing materials. Many forms of silicon compounds have been explored as potential flame retardants to polymeric materials. The focus of this chapter will be on the following types of silicon-based materials: silicones, silanes, silsesquioxane, silica, and silicates.

8.2 SILICONES AND SILANES

Silicones are a class of synthetic polymers having the general formula $(R_mSi(O)_{4-m/2})_n$, where $m = 1-3$ and $n \geq 2$. The most common example is polydimethylsiloxane (PDMS). This polymer has a repeating $(CH_3)_2SiO$ unit. Silicones and silanes are the subject of many reviews.¹²⁻²² It is not possible to cover adequately the many uses to which silicones have been put. However, a summary of the most important properties and representative applications that utilize these properties are provided in the literature.^{23,24}

Silicone materials exhibit relatively low rates of heat release, a uniquely low dependence of rate of heat release on external heat flux. One of the causes of the lower burning rate is attributed to the accumulation of the silica ash layer at the silicone fuel surface. This accumulation of amorphous silica ash at the surface results from the deposition of silica particles, one of the major combustion products of silicone oligomers (cyclic and/or linear structures) in the gas phase.

According to a gasification study conducted on silicones, two modes of gasification have been proposed: (1) the volatilization of molecular species native to the polymer and (2) the volatilization

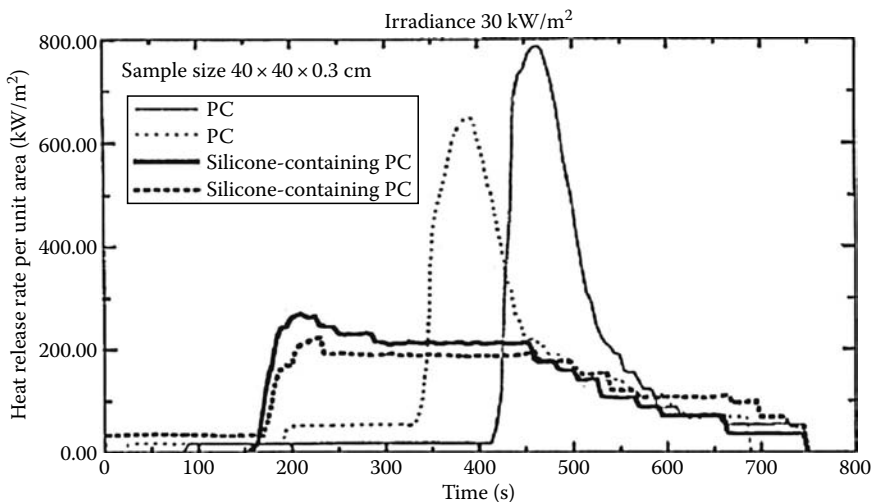


FIGURE 8.1 HRR for polycarbonate and polycarbonate-containing silicone (two repeated tests for each sample). (From Kashiwagi, T. et al., A nonhalogenated, flame retarded polycarbonate, in *Conference of Advanced Fire Resistant Aircraft Interior Materials*, Atlantic City, NJ, February 9–11, 1993, 175.)

of molecules resulting from thermally induced degradation of the polymer via siloxane rearrangement. The former process is dominant for short-chain oligomers, whereas the latter one is dominant in all higher molecular weight polymers.^{25,26}

Kashiwagi et al. investigated the flammability properties of various silicone-containing polycarbonates using the cone calorimeter.²⁷ The silicone was incorporated in the polycarbonate matrix as an additive or as a copolymer. Figure 8.1 shows a comparison between the heat release rate (HRR) of silicone/polycarbonate and pure polycarbonate. The data indicated that silicone has a significant effect in reducing the rate of the heat release. However, the delay in the ignition time for the silicone-containing sample is shorter than that for the pure polycarbonate sample.

One effective approach in increasing the fire resistance of polyurethane (PU) is to incorporate PDMS into its structure.²⁸ Microphase-segregated PU block copolymers containing hydroxyl-terminated silicone as the soft segment have been synthesized. The enhanced siliconated surface of the block copolymer has been confirmed by ESCA and x-ray analyses.

Thermal analysis (TGA) data of these siliconated block copolymers revealed that they are thermally more stable than the reference materials, poly(tetrahydrofuran block urethane) and poly(ethyleneglycol block urethane) copolymers. The thermal stability was found to depend on the silicone content, with stability increasing as the silicone content in the structure increases.

The flammability behavior of these materials, as revealed by oxygen index, showed that siliconated PUs have higher oxygen index values compared to reference materials. The siliconated block copolymers with higher PDMS content have higher oxygen index values. The oxygen index values depend upon the diisocyanate used. For example, block copolymers made of hydroxy-terminated PDMS, H(12)MDI, and 1,6-hexanediol showed higher oxygen index values compared to block copolymers made of hydroxy-terminated PDMS, TDI, and 1,6-hexanediol. This difference is related to the extent of soft block segregation.

The observed enhancement in oxygen index could be attributed to phase segregation in these block copolymers, which leads to domination of siloxane on the polymer surface. Siloxanes have solid-phase activity rather than vapor-phase activity and reduce flammability through increased formation of pyrolytic char.

Recently, PU/PDMS hybrid materials (with different PDMS content) were synthesized by a two-step addition reaction.²⁹ Thermogravimetric analysis indicated that no enhancement in the thermal

stability of PU was obtained under the thermo-oxidative conditions, but under the pyrolytic conditions some improvement in the thermal stabilization of PU was observed.

The thermal stability of PU is generally controlled by the thermally weakest link: the urethane bond. In the case of PU/PDMS hybrid system, any decrease in the thermal stability might be explained by thermal instabilities in PDMS structure.

In terms of flammability properties, both the limiting oxygen index (LOI) (21% for PU/PDMS vs. 22% for PU) and UL 94 (no rating for PU and PU/PDMS) indicated that no benefit was achieved by incorporating PDMS into PU. However, the most interesting results were revealed by the cone calorimeter, where the data showed that there is significant reduction in the HRR of PU/PDMS compared to PU. This can be explained by the accumulation of silica on the char layer that provides protection to the underlying polymer from heat transfer with the flame. To examine the efficiency of this char layer in protecting the underlying polymer, a heat transfer measurement was carried out on both PU and PU/PDMS during heat exposure. The temperature profiles indicated that for pure PU the evolution of temperature was relatively rapid compared to PU/PDMS.

Hermansson et al. carried out extensive investigations on the fire-retardant behavior of ethylene–acrylate copolymer modified with chalk and silicone elastomer.^{30–32} They have shown that incorporation of a silicone elastomer (at 5 wt.%) and chalk filler (at 30 wt.%) can greatly improve the flame-retardant properties of ethylene butyl acrylate formulations. The results show that, compared to the pure polymer, an increase in the LOI from 18 to 30, and a decrease in the peak heat release rate (PHRR) from 1300 to 330 kW/m² were observed.

These property improvements were assigned to an intumescent process, which was proposed to consist of the following steps: (1) ester pyrolysis occurs when degradation starts at 300°C producing carboxylate ions on the copolymer backbone; (2) the foam structure started to form when the volatile degradation products of ethylene butyl acrylate (EBA) copolymer are produced; (3) the ionomers produced during the degradation process increase the melt viscosity by cross-linking reactions and provide stabilization to the foam structure.

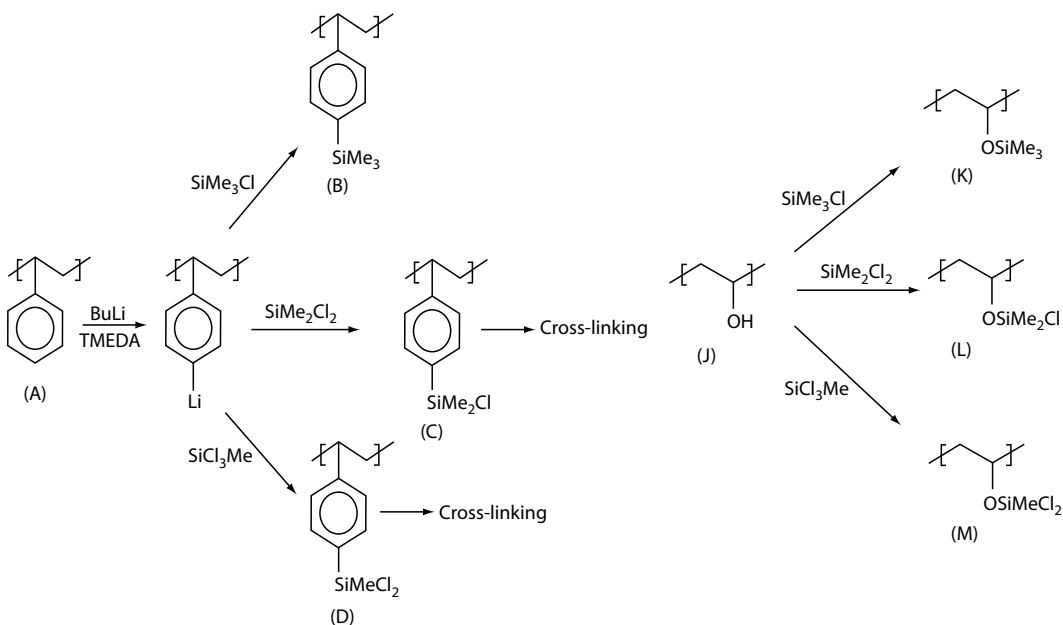
The melt-dripping behavior of various ethylene–acrylate formulations with chalk and silicone have also been addressed by exposing these formulations to a Bunsen burner. It has been demonstrated that viscosity plays a crucial role in this process by affecting the transport of volatile gases, eventual dripping, and the formation of the intumescent structure.³²

The strategy of incorporating silicon as a reactive component in the polymeric system to attain flame retardancy has been explored. For example, Ebdon et al. carried out silylation to the polystyrene using *n*-butyl lithium in the presence of tetramethylethylenediamine, followed by reaction with trimethylchlorosilane, dichlorodimethylsilane, or trichloromethylsilane, as shown in Scheme 8.1. Poly(vinyl alcohol) films have also been modified with chlorosilanes (Scheme 8.1).

The limiting oxygen indices of these systems showed a significant reduction in the flammability of the silylated polymers. In both systems, it appears that silicon has a much greater effect in the presence of halogen, probably through the evolution of silicon chlorides during the combustion process.³³

The reactive approach has been employed recently to prepare various polymeric systems.^{34,35} Silicon-containing polystyrenes and poly(methyl methacrylate)s (PMMA)s copolymers have been prepared by free radical polymerization. The LOI data indicated that a marginal improvement in flame retardancy has been observed compared to the parent homopolymers. The authors speculated that the nature of the silicon-containing group has an effect on the flame-retardant mechanism.³⁴

Flame-retardant epoxy resins with different silicon contents were prepared using silicon-containing epoxides or silicon-containing prepolymers. The thermal stability and flame-retardant properties of the produced epoxide systems were evaluated and related to the silicon content. The char yields under nitrogen and air atmospheres increased with increase in silicon content. The authors pointed out that the silicon-containing resin has improved flame retardancy over the silicon-free resin as evidenced by the LOI. LOI values increased from 24 for a standard commercial resin to 36 for silicon-containing resins.³⁵



SCHEME 8.1 Silylation of polystyrene (left) and poly(vinyl alcohol) (right). (From Ebdon, J.R. et al., *Polym. Degrad. Stab.*, 54, 395, 1996. With permission.)

8.3 POLYHEDRAL OLIGOMERIC SILSESQUIOXANE

The term silsesquioxanes refers to silicon structures that have the empirical formula $RSiO_{3/2}$ where R is a hydrogen atom or a carbon moiety. Polyhedral oligomeric silsesquioxane (POSS) is a unique member of this group with its name derived from the noninteger (one and one-half or sesqui) ratio between oxygen and silicon organic substituent. Actually, POSS represents an intermediate structure between those of silicone and silica. Figure 8.2 shows the general structure of POSS macromomers. The POSS molecules, which were first isolated along with other volatile compounds in 1946 through thermolysis of the polymeric products of methyltrichlorosilane co-hydrolysis, contain a polyhedral silicon–oxygen nanostructured skeleton.³⁶ The uniqueness of POSS molecules arises from the thermally stable silicon–oxygen framework and the flexible chemical composition; a variety of organic substituents can be attached to each corner silicon atom to give different functionality.

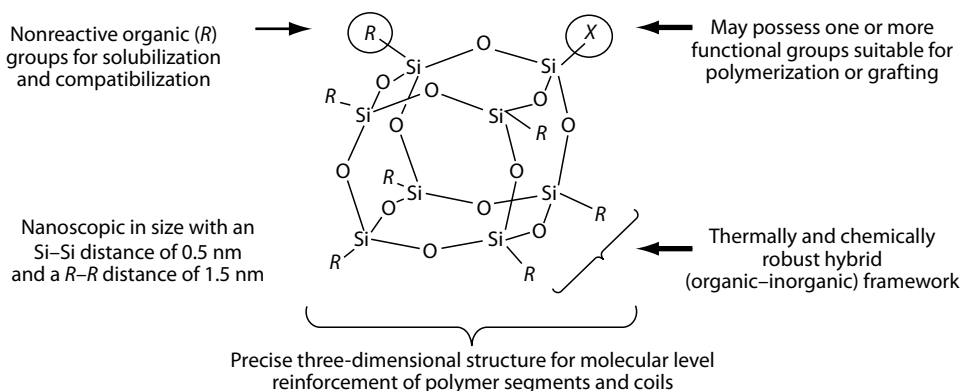


FIGURE 8.2 General structure of polyhedral oligomeric silsesquioxane. (From <http://www.hybridplastics.com>.)

POSS molecules can be incorporated into polymer systems through blending, grafting, or copolymerization aiming at nanostructured polymeric materials, which have properties that bridge the property space between organic plastics and ceramics. Recent studies on POSS-containing hybrid polymers have been reported indicating reinforced mechanical, thermal, and flammability properties.^{37–48}

In a detailed investigation about the thermolysis of POSS macromers and POSS–siloxane copolymers, Mantz et al.³⁸ investigated the pyrolysis of four POSS macromers: $\text{Cy}_8\text{-Si}_8\text{O}_{11}(\text{OH})_2$, $\text{Cy}_8\text{-Si}_8\text{O}_{11}(\text{OSiMe}_3)_2$, $\text{Cy}_6\text{-Si}_6\text{O}_9$, and $\text{Cy}_8\text{-Si}_8\text{O}_{12}$ (where $\text{Cy} = \text{c-C}_6\text{H}_{11}$) (Figure 8.3) and two POSS–siloxane copolymers ($\text{Cy}_8\text{-Si}_8\text{O}_{11}(\text{OSiMe}_2)_n\text{O-}$) (Figure 8.4).

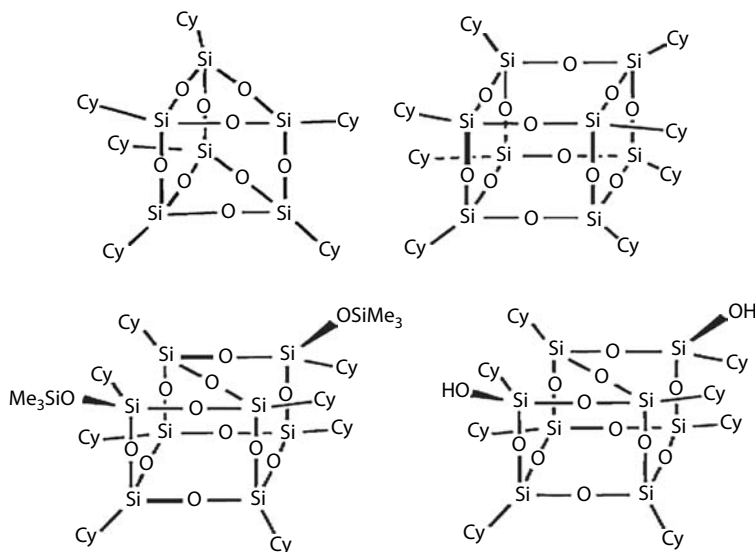


FIGURE 8.3 POSS macromers: $\text{Cy}_6\text{-Si}_6\text{O}_9$, $\text{Cy}_8\text{-Si}_8\text{O}_{12}$, and $\text{Cy}_8\text{-Si}_8\text{O}_{11}(\text{OSiMe}_3)_2$, $\text{Cy}_8\text{-Si}_8\text{O}_{11}(\text{OH})_2$, (where $\text{Cy} = \text{c-C}_6\text{H}_{11}$). (From Mantz, R.A. et al., *Chem. Mater.*, 8, 1250, 1996. With permission.)

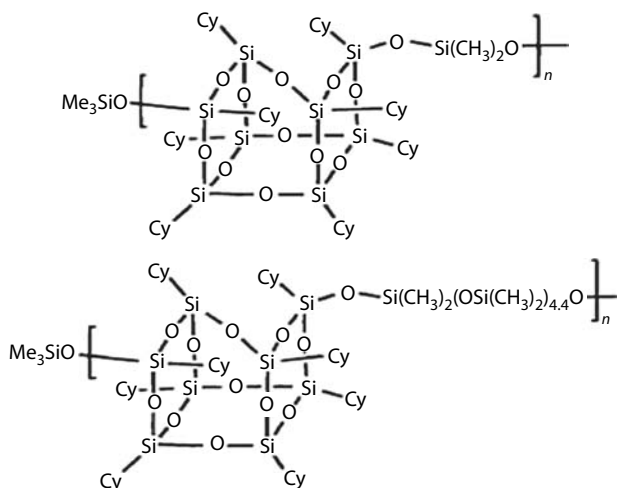


FIGURE 8.4 POSS–siloxane copolymers: $(\text{Cy}_8\text{-Si}_8\text{O}_{11}(\text{OSiMe}_2)_1\text{O-})_n$ and $(\text{Cy}_8\text{-Si}_8\text{O}_{11}(\text{OSiMe}_2)_{5.4}\text{O-})_n$. (From Mantz, R.A. et al., *Chem. Mater.*, 8, 1250, 1996. With permission.)

They indicated that both fully and incompletely condensed POSS macromers have a tendency to sublime upon heating, assuming they contain functionalities which do not undergo cross-linking reactions. The original POSS structure was observed in the sublimates for both fully and incompletely condensed structures. However, once this POSS structure was incorporated into a polymeric form, these macromers were no longer observed in the sublimates. Rather, they decompose primarily through partial loss of their organic substituents followed by subsequent cross-linking reactions which incorporates the remaining composition into a SiO_xC_y network (char).

Extensive thermal degradation study was carried out on octaisobutyl POSS under both inert and air atmospheres.⁴³ The degradation under inert conditions led to almost complete weight loss regardless of the heating rate. More complex degradation was observed under the oxidative atmosphere. The authors proposed a possible competition between the evaporation and oxidation processes, which eventually led to the production of silica-like thermally stable char. Analysis of the char residue after thermo-oxidative conditions indicated that the organic content decreased by increasing the treatment temperature. This char was converted to amorphous silica by heating the POSS up to 800°C.

The same group reported on the thermal and thermo-oxidative degradation of a number of POSS cages with different substituent groups; namely, $R = \text{H}$, CH_3 , C_4H_9 , C_8H_{17} , C_6H_5 , and vinyl (see Figure 8.5). Different thermal behavior was observed depending on the type of substituent. The basic difference between alkyl-substituted POSS and phenyl-substituted POSS is the intrinsic thermal stability of the substituent. For the alkyl substituent, cleavage of the Si–C and C–C bonds could occur, producing unsaturated moieties. On the other hand, phenyl POSS degradation would proceed by hydrogen abstraction of the phenyl group, and the resulting aromatic radicals would combine to form very stable polyaromatic structures. The highest ceramic yield was obtained for the polyvinyl POSS through material reorganization into O–Si–C_n–Si structure.⁴⁴

The above thermal analysis studies demonstrated the enhanced thermal stability of POSS materials, and suggested that there is potential to improve the flammability properties of polymers when compounded with these macromers. In a typical example of their application as flame retardants, a U.S. patent³⁹ described the use of preceramic materials, namely, polycarbosilanes (PCS), polysilanes (PS), polysilsesquioxane (PSS) resins, and POSS (structures are shown in Figure 8.6) to improve the flammability properties of thermoplastic polymers such as, polypropylene and thermoplastic elastomers such as Kraton (polystyrene–polybutadiene–polystyrene, SBS) and Pebax (polyether block–polyamide copolymer).

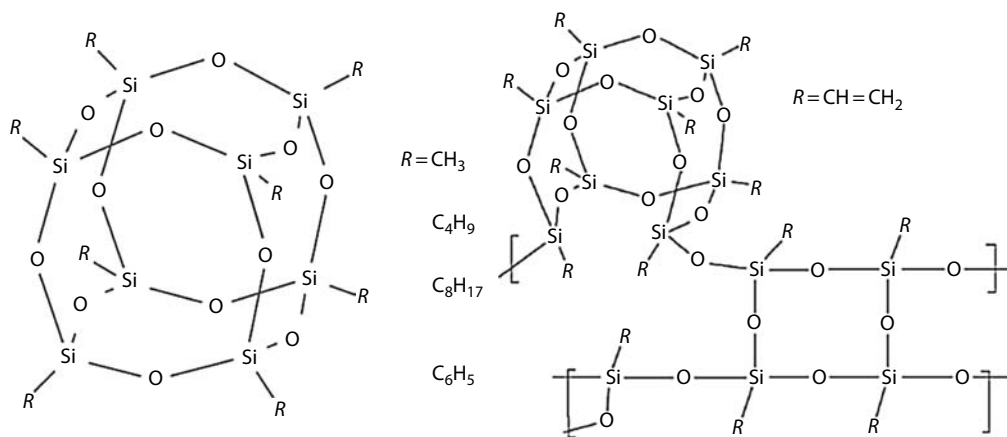


FIGURE 8.5 T₈ POSS structure and polyvinyl POSS. (From Fina, A. et al., *Thermochim. Acta*, 440, 36, 2006. With permission.)

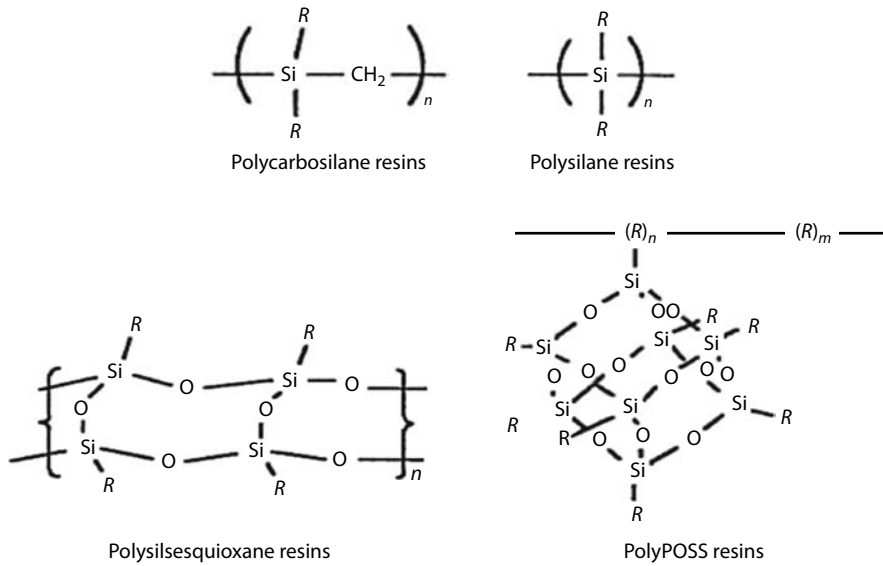


FIGURE 8.6 PCS, PS, PSS, and POSS structures. (From Lichtenhan, J.D. and Gilman, J.W., Preceramic additives as fire retardants for plastics, U.S. patent 6,362,279, 2002.)

The resulting blends were shown to possess enhanced flammability and mechanical properties. The cone calorimeter data shown in Table 8.1 indicate that the highest reduction in the PHRR was obtained for the Pebax system where a reduction of 65%–70% in PHRR was reported. The reduction in heat release was obtained by enhanced char formation. The char reduces the escape of small volatile molecules to the gas phase, which in turn reduces the amount of heat release feedback to the polymer surface.

Another example of enhanced flammability properties was obtained by adding POSS to the coating of textile fabrics.⁴⁰ In this study, POSS was used as an additive for the PU resin and the product was applied as a coating to the polyester fabrics. For comparison purposes, another kind of additive (Cloisite 30B) has been used. The structure of POSS materials employed in this investigation

TABLE 8.1
Cone Calorimeter Data for Polymers and Pre-Ceramic Polymer–Polymer Blends

Sample	Char Yield (%)	Peak HRR (Δ%) (kW/m ²)	Mean HRR (Δ%) (kW/m ²)	Mean Heat of Combustion (MJ/kg)	Total Heat Released (MJ/m ²)	Mean Ext. Area (m ² /kg)	Mean CO Yield (kg/kg)
PP	0	1.466	741	34.7	141	650	0.03
PP w/20%PSS	17	892 (40%)	432 (42%)	29.8	106	821	0.03
PEBAX	0	2.020	780	29.0	332	187	0.02
PEBAX w/20%PCS	15	699 (65%)	419 (46%)	28.5	272	260	0.02
PEBAX w/10%PSS	6	578 (72%)	437 (44%)	25.2	301	367	0.02
Kraton	1	1.405	976	29.3	351	1.750	0.08
Kraton w/20%PCS	20	825 (42%)	362 (63%)	26.4	266	1.548	0.07
Kraton w/10%PSS	6	1.027 (27%)	755 (23%)	26.9	324	1.491	0.07

Source: Lichtenhan, J.D. and Gilman, J.W., Preceramic additives as fire retardants for plastics, U.S. Patent 6,362,279, 2002.

is shown in Figure 8.7a and b. The data in Figure 8.8 show the HRR curves for the knitted fabrics coated with PU alone and PU compounded with each of the following additives; POSS MS2, POSS FQ2, and 30B. It is apparent that POSS MS2 has no significant effect on the reduction of PHRR. However, 55% reduction in PHRR was obtained for POSS FQ2. This reduction was achieved coupled with increase in time to ignition (20 vs. 10 s for pure PU).

Bourbigout et al. reported on the fire behavior of the polypropylene–POSS multifilament yarns.⁴⁵ The material was prepared by melt spinning of both polypropylene and poly(vinylsilsesquioxane) (FQ-POSS). The HRRR data shown in Figure 8.9 indicate that no reduction in PHRR was obtained using FQ-POSS. However, the time to ignition of PP-POSS system was increased relative to the pure PP. Thermoplastic polyurethane (TPU) coating systems were also prepared using two types of POSS macromers, namely, dodecaphenyl-POSS (DP-POSS) and FQ-POSS. The HRR data (Figure 8.10) showed that the PHRR was reduced by 31% and 50% for TPU/DP-POSS and TPU/FQ-POSS systems, respectively.

The effects of metal-containing POSS on the combustion behavior of polypropylene have been investigated.⁴⁶ Metal–POSS was prepared from incompletely condensed structures by reaction with organometallic compounds. The dimeric and oligomeric of Al and Zn–isobutyl silsesquioxane (POSS) have been evaluated as potential flame retardants for polypropylene, and the results were compared with PP/octaisobutyl POSS. The cone calorimeter data (Table 8.2) revealed that

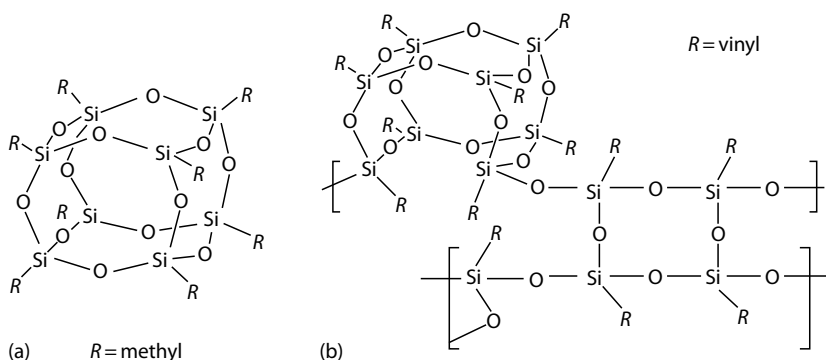


FIGURE 8.7 (a) Octamethyl POSS (POSS-MS) and (b) poly(vinylsilsesquioxane) (POSS-FQ). (From Devaux, E. et al., *Fire Mater.*, 26, 149, 2002. With permission.)

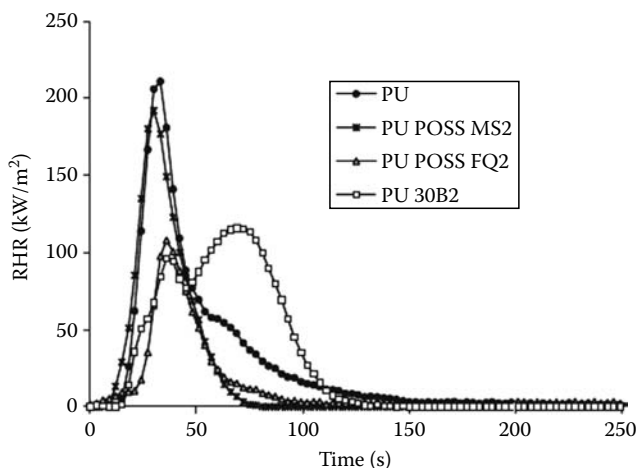


FIGURE 8.8 Rate of heat release curves of PU-nanocomposite coatings on PET knitted fabrics at 35 kW/m². (From Devaux, E. et al., *Fire Mater.*, 26, 149, 2002. With permission.)

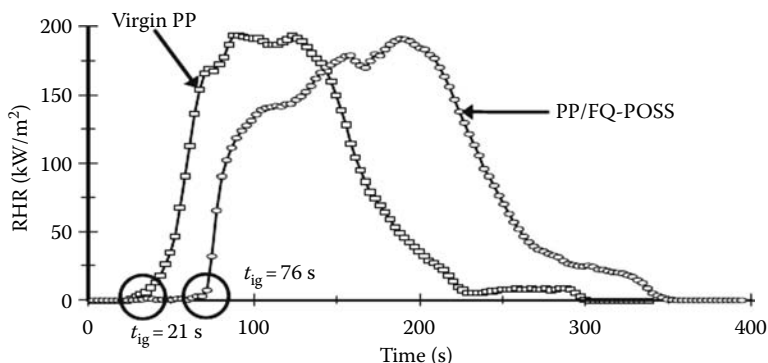


FIGURE 8.9 Rate of heat release curves of PP and PP/FQ-POSS knitted fabrics at 35 kW/m². (From Bourbigot, S. et al., *Fire Retardancy of Polymers: New Applications of Mineral Fillers*, Bras, M. et al., Eds., The Royal Society of Chemistry, Cambridge, MA, 2005, 189. With permission.)

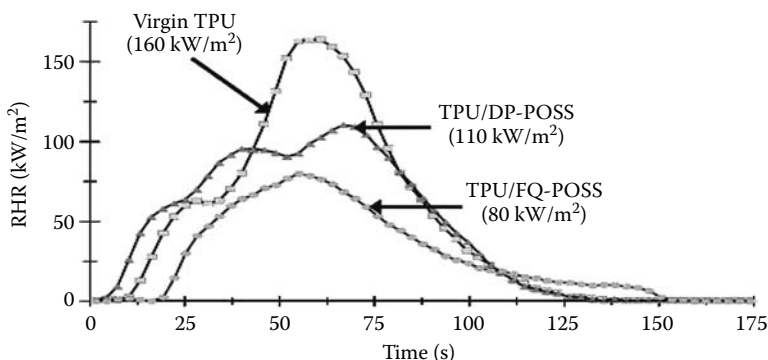


FIGURE 8.10 Rate of heat release curves of TPU, TPU/DP-POSS, and TPU/FQ-POSS as coating of woven PET fabrics at heat flux 35 kW/m². (From Bourbigot, S. et al., *Fire Retardancy of Polymers: New Applications of Mineral Fillers*, Bras, M., Bourbigot, S., Duquesne, S., Jama, C., and Wilkie, C.A., Eds., The Royal Society of Chemistry, Cambridge, MA, 2005, 189. With permission.)

TABLE 8.2
Cone Calorimeter Data for Different PP/POSS Formulations

Sample	TTI (s)	PHRR (kW/m ²)	MAHRE (kW/m ²)	THR (MJ/m ²)	EHC (MJ/kg)	Residual Weight (%)	TSR	Avg CO ₂ Yield (kg/kg)	Avg CO Yield (g/kg)
PP	56±5	1103±50	509±20	111±2	47±1	~0	1427±30	3.39±0.02	43±5
PP/T ₈ -POSS	50±3	1325±50	591±20	112±3	48±1	0.2±0.1	1564±70	3.45±0.04	42±1
PP/Al-POSS	37±1	624±20	399±10	98±1	41±1	2.5±0.1	1850±20	3.05±0.03	35±2
PP/Zn-POSS	54±4	1069±50	509±20	108±4	46±1	3.3±0.1	1525±25	3.35±0.08	42±2

Source: Fina, A. et al., *Polym. Degrad. Stab.*, 91, 2275, 2006. With permission.

Note: TTI, time to ignition; PHRR, peak of heat release rate; MAHRE, maximum average rate of heat emission; THR, total heat release; EHC, effective heat of combustion; TSR, total smoke released.

the addition of octaisobutyl POSS had a deteriorating effect on the flammability properties of polypropylene, which was ascribed to the partial evaporation of T₈-POSS and the subsequent oxidation of POSS organic substituents. Al-containing POSS can be an effective flame retardant, as evidenced by the significant reduction in PHRR. This enhanced performance was attributed to the

catalytic effect of Al which promotes char formation. Zn-POSS had no effect on polypropylene combustion behavior.

It should be noted that the inconsistency in the flammability performance of various types of polymer/POSS hybrid systems could be ascribed to several factors, such as, the type of polymeric material, the structure of POSS macromer, and the degree of dispersion of POSS in the polymer matrix.

The potential of synergistic effects on the POSS materials has been illustrated recently.⁴⁷ Octamethyl POSS (OMPOSS) and Exolit OP950, a phosphinate-based compound, have been incorporated with the recycled poly(ethylene terephthalate) (PET) by melt blending. Exolit OP950 showed intumescent behavior. The LOI increased from the initial value 29 vol.% for PET/10% OP950 to 36 vol.%, when 1 wt.% of OP950 is substituted by OMPOSS (Figure 8.11). This suggests that there is a synergistic effect between OP950 and OMPOSS.

The cone calorimeter data (Table 8.3) provided further evidence for this synergistic behavior. A reduction in PHRR of 30% and 37% was obtained for PET compounded with 20 wt.% and

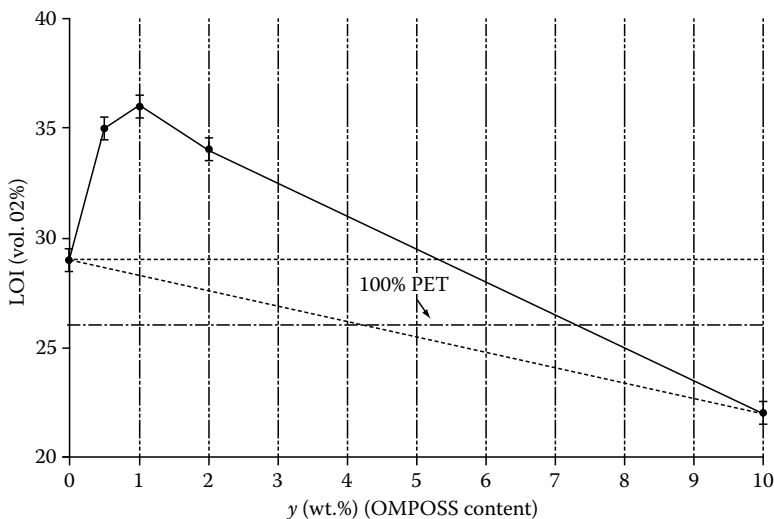


FIGURE 8.11 LOI values of formulations PET/OP950/OMPOSS (90/10 – y/y). (From Vannier, A. et al., *Polym. Degrad. Stab.*, 93, 818, 2008. With permission.)

TABLE 8.3
Cone Calorimeter Data for Various PET/OP950/OMPOSS
Formulations (35 KW/m²)

Sample	T_{ign} (s)	PHRR (kW/m ²)		THR (MJ/m ²)	AMLR (g/s)	ASEA (m ² /kg)
		(% Reduction)				
PET	75	708		49	0.11	269
PET + OP950 20 wt. %	145	496 (30)		35	0.09	616
PET + OP950 10 wt. %	109	448 (37)		37	0.10	454
PET + OP950 18 wt. % + OMPOSS 2 wt. %	62	247 (65)		44	0.06	481
PET + OP950 9 wt. % + OMPOSS 1 wt. %	73	279 (61)		46	0.06	440

Source: Vannier, A. et al., *Polym. Degrad. Stab.*, 93, 818, 2008. With permission.

Note: T_{ign} = time to ignition, PHRR = peak of heat release rate, THR = total heat release, AMLR = average mass loss rate, ASEA = average specific extinction area.

TABLE 8.4
Thermal Analysis (TGA, DTG, and DTA) Data for Different Formulations of PC/TPOSS, under Ar Atmosphere

Sample	$T_{-10\%}$ (°C)	$T_{-50\%}$ (°C)	$T_{-70\%}$ (°C)	T_{\max} (°C)	T_{mex} (°C)	Solid Residue (%) at 800°C
TPOSS	436	—	—	43, 210, 568	684	56.1
PC	478	525	553	524	552	19.7
PC/1 wt% TPOSS	467	508	557	517	558	21.7
PC/2 wt% TPOSS	477	514	596	518, 671	540	14.3
PC/3 wt% TPOSS	469	520	600	518, 670	538	2.9

Source: Song, L. et al., *Polym. Degrad. Stab.*, 93, 627, 2008. With permission.

10 wt.% of OP950, respectively. However, by partial substitution of OP950 with 2 wt.% and 1 wt.% of OMPOSS, the reduction observed in PHRR values was 65% and 61%, respectively.

The degradation and combustion behavior of polycarbonate/POSS hybrid system has been reported recently.⁴⁸ Different loading contents of trisilanolphenyl-POSS (TPOSS) were melt blended with polycarbonate matrix (PC). The data shown in Table 8.4 indicate that no improvement in thermal stability parameters (i.e., onset decomposition temperature and peak decomposition temperature) was observed compared to the neat polycarbonate. The thermo-oxidative degradation process of the hybrid system proved to be a complicated process, which includes hydrolysis/alcoholysis of the carbonate linkage, free radical oxidative chain degradation, reformation, and branching and cross-linking reactions.

The flame-retardant properties as evaluated by the cone calorimeter indicate that adding TPOSS to polycarbonate leads to a significant reduction in the PHRR value, but no improvement in the time to ignition was observed (Figure 8.12). The decrease in the time to ignition was attributed to the evolution of small molecules produced from dissociation of TPOSS. The authors proposed that during the combustion process a char layer is formed on the surface of the sample and TPOSS undergoes

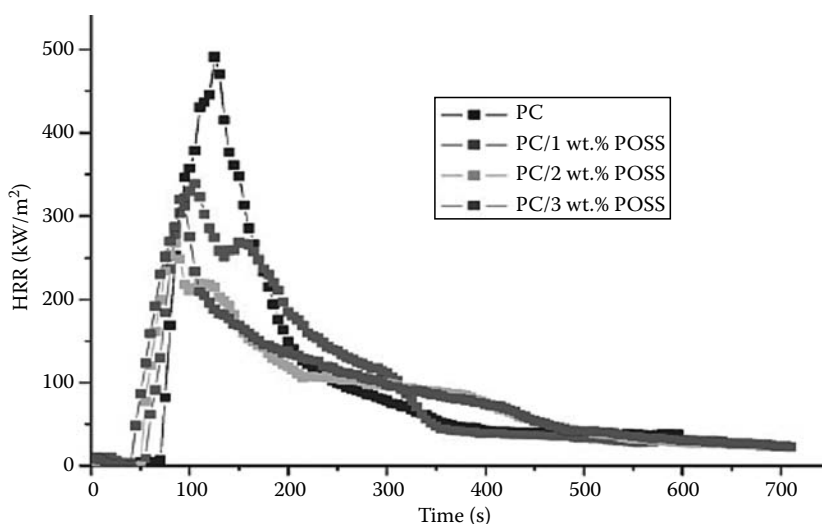


FIGURE 8.12 (See color insert following page 530.) Rate of heat release curves of PC, PC/1 wt.% TPOSS, PC/2 wt.% TPOSS, and PC/3 wt.% TPOSS. (From Song, L. et al., *Polym. Degrad. Stab.*, 93, 627, 2008. With permission.)

a series of oxidation reactions to form SiO_2 . The presence of SiO_2 can enhance the viscosity and the thermal oxidative stability of the char. This enhanced char structure protects and insulates the underlying polymer from any further degradation.

8.4 SILICA AND SILICATE

In an attempt to look for alternatives to the use of halogenated fire retardants, which function in the gas phase, an approach has been pursued which controls the polymer flammability by modifying the condensed phase chemistry. Silica gel combined with potassium carbonate have been reported to be an effective fire retardant for a wide variety of common polymers, such as polypropylene, nylon, poly(methylmethacrylate), poly(vinyl alcohol), cellulose, and to a lesser extent, polystyrene and styrene–acrylonitrile.⁴⁹ The cone calorimeter data shown in Table 8.5 indicate that the PHHR is reduced by up to 68% without significantly increasing the smoke or carbon monoxide levels during the combustion.

TABLE 8.5
Cone Calorimeter Data for Different Polymers with Silica Gel and Potassium Carbonate

Sample Disk (75 mm × 8 mm)	Char Yield (%)	LOI (%)	Peak RHR (Δ) (kW/m ²)	Mean RHR (kW/m ²)	Mean Heat of Combustion (MJ/m ²)	Total Heat Released (MJ/m ²)	Mean Ext. Area (m ² /kg)	Mean CO Yield (kg/kg)
PP	0	—	1761	803	37.9	357	689	0.04
PPw/6%SG & 4%PC	10	—	736 (58%)	512	33.1	297	710	0.04
PS	0	18	1737	1010	24.6	277	1422	0.07
PSw/6%SG & 4%PC	6	24	1190 (31%)	725	24.7	246	1503	0.07
PMMA	0	18	722	569	23.1	319	210	0.01
PMMAw/3%SG & 1%PC	15	25	420 (42%)	246	20.9	231	199	0.05
PVA	4	—	609	381	17.0	221	594	0.03
PVAw/6%SG & 4%PC	43	—	194 (68%)	114	12.4	101	201	0.03
Cellulose	4	—	310	161	11.3	101	27	0.02
Cellulose w/6% SG & 4% PC	32	—	149 (52%)	71	5.3	34	20	0.04
SAN	2	—	1499	837	25.2	197	1331	0.07
SAN w/6% SG & 4% PC	3	—	1127 (25%)	772	23.0	169	1301	0.06
Nylon 6,6	1	30	1131	640	23.2	108	234	0.02
Nylon6,6w/3%SG & 2%PC	5	33	526 (53%)	390	22.0	105	171	0.02
Nylon6,6w/6% SG & 4%PC	6	30	546 (52%)	370	23.5	102	185	0.02

Source: Gilman, J.W. et al., Environmentally safe fire retardants for polymeric materials—I. Silica gel-potassium carbonate additive, in *Society for the Advancement of Material and Process Engineering (SAMPE)*, Anaheim, CA, March 24–28, 1996, 708.

Note: SG, silica gel; PC, potassium carbonate.

TABLE 8.6
Material Properties of Various Silicas

Silica	Porosity (cm ³ /g)	Thermal Treatment (°C, h)	Silanol Surface Concentration (SiOH/nm ²)	Surface Area (m ² /g)	Primary Particle Size (μm)
Fused silica amorphous	~0	100°C (2h)	Low	Low	7
Fumed silica hydrophilic	NA	None	3–4	255±25	Aggregate length 0.2–0.3
Fumed silica hydrophobic	NA	100°C (15h)	1–2	140±30	NA
Silica gel	2.0	900°C (15h)	0.4	400±40	17

Source: Kashiwagi, T. et al., *Fire Mater.*, 24, 277, 2000. With permission.

To further explore the influence of silica material properties (morphology, surface area, silanol concentration, and surface treatment) on the silica flame-retardant properties, various types of silicas (silica gel, fumed silicas, and fused silica) were investigated.^{50,51} Material properties of the various silicas are summarized in Table 8.6. These different types of silicas were added to polypropylene and polyethylene oxide to determine their flame-retardant effectiveness and mechanisms. Polypropylene was chosen as a non-char-forming thermoplastic, and polyethylene oxide was chosen as a polar slightly char-forming thermoplastic. Flammability properties were measured in the cone calorimeter and the mass loss rate was measured in the radiative gasification device in nitrogen to exclude any gas phase oxidation reactions.

Figures 8.13 and 8.14 show the HRR and mass loss rate of the polypropylene samples with each silica additive. The addition of low density, large surface area silica, such as fumed silicas and silica gel, to PP and PEO significantly reduced the HRR and mass loss rate. However, the addition of fused silica did not reduce the flammability properties as much as other silicas.

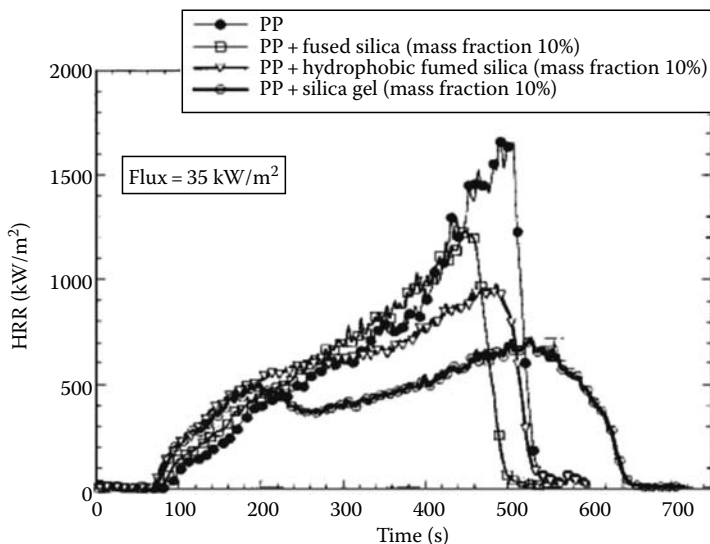


FIGURE 8.13 Effects of the addition of various silica types on the HRR of PP. (From Kashiwagi, T. et al., *Fire Mater.*, 24, 277, 2000. With permission.)

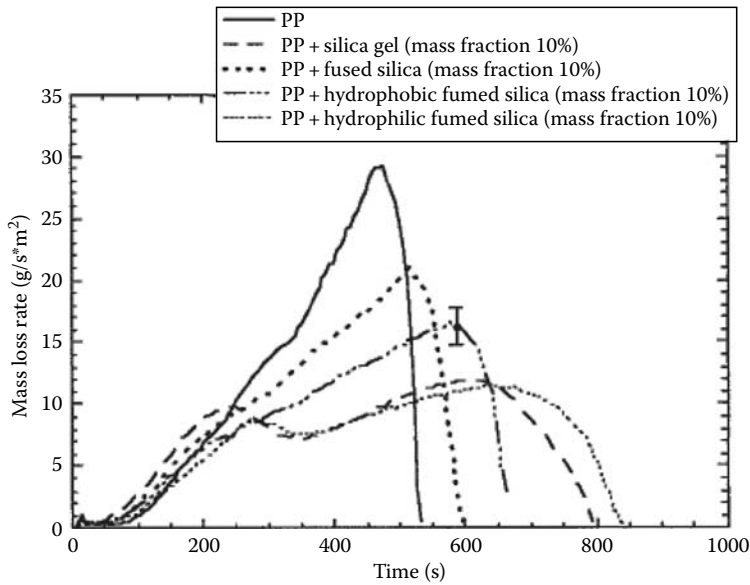


FIGURE 8.14 Effects of the addition of various silica types on the mass loss rate of PP in nitrogen. (From Kashiwagi, T. et al., *Fire Mater.*, 24, 277, 2000. With permission.)

The authors proposed a mechanism that accounts for the reduction in flammability properties, which depends on physical processes in the condensed phase rather than chemical reactions. Three factors are critical in determining the silica behavior during the combustion process: the density and surface area of the additive, the melt viscosity of the polymer. The interplay between these factors can determine whether the silica will accumulate near the surface or sink through the polymer melt. Fumed silica and silica gel provide examples for the first case where the silica particles accumulated on the surface and formed an insulating layer that provide protection to the underlying polymer. This is in contrast to the other case where the fused silica particles sank through the polymer melt.

The proposed hypothesis mentioned above for the flame retardancy of silica was further examined by studying the effects of polymer melt viscosity on the flammability properties of PMMA with the addition of the various types of silica.⁵² PMMA was chosen because of its large average zip length, which means that the molecular weight of PMMA does not significantly change during thermal degradation. The effects of melt viscosity were investigated by comparing the flammability properties of low molecular weight PMMA (LMWPMMA) with two types of silica (silica gel and fused silica) with that of high molecular weight PMMA (HMWPMMA) with the same types of silica.

The addition of fused silica to LMWPMMA did not bring a significant increase in the melt viscosity. However, adding silica gel (10% mass fraction) increased the melt viscosity by one order of magnitude compared to pure LMWPMMA. On the other hand, no significant increase in melt viscosity was observed for HMWPMMA by adding fused silica, but the addition of silica gel (10% mass fraction) increased the melt viscosity of HMWPMMA by a factor of five.

The pyrolysis of both LMWPMMA and HMWPMMA with different silica types was investigated under nitrogen in the gasification apparatus. The results for the LMWPMMA system indicate mass loss rate curves similar to that obtained for both pure LMWPMMA and LMWPMMA/fused silica. However, half the mass loss rate can be observed for the LMWPMMA/silica gel system. As opposed to the negligible effect observed for fused silica with LMWPMMA, a significant effect was observed with HMWPMMA. Silica gel, however, was more effective in reducing the mass loss rate for HMWPMMA.

The burning behavior for LMWPMMA and HMWPMMA samples was investigated using the cone calorimeter at 40 kW/m^2 . Figure 8.15 shows the heat release curves for LMWPMMA samples. The trends are similar to those of the mass loss rate in nitrogen. The data indicate that a roughly 50% reduction in heat release rate was observed by adding silica gel to LMWPMMA but no significant reduction in heat release rate was obtained with fused silica.

The results for the HMWPMMA system are shown in Figure 8.16. Comparing these results with the mass loss rates for the same samples indicate that the trends are similar. Adding fused silica reduced the heat release rate for HMWPMMA by about 25% compared to the pure sample. However, the addition of silica gel reduced the heat release rate by about one-third of the peak rate of the pure HMWPMMA.

Based upon these results, the authors concluded that the two critical factors for reducing the mass loss rate and HRR for PMMA are the amount of accumulation of silica particles on the surface and

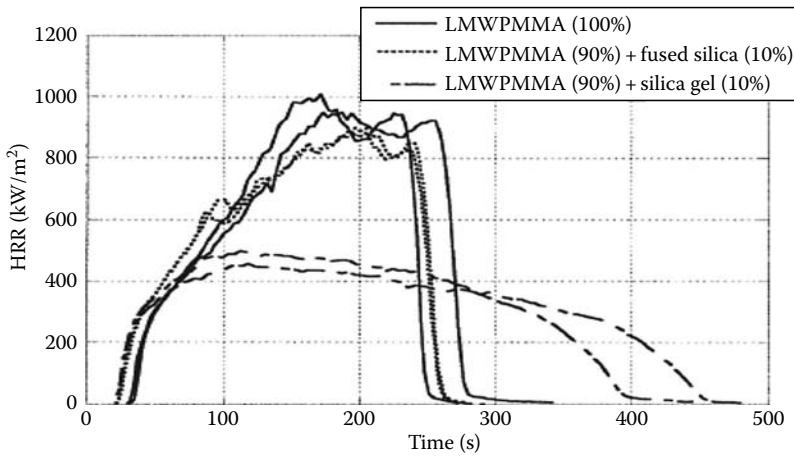


FIGURE 8.15 Effects of silica types on the HRR of LMWPMMA at 40 kW/m^2 . (From Kashiwagi, T. et al., *J. Appl. Polym. Sci.*, 87, 1541, 2003. With permission.)

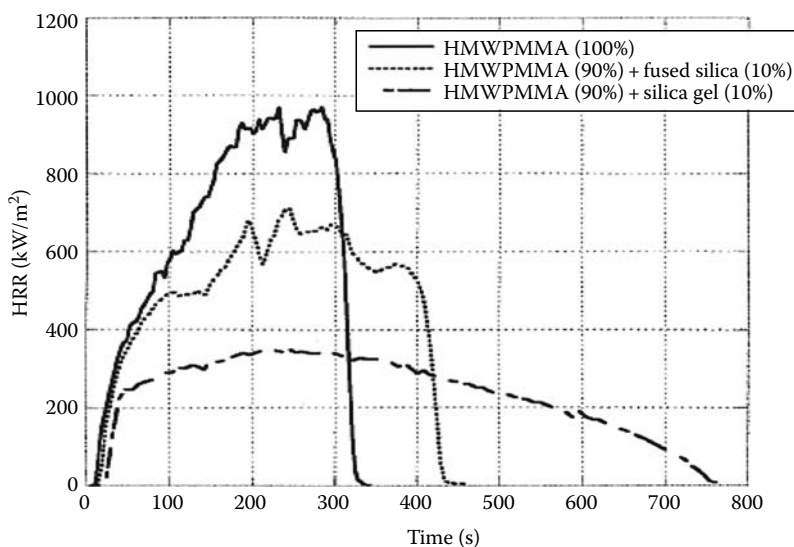


FIGURE 8.16 Effects of silica types on the HRR of HMWPMMA at 40 kW/m^2 . (From Kashiwagi, T. et al., *J. Appl. Polym. Sci.*, 87, 1541, 2003. With permission.)

their extent of surface coverage. These factors are determined not only by the silica characteristics, but also by the melt viscosity of PMMA.

Recently, some reports have explored the potential of synergistic effect between silica and other flame retardants.^{53–55} For example, silica showed synergistic effect with alumina in polypropylene (PP)/ammonium polyphosphate (APP)—pentaerythritol (PER) intumescent-based system. The data indicate that the HRR values improved by incorporating silica into the intumescent-based formulation and the improvement was much more pronounced by combining both silica and alumina in the formulation.

A synergistic effect was also observed between silica and ATH in LLDPE/EVA composite.⁵⁴ Based upon the data collected from TGA and cone calorimetry, the report concluded that the synergistic mechanism of silica with ATH is mainly due to physical effect in the condensed phase. A more compact barrier is produced by combining silica with ATH which leads to the reduction of HRR, MLR as revealed by cone calorimetry. The system combining fumed silica and magnesium hydroxide (MH) in ethylene vinyl acetate (EVA) showed synergistic behavior.⁵⁵ As can be seen in Table 8.7, partial substitution of magnesium hydroxide with fumed silica gave V-0 rating in UL-94 and increased the LOI value.

Zeolite is a crystalline, porous aluminosilicate mineral with a unique interconnecting lattice structure. This lattice structure is arranged to form a honeycomb framework of consistent diameter interconnecting channels and pores. Negatively charged alumina and neutrally charged silica tetrahedral building blocks are stacked to produce the open three-dimensional honeycomb framework.

An extensive study was conducted on the effect of chemical and structural aspects of zeolites on the fire performance of the intumescent system, ammonium polyphosphate–pentaerythritol (APP–PER), where a marked improvement of the fire-retardant properties within different polymeric matrices has been observed.^{56–58} The synergistic mechanism of zeolite 4A with the intumescent materials was investigated using solid-state NMR. Chemical analysis combined with cross-polarization dipolar-decoupled magic-angle spinning NMR revealed that the materials resulting from the thermal treatment of the APP–PER and APP–PER/4A systems were formed by carbonaceous and phosphocarbonaceous species, and that the zeolite enhances the stability of the phosphocarbonaceous species.

TABLE 8.7
LOI and UL-94 Data for Different Formulations
of EVA/MH/SiO₂

Sample Formulation	Composition (wt.%)			LOI	UL-94
	EVA	MH	SiO ₂		
A	100	0	0	18	Fail
B	40	60	0	35	V-0
C	40	58	2	37	V-0
D	40	55	5	39	V-0
E	40	52	8	39	V-0
F	40	48	12	37	V-1
G	45	55	0	32	Fail
H	45	53	2	34	V-2
I	45	50	5	35	V-0
J	45	47	8	35	V-0

Source: Fu, M. and Baojun, Q., *Polym. Degrad. Stab.*, 85, 633, 2004. With permission.

When evaluated by LOI, the system with zeolites has higher LOI than that without it. For example, compared with PP-APP-PER, which has an LOI of 30%, the LOI of PP-APP-PER system with zeolite 13X increases to 45%, an increase of 50%. Also the LOI of LRAM3.5 (ethylene-butyl acrylate-maleic anhydride terpolymer)-APP-PER system with 4A increases to 39%, relative to 29% for LRAM3.5-APP-PER system. All systems with zeolites obtained the UL-94 V-0 grade.

Wei et al. conducted investigation on the effects of zeolites 4A, 13X, mordenite, and ZSM-5 on the thermal degradation and charring of intumescent APP-pentaerythritol systems.⁵⁹ The residues formed with all types of zeolites at 600°C are higher (and more significantly with 4A and 13X) than that obtained with pure APP/PER. The authors argued that during the decomposition process of zeolite, the aluminum separates and migrates to the surface. This process leads to increasing the Si-Al ratio and enhancing the acid catalytic property, which improves the intumescent structure by retaining the volatile degradation products and promoting cross-linking reactions in the condensed phase.

Mizuno et al.⁶⁰ investigated the possibility of changing the pyrolysis behavior of polynorbornene (PNB) using the catalytic effect of zeolite. The flammability behavior of PNB compounded with zeolite was studied using a small-sized vertical combustion test. The results suggested that adding zeolite to PNB changed its primary ignition phenomena and increased the lower flammability limits (using Le Chatelier's equation) from 0.9 to 1.3.

In an attempt to provide compatibility between the FR and polymer matrix, Wang et al. reported recently on a novel microencapsulated intumescent system containing 4A zeolite as a potential flame retardant for natural rubber (NR).⁶¹ The flame-retardant properties of NR composites loaded with different amounts of intumescent flame retardant (IFR), IFR-4A zeolite, and microencapsulated intumescent flame retardant (MIFR)-4A zeolite agents were studied and compared. The LOI data demonstrate that the NR composite filled with 50 phr of MIFR-4A zeolite agent and 50 phr of IFR-4A zeolite shows better FR properties as compared to NR and 50 phr of IFR-filled systems.

Talc is a natural magnesium silicate, which when compounded with plastics improves, among other properties, the flame retardancy. For example, talc combined with magnesium hydroxide or ATH improved the fire-retardance behavior of PP and EVA.^{62,63}

Talc particles of different lamellarity and specific surface area have been incorporated into polyethylene vinyl acetate (EVA) copolymer/magnesium hydroxide (MH) composite system.⁶³ The fire retardancy of this system has been studied and compared with formulations containing only EVA and MH and formulations containing EVA, MH, and organomodified montmorillonites (oMMT). It was observed that talc with higher lamellar index showed fire behavior similar to that of EVA/MH/oMMT system with some intumescence.

8.5 CONCLUSION

This chapter has provided a concise account of an important type of flame retardants based on silicon. This class of flame retardants may provide an opportunity to develop systems for fire retardancy that are environmentally friendly. It seems that there is a growing interest in this type of flame retardant, and this trend most likely will continue, given the increasing concern over the release of the halogenated species into the environment.

REFERENCES

1. Eaborn, C., *Organosilicon Compounds*, Butterworths, London, U.K., 1960.
2. *The Chemistry of Organic Silicon Compounds*, Wiley, Chichester, U.K., Rappoport, Z.; Apeloig, Y., Eds., 1998, Vol. 2; Patai, S. and Rappoport, Z., Eds., 1989, Vol. 1.
3. Sommer, L.H., *Stereochemistry, Mechanism & Silicon*, McGraw Hill, New York, 1956.
4. Brook, M.A., *Silicon in Organic, Organometallic, and Polymer Chemistry*, John Wiley & Sons, Inc., New York, 2000.

5. Michl, J., Silicon chemistry, *Chem. Rev.* 1995, 95, 1135.
6. Jones, R.G., Ed., Silicon-containing polymers (*Proceedings of an RSC Macro Group Symposium*, University of Kent, 1994), Royal Society of Chemistry, Cambridge, MA, 1995.
7. Marciniak, B. and Chojnowski, J., Eds., Progress in organosilicon chemistry (*Proceedings of the 10th International Symposium on Organosilicon Chemistry*, Poznan, Poland, 1993), Gordon & Breach, Basel, Switzerland, 1995.
8. Bassindale, A.R. and Gaspar, P.P., Eds., Frontiers of organosilicon chemistry (*Proceedings of the 9th International Symposium on Organosilicon Chemistry*, Edinburgh, 1990), Royal Society of Chemistry, Cambridge, MA, 1991.
9. Colvin, E.W., Silicon, in *Comprehensive Organometallic Chemistry II: A Review of the Literature 1982–1994*, Wilkinson, G., Stone, F.G.A., Abel, E.W., Eds.; McKillop, A., Vol. Ed., Pergamon, Oxford, 1982, Vol. 2, Chap. 1, p. 1.
10. Larson, G.L., Ed., *Advances in Silicon Chemistry*, JAI, Greenwich, CT, 1996, Vol. 3; 1993, Vol. 2; 1991, Vol. 1.
11. Kashiwagi, T. and Gilman, J.W., Silicon-based flame retardants, in *Fire Retardancy of Polymeric Materials*, Grand, A.F. and Wilkie, C.A., Eds., Marcel Dekker, New York, 2000, Chap. 10, p. 353.
12. Butts, M., Cella, J., Wood, C.D., Gillette, G., Kerboua, R., Leman, J., Lewis, L., Rajaraman, S., Rubinsztajn, S., Schattenmann, F., Stein, J., Wengrovius, J., and Wicht, D., Silicones, in *Encyclopedia of Polymer Science and Technology*, 3rd edn., Mark, H.F., Edn., John Wiley & Sons, Inc, Hoboken, NJ, 2003, Vol. 11.
13. Noll, W., *Chemistry and Technology of Silicones*, Academic Press, Inc., New York, 1978.
14. Claron, S.J. and Semlyen, J.A., Eds., *Siloxane Polymers*, Prentice Hall, Englewood Cliffs, NJ, 1993.
15. Rochow, E.G., *Silicon and Silicones*, Springer-Verlag, Berlin, 1987.
16. Hunter, D., Carbide's silicones: The "sale of the century," *Chemical Week* 24, February 19, 1992.
17. Gorbunov, A.I., Belyi, A.P., and Filippov, G.G., Reactions of silicon and germanium with halogens, their hydrides, and organic halogen derivatives *Russ. Chem. Rev.* 1974, 43, 291.
18. Petrov, A.D., Mironov, B.F., Ponomarenko, V.A., and Chernyshev, E.A., *Synthesis of Organosilicon Monomers*, Consultants Bureau, New York, 1964, p. 36.
19. Zeigler, J.M. and Fearon, F.W.G., Eds., *Silicon-Based Polymer Science* (ACS Advances in Chemistry, Series 224), American Chemical Society, Washington, D.C., 1990.
20. Stark, F.O., Falender, J.R., and Wright, A.P., Silicones, in *Comprehensive Organometallic Chemistry*, Wilkinson, G., Stone, F.G.A., and Abel, E.W., Eds., Pergamon Press, Oxford, U.K., 1982, Chapter 9.3, p. 305.
21. Eaborn, C. and Bott, R.W., *The Bond to Carbon*, MacDiarmid, A.G., Ed., Marcel Dekker, Inc., New York, 1968, Vol. I, Part 1, p. 105.
22. Drake, R., MacKinnon, I., and Taylor, R., Recent advances in the chemistry of siloxane polymers and copolymers, in *The Chemistry of Organic Silicon Compounds*, Rappoport, Z. and Apeloig, Y., Eds., Wiley, Chichester, U.K., 1998, Vol. 2, Chapter 38, p. 2217.
23. Arkles, B., Look what you can make out of silicones (biomedical applications of silicones), *Chem. Tech.* 1983, 13, 542.
24. Tomanek, A., *Silicones and Industry*, Hanser (Wacker Chemie), Munich, Germany, 1991.
25. Austin, P.J., Buch, R.R., and Kashiwagi, T., Gasification of silicone fluids under external thermal radiation part I. Gasification rate and global heat of gasification, *Fire Mater.* 1998, 22, 221.
26. Austin, P.J., Buch, R.R., and Kashiwagi, T., Gasification of silicone fluids under external thermal radiation part 2. Gasification products—characterization and quantitation, *Fire Mater.* 1998, 22, 239.
27. Kashiwagi, T., Cleary, T.G., Davis, G.C., and Lupinski, J.H., A non-halogenated, flame retarded polycarbonate, *Conference of Advanced Fire Resistant Aircraft Interior Materials*, Atlantic City, NJ, February 9–11, 1993, 175.
28. Berrashid, R. and Nelson, G.L., Flammability improvement of polyurethanes by incorporation of a silicone moiety into the structure of block copolymers, in *Fire and Polymers* (ACS Symposium, Series 599), American Chemical Society, Washington D.C., 1995, p. 217.
29. Belva, F., Bourbigot, S., Duquesne, S., Jama, C., Le Bras, M., Pelegri, C., and Rivenet, M., Heat and fire resistance of polyurethane-polydimethylsiloxane hybrid material, *Polym. Adv. Technol.* 2006, 17, 304.
30. Hermansson, A., Hjertberg, T., and Sultan, B.A., The flame retardant mechanism of polyolefins modified with chalk and silicone elastomer, *Fire Mater.* 2003, 27, 51.
31. Hermansson, A., Hjertberg, T., and Sultan, B.A., Linking the flame-retardant mechanisms of ethyleneacrylate copolymer, chalk and silicone elastomer system with its intumescent behavior, *Fire Mater.* 2005, 29, 407.

32. Hermansson, A., Hjertberg, T., and Sultan, B.A., Influence of the structure of acrylate groups on the flame retardant behavior of ethylene acrylate copolymers modified with chalk and silicone elastomer, *J. Fire Sci.* 2007, 25, 287.
33. Ebdon, J.R., Hunt, B.J., Jones, M.S., and Thorpe, F.G., Chemical modification of polymers to improve flame retardance-II. The influence of silicon-containing groups, *Polym. Degrad. Stab.* 1996, 54, 395.
34. Ebdon, J.R., Hunt, B.J., and Joseph, P., Thermal degradation and flammability characteristics of some polystyrenes and poly(methylmethacrylate)s chemically modified with silicon-containing groups, *Polym. Degrad. Stab.* 2004, 83, 181.
35. Mercado, L.A., Reina, J.A., and Galia, M., Flame retardant epoxy resins based on diglycidylmethoxyphenylsilane, *J. Polym. Sci. Polym. Chem.*, 2006, 44, 5580.
36. Scott, D.W., Thermal rearrangement of branched-chain methylpolysiloxanes, *J. Am. Chem. Soc.* 1946, 68, 356.
37. <http://www.hybridplastics.com>
38. Mantz, R.A., Jones, P.F., Chaffee, K.P., Lichtenhan, J.D., and Gilman, J.W., Thermolysis of polyhedral oligomeric silsesquioxane (POSS) micromers and POSS-siloxane copolymers, *Chem Mater.* 1996, 8, 1250.
39. Lichtenhan, J.D. and Gilman, J.W., Pre-ceramic additives as fire retardants for plastics, U.S. Patent 6,362,279, 2002.
40. Devaux, E., Rochery, M., and Bourbigot, S., Polyurethane/clay and polyurethane/POSS nanocomposites as flame retarded coating for polyester and cotton fabrics, *Fire Mater.* 2002, 26: 149.
41. *Proceedings of POSS Nanotechnology Conference*, Huntington Beach, CA, September 2002.
42. Lu, S. and Hamerton, I., Recent developments in the chemistry of halogen-free flame retardant polymers, *Prog. Polym. Sci.* 2002, 27, 1661.
43. Fina, A., Tabuani, D., Frache, A., Boccaleri, E., and Camino, G., *Fire Retardancy of Polymers: New Applications of Mineral Fillers*, Le Bras, M., Wilkie, C., and Bourbigot, S., Eds., Royal Society of Chemistry, Cambridge, MA, 2005, p. 202.
44. Fina, A., Tabuani, D., Carniato, F., Frache, A., Boccaleri, E., and Camino, G. Polyhedral oligomeric silsesquioxanes (POSS) thermal degradation, *Thermochim. Acta* 2006, 440, 36.
45. Bourbigot, S., Le Bras, M., Flambard, X., Rochery, M., Devaux, E., and Lichtenhan, J.D., *Fire Retardancy of Polymers: New Applications of Mineral Fillers*, Bras, M., Bourbigot, S., Duquesne, S., Jama, C., and Wilkie, C.A., Eds., The Royal Society of Chemistry, Cambridge, MA, 2005, p. 189.
46. Fina, A., Abbenhuis, H.C.L., Tabuani, D., and Camino, G., Metal functionalized POSS as fire retardants in polypropylene, *Polym. Degrad. Stab.* 2006, 91, 2275.
47. Vannier, A., Duquesne, S., Bourbigot, S., Castrovinci, A., Camino, G., and Delobel, R., The use of POSS as synergist in intumescent recycled poly(ethylene terephthalate), *Polym. Degrad. Stab.* 2008, 93, 818.
48. Song, L., He, Q., Hu, Y., Chen, H., and Liu, L., Study on thermal degradation and combustion behaviors of PC/POSS hybrids, *Polym. Degrad. Stab.* 2008, 93, 627.
49. Gilman, J.W., Kashiwagi, T., and Lomakin, S.M., Environmentally safe fire retardants for polymeric materials—I. Silica gel-potassium carbonate additive, *Society for the Advancement of Material and Process Engineering (SAMPE)*, March 24–28, 1996, Anaheim, CA, p. 708.
50. Gilman, J.W., Kashiwagi, T., Nyden, M., and Harris, R.H., New flame retardants consortium: Final report, Flame retardant mechanism of silica, NISTIR 6357, June 1999.
51. Kashiwagi, T., Gilman, J.W., Butler, K.M., Harris, R.H., Shields, J.R., and Asano, A., Flame retardant mechanism of silica gel/silica, *Fire Mater.* 2000, 24, 277.
52. Kashiwagi, T., Shields, J.R., Harris, R.H., and Davis, R.D., Flame-retardant mechanism of silica: Effects of resin molecular weight, *J. Appl. Polym. Sci.* 2003, 87, 1541.
53. Wei P., Hao, J., Du, J., Han, Z., and Wang, J., An investigation on synergism of an intumescent flame retardant based on silica and alumina, *J. Fire Sci.* 2003, 21, 17.
54. Wei, P., Han, Z., Xu, X., and Li, Z., Synergistic flame retardant effect of SiO₂ in LLDPE/EVA/ATH blends, *J. Fire Sci.* 2006, 24, 487.
55. Fu, M. and Baojun, Q., Synergistic flame retardant mechanism of fumed silica in ethylene-vinyl acetate/magnesium hydroxide blends, *Polym. Degrad. Stab.* 2004, 85, 633.
56. Bourbigot, S., Le Bras, M., Delobel, R., Breatnb, P., and Tremillon, J.M., 4A zeolite synergistic agent in new flame retardant intumescent formulations of polyethylenic polymers-study of the effect of the constituent monomers, *Polym. Degrad. Stab.* 1996, 54, 275.
57. Bourbigot, S., Le Bras, M., Delobel, R., Decressainb, R., and Amoureuxb, J.P., Synergistic effect of zeolite in an intumescence process: Study of the carbonaceous structures using solid-state NMR, *J. Chem. Soc., Faraday Trans.* 1996, 92(1), 149.

58. Bourbigot, S., Le Bras, M., Delobel, R., and Tremillon, J.M., Synergistic effect of zeolite in an intumescence process: Study of the interactions between the polymer and the additives, *J. Chem. SOC., Faraday Trans.* 1996, 92(18), 3435.
59. Wei, P., Jiang, P., Han, Z., and Wang, J., An investigation of the effects of zeolites on the thermal degradation and charring of APP-PER by TGA-XPS, *J. Fire Sci.* 2005, 23, 173.
60. Mizuno, K., Ueno, T., Hirata, A., Ishikawa, T., and Takeda, K., Thermal degradation and flame retardancy of polynorborene by a zeolite, *Polym. Degrad. Stab.* 2007, 92, 2257.
61. Wang, J. and Chen, Y., Effect of microencapsulation and 4A zeolite on the properties of intumescent flame-retardant natural rubber composites, *J. Fire Sci.* 2008, 26, 153.
62. Jouffret, F. and Meli, G., Talc as a functional additive in flame retardant systems, in *Flame Retardants 2004*, London, January 27–28, 2004, Interscience Communications, Greenwich, U.K., pp. 129–132.
63. Clerc, L., Ferry, L., Leroy, E., and Lopez-Cuesta, J.M., Influence of talc physical properties on the fire retarding behavior of (ethylene-vinyl acetate copolymer/magnesium hydroxide/talc) composites, *Polym. Degrad. Stab.* 2005, 88, 504.

9 Boron-Based Flame Retardants and Flame Retardancy

Kelvin K. Shen, Saied H. Kochesfahani, and Frederic Jouffret

CONTENTS

9.1	Introduction	208
9.2	Products and Applications	209
9.2.1	Alkali Metal Borates	209
9.2.1.1	Borax Decahydrate ($\text{Na}_2\text{O} \cdot 2\text{B}_2\text{O}_3 \cdot 10\text{H}_2\text{O}$)	209
9.2.1.2	Borax Pentahydrate ($\text{Na}_2\text{O} \cdot 2\text{B}_2\text{O}_3 \cdot 5\text{H}_2\text{O}$)	210
9.2.1.3	Disodium Octaborate Tetrahydrate ($\text{Na}_2\text{O} \cdot 4\text{B}_2\text{O}_3 \cdot 4\text{H}_2\text{O}$)	210
9.2.1.4	Anhydrous Borax ($\text{Na}_2\text{O} \cdot 2\text{B}_2\text{O}_3$)	210
9.2.1.5	Miscellaneous Alkali Metal Borate	210
9.2.2	Boric Acid and Boric Oxide	211
9.2.2.1	Boric Acid ($\text{B}_2\text{O}_3 \cdot 3\text{H}_2\text{O}$ / $\text{B}(\text{OH})_3$)	211
9.2.2.2	Boric Oxide (B_2O_3)	214
9.2.3	Alkaline Earth Metal Borates	214
9.2.3.1	Calcium Borates ($2\text{CaO} \cdot 3\text{B}_2\text{O}_3 \cdot 5\text{H}_2\text{O}$)	214
9.2.3.2	Magnesium Borate ($x\text{MgO} \cdot y\text{B}_2\text{O}_3 \cdot z\text{H}_2\text{O}$)	214
9.2.3.3	Barium Metaborate ($\text{BaO} \cdot \text{B}_2\text{O}_3 \cdot \text{H}_2\text{O}$)	215
9.2.4	Transition Metal Borates and Miscellaneous Metal Borates	215
9.2.4.1	Zinc Borates ($x\text{ZnO} \cdot y\text{B}_2\text{O}_3 \cdot z\text{H}_2\text{O}$)	215
9.2.4.2	Aluminum Borate ($9\text{Al}_2\text{O}_3 \cdot 2\text{B}_2\text{O}_3$)	223
9.2.4.3	Miscellaneous Metal Borates	223
9.2.5	Boron and Nitrogen-Containing Compounds	223
9.2.5.1	Ammonium Pentaborate [$(\text{NH}_4)_2\text{O} \cdot 5\text{B}_2\text{O}_3 \cdot 8\text{H}_2\text{O}$]	223
9.2.5.2	Melamine Diborate [$(\text{C}_3\text{H}_8\text{N}_6)_2\text{O} \cdot \text{B}_2\text{O}_3 \cdot 2\text{H}_2\text{O}$] / ($\text{C}_3\text{H}_6\text{N}_6 \cdot 2\text{H}_3\text{BO}_3$)	224
9.2.5.3	Guanidinium Borate [$x[\text{C}(\text{NH}_2)_3]_2\text{O} \cdot y\text{B}_2\text{O}_3 \cdot z\text{H}_2\text{O}$]	224
9.2.5.4	Boron Nitride (BN)	224
9.2.5.5	Borazine [$(\text{HBNH})_3$]	225
9.2.6	Borester and Boron–Carbon Compounds	225
9.2.6.1	Boric Acid Esters [$\text{B}(\text{OR})_3$]	225
9.2.6.2	Boric Acid Ester Salts [$\text{M}^+ \text{B}(\text{OR})_4^-$]	225
9.2.6.3	Boronic Acid [$\text{ArB}(\text{OH})_2$]	226
9.2.6.4	Boron Carbide (B_4C)	227
9.2.7	Boron and Phosphorus-Containing Compounds	227
9.2.7.1	Boron Phosphate (BPO_4)	227
9.2.7.2	Phosphine–Borane	228

9.2.8	Boron and Silicon-Containing Compounds	228
9.2.8.1	Borosilicate, Borosilicate Glass, and Frits.....	228
9.2.8.2	Borosiloxane	228
9.2.9	Miscellaneous.....	229
9.2.9.1	Layered Double Hydroxides with Borate.....	229
9.2.9.2	Fluoroborates	229
9.3	Fire Retardancy Mechanism of Boron Compounds.....	230
9.3.1	Borates in Wood/Cellulose	230
9.3.2	Plastics and Elastomers.....	231
9.3.2.1	Halogen-Containing Polymers.....	231
9.3.2.2	Halogen-Free Polymers.....	231
9.4	Conclusions.....	232
	Acknowledgment	233
	References.....	233

9.1 INTRODUCTION

Boron is present in the earth's crust at a level of only three parts per million, but there are areas where it is concentrated as borate salts (salts of the oxidized form of elemental boron) in substantial volumes for mining. The United States and Turkey supply 90% of the global borate demand. Rio Tinto Minerals (RTM)/U.S. Borax, the largest borate producer, operates an open pit mine and refinery complex in the Mojave desert of California. The principal minerals in the deposit are tincal and kernite (Table 9.1).

RTM produces borax decahydrate, borax pentahydrate, anhydrous borax, boric acid (BA), boric oxide, and other specialty borates such as zinc borates from sodium borate minerals. Etibank, a Turkish national mining enterprise, offers borate minerals (colemanite and ulexite) as well as refined borates.

Boron compounds such as borax and boric acid are well-known fire retardants in cellulosic products and coatings.^{1,2} However, the use of boron compounds such as zinc borate, ammonium pentaborate (APB), melamine borate, boric oxide, boron phosphate, and other metal borates in polymers has become prominent only since early 1980s.³⁻⁶ This chapter will review the chemical and physical properties, the end-use applications, as well as the mode of actions of major boron compounds as fire retardants in different applications. Since boron-based flame retardants are extensively used and quoted in literature, only those formulations of commercial importance and representative literature examples will be discussed and/or cited in this chapter.

Table 9.2 lists the properties and applications for major boron-containing fire retardants.

TABLE 9.1
Major Borate Minerals

	Formula	B ₂ O ₃ (%) (Theo.)	Source
Tincal	Na ₂ O·2B ₂ O ₃ ·10H ₂ O	36.5	United States, Turkey
Colemanite	2CaO·3B ₂ O ₃ ·5H ₂ O	50.9	Turkey
Kernite	Na ₂ O·2B ₂ O ₃ ·4H ₂ O	50.9	United States
Ulexite	Na ₂ O·2CaO·5B ₂ O ₃ ·16H ₂ O	43.0	Turkey, Chile
Hydroboracite	CaO·MgO·3B ₂ O ₃ ·6H ₂ O	50.5	Argentina
Szaibelyite	2MgO·B ₂ O ₃ ·H ₂ O	41.4	Russia, China

TABLE 9.2
Major Boron-Based Commercial Flame Retardants

Chemical Name	Formula (Typical B ₂ O ₃ wt.%)	Starting Dehydration Temp. (°C)	Water Solubility (wt.%, ~25°C)	Applications
Borax pentahydrate	Na ₂ O·2B ₂ O ₃ ·5H ₂ O (49.0%)	65	4.4	Wood/cellulose/cotton, coating
Borax decahydrate	Na ₂ O·2B ₂ O ₃ ·10H ₂ O (37.5%)	~45	5.8	Wood/cellulose
Boric acid	B ₂ O ₃ ·3H ₂ O (56.6%)	70	5.5	Wood/cellulose/cotton, polymer, coating
Boric oxide	B ₂ O ₃ (98.5%)	—	—	Engineering plastics
Anhydrous borax	Na ₂ O·2B ₂ O ₃ (68.8%)	—	—	Urethane, wire, and cable
Disodium octaborate tetrahydrate	Na ₂ O·4B ₂ O ₃ ·4H ₂ O (67.3%)	40	9.7 (20°C)	Wood products, cotton
Calcium borate (colemanite)	2ZnO·3B ₂ O ₃ ·5H ₂ O (44%–48%)	290	0.2	Rubber-modified roofing membrane
Barium metaborate	BaO·B ₂ O ₃ ·H ₂ O (26% with ~90% purity)	200	0.3	PVC, coating
Zinc borates (see Table 9.3)	xZnO·yB ₂ O ₃ ·zH ₂ O	—	—	Polymer, elastomers, coatings, sealants/caulks
Ammonium pentaborate	(NH ₄) ₂ O·5B ₂ O ₃ ·8H ₂ O (64.6%)	120	10.9	Epoxy, urethane, coating
Melamine diborate	(C ₃ H ₈ N ₆)O·B ₂ O ₃ ·2H ₂ O (22.0%)	130	0.7	Epoxy intumescent coating, cotton textile
Boron phosphate	BPO ₄ (18.7% as B)	NA	Low	PPE/polyamide, PPE/HIPS, PO

9.2 PRODUCTS AND APPLICATIONS

9.2.1 ALKALI METAL BORATES

9.2.1.1 Borax Decahydrate (Na₂O·2B₂O₃·10H₂O)

Borax decahydrate (also called borax) is slightly soluble in cold water (4.71% by wt. at 20°C) and highly soluble in hot water (30% at 60°C). It has a pH of 9.24 (1% solution at ambient temperature) and exhibits excellent buffering property.⁷ As a crystalline material, borax decahydrate is stable under normal storage conditions. It will slowly lose water of crystallization if exposed to a warm and dry atmosphere. Conversely, exposure to a humid atmosphere can cause recrystallization at particle contact point, thus resulting in caking.

A mixture of ammonium chloride and borax was one of the treatments of cellulosic fabrics reported by Gay-Lussac in 1821. Due to its low dehydration temperature and water solubility, sodium borates are only used as flame retardants in cellulose insulation (ground-up newspaper—see Sections 9.2.1.2 and 9.2.2.1), wood timber, textiles, urethane foam, and coatings. For example, a mixture of urethane (100 parts), borax (100 phr), and perlite (30 phr) was claimed to provide flame-retardant urethane foam.⁸ Borax in conjunction with boric oxide, silica, ammonium chloride, and APB as ceramizing additives and volume builders, are claimed in a fire-protection coating based on polybutadiene and silicone microemulsion.⁹ Using a modified DIN 4102 test, the chipboard with the coating showed a loss of mass less than 1% and there was no pyrolysis of the wood sample.

The market demand for fire-retardant wood plastic composites (WPCs) has been increasing. A recent patent claims the use of an unspecified “sodium polyborate” in a fiber mass comprising polypropylene fiber and natural fibers. After compression molding at about 195°C, the mass is sprayed with sodium silicate solution and is subjected to heating again. The resulting product meets a flame spread index of less than 25 and a smoke density index of less than 450 in the ASTM E-84 tunnel test.¹⁰ It is believed that sodium borosilicate is formed in situ. In some applications, the water solubility of borax is not desirable. A recent patent claims that combining borax with polyacrylate, liquid vinyl acetate copolymer suspension (wood glue), and polytetrafluoroethylene (PTFE) suspensions result in a water non-leachable emulsion for treating roofing products.¹¹

9.2.1.2 Borax Pentahydrate ($\text{Na}_2\text{O} \cdot 2\text{B}_2\text{O}_3 \cdot 5\text{H}_2\text{O}$)

Borax pentahydrate (also known as Neobor[®]) is the most common form of sodium borate used in a variety of industries. Its advantages when compared with borax lie in the lower transportation, handling, and the storage cost of a more concentrated product. Borax pentahydrate readily effloresces upon heating. It starts to dehydrate at about 65°C, loses all water of hydration when heated above 320°C, and fuses when heated above 740°C. In water, it hydrolyzes to give a mildly alkaline solution with excellent buffering properties.⁷

Borax pentahydrate is an effective flame retardant for wood/cellulosic materials in terms of surface flammability. However, due to the Na_2O moiety, it can promote smoldering combustion in cellulose. Thus, in cellulosic material and wood products, it is commonly used in combination with boric acid, which is an effective smoldering inhibitor. For example, the treatment of wood fibers with a partially dissolved boric acid and borax pentahydrate slurry (~1.75% by wt. of boron) results in Medium Density Fiberboard (MDF) that is claimed to pass the ASTM E-84 Class 1 surface flammability standard.¹² The additional examples of using borax pentahydrate and boric acid combination are presented in Section 9.2.2.1.

9.2.1.3 Disodium Octaborate Tetrahydrate ($\text{Na}_2\text{O} \cdot 4\text{B}_2\text{O}_3 \cdot 4\text{H}_2\text{O}$)

This sodium borate, known as Polybor[®], is an amorphous material and thus can be dissolved into water rapidly (solubility 9.7 wt.% at room temperature and 21.9% at 30°C). It is particularly effective in reducing the flammability of wood/cellulose/paper products.

9.2.1.4 Anhydrous Borax ($\text{Na}_2\text{O} \cdot 2\text{B}_2\text{O}_3$)

Anhydrous borax ($\text{Na}_2\text{O} \cdot 2\text{B}_2\text{O}_3$), commercially known as Dehybor[®] and often called AB, does not rehydrate under ordinary storage conditions, but it can absorb surface moisture. With a melting point of 742°C, it is an excellent flux and glass former.⁷ Thus, it is an effective additive for ceramification during polymer combustion in applications such as wire and cable, sealants, and so on. Its potential as a flame retardant in polymers has not been fully explored.

Interestingly enough, Schmittman et al. claimed that a combination of ammonium polyphosphate (APP), ammonium phosphate, borax, anhydrous borax ($\leq 45 \mu\text{m}$), and melamine can be used in urethane panels to meet the German standard DIN 4102, Part 1, point 6.1.2. (B1 classification).¹³ They specifically reported that the combination of borax and anhydrous borax yields surprisingly effective results.

9.2.1.5 Miscellaneous Alkali Metal Borate

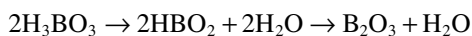
Sodium metaborate 4 mol ($\text{Na}_2\text{O} \cdot \text{B}_2\text{O}_3 \cdot 4\text{H}_2\text{O}$) and sodium metaborate 8 mol ($\text{Na}_2\text{O} \cdot \text{B}_2\text{O}_3 \cdot 8\text{H}_2\text{O}$) are available from RTM/U.S. Borax. They have higher water solubility than the aforementioned sodium borates and a high pH of 10–12 depending on concentration.

Potassium tetraborate ($\text{K}_2\text{O} \cdot 2\text{B}_2\text{O}_3 \cdot 4\text{H}_2\text{O}$) and potassium pentaborate ($\text{K}_2\text{O} \cdot 5\text{B}_2\text{O}_3 \cdot 4\text{H}_2\text{O}$) are also commercially available. An application example is treating wood and paper matches with potassium pentaborate solutions to control the burning rate and afterglow.¹⁴

9.2.2 BORIC ACID AND BORIC OXIDE

9.2.2.1 Boric Acid ($B_2O_3 \cdot 3H_2O$ / $B(OH)_3$)

Boric acid or orthoboric acid (commercially known as Optibor®) is a white triclinic crystal that is soluble in water (5.46 wt.%), alcohols, and glycerin. It is a weak acid and has a pH of 4 (saturated solution at room temperature). Upon heating in air to above 75°C, it loses part of its water of hydration to form metaboric acid (HBO_2) at around 120°C–130°C. The metaboric acid can be further dehydrated to boric oxide at around 260°C–270°C.



Due to their low dehydration temperatures and water solubilities, boric acid and sodium borates (borax pentahydrate and borax decahydrate) are mostly used as fire retardants in wood/cellulosic products such as timbers, plywood, particle board, wood fiber, paper products, and cotton products. In recent years, boric acid has also been used as fire retardant in epoxy intumescent coating, phenolics, urethane foam, and so on. When necessary, boric acid can be coated with silicone oil such as silicone to alleviate its water solubility in water-based coating.

9.2.2.1.1 Cellulose Insulation

Cellulose insulation commonly refers to a loose fill product produced from ground newspaper. Due to the energy crisis of late 1970s and early 1980s, the use of cellulose insulation in residential markets came to prominence. The appeal of cellulose as an insulation material can be attributed to its good thermal insulation, the relative ease of installation, and the simplicity of its production. Most importantly, it is produced from nonpetroleum-based materials (i.e., recycled newspapers).

All cellulose insulation products sold in the United States have to meet the Federal Specification HH-I-515-I. For fire retardancy, this calls for a Radiant Panel Test together with a smoldering combustion test. In order to meet the standard, the Critical Radiant Flux (CRF) has to be greater than or equal to 0.12 W/cm² in the Radiant Panel surface flammability test. For the smoldering test, the weight loss of the cellulose in a steel box (20 × 20 × 10 cm) has to be less than 15% after 2 h with a lighted cigarette as an ignition source. In addition, the standard also calls for a corrosivity test for steel, aluminum, and copper in cellulose to ensure that the flame retardants used are not corrosive to these metals.¹⁵

Boric acid is effective against both flaming (radiant panel surface flammability) and smoldering combustion, whereas sodium borates are effective against flaming combustion but can promote smoldering combustion. For corrosion, boric acid alone is slightly corrosive to mild steel and sodium borate alone tends to be corrosive to aluminum. To balance the flammability test performance, corrosion test performance, and chemical cost, the most reliable combination is boric acid and borax pentahydrate (~1:1 ratio) at a total loading of 15%–18%.^{16,17}

In recent years, driven by cost reduction, a combination of boric acid and ammonium sulfate is also used. Ammonium sulfate decomposes in the range of 204°C–260°C. It can release ammonia in the presence of mild alkaline conditions, and is corrosive to copper. Thus, the use of the boric acid/ammonium sulfate combination normally requires the addition of a proprietary corrosion inhibitor.

9.2.2.1.2 Cotton-Batting (Mattresses)

In 1973, the U.S. Department of Commerce promulgated Flammability Standard FF4-72. This Act requires all mattresses to pass a cigarette smoldering test. Boric acid (12–14 wt.% loading) in conjunction with a dust control agent (1 wt.% of paraffinic oil) is normally used in the cotton batting to pass the test.

The open flame hazard associated with a bedroom fire is well established through fire statistics and field studies. The majority of bedroom fires not caused by smoldering cigarettes involve

a match, a candle, a lighter, or an electrical malfunction that ignites an article of bedclothing. While the fire begins with bedclothing, it grows to eventually involve mattress. The combination of the burning bedclothes, a burning mattress, and other combustibles in the room often leads to fire-threatening conditions within 3 min. On January 1, 2005, California promulgated Assembly Bill 603 (TB 603) requiring that all mattresses sold in the State of California meet the AB 603 open flame test, which limits on Rate of Heat Release and Total Heat Release (THR). Eventually, the CPSC issued a rulemaking (16 CFR 1633), that went into effect throughout the United States on July 1, 2007. It is technically equivalent to CA TB 603, but has some added requirements in terms of labeling and record keeping. Although there are a variety of fire-barrier materials that can meet the open flame test requirement, Wakelyn reported boric acid treated cotton batting as fire-blocking barriers to pass the TB 603 test.¹⁸

9.2.2.1.3 *Fabrics*

To impart fire retardancy, cotton fabrics are commonly treated with borates for applications such as drapes, clothing, rugs, fire-smothering blankets, and Christmas tree decorations. Recommended formulations include borax/boric acid, Polybor, boric acid/APP, or boric acid/ammonium phosphate. It should be noted that these borate treatments will be removed during laundering; hence the treatment has to be reapplied. Much effort has been expended in trying to bond borate to cellulose fiber permanently with only partial success (see Section 9.2.6.1).

9.2.2.1.4 *Paper Products*

Polybor, borax/boric acid, and borates in combination with other additives are used to treat paper products where flame-retardant properties are required. The high level of flame retardants (15–20 wt.%) necessary for paper result in stiffening effects that can be alleviated by the inclusion of softening agents such as urea. A mixture of borax, boric acid, and magnesium chloride hexahydrate (in a ratio of 7:3:5) at a total loading of 12% is recommended as a starting point formulation. A combination of borax, boric acid, and urea (in a ratio of 7:3:4) with a lower total loading of 10% is also recommended. Good fire retardancy results are obtained with all four ingredients—borax, boric acid, urea, and magnesium chloride at 12 wt.% total loading. This combination has a lower tendency to precipitate magnesium borate than the formulation containing magnesium chloride but no urea.¹⁴ Magnesium ion is believed to be responsible for cross-linking and forming char/residue with borate during the combustion of cellulose.

9.2.2.1.5 *Wood Products*

Wood and its related products have been used extensively in the construction and transportation industries. Boric acid, borax, ammonium phosphate, melamine phosphate, dicyandiamide, and urea derivatives are commonly used flame retardants in wood. Depending on the specific application, borax pentahydrate (or borax decahydrate), and boric are normally used together.

Dimensional Lumber/Plywood—the standard method for fire-retardant treatment of dimensional lumber and plywood is by vacuum/pressure impregnation with the aqueous solution of flame retardants.^{19,20} These include boron compounds (borax pentahydrate or decahydrate, and boric acid), phosphorus compounds (ammonium phosphate, guanylurea phosphate [GUP]), and nitrogen compounds (dicyandiamide, urea). It should be noted that, for high temperature roofing product applications such as plywood sheathing and roof-truss lumber, phosphate treatment has a deleterious effect on modulus of rupture, caused by the release of phosphoric acid. This causes wood to darken and become brittle. When used in conjunction with a boron-based flame retardant, this unwanted effect can be alleviated significantly. Boric acid is a much weaker acid than phosphoric acid. In addition, it can also function as a good buffering agent. LeVan and Tran estimated that the loading levels of at least 7.5% (48 kg/m³) of borax–boric acid mixture is required for Southern Pine to meet the ASTM E84 Class I (FSI) and 5% loading for Class II.²¹ Boric acid in conjunction with a phenolic binder has been used as a flame retardant in MDF board to meet the ASTM E-84 Class A requirement.

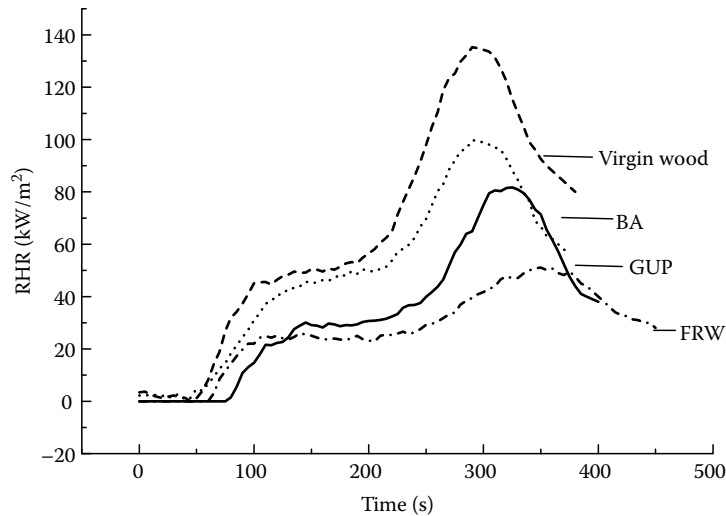


FIGURE 9.1 Cone calorimeter test of treated Larch wood at 35 kW/m^2 —BA is boric acid (33% kg/kg retention), GUP is guanylurea phosphate (31.4%), FRW is a mixture of GUP and BA (28.6%).

One of the most successful commercial products for fire-retardant wood is a combination of GUP and boric acid (approximate weight ratio 7:3), known in the trade as Dricon.²² This product can be produced by spray drying or a mechanical blending of a mixture of GUP (a reaction product of dicyandiamide and phosphoric acid) and boric acid. Based on cone calorimeter (ASTM E-1354) and Thermogravimetric Analysis (TGA)/Differential Thermogravimetric Analysis (DTG), Gao et al. demonstrated that there is a strong synergistic effect of fire retardance between GUP and BA in wood (larch).^{23,24} It was reported that GUP/BA in larch can drastically reduce heat release rate (HRR), THR, and Effective Heat of Combustion (EHC) by about 40%–60% (Figure 9.1).

Recently it was reported that, with the addition of 8%–10% of GUP/BA to MDI bonded Oriented Strand Board (OSB), it was possible to result in a Class B rating in the ASTM E-84 test.²⁵ The treated OSB experienced much less swelling when exposed to high humidity or soaked in water. For flexural properties, modulus of elasticity, was generally not unaffected, whereas bending strength was reduced by 1%–10%. It was concluded that a Class B rating was possible at loading of higher than 10 wt.%.

The Osmose company has been marketing a phosphate-free fire retardant (FirePro™) that contains borate and other materials. It is for the pressure impregnation of lumber and plywood and is claimed for Interior Type A high temperature (HT) applications.^{26,27}

Wood Composites—these are resin-bonded composite boards where the particles are wood shavings, flakes, chips, or fibers bonded with thermosetting adhesives that can be urea formaldehyde, melamine formaldehyde, phenol formaldehyde, or diisocyanate. In recent years, the markets for OSB and MDF board have been rapidly increasing. Most particle board production uses urea-formaldehyde as a binder that is acid setting. Hence, sodium borates (alkaline) can interfere with the setting. As a result, boric acid has been the major boron compound used as the flame retardant in particle board.^{28,29} Typically, a loading of 12%–15% of boric acid in MDF is required to meet the ASTM E-84 Class A rating. If sodium borate is used as a flame retardant, phenol-formaldehyde binder, that is compatible with alkaline chemicals, is commonly used.

WPC—there has been an increasing market demand for fire retardant grades of WPC that can meet ASTM E-84 economically. The California State Fire Marshall promulgated the “Urban Wildland Interface Building Test Standard (12-7A-5)” that requires wood decking to meet HRR and flying ember standards. Borates should have a good potential in fire retardant WPC (see, e.g., Section 9.2.1.1).

9.2.2.1.6 *Plastics and Coatings*

Boric acid in conjunction with APP was reported in epoxy intumescent coating.^{30,31} Boric acid and its derivatives were used in phenolics to impart thermal stability and fire retardancy. For example, Nisshin steel claims the use of boric acid and aluminum trihydroxide (ATH) in phenolics for sandwich panel.³² It was also reported that the small amounts of boric acid (around 0.25% by weight) in polyether imide (PEI) and glass-filled and PEI can reduce peak HRR by almost 50% in the OSU Heat Release test for the aircraft industry.³³ In applications where high modulus and high strengths are needed, boric acid can be added without the softening effects of other additives such as siloxanes.

9.2.2.2 Boric Oxide (B_2O_3)

Boric oxide, also known as anhydrous boric acid, is a hard glassy material, softens at about 325°C, and melts at about 450°C–465°C. It is produced commercially by the fusion of boric acid. Through this procedure, it generally contains up to 0.5% water. It can absorb water and revert back to boric acid; however, this normally does not affect its fire retardancy.

Boric oxide is reported to be an effective fire retardant in engineering plastics such as polyphenylene ether (PPE)/high impact polystyrene (HIPS), polyetherketone, and polyetherimide.^{34,35} It is particularly effective when used in conjunction with PTFE or polyvinylidene fluoride. The use of boric oxide in conjunction with red phosphorus was reported to be an effective combination in fiberglass reinforced polyamide 6,6.³⁶

9.2.3 ALKALINE EARTH METAL BORATES

9.2.3.1 Calcium Borates ($2CaO \cdot 3B_2O_3 \cdot 5H_2O$)

A variety of calcium borates can be prepared by reacting calcium hydroxide and boric acid. Synthetic gowerite ($CaO \cdot 3B_2O_3 \cdot 5H_2O$) and calcium metaborate ($CaO \cdot B_2O_3 \cdot 4H_2O$ or $CaO \cdot B_2O_3 \cdot 6H_2O$) are commercially available mostly for the glass industry. Synthetic nobleite ($CaO \cdot 3B_2O_3 \cdot 4H_2O$) was also reported.³⁷ Among all the known calcium borates, the natural mineral colemanite ($2CaO \cdot 3B_2O_3 \cdot 5H_2O$) is the most well known in the field of flame retardants. All calcium borates have low dehydration temperatures except colemanite, which has a dehydration temperature of 290°C–300°C. It is mostly used in rubber modified roofing membrane.³⁸ Its impurities are a limiting factor for its use in other thermoplastic polymers. Synthetic calcium borates with lower dehydration temperatures have been used in fire-retardant grade sealants and caulks. Recently Hitachi reported the use of synthetic calcium borate ($2CaO \cdot B_2O_3 \cdot H_2O$) in epoxy filled with silica for semiconductor encapsulation. This calcium borate's dehydration temperature is in the range of 200°C–400°C.³⁹

Calcium metaborate is claimed to be advantageously incorporated into frits as fire retardants in fire doors particularly for those based on sodium silicate. It is believed that calcium borosilicate will be formed upon heating in these compositions.⁴⁰

9.2.3.2 Magnesium Borate ($xMgO \cdot yB_2O_3 \cdot zH_2O$)

Due to its high charge to size ratio, the Mg^{2+} cation has a strong tendency to include water in its coordination sphere. Thus, most synthetic magnesium borates contain nonhydroxyl water that can cause them to have low dehydration temperature. For use in plastics, these magnesium borates have to be fully or partially pre-dehydrated. The Kyocera company reported the use of an unspecified magnesium borate in silica-filled epoxy/phenolic for electronic packaging. The addition of 25% magnesium borate resulted in a V-0 (1.6 mm) formulation with good moldability and high temperature reliability.⁴¹ Magnesium borate nano-whiskers [$2MgO \cdot B_2O_3 \cdot H_2O$ / $MgBO_2(OH)$] have also been synthesized, but not evaluated in polymers for fire retardancy.⁴²

9.2.3.3 Barium Metaborate ($\text{BaO} \cdot \text{B}_2\text{O}_3 \cdot \text{H}_2\text{O}$)

Barium metaborate can be produced from borax and barium sulfide. Its silica-modified form finds use primarily as a corrosion inhibitor and fungistatic pigments in coating. It is also promoted as a flame retardant (known as Busan 11M1 or Bulab Flamebloc[®]).⁴³ It is claimed for replacing antimony trioxide in flexible PVC, but its efficacy is not as good as that of zinc borates (see Sections 9.2.4.1 and 9.2.4.1.1.1). Its usage in plastics is limited by its low dehydration temperature (starting at around 200°C).

9.2.4 TRANSITION METAL BORATES AND MISCELLANEOUS METAL BORATES

9.2.4.1 Zinc Borates ($x\text{ZnO} \cdot y\text{B}_2\text{O}_3 \cdot z\text{H}_2\text{O}$)

Among all of the boron-containing fire retardants used in polymers, zinc borate has the most commercial importance. Depending on the reaction conditions, a host of zinc borates can be produced (Table 9.3). Around 1970, RTM/U.S. Borax patented and commercialized a unique form of zinc borate with a molecular formula of $2\text{ZnO} \cdot 3\text{B}_2\text{O}_3 \cdot 3.5\text{H}_2\text{O}$.^{44,45} In contrast to previously known zinc borates, this zinc borate (known in the trade as Firebrake[®] ZB)⁴⁶ is stable to 290°C–300°C. Due to the demand of high production throughput and thin-walled electrical parts, engineering plastics are processed at increasingly higher temperatures. To meet this market demand, RTM/U.S. Borax also developed an anhydrous zinc borate, Firebrake 500 ($2\text{ZnO} \cdot 3\text{B}_2\text{O}_3$), that is stable to at least 500°C and Firebrake 415 ($4\text{ZnO} \cdot \text{B}_2\text{O}_3 \cdot \text{H}_2\text{O}$) that is stable to >415°C (Figure 9.2).

TABLE 9.3
Major Commercial Zinc Borates

Formula	Approximate Starting Dehydration Temp. (°C)	Trade Name
$2\text{ZnO} \cdot 3\text{B}_2\text{O}_3 \cdot 7\text{H}_2\text{O}$	170	ZB-237
$2\text{ZnO} \cdot 2\text{B}_2\text{O}_3 \cdot 3\text{H}_2\text{O}$	200	ZB-223
$2\text{ZnO} \cdot 3\text{B}_2\text{O}_3 \cdot 3.5\text{H}_2\text{O}$	290	Firebrake ZB
$2\text{ZnO} \cdot 3\text{B}_2\text{O}_3$	None	Firebrake 500
$4\text{ZnO} \cdot \text{B}_2\text{O}_3 \cdot \text{H}_2\text{O}$	>415	Firebrake 415

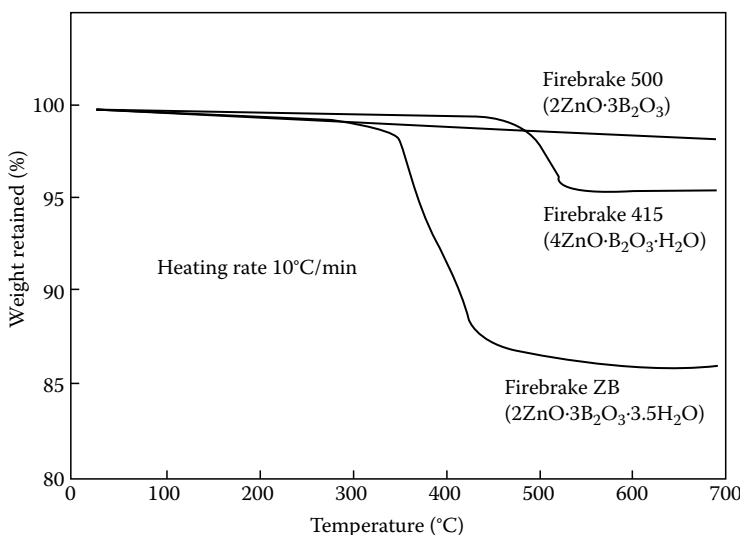


FIGURE 9.2 TGA of Firebrake zinc borates.

Zinc borates are multifunctional flame retardants. They can function as flame retardants, smoke suppressants, afterglow suppressants, and anti-arcing agents. In halogen-containing polymers, zinc borates are synergists of organic halogen sources. Their efficacy depends on the type of halogen (aromatic vs. aliphatic/additive vs. reactive) and base polymer used. In recent years, much effort has been expended to find either partial or complete substitutes for antimony oxide in halogen-containing fire-retardant polymers. This effort has been spurred by the desire to achieve better smoke suppression, a better cost/performance balance, and by the environmental/health concern of antimony oxide. The partial replacement of antimony oxide with zinc borate can result in the synergy of fire test performance and smoke reduction. In contrast to antimony oxide, zinc borates can function as smoke suppressants.

There has been a great recent market demand for halogen-free fire-retardant polymers. Zinc borates are also multifunctional fire retardants in halogen-free polymers. They can promote char formation, reduce the Rate of Heat Release, smoke evolution, carbon monoxide generation, and afterglow combustion. When used in conjunction with metal hydroxides, they can also display synergy in fire test performance.

Since zinc borates have a wide spectrum of applications, only representative examples are presented in the following text.

9.2.4.1.1 Firebrake ZB ($2ZnO \cdot 3B_2O_3 \cdot 3.5H_2O$)

This zinc borate can normally be prepared either by reacting boric acid with zinc oxide or by reacting borax pentahydrate with zinc sulfate. A recent single crystal x-ray crystallography study showed that it has a structure of $Zn[B_3O_4(OH)_3]$ (Figure 9.3).^{47,48} It has been used extensively in PVC,⁴⁹ polyamide,⁵⁰ polyolefin,^{51,52} epoxy,⁵³ phenolics,⁵⁴ and various elastomers.⁵⁵

This zinc borate functions as a flame retardant, smoke suppressant, afterglow suppressant, and anti-arcing agent. In halogen-containing polymers, its efficacy depends on the type of halogen

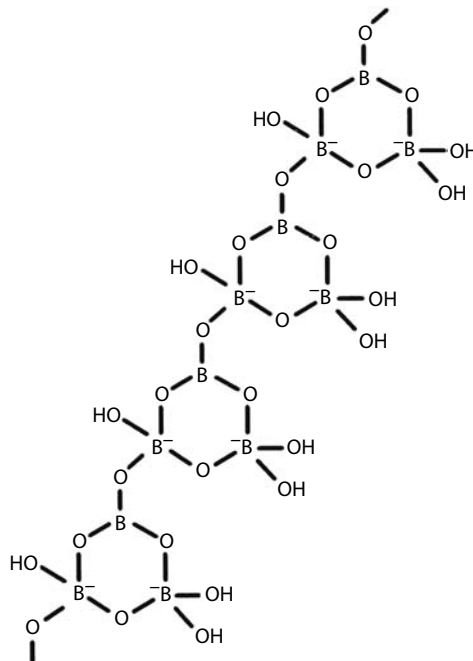


FIGURE 9.3 Molecular structure of Firebrake ZB (zinc atoms complexing with oxygen atoms are not displayed).

(aromatic vs. aliphatic/additive vs. reactive) and base polymer used. In contrast to antimony oxide, zinc borate is a smoke suppressant in halogen-containing polymers.

9.2.4.1.1.1 *Polyvinyl Chloride (PVC)* In flexible PVC, the partial replacement of antimony oxide with the zinc borate cannot only display synergy in flammability test performance but also results in dramatic smoke reduction.⁵⁶ This synergy can be more dramatic when used in conjunction with ATH or magnesium hydroxide (MDH) (Figures 9.4 through 9.6). A recent Cone Calorimeter study⁴⁹ showed that, in flexible PVC, the partial replacement of antimony with the zinc borate could reduce both the HRR and carbon monoxide production drastically at a

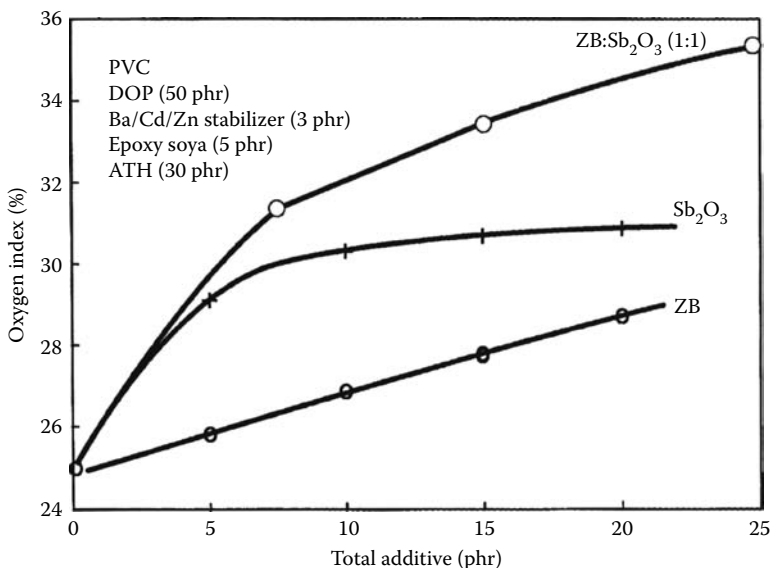


FIGURE 9.4 Limiting oxygen index of flexible PVC formulations (all contain 30phr ATH; ZB-Firebrake ZB).

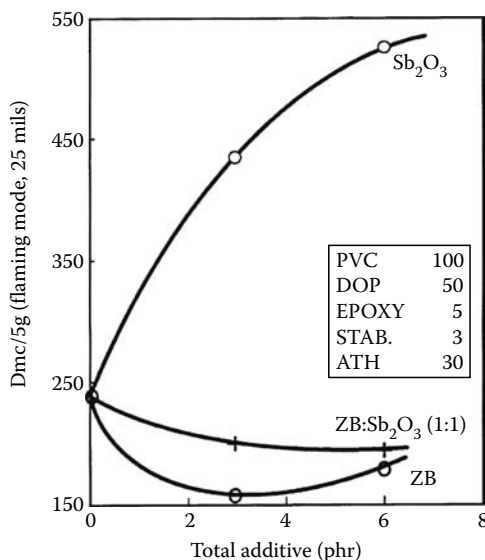


FIGURE 9.5 Smoke test of flexible PVC (ASTM E-662, all formulations contain ATH, ZB-Firebrake ZB).

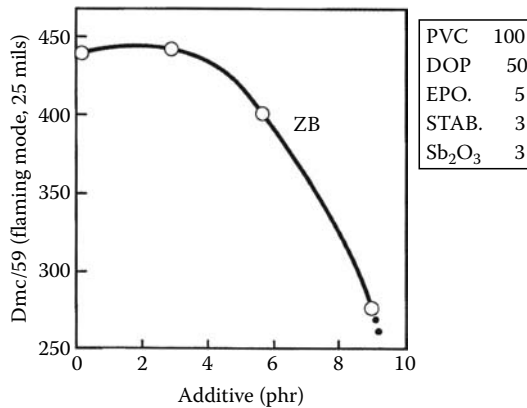


FIGURE 9.6 Smoke test of flexible PVC (ASTM E-662, all formulations contain 3 phr of antimony trioxide; ZB-Firebrake ZB).

TABLE 9.4
Fire Test Performances of Zinc Borate vs. Barium Metaborate

Components ^a (phr)	ASTM E-662 Smoke Test (Dmc)	Limiting Oxygen Index (%)
Sb ₂ O ₃ (5) + Ba metaborate ^b (5)	433	28.2
Sb ₂ O ₃ (5) + zinc borate ^c (4.5)	247	29.3
Sb ₂ O ₃ (3) + Ba metaborate ^b (3)	440	27.5
Sb ₂ O ₃ (3) + zinc borate ^c (2.7)	211	28.5

^a PVC (100), DOP (50), epoxy soya (5), Ba/Cd/Zn (3), CaCO₃ (40).

^b Busan 11M1 (90 wt.% modified barium metaborate).

^c Firebrake[®]ZB (2ZnO · 3B₂O₃ · 3.5H₂O).

heat flux of 35 kW/m². In certain PVC formulations, the zinc borate can replace antimony oxide completely.

This zinc borate is a more effective flame retardant and smoke suppressant than barium metaborate (Busan 11M1).⁴³ For example, in flexible PVC, a combination of antimony trioxide and the zinc borate results in much better fire test performances than the antimony trioxide and barium metaborate combination (Table 9.4). In contrast to flexible PVC, this zinc borate alone improves both fire retardancy and smoke suppression in rigid PVC.⁴⁸

9.2.4.1.1.2 Polyamides This zinc borate has been used extensively in fiberglass reinforced polyamides. For example, in polyamide 6,6 containing a halogen-based flame retardant, the zinc borate can almost replace antimony oxide (or sodium antimonate) completely and still maintain the same UL-94 rating (Table 9.5). In addition, the zinc borate can improve the Comparative Tracking Index (CTI), the thermal stability, the melt viscosity stability (Figure 9.7), the color stability, and the corrosion resistance of processing equipment.⁵⁰

In halogen-free polyamides, when the zinc borate is used in conjunction with red phosphorus, it cannot only display synergy in fire retardancy but also impart corrosion resistance toward metals such as copper.⁵⁷ It is believed that zinc borate can trap trace amounts of phosphine derived from red phosphorus. Martens et al. reported the use of zinc borate in conjunction with melamine pyrophosphate in glass reinforced polyamide 6,6 to achieve V-0 (1.6 mm). The partial replacement of melamine pyrophosphate with zinc borate can increase the CTI from 250 to 600 V.⁵⁸

TABLE 9.5
Fire Retardant Glass-Reinforced
Polyamide 6,6 Containing Firebrake ZB
(Antimony Oxide-Free)

	Examples (wt.%)			
	1	2	3	4
<i>Components</i>				
Polyamide 6,6	47	47	44	44
Fiberglass	25	25	25	25
Brominated polystyrene	21	21	24	24
Sb ₂ O ₃	7	—	—	—
Firebrake ZB	—	7	7	—
Firebrake ZB-XF (extra fine)	—	—	—	7
<i>Properties</i>				
UL-94 1.6 mm	—	V-2	V-0	V-0
0.8 mm	V-0	V-2	V-0	V-0
CTI (V) (dry as molded)	225	475	450	475
IZOD (kJ m ⁻²)	—	11.8	13.1	13.9

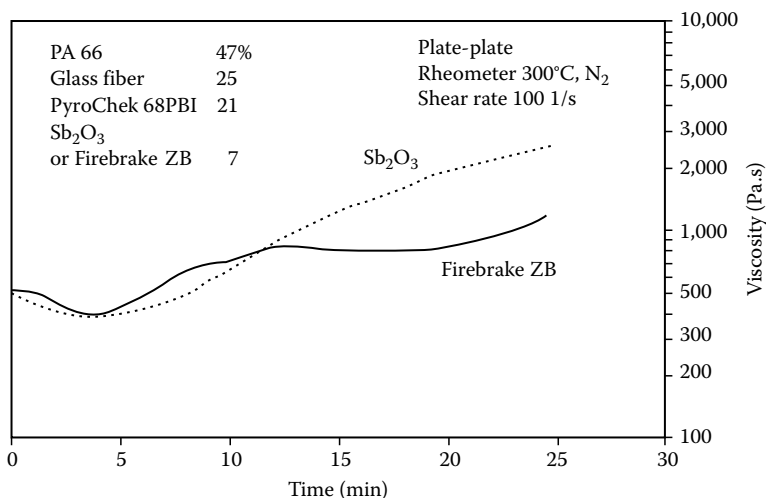


FIGURE 9.7 Melt viscosity stability of polyamide 6,6 containing Firebrake ZB vs. antimony oxide (PyroChek 68PBI is a brominated PS).

9.2.4.1.1.3 *Polyolefins* When used in conjunction with a halogen-based flame retardant, this zinc borate can partially replace antimony oxide (30%–40%) and still maintain the same fire test performance. In addition, it can improve aged elongation properties, increase char formation, and decrease smoke generation. The B₂O₃ moiety in zinc borate can also provide afterglow suppression (Table 9.6).

The market demand for halogen-free fire-retardant polymers has been increasing steadily in applications such as electrical/electronics, transportation, and construction products. In wire and cable, the high loadings of ATH or MDH are required (60–70 wt.%). Recent developmental efforts

TABLE 9.6
Firebrake ZB for Afterglow Control
in Polypropylene

	Examples (wt.%)		
	1	2	3
<i>Components</i>			
Polypropylene	56	51	45
Decabromodiphenyl oxide	16	16	16
Styrene-butadiene rubber	—	5	5
Talc	20	20	20
Sb ₂ O ₃	8	8	8
Zinc borate	—	—	6
<i>Properties</i>			
UL-94 (0.156 cm thick)	V-2	HB	V-0
Dripping	No	No	No
Afterglow (s)	5	>60	22

have focused on co-additives of ATH or MDH with the aim of reducing total loading and developing stronger char/residue formation.

In 1985, Shen first reported that this zinc borate and ATH could form porous and hard residue during the combustion of a cross-linked ethylene-vinyl acetate (EVA). In wire and cables, for example, this sintered residue is an important thermal insulator for the substrate or unburned polymer (particularly in security cables). It can prevent short-circuiting and sparking, as well as protect the underlying insulation material.⁵¹ In 1999, Bourbigot et al. reported that the partial replacement of ATH (total 65 wt.% in EVA) with the zinc borate (5%) in a noncross-linked EVA resulted in a significant increase in limiting oxygen index (LOI) from 42% to 51.5%. In the Cone Calorimeter test, a significant reduction of peak HRR, delayed time to ignition (TTI), and reduction in smoke evolution was also reported.⁵⁹ Recently, Hull et al. reported that the partial replacement of ATH with zinc borate in EVA reduces carbon monoxide yield under fuel rich conditions in the Purser furnace.⁶⁰

RTM's recent study showed that the sintering/fusion of this zinc borate and ATH starts at temperatures around 700°C.⁶ Figure 9.8 illustrates that, at 65% loading in EVA, ATH alone generates lower peak HRR than MDH (257 vs. 188 kW/m²) in the Cone Calorimeter test. A partial substitution of MDH with a fine grade of this zinc borate (Firebrake ZB-Fine) resulted in not only a significant reduction of first peak HRR but also a drastic reduction and delay of the second major peak of HRR. The latter indicates there is a significant char/hard residue formation due to the presence of the zinc borate. In the case of ATH, although the HRR reduction is not as dramatic, the second peak is flattened out with the use of zinc borate, an indication of a stronger char formation. It should be pointed out that both magnesium oxide (a dehydration product of MDH) and aluminum oxide (a dehydration product of ATH) are known to cause glowing combustion in polyolefins and that zinc borate is known to suppress the glowing combustion. The synergistic fire test performance of this zinc borate and metal hydroxide interaction can be further augmented with the use of co-additives such as silicone (Figure 9.9), melamine polyphosphate, red phosphorus, or nanoclay.⁵²

A recent joint study by J.M. Huber and RTM showed that, in EVA (28% VA) and a compatibilizer, a partial substitution of MDH with the fine grade of zinc borate (5–10 wt.%) resulted in not only HRR reduction but also better electrical properties/physical properties (except tensile strength).⁶¹ In addition, there was a significant torque reduction during compounding, an indication of improvement in processability.

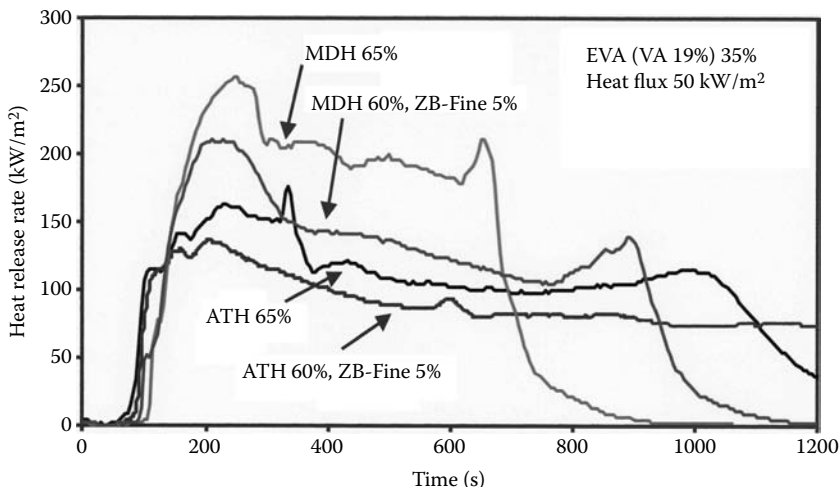


FIGURE 9.8 HRR curves of EVA (35%) containing MDH or ATH with Firebrake ZB-Fine (total loading 65% by wt).

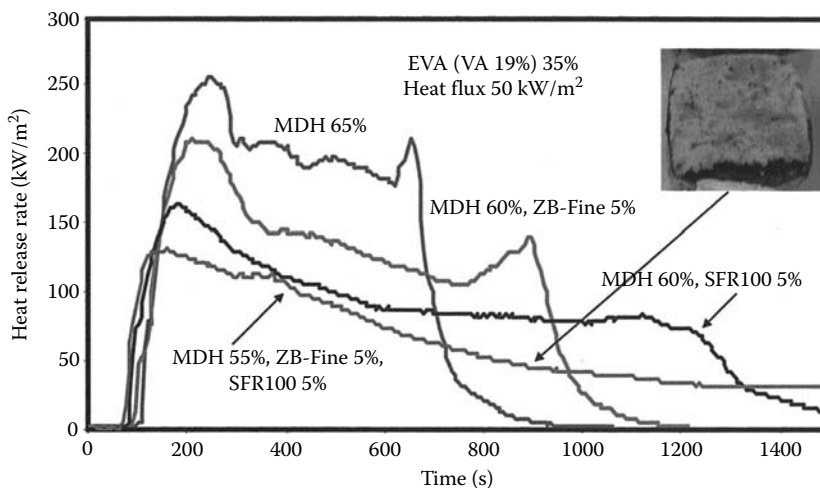


FIGURE 9.9 (See color insert following page 530.) HRR curves of MDH/Firebrake ZB-Fine/silicone-SFR100 (total loading 65%) in EVA.

Crompton reported the use of a combination of vitrifying and devitrifying frits in thermoplastics. The addition of zinc borate in the formulation is claimed to bring down the melt and the flow temperature.⁶²

The synergy between the zinc borate and the APP was claimed in several applications. For example, Bourbigot and Duquesne reported that the combination displayed synergy in LOI performance (see Section 9.3.2.2).

9.2.4.1.1.4 Elastomers The zinc borate is an effective synergist of halogen sources and smoke suppressants in elastomers such as styrene butadiene rubber (conveyor belting, flooring), neoprene (wire and cable, dampening compound, conveyor belt), EPDM and PVC-nitrile foam (insulation foam), and so on.⁵⁵ It has also been used in halogen-free silicone elastomer and EPDM, EP (in conjunction with ATH or MDH).

9.2.4.1.1.5 Thermosets/Coating This zinc borate is an effective flame retardant synergist of halogen sources in epoxy (bromine or chlorine source)⁵³ and unsaturated polyesters⁶³ (chlorendic anhydride or bromine source). The benefit of smoke suppression was also reported in these polymers. This zinc borate has been used in halogen-free epoxy, phenolics, and unsaturated polyester. For example, in a semiconductor encapsulation application, zinc borate can be used as a sole fire retardant in silica-filled epoxy to meet UL-94 V-0.⁶⁴ In intumescent coating, zinc borate is commonly used in conjunction with APP, silica, ATH, and so on, for strong char formation (see Section 9.2.5.1).

9.2.4.1.1.6 Wood Plastic Composites (WPC) In WPC applications, it was claimed that the addition of organic phosphate, zinc borate/boric acid, sodium silicate, or ATH to milled rice straw with a resin binder can produce a fire-resistant board.⁶⁵

9.2.4.1.2 Firebrake 500 ($2ZnO \cdot 3B_2O_3$)

This anhydrous zinc borate is recommended for use in engineering plastics processed at temperatures higher than 300°C which is the upper limit of Firebrake ZB processing temperature. It is reported to be an effective smoke suppressant in chlorofluoropolymers for plenum cable applications.⁶⁶ Recently it was claimed that this anhydrous zinc borate can replace antimony oxide (or sodium antimonate) completely in high temperature polyamide applications. Like its hydrated analog, this anhydrous zinc borate can also improve CTI, thermal stability, and the color stability of polyamide containing halogen sources.^{67,68}

This anhydrous zinc borate was also claimed to improve the stability of a halogen-free polyamide containing aluminum diethylphosphinate, a new halogen-free flame retardant developed by Clariant.⁶⁹ For aircraft applications, this zinc borate alone is also reported to be effective in reducing the HRR of polyetherketones and polysulfones (Table 9.7).⁷⁰

Although this zinc borate is recommended for use in polymers processed at 300°C or higher, RTM's recent study indicates that there are potential benefits of using the anhydrous zinc borate in conjunction with MDH in polyolefins.⁶¹

More recently, Bourbigot et al. reported the preparation a neutralized intumescent flame retardant (NIFR) by reacting pentaerythritol, phosphoryl trichloride, and melamine.⁷¹ The addition of a small amount of the anhydrous zinc borate (2 wt.% at the expense of NIFR) in PP leads to a

TABLE 9.7
Poly(Biphenylether Sulfone) and Poly(Arylether Ketone) Blend

	Examples (Parts by wt.)			
	1	2	3	4
<i>Composition</i>				
Poly(biphenylether sulfone)/ poly(arylether ketone) 65/35	100	100	100	100
Firebrake 500 ($2ZnO \cdot 3B_2O_3$)	—	4	8	8
Polytetrafluoroethylene	—	—	—	2
<i>Properties</i>				
Max. heat release rate ($kW m^{-2}$)	91	54	44	35
Impact strength (J)	—	171	144	129

dramatic improvement in the fire test performances (LOI and V-0 rating). The zinc borate promotes the formation of a cohesive intumescent barrier.

9.2.4.1.3 Firebrake 415 ($4\text{ZnO} \cdot \text{B}_2\text{O}_3 \cdot \text{H}_2\text{O}$)

This zinc borate has an unusually high onset of dehydration temperature ($>415^\circ\text{C}$).⁷² It is recommended for use as a synergist of halogen sources in engineering plastics such as polyamides. Duquesne et al. reported that increasing the level of substitution of MDH by this zinc borate in an EVA (6% VA content, with 60% total loading) displayed significant reductions of HRR and an increasingly stronger char.⁷³ They used a dynamic plate–plate rheometer to show that increasing Firebrake 415 loading could result in 100-fold increase in melt/pyrolysis viscosity in the range of 300°C – 400°C . They also demonstrated the strong char formed that is able to withstand a pressure of 50 kN/m^2 . This zinc borate was also claimed to be an effective flame retardant in high temperature polyamide 9T containing brominated polystyrene (PS) to completely replace antimony trioxide.⁷⁴ Lewin reported the use of a combination of methylsulfamate and this zinc borate in halogen-free polyamide 6 to achieve a V-0 rating.⁷⁵

9.2.4.2 Aluminum Borate ($9\text{Al}_2\text{O}_3 \cdot 2\text{B}_2\text{O}_3$)

Aluminum borate whiskers are produced commercially by an “external flux” method. Chlorides, sulfates, or carbonates of alkali metals are added to alumina and boric oxide (or boric acid) and the mixture is heated to 800°C – 1000°C to produce aluminum borate whisker (length 10 – $30\ \mu\text{m}$ and diameter 0.5 – $1.0\ \mu\text{m}$). It has a melting point of 1440°C , a very low coefficient of thermal expansion, and an excellent chemical resistance toward acids. The aluminum borate whisker was reported to be effective in improving not only the thermal degradation but also the glass transition temperature of epoxy.⁷⁶

9.2.4.3 Miscellaneous Metal Borates

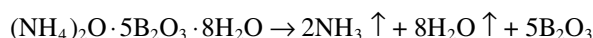
A variety of transition and other metal borates are reported in the literature. These include manganese borate, silver borate, iron borate, copper borate, nickel borate, strontium borate, lead borate, zirconium borate, double metal borates, and so on. Many of these borates have the potential to be flame retardants and/or smoke suppressants.

9.2.5 BORON AND NITROGEN-CONTAINING COMPOUNDS

The B/N-containing boric acid esters are presented in Section 9.2.6.1.

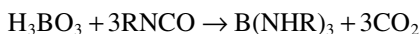
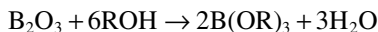
9.2.5.1 Ammonium Pentaborate [$(\text{NH}_4)_2\text{O} \cdot 5\text{B}_2\text{O}_3 \cdot 8\text{H}_2\text{O}$]

Ammonium pentaborate (APB) is produced from the reaction between ammonia and boric acid in water. It has a water solubility of 10.9 wt.% at 25°C . Upon thermal decomposition, APB first gives off a large amount of water starting at about 120°C . At about 200°C , it starts to give off ammonia and, at about 450°C , it is all converted to boric oxide which is a glass former. APB functions as both an inorganic blowing agent and a glass-forming fire retardant.



APB solution can be sprayed on paper or the paper can be dipped into the solution to yield fire-retardant products. In addition to the cellulose, it has also been used as a flame retardant in polyurethane foam and epoxy intumescent coatings.

Myers et al. reported that partially dehydrated APB is an effective intumescent flame retardant in thermoplastic polyurethane.⁷⁷ APB at 5–10 phr loading in TPU can provide 7- to 10-fold improvement in burn-through test. It is believed that in the temperature range of 230°C–450°C, the dehydrated APB and its released boric oxide/boric acid may react with the diol and/or isocyanate, the decomposed fragments from TPU, to produce a highly cross-linked borate ester and possibly boron–nitrogen polymer that can reduce the rate of formation of flammable volatiles and result in intumescent char.



Its usage in polymers, however, is limited by its high water solubility (10.9%) and low dehydration temperature. PPG reported the use of APB in conjunction with APP, zinc borate, silica, talc, and so on, in a flame-retardant intumescent coating for protection against hydrocarbon fires.⁷⁸

9.2.5.2 Melamine Diborate $[(\text{C}_3\text{H}_8\text{N}_6)_2\text{O} \cdot \text{B}_2\text{O}_3 \cdot 2\text{H}_2\text{O}] / (\text{C}_3\text{H}_6\text{N}_6 \cdot 2\text{H}_3\text{BO}_3)$

Melamine diborate (MB), known in the fire-retardant trade as melamine borate, is a white powder, which can be prepared readily from melamine and boric acid. It is partly soluble in water and acts as an afterglow suppressant and a char promoter in cellulosic materials. Budenheim Iberica⁷⁹ claims that, in a 1:1 combination with APP, MB (10%–15%) can be used for phenolic bound nonwoven cotton fibers. In general, melamine borate can be used as a char promoter in intumescent systems for various polymers including polyolefins or elastomers. However, its low dehydration temperature (about 130°C) limits its application in thermoplastics that are processed at above 130°C. Melamine borate is also reported to suppress afterglow combustion in flame-proofing textiles with APP or monoammonium phosphate to meet the German DIN 53,459 and Nordtest NT-Fire 002.⁸⁰

9.2.5.3 Guanidinium Borate $[x[\text{C}(\text{NH}_2)_3]_2\text{O} \cdot y\text{B}_2\text{O}_3 \cdot z\text{H}_2\text{O}]$

Several guanidinium borates have been reported in the literature. For example, guanidinium tetraborate $[\text{C}(\text{NH}_2)_3]_2\text{O} \cdot 2\text{B}_2\text{O}_3 \cdot 4\text{H}_2\text{O}$ can be prepared by reacting guanidinium carbonate with boric acid in hot water or it can be prepared by reacting guanidinium chloride with borax in cold water.⁸¹ Sanyo Chemical in Japan claims that the combination of calcium imidosulfonic acid and guanidinium borate or guanidinium sulfamate provides excellent flame retardancy in cellulosic materials.⁸² Guanidinium nonaborate $[\text{C}(\text{NH}_2)_3]_2\text{O} \cdot 3\text{B}_2\text{O}_3 \cdot 2\text{H}_2\text{O}$ with a unique nonaborate anion was reported.⁸³ It has a structural formula of $[\text{C}(\text{NH}_2)_3]_3[\text{B}_9\text{O}_{12}(\text{OH})_6]$. It was demonstrated that, in polypropylene-containing decabromodiphenyl oxide, antimony oxide, and talc, the partial replacement of antimony trioxide by the guanidinium nonaborate (up to 75%) can result in a significant reduction in afterglow while maintaining the UL-94 V-0 (3.2 mm) performance.

9.2.5.4 Boron Nitride (BN)

Boron nitride (BN) can normally be prepared from the reaction of boric acid and urea or melamine. For example, the pyrolysis of MB can yield hexagonal BN. It is commonly referred to as “white graphite” because of its platy hexagonal structure similar to graphite. Under high pressure and at 1600°C, the hexagonal BN is converted to cubic BN, which has a diamond-like structure.

Hexagonal BN is stable in inert or reducing atmosphere to about 2700°C and in oxidizing atmosphere to 850°C. It is an excellent thermal conductor and has been frequently quoted as a functional filler for fire-retardant encapsulants for E/E applications.

Single-walled BN nanotubes were recently reported. They are far more resistant to oxidation than carbon nanotubes.⁸⁴ A recent Japanese patent describes the use of BN nanotube (0.01 wt.%) to improve the thermal resistance of polybenzimidazole.⁸⁵

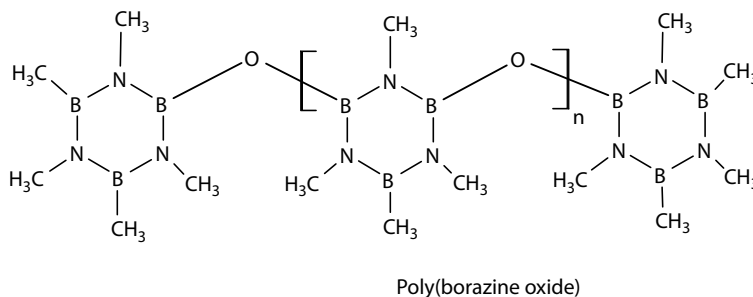


FIGURE 9.10 Poly(borazine oxide).

9.2.5.5 Borazine [(HBNH)₃]

Borazine is isoelectronic and isostructural with benzene. Poly(borazylene), a polymer of borazine and its derivatives, is reported extensively as a precursor of BN-coated ceramic fibers.⁸⁶ Polymeric borazine oxide derivative is claimed to be flame resistant (Figure 9.10).⁸⁷

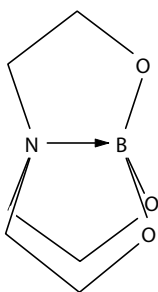
9.2.6 BORESTER AND BORON-CARBON COMPOUNDS

9.2.6.1 Boric Acid Esters [B(OR)₃]

In general, boric acid esters (also called borester) derived from alcohols and boric acid are hydrolytically unstable for general use in plastics/elastomers, wood, paper, or cotton. However, the pressure treating of wood with trimethylborate [B(OCH₃)₃] is reported to be effective in rendering it fire resistant.⁸⁸ In this case, once trimethylborate penetrates the wood, it will revert back to boric acid.

Halogen-containing borate ester such as tris(2,3-dibromopropyl)borate [B(OCH₂CHBrCH₂Br)₃] is reportedly used in polyurethanes, unsaturated polyesters, and epoxy novolacs.⁸⁹ More recently, it was also claimed to be used in cotton textiles.⁸⁹

Cyclic boric acid esters derived from triethanolamine (Figure 9.11) or diethanolamine can be stabilized toward hydrolysis by an intramolecular, boron-nitrogen coordination bonding. The blockage of the empty-orbital on the boron atom can alleviate hydrolysis. This effect has been used to prepare compositions with direct bonding to cellulose that are not removable by washing with water. For example, treating cellulose fibers with the compound depicted in Figure 9.12 gives a stiff mass that is appreciably slower burning than the control.⁹⁰ It is assumed that the methoxyl group in the molecule is displaced by the hydroxyl groups of cellulose. However, this treatment is not expected to sustain multiple washings.

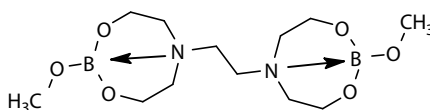


Triethanolamine borate

FIGURE 9.11 Triethanolamine borate.

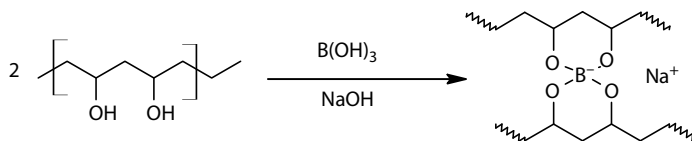
9.2.6.2 Boric Acid Ester Salts [M⁺-B(OR)₄]

Boric acid ester salts can be formed by reacting alcohols (including diols) with boric acid in the presence of alkaline metal salts. The surface modification of poly(vinyl alcohol) and poly(ethylene-*co*-vinyl alcohol) with boric acid and sodium hydroxide leads to



5-Aza-boracyclooctane derivative

FIGURE 9.12 5-Azaboracyclooctane derivative.



SCHEME 9.1 Polyvinyl alcohol cross-linked by borate.

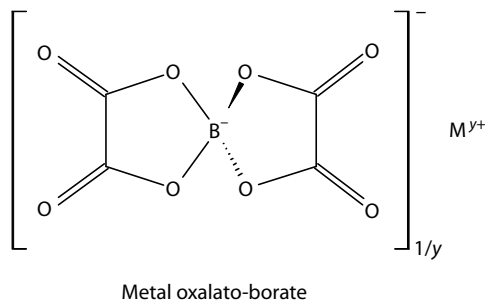


FIGURE 9.13 Metal oxalato-borate.

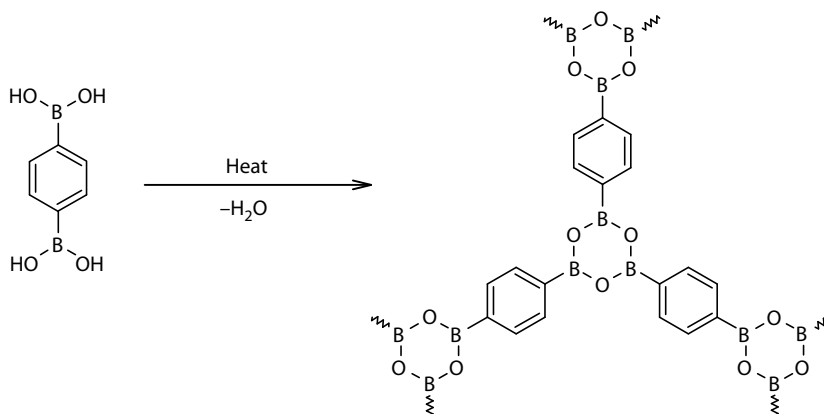
significant reductions in flammability as evidenced by increased LOI values and char yields. It was postulated that the borate is active in the condensed phase by assisting intermolecular cross-linking and helping to promote the formation of protective char layer (Scheme 9.1).⁹¹

A recent patent reported the preparation of a “bis-oxalato-borate salt” (Figure 9.13). It was claimed that this type of multifunctional salt can provide stabilizer, flame retardancy, and conductivity effects in a variety of polymers.⁹²

9.2.6.3 Boronic Acid [ArB(OH)_2]

Boronic acids are known to release water on thermolysis, thereby leading to the formation of boroxines or boronic anhydrides. It was reported that the chemical modification of polystyrene (PS) by introducing boronic acid functionality ($-\text{B(OH)}_2$) to predominately the para-position improves fire retardancy. It was reported that the boronated PS is significantly less flammable than the unmodified PS. For example, the virgin PS has a LOI of 18.3% vs. 25.3% for the boronated PS (the degree of substitution 9.2%). The char yield also increased from <1% to 7% at 600°C. It was postulated that the boronic acid groups are active in the condensed phase by assisting intermolecular cross-linking, forming the six-membered boroxine ring and promoting the formation of a protective char layer.⁹¹

Morgan et al. reported the syntheses of 1,4-benzenediboronic acid (BDB) and 1,3,5-benzenetriboronic acid (BTB) and evaluated them as fire retardants in ABS and polycarbonate (PC).⁹³ TGA and DSC analysis showed that both BDB and BTB have an endothermic event in the range of 180°C–260°C and showed they were good char-yielding compounds, forming a cross-linked boroxine network through the loss of water (Scheme 9.2). The char yields for BDB and BTB at 900°C were 40% and 48%, respectively, whereas for phenylboronic acid (a monoboronic acid) was 0%. UL-94 V-0 (3.2 mm) results were obtained with 5 wt.% of BDB in PC with 0.1 wt.% of PTFE anti-drip additive. However, BDB failed to give a quantifiable UL-94 in ABS in conjunction with 10 wt.% of chlorinated polyethylene as an anti-drip additive; interestingly enough, the flame moved very slowly along the exterior of the sample and was accompanied with char formation. It was concluded that these diboronic acid and triboronic acid are condensed phase flame retardants via the formation of boroxine layers. The detailed mode of action deserves further scrutiny. A boronic acid with a $\text{N} \rightarrow \text{B}$ coordination bond was reported as semi-durable fire retardant in cotton fabrics.⁸⁹



SCHEME 9.2 Formation of boroxine from *para*-diboronic acid.

9.2.6.4 Boron Carbide (B_4C)

Boron carbide is produced industrially by the carbo-thermal reduction of B_2O_3 (boron oxide) in an electric arc furnace. It is a black powder and has a melting point of $2445^\circ C$. It was reported⁹⁴ that the addition of boron carbide (10–15 wt.%) in a variety of intumescent coatings containing APP and a blowing agent resulted in the following benefits:

- Forming a uniform and hard foamed layer
- Preventing excessive expansion on heating
- Retarding oxidative weight loss of the foamed layer at $1000^\circ C$ or even higher
- Improving weight retention, compression strength, and peel strength during fire

9.2.7 BORON AND PHOSPHORUS-CONTAINING COMPOUNDS

9.2.7.1 Boron Phosphate (BPO_4)

Boron phosphate, an inorganic polymer of empirical formula BPO_4 , can be prepared by heating phosphoric and boric acids to calcining temperature. It is a white infusible solid that vaporizes at $1450^\circ C$ – $1462^\circ C$ without decomposition. As opposed to the tri-valency in boric oxide, most of the boron atoms in boron phosphate are tetra-coordinated (i.e., as BO_4^- group, Figure 9.14). Commercially it is available from Budenheim.⁷⁹

It was reported that, in polyamide (PA)/PPE alloy, a combination of boron phosphate (5%) and silicone oil (2%) resulted a V-0 (1.6 mm) rating in the UL-94 test.⁹⁵ The use of boron phosphate

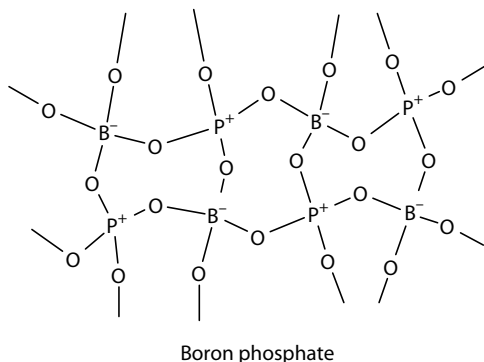
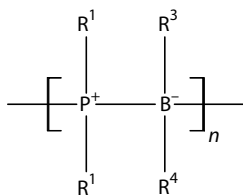


FIGURE 9.14 Boron phosphate.



Phosphine–borane polymer

FIGURE 9.15 Phosphine–borane polymer.

in conjunction with zinc borate prevents the UL-94 5VA burn through in PPE/HIPS/SEBS containing triphenyl phosphate.⁹⁶ A recent patent by Nexans claimed the use of a combination of zinc borate and boron phosphate in electrical insulation that is resistant to high temperature such as 1100°C.⁹⁷

9.2.7.2 Phosphine–Borane

The preparation of phosphine–borane polymer (Figure 9.15) was reported. It was claimed to be a fire retardant but no fire test results were given.⁹⁸

9.2.8 BORON AND SILICON-CONTAINING COMPOUNDS

Borate and silica are expected to function synergistically as a flame retardant by forming borosilicate ceramic/glass residue as the results in the following text indicate.

9.2.8.1 Borosilicate, Borosilicate Glass, and Frits

Borosilicate glass is a range of glasses based on boric oxide, silica, and a metal oxide. It has excellent thermal shock resistance and chemical resistance. A recent patent claimed the use of borosilicate glass powder (50–100 phr) in conjunction with expandable graphite (100 phr) or vermiculite in polyolefin, epoxy, or elastomers to achieve good fire retardancy (as evidenced by the Cone Calorimeter test at 35 kW/m²).⁹⁹

Olex Australia reported that using calcium borosilicate (e.g., 1.4CaO · 0.5B₂O₃ · SiO₂ · 0.5H₂O), MDH, and silica in polyolefin and/or silicone polymer could result in ceramification at an elevated temperature for security cable applications.¹⁰⁰ Calcium borosilicate is critical for maintaining the shape of insulation in wire and cable and preventing it from shrinking and cracking during fire. On exposure to high temperature (1000°C for 30 min), calcium borate helps to form self-supporting ceramics.

Ceramic frits are vitreous compounds, which are not soluble in water and obtained by melting and then rapidly cooling carefully the controlled blends of raw materials such as SiO₂, Na₂O, K₂O, B₂O₃, P₂O₅, CaO, ZnO, MgO, Al₂O₃, ZrO₂, and so on. The frit production process allows the use of soluble raw materials. One can achieve different softening temperatures of the frit by modifying the chemical composition. The use of frit in conjunction with halogenated flame retardants or halogen-free flame retardants can boost fire retardancy and char/residue formation. For example, Ceepree is a commercial fire retardant that consists of mainly glass or ceramic frits.⁶² This powdered additive is a blend of different components, which have almost a continuous melting range. The lowest melting components begin to melt at around 350°C. The vitreous materials will form fire barrier around host polymer. At about 800°C, some components in the frit begin to devitrify (i.e., passing from a vitreous state to a crystalline state). As a result, Ceepree can provide char/residue integrity at high temperatures via ceramification. Polymer Australia PTY reported that the addition of glass frit (0.8%–8%) to silicone-containing mica produced a self-supporting ceramic material at a temperature above the silicone decomposition temperature.¹⁰¹

9.2.8.2 Borosiloxane

Borosiloxane is a polyorganosiloxane containing mainly –Si–O–B–O–Si– chain linkage. It can be prepared by reacting a silanol terminated siloxane polymer with boric acid. Showa Electric reported the use of a borosiloxane in a low density polyethylene cable sheathing application. The borosiloxane improved the LOI significantly, and prevented the dripping and the formation of corrosive gases during combustion without giving any adverse effect on mechanical properties.¹⁰²

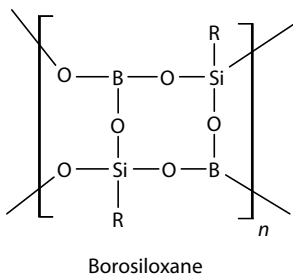


FIGURE 9.16 Borosiloxane.

elastomer (BSil) was prepared by reacting α,ω -dihydroxy-oligodimethylsiloxane and boric acid (10:1 ratio). In PP containing the IFR, the addition of BSil (1.5 wt.% at the expense of PP) results in a significant melt viscosity increase and thus reduces dripping. The presence of boron in the siloxane is an essential component of ceramic layer formation. In the absence of boron, the siloxane chain transforms to silica ash instead of a coherent continuous layer. They also reported that, in the presence of the IFR, the addition of an organic surfactant modified montmorillonite (MMT) coated with BSil results in not only increases in the LOI from 31% to 37% but also promotes the formation of a continuous char barrier layer in the Cone Calorimeter test (i.e., 33% IFR/1%MMT vs. 31%IFR/1%MMT/2%BSil).¹⁰⁵ It is believed that the BSil coating may act as a carrier delivering MMT to the surface.

9.2.9 MISCELLANEOUS

9.2.9.1 Layered Double Hydroxides with Borate

Recently layered double hydroxides (LDHs) such as $\text{Mg}_4\text{Al}_2(\text{OH})_{12}\text{CO}_3 \cdot \text{H}_2\text{O}$ has received considerable attention as fire retardants in halogen-free thermoplastics and thermoset polymers. The mineral hydroxalite [$\text{Mg}_6\text{Al}_2(\text{OH})_{16}\text{CO}_3 \cdot 4\text{H}_2\text{O}$] is an example of such a material and LDHs are also known as hydroxalite-like material. It was reported that the reaction of LDH with boric acid leads to a borate-pillard LDH. The ^{11}B magic angle spinning nuclear magnetic resonance data are consistent with the presence of polymeric triborate anions of the type $[\text{B}_3\text{O}_4(\text{OH})_2]^-$ in the interlayer galleries. It was demonstrated that this borated LDH in EVA leads to a significant enhancement in smoke reduction.¹⁰⁶

9.2.9.2 Fluoroborates

Both ammonium fluoroborate (NH_4BF_4) and potassium fluoroborate (KBF_4) were reported to be flame retardants in both Cl/Br-containing and halogen-free polymers. Ammonium fluoroborate sublimates at 238°C and potassium fluoroborate has a melting point of 359°C .

During the 1970–1980s, a mixture of ammonium fluoroborate and antimony oxide was offered on the market. This mixture was used in polypropylene with dechlorane (a chlorine source) to achieve V-0. In the absence of added halogen source, the mixture can also achieve V-0 and a LOI of 33% in PP at a loading of about 37.5%. It was claimed that the mixture can be easily dispersed, has excellent UV stability, and is non-blooming, nonvolatile, and odorless. However, its water absorption in high humidity areas was a deficiency of this additive.

Owens-Corning claimed the use of ammonium fluoroborate or potassium fluoroborate as smoke suppressant in isocyanurate–urethane.¹⁰⁷ It was believed that the fluoroborate decomposition products such as BF_3 , KF , or NH_4F act as free radical chain stopper and add across double bonds of olefinic decomposition products. NASA reported that both ammonium fluoroborate and potassium fluoroborate are the effective endothermic fillers of ablative intumescent coating.¹⁰⁸

In 2004, Kaneka reported the preparation of borosiloxane derivatives comprising silicon, boron, and oxygen having skeletons that are substantially formed by silicon–oxygen bonds, and boron–oxygen bonds with an aromatic ring attached to silicon (Figure 9.16).¹⁰³ It was shown that these borosiloxanes yielded V-0 (1.6 mm) ratings at 5–15 phr loading in PC, PC/PET, PC/PBT, PC/ABS, PPE/HIPS, and so on with good impact strength. The hydrolytic stability of borosiloxane was not discussed in the patent.

Marosi et al. reported the use of a “boroxo siloxane (BSil)” as a ceramic precursor in intumescent fire retardant polypropylene (IFR—70% APP and 30% pentaerythritol).¹⁰⁴ This borosiloxane

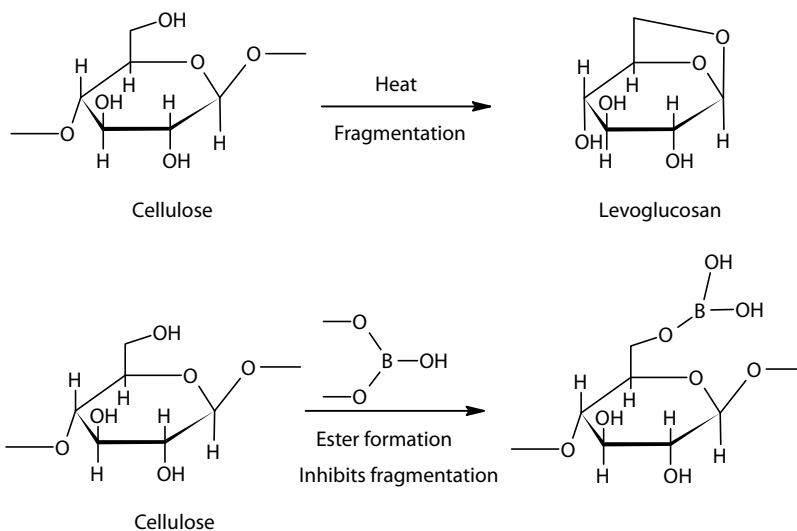
9.3 FIRE RETARDANCY MECHANISM OF BORON COMPOUNDS

9.3.1 BORATES IN WOOD/CELLULOSE

Upon heating, wood, consisting of cellulose, lignin, and hemicelluloses, can decompose to gaseous, liquid, tarry, and solid products. Cellulose is mainly responsible for the formation of flammable fragments. The volatile, flammable gases ignite and provide heat to further pyrolyze the liquid and tar into more flammable vapors and char residues. The nonflaming oxidative combustion of char is called smoldering or glowing combustion. The benefits of borates are summarized as follows.

- Sodium borate and boric acid undergo an endothermic release of water that acts as a diluent in the gas phase. For example, the conversion of boric acid to boric oxide is endothermic by 1530 J/g and is accompanied by giving off 44 wt.% by wt. of water.
- Molten sodium borate or boric oxide (a low-melting glass) can cover and stabilize the unburned substrate/char and inhibit oxygen permeation.
- Boric acid is an effective smoldering inhibitor; whereas sodium borate, due to the presence of the sodium cation, is not a smoldering inhibitor.
- Chemically, boric acid can react with the C6-hydroxyl group of cellulose polymer to give a borate ester and block the release of flammable fragments (Scheme 9.3).
- The dehydration of hydroxyl groups in cellulose is enhanced by boric acid, which increases the char yield of borate-treated cellulose. As it is a weak acid, this effect is not as strong as that for phosphoric acid.
- By forming a boron to oxygen bond (such as a borester $-B-O-CH_2-$), it is known that boron can inhibit oxidation at $-CH_2-$ positions.

It is well known that wood samples containing phosphorus compounds can release phosphoric acid that accelerates the dehydration and carbonization of wood (i.e., with decreased threshold temperature and activation energy). As a result, phosphate renders the main decomposition of wood at lower temperatures ($<300^{\circ}C$) and results in the formation of less flammable products and correspondingly more char. On the other hand, boric acid can increase the thermal stability of wood via a different pathway (i.e., increase in threshold temperature and activation energy), and thus suppresses the mass loss and stabilizes the char.



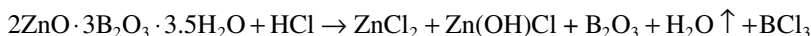
SCHEME 9.3 Effect of borate on cellulose degradation.

Another school of thought believes that the efficacy of boric oxide in afterglow suppression is related to its high ionization energy/or electron affinity; active sites for oxygen adsorption on the char surface may be deactivated by boric oxide via electron transfer. It was reported that boric oxide increases the oxidation temperature of crystalline carbon from 700°C to 800°C.¹⁰⁹

9.3.2 PLASTICS AND ELASTOMERS

9.3.2.1 Halogen-Containing Polymers

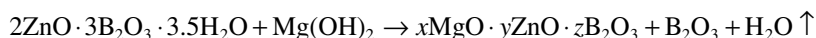
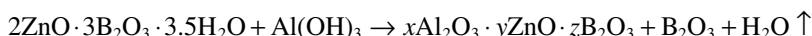
Zinc borates are predominately a condensed phase fire retardant. In a halogenated system such as flexible PVC, it is known to markedly increase the amount of char formed during polymer combustion; whereas the addition of antimony trioxide, a vapor-phase flame retardant, has little effect on char formation. Analyses of the char show that about 80%–95% of the antimony is volatilized, whereas the majority of the boron and zinc from Firebrake ZB remains in the char (80% and 60%, respectively).^{48,56} The fact that the majority of the boron remains in the condensed phase is in agreement with the fact that boric oxide is a good afterglow suppressant. The mode of action can be summarized in the following equation (not balanced).



- Firebrake ZB reacts with HCl released from PVC degradation to form zinc chloride, zinc hydroxychloride, boric oxide, water, and boron trichloride (low level, if any).
- The zinc species (such as, zinc chloride and zinc hydroxychloride) in the condensed phase can alter the pyrolysis chemistry by catalyzing the dehydrohalogenation and promoting cross-linking, resulting in increased char formation and a decrease in both smoke production and flaming combustion.
- It is believed that a portion of the zinc can be volatilized to the gas phase in the form of zinc chloride, which could function as a gas-phase flame retardant similar to that of SbCl_3 .
- The released boric oxide is a low-melting glass that can stabilize the char and inhibit afterglow.
- The water released can promote the formation of a foamy char that is a good thermal barrier. In addition, the release of water can absorb 503 J/g of heat.

9.3.2.2 Halogen-Free Polymers

Zinc borate in conjunction with ATH or MDH is used in many halogen-free polymers. Based on DTA and DSC analyses, it was also demonstrated that the partial replacement of ATH with Firebrake ZB in cross-linked EVA can delay and reduce the thermal oxidative peak (Figure 9.17). The mode of action of this zinc borate and metal hydroxide is summarized as follows:



- Zinc borate and alumina or magnesium oxide form a porous and ceramic-like residue at temperatures above 600°C, which acts as a thermal insulator for the unburned, underlying polymer.
- This zinc borate and/or the boric oxide released can function as a sintering aid for alumina or MgO.

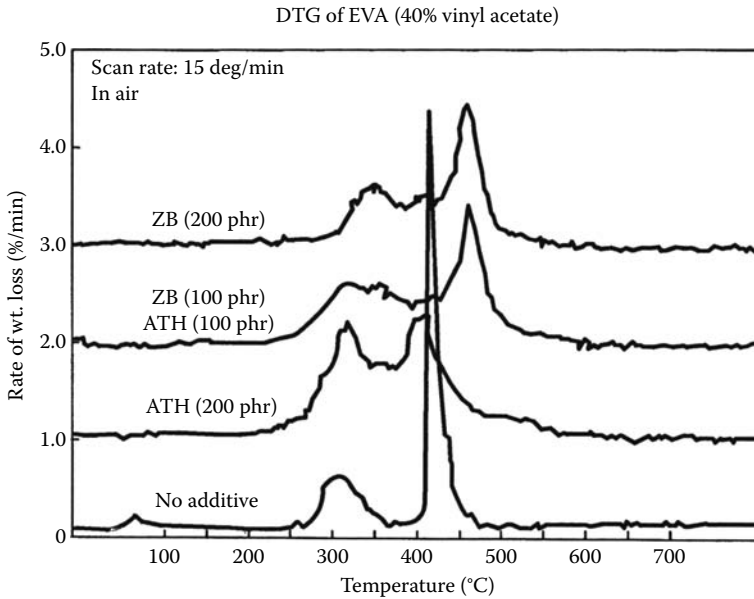


FIGURE 9.17 Differential thermogravimetric analysis of EVA-containing alumina trihydrate (ATH) and Firebrake ZB.

- This zinc borate can release 13.5 wt.% of water at 290°C–450°C. The endothermicity for water removal is 503 J/g. The release of water at high temperatures may contribute to the intumescence of the residue/char and inhibit flaming combustion.
- In the presence of co-additives, such as polydimethylsiloxane, melamine polyphosphate, the zinc borate is expected to form borosilicate, or zinc borophosphate residue.

Zinc borate and phosphorus compounds—the synergy between Firebrake ZB and APP is well documented in epoxy. In polypropylene, it has been shown that the synergy, as evidenced by LOI, derives from the formation of zinc phosphate and borophosphate during polymer combustion.¹¹⁰

Zinc borate in PC/ABS and polyamide—when zinc borate is used in conjunction with bisphenol-A-bis-diphenyl phosphate in PC/ABS, it was reported that borophosphate and zinc phosphate were generated during polymer combustion.¹¹¹ The formation of these materials could be beneficial for passing the more stringent fire tests, such as UL-95 5 V. When Firebrake 500 is used in conjunction with aluminum diethylphosphinate and melamine polyphosphate in polyamide, Scharitel et al. reported the formation of boron aluminum phosphate in the condensed phase.¹¹²

9.4 CONCLUSIONS

Boron-based fire retardants have a wide spectrum of applications. They are multifunctional fire retardants. They can function as flame retardants, smoke suppressants, afterglow suppressants, and anti-tracking agents.

Borates function as fire retardants by releasing water, acting as low-melting glass (covering and stabilizing substrate/char), inhibiting afterglow combustion, cross-linking with vicinal glycol, and forming borate ester with cellulose polymer (blocking the release of flammable fragments). In addition to being fire retardants, they also provide many additional benefits such as pH buffering, corrosion inhibition, biocide/preservative properties, and so on.

- In the field of fire-retardant wood and its products, borates are synergistic with N/P compounds. The future challenges will continue to be developing a borate-containing fire-retardant package that is water soluble during treatment (for ease of processing) and becomes water non-leachable once impregnated in wood or its products. Minimizing their impact on physical properties and optimizing their fire test performances with nitrogen, phosphorus, and silicate compounds would be the continuing development efforts.
- In the field of plastics and elastomers, water insoluble borates such as zinc borates have been very successful commercially in halogen-containing systems. They will play an increasingly more important role in halogen-free fire-retardancy applications. Due to the strong demand from electrical/electronics industry, future development on the use of borates as fire retardants will be to improve their high temperature thermal stability for high processing throughput and producing thin product parts, to maximize long-term water non-leachability for enhancing electrical properties, and to develop the use of co-additives such as silica, nitrogen, or phosphorus source for maximizing fire test performances.

ACKNOWLEDGMENT

The authors would like to thank Professor Ming Gao of North China Institute of Science and Technology for providing the Cone Calorimeter curves of GUP/BA treated wood and Dr. Robert White of USDA for providing some literature information in wood applications.

REFERENCES

1. Lyons, J.W. 1970. *The Chemistry and Uses of Fire Retardants*. Wiley-Interscience, New York.
2. Shen, K.K. 1996. Boron compounds as fire retardants. *Fire Retardant Chemical Association Spring Conference*, Baltimore, MD.
3. Shen, K.K. and Griffin T.S. 1990. Zinc borate as a flame retardant, smoke suppressant, and afterglow suppressant in polymers. In *Fire and Polymers* (ACS Symposium Series, vol. 425), Nelson G.L. (ed.). American Chemical Society, Washington, DC, p. 157.
4. Shen, K.K. and O'Connor, R. 1998. Flame retardants: Borates. In *Plastic Additives*, Prichard, G. (ed.). Chapman & Hall, London, p. 268.
5. Shen, K.K. 2000. Zinc borates—30 years of successful development as multifunctional fire retardants. *Polym. Mater. Sci. Eng.*, 83, 64–67.
6. Shen, K.K. and Olson E. 2005. Borate as fire retardants in polymers. *Fire and Polymers IV* (ACS Symposium Series, vol. 922), Wilkie C.A. and Nelson G.L. (eds.). American Chemical Society, Washington, DC, p. 224.
7. Mellor, J.W. 1980. *A Comprehensive Treatise on Inorganic and Theoretical Chemistry*, vol. 5: Suppl.1: Boron; Part A: Boron-oxygen compounds, Longmans, Green and Co., London.
8. Kimura, J. 1980. Flame retardant foam. Korean Patent 8000949.
9. Kruse, D., Simon, Menke, K., Friedel S., and Gettwert, V. 2007. Composition for a fire-protection agent for materials and fire-protection method. U.S. Patent Appl. 2007/051271.
10. Cline, A.J. 2006. Fire resistant fiber-containing article and method of manufacture. U.S. Patent Appl. 2006/0182940.
11. Moore, R. 2005. Stabilized borax based fire retardant system. U.S. Patent 6,894,099.
12. Hume, G. 2005. Fire retardant composite panel product and a method and system for fabricating same. U.S. Patent Appl. 2005/0249934.
13. Schmittmann, H.-B. and Their, A. 1984. Fire retardant and compounds based thereon. U.S. Patent 4,438,028.
14. Rio Tinto Minerals-Borax Service Bulletin, Borates in Cellulosic Materials, Denver, Colorado.
15. Shen, K.K. 1980. Corrosion tests of cellulose insulation containing borates. *J. Therm. Insulation*, 3, 190.
16. Sprague, R.W. and Shen, K.K. 1979. The use of boron products in cellulose insulation. *J. Therm. Insulation*, 2, 161.

17. Ferm, D.J. and Shen, K.K. 1994. Study on the permanence of borates in cellulosic insulation. *Tenth International Conference on Thermal Insulation*, San Francisco, CA, March 29.
18. Wakelyn, P.J. 2008. Environmental consideration for flame resistant textiles. *Proceedings of the Nineteenth Annual BCC Conference*, Stamford, CT, June 9–11.
19. Kozlowski, R. and Wladyka-Przybylak, M. 2001. In *Fire Retardant Materials*, Woodhead Publishing Limited, Cambridge, England, pp. 531–574.
20. White, R.H. and Dietenberger, M.A. 1999. Fire safety. In: *Wood Handbook—Wood as an Engineering Material*, Chapter 17, Gen. Tech. Rep. FPL-GTR-113. Forest Service, Forest Products Laboratory, U.S. Department of Agriculture, Madison, WI, pp. 17.1–17.16.
21. LeVan, S.L. and Tran, H.C. 1990. The role of boron in flame retardant treatment. *First International Conference on Wood Protection with Diffusible Preservatives: Proceedings*, vol. 47355, November 28–30, Nashville, TN, Forest Product Research Society, Madison, WI, pp. 39–41.
22. Pasek, A.E. and Thomason, S.M. 2003. Fire retardant. U.S. Patent 6,652,633.
23. Gao, M., Niu, J., and Yang, R. 2006. Flame retardant synergism of GUP and boric acid by cone calorimeter. *J. Appl. Polym. Sci.*, 102, 5522.
24. Gao, M., Niu, J., and Yang, R. 2006. Synergy of GUP and boric acid characterized by cone calorimetry and thermogravimetry. *J. Fire Sci.*, 24, 499.
25. Winandy, J.E., Wang, Q.W., and White, R.H. 2008. Fire retardant-treated strand board: Properties and fire performance. *Wood Fiber Sci.*, 40(1), 62–71.
26. Richards, M.J. and Herdman, D.J. 2001. Phosphate free fire retardant composition, U.S. Patent 6,306,317.
27. Winandy, J.E. and Richards, M.J. 2003. Evaluation of a boron-nitrogen (phosphate-free) fire retardant treatment. Part I. Testing of Douglas fir plywood per ASTM standard D-5516-96. *J. Testing Eval.*, 31(2), 133–139.
28. Warnes, R.D. and Bird, F. 1959. Method of producing chip-boards or chip-panels. GB 818,574.
29. Dulat, J. 1976. A process of producing flame-proof chip-board. GB 1435519.
30. Hanafin, J. and Bertrand, D.C. 2000. Low density light weight intumescent coating. U.S. Patent 6,096,812.
31. Jimene, M., Duquesne, S., and Bourbigot, S. 2006. Characterization of the performance of an intumescent fire protective coating. *Surf. Coating Technol.*, 201, 979–987.
32. Nobuyoki, T., Yasuaki, N., Takashi, H., and Hitoshi, T. 2002. Resol-type phenolic resin compound for manufacturing phenolic. *Jpn. Kokai Tokkyo Koho JP2002241530*.
33. Bassett, W.H. 1992. Non-halogen, flame retardant engineering thermoplastics. *Third Annual BCC Conference on Flame Retardancy*, Stamford, CT, May.
34. Claesen, C.A., Lohmeijer, H.G.M., Boogers, M.P.J., Bussink, J., Salenije, H.B., Hoeks, T.L., and Gossens, J.C. 1993. Polymer containing fluorinated polymers and boron compounds. U.S. Patent 5,182,325.
35. Hoeks, T.L., Claesen, C.A., Lohmeijer, H.G.M., and Pickett, J.M. 1997. Thermoplastic composition with boron compound. U.S. Patent 5,648,415.
36. Boderio, S. and Dien, R. 1994. Polyamide-based fire-proofed compositions. WO 94/22944.
37. Schubert, D.M. 1997. Method for producing calcium borate. U.S. Patent 5,688,481.
38. Grube, L.L. and Frankoski, S.P. 1992. Fire retardant bitumen. U.S. Patent 5,110,674.
39. Ishii, T., Kokaku, M., Nagsi, A., Nishita, T., and Kakimoto, M. 2006. Calcium borate flame retardation system for epoxy molding compound. *Polym. Eng. Sci.*, 46(5), 799–806.
40. Crompton, G. 1992. Materials for and manufacture of fire and heat resistant components. U.S. Patent 5,082,494.
41. Haruomi, H. 2003. Epoxy resin composition and electrical/electronic part equipment. *Jpn. Kokai Tokkyo Koho JP 2003096272*.
42. Zhu, W., Xian, L., He T., and Zhu, S. 2006. Hydrothermal synthesis and characterization of magnesium borate nano-whiskers. *Chem. Lett.*, 35(10), 1158.
43. Buckman Lab—www.buckman.com.
44. Nies, N. and Hulbert, P. 1970. Zinc borate of low hydration and method for preparing same. U.S. Patent 3,549,316.
45. Nies, N. and Hulbert, P. 1972. Zinc borate of low hydration and method for preparing same. U.S. Patent 3,649,172, 1972.
46. Lehman, H.A., Sperscheider, K., and Kessler, G.Z. 1967. Uber wasserhaltige zink borate. *Anorg. Allg. Chem.*, 354, 37–43.
47. Schubert, D.M., Alam, F., Visi, M.Z., and Knobler, C. 2003. Structural characterization and chemistry of the industrially important zinc borate, $Zn[B_3O_4(OH)_3]$. *Chem. Mater.*, 15(4), 866–871.

48. Shen, K.K. 1985. Firebrake®ZB (Zinc Borate)—The unique multifunctional additive. *Plastics Compounding*, Edgell Communication, Cleveland, September/October.
49. Shen, K.K. 2006. Overview of flame retardancy and smoke suppressant in flexible PVC. *Society of Plastics Engineering Vinyltech Conference*, Atlanta, GA, October 18.
50. Shen, K.K. 2002. Zinc borates as multifunctional fire retardants in polyamides. *Thirteenth Annual BCC Conference on Flame Retardancy*, Stamford, CT, June.
51. Shen, K.K. 1988. Zinc borate as a flame retardant in halogen-free wire and cable systems. *Plastics Compounding*, Edgell Communication, Cleveland, OH, November/December.
52. Shen, K.K. 2003. Zinc borates as multifunctional fire retardants in halogen-free polyolefins. *Fourteenth Annual BCC Conference on Flame Retardancy*, Stamford, CT, June.
53. Shen, K.K. and Sprague, R.W. 1982. Zinc borate as a flame retardant and smoke suppressant in epoxy systems. *J. Fire Retardant Chem.*, 9, 161.
54. Metcalf, G.S. and White, W.E. 2003. Method of constructing insulated metal dome structure for a rocket motor. U.S. Patent 6,544,936.
55. Shen, K.K. and Schultz, D. 2001. Flame retardants. In *Rubber Technology—Compounding and Testing for Performance*, Hanser, Munich, Germany, p. 248.
56. Shen, K.K. and Sprague, R.W. 1982. The use of zinc borate as a flame retardant and smoke suppressant in PVC. *J. Vinyl Technol.*, 4(3), 120.
57. Bonin, Y. and LaBlanc, J. 1995. Fire retardant, noncorrosive polyamide composition. U.S. Patent 5,466,741.
58. Martens, M.M., Cosstick, K.B., and Penn, K.B. 1997. Polyamide or polyester compositions. WO 9,723,565.
59. Bourbigot, S., Le Bras, M., Leeuwendal, R.M., Shen, K.K., and Schubert, D.M. 1999. Recent advances in the use of zinc borate in flame retardancy of EVA. *Polym. Degradation Stab.*, 64, 419–425.
60. Hull, T.R., Quinn, R.E., Areri, I.G., and Purser, D.A. 2002. Combustion toxicity of fire retarded EVA. *Polym. Degradation Stab.*, 77, 235–242.
61. Shen, K.K., Olson, E., Amigouet, P., and Tong, C. 2006. Recent advances on the use of metal hydroxides and borates as fire retardants in halogen-free polyolefins. *The 17th Annual BCC Conference on Flame Retardancy*, Stamford, CT, May.
62. Crompton, G. 2003. Fire barrier material. U.S. Patent 6,616,866.
63. Shen, K.K. and Sprague, R.W. 1981. On the use of a unique form of zinc borate as a flame retardant in fiberglass reinforced unsaturated polyesters and vinyl esters—A structure-activity relationship study. Reinforced Plastics/Composites Institute, The Society of Plastics Industry, Inc., Boltan, U.K., February 16–20; Section 13B, pp. 1–5.
64. Kamikooryma, Y., Hirose, M., and Koshibie, S. 1994. Production of flame resistant epoxy resin composition. *Jpn. Kokai Tokkyo Koho* JP 06,107,914, 1994.
65. Churchill, C.S. 2005. Fire resistance material and method of manufacture. U.S. Patent 6,886,306.
66. Chandrasekaran, S., Kundel, N.K., Garg, B., and Chin, H.B. 1990. Modified fluoropolymers for low flame/low smoke plenum cables. U.S. Patent 4,957,961.
67. Miyabo, A. and Koshida, R. 1998. WO 9,814,510.
68. Martens, M.M., Koshido, R., Tobin, W., and Willis, J. Synergist for flame retardant nylon. WO 9,947,597.
69. Nass, B., Hoerold, S., and Schacker, O. 2007. Polymer molding compositions based on thermoplastic polyamides. U.S. Patent Appl. 2007072967.
70. Kelley, W., Matzner, M., and Patel, S. 1991. Poly(biphenyl ether sulfone) compounds. WO 9115,539.
71. Fontaine, G., Bourbigot, S., and Duquesne, S. 2008. Neutralized flame retardant phosphorus agent: Facile synthesis, reaction to fire in PP and synergy with zinc borate. *Polym. Degradation Stab.*, 93, 68–76.
72. Schubert, D.M. 1994. Process of making zinc borates and fire retarding compositions thereof. U.S. Patent 5,342,553.
73. Duquesne, S., Le Bras, M., and Delobel, R. 2002. Visco-elastic behavior of intumescent materials. *Thirteenth Annual BCC Conference on Fire Retardant*, Stamford, CT, June.
74. Matsuoka, H., Sasaki, S., and Oka, H. 2002. Polyamide resin composition. U.S. Patent 6,414,064.
75. Lewin, M. 2001. Flame retardant polymer compositions. EP 1081183.
76. Kiyono, S. 1997. Heat resistant epoxy resin composition having excellent stability at normal temperature and curing agent for epoxy resin. U.S. Patent 5,610,209.
77. Myers, R.E., Dicksons, E.D., Licursi, E., and Evans, R. 1985. Ammonium pentaborate: An intumescent flame retardant for thermoplastic polyurethanes, *J. Fire Sci.*, November/December, 3(6), 432–449.

78. Nugent, R.M., Ward, T.A., Greigiger, P.P., and Seiner, J.A. 1992. Flexible intumescent coating composition. U.S. Patent 5,108,832.
79. Budenheim@Budenheim.es.
80. Thijssen, S. and Laser, J. 1992. Flameproof product. U.S. Patent 5,082,727.
81. Weakley, T.J.R. 1985. Guanidinium tetraborate. *Acta Cryst.*, C41, 377–379.
82. Yoshiyuki, U. and Yashushi, N. 1997. Flame retardant composition. *Jpn. Kokai Tokkyo Koho*, JP1997227870.
83. Schubert, D.M. 2006. Nonaborate composition and their preparation. U.S. Patent 6,919,036.
84. Bengu, E. and Marks, L.D. 2001. Single-walled nanostructures. *Phys. Rev. Lett.*, 86, 2385.
85. Hiroaki, K., Yoshio, B., Chunyi, Z., Tang, C., and Goldberg, D. 2008. Heat resistant composite composition and method for making the same. *Jpn. Kokai Tokkyo Koho*, JP 2008007699.
86. Sneddon, L.G., Beck, J.S., and Fazen, P.J. 1996. Direct thermal synthesis and ceramic applications of poly(borazylene). U.S. Patent 5,502,142.
87. Bradford, J.L. and Wagner, R.I. 1967. Borazine oxide derivative polymers and preparation thereof. U.S. Patent 3,341,474.
88. Martin, G.A. 1967. Wood treating process and process thereof. U.S. Patent 3,342,629.
89. Zhao, X., Zhu, P., Zan, Y.Z., and Dong, C.H. 2006. Study of boron synergists in fire retardancy applications. *Beijing International Fire Retardancy Technology and Material Conference*—Thesis Publication, Beijing, China, pp. 82–87.
90. Rudner, B. and Moores, M.S. 1962. Boracyclooctane condensation. U.S. Patent 3,042,636.
91. Armitage, P., Ebdon, J.R., Hunt, B.J., Jones, M.S., and Thorpe, F.G. 1996. Chemical modification of polymers to improve flame retardance. I. The influence of boron containing groups. *Polym. Degradation Stab.*, 54, 387–393.
92. Roder, J., Wietelmann, U., and Aul, R. et al. 2008. Usage of borate salt. WO 2008/028943.
93. Morgan, A.B., Jurs, J.L., and Tour, J.M. 2000. Synthesis, flame retardancy testing, and preliminary mechanism studies of nonhalogenated aromatic boronic acids. *J. Appl. Polym. Sci.* 76, 1257.
94. Kobayashi, N., Yoshida, K., Sagawa, K., and Ishibara, S. 1995. Intumescent fire resistant coating, fire resistant material, and process. U.S. Patent, 5,401,793.
95. Shaw, J.P. 1998. Flame retardant polyamide-polyphenylene ether compositions. U.S. Patent 5,714,550.
96. Yin, M., Kitamura, T., Ishiwa, K., Oshiro, A., Kosaka, K., and Kubo, H. 2003. Flame retardant composition and article. WO 03/004560.
97. David, C., Demay, J., Gardelein, M., and Lejeune, M. 2003. Heat resistant composition for electric cables contains organic polymer, a fusible ceramic filler which melts below the limiting temperature and a refractory filler with a high melting point. EP 1347464.
98. Manners, I. and H. Dorn, 2002. Linear phosphine-borane polymers and methods of preparation therefore. U.S. Patent 6,372,873.
99. Kazuhiro, O., Bunji, Y., and Hitomi, M. 2004. Fire resistant resin composition. JP 200404361.
100. Graeme, A. 2007. Fire resistant compositions. WO 2007121520.
101. Alexander, G., Cheng, Y., Burford, R.P., Shanks, R., Masonuri, J., Hodzic, A., Wood, C., Genovase, A., Barbier, K.W., and Rogdrigo, P.D.D. 2004. Fire resistant silicone polymer compositions. WO 2004013255.
102. Setsu, H., Ichirou, N., Kazumi, I., Kouzou, A., and Hisashi, A. 1982. Flame retardant polyolefin composition. JP 57076039.
103. Masumoto, K., Ono Y., and Tsyneishi, H. 2004. Flame retardant and flame retardant resin composition containing the same. U.S. Patent 6,716,952.
104. Marosi, G., Marton, A., Anna, P., Bertalan, G., Marosfoi, B., and Szep, A. 2002. Ceramic precursor in flame retardant system. *Polym. Degradation Stab.*, 77, 259–265.
105. Marosi, G., Marton, A., Szep, A., Csontos, I., Keszzi, S., Zimonyi, E., Toth, A., Almeras, X., and Le Bras, M. 2003. Fire retardancy effect of migration in polypropylene nanocomposites induced by modified interlayer. *Polym. Degradation Stab.*, 82, 379–385.
106. Shi, L. Li, D., Wang, J., Li, S., Evans, D.G., and Duan, X. 2005. Synthesis, flame retardant and smoke-suppressant properties of a borate-intercalated layered double hydroxide. *Clays Clay Miner.*, 53(3), 294–300.
107. Frisch, K.C. 1973. Low smoke generation plastic composition. U.S. Patent 3,725,319.
108. Sawko, P.M. and Salvatore, R. 1978. Intumescent ablator using endothermic filler. U.S. Patent 4,088,806.
109. Raksawski, J.F. and Parker, W.E. 1964. *Carbon* 2, 53.

110. Samyn, F., Bourbigot, S., Duquesne, S., and Delobel, R. 2007. Effect of zinc borate on the thermal degradation of ammonium polyphosphate. *Thermochimica*, 456, 134–144.
111. Pawlowski, K. and Scharrel, B. 2007. Fire retardant mechanisms of BDP in PC/ABS. *Fire Retardancy and Protection of Materials (FRPM)*, Germany.
112. Braun, U., Scharrel, B., Fichera, M.A., and Jager, C. 2007. Flame retardancy mechanism of aluminum phosphinate in combination with melamine polyphosphate and zinc borate in glass-fiber reinforced polyamide 6,6. *Polym. Degradation Stab.*, 92, 1528–1545.

10 Char Formation and Characterization

Sophie Duquesne and Serge Bourbigot

CONTENTS

10.1	Introduction.....	239
10.2	Carbonaceous Structures	241
10.3	Chemical Characterization of the Carbonization Process.....	241
10.3.1	Solid-State NMR	241
10.3.2	Raman Studies	244
10.3.3	X-Ray Photoelectron Spectroscopy	245
10.4	Dynamic Characterization.....	246
10.4.1	Study of the Dynamic Viscosity during Carbonization.....	248
10.4.2	Measurement of the Expansion Degree	250
10.4.3	Investigation of the Char Strength.....	252
10.5	Morphology of Carbonaceous Structures	254
10.5.1	X-Ray Diffraction	254
10.5.2	Microscopy	255
10.6	Conclusion.....	257
	References.....	257

10.1 INTRODUCTION

Flame-retardant (FR) additives in polymers may have an action either in the condensed phase or in the gas phase or also in both phases at the same time. When a condensed phase action is the mechanism of action of the FR, the properties of the solid phase during burning and also during the steady state are directly linked with the efficiency of the FR systems. As an example, the synergistic effect observed when montmorillonite (MMT) is included in polyamide 6 (PA6)/OP1311 (an aluminum phosphonate salt supplied by Clariant) has been, at least partially, explained by a sharp difference in terms of char structure^{1,2} (Figure 10.1). In the presence of MMT, the protective char exhibits a foamed structure constituted of numerous small closed cells whereas without MMT, a big bubble is observed. The foam charred structure is known to be very efficient in terms of thermal insulation and thus may explain why a synergistic effect is observed.

Similarly, numerous different nanoparticles, including organomodified clays,³ nanoparticles of silica,⁴ layered double hydroxides (LDH),⁵ or polyhedral silsesquioxanes (POSS),⁶ have been combined with intumescent formulations in polymeric materials to create large synergistic effects (see Chapter 12 for more details); the nanoparticles acting as “char reinforcer” or “char expander” that result in differences in terms of FR properties.

As another example, Kashiwagi et al.⁷ have investigated the flammability of polymer/single wall carbon nanotube (SWNT) nanocomposites. It has been observed that in the case where the nanotubes were relatively well-dispersed, a nanotube containing network structured layer was formed without any major cracks or openings during the burning tests and covered the entire

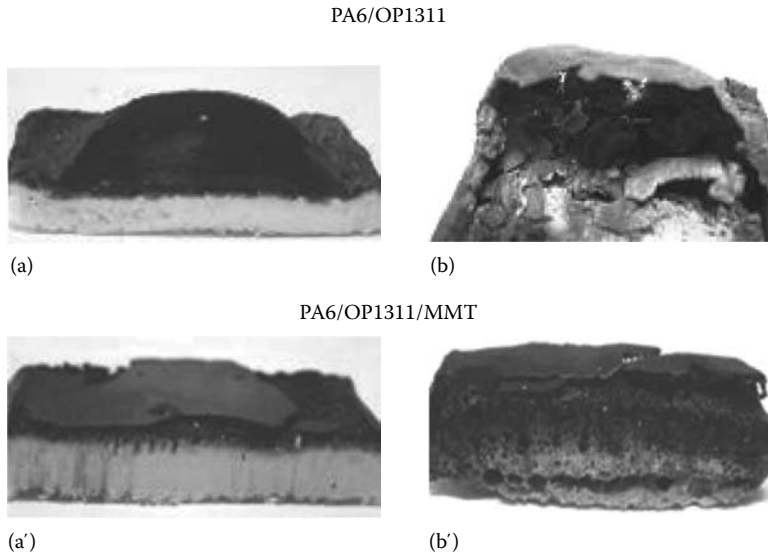


FIGURE 10.1 (See color insert following page 530.) Combustion residues of PA6/OP1311 and PA6/OP1311/MMT from the cone calorimeter obtained at different characteristic times ((a) and (a') after ignition and (b) and (b') at maximum PHRR). (From Samyn, F., Compréhension des procédés d'ignifugation du polyamide 6, Apport des nanocomposites aux systèmes retardateurs de flamme phosphorés, PhD dissertation, University of Lille, Lille, France, 2007.)

sample surface of the nanocomposites whereas nanocomposites having a poor nanotube dispersion or a low concentration of the nanotubes (0.2% by mass or less) formed numerous black discrete islands (Figure 10.2). The peak heat release rate of the nanocomposite, which formed the network structured layer is about one-half less of those that formed the islands. It has been proposed that the network layer acts as a heat shield to slow the thermal degradation of the polymer.

Thereby, it is obvious that dealing with FR acting in the condensed phase, the properties and the structure of the resulting carbonaceous layers will affect the FR properties and that is the reason why it is very important to be able to characterize this layer in detail.

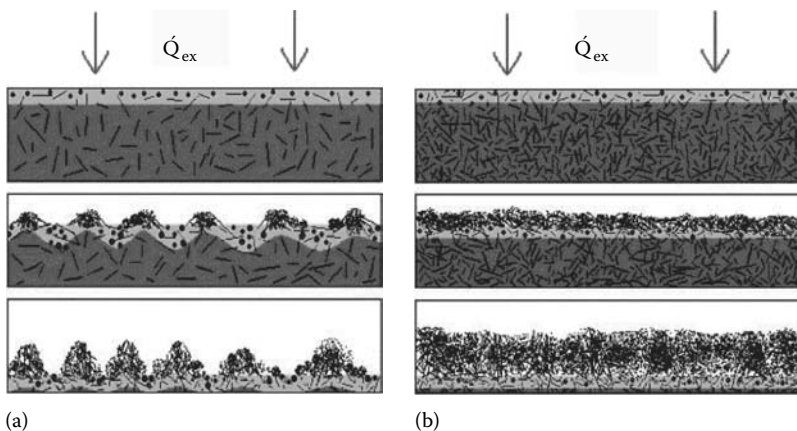


FIGURE 10.2 Schematic illustration of the formation of islands (a) and of a network structured layer (b). (Reproduced from Kashiwagi, T. et al., *Polymer*, 46, 471, 2005. With permission.)

The existing literature dealing with carbonaceous structural studies is very abundant, in particular in the field of coal combustion process.⁸ In the field of flame retardancy, no review, to our knowledge, has been published dealing with the techniques that can be used to monitor charring, and presenting their advantages and drawbacks. Moreover, fundamental questions specific to the flame retardancy field (such as, why do some polymers char and others do not? For those polymers that do char, how can the char yield be increased? How do polymer nanocomposites char?) are still not answered⁹ and a better understanding of the char formation in the case of fire-retarded system is fundamental. For these reasons, the purpose of this chapter is to give a selective presentation of the methods that can find benefits in the studies of char formation without being exhaustive. As a consequence, after a brief presentation of the several existing carbonaceous structures (Section 10.2), the spectroscopic techniques that can be used in order to investigate the chemical composition of the char (Section 10.3) are described and discussed. Then, in the following part, we focus on the physical aspect of the char characterization (Section 10.4) regarding strength, expansion, and viscosity measurements. In particular, the influence of those parameters on the morphology of the resulting char as well as on the efficiency of the FR systems are discussed. Finally, in Section 10.5, the use of several microscopic techniques (SEM and TEM, in particular) and of X-ray diffraction analysis to characterize the char morphology are presented. In particular, in intumescent systems, the bubble size and the bubble distribution are linked with the efficiency of the system and this will be discussed.

10.2 CARBONACEOUS STRUCTURES

Carbon is found in many different compounds. It is in the food you eat, the clothes you wear, the cosmetics you use, the gasoline that fuels your car. Carbon is the sixth most common element in the universe. It is a very special element because it plays a dominant role in the chemistry of life. Pure carbon is found in the universe as two main structures: graphite and diamond. It exists as several kinds of graphite materials, such as natural graphite, artificial graphite, kish graphite, mesophase carbon. In general, char is a highly cross-linked, porous solid. It may also form three-dimensional structures in addition to diamond and graphite, such as fullerenes or carbon nanotubes. Since these structures require specific conditions to be synthesized, they are rarely found in the condensed phase resulting from the combustion of polymeric materials, whether fire retarded or not.

Chemical fragmentation, cross-linking as well as bubble formation, and mass transport are processes occurring during char formation.⁹ The carbonaceous structure resulting from the combustion process of polymeric materials thus generally consists of disordered polycyclic aromatic hydrocarbons that become more ordered with increasing temperature (lower amorphous concentration, higher aromaticity, and larger crystallite size).¹⁰

10.3 CHEMICAL CHARACTERIZATION OF THE CARBONIZATION PROCESS

This part is dedicated to the presentation of the spectroscopic analyses that are often used to characterize char structures formed during burning. Since charred structures are poorly soluble, most of the techniques used are solid-state analyses. Moreover, since these techniques are complex and need specific conditions, in most cases, *ex-situ* analyses are carried out; that is to say that the charred residue is analyzed after combustion.

10.3.1 SOLID-STATE NMR

Solid-state nuclear magnetic resonance (ssNMR) is a useful technique that can give information regarding not only the chemical composition but also the structure of polymeric materials. Depending on their composition, nonzero spin atomic nucleus can be added during the synthesis of the material (isotopes) or can be present in the material either at low content (¹³C, ²⁹Si, ²⁵Mg, ...) or at high content (¹H, ²⁷Al, ³¹P, ...). These atomic nuclei are thus more or less easy to study.

As an example, when dealing with ^{13}C NMR studies, the low natural abundance of ^{13}C isotopes (1.1% presence) coupled with weak interactions between each ^{13}C nucleus and important distances between isolated ^{13}C spins and nearest unpaired electron result in long spin relaxation time causing very time-consuming experiments. However, a big advantage of this technique is linked with its selectivity, i.e., using ssNMR we can distinguish each atomic nucleus and their environment separately. Moreover, the existence of one relaxation time associated with the mobility of one region of the material can also lead to interesting information regarding heterogeneous material.

The use of ssNMR in the field of intumescent systems has demonstrated its usefulness in investigating the chemical composition of this structure versus time or temperature in the case of fire. Even if the use of this technique in this field is not recent,¹¹ it is still nowadays very useful. As an example, the mechanism of the degradation of ammonium polyphosphate (APP) derivative combined with boric acid in an epoxy-based coating has been recently elucidated using ssNMR. It was shown that both the additives provide an intumescent behavior to an epoxy-based coating but their combination inside the resin leads to an important expansion, a hard char and a good adhesion of the char to steel plates leading to the higher performance of the system.¹²

Figure 10.3 shows ^{11}B ssNMR spectra of the mixture boric acid/APP heat treated at 450°C . The comparison of the spectra obtained for pure boric acid and for the mixture boric acid/APP shows that the spectrum of the mixture of boric acid and coated APP exhibits a peak at $\delta_{\text{iso}} = -3$ ppm assigned to borophosphate.

The formation of borophosphate has been confirmed using ^{31}P ssNMR (Figure 10.4). The spectrum of borophosphate exhibits a single band at -30 ppm assigned to B–O–P bonds. When heated at 450°C , the spectrum of the mixture of boric acid/coated APP exhibits a band at the same chemical shift demonstrating unambiguously that a reaction takes place between boric acid and APP or its degradation products. All the phosphorous has reacted with the boron to yield borophosphate.

The formation of borophosphate partially explains the good performance when APP and boric acid are mixed together in the epoxy resin. Indeed, in that case good mechanical resistance of the intumescent char is observed as borophosphate is a hard material, which also shows a good thermal stability. As a conclusion, the boron containing compounds provide the good structural properties of the char, whereas the phosphorus ensures the adhesion of the char to the steel.

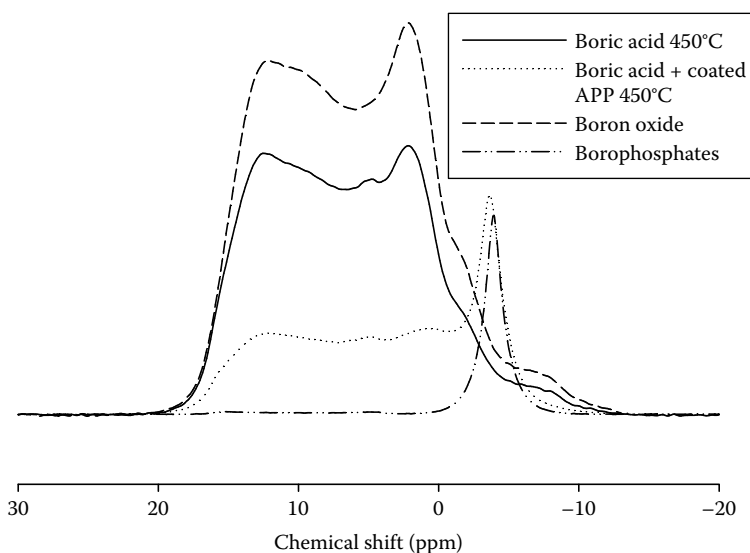


FIGURE 10.3 ^{11}B solid-state NMR spectra of boric acid mixed with APP heat treated at 450°C . (Reproduced from Jimenez, M. et al., *Thermochim. Acta*, 449, 16, 2006. With permission.)

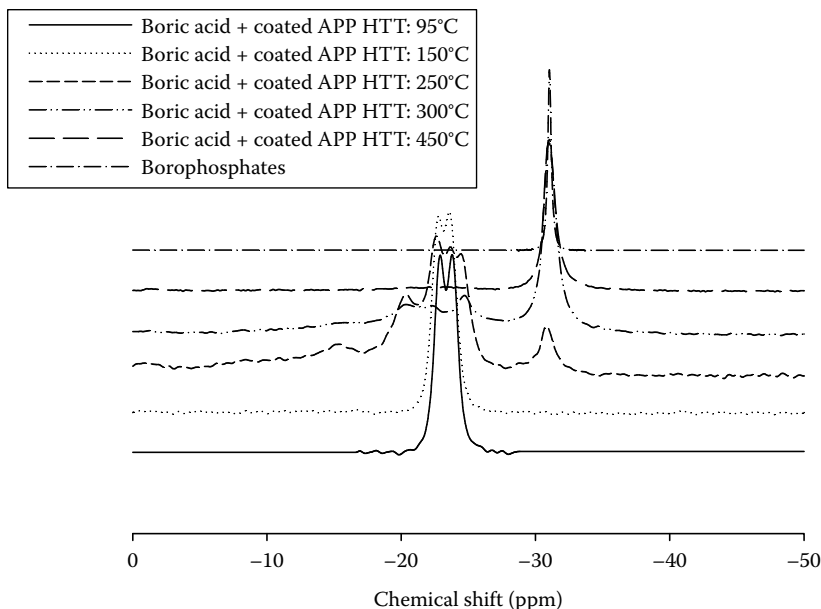


FIGURE 10.4 ^{31}P NMR of a mixture of boric acid and coated APP treated at five different temperatures. (Reproduced from Jimenez, M. et al., *Thermochim. Acta*, 449, 16, 2006. With permission.)

The structural information of charred materials can also be obtained from low-resolution ^1H NMR in the solid state.¹⁴ Since carbonaceous structures form when materials burned are strongly heterogeneous, they should contain regions of different mobilities and thus a study of the molecular dynamics by ssNMR may provide useful information.

This approach has been followed in the case of APP/PER (Pentaerythritol) systems, with or without zeolite (such as 4A zeolite for example), in order to better understand the synergistic effect of these aluminosilicate fillers in polyolefin-based intumescent systems.¹⁵

Figure 10.5 compares the spin-lattice relaxation time (T_1) obtained after inversion-recovery sequences of the APP/PER and the APP/PER-4A systems versus heat treatment temperature (HTT). At every HTT, only one T_1 value was obtained and it can be therefore expected that the slow relaxation domains size will be smaller than 10 nm.

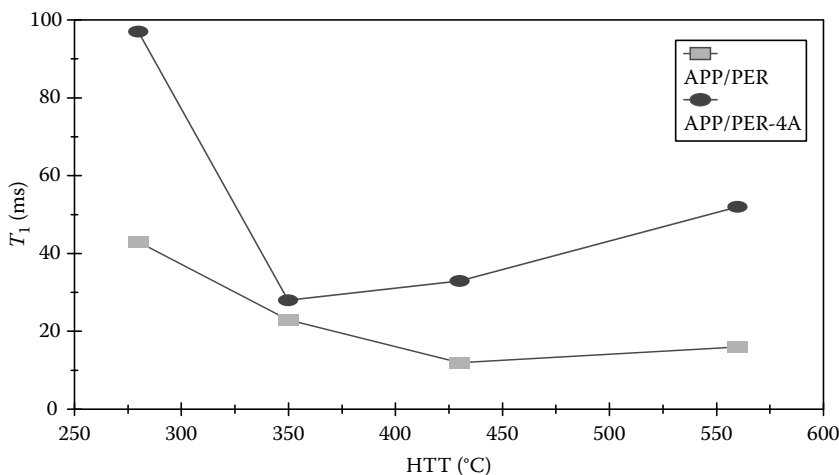


FIGURE 10.5 T_1 values of the APP/PER and APP/PER-4A systems versus HTT (heat treatment temperature).

The comparison between the T_1 values of the two systems (Figure 10.5) shows that their behavior compared to HTT is different. At 280°C, the T_1 value of the system with the zeolite is twice as large as that for the APP/PER system. It was concluded that the materials formed at this temperature are structurally different. Indeed a slower T_1 means that the molecular motions may be hindered and therefore that the structure may be more rigid. Between 280°C and 350°C, the T_1 values decrease and become identical. At 350°C, both systems are organized in stacks of polyaromatic species and it may be proposed that the two materials are structurally, in the NMR sense, similar. At higher temperatures, the T_1 values of the systems with zeolite are always larger. The carbonization process of the two intumescent materials develops in different ways. The zeolite allows molecular motion and the carbonaceous shields keep mobile structures.

As a consequence, it has been proposed that the zeolite has a controlling influence permitting the retention of a “low organized carbon” to temperatures higher than those of the system without zeolite that is responsible for the FR performances of the intumescent material. The low structuration of the carbonaceous matter appears essential to provide the desired fire proofing properties. Indeed the lack of “cohesion” and the quite large structuration in an intumescent coating provide a material that may not accommodate the stresses due to the temperature increase and which enhances the propagation of cracks in preferential directions in the structure. As a consequence it may be proposed that the loss of the protective character is related to changes in the dynamic properties of the intumescent material.

10.3.2 RAMAN STUDIES

Laser Raman spectroscopy complements ssNMR in characterizing the different types of carbonaceous structures formed in the charred materials. Indeed, in the Raman spectra of graphite, there are many features that can be identified and that can provide information about the properties of the materials, such as their electronic structure as well as information about imperfections or defects. Since mechanical, elastic, and thermal properties of graphite are influenced by its structure, Raman spectra could provide interesting information regarding the carbonization process.^{16,17}

As an example, Qu et al.¹⁸ have used laser Raman spectroscopy in order to characterize the structure of intumescent charred layers formed from intumescent halogen-free flame-retardant linear low-density polyethylene (LLDPE) showing excellent fire proofing properties.¹⁹ Laser Raman spectra of the residue obtained after degradation in a tubular furnace of various samples under air show that whereas for the material including expandable graphite (EG) a single peak centered approximately at 1575 cm⁻¹ is observed, in the case of LLDPE/NP28 (a phosphorus–nitrogen compound from Weizheng Fine Chemicals Co., China) blends, two distinct broad peaks centered around 1575 and 1350 cm⁻¹ are observed. The peak around 1575 cm⁻¹ can be assigned to the E_{2g} (C–C vibration) optical mode on the well-ordered defect-free graphite whereas in the presence of disorder an additional line at 1370 cm⁻¹ (defect band assigned to the A_{1g} vibrational mode) and a high-energy shoulder at the E_{2g} line are observed. The carbonaceous structure resulting from the combustion of intumescent systems can therefore be very different (from well-ordered graphite to a disordered system).

Raman spectroscopic measurement was also used to explain the improved thermal stability of nontreated (NoM–C) and silylated cotton fibers (Si–C).²⁰ In the region 3200–3500 cm⁻¹, peaks become more intense and narrower, demonstrating an apparent increase in the –OH group concentration in the ordered phase and an increase in the crystallinity. This phenomenon was explained by the fact that the silylation reaction cannot take place in the crystalline phase. The increase in crystallinity is the result of easier segmental motion, which is facilitated by the reduction of secondary chemical bonds in the amorphous phase. These structural changes explain the higher thermal stability, since the OH groups in the amorphous phase are more sensitive to thermal dehydration.

On the other hand, whereas ssNMR can only be used as *ex-situ* measurement, in the case of Raman spectroscopy, Raman microscopy can be used in order to heat the samples while the changes in the surface can be detected spectroscopically.

As an example, Marosi et al.²¹ have followed this approach to investigate the effect of surface and interface modifications in intumescent systems including MMT nanoparticles. The formulations

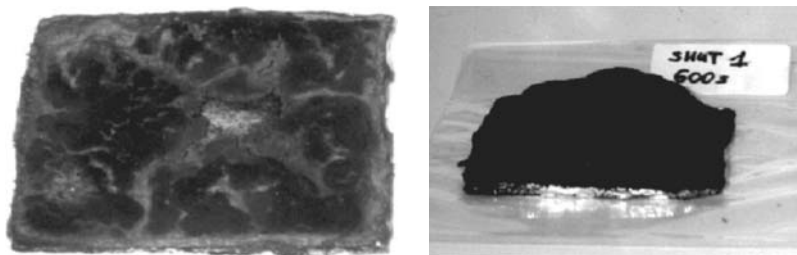


FIGURE 10.6 Characteristics of char formed during the cone calorimeter measurement of IFR-PP without BSil (on the left) and with BSil (on the right). (Reproduced from Marosi, Gy. et al., *Polym. Degrad. Stab.*, 82, 379, 2003. With permission.)

combine in a polypropylene (PP) matrix, MMT nanoparticle, an intumescent flame retardant system (IFR consisting of 75% APP and 25% polyol), and borosiloxane (BSil) elastomer, used as synergist. As far as the flame-retardant properties are considered, the combination of IFR and MMT shows some improvement but the best results are achieved when BSil is added to the system.

Figure 10.6 compares the charred residue obtained from IFR-PP formulations without and with BSil. The broken char observed in the absence of BSil hardly controls the gas transport, while with BSil the char forms a continuous barrier layer even if the evolving gases inflate it.

Raman spectra of the surface of a formulation containing 4% MMT and 4% MMT + 2% BSil (Figure 10.7) suggest no significant change due to heat treatment when MMT is used alone whereas the characteristic band of BSil-coated MMT appears in the spectra in the presence of BSil after treatment proving its accumulation on the surface. This was explained by the fact that BSil coating on particles reduces their surface energy considerably that gives a chance for MMT nanoparticles to migrate to the surface. The nanoparticles attached to each other with the coating layer form a stable and flexible protective layer on the surface resulting in a higher efficiency.

10.3.3 X-RAY PHOTOELECTRON SPECTROSCOPY

X-ray photoelectron spectroscopy (XPS) is also of great interest in the study of intumescence and in the chemical characterization of the charred material in order to better understand the condensed phase action of such FR systems.²²⁻²⁴ Similarly to ssNMR, it gives information on each element separately and provides detailed information about the elemental composition of charred materials. It is also a good complement to other spectroscopic techniques, in particular to ssNMR. As an example, in the case of nitrogen-containing system, the ¹⁵N NMR of the solid state cannot be used to characterize the N surroundings because of the low isotopic abundance of ¹⁵N (0.4%) that would require a very large number of scans to obtain only a very weak signal. Other spectroscopies, such as infrared, ¹³C and ¹H NMR, do not directly characterize nitrogen-based species in char. XPS can thus be used to characterize nitrogen compounds of coal and carbonaceous materials^{25,26} and is therefore a powerful tool in that way. Moreover, XPS of char also allows the characterization of the oxidized species intermediates for the degradation of the protective layer.

Kodolov et al.²⁷ investigated the role of modifying additives in epoxy intumescent compositions (epoxy resin + APP + polyethylene polyamine) using this technique. Modifying additives include manganese dioxide and calcium borate leading to the formation of mineral net structures in the surface layers of the intumescent coating and carbon-metal-containing tubulenes favoring the formation of foam cokes of a certain structure. Nickel-containing carbon tubules are the active precursors of a new carbon phase. This new phase presents different thermal and mechanical properties (heat capacity, porosity, etc.) resulting in a modification of the fire performance.

XPS analysis of char samples, including EG, is also of great interest.²⁸ Since, XPS provides the elemental composition of charred materials, information regarding the carbon accumulation and

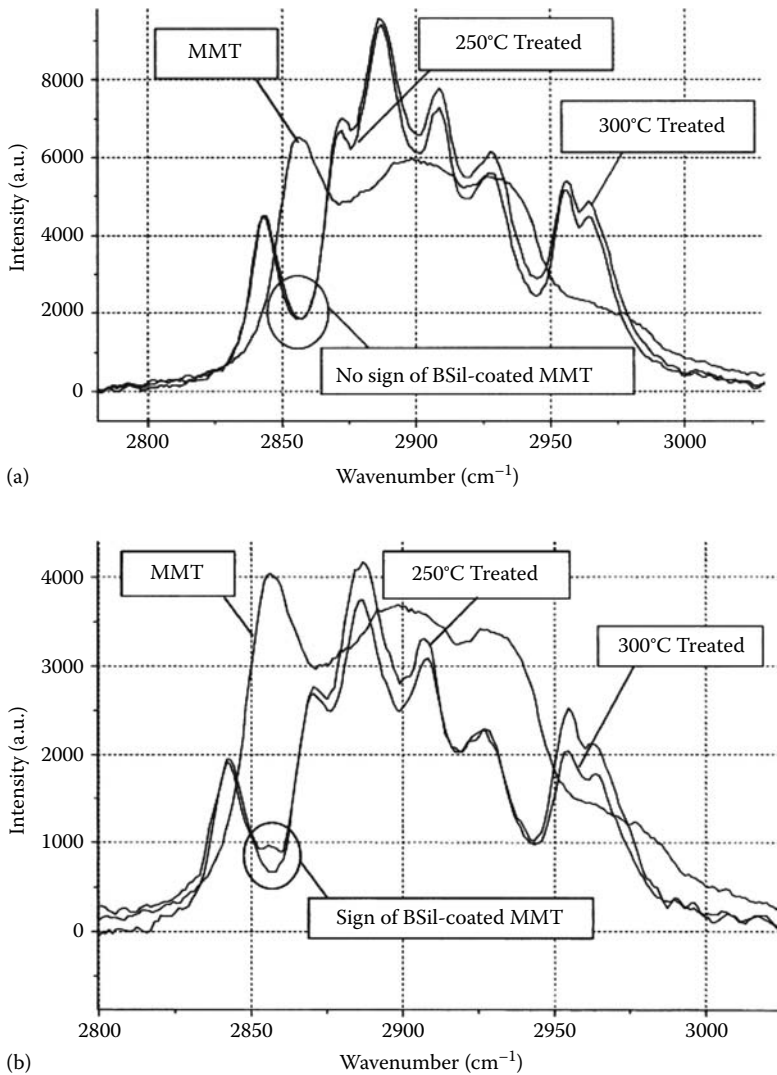


FIGURE 10.7 Raman spectra taken from the surface of PP+4% MMT (a) and PP+4%MMT+2%BSil (b) before and after a heat treatments at 250°C and 300°C for 2 min. (Reproduced from Marosi, Gy. et al., *Polym. Degrad. Stab.*, 82, 379, 2003. With permission.).

the oxidation properties of char structure is available. The comparison of the elemental composition of intumescent coatings (acrylic resin including APP, PER, and melamine) including EG or not including EG (Table 10.1) demonstrates that the degree of carbon accumulation and anti-oxidation properties of the char structure formed from No3 EG coating are better than those formed from No1 coating. A high degree of carbon accumulation and good anti-oxidation properties are favorable to the fire resistance of coatings. This XPS analysis shows that No3 EG coating can provide a good resistance to flame erosion and is uneasily damaged by oxidation when exposed to a fire.

10.4 DYNAMIC CHARACTERIZATION

Fire-retarded materials functioning in the condensed phase, such as intumescent systems, form, on heating, foamed cellular charred layers on the surface, which protects the underlying material from the action of the heat flux or the flame. It is recognized that the formation of the effective char occurs via a

TABLE 10.1
Element Composition of Charred Materials
Obtained from Intumescent Coatings without EG
(No1 Coating) and with EG (No3 EG Coating)

Sample	O (%)	C (%)	P (%)
No1 coating	40.2	51.8	8
No3 EG coating	18.8	74.7	6.4

Source: Reproduced from Wang, Z. et al., *Corrosion Sci.*, 49, 2237, 2007. With permission.

semiliquid phase, which coincides with gas formation and expansion of the surface.²⁹ Simultaneously with the expansion, the liquid char starts to solidify giving rise to a solid, cellular, and foamed char. Gases released from the degradation of the intumescent material, and in particular from the blowing agent, have to be trapped and must diffuse slowly in the highly viscous melted degraded material in order to create a layer with an “adapted” morphological properties as shown in Figure 10.8.

The way the gases diffuse into the semiliquid degraded matrix will sharply affect the structure of the residual char as well as its thermal and mechanical properties. As an example, a comparison on the heat capacity of an intumescent epoxy-based composition versus temperature shows a sharp increase between 373 and 480 K.²⁷ This result was attributed to the evolution of water and ammonia vapor into the bubbles being formed leading to an increase in the pressure inside the bubbles. On the contrary, in the presence of modifying agent (such as manganese dioxide, calcium borate, or carbon-metal-containing tubulenes) the heat capacity changed without any considerable change in peaks. The difference in the behavior of the modified composition was attributed to a smoother gas formation process resulting in the formation of foam cokes of an efficient structure.

The control of the structure of the foamed residue is linked not only with the gas formation process but also with the viscosity of the semiliquid degraded matrix. Indeed, if the degraded matrix is too liquid, an easy diffusion of gases takes place, in which gases are not trapped but escaped to feed the flame. The viscosity of the degraded matrix in the blowing phase is, as a consequence, a deciding factor.^{30–32}

Moreover, in the stabilization phase of the intumescent structure, the change in the viscosity of the charred material under stress may explain the loss of the protective character of the intumescent shield. Indeed, if the shield becomes too hard, the creation and the propagation of cracks leading to a rapid degradation of the material occurs.³³

Finally, the mechanical destruction of the intumescent char is also an important task for investigation. If a char has good structural, morphological, and heat insulative properties but is easily destroyed under mechanical action, its efficiency is totally lost in the turbulent regime of combustion.

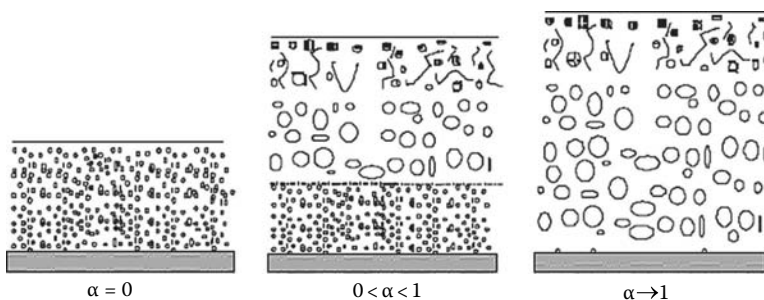


FIGURE 10.8 Development of the intumescent process (α = conversion degree).

So, the viscoelastic properties of intumescent materials in the range of temperature corresponding to the development, the stabilization, and the destruction of the protective shield are, as a consequence, an important task of investigation. The way to investigate those parameters is detailed in Section 10.4.1.

10.4.1 STUDY OF THE DYNAMIC VISCOSITY DURING CARBONIZATION

As previously mentioned, the viscosity of the polymer at the beginning of the development of the intumescence is an important factor affecting the development of the expanded layer. In particular, the viscosity of the degraded polymer could affect the char morphology in that range of temperature since it results from the diffusion of the gases of degradation in that matrix as previously mentioned. The carbonization process could thus be investigated by studying the modification of the viscosity versus time of the FR material.

In that way, the viscoelastic behavior of a PP-based intumescent formulation including polyurethane (PU) as carbon source in association with APP has been evaluated.³⁰ The use of PU/APP mixture in PP brings a decrease in the peak heat release from 1700 kW/m², in the case of the virgin matrix, to 300 kW/m², in the case of the intumescent formulation.

The curve of the apparent viscosity data versus temperature for PP/PU/APP is reported in the Figure 10.9. In the first step (200°C–240°C), the viscosity of the material decreases when the temperature increases following the behavior of a thermoplastic material. Even though we observe in this step a carbonization of the material surface, the polymeric matrix has been preserved under the surface. In the 240°C–300°C temperature range, the viscosity value slightly decreases and its value remains close to the low apparent viscosity of the material molten at 240°C. The sample appears as completely carbonized and liquid. The plateau may then be explained by the chemical transformation of the material (formation of phosphoric acid esters and aromatic species).³³

Between 300°C and 360°C, the viscosity value is very low and decreases slightly. The material forms a pasty intumescent shield only on the material surface, and most of the material remains as a liquid. In this step, there is coexistence between a liquid phase and a solid phase, the liquid phase may be assumed to be responsible for the viscosity data.

At 360°C–370°C, an important increase in the apparent initial viscosity begins that corresponds to the complete degradation of the initial material and to the carbonization of the system. The foamed material appears to be constituted by solid particles only. From 450°C–460°C, the viscosity value is more stable and increases slightly. At this temperature, a char oxidation/degradation probably starts. Complementarily, the viscosity can be analyzed versus temperature and versus time (Figure 10.10) in order to better visualize the mechanical and thermal stabilities of the protective intumescent layer and to have a better understanding of the carbonization process.

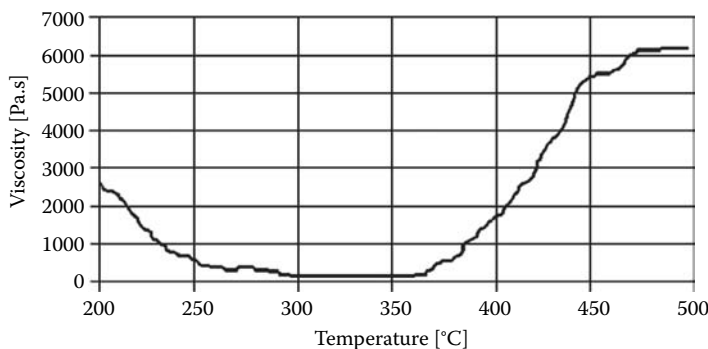


FIGURE 10.9 Apparent viscosity values versus temperature of PP/PU/APP system. (Adapted from Bugajny, M. et al., *Fire Mater.*, 23, 49, 1999.)

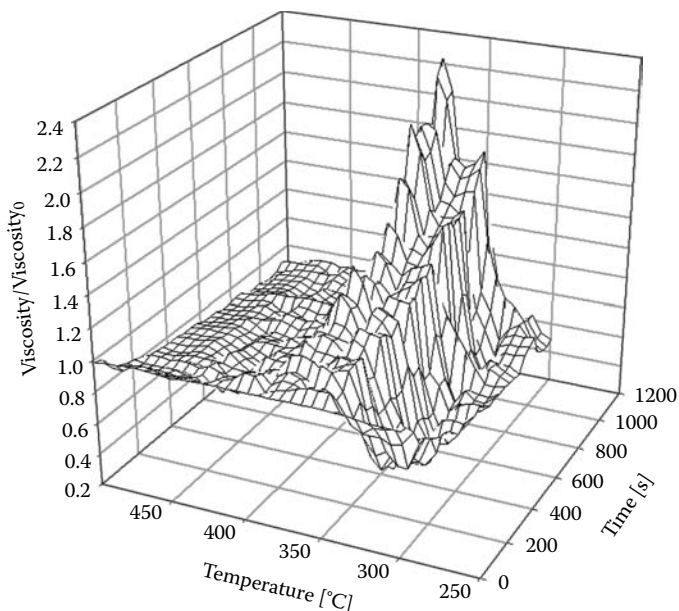


FIGURE 10.10 Relative change of the apparent viscosity of heat-treated PP/PU/APP versus temperature and time. (Adapted from Bugajny, M. et al., *Fire Mater.*, 23, 49, 1999.)

In the 300°C–340°C temperature range, the apparent viscosity of the material under strain decreases with time. After 20 min, the final value of viscosity corresponds to 0.6 times the initial value. This result was attributed to strain breaking of the residual polymeric chains and/or to a free radical process leading to a decrease in the polymer chain length.

On the contrary, the apparent viscosity increases with time in the temperature range of 340°C–390°C at which the intumescent process takes place. At 370°C (at this temperature the initial viscosity begins to increase strongly, see Figure 10.9) the relative increase is maximum and corresponds to two times the initial value. In that step, the formation of the polyaromatic stacks linked by polymer (PP) chains and phosphate species^{33,34} occurs despite the applied strain. The observed high value of the viscosity under strain explains the preservation of the protective character of the intumescent material observed in the temperature range. The viscosity is high enough to enable “encapsulation” of the trapped gaseous products resulting in the degradation of the material and the accommodation of stress induced by solid particles and the presumed high pressure of the trapped gases.

The behavior of the material heat treated at a temperature higher than 400°C under stress with time is very interesting. Indeed, the viscosity decreases dramatically in the first 200 s of the strain treatment, then slightly decreases with highest time. It has been proposed that the temperature/strain treatment leads to the degradation of the intumescent material (break of the polyethylenic links and evolving of the corresponding polyethylenic chains),³⁴ which is responsible for the observed loss of the dynamic property of interest and then of the formation of cracks in the material and, as a consequence, of the loss of the protective performance despite the important expansion and the comparatively high value of the nearly constant initial viscosity of the heat-treated material.

The study of the viscosity of intumescent systems appears, as a consequence, to be an important way to better understand the carbonization process. The data obtained from this technique agree and complement the results obtained during the examination of the chemical composition of the intumescent shield. Moreover, it has to be highlighted that, to the contrary of most of the chemical investigations of the carbonization process, this technique studies the material in situ whereas most of the charred chemical compositions are evaluated after combustion and cooling of the sample.

10.4.2 MEASUREMENT OF THE EXPANSION DEGREE

The formation of an expanded char layer is a crucial requirement for an intumescent system. The expansion degree strongly influences the flame-retardant properties of the material. However, the higher expansion does not necessarily lead to the highest FR performance since the structure of the char (in particular, the bubble's size and distribution) will also affect the thermal properties of the insulative layer. The expansion degree can be measured after the experiment but the measurement of expansion versus temperature is also reported in the literature.^{32,35} The measurement of the expansion versus temperature can be obtained using a plane–plane rheometer (Figure 10.11) applying a low normal force on the sample with or without strain.

As an example, Figure 10.12 compares the expansion versus the temperature of four intumescent epoxy-based coatings with that of the virgin resin. The intumescent coatings are formulated using two main FR agents: (1) a mineral acid, boric acid (H_3BO_3) (Aldrich, 99%) and (2) a commercial APP derivative supplied by Clariant (Germany), containing 20% phosphorus. Boric acid acts as an intumescent agent. It has been proposed that the formation of B_2O_3 due to the dehydration of the boric acid leads to the formation of a “glass-like” material, which increases the viscosity of the melt (compared with the unmodified resin) and prevents the escape of gaseous decomposition products to feed the flame.³⁶

Whereas no expansion is observed for the virgin resin, the four coatings show maximum expansion between 300°C and 350°C. The expansion is attributed to the evolution of volatile degradation products of the resin as well of the intumescent additives, which are trapped in the structure.

Table 10.2 compares the fire resistance properties obtained in the UL 1709 test with the expansion measured with the rheometer. The goal of intumescent coatings is to decrease, as much as possible, the slope of the time/temperature curve, i.e., reaching a failure temperature as late as possible. For regular reinforcing steel, the critical temperature is 538°C, whereas for prestressed steel bars that are made of high carbon, cold drawn steel instead of low carbon, hot-rolled steel, the critical temperature is significantly lower at 427°C. The temperature of 500°C has been officially adopted as a standard for normal loaded structural components, whereas the temperature of 400°C has been unofficially adopted as a standard for heavily loaded structural components.³⁷ As a consequence, the time of failure is obviously one of the parameters to be optimized. The best result is obtained when the longest time of failure is reached, which means that the coating has the best protective effect. The best results are achieved for IF8, which has a time to failure of 38.1 min.

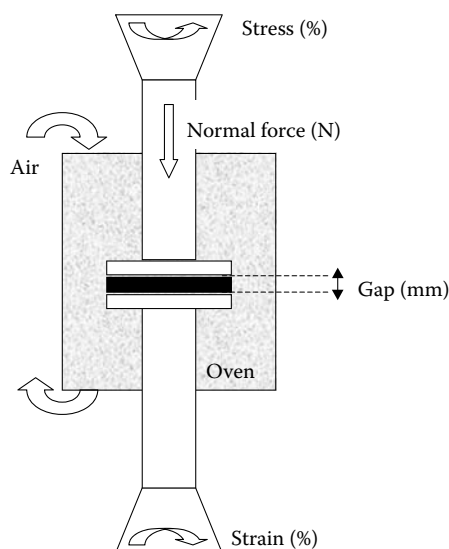


FIGURE 10.11 Scheme of the rheometer in the parallel plates configuration.

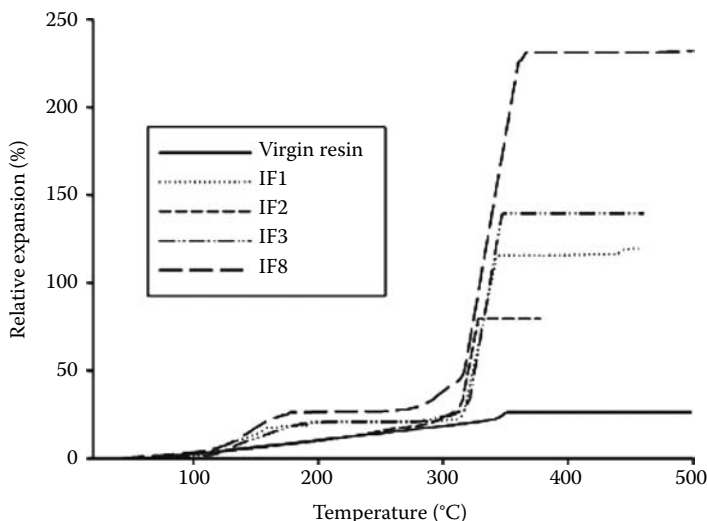


FIGURE 10.12 Comparison of the expansion measured in the rheometer of different formulations. (Reproduced from Jimenez, M. et al., *Ind. Eng. Chem. Res.*, 45, 4500, 2006. With permission.)

The relative expansion in the furnace test was determined by measuring the thickness of the coating before and after the test. The expansion in the furnace is considered as a key parameter in the development of fire protective coatings. Indeed, as discussed previously, one of the major characteristics of an intumescent coating is its ability to swell. This parameter is necessary but not sufficient to ensure fire protection. Indeed, a high swelling does not necessarily lead to the best performance, because the char formed can be too light and not sufficiently mechanically resistant.³⁸ The aim is to obtain a multicellular-charred layer in order to minimize the heat transfer to the steel plate and to provide good protection for the substrate. However, in the present study, Table 10.2 clearly shows that the coatings with the longest time to failure exhibit a higher expansion. Table 10.2 also shows that the measurements of the expansion carried out in the furnace test or in the rheometer agree. Indeed, the same ranking is obtained in both cases even if direct correlation is not possible.

It has to be noted that the measurement of the dynamic expansion can be also obtained using an infrared camera and a image analysis. This approach has been recently developed and first results are presented in Chapter 6 of this book.³⁹

TABLE 10.2
Fire Resistance and Intrinsic Properties of Epoxy-Based Intumescent Formulations

	UL 1709–Furnace Test		Rheological Measurement
	Failure Time (min)	Expansion (%)	Expansion (%)
Virgin resin	5	10	26
IF1	11.3	500	99
IF2	18.2	550	116
IF3	30	730	139
IF8	38.1	1164	190

10.4.3 INVESTIGATION OF THE CHAR STRENGTH

Finally, when dealing with fire retardancy or fire protection, an important parameter that has to be investigated regarding the carbonization process, or more precisely regarding the properties of the protective layer, is its strength. Indeed, when exposed to a fire, the charring residue can be exposed to internal pressure (from the degradation gases) or to external pressure (for example, to a jet fire flame). If the char is brittle, crack formation occurs or the char collapse and the FR performance are lost. Developing techniques that allow char strength characterization is thus an important topic of investigation.

In that frame, the use of a plane–plane rheometer has been evaluated. The purpose of the experiment carried out in the rheometer is not to mimic fire testing (this is not possible since the heating rate [slow ramp vs. quenching], heating source [convection vs. radiation], sample size, and boundaries effect are different) but to develop a test method that will permit the characterization of the char strength when exposed to pressure (in that case compression force).

In order to do that, a sample is placed in the oven of the rheometer heated to the desired temperature before measurement in order to enable the development of the intumescence without any perturbation. Then the upper plate is put in contact with the material and is then linearly pushed down, and the compression force is followed in comparison to the distance between the two plates. This is illustrated in Figure 10.13.

This approach can be followed in order to demonstrate the presumed reinforcing effect of nanoparticles in intumescent systems.⁴⁰ As an example, Figure 10.14 compares the compression force versus the gap of intumescent-based formulations without and with nanoparticles. Moving the upper plate downward the normal force takes up a nearly constant value, which can be considered proportional to the strength of the individual bubble. After breaking the charred structure, the normal force increases significantly because of the compression of the charred layer. This clearly demonstrates that, whereas spherical nanoparticles (SiO_2) do not modify the strength of the char obtained after heat treatment, the addition of lamellar nanoparticles (organomodified MMT (OMMT) or LDH) leads to its significant increase. The higher mechanical stability of the intumescent shield obtained in the presence of OMMT and LDH avoids the formation of cracks and so heat and mass transfers between the flame and the underlying material are limited leading to the interruption of the combustion triangle. Those results agree well the cone calorimeter measurements (Figure 10.15).

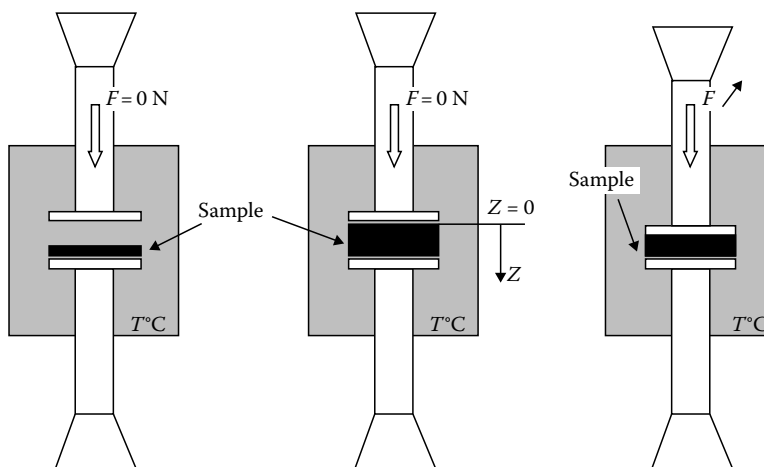


FIGURE 10.13 Char strength measurement. (Reproduced from Jimenez, M. et al., *Ind. Eng. Chem. Res.*, 45, 4500, 2006. With permission.)

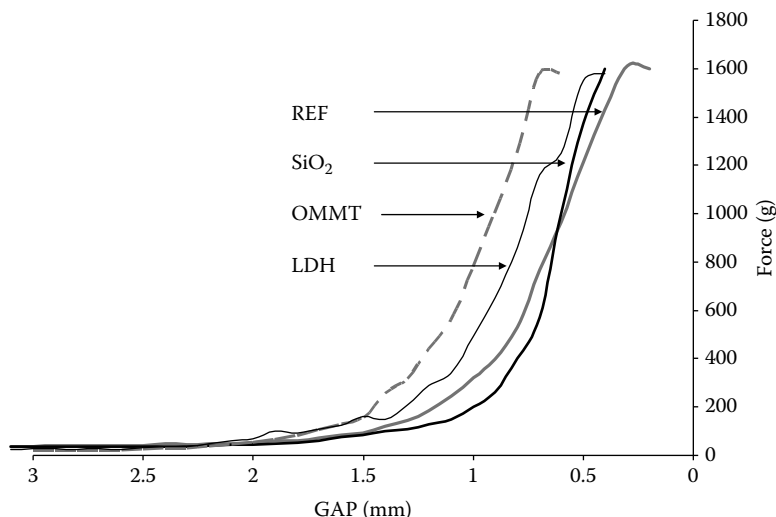


FIGURE 10.14 Compression force versus gap of EVA/PA6/APP-based intumescent formulations measured at 400°C without (REF) and with nanoparticles (SiO₂, silica; OMMT, organomodified montmorillonite; LDH, lamellar double hydroxide).

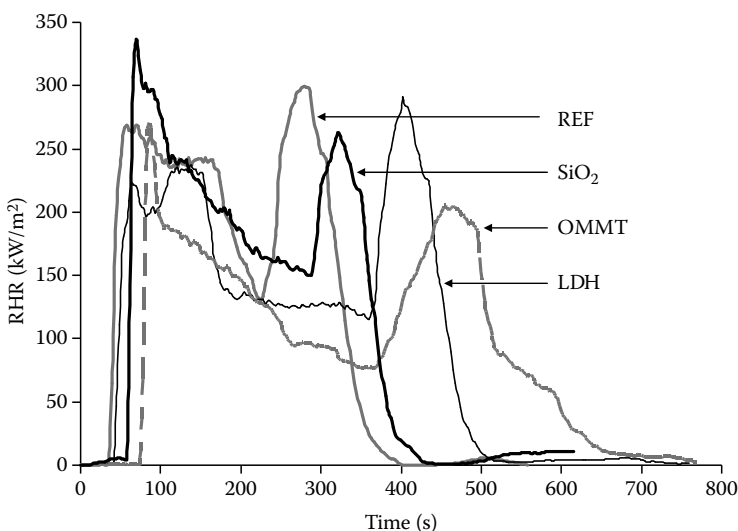


FIGURE 10.15 Rate of heat release versus time of EVA/PA6/APP-based intumescent formulations without (REF) and with nanoparticles. SiO₂, silica; OMMT, organomodified montmorillonite; LDH, lamellar double hydroxide.

Whatever the formulations, curve of the rate of heat release versus time shows two peaks, the first before 200 s (t_1) and the second between 300 s (REF) and 500 s (OMMT), which is the typical behavior of intumescent systems. The first peak is attributed to the formation of the intumescent protective shield that leads to a decrease in heat and mass transfers between the flame and the material. When this shield is formed, the RHR decreases and a plateau is observed in some cases. The second peak corresponds to the destruction of the intumescent layer leading to a sharp emission of flammable gases, the higher the time for the second peak, the higher the thermal and mechanical stabilities of the intumescent shield. Then, a thermally stable residue is formed. When lamellar

nanoparticles are added to the formulation, the time to the second peak heat release occurs around 200 s later than in the case of the reference formulation. This result demonstrates that the formation of the intumescent shield is modified when OMMT or LDH is added to EVA/APP/PA6 and that the intumescent shield formed is thermally and/or mechanically more stable.

A similar approach was followed to study the effect of MMT and sepiolite additives on an epoxy resin combined with a newly synthesized phosphorus-containing reactive amine, which can be used both as cross-linking agent and flame retardant.⁴¹ Similarly, it has been observed that the char of the reference sample is a more rigid char, with a bigger average bubble diameter, while the flame-retarded system provides a stronger, more uniform char with a smaller average bubble size.

10.5 MORPHOLOGY OF CARBONACEOUS STRUCTURES

As shown in Sections 10.3 and 10.4, the chemical composition of the degrading system as well as its dynamic properties will directly influence the morphology of the resulting charred protective structure that affects the properties of the system and, in particular, its thermal properties. Since intumescent systems act in the condensed phase limiting the heat transfer from the flame to the substrate, all those parameters are linked with the efficiency of the system. Moreover, to separate oxygen more efficiently from the degraded volatile component, the insulating barrier should be compact enough to prevent the penetration of gases. As a consequence, analyzing the morphology of the charred structure using adapted techniques appears as an interesting way to better understand the relation between structure and properties.

10.5.1 X-RAY DIFFRACTION

X-ray diffraction (XRD) has been poorly used to characterize the carbon phase of intumescent structure. Indeed, as shown previously, the carbon structure resulting from the development of the intumescent system is mainly disordered whereas XRD characterizes ordered structure. However, this technique may be of interest to study the carbonization process in the case of flame-retardant systems containing layered additives, such as expandable graphite,^{28,42} or even more in the case of lamellar nanocomposites, such as MMT-based nanocomposites.

Kashiwagi et al.⁴³ have investigated the composition of the carbonaceous floccules formed from PA6/clay after exposure at an external flux of 50 kW/m² in gasification experiments using wide-angle XRD measurements (Figure 10.16). The XRD data of original materials show the typical pattern of α crystalline phase of PA6; that of the original Na-clay shows many peaks with the d-spacing of about 1.19 nm (at 2θ of about 7.448), the γ crystalline phase is observed in the case of the PA6/clay(5%) original sample. It is reported in the literature that the presence of silicate layers favors the formation of the γ -phase.⁴⁴ Meanwhile, the addition of silicate layers changed the crystal structure of the PA6 matrix.

The data for the carbonaceous floccules residue collected show a reduction in the γ crystalline phase of PA6 in the residues with the sample mass loss as well as a decrease of the d-spacing of the clay in the black residues. Any PA6 characteristic structure disappears from the residues collected after losing more than 38% of the sample mass loss. However, since the d-spacing in the floccules always remains higher than that of the original clay (without organic treatment), it appears that some organic materials could be trapped in the space between the clay platelets. The pattern for the black residues indicate that the PA6/clay (5%) sample tends to form a small quantity of highly thermally stable organic components possibly having a graphitic structure (new peaks at $2\theta = 26.5$ and 27.38 close to that of ordered graphite spacing 3.354\AA). It was speculated that such a structure could be formed in the narrowly spaced clay platelets.

XRD analysis could also provide interesting information regarding the inorganic materials formed during the carbonization process in complex formulations.^{28,36} As an example, in the case of intumescent coatings, the formation of titanium pyrophosphate resulting from the reaction between APP and titanium dioxide can be demonstrated (Figure 10.17).

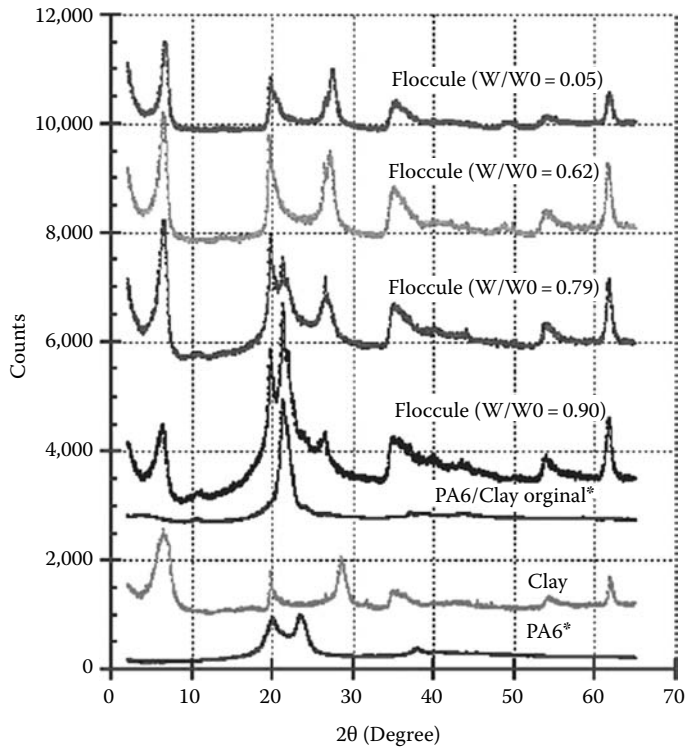


FIGURE 10.16 XRD of PA6, clay, PA6/clay (5%), and carbonaceous floccules collected at various fractions of sample mass loss at 50 kW/m^2 in N_2 . *PA6 and PA6/clay original values reduced to 10% of measured values. (Reproduced from Kashiwagi, T. et al., *Polymer*, 45, 881, 2004. With permission.)

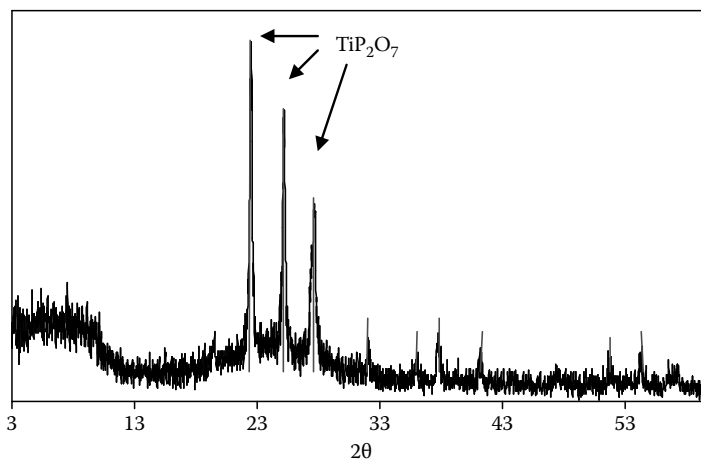


FIGURE 10.17 XRD pattern of residue obtained from an intumescent paint.

10.5.2 MICROSCOPY

Optical microscopy can be used to characterize the surface of the charred residue after heat treatment. As an example, Figure 10.18 compares the optical microscopy of virgin PU coatings with that of fire-retarded coatings. Whereas cracks are observed on the surface in the case of PU, large

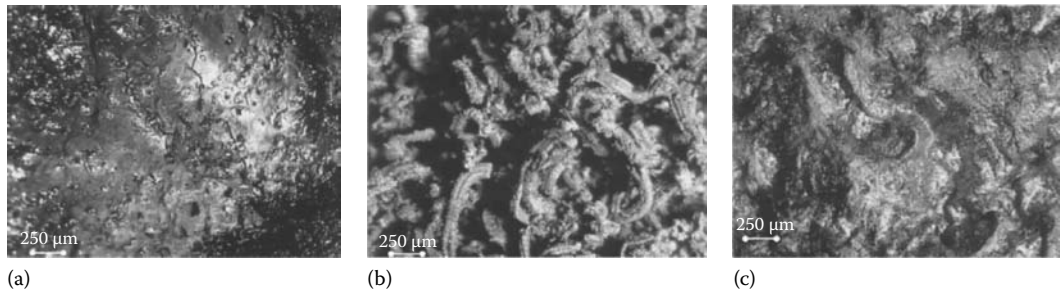


FIGURE 10.18 Optical microscopy picture of the surface of PU (a), PU/EG (b), and PU/APP (c) coatings after exposure at 800°C during 15 min (magnification $\times 40$). (Reproduced from Duquesne, S. et al., *Polym. Degrad. Stab.*, 77, 333, 2002. With permission.)

domains of deformation are observed for PU including APP coating. In that case, a “hills and valleys” topography is observed. This is linked with the rheological properties of the char obtained when combining APP with PU that allows deformation rather than cracking of the surface, which favors the FR performance. In the case of PU with EG, the structure of the surface is mainly composed of expanded graphite flakes. Thus, the behavior of the protective layer formed from several formulations will be different regarding the insulation of the substrate from oxygen. Indeed, the structure obtained in the case of PU/APP is compact enough to separate oxygen from the degraded volatile component resulting in high fire performance.

Similarly, it is possible to characterize the morphology of intumescent chars using scanning electron microscopy (SEM). SEM micrographs of the intumescent char samples obtained from fire-retarded LLDPE/EG blends with NP28 (a phosphorus–nitrogen compound from Weizheng Fine Chemicals Co., China) appears more compact than the one resulting from LLDPE/EG/APP samples. This provides evidence that NP28 has a better synergistic effect with EG than does APP.^{19,45}

Finally, the use of transmission electron microscopy (TEM) is of interest when dealing with the study of residual char obtained when MMT nanocomposites decompose. Figure 10.19 compares TEM images of an original PA6/clay sample with that of its residue collected at 17% sample mass

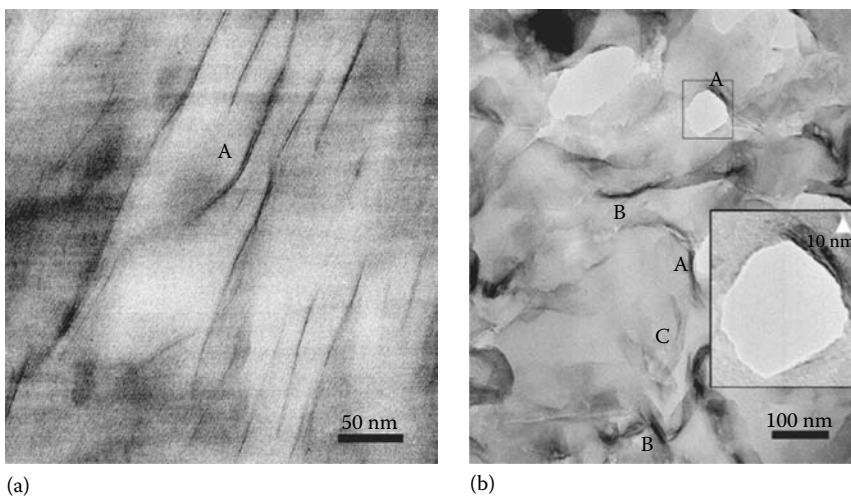


FIGURE 10.19 Comparison of the TEM images of the original (injection molded) PA6/clay (5%) (a) and of the outside of carbonaceous floccule collected when the PA6/clay (5%) sample lost 17% mass loss at 50 kW/m² in a nitrogen atmosphere (b). (Reproduced from Kashiwagi, T. et al., *Polymer*, 45, 881, 2004. With permission.)

loss. In the original sample, the clay platelets are fully exfoliated whereas large groups of wavy clay platelets are found in the carbonaceous floccule residues. The platelets are much closer to each other than those in the original sample. Those data show the initially well-dispersed clay particles in the sample tend to accumulate on the sample surface during burning/gasification to form protective floccules consisting of thermally stable organics (some of which could be carbonaceous char).

10.6 CONCLUSION

This chapter describes some of main techniques that can be used to study the carbonization process occurring when polymers, and, in particular, fire-retarded polymers burn. It has been shown that most of the techniques are complementary and combinations of techniques are often required to fully understand the carbonization process of a system. There are a number of variables influencing the amount and the nature of the charred residue released affecting char properties. The use of such a number of techniques is time consuming and expensive, and, in most cases, only comparison between similar formulations is possible, whereas general trends are not. Predicting how polymeric materials respond to high temperatures and what kind of structure (strength, porosity, etc.) can be formed from a composition under certain conditions is nowadays not possible and is an important question to answer in the coming years. In order to do that, a recent simulation analyzing in atomistic detail the morphological changes that result during the transformation of polymer into char has been reported.⁹ Special attention has to be paid to this approach in order to better understand the mechanisms involved in the formation of char and to answer many fundamental questions.

REFERENCES

1. Samyn, F. 2007. Compréhension des procédés d'ignifugation du polyamide 6, Apport des nanocomposites aux systèmes retardateurs de flamme phosphorés. PhD dissertation, University of Lille, Lille, France.
2. Bourbigot, S., Duquesne, S., Samyn, S., and Vannier, A. 2008. How to design polymer nanocomposites with flame retardants? *Paper Presented at the Annual BCC Conference on Flame Retardancy*, Stamford, CT.
3. Bourbigot, S., LeBras, M., Dabrowski, F., Gilman, J., and Kashiwagi, T. 2000. PA-6 clay nanocomposite hybrid as char forming agent in intumescent formulation. *Fire and Materials* 24:201–208.
4. Wang, Z., Han, E., and Ke, W. 2006. Effect of acrylic polymer and nanocomposite with nano-SiO₂ on thermal degradation and fire resistance of APP-DPER-MEL coating. *Polymer Degradation and Stability* 91(9):1937–1947.
5. Wang, Z., Han, E., and Ke, W. 2005. Influence of nano-LDHs on char formation and fire-resistant properties of flame-retardant coating. *Progress in Organic Coatings* 53(1):29–37.
6. Vannier, A., Duquesne, S., Bourbigot, S., Castrovinci, A., Camino, G., and Delobel, R. 2008. The use of POSS as synergist in intumescent recycled poly(ethylene terephthalate). *Polymer Degradation and Stability* 93(4):818–826.
7. Kashiwagi, T., Du, F., Winey, K.I., Groth, K.M., Shields, J.R., Bellayer, S., Kim, S., and Douglas, J.F. 2005. Flammability properties of polymer nanocomposites with single-walled carbon nanotubes: Effects of nanotube dispersion and concentration. *Polymer* 46(2):471–481.
8. Gupta, R. 2007. Advanced coal characterization: A review. *Energy and Fuels* 21(2):451–460.
9. Lawson, J.W. and Srivastava, D. 2008. Formation and structure of amorphous carbon char from polymer materials. *Physical Review B—Condensed Matter and Materials Physics* 77(14):144209/1–144209/6.
10. Lu, L., Kong, C., Sahajwalla, V., and Harris, D. 2002. Char structural ordering during pyrolysis and combustion and its influence on char reactivity. *Fuel* 81(9):1215–1225.
11. Delobel, R., LeBras, M., Ouassou, N., and Alistiqa, F. 1990. Thermal behaviors of ammonium polyphosphate-pentaerythritol and ammonium pyrophosphate-pentaerythritol intumescent additives in polypropylene formulations. *Journal of Fire Sciences* 8(2):85–108.
12. Jimenez, M., Duquesne, S., and Bourbigot, S. 2006. Characterization of the performance of an intumescent fire protective coating. *Surface and Coatings Technology* 201(3–4):979–987.

13. Jimenez, M., Duquesne, S., and Bourbigot, S. 2006. Intumescent fire protective coating: Toward a better understanding of their mechanism of action. *Thermochimica Acta* 449(1–2):16–26.
14. Bourbigot, S., Le Bras, M., Delobel, R., Decressain, R., and Amoureux, J.P. 1996. Synergistic effect of zeolite in an intumescence process: Study of the carbonaceous structures using solid-state NMR. *Journal of the Chemical Society—Faraday Transactions* 92(18):3435–3444.
15. Bourbigot, S., Le Bras, M., Duquesne, S., and Rochery, M. 2004. Recent advances for intumescent polymers. *Macromolecular Materials and Engineering* 289(6):499–511.
16. Dresselhaus, M.S., Dresselhaus, G., Saito, R., and Jorio, A. 2005. Raman spectroscopy of carbon nanotubes. *Physics Reports* 409(2):47–99.
17. Reich, S. and Thomsen, C. 2004. Raman spectroscopy of graphite. *Philosophical Transactions of the Royal Society A: Mathematical, Physical and Engineering Sciences* 362(1824):2271–2288.
18. Qu, B. and Xie, R. 2003. Intumescent char structures and flame-retardant mechanism of expandable graphite-based halogen-free flame-retardant linear low density polyethylene blends. *Polymer International* 52(9):1415–1422.
19. Xie, R.C. and Qu, B.J. 2001. Synergistic effects of expandable graphite with some halogen-free flame retardants in polyolefin blends. *Polymer Degradation and Stability* 71(3):375–380.
20. Anna, P., Zimonyi, E., Márton, A., Szép, A., Matkó, Sz., Keszei, S., Bertalan, Gy., and Marosi, Gy. 2003. Surface treated cellulose fibres in flame retarded PP composites. *Macromolecular Symposia* 202:245–254.
21. Marosi, Gy., Márton, A., Szép, A., Csontos, I., Keszei, S., Zimonyi, E., Toth, A., Almeras, X., and Le Bras, M. 2003. Fire retardancy effect of migration in polypropylene nanocomposites induced by modified interlayer. *Polymer Degradation and Stability* 82(2):379–385.
22. Bourbigot, S., Le Bras, M., Gengembre, L. and Delobel, R. 1994. XPS study of an intumescent coating. Application to the ammonium polyphosphate/pentaerythritol fire-retardant system. *Applied Surface Science* 81(3):299–307.
23. Bourbigot, S., Le Bras, M., Delobel, R. and Gengembre, L. 1997. XPS study of an intumescent coating II. Application to the ammonium polyphosphate/pentaerythritol/ethyleneic terpolymer fire retardant system with and without synergistic agent. *Applied Surface Science* 120(1–2):15–29.
24. Duquesne, S., Le Bras, M., Jama, C., Weil, E.D., and Gengembre, L. 2002. X-ray photoelectron spectroscopy investigation of fire retarded polymeric materials: Application to the study of an intumescent system. *Polymer Degradation and Stability* 77(2):203–211.
25. Schmiers, H., Friebel, J., Streubel, P., Hesse, R., and Kopsel, R. 1999. Change of chemical bonding of nitrogen of polymeric N-heterocyclic compounds during pyrolysis. *Carbon* 37(12):1965–1978.
26. Thomas, K.M. 1997. The release of nitrogen oxides during char combustion. *Fuel* 76(6):457–473.
27. Kodolov, V.I., Shuklin, S.G., Kuznetsov, A.P., Makarova, L.G., Bystrov, S.G., Demicheva, O.V., and Rudakova, T.A. 2002. Formation and investigation of epoxy intumescent compositions modified by active additives. *Journal of Applied Polymer Science* 85(7):1477–1483.
28. Wang, Z., Han, E., and Ke, W. 2007. Influence of expandable graphite on fire resistance and water resistance of flame-retardant coatings. *Corrosion Science* 49(5):2237–2253.
29. Vandersall, H.L. 1971. Intumescent coating systems, their development and chemistry. *Journal of Fire & Flammability* 2(April):97–140.
30. Bugajny, M., Le Bras, M., and Bourbigot, S. 1999. New approach to the dynamic properties of an intumescent material. *Fire and Materials* 23(1):49–51.
31. Anna, P., Marosi, Gy., Csontos, I., Bourbigot, S., Le Bras, M., and Delobel, R. 2001. Influence of modified rheology on the efficiency of intumescent flame retardant systems. *Polymer Degradation and Stability* 74(3):423–426.
32. Duquesne, S., Delobel, R., Le Bras, M., and Camino, G. 2002. A comparative study of the mechanism of action of ammonium polyphosphate and expandable graphite in polyurethane. *Polymer Degradation and Stability* 77(2):333–344.
33. Bourbigot, S., Le Bras, M., Delobel, R., and Trémillon, J.M. 1996. Synergistic effect of zeolite in an intumescence process: Study of the interactions between the polymer and the additives. *Journal of the Chemical Society—Faraday Transactions* 92(18):3435–3444.
34. Le Bras, M. and Bourbigot, S. 1998. Fire retarded intumescent thermoplastics formulations, synergy and synergistic agents—a review. In *Fire Retardancy of Polymers—The Use of Intumescence*, Le Bras, M., Camino, G., Bourbigot, S., and Delobel, R. (Eds.), Cambridge, London: The Royal Society of Chemistry, pp. 64–75.
35. Jimenez, M., Duquesne, S., and Bourbigot, S. 2006. Multiscale experimental approach for developing high-performance intumescent coatings. *Industrial and Engineering Chemistry Research* 45(13):4500–4508.

36. Jimenez, M. 2006. Etude des mécanismes de protection et de réaction au feu dans les revêtements intumescent. PhD dissertation, University of Lille, Lille, France.
37. Gosselin, G.C. 1987. Structural fire protection, predictive methods. *Proceedings of Building Science Insight*. http://irc.nrc-cnrc.gc.ca/pubs/bsi/87-5_e.html
38. Duquesne, S., Magnet, S., Jama, C., and Delobel, R. 2005. Thermoplastic resins for thin film intumescent coatings—Towards a better understanding of their effect on intumescence efficiency. *Polymer Degradation and Stability* 88(1):63–69.
39. Paul, Y. 2008. Evaluation de la résistance au feu de revêtements pour la protection de substrats métalliques—Conception de test à échelle laboratoire. CNAM dissertation, CNAM, Lille, France.
40. Duquesne, S., Lefebvre, J., Bourbigot, S., Le Bras, M., Delobel, R., and Recourt, P. 2004. Nanoparticles as potential synergists in intumescent systems. *Paper Presented at the ACS 228th Fall National Meeting, Division of Polymeric Materials, Science and Engineering, Session—Fire and Materials, Philadelphia, PA*.
41. Toldy, A., Anna, P., Csontos, I., Szabo, A., and Marosi, Gy. 2007. Intrinsically flame retardant epoxy resin—Fire performance and background—Part I. *Polymer Degradation and Stability* 92(12):2223–2230.
42. Duquesne, S., Le Bras, M., Bourbigot, S., Delobel, R., Vezin, H., Camino, G., Eling, B., Lindsay, C., and Roels, T. 2003. Expandable graphite: A fire retardant additive for polyurethane coatings. *Fire and Materials* 27(3):103–117.
43. Kashiwagi, T., Harris, Jr., R.H., Zhang, X., Briber, R.M., Cipriano, B.H., Raghavan, S.R., Awad, W.H., and Shields, J.R. 2004. Flame retardant mechanism of polyamide 6-clay nanocomposites. *Polymer* 45(3):881–891.
44. VanderHart, D.L., Asano, A., and Gilman, J.W. 2001. Solid-state NMR investigation of paramagnetic nylon-6 clay nanocomposites. 1. Crystallinity, morphology, and the direct influence of Fe³⁺ on nuclear spins. *Chemistry of Materials* 13(10):3781–3795.
45. Xie, R.C. and Qu, B.J. 2001. Expandable graphite systems for halogen-free flame-retarding of polyolefins. I. Flammability characterization and synergistic effect. *Journal of Applied Polymer Science* 80(8):1181–1189.

11 Polymer Nanocomposites

David D. Jiang

CONTENTS

11.1	Introduction.....	261
11.2	Structure and Properties of Nanoadditives	263
11.2.1	Structure and Properties of Clays	263
11.2.2	Structure and Properties of Carbon Nanotube and Other Nanoadditives	265
11.3	Surface Treatment of Nanoadditives.....	266
11.3.1	Surface Treatment of Clays.....	266
11.3.2	Surface Treatment of Carbon Nanotube and Other Nanoadditives	272
11.4	Preparation of Polymer Nanocomposites.....	272
11.5	Structure and characterization of Polymer Nanocomposites.....	275
11.5.1	Structure of Polymer Nanocomposites	275
11.5.2	Characterization of Polymer Nanocomposites	276
11.6	Thermal and Fire Performance of Polymer Nanocomposites and Mechanisms	279
11.6.1	Thermal and Fire Performance of Polymer Nanocomposites	279
11.6.2	Mechanism of the Effect of Nanoadditives on Flammability of Polymers	287
11.7	Concluding Comments and Trends for the Study of Polymer Nanocomposites.....	290
	Bibliography	291
	References.....	292

11.1 INTRODUCTION

Provided in this chapter is an overview on the fundamentals of polymer nanocomposites, including structure, properties, and surface treatment of the nanoadditives, design of the modifiers, modification of the nanoadditives and structure of modified nanoadditives, synthesis and structure/morphology of the polymer nanocomposites, and the effect of nanoadditives on thermal and fire performance of the matrix polymers and mechanism. Trends for the study of polymer nanocomposites are also provided. This covers all kinds of inorganic nanoadditives, but the primary focus is on clays (particularly on the silicate clays and the layered double hydroxides) and carbon nanotubes. The reader who needs to have more detailed information and/or a better picture about nanoadditives and their influence on the matrix polymers, particularly on the thermal and fire performance, may peruse some key reviews, books, and papers in this area, which are listed at the end of the chapter.

One of the significant impacts of nanotechnology on polymeric materials is achievement of the polymer nanocomposites (PNs) by using inorganic nanomaterials, which have at least one dimension measuring less than 100 nanometers (nm) (referred to as nanoadditives in this chapter), into polymer matrices through a variety of methods/processes. Figure 11.1 shows a generic illustration for using nanoadditives in polymer matrices to achieve the PNs, using clay as the example.

The nanoadditives used for fabricating the PNs can be a vast number of inorganic nanomaterials that, in general, are classified into four categories according to their dimensionality as shown in

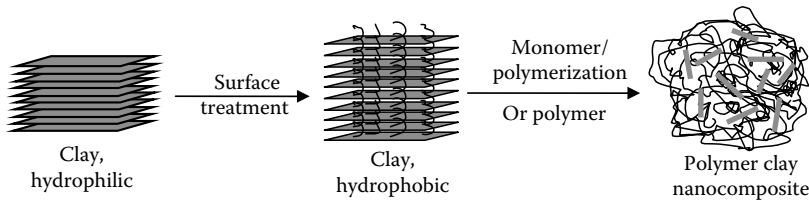


FIGURE 11.1 A schematic illustration of a general process of preparing PNs with clay as nanoadditive.

Figure 11.2: nanoparticles (0-dimension), nanofibers (1-dimension), nano-layers (2-dimensions), and nano-networks (3-dimension).

The 0-d nanoparticles can be nano-metal oxides (such as silica,¹ titania,² alumina³), nano-metal carbide,⁴ and polyhedral oligomeric silsesquioxanes (POSS),⁵ to name just a few; the 1-d nanofibers can be carbon nanofiber,⁶ and carbon nanotubes (CNT),⁷ which could be single-wall CNTs (SWCNT) or multiwall CNTs (MWCNT) etc.; the 2-d nano-layers include, but are not limited to, layered silicates,⁸ layered double hydroxides (LDH),⁹ layered zirconium phosphate,¹⁰ and layered titanates,¹¹ etc.; 3-d nano-networks are rarely used and thus examples are not provided here.

The impact of the nanocomposite technology on polymers is huge, reflected in enhanced properties of the resulting PNs, such as enhanced mechanical, barrier, solvent-resistant, and ablation properties.¹² The effect of nanocomposite technology on the thermal and fire performance of the polymers is primarily observed in two important parameters of the polymers: (1) the onset temperature (T_{onset}) in the thermogravimetric analysis (TGA) curve—representative of the thermal stability of the polymer, and (2) the peak heat release rate (peak HRR) in cone calorimetric analysis (CCA)—a reflection of the combustion behavior (the flammability) of the polymer. The T_{onset} will be increased and the peak HRR will be reduced for a variety of polymers when nanoscale dispersion of the nanoadditive is achieved in the polymer matrix.

In this chapter, an overview of the fundamentals of PNs is described, according to the author's understanding and experience as well as support from numerous references and review articles. The content of this chapter covers all kinds of inorganic nanoadditives, but, because the most widely investigated and thus understood nanoadditives used to enhance the thermal and fire resistance of the polymers are clays (natural or synthetic) followed by the CNTs and colloidal particles, the focus of the chapter is primarily on clays, particularly on the silicate clays and LDHs, as well as the CNTs. This includes structure, properties, and surface treatment of the nanoadditives, design of the modifiers, synthesis, characterization of the structure/morphology, and thermal and fire

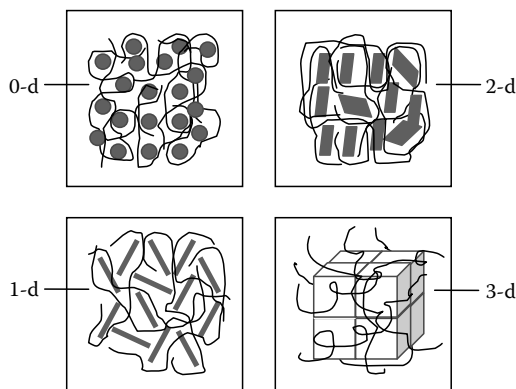


FIGURE 11.2 Nanoadditives used for fabrication of the polymer nanocomposites.

performance of PNs, and the subsequent mechanism of flammability reduction. A simple discussion about trends in PN studies is also provided. Since the focus is only on the basics of the nanoadditives and their applications in polymer matrices, it is recommended to the readers to peruse some key reviews, books, and papers in this area for more detailed information and/or a better picture about the nanoadditives and their influence on the matrix polymers. A few of these are listed at the end of the chapter.

11.2 STRUCTURE AND PROPERTIES OF NANOADDITIVES

11.2.1 STRUCTURE AND PROPERTIES OF CLAYS

Clays, natural or synthetic, are the most widely investigated and understood nanoadditives used to enhance the flame retardancy of polymers through nanocomposite technology, because of their unique properties, particularly the ease of surface treatment and application in polymer matrices. Clay can be cationic and anionic materials, in accordance with the charge on the clay layers. In this chapter, the focus is on two kinds of clays: montmorillonite (MMT), a naturally occurring cationic clay that belongs to the smectite group of silicates, and LDH, an anionic clay that does occur naturally but for which the synthetic form is more common. Other clays will also be mentioned as appropriate.

Silicate clay: The silicate clay¹³ belongs to an important group of layered inorganic nanomaterials called phyllosilicates that can be divided into four major subgroups: kaolinite, MMT/smectite, illite (or the clay-mica), and chlorite. Structurally, there are two types of silicate clay layers: tetrahedrally substituted (TS) and octahedrally substituted (OS). Both types of layers are observed in the 2:1 phyllosilicates. The TS layer (Figure 11.3¹⁴) consists of tetrahedrally coordinated silicon atoms fused to an edge-shared octahedral sheet of either aluminum or magnesium hydroxide. The layer thickness is around 1 nm while the lateral dimensions of the layers vary dramatically, from tens of nanometers to several microns, depending on the individual clay. Because of isomorphous substitution within the layers (such as Al^{3+} replaced by Mg^{2+} or Fe^{2+} , or Mg^{2+} replaced by Li^+), the silicate layers generally bear negative charges that are counterbalanced by alkali and/or alkaline earth cations residing within the galleries. The TS silicate can more readily interact with the polymer matrix than its OS counterpart, perhaps because of the negative charge located on the layer surface.

The metal cations residing inside the galleries between the layers can be replaced by many other cationic species and this property has been utilized to modify the clay with organocations.

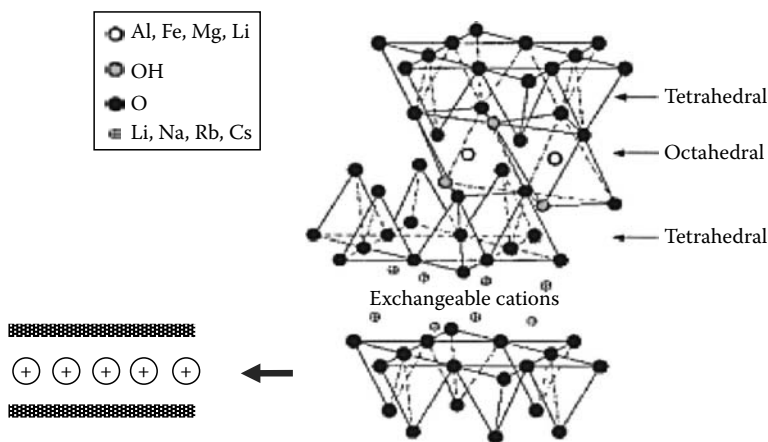


FIGURE 11.3 A schematic illustration of the structure of clay. (From Giannelis, E.P. et al., *Adv. Polym. Sci.*, 118, 108, 1999. With permission.)

Such a replacement is characterized by the ion exchange capacity (IEC), an important parameter for clay, generally expressed as milliequivalents (meq)/100 g. Typical IECs for 2:1 layered silicates range from 60 to 200 meq/100 g and the IEC of MMT is close to 100 meq/100 g. It should be pointed out that the IEC is an average value over the whole silicate platelet, because the negative charges on the surface of the silicate platelet varies from one layer to another and further from one kind of silicate clay to another. To counterbalance the negative charges of the silicate layers, correspondingly, metal ions, such as alkali and alkaline earth cations reside within the galleries, and may vary from one layer to another and from one kind of silicate clay to another.

Among all the silicate clays, MMT is the most widely used for preparing the PNs, referred to as polymer/clay nanocomposites (PCNs). Two characteristics of the silicate clays are generally considered in the fabrication of the PCNs: (1) the ability to fine-tune their surface chemistry through ion exchange reactions between organic and inorganic cations and (2) the ability of the silicate particles to be dispersed into individual layers in the matrix polymer. These two characteristics are co-related because the degree of dispersion for a given clay in a given polymer matrix is strongly dependent on the number of cations in the interlayers. A clay with a small IEC may not have enough anchoring points and this leads to a low organo-affinity of the modified clay, preventing the clay from dispersing and breaking up from its primary particles and hence influencing the formation of the nanocomposite. A clay with a large IEC may result in too many anchoring sites, leading to the anchored modifiers producing a blocking effect on the intercalation of the polymer chains. It may also lead to losses of the mechanical and thermal properties. The size of the clay platelets may be another factor to be considered in choosing the clay. The most commonly used clay, MMT, has a particle size larger than hectorite and saponite silicate clays but smaller than the synthetic clays, such as fluorinated synthetic mica (FSM).

LDH clay: Structurally, the LDH clays,¹⁵ natural or synthetic, have some similarity with the silicate clays. Both are layered inorganic nanomaterials bearing surface charges with ions residing in the interlayers. But according to composition, geometry, and thickness of the layers, the LDHs are quite different from the silicate clays. The layers of the silicate clays have a sandwich structure—one octahedral sheet containing oxides of Fe, Al, Mg, etc., is sandwiched between two silica tetrahedral sheets—that is the origin of the terminology 2:1 layered silicate, while each layer of the LDH consists of only a single octahedral metal hydroxide sheet. Another feature is that the silicate clays are cationic clays that bear negative charges on the layers with metal ions that are exchangeable residing in the gallery, while the LDHs are a class of minerals that consist of brucite-like sheets and bear positive charges on the layers that are compensated with exchangeable hydrated gallery anions and thus the LDHs are called anionic clays. The difference of layer structure determines the difference in the layer thickness and rigidity. A significant difference of the LDHs from the silicate clays is that the LDHs show a much lower layer thickness and rigidity.

Among the LDHs, synthetic LDHs are most commonly used. They are usually prepared via the co-precipitation method with M(II) and M(III) sources (in the form of chloride, nitrate, sulfate, carbonate, etc.) in basic solution, using the desired cations and anionic species to obtain the desired LDH structure and a tunable layer charge density through a large variety of compositions. This is also quite different from the silicate clays that are mostly naturally occurring. The charge density of the LDHs, which determines the IEC, can be much higher, for instance doubled, compared with MMT and other silicate clays. LDHs have a charge density similar to that seen in mica (0.32–0.34 cm⁻²).¹⁶

The most common naturally occurring LDH clay is Mg-Al-LDH, a hydrotalcite having chemical formula of Mg₆Al₂(OH)₆CO₃·4H₂O. Because of partial substitution of M^{II} to M^{III}, there are positive charges on the layers. The ideal formula of the general LDH is [M^{II}_xM^{III}_{1-x}(OH)₂]_{intra}[A^{m-}_{x/m}·nH₂O]_{inter}, where M^{II} and M^{III} are metal cations, such as Mg²⁺, Ca²⁺, Zn²⁺, etc., for M^{II} and Al³⁺, Cr³⁺, Fe³⁺, Co³⁺, etc., for M^{III}; A is the anion, which can be Cl⁻, CO₃²⁻, NO₃⁻, etc.; while the “intra” and “inter” denote the intralayer and interlayer domain, respectively. Many layers of the LDHs are

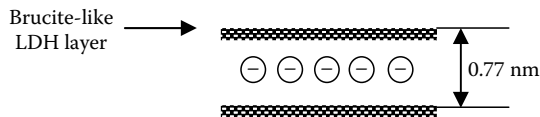


FIGURE 11.4 A schematic illustration of the structure of LDH.

stacked together one on another through Van der Waal's interactions, the interlayer distance or the basal spacing is about 0.77 nm for the Mg-Al-LDH (Figure 11.4). Being hydrated (like $\text{Mg}(\text{OH})_2$ or $\text{Al}(\text{OH})_3$), the LDH shows the potential to release water under fire conditions and this may lead to utility as flame-retardant nanoadditives.

11.2.2 STRUCTURE AND PROPERTIES OF CARBON NANOTUBE AND OTHER NANOADDITIVES

The CNTs,¹⁷ allotropes of carbon from the fullerene structural family and first reported in 1991,¹⁸ are nano-cylindrical carbon molecules (with similarity to graphite in the carbon-carbon bonds: sp^2 orbital hybridization) that have an aspect ratio, length-to-diameter ratio, up to greater than 1,000,000 and can be categorized as SWNTs, which have a diameter close to 1 nm and a “zigzag” or “armchair” or “chiral” structure, and MWNTs, which consist of multiple layers of the tube. The CNTs can be “fused” together when high pressure is exerted and this leads to converting the sp^2 bonds to the sp^3 bonds and producing stronger CNTs. Because of the Van der Waals forces, the CNTs in general aggregate. But unlike the layered materials that tightly stack together layer by layer, the CNTs align themselves into a “rope”-like shape.

Figure 11.5 shows a schematic illustration of structure of the SWCNT and high-resolution transmission electron microscopy (HRTEM) images of MWCNTs.¹⁹ Compared with the SWNTs, the MWNTs have a significantly improved chemical resistance, a critical property for surface treatment of the CNTs with different inorganic/metallic and organic species, such as functionalization or grafting onto the surface that leads to an attractive strategy for expanding, improving, and alternating applications. This is because, when the functionalization is performed, the SWNT will leave defects, due to the breaking of carbon-carbon double bonds ($\text{C}=\text{C}$). When the MWNT is modified, only the outer wall is involved.

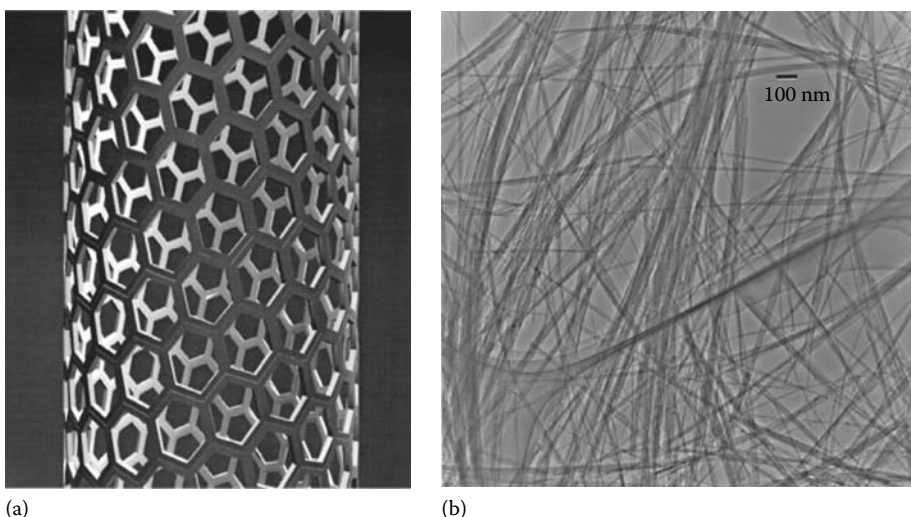


FIGURE 11.5 (a) A schematic illustration of a SWCNT; (b) TEM image of MWCNTs. (From Ajayan, P.M. and Ebbesen, T.W., *Rep. Prog. Phys.*, 60, 1025, 1997. With permission.)

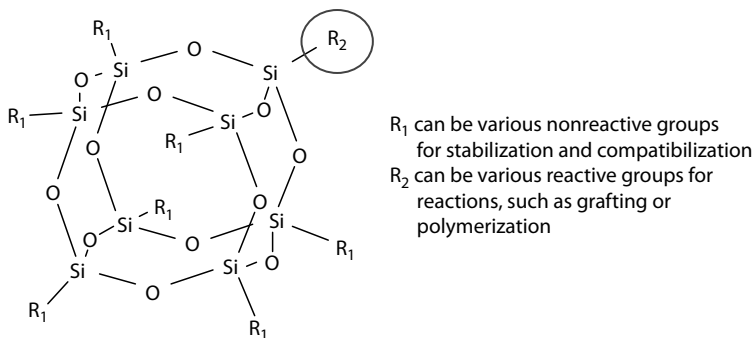


FIGURE 11.6 A representative structure of POSS.

Because of the unique combination of mechanical, electrical, and thermal properties, the CNTs have been excellent candidates to substitute or complement the conventional nanofillers in the fabrication of multifunctional PNs. The first PNs using CNTs as the nanoadditive was reported in 1994.²⁰ By far, the CNTs have been the second most investigated nanoadditives to reduce the flammability of the polymers through nanocomposite technology. A difficulty of the application of the CNTs in polymers is the dispersion of CNTs in the matrix polymer, and the high cost of the CNTs is another problem.

Other nanoadditives that have been used include nanofibers, such as carbon nanofibers,²¹ and colloidal nanoparticles, such as POSS,²² silica,²³ and alumina,²⁴ but they are much less investigated and understood. Among these nanoparticles, POSS is unique. Unlike other nanoadditives, POSS is an inorganic–organic hybrid material, containing an inorganic siloxane-like core, Si_8O_{12} (Figure 11.6), and organic substituents that can be tailored to various structures and can be of interest for many applications, such as mechanical reinforcing and flammability reduction in polymers.

It has been shown in the literature that POSS may be utilized as a precursor of flame retardants.²² The literature also reports observations of significantly reduced peak HRR for a few polymers²⁵ and increased time to ignition²⁶ when using POSS as the nanoadditive. However, a great restriction in using POSS from a large-scale production perspective is the high loading level required to have good flame-retardant performance as well as, like CNTs, its high cost. As for other nanoadditives, such as alumina and silica, although they have also been used to promote the thermal and fire performance of polymers, because these nanoadditives are less investigated and understood, no detailed discussion is included in this chapter.

11.3 SURFACE TREATMENT OF NANOADDITIVES

As an inorganic mineral, most unmodified nanoadditives are strongly hydrophilic and are generally compatible and miscible only with a few hydrophilic polymers, for instance, clay can only be made into PNs with poly(ethylene oxide),²⁷ poly(vinyl alcohol),²⁸ and a few other water soluble polymers. Most polymers are hydrophobic and thus they are neither compatible nor miscible with the unmodified nanoadditives, leading to an inability to achieve a PN with a good nanodispersion in most cases. Therefore, for most nanoadditives that have been used to prepare the PNs, an important and necessary feature is their surface treatment that provides compatibility to the nanoadditives and enables them to be uniformly dispersed (and/or separated into single nanoparticles) in the polymer matrix.

11.3.1 SURFACE TREATMENT OF CLAYS

Surface treatment of clays: The surface treatment of the nanoadditives helps establish an interface with the polymer matrix and hence enhance the compatibility and/or the miscibility of the nanoadditive with the polymer matrix. In terms of the cationic silicate clay, such as MMT, the interface is

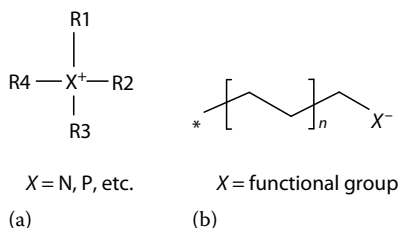


FIGURE 11.7 A representative structure. (a) An onium and (b) an anionic surfactant.

generally achieved in an aqueous system through an ion-exchange process by which the cationic surfactant, typically an organo-onium, is applied to the pre-prepared clay suspension and anchored onto the clay surface, converting the hydrophilic clay to organophilic and thus making the intercalation of clay interlayers with the polymer chains possible. The oniums can be primary, secondary, tertiary, or quaternary-based alkylammonium²⁹ or alkylphosphonium^{6a} as well as other oniums such as imidazolium,^{30a} and stibonium.^{30b} Modification of the LDH clays are achieved using anionic surfactants, such as sodium dodecylbenzenesulfonate (SDBS), lauric acid (LA), sodium dodecylsulfate (SDS), and bis(2-ethylhexyl)hydrogen phosphate (BEHHP).³¹ A general structure of the onium and anionic surfactant is shown in Figure 11.7 and a general procedure of the organo-modification (suitable for both the silicate clays and the LDH clays) is provided in Figure 11.8.

The clay is first dispersed in water or an aqueous system (to form a suspension) and the modifier that has been pre-dissolved in water (or an aqueous system) is then gradually (drop-wise) added to the clay suspension. The organo-modifier will be anchored onto the surface of the clay platelets immediately after it is added but further stirring for some more time up to a few hours may be needed to achieve homogeneous and complete ion exchange. Some representative modifiers (in both cationic and anionic form) that have been used as surface treatment for the clays in the literature are shown in Figure 11.9.

Structure of modified clays: After drying, the modified clay layers will be stacked together because of the high surface energy of the nanoparticles causes them to re-agglomerate back into their original stack forms, which is described as a “memory effect.” A single clay aggregate, in general, contains many primary clay particles with a multilayer structure. After organo-modification, the gap (commonly referred to d-spacing or basal spacing) between the clay layers, compared with that of the pure clay, becomes larger due to the presence of the modifier in the interlayers. Two major factors influence the interlayer spacing: (1) the size and chain length of the modifier, a larger size and a longer chain length leads to a larger d-spacing and (2) the IEC that determines the packing density of the modifier in the interlayers of the modified clay, which differs from one clay to another because of the variation of the IEC of the different clays (see Section 11.2.1). This may greatly affect the efficiency of the ion exchange between the inorganic ions and the organo-ions and thus further affect the dispersion of the clay in the polymer matrix. In determining the d-spacing of the modified clay, x-ray diffraction (XRD) has been the most used characterization method.

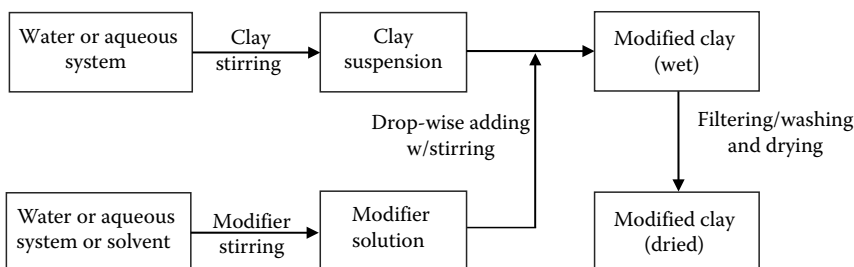


FIGURE 11.8 A schematic illustration of the organo-modification of clay.

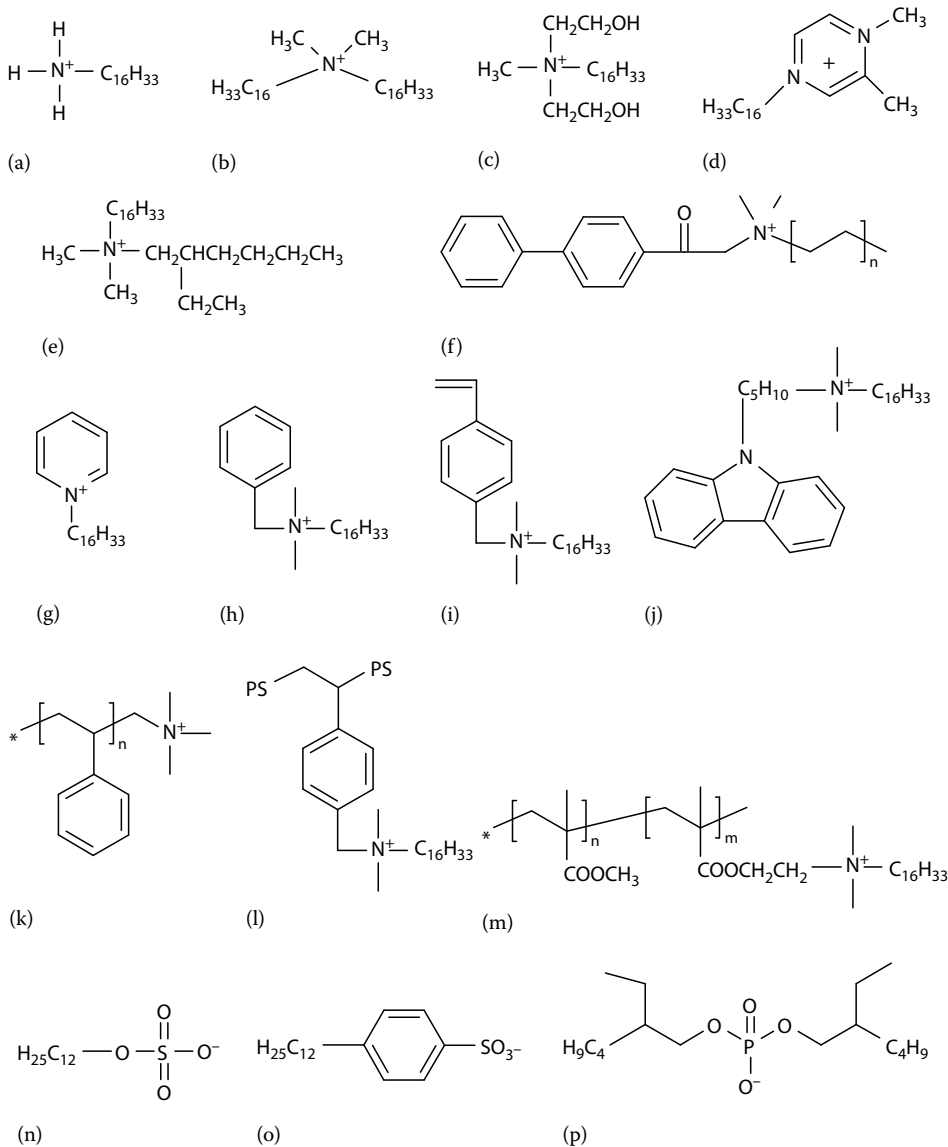


FIGURE 11.9 Representative organo-modifiers for clay surface treatment. (a) Hexadecylammonium. (From Li, Y. and Ishida, H., *Langmuir*, 19, 2479, 2003.) (b) Dimethyldihexadecylammonium. (From http://www.scprod.com/product_bulletins.asp) (c) Methyl-bis-2-hydroxyethylhexadecylammonium. (From http://www.scprod.com/product_bulletins.asp) (d) 1,2-Dimethyl-3-hexadecylimidazolium. (From Wang, D. et al., *Polym. Eng. Sci.*, 44, 1122, 2004; Costache, M.C. et al., *Polymer*, 46, 6947, 2005.) (e) Dimethyl-2-ethylhexyl-dehydrogenated tallow. (From http://www.scprod.com/product_bulletins.asp) (f) Phenylacetophenonedimethylhexadecyl ammonium. (From Chigwada, G. et al., *Polym. Degrad. Stab.*, 91, 755, 2006.) (g) Hexadecylpyridium. (From Xiao, J. et al., *Eur. Polym. J.*, 41, 1030, 2005.) (h) Dimethylbenzylhydrogenated tallow ammonium. (From http://www.scprod.com/product_bulletins.asp) (i) Dimethylvinylbenzylhexadecylammonium (VB16). (From Zhu, J. et al., *Chem. Mater.*, 13, 3774, 2001.) (j) Carbazole-based ammonium. (From Chigwada, G. et al., *Thermochim. Acta*, 436, 13, 2005.) (k) Amine-terminated PS surfactants (PS-NH₄). (From Beyer, F.L. et al., *Chem. Mater.*, 14, 2983, 2002.) (l) Ammonium of oligomeric copolymer of styrene and vinylbenzyl chloride (COPS). (From Su, S. et al., *Polym. Degrad. Stab.*, 83, 333, 2004.) (m) Ammonium based on methyl methacrylate oligomer (MAPS). (From Su, S. et al., *Polym. Degrad. Stab.*, 83, 321, 2004.) (n) Dodecylsulfate. (From Costa, F.R. et al., *Adv. Polym. Sci.*, 210, 101, 2008.) (o) Dodecylbenzenesulfonate. (From Costa, F.R. et al., *Adv. Polym. Sci.*, 210, 101, 2008.) (p) Bis(2-ethylhexyl)hydrogen phosphate. (From Costa, F.R. et al., *Adv. Polym. Sci.*, 210, 101, 2008.)

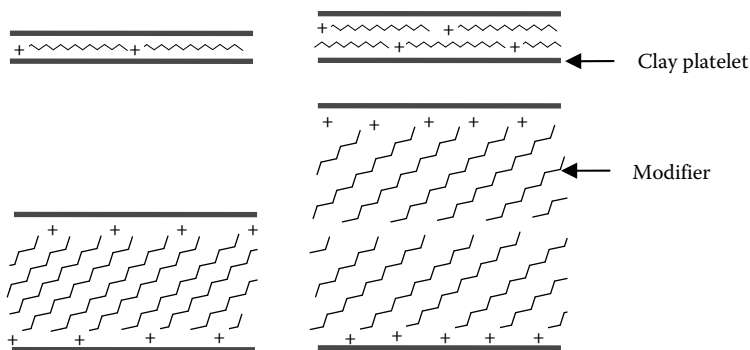


FIGURE 11.10 A schematic illustration of orientation and alignment of the modifier in the clay interlayer. (Modified from Lagaly, G., *Solid State Ionics*, 22, 43, 1986.)

The structure of the modified clay generally means the orientation and alignment of the modifier in the clay interlayers. After anchoring onto the clay surface, the modifier will take different orientations or arrangements in the clay interlayers. The long chains of the modifier has been thought to take two types of orientations/arrangements according to the results of silicate clays, as shown in Figure 11.10:⁴⁰ (1) lying parallel to the clay layers, this can be mono or bilayers, and (2) radiating away from the clay layers, this can also be mono or bimolecular arrangements. It is found that the orientation or the arrangement of the modifier is related to temperature because, on heating, the long chain of the modifiers between the clay layers can show a thermal transition, similar to melting or liquid-crystalline to liquid-like transitions.

The patterns of the organoclay structure above are based on the dry state and an idealized model that is assumed to be all trans conformations for the long chain arrangement. This has been demonstrated to be unrealistic according to the results of FTIR analysis⁴¹ and through molecular dynamics simulations.⁴² It was found that the chains of the modifier show varying degrees of order, according to the frequency shifts of the asymmetric CH_2 stretching and bending vibrations. In general, the chains of the modifier adopt a more disordered liquid-like structure, with a decrease in packing density or chain length or an increase in temperature. When the available surface area/molecule is within a certain range, the chains are not completely disordered, but retain some orientational order similar to that in a liquid crystalline state. However, the modified clays have a different arrangement/alignment in the “wet” state, such as in various solvents, and this may be studied with neutron scattering.⁴³

Compatibility/miscibility and design of the modifier: As mentioned above, the modifiers provide the nanoadditive compatibility with the polymer matrix. For example, after anchoring the modifier onto the clay surface, the resulting organoclay can be nanodispersed (well intercalated and/or exfoliated) in the polymer matrix. It has been demonstrated in the literature that the modifiers for clays can be small—molecule-based or oligomer-based,⁴⁴ nonreactive or reactive,⁴⁵ including those containing reactive functional groups, such as a vinyl group in the modifier,^{6a} or producing reactive sites in the course of fabricating the PNs, such as radicals produced on heating.⁴⁶ The discussion below is focused on the cationic clays, but it is also suitable for LDHs.

It should be noted that although the quaternary ammonium is nominally chosen as the modifier to compatibilize the cationic clays with the polymer matrix, this does not refer to the processing aids or compatibilizers that help disperse the clay particle into the polymer matrix and set up the PN structure; the compatibilizers may not necessarily be part of the interface between the polymer and the clay. For instance, the graft copolymer of ethylene or propylene with maleic anhydride (PE-g-MA or PP-g-MA) has proven to be an excellent compatibilizer/disperser for the PE/ or PP/ clay nanocomposite,⁴⁷ but the graft copolymer is not part of the interface of the modified clay.

In designing a modifier, the first thing to be considered is the compatibility and the miscibility of the modifier with the polymer matrix. Compatibility⁴⁸ may generally be considered to be a measure

of the stability of the substance when it is mixed with another material. Miscibility⁴⁹ refers to the property of two or more liquids to be mixed and form a clear, homogeneous solution in all proportions, for instance, a mixture of water and ethanol. Miscibility/immiscibility has been extended to mixtures of solids or of gases. However, one should be aware that a transparent “solution” does not mean that two materials are miscible. They may form an immiscible but visibly clear mixture when the indexes of refraction of the two materials are similar.

The structure of the modifier needs to be similar to that of the polymer matrix to achieve a good compatibility and miscibility between the modified clay and the polymer matrix. For instance, a clay based on the quaternary ammonium salt containing a benzyl group^{6a} shows excellent compatibility and miscibility with aromatic polymers, such as polystyrene. However, other features of the molecular structure, such as alkyl chain length and number of alkyl chains, also play an important role. It has been found, based on numerous experiments, that the length of the alkyl chains is critical. Longer chains seem to be able to expand the gallery space far enough to allow for intercalation of the polymer chains and the usual statement is that the modifier needs to have at least one alkyl-chain with 12 carbons (in practice, it is typically C12 to C16) in order to be effectively intercalated or exfoliated by the polymer chains.⁵⁰ In some cases, two long chains will be more helpful.⁵¹ It is also observed that the loading of the modified clay in the polymer matrix is another factor that affects the miscibility and should be considered.

A few attempts have been made using the solubility parameter to predict the compatibility between the clay and polymer.⁵² Dispersing organoclay in a monomer or a solvent in which polymerization is carried out is an additional consideration that has proven useful. Techniques that can be used as screening methods for analyzing the dispersion of the modified clay in the monomer or solvent have been investigated in previous work.⁵³ In general, a modified clay that is miscible with a polymer matrix will be dispersed in the same type of solvents for that polymer. The use of the ultra-sonication is greatly helpful in improving the miscibility.⁵⁴ Other factors that matter in the miscibility between the modified clay and the polymer matrix include the ability of the polymer chains to entangle with the modifier, hydrogen bonding, or alignment of the modifier on the clay surface.⁵⁵ The entropy and enthalpy of mixing between the polymer and the organic treatment on the clay plays a role.

In addition to the use of the compatibilizers to improve the miscibility problem, one must also design the modifier to perform a particular role. The presence or absence of functional groups (reactive or nonreactive) on the modifier is important for the miscibility of the clay (the dispersion) in the polymer matrix, particularly for achieving PCNs through in situ polymerization and sometimes with melt processing, etc. The reactive functional groups can either provide a reactive site (such as a radical), allowing the polymerization to occur on the clay surface, yielding larger amounts of exfoliation in the final PCNs or to graft the polymer chains onto the clay surface. Both lead to better results in regard to clay exfoliation.^{45a,46,56} However, the functionalized clays may bring their own problems, such as polymerization control for thermosetting resins like polyurethanes and epoxies.⁵⁷ It may also lead to potential cross-linking of the final polymer. An example for this is the organoclay with *N,N*-dimethyl-*N*-vinylbenzylhexdecylammonium chloride^{6a} as modifier. Since this contains a vinyl group that participates in the polymerization, a pseudo-grafted and also perhaps cross-linked polystyrene/clay nanocomposite (PSCN) is obtained. The use of a modifier without functional groups will not lead to grafting/cross-linking, but the interface between the clay and the polymer may not be as strong as that with the functional groups.

The thermal stability of the modifier (and hence of the organoclay) is an important factor to consider. The pure clay, such as MMT, does not undergo any significant mass loss in decomposition processes up to 300°C. After organo-modification, the degradation process of modifier-intercalated clay is significantly different. The onium cation decomposes at a temperature much lower than the onset temperature of the matrix polymer; alkylammoniums typically decompose in the temperature range of 180°C–200°C⁵⁸ either via a Hofmann elimination reaction to give an alpha olefin and amine, or through an S_N2 nucleophilic substitution reaction to produce the amine and substituted

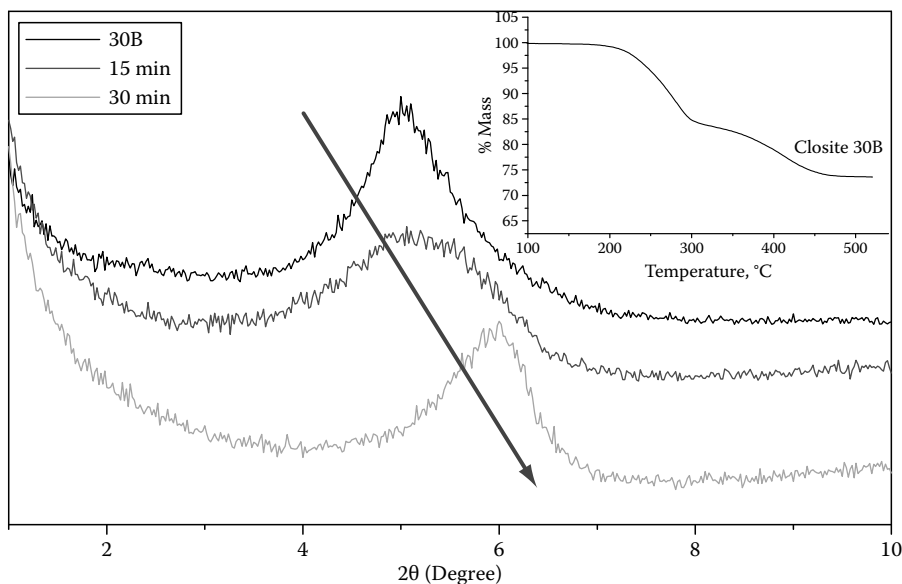


FIGURE 11.11 (See color insert following page 530.) Thermal stability of Cloisite 30B seen in XRD patterns before and after heating at 190°C under air for 15 and 30 min; (inset) TGA result under N₂ at 20°C/min.

alkyl group because the C–N bond is the weak link in the ammonium structure and breaks easily on heating. The thermal degradation of the modifier, which can be monitored through TGA, can dramatically change the structure of the modified clay. This can be examined with XRD as demonstrated in Figure 11.11 in which the XRD patterns of Cloisite 30B, a commercial organoclay produced by Southern Clay Products, in the pristine state and after heat treatment at 190°C for 15 and 30 min, are shown.

The degradation of the modifier will not only greatly restrict the use of the organoclay in the polymerizations, which require a temperature exceeding the degradation temperature of the modifier,⁵⁹ but it also affects the use of the organoclay in melt processing as many PCNs are prepared either through melt-compounding and not many polymers can be processed below 200°C or with intercalation process that may be conducted at high or low temperature. But even in a case such as solution intercalation that may not need a high temperature in the course of fabricating the PCN, all the components of the PCN may be subjected to a high temperature exposure in the course of postprocessing to fabricate a useful part from the solvent-processed nanocomposite. Therefore, the degradation of the modifier is a concern for many thermoplastics because they are often injection/compression molded or extruded at higher temperatures and the temperature can exceed the set point by 20°C–30°C due to the shearing, which can further accelerate the decomposition of the modifier.

The decomposition or degradation of the modified clay can lead to more than one effect in the PCN. For instance, the thermal degradation of the organoclay through the Hofmann mechanism produces an olefin and an amine and leaves an acid proton on the surface of the MMT.^{59a} This acid site may have a catalytic effect on the initial stages of decomposition of organic material within the clay layers and this will also decrease the molecular weight of the matrix polymer because the acid sites have been known to be responsible for the breaking of C–C bonds of the matrix polymer, thus exerting an impact on the mechanical properties and the flammability of the matrix polymer. Further, re-aggregation of the clay platelets will occur and this leads to the formation of a conventional composite, or microcomposite.

Measures have been taken to improve the thermal stability of the organoclays. Extraction of excess modifier can improve the thermal stability of alkyl ammoniums, sometimes with improvements up

to 220°C.⁶⁰ Additionally, the use of sub-stoichiometric amounts of modifier on clay can give some improvement to the thermal stability of the modified clay.⁶¹ Further, in melt compounding, careful experimental design and processing equipment choice can be of great importance in overcoming the thermal degradation of the modifier.⁶² However, the structure of the modifier is the important factor affecting the thermal stability. The use of modifier based on an aromatic amine can enhance the thermal resistance of ammonium compounds.⁶³ The thermal degradation temperature of the alkylphosphonium is 20°C–30°C^{6a,64} higher than that of alkylammoniums. Stibonium^{31b} can be another choice as it is noted that stibonium containing the hexadecyl group that occupies 35% of the total mass has only 13% of the mass loss at 400°C and a complete degradation of this cation did not occur.⁶⁵ Further, functionalized and nonfunctionalized imidazoliums can provide better thermal stability²⁹ than many oniums. Application of oligomer-based modifiers with a single or more than one cationic group has been shown to be a good process to improve the thermal stability of the organoclay.⁶⁶ For LDH clays, seeking thermally more stable modifiers is of equal importance as for the silicate clays. The oligomeric-based modifier may be one good choice.

11.3.2 SURFACE TREATMENT OF CARBON NANOTUBE AND OTHER NANOADDITIVES

Similar to clays, surface treatment of the CNTs and other nanoadditives is necessary to establish an interface between the polymers and these nanoadditives. However, the method for modification or functionalization of these nanoadditives is dramatically different than that for clay modification in which the organo-surfactant is used and anchored onto the clay surface. Introduction of the surface treatment onto the CNTs takes advantage of the double bonds on the CNTs but, in general, aggressive reaction conditions, such as oxidation with nitric acid⁶⁷ and other agents that are strongly oxidative or treatment with high energy beams, like ion beam⁶⁸ or plasma, are needed to break the double bonds, while modification of the colloidal nanoparticles is typically achieved through sol–gel reactions. Figure 11.12 shows a schematic illustration for the modification or functionalization of the CNTs and the inorganic nanoparticles. The surface treatment, as for clays, can be small molecular-⁶⁹ or polymer based.⁶⁷

11.4 PREPARATION OF POLYMER NANOCOMPOSITES

An advantage of the PNs is the strong interaction between the polymer matrix and the nanoadditives because of the nanoscale dispersion of the nanoadditives in the polymer matrix. As a result, the PNs exhibit unique properties that are not shared by their microscale counterparts—conventional polymeric composites.⁷⁰ However, the PNs are not easy to obtain. Simple physical mixing of a polymer with nanoadditives does not result in a PN but rather one obtains a more conventional composite with poor mechanical and thermal properties because of phase separation and, hence, the poor physical interaction between the matrix polymer and the nanoadditives.

To successfully achieve the PNs, the first problem encountered is how to incorporate the nano-additive into the polymer matrix. Not only is it necessary to break up the agglomerates to much

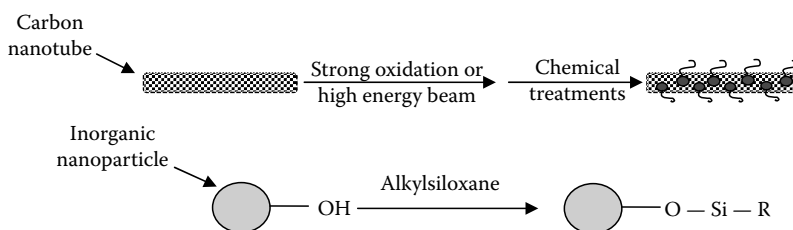


FIGURE 11.12 A schematic illustration of introducing surface treatment onto CNTs and inorganic nanoparticles.

smaller agglomerates or single nanoparticles but also these particles must be well dispersed at the nanoscale in the polymer matrix. This requires that the methods and processes used for fabricating the PNs comply with both the polymer chemistry and the nanoparticle chemistry. A variety of methods/processes that are suitable for all the nanoadditives have been and continue to be applied to prepare the PNs. They, in general, can be classified into three categories: in situ polymerization, solvent blending, and melt compounding. A simple discussion is given below:

In situ polymerization: This method has been widely applied to obtain the PNs, involving polymerization either in a solvent-free system (i.e., a bulk phase) or in a solvent-based system (including an aqueous phase) that can be a pure solvent system or an emulsion⁷¹ or suspension system.⁷² The structure of the modifier is strongly related to the compatibility and the miscibility of the nanoadditives with the matrix polymer; stirring is also an important factor as it provides the shearing force to separate the nanoparticles, such as to delaminate the clay platelets. Ultrasonication can be helpful in breaking apart the nanoparticle and thus improve the dispersion through the in situ process.

Figure 11.13 shows a schematic illustration of the in situ polymerization process with clay as example. An advantage of this process is that it usually produces PNs with a well-dispersed morphology—at both the micro- and nanoscale, particularly in the presence of functional groups in the modifier. This process will be quite suitable for preparing the PNs based on thermosetting polymer, as the process of synthesizing the thermosetting material is almost always an in situ polymerization in which the nanoadditives and the monomers can be mixed together before polymerization.

One feature of some nanoadditives, such as clays, is that they can significantly change, often increase, the viscosity of a fluid^{45a,56} and this may be a benefit (for instance, it may be used to adjust the viscosity to set up an ordered and well-aligned PN structure) or be a problem (for instance, a thermoset formulation may be impeded by characteristics that are quite different from those of the virgin polymer). A disadvantage of in situ polymerization is that, depending on the final interface between matrix polymer and nanoparticle, a well-dispersed morphology of the PN may be achieved, but it is perhaps not a thermodynamically stable form and the PCN may revert to a different morphology in the course of processing.⁷³ Furthermore, the process is not easily applied in industry, particularly at the multiton scale. In the case of clays, the PA-6/clay nanocomposite from Ube/Toyota seems to be the only commercial example of the in situ process.

Solvent blending: Solvent blending, also called solution intercalation in the case of clay and other nanolayers, involves both dispersing the nanoadditive and dissolving the matrix polymer in a solvent or a solvent mixture. Three parameters have been considered to be important, particularly for clays, in choosing the surface treatment of the nanoadditives with this process: The structure of the modifier, its miscibility with the polymer, and its thermal stability. The miscibility of the modifier here has two meanings: miscibility with both the final polymer and the solvent chosen to dissolve the polymer. The modifier structure and its miscibility are perhaps more important than the thermal

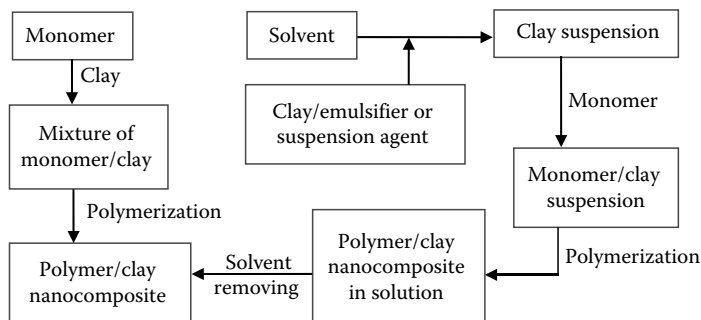


FIGURE 11.13 A schematic illustration of the in situ polymerization process with clay as example.

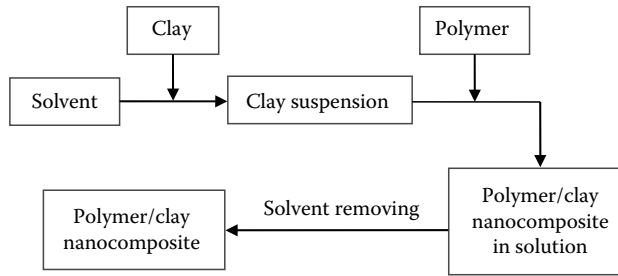


FIGURE 11.14 A schematic illustration of the solution intercalation process with clay as example.

stability as that is only important for the postprocessing, such as molding where it may experience a high thermal exposure. Figure 11.14 shows a schematic illustration of the solvent intercalation process with clay as example.

An advantage of using this process to obtain the PN is that the polymer can be dissolved and the nanoadditives, such as the clay, can be well dispersed/exfoliated in the same solvent/solvent mixture. Similar to the in situ process, a critical issue in obtaining PNs through this process is breaking apart the agglomerates of the nanoadditive primary nanoparticles, more specifically the uniformity of mixing is of key importance. Again, ultrasonication has proven to be a very useful tool to break apart the nanoadditive agglomerates, as has been seen for clay.⁵³ It has been noted that the loading of the clay can be about 1–3 wt % to obtain delamination in the solution and in the final PCN. This process is perhaps better used for preparing the PNs based on thermosetting polymers or polymers that can swell extensively in a solvent, allowing the polymer chains and the nanoadditives to mix freely.

Although solution blending has only been used at the lab scale at this time, compared with the in situ process, it may be more industrially friendly, particularly for the primary polymer producers who have operations, which can easily recover and recycle the solvent. High dilution is required and this may have an effect on the production of the PNs and the process is quite dependent on the individual polymer. Some polymers have many solvents from which to choose while others do not. A typical example is polystyrene, which can dissolve in a variety of solvents, so it is easy to find a solvent that is compatible with both the clay and the polymer. Polyolefins, on the other hand, require high boiling solvents and the high temperature may exert an effect of thermal degradation on the modifier.

Melt Compounding: Among all the methods/processes used for preparation of the PNs (at least this is true for the PCNs), melt compounding (Figure 11.15) is perhaps the most widely studied approach⁷⁵ because of its simplicity and the ready availability of the processing equipment. Preparation of the PN through melt compounding requires one to feed the polymer/nanoadditive mixture into the compounding equipment, such as an extruder, and then compound at the temperature required for melt mixing of the matrix polymer. The modifier needs to be compatible and miscible with the matrix polymer and the thermal stability of the modifier is the most important consideration for

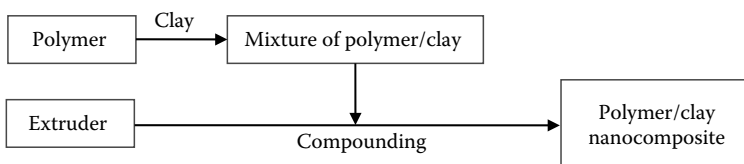


FIGURE 11.15 A schematic illustration of the melt compounding process using clay as example.

such operations. The need for functional groups that may covalently link polymer and nanoparticle becomes less important with this process, but it can be a factor in in situ grafting the polymer chains onto nanoadditives and in helping the dispersion.

In addition to its simplicity and the ready availability of the processing equipment, an advantage of melt compounding is that the nanoadditives, which may not be well dispersed in the in situ polymerization or in the solvent-blending process, may be well dispersed into polymer matrix through melt compounding, because the large shear can break apart the nanoadditive particles into small aggregates and/or even to separate into single nanoadditive particles. However, this technique will usually be restricted to thermoplastics (which are the only polymers that are thermally processable) and perhaps to those thermosets that can be made into the final nanocomposite parts through injection molding or resin transfer molding processes.

11.5 STRUCTURE AND CHARACTERIZATION OF POLYMER NANOCOMPOSITES

In general, the structure of the resulting PNs, i.e., the dispersion of the nanoadditives in the polymer matrix, can be broadly classified into two categories: nanoscale-dispersed PNs and micro/macro-scale-dispersed conventional polymer composites. Many factors play a role in achieving a particular morphology. For a given organo-modified nanoadditive, it is a function of the matrix polymer, the structure of the organo-modifier, and the method used for fabricating the PN as well as the shearing force, etc. To successfully obtain a PN, all these factors must be considered.

11.5.1 STRUCTURE OF POLYMER NANOCOMPOSITES

In the case of PCNs (and for other PNs containing inorganic nanolayers), three kinds of commonly accepted terms have been widely used to describe the structures (ordered and disordered): immiscible, intercalated, and exfoliated.⁷⁵ In most cases, all three structures coexist in the same PCN, but one is generally dominant. A schematic illustration of the structures of the PCNs is given in Figure 11.16. The immiscible structure (Figure 11.16a) indicates that the matrix polymer and the clay are incompatible or processing resulted in a clay that was immiscible in the polymer matrix. This generally means a phase separation occurred in the PCN because either the chains of matrix polymer were unable to penetrate into (to intercalate) the clay layers or the organoclay undergoes thermal degradation in the course of fabricating the PCN. Therefore, the PCNs with an immiscible structure are equivalent to the microcomposites or conventional composites. The formation of the immiscible PCNs may mean that the process used to achieve the PCN is not suitable for this particular clay and matrix polymer. The resulting PCN tends to have the same properties as those seen in the conventional composites.

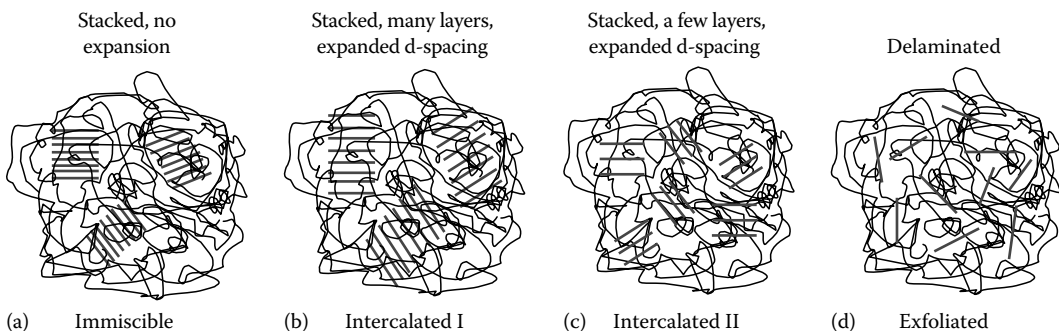


FIGURE 11.16 A schematic illustration of currently defined morphology of the PCN.

The two kinds of common intercalated structures observed in the PCNs are shown in Figure 11.16b and c. Both are considered as nanocomposite materials but the PCNs with intercalated structure as shown in Figure 11.16c is a nanomaterial with better dispersion than that in Figure 11.16b. The definition of “intercalated” derives from the XRD measurement, indicates that the clay layers maintain their registry. The formation of the intercalated structures of the PCN occurs because of the penetration of the polymer chains into the interlayer spacing of the clay platelets, which leads to an expansion of the d-spacing of the clay platelets (Figure 11.16b). On further intercalation of the matrix polymer into the interlayers of the clay platelets or under an external force, such as a shearing force (perhaps a more important factor), some delamination occurs, leading to an intercalated structure but with only a few clay layers stacks and perhaps a uniform dispersion (Figure 11.16c).

With more and more polymer chains entering the interlayers of the clay platelets, the d-spacing becomes increasingly larger, and/or with the shearing force, exfoliation of the clay platelets is achieved (Figure 11.16d); this is considered as the best among the nanocomposite structures. However, the PCNs with the intercalated structure as shown in Figure 11.16c, in terms of performance, may be equal to the PCNs with exfoliated structure. There is no standard criterion to describe “exfoliated.” Some researchers refer to “exfoliated” when the d-spacing of the clay platelets is larger than 6–8 nm or simply to mean a well-dispersed clay at the nanometer level (either intercalated or exfoliated) because of the fact that the properties of the PCN for these two cases have little difference, while others think that the term exfoliated means that the registry of the clay platelets has been lost. An alternative of the “exfoliated” is “delaminated” and both are used interchangeably.

The terms above are widely used to classify the degree of dispersion of clay in the polymer matrix; it should be pointed out that the use of these terms is strictly qualitative, and quite often controversial and strongly dependent on the individual users. Because there are no standards to follow, there will be some difference in interpretation of the morphology of PCNs. For instance, both delamination and exfoliation have been used to describe the morphology of the PCNs in which the clay platelets have a d-spacing larger than 6–8 nm or been separated to single pieces; some researchers argue that the delamination is a clay dispersion beyond exfoliation. Attempts to provide standard descriptions for levels of clay dispersion can be seen in a few papers.⁷⁷ Image analysis^{76c,77} has also been used to try to quantify the degrees of nanoadditive dispersion, but more work is needed in these areas.

In the case of PNs containing nanoadditives other than nanolayers, such as CNTs and POSS, the terms above are not used. They also show similar observations as those seen for the clay in the polymer matrix: Aggregated to a large extent (immiscible or partially immiscible) or a few nanoadditive nanoparticles or separated into single nanoparticle, and all of these may coexist in the same PN.

11.5.2 CHARACTERIZATION OF POLYMER NANOCOMPOSITES

Various methods/techniques at the nanoscale or microscale have been used to directly or indirectly characterize the structure/morphology of the PN. In the case of clays, these methods include XRD,⁷⁸ transmission electron microscopy (TEM),^{76a,59} nuclear magnetic resonance (NMR) spectroscopy,⁷⁹ Fourier transmission infrared (FTIR) spectroscopy,⁸⁰ atomic force microscopy (AFM),⁸¹ scanning electronic microscopy (SEM),⁸² fluorescence,⁸³ etc., just to name a few. Material property tests can also be an option to indirectly confirm the PCN morphology, for instance, through characterizing various properties of the PCN including mechanical, thermal, conductivity, and gas barrier properties, etc. If nanodispersion is achieved, this can be inferred from properties of the PCN, showing enhancement of various properties when compared with those of a conventional composite or the base polymer.

Among the methods for the determination of morphology, XRD and TEM are two most commonly used techniques. In this chapter, a simple introduction to these two techniques is provided. For more detailed information about these two methods as well as other methods, the reader can

refer to related papers/references.^{60,77,84} However, one should be aware that the required and/or desired information about the PCN cannot be obtained through a single method; the combination of multiple methods is necessary to properly understand the morphology and properties and to correlate the morphology to the properties.

The use of XRD as one of the two primary tools to characterize the structure or morphology of PCN is based on the fact that the multilayer structure, the registry, of the clay platelets may be maintained in the polymer matrix, such as in the PCNs with immiscible and/or intercalated structures and through the Bragg equation, one may determine the distance, i.e., the d-spacing of the clay platelets. There are two kinds of typically used XRD, wide angle x-ray scattering (WAXS)^{79a} and small angle x-ray scattering (SAXS),^{38,79b} both can be complementary because they cover a different domain and degree of the nanodispersion but the use of the WAXS is much more common. WAXS is usually used to determine the d-spacing of the clay layers less than 6–8 nm, while the SAXS is used to obtain the d-spacing larger than this, which WAXS is unable to detect. However, WAXS is enough in most cases to determine if intercalation has occurred.

The clay can be ordered or disordered in the polymer matrix, but only an ordered clay structure is able to scatter or diffract the x-rays. In this case, a peak will appear in the WAXS pattern that indicates the morphology of the PCN. A sharp and strong peak means that the clay platelets in the polymer matrix has an ordered structure (immiscible or intercalated), while a broad and weak peak usually indicates a mixture of intercalated (ordered) and disordered structures. When a completely exfoliated structure is achieved, there will be no diffraction peak in the WAXS pattern because the d-spacing between the layers is too large (i.e., exceeding 6–8 nm). However, it should be pointed out that exfoliation only means that the clay is exfoliated relative to other clay plates but it does not necessarily mean that a uniform dispersion of the clay in the polymer matrix was achieved. The absence of a peak does not necessarily mean that an exfoliated structure has been obtained in the PCN. Based on the author's experience, the absence of a peak only indicates an absence of clay order, and more often, indicates disordered poorly dispersed clay as observed by TEM in many cases. The literature also points out that the absence of signal cannot be simply used as proof of the exfoliation of the clay.^{77a} In such cases, TEM must be used to obtain the information about the morphology of the PCN. An option is to use SAXS, as the invisible diffraction peak in the WAXS pattern may be visible in the SAXS because it may have been beyond the range of WAXS and entering the range of SAXS. In such cases, the clay is exfoliated.

With the XRD method, some practical experimental details⁸⁵ that need to be considered include scattering/diffraction mode (transmission or reflection), sample form (powder or solid), data collection parameters (2θ step size and count time), clay diffraction peaks/signals, and equipment parameters (e.g., beam intensity, slit size, detection modes), etc. Information on why these parameters matter and what the XRD data indicate about a nanocomposite material can be found in references^{79a} as well as from books and manuscripts about x-ray diffraction.^{84,86} Figure 11.17 provides an example of the WAXS patterns for two organoclays and two PSCNs containing these two organoclays, either intercalated that showing a strong and sharp peak or disordered that does not show a peak.

XRD is easily used but does not directly provide the dispersion information while TEM is an expensive and difficult method to use. With TEM, however, direct information, although qualitative, about the dispersion of clay (and other nanoadditives) in the matrix polymer can be obtained. The XRD method is usually used together with the TEM technique to characterize the morphology of the resulting PCNs. Attempts have been made to quantify the information that has been obtained through TEM technique,⁷⁸ but it seems to be not so successful in current practice, particularly for describing the dispersion of clays.

TEM is very qualitative rather than quantitative because of the lack of well-defined standards for exfoliation, intercalation, and distribution for the clay layers in the polymer matrix. Figure 11.18 shows the TEM micrographs which, based on author's understanding and experience with TEM, illustrate the morphologies: immiscible, intercalated with many stacked clay layers, intercalated with a few stacked clay layer and uniform dispersion, and exfoliated with uniform dispersion.

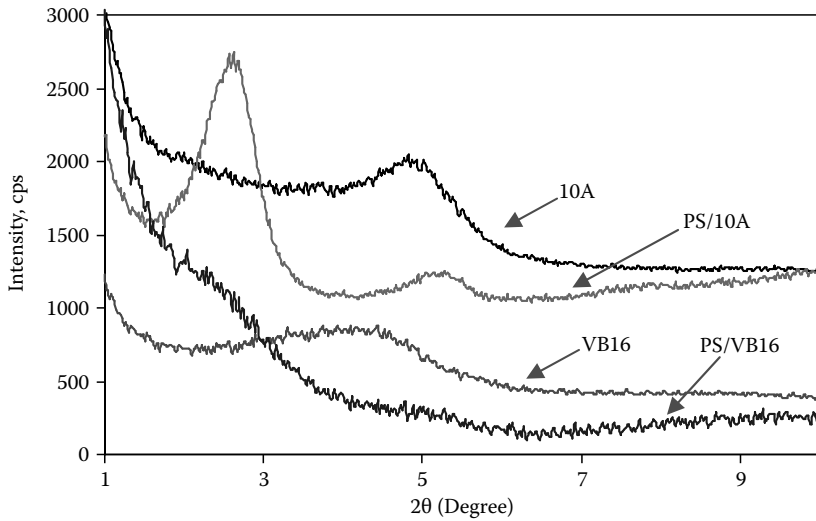


FIGURE 11.17 XRD patterns of two organoclays (Cloisite 10A, from Southern Clay Products, and VB16⁶⁴) and two PSCNs with intercalated (PS/10A) or exfoliated (PS/VB16) morphology.

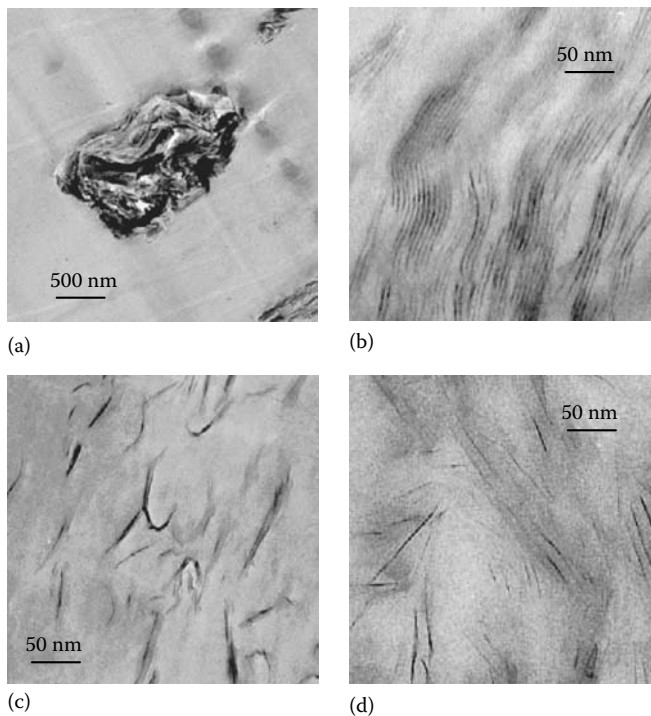


FIGURE 11.18 Representative TEM images: (a) immiscible; (b) intercalated with many clay layers stacking together; (c) intercalated and uniformly dispersed with a few clay layers stacking together; (d) exfoliated (delaminated) with a uniform dispersion.

Examples of these structures and morphology can be in the literature^{76,77a,87} to which researchers can compare their materials.

However, it is better to combine techniques to get an overall picture of the nanoscale structure of the nanocomposite. Furthermore, as each TEM image is focused on a very small snapshot (in

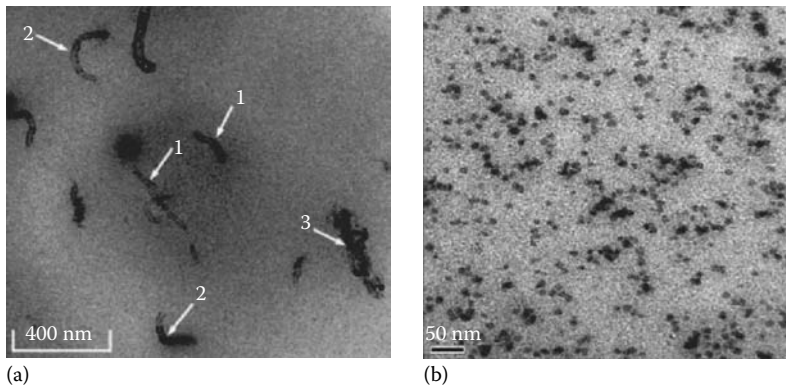


FIGURE 11.19 (a) TEM images of (a) carbon nanotube in polypropylene (arrow 1, straight tubes, arrow 2, curved tubes, and arrow 3, bundled or entangled tubes). (From Yang, J. et al., *Macromol. Rapid Commun.*, 28, 955, 2007. With permission.) (b) Nanosilica in acrylate polymer. (From Qi, D.M. et al., *Polymer*, 47, 4622, 2006. With permission.)

length scales of microns to nanometers) of the entire material, multiple images in both low magnification and high magnification and collection of several sections from different parts of the nanocomposite samples are necessary to make an informed decision about the clay dispersion and morphology. The low magnification images are particularly important for determining the overall clay distribution and dispersion in the polymer matrix. Although this greatly increases the amount of sample analysis time and cost, it does provide more confidence in interpreting the morphology, particularly when used in combination with other techniques, such as XRD and/or material property measurements. However, when a uniform dispersion is achieved (such as clay in polyamide-6 in most cases), a uniform distribution of the clay in the polymer matrix is seen in the low-magnification TEM image. In such cases, all randomly chosen points from which a TEM image is obtained will appear similar.

The structures of the PNs based on CNTs and other nanoadditives have both similarities and differences with those seen for the PCNs because of the dramatic difference of the nanoadditives in geometry. Like clays, the CNTs and other nanoadditives can be immiscible or aggregated with a few CNTs and nanoparticles or separated into single pieces in the polymer matrix, but intercalated and exfoliated are not suitable to describe the morphology of the PNs derived from CNTs and other nanoadditives as those terms are only suitable for describing the structure of layered nanoadditives as in the PCNs. The methods that are used for characterizing the nanostructure of the PCNs can be selectively used to characterize the structure of the PNs that contain CNTs and other nanoadditives other than the clay, except those, such as XRD, that are particularly used for analyzing the ordered structure related to the layered materials. TEM will be the most used and best tool to examine the morphology/dispersion of CNTs and other nanoadditives in the polymer matrices (Figure 11.19⁸⁸).

11.6 THERMAL AND FIRE PERFORMANCE OF POLYMER NANOCOMPOSITES AND MECHANISMS

11.6.1 THERMAL AND FIRE PERFORMANCE OF POLYMER NANOCOMPOSITES

The impact of nanocomposite technology on flame retardance (the thermal and fire resistance) of the polymers, as mentioned in Section 11.1, is primarily reflected in two important parameters: (1) the T_{onset} in the TGA curve—representative of the thermal stability of the polymer and (2) the peak HRR in the curve of CCA—reflection of the combustion behavior (the flammability) of the

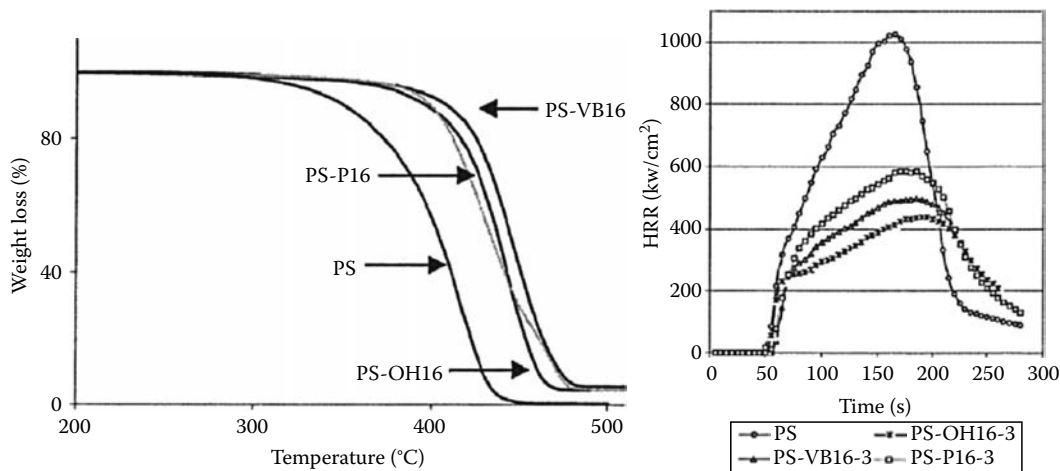


FIGURE 11.20 TGA curves and the CCA curves for pure polystyrene and three PS/clay nanocomposites obtained with in situ bulk polymerization, VB16 and OH16 are two ammonium-modified MMT and P16 is phosphonium-modified MMT. (From Zhu, J. et al., *Chem. Mater.*, 13, 3774, 2001. With permission.)

polymer. The T_{onset} will be increased while the peak HRR will be reduced for a variety of polymers when nanodispersion of the nanoadditive is achieved in the polymer matrix as seen in Figure 11.20 in which both the TGA curves and the CCA curves for pure polystyrene and a few PSCNs^{6a} obtained by in situ bulk polymerization are presented. In addition to these two methods, LOI and UL-94 testing, etc., have also been used. In most cases the PNs (tested with no additional FR additives) do not show an increased LOI nor can they be classified in the UL-94 test. Detailed information about LOI and UL-94 is not provided in this chapter.

TGA is the most widely used tool in analyzing the thermal performance of the PNs. A nanodispersed nanoadditive, as seen in Figure 11.20, usually brings a significant improvement of the thermal stability to the matrix polymer. More examples are given in Figure 11.21 in which the TGA curves

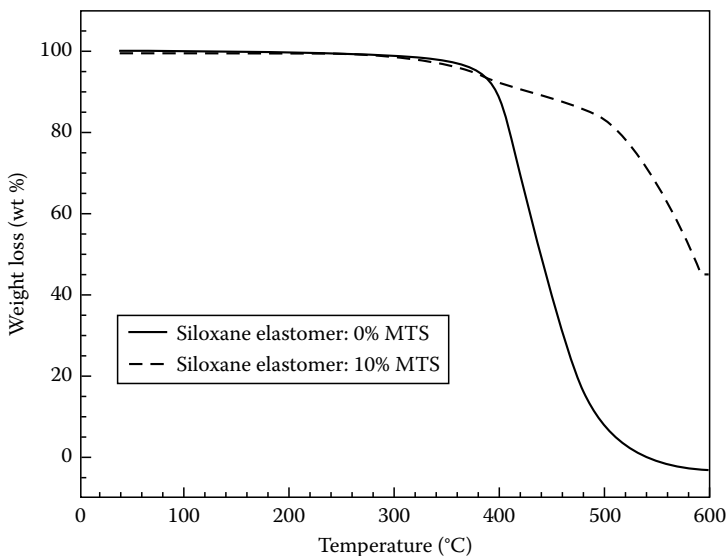


FIGURE 11.21 TGA traces for PDMS and its clay nanocomposite. (From Burnside, S.D. and Giannelis, E.P., *Chem. Mater.*, 7, 1597, 1995. With permission.)

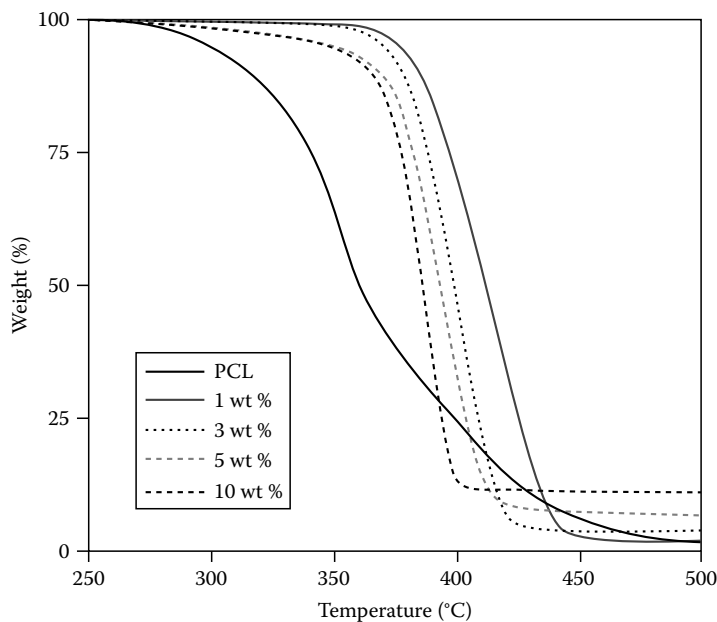


FIGURE 11.22 Relationship of weight loss and temperature under an air flow for neat PCL and PCL nanocomposites containing 1, 3, 5, and 10 wt % clay. (From Lepoittevin, B. et al., *Polymer*, 43, 4017, 2002. With permission.)

of polydimethylsilicone (PDMS) and its clay nanocomposite (at 10% organo-MMT)⁸⁹ are shown—a drastic shift of the T_{onset} to a higher temperature (with a stabilization as high as 140°C at 50% weight loss) is observed and in Figure 11.22 in which TGA curves of poly(1-caprolactone), PCL, and its clay nanocomposites⁹⁰ are provided—again, the PCNs show a much enhanced thermal stability.

However, one should be aware that the enhancement of the thermal stability of the PNs is strongly dependent on individual matrix polymers and nanoadditives. For a given nanoadditive, the resulting PNs based on one polymer matrix may show a significant enhancement of the thermal stability, while for another polymer matrix, such an enhancement may be less significant. Similarly, for a given matrix polymer, one nanoadditive, when it is nanodispersed, may significantly enhance the thermal stability of this matrix polymer; while another nanoadditive may be ineffective. Such a performance dependence on the individual polymer matrices and nanoadditives should be attributed to the interactions between the polymer matrix (and/or its pyrolysis products) and the nanoadditives.

Examples for illustrating dependence about thermal stability of the PNs on the polymer matrix (with MMT as nanoadditive) are given here: The PSCN at 3% loading of organoclay, as seen in Figure 11.20, shows an increased T_{onset} (at 5% mass loss) of about 50°C; but for PCNs based on polyolefins, a less significant enhancement in the thermal stability is observed (Figure 11.23⁹¹ in which results for PCNs based on polyethylene are shown); and for the PCNs based on PA-6, no change in the TGA parameters is observed.

Examples of the dependence of the thermal stability of the PNs on the nanoadditives (with poly(methyl methacrylate) (PMMA) as matrix polymer) are given here: The ZnAl_2 , CoAl_2 , and NiAl_2 LDHs bring an enhanced thermal stability to PMMA, as seen in Figure 11.24,⁹² but the CuAl_2 LDH results in a significantly reduced thermal stability. It is also seen that use of CNT can increase the T_{onset} as seen in PAN/MWCNT composite fibers,⁹³ which shows a 24°C shift in T_{onset} at 5% MWCNT loading, compared with that of the pure PAN, which shows a very limited enhancement when using clay as nanoadditive.⁹⁴

The thermal stability of PNs also shows a dependence on the surface treatment, as noted in Figure 11.25⁹⁵ in which TGA curves of PMMA and its clay nanocomposites (with the same MMT

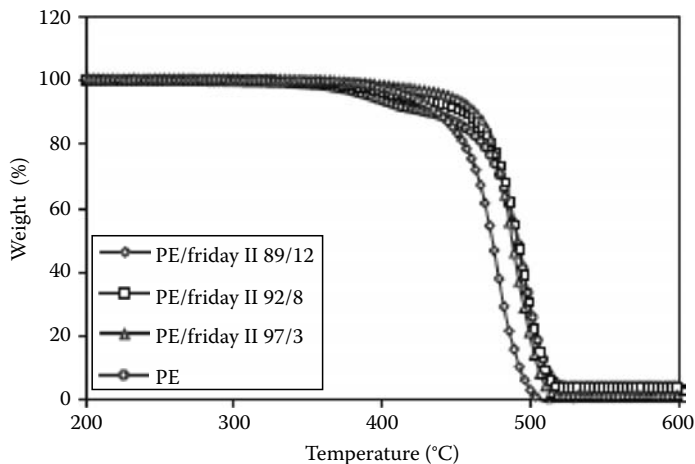


FIGURE 11.23 TGA curves of neat PE and composites. (From Zhang, J. et al., *Polym. Degrad. Stab.*, 91, 298, 2006. With permission.)

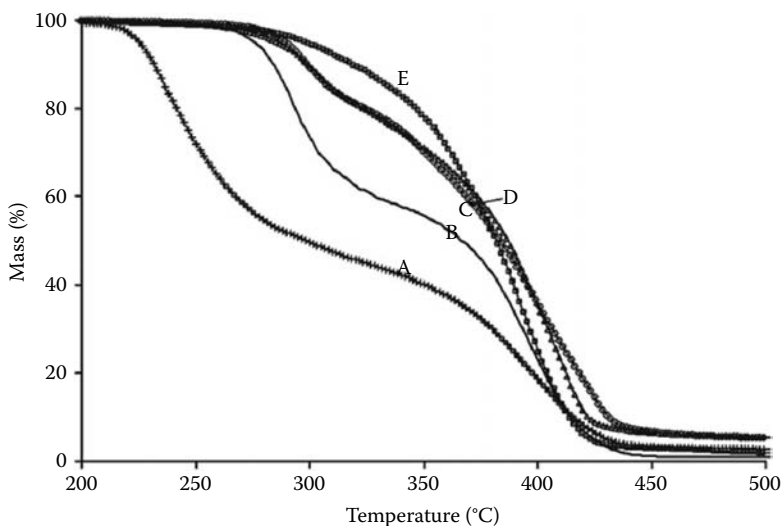


FIGURE 11.24 TGA curves of neat PMMA and PMMA/LDH nanocomposite (5% loading) in N_2 at $20^\circ C/min$. A: PMMA/ $CuAl_2$; B: PMMA; C: PMMA/ $ZnAl_2$; D: PMMA- $CoAl_2$; E: PMMA/ $NiAl_2$. (From Manzi-Nshuti, C. et al., *J. Mater. Chem.*, 18, 3091, 2008. With permission.)

but different surface treatments) are shown. It is clearly seen that MMT based on different surface treatment leads to a different thermal stability of the resulting PCN. The pyrolytic and oxidative conditions also play an important role in the thermal performance of the PNs, as seen in Figure 11.26⁹⁶ for PSCNs in both inert atmosphere and oxidative conditions. Under the pyrolytic condition, the thermal stability of PSCN was enhanced in terms of the onset temperature of degradation ($50^\circ C$ higher compared with pure PS); under thermo-oxidative condition, the degradation of pristine polymer and PSCN occurred at the comparable temperatures; but a significantly enhanced charring performance for the PSCN is observed, from 5% for pristine polymer to 15% for PSCN, at temperature around $400^\circ C$. However, the final char residue is about the same for both oxidative and pyrolytic conditions.

The loading of the nanoadditive is another factor affecting the thermal stability of the PNs. A significant enhancement is observed at a low loading of the nanoadditives above this loading,

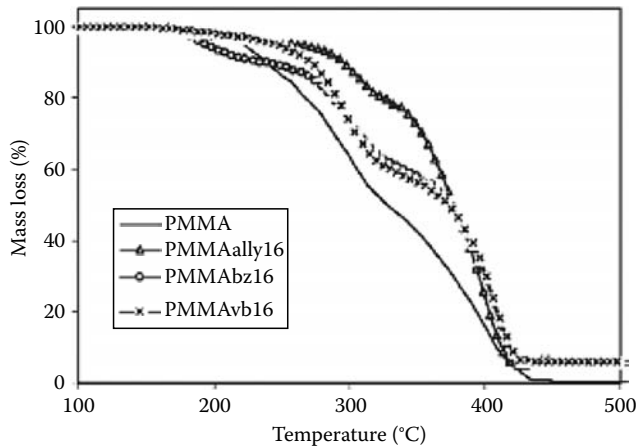


FIGURE 11.25 TGA curves of neat PMMA and PMMA/MMT nanocomposites at 5% loading. (From Zhu, J. et al., *Polym. Degrad. Stab.*, 77, 253, 2002. With permission.)

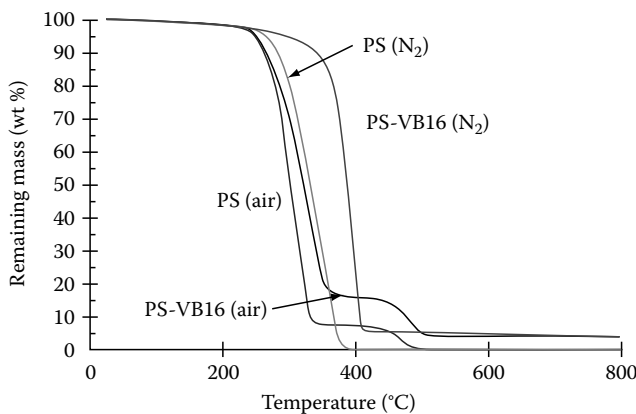


FIGURE 11.26 TGA curves of PS and its clay nanocomposites under pyrolytic and thermo-oxidative conditions at 1°C/min. (From Bourbigot, S. et al., *Polym. Degrad. Stab.*, 84, 483, 2004. With permission.)

the enhancement may level off. This is shown in Figure 11.27⁹⁷ in which the onset temperature as a function of clay loading for a few PSCNs are given. Further, it is noted that only surface-treated MMTs bring an enhanced thermal stability to the PS while inorganic (no organic onium present) MMT does not lead to an enhancement to the PS.

The nanodispersed nanoadditives usually show enhanced fire performance and CCA has been the most powerful tool in analyzing the flammability of the PNs. In most cases, the PNs, as seen in Figure 11.20, show a significantly reduced peak HRR in the CCA curve. More examples of this are seen in PA-6/clay nanocomposite, which shows a 63% reduction in the peak HRR at 5% loading (Figure 11.28⁹⁸ in which the heat release rate as a function of time for pure PA-6 and its clay nanocomposites is shown) and in poly(ethylene-co-vinyl acetate) (EVA)/clay nanocomposite,⁹⁹ which shows a reduction of the peak HRR at about 50% at 5% organoclay loading.

Like the thermal stability, however, the magnitude of the reduction in the flammability of the PNs is strongly dependent on the polymer matrices and the nanoadditives. Examples of matrix polymer dependence is illustrated with MMT-based PCNs: The PCNs based on PS,^{6a} EVA,⁹⁹ and PA-6,⁹⁸ etc. show a significant reduction of the peak HRR in the CCA curve (40%–70% at a clay loading about 5%);

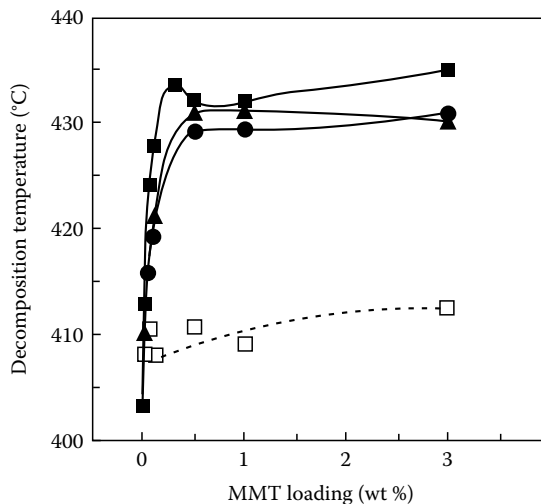


FIGURE 11.27 Decomposition temperature as a function of MMT loading of PS nanocomposites. The MMT is modified with (filled square) dimethyl(hydrogenated tallow alkyl)benzyl ammonium ion, (filled circle) dimethyl di(hydrogenated tallow alkyl) ammonium ion, (filled triangle) dimethyl(hydrogenated tallow alkyl) 2-ethylhexyl ammonium ion, and (open square) NaMMT. (From Doh, J.G. and Cho, I., *Polym. Bull.*, 41, 511, 1998. With permission.)

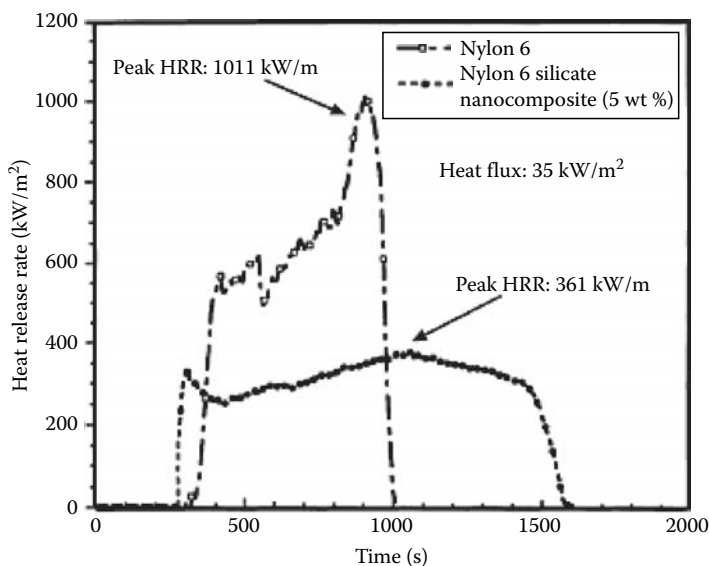


FIGURE 11.28 CCA curves of PA-6 and its clay nanocomposite (5 wt %) at 35 kW/m² heat flux. (From Gilman, J.W., *Appl. Clay Sci.*, 15, 31, 1999. With permission.)

while the PCNs based on polymers like polypropylene (PP) show a moderate reduction of the peak HRR (30%–50% at a 5% clay loading) and the PCNs based on PMMA and polyacrylonitrile (PAN) etc. show a limited reduction (10%–20% at a 5% clay loading).⁹⁴

The CNTs can surpass the clays and other nanoadditives as effective flame-retardant additives, as reflected in the lower loading of the CNTs than the other nanoadditives needed to enhance the thermal and fire resistance.¹⁰⁰ For instance, the results for PMMA in the presence of different nanoadditives are seen in Figure 11.29 in which the relationship of mass loss rate (MLR) and loading of

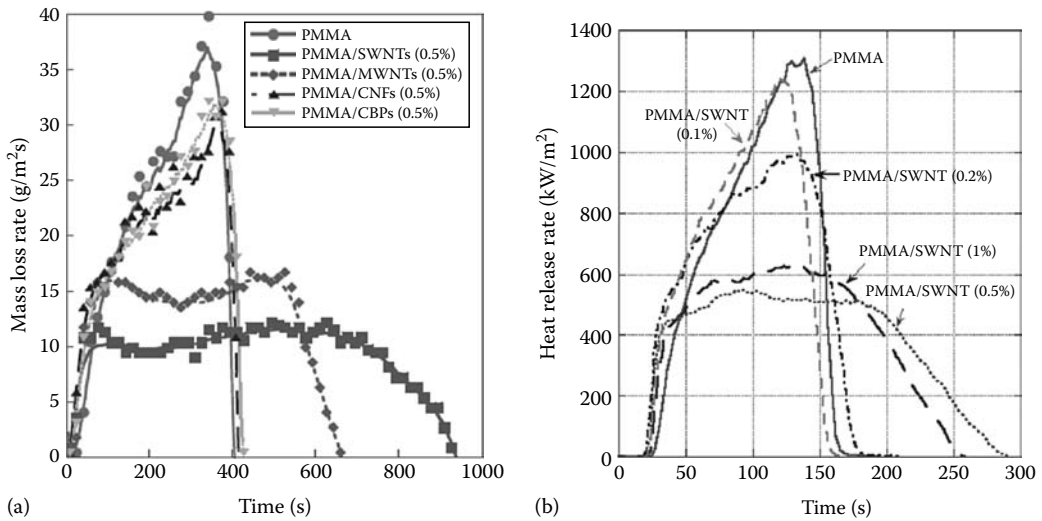


FIGURE 11.29 (a) Mass loss rate as a function of gasification time for several PMMA nanocomposites, at an external radiant flux of 50kW/m² in nitrogen. (From Kashiwagi, T. et al., *Nat. Mater.*, 4, 928, 2005.); (b) Effects of SWNT concentration on heat release rate of PMMA at 50kW/m². (Reprinted from Kashiwagi, T. et al., *Polymer*, 46, 471, 2005. With permission.)

CNT is shown.¹⁰¹ The PMMA nanocomposite in the presence of CNT gives a significant reduction in the peak MLR (55%–70%) at a CNT loading of only 0.5%; the effect of the CNT loading on the HRR of the PMMA¹⁰² is also shown in Figure 11.29, where a significant reduction of the peak HRR (~55%) is seen. PMMA nanocomposites in presence of other nanoadditives may show a limited reduction of the peak HRR and this is true with clay as the nanoadditive.⁹⁴ For other polymers, such as PP shown in Figure 11.30,¹⁰³ CNT can also exert a significant effect on the peak MLR and peak HRR, while MMT⁹¹ shows a moderate reduction of the peak HRR.

In addition to the identity of the matrix polymer and nanoadditive, other factors, such as concentration, size, and degree of dispersion of the nanoadditive, also show an effect. The greatest

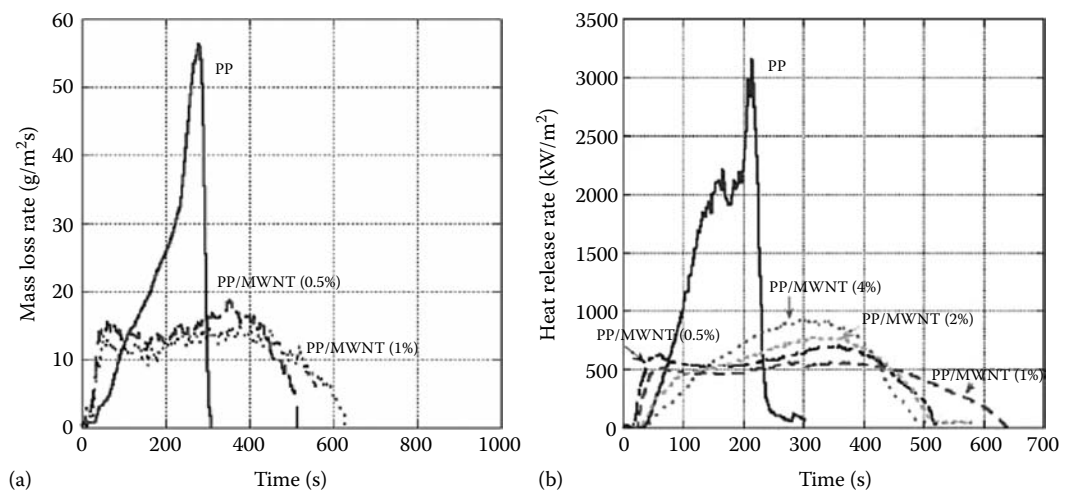


FIGURE 11.30 (a) Effects of concentration of MWNT on mass loss rate of PP at 50kW/m² in nitrogen; (b) Effects of concentration of MWNT on heat release rate of PP at 50kW/m². (From Kashiwagi, T. et al., *Polymer*, 45, 4227, 2004. With permission.)

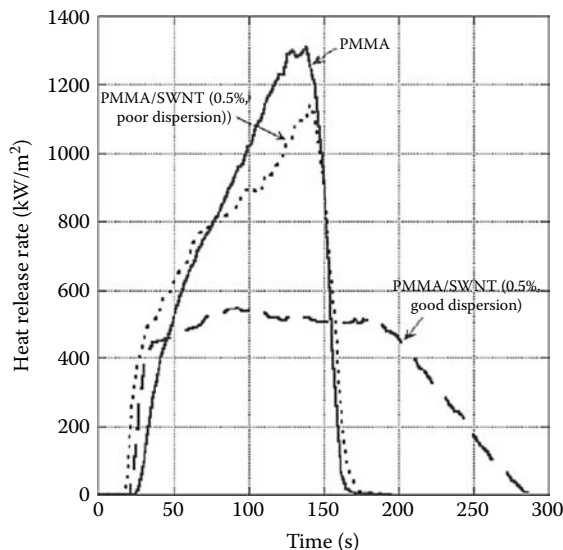


FIGURE 11.31 Effect of SWNT dispersion (at 0.5% loading) on heat release rate of PMMA at 50kW/m². (From Kashiwagi, T. et al., *Polymer*, 46, 471, 2005. With permission.)

flammability reduction, in general, may be obtained at 5 wt% clay loading, regardless of polymer type,^{98,104} although exceptions are known. A more uniform dispersion of the nanoadditive in the PN is responsible for a larger reduction in peak HRR and better reproducibility of the fire performance. This can be seen in Figure 11.31¹⁰² in which the CCA data of the PMMA in presence of SWCNT, either with poor or with good dispersion, are shown; there is dramatic difference in the peak HRR between the good and poor dispersion. As the reduction of the peak HRR in CCA is related to the morphology, the CCA may be used to identify whether or not a nanocomposite has been obtained.⁸⁵ For instance, when the peak HRR of a PN is less than the best that has been observed for a particular polymer, it may indicate that the PN is not as well-dispersed or that “defects” are present; usually this implies the presence of a significant amount of immiscible material in the PN.

Results¹⁰⁵ from the National Institute of Standards and Technology (NIST) show that a formation of a homogeneous carbonaceous char from the combustion of a PN is critical for preventing rapid combustion (this is related to uniform dispersion of the nanoadditive in the polymer matrix, however, a uniform dispersion may not necessarily lead to a homogeneous char residue because of uneven aggregation of the nanoadditive). The assertion is drawn from comparison of the MLR data in the gasification test for three different polypropylene/clay nanocomposites (PPCNs) (in presence of maleic anhydride grafted PP (PP-g-MA) using MMT, synthetic hectorite and FSM as the nanoadditive) and the PP/PP-g-MA mixture that produces little or no carbonaceous material after gasification. The PPCN with the FSM gives the largest reduction in the peak MLR in the gasification test (>50%), as shown in Figure 11.32.¹⁰⁵ This can be attributed to the PPCN that, with FSM as the nanoadditive, forms a more continuous and crack-free residue (also shown in Figure 11.32) than the other two samples. This also indicates the importance of the aspect ratio of the clay in forming the continuous and crack-free char residue: The FSM possesses a much larger aspect ratio (about 1200) than MMT (about 200) and hectorite (about 50).

Although the nanoadditive can enhance both the thermal stability and the fire performance of the matrix polymer, it has been noted that the enhancement on the fire performance is not parallel to that on the thermal stability, i.e., an observation about the reduction of the peak HRR of the resulting PN does not necessarily mean that an enhancement of the thermal stability of the PN can be observed. A typical example is PA-6. It has been seen that the PA-6/clay nanocomposite shows a significantly reduced peak HRR,⁹⁸ but it does not show enhanced thermal stability.

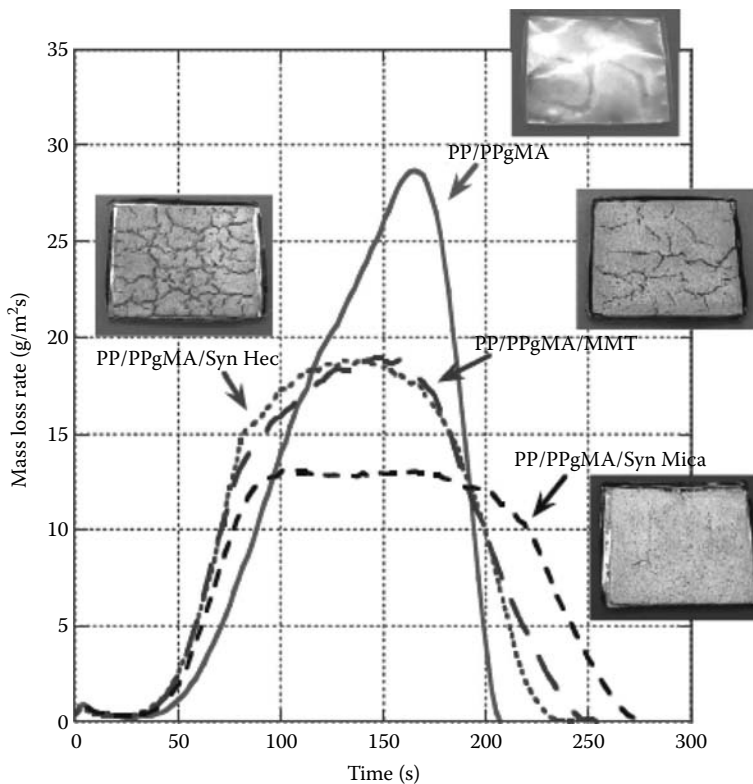


FIGURE 11.32 (See color insert following page 530.) Effect of clay type on MLR of PP (84.6%)/PPgMA (7.7%)/clay (7.7%) at 50 kW/m^2 in N_2 . (From Cipiriano, B.H. et al., *Polymer*, 48, 6086, 2007. With permission.)

In characterizing the fire performance of the materials, microscale combustion calorimetry (MCC, also called pyrolysis combustion flow calorimeter (PCFC)) can also be a useful tool. MCC is a newly introduced technique developed by scientists at the Federal Aviation Administration (FAA) laboratories¹⁰⁶ and recently became a Standard Test Method.¹⁰⁷ The technique utilizes the traditional oxygen depletion calorimetry. The specimen is first heated at a constant rate (typically 1°C/s) in a pyrolyzer. The pyrolyzed products are swept by an inert gas, such as nitrogen, and then mixed with oxygen to form a gas stream that enters the combustor in which the decomposition products are completely oxidized at 900°C . Oxygen concentration and flow rates of the combustion gases are used to determine the oxygen depletion involved in the combustion process and the heat release rates are determined from these measurements. With the MCC, various parameters can be determined in a short time with a very small specimen (1–50 mg), such as, HRR (W/g), heat of combustion (HC, J/g), and ignition temperature (T_i , $^\circ\text{C}$). The MCC technique has some similarity, but is still quite different, to the CCA. In addition to the advantages of requiring only a small amount of sample and obtaining results in a very short time, an important advantage is that the results from the MCC can be correlated to those from the other fire test testing methods, such as CCA, flammability tests (limiting oxygen index (LOI), UL-94), and combustion tests (bomb calorimeter), and therefore MCC can be not only a useful but also a low-cost tool to screen and predict the flammability of the polymers and other materials. Figure 11.33 shows a typical MCC curve.¹⁰⁸

11.6.2 MECHANISM OF THE EFFECT OF NANOADDITIVES ON FLAMMABILITY OF POLYMERS

The mechanism for the effect of nanoadditives on the thermal and fire performance of the matrix polymers has been widely investigated and different interpretations have been put forward,¹⁰⁹ but a complete understanding is not yet available. Because the enhancement of the thermal and fire performance

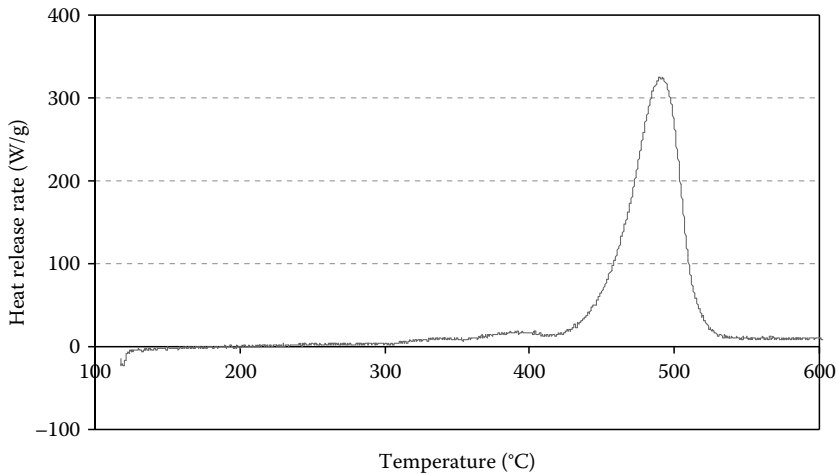


FIGURE 11.33 A representative MCC curve (relation of heat release rate and temperature) of a polyethylene-based FR composite.

for the PNs is quite dependent on the identity of the polymer; the effect of the nanoadditives on the flammability of the polymers shows differences. For instance, in the case of clay, it is hypothesized that migration of clay particles to the surface of the matrix polymer occurs during burning.¹¹⁰ It is believed that the clay is pushed by the numerous rising bubbles of degradation products and the associated convective flow in the melt from the interior of the sample toward the sample surface, while the matrix polymer because of the pyrolysis with de-wetted clay particles is left behind. Further, aggregation of clay layers occurs after the degradation of the organic treatment on the clay interlayers, which makes the clay more hydrophilic and less compatible with the matrix polymer, and thus leads to a clay-rich barrier that slows the rate of mass loss and, in turn, lowers the HRR.

The migration mechanism of the clay, however, can be explained equally by the well-accepted barrier mechanism^{104a,111} in the condensed phase during burning.¹¹² The barrier mechanism (Figure 11.34) suggests that, under pyrolysis conditions, the clay forms a char-like material that acts as both a barrier to mass transport of the degradation products to the surface of the degrading polymer and a thermal barrier, preventing additional exposure of the polymer matrix to the heat and oxygen. The barrier function of the clay platelets can provide thermal insulation for the condensed phase and thus increase the thermal stability of the matrix polymer.

A supplemental mechanism to the barrier mechanism is paramagnetic radical trapping,¹¹³ when the clay loading is low, paramagnetic radical trapping is a component of the mechanism in the stabilization and such a radical trapping might be attributable to the presence of the paramagnetic impurities within the clay. This is confirmed after examination of the PSCNs prepared by bulk-polymerization using either an iron-containing or an iron-depleted clay, a specially designed experiment to determine the function of paramagnetic iron on the enhancement of thermal stability.

Research shows that clay can qualitatively affect polymer degradation.⁹⁴ The presence of the clay can significantly change the degradation pathway of the matrix polymer, and clay promotes the

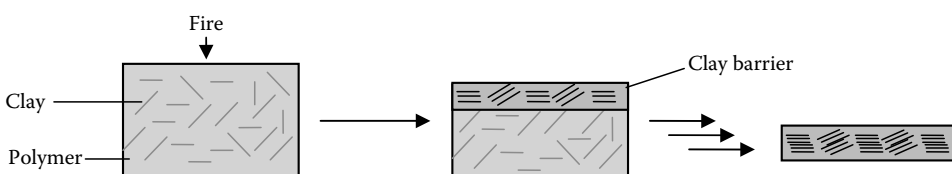


FIGURE 11.34 Mechanism of how the clay barrier forms.

TABLE 11.1
Thermal Degradation Pathways of Some Polymers and Their Clay Nanocomposites and Resulting Reduction of Peak HRR

Polymer	Degradation Pathway of Virgin Polymer	Degradation Pathway Change in Presence of Clay	Reduction in Peak HRR (%)
PA6	Intra-aminolysis/acidolysis, random scission	Inter-aminolysis/acidolysis, random scission	50–70
PS, HIPS	β -Scission (chain end and middle)	Recombination, random scission	40–70
EVA	Chain stripping, disproportionation	Hydrogen abstraction, random scission	50–70
SAN, ABS	β -Scission (chain end and middle)	Recombination, random scission	20–50
PE	Disproportionation	Hydrogen abstraction	20–40
PP	β -Scission, disproportionation	Random scission	20–50
PAN	Cyclization, random scission	No change	<10
PMMA	β -Scission	No change	10–20

Source: Jang, B.N. et al., *Polymer*, 46, 10678, 2005. With permission.

production of oligomers rather than the monomers.¹¹⁴ In the case of PCNs that degrade by a radical pathway, the effect of clay on the enhancement of the thermal and fire resistance of matrix polymers is strongly related to the stability of the radicals that are produced during the thermal degradation of the matrix polymer. The more stable the polymeric radical that is produced, the larger is the enhancement on the fire retardancy (reflected in the reduction of the peak HRR) that the matrix polymer can obtain. When a polymer, such as PS, degrades by more than one pathway, the presence of clay will enhance one degradation pathway instead of another and this generally favors oligomers, leading to the matrix polymer degrading slower than the pure polymer. But this is not seen for other polymers, such as PMMA, that degrade by only a single pathway, i.e., the clay cannot promote the formation of different degradation products of such polymers. Table 11.1 shows the thermal degradation pathways of some pure polymers and their clay nanocomposites and resulting reduction of peak HRR. The presence of clay also significantly affects the apparent activation energy.¹¹⁵

The mechanism by which clays enhance the thermal and fire resistance of the matrix polymers may also be used to interpret the function of the CNTs and other nanoadditives. The formation of the continuous and networked char barrier as seen in Figure 11.32 for PPCN¹⁰⁵ and in Figure 11.35 for

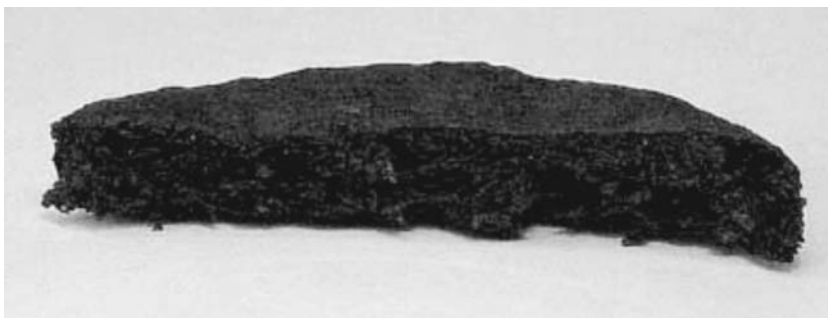


FIGURE 11.35 Cross section of the char residue of the PP/MWNT (1%). (From Kashiwagi, T. et al., *Polymer*, 46, 471, 2005. With permission.)

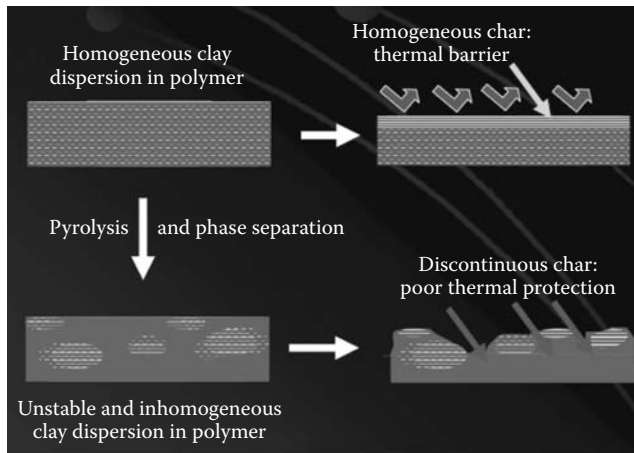


FIGURE 11.36 (See color insert following page 530.) Mechanism of how crack-free and networked char barrier affects the thermal stability of polymer matrix. (From Gilman, J.F., Flame retardant polymer nanocomposite, http://www.epa.gov/oppt/nano/p2docs/casestudy2_gilman.pdf)

PP/CNT nanocomposite¹⁰² on the surface of the matrix polymer is the primary pathway by which the nanoadditives enhance the thermal and fire resistance of the matrix polymer, because such crack-free and networked nanoadditive char barriers can significantly shield the heat and oxygen from the matrix polymer and thus reduce the heat release rate, i.e., slow the burning process (Figure 11.36).¹¹⁶

11.7 CONCLUDING COMMENTS AND TRENDS FOR THE STUDY OF POLYMER NANOCOMPOSITES

Based on the observations for PNs, it is quite clear that the nanoadditives can exert a definite flame-retardant effect, appearing in the form of an increase in the T_{onset} and a reduction in the peak HRR of polymers and this reduces the burning process, as evidenced by most thermoplastic polymers studied to date, such as PS, PA-6, EVA, and many others. An additional phenomenon that should be noted and will be useful in designing a flame-retardant polymer system is that the PNs usually do not drip and they can retain the shape of the original sample during the course of combustion. Production of a continued and networked char residue is critical in achieving a significant enhancement of the thermal and fire performance of the matrix polymer and this requires that one maintain the homogeneous dispersion of the nanoadditives in the polymer melt during pyrolysis. This is true whether a carbonaceous char forms or if only nanoadditive makes up the residue.

However, a common feature of the PNs is that, based on the flammability of various polymers that have been studied with a single nanoadditive, like clay, they can only show a retarded combustion process (i.e., the peak HRR and the average HRR can be lowered), while almost all the carbon sources will eventually burn out in most cases. The total heat released (THR) in CCA is not changed compared with that of the same amount of base polymer. Furthermore, like many flame-retardant composites, an earlier time to ignition (and perhaps also the time to peak HRR) for most PNs than the base polymer is also seen in the CCA experiment.¹¹⁷

Finding new approaches of applying nanoadditives, effectively and at low cost, in polymers with desired properties, such as required thermal and fire resistance, have been of increasing interest and a large challenge. Prediction about the adaptation of the nanoadditives in polymers to promote the thermal and fire resistance as well as the other properties can be seen in the literature.⁸⁵ A simple discussion, summarized from the literature, is provided below.

To promote the thermal and fire resistance (as well as other properties) of the polymer matrix, one trend is the application of two or more nanoadditives, i.e., multitypes of nanoadditives, into one

polymer matrix to achieve a nanocomposite containing multi-nano-components. An advantage of using the nanoadditives in such a way is that the advantages of the different nanoadditives, including synergism, can be combined into one system, so that the resulting PN may exhibit better performance. Clay is of great interest as one component of the combined nanoadditives because it is easy to obtain at low cost and, more importantly, its comprehensive performance. For instance, it is seen that use of a combination of clay with CNT brings enhanced performance.¹¹⁸ Of increasing interest is the use of synthetic clays, such as, fluorinated synthetic mica, magadiite, and LDHs. The LDHs, as a hydrated material (very similar to $\text{Mg}(\text{OH})_2$ or $\text{Al}(\text{OH})_3$), are of particular interest because of their potential to release water under fire conditions and the presence of a layered structure, like that of the silicate clays. However, the high cost and limited sources of the synthetic clays have slowed the use of such nanoadditives.

Another process is the use of other additives, which may not be nano-sized, to enhance the fire resistance of the matrix polymer, such as, using an additive that can form a glassy barrier to seal the cracks in the char, resulting in a self-extinguishing PN. It has been noted in the literature that the concept has been practiced.¹¹² One common and practical way is to use nanoadditives in the presence of traditional flame retardants, such as halogen-¹¹⁹ or phosphorous-based,¹²⁰ or as a nanoscale component in a traditional flame-retardant system to achieve a fire-resistant polymer composite; this includes nanoparticles, such as nano- $\text{Mg}(\text{OH})_2$ and nano- $\text{Al}(\text{OH})_3$,¹²¹ obtained from traditional inorganic flame retardants that have an original particle size in microns. Still, the clay will be of great interest because of its excellent performance, such as the antidripping and charring properties and/or the synergism with many traditional fillers/flame retardants. For instance, flame-retardant composites based on EVA or PP in presence of clay can significantly reduce the loading of $\text{Mg}(\text{OH})_2$, the primary filler.¹²² Nanoadditives like CNTs and POSS, although expensive when used alone in the polymer matrix, can also be combined with traditional flame-retardant system, not only reducing the cost but also improving the fire performance of the resulting PNs. Closely related is a trend of using PNs to reinforce the traditional composites and to improve the fire resistance.

Two more areas will be suggested as future trends: specific nanocomposite structural design and true multifunctional materials.⁸⁵ Specific nanocomposite structural design does not just mean to obtain a nice dispersion of the nanoparticles in the polymer matrix, but to achieve a specific structure, such as an ordered alignment of the nanoadditives (e.g., the clay), to produce some specially desired performance in the final nanocomposite. True multifunctional materials have been and will continue to be one of the targets for nanocomposite materials, but this is somewhat elusive and premature in the PN area. Because such performance PNs may not show a better, if any, improvement in the thermal and fire performance than the regular PNs, they are not further discussed in this chapter. However, this means that new multifunctional materials may already begin with enhanced thermal and fire properties simply because of their nanocomposite structure, not because of deliberate researcher design.

BIBLIOGRAPHY

- Ahir, S. V. and Terentjev, E. M. Polymers containing carbon nanotubes: Active composite materials. *Polym. Nanostruct. & Their Appl.* (2007), 2, 153–200.
- Alexandre, M. and Dubois, P. Nanocomposites, *Macromol. Eng.* (2007), 4, 2033–2070.
- Alexandre, M. and Dubois, P. Polymer-layered silicate nanocomposites: Preparation, properties, and uses of a new class of materials, *Mater. Sci. Eng. Rep.* (2000), 28, 1–63.
- Beyer, G. Flame retardant properties of organoclays and carbon nanotubes and their combinations with alumina trihydrate, *Flame Retard. Polym. Nanocomp.* (2007), 163–190.
- Coleman, J. N., Khan, U., and Gun'ko, Y. K. Mechanical reinforcement of polymers using carbon nanotubes, *Adv. Mater.* (Weinheim, Germany) (2006), 18, 689–706.
- Costa, F. R., Saphiannikova, M., Wagenknecht, U., and Heinrich, G. Layered double hydroxide based polymer nanocomposites, *Adv. Polym. Sci.* (2008), 210, 101–168.
- Grossiord, N., Loos, J., Regev, O., and Koning, C. E. Toolbox for dispersing carbon nanotubes into polymers to get conductive nanocomposites, *Chem. Mater.* (2006), 18, 1089–1099.

- Joshi, M. and Butola, B. S., Polymeric nanocomposites—polyhedral oligomeric silsesquioxanes (POSS) as hybrid nanofiller, *J. Macromol. Sci., Polym. Rev.* (2004), C44, 389–410.
- Leroux, F. and Besse, J. P. Polymer interleaved layered double hydroxide: A new emerging class of nanocomposites, *Chem. Mater.* (2001), 13, 3507–3515.
- Leszczynska, A., Njuguna, J., Pielichowski, K., and Banerjee, J. R. (a) Polymer/montmorillonite nanocomposites with improved thermal properties, Part I: Factors influencing thermal stability and mechanisms of thermal stability improvement, *Thermochim. Acta* (2007), 453, 75–96.; (b) Polymer/montmorillonite nanocomposites with improved thermal properties. Part II: Thermal stability of montmorillonite nanocomposites based on different polymeric matrixes, *Thermochim. Acta* (2007), 454, 1–22.
- Moniruzzaman, M. and Winey, K. I. Polymer nanocomposites containing carbon nanotubes, *Macromolecules* (2006), 39(16), 5194–5205.
- Morgan, A. B. and Wilkie, C. A. (Eds.), *Flame Retardant Polymer Nanocomposites*, John Wiley & Sons, Hoboken, NJ (2007), 421pp.
- Pielichowski, K., Njuguna, J., Janowski, B., and Pielichowski, J. Polyhedral oligomeric silsesquioxanes (POSS)-containing nanohybrid polymers, *Adv. Polym. Sci.* (2006), 201 (Supramolecular Polymers, Polymeric Betains, Oligomers), 225–296.
- Pinnavaia, T. J. and Beall, G. W. (Eds.), *Polymer-Clay Nanocomposites*, John Wiley & Sons, Chichester, U.K. (2000), 343pp.
- Serge, B. and Sophie, D. Fire retardant polymers: Recent developments and opportunities, *J. Mater. Chem.* (2007), 17, 2283–2300.
- Sinha Ray, S. and Okamoto, M. Polymer/layered silicate nanocomposites: A review from preparation to processing, *Prog. Polym. Sci.* (2003), 28, 1539–1641.
- Utracki, L. A. *Clay-Containing Polymeric Nanocomposites*, RAPRA Tech. Ltd., Shawbury, Shrewsbury, Shropshire, U.K., 2004, p. 496.

REFERENCES

- Garnweitner, G., Smarsly, B., Assink, R., Ruland, W., Bond, E., and Brinker, C. J. Self-assembly of an environmentally responsive polymer/silica nanocomposite, *JACS* (2003), 125, 5626–5627.
- (a) Khaled, S.M., Sui, R., Charpentier, P.A., and Rizkalla, A.S. Synthesis of TiO₂-PMMA nanocomposite: Using methacrylic acid as a coupling agent, *Langmuir* (2007), 23, 3988–3995; (b) Xiong, H.-M., Shen, W.-Z., Wang, Z.-D., Zhang, X., Xia, Y.-Y. Liquid polymer nanocomposites PEGME-SnO₂ and PEGME-TiO₂ prepared through solvothermal methods, *Chem. Mater.* (2006), 18, 3850–3854.
- (a) Guo, Z., Pereira, T., Choi, O., Wang, Y., and Hahn, H. T. Surface functionalized alumina nanoparticle filled polymeric nanocomposites with enhanced mechanical properties, *J. Mater. Chem.* (2006), 16, 2800–2808; (b) Ash, B. J., Siegel, R. W., and Schadler, L. S. Mechanical behavior of alumina/poly(methyl methacrylate) nanocomposites, *Macromolecules* (2004), 37, 1358–1369.
- Corriu, R. J. P., Gerbier, P., Guerin, C., and Henner, B. From preceramic polymers with interpenetrating networks to SiC/MC nanocomposites, *Chem. Mater.* (2000), 2, 805–811.
- (a) Ni, Y. and Zheng, S. A novel photocrosslinkable polyhedral oligomeric silsesquioxane and its nanocomposites with poly(vinyl cinnamate), *Chem. Mater.* (2004), 16, 5141–5148; (b) Zheng, L., Hong, S., Cardoen, G., Burgaz, E., Gido, S. P., Coughlin, E. B. Polymer nanocomposites through controlled self-assembly of cubic silsesquioxane scaffolds, *Macromolecules* (2004), 37, 8606–8611; (c) Fina, A., Tabuani, D., Frache, A., Boccaleri, E., and Camino, G. Octaisobutyl POSS thermal degradation, in *Fire Retardancy of Polymers: New Applications of Mineral Fillers*, Le Bras, M., Wilkie, C. A., Bourbigot, S., Duquesne, S., and Jama, C. (Eds.), Royal Society of Chemistry, Cambridge (2005), pp. 202–220.
- (a) Dalmas, F., Chazeau, L., Gauthier, C., Cavaille, J. Y., and Dendievel, R. Large deformation mechanical behavior of flexible nanofiber filled polymer nanocomposites, *Polymer* (2006), 47, 2802–2812; (b) Kelarakis, A., Yoon, K., Somani, R.H., Chen, X., Hsiao, B.S., and Chu, B. Rheological study of carbon nanofiber induced physical gelation in polyolefin nanocomposite melt, *Polymer* (2005), 46, 11591–11599.
- (a) Moniruzzaman, M. and Winey, K.I., Polymer nanocomposites containing carbon nanotubes, *Macromolecules* (2006), 39, 5194–5205; (b) Haggemueller, R., Fischer, J. E., and Winey, K. I. Single wall carbon nanotube/polyethylene nanocomposites: Nucleating and templating polyethylene crystallites, *Macromolecules* (2006), 39, 2964–2971; (c) Datsyuk, V., Guerret-Piecourt, C., Dagreou, S., Billon, L., Dupin, J.-C., Flahaut, E., Peigney, A., and Laurent, C. Double walled carbon nanotube/polymer composites via in-situ nitroxide mediated polymerization of amphiphilic block copolymers, *Carbon* (2005), 43, 873–876.

8. (a) Zhu, J., Morgan, A. B., Lamelas, F. J., and Wilkie, C. A. Fire properties of polystyrene-clay nanocomposites, *Chem. Mater.* (2001), 13, 3774–3780; (b) Su, S., Jiang, D. D., and Wilkie, C. A. Polybutadiene modified clay and its nanocomposites, *Polym. Degrad. Stab.* (2004), 84, 279–288; (c) Wang, D., Jang, B. N., Su, S., Zhang, J., Zheng, X., Chigwada, G., Jiang, D. D., and Wilkie, C. A. Fire retardancy of polystyrene-hectorite nanocomposites, Editor(s): Le Bras, M. *Fire Retard. Polym.: New Appli. Miner. Fillers*, [9th European Meeting on Fire Retardancy and Protection of Materials] (2005), 126–138; (d) Maiti, P., Yamada, K., Okamoto, M., Ueda, K., and Okamoto, K. New polylactide/layered silicate nanocomposites: Role of organoclays, *Chem. Mater.* (2002), 14, 4654–4661.
9. (a) Costache, M. C., Heidecker, M. J., Manias, E., Camino, G., Frache, A., Beyer, G., Gupta, R. K., and Wilkie, C. A. The influence of carbon nanotubes, organically modified montmorillonites and layered double hydroxides on the thermal degradation and fire retardancy of polyethylene, ethylene-vinyl acetate copolymer and polystyrene, *Polymer* (2007), 48, 6532–6545; (b) Leroux, F. and Besse, J.P. Polymer interleaved layered double hydroxide: A new emerging class of nanocomposites, *Chem. Mater.* (2001), 13, 3507–3515.
10. Sue, H. J., Gam, K. T., Bestaoui, N., Spurr, N., and Clearfield, A. Epoxy nanocomposites based on the synthetic α -zirconium phosphate layer structure, *Chem. Mater.* (2004), 16, 242–249.
11. Sukpirom, N. and Lerner, M. M., Preparation of organic-inorganic nanocomposites with a layered titanate, *Chem. Mater.* (2001), 13, 2179–2185.
12. Giannelis, E. P. Polymer layered silicate nanocomposites, *Adv. Mater.* (Weinheim, Germany) (1996), 8, 29–35.
13. <http://en.wikipedia.org/wiki/Clay>
14. Giannelis, E. P., Krishnamoorti, R., and Manias, E., Polymer/silica nanocomposites: Model systems for confined polymers and polymer brushes, *Adv. Polym. Sci.* (1999), 118, 108–147.
15. http://en.wikipedia.org/wiki/Layered_double_hydroxide
16. Meyn, M., Beneke, K., and Legaly, G. Anionic-exchange reactions of layered double hydroxides, *Inorg. Chemistry* (1990), 29, 5201–5207.
17. http://en.wikipedia.org/wiki/Carbon_Nano_Tube
18. Iijima, S. Helical microtubules of graphitic carbon, *Nature (London)* (1991), 354, 56–58.
19. Ajayan, P. M. and Ebbesen, T. W., Nanometer-size tubes of carbon. *Rep. Prog. Phys.* (2003), 60, 1025–1065.
20. Ajayan, P. M., Stephan, O., Colliex, C., and Trauth, D. Aligned carbon nanotube arrays formed by cutting a polymer resin—Nanotube composite, *Science* (1994), 265, 1212–1214.
21. (a) Lozano, K., Yang, S., and Zeng, Q. Rheological analysis of vapor-grown carbon nanofiber-reinforced polyethylene composites, *J. Appl. Polym. Sci.* (2004), 93, 155–162; (b) Zeng, J., Saltysiak, B., Johnson, W. S., Schiraldi, D. A., and Kumar, S. Processing and properties of poly(methyl methacrylate)/carbon nanofiber composites, *Composites B* (2003), 35, 173–178.
22. (a) Fina, A., Tabuani, D., Carnaito, F., Frache, A., Boccaleri, E., and Camino, G. Polyhedral oligomeric silsesquioxanes (POSS) thermal degradation, *Thermochim Acta* (2006), 440, 36–42; (b) Fina, A., Abbenhuis, H. C. L., Tabuani, D., Frache, A., and Camino, G. Polypropylene metal functionalized POSS nanocomposites: A study by thermogravimetric analysis, *Polym. Degrad. Stab.* (2006), 91, 1064–1070.
23. Yang, F. and Nelson, G. L. Polymer/silica nanocomposites prepared via extrusion, *Polym. Adv. Tech.* (2006), 17(4), 320–326.
24. Yang, F., Bogdanova, I., and Nelson, G. L. Mechanism study on the flammability and thermal stability of polymer/alumina nanocomposites via extrusion, *PMSE Preprints* (2008), 98, 319–320.
25. Lichtenham, J. D. and Gilman, J. W. Pre-ceramic additives as fire retardants for plastics *U.S. Patent 6362279* (2002).
26. Bourbigot, S., Le Bras, M., Flambard, X., Rochery, M., Devaux, E., and Lichtenham, J. D. Polyhedral oligomeric silsesquioxanes: Application to flame retardant textiles in *Fire Retardancy of Polymers: New Applications of Mineral Fillers*, Le Bras, M., Wilkie, C. A., Bourbigot, S., Duquesne, S., and Jama, C. (Eds.), Royal Society of Chemistry, Cambridge (2005), pp. 189–201.
27. Aranda, P. and Ruiz-Hitzky, E. Poly(ethylene oxide)-silicate intercalation materials, *Chem. Mater.* (1992), 4, 1395–1403.
28. Greenland, D.J. Adsorption of poly(vinyl alcohols) by montmorillonite. *J. Colloid Sci.* (1963), 18, 647–64.
29. (a) Wang, D., Jiang, D.D., Pabst, J., Han, Z., Wang, J., and Wilkie, C.A., Polystyrene magadiite nanocomposites, *Polym. Engin. Sci.* (2004), 44(6), 1122–1131; (b) Costache, M.C., Jiang, D.D., and Wilkie, C.A. Thermal degradation of ethylene-vinyl acetate copolymer nanocomposites, *Polymer* (2005), 46, 6947–6958.

30. (a) Gilman, J. W., Awad, W. H., Davis, R. D., Shields, J., Harris, R. H., Jr., Davis, C., Morgan, A. B., Sutto, T. E., Callahan, J., Trulove, P. C., and DeLong, H. C. Polymer/layered silicate nanocomposites from thermally stable trialkylimidazolium-treated montmorillonite, *Chem. Mater.* (2002), 14, 3776–3785; (b) Wang, D. and Wilkie, C.A. A stibonium-modified clay and its polystyrene nanocomposite, *Polym. Degrad. Stab.* (2003), 82, 309–315.
31. Costa, F. R., Saphiannikova, M., Wagenknecht, U., and Heinrich, G., Layered double hydroxide based polymer nanocomposites, *Adv. Polym. Sci.* (2008), 210(Wax Crystal Control: Nanocomposites Stimuli-Responsive Polymers), 101–168.
32. Li, Y. and Ishida, H. Concentration-dependent conformation of alkyl tail in the nanoconfined space: Hexadecylamine in the silicate galleries, *Langmuir* (2003), 19, 2479–2484.
33. http://www.scprod.com/product_bulletins.asp
34. Chigwada, G., Wang, D., Jiang, D. D., and Wilkie, C.A., Styrenic nanocomposites prepared using a novel biphenyl-containing modified clay, *Polym. Degrad. Stab.* (2006), 91, 755–762.
35. Xiao, J., Hu, Y., Wang, Z., Tang, Y., Chen, Z., and Fan, W., Preparation and characterization of poly(butylene terephthalate) nanocomposites from thermally stable organic-modified montmorillonite, *Eur. Polym. J.* (2005), 41, 1030–1035.
36. Chigwada, G., Jiang, D. D., and Wilkie, C. A. Polystyrene nanocomposites based on carbazole-containing surfactants, *Thermochimica Acta* (2005), 436, 13–121.
37. Beyer, F. L., Beck, Tan, N. C., Dasgupta, A., and Galvin, M. E. Polymer-layered silicate nanocomposites from model surfactants, *Chem. Mater.* (2002), 14, 2983–2988.
38. Su, S., Jiang, D. D., and Wilkie, C. A. Novel polymerically-modified clays permit the preparation of intercalated and exfoliated nanocomposites of styrene and its copolymers by melt blending, *Polym. Degrad. Stab.* (2004), 83, 333–346.
39. Su, S., Jiang, D. D., and Wilkie, C. A. Poly(methyl methacrylate), polypropylene and polyethylene nanocomposite formation by melt blending using novel polymerically-modified clays, *Polym. Degrad. Stab.* (2004), 83, 321–331.
40. Lagaly, G. Interaction of alkylamines with different types of layered compounds, *Solid State Ionics* (1986), 22, 43–51.
41. Vaia, R. A., Teukolsky, R. K., and Giannelis, E.P. Interlayer structure and molecular environment of alkylammonium layered silicates, *Chem. Mater.* (1994), 6, 1017–1022.
42. Hackett, E., Manias, E., and Giannelis, E. P. Molecular dynamics simulations of organically modified layered silicates, *J. Chem. Phys.* (1998), 108, 7410–7415.
43. (a) Ho, D. L., Briber, R. M., and Glinka, C. J. Characterization of organically modified clays using scattering and microscopy techniques, *Chem. Mater.* (2001), 13, 1923–1931; (b) Hanley, H. J. M., Muzny, C. D., Ho, D. L., and Glinka, C. J. A small-angle neutron scattering study of a commercial organoclay dispersion, *Langmuir* (2003), 19, 5575–5580.
44. (a) Zhang, J., Jiang, D.D., Wang, D., and Wilkie, C.A., Styrenic polymer nanocomposites based on an oligomerically-modified clay with high inorganic content, *Polym. Degrad. Stab.* (2006), 91, 2665–2674; (b) Zhang, J., Manias, E., and Wilkie, C.A. Polymerically modified layered silicates: An effective route to nanocomposites, *J. Nanosci. Nanotech.* (2008), 8, 1597–1615; (c) Zheng, X., Jiang, D. D., and Wilkie, C. A., Methyl methacrylate oligomerically-modified clay and its poly(methyl methacrylate) nanocomposites, *Thermochimica Acta* (2005), 435, 202–208; (d) Su, S., Jiang, D. D., and Wilkie, C. A. Methacrylate modified clays and their polystyrene and poly(methyl methacrylate) nanocomposites, *Polym. Adv. Tech.* (2004), 15, 225–231.
45. (a) Imai, Y., Nishimura, S., Abe, E., Tateyama, H., Abiko, A., Yamaguchi, A., Aoyama, T., and Taguchi, H. High modulus poly(ethylene terephthalate)/expandable fluorine mica nanocomposites with a novel reactive compatibilizer, *Chem. Mater.* (2002), 14, 477–479; (b) Paul, M.-A., Alexandre, M., Degee, P., Calberg, C., Jerome, R., and Dubois, P. Exfoliated polylactide/clay nanocomposites by *In-Situ* coordination-insertion polymerization, *Macromol. Rapid Commun.* (2003), 24, 561–566.
46. (a) Weimer, M. W., Chen, H., Giannelis, E. P., and Sogah, D. Y. Direct synthesis of dispersed nanocomposites by *In-Situ* living free radical polymerization using a silicate-anchored initiator, *J. Am. Chem. Soc.* (1999), 121, 1615–1616; (b) Fan, X., Zhou, Q., Xia, C., Cristofoli, W., Mays, J., and Advincula, R. Living anionic surface-initiated polymerization (LASIP) of styrene from clay nanoparticles using surface bound 1,1-diphenylethylene (DPE) initiators, *Langmuir* (2002), 18, 4511–4518.
47. (a) Cui, L. and Paul, D. R. Evaluation of amine functionalized polypropylenes as compatibilizers for polypropylene nanocomposites, *Polymer* (2007), 48, 1632–1640; (b) Kim, D. H., Fasulo, P. D., Rodgers, W. R., and Paul, D. R. Structure and properties of polypropylene-based nanocomposites: Effect of PP - g - MA to organoclay ratio, *Polymer* (2007), 48, 5308–5323.

48. <http://en.wikipedia.org/wiki/Compatibility>
49. <http://en.wikipedia.org/wiki/Miscibility>
50. (a) Reichert, P., Nitz, H., Klinke, S., Brandsch, R., Thomann, R., and Mulhaupt, R. Poly(propylene)/organoclay nanocomposite formation: Influence of compatibilizer functionality and organoclay modification *Macromol. Mater. Eng.* (2000), 275, 8–17; (b) Usuki, A., Kawasumi, M., Kojima, Y., Okada, A., Kurauchi, T., and Kamigaito, O. Swelling behavior of montmorillonite cation exchanged for ω -amino acids by ϵ -caprolactam, *J. Mater. Res.* (1993), 8, 1174–1178.
51. Fornes, T. D., Hunter, D. L., and Paul, D. R. Nylon-6 nanocomposites from alkylammonium-modified clay: The role of alkyl tails on exfoliation, *Macromolecules* (2004), 37, 1793–1798.
52. (a) Ishida, H., Campbell, S., and Blackwell, J. General approach to nanocomposite preparation, *Chem. Mater.* (2000), 12, 1260–1267, (b) Jang, B. N., Wang, D., and Wilkie, C. A. The relationship between the solubility parameter of polymers and the clay-dispersion in polymer-clay nanocomposites and the role of the surfactant, *Macromolecules* (2005), 38, 6533–6543.
53. Vaia, R. A., Liu, W., and Koerner, H. Analysis of small-angle scattering of suspensions of organically modified montmorillonite: Implications to phase behavior of polymer nanocomposites, *J. Polym. Sci. B: Polym. Phys.* (2003), 41, 3214–3236.
54. Morgan, A. B. and Harris, J. D. Exfoliated polystyrene-clay nanocomposites synthesized by solvent blending with sonication, *Polymer* (2004), 45, 8695–8703.
55. (a) Fornes, T. D., Yoon, P. J., Hunter, D. L., Keskkula, H., and Paul, D. R. Effect of organoclay structure on nylon 6 nanocomposite morphology and properties, *Polymer* (2002), 43, 5915–5933; (b) McAlpine, M., Hudson, N. E., Liggat, J. J., Pethrick, R. A., Pugh, D., and Rhoney, I. Study of the factors influencing the exfoliation of an organically modified montmorillonite in methyl methacrylate/polym(methyl methacrylate) mixtures, *J. App. Polym. Sci.* (2006), 99, 2614–2626; (c) Zeng, Q. H., Yu, A. B., Lu, G. Q., and Standish, R. K. Molecular dynamics simulation of organic-inorganic nanocomposites: Layering behavior and interlayer structure of organoclays, *Chem. Mater.* (2003), 15, 4732–4738; (d) Heinz, H., Koerner, H., Anderson, K. L., Vaia, R. A., and Farmer, B. L. Force field for mica-type silicates and dynamics of octadecylammonium chains grafted to montmorillonite, *Chem. Mater.* (2005), 17, 5658–5669.
56. Paul, M.-A., Alexandre, M., Degee, P., Calberg, C., Jerome, R., and Dubois, P. Exfoliated polylactide/clay nanocomposites by *In-Situ* coordination-insertion polymerization, *Macromol. Rapid Commun.* (2003), 24, 561–566.
57. (a) Dean, D., Walker, R., Theodore, M., Hampton, E., and Nyairo, E. Chemorheology and properties of epoxy/layered silicate nanocomposites, *Polymer* (2004), 46, 3014–3021; (b) Ton-That, M.-T., Ngo, T.-D., Ding, P., Fang, G., Cole, K. C., and Hoa, S. V. Epoxy nanocomposites: Analysis and kinetics of cure, *Polym. Eng. Sci.* (2004), 44, 1132–1141.
58. (a) Xie, W., Gao, Z., Pan, W.-P., Hunter, D., Singh, A., and Vaia, R. Thermal degradation chemistry of alkyl quaternary ammonium montmorillonite, *Chem. Mater.* (2001), 13, 2979–2990; (b) He, H., Ding, Z., Zhu, J., Yuan, P., Xi, Y., Yang, D., and Frost, R. L. Thermal characterization of surfactant-modified montmorillonites, *Clays and Clay Minerals* (2005), 53, 287–293; (c) Dharaiya, D. and Jana, S. C. Thermal decomposition of alkyl ammonium ions and its effect on surface polarity of organically treated nanoclay, *Polymer* (2005), 46, 10139–10147; (d) Gelfer, M., Burger, C., Fadeev, A., Sics, I., Chu, B., Hsiao, B. S., Heintz, A., Kojo, K., Hsu, S.-L., Si, M., and Rafailovich, M. Thermally induced phase transitions and morphological changes in organoclays, *Langmuir* (2004), 20, 3746–3758.
59. Morgan, A. B., Gilman, J. W., and Jackson, C. L. Characterization of the dispersion of clay in a polyetherimide nanocomposite, *Macromolecules* (2001), 34, 2735–2738.
60. (a) Davis, R. D., Gilman, J. W., Sutto, T. E., Callahan, J. H., Trulove, P. C., and De Long, H. C. Improved thermal stability of organically modified layered silicates, *Clays Clay Miner.* (2004), 52, 171–179; (b) Morgan, A. B. and Harris, J. D. Effects of organoclay Soxhlet extraction on mechanical properties, flammability properties and organoclay dispersion of polypropylene nanocomposites, *Polymer* (2003), 44, 2313–2320.
61. He, H., Ding, Z., Zhu, J., Yuan, P., Xi, Y., Yang, D., and Frost, R. L. Thermal characterization of surfactant-modified montmorillonites, *Clays Clay Miner.* (2005), 53, 287–293.
62. (a) Hotta, S., Paul, D. R. Nanocomposites formed from linear low density polyethylene and organoclays *Polymer* (2004), 45, 7639–7654. (b) Lee, H.-S., Fasulo, P. D., Rodgers, W. R., and Paul, D. R. TPO based nanocomposites. Part I. Morphology and mechanical properties, *Polymer* (2005), 46, 11673–11689; (c) Ton-That, M.-T., Perrin-Sarazin, F., Cole, K. C., Bureau, M. N., Denault, J. Polyolefin nanocomposites: Formulation and development, *Polym. Eng. Sci.* (2004), 44, 1212–1219; (d) Dennis, H. R., Hunter, D. L., Chang, D., Kim, S., White, J. L., Cho, J. W., and Paul, D. R. Effect of melt processing conditions on the extent of exfoliation in organoclay-based nanocomposites, *Polymer* (2001), 42, 9513–9522;

- (e) Tanoue, S., Utracki, L. A., Garcia-Rejon, A., Tatibouët, J., and Kamal, M. R. Melt compounding of different grades polystyrene with organoclay, Part 3: Mechanical properties, *Polym. Eng. Sci.*, (2005), 45, 827–837; (f) Hasegawa, N., Okamoto, H., Kato, M., Usuki, A., and Sato, N. Nylon-6/Na-montmorillonite nanocomposites prepared by compounding Nylon 6 with Na-montmorillonite slurry, *Polymer* (2003), 44, 2933–2937; (g) Kato, M., Matsushita, M., and Fukumori, K. Development of a new production method for a polypropylene-clay nanocomposite, *Polym. Eng. Sci.* (2004), 44, 1205–1211.
63. Liang, Z.-M., Yin, J., and Xu, H. J. Polyimide/montmorillonite nanocomposites based on thermally stable, rigid-rod aromatic amine modifies, *Polymer* (2003), 44, 1391–1399.
64. Xie, W., Xie, R., Pan, W.-P., Hunter, D., Koene, B., Tan, L.-S., and Vaia, R. Thermal stability of quaternary phosphonium modified montmorillonites *Chem. Mater.* (2002), 14, 4837–4845.
65. Xie, W., Gao, Z., Pan, W. P., Vaia, R., Hunter, D., and Singh, A., Characterization of organically modified montmorillonite by thermal techniques, *Polym. Mater. Sci. Eng.* (2000), 83, 284.
66. (a) Zhang, J., Jiang, D. D., Wang, D., and Wilkie, C. A. Mechanical and fire properties of styrenic polymer nanocomposites based on an oligomerically modified clay, *Polym. Adv. Tech.*, (2005), 16, 800–806; (b) Zhang, J., Jiang, D. D., and Wilkie, C. A. Fire properties of styrenics polymer-clay nanocomposites based on an oligomerically modified clay, *Polym. Degrad. Stab.* (2006), 91, 358–366; (c) Zheng, X., Jiang, D. D., Wang, D., and Wilkie, C.A. Flammability of styrenic polymer clay nanocomposites based on a methyl methacrylate oligomerically-modified clay, *Polym. Degrad. Stab.* (2005), 91(2), 289–297; (d) Su, S., Jiang, D. D., and Wilkie, C. A. Study on the thermal stability of polystyryl surfactants and their modified clay nanocomposites, *Polym. Degrad. Stab.* (2004), 84(2), 269–277; (e) Zheng, X., Jiang, D. D., Wang, D., and Wilkie, C.A., Flammability of styrenic polymer clay nanocomposites based on a methyl methacrylate oligomerically-modified clay, *Polym. Degrad. Stab.* (2005), 91(2), 289–297.
67. Tao, L., Chen, G., Mantovani, G., York, S., Haddleton, D.M., Modification of multi-wall carbon nanotube surfaces with poly(amidoamine) dendrons: Synthesis and metal templating *Chem. Commun.* (2006), 47, 4949–4951.
68. Raghuvver, M. S., Kumar, A., Frederick, M. J., Louie, G. P., Ganesan, P. G., and Ramanath, G. Site-selective functionalization of carbon nanotubes, *Adv. Mater.* (2006), 18, 547–552.
69. Yokoi, T., Iwamatsu, S., Komai, S., Hattori, T., and Murata, S. Chemical modification of carbon nanotubes with organic hydrazines. *Carbon* (2005), 43, 2869–2874.
70. (a) Okada, A., Kawasumi, M., Usuki, A., Kojima, Y., Kurauchi, T., and Kamigaito, O. Synthesis and properties of nylon-6/clay hybrids, *Polymer Based Molecular Composites*. Schaefer D.W., Mark J.E. (Eds.), MRS Symposium Proceedings, Pittsburgh, PA (1990), 171, 45–50; (b) Giannelis, E.P., Krishnamoorti, R., and Manias, E. Polymer-silicate nanocomposites: Model systems for confined polymers and polymer brushes, *Adv. Polym. Sci.* (1999), 138, 107–147; (c) LeBaron, P. C., Wang, Z., and Pinnavaia, T. J. Polymer-layered silicate nanocomposites: An overview, *Appl. Clay Sci.* (1999), 15, 11–29; (d) Vaia, R. A., Price, G., Ruth, P. N., Nguyen, H. T., and Lichtenhan, J. Polymer/layered silicate nanocomposites as high performance ablative materials, *Appl. Clay Sci.* (1999), 15, 67–92; (e) Biswas, M. and Sinha R. S. Recent progress in synthesis and evaluation of polymer–montmorillonite nanocomposites, *Adv. Polym. Sci.* (2001), 155, 167–221.
71. (a) Voorn, D. J., Ming, W., and Van Herk, A. M. Polymer-clay nanocomposite latex particles by inverse pickering emulsion polymerization stabilized with hydrophobic montmorillonite platelets, *Macromolecules* (2006), 39, 2137–2143; (b) Xu, M. Z., Choi, Y. S., Kim, Y. K., Wang, K. H., and Chung, I. J. Synthesis and characterization of exfoliated poly(styrene-co-methyl methacrylate)/clay nanocomposites via emulsion polymerization with AMPS, *Polymer* (2003), 44(20), 6387–6395.
72. Wang, D., Zhu, J., Yao, Q., and Wilkie, C. A., A comparison of various methods for the preparation of polystyrene and poly(methyl methacrylate) clay nanocomposites, *Chem. Mater.* (2002), 14, 3837–3843.
73. Utracki, L. A. Clay-containing polymeric nanocomposites, RAPRA Tech. Ltd., Shawbury, Shrewsbury, Shropshire, U.K., 2004, p. 496.
74. (a) Vaia, R. A., Ishii, H., and Giannelis, E. P. Synthesis and properties of two-dimensional nanostructures by direct intercalation of polymer melts in layered silicates, *Chem. Mater.* (1993), 5, 1694–1696; (b) Giannelis, E. P., Krishnamoorti, R., and Manias, E. Polymer-silicate nanocomposites: Model systems for confined polymers and polymer brushes, *Adv. Polym. Sci.* (1999), 138, 107–147; (c) Chigwada, G., Jiang, D. D., and Wilkie, C. A., Fire retardancy of polystyrene nanocomposites using naphthenate-containing clays, *Fire and Polymers IV* (2006), (ACS Symposium Series, 922), 103–116; (d) Zhang, J., Jiang, D. D., and Wilkie, C. A. Polyethylene and polypropylene nanocomposites based upon an oligomerically modified clay, *Thermochimica Acta* (2005), 430, 107–113.
75. Alexandre, M. and Dubois, P. Polymer-layered silicate nanocomposites: Preparation, properties, and uses of a new class of materials *Mater. Sci. Engin. Rep.* (2000), 28, 1–63.

76. (a) Morgan, A. B. and Gilman, J. W. Characterization of polymer-layered silicate (clay) nanocomposites by transmission electron microscopy and X-Ray diffraction: A comparative study, *J. App. Polym. Sci.* (2003), 87, 1329–1338; (b) Vermogen, A., Masenelli-Varlot, K., Seguela, R., Duchet-Rumeau, J., Boucard, S., and Prele, P. Evaluation of the structure and dispersion in polymer-layered silicate nanocomposites, *Macromolecules* (2005), 38, 9661–9669.
77. (a) Perrin-Sarazin, F., Ton-That, M.-T., Bureau, M. N., and Denault, J. Micro- and nano-structure in polypropylene/clay nanocomposites, *Polymer* (2005), 46, 11624–11634; (b) Causin, V., Marega, C., Mariog, A., and Ferrara, G. Assessing organo-clay dispersion in polymer layered silicate nanocomposites: A SAXS approach, *Polymer* (2005), 46, 9533–9537.
78. (a) Vaia, R. A. and Liu, W. X-ray powder diffraction of polymer/layered silicate nanocomposites: Model and practice, *J. Polym. Sci. B: Polym. Phys.* (2002), 40, 1590–1600; (b) Vaia, R. A., Liu, W., and Koerner, H. Analysis of small-angle scattering of suspensions of organically modified montmorillonite: Implications to phase behavior of polymer nanocomposites, *J. Polym. Sci. B: Polym. Phys.* (2003), 41, 3214–3236.
79. (a) Bourbigot, S., Vanderhart, D. L., Gilman, J. W., Awad, W. H., Davis, R. D., Morgan, A. B., and Wilkie, C. A., Investigation of nanodispersion in polystyrene-montmorillonite nanocomposites by solid-state NMR, *J. Polym. Sci. Part B: Polym. Phys.* (2003), 41, 3188–3213; (b) Gilman, J. W., Bourbigot, S., Shields, J. R., Nyden, M., Kashiwagi, T., Davis, R. D., Vanderhart, D. L., Demory, W., Wilkie, C. A., Morgan, A. B., Harris, J., and Lyon, R. E., High throughput methods for polymer nanocomposites research: Extrusion, NMR characterization and flammability property screening, *J. Mater. Sci.* (2003), 38, 4451–4460.
80. Vaia, R. A., Vasudevan, S., Krawiec, W., Scanlon, L. G., and Giannelis, E. P. New polymer electrolyte nanocomposites: Melt intercalation of poly(ethylene oxide) in mica-type silicates, *Adv. Mater.* (1995), 7, 154–156.
81. Maiti, M. and Bhowmick, A. K. New insights into rubber-clay nanocomposites by AFM imaging, *Polymer* (2006), 47, 6156–6166.
82. (a) Wu, D., Wu, L., Zhang, M., Zhou, W., and Zhang, Y., Morphology evolution of nanocomposites based on poly(phenylene sulfide)/poly(butylene terephthalate) blend, *J. Polym. Sci. Part B: Polym. Phys.* (2008), 46, 1265–1279; (b) Lutkenhaus, J. L., Olivetti, E. A., Verploegen, E. A., Cord, B. M., Sadoway, D. R., and Hammond, P. T. Anisotropic structure and transport in self-assembled layered polymer-clay nanocomposites, *Langmuir* (2007), 23, 8515–8521.
83. Maupin, P. H., Gilman, J. W., Harris, R. H., Bellayer, S., Bur, A. J., Roth, S. C., Murariu, M., Morgan, A. B., and Harris, J. D. Optical probes for monitoring intercalation and exfoliation in melt-processed polymer nanocomposites, *Macromol. Rapid Commun.* (2004), 25, 788–792.
84. Drits, V. A. and Tchoubar, C. *X-Ray Diffraction by Disordered Lamellar Structures: Theory and Application to Micro-divided Silicates and Carbons*, Springer-Verlag: New York, 1990.
85. Morgan, A. B. and Wilkie, C. A. Practical issues and future trends of polymer nanocomposite flammability research, in *Flame Retardant Polymer Nanocomposites*, Morgan, A. B. and Wilkie, C. A. (Eds.) John Wiley & Sons: Hoboken, NJ, 2007, p. 421.
86. (a) Bish, D. L. and Post, J. E. (Eds.), Modern powder diffraction, *Reviews in Mineralogy 20*; Mineralogical Society of America: Washington, D.C., 1989; (b) Roe, R.-J. *Methods of X-Ray and Neutron Scattering in Polymer Science*, Oxford University Press: New York, 2000, pp. 155–210.
87. Ray, S. S. and Okamoto, M. Polymer/layered silicate nanocomposites: A review from preparation to processing, *Prog. Polym. Sci.* (2003), 28, 1539–1641.
88. (a) Yang, J., Zhang, Z., Friedrich, K., and Schlarb, A. K. Creep resistant polymer nanocomposites reinforced with multiwalled carbon nanotubes, *Macromol. Rapid Commun.* (2007), 28, 955–961; (b) Qi, D. M., Bao, Y. Z., Weng, Z. X., and Huang, Z. M. Preparation of acrylate polymer/silica nanocomposite particles with high silica encapsulation efficiency via miniemulsion polymerization, *Polymer* (2006) 47, 4622–4629.
89. Burnside, S. D. and Giannelis, E. P. Synthesis and properties of new poly(dimethylsiloxane) nanocomposites, *Chem. Mater.* (1995), 7, 1597–1600.
90. Lepoittevin, B., Devalckenaere, M., Pantoustier, N., Alexandre, M., Kubies, D., Calberg, C., Jerome, R., and Dubois P. Poly (1-caprolactone)/clay nanocomposites prepared by melt intercalation: Mechanical, thermal and rheological properties, *Polymer* (2002), 43, 4017–4023.
91. Zhang, J., Jiang, D. D., and Wilkie, C. A. Thermal and flame properties of polyethylene and polypropylene nanocomposites based on an oligomerically-modified clay, *Polym. Degrad. Stab.* (2006), 91, 298–304.
92. Manzi-Nshuti, C., Wang, D., Hossenlopp, J. M., and Wilkie, C. A. Aluminum-containing layered double hydroxides: The thermal, mechanical, and fire properties of (nano)composites of poly(methyl methacrylate), *J. Mater. Chem.* (2008), 18, 3091–3102.

93. Ge, J. J., Hou, H., Li, Q., Graham, M. J., Greiner, A., Reneker, D. H., Harris, F. W., and Cheng, S. Z. D. Assembly of well-aligned multiwalled carbon nanotubes in confined polyacrylonitrile environments: Electrospun composite nanofiber sheets, *J. Am. Chem. Soc.* (2004), 126, 15754–15761.
94. Jang, B. N., Costache, M., and Wilkie, C. A. The relationship between thermal degradation behavior of polymer and the fire retardancy of polymer/clay nanocomposites, *Polymer* (2005), 46, 10678–10687.
95. Zhu, J., Start, P., Mauritz, K. A., and Wilkie, C. A. Thermal stability and flame retardancy of poly(methyl methacrylate)-clay nanocomposites, *Polym. Degrad. Stab.* (2002), 77, 253–258.
96. Bourbigot, S., Gilman, J. W., and Wilkie, C. A. Kinetic analysis of the thermal degradation of polystyrene-montmorillonite nanocomposite, *Polym. Degrad. Stab.* (2004), 84, 483–492.
97. Doh, J. G. and Cho, I. Synthesis and properties of polystyrene-organoammonium montmorillonite hybrid, *Polym. Bull.* (1998), 41, 511–517.
98. Gilman, J. W. Flammability and thermal stability studies of polymer layered-silicate (clay) nanocomposites, *Appl. Clay Sci.* (1999), 15, 31–49.
99. Costache, M. C., Jiang, D. D., and Wilkie, C. A. Thermal degradation of ethylene–vinyl acetate copolymer nanocomposites, *Polymer* (2005), 46, 6947–6958.
100. (a) Kashiwagi, T., Grulke, E., Hilding, J., Harris, R., Awad, W., and Douglas, J. Thermal degradation and flammability properties of poly(propylene)/carbon nanotube composites, *Macromol. Rapid Commun.* (2002), 23, 761–765; (b) Kashiwagi, T. Progress in flammability studies of nanocomposites with new types of nanoparticles in *Flame Retardant Polymer Nanocomposites*, Morgan, A. B. and Wilkie, C. A. (Eds.) (2007), pp. 285–324, John Wiley & Sons, 421pp.
101. Kashiwagi, T., Du, F., Douglas, J. F., Winey, K. I., Harris, R. H. Jr., and Shields, J. R. Nanoparticle networks reduce the flammability of polymer nanocomposites, *Nat. Mater.* (2005), 4, 928–933.
102. Kashiwagi, T., Du, F., Winey, K. I., Groth, K. M., Shields, J. R., Bellayer, S. P., Kim, H., and Douglas, J. F. Flammability properties of polymer nanocomposites with single-walled carbon nanotubes: Effects of nanotube dispersion and concentration, *Polymer* (2005), 46, 471–481.
103. Kashiwagi, T., Grulke, E., Hilding, J., Groth, K., Harris, R., Butler, K., Shields, J., Kharchenko, S., and Douglas, J. Thermal and flammability properties of polypropylene/carbon nanotube nanocomposites, *Polymer* (2004), 45, 4227–4239.
104. (a) Gilman, J. W., Jackson, C. L., Morgan, A. B., Harris, R., Manias, E., Giannelis, E. P., Wuthenow, M., Hilton, D., and Phillips, S. H. Flammability properties of polymer-layered silicate nanocomposites: Polypropylene and polystyrene nanocomposites, *Chem. Mater.* (2000), 12, 1866–1873; (b) Gilman, J. W., Kashiwagi, T., Morgan, A. B., Harris, R. H., Brassell, L., Van Landingham, M., and Jackson, C. L. Flammability of polymer-clay nanocomposites consortium: Year one annual report, *National Institute of Standards and Technology Internal Report (NISTIR) 6531*(2000).
105. (a) Gilman, J.W., Flame retardant mechanism of polymer clay nanocomposite, in *Flame Retardant Polymer Nanocomposites*, Morgan, A. B. and Wilkie, C.A. (Eds.) (2007), 421pp; (b) Cipriano, B. H., Kashiwagi, T., Raghavan, S.R., Yang, Y., Grulke, E. R., Yamamoto, K., Shields, J. R., and Douglas, J. F., Effects of aspect ratio of MWNT on the flammability properties of polymer nanocomposites, *Polymer* (2007), 48, 6086–6096.
106. Lyon, R. E. and Walters, R. N. Screening flame-retardants for plastic using microscale combustion calorimetry. *Proceed. Conf. on Recent Adv. Flame Retard. Polymeric Mater.* (2007), 18, 74–93.
107. ASTM D7309–07 – Standard test method for determining flammability characteristics of plastics and other solid materials using microscale combustion calorimetry (2007).
108. Obtained with a commercial PE based FR composite.
109. Gilman, J. W., Kashiwagi, T., Brown, J. E., James E. T., Lomakin, S., Giannelis, E. P., and Manias, E. Flammability studies of polymer layered silicate nanocomposites, *Materials and Process Affordability: Keys to the Future*, Book 1 (1998) (International SAMPE Symposium and Exhibition, vol 43.), 1053–1066.
110. Kashiwagi, T, Harris, Jr., R. H., Zhang, X., Briber, R. M., Cipriano, B. H., Raghavan, S. R., Awad, W. H., and Shields, J. R. Flame retardant mechanism of polyamide 6-clay nanocomposites, *Polymer* (2004), 45, 881–891.
111. Akelah A. Polystyrene/clay nanocomposites in *Polymers and Other Advanced Materials. Emerging Technologies and Business Opportunities*, Prasad, P. N., Mark, J. E., and Ting F. J. (Eds.), Plenum Press: New York, 1995, pp. 625–630.; Xiao, P., Xiao, M., and Gong, K. Preparation of exfoliated graphite/polystyrene composite by polymerization-filling technique, *Polymer* (2001), 42, 4813–4816, Tseng, C. R., Wu, J. Y., Lee, H. Y., and Chang F. C., Preparation and crystallization behavior of syndiotactic polystyrene-clay nanocomposites, *Polymer* (2001), 42, 10063–10070.

112. (a) Komori, Y., Sugahara, Y., and Kuroda, K. Direct intercalation of poly(vinylpyrrolidinone) into kaolinite by a refined guest displacement method, *Chem. Mater.* (1999), 11, 3–6; (b) Nisha, A., Rajeswari, M. K., and Dhamodharan, R. Intercalative redox polymerization and characterization of poly(n-vinyl-2-pyrrolidinone) in the gallery of vermiculite: a novel inorganic–organic hybrid material, *J. Appl. Polym. Sci.* (2000), 76, 1825–1830; (c) Fournaris, K. G., Karakassides, M. A., Petridis, D., and Yiannakopoulou, K. Clay–polyvinylpyridine nanocomposites, *Chem. Mater.* (1999), 11, 2372–2381; (d) Parfitt, R. L. and Greenland, D. J. The adsorption of poly(ethylene glycols) on clay minerals, *Clay Miner.* (1970), 8, 305–315; (e) Zhao, X., Urano, K., and Ogasawara, S. Adsorption of poly(ethylene vinyl alcohol) from aqueous solution on montmorillonite clays, *Colloid. Polym. Sci.* (1989), 267, 899–906.
113. Zhu, J., Uhl, F., Morgan, A. B., and Wilkie, C. A. Studies on the mechanism by which the formation of nanocomposites enhances thermal stability, *Chem. Mater.* (2001), 13, 4649–4654.
114. Jang, B. N. and Wilkie, C. A. The thermal degradation of polystyrene nanocomposite, *Polymer*, (2005), 46(9), 2933–2942.
115. Guo, B., Jia, D., and Cai, C. Effects of organo-montmorillonite dispersion on thermal stability of epoxy resin nanocomposites, *Eur. Polym. J.* (2004), 40, 1743–1748.
116. http://www.epa.gov/oppt/nano/p2docs/casestudy2_gilman.pdf (Gilman, J.F. Flame retardant polymer nanocomposite).
117. (a) Marosi, G., Marton, A., Szep, A., Csontos, I., Keszei, S., Zimonyi, E., Toth, A., Almeras, X., and Le Bras, M. Fire retardancy effect of migration in polypropylene nanocomposites induced by modified interlayer, *Polym. Degrad. Stab.* (2003), 82, 379–385; (b) Szep, A., Szabo, A., Toth, N., Anna, P., and Marosi, G. Role of montmorillonite in flame retardancy of ethylene-vinyl acetate copolymer, *Polym. Degrad. Stab.* (2006), 91, 593–599; (c) Marosi, G., Anna, P., Marton, A., Bertalan, G., Bota, A., Toth, A., Mohai, M., Racz, I. Flame-retarded polyolefin systems of controlled interphase, *Polym. Adv. Technol.* (2002), 13, 1–9.
118. Kotaki, M., Wang, K., Toh, M. L., Chen, L., Wong, S. Y., and He, C. Electrically conductive epoxy/clay/vapor grown carbon fiber hybrids, *Macromolecules* (2006), 39, 908–911.
119. Chigwada, G., Jash, P., Jiang, D. D., and Wilkie, C. A. Synergy between nanocomposite formation and low levels of bromine in fire retardancy in polystyrenes, *Polym. Degrad. Stab.* (2005), 88, 382–393.
120. Chigwada, G., Jash, P., Jiang, D. D., and Wilkie, C. A. Fire retardancy of vinyl ester nanocomposites: Synergy with phosphorus-based fire retardants, *Polym. Degrad. Stab.* (2005), 89, 85–100.
121. (a) Mishra, S., Sonawane, S. H., Singh, R. P., Bendale, A., and Patil, K. Effect of nano-Mg(OH)₂ on the mechanical and flame-retarding properties of polypropylene composites, *J. App. Polym. Sci.* (2004), 94, 116–122; (b) Zhang, Q., Tian, M., Wu, Y., Lin, G., and Zhang, L. Effect of particle size on the properties of Mg(OH)₂-filled rubber composites, *J. App. Polym. Sci.* (2004), 94, 2341–2346; (c) Okoshi, M. and Nishizawa, H. Flame retardancy of nanocomposites, *Fire Mater.* (2004), 28, 423–429.
122. Lan, T., Nanomer nanoclay as flame retardation additives, *Environmentally Friendly Flame Retardants-Intertech Pira*, July 19, 2007. (<http://www.nanocor.com/techpapers.asp>).

12 Multicomponent FR Systems: Polymer Nanocomposites Combined with Additional Materials

J.-M. Lopez-Cuesta and F. Laoutid

CONTENTS

12.1	Introduction.....	301
12.2	Layered Silicates Associated with Flame-Retardant Compounds.....	303
12.2.1	Layered Silicates in Intumescent Systems Based on Ammonium Polyphosphate.....	303
12.2.1.1	Montmorillonite and Cationic Clays.....	303
12.2.1.2	Anionic Clays.....	307
12.2.2	Layered Silicates Associated with Other Phosphorus and Nitrogen Compounds.....	308
12.2.3	Layered Silicates Associated with Metal Hydroxides.....	313
12.2.4	Layered Silicates Associates with Brominated Compounds.....	315
12.3	Other Nanoparticles Associated with Various Flame Retardants.....	316
12.3.1	Combinations of Carbon Nanotubes with Flame Retardants and Nanoparticles.....	316
12.3.2	Combinations with, Nano-Hydroxides, Nano-Oxides, and Other Nanoparticles.....	317
12.3.2.1	Combinations with Nano-Hydroxides.....	317
12.3.2.2	Combinations with Nano-Oxides.....	320
12.3.2.3	Other Combinations with Different Nanoparticles.....	321
12.4	Conclusion.....	322
	Acknowledgments.....	324
	References.....	324

12.1 INTRODUCTION

For more than a decade, numerous research studies have been carried out on the flame-retardant properties conferred by nanoparticles and mainly by organo-modified layered silicates (OMLS). Earlier work at Cornell University and National Institute of Standards and Technology in the United States showed that nanocomposites containing OMLS reduced polymer flammability and enhanced the formation of carbonaceous residue (char).¹⁻⁴ Owing to a strong increase in polymer viscosity, impairing processability, and also due to the breakdown of ultimate mechanical properties, the acceptable rate of incorporation for nanoparticles to improve flame retardancy is generally restricted to less than 10 wt %.

The different flame-retardant (FR) mechanisms of action of current nanoparticles, such as layered silicates, carbon nanotubes (CNTs), and nano-oxides or -hydroxides, according to their nature and interfacial modifications, are relatively well known and detailed in numerous works.⁵⁻¹³ These mechanisms are rather different from those exhibited by usual FRs and correspond mainly to the following physical, physicochemical, or chemical actions:

- Creation of a mass transfer barrier for combustible volatiles and oxygen by migration of nanoparticles toward the surface exposed to heat flux
- Formation of an insulating char structure (possibly expanded) leading to a limitation of the temperature for the remaining material, or able to dissipate incident heat by radiative emission
- Modification of heat diffusivity through the material
- Restriction of macromolecular mobility and increase in viscosity
- Catalytic effects promoting the formation of charred structures
- Modification of the thermal degradation pathway of polymers
- Trapping of radicals formed through the thermal degradation and combustion process

Nevertheless, the incorporation of relatively low amounts of nanoparticles in polymers by several processing methods is unable to meet fire performance standards in comparison with usual FRs, such as hydrated minerals, halogen, phosphorus, or nitrogen compounds, for which the loading is generally higher, up to 65 wt % for some metallic hydroxides.

In consequence, the concept of combining nanoparticles with FRs, mainly nonhalogenated, has emerged, to generate synergies for some FR properties, leading also to the possibility of reducing the global loading of FR additives or fillers in polymers. This last objective is aimed particularly to combine high levels of flame retardancy, compatibility with demanding standards, the conservation, and even the improvement of some mechanical properties, mainly stiffness and reinforcement, owing to the presence of nanoparticles.

In numerous works dealing with the combination of nanoparticles and FR compounds, surface modifications of nanoparticles were only aimed to promote good dispersion of the nanoparticles into the polymer matrix (with intercalated or exfoliated morphologies for layered silicates as nanoparticles), even in the presence of the usual FRs, for example ammonium polyphosphate (APP) or magnesium hydroxide (MH). The initial aim was to combine the individual effects of each component to achieve strong synergistic effects.

Nevertheless, it has also been noticed that some interactions between nanoparticles and conventional FRs could occur, particularly reactions leading to new mineral species, such as metallic phosphates, depending on the flammability conditions.

Moreover, the development of new strategies for surface modifications of nanoparticles with compounds having FR activity could provide a new field of research on FR systems. The use of novel phosphorus-, nitrogen-, or halogen-containing modifiers, instead of alkylammonium ions, for layered silicates seems promising. FR action conferred by the surface modifier can be combined with action due to composite morphology, particularly when the host polymer is a polymer blend instead of a pure polymer.

In addition, FRs used in combination with nanoparticles differ from current FR used alone in polymers. Some FR agents are now available at the submicronic scale and, in some cases, chemically surface modified, entailing significant changes in their reactivity. For example, new varieties of metallic hydroxides are synthesized, either able to play a similar role as some lamellar nanoparticles or to act as conventional hydrated FR fillers.

Finally, the use of complex FR systems, in which several kinds of organomodified nanoparticles, presenting different FR mechanisms, are associated, can also represent an interesting alternative to conventional FR systems and provide a more promising range of properties for the host polymers.

This chapter develops at first the more frequent combinations of nanoparticles that concern layered silicates associated with phosphorus compounds, as well as metallic hydroxides and halogen compounds. The association of natural layered silicates with intumescent FR (IFR) systems represents one of the main contributions of the combined use of nanoparticles and FRs. Moreover, combinations of layered silicates with other phosphorus compounds have been studied and have led to significant improvements for fire retardancy.

The growing interest in other categories of nanoparticles, such as synthetic anionic layered silicates, CNTs, nano-oxides or -hydroxides, metallic phosphates, etc., has materialized either through the study of combinations of those nanoparticles with layered silicates or with metal hydroxides or phosphorus FRs. Such combinations are also detailed in Section 12.3. Nevertheless, for some combinations, interpretations of the possible interactions between components are sometimes missing or not completely detailed.

12.2 LAYERED SILICATES ASSOCIATED WITH FLAME-RETARDANT COMPOUNDS

The FR properties of polymer-layered silicate nanocomposites have been studied for a wide range of polymers, especially for organomodified montmorillonites (OMMT) in thermoplastics. Depending on the nature of the polymer, the decomposition pathway and decomposition products may change.⁸ A major consequence of the introduction of modified clays is the formation or the enhancement of charred structure, caused by cross-linking processes possibly catalyzed by the nanoparticles.

The main categories of clays studied are cationic clays, mainly 2:1 silicates, belonging to the category of dioctahedral smectites: montmorillonite or bentonite.¹⁴ Procedures of cation exchange using mainly alkylammonium ions can lead to organophilic materials, able to disperse in polymers in the molten state, leading to nanocomposites. The silicates exhibit exfoliated or intercalated structures in nanocomposites.¹⁵ Such morphologies are required to achieve flame retardancy.¹⁻⁴ In addition, 1:1 silicates such as ultrafine kaolinite seem promising owing to possibilities of functionalization using surface hydroxyl groups.¹⁶

New developments in the use of silicates to improve flame retardancy have arisen from the use of synthetic anionic clays that correspond to the family of lamellar mixed metal hydroxides, commonly named layered double hydroxides (LDH) or hydrotalcite-like compounds.¹⁷

The interest of combining organomodified clays with FR compounds can be driven by industrial demand, to replace standard flame retarded compositions, with the intent to phase out halogenated compounds due to environmental concerns or to reduce the high percentages of hydrated fillers needed in some polymers, such as ethylene vinyl acetate copolymer (EVA). New scientific approaches concerning the interactions between nanoparticles and FRs, especially organomodified clays, are also developed in relation with current concepts or general FR mechanisms, such as synergism or intumescence. The formation of new species in the condensed phase from the combination of degradation products of both polymer and components of the FR system is also expected to play a positive role in flame retardancy.

12.2.1 LAYERED SILICATES IN INTUMESCENT SYSTEMS BASED ON AMMONIUM POLYPHOSPHATE

12.2.1.1 Montmorillonite and Cationic Clays

Among the various associations involving organomodified clays, the use with components of intumescent compositions, such as APP, was widely reported for various host polymers or blends, in which the role of the carbon source is played by a polymer (PA6, EVA, thermoplastic polyurethanes).

Intumescent compositions correspond to a particular behavior of the polymer, which swells and expands when heated beyond a critical temperature, with the formation of a stable charred

structure.¹⁸ This structure, generally foamed, provides a barrier to the transfer of the heat, combustible gases and free radicals during a fire and protects the residual material from the action of the heat source.

The main components of intumescent compositions are most often a polyacid, a carbon source, and an expansion agent. In some cases, the carbon source is the host polymer itself and the expansion process is generated by the decomposition products of the polymer or the acid source, e.g., melamine pyrophosphate (MPP). The most frequent polyacid used is APP. Polymers such as those mentioned above are generally preferred rather than polyols due to exudation, water solubility, and difficulties with processing for the filled polymer. Several studies mention the use of OMMT as a nanofiller introduced in the polymer playing the role of carbon source. In other studies, the silicate is blended with all the components of the flame-retarded polymer.

Because of its widespread use in the cable industry and its ability to form a stable char, EVA has been investigated as host polymer containing both APP and organomodified silicate. Owing to the ability to achieve a nanocomposite structure in PA6 showing superior mechanical properties, the direct incorporation by Bourbigot et al.^{19,20} of a PA6 containing nanoparticles at a percentage of 2 wt % into a blend of APP and EVA (constant percentage of 60 wt % for EVA in the blend) showed significant improvement in the limiting oxygen index (LOI) and heat release rate (HRR) (Figure 12.1). Interpretations of these improvements were made in relation with the formation of aluminophosphate species, highlighted using different spectroscopic techniques^{20,21} and also with the modification of the mechanical behavior of the intumescent char formed, depending on the presence of cationic- or anionic-layered silicates.¹⁹

It was also noticed by the same authors¹⁹ that the incorporation of the OMMT in EVA instead of PA6, keeping constant the global composition, led to a strong decrease in heat released, but with a different evolution of HRR as a function of time. This was ascribed to different morphologies of clays (mixed intercalated/exfoliated versus completely exfoliated) for the polymer blend. Consequently, the formulation process of complex FR systems involving polymer blends and made up of nanoparticles in combination with FRs seems crucial.

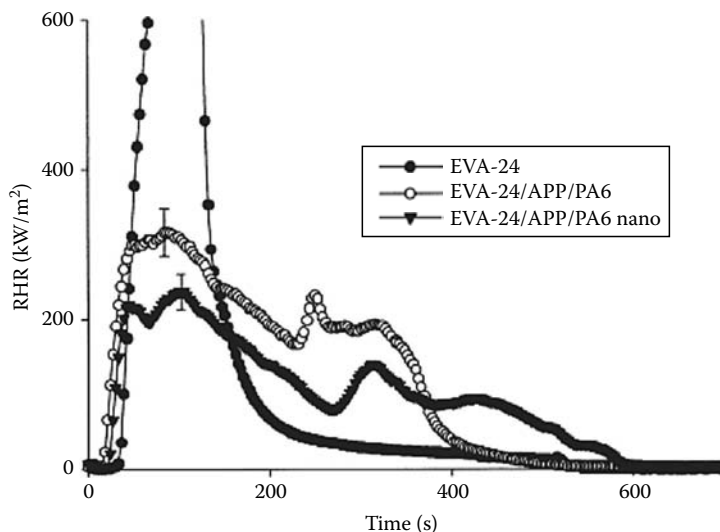


FIGURE 12.1 RHR values versus time of the formulations EVA24-APP/PA6 and EVA24-APP/PA6-nano in comparison with the virgin EVA24 (heat V_{ux} 50 kW/m²). (From Bourbigot, S. et al., *Fire Mater.*, 24, 201, 2000. With permission.)

Intumescent FR-montmorillonite compositions for polypropylene (PP) were investigated by Tang et al.^{22–26} An IFR system based on APP, pentaerythritol (PER), and MPP has been added to a PP + pristine montmorillonite + C16 compatibilizer (hexadecyltrimethyl ammonium bromide) using a twin roll mill.²² Synergistic effects on HRR values between clay and IFR system were highlighted even if partially intercalated structures were observed for such compositions. The same authors used two types of maleated PP (MAPP), differing in the percentage of anhydride, to improve the clay dispersion.^{23,25} Several ratios PP/MAPP were also tested. It was noticed that the use of the MAPP containing the highest anhydride content (4 vs 1.1 phr) led to the more exfoliated system. The optimum amount of OMMT, around 4 wt %, was shown to maximize the synergistic effect between the organomodified clay and the IFR system. The negative effect of high loadings of OMMT was ascribed to a limitation of the expansion of the charred structure in relation with the release of ammonia from the intumescent system.

The combination of the same IFR, modified MMT, and a PA6/EVA alloy in PP containing MAPP was also investigated.^{23,26} The improvement in the mechanical properties of the PP compositions containing only IFR and modified clay was achieved using the compatibilizing effect of the EVA/PA6 alloy. This effect was particularly ascribed to the formation of a copolymer resulting from the reaction between MAPP and PA6. The PA6/EVA ratio strongly influenced the balance between mechanical and flammability properties of the nanocomposite blend at a constant percentage of clay (0.5 wt %) and IFR (25 wt %). High values of this ratio led to better FR behavior (HRR values) while low values improved the impact resistance. Despite the low percentage of clay introduced in all compositions, synergistic effects with the IFR system were observed.

Other compatibilizing agents instead of MAPP were studied in IFR systems for PP containing ammonium-modified OMMT as synergist and PA6 as charring agent. Ma et al.²⁷ used carboxylated polypropylene (CPP) as reactive compatibilizer for PP/PA6 blend, leading to co-crystallization processes. The presence of OMMT at an optimum value of 4 wt % prevented dripping in flammability tests (auto-extinguishability) observed for compositions containing only the compatibilized blend and IFR (APP and melamine).

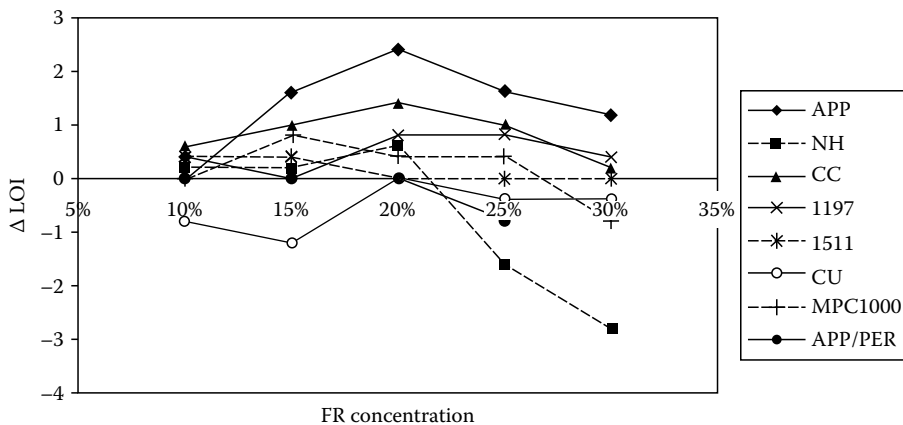
Complex FR compositions containing both organomodified clays and APP in PP were also studied by Marosi et al.^{28,29} A reactive blend of OMMT with a cationic surfactant, silicone, and polyborosiloxane elastomer (BSil) was combined with an IFR system made of APP and polyol in PP. Microthermal analysis and rheological measurements proved the existence of a coating on clays by the elastomer. Raman spectroscopy showed that heat treatment of filled PP samples resulted in an accumulation of clay particles at the surface when coated by BSil elastomer. Moreover, the cone calorimeter residue with BSil was found to be more flexible and durable, while the residue for the composition containing only IFR and MMT was brittle and rigid. This improvement was ascribed to the better thermal stability of silicone in comparison with the cationic surfactant. The BSil/MMT ratio was shown to be crucial for the initial good dispersion of nanoparticles, and thereby influenced the effectiveness of the coating. It was also concluded that the coating may act as a carrier delivering the nanoparticles to the surface, and as a stable and protective layer, when the composite is exposed to a heat source.

Flammability, degradation, and structural characterization of fiber-forming PP containing both organoclays and IFR combinations were studied by Horrocks and coworkers.^{30–32} Combinations of methyl, bis(hydroxyethyl), hydrogenated tallow ammonium-modified montmorillonite (Cloisite 30B), and APP (2.5% for each one) in PP only led to a low increase of LOI with respect to pure polymer (20.6% vs. 19.2%).³⁰ Thermogravimetric analysis showed an increase in the starting degradation temperature for the combination of clay and APP; however, the formation of a nanocomposite structure was not observed. In more recent work by the same authors,^{31,32} MAPP and PP grafted using diethyl-*p*-vinylbenzyl phosphonate (DEP) were used as compatibilizing agents. Other cationic modifiers for OMMT were also used: methyl, tallow, dihydrogenated tallow ammonium chloride (Cloisite 20A), and vinyltriphenyl phosphonium bromide. The amount of OMMT was 3 or 5 wt %.

It was shown that the clay dispersion was improved with increasing compatibilizing agent, but at the expense of the polymer processability into filaments. Nevertheless, there was no evidence of intercalation or exfoliation, irrespective of the nature of compatibilizer or clay modifier, nor strong improvements of LOI. Despite the absence of formation of true nanocomposites, filaments were sufficiently strong to be knitted into fabrics and presented slower burning behavior than the pure polymer.

The combined incorporation of ammonium-modified clays in combination with several FRs in PA6 and PA66 films was also carried out by the same group.^{33,34} Among the several FR agents, APP showed the best improvement of $\Delta\text{LOI} = \text{LOI}(\text{nanoclay} + \text{FR}) - \text{LOI}(\text{FR})$ for PA66 and PA66 (Figure 12.2). Nevertheless, the incorporation of nanoclay alone in both kinds of polyamides tended to depress the LOI values. It was proposed that the nanoclay would reinforce the material structure, and reduce its dripping capacity. The LOI reduction was explained by the difficulty of receding from the igniting flame and also by the poor thermal stability of nanoclay functionalizing species.

Incorporation of modified clays into thermosetting resins, and particularly in epoxy³⁵ or unsaturated polyester resins, in order to improve thermal stability or flame retardancy, has been reported.³⁶ A thermogravimetric study of polyester–clay nanocomposites has shown that addition of nanoclays lowers the decomposition temperature and thermal stability of a standard resin up to 600°C. But, above this temperature, the trend is reversed in a region where a charring residue is formed. Char formation seems not as important as compared with other polymer–clay nanocomposite structures. Nazaré et al.³⁷ have studied the combination of APP and ammonium-modified MMT (Cloisite 10A, 15A, 25A, and 30B). The diluent used for polyester resin was methyl methacrylate (MMA). The



Key:

Code: Constitution	Commercial Name	Manufacturer
APP: Ammonium polyphosphate	Antiblaze MCM	Rhodia
NH: Melamine phosphate	Antiblaze NH	Rhodia
CU: Cyclic organophosphonate	Antiblaze CU	Rhodia
CC: Poly (phosphine oxide)	Proban CC polymer	Rhodia
APP/PER	Antiblaze MCM/pentaerythritol	Rhodia
APP/PER/melamine	MPC 1000	Rhodia
1197: Pentaerythritol phosphate	NH 1197	Great Lakes
1511: PER phosphate/melamine	NH 1511	Great Lakes

FIGURE 12.2 ΔLOI values for all additives examined in polyamide 6.6 films. (From Horrocks, A.R. et al., *Polym. Degrad. Stabil.*, 88, 3, 2005. With permission.)

amount of clay was restricted to 5 wt %, since in the presence of FRs, the cross-linking reaction could be noticeably slowed for higher clay percentages and difficult to process. It was noticed by Bharadwaj et al.³⁸ that the cross-link density was inversely proportional to the degree of exfoliation and macroscopic dispersion. In addition, less cross-linking tended to reduce the charring ability of the resin, resulting in a poorer fire behavior for the sample. The study carried out by Nazaré et al.³⁷ showed that the incorporation of nanoclays alone reduced flammability only to a limited extent, while the effect of APP and other FR agents allowed the flammability to be considerably reduced. Owing to the percentage of components selected, no highlighted synergistic effect could be found.

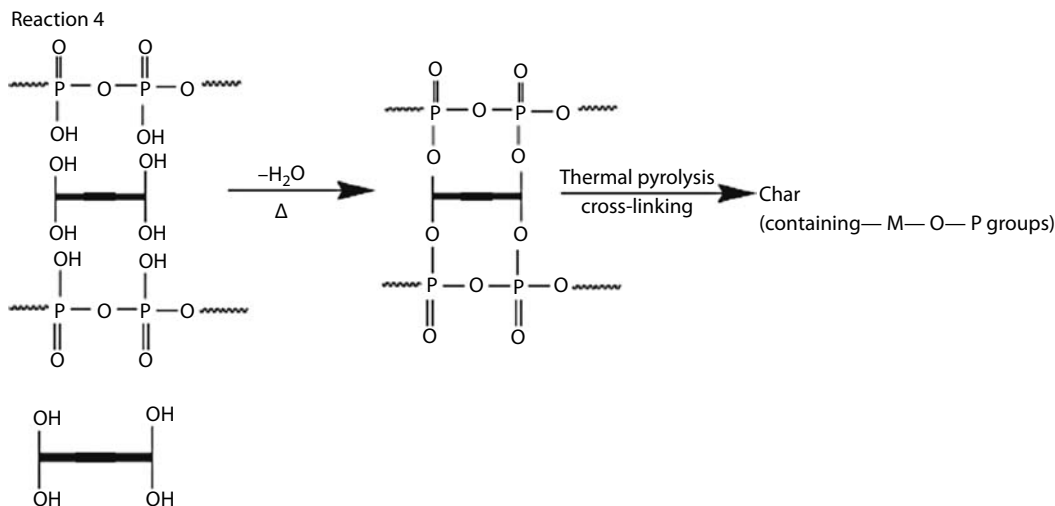
The nature of the organomodifier plays a role in the existence of true nanocomposite structures (intercalated for 15A and 30B, exfoliated for 25A, microcomposite for 10A), cone calorimeter results associated with x-ray diffraction (XRD) suggest that increased flame retardancy are more dependent on physical and thermal cross-linking of clay particles and polymer chains than on formation of nanocomposite structure. However, it can be concluded that the role of clay is crucial since PHRR values are reduced up to 70% in the presence of clays.

Another study concerning cross-linked polymers and intumescent/OMMT compositions was carried out on polyurethanes by Song et al.³⁹ The polyurethane (PU) structure was built using a PP oxide glycol and toluene diisocyanate (TDI) (NCO/OH = 2:1) cross-linked using glycerine. OMMT was prepared using hexadecyltrimethyl ammonium chloride and the FR used was MPP. OMMT was initially dispersed into the polyether to obtain a colloidal polymer nanocomposite before reaction with TDI and then cross-linking. XRD patterns showed an intercalated structure with no significant change in the presence of MPP. The selected values for each component did not show evidence of synergistic effects; however, rather high values of LOI (27.5%) were found in the presence of 5 wt % MMT and 6 wt % MPP and HRR values decreased strongly. The improvement in fire retardancy was ascribed to the increase of char residue, due to reactions of polyphosphoric acid derivatives, acid sites of OMMT, and PU. It is proposed that OMMT layers could retard the release of water and ammonia and enhance the cross-linking reaction of PU.

12.2.1.2 Anionic Clays

Owing to the availability of commercial OMMT, the majority of the studies on combinations between intumescent compositions and layered silicates concern this type of clay. More recently, interest has arisen in LDH and this has also led to investigations about the advantages of combining them with intumescent compounds. Wang and coworkers^{40,41} have combined LDH with an intumescent system made of APP and PER in acrylate–silicone–melamine formaldehyde coatings. Using various experimental techniques, the authors concluded that LDH could catalyze the esterification reaction between APP and PER. The constitution of an interpenetrating network formed from the decomposition products of LDH and the organic fraction of the coating improved the char structure and the FR properties of the coating.

Zhao et al.⁴² have studied potential synergistic effects of APP and LDH on flame retardancy of poly(vinyl alcohol) (PVA). Several LDH structures (Zn/Al-LDH, Ni/Al-LDH, Zn/Fe-LDH) were prepared from carbonate intercalated LDH precursors. The global loading of APP + LDH was kept constant at 15 wt % with the percentage of LDH between 0.1 and 3 wt %. For all kinds of LDH prepared, synergistic effects between APP and LDH were observed from LOI values and the UL-94 test, in which a V-0 classification was achieved for many of the compositions, particularly for Zn/Fe-LDH. The optimum compositions, leading to the better fire performance, corresponded to an LDH percentage of 3 wt %. Although no information was given about the morphology of the LDH/APP/PVA composites, mechanisms of flame retardancy were proposed on the basis of FTIR and XPS characterizations of the char residues formed from composites degraded in air at 500°C. The significant increase of char formed in the presence of LDH suggested that LDH plays a very important role in catalyzing the cross-linking of polyphosphate or phosphate with PVA to form an expanded and protective char layer. Moreover, in addition to the



Layered structure of LDH

SCHEME 12.1 Possible reaction mechanism of char formation during combustion of PVA/APP/LDH systems. (From Zhao, C.X. et al., *Polym. Degrad. Stabil.*, 93, 1323, 2008. With permission.)

direct and traditional reaction of the phosphate ester with the PVA chain, the authors proposed a reaction of polyphosphoric acid with LDH layers, releasing water molecules and producing bridges between APP chains (Scheme 12.1). Consequently, the process of char formation seems to differ from that existing in the presence of APP alone, leading to a more compact and dense char layer.

The concomitant use of APP and Mg/Al undecenoate LDH in polystyrene was reported by Nyambo et al.⁴³ All the components were mixed in the molten state for PS in a Brabender mixer. FTIR spectra, XRD patterns, and TEM analysis showed that undecenoate ion was intercalated into the LDH galleries and that nanoclay were dispersed and exfoliated in PS at a loading of 3 wt %. Nevertheless, increasing the loading up to 5 wt % led to a microcomposite. The individual components (APP and LDH) had small effects on thermal stability, but their combination entailed a stabilization effect on the thermo-oxidative degradation, by promoting char formation at high temperature. Addition of both components at a loading no higher than 10 wt % resulted in dramatic reduction of PHRR and average mass loss rate (AMLR). These phenomena were ascribed to the slower rate at which combustible volatiles were released.

12.2.2 LAYERED SILICATES ASSOCIATED WITH OTHER PHOSPHORUS AND NITROGEN COMPOUNDS

Phosphorus FR compounds cover a wide range of chemical structures not only as additives incorporated in the molten state in thermoplastics but also as reactive components introduced as monomers in thermoset polymers: phosphates, phosphonates, phosphinates, phosphine oxides, phosphites, red phosphorus, etc. They can be also used as layered silicate modifiers. Organic phosphates and red phosphorus are among the most frequent additive FRs used in various non-polyolefinic polymers.

Despite red phosphorus having high effectiveness as an FR, able to act either in the vapor or condensed phase according to the nature of polymer, and its possibility to react with metal oxides, leading to synergistic effects,⁴⁴ the main drawback of red phosphorus is the risk of phosphine

(PH_3) release during the transformation process. This phenomenon occurs through reaction with moisture and is due to the poor thermostability of red phosphorus. The formation of phosphine can be avoided by the encapsulation of red phosphorus in another polymer. Investigations on the synergistic effects of LDH (hydrotalcite) with microencapsulated red phosphorus were carried out by Jiao et al.⁴⁵ and Du et al.⁴⁶ in EVA. In the compositions produced by this last research group, the percentage of hydrotalcite (HTP) was high, between 25 and 38 wt %, while the percentage of phosphorus varied between 2 and 15 wt %, the global loading was kept at 40 wt %. It was found that increasing amounts of red phosphorus up to 10% entailed a decline of HRR values and an increase for the flame out time in cone calorimeter tests (Figure 12.3). Moreover, LOI values increased up to 33% and the V-0 classification was achieved in the UL-94 test. Nevertheless, these improvements in flammability occurred at the expense of increased average smoke produced per unit weight of degraded volatiles (SEA). No interpretation of the FR synergy between LDH and red phosphorus was given.

Similar FR synergistic effects for LOI and UL-94 test values were found by Jiao et al.⁴⁵ The change in the composites before and after gamma irradiation was compared. LOI values of compositions containing both LDH and red phosphorus were improved after irradiation using a suitable dose. Comparisons with compositions containing metallic hydroxides (magnesium and aluminum hydroxide) instead of LDH were also carried out in EVA.⁴⁰ Investigations on the ternary combination of modified MMT, MH, and red phosphorus were performed by Song et al.⁴⁷ in PA6. The authors mentioned synergistic effects between the three components. Partial substitution of 2 wt % of MH by an ammonium-modified MMT in PA6 + 6% MH + 5% Red phosphorus led to improved fire behavior, observed using cone calorimeter and LOI. An intercalated-exfoliated structure was observed by TEM and XRD for the clays in the ternary composition. The authors suggested that water vapor released from MH and the acidic behavior of clay after degradation of organic modifier facilitates the thermo-oxidation degradation of PA6, cross-linking, and charring. Moreover, the

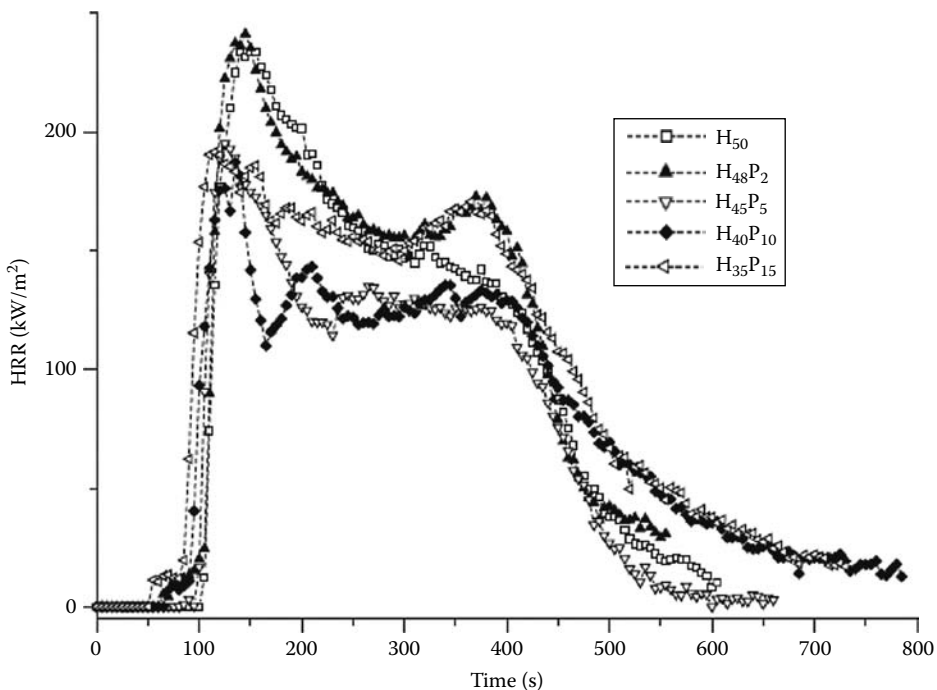


FIGURE 12.3 Effect of MRP on HRRs of EVA/hydrotalcite composites. (From Du, L. et al., *Polym. Degrad. Stabil.*, 91, 995, 2006. With permission.)

combustion entails the formation of polyphosphoric acid derivatives from red phosphorus, which can react with the decomposition products of the other components, leading to the formation of a stable glassy and carbonaceous layer. This can act as a mass and heat transfer barrier. MLR evolution tends to confirm this mechanism.

Various combinations of phosphorus compounds other than red phosphorus have also been combined with organomodified clays in PA6 and PA66 by Padbury et al.^{34,48} The objective was to reduce the required amount of phosphorus FR needed for some applications of fibers and films. This group has reported measurement of LOI for the combination of a given amount of organoclays (not clearly indicated) with various phosphates and phosphonates species, including intumescent systems, mentioned in the Section 12.2.1.1. All the discussion in this chapter is based on the evolution of Δ LOI (in presence or absence of clay) as a function of the percentage of each phosphorus FR (see above). The evolution of the increase in LOI per unit phosphorus was also investigated. It was concluded that the presence of organomodified clay increased the FR efficiency by at least a factor 2 on average, thereby indicating a positive clay–FR interaction for each retardant.

Aromatic phosphates are widely used in engineering plastics such as styrenics and polyesters. Polystyrene–clay nanocomposites combined with numerous (31) phosphorus-containing FR were prepared by Chigwada and Wilkie.⁴⁹ The percentages of clays and FR were varied (3–10 wt %) to study the effect of each on thermal stability and mechanical properties of the polymer. The clay modifier was dimethyl benzyl hydrogenated tallow ammonium (Cloisite 10A), which was intercalated in the polymer. The authors have also verified that intercalation was conserved in the presence of all phosphates (percentages between 5 and 30 wt %). Cone calorimeter measurements evidenced synergistic effects between phosphate FRs and organomodified clay. It was also shown that a percentage of 30 wt % for the phosphate was needed to achieve a V-0 rating in the UL-94.

The same research group of Marquette University has also investigated the influence of the combination of various organomodified clays and conventional aromatic phosphates on the fire retardancy of vinyl ester composites.^{36,49,50} Synergic effects were shown through the use of cone calorimeter: Reductions in peak of HRR, total heat release (THR), and AMLR. No improvement in the time to ignition was found. Thermogravimetric analysis showed that char yield increases in the presence of phosphate and that a synergistic effect leading to a superior enhancement of char formation occurs in the presence of resorcinol diphosphate and commercial Cloisite 15A. On the whole, the incorporation of phosphate did not modify the intercalated structure of cationic clays. The mixing time and the atmosphere in which the reaction between clay and resin occurred seemed not to influence the flammability and thermal stability of the nanocomposite.³⁶

Binary combinations between the three components Cloisite 15A, copper hydroxy dodecyl sulfate (CHDS), which is a layered hydroxy salt (LDS), and resorcinol di-phosphate, have been investigated to improve flammability of vinyl ester resins.^{50,51} Significant increments in TGA char formation, up to 260%, were observed in some cases when the fire retardants were used individually or in combination. Char yields produced from cone calorimeter testing were highest in the presence of resorcinol bis(diphenylphosphate) (RDP). Intercalated or exfoliated structures were observed in the presence of both RDP and CHDS. Synergies on PHRR and THR were not found by the association of CHDS and RDP for a global loading of 10 wt % in the resin, even if the percentage of char was strongly increased. This strong char enhancement was ascribed to the reaction of water released by CHDS with phosphates to form acid phosphates. The origin of water released could be either dehydroxylation of the copper hydroxide layers or combustion of dodecyl sulfate.

Among the conventional FR, which can be potentially associated with organomodified layered silicates, nitrogen compounds play a specific role in improving the flame retardancy of some polymers, particularly polyamides. Melamine and its salts are widely used, due to its ability to release

several gaseous degradation products limiting the ignition. Also, melamine accelerates the decomposition of PA6 by aminolysis.⁵²

Hu et al.⁵³ and Zhang et al.⁵⁴ have studied the combination of OMMT with melamine cyanurate (MCA) in PA6. The first authors used an OMMT modified using hexadecyltrimethyl ammonium bromide. They have shown that a binary composition of 15 wt % MCA and 5 wt % OMMT gave a reduced PHRR in comparison with compositions with MCA or MMT alone at the same loading. Nevertheless, the V-0 rating was not achieved when OMMT was added to the polymer in combination with MCA. It was explained by the specific role of MCA, which acts as a dripping promoter, taking heat away, while clays, dispersed at the nanometric level, enhance the formation of char and prevent dripping. Zhang et al.⁵⁴ used a range of ammonium organomodified OMMT percentages between 0.2 and 5 wt % for a percentage of 13 wt % for MCA. The antagonism concerning UL-94V between both components was also highlighted. LOI of PA6 was also impaired by the concomitant use of MCA and clay. The addition of polyvinylpyrrolidone (PVP) partially restored the UL rating. The influence of organomodified clay on polymer viscosity as well as barrier effects influencing the rate of MCA release were proposed to explain the antagonism. The effects of PVP addition or the use of natural MMT instead of organomodified one, which limits the increase in viscosity, support this explanation.

Besides the use of additive FR containing phosphorus into the host polymer nanocomposite, the modification of the layered silicates with P-based compounds seems promising. However, even taking into account the high specific surface area available, the quantity of phosphorus incorporated into the polymer is significantly lower than that obtained by the additive route.

In the work of Wilkie et al.,^{55,56} oligomers of styrene, vinylbenzyl chloride, and diphenyl vinylbenzylphosphate and diphenyl vinylphenylphosphate (DPVPP) have been prepared and reacted with an amine and then ion-exchanged onto clay. The resulting modified DPVPP clays have been melted blended with polystyrene and the flammability was evaluated. XRD and TEM observations proved the existence of intercalated nanocomposite structures. Cone calorimeter tests have shown a substantial reduction in the PHRR of about 70% in comparison with pure PS. According to the authors, this reduction was higher than the maximum reduction usually obtained with PS nanocomposites. Other vinylphosphate modified clay nanocomposites were also elaborated. The reduction in PHRR was greater with higher phosphorus content than for DPVPP. Consequently, the reduction in PHRR seemed attributed to both the presence of the clay and to the presence of phosphorus.

The intercalation of LDH by phosphorus-containing ions was also performed in EVA. Ye and Qu⁵⁷ have intercalated phosphate ions to produce a MgAl-PO₄ hydrotalcite phosphate (HTP). This mineral was prepared by ion exchange from MgAl-NO₃ hydrotalcite. Percentages of LDH were varied between 40 and 60 wt % and a comparison was made with carbonate HTC, also able to release carbon dioxide, at the same loadings. LOI value of MgAl-PO₄ composite was found 2% higher than those of MgAl-CO₃ (HTC). Moreover, a V-1 rating in the UL-94 test could be achieved. FTIR spectra revealed that in MgAl-PO₄ composition, the charred structure was more compact, involves P-O-P and P-O-C bonds and has faster formation than MgAl-CO₃ or EVA (Figure 12.4).

Another strategy may consist in reducing the volatile character of a phosphorus compound by intercalating it between the platelets of a layered silicate. Kim et al.⁵⁸ have intercalated an OMMT (Cloisite 30B) with triphenylphosphate (TPP) in ABS. A silane coupling agent was added and synergistic effects were investigated by incorporation of epoxy resins. It was found that TPP intercalated in the clay presents a higher evaporation temperature when compared with TPP. In addition, the thermal stability of ABS was increased by incorporation of TPP-modified clay. The incorporation of epoxy resin at global loading of all components, kept constant at 15 wt %, resulted in a significant increase of LOI. Microscopy results suggested that this enhancement could be related to the compact character of chars formed after burning of the filled ABS/epoxy resins.

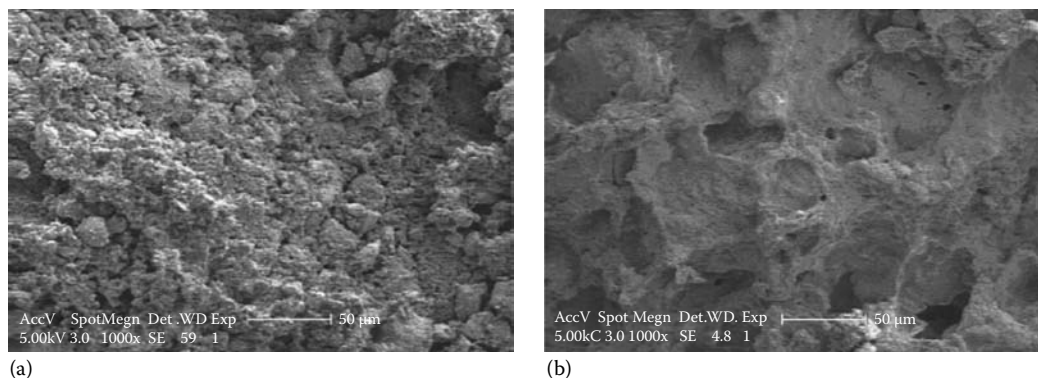


FIGURE 12.4 SEM images of charred residues of (a) HTC60 and (b) HTP60 samples. (From Ye, L. and Qu, B., *Polym. Degrad. Stabil.*, 93, 918, 2008. With permission.)

To take advantage of both modified layered silicate and the substantial presence of phosphorus, the combined use of phosphorus-modified silicates and phosphorus compounds may represent an innovative solution to achieve high levels of flame retardancy. Phosphonium-modified layered silicates in epoxy resins were associated with organo-phosphorus FRs by ScharTEL et al.⁵⁹ Ion exchange of Na-montmorillonite was carried out using tetraphenyl phosphonium bromide. Triphenyl phosphate and a reactive phosphorus compound were used as FR incorporated in the epoxy resin.

Even though well-distributed phosphonium-modified clay composition shows better properties than ammonium compositions, the combination of fire retardants containing phosphorus and phosphonium-modified layered silicates in this case shows antagonistic behavior for most of the fire properties. Conversely, the use of a phosphonium-modified OMMT or a phosphorus-functionalized nano-kaolin, incorporated in PET or PC-PET blend^{60,61} led to different conclusions. Both materials were recycled, but are high-purity polymers. The phosphorus compound used was triphenylphosphite (TPPi) or methyltriphenoxyposphonium iodide. Surface hydroxyls of kaolinite were reacted with the first, while the ionic form was exchanged with sodium ions of the OMMT. It can be shown in Figure 12.5 that the combination in a 80 w/20 w PET/PC blend of 4 wt % P-modified OMMT and 5 wt % TPPi present as an additive in the polymer seemed advantageous in comparison with the same components used separately. This combination obtains a V-0, rather than V-2, rating in the UL-94V. This behavior has been ascribed to the compatibilizing effect for the blend of modified OMMT and chain extender role of TPPi.

A last route allowing phosphorus to have an FR effect in host polymers in combination with organomodified layered silicates is to carry out in situ polymerization using phosphorus-containing monomers. For example, a novel phosphorus-containing PET copolymer was synthesized by Ge et al.⁶² by in situ intercalation polycondensation of terephthalic acid, ethylene glycol, and 2-carboxyethyl(phenylphosphinic)acid (HPPPA) with OMMT. It has been shown that the nanocomposite had better flame retardancy than neat PET-co-HPPPA. There was an increase in LOI values (from 31.4 to 34.0) for a very low OMMT content. For an OMMT loading of 2 wt %, a V-0 rating could be achieved. Another synthesis made by the same research team, using a diol grafted by a DOPO structure (DDP) as monomer instead of HPPPA, also led to interesting results.

The combinations of OMLS with various phosphorus compounds have generally proved to be of interest. Because of the existence of various routes to associate the silicates and the phosphorus FR, and also owing to the very large number of phosphorus compounds, the future of this class of FR systems seems very promising.

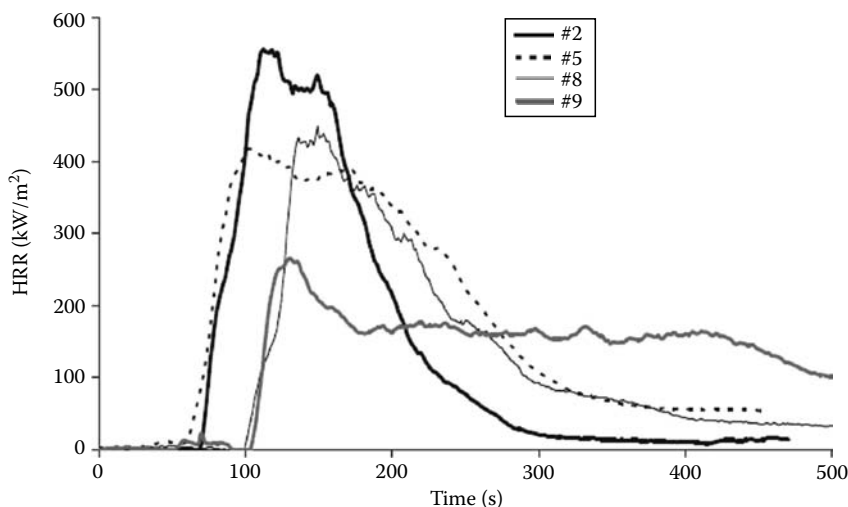


FIGURE 12.5 Heat release rate curves obtained in cone calorimeter tests for formulations #2,5,8,9. (respectively: PET/PC (80:20), PET/PC (80:20) + 5% MMT-P, PET/PC (80:20) + 4% TPPi, PET/PC (80:20) + 5% MMT-P + 4% TPPi). (From Swoboda, B. et al., *Proceedings of the 19th BCC Conference on Flame Retardancy*, Lewin, M. (ed.), Business Communications Co Editions, Norwalk, CT, 2008; Swoboda, B. et al., *Proceedings of the ACS Conference*, New Orleans, LA, 2008.)

12.2.3 LAYERED SILICATES ASSOCIATED WITH METAL HYDROXIDES

Metal hydroxides, such as alumina trihydrate (ATH) or MH, are among the more environment-friendly FRs. Nevertheless, they present two kinds of drawbacks. On the one hand, the loadings required to meet high fire performances tend to impair the ultimate mechanical properties and, on the other hand, the water release caused by their FR action leads to hydrolysis reactions for some categories of polymers, such as polyesters. To limit the global amount of FR incorporated in flame-retarded polymers, particularly polyolefins, attempts to associate metal hydroxides and OMMT were aimed to reduce the global loading at constant fire behavior, particularly for EVA or LDPE, frequently used in cable industry. The aim could also be related to the following objectives:

- Take advantage of the barrier effect produced by the clays to regulate the water release.
- Improve the cohesion of the oxide residue formed at the surface of sample after polymer ablation.

Several micron-sized layered silicates, such as talcs, can improve the fire retarding behavior of EVA by partial substitution of metal hydroxides. Clerc et al.⁶³ have shown that better fire performance was achieved using higher values of the lamellarity index and specific surface area for four different types of talcs in MH/EVA blends. Expanded mineral and charred layers were formed, similar to intumescent compositions with APP, proving the barrier effect on mass transfer, even at the micron scale for the mineral filler.

OMLS, such as montmorillonite, are able to develop the highest specific interfacial area for intercalated or exfoliated morphologies, and exhibit similar expanded character for the EVA-related compositions in which MH or ATH is partially substituted by OMMT.⁶⁴ Moreover, many authors^{64–69} have shown synergistic effects on fire properties between organomodified layered silicates and metal hydroxides (MH or ATH) in polyolefins. Nanocomposite morphologies in the presence of large loadings of metal hydroxides in EVA were not clearly established by the several authors. The mechanisms of action for the role of organomodified clay are heterogeneous bubble nucleation for decomposition products of EVA, increased viscosity,⁶⁴ and promotion of charring.⁷⁸

The quality of char formed for metal hydroxide/MMT combinations seems of prime importance to maximize the barrier effect. Incorporation of silica in combination with MH and MMT by partial substitution of MMT has been investigated by Ferry et al.,⁶⁴ Laoutid et al.⁷⁰ to improve the cohesion of charred and expanded structure. Even though silica generated cracks in the char and reduces its resistance, as measured by indentation, fire behavior, as studied by cone calorimeter was improved.

The use of compatibilizers is required to promote the formation of exfoliated or intercalated structures in PP with OMMT. Ristolainen et al.⁶⁶ have used two types of compatibilizers of OMMT (Cloisite 15A) in a blend with ATH: Commercial PP grafted with maleic anhydride, and hydroxyl functionalized PP. The intercalated/exfoliated morphologies were shown with compatibilizers at 5 wt % organoclay, even in the presence of ATH, the global loading being kept at 30 wt %. ATH was shown to facilitate exfoliated instead of intercalated structures. The ATH and organomodified clay combination resulted in synergistic flammability effects (HRR values) and reduced mass loss, ascribed to char formation limiting volatile transfer.

As observed for talc particles (see above), the morphology of clay particles has a significant influence on fire performance in blends with metallic hydroxides. Marosfoi et al.⁷¹ have associated layered materials (OMMT with acetyl trimethyl ammonium bromide) and organically modified sepiolite (OSEP). Both clays were used in combination with MH in PP. Sepiolite at 5 wt % produced a synergistic effect on PHRR when associated with MH at 10 wt %. Nevertheless, THR remained unchanged. Conversely, the concomitant use of 2.5 wt % OMMT and 2.5 wt % OSEP also led to a significant decrease of PHRR and also to a decrease of THR (Table 12.1). These interesting results were ascribed by the authors to the formation of bridges between particles of lamellar particles of OMMT and magnesium oxide through fibrous sepiolite particles. Consequently, a network of nanoparticles was probably built at the surface and conserved when irradiation occurred.

MH and ATH are not the only metallic hydroxides studied in association with organomodified layered silicates. Hydromagnesite (HM) has a formula of $5\text{MgO}\cdot 4\text{CO}_2\cdot 5\text{H}_2\text{O}$ and can be found in natural deposits with huntite, or as an industrial by-product. HM is able to release 54% of its weight as water vapor and carbon dioxide in the range 200°C–550°C. Its decomposition enthalpy is less than ATH or MH, but the mass loss is higher. Pure HM associated with OMMT (nanofil 5, ammonium modified) was used by Laoutid et al.⁷² in EVA and Haurie et al.⁷³ in EVA/LDPE blends. Comparisons were made with MH or ATH at the same loading, and in association with OMMT. From Laoutid et al.,⁷² HM/MMT (55 wt %/5 wt %) displayed a synergistic effect between the two components,

TABLE 12.1
Characteristic Combustion Parameters of PP and PP-Based Composites

Sample Name	Matrix PP400H Mass Ratio	Additive PPgMA Mass Ratio	Microfiller MH Mass Ratio	Nanofiller SEP Mass Ratio	Nanofiller OSEP Mass Ratio
PP400H	100	0	0	0	0
PP + MH (10%)	90	0	10	0	0
PP + MH (15%)	85	0	15	0	0
PP + SEP (5%)	90	5	0	5	0
PP + OSEP (5%)	90	5	0	0	5
PP + MH (10%) + OSEP (5%)	80	5	10	0	5
PP + MH (15%) + OSEP (5%)	75	5	15	0	5

Source: Marosfoi, B.B. et al., *Polym. Adv. Technol.*, 19, 693, 2008. With permission.

Note: All samples were compounded at 190°C applying a mixing rate of 50 rpm for 10 min.

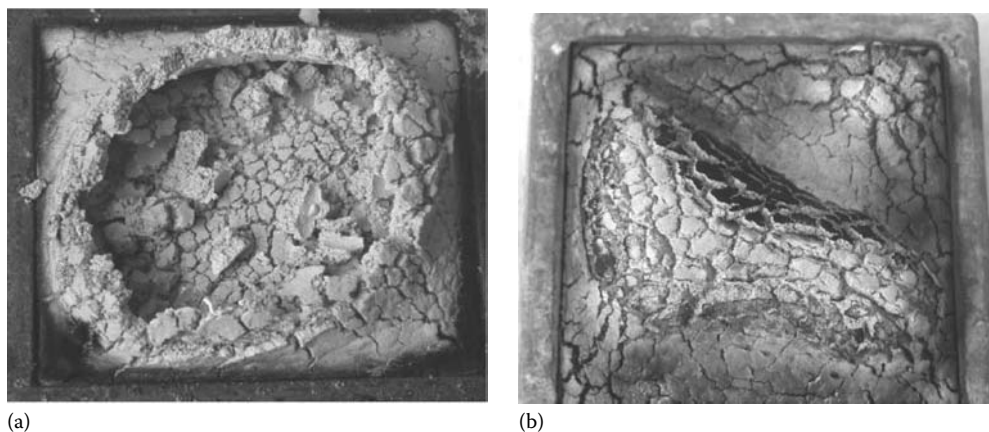


FIGURE 12.6 Photos of the LDPE/EVA filled samples: (a) Hy60, and (b) Hy/MMT50 after cone calorimeter test. (From Laachachi, A. et al., *Polym. Degrad. Stabil.*, 89, 344, 2005.)

based on HRR values. Moreover, the resistance to ignition and self-extinguishability was better than the corresponding MH/MMT composition, whereas the HRR values seemed relatively similar. The study of residues formed during thermal degradation at 1200°C revealed the formation of forsterite (Mg_2SiO_4) when either MH or HM were used in combination with MMT. Scanning electron microscope observations of residues have shown sintering of the mineral particles, particularly in the case of HM/MMT composition. For LDPE/EVA blends,⁷³ a reduction in PHRR was also noticed for the sample containing MMT (modified by dimethyl distearyl ammonium chloride) in comparison with pure HM. Cone calorimeter results were explained by the increase in stability of char observed (Figure 12.6).

Investigations concerning LDH in combination with metallic hydroxides were also carried out. Zhang et al.⁷⁴ and Ye et al.,⁷⁵ from the same research group, have associated ultrafine MH (range 0.1–1 μm) with LDH in EVA or EVA/LDPE by melt blending. XRD patterns and TEM micrographs have shown that the LDH loading controls the morphology: Exfoliated, up to 5 wt %, intercalated for higher percentages.⁷⁴ From these authors, LDH particles acted as dispersion promoters of MH particles in EVA or LDPE/EVA blends. Thermal stability of LDH/MH compositions was increased in comparison with those containing only MH. In addition, strong synergistic effects were noticed for LOI values, which were attributed to a low dispersion of MH particles, because of their size and absence of surface treatment. Finally, additional improvements of fire performance, characterized by LOI values and also char formation, were achieved by replacing 5 wt % MH by either red phosphorus or expandable graphite, in a 95/5 (phr/phr) composition for LDPE/EVA blends. Consequently, significant synergistic effects have been observed in these multicomponent systems.

12.2.4 LAYERED SILICATES ASSOCIATES WITH BROMINATED COMPOUNDS

Since one objective of the combined use of organomodified layered silicates and FR compounds could be to replace effective FR systems containing halogenated FR, few studies mention the concomitant use of silicates, and more generally nanoparticles, with halogenated compounds. In some cases, comparisons have been made between those systems and the corresponding ones in which silicates are associated with other kind of FRs. All these studies have been carried out rather recently by research groups in countries where the use of brominated FR seems less undesirable than in Europe.

Hu et al.⁵³ have studied the nanocomposites obtained by blending PA6, OMMT, and decabromodiphenyl oxide (DB) synergized by antimony oxide (AO). Moreover, comparisons were made with a similar composition containing MCA instead of DB + AO.

Combination between a polybrominated aromatics and AO is the most frequently used halogenated systems, and this provides excellent and synergistic fire performance for several thermoplastic polymers, including polyamide 6. According to Levchik and Weil,⁷⁶ the fire-retardant mechanisms of this FR combination in PA6 are the generation of free radicals, the promotion of char formation through dehydrogenation reactions, the formation of HBr, which acts as a gas barrier between the material and the combustible volatiles. Even if no synergistic effect can be proved, due to a nonconstant global loading, the association of 5 wt % OMMT (hexadecyltrimethylammonium bromide), 15 wt % DB and 5 wt % AO (PA6-*n*/DB-AO) leads to a strong decrease of PHRR (390 kW/m²) compared with 627 kW/m² for the same amounts of DB + AO (cone calorimeter tests at 50 kW/m²). Moreover, the V-0 rating in the UL-94 test is maintained. A slower thermal decomposition for PA6-*n*/DB-AO is ascribed to the labyrinth and barrier effect of the silicate layers, initially well-dispersed in the polymer (intercalated/exfoliated morphology). Several reactions occurring between clay, DB, AO, and PA6 are mentioned by the authors, particularly between AO and NaBr present as an impurity in commercial clay, which can lead to the formation of the active FR antimony tribromide. All these reactions can account for the compatibility and fire performance of the global system.

Another route to combine organomodified layered silicates and brominated species is similar to those with phosphorus, by cation exchange, introducing brominated cations into the layered structure. Chigwada et al.⁷⁷ have investigated the potential synergy between an organomodified layered silicate and low levels of bromine in fire retardancy in polystyrene. An organically modified clay has been prepared using ammonium salts, which contain an oligomeric material consisting of vinylbenzyl chloride, styrene, and dibromostyrene (DBS). The nanocomposites (intercalated structure) were prepared by bulk polymerization and melt blending with various contents of the three monomers, producing various percentages (between 4 and 44 wt %) of bromine in the clay. Because of the low inorganic content of the bromine modified clay, at least 10 wt % clay is required to achieve a significant reduction in PHRR for cone calorimeter measurements at 35 kW/m². On the whole, the presence of clay caused the reduction in PHRR, while the presence of bromine brought about the reduction in total heat released. A comparison made with DB oxide introduced in PS at 3 wt % without clay and a composition with a similar amount of bromine showed that the reduction in THR was lower with DB and no PHRR reduction was noticed. It could be concluded that a useful FR system can be obtained by the use of a bromine-containing nano-dispersed clay. It is also likely that the use of bromine supported by the clay would limit the emission of bromine compound during processing operations.

In another study carried out by the same research group,⁷⁸ fluorine-containing quaternary ammonium salts used to modify sodium montmorillonite (new VB16 clay) have been introduced in PS by bulk polymerization with DBS and styrene. It was noticed that a modified PS with 90 wt % of DBS-VB16 composition avoided dripping and burning in the UL-94 test, allowing a V-0 rating to be achieved. Moreover, bromine present as pentabromobenzyl derivatives (3 wt %) in PP, PE, and PS was evaluated by the same authors in combination with a commercial montmorillonite (Cloisite 30B), also at 3 wt %. The reduction in PHRR and THR appears strongly dependent on the nature of brominated derivative. For some compositions, and particularly for PE, PHRR and THR are not decreased by the combined brominated compound-organoclay. Consequently, the use of an additive brominated/clay FR system has to be carefully designed, while FR systems based on halogenated compounds supported by the clay using ion exchange seem to present more potential.

12.3 OTHER NANOPARTICLES ASSOCIATED WITH VARIOUS FLAME RETARDANTS

12.3.1 COMBINATIONS OF CARBON NANOTUBES WITH FLAME RETARDANTS AND NANOPARTICLES

Thanks to their high aspect ratio, CNTs percolate to form a network at very low loading in the polymer matrix and lead to substantial enhancement of several functional properties, such as flame retardancy. Two different types of CNTs, single-walled nanotubes (SWNT) with

small diameters (1 ~ 2 nm) and multi-walled nanotubes (MWNT) with larger diameters (10 ~ 100 nm) can be considered.

Regardless of the nature of these nanotubes, their dispersion state in the host polymer is crucial and its improvement is a challenge to achieve the best fire performance of the corresponding nanocomposites. For example, Kashiwagi et al.⁹ have shown that in PMMA well-dispersed SWNTs led to a strong decrease in PHRR in cone calorimeter tests, while poorly dispersed SWNTs did not modify HRR in comparison with pristine PMMA.

The FR properties of polymer/CNTs nanocomposites appear to be governed by two distinct physical processes. First, the network structured layer acts as a shield and re-emits much of the incident radiation back into the gas phase decreasing the polymer degradation rate. Second, the presence of CNTs increases the thermal conductivity of the materials. A balance between thermal conductivity and shielding effects is necessary to obtain the lowest HRR and the largest time to ignition. Nanotube surface reactivity also leads to some modifications and improvement of nanocomposite fire properties and especially in the case of crushed MWNTs.⁷⁹ Indeed, some radical species formed during the nanotube crushing process interact with the polymer when it decomposes, increasing resistance to inflammation of the nanocomposite and producing a homogeneous char.

Additives combinations of CNT with organomodified clays and with ATH in EVA cable compositions have been carried out by Beyer and coworkers.^{80–83}

Compositions of EVA with 5 phr of crude or purified CNTs (MWNTs), 2.5 phr of each CNTs and organomodified layered silicate (dimethyl distearyl ammonium) were tested using the cone calorimeter^{80,81} at 35 kW/m². It was found that crude CNTs were as effective in the reduction of PHRR as purified CNTs. A synergistic effect for flame retardancy between CNTs and organoclays was observed. Moreover, the residues revealed a reduction in the crack density for the sample with CNTs and organoclay.

It was concluded that organoclays played an active role in the formation of a compact char, while CNTs, owing to their high aspect ratio, could also strengthen it. Finally, the production of an FR insulated wire containing CNTs has shown that synergistic effects of CNTs combined with organoclay were also conserved when the composition contains ATH. In a further investigation of the role of MWCNTs and organoclays in the fire retardancy of EVA,⁸³ it was found that the CNTs played an important role in the reduction of PHRR by forming low permeability char containing graphitic carbon. The char oxidation is important in fire retardancy and the oxidation resistance of the char and is a function of the degree of graphitization. Nanotubes may act as the nucleation of graphitization leading to the formation of turbostratic and graphitic carbons. This effect was enhanced when CNTs and organoclays were associated.

The grafting of chemical species onto a functionalized nanotube surface is a new way to improve polymer/CNTs compatibility leading to better dispersion of CNT and more effective CNTs network structured layer. Thus, FRs can be grafted onto the surface of CNT, thus combining the effect of the CNTs network with FR action. This was suggested by Ma et al.⁸⁴ who covalently grafted a phosphorus–nitrogen carbonization FR agent, poly(diaminodiphenyl methane spirocyclic pentaerythritol bisphosphonate) (PDSPB) onto the surface of MWNTs (Figure 12.7) leading to better dispersion of MWNT-PDSPB in ABS matrix. The corresponding nanocomposites showed a reduction of PHRR in comparison with nongrafted MWNTs. However, it was not clearly established that the reduction of PHRR was due to the combination of the FR action of both PDSPB and MWNTs or just because of better dispersion of grafted MWNTs.

12.3.2 COMBINATIONS WITH, NANO-HYDROXIDES, NANO-OXIDES, AND OTHER NANOPARTICLES

12.3.2.1 Combinations with Nano-Hydroxides

Many nanoparticles (oxides, hydroxides, POSS, metallic phosphates, catalysts residues,...) have been developed for various purposes corresponding to various functional properties of polymers and composites. Some of them have been evaluated as potential FRs owing to their characteristics

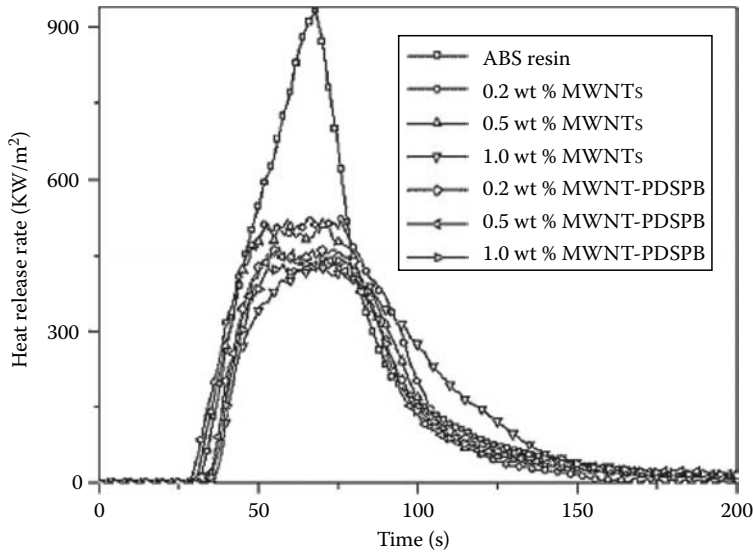


FIGURE 12.7 Heat release rate curves for ABS and its nanocomposites with different MWNTs and MWNT-PDSPB content. (From Ma, H. et al., *Adv. Funct. Mater.*, 18, 414, 2008. With permission.)

of size, aspect ratio, specific surface area, chemical nature, indicating possible reactivity with the polymer, its degradation products, or usual FRs.

Nano-hydroxides have been developed to combine the advantages of the usual hydroxides without their main drawback: The required high loadings. Moreover, owing to their size, an enhanced chemical reactivity of these hydrated minerals, able to form useful species for flame retardancy (e.g., aluminum phosphate) is expected. Thus, Huang et al.⁸⁵ have investigated the effect of the particle size on flame retardancy of MH filled EVA copolymer composites. Four kinds of MH with different particle size were selected (a nano-MH with particle size less than 100 nm and three micro-MH with D50 ranging between 2.33 and 3.89 μm) and incorporated by melt blending at loadings between 35 and 70 wt %. Nano-MH presented the better fire retardant results, evaluated using cone calorimeter and LOI measurements, but only for the 55 wt % loading. In addition, the evolution of fire retardancy was not linear as a function of size for the micro-MH. Globally, the coarser MH presented the better dispersion and led to better fire performance. It was concluded by the authors that good dispersion was the key factor to improve fire behavior.

Zhang et al.⁸⁶ have prepared EVA/nano-ATH composites by melt-blending. Two kinds of interfacial modifiers were used: A titanate coupling agent and a maleated EVA (MEVA). It was found that the combination of the two kind of interfacial modifiers led to a dramatic increase in FR behavior, evaluated using LOI measurements and UL-94 test. Without any interfacial modifier only a V-2 rating and a LOI value of 30.6 were obtained for a 60 wt % ATH loading. Using both modifiers (10 wt % MEVA and 60 wt % modified ATH), a V-0 rating was achieved as well as a LOI value of 39.1%. TEM observations showed a good dispersion of samples containing modified ATH or both modified ATH and MEVA. This confirmed the crucial role of nano-hydroxides dispersion on the fire performance of composites containing these materials.

An interesting route to promote good dispersion of nano-hydroxides in polymers consists in blending the nanofiller at elementary scale with an elastomer, before blending it with the host polymer. Gui et al.⁸⁷ have prepared a compound powder of cross-linked rubber/nano-MH by co-spray drying a fluid mixture of nano-MH slurry and irradiated rubber latex (Figure 12.8). The compound powder was incorporated in PA6 or EVA. It was found that the ternary nanocomposite composition of polymer/cross-linked rubber/nano-MH had better FR properties and thermal stability than the conventional one (prepared by melt blending of the components using an internal mixer

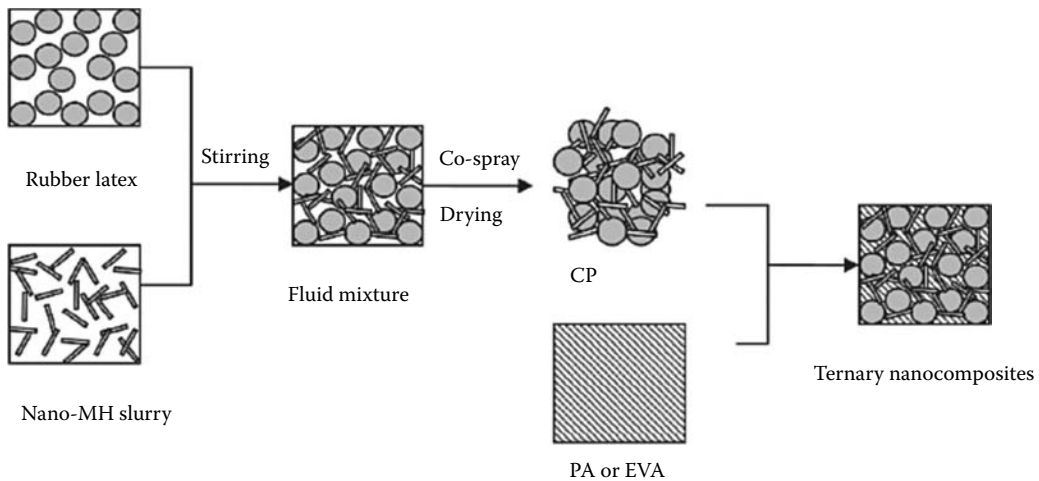


FIGURE 12.8 Schematic illustration for the preparation of polyamide 6/CPA and EVA/CPB nanocomposites: CPA, CNB-UFPR/nano-MH = 40/60, wt, CPB, NB-UFPR/nano-MH = 40/60, wt. (From Gui, H. et al., *Comp. Sci. Technol.*, 67, 974, 2007. With permission.)

at constant MH loading),⁸⁸ which has been ascribed to a better dispersion of nano-hydroxide. As noted in Section 12.2, the concomitant use of nano-MH and LDH by Zhang et al.⁷⁴ has led to strong synergistic effects on flame retardancy, and the introduction of nano-ATH seems able to control the clay morphology in EVA.

Combinations with red phosphorus were also investigated in EVA by Lv and Liu.⁸⁹ The nano-MH used (350 nm diameter, specific surface area of 42 m²/g) was synthesized in the presence of water-soluble polymer dispersants to prevent aggregation. It was noted that such treatment prevented aggregation in the polymer, leading to superior flame-retardant properties when compared with a micro-MH incorporated at the same loading (between 80 and 150 phr). It was postulated by the authors that nano-MH led to the formation of a more compact oxide layer than micro-MH. For a loading of 100 phr of nano-MH, a partial substitution by microencapsulated red phosphorus from 1 to 14 wt % has allowed a V-0 rating in the UL-94V test, and a strong increase in the LOI value, from 37% with pure MH to 60% with 5 wt % red phosphorus. The use of dynamic FTIR enabled the clarification of the mechanism of fire retardancy. First, MH decomposes endothermically with the release of water. Second, red phosphorus is oxidized to various phosphoric acid derivatives, which react with EVA to form very stable char structures containing P–O–P and P–O–C structures at higher temperatures. In addition, PO radicals were emitted to quench radicals in the gas phase.

The formation of a chemical compound containing both phosphorus and alumina was not proven. It appears that the synergy is due to the action of two successive mechanisms rather than an interaction between those mechanisms.

A similar kind of synergy was investigated by Cui et al.,⁹⁰ who prepared by melt blending nano-modified ATH using oxalic acid, a red phosphorus masterbatch and high impact polystyrene (HIPS). Unfortunately, the use of variable amounts of HIPS in the compositions has limited the possibility to see evidence of synergistic effects. The authors have stressed the well-developed and robust character of the char layer formed after UL-94V flame test for the composition HIPS/modified ATH/Red phosphorus (68/20/12). The use of FTIR confirmed also that both P–O–P and P–O–C groups were present in the char.

Besides trihydrated alumina, less hydrated structures, such as boehmite (monohydrate AlOOH), can be combined with FRs. Boehmite has a layered structure, like montmorillonite. Camino et al.⁹¹ have studied the incorporation of boehmite in EVA. It was concluded that boehmite improved the char forming properties but its fire retardant activity was less than that of ATH.

Pawlowski and Scharfel⁹² have added 1 or 5 wt % of boehmite to blends of PC/ABS with PTFE and RDP or bisphenol A bis(diphenylphosphate). The release of water from AlOOH influences the decomposition of the material by enhancing the hydrolysis of PC and RDP. Consequently, the condensed action of RDP or BDP is perturbed. The reaction of the arylphosphate with boehmite replaces both the formation of anhydrous alumina and alumina phosphate on the one hand, and the cross-linking of arylphosphate with PC on the other hand, since less phosphate is available to perform condensed-phase action. The reaction with arylphosphate therefore decreases the char formation, but the formation of aluminum phosphate could enhance barrier properties. On the whole, even high levels of fire retardancy can be achieved (V-0 ratings); the combination of boehmite with arylphosphates acting in the condensed phase seems very complex, particularly when the host polymer can undergo hydrolysis reactions due to water release.

12.3.2.2 Combinations with Nano-Oxides

Some other investigations have been carried out on combinations of oxide nanoparticles with FRs, mainly phosphorus FR, but also with organomodified layered silicates.

Silica nanoparticles are a promising component of FR systems because of their effect on viscosity in the molten state and the potential ability to react with many other chemical compounds, particularly during degradation stages of filled polymers.

In Section 12.2.2 combinations of silica with MH and OMMT in EVA have been reported. Fumed silica (SiO_2) with a specific surface area of $150 \text{ m}^2/\text{g}$ and an average particle size of 14 nm were combined by Fu and Qu⁹³ with MH in EVA by melt blending. The partial replacement of MH (at constant loading of 60 wt %) by a given amount of fumed silica increased the LOI value and maintained the V-0 rating in the UL-94 test. The presence of fumed silica not only greatly reduced HRR values and MLRs in the cone calorimeter, but also depressed the smoke released during the combustion of EVA/MH blends. The FR mechanism of fumed silica was ascribed by the authors to the physical process of fumed silica acting as enhanced char/silica layers in the condensed phase by accumulation of silica at the surface of the sample. It was proposed that these layers were able to limit heat and mass transfer.

Laachachi et al.⁹⁴ have combined oxide nanoparticles (Fe_2O_3 and TiO_2) and organoclays to improve thermal stability and fire retardancy of PMMA by melt blending. Cone calorimeter measurements showed that PHRR was lowered in the presence of oxide nanoparticles in comparison with pure PMMA and this decrease was higher when the filler content increased. Moreover, a synergistic effect was also found by the combination of TiO_2 and organoclays resulting mainly in an increase in the ignition time and the reinforcement of the barrier effect of organomodified clays. The promotion of charring due to OMMT together with TiO_2 was presented as the key elements to understand the reduced flammability of PMMA– TiO_2 –OMMT composites. The same authors have also successively investigated the combinations between metal oxide nanoparticles (Al_2O_3 and TiO_2), respectively, with APP (or APP + melamine phosphate additive) and then with phosphinate derivatives in PMMA.^{95,96}

Phosphorus-based additives and nanoparticles have been incorporated separately or combined at a 15 wt % global percentage in polymer. An APP-based additive containing melamine phosphate has led to an intumescent behavior during cone calorimeter tests.⁹⁵ APP with melamine phosphate and Al_2O_3 combination showed significant synergism on flame retardancy can be achieved (HRR values at $35 \text{ kW}/\text{m}^2$ and char yield), owing to the catalytic action of well-dispersed alumina nanoparticles, which modified the decomposition pathway of PMMA and the formation of a charred and ceramized structure. Aggregation processes in the case of TiO_2 seemed to limit the catalytic action of the surface and did not allow synergism for flame retardancy to be observed.

Similar synergistic effects leading to the reduction of PHRR and THR up to 30% (Figure 12.9) and to the increase of time to ignition were observed between nanometric alumina and phosphinate additives,⁹⁶ using the same protocol. It has been proposed that phosphinates acted principally in the condensed phase, and the presence of oxides played a reinforcement role in the carbonaceous layer promoted by the phosphinate additives.

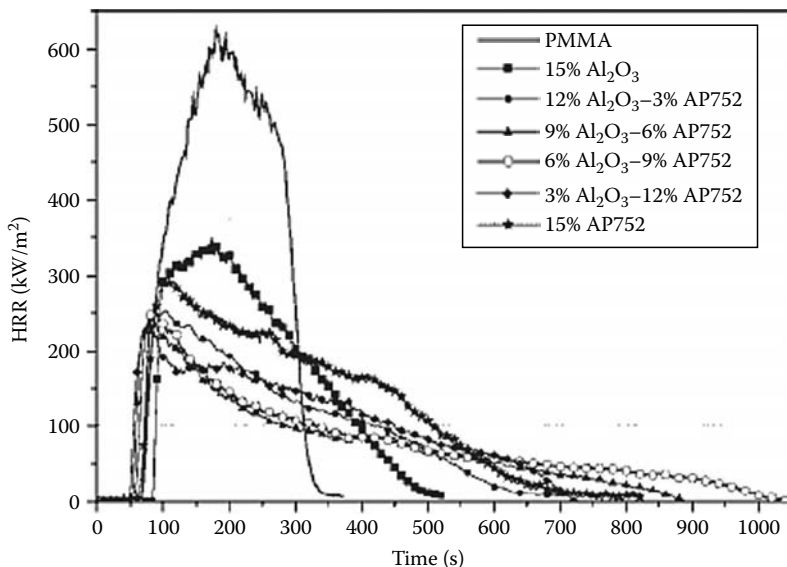


FIGURE 12.9 HRR curves of PMMA compositions with AP752 (APP-based additive containing melamine phosphate) and Al_2O_3 . (From Laachachi, A. et al., *Polym. Adv. Technol.*, 17, 327, 2006. With permission.)

Following the example of all kinds of nanoparticles mentioned above, oxide nanoparticles can also be functionalized to improve their contribution to flame retardancy of polymers. The grafting of oligomers on nanometric alumina particles has been carried out by Cinausero et al.⁹⁷ Nanoparticles were modified by phosphonic acid-based oligomers of aromatic polyester, polyether, or polydimethylsiloxane. Then, nanocomposites were prepared by melt-blending in a PMMA matrix at a loading of 5 wt %. The best results in terms of thermal stability and flammability were obtained with the bis-phosphonic polydimethylsiloxane-based formulation, when this is grafted at 12 wt % on alumina, a slight decrease in PHRR was noticed during the combustion. PyGC/MS experiments led to the conclusion that PDMS-covered nanoparticles played a role in the composition of the gaseous phase as well.

12.3.2.3 Other Combinations with Different Nanoparticles

Among the various other categories of nanoparticles synthesized by research groups or companies, some have been combined with different FR agents and the fire behavior of the host polymers has been evaluated.

Chigwada et al.³⁶ have combined polyhedral oligosilsesquioxanes (POSS), which are cage-like hybrid molecules of silicon and oxygen, with TCP (tricresylphosphate) in poly(vinyl ester) resins (PVE). POSS molecule contains nonreactive organic functionalities allowing solubility and compatibility of the POSS with various polymers. POSS was incorporated alone (3–10 wt %) in PVE, and four compositions were made with TCP at 4 wt % POSS + 4 wt % TCP and 5 wt % POSS + 5, 10, 15 wt % TCP. High reductions in PHRR and THR were noticed. Nevertheless, the POSS/TCP combination did not exhibit better performances than compositions with only 5 or 10 wt % of TCP alone.

Metallic phosphates nanoparticles have been identified as potential components of FR systems for PP. Hu and coworkers^{98,99} have used α -zirconium phosphate (α -ZrP) in combination with IFR based on APP and PER.

α -ZrP can act as an acid able to catalyze the dehydrogenation of polymers. Moreover, as a layered phosphate, it possesses rich intercalation chemistry, and can be organically modified by cationic surfactants. Hu et al.⁹⁸ have performed ion-exchange with hexadecyltrimethylammonium before

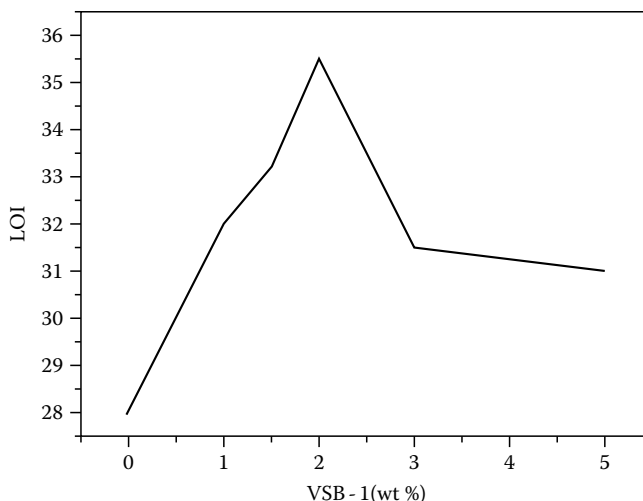


FIGURE 12.10 Effect of the content of VSB-1 on the LOI of PP/IFR/VSB-1 systems (PP/IFR/VSB-1/475/25-x/x; IFR:APP/petol/42/1, by weight). (From Nie, S. et al., *Polym. Adv. Technol.*, 19, 489, 2008. With permission.)

intercalation by PP using a compatibilizer such as MAPP. The IFR system was blended with modified α -ZrP named OZrP. TEM observations proved the intercalated structure of OZrP in a PP/2.5 wt % OZrP composition. At a constant loading of 25 wt % of IFR + OZrP with OZrP percentages ranging from 1 to 5 wt %, an increase in LOI values and char residue at 600°C was noticed in comparison with IFR alone. These synergistic effects are explained by the reaction of α -ZrP with APP to form a ceramic-like structure, which improves the efficiency of the intumescent char shield. In another paper,⁹⁹ the role of OZrP as char promoter was detailed, and its influence on the formation of graphitized carbon structures was highlighted.

The same research group has also investigated the use of nanoporous nickel phosphates (called VSB-1) as synergist with IFR systems in PP.¹⁰⁰ The same global amount of 25 wt % for IFR + Metallic phosphate was used. Synergistic effects on LOI values were noticed (Figure 12.10); moreover, the V-0 rating at UL-94 test obtained with IFR alone was maintained. A comparison was made between a composition of PP + 18%IFR + 2%VSB-1 and a composition differing by the use of OMMT instead of VSB-1. Only the composition with nickel phosphate achieved the V-0 rating.

Carbonization catalysts can also be used to char polymers containing nanoparticles, such as OMMT. Cai et al.¹⁰¹ have used FeCl_3 (1 wt %) as a catalyst in OMMT/ABS nanocomposite exhibiting an intercalated structure. Using TGA analysis, it was shown that intercalated nanocomposites had better thermal stability with high char residue, especially in the presence of FeCl_3 , owing to the char residue yield and catalytic graphitization effect.

12.4 CONCLUSION

The use of nanoparticles in combination with additional materials has been widely studied, with the aim to improve the fire retardancy of nanocomposites.

Since the majority of research carried out on flame retardancy of nanocomposite has dealt with OMLS, the most investigated combinations have concerned the corresponding class of nanocomposites of polymers, particularly EVA copolymer, PP, and polystyrene. The great interest taken in the development of IFR systems has also entailed the development of various and complex compositions in which OMLS have been associated with different intumescent systems containing APP and co-synergists able to promote the formation of a stable and expanded char layer reinforced by aluminophosphate species formed by reaction between APP and OMLS.

Owing to the multiple combinations involving interfacial compatibilizers and char promoter agents, including various polymers, this category of FR systems appears promising and yet able to meet industrial demand based on the association of excellent FR and mechanical properties. Moreover, the emergence of synthetic anionic clays, like LDHs, offers new possible combinations.

On the whole, the large group of phosphorus compounds can be combined successfully with OMLS, because of the possibility to combine the barrier properties of layered silicates, and to their reinforcement action on the charred residue promoted by the phosphorus additives. In addition, the formation of various aluminophosphate species and the specific action in the gaseous phase of some phosphorus FR can complicate the optimization of the FR performance and the interpretation of the synergistic effects observed.

For polymers that do not undergo hydrolysis during thermal degradation, the combination of OMLS with metallic hydroxides can lead to synergistic effects on flammability and can represent a solution to limit the excessive amount of fillers required to meet fire standards. In some cases, the concomitant use of surface-modified metallic hydroxides and OMLS had a positive effect on the formation of exfoliated or intercalated nanocomposite structures. In addition, the use of complementary additives, such as silica, and the possibility to enlarge the group of metallic hydroxides available, particularly owing to the development of nano-hydroxides, bring out new possibilities of interesting combinations.

Even if some of the different combinations between OMLS and above FRs were developed to propose alternatives to brominated FR systems, the association of OMLS with brominated compounds also has led to synergistic effects. Nevertheless, the progressive phase out of various halogenated FRs in numerous countries will limit the potential of such new compositions.

Because of their high effectiveness on thermal stability and fire reaction, CNTs have been also associated with FRs, mainly metallic hydroxides, as well as with OMLS.

Synergistic effects have been noticed and ascribed to the char reinforcing influence of CNTs. Moreover, CNTs could promote the formation of graphitized carbon structures allowing a better protective shielding for the remaining material.

The amount of char formed and its structure are key parameters accounting for the effectiveness of an FR system. The enhancement of the charring activity of IFR systems or OMLS can be enhanced by the use in combination of nanoparticles having a strong catalytic activity for carbonization processes. Some layered phosphates seem promising, since they can also promote the formation of graphitized structures.

Among combinations involving nanoparticles, the interest of nano-oxides with OMLS and phosphorus FR has been highlighted. Their high specific surface area could compensate for the absence of water release available in hydroxides, since their influence on thermal properties and viscosity of the host polymer tend to improve both thermal stability and fire reaction. Besides, their potential reactivity with phosphorus FR allows them to be included in FR systems, particularly for polymers undergoing hydrolysis reactions. Also, the absence of high amounts of organic modifiers at their surface can offer a stable catalytic potential for decomposition processes leading to char formation in combination with OMLS.

A constant challenge that remains is the design of FR systems allowing a maximum effectiveness on flammability with the minimum of additive or active agent in the polymer. The incorporation of nanoparticles able to generate synergistic effects in FR systems is key to this challenge, particularly when FR agents are attached to the nanoparticles. Numerous investigations mentioned in the different sections of this chapter prove that ion exchange of layered silicates with phosphorus- or bromine-based modifiers and functionalization of hydroxides or oxides using active FR compounds lead to interesting synergies at low loading. Thus, one can expect the development of more complex FR systems with new and original surface modifications of nanoparticles (possibly blended), associated with intumescent system including various polymers and interfacial agents. In consequence, one can predict that the control of all the processing operations of FR systems and polymers will be much more important in the future.

ACKNOWLEDGMENTS

F. Laoutid thanks “Région Wallonne” and the European Union (FEDER, FSE) for financial support in the frame of “Fonds structurels européens 2007-2013–FEDER Convergence” and “EU Seventh Framework Programme FP7.”

REFERENCES

1. E.P. Giannelis, Polymer layered nanocomposites, *Adv. Mater.*, 1996, 8:29–35.
2. J. Gilman, T. Kashiwagi, S. Lomakin, E. Giannelis, E. Manias, J. Lichtenhan, and P. Jones, in: *Fire Retardance of Polymers: The Use of Intumescence*, Royal Society of Chemistry, London, U.K., 1998, p. 203.
3. J. Gilman, T. Kashiwagi, and J. Lichtenhan, Nanocomposites: A revolutionary new flame retardant approach, *Sampe J.*, 1997, 33:40–46.
4. J.W. Gilman, C.L. Jackson, A.B. Morgan, R. Harris, E. Manias, E.P. Giannelis, M. Wuthenow, D. Hilton, and S.H. Phillips, Flammability properties of polymer-silicate nanocomposites: PP and PS nanocomposites, *Chem. Mater.*, 2000, 12:1866.
5. J.W. Gilman, Flame retardant mechanism of polymer-clay nanocomposites, in: *Flame Retardant Polymer Nanocomposites*, A. Morgan and C. Wilkie (Eds.), Wiley-Interscience, Hoboken, NJ, 2007, p. 67.
6. M. Zanetti, S. Lomakin, and G. Camino, Polymer layered silicate nanocomposites, *Macromol. Mater. Eng.*, 2000, 279:1–9.
7. G. Beyer, Flame retardancy of nanocomposites, *Polym. Polym. Compos.*, 2005, 13:529–538.
8. B.N. Jang, M. Costache, and C.A. Wilkie, The relationship between thermal degradation behaviour of polymer and the fire retardancy of polymer/clay composites, *Polymer*, 2005, 46:10678–10687.
9. T. Kashiwagi, F. Du, K.J. Winey, K.M. Groth, J.R. Shields, S.P. Bellayer, H. Kim, and J.F. Douglas, Flammability properties of polymer nanocomposites with singled-walled carbon nanotubes: Effects of nanotube dispersion and concentration, *Polymer*, 2005, 46:471–481.
10. M. Lewin, E.M. Pearce, K. Levon, A. Mey-Maroon, M. Zammarano, C.A. Wilkie, and B.N. Jang, Nanocomposites at elevated temperatures: Migration and structural changes, *Polym. Adv. Technol.*, 2006, 17:226–234.
11. M. Lewin, Reflections on migration of clay and structural changes in nanocomposites, *Polym. Adv. Technol.*, 2006, 17:758–763.
12. B. Schartel, M. Bartholmai, and U. Knoll, Some comments on the main fire retardancy mechanisms in polymer nanocomposites, *Polym. Adv. Technol.*, 2006, 17:772–777.
13. A. Laachachi, E. Leroy, M. Cochez, M. Ferriol, and J.M. Lopez-Cuesta, Use of oxide nano-particles and organoclays to improve thermal stability and fire retardancy of PMMA, *Polym. Degrad. Stabil.*, 2005, 89:344.
14. F. Bergaya, B.K.G. Theng, and G. Lagaly (Eds.), *Handbook of Clay Science*, Elsevier, Oxford, U.K., 2006.
15. R.A. Vaia, H. Ishii, and E.P. Giannelis, Synthesis and properties of 2-dimensional nanostructures by direct intercalation of polymer melts in layered silicates, *Chem. Mater.*, 1993, 5:1694–1696.
16. B. Swoboda, E. Leroy, J.-M. Lopez-Cuesta, C. Artigo, C. Petter, and C.H. Sampaio, Organomodified ultrafine kaolin for mechanical reinforcement and flame retardancy: An example with recycled PET, in: *Fire Retardancy of Polymers*, B. Kandola and R. Hull (Eds.), Royal Society of Chemistry, Cambridge, U.K., 2008.
17. E. Kandare, D. Hall, D.D. Jiang, and J.M. Hossenlopp, Development of new fire retardant additives based on hybrid inorganic-organic nanodimensional compounds: Thermal degradation of PMMA composites, in: *Fire and Polymers IV, Materials and Concepts for Hazard Prevention*, C.A. Wilkie and G.L. Nelson (Eds.), ACS Symposium Series, American Chemical Society, 922, 2005.
18. M. Le Bras, G. Camino, S. Bourbigot, and R. Delobel, *Fire Retardancy of Polymers, The Use of Intumescence*, The Royal Society of Chemistry, Cambridge, U.K., 1998.
19. S. Bourbigot and S. Duquesne, Intumescence and nanocomposites: A novel route for flame-retarding polymeric materials, in: *Flame Retardant Polymer Nanocomposites*, A.B. Morgan and C.A. Wilkie (Eds.), Wiley Interscience, Hoboken, NJ, 2007, pp. 131–162.
20. S. Bourbigot, M. Le Bras, F. Dabrowski, J.W. Gilman, and T. Kashiwagi, PA6 clay nanocomposite hybrid as char forming agent in intumescent formulations, *Fire Mater.*, 2000, 24:201–208.
21. M. Le Bras, S. Bourbigot, and B. Revel, Comprehensive study of the degradation of an intumescent EVA-based material during combustion, *J. Mater. Sci.*, 1999, 34:5777–5789.

22. Y. Tang, Y. Hu, Y.S. Wang, Z. Gui, Z. Chen, and W. Fan, Intumescent flame retardant-montmorillonite synergism in polypropylene-layered silicate nanocomposites, *Polym. Int.*, 2003, 52:1396–1400.
23. Y. Tang, Y. Hu, B. Li, L. Liu, Z. Wang, Z. Chen, and W. Fan, Polypropylene/montmorillonite nanocomposites and intumescent, flame retardant montmorillonite synergism in polypropylene nanocomposites, *J. Polym. Sci. A Polym. Chem.*, 2004, 42:6161–6173.
24. Y. Tang, Y. Hu, J. Xiao, J. Wang, L. Song, and W. Fan, PA6 and EVA alloy/clay nanocomposites as char forming agents in PP intumescent formulations, *Polym. Adv. Technol.*, 2005, 16:338–343.
25. Y. Hu, Y. Tang, and L. Song, Poly(propylene)/clay nanocomposites and their application in flame retardancy, *Polym. Adv. Technol.*, 2006, 17:235–245.
26. Y. Tang, Y. Hu, L. Song, R. Zong, Z. Gui, and W. Fan, Preparation and combustion properties of flame retarded polypropylene/polyamide-6 alloys, *Polym. Degrad. Stabil.*, 2006, 91:234–241.
27. Z.L. Ma, W.Y. Zhang, and X.Y. Liu, Using PA6 as a charring agent in intumescent polypropylene formulations based on carboxylated polypropylene compatibilizer and nano-montmorillonite synergistic agent, *J. Appl. Polym. Sci.*, 2006, 101:739–746.
28. G. Marosi, A. Marton, A. Szep, I. Czontos, S. Keszei, E. Zimonyi, A. Toth, X. Almeras, and M. Le Bras, Fire retardancy effect of migration in PP nanocomposites induced by modified interlayer, *Polym. Degrad. Stabil.*, 2003, 82:379–385.
29. S. Keszei, Sz. Matko, G. Bertalan, P. Anna, G. Marosi, and A. Toth, Progress in interface modifications: From compatibilization to adaptive and smart interphases, *Eur. Polym. J.*, 2005, 41:697–705.
30. S. Zhang, A.R. Horrocks, T.R. Hull, and B.K. Kandola, Flammability, degradation and structural characterization of fiber-forming polypropylene containing nanoclay-flame retardant combinations, *Polym. Degrad. Stabil.*, 2006, 91:719–725.
31. A.R. Horrocks, B.K. Kandola, G. Smart, S. Zhang, and R. Hull, Polypropylene fibers containing dispersed clays having improved fire performance. Part 1: Effect on nanoclays on processing parameters and fibres properties, *J. Appl. Polym. Sci.*, 2007, 106:1707–1717.
32. G. Smart, B.K. Kandola, A.R. Horrocks, S. Nazaré, and D. Marney, Polypropylene fibers containing dispersed clays having improved fire performance. Part 2: Characterization of fibers and fabrics from PP-nanoclay blends, *Polym. Adv. Technol.*, 2008, 19:658–670.
33. A.R. Horrocks, B.K. Kandola, P.J. Davies, S. Zhang, and S.A. Padbury, Developments in flame retardant textiles: A review, *Polym. Degrad. Stabil.*, 2005, 88:3–12.
34. S.A. Padbury, A.R. Horrocks, and B. K. Kandola, in *Proceedings of the 14th BCC Conference on Flame Retardancy*, M. Lewin (Ed.), Business Communications Co Editions, Norwalk, CT, 2003.
35. Z. Wang and T.J. Pinnavaia, Hybrid organic-inorganic nanocomposites: Exfoliation of magadiite monolayers in an elastomeric epoxy polymer, *Chem. Mater.*, 1998, 10:1820–1826.
36. G. Chigwada, P. Jash, D.D. Jiang, and C.A. Wilkie, Fire retardancy of vinyl ester nanocomposites: Synergy with phosphorus-based fire retardants, *Polym. Degrad. Stabil.*, 2005, 89:85–100.
37. S. Nazaré, B.K. Kandola, and A.R. Horrocks, Flame-retardant unsaturated polyester resin incorporating nanoclays, *Polym. Adv. Technol.*, 2006, 17:294–303.
38. R.K. Bharadwaj, A.R. Mehrabi, C. Hamilton, C. Trujillo, M. Murgs, R. Fan, A. Chavira, and A.K. Thomson, Structure-properties relationships in crosslinked polyester-clay nanocomposites, *Polymer*, 2002, 43:3699–3705.
39. L. Song, Y. Hu, Y. Tang, R. Zhang, Z.Y. Chen, and W. Fan, Studies on the flame retardant polyurethane/organoclay nanocomposite, *Polym. Degrad. Stabil.*, 2005, 87:111–116.
40. Z. Wang, E. Han, and W. Ke, Influence of nano-LDHs on char formation and fire-resistant properties of flame-retardant coating, *Prog. Org. Coat.*, 2005, 53:29–37.
41. Z. Wang, E. Han, and W. Ke, Effect of nanoparticles on the improvement in fire-resistant and anti-ageing properties of flame-retardant coating, *Surf. Coat. Technol.*, 2006, 200:5706–5716.
42. C.X. Zhao, Y. Liu, D.Y. Wang, D.L. Wang, and Y.Z. Wang, Synergistic effect of ammonium polyphosphate and layered double hydroxide on flame retardant properties of poly(vinyl alcohol), *Polym. Degrad. Stabil.*, 2008, 93:1323–1331.
43. C. Nyambo, E. Kandare, D. Wang, and C.A. Wilkie, Flame retarded polystyrene: Investigating chemical interactions between ammonium polyphosphate and MgAl double hydroxide, *Polym. Degrad. Stabil.*, 2008, 93:1656–1663.
44. F. Laoutid, L. Ferry, J.-M. Lopez Cuesta, and A. Crespy, Red phosphorus aluminium oxide compositions as flame retardant in recycled PET, *Polym. Degrad. Stabil.*, 2003, 82:357–363.
45. C. Jiao, Z. Wang, X. Chen, B. Yu, and Y. Hu, Irradiation crosslinking and halogen-free flame retardation of EVA using hydrotalcite and red phosphorus, *Radiat. Phys. Chem.*, 2006, 75:557–563.

46. L. Du, B. Qu, and Z. Xu, Flammability characteristics and synergistic effect of hydrotalcite with microencapsulated red phosphorus in halogen-free flame retardant EVA composite, *Polym. Degrad. Stabil.*, 2006, 91:995–1001.
47. L. Song, Y. Hu, Z. Lin, S. Xuan, S. Wang, Z. Chen, and W. Fan, Preparation and properties of halogen-free flame-retarded polyamide 6/organoclay nanocomposite, *Polym. Degrad. Stabil.*, 2004, 86:535–540.
48. S. Padbury, B.K. Kandola, and A.R. Horrocks, The effect of phosphorus-containing flame retardants and nanoclay on the burning behaviour of PA 6 and PA 6.6, *Proceedings of the 14th BCC Conference on Flame Retardancy*, M. Lewin (Ed.), Business Communications Co Editions, Norwalk, CT, 2003.
49. G. Chigwada and C.A. Wilkie, Synergy between conventional phosphorus fire retardants and organically-modified clays can lead to fire retardancy of styrenics, *Polym. Degrad. Stabil.*, 2003, 80:551–557.
50. E. Kandaré, G. Chigwada, D. Wang, C.A. Wilkie, and J.M. Hossenlopp, Probing synergism, antagonism, and additive effects in poly(vinyl ester)(PVE) composites with fire retardants, *Polym. Degrad. Stabil.*, 2006, 91:1209–1218.
51. E. Kandaré and J.M. Hossenlopp, Nanocomposite-containing additive combinations, *Proceedings of the 17th BCC Conference on Flame Retardancy*, M. Lewin (Ed.), Business Communications Co Editions, Norwalk, CT, 2006.
52. S. Levchik, A.I. Balabanovitch, G.F. Levchik, and L. Costa, Effect of melamine and its salts on combustion and thermal decomposition of polyamide 6, *Fire Mater.*, 1997, 21:75–83.
53. Y. Hu, S.F. Wang, Z.H. Lin, Y.L. Zhuang, Z.Y. Chen, and W.C. Fan, Preparation and combustion properties of flame retardant nylon 6/montmorillonite nanocomposite, *Macromol. Mater. Eng.*, 2003, 288:272–276.
54. J. Zhang, M. Lewin, E. Pearce, M. Zammarano, and J.W. Gilman, Flame retarding PA6 with melamine cyanurate and layered silicates, *Proceedings of the 19th BCC Conference on Flame Retardancy*, M. Lewin (Ed.), Business Communications Co Editions, Norwalk, CT, 2008.
55. X. Zheng and C.A. Wilkie, Synergy between nanocomposites formation and low levels of bromine and fire retardancy in polystyrene, *Polym. Degrad. Stabil.*, 2003, 81:539–550.
56. C.A. Wilkie, G. Chigwada, and X. Zheng, Recent advances in fire retardancy based on nanocomposites, *Proceedings of the 14th BCC Conference on Flame Retardancy*, M. Lewin (Ed.), Business Communications Co Editions, Norwalk, CT, 2003.
57. L. Ye and B. Qu, Flammability characteristics and flame retardant mechanism of phosphate-intercalated hydrotalcite in halogen-free flame retardant EVA blends, *Polym. Degrad. Stabil.*, 2008, 93:918–924.
58. J. Kim, K. Lee, J. Bae, J. Yang, and S. Hong, Studies on the thermal stabilization enhancement of ABS: Synergistic effect of triphenylphosphate nanocomposite, epoxy resin and silane coupling agent mixtures, *Polym. Degrad. Stabil.*, 2003, 79:201–207.
59. B. Schartel, U. Knoll, A. Hartwig, and D. Pütz, Phosphonium-modified layered silicate epoxy resins nanocomposites and their combinations with ATH and organo-phosphorus fire retardants, *Polym. Adv. Technol.*, 2006, 17:281–293.
60. B. Swoboda, E. Leroy, L. Ferry, N. Kerboua, and J.M. Lopez-Cuesta, Fire properties of alloys and composites based on recycled polyethylene terephthalate, *Proceedings of the 19th BCC Conference on Flame Retardancy*, M. Lewin (Ed.), Business Communications Co Editions, Norwalk, CT, 2008.
61. B. Swoboda, E. Leroy, F. Laoutid, and J.M. Lopez-Cuesta, Flame retardant PET/PC blends compatibilized by organomodified montmorillonites, *Proceedings of the ACS Conference*, New Orleans, LA, 2008.
62. X. Ge, D. Wang, C. Wang, M. Qu, J. Wang, C. Zhao, X. Jing, and Y. Wang, A novel phosphorus-containing copolyester/montmorillonite nanocomposites with improved flame retardancy, *Eur. Polym. J.*, 2007, 43:2882–2890.
63. L. Clerc, L. Ferry, E. Leroy, and J.M. Lopez-Cuesta, Influence of talc physical properties on the fire retarding behaviour of EVA copolymer/magnesium hydroxide/talc composites, *Polym. Degrad. Stabil.*, 2005, 91:2140–2145.
64. L. Ferry, P. Gaudon, E. Leroy, and J.M. Lopez-Cuesta, Intumescence in EVA copolymer filled with magnesium hydroxide and organoclays, in: *Fire Retardancy of Polymers*, Royal Society of Chemistry, London, U.K., 2005, pp. 302–312.
65. J. Zhang and C.A. Wilkie, Fire retardancy of polyethylene-alumina trihydrate containing clay as a synergist, *Polym. Adv. Technol.*, 2005, 16:549–553.
66. N. Ristolainen, U. Hippi, J. Seppala, A. Nikanen, and J. Ruokolainen, Properties of polypropylene/aluminium trihydroxide composites containing nanosized organoclay, *Polym. Eng. Sci.*, 2005, 45:1568–1575.
67. G. Beyer, Flame retardant properties of EVA-nanocomposites and improvement by combination of nanofillers with alumina trihydrate, *Fire Mater.*, 2001, 25:193–197.

68. M. Wladyka-Przybylak and H. Rydarowski, Flammability and mechanical properties of PP modified by nanoclay compounds and aluminium hydroxide flame retardant, in *Proceedings of the 19th BCC Conference on Flame Retardancy*, M. Lewin (Ed.), Business Communications Co Editions, Norwalk, CT, 2008.
69. R. Kozlowski, M. Wladyka-Przybylak, and H. Rydarowski, Flammability of polypropylene/clay nanocomposites-synergism with some flame retardants, *Proceedings of the 17th BCC Conference on Flame Retardancy*, M. Lewin (Ed.), Business Communications Co Editions, Norwalk, CT, 2006.
70. F. Laoutid, L. Ferry, E. Leroy, and J.M. Lopez-Cuesta, Intumescent mineral fire retardant systems in EVA copolymer: Effect of silica particles on char cohesion, *Polym. Degrad. Stabil.*, 2006, 91:2140–2145.
71. B.B. Marosfoi, S. Garas, B. Bodzay, F. Zubonyai, and G. Marosi, Flame retardancy study on magnesium hydroxide associated with clays of different morphology in polypropylene matrix, *Polym. Adv. Technol.*, 2008, 19:693–700.
72. F. Laoutid, P. Gaudon, J.M. Taulemesse, J.M. Lopez-Cuesta, J.I. Velasco, and A. Piechaczyk, Study of hydromagnesite and magnesium hydroxide based fire retardant systems for EVA containing organo-modified montmorillonite, *Polym. Degrad. Stabil.*, 2006, 91:3074–3082.
73. L. Haurie, A.I. Fernandez, J.I. Velasco, J.M. Chimenos, J.M. Lopez-Cuesta, and F. Espiell, Thermal stability and flame retardancy of LDPE/EVA blends filled with synthetic hydromagnesite/aluminium hydroxide/aluminium hydroxide/ montmorillonite mixtures, *Polym. Degrad. Stabil.*, 2007, 92:1082–1087.
74. G. Zhang, P. Ding, M. Zhang, and B. Qu, Synergistic effects of layered double hydroxide with hyper-fine magnesium hydroxide in halogen-free flame retardant EVA/HFMH/LDH nanocomposites, *Polym. Degrad. Stabil.*, 2007, 92:1715–1720.
75. L. Ye, P. Ding, M. Zhang, and B. Qu, Synergistic effects of exfoliated LDH with some halogen-free flame retardants in LDPE/EVA/HFMH/LDH nanocomposites, *J. Appl. Polym. Sci.*, 2007, 107:3694–3701.
76. S. Levchik and E. Weil, Combustion and fire retardancy of aliphatic nylons, *Polym. Int.*, 2000, 49:1033–1073.
77. G. Chigwada, P. Jash, D.D. Jiang, and C.A. Wilkie, Synergy between nanocomposites formation and low levels of bromine on fire retardancy in polystyrenes, *Polym. Degrad. Stabil.*, 2005, 88:382–393.
78. D. Wang, K. Echols, and C.A. Wilkie, Cone calorimetric and thermogravimetric analysis evaluation of halogen-containing polymer nanocomposites, *Fire Mater.*, 2005, 29:283–294.
79. S. Peeterbroeck, F. Laoutid, B. Swoboda, J.-M. Lopez-Cuesta, N. Moreau, J.B. Nagy, M. Alexandre, and Ph. Dubois, How carbon nanotube crushing can improve flame retardant behavior in polymer nanocomposites, *Macromol. Rapid. Commun.*, 2007, 28:260–271.
80. G. Beyer, Flame retardancy of nanocomposites based on organoclays and carbon nanotubes with aluminium trihydrate, *Polym. Adv. Technol.*, 2005, 17:218–225.
81. G. Beyer, Filler blend of carbon nanotubes and organoclays with improved char as a new flame retardant system for polymers and cable application, *Fire Mater.*, 2005, 29:61–69.
82. G. Beyer, Progress on nanostructured flame retardants, *Proceedings of the 14th BCC Conference on Flame Retardancy*, M. Lewin (Ed.), Business Communications Co Editions, Norwalk, CT, 2003.
83. F. Gao, G. Beyer, and Q. Huan, A mechanistic study of fire retardancy of carbon nanotube/EVA copolymers and their clay composites, *Polym. Degrad. Stabil.*, 2005, 89:559–564.
84. H. Ma, L. Tong, Z. Xu, and Z. Fang, Functionalizing carbon nanotubes by grafting on intumescent flame retardant: Nano-composite synthesis, morphology, rheology, and flammability, *Adv. Funct. Mater.*, 2008, 18:414–421.
85. H. Huang, M. Tian, L. Liu, W. Liang, and L. Zhang, Effect of particle size on flame retardancy of magnesium hydroxide filled EVA copolymer composites, *J. Appl. Polym. Sci.*, 2006, 100:4461–4469.
86. X. Zhang, F. Guo, J. Chen, G. Wang, and H. Liu, Investigation of interfacial modification for flame retardant EVA copolymer/alumina trihydrate nano-composites, *Polym. Degrad. Stabil.*, 2005, 87:411–418.
87. H. Gui, X. Zhang, Y. Liu, W. Dong, Q. Wang, J. Gao, Z. Song, J. Lai, and J. Qiao, Effect of dispersion of nano-magnesium hydroxide on the flammability of flame retardant ternary composites, *Comp. Sci. Technol.*, 2007, 67:974–980.
88. H. Gui, X. Zhang, W. Dong, Q. Wang, J. Gao, Z. Song, J. Lai, Y. Liu, F. Huang, and J. Qiao, Flame retardant synergism of rubber and magnesium hydroxide in EVA composites, *Polymer*, 2007, 48:2537–2541.
89. J.P. Lv and W.H. Liu, Flame retardancy and mechanical properties of EVA nanocomposites based on magnesium hydroxide nano-particles/microcapsulated red phosphorus, *J. Appl. Polym. Sci.*, 2007, 105:333–340.
90. W. Cui, F. Guo, and J. Chen, Preparation of flame retardant high impact polystyrene, *Fire Safety J.*, 2005, 42:232–239.

91. G. Camino, A. Maffezzoli, M. Braglia, M. de Lazzaro, and M. Zammarano, Effects of hydroxides and hydroxycarbonate structure on fire retardant effectiveness and mechanical properties in EVA copolymer, *Polym. Degrad. Stabil.*, 2001, 74:457–474.
92. K.H. Pawlowski and B. Scharfel, Flame retardancy mechanisms of aryl phosphates in combination with boehmite in bisphenol A polycarbonate/acrylonitrile butadiene styrene blends, *Polym. Degrad. Stabil.*, 2008, 93:657–667.
93. M.Fu and B.Qu, Synergistic flame retardant mechanism of fumed silica in EVA/magnesium hydroxide blends, *Polym. Degrad. Stabil.*, 2004, 85:633–639.
94. A. Laachachi, E. Leroy, M. Cochez, M. Ferriol, and J.M. Lopez-Cuesta, Use of nano-particles and organoclays to improve thermal stability and fire retardancy of PMMA, *Polym. Degrad. Stabil.*, 2005, 89:344–352.
95. A. Laachachi, M. Cochez, E. Leroy, P. Gaudon, M. Ferriol, and J.M. Lopez-Cuesta, Effect of Al_2O_3 and TiO_2 nano-particles and APP on thermal stability and flame retardance of PMMA, *Polym. Adv. Technol.*, 2006, 17:327–334.
96. A. Laachachi, M. Cochez, E. Leroy, M. Ferriol, and J.M. Lopez Cuesta, Fire retardant systems in PMMA: Interactions between metal oxide nanoparticules and phosphinates, *Polym. Degrad. Stabil.*, 2007, 92:61–69.
97. N. Cinausero, N. Azema, M. Cochez, M. Ferriol, M. Essahli, F. Ganachaud, and J.-M. Lopez-Cuesta, Influence of the surface modification of alumina nano-particles on the thermal stability and fire reaction of PMMA composites, *Polym. Adv. Technol.*, 2008, 19:1–9.
98. Y. Hu, D. Yang, L. Song, and Y. Tang, Synthesis and combustion property of PP/IFR/ZrP nanocomposites, *Proceedings of the 18th BCC Conference on Flame Retardancy*, M. Lewin (Ed.), Business Communications Co Editions, Norwalk, CT, 2007.
99. Y. Hu, D. Yang, and L. Song, Carbonization and graphitization of polymer/alpha-zirconium phosphate nanocomposites, *Proceedings of the 19th BCC Conference on Flame Retardancy*, M. Lewin (Ed.), Business Communications Co Editions, Norwalk, CT, 2008.
100. S. Nie, Y. Hu, L. Song, S. He, and D. Yang, Study on a novel and efficient flame retardant synergist nanoporous nickel phosphate VSB-1 with intumescent flame retardants in polypropylene, *Polym. Adv. Technol.*, 2008, 19:489–495.
101. Y. Cai, Y. Hu, L. Song, S. Xuan, Y. Zhang, Z. Chen, and W. Fan, Catalyzing carbonization function of ferric chloride based on ABS copolymer/organophilic montmorillonite nanocomposites, *Polym. Degrad. Stabil.*, 2007, 92:490–496.

13 Design of Interlayers for Fire-Retarded Polymeric Systems

*György Marosi, Botond B. Marosfői,
Brigitta Bodzay, Tamás Igricz, and György Bertalan*

CONTENTS

13.1	Introduction.....	329
13.2	Compatibilizer Interlayer	331
13.3	Metallic Activator Interlayer	336
13.4	Polymer Interlayer of Fire-Retardant Activity	340
13.5	Reinforced-Char-Forming Ceramizer Interlayer	343
13.6	Conclusions.....	345
	Acknowledgments.....	345
	References.....	345

13.1 INTRODUCTION

Surface-interface phenomena play an essential role in the area of material science, including ceramics, multicomponent polymer systems, metal-coating, biomaterials, heterogeneous catalysis, and (nano-) tribology. Spontaneous interactions lead to the formation of uncontrolled interlayers, while their design allows governing the response of the materials to external impact. The basic rules governing the phenomena and determining the design of interlayers in different materials are more or less the same. However, either physical or chemical processes are involved in the interfacial interactions, but the complex physical chemical background is not entirely elucidated. Fire retardancy (FR) is a unique area in which both the physical and the chemical interactions are essential. On this basis, even more complex interfacial structure can be anticipated than in other areas.

Considering the role of interlayers, two basic types can be distinguished:

1. *Separating interlayer*, which is in fact an independent phase, promotes the segregation of individual phases.
2. *Integrating interlayer* establishes a more or less continuous transition between the adjacent phases and connects them.

The spontaneous formation of interlayers rarely results in an optimal and advantageous structure. The conscious selection of additives and technologies are needed for preventing the development of undesired interfacial structures. Optimizations of integrating interlayers are common tasks when multicomponent polymer systems are designed. A general rule for integrating interlayers of disperse systems is defined in the *Ostwald–Buzágh continuity principle* [1]. According to this principle, the inclusions in an optimal disperse system are embedded continuously into the surrounding matrix owing to their adsorbed interlayer. At an optimal interlayer the transition between the different

phases should be harmonic instead of a sharp change. This principle was utilized when a hierarchic multilayer interfacial structure was proposed for polymer composites based on an early patent [2]. The method developed for thermoplastic polymer systems forms multilayer interfacial structure around inclusions by means of surfactants and elastomers [3–6].

In the field of flame retardancy only a few papers paid attention to the interfaces until the appearance of nanocomposites [7,8]. *Nanocomposite* technologies adapted the use of both the surfactants and the multilayer interfacial structures (introducing maleic anhydride grafted macromolecular interlayer) [9,10]. A simplification is, however, characteristic to most of the works dealing with nanostructured FR polymers: the importance of dispersion is considered, neglecting the other special interfacial requirements of FR.

These requirements include

- Compatibilization of adjacent phases
- Control of the rheology up to high temperature
- Enhancement of the mechanical and thermal stability
- Activation of the charring process
- Insulation of the components for avoiding their uncontrolled chemical interaction
- Promotion of the regulated delivery of components being suitable for
- Partial ceramization.

The design of interlayers must consider the relevant thermodynamic and kinetic factors. Thermodynamic features, establishing the intensity of the driving force, represent the “necessary” conditions for interphase formation; kinetic factors (diffusion, nucleation, and reaction of the components) determining the time scale (relative to processing times) required to achieve certain

TABLE 13.1
Opportunities for Influencing the Fire-Induced Degradation through the Interfaces

Stages	Effect on the Behavior	Structural Changes	Possible Role of Designed Interlayer
0 stage	Preceding process influencing the stability	Improvement of the dispersion not just for good mechanical properties but also for better availability of FRs	Physical and chemical compatibilization, enhancement of the mechanical stability
1 stage	Competitive process influencing the ignition time	Formation of protecting surface layer before or after ignition being in competition with the heat-induced decomposition of the polymer chains and oxidation of the formed fragments by radical process	Activation of the charring process, hindrance of uncontrolled chemical interactions at the interface, targeted delivery of components
2 stage	Evolution of the char foam influencing steady-state phase of the heat release	Stabilization of the thickness; pore size; heat and gas barrier performance of the protecting surface layer, hindrance of the dipping of the melt phase	Interconnection of expanded interlayers, control the bubble formation in the char, control of the rheology up to high temperature
3 stage	Breakdown of the surface protection influencing second raise of heat release	Re-acceleration of the degradation process due to heat-induced decomposition of the protecting layer and its compliance to the gas and melt pressure	Reinforcement of the char through partial ceramization, enhancement of the thermal stability

interphase structures represent the “sufficient” conditions for interphase formation. The free energies at the boundary of contacting phases can be lower or higher than the surface energy of the individual phases. The first case means a thermodynamic driving force for the formation of stable interlayer, while in the second case, the thermodynamic incompatibility must be overcome by the energy of mixing of the homogenization process. Thermodynamic incompatibility causes segregation if kinetic control does not hinder the disintegration.

Temperature function represents a special feature for interlayers in fire-retarded systems, which distinguishes their design from any other similar task. In order to design interlayers matched to the demands of the extreme circumstances of fire action their possible roles at each stages of the combustion process has to be taken into account.

Interface-related stages influencing the fire-induced degradation are summarized in Table 13.1

This chapter provides an overview of the interface-related features of flame retardancy considering the described stages of the combustion and proposes FR-active interfacial structures. The challenge is to find advantageous interface/surface design suitable for improving the behavior of various multicomponent FR systems at each stage of the degradation process.

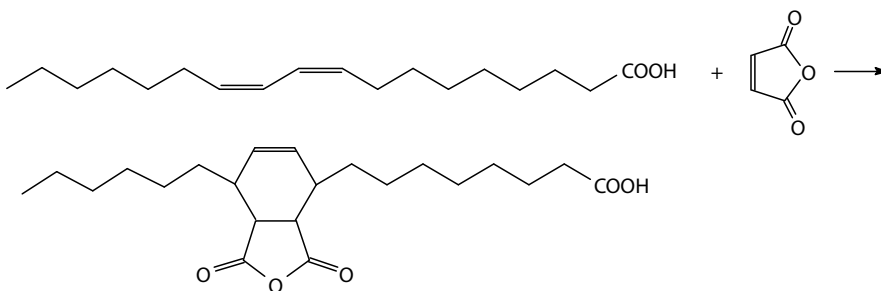
13.2 COMPATIBILIZER INTERLAYER

Compatibilizer interlayers (CIL) are used for improving the *dispersion*, *rheology*, and *mechanical properties* of composites. All of these characteristics are relevant primarily for fire-retardant systems. *Dispersion* influences the FR efficiency because the flame-retardant additives, similarly to any other stabilizer, have to be present at all sites where degradation may occur. In order to meet this requirement the distribution should approach the molecular level. Considering certain dimensions of nanofillers, which are of similar magnitude to the radius of gyration for the matrix polymer, this aim is attainable. On the other hand, fire-induced accumulation of FR-active constituents at the surface is also advantageous. *Rheology* determines the dripping (and consequently the flame spreading) as well as the delivery of flammable molecules to the surface of burning materials (and consequently the re-acceleration of the combustion process). *Mechanical properties* determine the dimensional stability (and consequently the vertical or horizontal spreading of the flame) during the combustion process. These properties depend on the quality of contact at the interfacial area. The total interfacial area is especially large for systems containing metal hydroxides in high concentration; these materials are extremely sensitive to the structure of interfacial layer and local stress distribution.

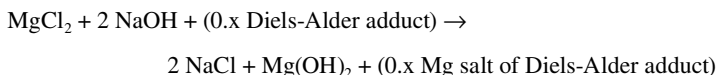
In this chapter, examples are given showing the role of CIL in FR polymer systems.

CIL was applied in fire-retarded systems at first when the interface around *metal hydroxides* had to be improved because at the needed high loadings these fillers cause marked deterioration of the mechanical properties. The decrease of the particle size below 1 μm is favorable from the FR point of view but deteriorates the rheological properties. A surfactant layer facilitates the processability, but at the expense of the flame retardancy. Coupling to the polymer phase by means of coupling agents (vinyltriethoxysilane or maleic anhydride) has been proposed recently for PP/aluminum hydroxide composites [11]. A good compromise could be achieved by using *reactive surfactants* that combine the coupling and surfactant functions [12]. These reduce the viscosity (similarly to common surfactants) at low temperature but increase it again, owing to coupling reaction at both (polymer and inclusion) sites, when the temperature is raised. Reduced dripping and improved balance between processability and FR was reported for such systems [13]. A reactive surfactant was used for achieving coupling at the interfaces also in intumescent FR polypropylene system reinforced with natural fibers [14].

A *Diels–Alder adduct*, an example of reactive surfactants, has been synthesized from linoleic acid and maleic anhydride, according to Scheme 13.1, and used for preparing *nanosized* $\text{Mg}(\text{OH})_2$ (MH) [12].



SCHEME 13.1



SCHEME 13.2

The hydrophobic nano-MH was produced by the co-precipitation method [15] as described in Scheme 13.2 and a TEM image of the nanoparticle is shown in Figure 13.1.

The interaction of MH nanoparticles with the PP matrix across their enhanced surface area resulted already at low loading level (2.5%) in T_g (determined by thermally stimulated current [TSC] method) shifting from -12°C to 8°C and heat release rate reduced as shown in Figure 13.2. For achieving V-0 rating (according to UL-94) inclusion of 50% nano-MH was needed in PP, while the reference system required 65% loading of commercial micro-MH.

The *anionic surfactant* CIL-coated commercially available *hydrotalcite* is similar to nano-MH but, owing to its platelet form, further advantages can be realized [16].

CIL is unavoidable when nanodispersion of any other nanofiller, such as *clay or carbon nanotube* (CNT) is considered [17,18]. Various types of *cationic surfactants* in the case of montmorillonite (MMT) and *reactive interface modifications* in the case of CNT have been introduced to ensure

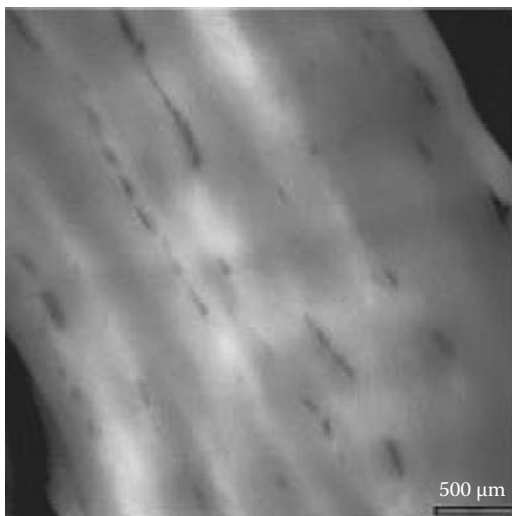


FIGURE 13.1 TEM micrograph of MH nanoparticles.

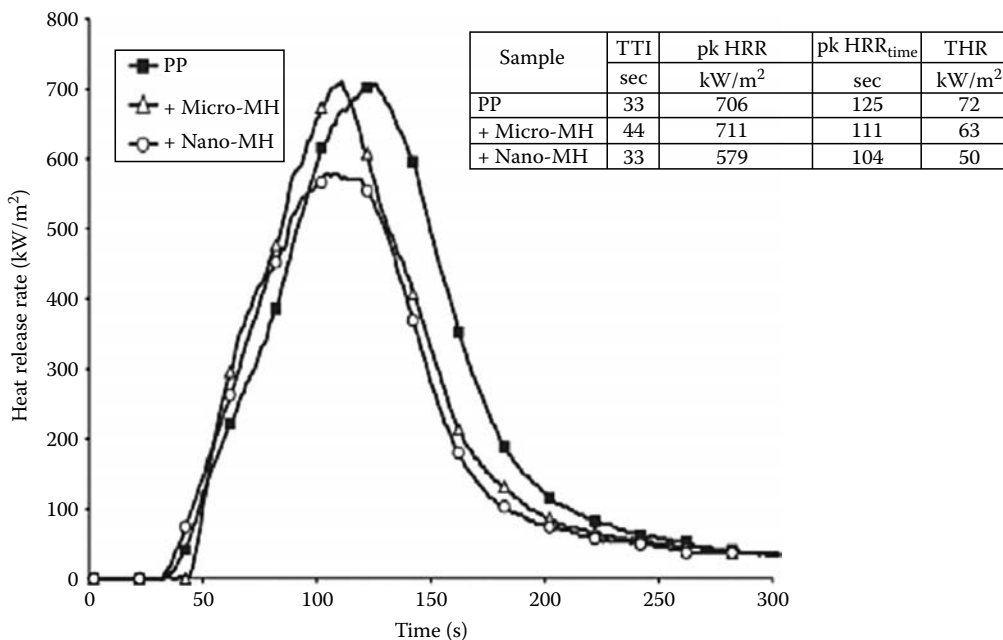


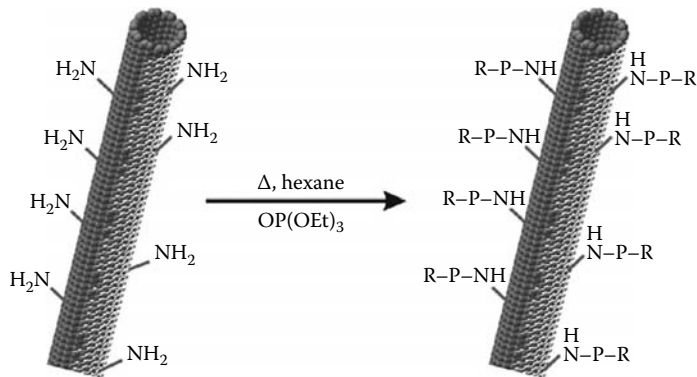
FIGURE 13.2 Heat release rate (HRR) and total heat release (THR) results at low metal hydroxide loading (2.5%); the PP systems containing nano-MH (prepared by coprecipitation method) is compared to PP and reference system containing micro-MH (heat flux: 50 kW/m², samples thickness: 4 mm).

dispersibility at the nanoscale [19]. In blends of incompatible polymers, the dispersed nanoparticles may act as a compatibilizing interlayer [20]. This action at the solid–gas interface decreases the pore size in char layers improving their barrier function [21]. Interfacial traction is a concern especially for CNT, the surface of which is essentially an inert graphene sheet; the defects or the chemical functionalization of the surface are required for coupling to the polymer matrix with covalent bonds.

The selection of optimal CIL is a much more complex task when FR is concerned than just for improving the distribution. The limited *thermal stability of the interface modifier* may cause decomposition either during processing or at an early stage of heat treatment delivering flammable fragments into the gas phase and inducing further decomposition in the solid phase [22]. The use of a thermally more stable interlayer has been proposed as a possible solution [23]. On the other hand, the decomposition of the compatibilizing interlayer at higher temperature (just before combustion) may promote the *migration of nanofillers to the surface*, the importance and background of which have been discussed in details by Lewin [24,25]. Not only the thermodynamics but also the kinetics of migration is of great importance because the competitive processes of degradation are controlled kinetically.

The degradation products of interlayers can be adjusted to the purposes of FR by including FR-active elements such as phosphorus (P) into the surface modifier molecule [26]. The reactive formation of such interlayer around CNT has been performed by a transamidation reaction, shown in Scheme 13.3.

By including *CNT with a P-modified surface* into a phosphorylated epoxy (PEP) resin, a limiting oxygen index (LOI) level of 40 could be achieved compared to 21 for the reference resin. However, the P content built-in coupled to CNT was limited by the reactive groups available on the surface of a functionalized CNT, which alone (without additional P containing species) is not enough for achieving significant improvement of FR.



SCHEME 13.3

CIL has influence on fire-retardant systems through viscosity as well. Nonmodified montmorillonite (NMM) and organophilic montmorillonite (OMM) have been introduced into ethylene vinyl-acetate (EVA) copolymer (clay content was 10%) and compared in AR 2000 type rheometer. (Measurements were performed at 210°C and 0.5% amplitude. The applied frequency range was $\omega = 1\text{--}600$ 1/s.)

Figure 13.3 gives the log complex viscosity values of EVA, EVA–NMM, and EVA–OMM compounds versus log ω (angular) frequency. The pristine EVA shows, due to lack of matrix reinforcement, lower viscosity than the composites. The nonlinear decrease of the viscosity of EVA against increasing shear rate is characteristic for pseudo-plastic materials.

The addition of non-OMM increases the viscosity, but the resulting curve (EVA–NMM) is nearly parallel to the curve of EVA. This shape of viscosity curve is characteristic for compounds with low grade fillers.

The addition of OMM increases the steepness of the curve owing to the higher viscosity of exfoliated microgel type network structure [13] at low shear rates and its orientation that enhances the decrease of viscosity with increasing shear rate.

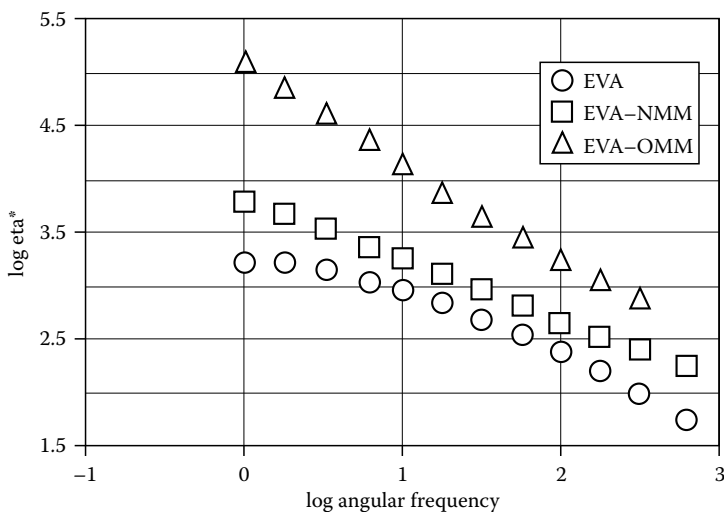


FIGURE 13.3 Viscosity of EVA, EVA–NMM, and EVA–OMM composites plotted against frequency at 210°C (clay content 10%).

The so-called shear-thinning exponent describes the steepness of the viscosity-shear rate curve

$$\eta \sim \omega^n$$

where

n is the “shear-thinning” exponent

η is the viscosity

ω is the frequency of the measurement

A high shear-thinning coefficient means good exfoliation, while a low shear-thinning coefficient denotes poor or no exfoliation [26].

CIL may act in fire-retardant systems also as *mechanical compatibilizer* overcoming the local stresses around the inclusions originating from a different heat or a tensile expansion of components. The stress concentration and the partial immobilization of the macromolecules at the surface of inclusions lead to the separation of the phases and embrittlement. The phase-separation, shown in Figure 13.4a, can be decreased by an elastomeric interlayer that distributes the stresses in a larger region, as shown in Figure 13.4b. However, a conventional elastomer CIL decreases the FR in most cases [7].

Considering the *physical effects of an interlayer*, designed for flame-retarded polymer systems, it should perform the following roles:

- Ensure good dispersion
- Promote the rapid migration of FR-active components to the surface (at the temperature of combustion)
- Avoid producing fuel
- Control the viscosity and
- Compensate the embrittlement-effect of the large surface area of inclusions

Such a complex set of requirements cannot be achieved with a single-coating layer. Thus, a multi-layer interfacial structure is required as proposed previously [28,29]. The function of each layer to be discussed is described in the scheme given in Figure 13.5.

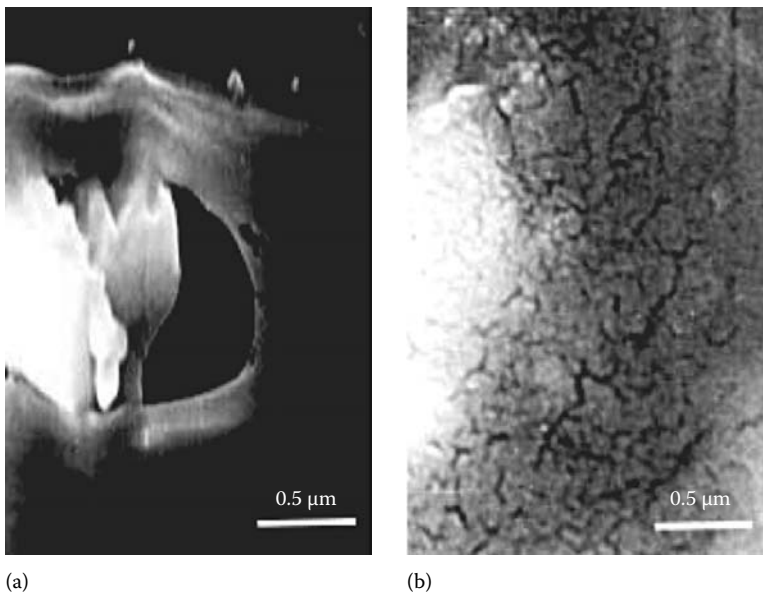


FIGURE 13.4 SEM micrograph of phase-separation around filler particle in PP (a); stress distributed by EPDM elastomer interlayer around a particle (b).

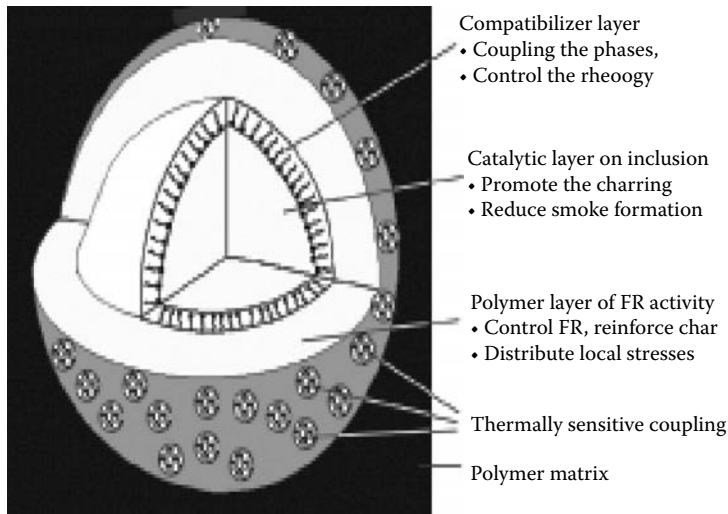


FIGURE 13.5 Scheme of the phase structure of a flame-retarded system.

TABLE 13.2
Cone Calorimetric Data of PP-Clay Compositions

Sample	TTI (s)	pk HRR (kW/m ²)	pk HRR _{time} (s)	THR (MJ/m ²)	Residue	
					% (100s)	% (Char) (250s)
PP	35	898	175	112.4	82.2	0.0 (0.0)
PP + MMT(1.0)	23	868	181	107.6	80.7	2.7 (1.7)
PP + MMT(2.5)	25	861	179	107.9	79.8	3.2 (0.7)
PP + MMT(5.0)	25	857	188	105.2	81.0	5.4 (0.4)
PP + SEP(1.0)	27	753	167	109.4	67.3	3.7 (2.7)
PP + SEP(2.5)	25	761	173	107.3	66.9	4.1 (1.6)
PP + SEP(5.0)	26	764	169	103.3	64.4	7.0 (2.0)

The model described in Figure 13.5 takes into account both the physical and chemical effects of the interlayers but the chemical ones, which are reflected, for example, in the ignition time, have not yet been discussed. A number of cone calorimetric investigations reported a decrease of the time to ignition (TTI) in presence of clay nanofillers. Such results can be seen in Table 13.2 for MMT and sepiolite (SEP) clay types.

Atoms in the surface layer of inclusions may act as catalytic sites in course of the degradation, modifying the run of the process. The catalytic origin of the shift of TTI and the formation of char residue in presence of MMT and SEP is a reasonable assumption; the experiment verification of this is, however, a challenging task.

13.3 METALLIC ACTIVATOR INTERLAYER

Metallic interlayer (MIL) influences the chemical processes of FR. The role of metal ions in the degradation process has been summarized by Lewin and Endo [30]. The advantageous effect of a MIL around metal hydroxide flame retardants was utilized at first by Hornsby et al. [31]. They proposed a zinc-hydroxy-stannate (ZnHSt) layer, the detailed chemical–physical structure and 4.7 nm thickness

TABLE 13.3
Composition of Surface Layer Enriched in Fe Ions (MMT-Fe) and
Reference Surface as Determined by XPS

Additive	Atom (%)							
	Na	Fe	Ca	O	Si	Al	C	Mg
MMT	8.0	0.3	0.4	59.3	13.0	5.9	13.1	0.0
MMT-Fe	0.0	0.9	0.3	64.7	14.5	8.4	11.2	0.0

of which could be determined by x-ray photoelectron spectroscopy (XPS) analyses [32]. This layer controlled the formation of degradation gases and thus reduced the smoke development. The improvement of thermal stability and FR performance was lower if the ZnHSt was applied as separate particles, rather than as a coating layer [33]. Iron and cobalt were also added together with known fillers, such as kaolin and magnesium hydroxide, as flame-retardant promoters and in the form of metal chelates that could be intercalated with MMT to produce nanocomposite flame retardants [34,35].

Wilkie and his coworkers [36] reported that clay-containing structural iron increases the onset temperature of the degradation of polystyrene and decreases the rate of heat release.

In order to study the chemical effects of MIL the concentration of the catalytic (Fe^{3+}) atoms on the surface of MMT clay was increased by surface treatment. The result of the treatment was evaluated by XPS method. The atomic composition of the surfaces, given in Table 13.3, reflects 3 \times increase of Fe ions after the treatment when compared to the reference.

Composites of 5 m/m% clay content were prepared in EVA copolymer matrix in a Brabender plastograph. In model studies, laser pyrolysis (LP) has been applied, using a CO_2 laser, for modeling the effect of fire, as described recently [37,38]. The method was established by the basic work carried out by Price et al. [39]. The effect of MMT of Fe-enriched surface layer (MMT-Fe) on the amount and composition of the evolved gas, compared to pristine EVA, can be seen in Figure 13.6.

The FTIR spectrum in Figure 13.6b shows no new or missing band in the gas phase but the amounts of the components are different. In the first stage of the process the MMT-Fe-induced development of higher amount of flammable degradation products, that is, hydrocarbons represented

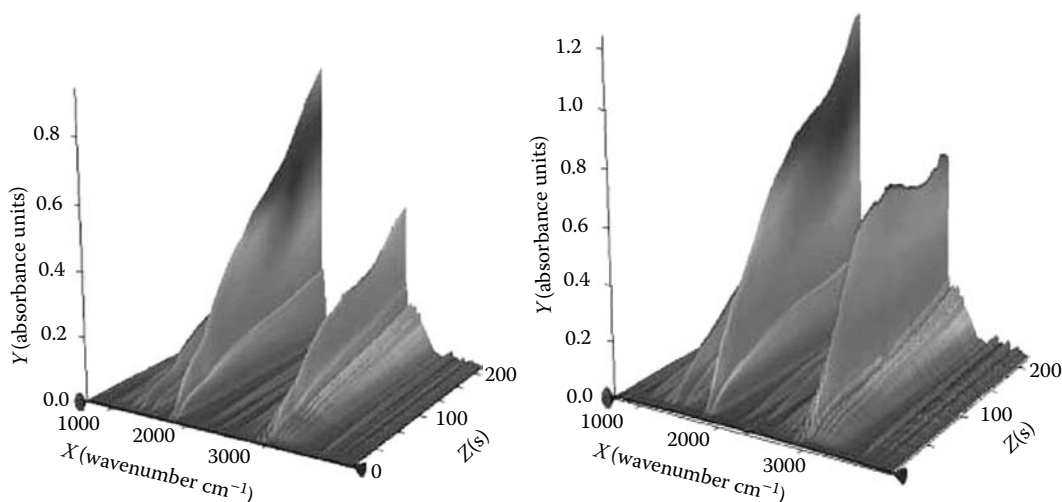


FIGURE 13.6 The results of FTIR analysis of gaseous degradation products of EVA and its composite containing MMT-Fe particles during LP treatment CO_2 laser at 0.5 W power.

by bands around 2900 cm^{-1} and acetic acid (band at 1761 cm^{-1}), than in pristine EVA. However, it is also clearly visible that the development of hydrocarbons slows in case of the composite, while the reference shows a permanent increase.

Comparing the effect of two clays (MMT-Fe and MMT) to each other based on the integral values of two characteristic band ranges (acetate group: $1606\text{--}1848\text{ cm}^{-1}$ and $\text{CH}_2\text{--}$ and $\text{CH}_3\text{--}$ groups: $2810\text{--}2990\text{ cm}^{-1}$) similar tendencies can be seen in Figure 13.7.

The main characteristics of the plots of MMT-Fe containing system appear also in the case of EVA–MMT but in a moderated and delayed manner confirming the basic correspondence of the two effects.

The changes in the composition of the gas phases can be interpreted by considering the parallel changes in the solid phase. The progress of the chemical transformation of the solid phase in course of LP process was monitored by a Raman microscope.

In the Raman spectra of EVA (Figure 13.8a) the intensity of bands of acetate $\text{C}=\text{O}$ groups at 1736 cm^{-1} and to OCO deformation vibration at 629 cm^{-1} is decreasing as the treatment time is increasing. This change represents the gradual scission of acetate groups from the main polymer chain. Parallel to this process the intensity of band at 1653 cm^{-1} increase continuously. This band splits after the treatment time of 0.6 s and a new band appears at 1665 cm^{-1} . The characteristic bands of carbon–carbon double bonds isolated and conjugated with $\text{C}=\text{O}$ or $\text{C}=\text{C}$ can be detected in this range, which forms after the scission of acetate groups. A sample containing Fe-enriched MMT (MMT-Fe) exhibits similar tendencies in the same bands (in Figure 13.8b) as described for pristine EVA. However, comparing the spectra at the same treatment time, accelerated changes can be found in the presence of MMT-Fe. The characteristic spectrum of char is detected on the surface of EVA–MMT-Fe after treatment time of 5 s , while EVA, after the same treatment time, still shows the bands of the original polymer chain.

The results of metal-coated MMT confirmed the catalytic effect of Fe atoms on the clay surface, which accelerates the appearance of degradation products in the gas phase but also at later stages,

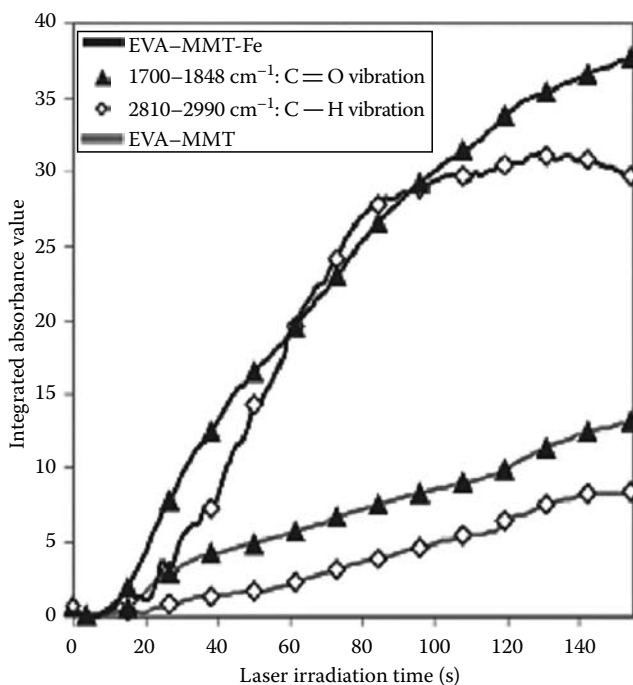


FIGURE 13.7 Comparison of the characteristic integral values of EVA–MMT-Fe (–) and EVA–MMT (–) composites based on LP-FTIR analysis (CO_2 laser at 0.5 W power).

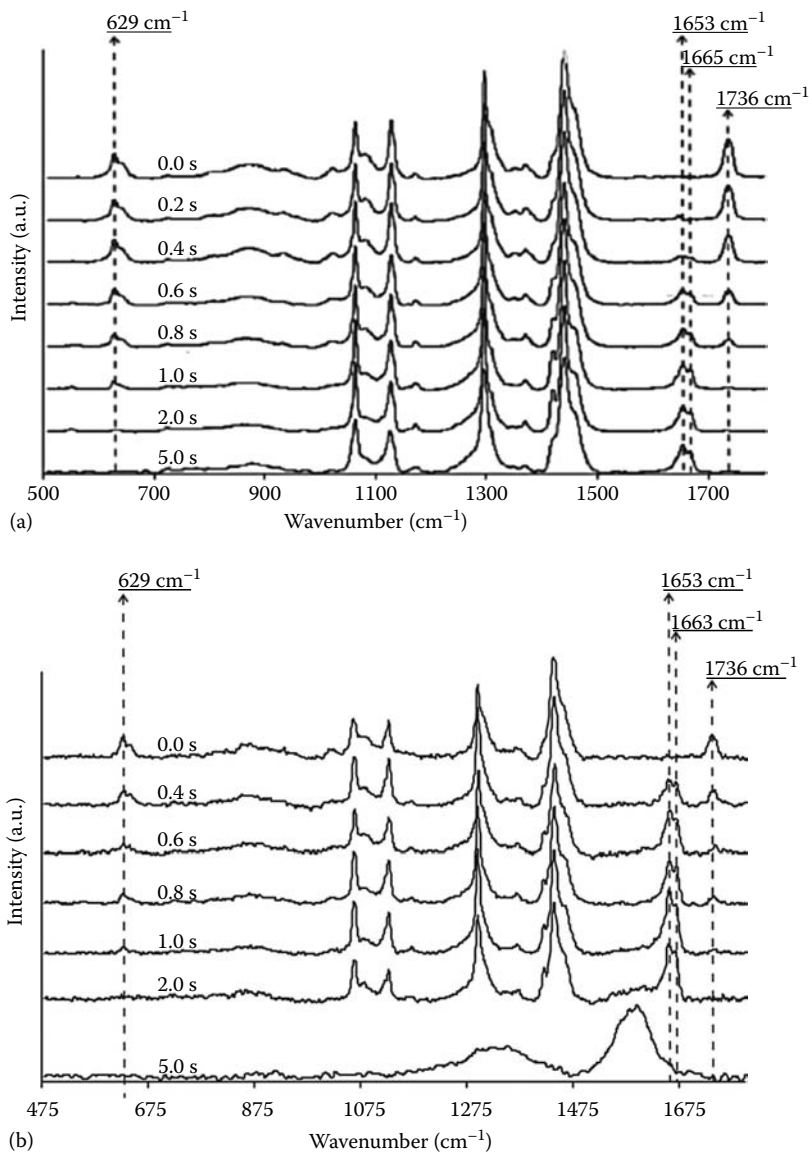


FIGURE 13.8 Comparison of the progress of degradation (induced by treatment with CO₂ laser at power of 10 W) in EVA (a) and EVA-MMT-Fe (b) based on the normalized Raman spectra of the solid phases.

the charring in the solid phase as well. The formed char layer slows down the fuel supply to the gas phase. Based on these results the decrease of the ignition time, which is a characteristic consequence of the inclusion of nanoparticles, is considered as an interfacial phenomenon. The catalytic effect, associated with impurities on most of the enhanced surface areas (even the neutral CNT contains some catalyst residue [40]), is probably responsible for accelerated fuel formation in the initial stage of degradation of these nanocomposites.

If this assumption is true the decrease of the ignition time can be avoided by suitable interface modification, which, however, should preserve the advantageous charring activity of nanofillers having catalytic effects. This challenging concept could not be realized by any conventional interface modifier. A polymeric interlayer, which has not yet been studied in this respect, may provide a solution.

13.4 POLYMER INTERLAYER OF FIRE-RETARDANT ACTIVITY

The concept to use a polymer interlayer (PIL) for influencing the competitive process between the evolution of fuels and the formation of heat and gas barrier char layers has been proposed recently [27]. The delay of the ignition time was planned to be achieved by forming less combustible gases from the interlayer in the first stage of degradation process than the fragments of the matrix polymer. In order to accelerate the development and improve the performance of heat and gas barrier surface layer, the migration of active substances to the surface has to be promoted by suitable interlayers.

Insulating interlayers separates the inclusions from each other and from the matrix polymer in such system degradation catalyzed by nanoparticles starts within the interlayer. This layer should provide less combustible degradation products. A new method for the formation of PEP resin has been proposed recently [21]. A detailed analysis of PEP revealed the combined (gas and solid phase) mechanism of FR action in this material [41]. This polymer was selected for forming an interlayer around clay nanoparticles. The monomer components were introduced during the compounding process and the interlayer was formed by *in situ* curing.

Thermogravimetric analysis (Figure 13.9) of the formed systems confirmed the catalytic activity of both clay types as the delayed mass loss of PEP containing PP is accelerated again when the clays are introduced.

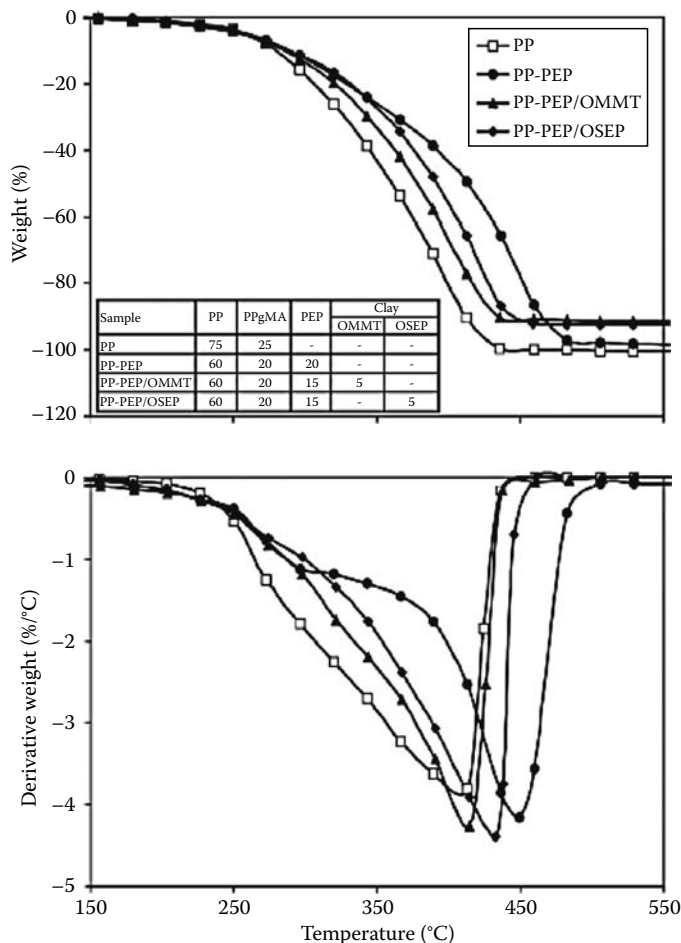


FIGURE 13.9 TG and dTG curves of PP composites containing PEP-coated OMM and OSEP.

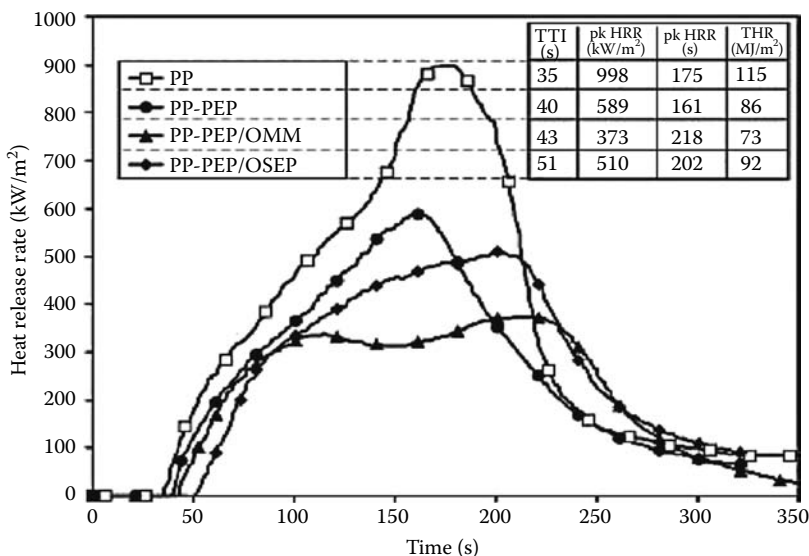


FIGURE 13.10 HRR curves of PP-PEP/OMM and PP-PEP/OSEP composites compared to the reference curves.

The TTI, shown in Figure 13.10, does not correlate with the mass loss curves (given in Figure 13.9). Nanoclays that accelerated the mass loss increase in this case the TTI compared to the reference materials. The reason is the composition of the developed gases during the initial mass loss. As mentioned earlier, PEP releases phosphorous compounds that act by a radical mechanism in the gas phase. The catalytic action of nanoclays produces in this case a larger amount of flame-retardant species resulting in delayed ignition. The heat release rate (HRR) values correlate with the charring activity of the clays.

The best result, 60% and 40% decrease of the HRR and total heat release (THR), respectively, was achieved by PP-PEP/OMMT the P content of which is only 0.5 wt%.

The influence of the applied PIL is even more obvious if the residues of the combusted materials are compared (Figure 13.11). Pristine PP is burned out completely, while the largest amount of char remained after the combustion of PP-PEP/OMM. This residue has an almost continuous compact surface.

Our assumption for explaining these results considers the expansion capacity of PEP coating around nanofillers. MMT influences the foaming process of epoxy resin advantageously, as reported previously [21]. Owing to heat and catalytic effects, the particles may reach each other, leading to the percolation of the coating layers. Compared to the conventional intumescent systems in which continuous char layer is formed only after the decomposition of a considerable amount of matrix polymer, in a “percolating intumescent system” the expanding particles reach each other in the

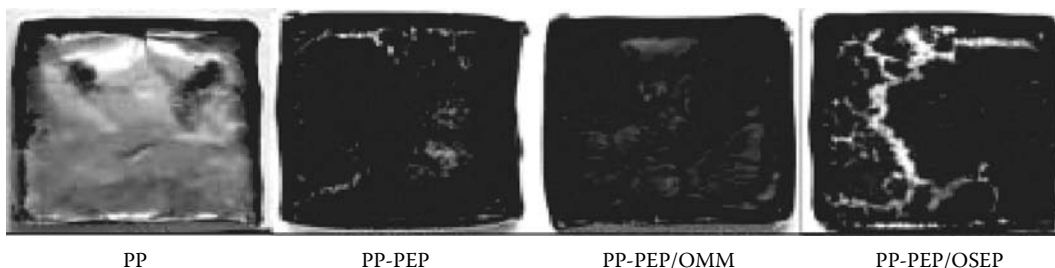


FIGURE 13.11 Residues of the samples after combustion.

earlier stage of the process providing rapid protection to the underlying polymer phase [42]. (A percolation model for isodimensional inclusions of polystyrene blend has been applied recently [43].) Parameters influencing the percolation are the interparticle distance, the volume increase, and the rate of action [41].

Similar *protecting interlayers* are applicable to overcome the chemical and thermal sensitivity of fire retardants [44]. Ammonium polyphosphate (APP) has to be protected against hydrolytic degradation at higher temperature. Various PILs have been proposed for protecting the APP particles [45,46]. A shear stress-resistant silicone elastomer PIL was found suitable for preserving the stability under processing conditions [44]. The protecting effect was confirmed by the decrease of the conductivity of water used for extracting the FR product (from 200 μs of the reference sample to 50 μs of protected APP).

The same method is applicable to control critical temperature where the reaction between polyphosphates and polyols takes place. For example, melamine polyphosphate-polyol system, which is stable at the degradation temperature of PP, has been activated for application in polyolefins [47]. An activating effect is ascribed also to the char-forming polymers in intumescent nanocomposites, according to the blending approach [48].

The results on activator/insulating/protecting interlayers suggest the economic strategy of adjusting the flame-retardant action to the degradation profile of polymers. This means the selection of a few general flame retardants and the use of activating or deactivating interphases for shifting their action temperature close to the degradation range of a particular polymer matrix.

Transporter (adaptive) interlayers promote the delivery of components, responsible for barrier layer formation, to the surface at high temperature. It is of great importance to prevent the formation of combustible gases as early as possible. Two concepts have been proposed up to now for this purpose: *polyorganosiloxane* and *expandable* [49] *interlayers*.

Polyorganosiloxane interlayers of low surface tension have to be coupled to the matrix using thermally sensitive reactive branches as shown in Figure 13.5; phase-separation during compounding can be avoided in this way. At the temperature of fire action the coupling units will decompose leaving behind an incompatible-coating layer. The elimination of the coupling unit could be confirmed by the disappearance of its characteristic Raman band, as shown in Figure 13.12.

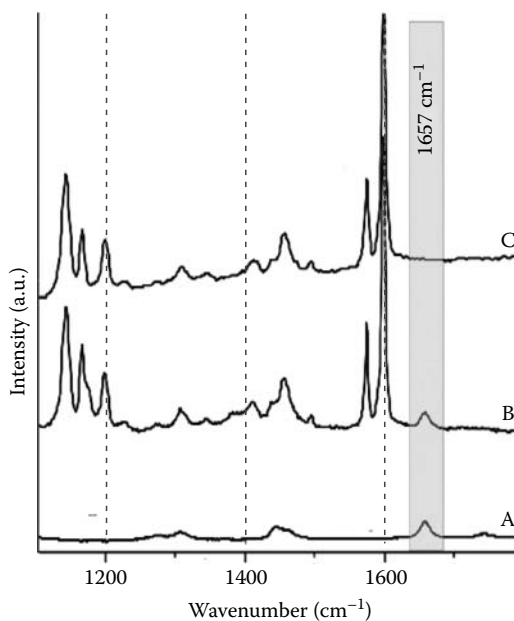


FIGURE 13.12 Raman spectra of unsaturated silane coupling agent (A), silane—PDMS adduct (B), and the adduct after treatment at 350°C for 0.5 min (C).

The disappearance of the band at 1657 cm^{-1} belonging to the double bond of the unsaturated silane unit suggests the decomposition of the coupling site. PIL that became incompatible with the matrix delivers the inclusion to the surface as confirmed by XPS and Raman spectroscopic results [50]. The thermal responsive character of the interlayer justifies the *adaptive* term. Compared to other elastomers, much better flame retardancy was found in PP when polyorganosiloxane elastomer interlayer was applied around intumescent additives [7]. CaCO_3 combined with a silicon elastomer was also found to act as an efficient FR additive in ethylene-acrylate copolymer [51]. Factors influencing the formation of PIL during the compounding process are ratios of melting temperatures, viscosities, and polarities of the polymer components [52].

Expandable interlayers provide an alternative way for rapid delivery. Migration, even if promoted by an incompatible interlayer, is sometimes not rapid enough to deliver active substances to the surface; therefore, a new adaptive concept has been developed recently [53,54]. A material utilizing this mechanism contains a phosphorylated polyol (PPOL) interlayer of relatively low decomposition temperature intercalated between layers of nanoparticle. At the early stage of fire action the gaseous degradation products of the interlayer separate the nanolayers and drive them to the surface in the most rapid way.

13.5 REINFORCED-CHAR-FORMING CERAMIZER INTERLAYER

Reinforced-char-forming, interlayer (RIL) that contributes to the ceramization of the char is very useful for maintaining the barrier capacity of the surface protection achieved either by the migration, the charring, and/or the foaming of the components. For example the protection achieved by either clay or other FR-active particles accumulated at the surface does not sustain if the bubbles push them away. In such case island-like floccules form instead of a continuous net-like structure [55]. The mechanical and thermal stability of the surface layer has to be improved in order to maintain its integrity. The thermal stability of a common char is also limited. Its durability decreases under permanent heat irradiation and the underlying melt breaks through, reaccelerating the combustion. RIL by bonding nanoparticles to each other and by ceramizing the char increases its *heat and pressure resistance*.

Boron atoms built in polysiloxane elastomers promote the ceramization of the surface layer in case of fire [56]. According to XPS measurements, the partially organic (and elastomeric) character of the ceramic layer is preserved even after long flame treatment, resulting in mechanically resistant char [44,46]. A polyboroxosiloxane (BSi) interlayer at high temperature promotes the merging of FR components on the surface. According to Thermal Scanning Rheometer results, RIL increases the mechanical resistance of the residue of both metal hydroxide and intumescent type FR systems [45]. Further improvement can be achieved when this elastomer can be applied together with pristine MMT. The softening temperature, indicated by sensor penetration into the interlayers, has been investigated using μ -TA method (Microthermal analyzer micro-TA 2990, TA Instruments) in Figure 13.13.

This additive system maintains the viscosity and increases it gradually in the temperature range of 390°C – 470°C , where other compositions lose their melt strength. Combining the advantages of the described interfacial structures in an intumescent PP system containing 30% total additive content, the RHR curve could be kept under 100 kW/m^2 and burning was terminated within 300 s (see in Figure 13.14).

The percolation of the coated intumescent particles, their attachment through heat resistant sealants and the MMT-controlled optimal pore structures are ascribed to the gradual decrease of the heat release and missing of the reacceleration period in case of the best system.

The ceramizing capacity of polyboroxosiloxane elastomer provides a new P-free intumescent mechanism [57]. The combustion of PP-polyboroxosiloxane 3:1 blend filled with 1.25% organo-modified SEP (OSEP, Pangel B40 product of Tolsa Ltd.) and 1.25% melamine borate lead to the formation of white foamed ceramic structure shown in Figure 13.15.

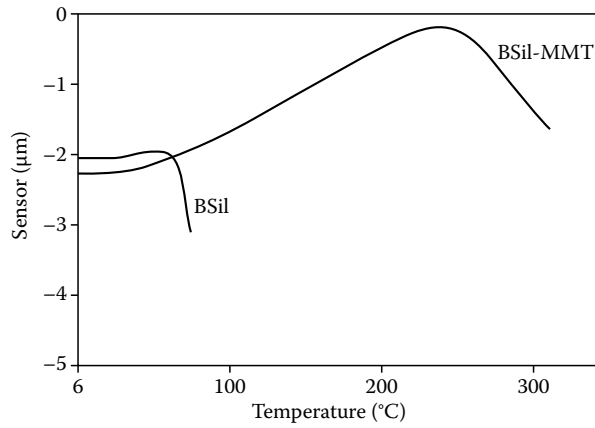


FIGURE 13.13 Penetration of μ -TA sensor into the polyboroxosiloxane phase with and without MMT.

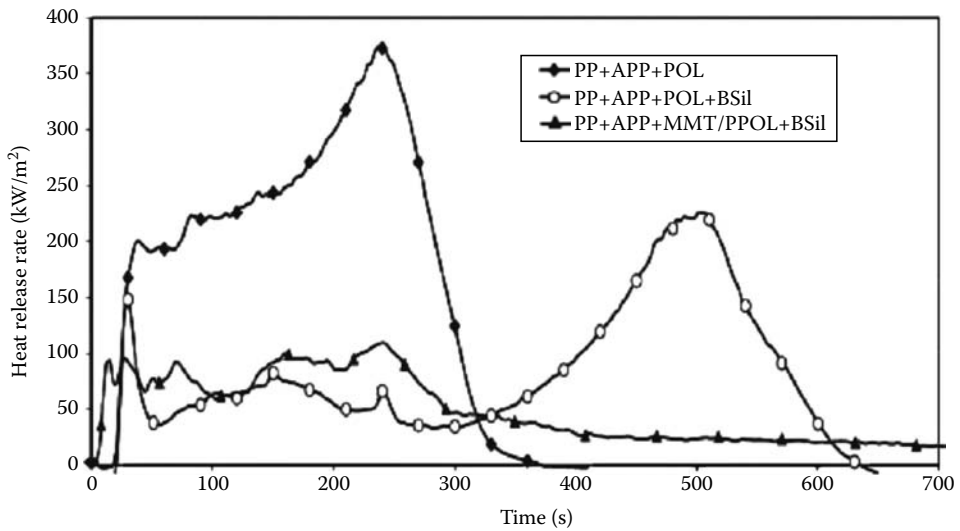


FIGURE 13.14 Comparison of the heat release of various intumescent PP systems of 30% total additive content (heat flux: 50 kW/m^2).

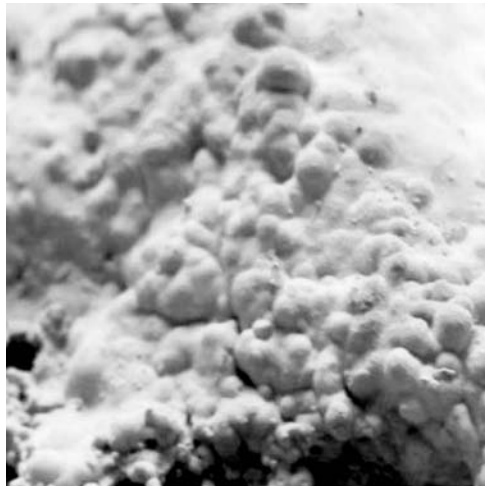


FIGURE 13.15 Real size photograph of a nonphosphorous intumescent residue.

Although the FR efficiency of this white intumescent system is far from the conventional types, the combination of different mechanisms may lead to an industrially applicable P-free FR system.

13.6 CONCLUSIONS

The role of interfaces (and surfaces) has been underestimated in the technology of fire retardancy for a long time. In this chapter, we tried to demonstrate that this role is even larger than in other multicomponent systems. At normal circumstances, the fire-retarded polymer systems, like any other composite structure, need compatibilizer interlayer for ensuring homogeneous structure and maintaining the contact between the phases. Nanosize additives require high amount of interfacial agent for covering their high surface area but their amount or the flammability has to be minimized in order to promote the fire retardancy of the composite. Nanodispersion, achieved by the introduction of organic coating layer, results in increased viscosity and thus reduced the dripping of burning polymer but the parallel decrease of the processability has to be minimized. In order to describe how to meet the complex requirements a model of a multilayer interphase has been proposed for fire-retardant polymer composites, consisting of layers of compatibilizing, catalytic, local-stress-releasing, and char-stabilizing activities.

Reactive interfacial agents formed compatibilizer interlayers around nanosize magnesium hydroxide and CNT.

The catalytic role of metal-doped clay surface in fire-induced degradation could be proven and an epoxy-based interlayer has been developed for controlling this activity. As a result of the modification, an increased amount of char residue was formed in fire-retarded PP system.

The efficiency of intumescent fire retardants could be enhanced by interlayers that deliver the active components to the surface (shown by two examples). The fire-retardant additives, delivered to the surface at early stage of combustion, accelerate the formation of protecting surface layer that hinders the degradation of the underlying material. This coating structure could be reinforced by an interlayer of ceramizing capability (e.g., polyborosiloxane). Phosphorus-free intumescent fire-retardant system could be formed by using such additive.

Further development is expected by developing multifunctional interlayers, which will assist in the improvement of tribological, adhesive/dehesive biocompatible characteristics beyond the good mechanical and fire-retardant features.

ACKNOWLEDGMENTS

The supports from EU Multihybrids (IP 026685-2), W2Plastics (212782), Hungarian Research Found OTKA K76346, RECYTECH, Found of European Union and Hungarian state GVOP/3.1.1. 2004-0531/3.0, Public Benefit Association of Sciences and Sport of the Budapest University of Technology and Economics are acknowledged.

REFERENCES

1. Buzágh, A. 1952. Über den Zusammenhang zwischen Adhäsion und Stabilität disperser Systeme. *Kolloid Zeitschrift* 125:14–21.
2. Hungarian Pat. 167063 (1975); US Pat. 4116897 (1978); German Pat. 2453491 (1986).
3. Geckeler, K. E., Rupp, F., and Geis-Gerstorfer, J. 1997. Interfaces and interphases of (bio)materials: Definitions, structures, and dynamics. *Advanced Materials* 9:513–18.
4. Finka, B. K. and Mccullough, R. L. 1999. Interphase research issues. *Composites: Part A*. 30:1–2.
5. Gutowski, W. V. 2003. Interface/interphase engineering of polymers for adhesion enhancement: Review of micromechanical aspects of polymer interface reinforcement through surface grafted molecular brushes. *Journal of Adhesion* 79:445–82.
6. Landman, U. and Luedtke, W. D. 1991. Nanomechanics and dynamics of tip substrate interactions. *Journal of Vacuum Science and Technology* B9:414–23.

7. Marosi, G., Bertalan, G., Balogh, I., Tohl, A., Anna, P., and Szentirmay, K. 1996. Silicone containing intumescent flame retardant systems for polyolefins. In: *Flame Retardants*, ed. Grayson, S. London, U.K.: Interscience Commun. Ltd. Publ., p. 115.
8. Marosi, G., Anna, P., Balogh, I., Bertalan, G., Tohl, A., and Maatoug, M. A. 1997. Thermoanalytical study of nucleating effects in polypropylene composites. 3. Intumescent flame retardant containing polypropylene. *Journal of Thermal Analysis* 48:717–26.
9. Tidjani, A., Wald, O., Pohl, M. M., Hentschel, M. P., and Schartel, B. 2003. Polypropylene-graft-maleic anhydride-nanocomposites. I. Characterization and thermal stability of nanocomposites produced under nitrogen and in air. *Polymer Degradation and Stability* 82:133–40.
10. Bartholmai, M. and Schartel, B. 2004. Layered silicate polymer nanocomposites: New approach or illusion for fire retardancy? Investigations of the potentials and the tasks using a model system. *Polymers for Advanced Technologies* 15:355–64.
11. Nachtigall, S. M. B., Miotto, M., Schneider, E. E., Mauler, R. S., and Forte, M. C. 2006. Macromolecular coupling agents for flame retardant materials. *European Polymer Journal* 42:990–99.
12. Marosi, G., Marton, A., Csontos, I., Matko, S., Szep, A., Anna, P., Bertalan, G., and Kiss, E. 2004. Reactive surfactants—New type of additive for multicomponent polymer systems. *From Colloids to Nanotechnology* 125:189–93.
13. Marosi, G., Keszei, S., Matko, S., and Bertalan, G. 2006. Effect of interfaces in metal hydroxide-type and intumescent flame retarded nanocomposites. In: *Fire and Polymers IV: Materials and Concepts for Hazard Prevention*, Vol. 922, eds. Wilkie, C. and Nelson, G. Washington, DC: ACS, pp. 117–30.
14. Anna, P., Zimonyi, E., Marton, A., Szep, A., Matko, S., Keszei, S., Bertalan, G., and Marosi, G. 2003. Surface treated cellulose fibres in flame retarded PP composites. *Macromolecular Symposia* 202:245–54.
15. Lv, X. T., Hari, B., Li, M. G., Ma, X. K., Ma, S. S., Gao, Y., Tang, L. Q., Zhao, J. Z., Guo, Y. P., Zhao, X., and Wang, Z. C. 2007. In situ synthesis of nanolamellas of hydrophobic magnesium hydroxide. *Colloids and Surfaces A: Physicochemical and Engineering Aspects* 296:97–103.
16. Zammarano, M., Bellayer, S., Gilman, J. W., Franceschi, M., Beyer, F. L., Harris, R. H., and Meriani, S., 2006. Delamination of organo-modified layered double hydroxides in polyamide 6 by melt processing. *Polymer* 47:652–62.
17. Marosfoi, B. B., Marosi, G. J., Szep, A., Anna, P., Keszei, S., Nagy, B. J., Martvona, H., and Sajo, I. E. 2006. Complex activity of clay and CNT particles in flame retarded EVA copolymer. *Polymers for Advanced Technologies* 17:255–262.
18. Andrews, R. and Weisenberger, M. C. 2004. Carbon nanotube polymer composites. *Current Opinion in Solid State & Materials Science* 8:31–37.
19. Eitan, A., Jiang, K. Y., Dukes, D., Andrews, R., and Schadler, L. S. 2003. Surface modification of multiwalled carbon nanotubes: Toward the tailoring of the interface in polymer composites. *Chemistry of Materials* 15:3198–201.
20. Si, M., Araki, T., Ade, H., Kilcoyne, A. L. D., Fisher, R., Sokolov, J. C., and Rafailovich, M. H. 2006. Compatibilizing bulk polymer blends by using organoclays. *Macromolecules* 39:4793–801.
21. Toldy, A., Anna, P., Csontos, I., Szabo, A., and Marosi, G. 2007. Intrinsically flame retardant epoxy resin—Fire performance and background—Part I. *Polymer Degradation and Stability* 92:2223–2230.
22. Zanetti, M., Camino, G., Thomann, R., and Mullhaupt, R. 2001. Synthesis and thermal behaviour of layered silicate-EVA nanocomposites. *Polymer* 42:4501–07.
23. Gilman, J. W., Awad, W. H., Davis, R. D., Shields, J., Harris, R. H., Davis, C., Morgan, A. B., Sutto, T. E., Callahan, J., Trulove, P. C., and DeLong, H. C. 2002. Polymer/layered silicate nanocomposites from thermally stable trialkylimidazolium-treated montmorillonite. *Chemistry of Materials* 14:3776–85.
24. Lewin, M., Pearce, E. M., Levon, K., Mey-Marom, A., Zammarano, M., Wilkie, C. A., and Jang, B. N. 2006. Nanocomposites at elevated temperatures: Migration and structural changes. *Polymers for Advanced Technologies* 17:226–34.
25. Lewin, M. 2009. In: *Fire Retardancy of Polymers*, eds. Kandola, K. and Hull, R. Cambridge, U.K.: Royal Society of Chemistry.
26. Xie, W., Xie, R. C., Pan, W. P., Hunter, D., Koene, B., Tan, L. S., and Vaia, R. 2002. Thermal stability of quaternary phosphonium modified montmorillonites. *Chemistry of Materials* 14:4837–45.
27. Wagener, R. and Reisinger, T. J. G. 2003. A rheological method to compare the degree of exfoliation of nanocomposites. *Polymer* 44:7513–18.
28. Marosi, G., Bertalan, G., Ruzsnak, I., and Anna, P. 1986. Role of interfacial layers in the properties of particle-filled polyolefin systems. *Colloids and Surfaces* 23:185–98.

29. Marosi, G. and Bertalan, G. 2004. Role of interfaces in multicomponent polymer systems and biocomposites. In: *Modification and Blending of Synthetic and Natural Macromolecules*, Vol. 175, eds. Ciardelli, F. and Penczek, S., Dordrecht, the Netherlands: Springer, pp. 135–54.
30. Lewin, M. and Endo, M. 2003. Catalysis of intumescent flame retardancy of polypropylene by metallic compounds. *Polymers for Advanced Technologies* 14:3–11.
31. Hornsby, P. R., Cusack, P. A., Cross, M., Toth, A., Zelei, B., and Marosi, G. 2003. Zinc hydroxystannate-coated metal hydroxide fire retardants: Fire performance and substrate-coating interactions. *Journal of Materials Science* 38:2893–99.
32. Mohai, M., Toth, A., Hornsby, P. R., Cusack, P. A., Cross, M., and Marosi, G. 2002. XPS analysis of zinc hydroxystannate-coated hydrated fillers. *Surface and Interface Analysis* 34:735–39.
33. Marosi, G., Anna, P., Bertalan, G., Szabó, S., Ravadits, I., and Papp, J. 2001. Role of interface modification in flame retarded multiphase polyolefin systems. In: *Fire and Polymers: Materials and Solutions for Hazard Prevention*, Vol. 797, eds. Nelson, G. and Wilkie, C. Washington, DC: American Chemical Society, pp. 161–71.
34. Wang, D. Y., Liu, Y., Ge, X. G., Wang, Y. Z., Stec, A., Biswas, B., Hull, T. R., and Price, D. 2008. Effect of metal chelates on the ignition and early flaming behaviour of intumescent fire-retarded polyethylene systems. *Polymer Degradation and Stability* 93:1024–30.
35. Shehata, A. B., Hassan, M. A., and Darwish, N. A. 2004. Kaolin modified with new resin-iron chelate as flame retardant system for polypropylene. *Journal of Applied Polymer Science* 92:3119–25.
36. Zhu, J., Uhl, F. M., Morgan, A. B., and Wilkie, C. A. 2001. Studies on the mechanism by which the formation of nanocomposites enhances thermal stability. *Chemistry of Materials* 13:4649–54.
37. Bodzay, B., Marosfoi, B. B., Igricz, T., Bocz, K., and Marosi, G. 2009. Polymer degradation studies using Laser pyrolysis-FTIR microanalysis. *Journal of Analytical and Applied Pyrolysis* 85:313–320.
38. Marosfoi, B. B., Marosi, G., Szabo, A., Vajna, B., and Szep, A. 2007. Laser pyrolysis microspectroscopy for modelling fire-induced degradation of ethylene-vinyl acetate systems. *Polymer Degradation and Stability* 92:2231–2238.
39. Price, D., Milnes, G. J., Lukas, C., and Hull, T. R. 1984. Application of time-of flight mass-spectrometry to investigate fire-retardant systems. *International Journal of Mass Spectrometry and Ion Processes* 60:225–35.
40. Moissala, A., Nasibulin, A. G., and Kauppinen, E. I. 2003. The role of metal nanoparticles in the catalytic production of single-walled carbon nanotubes—A review. *Journal of Physics: Condensed Matter* 15:S3011–S35.
41. Szabo, A., Marosfoi, B., Anna, P., and Marosi, G. 2009. Complex micro-analysis assisted design of fire retardant nanocomposites—Contribution to the nano-mechanism. In: *Fire Retardancy of Polymers*, eds. Kandola, K. and Hull, R. Cambridge, U.K.: Royal Society of Chemistry, pp. 74–91.
42. Zhang, F., Zhang, J., and Wang, Y. 2007. Modeling study on the combustion of intumescent fire-retardant polypropylene. *eXPRESS Polymer Letters* 1:157–65. <http://www.expresspolymlett.com/>
43. Guo, Z., Fang, Z., and Tong, L. 2007. Application of percolation model on the brittle to ductile transition for polystyrene and polyolefin elastomer blends. *eXPRESS Polymer Letters* 1:37–43. <http://www.expresspolymlett.com/>
44. Marosi, G., Anna, P., Marton, A., Bertalan, G., Bota, A., Toth, A., Mohai, M., and Racz, I. 2002. Flame-retarded polyolefin systems of controlled interphase. *Polymers for Advanced Technologies* 13:1103–11.
45. Anna, P., Marosi, G., Csontos, I., Bourbigot, S., Le Bras, M., and Delobel, R. 2001. Influence of modified rheology on the efficiency of intumescent flame retardant systems. *Polymer Degradation and Stability* 74:423–26.
46. Ravadits, I., Toth, A., Marosi, G., Marton, A., and Szep, A. 2001. Organosilicon surface layer on polyolefins to achieve improved flame retardancy through an oxygen barrier effect. *Polymer Degradation and Stability* 74:419–22.
47. Marosi, G., Bertalan, G., Anna, P., Ravadits, I., Bourbigot, S., Le Bras, M., and Delobel, R., 2000. Polyphosphate flame retardants in polyolefins. In: *Recent Advances in Flame Retardancy of Polymeric Materials*, Vol. XI, ed. Lewin, M. Stamford, CT: BCC, Inc., pp. 154–63.
48. Bourbigot, S., Le Bras, M., Duquesne, S., and Rochery, M. 2004. Recent advances for intumescent polymers. *Macromolecular Materials and Engineering* 289:499–511.
49. Lewin, M. 2003. Some comments on the modes of action of nanocomposites in the flame retardancy of polymers. *Fire and Materials* 27:1–7.
50. Marosi, G., Marton, A., Szep, A., Csontos, I., Keszei, S., Zimonyi, E., Toth, A., and Almeras, X. 2003. Fire retardancy effect of migration in polypropylene nanocomposites induced by modified interlayer. *Polymer Degradation and Stability* 82:379–85.

51. Hermansson, A., Hjertberg, T., and Sultan, B. A. 2003. The flame retardant mechanism of polyolefins modified with chalk and silicone elastomer. *Fire and Materials* 27:51–70.
52. Marosi, G., Bertalan, G., Anna, P., and Rusznak, I. 1993. Elastomer interphase in particle filled polypropylene, structure, formation and mechanical characteristics. *Journal of Polymer Engineering* 12:34–61.
53. German Patent Application Registration No. R 4700 (13.03.2002).
54. Marosi, G., Anna, P., Márton, A., Matkó, S., Szep, A., Keszei, S., Csontos, I., and Marosfői, B. 2003. Mechanism of interactions in flame retarded polymer nanocomposites. In: *12th International Conference on Additives*, Vol. 12. eds. Wilkie, C. and Al-Malaika, S. San Francisco, CA: ECM Ltd., p. 203.
55. Kashiwagi, T., Harris, R. H., Zhang, X., Briber, R. M., Cipriano, B. H., Raghavan, S. R., Awad, W. H., and Shields, J. R. 2004. Flame retardant mechanism of polyamide 6-clay nanocomposites. *Polymer* 45:881–91.
56. Anna, P., Marosi, G., Bertalan, G., Marton, A., and Szep, A. 2002. Structure-property relationship in flame retardant polymers. *Journal of Macromolecular Science: Physics* B41:1321–30.
57. Marosfői, B., Szabo, A., Kiss, K., and Marosi, G. 2009. Use of organosilicone composites as flame retardant additives and coating for polypropylene. In: *Fire Retardancy of Polymers*, eds. Kandola, K. and Hull, R. Cambridge, U.K.: Royal Society of Chemistry, pp. 49–58.

14 Fundamentals of Fire Testing and What Tests Measure

Marc Janssens

CONTENTS

14.1	Fundamentals of Fire Testing.....	350
14.1.1	Typical Development of a Compartment Fire.....	350
14.1.1.1	Initiation	350
14.1.1.2	Pre-Flashover Stage.....	351
14.1.1.3	Flashover	351
14.1.1.4	Post-Flashover Stage	351
14.1.2	The NFPA 550 Fire Concepts Tree.....	352
14.1.3	Reaction to Fire of Materials	352
14.1.3.1	Ignition	352
14.1.3.2	Heat Release	353
14.1.3.3	Surface Flame Spread	353
14.1.3.4	Production of Smoke and Toxic and Corrosive Products of Combustion	353
14.1.4	Types of Flammability Tests.....	354
14.1.4.1	Small Heat Source Ignition Tests	354
14.1.4.2	Bench-Scale Reaction-to-Fire Tests	354
14.1.4.3	Large-Scale Reaction-to-Fire Tests.....	355
14.2	Small Heat Source Ignition Tests.....	355
14.2.1	General Concepts.....	355
14.2.2	Examples of Small Heat Source Ignition Tests.....	355
14.2.2.1	UL 94 20-mm Vertical Burning Test	355
14.2.2.2	Limiting Oxygen Index Test.....	356
14.2.2.3	Other Small Heat Source Ignition Tests.....	357
14.2.3	Use and Limitations of Small Heat Source Ignition Tests.....	357
14.3	Bench-Scale Reaction-to-Fire Tests.....	358
14.3.1	General Concepts.....	358
14.3.2	Ignition.....	359
14.3.2.1	Pertinent Material Properties	359
14.3.2.2	Ignition Measurements	359
14.3.2.3	Examples of Ignition Tests	360
14.3.3	Heat Release Rate	363
14.3.3.1	Pertinent Material Properties	363
14.3.3.2	Heat Release Rate Measurements	364
14.3.4	Surface Flame Spread	367
14.3.4.1	Pertinent Material Properties	367
14.3.4.2	Surface Flame Spread Measurements.....	368
14.3.4.3	Examples of Flame Spread Tests	368

14.3.5	Smoke and Toxicity.....	370
14.3.5.1	Pertinent Material Properties	370
14.3.5.2	Smoke and Toxicity Measurements.....	371
14.3.5.3	Examples of Smoke and Toxicity Tests.....	374
14.4	Large-Scale Reaction-To-Fire Tests	377
14.4.1	Furniture Calorimeter.....	378
14.4.2	Room/Corner Test.....	378
14.4.3	Other Large-Scale Reaction-To-Fire Tests	380
14.5	Conclusions	380
	Bibliography	381
	Codes and Standards	381
	References Cited	382
	Sources for Additional Information and Further Reading.....	385

14.1 FUNDAMENTALS OF FIRE TESTING

14.1.1 TYPICAL DEVELOPMENT OF A COMPARTMENT FIRE

The fire tests discussed in this chapter are used to evaluate one or several aspects of the behavior of a material in a compartment fire. This behavior is strongly affected by the environmental conditions in the compartment, i.e., the surrounding gas temperature, the incident heat flux to the surface of the material, and the amount of oxygen available for combustion. These conditions change as the fire develops. Compartment fires that progress to burnout typically consist of four stages: initiation, pre-flashover growth stage, flashover, and post-flashover stage. A typical sequence of fire development involving these four stages is briefly described as follows.

14.1.1.1 Initiation

A compartment fire usually starts with the ignition of a small amount of combustible contents or interior finishes due to, for example, a lighter flame, an electrical fault, or a smoldering cigarette. This is illustrated in Figure 14.1a, which shows an upholstered chair shortly after the onset of flaming combustion due to exposure to a small open flame ignition source.

The fire remains limited in size for some time, during which only one item or a small area is involved. A single person can easily extinguish the flames with a small amount of water or a portable extinguisher, but the fire may not be detected at this time. The environment inside the compartment is not yet affected, and there is no major threat to occupants. The fire may be detected when flames are large enough to be visible or when smoke or heat is produced in sufficient quantities to activate a detector.

Some types of materials will first start smoldering when exposed to heat without an open flame ignition source. Smoldering combustion is a slow exothermic surface reaction between a solid fuel and oxygen in the air. Oxygen is needed to support smoldering combustion, but it is consumed at a much smaller rate than in flaming fires. Smoldering fires involve a low rate of mass loss per unit time, but a larger share of lost mass is released as the products of incomplete combustion, in particular carbon monoxide (CO), than in flaming fire conditions.

A smoldering upholstered chair fire in a closed room can cause untenable conditions in approximately 1–2 h, depending on the size of the room.¹ The heat produced by smoldering fires is usually insufficient to activate a sprinkler head. Smoldering fires often make a transition to flaming combustion. It is difficult to predict the occurrence and the time of occurrence of this transition, but it usually happens after conditions near the fire's point of origin have already become untenable due to the elevated concentration of carbon monoxide. However, the number of fire fatalities in the United States due to smoldering fires that do not transition to flaming fires is relatively insignificant.²

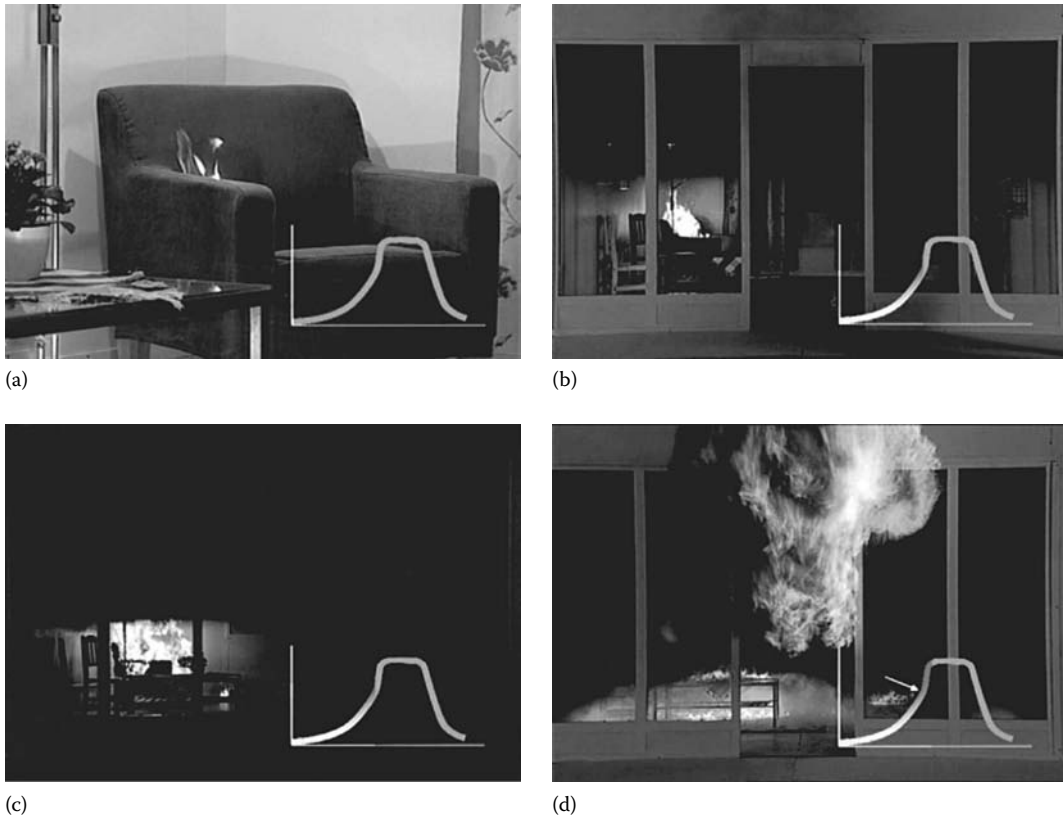


FIGURE 14.1 Compartment fire stages from initiation through flashover. (Courtesy of SP, Borås, Sweden.)

14.1.1.2 Pre-Flashover Stage

As the fire grows, a hot smoke layer accumulates beneath the ceiling and temperatures gradually increase. The fire is still limited to the first item ignited and it becomes increasingly difficult to see exit signs through the smoke layer, as illustrated in Figure 14.1b.

The fire eventually starts spreading beyond the first item ignited (note the burning curtain on the floor in Figure 14.1c) and visibility through the upper smoke layer drops to zero. Conditions become untenable when the heat flux to the lower part of the compartment exceeds a critical level, or when people become exposed to the hot toxic smoke. At this point, it is no longer possible to control the fire with a portable extinguisher.

14.1.1.3 Flashover

When heat fluxes to the lower part of the compartment are high enough to ignite common combustible materials, a rapid transition occurs to a fully developed fire. This transition usually takes less than a minute and is referred to as flashover. When flashover occurs, it is no longer possible to survive in the fire compartment. All exposed combustible materials become involved in the fire (note burning rug and table top in Figure 14.1d). Commonly used criteria for the onset of flashover are a hot smoke layer temperature of 600°C and an incident heat flux at floor level of 20kW/m^2 .

14.1.1.4 Post-Flashover Stage

Flashover leads to the fully developed stage of a fire in which all exposed combustibles in the compartment are involved. The temperatures and heat fluxes in the compartment and the types of combustible materials that are present control the generation rate of fuel volatiles. Typical

temperatures in a fully developed fire are 800°C–1000°C, and corresponding incident heat fluxes range from 75 to 150 kW/m². The flow rate of air into the compartment is primarily determined by the size and shape of the ventilation openings. The supply of air in a fully developed fire is usually below what is needed to burn all fuel volatiles inside the compartment. The fire is therefore ventilation-limited and some fuel volatiles burn outside the compartment; in other words, flames emerge from doors and windows (see Figure 14.1d).

Once a fire reaches the post-flashover stage, it becomes a threat to the entire building. Occupants remote from the fire compartment may be affected and evacuation of the entire building is necessary to avoid casualties. Flames can propagate to other compartments through interior or exterior pathways, and smoke may travel over long distances and pose a threat to occupants in remote parts of the building. According to U.S. fire statistics, post-flashover fires account for approximately 70% of fire fatalities, with the majority of deaths remote from the fire room of origin. Without intervention, the fire will eventually decay and burn out when all combustibles in the compartment are consumed.

14.1.2 THE NFPA 550 FIRE CONCEPTS TREE

NFPA 550, *Fire Safety Concepts Tree*, was first developed in 1974. The document presents a systematic approach and identifies fundamental strategies for achieving a fire-safe environment. NFPA 550 suggests two strategies that pertain specifically to materials whose fire performance can be improved with flame retardants. The first strategy involves preventing, or at least minimizing the likelihood of ignition. Since in practice it is not possible to completely eliminate ignition, the second strategy involves managing the impact of a subsequent fire. The latter is accomplished in part by delaying and reducing the likelihood of flashover, which in turn requires controlling the intensity with which a material burns and releases heat once ignited, its propensity to spread fire, and the rate at which it generates smoke and toxic or corrosive combustion products during gasification and burning.

14.1.3 REACTION TO FIRE OF MATERIALS

The two strategies discussed in Section 14.1.2 are implemented in fire safety codes and regulations. The requirements are based on performance in “flammability” tests, which are intended to evaluate one or multiple aspects of the fire behavior of a material. A distinction can be made between two types of flammability tests. The first type pertains to the initiation stage and evaluates the ignition propensity of a material exposed to a small heat source such as a small flame, a cigarette, or a glowing wire. The second type assesses how a material reacts to the thermal exposure conditions in the pre-flashover stage of a fire and contributes to the fire’s growth toward flashover. The different elements of the reaction to fire of a material are described as follows.

14.1.3.1 Ignition

When a combustible material is exposed to an external radiant heat source, its surface temperature starts to rise. The temperature inside the solid also increases with time, but at a slower rate. Provided the net heat flux into the material is sufficiently high, the surface temperature eventually reaches a level at which thermal decomposition begins. The fuel gases and vapors generated emerge through the exposed surface and mix with air in the gas phase. Under certain conditions, this mixture exceeds the lower flammability limit and ignites.

The initiation of flaming combustion as described in the previous paragraph is termed flaming ignition. Piloted ignition refers to the case when a pilot (small flame, spark igniter, hot wire, etc.) is used to ignite the fuel gases and vapors generated by a pyrolyzing specimen. Autoignition occurs when there is no pilot and the gas mixture is ignited at the hot surface of the material. A specimen of a specific material exposed to a specified irradiance will ignite faster when a pilot is present. Tests to evaluate the ignitability of a material exposed to radiant heat therefore typically include a pilot.

14.1.3.2 Heat Release

The rate at which heat is released in a compartment is the most important factor affecting fire growth toward flashover and the severity of subsequent post-flashover fire conditions. This can be illustrated as follows:

- When large surfaces are involved in the early stages of a fire, pre-flashover growth is determined primarily by the increase of the burning area. As discussed in Section 14.1.3.3, that this increase is primarily due to wind-aided flame spread, the rate of which depends in part on the flame length. The latter is a direct function of the local heat release rate of the pyrolyzing fuel downstream of the area being heated by the flame.³
- The rate of heat release of a fire is the driving force for a buoyant plume. When the plume hits the ceiling, it turns into a ceiling jet whose characteristics determine when heat detectors respond⁴ or when sprinklers are activated.⁵
- Temperature rise in the upper layer in pre-flashover compartment fires has been correlated with the energy release rate.⁶⁻⁸
- The heat from the fire source and the upper layer determines the time when conditions become untenable inside the compartment and consequently the duration for safe egress.⁹
- Given the heat release rate in a compartment as a function of time, models have been developed to predict the transport of hot smoke and toxic gases from this compartment to neighboring compartments.^{10,11} It has been demonstrated, using such models, that heat release rate is the single most important variable in characterizing fire hazard.¹²
- An upper layer temperature of 600°C is frequently been used as a criterion for flashover. This criterion and the aforementioned upper layer temperature correlations resulted in expressions for the heat release rate required for flashover as a function of the geometry of the compartment, the thermal properties of the walls, and the ventilation opening.^{8,13,14}
- Post-flashover fire temperatures also depend mainly on the energy release rate inside the compartment.¹⁵ If the fire is ventilation limited, the heat release rate inside the compartment is controlled by the ventilation factor, which is equal to the product of the area and the square root of the height of the ventilation opening.¹⁶

14.1.3.3 Surface Flame Spread

Flames can spread over a solid surface in two modes. In the wind-aided flame spread mode, flames spread in the same direction as the surrounding airflow. The second mode is referred to as opposed-flow flame spread, which occurs when flames spread in the opposite direction of the surrounding airflow. These two modes are illustrated for flame spread over a flat surface in Figure 14.2.

Flame spread in the upward direction over a vertical wall surface is concurrent with the surrounding airflow and is therefore wind-aided. Flame spread in the downward direction is against the entrained airflow and is of the opposed-flow type. The height of the region that is heated by the flame above the pyrolyzing region is much greater than the height of the heated region below the pyrolyzing region. The former is comparable with the height of the pyrolyzing region and is typically of the order of 1 m. The latter is only a few millimeters at the most. The result is that upward or wind-aided flame spread is much faster than downward or opposed-flow flame spread.

14.1.3.4 Production of Smoke and Toxic and Corrosive Products of Combustion

Fires generate particulate matter, which reduces the intensity of light transmitted through smoke. The distance at which an exit sign can be seen through a smoke layer is a direct function of the concentration of particulates in the smoke.¹⁷

Fires also generate toxic products of combustion, primarily in gaseous form. There are two types of toxic gases: narcotic gases such as carbon monoxide (CO) and hydrogen cyanide (HCN), and irritant gases such as hydrochloric acid (HCl) and hydrogen bromide (HBr). Narcotic gases are absorbed into the blood stream and reduce the intake of oxygen, which can lead to loss of

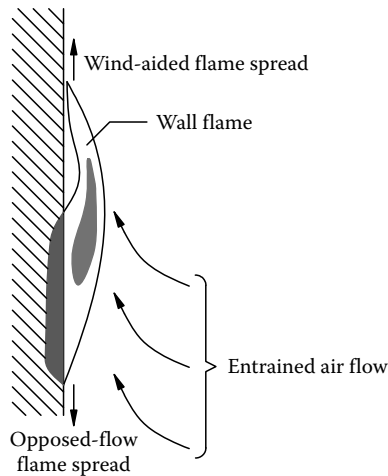


FIGURE 14.2 Modes of flame spread.

consciousness and death. Irritant gases cause respiratory distress and indirectly contribute to incapacitation and lethality during exposure to fire gases. Inflammation of the respiratory tract may result in death within days or even weeks after the fire.

Acid gases can also cause corrosion damage to electronic and computer equipment.

14.1.4 TYPES OF FLAMMABILITY TESTS

This section provides a brief overview of the three different types of flammability tests that are in use. A more detailed discussion with specific examples follows in subsequent sections.

14.1.4.1 Small Heat Source Ignition Tests

A large variety of combustible materials are typically used throughout buildings and in transportation vehicles. A major concern is that these materials might easily ignite when exposed to a small heat source and, thus, support flame propagation that quickly leads to a catastrophic fire. This concern can be addressed by requiring that materials used in significant quantities do not ignite or support flame propagation when exposed to a small heat source. A large number of small heat source ignition tests have been developed for this purpose.¹⁸

For some materials, or under certain conditions, combustion is not in the gas phase but in the solid phase. In such cases, no flame can be observed and the surface is glowing. This very different phenomenon is termed smoldering ignition. Flaming combustion can be preceded by glowing ignition for char-forming materials exposed to low heat fluxes. Several small heat source ignition tests evaluate the smoldering ignition propensity of materials. The most common of these test methods are used to evaluate the ignition propensity of upholstered furniture components and composites exposed to the heat from a smoldering cigarette. Performance in these tests is assessed on the basis of specimen mass loss or the extent of charring and thermal degradation.

14.1.4.2 Bench-Scale Reaction-to-Fire Tests

Bench-scale reaction-to-fire tests are used to characterize the behavior of materials under more severe thermal exposure conditions that are representative of the growing pre-flashover stage of a compartment fire. These tests essentially determine how a material responds to the temperatures and heat fluxes in a growing fire. In these tests, the fire conditions are simulated with a radiant panel or by inserting the specimen into a small furnace. A pilot may be used to ignite the flammable gases and vapors that are generated as a result of thermal decomposition of the

specimen. Performance of a material is quantified on the basis of one or several of the different reaction-to-fire characteristics, which are typically obtained over a range of thermal exposure conditions.

14.1.4.3 Large-Scale Reaction-to-Fire Tests

In some cases, it is not possible to evaluate a material or product (combination of materials) in a bench-scale test in a manner that is representative of its end-use. For example, it is difficult to use a bench-scale test method to evaluate the effect of joints on the fire performance of a thick sandwich panel that consists of a plastic foam core and metal skins. In this case, a room test is used to assess the reaction to fire of the materials. It is also very difficult to assess the fire performance of complex objects such as upholstered furniture based on the reaction-to-fire characteristics of the object's components. Large-scale reaction-to-fire tests have been developed to evaluate these complex objects.

14.2 SMALL HEAT SOURCE IGNITION TESTS

14.2.1 GENERAL CONCEPTS

Tests of this type expose a relatively small specimen (linear dimensions of the order of centimeters) to a small heat source (Bunsen burner type flame, glowing wire, smoldering cigarette, etc.) for a short duration (seconds). Pass/fail criteria are based on the ignition of the specimen during exposure, formation of flaming droplets, extent or rate of flame propagation over the specimen surface, or sustained flaming or smoldering after removing the heat source. A few commonly used small heat source ignition tests are described as follows.

14.2.2 EXAMPLES OF SMALL HEAT SOURCE IGNITION TESTS

14.2.2.1 UL 94 20-mm Vertical Burning Test

The UL 94 standard specifies bench-scale test methods to determine the acceptability of plastic materials for use in appliances or other devices with respect to flammability under controlled laboratory conditions. The test method that is used depends on the intended end-use of the material and its orientation in the device. The standard outlines two horizontal burning tests, three vertical burning tests, and a radiant panel flame spread test. The most commonly used test method described in the UL 94 standard is the "20-mm Vertical Burning Test; V-0, V-1, or V-2." The method is also described in ASTM D 3801. A schematic of the test setup is shown in Figure 14.3.

The flame is maintained for 10 s, and then removed to a distance of at least 150 mm. Upon flame removal, the specimen is observed for flaming and its duration time recorded. As soon as the flame ceases, the burner flame is reapplied for an additional 10 s, then removed again. Duration of flaming or glowing after the second flame application is recorded. Ignition of the cotton by dripping particles from the test specimen is noted. On the basis of the results for five specimens tested, the material is classified as either V-0, V-1, or V-2.

The results of the UL 94 20-mm vertical burning test are very sensitive to the exact duration of flame application and to the technique that is used to apply and remove the flame.¹⁹ The magnitude of the effect depends on the type of material that is being tested. Loosely following the test procedure might result in an unwarranted V-0 classification.

Specimen thickness affects performance in the test as was recently demonstrated in a study involving 18 plastics.²⁰ The materials were tested in two thicknesses, 1.6 and 3.2 mm. Specimen thickness did not affect the rating for most materials but for some the rating changed from V-0 to V-2 (two materials), from V-0 to not rated (one material), and from V-1 to not rated (one material). Small heat source ignition test standards therefore nearly always require that at least the minimum end-use thickness be tested.

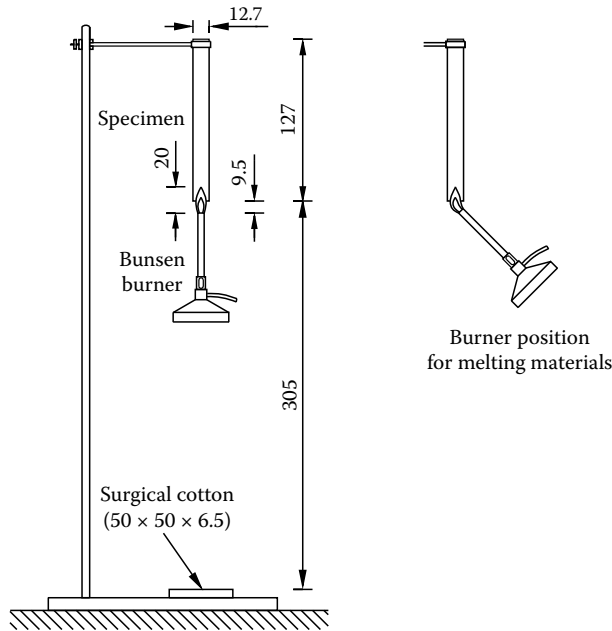


FIGURE 14.3 UL 94 20-mm vertical burning test (dimensions in millimeters).

14.2.2.2 Limiting Oxygen Index Test

The limiting oxygen index (LOI) test is standardized in North America as ASTM D 2863 and internationally as ISO 4589-2. The LOI apparatus consists of a glass tube of 75–100 mm in diameter and 450–500 mm in height. Figure 14.4 shows a schematic of the apparatus. A specimen with a height between 70 and 200 mm and a width of 7–52 mm is supported inside the glass tube. A gas mixture of oxygen and nitrogen is supplied at the bottom of the tube and a small candle-like flame is applied to the top of the specimen in an attempt to ignite it. The objective is to find the minimum oxygen

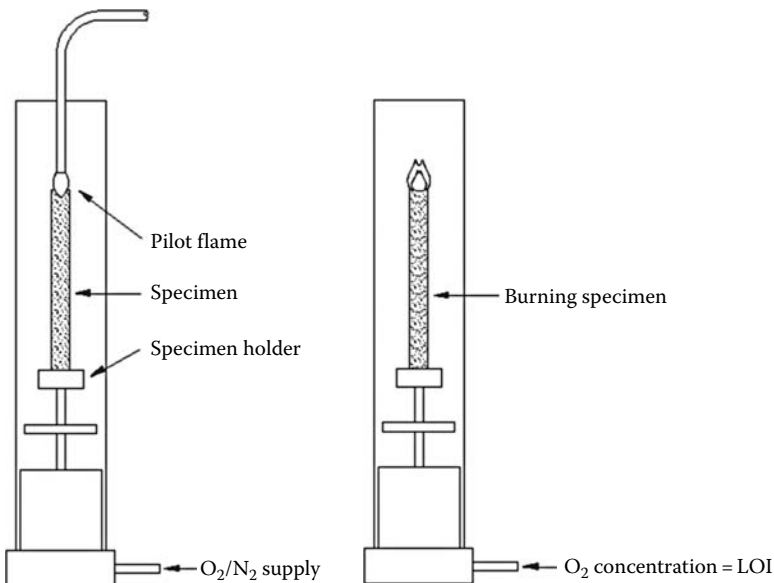


FIGURE 14.4 Limiting oxygen index test (LOI).

concentration in nitrogen that will result in sustained combustion for at least 3 min or excessive flame propagation down the specimen. The dimensions of the specimen and the limit of excessive flame propagation depend on the type of material that is being tested.

14.2.2.3 Other Small Heat Source Ignition Tests

A large number of flammability tests have been developed to evaluate the ignition propensity of a wide range of materials exposed, usually for a short duration, to a small heat source. For example, the most recent compilation of ASTM fire standards includes 30 small heat source ignition tests.²¹ When adding methods that use an electric arc, hot wire, hot surface, etc., instead of a flame and those developed by other standard organizations (NFPA, UL, ISO, IEC, etc.), the total number of tests is in the hundreds.

Conceptually all small heat source ignition tests are very similar. The examples described in Sections 14.2.2.1 and 14.2.2.2 illustrate these concepts. Other examples of commonly used small heat source ignition tests are California Technical Bulletin 117 (CAL TB 117), Federal Motor Vehicle Safety Standard 302 (FMVSS 302), and IEC 60695-2-13. CAL TB 117 describes a test procedure for evaluating cigarette and small flame ignition resistance of resilient filling materials for use in upholstered furniture. FMVSS 302 describes a small flame ignition test method for exposed materials in the passenger compartment of motor vehicles. The IEC test method assesses the susceptibility of electrical insulating materials to ignition as a result of exposure to a glowing wire.

14.2.3 USE AND LIMITATIONS OF SMALL HEAT SOURCE IGNITION TESTS

Fire safety codes and regulations have requirements that are based on small heat source ignition tests. The objective of these requirements is to greatly reduce the probability of a relatively benign ignition source causing a major catastrophic fire (first strategy in the NFPA 550 *Fire Concepts Tree*).

It is easy to see that the aforementioned requirements have a noticeable and positive impact on fire statistics. For example, the significantly lower number of fatalities per capita in fires involving television sets in the United States compared with Europe can be attributed to the UL 94 V-0 requirement for the plastic housing in North America.²²

However, good performance in a small heat source ignition test can give a false sense of confidence as far as a material's behavior in real fires is concerned. Performance in the test depends on how it is measured, i.e., how the pass/fail or classification criteria are defined. Whether a material will ignite in the test depends on many factors such as

- Specimen size, in particular thickness
- Specimen orientation and direction of flame propagation
- Specimen mounting and substrate
- Type and intensity of the heat source and duration of its application

A material that does very well in the test might perform very differently in a real fire if any of these factors are different. For example, a V-0 rated material is not expected to ignite when subjected in a real fire to a heat source similar to that in the test. But what would happen if the real source is more severe or persists beyond the exposure time in the test? The results could be dramatically different. Ignition might occur and flames might subsequently propagate over the surface and quickly result in a catastrophic fire. There are numerous examples of materials that pass a flammability test successfully, but perform miserably under slightly more severe real fire conditions.

In 1974, the U.S. Federal Trade Commission issued a consent order that resulted in the withdrawal of ASTM D 1692. The order was motivated by the fact that some ASTM flammability test standards used terms such as “nonburning” and “self-extinguishing” to label materials that perform well in the test. The Commission determined that these terms give the public a false sense of confidence in the actual fire performance of these materials. ASTM subsequently drafted a policy to

ensure that the limitations of using test results for assessing the fire hazard and risk of materials, products, and assemblies be clearly stated in its fire test standards. The policy is no longer in effect, but the issue is addressed by the requirement that the following caveat be included in the scope section of every ASTM fire test standard: This standard is used to measure and describe the response of materials, products, or assemblies to heat and flame under controlled conditions, but does not by itself incorporate all factors required for fire hazard or fire risk assessment of the materials, products, or assemblies under actual fire conditions. The caveat concisely sums up the main limitation of all flammability tests.

Small heat source ignition tests generally appear to be very sensitive to the composition of the material and some are therefore ideally suited to serve as a tool for formulation development and quality assurance of fire-retardant-treated products and materials. The equipment is inexpensive, only a small quantity of material is needed, the results are usually reasonably repeatable and reproducible, and a qualified laboratory technician can run many tests in a short time.

14.3 BENCH-SCALE REACTION-TO-FIRE TESTS

The purpose of bench-scale reaction-to-fire tests is to measure the flammability characteristics of materials, i.e., ease of ignition, flame spread propensity, heat release, and production of smoke and toxic combustion products. Some tests are designed to measure only one of these characteristics. Other tests are more sophisticated and can be used to measure several characteristics at the same time.

14.3.1 GENERAL CONCEPTS

Bench-scale reaction-to-fire tests characterize the behavior of materials under thermal exposure conditions that are representative of the growing pre-flashover stage of a compartment fire. The fire conditions are typically simulated in these bench-scale reaction-to-fire tests by exposing the specimen to the heat flux from a gas-fired radiant panel or an electrical heater. The range of heat fluxes that can be obtained in a particular test apparatus depends on the specimen-heater geometry and the type of radiant heat source that is used. Between different tests, heat fluxes vary over a broad range, from approximately 1 kW/m^2 to more than 100 kW/m^2 . The heat flux to the specimen is specified in some test standards and is variable in others. Tests for measuring flame spread characteristics typically expose the specimen to a heat flux that varies in the direction of its largest dimension.

An important aspect of the heater is its ability to maintain the emitted radiant heat flux at a constant level during a test. If the heater is operated at a constant power level, incident radiant heat flux changes during testing. At the start of a test, a cold specimen is inserted. The specimen acts as a heat sink, resulting in a decrease of the heater temperature, and consequently a decrease of the incident radiant heat flux. After ignition, the heat released by the specimen results in an increase of the heater temperature and the incident radiant heat flux. To maintain the incident radiant heat flux during a test, it is therefore necessary to keep the temperature of the heater constant. This is not trivial with a gas-fired radiant panel, but relatively straightforward for electrical heating elements.

Two types of electrical heaters are used: high and low temperature. The former are commonly tungsten filament lamps that operate at temperatures close to 2600 K . According to Wien's displacement law, peak radiant heat flux from such lamps is at a much shorter wavelength than for real fires, with temperatures in the range of $600\text{--}1400 \text{ K}$. Piloted ignition studies on plastics and wood have shown that these materials absorb much less radiation in the visible and near-infrared range, than at higher wavelengths.^{23,24} Specimens that are tested in an apparatus with tungsten filament lamps therefore have to be covered with a thin black coating. A procedure is described in the Fire Propagation Test standard ASTM E 2058.

The heat flux can also be provided with a gas burner flame in contact with the specimen. Incident heat flux from impinging gas burner flames is primarily convective and can only be adjusted over a

narrow range. A gas burner flame is therefore not a suitable heat source if the response of a material over a range of heat fluxes is to be determined.

Finally, a small furnace is sometimes used to create the desired thermal exposure conditions. A furnace arrangement is ideal when the objective is to create a constant or specified time-varying temperature environment.

A pilot flame, spark plug, or hot wire is often used to ignite the gases and vapors that are generated by the pyrolysis of the heated specimen. When a pilot flame is used, it is either located in the gas phase or impinging on the specimen surface. The latter is less desirable because it locally increases the heat flux to the specimen by an unknown amount.

A pilot flame is sometimes extinguished by fire retardants or halogens in the fuel volatiles. An electric spark remains stable when fire retardants or halogens are present. However, it occupies a small volume, so that the positioning of the spark plug is more critical than with a pilot flame. A glowing wire is not an efficient method for igniting fuel volatiles, leading to poor repeatability.

14.3.2 IGNITION

The performance of a material in a growing pre-flashover fire is affected by its ignition characteristics in primarily two ways. First, flame spread over the surface of the material can be viewed as a series of subsequent ignitions of incremental areas. Second, the flame spread process is typically initiated in an area that is heated by an impinging flame from a burning object. In both cases, a flame is present in the vicinity of the material that is heated to ignition. The focus of this section is therefore on piloted ignition.

14.3.2.1 Pertinent Material Properties

The propensity for piloted ignition is characterized by two intrinsic material properties. The first property quantifies a critical condition for ignition. Piloted ignition occurs when the lower flammability limit is reached in the fuel–air mixture around the pilot. Consequently, a critical mass flux criterion appears to be logical. This has been proposed,²⁵ but unfortunately it is not very practical. The most common criterion is based on the assumption that ignition occurs when a critical temperature at the surface, T_{ig} , is reached. The surface temperature at ignition of a thermoplastic is reasonably constant and independent of heat flux.^{26,27} Numerous investigators measured T_{ig} for a range of wood products.^{28–35} Reasonably constant values were found for each material at heat fluxes $\geq 25 \text{ kW/m}^2$. All studies reported a significant increase of T_{ig} at lower heat fluxes (50°C – 150°C at 15 kW/m^2). This is due to the fact that pyrolysis and char formation at the surface are no longer negligible for ignition times exceeding 3 min. Under those conditions, one of the basic assumptions of thermal ignition theory, i.e., that the specimen behaves as an inert solid, is no longer valid.

The second property is the thermal inertia, $k\rho c$. This property is a measure of how fast the surface temperature of a material rises when exposed to heat. A material with lower $k\rho c$ will ignite faster than a material with higher $k\rho c$ and the same T_{ig} exposed to the same heat flux.

The minimum heat flux for ignition, \dot{q}_{min}'' , is closely related to T_{ig} . This heat flux is just sufficient to heat the material surface to T_{ig} for very long exposure times (theoretically ∞). The minimum heat flux is not a true material property, because it depends on the rate of convective cooling from the surface. This, in turn, depends primarily on the orientation, size, and flow field around the exposed surface. Since these are different in a bench-scale test versus a real fire, the minimum heat flux determined based on test data is an approximate value. To make the distinction, it is referred to as the critical heat flux for ignition, \dot{q}_{cr}'' . Since the rate of convective cooling in a bench-scale test is generally smaller than in a real fire, \dot{q}_{cr}'' is a conservative estimate of \dot{q}_{min}'' .

14.3.2.2 Ignition Measurements

Ignition properties can be determined by direct measurements. T_{ig} can be measured with fine thermocouples attached to the exposed surface of ignition test specimens, or by using an optical pyrometer. ASTM D 1929 is a bench-scale furnace test method to determine piloted ignition and

autoignition temperatures of plastics (Section 14.3.2.3.1). The latter are reasonably accurate, but the former are not, because the pilot is located too far above the specimen.¹⁸

\dot{q}_{cr}'' can be determined by bracketing, i.e., by conducting experiments that incrementally decrease the heat flux levels until ignition does not occur within a specified period (usually 10 or 20 min). $k\rho c$ can be determined by measuring thermal conductivity, density, and specific heat separately. However, since k and c are temperature-dependent, measurements at elevated temperature are needed.

Because it is very tedious to measure T_{ig} and $k\rho c$ directly, it is much more common to determine ignition properties on the basis of an analysis of time-to-ignition data obtained over a range of heat fluxes. The analysis is usually based on a simple heat conduction model, which assumes that the solid is inert (negligible pyrolysis prior to ignition) and thermally thick (heat wave does not reach the back surface prior to ignition). An example of this type of analysis is discussed in Section 14.3.2.3.2.

Ignition is determined on the basis of visual observation. This can be tricky when the material exhibits extensive flashing before sustained flaming. An alternative method based on the second time derivative of the mass of the specimen has been suggested to alleviate this problem.^{36,37}

14.3.2.3 Examples of Ignition Tests

14.3.2.3.1 ASTM D 1929

The test apparatus consists of a small tubular furnace, with an inside diameter of 76 mm and a height of 210–250 mm (see Figure 14.5). A controlled flow of ambient air is supplied at the bottom of the apparatus. A specimen with an area of 20 × 20 mm is inserted into the furnace from the top. Specimen height is 50 mm for materials with a density of 100 kg/m³ or less. For materials with a higher density, the height of the specimen is adjusted so that its mass is equal to 3 g. The air temperature in the furnace is increased at increments 10°C and tests are repeated until ignition is observed. Tests are performed with and without pilot flame to determine the flash ignition temperature (FIT) and spontaneous ignition temperature (SIT), respectively. The former is equal to the piloted ignition temperature, T_{ig} .

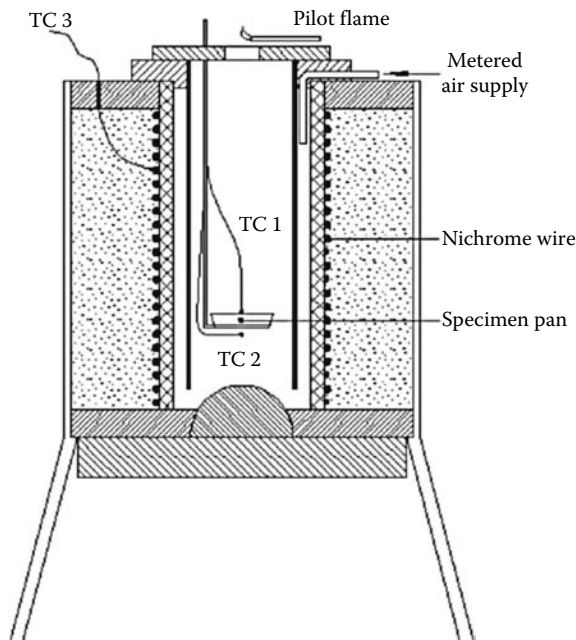


FIGURE 14.5 ASTM D 1929 test apparatus.

14.3.2.3.2 Lateral Ignition and Flame Spread Test (ASTM E 1321)

The Lateral Ignition and Flame spread Test (LIFT) apparatus was developed primarily for lateral flame spread measurements. The apparatus, test procedures, and methods for data analysis are described in ASTM E 1321. A sample of 155 × 800 mm is exposed to the radiant heat of a gas-fired panel. The panel measures 280 × 483 mm. The heat flux is not uniform over the specimen, but varies along the long axis as a function of distance from the hot end as shown in Figure 14.6. The flux distribution is an invariant of distance when normalized to the heat flux at the 50 mm position. When methane or natural gas is burnt, the upper limit of the radiant heat flux is 60–65 kW/m². The lower limit is approximately 10 kW/m² since the porous ceramic tile surface of the panel is only partly covered with flame at lower heat fluxes.

In flame spread tests, the specimen is ignited at the hot end by a nonimpinging premixed acetylene-air pilot flame. Flame spread rate over the surface is then monitored as a function of distance x . Thus, one experiment yields information on flame spread rate over a whole range of heat flux levels (or surface temperatures). Information to this extent can be obtained in one run owing to the particular shape of the flux invariant, which is the result of the specific geometry and specimen-panel arrangement shown in Figure 14.7.

The heat flux distribution is fairly uniform over the first 100–150 mm. Therefore, the same apparatus, with some slight modifications, may also be used for ignitability measurements. A 155 × 155 mm specimen is positioned at the hot end in the flame spread sample holder. An acetylene-air pilot is located

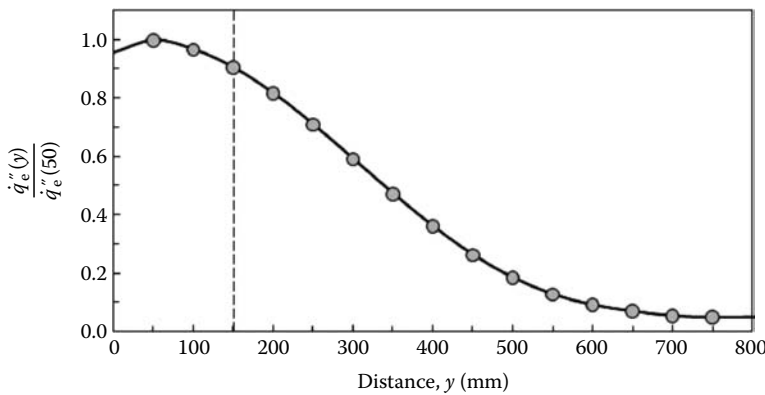


FIGURE 14.6 Radiant heat flux profile in the LIFT.

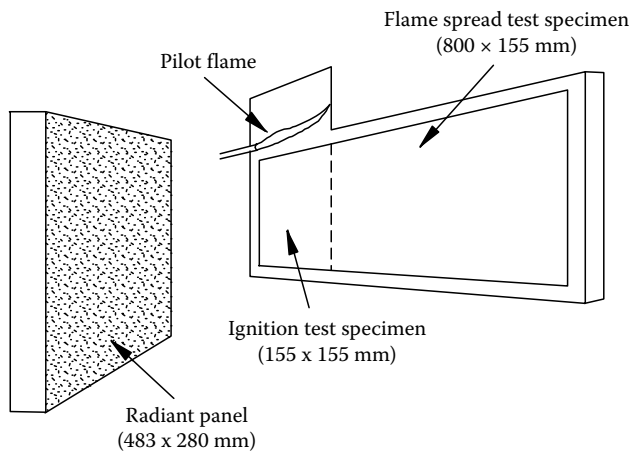


FIGURE 14.7 Schematic of the LIFT.

in the boundary layer above the specimen. A steel plate is attached to the sample holder to extend the boundary layer. The specimen is wrapped in aluminum foil and backed by a low-density ceramic fiber board. The LIFT apparatus as used for piloted ignition testing is illustrated in Figure 14.7.

Quintiere and Harkleroad developed a practical method for analyzing ignition data obtained with the LIFT apparatus.³⁸ The method is described in ASTM E 1321. The first step of the method consists of conducting ignition tests starting at a radiant heat flux level near the maximum for the apparatus (60–65 kW/m²). Time to ignition is obtained at heat flux levels in descending order at intervals of 5–10 kW/m², preferably with some replicates. When ignition time becomes sufficiently long (of the order of 10 min), data are obtained at heat flux levels more closely together (1.5–2 kW/m² intervals). At a certain level, ignition will no longer occur within the (arbitrary) maximum test duration of 20 min. The critical heat flux is taken to be slightly above this level. Usually, a few more tests are conducted around this level to confirm its value. Once the critical heat flux is known, T_{ig} can be calculated from a heat balance at the surface (see Figure 14.8) after very long exposure, since heat conduction into the specimen then becomes negligible:

$$\varepsilon \dot{q}_{cr}'' = h_c(T_{ig} - T_\infty) + \varepsilon \sigma(T_E^4 - T_\infty^4) \equiv h_{ig}(T_{ig} - T_\infty) \quad (14.1)$$

where

ε is the surface emissivity

h_c is the convection coefficient (kW/m²·K)

T_∞ is the ambient temperature (K)

σ is the Boltzmann constant (5.67·10⁻¹¹ kW/m²·K⁴)

h_{ig} is the total heat transfer coefficient at ignition (kW/m²·K)

Surface temperature measurements under steady-state conditions for a number of inert materials and some combustible materials resulted in the following fit³⁸:

$$\dot{q}_{cr}'' = 0.015(T_{ig} - T_\infty) + \sigma(T_{ig}^4 - T_\infty^4) \equiv h_{ig}(T_{ig} - T_\infty) \quad (14.2)$$

Thus, if specimens are heated for a sufficiently long time in the LIFT apparatus, it may be assumed that $\varepsilon = 1$ and that $h_c = 15$ W/m²·K. Once T_{ig} is calculated from the empirical value for \dot{q}_{cr}'' via Equation 14.2, a total heat transfer coefficient from the surface at ignition can be obtained by rearranging this equation as follows:

$$h_{ig} \equiv \frac{\dot{q}_{cr}''}{T_{ig} - T_\infty} = 0.015 + \sigma \frac{T_{ig}^4 - T_\infty^4}{T_{ig} - T_\infty} \quad (14.3)$$

The surface temperature at ignition for exposure to a constant radiant heat flux is approximated by

$$T_{ig} = T_\infty + \frac{\dot{q}_e''}{h_{ig}} F(t_{ig}) \quad \text{with} \quad F(t) = \begin{cases} \frac{2h_{ig}\sqrt{t}}{\sqrt{\pi k \rho c}} & \text{small } t \\ 1 & \text{large } t \end{cases} \quad (14.4)$$

where

t_{ig} is the time to ignition at incident heat flux \dot{q}_e'' (s)

F is the function of time

This leads to the following expression for correlation of piloted ignition data:

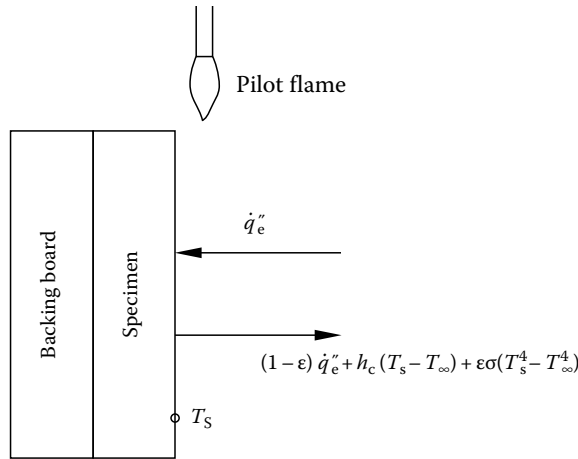


FIGURE 14.8 Schematic of a piloted ignition experiment.

$$\frac{\dot{q}_{cr}''}{\dot{q}_e''} = F(t_{ig}) = \begin{cases} \frac{2 h_{ig} \sqrt{t_{ig}}}{\sqrt{\pi k \rho c}} & t_{ig} \leq t^* \\ 1 & t_{ig} > t^* \end{cases} \quad (14.5)$$

where t^* is the time to reach steady conditions (s).

Thus, all data are plotted in a graph of $\dot{q}_{cr}''/\dot{q}_e''$ versus $\sqrt{t_{ig}}$. An “apparent” value for $k\rho c$ can be calculated from the slope of the line through zero that best fits the data. This line crosses $\dot{q}_{cr}''/\dot{q}_e''=1$ at t^* , the time needed to reach “steady-state” conditions. The functional form of Equation 14.5 for small times is identical to that of the solution of the one-dimensional heat conduction equation for a semi-infinite solid exposed to a constant heat flux without heat losses from the surface. Consequently, $k\rho c$ values obtained with this procedure are higher than the actual average values. The same procedure can be used to analyze piloted ignition data obtained with the Cone Calorimeter (see Section 14.3.3.2.1), provided an adjustment is made to h_c to account for the differences in convective cooling conditions.

14.3.2.3.3 Other Ignition Tests

The time to ignition as a function of incident radiant heat flux can also be measured in the ISO ignitability test apparatus. This apparatus and its use are described in ISO 5657. Bench-scale heat release calorimeters such as the Cone Calorimeter (Section 14.3.3.2.1) and the Fire Propagation Apparatus (Section 14.3.3.2.3) can also be used to obtain this kind of data.

14.3.3 HEAT RELEASE RATE

14.3.3.1 Pertinent Material Properties

There are two intrinsic material characteristics that are related to heat release rate. These two properties are the effective heat of combustion, ΔH_c (MJ/kg), and the heat of gasification, L (MJ/kg). The effective heat of combustion is the ratio of heat release rate to mass loss rate measured in a bench-scale calorimeter:

$$\Delta H_c \equiv \frac{\dot{Q}''}{\dot{m}''} \quad (14.6)$$

where

\dot{Q}'' is the heat release rate per unit exposed area (kW/m²)

\dot{m}'' is the mass loss rate per unit exposed area (g/m²·s)

ΔH_c is different from the lower calorific value measured in an oxygen bomb calorimeter

The latter is measured in a small container under high pressure and in pure oxygen, conditions that are not representative of real fires. The conditions in bench-scale calorimeters such as the cone calorimeter resemble those in real fires much more closely. For some fuels, in particular gases, both values are nearly identical. However, for charring solids such as wood, ΔH_c is significantly lower and equal to the heat of combustion of the volatiles during flaming combustion.

The second material property is heat of gasification, L , defined as the net heat flow into the material required to convert one unit mass of solid material to volatiles. The net heat flux into the material can be obtained from an energy balance at the surface of the specimen. Typically, a sample exposed in a bench-scale calorimeter is heated by external heaters and by its own flame. Heat is lost from the surface in the form of radiation. Owing to the small sample size, the flame flux is primarily convective, and flame absorption of external heater and specimen surface radiation can be neglected. Hence, L can be defined as

$$L \equiv \frac{\dot{q}_{\text{net}}''}{\dot{m}''} = \frac{\dot{q}_e'' + \dot{q}_f'' - \dot{q}_l''}{\dot{m}''} \quad (14.7)$$

where

L is the heat of gasification (MJ/kg)

\dot{q}_e'' is the heat flux from external sources (kW/m²)

\dot{q}_f'' is the heat flux from the flame (kW/m²)

\dot{q}_l'' is the heat losses from the exposed surface (kW/m²)

14.3.3.2 Heat Release Rate Measurements

A variety of calorimeters have been developed to determine the heat release rate and related properties under a range of conditions. The heat release rate is generally measured on the basis of the oxygen consumption technique,^{39,40} although the generation of carbon dioxide is also used.^{41,42} The oxygen consumption technique is based on the observation that for a wide range of materials undergoing complete combustion, a nearly constant amount of heat is released per unit mass of oxygen consumed.^{43,44} The value is 13.1 ± 0.7 kJ/g of O₂ consumed. This observation, generally referred to as Thornton's rule, implies that it is sufficient to measure the flow rate and oxygen concentration in the exhaust duct of a fire test apparatus to determine the heat release rate of the burning test specimen. In addition, bench-scale calorimeter specimens are usually placed on a load cell to measure the mass loss (rate) during a test.

Some materials exhibit nearly steady mass loss rates when exposed to a fixed radiant heat flux. The surface temperature for these materials reaches a steady value after a short initial transient period, and all terms in Equation 14.7 are approximately constant at a specified heat flux level. L can then be obtained by measuring steady mass loss rates at different radiant heat flux levels, and by plotting \dot{m}'' as a function of \dot{q}_e'' . The reciprocal of the slope of a straight line fitted through the data points is equal to L . The intercept of the line with the abscissa is equal to $\dot{q}_l'' - \dot{q}_f''$. Several investigators have used this technique to obtain average L values for a large number of materials.^{45,46}

14.3.3.2.1 Cone Calorimeter

The cone calorimeter was developed at the National Bureau of Standards (NBS), currently the National Institute of Standards and Technology or NIST by Dr. Vytenis Babrauskas in the early 1980s.⁴⁷ It is presently the most commonly used bench-scale calorimeter. A bibliography compiled

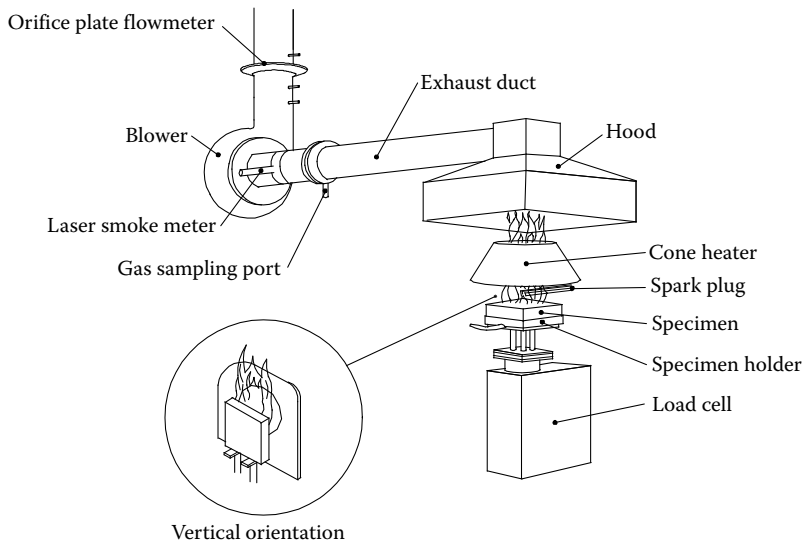


FIGURE 14.9 Cone calorimeter.

by the inventor indicates that over one thousand papers on Cone Calorimeter studies had been published at the end of 2002. The apparatus and test procedure are standardized in the United States as ASTM E 1354 and NFPA 271 and internationally as ISO 5660 Parts 1 and 2. A schematic of the apparatus is shown in Figure 14.9.

A square specimen of 100×100 mm is exposed to the radiant flux of an electric heater. The heater has the shape of a truncated cone (hence the name of the instrument) and is capable of providing heat fluxes to the specimen in the range of $10\text{--}110\text{ kW/m}^2$. Prior to testing, the heater temperature is set at the appropriate value resulting in the desired heat flux. At the start of a test, the specimen in the appropriate holder and the retainer frame (if used) is placed on the load cell, which is located below the heater. An electric spark is used to ignite the pyrolysis products released by the specimen. As soon as sustained flaming is observed, the electric spark igniter is removed. All combustion products and entrained air are collected by an exhaust hood. At a sufficient distance downstream from a mixing orifice, a gas sample is taken and analyzed for oxygen concentration. Measurements of the gas temperature and differential pressure across the orifice plate are used for calculating the mass flow rate of the exhaust gases. The heat released rate can be determined on the basis of the oxygen depletion and the mass flow rate in the exhaust duct.

Most Cone Calorimeters include instrumentation for measuring light extinction in the exhaust duct, using a laser light source, described in ASTM E 1354 and ISO 5660-2 (Section 14.3.5.3.2). Instrumentation to measure concentrations of soot, carbon dioxide, carbon monoxide, and other gases are commonly added. Some laboratories have used a modified version of the standard apparatus to conduct studies in vitiated or oxygen enriched atmospheres.⁴⁸⁻⁵⁰

14.3.3.2.2 FAA Microflow Combustion Calorimeter (ASTM D 7309)

The U.S. Federal Aviation Administration (FAA) developed the Microflow Combustion Calorimeter to assist with the development of fire-resistant polymers for use in commercial passenger aircraft. A schematic of this microscale calorimeter is shown in Figure 14.10. The apparatus is described in ASTM D 7309.

A 1–10 mg specimen (typically between 2 and 5 mg) is heated at a constant rate between 0.2 and 2 K/s in the lower chamber. Decomposition can take place in nitrogen (method A) or in a mixture of nitrogen and oxygen (method B). When method A is used, charforming specimens do not decompose completely and leave a solid residue. In this case, the volatiles are mixed with a metered supply

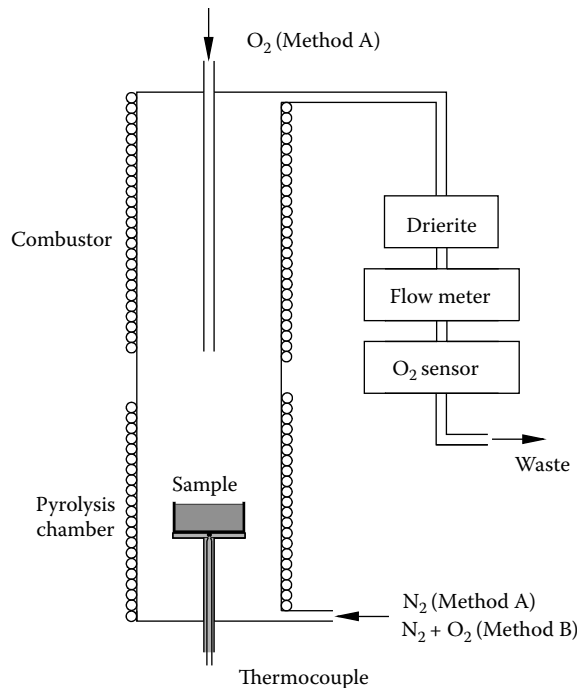


FIGURE 14.10 FAA microflow combustion calorimeter.

of oxygen in the combustor to obtain the heat release rate of the volatiles. When method B is used, the specimen is completely consumed with the exception of any noncombustible components. The total heat released in this case is comparable with that measured in an oxygen bomb calorimeter. The temperature of the combustor is set at approximately 900°C to ensure that all specimen gases are completely oxidized.

Oxygen consumption calorimetry with $E = 13.1 \text{ kJ/g}$ is used to measure heat release rate as a function of time. The specific heat release rate, $Q(t)$, in W/g is equal to the heat release rate divided by the initial specimen mass, m_o . The following five parameters are calculated when method A is used:

1. The heat release capacity $\eta_c \equiv Q_{\max}/\beta$ in $\text{J/g}\cdot\text{K}$, where Q_{\max} is the maximum value of $Q(t)$ and β is the heating rate in K/s .
2. The heat release temperature T_{\max} in K as the pyrolysis chamber temperature at which $Q(t) = Q_{\max}$.
3. The specific heat release h_c in J/g as the area under the $Q(t)$ curve.
4. The pyrolysis residue $Y_p \equiv m_p/m_o$ in g/g , where m_p is the residual mass of the specimen at the end of the test.
5. The specific heat of combustion of the specimen gases $h_{c,\text{gas}} \equiv h_c/(1 - Y_p)$ in J/g .

For method B, only three parameters are calculated:

1. The combustion temperature T_{\max} in K as the pyrolysis chamber temperature, at which the specific heat release rate is the maximum, i.e., $Q(t) = Q_{\max}^0$.
2. The combustion residue $Y_c \equiv m_c/m_o$ in g/g , where m_c is the residual mass of the specimen at the end of the test.
3. The net calorific value h_c^0 in J/g as the area under the $Q(t)$ curve.

The thermal combustion properties measured in the test are related to the flammability characteristics of the material.⁵¹⁻⁵⁵ For example, the heat release temperature from method A approximates the surface temperature at ignition (Section 14.3.2.1). The net calorific value from method B approximates the net heat of combustion measured in an oxygen bomb calorimeter.

14.3.3.2.3 Other Heat Release Rate Calorimeters

The apparatus designed by Professor Ed Smith at Ohio State University is one of the most widely used and best known bench-scale calorimeters.⁵⁶ The test method based on this apparatus was first published as a proposed ASTM standard in 1980. In 1983, it was adopted as ASTM E 906. The standard was later amended to include two configurations of the test apparatus. Configuration A is that which is used by the FAA for assessing aircraft cabin materials at a radiant heat flux of 35 kW/m². The test procedure in this configuration is also described in the FAA *Aircraft Material Fire Test Handbook*.⁵⁷ Configuration B is the original configuration. In both the configurations, heat release rate is determined on the basis of the temperature rise of the exhaust gases.

Factory Mutual Research Corporation (FMRC, currently FM Global Research) developed the Fire Propagation Apparatus (originally referred to as the Combustibility Apparatus) to measure heat release rate and generation rates of smoke and combustion products.⁵⁸ Originally, only convective heat release rate was measured on the basis of temperature rise of the exhaust gases. Test results reported since the late 1970s also include total heat release rates calculated from oxygen consumption or carbon dioxide generation. The standard test method based on the Fire Propagation Apparatus is described in ASTM E 2058.

14.3.4 SURFACE FLAME SPREAD

14.3.4.1 Pertinent Material Properties

As described in Section 14.1.3.3, flames can spread over a surface in two modes, i.e., concurrent with and in the opposite direction of the surrounding air flow. The rate of wind-aided flame spread is typically much higher than that of opposed-flow flame spread, and is therefore of primary concern in fire hazard assessment. To predict the rate of wind-aided flame spread over the surface of a material, it is necessary to determine the heat flux distribution downstream of the pyrolysis front and the thermal response of the material, as its surface temperature increases and eventually reaches the ignition threshold. The former depends primarily on the length of the flame, which, in turn, is a function of the heat release rate of the pyrolyzing fuel and the geometry, e.g., the flame height from a fire with a specified heat release rate is shorter for a flat surface than in a corner.^{59,60} The latter is determined by the ignition properties. In other words, there are no specific material properties pertaining to wind-aided flame spread other than those discussed in Sections 14.3.2.1 and 14.3.3.1.

The rate of opposed-flow flame spread can be determined from the following equation, derived theoretically by deRis.⁶¹

$$V_p = \frac{\phi}{k\rho c (T_{ig} - T_s)^2} \quad (14.8)$$

where

V_p is the flame spread rate (m/s)

ϕ is the flame heating parameter (kW²/m³)

T_s is the surface temperature ahead of the flame front (K)

It is of interest to know under what conditions opposed-flow flame spread ceases. Quintiere and Harkleroad proposed the minimum surface temperature for spread, $T_{s,min}$, as a convenient criterion.³⁸

If the surface temperature just ahead of the pyrolysis front is lower than $T_{s,\min}$, the gas-phase heat conduction from the flame is insufficient to raise the fuel temperature to T_{ig} . Both ϕ and $T_{s,\min}$ are material properties that can be measured in the LIFT apparatus as described in ASTM standard E 1321 (Section 14.3.4.3.2).

14.3.4.2 Surface Flame Spread Measurements

By far the most common and most practical approach to measure the rate of flame spread over a flat surface involves recording the location of the flame tip (wind-aided spread) or flame front (opposed-flow spread) as a function of time based on visual observations. However, in the case of wind-aided flame spread, it is very difficult to track propagation of the pyrolysis front (boundary between the pyrolyzing and nonpyrolyzing fuel) as it is hidden by the flame. This problem can be solved by attaching fine thermocouples to the surface at specified locations as ignition results in an abrupt rise of the surface temperature. This approach is very tedious and not suitable for routine use. An infrared video camera has been used to look through the flame and monitor the upward advancement of the pyrolysis front in a corner fire.⁶²

14.3.4.3 Examples of Flame Spread Tests

Conceptually, there are two types of flame spread tests. The length of the specimen is generally much greater than the width and flame propagation is measured in the direction of the longest dimension. In the first type of flame spread tests, the specimen is exposed to a gas burner flame at one end. In the second type, the specimen is exposed to a radiant panel producing a heat flux that varies from one end of the specimen to the other. A pilot flame is used to ignite the specimen at the hot end. An example of each of the two types is described as follows.

14.3.4.3.1 Steiner Tunnel Test

As mentioned earlier, the fire hazard of interior finish materials is primarily due to the potential for rapid wind-aided flame spread over the surface. It is therefore not a surprise that reaction-to-fire requirements for interior finish materials in U.S. building codes are primarily based on performance in a wind-aided flame spread test. The apparatus of this test is often referred to as the Steiner tunnel. The Steiner tunnel test is described in ASTM E 84. Although the test does not measure any material properties that can be used in a model-based hazard assessment, a discussion of the test is included here due to its practical importance for the passive fire protection of buildings in the United States.

A schematic of the test apparatus is shown in Figure 14.11. It consists of a long tunnel-like enclosure measuring $8.7 \times 0.45 \times 0.31$ m. The test specimen is 7.6 m long and 0.51 m wide, and is mounted in the ceiling position. It is exposed at one end, designated as the burner end, to a 79 kW gas burner. There is a forced draft through the tunnel from the burner end with an average initial air velocity of 1.2 m/s. The measurements consist of flame spread over the surface and smoke obscuration in the exhaust duct of the tunnel. Test duration is 10 min. A flame-spread index (FSI) is calculated on the basis of the area under the curve of flame tip location versus time as follows:

$$FSI = \begin{cases} 0.0282A_T & \text{for } A_T \leq 1783 \text{ m/s} \\ \frac{89611}{3566 - A_T} & \text{for } A_T > 1783 \text{ m/s} \end{cases} \quad (14.9)$$

where

FSI is the ASTM E 84 flame-spread index

A_T is the area under the curve of flame tip location versus time (m/s)

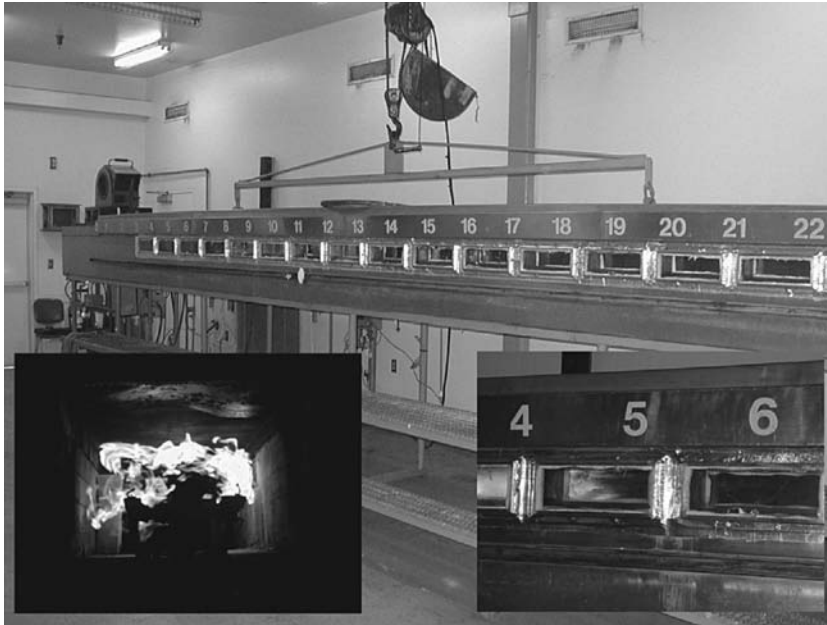


FIGURE 14.11 ASTM E 84 Steiner tunnel test apparatus. Left insert: Burner flame viewed from tunnel inlet. Right insert: Initial flame tip location is 1.37 m (4.5 ft) from the burner. (Photo courtesy of Southwest Research Institute, San Antonio, TX.)

A_T is calculated based on the flame extension, i.e., the distance of the flame tip from the burner minus the length of the burner flame. It is important to note that flame recession is ignored in the calculation of A_T .

The classification of linings in the U.S. model building codes is based on the FSI and SDI (smoke developed index). The latter is based on the area under the light transmission versus time curve normalized to the area for red oak flooring, which by definition has an SDI of 100. There are three classes: Class A for products with $FSI \leq 25$, Class B for products with $25 < FSI \leq 75$, and Class C for products with $75 < FSI \leq 200$. In all cases, the SDI must be 450 or less. Class A products are generally permitted in enclosed vertical exits. Class B products can be used in exit access corridors and Class C products are allowed in other rooms and areas.

14.3.4.3.2 Lateral Ignition and Flame Spread Test

The LIFT apparatus can be used for obtaining opposed-flow flame spread properties. The apparatus is briefly discussed in Section 14.3.2.3.2 and is described in detail in ASTM E 1321. A schematic is shown in Figure 14.7.

The gas flow to the radiant panel is set to obtain a heat flux at the 50 mm location that is 5–10 kW/m² above the critical heat flux for ignition (Section 14.3.2.3.2). The heat flux is verified with a heat flux meter inserted into a calcium silicate dummy specimen. The heat flux profile is shown in Figure 14.6 and can be used to determine the incident radiant heat flux at any location along the specimen center-line. The flux invariant may vary slightly and is usually determined for each apparatus during the initial calibration.

A horizontal line is drawn along the center of the 155 × 800 mm specimen and vertical marks are made on the line at 25 mm intervals. A marked specimen backed by a ceramic fiber insulation board is mounted in the specimen holder. The holder is inserted when the panel reaches equilibrium and the heat flux at the 50 mm position is at the desired level. After preheating to steady conditions (see Equation 14.5 and subsequent discussion), the specimen is ignited at the hot end

with a nonimpinging premixed acetylene flame. The time for the flame to travel to each mark is recorded. The flame spread rate at the location of every mark (except for the two extreme locations) is then calculated from a simple running 3-point least squares fit. The distance from the hot end of the specimen where the flame spread stops is also recorded.

The main objective of conducting LIFT flame spread experiments is to obtain material properties for predicting opposed-flow flame spread. On the basis of the analysis by deRis (see Equation 14.8), the flame heating parameter ϕ can be determined from the slope of a linear fit of $1/\sqrt{V_p(y)}$ plotted as a function of $\dot{q}_e''(y)$, where y is the distance from the hot end of the specimen. The minimum surface temperature for spread, $T_{s,\min}$, is calculated according to an expression akin to Equation 14.4 from the incident heat flux at the maximum distance from the hot end reached by the flame.

14.3.4.3.3 Other Flame Spread Tests

The LIFT apparatus is used in conjunction with an instrumented exhaust stack to qualify finish materials for use on ships that sail on international voyages and need to comply with the SOLAS (Safety of Life at Sea) regulations developed by the International Maritime Organization (IMO). The method is described in ASTM E 1317 and in Part 5 of Annex 1 to the IMO Fire Test Procedures (FTP) code.

The NBS (currently the National Institute of Standards and Technology, or NIST) conducted a series of full-scale fire tests in the 1970s to investigate the fire hazard of floor coverings.⁶³ The main concern was flame spread from a fire room to a connected corridor. This work resulted in the development of the radiant flooring panel test. This test is described in ASTM E 648.

The test method described in ASTM E 162 also evaluates opposed-flow flame spread characteristics of a product, and is referred to in regulations that pertain to various modes of transportation.

14.3.5 SMOKE AND TOXICITY

14.3.5.1 Pertinent Material Properties

The generation rate of smoke (soot) can be written as

$$\dot{m}_s = \dot{m}Y_s \quad (14.10)$$

where

\dot{m}_s is the mass generation rate of soot (g/s)

\dot{m} is the mass loss rate of the fuel (g/s)

Y_s is the soot yield (g/g)

Similarly, the generation rate of toxic gas species can be expressed as

$$\dot{m}_i = \dot{m}Y_i \quad (14.11)$$

where

\dot{m}_i is the mass generation rate of species i (g/s)

Y_i is the yield of species i (g/g)

The yields of soot and toxic gas species are material properties that may vary as a function of vitiation or ventilation. The latter is characterized by the equivalence ratio, i.e., the actual mass ratio of fuel to air divided by the stoichiometric ratio. This implies, for example, that underventilated fires are characterized by an equivalence ratio greater than one.

14.3.5.2 Smoke and Toxicity Measurements

14.3.5.2.1 Smoke

There are essentially two different experimental configurations that are used for quantifying the attenuation of light in fire effluents. The test methods that are based on these two configurations are referred to as static and dynamic, respectively. Different units have been used to report the results of these two types of tests.

The intensity of light passing through smoke is attenuated due to scattering and absorption by the suspended particulates. Light attenuation by smoke is described by the following equation, which is known as the Bouguer or Lambert–Beer law:

$$I = I_0 \exp(-kL) \quad (14.12)$$

where

I is the light intensity measured at the detector (mW)

I_0 is the light intensity at the source (mW)

k is the extinction coefficient (1/m)

L is the path length (m)

The extinction coefficient is the most fundamental smoke measurement in dynamic test methods. The products of combustion generated in these test methods are collected in a hood and extracted through an exhaust duct. The smoke meter consists of a light source on one side of the duct and a detector on the opposite side of the duct. Assuming that the light source is stable, I_0 can be measured at the start of a test. Alternatively, the intensity of the source can be measured during the test if the smoke meter comprises a beam splitter at the light source to divert a fraction of the beam to a reference detector. This arrangement is typically used in laser light source systems. The path length is equal to the diameter of the duct. The extinction coefficient can be calculated from the measured light intensity during a test, and is a direct measure of the concentration of particulates in the exhaust duct. This implies that k is a function of the generation rate of particulates in the fire and the volumetric flow rate in the duct. The smoke production rate is independent of the duct flow rate and is defined as follows:

$$\dot{s} \equiv k\dot{V}_s \quad (14.13)$$

where

\dot{s} is the smoke production rate (m^2/s)

\dot{V}_s is the actual volumetric flow rate at the smoke meter (m^3/s)

The fact that \dot{S} is independent of duct flow rate can be illustrated as follows. Suppose the fire is generating particulates at a constant rate, at some point during a test, the exhaust fan speed is adjusted so that the duct flow rate is doubled. As a result additional ambient air is drawn into the hood and the concentration of particulates in the exhaust is reduced by 50%. The extinction coefficient is therefore also cut in half and the smoke production rate is unchanged.

Sometimes, it is helpful to express the smoke production rate per unit of exposed specimen surface area:

$$\dot{s}'' = \frac{k\dot{V}_s}{A_s} = \frac{\dot{s}}{A_s} \quad (14.14)$$

where

\dot{s}'' is the smoke production rate per unit exposed specimen surface area (1/s)

A_s is the exposed area of the specimen (m^2)

The smoke production rate can also be expressed per unit of specimen mass loss by dividing the RHS in Equation 14.14 by the mass loss rate. The result is referred to as the specific extinction area, because it has the units of area divided by mass.

$$\sigma_f \equiv \frac{\dot{s}}{\dot{m}} = \frac{k\dot{V}_s}{\dot{m}} \quad (14.15)$$

where

σ_f is the specific extinction area (m^2/g)

\dot{m} is the mass loss rate of the specimen (g/s)

The ratio of the light extinction coefficient of flame-generated smoke to the mass concentration of soot in the smoke is approximately constant and equal to $\sigma_s = 8.7 \pm 1.1 \text{ m}^2/\text{g}$.⁶⁴ The implication of this nearly universal value is that the soot yield, i.e., the mass of soot generated per mass unit of fuel burnt, can be estimated from light extinction measurements as follows:

$$Y_s \equiv \frac{\dot{m}_s}{\dot{m}} = \frac{\left(\frac{k}{\sigma_s}\right)\dot{V}_s}{\dot{m}} = \frac{\dot{s}}{\sigma_s \dot{m}} = \frac{\sigma_f}{\sigma_s} \quad (14.16)$$

where σ_s is the ratio of extinction coefficient to soot concentration ($\sigma_s = 8.7 \pm 1.1 \text{ m}^2/\text{g}$).

The extinction coefficient in static methods is typically expressed per unit path length using base 10 logarithms:

$$D = \log\left(\frac{I_0}{I}\right) = \log\left(\frac{100}{T}\right) \quad (14.17)$$

where

D is the optical density

T is the light transmittance (%)

The relationship between k and D is as follows:

$$k = \frac{2.303D}{L} \quad (14.18)$$

The specific optical density is a dimensionless quantity that is defined as follows:

$$D_s \equiv \frac{DV}{A_s L} \quad (14.19)$$

where

D_s is the specific optical density

V is the volume of the chamber in which the smoke is collected (m^3)

Slight variations of the units described in this section have been used. Conversion factors can easily be derived on the basis of the definition of these alternative units.

14.3.5.2.2 Toxicity

Toxic potency of fire effluents can be quantified by evaluating the response of live animals to smoke generated from fires in a controlled atmosphere. Mice, rats, and primates have been used for this purpose. The results are expressed as an LC_{50} value. The LC_{50} is the concentration (by mass) estimated to produce lethality in 50% of the animals within the specified time (typically 30 min). Under pressure from animal rights groups and the general public, bioassay methods have fallen out of favor. Over 20 years of research using bioassay methods supplemented by gas analysis have resulted in an extensive database defining the concentration–response relationship for various materials and toxic gases. This has greatly eliminated the need for animal testing and made it possible to rely primarily on analytical techniques to obtain toxic potency data for fire hazard analysis.

Researchers at the NIST developed a concept to minimize the usage of animals for the assessment of the toxic potency of a material in fires. This concept is based on the well-established hypothesis that a small number (N) of gases in the smoke accounts for a large percentage of the observed toxic potency. Research at NIST of toxicologically important gases and their interactions resulted in the development of the N -Gas Model,⁶⁵ which is expressed by the following equation:

$$FED = \frac{m[CO]}{[CO_2] - b} + \frac{[HCN]}{LC_{50}(HCN)} + \frac{21 - [O_2]}{21 - LC_{50}(O_2)} + \frac{[HCl]}{LC_{50}(HCl)} + \frac{[HBr]}{LC_{50}(HBr)} \quad (14.20)$$

where

FED is the fractional effective exposure dose

m is the constant ($m = -0.0018$ if $[CO_2] \leq 5\%$ and $m = 0.0023$ if $[CO_2] > 5\%$)

$[CO]$ is the concentration of CO (ppm)

b is the constant ($b = 12.2\%$ if $[CO_2] \leq 5\%$ and $b = -3.86\%$ if $[CO_2] > 5\%$)

$[CO_2]$ is the concentration of CO_2 (%)

$[HCN]$ is the concentration of HCN (ppm)

$[O_2]$ is the concentration of O_2 (%)

$[HCl]$ is the concentration of HCl (ppm)

$[HBr]$ is the concentration of HBr (ppm)

$LC_{50}(X)$ is the lethal concentration of species X resulting in 50% mortality (% or ppm)

The constants in Equation 14.20 are based on laboratory tests with deaths within a 30 min exposure period and a 14-day post-exposure period. The LC_{50} values are 150 ppm for HCN, 5.4% for O_2 , 3800 ppm for HCl, and 3000 ppm for HBr. The first term on the RHS of Equation 14.20 indicates that CO and CO_2 interact in a nonlinear way. Theoretically, 50% of the animals should die at $FED = 1$. Instead, due to slight nonlinearities, the 50% lethality level corresponds to $FED = 1.1$.⁶⁶

Equation 14.20 with $FED = 1.1$ can be used in a bench-scale toxicity test to determine the LC_{50} of a material. The test involves burning a specified amount of material and collecting the effluents in a closed chamber. Tests are conducted with varying amounts of material to find the mass loss Δm_{50} that is expected to result in 50% lethality of test animals exposed over a 30-min test duration to the atmosphere in the chamber. The LC_{50} can then be calculated as follows:

$$LC_{50} = \frac{\Delta m_{50}}{V} \quad (14.21)$$

where

LC_{50} is the lethal concentration (g/m^3)

Δm_{50} is the mass loss resulting in $FED = 1.1$ in the chamber after 30 min (g)

V is the volume of the chamber (m^3)

The total mass loss of a material in a pre-flashover fire that will result in a lethal mixture can be theoretically determined as the product of the LC_{50} and the volume in which the products of combustion are distributed. For post-flashover fires, it is necessary to correct the LC_{50} measured in the bench-scale test to account for the increased CO production in these fires.⁶⁷ NIST conducted a series of full-scale validation tests and determined that the smoke from the bench-scale method reproduces that from room fires to within a factor of 3.⁶⁶

$$LC_{50}(\text{corrected}) = \frac{1}{\frac{1}{LC_{50}} + 0.044 - \frac{0.00005[\text{CO}]}{\Delta m}} \quad (14.22)$$

The correction is important because majority of U.S. fire deaths occur remote from the fire room, overall and especially for fires that have proceeded past flashover.⁶⁸

Various methods and instruments are available for measuring gas concentrations in fire effluents, e.g., gas detector tubes, ion-selective electrodes, GC/MS (gas chromatography/mass spectrometry), and Fourier Transform Infrared (FTIR) spectroscopy. An extensive review of the methods is provided in ASTM E 800 and ISO 19701.

14.3.5.3 Examples of Smoke and Toxicity Tests

14.3.5.3.1 NBS Smoke Chamber

The NBS smoke chamber is the most commonly used bench-scale test apparatus for measuring the optical density of smoke. The apparatus and test procedure are described in ASTM E 662. The method was developed at the NBS in the 1960s.⁶⁹

The test apparatus consists of a $0.914 \times 0.610 \times 0.914$ m enclosure (see Figure 14.12). A radiant heater with a diameter of 76 mm is used to provide a constant radiant heat flux of 25 kW/m^2 to the specimen surface. The specimen measures 76×76 mm and is oriented vertically.



FIGURE 14.12 NBS Smoke density chamber with heater described in IMO FTP code. Insert: Close-up view of ASTM E 622 heater. (Photo courtesy of Southwest Research Institute, San Antonio, TX.)

Tests are conducted in two modes. A six-tube premixed pilot burner is used in the flaming mode. The burner flames impinge on the lower half of the specimen surface. The burner is removed to conduct tests in the nonflaming mode. Three replicate tests are typically conducted in each mode. An additional set of three specimens are tested if there is a high variation in the results from the first set.

Smoke density is measured based on the attenuation of a light beam by the smoke accumulating in the closed chamber. A white light source is located at the bottom of the enclosure, and a photomultiplier tube is mounted at the top. A modified version of Equation 14.19 is used to calculate the specific optical density from the measured transmittance:

$$D_s = \frac{V}{A_s L} \left[\log \left(\frac{100}{T} \right) + F \right] = 132 \left[\log \left(\frac{100}{T} \right) + F \right] \quad (14.23)$$

where

V is the volume of the smoke chamber (0.51 m³)

L is the interior height of the chamber (0.91 m)

F is the optical density of the range extension filter if moved out of the light path

A test is terminated 3 min after the light transmittance value reaches a minimum value or 20 min after the start of the test, whichever occurs first. D_s calculated according to Equation 14.23 is reported as a function of time. In addition, the maximum value of the specific smoke density, D_m , is reported separately after correction for soot deposits on the windows of the optical system during the test. The correction is equal to the apparent optical density that is recorded after the test is terminated and the smoke has been cleared from the chamber.

The test method described in ASTM E 662 appears to have some significant limitations, although it is hard to find objective evidence for such limitations. To make the user aware of these limitations, the ASTM committee that developed the standard added the following caveat to the scope section of the document: "This test method is intended for use in research and development and not as a basis for ratings for regulatory purposes." In spite of this caveat, the method is referenced in several fire safety regulations and specifications for materials used in passenger aircraft, Navy ships, and rail transportation vehicles. The acceptance criteria in these regulations and specifications are typically based on the limits for D_s at specified times (typically 1½ or 4 min) or D_m .

The smoke chamber method described in ASTM E 662 is often supplemented with toxic gas analysis. A PTFE-lined stainless steel tube is used to take a gas sample from the geometric center of the chamber at a specified time. This time can be fixed, for example 1½ or 4 min into the test, or variable, for example immediately following the maximum specific optical density. Regulations and specifications that call for these measurements require the concentration of a predefined set of gases to be determined. The product is acceptable if the concentration of every gas is within specified limits. These limits have been established from experience based on data for products that are deemed to be acceptable or not acceptable.

For example, Airbus Industries ABD 0031 and Bombardier SMP 800-C are industry specifications that place limits on the amount of toxic gases that may be generated in the NBS smoke chamber by materials used in aircraft and ground transportation vehicles, respectively. Part 2 of Annex 1 to the IMO FTP Code places limits on the amount of toxic gases that may be generated in the ISO 5659-2 single smoke chamber method by materials used in ships. ISO 5659-2 specifies the same chamber and smoke meter as ASTM E 662, but uses a scaled-down version of the cone calorimeter heater. The gas concentration limits for these three methods are given in Table 14.1.

Static smoke chamber methods have major limitations in terms of being indicative of the fire hazard due to smoke toxicity of products and materials in actual fires. As combustion products accumulate in the chamber during a test, the burning behavior of the test specimen may have a significant effect on the level of vitiation (oxygen concentration) and temperature rise in the chamber.

TABLE 14.1
Toxic Gas Concentration Limits
for Three Static Methods

Airbus	Bombardier	IMO
NA	90,000	NA
1000	3,500	1450
100	100	600
150	500	600
NA	100	600
100	100	350
150	100	140
100	100	120

Consequently, rather than simulating a specific fire scenario, conditions in smoke chamber tests vary over time and are not well-defined. A relatively new tube furnace method greatly alleviates this problem and, for that reason, is gaining increased international acceptance. The method is described in ISO TS 19700.

14.3.5.3.2 Cone Calorimeter

The standard Cone Calorimeter (Section 14.3.3.2.1) described in ASTM E 1354 includes a smoke photometer to measure light extinction in the exhaust duct. The system is based on a laser light source. The same system is also standardized internationally, although it is described in a separate document from the main Cone Calorimeter standard (ISO 5660-2). Smoke measurements are reported in terms of the average specific extinction area (ASTM E 1354 and ISO 5660-2) and the smoke production rate and total smoke production for the period prior to ignition and the flaming period (ISO 5660-2).

The cone calorimeter and other bench- and large-scale calorimeters have also been used to obtain dynamic smoke toxicity data. A continuous gas sample is taken through the oxygen consumption probe or through a separate gas sampling probe and analyzed for the gases of interest. Since the gas concentrations are a function of the flow rate in the exhaust duct, they need to be converted to generation rates or yields. For example, if the gas concentrations are measured on a wet basis (as in an FTIR spectrometer), the generation rate and yield of a particular gas species can be calculated from

$$\dot{m}_i = \frac{X_i \dot{V}_e M_i}{8.2 \cdot 10^{-5} T_e} \quad (14.24)$$

and

$$Y_i = \frac{\dot{m}_i}{\dot{m}} \quad (14.25)$$

where

X_i is the mole fraction of species i in the exhaust duct on a wet basis

\dot{V}_e is the actual volumetric flow rate at the sampling point (m^3/s)

M_i is the molecular mass of species i (g/mol)

T_e is absolute gas temperature at the sampling point (K)

If the gases are measured on a dry basis, the equations need to be adjusted to account for moisture. The derivation of the equations is then similar to those used for calculating heat release rate based on oxygen consumption.

The cone calorimeter is also used to quantify the corrosivity of products of combustion as described in ASTM D 5485. The “Cone Corrosimeter” uses the same load cell, specimen holder, retainer frame, spark igniter, conical heater, and exhaust system as the cone calorimeter. A heated stainless steel sampling tube is connected to a funnel placed on top of the conical heater. A gas sample is continuously drawn from the tube at a rate of 4.5 L/min. The sampling tube is connected with silicone rubber tubing to the pump via an 11.2 L exposure chamber, a filter, and a flow meter. A target is placed in the exposure chamber at the start of the test and exposed to the corrosive atmosphere of the gas sample for 60 min or until the specimen has lost 70% of its total mass loss, whichever occurs first.

The target consists of a printed circuit board with two circuits. One circuit is exposed. The second circuit is protected and is used to compensate for the effect of elevated temperature on the electrical resistance of the circuit. The target is removed from the chamber 1 h after the start of a test and the reduction of the electrical resistance of the exposed circuit is measured. The target is then exposed to an atmosphere of 23°C and relative humidity of 75% for 24 h. The electrical resistance is measured again after the 24 h post-test exposure. The electrical resistance measurements are converted to the equivalent reductions in metal thickness, C_1 and C_2 respectively, expressed in nanometers.

14.3.5.3.3 Other Smoke Toxicity Tests

Two smoke toxicity tests that involve animal exposure are still used in the United States. The University of Pittsburgh, or UPitt, method is required to demonstrate compliance with the requirement in the New York City building code that no construction product shall be more toxic than wood. A small specimen of the product is heated in a muffle furnace, and four mice are exposed to the products of combustion diluted with air. The furnace temperature is ramped at a rate of 5°C/min. The test is terminated after 30 min. The objective is to find the LC_{50} , defined in this case as the quantity of the product in grams that results in 50% mortality of the test animals. A product is acceptable if the LC_{50} is equal to or greater than 19.5 g, which is the value assigned to wood.

The test procedure described in ASTM E 1678 minimizes the number of animal tests. In this test procedure, a specimen is exposed to a radiant heat flux of 50 kW/m², and the products of combustion are collected in a 0.2 m³ chamber. Test duration is 30 min. Additional tests are performed with specimens of different size to find the exposed area that is expected to result in 50% lethality of test animals exposed over the 30-min test duration to the atmosphere in the chamber. The lethality is determined on the basis of analytical measurements of the composition of the contents of the chamber and the *N*-Gas model (see Equation 14.20). To verify the results, two additional tests are conducted with 70% and 140% of that specimen area and six rats exposed to the gases in the chamber.

14.4 LARGE-SCALE REACTION-TO-FIRE TESTS

Often it is very difficult to determine the burning behavior of complex objects on the basis of the performance of its individual components in bench-scale reaction-to-fire tests. It is much more practical to measure the heat release rate and related properties for the complete object. This requires a large-scale test. In other cases, it is not possible to capture certain aspects of real fire behavior such as melting, delamination, joint effects, etc., in a bench-scale test. A large-scale test is needed to assess these effects. Two commonly used large-scale reaction-to-fire tests are test methods are discussed as follows.

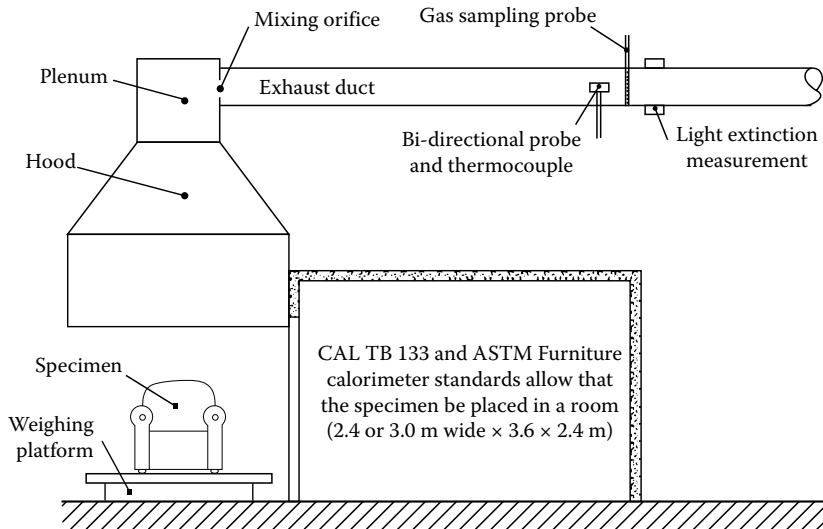


FIGURE 14.13 Furniture calorimeter.

14.4.1 FURNITURE CALORIMETER

It is very hard to determine the burning behavior of upholstered furniture on the basis of the fire characteristics of the foam, fabric, and framing materials and to account for the geometry and configuration of the furniture and how it is ignited. It is much easier to test the entire furniture item. The calorimeter described in the section was developed for this purpose.

A furniture calorimeter consists of a weighing platform that is located on the floor of the laboratory, beneath a hood connected to an instrumented exhaust duct (see Figure 14.13). The object is placed on the platform and ignited with the specified ignition source. The products of combustion are collected in the hood and extracted through the exhaust duct. Measurements of oxygen concentration, flow rate, and light transmission in the exhaust duct are used to determine the heat release rate and smoke production rate from the object as a function of time.

Furniture calorimeters were developed in the 1980s in several laboratories to obtain this kind of data.^{70,71} The first furniture calorimeter test standard was published in 1987 in the Nordic countries as NT Fire 032. Furniture calorimeter test standards have been developed by ASTM for chairs, mattresses, and stacked chairs. The corresponding designations are ASTM E 1537, ASTM E 1590, and ASTM E 1822, respectively. The California Bureau of Home Furnishings and Thermal Insulation (CBHFTI) developed California Technical Bulletins (CAL TB) 133 and 603. These documents describe fire test procedures to qualify seating furniture and mattresses, respectively, for use in public occupancies in California. CAL TB 603 has been superseded by the Federal CPSC standard 16 CFR 1633. The primary difference between the various chair and mattress tests is the ignition source.

14.4.2 ROOM/CORNER TEST

Several standard room/corner test protocols are now available and are specified in codes and regulations for qualifying interior finishes. For example, U.S. model building codes require that textile wall coverings for use in unsprinklered compartments meet specific performance requirements when tested according to NFPA 265. The principal requirement of these tests is that flash-over does not occur. The same codes also require that all other interior wall and ceiling finish materials comply with requirements based on NFPA 286, including a limit on the total smoke released.

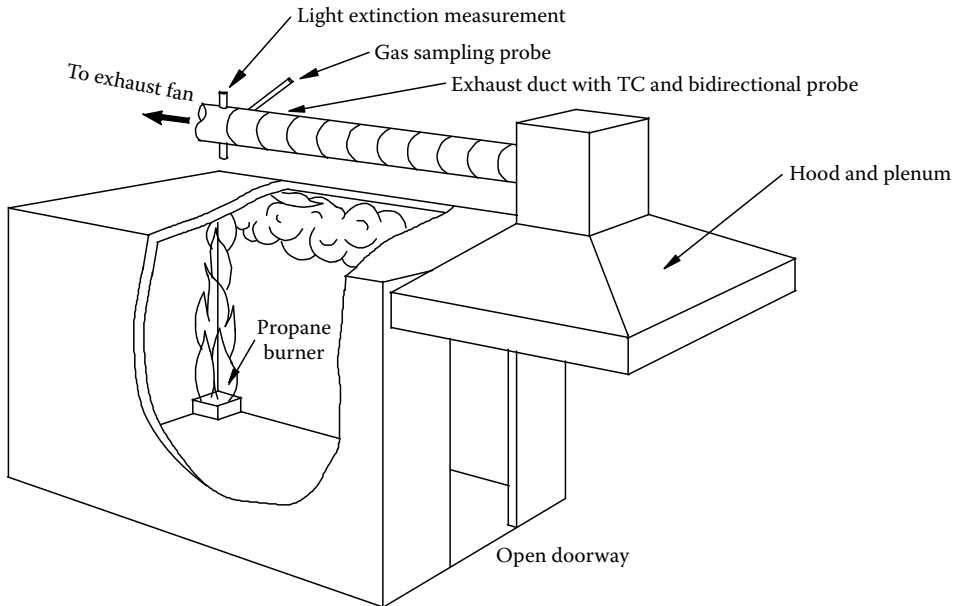


FIGURE 14.14 Room/corner test.

SOLAS permits the use of combustible bulkhead and ceiling linings on high speed craft, provided they meet stringent fire performance requirements based on assessment according to ISO 9705. ASTM E 2257 is the American version of ISO 9705.

The test apparatus and instrumentation described in the NFPA and ISO room/corner test standards are very similar (see Figure 14.14). However, there are some significant differences in terms of specimen configuration and ignition source. The apparatus consists of a room measuring 3.6 m deep by 2.4 m wide by 2.4 m high, with a single ventilation opening (open doorway) measuring approximately 0.8 m wide by 2 m high in the front wall. Walls and ceiling are lined for tests according to ISO 9705. For tests according to the NFPA standards, the interior surfaces of all walls (except the front wall) are covered with the test material. NFPA 286 is also suitable for evaluating ceiling finishes (see subsequent text).

The test material is exposed to a propane burner ignition source, located on the floor in one of the rear corners of the room opposite the doorway. The burner is placed directly against (ISO 9705 and NFPA 286) or at a distance of 50 mm (NFPA 265) from the walls. The ISO burner consists of a steel sandbox measuring $0.17 \times 0.17 \times 0.135$ m. Propane is supplied to the burner at a specified rate such that a net heat release rate of 100 kW is achieved for the first 10 min of the test, followed by 300 kW for the remaining 10 min (20 min test duration, unless terminated when flashover occurs). The NFPA burner consists of a steel sandbox measuring $0.305 \times 0.305 \times 0.152$ m, with the top surface positioned 0.305 m above the floor of the room. Propane is supplied at a specified rate so that a net heat release rate of 40 kW is achieved for the first 5 min of the test, followed by 150 kW (NFPA 265) or 160 kW (NFPA 286) for the remaining 10 min (15 min test duration unless terminated when flashover occurs).

A fundamental difference between NFPA 265 and NFPA 286 is the fact that the flame from the burner alone just touches the ceiling in NFPA 286. This makes it suitable for assessing the fire performance of interior ceiling finish, an application for which NFPA 265 is unsuitable. This effect is partly due to the higher energy release rate of the NFPA 286 burner, but primarily because of the burner being in direct contact with the walls, thereby reducing the area over which the flames can entrain air and increasing the overall flame height.

All combustion products emerging from the room through the open doorway are collected in the standard hood. Instrumentation is provided in the exhaust duct for measuring heat release rate based

on the oxygen consumed (ISO and NFPA standards) and smoke production rate (ISO 9705 and NFPA 286 only). The room contains a single heat flux meter located in the center of the floor. The NFPA standards also specify that seven thermocouples be installed in the upper part of the room and doorway to measure the temperature of hot gases that accumulate beneath the ceiling and exit through the doorway. In addition to quantitative heat release and smoke production rate measurements, time to flashover (if it occurs) is one of the main results of a room/corner test. Different criteria are commonly used to define flashover, e.g., upper layer temperature of 600°C, flames emerging through the doorway, heat flux to the floor of 20 kW/m², heat release rate of 1 MW, etc.

14.4.3 OTHER LARGE-SCALE REACTION-TO-FIRE TESTS

The Intermediate-Scale Calorimeter (ICAL), described in ASTM E 1623, is essentially a scaled-up version of the Cone Calorimeter. The apparatus consists of a vertical gas-fired radiant panel with a height of approximately 1.33 m and width of approximately 1.54 m. The standard test specimen measures 1 × 1 m, and is positioned parallel to the radiant panel. The heat flux to the specimen is preset in the range of 10–60 kW/m² by adjusting the distance to the panel. The products of pyrolysis from the specimen are ignited with hot wires located near the top and bottom of the specimen. The specimen is placed on a load cell to measure mass loss during testing. Panel and specimen are positioned beneath the ISO 9705 hood and exhaust duct.

The European reaction-to-fire classification system described in EN 13501 is based primarily on performance in the Single Burning Item test (SBI) for construction products except floor coverings. The apparatus and test method are described in EN 13823. The classification is based primarily on fire growth (FIGRA) and smoke development (SMOGRA) indices that are equal to the peak heat release and smoke production rate, respectively, divided by the time to reach the peak. FIGRA and SMOGRA limits were established based on performance in the ISO 9705 room/corner test as the reference scenario.⁷²

14.5 CONCLUSIONS

There are literally hundreds of test methods to evaluate material flammability and this chapter can only scratch the surface. The intent was to identify and describe the different aspects of material flammability and to illustrate how they can be measured. Several commonly used flammability tests not covered in this chapter are described elsewhere in the book. For example, Chapter 24 addresses flammability testing of textiles. The reader is referred to the end of this chapter for a short list of more comprehensive surveys of flammability tests.

Each test method is unique and provides information concerning the specimen's response to the specific fire conditions simulated by the test. A material that does very well in a test might perform very poorly in a real fire if, for example, the thermal exposure conditions in the fire are more severe than those in the test. For the same reason, good performance in one test does not guarantee good performance in another. This helps to explain inconsistencies between fire codes and regulations that rely on different standard tests. Each test method has merits but also limitations. It is important to recognize the limitations and not to draw any unwarranted conclusions from the test results.

There is an increased use of flammability tests, which measure fundamental properties as opposed to tests that simulate a specific fire scenario. The former can be used in conjunction with mathematical models to predict the performance of a material in a range of fire scenarios. This approach has become feasible due to the significant progress that has been made in the past few decades in our understanding of the physics and chemistry of fire, mathematical modeling of fire phenomena and measurement techniques. However, there will always be materials that exhibit a behavior that cannot be captured in bench-scale tests and computer models. The fire performance of those materials can only be determined in full-scale tests.

BIBLIOGRAPHY

CODES AND STANDARDS

- ABD 0031: Airbus Directives (ABD) and Procedures for Fire–Smoke–Toxicity (FST). Airbus Industries.
- ASTM D 1692: Method of Test for Rate of Burning or Extent and Time of Burning of Cellular Plastics Using a Specimen Horizontal (Withdrawn 1976). ASTM International, West Conshohocken, PA.
- ASTM D 1929: Test Method for Determining Ignition Temperature of Plastics. ASTM International, West Conshohocken, PA.
- ASTM D 2863: Test Method for Measuring the Minimum Oxygen Concentration to Support Candle-Like Combustion of Plastics (Oxygen Index). ASTM International, West Conshohocken, PA.
- ASTM D 3801: Test Method for Measuring the Comparative Burning Characteristics of Solid Plastics in a Vertical Position. ASTM International, West Conshohocken, PA.
- ASTM D 5485: Standard Test Method for Determining the Corrosive Effect of Combustion Products Using the Cone Corrosimeter. *Annual Book of Standards, Vol. 04.07*, ASTM International, West Conshohocken, PA.
- ASTM D 7295: Standard Practice for Sampling and Determination of Hydrogen Cyanide (HCN) in Combustion Effluents and Other Stationary Sources. *Annual Book of Standards, Vol. 11.07*, ASTM International, West Conshohocken, PA.
- ASTM D 7309: Standard Test Method for Determining Flammability Characteristics of Plastics and Other Solid Materials Using Microscale Combustion. *Annual Book of Standards, Vol. 08.03*, ASTM International, West Conshohocken, PA.
- ASTM E 84: Standard Test Method for Surface Burning Characteristics of Building Materials. *Annual Book of Standards, Vol. 04.07*, ASTM International, West Conshohocken, PA.
- ASTM E 162: Standard Test Method for Surface Flammability of Materials Using a Radiant Heat Energy Source. *Annual Book of Standards, Vol. 04.07*, ASTM International, West Conshohocken, PA.
- ASTM E 648: Standard Test Method for Critical Radiant Flux of Floor Covering Systems Using a Radiant Heat Energy Source. *Annual Book of Standards, Vol. 04.07*, ASTM International, West Conshohocken, PA.
- ASTM E 662: Standard Test Method for Specific Optical Density of Smoke Generated by Solid Materials. ASTM International, West Conshohocken, PA.
- ASTM E 800: Standard Guide for Measurement of Gases Present or Generated during Fires. *Annual Book of Standards, Vol. 04.07*, ASTM International, West Conshohocken, PA.
- ASTM E 906: Standard Test Method for Heat and Visible Smoke Release Rates for Materials and Products. *Annual Book of Standards, Vol. 04.07*, ASTM International, West Conshohocken, PA.
- ASTM E 1317: Standard Test Method for Flammability of Marine Surface Finishes. *Annual Book of Standards, Vol. 04.07*, ASTM International, West Conshohocken, PA.
- ASTM E 1321: Test Method for Determining Material Ignition and Flame Spread Properties. ASTM International, West Conshohocken, PA.
- ASTM E 1354: Standard Test Method for Heat and Visible Smoke Release Rates for Materials and Products Using an Oxygen Consumption Calorimeter. *Annual Book of Standards, Vol. 04.07*, ASTM International, West Conshohocken, PA.
- ASTM E 1537: Standard Test Method for Fire Testing of Upholstered Furniture. *Annual Book of Standards, Vol. 04.07*, ASTM International, West Conshohocken, PA.
- ASTM E 1623: Test Method for Determination of Fire and Thermal Parameters of Materials, Products, and Systems Using an Intermediate Scale Calorimeter (ICAL). ASTM International, West Conshohocken, PA.
- ASTM E 1590: Standard Test Method for Fire Testing of Mattresses. *Annual Book of Standards, Vol. 04.07*, ASTM International, West Conshohocken, PA.
- ASTM E 1678: Standard Test Method for Measuring Smoke Toxicity for Use in Fire Hazard Analysis. ASTM International, West Conshohocken, PA.
- ASTM E 1822: Standard Test Method for Fire Testing of Stacked Chairs. *Annual Book of Standards, Vol. 04.07*, ASTM International, West Conshohocken, PA.
- ASTM E 1995: Standard Test Method for Measurement of Smoke Obscuration Using a Conical Radiant Source in a Single Closed Chamber, With the Test Specimen Oriented Horizontally. ASTM International, West Conshohocken, PA.
- ASTM E 2058: Standard Test Methods for Measurement of Synthetic Polymer Material Flammability Using a Fire Propagation Apparatus. *Annual Book of Standards, Vol. 04.07*, ASTM International, West Conshohocken, PA.
- ASTM E 2257: Standard Test Method for Room Fire Test of Wall and Ceiling Materials and Assemblies. *Annual Book of Standards, Vol. 04.07*, ASTM International, West Conshohocken, PA.

- CAL TB 117: Requirements, Test Procedures and Apparatus for Testing the Flame Retardance of Resilient Filling Materials Used in Upholstered Furniture. Bureau of Home Furnishings and Thermal Insulation, Sacramento, CA.
- EN 13501: Fire Classification of Construction Products and Building Elements – Part 1 – Classification Using Test Data from Reaction-to-Fire Tests. European Committee for Standardization, Brussels, Belgium.
- EN 13823: Reaction to Fire Tests for Building Products—Building Products Excluding Flooring Exposed to the Thermal Attack of a Single Burning Item. European Committee for Standardization, Brussels, Belgium.
- FMVSS 302: Motor Vehicle Interior Materials Fire Test National Highway Traffic Safety Administration, Washington, DC.
- IEC 60695-2-13: Fire Hazard Testing—Part 2-13: Glowing/Hot-Wire Based Test Methods—Glow-Wire Ignitability Test Method for Materials. International Electrotechnical Commission, Geneva, Switzerland.
- IMO FTP Code: International Code for Application of Fire Test Procedures, Annex 1. Part 2. International Maritime Organization: London, U.K.
- IMO FTP Code: International Code for Application of Fire Test Procedures, Annex 1. Part 5. International Maritime Organization: London, U.K.
- ISO 4589-2: Plastics—Determination of Burning Behavior by Oxygen Index—Part 2: Ambient-Temperature Test. International Organization for Standardization, Geneva, Switzerland.
- ISO 5657: Fire Tests—Reaction to Fire—Ignitability of Building Products. International Organization for Standardization, Geneva, Switzerland.
- ISO 5659-2: Plastics—Smoke Generation—Part 2: Determination of Optical Density by a Single-Chamber Test. International Organization for Standardization, Geneva, Switzerland.
- ISO 5660-1: Reaction-to-Fire Tests—Heat Release, Smoke Production and Mass Loss Rate—Part 1: Heat Release Rate (Cone Calorimeter Method). International Organization for Standardization, Geneva, Switzerland.
- ISO 5660-2: Reaction-to-Fire Tests—Heat Release, Smoke Production and Mass Loss Rate—Part 2: Smoke Production Rate (Dynamic Measurement). International Organization for Standardization, Geneva, Switzerland.
- ISO 9705: Fire Tests—Reaction-to-Fire—Room Fire Test. International Organization for Standardization, Geneva, Switzerland.
- ISO TS 19700: Fire Tests—Controlled Equivalence Ratio Method for the Determination of Hazardous Components of Fire Effluents. International Organization for Standardization, Geneva, Switzerland.
- ISO 19701—Methods for Analysis and Sampling of Fire Effluents. International Organization for Standardisation, Geneva, Switzerland.
- MIL-STD-2031: Fire and Toxicity Test Methods and Qualification Procedure for Composite Material Systems Used in Hull, Machinery and Structural Applications Inside Naval Submarines. U.S. Department of Defense, Washington, DC.
- NFPA 265: Standard Method of Tests for Evaluating Room Fire Growth Contribution of Textile Wall Coverings. National Fire Protection Association, Quincy, MA.
- NFPA 271: Standard Method of Test for Heat and Visible Smoke Release Rates for Materials and Products Using an Oxygen Consumption Calorimeter. National Fire Protection Association, Quincy, MA.
- NFPA 286: Standard Method of Tests for Evaluating Contribution of Wall and Ceiling Interior Finish to Room Fire Growth. National Fire Protection Association, Quincy, MA.
- NFPA 550: Guide to the Fire Safety Concepts Tree. National Fire Protection Association, Quincy, MA.
- SMP 800-C: Bombardier Material and Process Specification, Toxic Gas Generation. Bombardier: Montréal, Quebec, Canada.
- SOLAS: Consolidated Edition, 2001, Chapter II-2—Construction: Fire Protection, Fire Detection and Fire Extinction. International Maritime Organization, London, U.K.
- UL 94: Test for Flammability of Plastic Materials for Parts in Devices and Appliances, Underwriters Laboratories, Northbrook, IL.

REFERENCES CITED

1. Quintiere, J., *Principles of Fire Behavior*. Delmar Cengage Learning: Albany, NY, 1997.
2. Gann, R., Babrauskas, V., Peacock, R., and Hall, J., Fire conditions for smoke toxicity measurement. *Fire and Materials* 1994, 18, 193–199.
3. Tu, K. and Quintiere, J., Wall flame heights with external radiation. *Fire Technology* 1991, 27, 195–203.
4. Evans, D. and Stroup, D., Methods to calculate the response time of heat and smoke detectors installed below large unobstructed ceilings. *Fire Technology* 1986, 22, 54–65.
5. Evans, D., Calculating sprinkler actuation time in compartments. *Fire Safety Journal* 1985, 9, 147–155.
6. Deal, S. and Beyler, C., Correlating preflashover room fire temperatures. *Journal of Fire Protection Engineering* 1990, 2, 33–48.

7. Foote, K., Pagni, P., and Alvarez, N., In temperature correlations for forced ventilation compartment fires, *First International Symposium on Fire Safety Science*, Gaithersburg, MD, Hemisphere Publishing Corporation: New York, 1986, pp. 139–148.
8. McCaffrey, B., Quintiere, J., and Harkleroad, M., Estimating room fire temperatures and the likelihood of flashover using fire test data correlations. *Fire Technology* 1981, 17, 98–119.
9. Cooper, L., A mathematical model for estimating available safe egress time in fires. *Fire and Materials* 1982, 6, 135–144.
10. Jones, W., Peacock, R., Forney, G., and Reneke, P., *CFAST: Consolidated Model of Fire Growth and Smoke Transport (Version 5). Technical Reference Guide.*, NIST Special Publication 1030, National Institute of Standards and Technology: Gaithersburg, MD, 2004, p. 153.
11. McGrattan, K. B., Hostikka, S., Floyd, J. E., Baum, H. R., and Rehm, R. G., *Fire Dynamics Simulator (Version 5): Technical Reference Guide*, NIST Special Publication 1018-5, National Institute of Standards and Technology: Gaithersburg, MD, 2007, p. 100.
12. Babrauskas, V. and Peacock, R., Heat release rate: The single most important variable in fire hazard. *Fire Safety Journal* 1992, 18, 255–272.
13. Thomas, P., Testing products and materials for their contribution to flashover in rooms. *Fire and Materials* 1980, 5, 103–111.
14. Babrauskas, V., Estimating room flashover potential. *Fire Technology* 1980, 16, 94–104.
15. Babrauskas, V., A closed form approximation for post-flashover compartment fire temperatures. *Fire Safety Journal* 1981, 4, 63–73.
16. Thomas, P., SFPE Classic paper review: Fire behavior in rooms by Kunio Kawagoe. *Journal of Fire Protection Engineering* 2004, 14, 5–8.
17. Jin, T., Visibility through smoke. *Journal of Fire and Flammability* 1978, 9, 135–155.
18. Babrauskas, V., *Ignition Handbook*. Fire Science Publishers: Issaquah, WA, 2003.
19. Blaszkiewicz, M., Bowman, P., and Masciantonio, M., In Understanding the repeatability and reproducibility of UL 94 testing, *18th BCC Conference on Flame Retardancy*, Stamford, CT, May 21–23, 2007, Business Communications Co.: Stamford, CT, 2007.
20. Morgan, A. and Bundy, M., Cone calorimeter analysis of UL 94V-rated plastics. *Fire and Materials* 2007, 31, 257–283.
21. *ASTM Fire Standards and Related Technical Material, 7th Edition*. ASTM International: West Conshohocken, PA, 2007.
22. Roed, J., In *Low Voltage Directive*, FIRESEL 2003, Borås, Sweden, May 27–28, 2003, SP, Borås, Sweden, 2003.
23. Hallman, J., Ignition of polymers by radiant energy. PhD thesis, University of Oklahoma, Norman, OK, 1971.
24. Koohyar, A., Ignition of wood by flame radiation. PhD thesis, University of Oklahoma, Norman, OK, 1967.
25. Rasbash, D., Drysdale, D., and Deepak, D., Critical heat and mass transfer at pilot ignition and extinction of a material. *Fire Safety Journal* 1986, 10, 1–10.
26. Thomson, H. and Drysdale, D., Flammability of plastics, I: Ignition temperatures. *Fire and Materials* 1987, 11, 163–172.
27. Thomson, H., Drysdale, D., and Beyler, C., An experimental evaluation of critical surface temperature as a criterion for piloted ignition of solid fuels. *Fire Safety Journal* 1988, 13, 185–196.
28. Atreya, A., Pyrolysis, ignition and fire spread on horizontal surfaces of wood. PhD thesis, Harvard University, Cambridge, MA, 1983.
29. Atreya, A., Carpentier, C., and Harkleroad, M., In Effect of sample orientation on piloted ignition and flame spread, *First International Symposium on Fire Safety Science*, Gaithersburg, MD, Hemisphere Publishing Co.: New York, 1985, pp. 97–109.
30. Abu-Zaid, M., Effect of water on ignition of cellulosic materials. PhD thesis, Michigan State University, East Lansing, MI, 1988.
31. Fangrat, J., Hasemi, Y., Yoshida, M., and Hirata, T., Surface temperature at ignition of wooden based slabs. *Fire Safety Journal* 1996, 27, 249–259.
32. Janssens, M., In thermal model for piloted ignition of wood including variable thermophysical properties, *Third International Symposium on Fire Safety Science*, Edinburgh, Scotland, Cox, G., Langford, B. (Eds.), Elsevier Applied Science: New York, 1991, pp. 167–176.
33. Moghtaderi, B., Novozhilov, V., Fletcher, D., and Kent, J., A new correlation for bench-scale piloted ignition data of wood. *Fire Safety Journal* 1997, 29, 41–59.
34. Urbas, J. and Parker, W., Surface temperature measurements on burning wood specimens in the cone calorimeter and effect of grain orientation. *Fire and Materials* 1993, 17, 205–208.

35. Yudong, L. and Drysdale, D., Measurement of the ignition temperature of wood. *Fire Safety Science* 1992, 1, 25–30.
36. Khan, M. and deRis, J., In operator independent ignition measurements, *Eighth International Symposium on Fire Safety Science*, Beijing, China, International Association of Safety Science: Beijing, China, 2005, pp. 163–174.
37. Khan, M. and deRis, J., In device and method for measuring absorbed heat flux, *10th Fire and Materials Conference*, San Francisco, CA, Interscience Communications: London, U.K., 2007, pp. 25–26 (abstract, full paper on CD).
38. Quintiere, J. and Harkleroad, M., *New Concepts for Measuring Flame Spread Properties*. NBSIR 84-2943, National Bureau of Standards: Gaithersburg, MD, 1984.
39. Janssens, M., Measuring rate of heat release by oxygen consumption. *Fire Technology* 1991, 27, 234–249.
40. Parker, W., Calculations of the heat release rate by oxygen consumption for various applications. *Journal of Fire Sciences* 1984, 2, 380–395.
41. Beaulieu, P. and Dembsey, N., In enhanced equations for carbon dioxide and oxygen calorimetry, *9th International Fire and Materials Conference*, San Francisco, CA, Interscience Communications Limited: London, U.K., 2005, pp. 51–62.
42. Tewarson, A., Generation of heat and chemical compounds in fires. In *The SFPE Handbook of Fire Protection Engineering*, National Fire Protection Association: Quincy, MA, 2002, Section 3, pp. 82–161.
43. Huggett, C., Estimation of the rate of heat release by means of oxygen consumption. *Fire and Materials* 1980, 12, 61–65.
44. Thornton, W., The relation of oxygen to the heat of combustion of organic compounds. *The London, Edinburgh and Dublin Philosophical Magazine and Journal of Science* 1917, 33, 196–203.
45. Petrella, V., The mass burning rate of polymers, wood and liquids. *Journal of Fire and Flammability* 1980, 11, 3–21.
46. Tewarson, A. and Pion, R., Flammability of plastics. I. Burning intensity. *Combustion & Flame* 1976, 26, 85–103.
47. Babrauskas, V., Development of the cone calorimeter—A bench-scale heat release rate apparatus based on O₂ consumption. *Fire and Materials* 1984, 8, 81–95.
48. Babrauskas, V., Twilley, W., Janssens, M., and Yusa, S., A cone calorimeter for controlled atmosphere studies. *Fire and Materials* 1992, 16, 37–43.
49. Leonard, J., Bowditch, P., and Dowling, V., Development of a controlled-atmosphere cone calorimeter. *Fire and Materials* 2000, 24, 143–150.
50. Hshieh, F. and Buch, R., Controlled-atmosphere cone calorimeter studies of silicones. *Fire and Materials* 1997, 21, 265–272.
51. Lyon, R., Heat release kinetics. *Fire and Materials* 2000, 24, 179–186.
52. Lyon, R., Walters, R., and Stoliarov, S., A thermal analysis method for measuring polymer flammability. *Journal of ASTM International* 2006, 3, 1–18.
53. Lyon, R. and Janssens, M., Polymer flammability. In *Encyclopedia of Polymer Science & Engineering (On-line Edition)*, John Wiley & Sons: New York, 2005.
54. Lyon, R., Plastics and rubber. In *Handbook of Building Materials for Fire Protection*, Harper, C. (Ed.), McGraw-Hill: New York, 2004, pp. 3.1–3.51.
55. Lyon, R., Walters, R., Safronava, N., and Stoliarov, S., In a statistical model for the results of flammability tests, *11th International Fire and Materials Conference*, San Francisco, CA, Interscience Communications Limited: London, U.K., 2009, pp. 141–159.
56. Smith, E., Heat release rate of building materials. In *Ignition, Heat Release and Noncombustibility of Materials, ASTM STP 502*, American Society of Testing and Materials, Philadelphia, PA: October 6, 1971, Washington, DC, 1972, pp. 119–134.
57. *Aircraft Material Fire Test Handbook*, DOT/FAA/CT-89/15, U.S. Department of Transportation, Federal Aviation Administration: Atlantic City, NJ, 1990.
58. Tewarson, A., Heat release rates from burning plastics. *Journal of Fire and Flammability* 1977, 8, 115–130.
59. Hasemi, Y., Experimental wall flame heat transfer correlations for the analysis of upward wall flame spread. *Fire Science and Technology* 1984, 4, 75–90.
60. Hasemi, Y. and Tokunaga, T., In modeling of turbulent diffusion flames and fire plumes for the analysis of fire growth, *21st National Heat Transfer Conference, Fire Dynamics and Heat Transfer*, Seattle, WA, 1983, pp. 37–45.
61. deRis, J., In spread of a laminar diffusion flame, *Twelfth Symposium (International) on Combustion*, Combustion Institute: Pittsburgh, PA, 1969, pp. 241–252.

62. Qian, C., Ishida, H., and Saito, K., *Upward Flame Spread Along the Vertical Corner Walls*. NIST-GCR-94-648, National Institute of Standards and Technology: Gaithersburg, MD, 1994.
63. Hartzell, G. *Development of a Radiant Panel Test for Flooring Materials*. NBSIR 74-495, National Bureau of Standards: Washington, DC, 1974.
64. Mulholland, G. and Croarkin, C., Specific extinction coefficient of flame generated smoke. *Fire and Materials* 2000, 24, 227–230.
65. Babrauskas, V., Levin, B., Gann, R., Paabo, M., Harris, R., Peacock, R., and Yusa, S., *Toxic Potency Measurements for Fire Hazard Analysis*, Special Publication 827, National Institute of Standards and Technology: Gaithersburg, MD, 1991.
66. Babrauskas, V., Gann, R., Levin, B., Paabo, M., Harris, R., Peacock, R., and Yusa, S., A methodology for obtaining and using toxic potency data for fire hazard analysis. *Fire Safety Journal* 1998, 31, 345–358.
67. Babrauskas, V., The generation of CO in bench-scale fire tests and the prediction for real-scale fires. *Fire and Materials* 1995, 19, 205–213.
68. Gann, R., Babrauskas, V., and Peacock, R., Fire conditions for smoke toxicity measurement. *Fire and Materials* 1994, 18, 193–199.
69. Gross, D., Loftus, J., and Robertson, A., In *Method for Measuring Smoke From Burning Materials*, Fire test methods: Restraint and smoke, ASTM STP 422, June 26–July 1, 1966, Atlantic City, NJ, American Society for Testing and Materials: Philadelphia, PA, June 26–July 1, 1966, 1967, pp. 166–204.
70. Ames, S. and Rogers, S., In large and small scale fire calorimetry assessment of upholstered furniture, *5th Interflam Conference*, Canterbury, U.K., September 17–19, 2001, Interscience Communications: London, U.K., 1990, pp. 221–232.
71. Babrauskas, V., Lawson, J., Walton, W., and Twilley, W., *Upholstered Furniture Heat Release Rates Measured with a Furniture Calorimeter*. NBSIR 82-2604, National Bureau of Standards: Gaithersburg, MD, 1982.
72. Smith, D., Marshall, N., Shaw, K., and Colwell, S., In correlating large-scale fire performance with the single burning item test, *9th Interflam Conference*, Edinburgh, Scotland, Interscience Communications: London, U.K., 2001, pp. 531–542.

SOURCES FOR ADDITIONAL INFORMATION AND FURTHER READING

Comprehensive compilations and an extensive discussion of various uses of flammability test methods can be found in the following two books:

Apte, V., *Flammability Testing of Materials Used in Construction, Transport and Mining*. Woodhead Publishing Limited: Cambridge, U.K., 2006.

Troitzsch, J. (Ed.), *Plastics Flammability Handbook – Principles, Regulations, Testing, and Approval*, 3rd edn., Hanser Publisher: Munich, Germany, 2006.

The most complete collection of fire test standards is published by ASTM international:

ASTM Fire Standards and Related Technical Material, 7th edn., ASTM International, West Conshohocken, PA, 2007. Available from <http://www.astm.org>.

An extensive discussion of the principles of fire physics and chemistry and the behavior of materials in fire can be found in the following books:

Cote, A. (Ed.), *Fire Protection Handbook*. 20th edn., National Fire Protection Association: Quincy, MA, 2008.

DiNunno, P. (Ed.), *The SFPE Handbook of Fire Protection Engineering*. 3rd edn., Society of Fire Protection Engineers: Bethesda, MD, 2002.

Finally, a tremendous amount of useful information can be found on the Internet. For example, the website of the Building and Fire Research Laboratory at the National Institute of Standards and Technology (URL: <https://www.bfrl.nist.gov>) is a great resource. Instead of providing a list of websites in this chapter, the reader is referred to the site of Dr. Vyto Babrauskas' company, Fire Science and Technology (URL: <http://www.doctorfire.com>). Not only is there a lot of useful information on this site, but you will also find what is, to the author's knowledge, the longest list of fire-related links on the web (URL: <http://www.doctorfire.com/links.html>).

15 Uses of Fire Tests in Materials Flammability Development

Bernhard Schartel

CONTENTS

15.1	Introduction.....	387
15.2	Ignition: Reaction to a Small Ignition Source.....	391
15.3	Developing Fire: Forced Flaming Combustion.....	396
15.4	Fully Developed Fire.....	403
15.5	Other Fire Hazards.....	404
15.6	Understanding Fire Behavior and Fire Retardancy Mechanisms.....	405
15.7	Conclusion.....	414
	Acknowledgments.....	415
	References.....	415

15.1 INTRODUCTION

For economic reasons, flame-retarded commodity and engineering polymers are widely used, whereas only few niche products are made from inherently flame-resistant high-performance polymers. However, there are increasing demands for sustainable materials, for materials that pass fire regulations with increasingly strict tests, and for materials that are suitable for new applications that require advanced property combinations. Thus, developing new flame-retarded polymeric materials is a current challenge for material science and its research and industrial development. Some current challenges include halogen-free, self-extinguishing thermoplastics; thermosets, composites, and foams based on flammable polymers, such as poly(propylene) (PP), poly(styrene) (PS), high-impact PS (HIPS), bisphenol A polycarbonate (PC), PC/acrylonitrile-butadiene-styrene blends (PC/ABS), poly(butylene terephthalate) (PBT), epoxy resin (EP), and poly(urethane) (PU); especially materials that meet the UL 94 classification V-0 for electrical engineering and electronics applications like computer housings and printed circuit boards; materials that achieve new advanced standards such as CEN TS 45545 “Railway Applications—Fire Protection of Railway Vehicles”; flame-retarded high-performance composites and foams for transportation. Even though flame-retarded polymeric materials are clearly the mass products, the field is characterized by a reasonable high level of innovation, meaning that a large number of commercialized materials have been developed within the last 10 years.

Most of the development is based on the optimization of established approaches. These include, for instance, the modification of flame-retardants using advanced technologies such as microencapsulation to increase their stability against hydrolysis or avoid agglomeration, adjusting the combinations of flame-retardants with synergists or adjuvants, and proposing new combinations of additives to reduce the load or costs at the same time as increasing the efficiency of flame retardation. Some work focuses on the synthesis of new derivatives, adjusting the properties of flame-retardants such as molecular weight, thermal stability, or compatibility with the polymer. New approaches such as nanocomposites,¹⁻⁴ the incorporation of 9,10-dihydro-9-oxa-10-phosphaphenanthrene-10-oxide (DOPO) structures in thermosets,⁵⁻¹¹ or metal phosphinate salts,¹²⁻¹⁵ which have been advanced

in recent years, are rare, but also a focus of discussion, as they show promise for fulfilling future demands with respect to sustainability and efficiency. All of these developments are based primarily on rather empirical concepts and screening procedures. It should be noted that empirically based development includes “trial and error” as well as decades of experience and ingenious sophisticated approaches. However, a detailed scientific understanding of the flame-retardant mechanisms or structure–property relationships is usually lacking, even where successfully commercialized products are concerned. This fact is mainly due to two inherent characteristics of the task of developing flame-retarded materials.

First, it is rather typical for the area that the plethora of parameters that need to be optimized to obtain a product, such as the number and kind of components (polymer, flame retardant, synergist, adjuvant, additive), the concentration of each compound, the morphology of both the material (in particular the distribution of the components) and of each component (particle size, shape, and particle-size distribution), and the modification of each compound through processes such as coating and microencapsulation, but also molecular weight and branching, make for a very large multidimensional matrix. Analytical description of the matrix is impossible as long as the manifold interactions between the different compounds and their influences on fire behavior are unknown, apart from an empirical understanding of the main mechanisms. Indeed, even these are often described in detail and fully understood only for rather simple or model systems. Thus, it has been concluded that typical working packages in the area of developing flame-retarded polymeric materials demand high-throughput screening or combinatorial methods,^{16–18} as discussed in a separate chapter in this book. Even so, if an ingenious empirical concept reduces the number of systems to be investigated, the comprehensive screening of a variety of systems generally remains. So, in a typical example, the patent DE 42 31 774 A1 from 1994 protects a thermoplastic polymer flame-retarded with a combination of 0.1–30 parts per weight of a phosphorous flame retardant and 0.1–15 parts per weight of aluminosilicate.¹⁹ This special idea proposed by the patent covers an overwhelming matrix of components. According to the patent, thermoplastic polymers include all kinds of homo- or (graft-) copolymers, polymer blends, and composites (based on fibers but also with poly(tetrafluoroethylene) (PTFE)), which are based on ethylenically unsaturated monomers such as propylene, vinyl acetate, styrene, 2-methyl styrene, acrylnitriles, methaacrylnitriles, methyl methacrylate, methacrylate, maleic acid anhydride, maleinimide, chloroprene, butadiene, isoprene, and C1–C8 alacyl acrylates or on bifunctional compounds such as PC, polyesters (PET, PBT, etc.), polysulfones (PSU), polyether-sulfones (PES), and polyketones (PEEK, PEK, etc.). All kinds of phosphorus-containing compounds are proposed as flame-retardants, like various phosphine oxides, phosphinates, phosphonates, and phosphates with or without halogen. Aluminosilicates include all kinds of zeolithes according to $\text{Me}_{2/n}\text{O} \cdot \text{Al}_2\text{O}_3 \cdot x\text{SiO}_2 \cdot y\text{H}_2\text{O}$ (Me = hydrogen or metal ion of the first to fifth main group or first to eighth subgroup), all kinds of layered silicates (LS) (kaolin types, spinel types, serpentine types, and montmorillonite types), and types containing Cu^{2+} , Co^{2+} , and Ni^{2+} , including all mixtures and modified compounds.

The second reason is that flame-retardancy mechanisms^{20–24} on a molecular or microscopic scale are used to protect macroscopic specimens, so that they pass a distinct fire test conceived with respect to a distinct application.²⁵ How distinct flame retardancy mechanisms influence performance in a distinct fire test is not a trivial question and cannot be answered generally, since a whole set of materials properties such as char yield (μ), effective heat of combustion of the volatiles (h_c), heat of gasification (h_g), thermal conductivity, melt viscosity, and surface emissivity usually determines the fire behavior of a specimen. Furthermore, the role played by each material property differs from one fire test to the next. Fire tests do not focus on certain material properties; instead, each fire test simulates a distinct fire scenario to check whether a certain protection goal is achieved. The fire scenarios and protection goals considered are very different with respect to various applications. Generally, fires differ crucially in their heat and mass transport, defined by characteristics such as applied heat flux (\dot{q}_{ex}''), temperature, length scales, and ventilation (Figure 15.1). Their behavior can be divided into three main general stages:

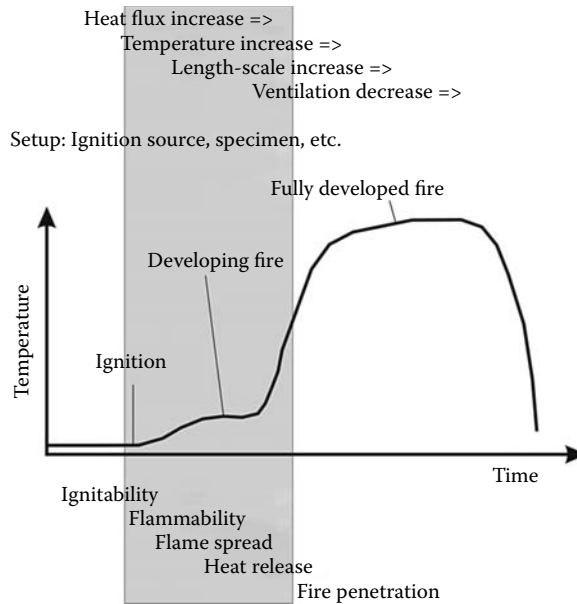


FIGURE 15.1 Schematic temperature development during a (room) fire; illustrating the fire scenarios: ignition, developing fire, and fully developed fire with their characteristics heat flux, temperature, length scale involved, and ventilation; the predominant fire properties ignition, flammability, flame spread, heat release, and fire penetration. The gray area marks the main area in which the flame retardancy of polymers is applied.

- Ignition: Piloted ignition is the onset of flaming combustion, characterized by an ignition source (flame, cigarette, glow wire, etc.), small length scale (cm), ambient temperatures in the range of ignition temperatures (600–700 K), and high ventilation.
- Developing fire: The continuation of flaming combustion occurring in this stage of fire growth is characterized by an external heat flux $\dot{q}_{ex}'' = 20\text{--}60\text{ kW m}^{-2}$, larger length scales (dm to m), ambient temperatures above the ignition temperature (700–900 K), and continuing high ventilation.
- Fully developed fire: The penultimate stage of fire growth is characterized by a high external heat flux $\dot{q}_{ex}'' > 50\text{ kW m}^{-2}$, large length scales $> \text{m}$, ambient temperatures above autoignition temperatures ($>900\text{ K}$), and low ventilation.

These different fire scenarios highlight different fire properties

Ignition:

- Ignitability (time to ignition (t_{ig}), critical mass loss (ML) rate or heat flux for ignition, ignition temperature (T_{ig}), etc.)
- Flammability (extinction behavior under ambient conditions after removing an ignition source, reaction to a small flame)

Developing fire:

- Flame spread (opposed flow and wind-aided flame spread, fire growth rate, etc.)
- Heat release rate (HRR)
- Total heat release (THR)/total heat evolved (THE)/fire load (THR is the total heat released up to certain time point of testing and thus a function of time; THE = THR after burning, and thus something like the fire load of the specimen monitored by the applied fire test)

Fully developed fire:

- Heat penetration
- Fire penetration/fire resistance
- THE/fire load
- Structural integrity

As mentioned earlier, these properties such as reaction to small flame (flammability), flame spread, and fire penetration are not materials properties, but merely the performance of a certain specimen in a certain fire scenario. And, not only terms such as “fire-proof,” “flash, flame or fire resistant,” and “self-extinguishing,” but also “flammable” and “(in)combustible” often have different meanings depending on the standard or regulation applied; this situation can cause confusion. “Flammability” is used in this chapter in the specific sense of “showing sustained flaming after removal of a small ignition source” and not in the general sense of “fire behavior.”

Most fire science and thus most fire testing focuses on specific protection goals in the different applications, for good reason. Common protection goals include preventing sustained ignition (beginning of a fire), limiting the contribution to fire propagation (developing fire), or acting as a fire barrier (fully developed fire). Established fire tests try to simulate a specific, realistic fire scenario and monitor a specific fire risk or hazard from a specific specimen within that scenario. However, fire tests simulating similar fire scenarios neither necessarily deliver equal results for a material nor an equivalent ranking of materials. Even rather small differences in the fire scenario can play a crucial role and highlight different materials properties. For instance, the ignition and flammability hazards are often changed crucially depending on whether a pilot flame, irradiation, a glow wire, or a cigarette is used.²⁶ Further, some materials properties are important for the performance of the tested specimen in certain tests, but not in others. The melt viscosity of the material, for instance, and the resulting heat removal through dripping or melt flow, have a crucial influence on some flammability tests,²⁷ whereas other fire tests are hardly influenced by these phenomena. For some applications, the market is controlled by national standards rather than international ones,^{25,28} so that a material may pass the national test necessary in country A and fail the corresponding national test in country B, or vice versa. In fact, it should be noted that, in practice, developing flame-retarded polymeric materials basically means developing a material for the sole purpose of ensuring that a defined specimen can pass a distinct fire test. Sometimes, this is achieved with little or no improvement in performance in another fire test. In most cases, this aspect also favors screening and empirical approaches rather than attempting to understand all of the structure–property relationships or mechanisms in detail. However, it is also the objective of this chapter to discuss the understanding of flame retardancy mechanisms and structure–property relationships controlling the performance of polymeric materials in different fire tests. In particular, the use of the understanding of flame-retardancy and comprehensive assessment of fire behavior are indicated as scientific fundamentals for the future, more tailored development of innovative materials.

Only the uses of those fire tests that are the most important for the development of flame-retarded polymers are discussed. As such, the chapter abstains from describing test apparatuses or the testing procedures themselves, since the relevant international standards can be used to ensure accurate quality assurance, and the comprehensive assemblies already have been described in established textbooks.²⁵ Instead, the main aim of this chapter is to stimulate the reader’s interest in advanced uses of fire tests in the development of new materials. Further, the chapter tries to give comprehensive insight into how fire test can be used for the tailored development of flame-retarded materials, not a comprehensive review what has been achieved so far. Consequently, apart from the data used for Figure 15.2, all of the examples, data, tables, and figures presented were chosen from the work performed in the author’s working group.

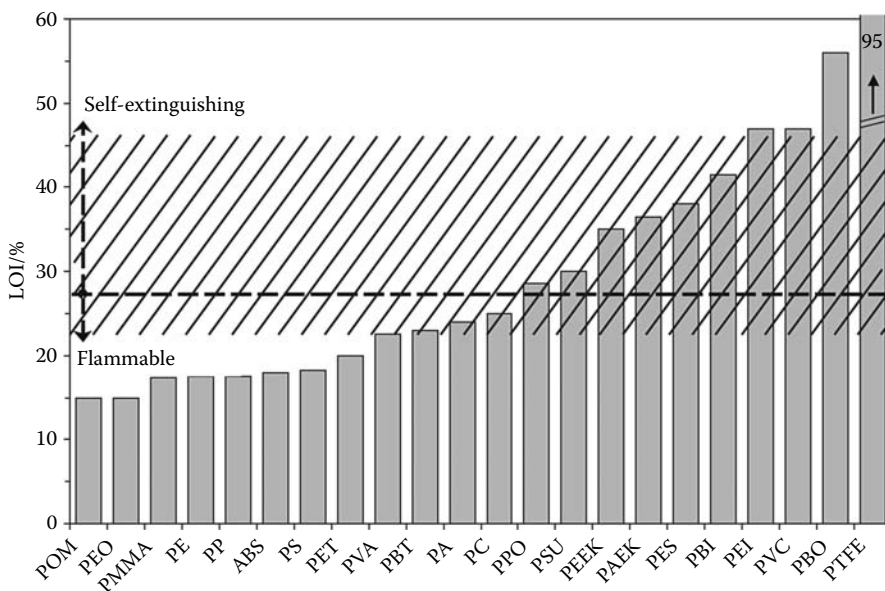


FIGURE 15.2 LOI of several polymers. In general, roughly LOI values of up to 27% (dashed line) signify flammability; higher LOI values signify self-extinguishing behavior in the UL 94 test.³³ There is no clear correlation between LOI and UL 94, and some extremes down to 22% and up to 47% (hatched zone) are reported for polymers that are self-extinguishing or flammable, respectively.^{34,35}

15.2 IGNITION: REACTION TO A SMALL IGNITION SOURCE

Considering the necessary amount of material and time for investigation, which, taken together, constitute the costs, in practice, small or bench-scale methods (specimen size up to 1 dm²) are required to develop flame-retarded polymers. This length scale is typical only for the beginning of a fire and hence ignition, flammability, or response to an ignition source such as a small flame. Correspondingly, small-scale or bench-scale fire tests have become established, like the limiting oxygen index (LOI, ISO 4589), the glow wire tests (glow wire ignition temperature = GWIT, IEC 60695-2-13; glow wire flammability index = GWFI, IEC 60695-2-12), and reaction to a small flame—in particular, vertical and horizontal flame test methods according to IEC 60695-11-10 (=UL 94), which monitor the ignition or sustained flammability after a defined contact with a certain ignition source. Tests such as the glow wire test represent a very specific scenario and are used only in the process of developing materials intended for a given application, whereas UL 94 and LOI are very common and widespread, and are often used universally.

Whereas UL 94 delivers only a classification based on a pass-and-fail system, LOI can be used to rank and compare the flammability behavior of different materials. In Figure 15.2 the increasing LOI values are presented for different polymers as an example: POM = poly(oxymethylene), PEO = poly(ethyl oxide), PMMA = poly(methyl methacrylate), PE = poly(ethylene), PP, ABS, PS, PET = poly(ethylene terephthalate), PVA = poly(vinyl alcohol), PBT, PA = poly(amide), PC, PPO = poly(phenylene oxide), PSU, PEEK = poly(ether ether ketone), PAEK = poly(aryl ether ketone), PES, PBI = poly(benzimidazole), PEI = poly(ether imide), PVC = poly(vinyl chloride), PBO = poly(aryl ether benzoxazole), PTFE. The higher the LOI, the better is the intrinsic flame retardancy. Apart from rigid PVC, nearly all commodity and technical polymers are flammable. Only a few high-performance polymers are self-extinguishing. Table 15.1 shows an example of how the LOI is used in the development of flame-retarded materials. The flame retardant red phosphorus (P_{red}) increases

TABLE 15.1
LOI Results with Increasing P_{red} Content
in HIPS and PBT-GF

	LOI/% ($\pm 1\%$)		LOI/% ($\pm 1\%$)
HIPS	17.2	PBT-GF	20.1
HIPS/7.5 wt.% P_{red}	22.2	PBT-GF/7 wt.% P_{red}	26.7
HIPS/10 wt.% P_{red}	22.5	PBT-GF/10 wt.% P_{red}	26.8

flame retardancy in HIPS and glass fiber-reinforced PBT (PBT-GF), but only up to a certain amount of P_{red} . This observation corresponds to similar studies reported in the literature.^{29–31} P_{red} is reported not only to cause flame inhibition, but also to harbor the propensity to enhance fire in the gas phase,³² which may explain the behavior observed in HIPS and PBT-GF.

LOI and UL 94 are so common for plastics that in practice their results are often discussed as intrinsic fire properties of materials, which is not correct.^{27,33–35} Even such small-scale fire tests are specific fire scenarios. This becomes obvious when, for instance, the dimensions of the specimen are changed,^{36,37} as is shown in Figure 15.3 for carbon-fiber (60 vol.%) reinforced epoxy composites (EP-CF). The LOI and the UL 94 are not intrinsic material properties, but describe the ease of extinction of a specific specimen, which is of course crucially dependent on parameters such as the thickness of the specimen. Indeed, the LOI is reported to depend on every parameter of the set-up such as temperature, mode of ignition, column size and diameter, gas flow rate, sample condition, and sample dimension.^{36–40} It is obvious that tests that differ from the UL 94 or LOI standard must not be performed and called UL 94 or LOI, respectively, because of a lack of comparability. Furthermore, a comparison of these two different specific fire scenarios, LOI and UL 94, shows that there is no clear general correlation between them as indicated earlier in Figure 15.2. The main difference is not that a critical oxygen concentration is monitored in the LOI and an afterburning time in UL 94, as both results are based on observing the critical condition for extinguishing. The main difference is that LOI focuses on a downward flame spread and UL 94 on an upward flame spread.^{41–44} Indeed it was concluded, that the inability of flame propagation is the explicit cause of extinction in the LOI and should not be interpreted as a limit below which burning of the material cannot take place.⁴⁵ Modified LOI with upward burning was proposed⁴⁶ and showed better correlation with the UL 94.⁴⁷

In general, roughly LOI values of up to 27% signify flammability;³³ higher LOI values signify self-extinguishing behavior in the UL 94 test (Table 15.2). However, there is no clear correlation between LOI and UL 94, and some extremes down to 22% and up to 47% (Figure 15.2, Table 15.2)

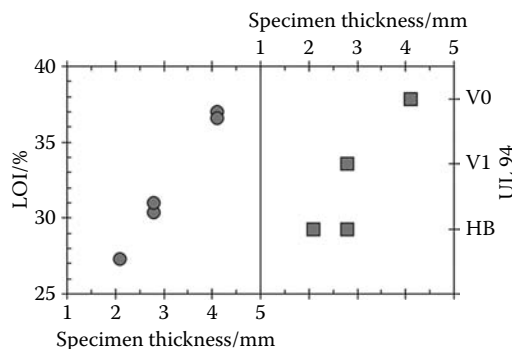


FIGURE 15.3 Influence of specimen thickness (2.1–4.2 mm) of EP-CF on the results of LOI and UL 94.

TABLE 15.2
Flammability of Different Materials

Material	EP	+10 wt.% APP	+15 wt.% APP	
LOI/% ($\pm 1\%$)	20.5	23.8	28.9	
UL 94	HB	HB	V-0	
	HIPS	HIPS/P _{red}	HIPS/Mg(OH) ₂	HIPS/P _{red} /Mg(OH) ₂
LOI/% ($\pm 1\%$)	17.2	22.2	19.5	22.8
UL 94	HB	V-2	HB	V-1
	EP-CF	EP-CF/DOP-Et	EP-CF/DOP-Cy	
LOI/% ($\pm 1\%$)	31	44	49	
UL 94	HB	V-1	V-0	
	PA 66-GF	+MPP	+AlPO ₂	+AlPO ₂ /MPP
LOI/% ($\pm 1\%$)	21.5	28.9	37.9	28.2
UL 94	HB	HB	HB	V-0

Sources: Braun, U. and ScharTEL, B., *Macromol. Chem. Phys.*, 205, 2185, 2004; ScharTEL, B. et al., *J. Appl. Polym. Sci.*, 104, 2260, 2007; Braun, U. et al., *Polymer*, 47, 8495, 2006; ScharTEL, B. et al., *J. Appl. Polym. Sci.*, 2009, submitted; Braun, U., et al., *Polym. Degrad. Stab.*, 92, 1528, 2007.

Note: APP, ammonium polyphosphate; DOP-Et, 10-ethyl-9,10-dihydro-9-oxa-10-phosphaphenanthrene 10-oxide; DOP-Cy, 1,3,5-tris[2-(9,10-dihydro-9-oxa-10-phosphaphenanthrene 10-oxide-10-ethyl)]1,3,5-triazine-2,4,6-(1H,3H,5H)-trione).

are reported for polymers that are self-extinguishing or flammable in the UL 94, respectively.^{34,35,48–51} The correlation seems to disappear when a set of materials is compared such as glass fiber reinforced PA 66 (PA 66-GF), PA 66-GF/melamine polyphosphate (MPP), PA 66-GF/ aluminum phosphinate (AlPO₂), and PA 66-GF/AlPO₂/MPP, in which the flame retardancy mechanisms alternate between flame inhibition, charring, and barrier formation (Table 15.2).⁵² The protection of the char is sensitive to ignition and burning from the top (LOI) or from the bottom (UL 94: V-classifications).³⁴

Table 15.3 presents a rough empirical approach summarizing the LOI improvement achieved by adding 5–15 wt.% flame retardant to some polymer systems.^{48,52–57} LOI seems to be very sensitive to flame inhibition and efficient char formation. The important role of char yield (μ) was noted back in the 1970s by van Krevelen, who reported on the correlation between the char yield (μ) of halogen-free polymers—measured by thermogravimetry under nitrogen—and their fire properties like LOI.^{58,59} This approach was refined to take char yield (μ) and the effective heat of combustion of the pyrolysis products (h_c) divided through the heat of gasification (h_g) into account.^{60–63} Indeed, the effective heat of combustion of the volatile pyrolysis products is observed to lie between 3 and 45 kJ g⁻¹.^{28,60,62,64} However, fire behavior is controlled not by the effective heat of combustion of the volatiles (h_c), but by its product with combustion efficiency (χh_c). Whereas combustion efficiency is near a value of $\chi = 1$ in the well-ventilated LOI or UL 94 setup, it typically changes to values below $\chi < 0.8$ for effective flame inhibition. Further, in some systems the best results in flammability seem to be achieved when flame inhibition is accompanied by some stable residue formation (Table 15.3).^{48,52–57}

Furthermore, melt flow and dripping are sensitive to ignition and burning from the top (LOI) or from the bottom (UL 94: V-classifications)³⁴ as well as to a horizontal (UL 94: HB-classifications) or vertical (LOI, UL 94: V-classifications) specimen position during testing. Both melt flow and

TABLE 15.3
LOI Performance of the Materials

	LOI/% ($\pm 1\%$)		LOI/% ($\pm 1\%$)
PP-g-MA	19.2	PA 66-GF	22.4
PP-g-MA/5% LS	19.3	PA 66-GF/7% P _{red}	26.0
Only barrier		Charring	
	LOI/% ($\pm 1\%$)		LOI/% ($\pm 1\%$)
HIPS	17.2	PBT-GF	19.7
HIPS/15% Mg(OH) ₂	19.5	PBT-GF/13.3% ZnPi	27.0
Barrier + additional effects		Flame inhibition	
	LOI/% ($\pm 1\%$)		LOI/% ($\pm 1\%$)
PA 66-GF	21.5	PBT-GF	19.7
PA 66-GF/11.4% AlPi	37.9	PBT-GF/13.3% AlPi	42.0
Flame inhibition + charring		Flame inhibition + charring	

Sources: Braun, U. and Scharrel, B., *Macromol. Chem. Phys.*, 205, 2185, 2004; Braun, U. et al., *Polym. Degrad. Stab.*, 92, 1528, 2007; Bartholmai, M. and Scharrel, B., *Polym. Adv. Technol.*, 15, 355, 2004; Scharrel, B. et al., *J. Appl. Polym. Sci.*, 83, 2060, 2002; Scharrel, B. and Braun, U., *e-Polymers*, Art. no. 13, 2003; Braun, U. and Scharrel, B., *Macromol. Mater. Eng.*, 293, 206, 2008; Braun, U. et al., *Polym. Adv. Technol.*, 19, 680, 2008.

Note: PP-g-MA, poly(propylene-graft maleic anhydride); LS, layered silicate; ZnPi, zinc phosphinate; AlPi, aluminium phosphinate.

dripping are significant mechanisms to remove heat from the pyrolysis zone, thus reducing heat release, flame spread, and enhancing self-extinction. In the LOI, two kinds of burning for a thermoplastic material were reported, clean burning and a burning with melting and dripping, which differ in the resulting LOI values.⁶⁵ The left side of Figure 15.4 illustrates the influence of dripping on an upward-burning fire behavior for the investigated polypropylene graft maleic anhydride (PP-g-MA), which extinguishes due to dripping, but its burning drops probably ignite the surroundings; a corresponding layered silicate (LS) PP-g-MA nanocomposite (PP-g-MA/LS), for which the dripping and hence the extinction of the specimen is inhibited.^{53,66} The right side of Figure 15.4 shows the residues of PC/ABS, PC/ABS/PTFE (PTFE content <0.5 wt.%), PC/ABS/bisphenol A bis(diphenyl phosphate) (BDP), and PC/ABS/PTFE/BDP after UL 94 testing.⁶⁷ The antidripping effect of adding a small amount of PTFE becomes apparent,^{24,68} whereas the flame-retardant BDP shows a clear plasticization effect. In Table 15.4, the corresponding LOI and UL 94 results are summarized. Not only PC/ABS shows self-extinction in the vertical UL 94 test due to burning dripping, but also PC/ABS/BDP. Indeed, it shows a clearly enhanced propensity for dripping (Figure 15.4). Adding PTFE inhibits dripping so that no self-extinction is observed in PC/ABS/PTFE (= HB classification). PTFE is a very important real synergist for the effectiveness of aryl phosphates in PC/ABS. By avoiding dripping in combination with aryl phosphates, PC/ABS/PTFE/BDP achieves V-0, which is a prerequisite for challenging applications. Only when PTFE stabilizes the pyrolysis zone in the vertical UL 94 test, the flame retardancy action of BDP is exploited.⁶⁷ Fibers such as glass fibers in glass-fiber reinforced composites also inhibit dripping and melt flow⁶⁹ and thus often decrease the LOI or UL 94 performance, at least for the usual glass fiber content. Consequently, flame retarding such composites is generally more challenging than for their corresponding pure polymers, and often requires different flame retardancy approaches than for the polymer without glass fibers.

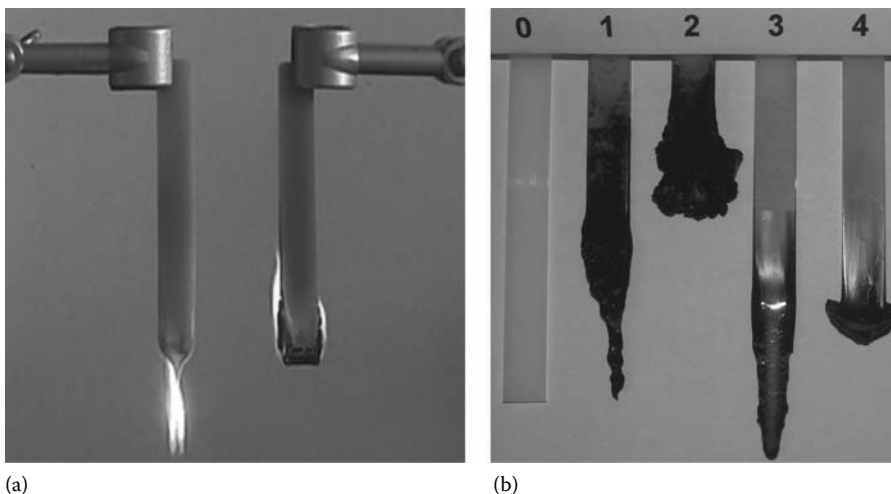


FIGURE 15.4 Influence of dripping on the fire behavior of PP-g-MA and PP-g-MA/LS nanocomposite (a) and UL 94 residues (specimen 0 before UL 94 test) of (1) PC/ABS, (2) PC/ABS/PTFE, (3) PC/ABS/BDP, and (4) PC/ABS/PTFE/BDP (b). PC/ABS and PC/ABS/BDP show extinction due to dripping (V-2); PC/ABS/PTFE HB behavior; PC/ABS/PTFE/BDP shows self extinction (V-0).

TABLE 15.4
Flammability (LOI, UL 94) for PC/ABS, PC/ABS/PTFE, PC/ABS/BDP, and PC/ABS/BDP/PTFE

	PC/ABS	PC/ABS/PTFE	PC/ABS/BDP	PC/ABS/BDP/PTFE
LOI/% ($\pm 1\%$)	23.2	23.6	26.0	28.1
UL 94	V-2	HB	V-2	V-0

UL 94 and LOI are discussed in detail, because these two are used most commonly and universally in materials flammability development. However, there are many more small heat source ignition tests. First of all, it should be noted that there are further tests based on a small flame as ignition source, similar to LOI and UL 94, such as small burner/flame tests (building, textiles) or the needle flame test (electrical engineering). There are also two further tests based directly on the LOI setup and test procedure: LOI for elevated temperatures and determination of a nitrous oxide index. Both deliver quite interesting results with respect to flame retardancy mechanisms,³⁶ but are used very rarely. The FMVSS 302 test for motor vehicle interior components is a common Bunsen burner type test too, but its specific protection goal is so low that it is probably not relevant for the challenges in development. As indicated before, there are also tests that are crucially different, as they do not use a pilot flame but irradiation, a glow wire, or a cigarette as the ignition source. Often they simulate specific scenarios that are important for a given application, such as cigarette tests for upholstery and mattresses, and glow wire tests and high current/voltage arc ignition tests in electrical engineering and electronics.

LOI (of minor importance in building, rail vehicles codes) and UL 94 (important test for electronics and electrical engineering regulations) are commonly and successfully used far beyond their mandatory performance for screening and estimation of fire behavior in flame-retarded materials development. However, owing to their specific fire scenario, the explanatory power of LOI and UL 94 is restricted, particularly when the fire scenario or the protection goal is changed. In particular despite its advantages, the use of LOI was doubted, since its minor importance in real fires and its less

demanding downward-burning configuration resulting only in no or rough correlations with other fire tests.^{34,35,70} However, probably only since the V-1 and V-0 classifications are quite demanding in UL 94 and achieved only through a substantial flame retardancy approach, the results correlate surprisingly well with fire tests covering the fire scenarios of a developing fire.⁷¹

15.3 DEVELOPING FIRE: FORCED FLAMING COMBUSTION

The cone calorimeter is a rather performance-based bench-scale fire testing apparatus,^{72–75} which realizes forced flaming conditions⁶² and thus simulates a developing fire scenario with a very small specimen size. Therefore, it is not surprising that beyond its use in mandatory codes (transportation, building in Japan) the cone calorimeter has found increasing implementation as a characterization tool in the research and development of fire-retarded polymeric materials. When characteristics such as peak HRR (PHRR), THR(t), and THE are discussed with respect to the development of new flame-retarded materials, they are used as a means of comparing systematically varied samples, whereas the absolute numbers are often of minor interest. Thus, some important aspects and approaches are addressed in the in the subsequent text, which received consideration in evaluating cone calorimeter data, interpreting the results and drawing conclusions.

Square-shaped 100 mm × 100 mm samples are used, mostly of a thickness between 2 and 10 mm; therefore the cone calorimeter is described as a small-scale or bench-scale fire test. Its length scale corresponds to the upper limit of the flammability tests typically used to characterize performance in ignition scenarios. The sample size is of the smallest order of magnitude discussed in fire engineering and of the largest used in polymer analysis. Hence, the cone calorimeter constitutes an important link between fire engineering and polymer science, which is crucial in the interdisciplinary area of the flame retardancy of polymers. Furthermore, it provides comprehensive insight into not only several fire risks such as HRR, THR(t), THE, and t_{ig} , but also fire hazards such as smoke release and CO production. Further, the ML and its rate are monitored. The cone calorimeter setup was developed thoroughly⁷⁴ to provide comprehensive and meaningful insight into the fire properties of materials,⁷⁵ rather than to correspond to a special full-scale scenario of a real fire. However, the cone calorimeter setup also defines a specific fire scenario. As is typical for all fire tests, samples' performance in the cone calorimeter depends on the characteristics of the test, including ignition source, ventilation, irradiance (external heat flux, \dot{q}_{ex}''), temperature, and the geometry of the specimen. Strictly speaking, the cone calorimeter test characterizes the performance resulting from an interaction of material properties, specimen, and the defined fire scenario. The meaning of the results may have little relevance for other fire scenarios or fire tests that essentially differ in their setup.

After ignition, the cone calorimeter represents a well-defined flaming condition, forced by external radiation, typical for a developing fire scenario. The external radiant heat flux is varied, typically between $\dot{q}_{ex}'' = 25$ and 70 kW m^{-2} . Applying an irradiance of $\dot{q}_{ex}'' = 35$ or 50 kW m^{-2} , corresponding to the heat fluxes typical for developing fires,^{76,77} it aims to replicate the performance in developing fires. Thus one of the key features of cone calorimeter is that reasonable insight into the developing fire behavior of a material can be obtained from a small specimen, reducing development time and cost. Although this is a significant advantage of the cone calorimeter, it is not without some important limitations. For instance, there is ignition by radiation accompanied by a spark, burning is well ventilated, the specimens are usually in a vertical position to rule out melt flow and dripping, no real flame spread occurs, and burning is one dimensional (the flame front penetrates only the depth of the sample). This dimension, the thickness, can be varied in the cone calorimeter, and the thickness used has a significant influence on the results, as is also typical of performance in real fires (fire load, flame spread, flammability, and ignition) and hence most fire tests. The thickness of the investigated samples has to be taken into account thoroughly in the discussion of cone calorimeter results. In particular, thermally thin samples show a decreased ignition time, as it is no longer dependent on the conductivity controlling the heat transport into the sample, but on the thickness characterizing the limited volume that is heated up. Further, samples

that are thermally thin or of intermediate thickness show a higher PHRR than do thermally thick samples.⁷⁸ There are no general limits for the different regimes, but they are dependent on the irradiation⁷⁹ and thermal properties of the specimen during burning, such as thermal conductivity and heat capacity. Further, it should be noted that, according to ISO 5660, all specimens less than 6 mm thick are considered to be thin specimens, which does not necessarily mean that they are thermally thin, but provides useful guidance about the type of behavior to be expected. Furthermore, any variation in specimen thickness results in a different typical set of HRR curves for different burning behavior. This influence is shown for noncharring and residue-forming material (Figure 15.5).^{80,81} Most obviously, time to PHRR is shifted for the noncharring material by varying the thickness, whereas it remains constant for the residue-forming material. This result shows that specimen thickness is a key parameter that needs to be chosen carefully, in accordance with the aim of the cone calorimetric measurement. For applied research and development, as well as for regulatory testing, the end-use condition dictates the thickness to be tested. Thicker samples may be more advantageous to study material properties, but have little relevance with respect to end-use conditions. In any case, a comparison of cone calorimeter results obtained for different materials requires testing with the same specimen thickness.

Higher irradiation levels give better reproducibility, more clearly defined ignition, and shorter measurement times, but correspond to more developed fires. Thus particularly for flame-retarded polymers, a smaller irradiation level often corresponds better to the fire protection goals addressed. Cone calorimeter results for the HRR at small irradiances correspond to flammability tests such as LOI and UL 94, if a reasonable set of materials are compared and the behavior is not dominated by dripping effects. Thus different considerations govern the choice of external heat flux.^{76,77}

The external heat flux (\dot{q}_{ex}'') from the cone heater does not exclusively determine the heat flux important for samples' pyrolysis in the cone calorimeter, since the reradiation from the hot sample surface (\dot{q}_{rerad}''), the loss by thermal conductivity into the specimen and the surroundings (\dot{q}_{loss}''), and the heat flux from the flame (\dot{q}_{flame}'') are also of the same order of magnitude.⁸²⁻⁸⁵ Thus, the heat flux effective with respect to pyrolysis during a cone calorimeter run (\dot{q}_{eff}'') is the result of the external heat flux and the material's response ($\dot{q}_{\text{eff}}'' = \dot{q}_{\text{ex}}'' + \dot{q}_{\text{flame}}'' - \dot{q}_{\text{rerad}}'' - \dot{q}_{\text{loss}}''$).

The cone heater is designed to provide rather homogeneous irradiation over the entire sample surface. It is reasonably optimized for a particular distance (2.5 cm) between the defined sample surface (a square 10 × 10 cm) and the cone heater. The irradiance is constant for an area larger than 5 cm × 5 cm at a distance of 2.5 cm, as specified by the ISO 5660 standard. There are considerable deviations in the heat flux when the distance is changed with respect to both the vertical and the horizontal characteristics.^{80,81} Thus, strictly speaking, the cone calorimeter must not be used for samples that exhibit significant deformation, such as foams that collapse before ignition, some polymers that show extensive deformation, or the presence of intumescent materials. Changing the initial distance by the

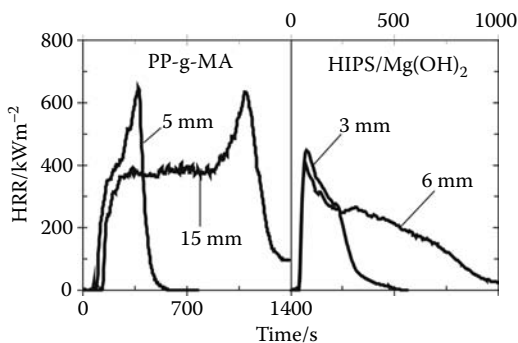


FIGURE 15.5 Comparing the influence of thickness for a noncharring (PP-g-MA) and a residue-forming (HIPS/Mg(OH)₂) polymeric material with respect to HRR.

user or the change in distance due to the deformation of the sample during the test have a significant influence on the fire scenario and hence on the cone calorimeter results.

The maximum surface temperatures reached without ignition are around 570–790 K (300°C–520°C) for low external heat fluxes ($\dot{q}_{\text{ex}}'' = 15\text{--}35 \text{ kW m}^{-2}$),^{80,81} which corresponds to the critical radiant flux required to ignite many combustible organic materials; $\dot{q}_{\text{ex}}'' = 50 \text{ kW m}^{-2}$ causes temperatures up to around 880 K (610°C), and $\dot{q}_{\text{ex}}'' = 70 \text{ kW m}^{-2}$ up to 970 K (700°C). A direct measurement of the response to a small flame, like the ignition source targeted by a flammability test (UL 94, LOI), is not possible because the combination of small irradiation and a high temperature is not available in the cone calorimeter. Temperatures reached for high irradiation are lower than temperatures on the standard time temperature curve typically used in testing with respect to fully developed fires. Thus, no correlations can be drawn between cone calorimeter and testing with the standard time temperature curve when high-temperature processes are crucial.⁸⁶ However, after ignition materials, decomposition, pyrolysis, and vaporization exert cooling effects on the surface. Indeed, for noncharring materials the pyrolysis temperature equals the surface temperature as the pyrolysis zone moves through the sample, consuming the material.

During the cone calorimeter experiment, the main result of heat release, especially HRR^{81,87} and THR, is determined by oxygen consumption calorimetry.^{88,89} In due course, different types of typical burning behavior give rise to characteristic curves of HRR. Some are illustrated schematically in Figure 15.6:⁸¹

- (a) Thermally thick noncharring (and nonresidue forming) samples show a strong initial increase after ignition up to a quasi-static HRR value, corresponding to the HRR_{st} (steady state HRR). This plateau remains near the end of the test when the PHRR occurs. This peak is caused by diminution of \dot{q}_{loss} as the glass wool supporting the sample prevents heat transfer to the sample holder as the pyrolysis zone approaches it.

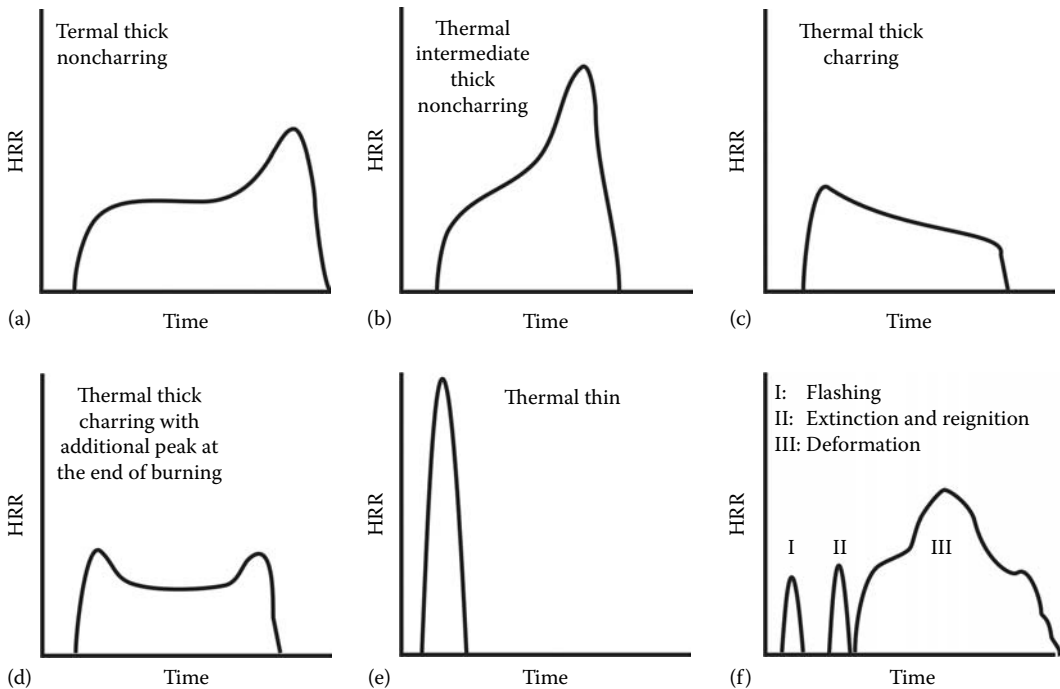


FIGURE 15.6 HRR in the cone calorimeter for typical burning behaviors: (a) thermally thick noncharring; (b) intermediate thermally thick noncharring; (c) thermally thick charring; (d) thermally thick charring with additional heat release maximum at the end of burning; (e) thermally thin samples; (f) samples that show flashing, extinction and reignition, and deformation.

- (b) For noncharring samples of intermediate thickness the plateau vanishes. The HRR_{st} is marked only by a shoulder. The PHRR increases more than the thermally thick noncharring samples because its origin is halfway between the behavior of thermally thick noncharring and thermally thin samples, as discussed here.
- (c) Thermally thick charring (residue-forming) samples show an initial increase in HRR until an efficient char layer is formed. As the char layer thickens, HRR decreases. The maximum reached at the beginning equals both the HRR_{st} and the PHRR.
- (d) Some thermally thick charring materials, such as wood (but not exclusively), tend to show a HRR peak at the beginning, prior to charring, and a second HRR peak at the end of the measurements. The second peak may be caused by cracking the char or increasing the effective pyrolysis temperature, analogous to that observed with the thick noncharring materials.
- (e) Thermally thin samples are characterized by a sharp peak in HRR, since the whole sample is pyrolyzed at the same time. In this case, the PHRR is dependent on their total fire load.
- (f) Some samples show HRR curves characterized by a kind of unsteady development of combustion. Reasons for this can be flashing (ignition followed by self-extinction) before a sustained flame or during the whole measurement, or deformation during burning, which changes the surface area and distance to the cone heater.

Obviously, this everyday interpretation of HRR curves is mainly empirical, but it clearly demonstrates that the full information on the fire behavior in terms of its HRR is available only by looking at the complete HRR curve over the full duration. Only the whole HRR curve can adequately represent the fire behavior controlled by the material-specific properties (char yield (μ), effective heat of combustion (h_c), heat of gasification (h_g), etc.), the influences from the specimen (thickness, deformation, etc.), and the physical and chemical mechanisms active during burning (increasing and cracking char layer, endothermic reactions, release of different pyrolysis products, afterglow, etc.). However, for practical reasons often only characteristic values are used to describe burning behavior, such as averaged HRR or PHRR. These values do not contain the complete information and may sometimes be misleading.

The PHRR in the cone calorimeter is strongly dependent on the test setup and the specimen, as well as the intrinsic fire properties of the materials. To obtain comparable results, it is essential for the specimen and sample holder to be used as defined in the standard. This is illustrated in Figure 15.7, where the cone calorimeter HRR curves are compared with results using a modified sample holder.^{80,81}

The modified sample holder allows heat to be conducted away from the back of the specimen. Consequently, the large PHRR disappears at the end of burning the noncharring materials (around

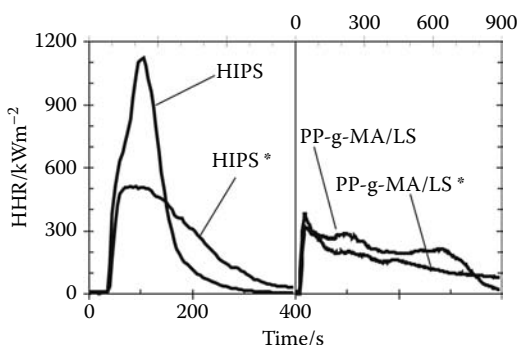


FIGURE 15.7 HRR for HIPS (noncharring) and PP-g-MA/LS (char/residue-forming) if the standard or a modified sample holder is used in the cone calorimeter. In the modified setup the sample is placed at a conductive 1 cm thick Cu plate.

100s for a 3 mm-thick HIPS specimen in Figure 15.7), whereas the PHRR is barely affected for residue-forming materials at the beginning of the HRR curve (PP-g-MA/5 wt.% LS material) (Figure 15.7). This difference is explained by the different origin of the PHRR, as described earlier. The PHRR of a specimen in the cone calorimeter is clearly not an “intrinsic” material property. This is also the reason why correlations with other tests such as LOI and UL 94 usually show some deficits when PHRR is used.⁸¹ However, “nonintrinsic” material properties are not artifacts, and may be quite important with regard to the assessment of real fire hazards.⁸⁷ Indeed, the thermal insulation at the back of the specimen in the cone calorimeter setup was originally chosen to represent free-standing material applications, and the PHRR is probably the most widely used result from cone calorimeter investigations.

To simplify the interpretation of cone calorimeter data, indices have been introduced to assess the hazard of developing fires, such as the FIGRA (fire growth rate) and the MARHE (maximum average rate of heat emission). These are used for regulatory purposes, such as FIGRA for the single burning item test (SBI; EN 13823) with respect to the building products, and MARHE for cone calorimeter tests with respect to fire protection in railway vehicles according to CEN TS 45545. However, these indices try to concentrate the relevant information into a single number, which has limited physical meaning with regard to fire behavior, and thus clearly oversimplify and can even be misleading. It should be noted that the flame spread in developing fires is controlled by several characteristics, such as the heat release of the burning part of the specimen, the specimen (thickness, orientation, etc.), the ignitability of the surface material, the fire scenario (ventilation, airflow, etc.), the direction in which the flame spread is considered (opposed flow, wind-aided, horizontal, vertical, etc.) and so on. Obviously, real flame spread cannot be measured in the cone calorimeter, and hence it is not incorporated directly into any of the fire growth indices.

The THR(t) during a cone calorimeter test is the integral of the HRR with respect to time—the total heat output up to that point. The THR at the end of the test is the THE and is, therefore, the fire load of the specimen in the cone calorimeter fire scenario. The THE and the HRR are mathematically related, but monitor quite independent fire hazards.

Figures 15.8 and 15.9 illustrate examples of how cone calorimeter data can be used in the development of flame-retarded materials. PA 66-GF without P_{red} showed typical fire behavior for noncharring polymers containing inorganic glass fiber as inert filler,⁶⁹ when high external heat flux is applied. The shape of the HRR curve is divided in two different parts. In the beginning, the surface layer pyrolysis shows a sharp peak, followed by a reduced pyrolysis rate when the pyrolysis zone is covered by the glass fiber network residue layer. When P_{red} was added, the PA 66-GF samples were transformed into carbonaceous char-forming materials, which led to a

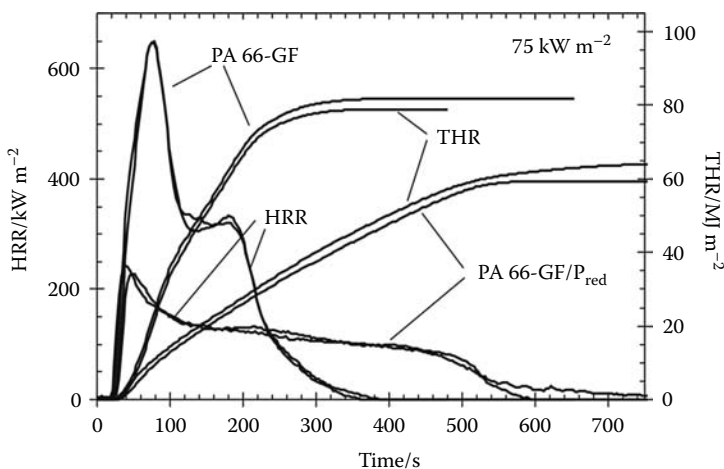


FIGURE 15.8 HRR and THR of PA 66-GF and PA 66-GF/ P_{red} for irradiation = 75 kW m^{-2} . P_{red} reduces the THE and the PHRR.

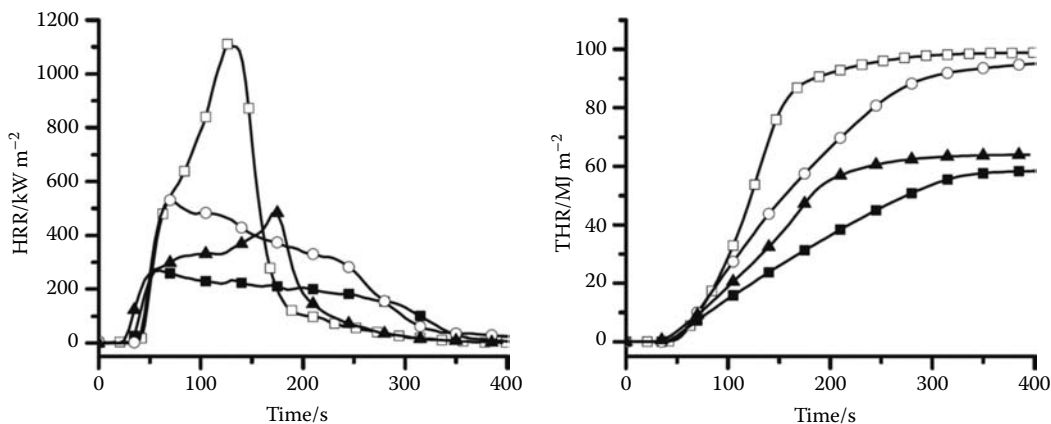


FIGURE 15.9 HRR and THR of HIPS (open squares), HIPS/ P_{red} (filled triangles), HIPS/ $Mg(OH)_2$ (open circles), and HIPS/ $P_{red}/Mg(OH)_2$ (filled squares). HIPS and HIPS/ P_{red} show the typical HRR curve of a noncharring material; HIPS/ $Mg(OH)_2$ and HIPS/ $P_{red}/Mg(OH)_2$, that of residue-forming material. Adding P_{red} reduces the HRR and THE by flame inhibition; $Mg(OH)_2$ reduces the HRR, mainly by introducing a barrier.

reduction in the THE and a reduction in the PHRR, accompanied by a prolongation of the burning time.⁵⁴ The reduction in the THE correlates with the increase in residue. The effective heat of combustion determined by the cone calorimeter software (dividing heat release by ML) is not changed, which means the ratio $THE/ML \sim \chi \cdot h_c$ is constant, indicating the absence of relevant gas-phase mechanisms such as flame inhibition or fuel dilution. The cone calorimeter investigations highlight P_{red} as an interesting halogen-free char inducing flame-retardant for PA 66 with respect to HRR and THE.

The influence of different flame retardants ($Mg(OH)_2$ and P_{red} in HIPS) and their combination is shown in Figure 15.9.⁴⁸ The most obvious effect of the 15 wt.% $Mg(OH)_2$ used in the cone calorimeter is not the release of incombustible cooling agents such as water, but barrier formation in the condensed phase. HIPS and HIPS/ P_{red} show the typical HRR curve of a noncharring material, whereas HIPS/ $Mg(OH)_2$ and HIPS/ $P_{red}/Mg(OH)_2$ show the typical HRR curve of a charring—or a better, residue-forming—one. The clear change in the HRR curve was accompanied by a clear decrease in PHRR and prolongation of burning time, but the amount added, 15 wt.% $Mg(OH)_2$, is far too little to exert a significant influence on the THE (Figure 15.9). The barrier properties of the inorganic residue layer in HIPS/ $P_{red}/Mg(OH)_2$ were clearly improved in comparison with HIPS/ $Mg(OH)_2$.⁴⁸ With respect to barrier properties, the combination of P_{red} and $Mg(OH)_2$ shows clear synergy, since MgO is replaced by Mg-phosphates. Of course, in the cone calorimeter experiment, the formation of Mg-phosphates is indicated only by the increased residue. Unambiguous evidence was supplied by solid-state NMR investigations proving the formation of glassy Mg-phosphates.⁹⁰ Adding P_{red} to HIPS or HIPS/ $Mg(OH)_2$ significantly reduced the THE/ML, respectively, and thus also the THE, through flame inhibition in the gas phase (Figure 15.9). P_{red} does not show a significant interaction with the HIPS decomposition. No additional carbonaceous char was produced. Detailed data evaluation indicates that the combination shows a slight antagonism with respect to flame inhibition.⁴⁸ However, over all the fire retardancy of HIPS containing P_{red} and $Mg(OH)_2$ was significantly better than when either additive was used alone. Since the flame retardancy effect cannot be increased efficiently by using more P_{red} (Table 15.1), and because a very large amount of $Mg(OH)_2$ is needed to obtain performance similar to that of the combination, the combination is the far more interesting system with respect to fire retardancy.

As indicated in the introduction, not only the identification of promising polymer-flame retardant systems and promising additive combinations is at the focus of materials development, but also the amount and the optimization of the substances used. Such examples are shown in Figures 15.10

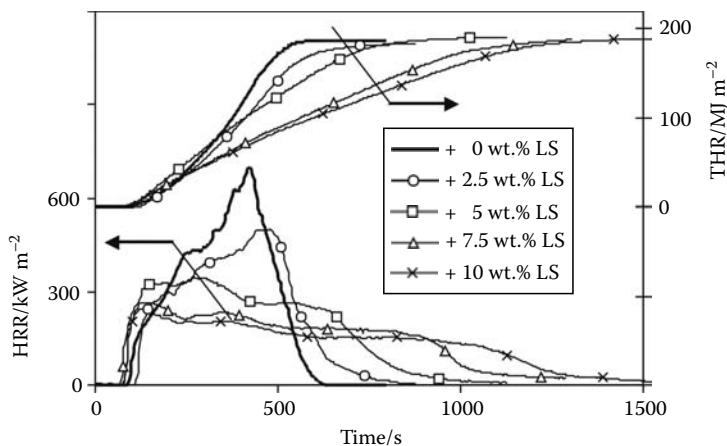


FIGURE 15.10 HRR and THR for PP-g-MA/LS nanocomposite plotted against the amount of clay added (0, 2.5, 5, 7.5, 10 wt.% clay; external heat flux = 30 kW m^{-2}).

and 15.11.^{53,91} In Figure 15.10, the HRR and the THR of PP-g-MA/LS nanocomposites are shown with increasing LS content. In this system, the additional carbonaceous char formation is negligible. The increase in residue corresponds to the inert filler effect of LS. As a consequence, the change in THE is less than 10% and thus still in the same order of magnitude as the typical error. The only relevant flame retardancy mechanism that influences fire behavior in the cone calorimeter is the change in the HRR shape from a noncharring material to a residue-forming one.⁶⁶ The PHRR at the end of burning vanishes more and more and thus is replaced by the PHRR in the beginning, typical for residue-forming materials. The PHRR drops dramatically—by more than 50%—even when only small amounts of LS are added, but this effect is not linear in keeping with LS concentration, leveling out for amounts larger than 7.5 wt.%. Only very high loadings are expected to show a larger impact, when the replacement of polymer results in a crucial additional reduction in fuel.

Figure 15.11 illustrates an example of the kind of development tasks that can exist and be addressed within the same materials system. The polymer and the additive as well as their concentration are

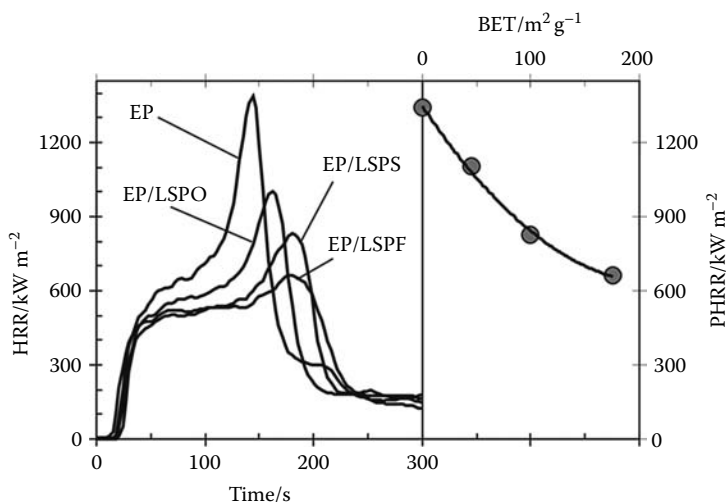


FIGURE 15.11 HRR (irradiation = 70 kW m^{-2}) of EP, EP/LSPo, EP/LSPs, and EP/LSPF plotted against time and PHRR plotted against the BET of the LSP used. BET as well as the reduction in PHRR increase in the order: oven-dried (LSPo) < spray-dried (LSPs) < freeze-dried (LSPF).



FIGURE 15.12 Fire residue of EP+15 wt.% APP (left) and EP+LS+10 wt.% APP (right). Combining APP with LS inhibited intumescence, causing strong antagonism.

the same for the layered silicate epoxy resin nanocomposites (EP/LS) investigated.⁹¹ Only the morphology of the LS was varied, owing to the different drying procedures during processing. The tetraphenyl phosphonium-modified LS was dried in a ventilated oven and subsequently ground in a ball mill (LSPO), spray-dried (LSPS) or freeze-dried (LSPF). The reduction in PHRR compared with the EP increases significantly with the increasing BET surface of the additives used. The reason for this is the increased homogeneous distribution of LS as monitored by TEM.⁹¹

During a cone calorimeter run, visual observation is often a crucial step in understanding the burning behavior of a specimen.⁸¹ Bubbling, char formation, surface rise, deformation due to residual stresses, intumescence, char cracking, collapse of structures, and afterglow are the examples of important observations of the test. These phenomena profoundly influence the HRR, but cannot necessarily be deduced unambiguously from the HRR curves. In Figure 15.12 such an example is shown by the mean of fire residues.

Combining 5 wt.% LS with 10 wt.% ammonium polyphosphate (APP) in EP (EP/LS/APP) inhibited the intumescence due to APP and causes a strong antagonism.⁵¹ It is assumed that adding LS to any polymer/APP systems influences the viscosity in the pyrolysis zone, the amount and the mechanical strength of the fire residue. These interactions can be deleterious as in the investigated system, but can also be advantageous.⁹² It should be noted that according to ISO 5660 visual observations are an essential part of the test results and must be recorded.

Apart from the cone calorimeter, fire testing within the fire scenario of a developing fire is usually based on the larger specimens, generally ruling these tests out for comprehensive systematic investigations or screening approaches. Radiant panel tests are common for different applications (buildings, ships, railway vehicles), in which a real flame spread is measured based on 230 mm × 1050 mm or 155 mm × 800 mm samples. Further, building codes require tests such as the European SBI test (EN 13823), which simulates fire propagation in a room corner, and the U.S. Steiner tunnel test based on specimens of 2.25 m² and 3.73 m², respectively. Thus, within the topic development of fire retardant materials, truly reliable procedures to predict performance in the SBI or Steiner tunnel test are needed and are under development—in particular using the cone calorimeter data.^{93–97}

15.4 FULLY DEVELOPED FIRE

Apart from some specific areas such as fuel tanks or intumescent coatings, the performance in a fire test simulating a fully developed fire is often not of real interest with respect to the development of fire-retarded polymers, since common flame-retarded polymeric materials are used in applications

that demand the inhibition of fire hazards only with respect to the beginning (electrical engineering, electronics, etc.) and the development of a fire (building, transportation, etc.) (as illustrated in Figure 15.1). However, since recent developments like the increasing use of carbon and glass fiber reinforced polymer composites to replace metallic materials in structural building and transportation applications, the focus of interest is shifting to passing tests simulating fully developed fire scenarios.

Testing codes within the scenario of a fully developed fire are based on intermediate, large, or full-scale testing. Specimens are typically in the dimension of several square meters and often, real components such as building columns are tested, or the whole product in the case of gas bottles. Tests like the small-scale test furnace based on specimens of 500 mm × 500 mm are exceptions. Intensive flame application or the use of furnaces realizing standard time–temperature curves are used to simulate the characteristics of fully developed fires. Thus, in particular the heat impact of convection and the surface temperature are clearly greater than in the tests discussed earlier. The fire properties investigated are often resistance to fire, or the fire or temperature penetration.

Again, the time and specimen size needed for these tests rule them out for comprehensive systematic investigations or screening approaches within the development of new materials. Thus, bench scale setups are common to estimate performance in the larger tests. Using high external heat fluxes ($\dot{q}_{ex}^* \geq 70 \text{ kW m}^{-2}$) in the cone calorimeter combined with temperature measurements has been proposed, in particular for intumescent coatings,^{98,99} even though this approach has some deficits with respect to the maximum surface temperature reached.⁸⁶ Furnaces that can realize the standard-time temperature curve for samples smaller than 250 mm × 250 mm are rare. In most cases, a flame is applied directly to smaller specimen by using Bunsen burner-type burners or burner areas, or similar bench-scale burner approaches. All of these approaches have some intrinsic limitations as compared with the larger test, in particular with respect to monitoring the structural integrity during fire, which often plays an important role for the component or product behavior in the larger tests.

15.5 OTHER FIRE HAZARDS

So far, the chapter has focused on preventing sustainable ignition and subsequent fire growth, which are, of course, the two main goals in fire protection. However, it is often not the heat or the flame that prevents people from escaping from a fire, but the smoke. In the majority of cases, toxic gases are the actual cause of the loss of human life. In general, combustion is never complete in a real fire, so that apart from products such as H₂O and CO₂, other products of incomplete combustion such as soot, smoke, HCN, and CO are quite characteristic and, in fact, important fire hazards. What is more, as a consequence, flame inhibition that reduces combustion efficiency (χ) is accompanied by an increase in CO yield and often, smoke yield as well. Of course, this yield is less than the absolute amount of material, and a burning item generally produces more smoke and toxic gases than a nonburning item; further, self-extinguishing during an early stage of a fire reduces smoke and toxic gases. However, particularly in some transportation applications like aviation, shipping, and railway vehicles, the combination of reducing fire growth and smoke yield (or toxic gases production and yield) is required, and thus constitutes a goal in the development of flame-retarded materials. Typical approaches are the use of a combination of a flame retardant and a smoke suppressant, or implementing a change in the flame retardant or polymer material itself.

The ventilation condition has a significant effect on fire hazards like HRR, fire growth rate, smoke, and CO production; in the latter cases, this crucially influences both the absolute amount and the ranking of different materials. CO production and smoke production depend not only on the material, but also strongly on the fire scenario.^{100,101} The most important influence is ventilation, but other parameters such as temperature, irradiation, residence time, and quenching effects are also important. Comprehensive studies in which more than one of the key influences varied systematically¹⁰² are rare, and show rather complex landscapes of dependencies. There are no easy correlations between different fire scenarios or fire tests. The absolute amount and the ranking of different

materials in one test are of limited use in predicting the results in another. Thus, the development of flame-retarded materials in this area is based on the established smoke or toxicity tests that have to be passed for different applications. The most important tests are probably the ones based on the NBS smoke chamber.

Efficient fire protection is also based on the consideration of product or scenario-specific hazards, which may lead to very specific materials development goals. Examples are the combination of impacts, such as vandalism and ignition source for seats in railway vehicles, or a preceding shock wave before the fire impact in navy applications. Some more product-specific phenomena of such kind are related directly to material properties, such as building up an increased risk for pool fires through burning thermoplastic plastics or dripping foams, and thus have become topics in the development of some flame-retarded materials.¹⁰³

Additional goals become relevant, in particular with respect to the protection of larger properties not subjected to direct fire influences, such as corrosion induced by the fire effluents. Hereby, the long-term corrosion damage to the building and to equipment (industrial machinery as well as electrical and electronic installations) is of great interest.

15.6 UNDERSTANDING FIRE BEHAVIOR AND FIRE RETARDANCY MECHANISMS

Figure 15.13 illustrates the fundamental difference in the fire retardancy mechanism of P_{red} used in HIPS and PA 66-GF evaluated by cone calorimeter testing.^{48,54,55,81} The THE for both materials with and without P_{red} as a fire retardant are plotted against the ML. The lack of significant change in the mass of residue shows that phosphorus in HIPS vaporizes nearly completely and no additional charring occurs. The THE is reduced through flame inhibition, reducing the product of the effective heat of combustion of the volatiles and combustion efficiency (χh_C), which is indicated by the reduced slope. For P_{red} in PA 66-GF χh_C remains constant, whereas the reduction in THE is caused by a decreased ML. This shows that P_{red} induces char formation in the condensed phase.

It is concluded that the difference in flame retardancy mechanisms of phosphorus flame retardants is due to the different decomposition pathways and interactions between flame retardant and polymer or their decomposition products, respectively. The release of phosphorous-containing molecules into the gas phase competes with char-inducing or inorganic residue-forming interactions

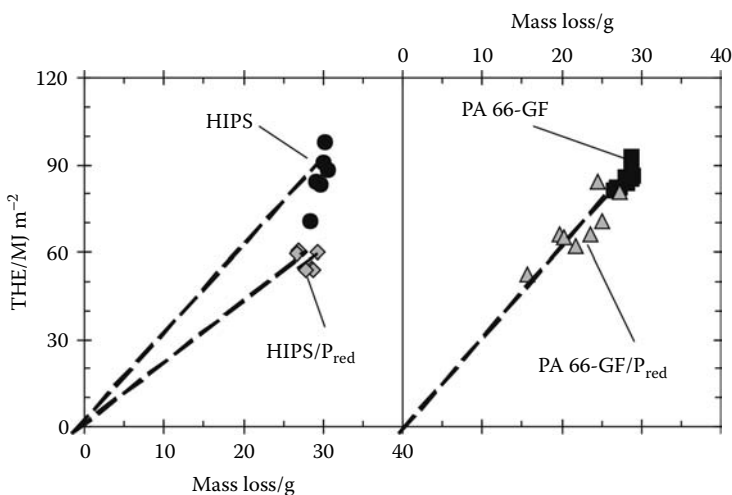


FIGURE 15.13 THE plotted against ML for HIPS, HIPS/ P_{red} , PA 66-GF, and PA 66-GF/ P_{red} , illustrating the pure flame inhibition effect of P_{red} in HIPS and the pure charring effect in PA 66-GF.

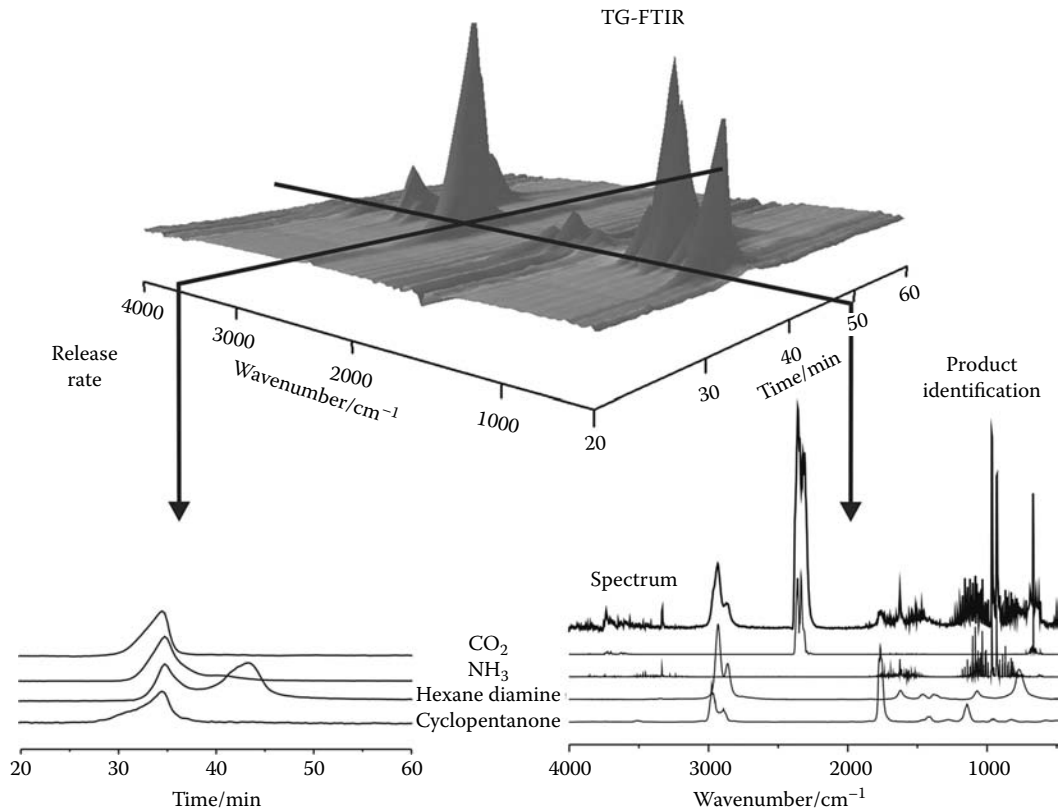


FIGURE 15.14 FTIR monitored online during a TG-FTIR experiment (this means several hundreds of FTIR spectra are taken) of PA 66-GF/MPP enables the identification of volatile pyrolysis products (H₂O, NH₃, CO₂, cyclopentanone, amines, and hydrocarbons) at distinct stages of the decomposition and the investigation of the product release rates.

in the solid state. Thus, the combination of cone calorimeter results and thermal analysis becomes interesting. Figure 15.14 illustrates the potential of evolved gas analysis to identify volatile pyrolysis products as well as the release rate during decomposition. TG-MS or pyrolysis GC-MS are also proposed as methods targeting the volatile pyrolysis products. Solid-state products are often tackled by solid-state NMR, ATR-FTIR, or XPS. Table 15.5 shows an example of how the results of combined cone calorimeter and thermal analysis can be used to improve our understanding of a system like PC/ABS/PTFE, PC/ABS/PTFE/TPP (TPP = triphenylphosphate), and PC/ABS/PTFE/BDP.⁶⁷ Even though TPP and BDP are very similar in their structure, thermal analysis monitors an earlier and slightly larger phosphorus release for PC/ABS/PTFE/TPP than for PC/ABS/PTFE/BDP, and only for PC/ABS/PTFE/BDP an increase in residue compared with PC/ABS/PTFE.⁶⁷ The same trends are monitored by cone calorimeter data $\chi \cdot h_c$ and residue. Using both thermal analysis and fire testing reveals an unambiguous understanding of the flame retardancy mechanism controlling the change in PHRR and THE.

Combining data obtained by the cone calorimeter with pyrolysis combustion flow calorimeter (PCFC; sometimes called microscale combustion calorimeter, MCC) results was also proposed to increase the understanding of flame retardancy and flame retardancy mechanisms.¹⁰⁴ Dividing the fraction of the effective heat of combustion of the volatiles (THE/ML) obtained from the cone calorimeter by the heat of complete combustion of the volatiles obtained from PCFC yields the combustion efficiency χ . Thus the combination of fire test and PCFC enables a quantitative

TABLE 15.5
Propensity for Phosphorus Release and Charring Determined by Thermal Analysis for PC/ABS Materials, Combustion Efficiency Multiplied by the Effective Heat of Combustion ($\chi \cdot h_c$), Residue, PHRR, and THE Determined by Cone Calorimeter

PC/ABS with	Thermal Analysis		Cone Calorimeter			
	P-release	Residue	$\chi \cdot h_c^a$ kJ g ⁻¹	PHRR ^b kW m ⁻²	THE ^a MJ m ⁻²	Residue ^b wt.%
			±0.5	±25	±1.5	±1
PTFE			23.6	555	55.7	33.7
BDP + PTFE	++	++	19.9	357	45.4	35.9
TPP + PTFE	+++		18.6	377	47.4	29.8

^a Average over all measurements for different irradiations.
^b Value for 50kW m⁻² irradiation.

evaluation of ventilation, but also of the flame inhibition that reduces χ . Figure 15.15 shows an example for PC/ABS/PTFE, PC/ABS/PTFE/BDP, PC/ABS/PTFE/RDP (RDP = resorcinol bis(diphenyl phosphate), PC/ABS/PTFE/TPP, and PC/ABS/PTFE/BDP/ZB (ZB = zinc borate).

For PC/ABS/PTFE, a combustion efficiency close to 1 ($\chi = 0.98$) was observed. Almost all volatile pyrolysis products were completely oxidized. This is in good accordance with the absence of a flame inhibition effect and the well-ventilated cone calorimeter fire scenario.³³ Corresponding results have been reported previously for different polymers in the cone calorimeter.³⁴ Adding BDP, RDP, and TPP results in a very similar flame inhibition activity in PC/ABS/PTFE ($\chi = \sim 0.8$), increasing slightly in the order BDP < RDP < TPP.¹⁰⁴ Using the combination of BDP and ZB results in the

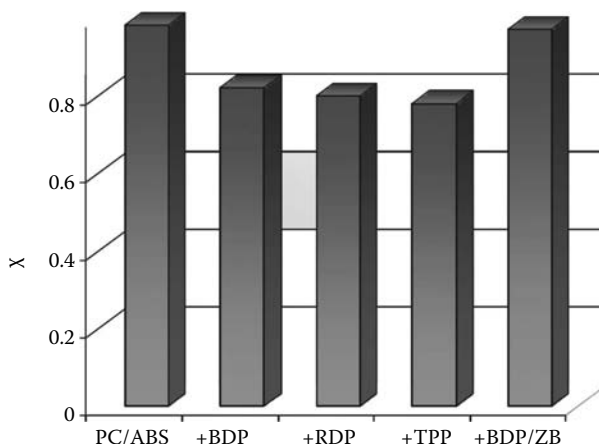


FIGURE 15.15 Combustion efficiency (χ) of various PC/ABS materials calculated using the THE/ML measured in the cone calorimeter, and the heat release per ML for the complete combustion of the volatiles monitored in the PCFC. Systems that do not show flame inhibition show combustion efficiencies of around 1, according to the well-ventilated fire scenario of the cone calorimeter. Systems, in which adding aryl phosphates result in flame inhibition, show combustion efficiencies of around 0.8. When the release of phosphorus is reduced by competing reactions in the solid state, combustion efficiencies of between 0.8 and 1 are observed.

TABLE 15.6
Comparison between HR ($\pm 0.3 \text{ kJ g}^{-1}$)
from PCFC and HOC_{bomb} ($\pm 0.03 \text{ kJ g}^{-1}$)
from Bomb Calorimeter

	PC/ABS
HOC_{bomb} (kJ g^{-1})	32.56
HR (kJ g^{-1})	22.4
$\text{HOC}_{\text{bomb}} - \text{HR}$ (kJ g^{-1})	10.2
μ (%)	18.3
HOC_{char} (kJ g^{-1})	55.7

formation of zinc phosphates in the solid state. This competing mechanism reduces the release of phosphorus in the gas phase. The combination showed a significant antagonism in terms of flame inhibition.

The additional power of charring becomes clear when results using a bomb calorimeter and PCFC for PC/ABS (Table 15.6) are compared.¹⁰⁴ The bomb calorimeter delivers the heat of combustion per mass for the complete oxidation of a material (HOC_{bomb}). The PCFC determines the heat of combustion per mass for the complete oxidation of the volatiles (HR), whereas the char formed during anaerobe decomposition is not oxidized. Subtracting the PCFC from the bomb calorimeter results delivers the heat of combustion held in the condensed phase by carbonaceous charring (Table 15.6). This value is zero for inert fillers or an inorganic residue. Inert fillers and inorganic residue are accompanied by a reduction in heat release only to the extent of polymeric mass per volume replacement, but do not cause a reduction by storing the fire load in the residue. The heat of combustion of the carbonaceous char of PC/ABS is around one-third of the total heat of combustion for PC/ABS (HOC_{bomb}), whereas the char yield (μ) is only around one-fifth. Thus, the heat of combustion per unit mass of PC/ABS char was calculated to be 55.7 kJ g^{-1} .¹⁰⁴ This heat of combustion per unit mass of char is clearly higher than the effective heat of combustion of the polymer (HOC_{bomb}). The enrichment of carbon in the char becomes apparent, resulting in a carbonaceous, graphite-like or fuel character. This result also correlates with investigations of the chemical composition of char reported in the literature,^{105,106} demonstrating 90% carbon for PC char. As a consequence, the increased charring of polymers containing hetero-atoms often results in a slight decrease in the effective heat of combustion of the fuel through corresponding fuel dilution, and, if the char is oxidized, also in a significant increase in products such as CO. Neither effect should be misinterpreted as flame inhibition. As a rule, carbonaceous charring is more than fixing a part of the polymer in the condensed phase or diluting the polymeric material. Charring due to the polymer structure entails fixing fuel in the condensed phase, and hence the formation of inorganic residue should always be distinguished from the charring of hydrocarbons.

Flame retardants or flame retardancy mechanisms, respectively, influence different fire properties quite differently, and, what is more, show different effectiveness in different fire scenarios, and thus fire tests. In extreme cases, flame retardancy with respect to a specific fire property or specific test is achieved with little or no improvement in performance in another fire property or fire test. This fundamental understanding in fire science sometimes may be overlooked in materials development, but is worth addressing. The influence on different fire risks and the dependency of effectiveness on the scenario addressed is discussed subsequently based on the fire retardancy mechanisms accompanying charring and barrier formation.

Char or inert residue influences fire behavior through two quite different mechanisms. As discussed earlier, char especially, but also inorganic fillers that replace polymeric material per volume, result in a reduction of the total fuel release and hence the THE. In a first approximation,

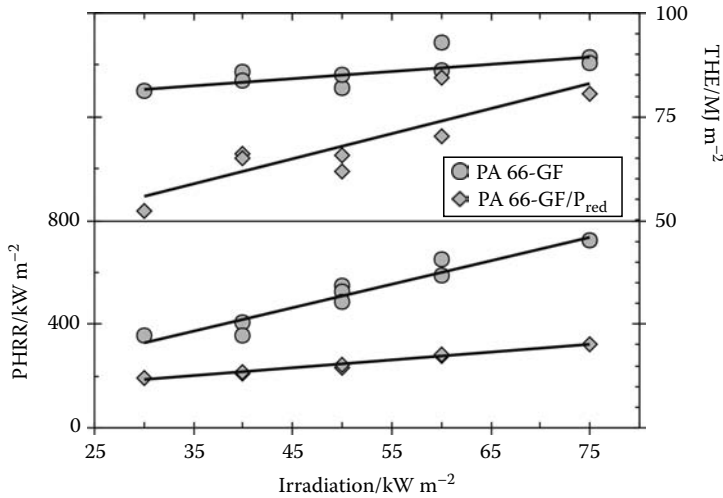


FIGURE 15.16 THE and PHRR of PA 66-GF and PA 66-GF/P_{red} plotted against irradiation. With increasing irradiation the flame retardancy effect vanishes with respect to THE and increases with respect to PHRR. The THE correlates to the ML during burning, which converges for PA 66-GF and PA 66-GF/P_{red} with increasing irradiation. The PHRR is determined more by the barrier properties of the char than by its quantity.

the increase in carbonaceous char yield also yields a proportional decrease in HRR. Further, every fire residue also works as a kind of barrier for heat or mass transfer, suppressing the HRR in particular. Although the same char is the origin of both effects, these mechanisms must be considered as independent to some degree. Again, this conclusion is illustrated exemplarily by the investigations on PA 66-GF/P_{red}. Figure 15.16 summarizes the THE and the PHRR for PA 66-GF/P_{red} in comparison with PA 66-GF.^{54,55} With increasing irradiance, an increasingly complete decomposition of the polymer resulted, so that fire retardancy vanished in terms of THE. In contrast to this, the reduction of PHRR increased for higher external heat fluxes, which was due to barrier properties.

It is striking that this system shows such a clear differentiation between the behavior of the two probably most important fire risks PHRR and THE, when the external heat flux is varied. The flame retardancy effect with respect to the THE decreases with increasing irradiation, whereas the relative flame retardancy effect with respect to the PHRR increases. The latter clearly indicates the predominant influence of the barrier effect on the HRR.

Taking into account the different heat fluxes in the cone calorimeter setup ($\dot{q}_{\text{eff}}'' = \dot{q}_{\text{ex}}'' + \dot{q}_{\text{flame}}'' - \dot{q}_{\text{rerad}}'' - \dot{q}_{\text{loss}}''$), Equation 4.1 was proposed for the idealized “steady-state” HRR (HRR_{st}) during a “steady-state” burning:^{60,62,107,108}

$$\text{HRR}_{\text{st}} = \chi(1 - \mu) \frac{h_c}{h_g} \dot{q}_{\text{eff}}'' = \chi(1 - \mu) \frac{h_c}{h_g} (\dot{q}_{\text{ex}}'' + \dot{q}_{\text{flame}}'' - \dot{q}_{\text{rerad}}'' - \dot{q}_{\text{loss}}'')$$

$$\text{HRR}_{\text{st}} = \chi(1 - \mu) \frac{h_c}{h_g} \dot{q}_{\text{ex}}'' + \chi(1 - \mu) \frac{h_c}{h_g} (\dot{q}_{\text{flame}}'' - \dot{q}_{\text{rerad}}'' - \dot{q}_{\text{loss}}'') = \text{HRP} \dot{q}_{\text{ex}}'' + \text{HRR}_0 \quad (15.1)$$

Hence, a linear dependency of the HRR_{st} from the external heat flux is expected (Figure 15.17) based on Schartel and Braun.⁵⁵ The slope (referred to as the heat release parameter, HRP) is interpreted as a fire response parameter,^{60,108} whereas the intercept (HRR_0) is considered a flammability parameter,^{62,107} at least on this length scale.

Both values are based on materials properties and are, or approximate, “intrinsic” materials properties. Some ideas of how an idealized HRR such as the HRR_{st} can be deduced from experimental

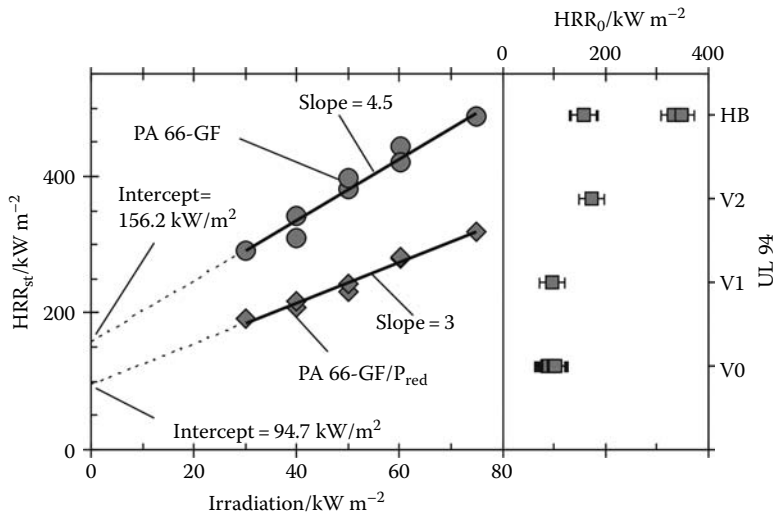


FIGURE 15.17 On left: HRR_{st} for PA 66-GF and PA 66-GF/ P_{red} at 30, 40, 50, 60, and 75 $kW\ m^{-2}$ and the extrapolation to irradiation = 0. The slope is the HRP; the intercept a flammability parameter (HRR_0). On right: UL 94 performance plotted against HRR_0 for a variety of PA 66-GF and HIPS materials. The critical value of $125 \pm 25\ kW\ m^{-2}$ is a good determination of the point when self-extinguishing behavior is reached.

cone calorimeter HRR data have been described,¹⁰⁷ but in practice the proposed methods do not work satisfactorily for many HRR curves.⁷¹ However, the improvement achieved by using HRR_{st} instead of PHRR was concluded through attempted correlation with other tests.^{58,96} In fact, the flammability parameter was found to correlate quite reasonably with UL 94 performance.⁶² A critical HRR of $125 \pm 25\ kW\ m^{-2}$ was proposed for self-extinguishing in the absence of the application of external heat.^{60,107} It must be concluded that the data error is generally so large that the influence of thickness (1.5–3 mm) in the UL 94 classification and the differentiation between the classification as V-0, V-1, or V-2 cannot be considered. The results for different PA 66-GF and HIPS materials investigated are summarized in Figure 15.17 following this approach.⁵⁵ Some of the selected data are quite close to self-extinction (V-0, V-1) or flammable (HB) behavior, respectively. Thus the data clearly challenge the practical use of the concept, and hence validate it. However, the precise prediction of UL 94 performance through droves of cone calorimeter data is, of course, academic claptrap. The important conclusion is that the inter- and extrapolation of results obtained under forced flaming conditions in the cone calorimeter can be used to get a reasonable and realistic idea of fire behavior in different fire scenarios such as flammability. Using several irradiances was proposed to obtain comprehensive information on material performance for different fire scenarios.^{53–55,81}

What is more, the use of several irradiances is proposed to provide further valuable insight into the active flame retardancy mechanisms themselves and their efficiency in different fire scenarios.^{55,66} To a certain degree, different flame retardancy effects show specific, characteristic behavior depending on the irradiation.^{53,55} Typically, the PHRR of noncharring plastics shows a strong linear increase with irradiation. When flame inhibition or charring is induced, the PHRR decreases and the ratio between the PHRR with and without flame retardant is rather constant, corresponding to the model where generally only the factor combustion efficiency (χ) or the factor “(1 – μ)” is changed (Equation 15.1). The efficiency is proposed to increase slightly with increasing irradiation owing to a kind of self-reinforcing flame retardancy effect, caused by additionally reduced thermal feedback from the flame, inducing an efficient barrier results in negligent increase in PHRR at higher irradiation. Thus the relative reduction is large for high irradiation, but can vanish for low irradiation. Such extreme behavior was found for some nanocomposites,^{53,66,91} as illustrated in

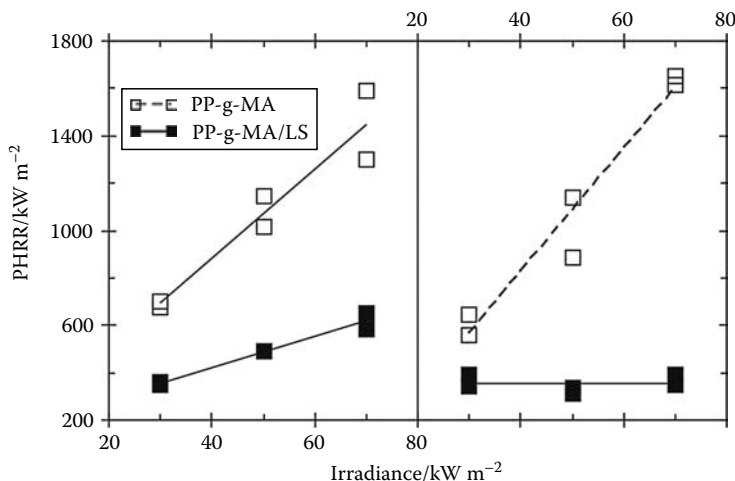


FIGURE 15.18 PHRR of PP-g-MA and PP-g-MA/5 wt.% LS plotted against irradiance. The materials were compounded by extrusion and subsequently pressed into specimen (left) or injection-molded into specimen (right). The flame retardancy increases with increasing irradiance. Additional injection molding increased the nanodispersion even further until the increase in PHRR as a function of irradiance vanished.

Figure 15.18. The vanishing flame retardancy for low irradiances corresponds to the flammability performance measured for these systems in the LOI.⁵³

In principle, all char or residue formed during a fire also acts as a barrier to heat and mass transport. The effectiveness of the barrier depends not only on the amount of char, but also on the properties of the char, such as its morphology, which determines gas permeability and thermal conductivity. Further, the properties of char may be tailored by adding elements such as inorganic adjuvants and synergists.^{52, 110–114} Consequently, the heterogeneous, gradually changing, or structured morphology of fire residues plays an important role in terms of fire behavior and fire retardancy. Indeed, the design of a fire residue consisting of multicellular structures or closed glassy surface layers, rather than merely separated loose particles, is a promising approach for flame-retarded materials. Such approaches often play a crucial role, in particular, in halogen-free systems containing phosphorus. Pursuing the objectives of the understanding and directed development of flame-retarded materials shifts the focus to the accurate investigation of heterogeneous or complex fire residues with respect to their morphology and chemical composition, as well as the investigation of their formation during fire. Scanning electron microscopy is proposed as a suitable and powerful tool for advanced characterization of such complex fire residues, since it offers high resolution in combination with good depth of field and, simultaneously, when SEM-EDX is used, an analysis of the chemical composition at the same location. Because fire residues in the form of sticky smut, char, or slug obviously are not the preferred samples for investigation in an SEM apparatus, such SEM investigations are probably used more rarely than the multitude of fire tests, and focus mainly on the characterization of special surface layers.^{52, 115–120}

The surface temperature during burning and the gradient inside the sample are interesting for the development of materials, especially for materials that are flame retarded by intumescent barrier layers.^{121, 122} In different groups sample holders were developed to address this objective for the cone calorimeter (Figure 15.19) but also for other tests, especially to gain deeper insight into the actual pyrolysis conditions and flame retardancy mechanism.

Shielding effects are observed, especially in the case of effective insulation accompanied by increased reradiation due to high surface temperatures. Indeed, optimizing the barrier properties so that the HRR drops below a critical value characteristic for passing a test, or even reducing the HRR

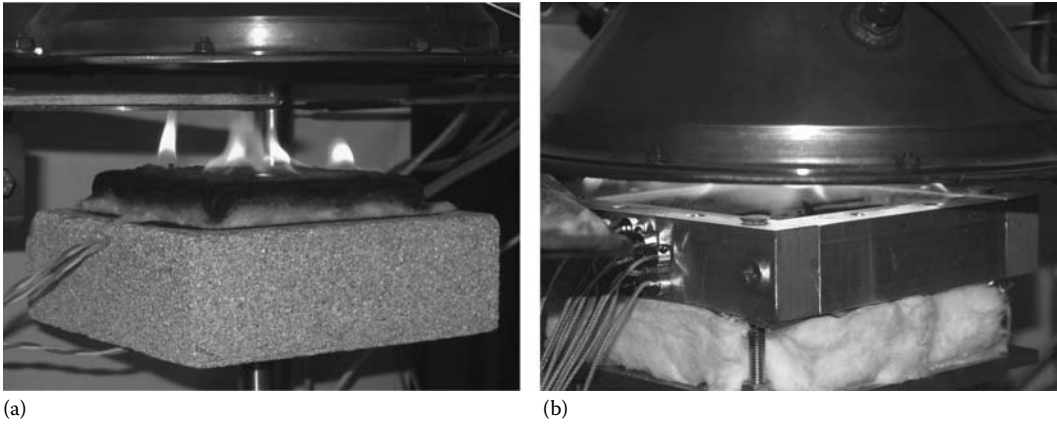


FIGURE 15.19 Sample holders used to measure the temperature on the back of coated steel plates (a) and at different positions within polymer samples (b) during flaming combustion in a cone calorimeter.

to cause self-extinction, is a self-contained flame retardancy approach. Most successful is intumescence, where applied heat results in expanding—often multicellular—char, insulating underlying material.^{123,124} Recent reviews of this concept and its use in polymers, and precise descriptions of the chemistry involved have been published.^{92,119,120,125–134} Temperature differences of up to several hundred degrees Kelvin are observed (Figure 15.20).⁹⁸ Intumescence in polymeric materials can be used to reduce HRR by slowing down the pyrolysis front velocity, or even to achieve extinction before the pyrolysis front goes through the whole specimen. In the latter case, the insulation of the char decreases the temperature in the underlying material to keep it from reaching the decomposition temperature of the polymer.

Since different flame-retardant approaches influence different fire properties quite differently and show different effectiveness in different fire tests, the focus of interest shifts to a comprehensive

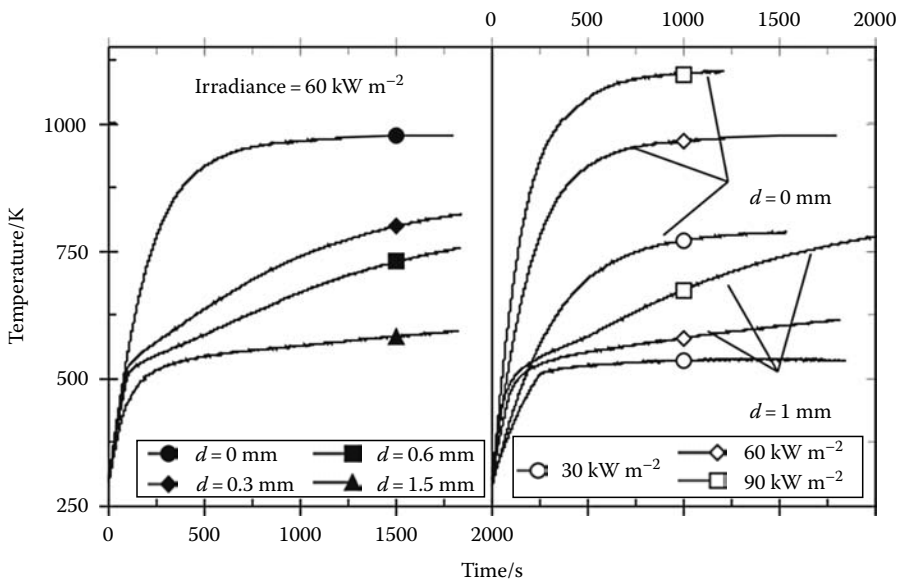


FIGURE 15.20 Temperature at the back of coated (system A) steel plates plotted against time, for different intumescent coating thicknesses (d) and external heat fluxes.

assessment of fire retardancy. The fire load and the flame spread or HRR are believed to have the greatest influence on the fire hazard. Petrella proposed plotting THE (as fire load) against $\text{PHRR}/t_{\text{ig}}$ (as a fire growth index) to give a comprehensive assessment of the two most important fire hazard of a material.¹³⁵ The use of $\text{PHRR}/t_{\text{ig}}$ as index for the fire growth was reported in the 1980s.¹³⁶ Even though the index $\text{PHRR}/t_{\text{ig}}$ may be a better way to address flame spread than FIGRA, it still suffers from the disadvantages of oversimplified empirical indices as discussed earlier. However, Petrella's idea of the assessment of both fire load and fire growth in a graphic at the same time were successfully developed further to achieve a comprehensive and reasonable scientific assessment of the flame retardancy of a material by comparing different approaches, or by comparing the effects for different irradiations. Examples for such a data evaluation are given in Figure 15.21 for the examples discussed earlier based on HIPS with P_{red} and $\text{Mg}(\text{OH})_2$ and P_{red} in PA 66-GF.^{48,54}

The fire hazard is reduced by the flame retardant, either by reducing the THE or by reducing the fire growth rate. The best fire retardancy yield reduction in both, represented by approaching the origin. Over all (synergism in barrier properties and antagonism in flame inhibition), the fire retardancy of HIPS containing P_{red} and $\text{Mg}(\text{OH})_2$ was approximated quite well by a superposition of the effects reached by each of the flame retardants alone (Figure 15.21 left), so that the combination is the by far a more interesting system with respect to fire retardancy.

Figure 15.21 (right) uses the Petrella approach, to assess the fire risks of both PA 66-GF and PA 66-GF/ P_{red} at different external heat fluxes.^{54,55,81} Thus, the assessment is valuable for different applications, fire scenarios, and fire tests, as these correspond to different external heat fluxes and define different demands on fire retardancy in terms of the long duration and growth of a fire. The data for both materials show that with increasing heat flux the fire hazards increase in terms of fire growth, as expected, since a higher irradiance results in an increase in fuel production rate. The THE of

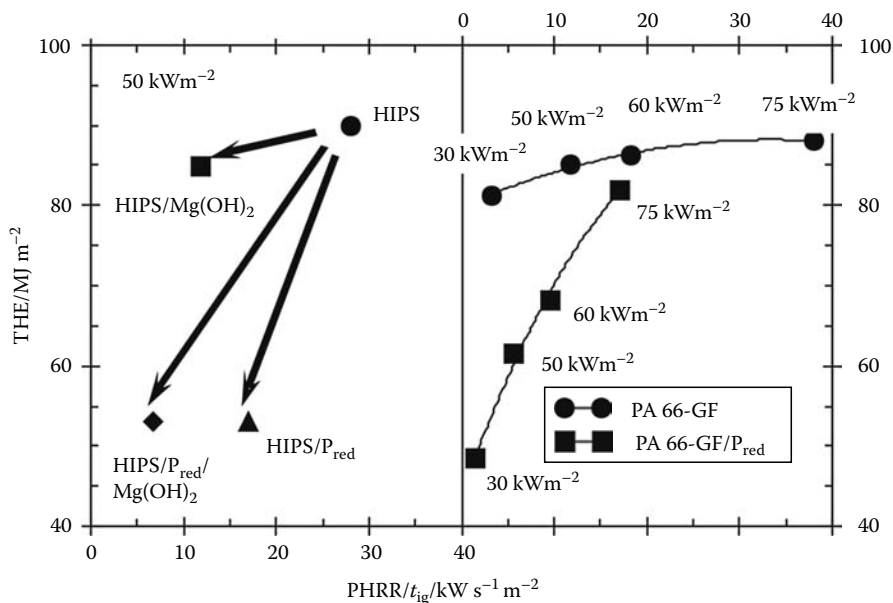


FIGURE 15.21 Using the Petrella plot for comprehensive and reasonable scientific assessment of flame retardancy by comparing different approaches, or by comparing the effects for different irradiations. THE stands for the fire load and $\text{PHRR}/t_{\text{ig}}$ for the fire growth rate; hence, the two most important fire risks are monitored at the same time. An ideal flame retardancy would decrease both hazards significantly as is the case for the combination of both flame retardants on the left (comparison of HIPS), $\text{HIPS}/\text{P}_{\text{red}}$, $\text{HIPS}/\text{Mg}(\text{OH})_2$, and $\text{HIPS}/\text{P}_{\text{red}}/\text{Mg}(\text{OH})_2$) and for low external heat flux on the right (comparison of PA 66-GF and PA 66-GF/ P_{red} for different irradiations).

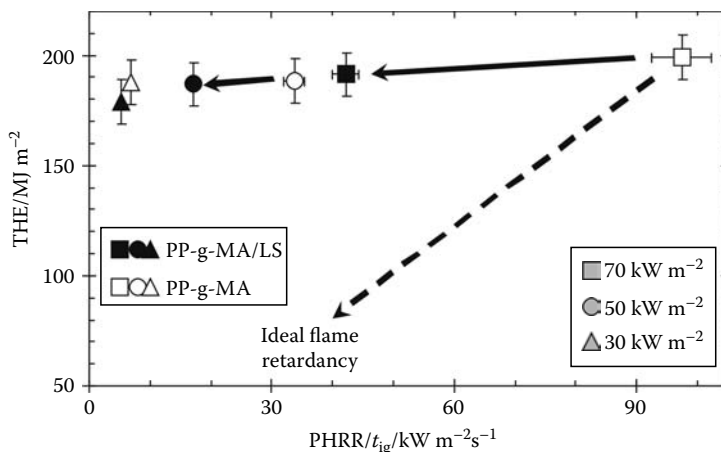


FIGURE 15.22 THE (fire load) plotted against the $\text{PHRR}/t_{\text{ig}}$, (fire growth index) for PP-g-MA and the corresponding 5 wt.% LS PP-g-MA nanocomposites (PP-g-MA/LS) at different irradiances: 30, 50, and 70 kW m^{-2} .

PA 66-GF is fairly constant, since the polymer is nearly completely combusted for all irradiances used, whereas the THE decreases most for the flame-retarded material at low irradiance, because the char formation is at the highest level. This effect diminishes with increasing irradiance. In the case of P_{red} in PA 66-GF, combustion is complete at the highest external heat flux, with or without flame retardant, so the THE is almost the same, but the fire growth index is almost halved. Conversely, at low irradiance, not only is the fire growth index reduced, but the THE is almost halved as well. The change in the fire scenario changes the effectiveness of P_{red} added to PA 66-GF in two of the most important fire properties. P_{red} in PA 66-GF works best for low external heat flux. Flammability tests like LOI and, much more important, UL 94, are fire scenarios with low external heat flux.

It should not escape our notice that such a comprehensive assessment of a specific system sometimes amounts to the essential assessment of a whole fire retardancy approach and immediately blazes the trail for progress in the field. Such an example is shown in Figure 15.22, assessing the barrier effect in layered silicate-based nanocomposites with noncharring materials, which was also discussed earlier.^{53,66} Apart from the impressive reduction in fire growth, comparing these to an ideal flame retardancy revealed the deficits of nanocomposites, which must be remedied by combining the concept with traditional flame retardants or by designing special systems that show additional crucial carbonaceous charring. Discussing the flame retardancy performance for different irradiances used, it becomes clear that the pronounced shielding effect in the cone calorimeter may have less impact in flammability tests like UL 94 or LOI.

15.7 CONCLUSION

This work outlined a great number of approaches for an advanced investigation of fire retardancy and evaluated these for use in flame-retarded materials development. Understanding the key to fire retardancy and fire retardancy mechanisms was deepened in keeping with the golden rule of using several methods of description. Fire behavior and fire retardancy were studied to ensure a comprehensive characterization. Several fire scenarios as well as several fire properties are discussed to work out in detail the fire retardancy, but also the potentials and limitations with respect to applications. Tailored experimental approaches and targeted data evaluation were not the focus of this chapter as ends in themselves, but as means to an end. Thus, neither a new fire testing apparatus nor a detailed theoretical description of fire behavior was evaluated, but merely small steps that could facilitate improved monitoring and understanding. While each of these steps may be not impressive itself, together they constitute a crucial force to tackle the challenge successfully and promise a significant scientific and commercial impact.

ACKNOWLEDGMENTS

The examples used in this chapter are based on studies performed in the author's research group—thus thanks to A. I. Balabanovich, H. Bahr, M. Bartholmai, U. Braun, U. Knoll, K. H. Pawlowski, and A. Weiß—and some of them were performed in cooperation with other research institutes or companies—thus thanks to A. Hartwig (IFAM in Bremen), R. E. Lyon (FAA, US), M. Doering (KIT in Karlsruhe), V. Altstädt (University Bayreuth), BASF AG, Clariant GmbH, and Bayer MaterialScience AG. Financial support was received by the German Research Foundation (DFG, Scha 730/6-1, Scha 730/8-1, BR 3376/1-1), the Volkswagen Foundation (I/77 974), BASF AG, Bayer MaterialScience AG, and Clariant Produkte (Deutschland) GmbH.

REFERENCES

1. Bödiger M, Eckel T, Wittmann D, Alberts H. Feinstteilige anorganische Pulver als Flammenschutzmittel in thermoplastischen Formmassen. German patent. DE 195 30 200 A1, 1997.
2. Gilman JW, Kashiwagi T, Lichtenhan JD. Nanocomposites: A revolutionary new flame retardant approach. *SAMPE J.* 1997; 33:40–46.
3. Gilman JW. Flammability and thermal stability studies of polymer layered-silicate (clay) nanocomposites. *Appl. Clay Sci.* 1999; 15:31–49.
4. Zanetti M, Camino G, Reichert P, Mülhaupt R. Thermal behaviour of poly(propylene) layered silicate nanocomposites. *Macromol. Rapid Commun.* 2001; 22:176–180.
5. Shieh JY, Wang CS. Effect of the organophosphate structure on the physical and flame-retardant properties of an epoxy resin. *J. Polym. Sci. Part A: Polym. Chem.* 2002; 40:369–378.
6. Lin CH, Wang CS. Novel phosphorus-containing epoxy resins. Part I. Synthesis and properties. *Polymer* 2001; 42:1869–1878.
7. Hussain M, Varley RJ, Mathys Z, Cheng YB, Simon GP. Effect of organo-phosphorus and nano-clay materials on the thermal and fire performance of epoxy resins. *J. Appl. Polym. Sci.* 2004; 91:1233–1253.
8. Shieh JY, Wang CS. Synthesis of novel flame retardant epoxy hardeners and properties of cured products. *Polymer* 2001; 42:7617–7625.
9. Wang CS, Lin CH. Synthesis and properties of phosphorus-containing epoxy resins by novel method. *J. Polym. Sci. Part A: Polym. Chem.* 1999; 37:3903–3909.
10. Perez RM, Sandler JKW, Altstädt V, Hoffmann T, Pospiech D, Ciesielski M, Döring M. Effect of DOP-based compounds on fire retardancy, thermal stability, and mechanical properties of DGEBA cured with 4,4'-DDS. *J. Mater. Sci.* 2006; 41:341–353.
11. Liu YL. Flame-retardant epoxy resins from novel phosphorus-containing novolac. *Polymer* 2001; 42:3445–3454.
12. Kleiner H-J, Verfahren zur Herstellung von Aluminiumsalzen von Phosphinsäuren. German Patent DE 196 16 025 C1, 1997.
13. Kleiner H-J, Budzinsky W, Kirsch G. Schwerentflammbare Polyamidformmassen. German Patent DE 196 07 635 A1, 1997.
14. Kleiner H-J, Budzinsky W, Kirsch G. Formteile aus schwerentflammbarer Polyesterformmasse. German Patent DE 196 08 008 A1, 1997.
15. Jenewein E, Naß B, Wanzke W. Flammenschutzmittel-Kombination. German Patent DE 199 33 901 A1, 2001.
16. Gilman JW, Bourbigot S, Shields JR, Nyden M, Kashiwagi T, Davis RD, Vanderhart DL, Demory W, Wilkie CA, Morgan AB, Harris J, Lyon RE. High throughput methods for polymer nanocomposites research: Extrusion, NMR characterization and flammability property screening. *J. Mater. Sci.* 2003; 38:4451–4460.
17. Wilkie CA, Chigwada G, Gilman JW, Lyon RE. High-throughput techniques for the evaluation of fire retardancy. *J. Mater. Chem.* 2006; 16:2023–2029.
18. Jimenez M, Duquesne S, Bourbigot S. High-throughput fire testing for intumescent coatings. *Ind. Eng. Chem. Res.* 2006; 45:7475–7481.
19. Eckel T, Ooms P, Wittmann D, Buysch H-J. Thermoplastische Polymerformmassen mit flammwidrigen Eigenschaften. German patent. DE 42 31 774 A 1, 1994.
20. Bourbigot S, Le Bras M. Flame retardants. In: *Plastics Flammability Handbook*, 3rd Edn. Troitzsch J, Ed. Hanser: Munich, Germany, 2004; chap. 5, pp. 133–157.
21. Camino G, Costa L, Luda di Cortemiglia MP. Overview of fire retardant mechanisms. *Polym. Degrad. Stab.* 1991; 33:131–154.

22. Lewin M. Physical and chemical mechanisms of flame retarding of polymers. In: *Fire Retardancy of Polymers. The Use of Intumescence*. Le Bras M, Camino G, Bourbigot S, Delobel R, Eds. Royal Society of Chemistry: London, 1998; pp. 3–32.
23. Lewin M, Weil ED. Mechanisms and modes of action in flame retardancy of polymers. In: *Fire Retardant Materials*. Horrocks AR, Price D, Eds. Woodhead Publishing Limited: Cambridge, U.K., 2001; chap. 2, pp. 31–68.
24. Levchick SV. Introduction to flame retardancy and polymer flammability. In: *Flame Retardant Polymer Nanocomposites*. Morgan AB, Wilkie CA, Eds. John Wiley & Sons: Hoboken, NJ, 2007; chap. 1, pp. 1–29.
25. Troitzsch J, Ed. *Plastics Flammability Handbook Principles, Regulations, Testing, and Approval*, 3rd Ed. Hanser: Munich, Germany, 2004.
26. Babrauskas V. *Ignition Handbook*. Fire Science Publishers and SFPE: Issaquah, WA, 2003.
27. Reimschuessel HK, Shalaby SW, Pearce EM. On the oxygen index of nylon 6. *J. Fire Flammability* 1973; 4:299–308.
28. DiNenno PJ, Drysdale D, Beyler CL, Walton WD, Custer RLP, Hall JR Jr, Watts JM Jr, Eds. *The SFPE Handbook of Fire Protection Engineering*, 3rd Edn. National Fire Protection Association, Inc.: Quincy, MA, 2002.
29. Levchik GF, Levchik SV, Camino G, Weil ED. Fire retardant action of red phosphorus in nylon 6. In: *Fire Retardancy of Polymers. The Use of Intumescence*. Le Bras M, Camino G, Bourbigot S, Delobel R, Eds. Royal Society of Chemistry: London, 1998; pp. 304–315.
30. Yeh JT, Hsieh SH, Cheng YC, Yang MJ, Chen KN. Combustion and smoke emission properties of poly(ethylene terephthalate) filled with phosphorous and metallic oxides. *Polym. Degrad. Stab.* 1998; 61:399–407.
31. Balabanovich AI, Zevaco TA, Schnabel W. Fire retardance in poly(butylene terephthalate). The effects of red phosphorus and radiation-induced cross-links. *Macromol. Mater. Eng.* 2004; 289:181–190.
32. Hastie JW. Molecular-basis of flame inhibition. *J. Res. Nat. Bur. Stand. Sect. A Phys. Chem.* 1973; 77A:733–754.
33. Isaacs JL. The oxygen index flammability test. *J. Fire Flammability* 1970; 1:36–47.
34. Weil ED, Hirschler MM, Patel NG, Said MM, Shakir S. Oxygen index: Correlations to other fire tests. *Fire Mater.* 1992; 16:159–167.
35. Wharton RK. Correlation between the critical oxygen index test and other fire tests. *Fire Mater.* 1981; 5:93–102.
36. Camino G, Costa L, Casorati E, Bertelli G, Locatelli R. The oxygen index method in fire retardance studies of polymeric materials. *J. Appl. Polym. Sci.* 1988; 35:1863–1876.
37. Wharton RK. The effect of sample size on the burning behaviour of thermoplastic materials in the critical oxygen index test. *Fire Mater.* 1981; 5:73–76.
38. Wharton RK. Factors that influence the critical oxygen index of various solids. *Fire Mater.* 1979; 3:39–48.
39. Wharton RK. The relative performance of critical oxygen index testing columns under ambient conditions. *J. Fire Flammability* 1981; 12:266–271.
40. Wharton RK. Comments on the effect of gas velocity on oxygen index measurements. *J. Fire Sci.* 1983; 1:459–464.
41. Sibulkin M, Lee CK. Flame propagation measurements and energy feedback analysis for burning cylinders. *Combust. Sci. Technol.* 1974; 9:137–147.
42. Sibulkin M, Kim J, Creeden Jr JV. The dependence of flame propagation on surface heat transfer I. Downward burning. *Combust. Sci. Technol.* 1976; 14:43–56.
43. Sibulkin M, Kim J. The dependence of flame propagation on surface heat transfer II. Upward burning. *Combust. Sci. Technol.* 1977; 17:39–49.
44. Tewarson A, Ogden SD. Fire behaviour of polymethylmethacrylate. *Combust. Flame* 1992; 89:237–259.
45. Sibulkin M, Little MW. Propagation and extinction of downward burning fires. *Combust. Flame.* 1978; 31:197–208.
46. Arcand, Jr CG. The bottom ignition oxygen index test. *Text. Res. J.* 1972; 42:328–330.
47. Ševčėk P, Filipi B, Zapletalova I. Modification of the oxygen index test for better evaluation of the relative flammability. *Fire Mater.* 1981; 5:39–40.
48. Braun U, Schartel B. Flame retardant mechanisms of red phosphorus and magnesium hydroxide in high impact polystyrene. *Macromol. Chem. Phys.* 2004; 205:2185–2196.

49. Schartel B, Balabanovich AI, Braun U, Knoll U, Artner J, Ciesielski M, Döring M, Perez P, Sandler JKW, Altstädt V, Hoffmann T, Pospiech D. Pyrolysis of epoxy resins and fire behaviour of epoxy resin composites flame-retarded with 9,10-dihydro-9-oxa-10-phosphaphenanthrene-10-oxide additives. *J. Appl. Polym. Sci.* 2007; 104:2260–2269.
50. Braun U, Balabanovich AI, Schartel B, Knoll U, Artner J, Ciesielski M, Döring M, Perez R, Sandler JKW, Altstädt V, Hoffmann T, Pospiech D. Influence of the oxidation state of phosphorus on the decomposition and fire behaviour of flame-retarded epoxy resin composites. *Polymer* 2006; 47:8495–8508.
51. Schartel B, Weiß A, Mohr F, Kleemeier M, Hartwig A, Braun U. Flame retarded epoxy resins by adding layered silicate in combination with the conventional protection layer building flame retardants melamine borate and ammonium polyphosphate. *J. Appl. Polym. Sci.*, 2009, submitted.
52. Braun U, Schartel B, Fichera MA, Jäger C. Flame retardancy mechanisms of aluminium phosphinate in combination with melamine polyphosphate and zinc borate in glass-fibre reinforced polyamide 6,6. *Polym. Degrad. Stab.* 2007; 92:1528–1545.
53. Bartholmai M, Schartel B. Layered silicate polymer nanocomposites: New approach or illusion for fire retardancy? Investigations on the potential and on the tasks using a model system. *Polym. Adv. Technol.* 2004; 15:355–364.
54. Schartel B, Kunze R, Neubert D. Red phosphorus controlled decomposition for fire retardant PA 66. *J. Appl. Polym. Sci.* 2002; 83:2060–2071.
55. Schartel B, Braun U. Comprehensive fire behaviour assessment of polymeric materials based on cone calorimeter investigations. *e-Polymers* 2003; art. no. 13.
56. Braun U, Schartel B. Flame retardancy mechanisms of aluminium phosphinate in combination with melamine cyanurate in glass-fibre reinforced poly (1,4-butylene terephthalate). *Macromol. Mater. Eng.* 2008; 293:206–217.
57. Braun U, Bahr H, Sturm H, Schartel B. Flame retardancy mechanisms of metal phosphinates and metal phosphinates in combination with melamine cyanurate in glass-fiber reinforced poly(1,4-butylene terephthalate): The influence of metal cation. *Polym. Adv. Technol.* 2008; 19:680–692.
58. van Krevelen DW. Some basic aspects of flame resistance of polymeric materials. *Polymer* 1975; 16:615–620.
59. van Krevelen DW. *Properties of Polymers: Their Correlation with Chemical Structure*. Elsevier: Amsterdam, the Netherlands, 1990.
60. Tewarson A. Generation of heat and chemical compounds in fires. In: *The SFPE Handbook of Fire Protection Engineering*, 3rd Edn. DiNunno PJ, Drysdale D, Beyler CL, Walton WD, Custer RLP, Hall Jr JR, Watts Jr JM, Eds. National Fire Protection Association, Inc.: Quincy, MA, 2002; chap. 3.4, pp. 3-82–3-161.
61. Lyon RE, Janssens ML. Polymer flammability. In: *Encyclopedia of Polymer Science and Technology*, 3rd Edn. Mark HF, Ed. Wiley: New York, 2004.
62. Lyon RE. Plastics and rubber. In: *Handbook of Building Materials for Fire Protection*. Harper CA, Ed. McGraw-Hill: New York, 2004; chap. 3, pp. 3.1–3.51.
63. Walters RN, Lyon RE. Molar group contributions to polymer flammability. *J. Appl. Polym. Sci.* 2003; 87:548–563.
64. Quintiere JG. *Fundamentals of Fire Phenomena*. Wiley: Chichester, U.K., 2006.
65. Wharton RK. Identification of two pass regimes for nylon-66 based rods in the critical oxygen index test. *J. Appl. Polym. Sci.* 1982; 27:3193–3197.
66. Schartel B, Bartholmai M, Knoll U. Some comments on the main fire retardancy mechanisms in polymer nanocomposites. *Polym. Adv. Technol.* 2006; 17:772–777.
67. Pawlowski KH, Schartel B. Flame retardancy mechanisms of triphenyl phosphate, resorcinol bis(diphenyl phosphate) and bisphenol a bis(diphenyl phosphate) in polycarbonate/acrylonitrile-butadiene-styrene blends. *Polym. Int.* 2007; 56:1404–1414.
68. Weil ED. Synergists, adjuvants, and antagonists in flame-retardant efficacy in polymeric materials. In: *Fire Retardancy of Polymeric Materials*. Grand AF, Wilkie CA, Eds. Marcel Dekker: New York, 2000; chap. 4, pp. 115–145.
69. Casu A, Camino G, De Giorgi M, Flath D, Laudi A, Morone V. Effect of glass fibres and fire retardant on the combustion behaviour of composites, glass fibres poly(butylene terephthalate). *Fire Mater.* 1998; 22:7–14.
70. Day AG. Oxygen index test: Temperature effect and comparison with other flammability tests. *Plast. Polym.* 1975; 43:64–67.
71. Morgan AB, Bundy M. Cone calorimeter analysis of UL-94 V-rated plastics. *Fire Mater.* 2007; 31:257–283.

72. Karlsson B. Performance-based test methods for material flammability. In: *Fire Retardant Materials*. Horrocks AR, Price D, Eds. Woodhead Publishing Limited: Cambridge, U.K., 2001; chap. 12, pp. 355–377.
73. Babrauskas V. The cone calorimeter. In: *Heat Release in Fires*. Babrauskas V, Grayson SJ, Eds. Elsevier Science Publishers Ltd.: Barking, U.K., 1992; chap. 4, pp. 61–91.
74. Babrauskas V. Development of the cone calorimeter—a bench-scale heat release rate apparatus based on oxygen-consumption. *Fire Mater.* 1984; 8:81–95.
75. Babrauskas V. Fire test methods for evaluation of fire-retardant efficacy in polymeric materials. In: *Fire Retardancy of Polymeric Materials*. Grand AF, Wilkie CA, Eds. Marcel Dekker Inc.: New York, 2000; chap. 3, pp. 81–113.
76. Scudamore MJ, Briggs PJ, Prager FH. Cone calorimetry—a review of tests carried out on plastics for the Association of Plastic Manufacturers in Europe. *Fire Mater.* 1991; 15:65–84.
77. Babrauskas V. Specimen heat fluxes for bench-scale heat release rate testing. *Fire Mater.* 1995; 19:243–252.
78. Babrauskas V. Heat release rates. In: *The SFPE Handbook of Fire Protection Engineering*, 3rd Edn. DiNenno PJ, Drysdale D, Beyler CL, Walton WD, Custer RLP, Hall Jr JR, Watts Jr JM, Eds. National Fire Protection Association, Inc.: Quincy, MA, 2002; chap. 3.1, pp. 3-1–3-37.
79. Scudamore MJ. Fire performance studies on glass-reinforced plastic laminates. *Fire Mater.* 1994; 18:313–325.
80. ScharTEL B, Bartholmai M, Knoll U. Some comments on the use of cone calorimeter data. *Polym. Degrad. Stab.* 2005; 88:540–547.
81. ScharTEL B, Hull TR. Development of fire retarded materials—interpretation of cone calorimeter data. *Fire Mater.* 2007; 31:327–354.
82. Drysdale DD. Fire safety design requirements of flame-retarded materials. In: *Fire Retardant Materials*. Horrocks AR, Price D, Eds. Woodhead Publishing: Cambridge, U.K., 2001; chap. 13, pp. 378–397.
83. Tewarson A, Pion RF. Flammability of plastics. 1. Burning intensity. *Combust. Flame* 1976; 26:85–103.
84. Tewarson A. Flammability of polymers. In: *Plastics and the Environment*. Andrady AL, Ed. John Wiley & Sons: Hoboken, NJ, 2003; chap. 11.
85. Hopkins D Jr, Quintiere JG. Material fire properties and predictions for thermoplastics. *Fire Safety J.* 1996; 26:241–268.
86. Bartholmai M, ScharTEL B. Assessing the performance of intumescent coatings using bench-scaled cone calorimeter and finite difference simulations. *Fire Mater.* 2007; 31:187–205.
87. Babrauskas V, Peacock RD. Heat release rate—the single most important variable in fire hazard. *Fire Safety J.* 1992; 18:255–272.
88. Janssens M, Parker WJ. Oxygen consumption calorimetry. In: *Heat Release in Fires*. Babrauskas V, Grayson SJ, Eds. Elsevier Science Publishers: Barking, U.K., 1992; chap. 3, pp. 31–59.
89. Huggett C. Estimation of rate of heat release by means of oxygen-consumption measurements. *Fire Mater.* 1980; 4:61–65.
90. Fichera MA, Braun U, ScharTEL B, Sturm H, Knoll U, Jäger C. Solid-state NMR investigations of the pyrolysis and thermo-oxidative decomposition products of a polystyrene/red phosphorus/magnesium hydroxide system. *J. Anal. Appl. Pyrolysis* 2007; 78:378–386.
91. ScharTEL B, Knoll U, Hartwig A, Pütz D. Phosphonium-modified layered silicate epoxy resins nanocomposites and their combinations with ATH and organo-phosphorus fire retardants. *Polym. Adv. Technol.* 2006; 17:281–293.
92. Bourbigot S, Le Bras M, Duquesne S, Rochery M. Recent advances for intumescent polymers. *Macromol. Mater Eng.* 2004; 289:499–511.
93. Van Hees P, Axelsson J. Modelling of euroclass test results by means of the cone calorimeter. In: *Multifunctional Barriers for Flexible Structure Textile, Leather, and Paper*. Duquesne S, Magniez C, Camino G, Eds. Springer: Berlin, 2007.
94. Messerschmidt B, Van Hees P, Wickström U. Prediction of SBI (single burning item) test results by means of cone calorimeter test results. *Interflam 1999, Proceedings of the Eighth International Conference*. Interscience Communication Limited: London, 1999; pp. 11–22.
95. Hakkarainen T, Kokkala MA. Application of a one-dimensional thermal flame spread model on predicting the rate of heat release in the SBI test. *Fire Mater.* 2001; 25:61–70.
96. Hansen AS. Prediction of heat release in the single burning item test. *Fire Mater.* 2002; 26:87–97.
97. Janssens M, Huczek J, Saucedo A. Development of a model of the ASTM E84 Steiner tunnel test. *Ninth International IAFSS Symposium*. Interscience Communications Ltd.: Greenwich, London, 2008.
98. Bartholmai M, Schriever R, ScharTEL B. Influence of external heat flux and coating thickness on thermal insulation properties of two different intumescent coatings using cone calorimeter and numerical analysis. *Fire Mater.* 2003; 27:151–162.

99. Duquesne S, Magnet S, Jama C, Delobel R. Thermoplastic resins for thin film intumescent coatings—towards a better understanding of their effect on intumescence efficiency. *Polym. Degrad. Stab.* 2005; 88:63–69.
100. Hull TR, Carman JM, Purser DA. Prediction of CO evolution from small-scale polymer fires. *Polym. Int.* 2000; 49:1259–1265.
101. Babrauskas V. The generation of CO in bench-scale fire tests and the prediction for real-scale fires. *Fire Mater.* 1995; 19:205–213.
102. Wittbecker F-W, Bansemmer B. A model for the scenario-related assessment of the smoke toxic potency. *Interflam 2004, Proceedings of the Tenth International Conference*, Edinburgh. Interscience Communication Limited: London, 2004; pp. 1479–1490.
103. Zammarano M, Krämer RH, Harris R, Ohlemiller TJ, Shields JR, Rahatekar SS, Lacerda S, Gilman JW. Flammability reduction of flexible polyurethane foams via carbon nanofiber network formation. *Polym. Adv. Technol.* 2008; 19:588–595.
104. ScharTEL B, Pawlowski KH, Lyon RE. Pyrolysis combustion flow calorimeter: A tool to assess flame retarded PC/ABS materials? *Thermochim. Acta* 2007; 462:1–14.
105. Price D, Anthony G, Carty P. Introduction: Polymer combustion, condensed phase pyrolysis and smoke formation. In: *Fire Retardant Materials*. Horrocks AR, Price D, Eds. Woodhead Publishing: Cambridge, U.K., 2001; chap. 1, pp. 1–30.
106. Factor A. Char formation in aromatic engineering polymers. In: *Fire and Polymers*, ACS Symposium Series 425. American Chemical Society: Washington, 1990; chap. 19, pp. 274–287.
107. Lyon RE. Ignition resistance of plastics. In: *Recent Advances in Flame Retardancy of Polymers*, Vol. 13. Lewin M, Ed. Business Communications Co. Inc.: Norwalk, CT, 2002; pp. 14–25.
108. Tewarson A. Flammability parameters of materials—ignition combustion, and fire propagation. *J. Fire Sci.* 1994; 12:329–356.
109. Bundy M, Ohlemiller T. Bench-scale flammability measures for electronic equipment, NISTR 7031. National Institute of Standards and Technology, NIST: Gaithersburg, MD, 2003.
110. Anna P, Marosi G, Csontos I, Bourbigot S, Le Bras M, Delobel R. Influence of modified rheology on the efficiency of intumescent flame retardant systems. *Polym. Degrad. Stab.* 2001; 74:423–426.
111. Laoutid F, Gaudon P, Taulemesse JM, Lopez Cuesta JM, Velasco JI, Piechaczyk A. Study of hydro-magnesite and magnesium hydroxide based fire retardant systems for ethylene-vinyl acetate containing organo-modified montmorillonite. *Polym. Degrad. Stab.* 2006; 91:3074–3082.
112. Bourbigot S, LeBras M, Delobel R, Tremillon J-M. Synergistic effect of zeolite in an intumescence process—study of the interactions between the polymer and the additives. *J. Chem. Soc. Faraday Trans.* 1996; 92:3435–3444.
113. Samyn F, Bourbigot S, Duquesne S, Delobel R. Effect of zinc borate on the thermal degradation of ammonium polyphosphate. *Thermochim. Acta* 2007; 456:134–144.
114. Pawlowski KH, ScharTEL B. Flame retardancy mechanisms of aryl phosphates in combination with boehmite in bisphenol A polycarbonate/acrylonitrile-butadiene-styrene blends. *Polym. Degrad. Stab.* 2008; 93:657–667.
115. Song L, Hu Y, Lin Z, Xuan S, Wang S, Chen Z, Fan W. Preparation and properties of halogen-free flame-retarded polyamide 6/organoclay nanocomposite. *Polym. Degrad. Stab.* 2004; 86:535–540.
116. Gentilhomme A, Cochez M, Ferriol M, Oget N, Mieloszynski JL. Thermal degradation of methyl methacrylate polymers functionalized by phosphorus-containing molecules. III: Cone calorimeter experiments and investigation of residues. *Polym. Degrad. Stab.* 2005; 88:92–97.
117. Tang Y, Hu Y, Song L, Zong RW, Gui Z, Fan WC. Preparation and combustion properties polypropylene-polyamide-6 of flame retarded alloys. *Polym. Degrad. Stab.* 2006; 91:234–241.
118. Laoutid F, Ferry L, Lopez-Cuesta JM, Crespy A. Flame-retardant action of red phosphorus/magnesium oxide and red phosphorus/iron oxide compositions in recycled PET. *Fire Mater.* 2006; 0:343–358.
119. Bertelli G, Marchetti E, Camino G, Costa L, Locatelli R. Intumescent fire retardant systems—Effect of fillers on char structure. *Angew. Makromol. Chem.* 1989; 172:153–163.
120. Bertelli G, Camino G, Marchetti E, Costa L, Locatelli R. Structural studies on chars from fire retardant intumescent systems. *Angew. Makromol. Chem.* 1989; 169: 137–142.
121. Le Bras M, Bourbigot S, Siat C, Delobel R. Comprehensive study of protection of polymers by intumescence—application to ethylene vinyl acetate copolymer formulations. In: *Fire Retardancy of Polymers: The Use of Intumescence*. Le Bras M, Camino G, Bourbigot S, Delobel R, Eds. The Royal Chemical Society: Cambridge, U.K., 1998; pp. 266–279.
122. Bourbigot S, Leroy J-M. Modelling of thermal diffusivity during combustion—application to intumescent materials. In: *Fire Retardancy of Polymers: The Use of Intumescence*. Le Bras M, Camino G, Bourbigot S, Delobel R, Eds. The Royal Chemical Society: Cambridge, U.K., 1998; pp. 129–139.

123. Vandersall HL. Intumescent coating systems, their development and chemistry. *J. Fire Flammability* 1971; 2:97–140.
124. Kay M, Price AF, Lavery I. Review of intumescent materials, with emphasis on melamine formulations. *J. Fire Retard. Chem.* 1979; 6:69–91.
125. Camino G, Costa L, Trossarelli L. Study on the mechanism of intumescence in fire retardant polymers. 1. Thermal-degradation of ammonium polyphosphate pentaerythritol mixtures. *Polym. Degrad. Stab.* 1984; 6:243–252.
126. Camino G, Costa L, Trossarelli L. Study on the mechanism of intumescence in fire retardant polymers 2. Mechanism of action in polypropylene-ammonium polyphosphate pentaerythritol mixtures. *Polym. Degrad. Stab.* 1984; 7:25–31.
127. Camino G, Costa L, Trossarelli L. Study on the mechanism of intumescence in fire retardant polymers. 3. Effect of urea on the ammonium polyphosphate pentaerythritol system. *Polym. Degrad. Stab.* 1984; 7:221–229.
128. Camino G, Costa L, Trossarelli L, Costanzi F, Landoni G. Study on the mechanism of intumescence in fire retardant polymers. 4. Evidence of ester formation in ammonium polyphosphate pentaerythritol mixtures. *Polym. Degrad. Stab.* 1984; 8:13–22.
129. Camino G, Costa L, Trossarelli L. Study on the mechanism of intumescence in fire retardant polymers. 5. Mechanism of formation of gaseous products in the thermal-degradation of ammonium polyphosphate pentaerythritol mixtures. *Polym. Degrad. Stab.* 1985; 12:203–211.
130. Camino G, Costa L, Trossarelli L, Costanzi F, Pagliari A. Study on the mechanism of intumescence in fire retardant polymers. 6. Mechanism of ester formation in ammonium polyphosphate pentaerythritol mixtures. *Polym. Degrad. Stab.* 1985; 12:213–228.
131. Camino G, Costa L, Martinasso G. Intumescent fire-retardant systems. *Polym. Degrad. Stab.* 1989; 23:359–376.
132. Camino G, Delobel R. Intumescence. In: *Fire Retardancy of Polymeric Materials*. Grand AF, Wilkie CA, Eds. Marcel Dekker: New York, 2000; chap. 7, pp. 217–243.
133. Camino G, Lomakin S. Intumescent materials. In: *Fire Retardant Materials*. Horrocks AR, Price D, Eds. Woodhead Publishing: Cambridge, U.K., 2001; chap. 10, pp. 318–336.
134. Marchal A, Delobel R, Le Bras M, Leroy J-M, Price D. Effect of intumescence on polymer degradation. *Polym. Degrad. Stab.* 1994; 44:263–272.
135. Petrella RV. The assessment of full-scale fire hazards from cone calorimeter data. *J. Fire Sci.* 1994; 12:14–43.
136. Babrauskas V. Bench-scale methods for prediction of full-scale fire behaviour of furnishings and wall linings. SFPE Technology Report 84-10. Society of Fire Protection Engineers: Boston, MA, 1984.

16 High Throughput Techniques for Fire Resistant Materials Development*

*Rick D. Davis, Richard E. Lyon, Michael T. Takemori,
and Naomi Eidelman*

CONTENTS

16.1	Introduction	422
16.2	Case Study 1. The Development of Fire Safe Transparent Plastics for Commercial Aircraft Cabin Interiors Using High Throughput Methods	424
16.2.1	Introduction	424
16.2.2	Methodology	424
16.2.2.1	High Throughput Screening for Flammability	424
16.2.2.2	Empirical Molar Group Contributions.....	425
16.2.2.3	Fire Testing	425
16.2.3	Results and Discussion	428
16.2.3.1	Deterministic Model of Flammability (Molar Group Contributions)	428
16.2.3.2	Statistical Model of Flammability (Probabilistic Regression).....	430
16.2.3.3	Flammability Results of Optimized Formulations	432
16.2.4	Conclusions.....	433
16.3	Case Study 2. High Throughput Polymer Flammability Characterization Using Gradient Heat Flux Environments and Rapid Cone Calorimetry	434
16.3.1	Introduction	434
16.3.2	Experimental	435
16.3.2.1	Sample Preparation	435
16.3.2.2	Flammability Properties	436
16.3.3	Results and Discussion	438
16.3.3.1	Minimum Flux for Flame Spread and t_{ign}	438
16.3.3.2	Rapid Cone Calorimetry (RCC)	441
16.3.4	Conclusion	442
16.4	Case Study 3. A Potential High Throughput Approach for Screening Intumescence Coatings.....	442
16.4.1	Introduction	442
16.4.2	Experimental	443
16.4.2.1	Sample Preparation	443
16.4.2.2	Coating Characterization	444

* In this chapter, we have provided links to websites that may have information of interest to users. NIST does not necessarily endorse the views expressed or the facts presented on these sites. Further, NIST does not endorse any commercial products that may be advertised or available on these sites.

16.4.3 Results and Discussion	445
16.4.3.1 Fluorescence Probes	445
16.4.3.2 FTIR-RTM.....	446
16.4.3.3 Potential Application for Fire Testing.....	448
16.4.4 Conclusion	449
16.5 Chapter Summary.....	449
References.....	450

16.1 INTRODUCTION

This chapter describes recent activities using high throughput (HT) tools and methods to optimize the fire performance of polymeric materials. In essence, HT is a methodology that uses high rate, often automated, synthesis and testing to discover processes, relationships, and products in multivariate, multicomponent systems whose complexity precludes detailed understanding or predictive capability. Most definitions of high throughput explain HT in terms of pharmaceutical and biological applications. For example, HT is a method for scientific experimentation especially used in drug discovery and relevant to the fields of biology and chemistry [1]. Over the past 15 years, HT has expanded into other technical areas, such as polymer and material science. In the last several years, HT in polymer science has become quite popular with a variety of companies now offering polymer HT testing tools [2–4] and the appearance of several polymer/HT review chapters and books that are now available [5]. Owing to this evolution of HT, perhaps a more appropriate definition is that HT is an approach to scientific experimentation that can significantly accelerate knowledge. There is a widespread and increasing use of HT throughout the chemical industry, as this acceleration of knowledge provides corporations with the opportunity to make decisions based on more technical information or in significantly less time. For the scientific community, HT gives an opportunity for those doing basic and applied science to significantly accelerate technology and remove obstacles found during the exploration of new scientific frontiers.

The underlying process of conducting research is the same regardless of the approach. After generating a question or an idea, the process involves a continuous loop of conducting experiments and analyzing data, till sufficient knowledge is obtained from these steps, through data interpretation, so that one can arrive at answers for the project founding questions or make a decision, respectively. HT does not significantly alter this process—it just removes the main bottleneck of research, conducting experiments and analyzing data. Both the HT tools (hardware) and “Informatics” (software) are critical to successful use of HT. However, this chapter will not discuss the software used to operate the tools, analyze the data, and perform data mining (Informatics), but rather focus on the in-house developed HT tools (hardware) and the knowledge obtained using these tools. Nevertheless, it must be emphasized that to fully reap the benefits of HT, a comparable amount of time and effort needs to be applied to Informatics. Without Informatics the tools are significantly less efficient and more importantly the bottleneck simply moves further downstream to data analysis; arguably, there is no reason to generate data of 1000 experiments in a week if the analysis still takes months.

HT accelerates experiments primarily by conducting activities in parallel rather than in series—in effect multitasking. The most common HT multitasking activities are simultaneously conducting multiple experiments on the same sample, such as dielectric spectroscopy while extruding filled polymers [6], simultaneously evaluating or creating multiple samples on the same instrument, such as causing UV degradation to 100 samples simultaneously [7], and using robots to create, handle, and test samples, thereby freeing the scientist to be involved in other activities, such as liquid handling robots [8,9], automated thermal analysis [10], automated sample dispensing and weighing [8,9], and polymer tensile testing [11]. In essence, multitasking accelerates experimentation by reducing the time between tests.

HT can also accelerate experiments by reducing the actual experiment time, such as reducing the dead time within experiments, the time between specimen testing, and reducing sample

size, for example, testing sample properties as a function of gradient composition, temperature, sample dimensions, and environment [12]. In addition to accelerating the experiments, decreasing the sample size requirements for testing creates the opportunity to evaluate experimental materials of limited supply, which could not be studied using conventional tools or techniques.

Automation can simply be the moving of samples from a holder to the testing tool and vice versa. Automating a conventional tool has the distinct advantage of not impacting the type or value of the responses measured. Therefore, these automated conventional tools are often preferred as they deliver a measurable, which can have an immediate impact without the need to establish a new correlation between the HT and the conventional measurable. For example, the automated Instron delivers the same response as a manual loaded Instron as the only difference being the robot, which loads and unloads the test specimen, measures the specimen thickness, and marks the specimen. In contrast, the Parallel Dynamic Mechanical Thermal Analysis (pDMTA) tool by Symyx is a completely new approach and may require some methods development to establish a correlation between the pDMTA on a micron-thick film and conventional DMTA on a dog bone. However, the ability to simultaneously perform DMTA-like tests on 96 specimens in a few hours is unprecedented and does warrant serious consideration.

Automating a conventional tool may not be possible, may be cost prohibited, and may not significantly accelerate the experiment. The alternative is to develop a new tool/s with the time-saving capabilities discussed earlier; i.e., reduced sample size and testing time. This route will eventually result in significant methods development to establish a correlation between the conventional test and the HT approach. Often the correlation is not one-to-one with the absolute value from the conventional tools, but the trends are normally aligned. The reality of HT is there is a hand full of HT tools available for evaluating the common properties of common polymers in common applications, and the tool owners will need to establish a correlation between one of these HT tool responses and the desired end-product performance characteristic they want to measure.

The biggest mistake most people make is underestimating the resources (money, time, and personnel) required to setup, maintain, and operate the HT capabilities. HT is not an opportunity to immediately decrease resources, especially manpower, but rather an opportunity to maximize the efficiency of the current resources. Before rushing out to buy HT tools, the following comments are to be considered.

1. HT tools can be extremely sophisticated and require trained personal dedicated to operating and repairing the tools. Some of these tools are extremely expensive and contain a significant amount of electronics, and precision moving parts, which require someone with more than basic mechanic, electronic, and computer skills.
2. A significant portion, as high as 70% with new tools, of research time is dedicated to purely methods development. Methods development is necessary, as polymer chemistries, properties, and applications are extremely diverse. A portion of this methods development is focused on how to handle different materials, such as butyl rubber versus low-density polyethylene. However, the largest portion of methods development is dedicated to data correlation.
3. HT tools can be quite expensive and though there are relatively lower cost HT tools available, there is often the trade-off of versatility, functionality, robustness, and ease of use.
4. HT is not an opportunity to blindly take a “shot gun” approach to research. These studies take skill scientists to decide the right types of experiments, interpret the data, and make decisions on the best technical course of action.
5. Besides the tools, there is a significant effort required to maintain and develop the necessary Informatics capabilities, which are critical to effectively using these HT tools. This infrastructure does not normally exist for conventional tools; therefore additional resources are often required.

In this chapter, the discussion is on how HT is or could be used to accelerate the understanding of a polymer fire performance. Many other researchers have also taken HT approaches to accelerate material fire science, such as attempting to balance the high flame retardant (FR) loading levels needed to achieve the desired fire performance with the resulting decrease in the inherent polymer properties owing to the high FR loading levels. An attractive solution is to identify fire retardant additives that work synergistically to provide the desired FR performance and do so with no impact on the other polymer properties. However, developing an understanding of the synergistic and antagonistic relationship of multiadditive packages in polymer systems is often not intuitive and is a resource-intensive undertaking not compatible with conventional methods, but perfectly suited for HT approaches. Though this chapter discusses the research in addressing this type of problem, the authors are not the ones who are actively working in this arena. Chigwada et al. [13] applied a HT philosophy to identify a synergy between phosphorous containing FR and vinyl ester nanocomposites, as indicated by cone calorimetry. The improvements in total and peak release rate, mass loss rate, and ignition time were all proportional to the phosphate concentration. The types of clay used impacted the flammability of the nanocomposites formed. Another similar multiadditive type study was also published by Chigwada and Wilkie [14] on polystyrene containing organoclays and phosphorus fire retardants. A more detailed description of the HT apparatus Chigwada used in these studies can be found in a publication by Wilkie et al. [15]. There are other notable applications of HT approaches to material fire science, which will not be reviewed here, but are worth reading [16,17].

This chapter has three case studies relevant to HT for fire material research. The first case study describes a HT methodology using microscale combustion calorimetry (MCC) to screen new polymers for flammability for use in aircraft cabins. The second case study describes the development and application of HT tools and methods to accelerate our understanding of polymer fire performance characteristics, such as minimum flux for flame spread (MFFS). The third case study describes the development of HT tools and methods to create and characterize coatings with gradient curing accelerator concentrations. Though fire performance testing was not applied in the latter study, the HT tools and methods discussed offer a foundation for HT-coating fire performance studies, such as evaluating the effect of FR type and concentration on the intumescent behavior of steel beam coatings.

16.2 CASE STUDY 1. THE DEVELOPMENT OF FIRE SAFE TRANSPARENT PLASTICS FOR COMMERCIAL AIRCRAFT CABIN INTERIORS USING HIGH THROUGHPUT METHODS

16.2.1 INTRODUCTION

The use of HT methods to develop transparent plastic glazing materials is described in this case study. The methodology combines an MCC test that requires only a few milligrams of material to rapidly determine several key combustion parameters [18] with a group contribution methodology specifically developed to model and estimate these parameters [19,20]. The correlation between the microscale combustion properties with larger-scale fire testing can be shown using a simple statistical model for flammability. This methodology was utilized in a joint program between Boeing and the General Electric Global Research Center to screen materials for aircraft cabin interiors [21–26].

16.2.2 METHODOLOGY

16.2.2.1 High Throughput Screening for Flammability

Candidate polymers were screened for flammability using microscale MCC according to a standard method [18]. In the test, a 3–5 mg sample is heated at a rate of 1 K/s from ambient temperature to 850°C. The pyrolysis gases are purged from the sample chamber with nitrogen, mixed with excess oxygen, and combusted at 900°C. Heat released by combustion of the pyrolysis gases is calculated

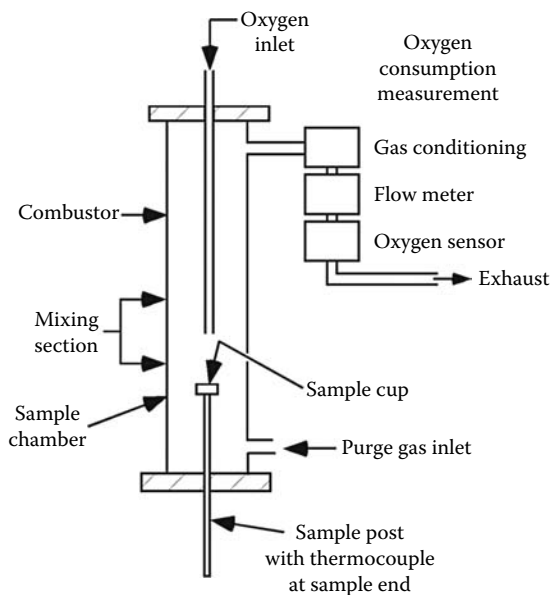


FIGURE 16.1 Schematic diagram of the MCC used to screen flammability.

from the flow rate of the gas stream and the oxygen consumed. Figure 16.1 is a schematic diagram of the MCC showing the separate pyrolysis, combustion, and oxygen consumption measurement sections. Four thermal combustion properties are measured during the 15 min test: the heat release capacity HRC (kJ/mol K), the total heat released by combustion of fuel gases HR (kJ/g), the thermal decomposition/ignition temperature (K), and the weight fraction of char or inert material remaining after the test μ (g-char/g-sample). The total time required to test 84 new and commercial polymers in triplicate for the screening study using MCC was 84 h (including sample preparation).

16.2.2.2 Empirical Molar Group Contributions

Empirical molar group contributions to flammability were determined for the polycarbonates and polyester carbonates by multiple linear regression of the thermal combustion properties: HRC, HR, and μ measured by MCC against 38 backbone and side-group component chemical groups using a commercial spreadsheet program [26]. Earlier efforts had established the efficacy of using molar group contributions for HRC using a wide range of thermoset and thermoplastic polymers [19,26]. In the present study, the molar group contributions were reoptimized to better fit the focal subclass of (mostly) polycarbonates and (some) polyester carbonates and extended to include HR and μ data. Data from over a 100 different formulations tested by MCC at Trace Laboratories were used in the linear regression to provide the optimized set of molar group contributions shown in Table 16.1. The three thermal combustion properties are related to the molar group contributions by the following additivity relationships:

$$\text{HR} = \frac{\sum n_i \Omega_i}{\sum n_i M_i}, \quad \mu = \frac{\sum n_i X_i}{\sum n_i M_i}, \quad \text{and} \quad \text{HRC} = \frac{\sum n_i \Psi_i}{\sum n_i M_i} \quad (16.1)$$

16.2.2.3 Fire Testing

Fire testing was performed according to 14 CFR Part 25 for heat release rate (HRR), smoke density, and flame resistance [22]. HRR was measured using retaining wires on the sample holder in an attempt to prevent melt dripping. At least two samples were tested and averaged to obtain reported values.

TABLE 16.1
Molar Group Contribution Values

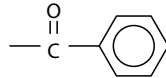
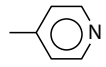
Chemical Group ^a	Type ^b	Molar Group Contributions		
		Ω_i (MJ/mol)	X_i (g/mol)	Ψ_i (kJ/mol K)
	B	0.22	-1	13.6
	B	1.08	35	13.1
	B	1.08	35	13.1
	B	-0.69	76	23.0
	B	2.19	21	43.2
	B	2.63	0	85.5
	B	0.51	0	14.4
	B	0.12	0	11.1
	B	-0.19	7	-12.6
	B	0.24	0	3.1
	B	0.78	9	7.9
	B	0.31	-1	-10.9
	B	0.72	0	6.1
	B	0.15	2	2.5
	B	-1.26	79	-33.3
	B	-0.04	100	-18.6

TABLE 16.1 (continued)
Molar Group Contribution Values

Chemical Group ^a	Type ^b	Molar Group Contributions		
		Ω_i (MJ/mol)	X_i (g/mol)	Ψ_i (kJ/mol K)
	B	0.42	0	5.8
	B	0.19	128	-3.3
	B	2.38	54	39.6
	B	0.79	87	-1.0
	B	0.25	129	-27.7
	S	0.67	0	5.7
	S	1.00	-2	-5.3
	S, B	0.13	0	-1.7
	S, B	1.69	21	24.7
	S, B	1.20	48	0.4
	-6	-0.81	28	-98.5
	S	-0.07	3	-13.5
	S	0.50	0	18.5
	S	1.49	37	12.5
	S	-0.12	0	4.8
	S	-1.85	26	-36.6
	S	-0.47	11	-11.8
	S	-0.96	40	-4.0
	S	4.84	0	108.6

(continued)

TABLE 16.1 (continued)
Molar Group Contribution Values

Chemical Group ^a	Type ^b	Molar Group Contributions		
		Ω_i (MJ/mol)	X_i (g/mol)	Ψ_i (kJ/mol K)
$-\text{NH}_2$	S	-0.04	1	-1.4
	S	0.27	96	-17.3
	S	2.16	0	39.6

^a R = organic substituent.
^b B = backbone group, S = side or pendant group.

16.2.3 RESULTS AND DISCUSSION

16.2.3.1 Deterministic Model of Flammability (Molar Group Contributions)

It is well known that the flammability of polymers is related to their thermal and combustion properties [26]. Moreover, these thermal combustion properties are amenable to calculation by additive molar group contributions. In the present study, we applied the empirical group contribution method to specific chemical groups in polyesters and polycarbonates for 84 polymers of interest [26]. Figure 16.2 shows the results for char yield modeled as an additive molar function versus the measured char yield for 73 experimental polymers and 11 commercial polymers. The experimental data are reasonably well approximated by additive molar contributions to charring using 38 individual chemical groups (Table 16.1) as shown by the proximity to the equivalence line. A char yield $\geq 30\%$ by weight (enclosed by the dashed circle) was considered one criterion for low flammability.

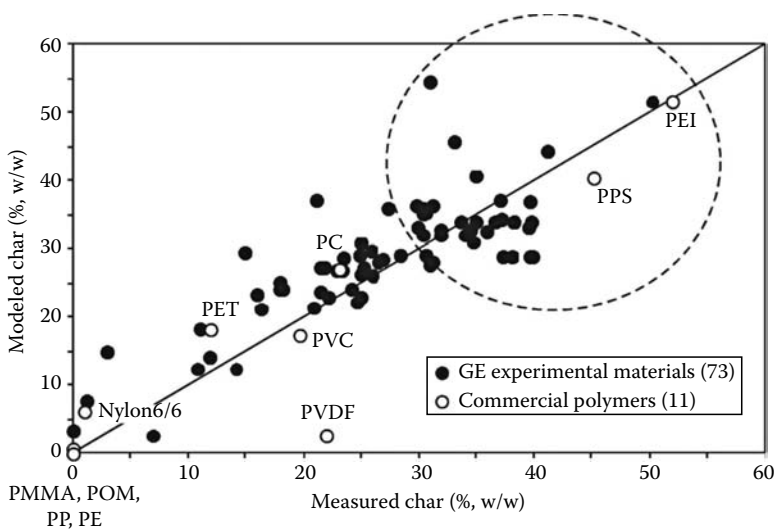


FIGURE 16.2 Char yield calculated from the additive model versus measured char yield for 84 polymers. Char reported as mass fraction (%).

A second measure of flammability is the amount of heat liberated by combustion of the fuel gases. The same molar groups that were assigned additive charring contributions were assigned additive heat release contributions based on the HR measured in the MCC. Figure 16.3 shows the results of these calculations as the additive model of HR versus the measured HR for 84 polymers. A heat release, $HR < 12\text{kJ/g}$ (enclosed by the dashed circle) was considered as a second criterion for low flammability.

The HRC of a polymer is thought to be a fundamental fire property, and empirical molar group contributions to polymer HRC have been determined for a wide range of polymers. These molar group contributions were refined and recalculated for the limited range of polymer chemistry in the development program, in an attempt to obtain better predictive capability. The results of the additive model calculations are shown in Figure 16.4 versus the measured values from MCC. Reasonably

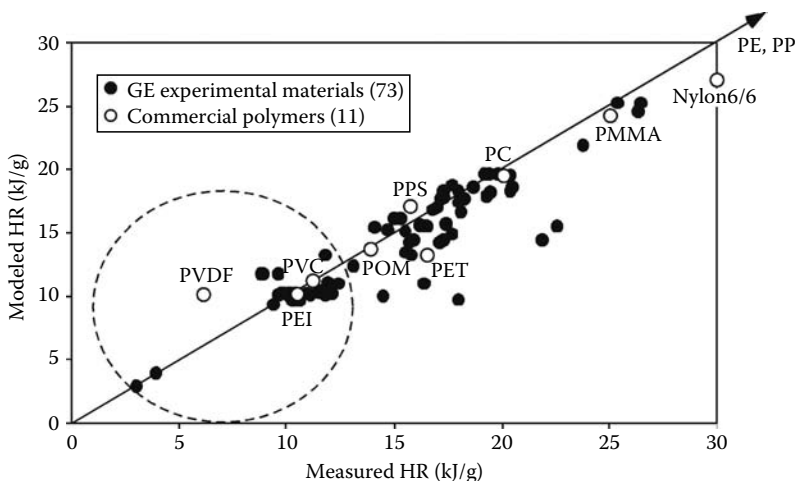


FIGURE 16.3 Heat release calculated by the additive model versus heat release measured in the MCC for 84 polymers.

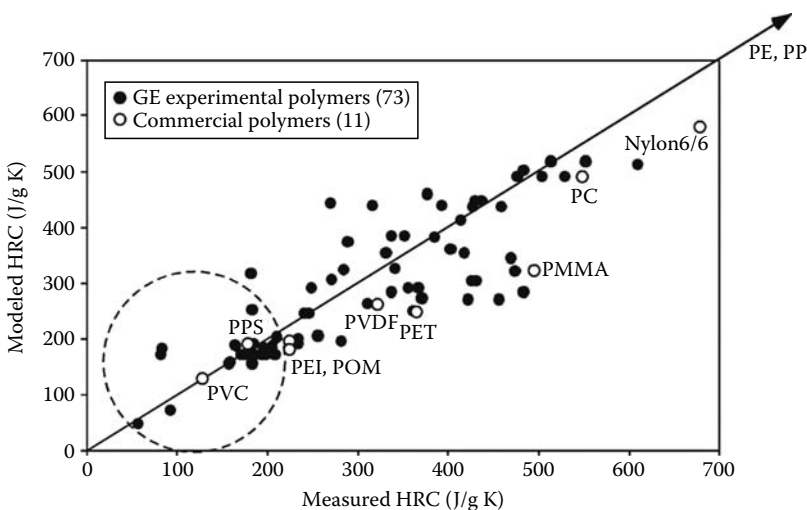


FIGURE 16.4 HRC calculated from additive molar group contribution model versus HRC measured in MCC for 84 polymers. Solid line is equivalence.

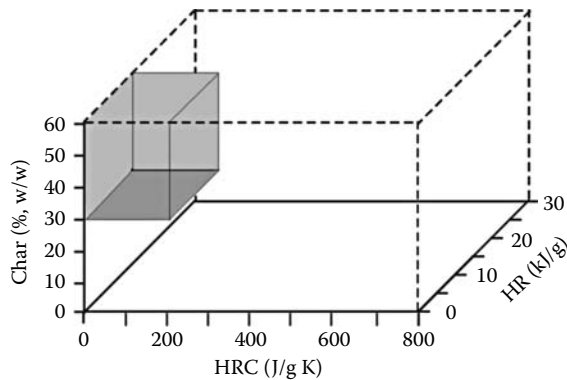


FIGURE 16.5 The shaded region satisfies the three flammability criteria for the program and represents 5% of the response space.

good agreement is observed between the additive model HRC and the measured HRC. A heat release capacity, $HRC \leq 200 \text{ J/g K}$, was considered to be a third criterion for low flammability (enclosed by the dashed circle).

Figure 16.5 shows the region of space bounded by the three separate flammability criteria: $HRC \leq 200 \text{ J/g K}$, $HR \leq 12 \text{ kJ/g}$, and $\mu \geq 30 \text{ wt\%}$. The volume of this target region is 5% of the parameter space of formulations tested in this program and 2% of the parameter space for the commercial polymers that were tested.

16.2.3.2 Statistical Model of Flammability (Probabilistic Regression)

Selecting materials for scale-up based on separate flammability criteria for HRC, HR, and μ increases the likelihood that a sample will pass the requirements of 14 CFR 25. However, it has been shown that these three properties are not independent [27]. For a single-step thermal decomposition reaction at a constant heating rate, these thermal combustion properties are related:

$$HRC = \frac{(1-\mu)h_c}{eRT_p^2/E_a} = \frac{HR}{\Delta T_p} \quad (16.2)$$

where

h_c (J/g-gas) is the net heat of complete combustion of the pyrolysis gases

T_p is the temperature at peak pyrolysis rate

E_a is the global activation energy for thermal decomposition

ΔT_p is the pyrolysis temperature interval, which is typically about 50 K

As HRC is a composite of key flammability parameters, it should be (and is) a good predictor of flame and fire test results [27]. For this reason, HRC was selected as the sole explanatory variable for a probabilistic analysis of flammability.

Although 14 CFR Part 25 contains requirements for flame resistance (12-s Bunsen burner test), smoke generation under radiant heating, and HRR in flaming combustion, it is the latter that is generally regarded as the most difficult aspect of the regulation and, in particular, the peak heat release rate (pHRR). Consequently, a probabilistic relationship between pHRR and HRC was derived for 41 of the materials by force-ranking the results by HRC and computing the fraction of passing results

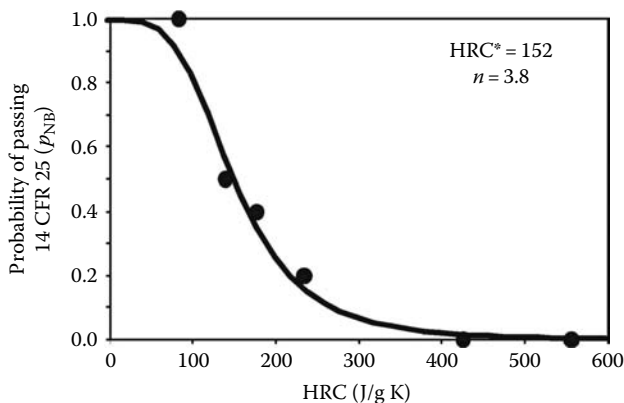


FIGURE 16.6 The probability of passing the pHRR requirement of 14 CFR 25 versus the HRC of the sample. Circles are binned data. Line is regression model.

(pHRR ≤ 65 kW/m²) and average HRC for successive bins of increasing HRC. Figure 16.6 shows the results of this exercise as solid circles for the fraction of samples having pHRR ≤ 65 kW/m² (i.e., the probability of not burning, p_{NB}) versus the average HRC of the successive bins. A regression equation for this binary (pass/fail) data is obtained from a semiempirical equation for the odds of burning derived from flame-spread theory [28]:

$$\text{Odds of burning} = \frac{\text{Probability of burning}}{\text{Probability of not burning}} = \frac{p_B}{1 - p_B} = \left(\frac{\text{HRC}}{\text{HRC}^*} \right)^n \quad (16.3)$$

The probability of not burning is, therefore,

$$p_{NB} = 1 - p_B = \frac{1}{1 + (\text{HRC} / \text{HRC}^*)^n} \quad (16.4)$$

The solid line in Figure 16.6 is a fit of Equation 16.4 to the experimental data using HRC* and n as adjustable parameters. The mean deviation of Equation 16.4 from the experimental data using the best-fit parameters, HRC* = 152 J/g K and $n = 3.8$, is $\sigma = 0.07$. Assuming that Equation 16.4 represents the mean for a normally distributed probability at each HRC, about 95% of the probability distribution will be found within $p_{NB} \pm 2\sigma$, or, $p_{NB} \pm 0.14$. The critical HRC in Equations 16.3 and 16.4, HRC* = 152 J/g K, is the value of HRC at which $p_{NB} = p_B = 0.5$, i.e., at which 50% \pm 14% of the samples are expected to pass (or fail) the pHRR requirement of 14 CFR 25.

A sample calculation for a generic polyester carbonate (Figure 16.7) [29] with corresponding group contributions (Table 16.2) illustrates how the deterministic and statistical models were used to screen for flammability.

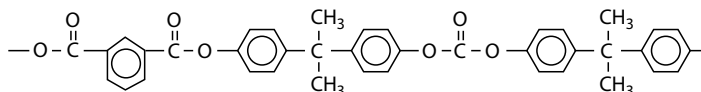
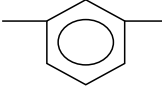

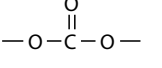
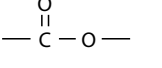
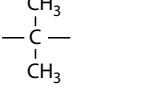


FIGURE 16.7 Polyester carbonate structure used for sample calculations to demonstrate how the model was used to predict flammability.

TABLE 16.2
Molar Chemical Group Contributions Used to Predict
Polymer Flammability

Group	<i>n</i>	Molar Quantity (<i>P_i</i>)			
		Molar Mass (g/mol)	Ω (MJ/mol)	X (g/mol)	Ψ (kJ/mol K)
	1	76	1.08	35	13.1
	4	76	1.08	35	13.1
	1	60	0.22	-1	13.6
	2	44	0.24	0	3.1
	2	42	2.63	0	85.5
$\Sigma n_i P_i$		612 g	11.36 MJ	174 g	256.3 kJ/K

From these data and Equation 16.1, we calculate for the generic polyester carbonate: $HR = 11.36 \text{ MJ/g} = 18.6 \text{ kJ/g}$, $\mu = 174 \text{ g/g} = 0.284$ (28.4% char), and $HRC = (256.3 \text{ kJ/K})/\text{g} = 419 \text{ J/g K}$. The generic polyester carbonate is thus eliminated from further consideration, because it satisfies none of the three flammability criteria of the deterministic model (see Figure 16.5) and has a low probability of passing the pHRR requirement of 14 CFR 25, $p_{NB} = [1 + (419/152)^{3.8}]^{-1} = 0.02 \pm 0.14$ (see Equation 16.4).

16.2.3.3 Flammability Results of Optimized Formulations

Table 16.3 contains the MCC results for a commercial transparent polyphenylsulfone polymer and three colors of the polyester carbonate polymer developed in this study based on the three-dimensional flammability criterion. The probabilistic analysis for these polymers using HRC as the sole explanatory variable (Equation 16.4) suggests that the PPSU (clear) has $p_{NB} = 0.18 \pm 0.14$, i.e., an 18% \pm 14% chance of passing the pHRR requirement of 14 CFR 25 while the clear, gray and white grades of the polyester carbonate have a 41%, 29%, and 22% (\pm 14%) chance of passing 14 CFR 25, respectively. The average

TABLE 16.3
Thermal Combustion Properties of Clear/Transparent Plastics

Material	HRC (J/g K)	HR (kJ/g)	T_p ($^{\circ}\text{C}$)	Char Fraction, μ (%)	p_{NB} (%)
Polyphenylsulfone (clear)	228	13.5	622	42	18
Polyester carbonate (clear)	168	10.3	531	38	41
Polyester carbonate (gray)	192	10.4	495	35	29
Polyester carbonate (white)	213	10.9	496	36	22

TABLE 16.4
Heat Release and Smoke Density Results for Clear/Transparent
Plastics in 14 CFR 25

Thickness (mm)	PEAK HRR (kW/m ²)	2-MIN HR (kW min/m ²)	Smoke Density (⁴ D _m)
Clear polyphenylsulfone			
1	63 ± 5	13 ± 9	Not measured
2	49 ± 11	2 ± 3	2 ± 1
3	39 ± 1	4 ± 1	Not measured
4	66 ± 2	18 ± 3	Not measured
5	59 ± 1	5 ± 2	Not measured
Clear polyestercarbonate			
1.5	38 ± 1	27 ± 3	6 ± 1
2.5	61 ± 4	18 ± 1	7 ± 5
3.2	51 ± 5	9 ± 2	10 ± 3
Gray polyestercarbonate			
1.5	50 ± 11	34 ± 11	10 ± 3
2.5	45 ± 14	18 ± 5	10 ± 2
3.2	52 ± 11	12 ± 6	11 ± 6
White polyestercarbonate			
1.5	48 ± 8	30 ± 1	10 ± 2
2.5	59 ± 1	23 ± 6	7 ± 3
3.2	47 ± 6	12 ± 1	6 ± 1
14 CFR 25 maximum	65	65	200

probability of passing the pHRR requirement of 14 CFR 25 using the criterion $HRC \leq 200 \text{ J/g K}$ in Equation 16.4 is $p_{NB} \geq 26\%$.

Table 16.4 shows the 14 CFR 25 data for heat release and smoke for various thicknesses of clear polyphenylsulfone and three colors of polyester carbonate. It is observed that the polyphenylsulfone passes the pHRR requirement at some, but not all, thicknesses, while easily passing the smoke density and heat release requirements. By comparison, the polyester carbonate passes pHRR, 2-min heat release, and smoke density at all colors and thicknesses. Thus, extrinsic factors that reduce flammability in the HRR tests, such as melt dripping and intumescence, but are not measured by MCC, could improve the chances of passing the 14 CFR 25 requirement for pHRR compared with what would be expected from a probabilistic analysis using HRC as the sole predictive variable. HRC was used as the sole explanatory variable owing to its theoretical relationship to flame spread, which by itself is a gross simplification of the burning process in 14 CFR 25. This creates a source of error between the model and 14 CFR 25 performance. It is to be noted that, a more robust, totally empirical model, such as logistic regression that uses all three of the MCC target variables in Figure 16.5, would be expected to provide better predictive capability, but at the expense of a physical basis and simplicity.

16.2.4 CONCLUSIONS

HT synthesis and testing supported by deterministic (molar group contributions) and statistical (probabilistic regression) analyses were successfully used to develop novel, functional, transparent plastics from commodity starting materials that satisfy the stringent flammability requirements for use in aircraft cabin interiors.

16.3 CASE STUDY 2. HIGH THROUGHPUT POLYMER FLAMMABILITY CHARACTERIZATION USING GRADIENT HEAT FLUX ENVIRONMENTS AND RAPID CONE CALORIMETRY*

16.3.1 INTRODUCTION

Predicting fire performance using small-scale fire tests requires a significant amount of data, which is often collected from a variety of different tests. The type of data necessary depends on the material application, but generally the following information can be quite useful: ignition time, HRR, flame velocity, self-extinguishing behavior, etc. as a function of type and amount of additive, flux environment, etc. The potential benefits of taking a HT approach is to significantly reduce the resources required to obtain the desired information, reduce research turnaround time, and allow for a more thorough exploration of the experimental space. A common approach to developing a HT test is to change the experiment by testing smaller sample sizes, using smaller testing equipment, and accelerating the testing procedure. This approach unfortunately is thought to be counterproductive for fire performance testing because the small-scale fire behavior may not easily translate to the behavior observed in larger more realistic fires.

One reason it may be difficult to correlate results across fire testing scales is the difficulty in quantifying or controlling the heat transfer rate through the sample. Since the maximum burn rate depends on the heat transfer to the sample, the inability to reproduce this phenomenon can lead to misinterpretation of testing results [30]. One example is the faster ignition rate for samples sufficiently thin to experience thermally thin behavior. As shown in Equation 16.1, the time to ignition, t_{ign} (s), for thermally thin samples is dependent on the heat capacity of the material per unit area ($\tau\rho c$), where for thermally thick samples t_{ign} depends on the thermal inertia ($\sqrt{\kappa\rho c}$), as the surface temperature is dictated by the thermal gradient within the sample so the thermal conductivity (κ , W/(mK)) of the material becomes important.

$$t_{\text{ign}} = \frac{\tau\rho c}{2h} \ln \frac{T_{\infty} - T_0}{T_{\infty} - T_i} \quad (16.5)$$

where

h (W/(m²K)) is the convective heat transfer coefficient

ρ (m³/g) is the density

c (J/g) is the thermal capacity

τ (m) is the sample thickness

T (K) is the temperature

Research suggests a more complete picture of material fire performance can be obtained by conducting experiments at different heat fluxes. Lyon [31] reported that the intercept (HRR_0) of the HRR versus heat flux curve correlates with UL-94 behavior. Lyon's work was corroborated by Bundy and coauthors [32] who showed HRR_0 correlated with the UL-94 results for High Impact Polystyrene (HIPS) filled with different loading levels of a bromine/antimony oxide fire retardant package or a nonhalogen fire retardant (Figure 16.8). A drawback to the conventional testing approach described in Bundy's study was the long turnaround time to obtain the Cone data (nearly 2 weeks) for 27 tests.

* Case studies 2 and 3 were carried out by the National Institute of Standards and Technology (NIST)—an agency of the U.S. government and by statute is not subject to copyright in the United States. Certain commercial equipment, instruments, materials, or companies are identified in this paper to adequately specify the experimental procedure. This in no way implies endorsement or recommendation by NIST. The policy of NIST is to use SI units of measurement in all its publications, and to provide statements of uncertainty for all original measurements. In this document, however, data from organizations outside NIST are shown, which may include measurements in nonmetric units or measurements without uncertainty statements.

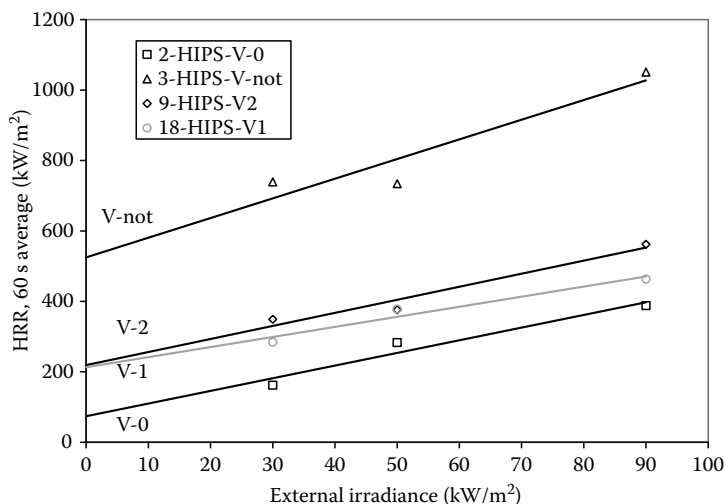


FIGURE 16.8 Average heat release rate (HRR, 60s average) versus external irradiance (heat flux) for four HIPS formulations. The FR in 2-HIPS was bromine/antimony oxide, 3-HIPS contained no FR, 9-HIPS contained bromine/antimony oxide, and 18-HIPS contained a nonhalogen FR. The UL 94 rating for each formulation is indicated on the plot. The uncertainty in the HRR is $\pm 5\%$ (2σ).

Another study demonstrating the importance of conducting multflux flammability tests was conducted by Panagiotou and Quintiere [33]. Quintiere used modeling of flame-spread to show that a polymer system can be accurately characterized only if the flammability is measured over a range of heat fluxes; ignition time, flame spread, and HRR need to be measured at various fluxes.

The efforts described here are those specifically focused at developing HT flammability analysis methods, which kept pace with our sample preparation rate (one sample per minute) and accelerated the acquisition of data at multiple heat fluxes. The purpose of these HT flammability studies was to evaluate the potential benefits of these HT approaches, while simultaneously evaluating the effectiveness of combining a standard intumescence FR (ammonium polyphosphate [APP] and pentaerythritol [PER]) with a nanocomposite FR (organoclay [34]). The need to develop HT flammable tests was driven by our inability to test the fire performance at a rate close to the rate we could generate samples (5 specimens/day as compared with 200 specimens/day). The result of developing these HT flammability methods (flame spread and rapid cone calorimetry [RCC]) is a 10 times smaller sample size requirement and a 10 times faster experiment turnaround time. Not demonstrated here, but implied is the opportunity to increase the experimental matrix by 10 times rather than decreasing the total study time by an order of magnitude.

16.3.2 EXPERIMENTAL

16.3.2.1 Sample Preparation

A twin-screw extruder (B&P, 19 mm diameter screws with a 25:1 length to diameter ratio) was used to prepare filled polymer strands with homogenous or gradient additive concentrations. The extruder operating conditions were as follows, feed: 443 K (170°C), zone-2: 453 K (180°C), zone-3: 453 K (180°C), exit die: 463 K (190°C), and screw speed: 10.5 rad/s (100 rev/min). The additive dispense rate was based on the additive concentration desired in the strands and the base polymer feed rate, which was 2–3 kg/h. The width–thickness–length strand geometry (7 mm by 4 mm by 1 mm) was created by a two-hole circular exit die. Before collecting or pelletizing, the polymer strands were air-knife cooled (10 s) while traveling down a conveyor belt.

Forty-two discrete compositions were prepared using the conditions described above (Table 16.5). The samples were primarily polystyrene and contained 0 mass fraction (%) to 30 mass fraction (%)

TABLE 16.5
42 Member Compositional Matrix of Polystyrene (PS)
Containing Various Levels of a 3:1 Mass Ratio of Ammonium
Polyphosphate (APP/PER (3:1)) or a Cloisite 15A Organoclay

↓ Mass Fraction (%) APP/PER (3:1)	Mass Fraction (%) Organoclay →					
	0	2	4	6	8	10
0	√	√	√	√	√	√
5	√	√	√	√	√	√
10	√	√	√	√	√	√
15	√	√	√	√	√	√
20	√	√	√	√	√	√
25	√	√	√	√	√	√
30	√	√	√	√	√	√

of a 3:1 mass ratio of APP and PER. Of each composition 10–12 strands were collected for flammability testing. A portion of each composition was pelletized, rather than collected as a strand, then compounded again to add 0 mass fraction (%) to 15 mass fraction (%) of an organoclay [34]. These APP/PER/organoclay compositions were only collected as strands. All tests were performed on the as-collected strands, except for the t_{ign} and RCC experiments, where smaller portions of the strands (length of 90 mm) were used for testing. Unless otherwise indicated, when referring to sample compositions, the % value is mass fraction (%).

16.3.2.2 Flammability Properties

The flammability performance of the PS strands was measured using a Radiant Panel Apparatus (RPA) and a Cone Calorimeter. The RPA was configured to provide a position dependent heat flux to homogenous composition samples (Figures 16.9 through 16.11). The MFSS experiments were performed on single homogeneous composition strands. Only one strand could be tested at a time because feedback from other strands created large irreproducible fluctuations in the heat flux profile. All samples tested in the RPA were ignited by a spark source.

The t_{ign} experiments were conducted in the same flux environment as the MFSS experiments, but used the 90 mm ($2\sigma = \pm 5$ mm) discrete samples placed at different heat fluxes (34.9, 31.1, and

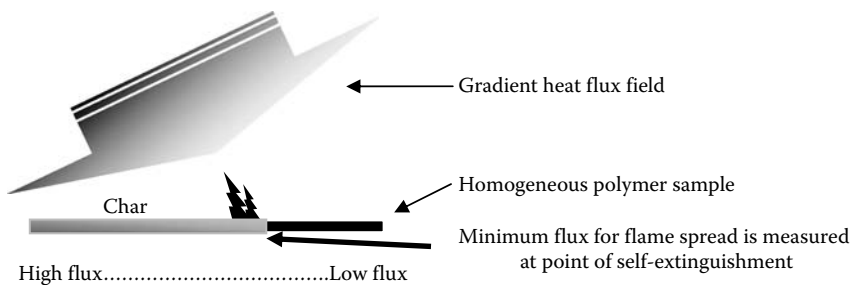


FIGURE 16.9 Schematic of the MFSS experiment where a homogeneous composition strand is exposed to a gradient heat flux intensity environment.

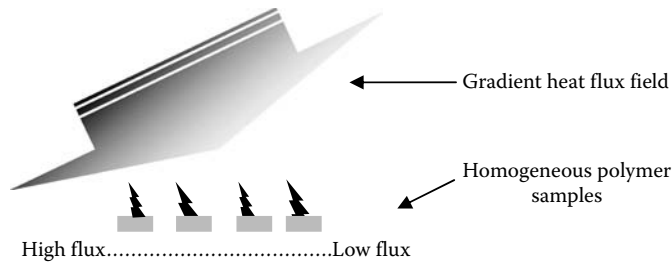


FIGURE 16.10 Schematic of the time to ignition experiment where the t_{ign} of three to four samples of the same composition are simultaneously measured at several incident fluxes.



FIGURE 16.11 RPA with a gas radiant heat source and a ceramic sample holder.

22.1 kW/m², $2\sigma = \pm 1$ kW/m²). The heat flux profile (Figure 16.12) was determined using a flux gauge at 50 mm increments along the centerline of the sample holder. The heat flux profile depended not only on the angle of the radiation panel, but also on the maximum heat flux. The heat flux profile used for these tests is indicated as “Test Gradient” in Figure 16.12. In the MFFS experiments, the strands were ignited at the high heat flux end. For the t_{ign} experiments, each sample was ignited at different fluxes by separate ignition sources. For both experiments, the samples were surrounded (sides and back only) by a heavy gauge aluminum conformed to the shape of the sample. The aluminum holder improves experimental reproducibility and minimizes cleanup between experiments. These holders are 1.5 mm taller than the sample sides, but slightly flared away from the strands so as not to shield the strands from the incident flux.

The Cone Calorimeter was equipped with a conveyor belt (Figure 16.13) to allow for continuous supply of small samples to pass under the cone heater for testing; this is called RCC. Similar to a conventional Cone [35], the combustion products (smoke, CO, CO₂, etc.) are analyzed with the primary measurement being the amount of O₂ consumed while burning. The operation procedure of the RCC and the conventional cone (ASTM 1354) are quite different as the RCC uses significantly smaller specimens and the test is continuous. In these studies, both the RCC and conventional cone were operated at a heat flux of 35 kW/m². The absolute values for the RCC and conventional cone are not identical, since the sample masses are different, but the result

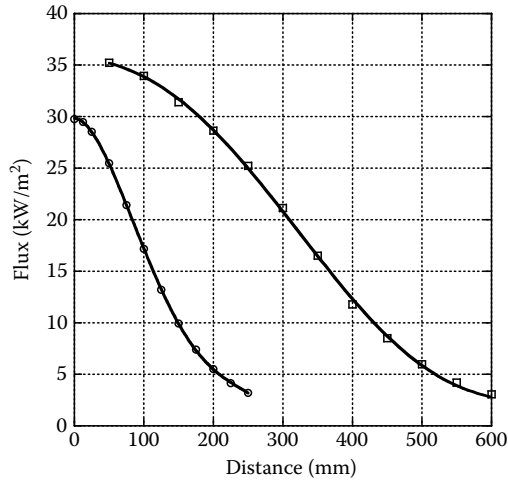


FIGURE 16.12 Flux gradient profile generated in the RPA. Top curve is the “Test Gradient” used in the study. Bottom curve is a different gradient created by changing the radiant panel tilt angle and maximum heat flux value.

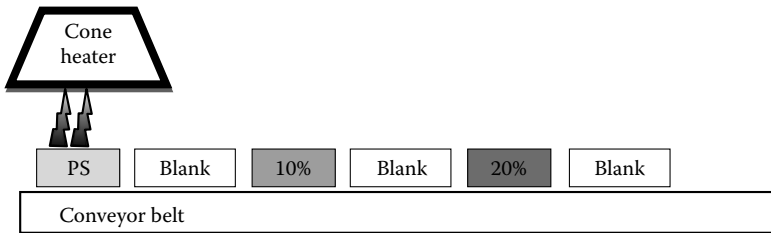


FIGURE 16.13 Schematic of the RCC.

trends are aligned. The same sample size and pans were used in RCC as described earlier for the t_{ign} experiments. An empty aluminum pan was placed between each test specimen to prevent feedback and preheating of subsequent test specimens. A specimen is tested in 50–60 s with a 100–110 s spacer between each specimen. The times reported were experimentally determined to be the most reproducible for specimens with the described dimensions. The test times were controlled by adjusting the conveyor belt speed.

16.3.3 RESULTS AND DISCUSSION

The purpose of these HT flammability studies was to evaluate the potential benefits of the HT approaches, while simultaneously evaluating the effectiveness of combining a standard intumescent FR (APP and PER) with a nanocomposite FR (organoclay). The 15 replicates of the 42 formulations in this study were generated by the extruder in 3 days and the MFFS, t_{ign} , and RCC tests were completed in 10 days. The HT benefits realized by using these HT methods were an order of magnitude of material, testing time, or compounding time.

16.3.3.1 Minimum Flux for Flame Spread and t_{ign}

The RPA was used to measure flammability at a variety of fluxes, nearly simultaneously, and in a HT fashion. A schematic of the experiment performed in the radiant panel is shown in Figures 16.10 and 16.11. The angled radiant panel configuration created a gradient heat flux field (top curve of

Figure 16.12); the heat flux field map was determined by taking several measurements using a heat flux gauge.

For the MFFS studies, the samples were ignited in the high heat flux region and allowed to burn until they self-extinguished. The local flux at self-extinguishment was determined from the flux map and is termed the MFFS. A UL 94 V-0 rating was found to correlate with a minimum MFFS of $13 \text{ kW/m}^2 \pm 1.4 \text{ kW/m}^2$ (2σ) for polyamide-6 containing either organobromine/antimony trioxide or magnesium hydroxide FR package [36]. Furthermore, the MFFS results of rigid polyisocyanurate foams were found to correlate with the flame-spread index in the E-84 tunnel test [36]. For the t_{ign} studies, the samples were placed at different positions on the holder and ignited using dedicated sparking source for each sample. Owing to the flux mapping, the local flux environment for each specimen was known.

The controls for the MFFS experiments were the pure PS loaded with a 0 mass fraction (%) to 30 mass fraction (%) of 3:1 mass ratio of APP/PER. The MFFS values for these controls are shown in Figure 16.14 on the “control curve.” This “control curve” does not contain data points below 15 mass fraction (%) APP/PER, because at these low-loading levels the samples could not

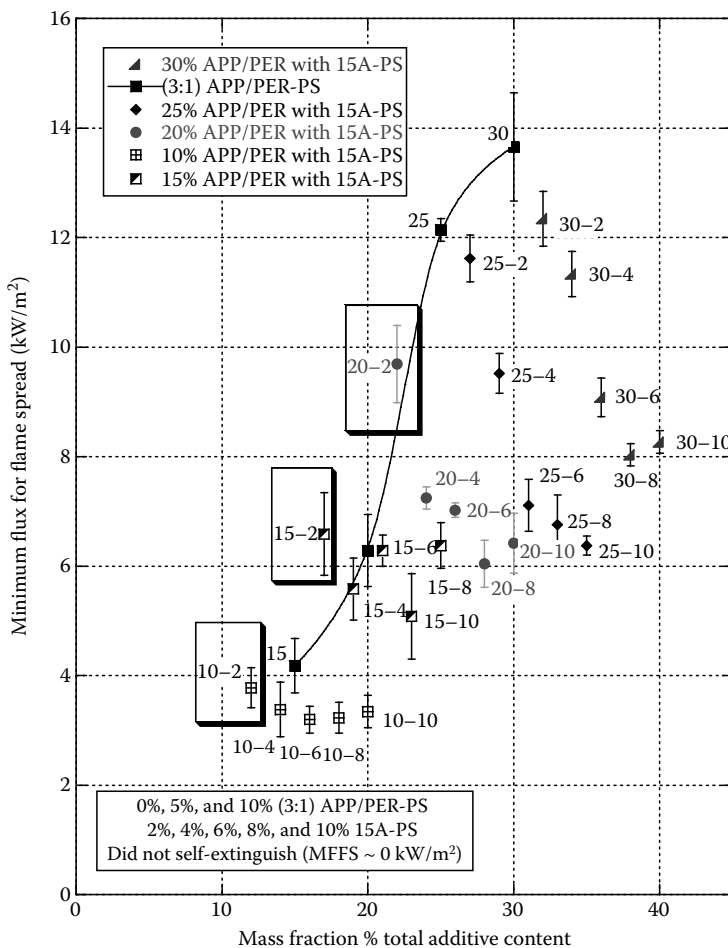


FIGURE 16.14 MFFS data for the PS flame retarded formulations measured in the RPA. The error bars represent a standard uncertainty of $\pm 1\sigma$. The data points labeled with a single number are the pure APP/PER (3:1) in PS, where the number refers to the mass fraction (%) of APP/PER. All two number labels (X–Y) refer to the mass fraction (%) of APP/PER (X) and organoclay (Y) in the APP/PER-15A-PS blends.

self-extinguish; therefore, they were presumed to have a MFSS equal to that of pure PS (0 kW/m^2). The data points off the control curve are the MFSS of these control formulations with the addition of differing amounts of organoclay, i.e., 20–10 refers to a 20 mass fraction (%) APP/PER plus 10 mass fraction (%) organoclay. In general, adding organoclay creates a deficiency (data points below control curve) in the MFSS performance, as compared with the control with the same APP/PER loading. This antagonistic interaction between organoclay and APP/PER can be quite severe, as the MFSS performance can be significantly worse than the same loading level of pure APP/PER, i.e., 20%–10% APP/PER–organoclay compared with 30% pure APP/PER. However, a synergistic interaction (data points above the control curve) occurred for three formulations with the resulting MFSS being more than 10% better than the pure APP/PER at the same total loading level. Moreover, only the formulations with low organoclay (2 mass fraction [%]) loading exhibited improved MFSS, and further organoclay loading either had no impact or created an increasing deficiency in MFSS performance.

Understanding thermoplastic fire performance based on MFSS alone is difficult, as flame spread is dependent on the burning configuration, material thermal properties, HRR, and the ignition properties [37]. Therefore, we developed the HT t_{ign} method to rapidly measure ignition times and the RCC to rapidly measure HRR and peak HRR (pHRR). The burning configuration was not a factor in this study as all samples were burned horizontally. For all recipes (only low organoclay data is shown), decreasing the heat flux resulted in delayed ignition (Figure 16.15).

Addition of APP/PER to PS, regardless of the loading level and the heat flux, shortened the ignition time, as compared with pure PS (Figure 16.15). For the APP/PER–PS formulations with MFSS

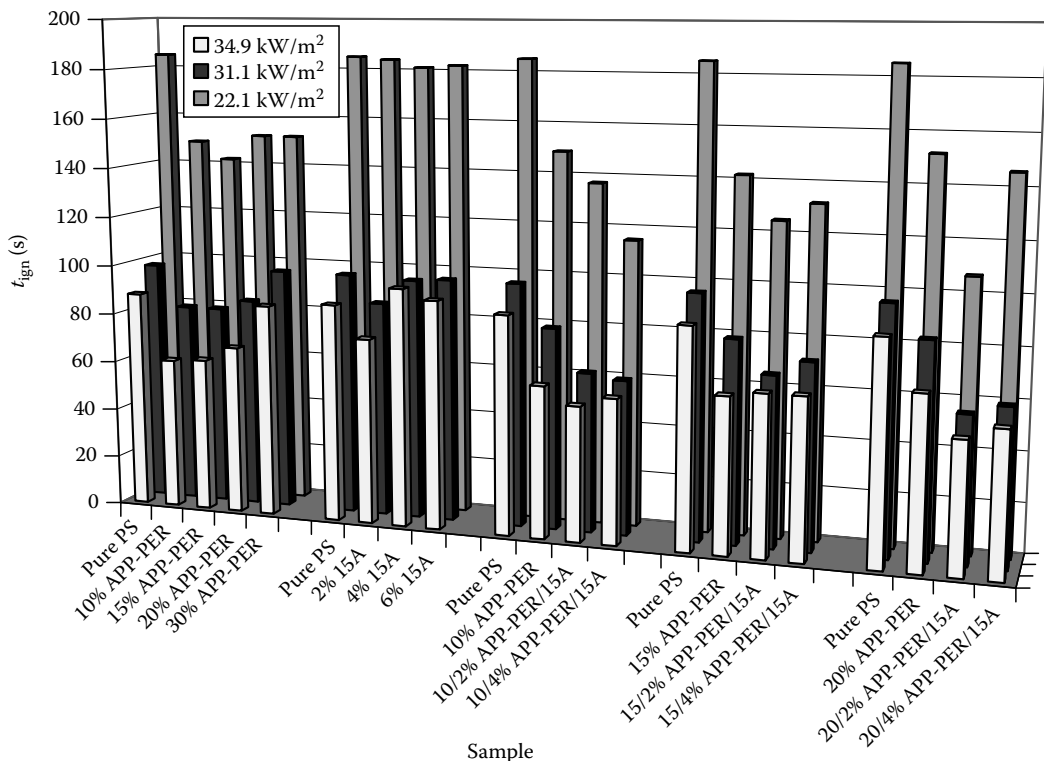


FIGURE 16.15 (See color insert following page 530.) t_{ign} data for PS flame retarded formulations measured in the RPA. The ignition time of each formulation was measured at three different heat fluxes simultaneously. The heat fluxes are provided in the insert in units of kW/m^2 and are color matched with the data bars in the graph. The t_{ign} standard uncertainty, averaged over all fluxes where t_{ign} was measured, is $\pm 10\%$ (2σ).

better than pure PS ($>0\text{ kW/m}^2$, >15 mass fraction [%] APP/PER), this additional information of a deficiency in ignition time suggests the APP/PER must significantly reduce the HRR to achieve the improved MFFS shown in Figure 16.14. In contrast, just adding organoclay to pure PS had little impact on t_{ign} and, in terms of MFFS, the addition of organoclay was insufficient for the pure PS to become self-extinguishing.

Finally, adding 2 mass fraction (%) organoclay to the APP/PER formulations shortened the ignition time, regardless of the heat flux (Figure 16.15). However, increasing the organoclay content to 4 mass fraction (%) resulted in complete or partial recovery of this ignition deficiency. These 2 mass fraction (%) organoclay formulations with 10 mass fraction (%) to 20 mass fraction (%) APP/PER were also the only samples with a measured improvement in MFFS. This suggests these formulations must have a significantly improved HRR to overcome the ignition deficiency and achieve the improved MFFS shown in Figures 16.14 and 16.15.

The HT benefits realized using these HT tools and methods (gradient compositions using the extruder, and t_{ign} and MFFS using the RPA) were one order of magnitude smaller in the sample size requirements and knowledge turnaround time, as compared with a conventional approach.

16.3.3.2 Rapid Cone Calorimetry (RCC)

The HRR curves for six formulations were collected over 20 min using the RCC (Figure 16.16). In a previous publication [36], we showed that the absolute pHRR values measured from the conventional cone and the RCC were not the same; however, the trends as a function of different compositions were aligned. For this reason, the RCC is primarily used as a screening tool and it reduces the sample size and experiment time from 50 g and 45 min per sample to 0.5 g and 1.5 min per sample. This is an approximate order of magnitude improvement.

The RCC data shows the incorporation of APP/PER reduced the pHRR and the reduction was fairly linear with the loading level (Figure 16.16) with an approximate 22% reduction in pHRR for every 10 mass fraction (%) increase in APP/PER loading. The addition of 2 mass fraction (%) organoclay provided a further reduction in pHRR. This pHRR reduction caused by the 2 mass fraction (%) organoclay is greater than expected for the same loading level of pure APP/PER, which suggests a synergistic interaction between organoclay and APP/PER. Specifically, the pHRR of 10%–2% APP/PER-organoclay was 2100 kW/m^2 as compared with a calculated 2580 kW/m^2 for 12 mass fraction (%) APP/PER.

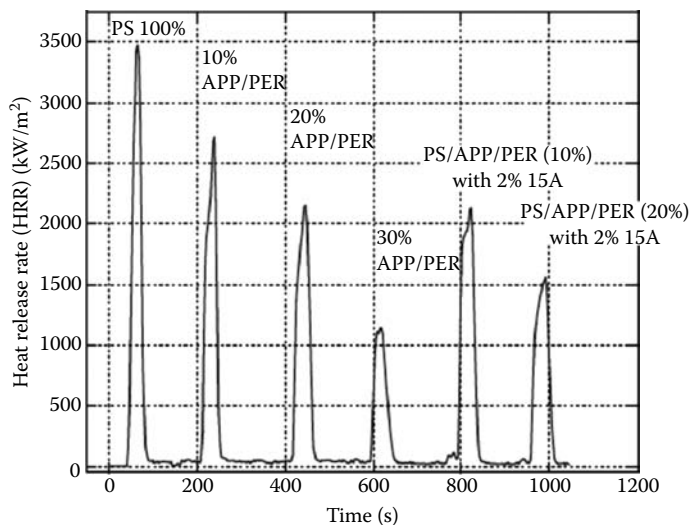


FIGURE 16.16 HRR curves for specimens tested with the RCC.

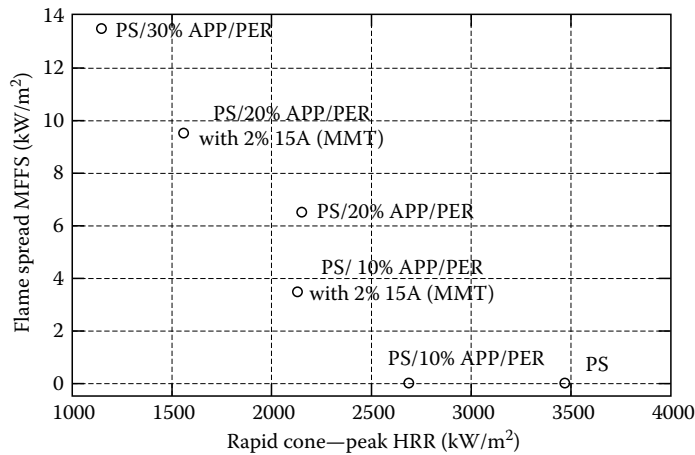


FIGURE 16.17 Correlation of MFFS and pHRR from RCC. Standard uncertainty is $\pm 10\%$ (2σ) for both MFFS and pHRR.

The RCC measures t_{ign} , smoke, CO, specific heat of combustion, mass loss rate, and a variety of other parameters; which can help to determine the mechanisms affecting the material flammability. The RCC data is an excellent complement to MFFS data as the MFFS is a measure of the interaction of several of these parameters measured in the RCC. Comparison of the RCC and MFFS data shows the inverse relationship between MFFS and pHRR (Figure 16.17); the higher the pHRR the lower the MFFS. A more detailed explanation of flame spread and more specifically flame spread using the flooring radiation panel apparatus [37] can be found elsewhere [38].

16.3.4 CONCLUSION

This RPA and RCC have been successfully demonstrated to significantly accelerate the acquisition of data critical to developing a mechanistic understanding of material fire performance. These HT flammability tests significantly reduced the amount of time and sample needed by at least an order of magnitude. The resource credits generated by applying these HT approaches could provide the fire research community with a number of significant benefits, such as but not limited to, the ability to evaluate experimental materials where sample supply is limited, to identify fire retardant combinations with synergistic performance advantages, and to develop sufficient technical information to better understand the mechanisms by which a fire retardant improves or diminishes material performance.

16.4 CASE STUDY 3. A POTENTIAL HIGH THROUGHPUT APPROACH FOR SCREENING INTUMESCENCE COATINGS

16.4.1 INTRODUCTION

The power of using compositional gradients to explore a continuous range of chemical compositions in a single sample has been demonstrated in the field of ceramics, metals, and simple polymer blends [39–45]. In each of these fields, the chief benefits obtained are a doubling in the speed of developing new materials, and an order of magnitude larger database of information on processing, properties, and costs. These benefits together have contributed to the development of robust successful products.

The activities described here focus on the development and use of HT tools and methods to rapidly create and analyze lateral gradient composition coatings on a substrate. The tools and methods were applied to addressing a specific problem for the military—how to reduce the “dry-to-fly” time of aircraft topcoats. The complexity of the topcoat formulations, such as determining the amount and type of polyol, isocyanate, solvents, pigments, curative, and defoamers, can result in thousands of formulation permutations and combinations. Including processing and application parameters, a complete coating study can quickly become a million parameter spaces. Coating studies are perfectly suited for HT because conventional approaches cannot address this magnitude of parameters in a reasonable amount of time or with sufficient information resolution. By using HT approaches, such as gradient compositions, simultaneous tests, a coating study can be reduced by the general rule of thumb of an order of magnitude (1 month rather than 10 months). The aim of this study was not to develop a solution to the dry-to-fly problem, but to develop the HT tools and methods necessary to accelerate all types of coating studies, such as the impact of fire retardants on the intumescent behavior of a coating. The results presented here clearly demonstrate that the accelerator concentration has a significant impact on the cure rate for high solids fluorinated polyurethane coatings. The readers are recommended to refer the project final report for significantly more details on this project [46].

A potential application (not demonstrated in this study) of these HT tools and methods is to create and analyze the impact property modifying additive types and concentrations have on the performance attributes of coatings, i.e., modulus, color, and fire resistance. Specifically, one could evaluate a matrix of multiadditive packages on the intumescence behavior of a coating intended for a steel beam.

16.4.2 EXPERIMENTAL

16.4.2.1 Sample Preparation

A standard aircraft topcoat and accelerator package was used for this study (Deft ELT 36173, MIL-C-85285B Type I Aircraft Topcoat containing 10 vol% of a dibutyltin dilaurate [DBTDL] solution). The topcoat formulation viscosity was decreased with a reducer Deft IS213, MIL T81772 Type I Urethane Reducer; the lower viscosity helped to reproducibly obtain the correct film thicknesses and improved component mixing in the static mixer. The film substrates were 5052-H32 aluminum tests panels (50 cm by 7.5 cm by 0.13 cm = length by width by thickness) cleaned three times with methyl ethyl ketone and once with methylene chloride.

A Fluidic System spray coater was modified to generate coatings (50–150 μm , $2\sigma = \pm 10\%$) with a gradient accelerator concentration. The gradient concentration was created across a substrate (lateral) and not through the sample (thickness) or across the width (horizontal). The types of modifications included, but are not limited to, a higher number of flights in a polypropylene static mixer, smaller diameter mixing chamber with polypropylene mixing elements to improve mixing and prevent premature component mixing, and a number of plumbing changes to prevent curing within the system. To create the gradients the substrates were placed on a conveyor belt, which horizontally transported the substrates past a downward facing spray gun (Walther Pilot Domino Type 20-339). This entire system was termed the Gradient Composition Spray Coater (GCSC).

The compositions were created by changing the relative pumping speed of the accelerator. This is a complicated process because changing the accelerator solution flow rate also impacted other parameters, such as formulation viscosity and film thickness. Fifteen parameters needed to be controlled to create gradient compositions where there was only a change in accelerator concentration. Coatings were cured at room temperature at various times depending on the level of cure desired for testing.

16.4.2.2 Coating Characterization

Coating thickness was measured both wet and dry. Wet thickness measurements were taken using a Gardner's Company Precision Hot Cake, which can measure between 125 and 500 μm films with a 2σ uncertainty of $\pm 10\%$. Dry film thickness measurements were taken using an ElektroPhysik's Exacto FN gauge, which can measure between 0.1 and 2000 μm with a 2σ uncertainty of $\pm 3\%$.

Two approaches were taken to measure the degree of cure. One approach was to use fluorescent probes (0.02 mol%) with fluorescent behavior sensitive to the environmental mobility (Figure 16.18).

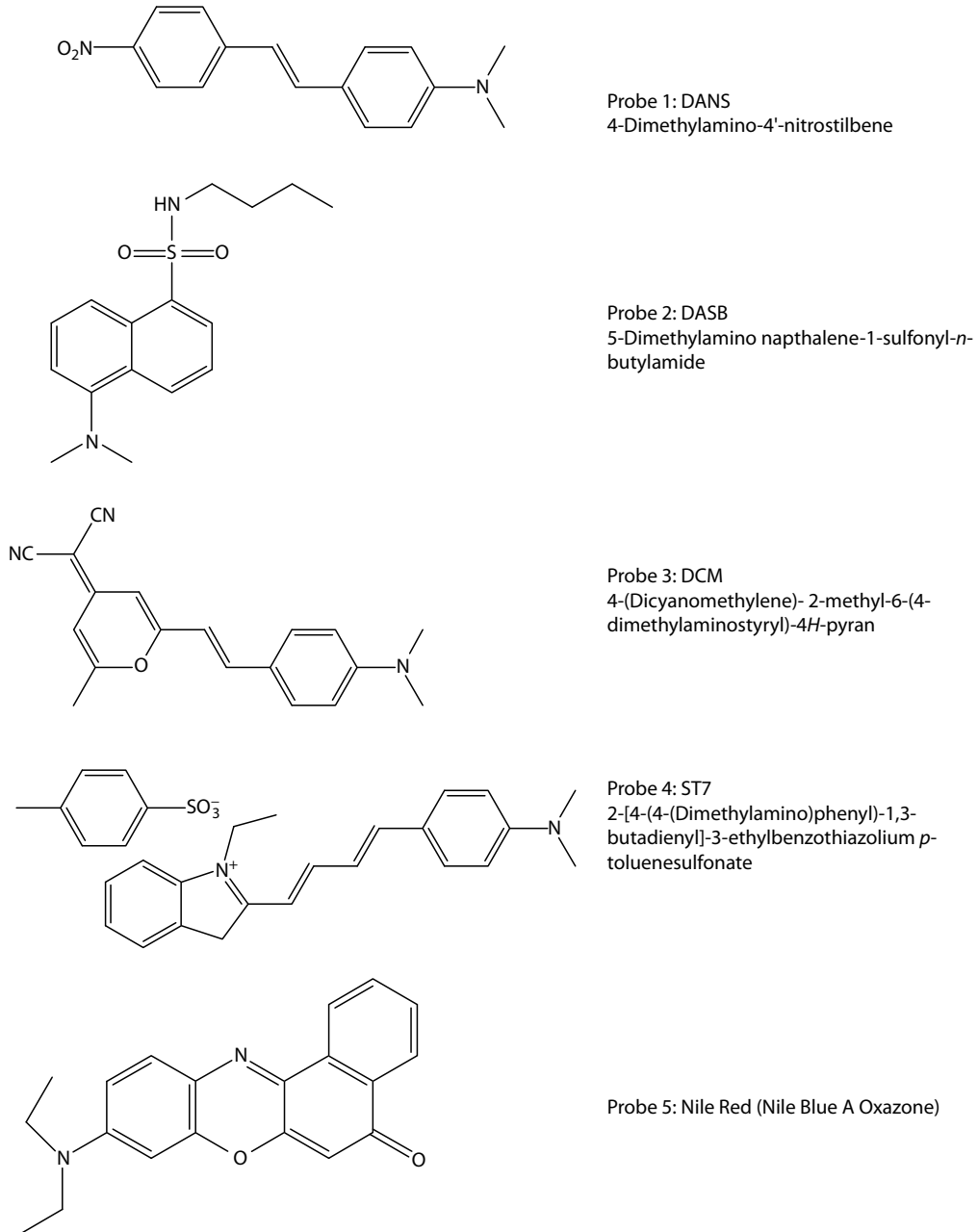


FIGURE 16.18 Fluorescent probes evaluated for monitoring topcoat cure based on change in fluorescence behavior due to environmental mobility changes.

Of the five probes evaluated only Probes 1, 3, and 5 were worth evaluating in detail, as the others had small Stokes shift (excitation wavelength, λ_{ex} , minus emission wavelength, λ_{em}) or no detectable emission. Fluorescence behavior was measured using a Zeiss LSM 510 Laser Scanning Confocal Microscope (LSCM) and an Ocean Optics USB2000 spectrometer.

Another approach used to measure cure was Fourier Transform Infrared-Reflectance Transmission Microscopy (FTIR-RTM). Measurements were performed using a Nicolet Magna-IR 550 interfaced with a NicPlan IR microscope. The microscope is equipped with a video camera, a liquid nitrogen cadmium telluride detector (Nicolet Instrumentation), and a computer-controlled mapping translation stage (Spectra-Tech, Inc.). Spectra were obtained from coated panels with different thicknesses at various curing times from 4000 to 650 cm^{-1} at a spectral resolution of 8 cm^{-1} with 64 scans and a beam spot size of 400 μm by 400 μm and ratioed against the background of a reflective glass slide. The intensity of the isocyanate peak at 2272 cm^{-1} decreased with longer cure times, while that of the methylene doublet peaks at 2857 and 2930 cm^{-1} was not dependent on cure time and served as internal standard. The ratio of the isocyanate peak area (2251–2100 cm^{-1}) to the $-\text{CH}_2-$ peaks area (3040–2700 cm^{-1}) was used throughout to eliminate the effects of sample thickness variations within and among samples. The spectra were imported into the I-Sys software (Spectral Dimensions) for quantitative measurements of the peaks areas. To evaluate the cure over a continuous portion of the gradient, spectral point-by-point mapping of the gradients was performed in a grid pattern from left to right (across the panel length) and row by row (along the panel width) with the computer-controlled microscope stage and the Omnic Atlas software. Since the maximum movements of the stage are limited to 12.4 cm in the x -axis direction and to 2.4 cm in the y -axis directions, only sections of the gradients were mapped. The reported gradient (#3) was mapped between 13.2 and 25.6 cm from the beginning of the coated panel at every 1 mm across the gradient direction (x -axis), and every 1.6 mm across the presumed constant composition y -axis direction. Mapping this section took about 12 h. This mapping procedure was repeated on the same section four times at about every 10 h. The maps spectra were collected from 4000 to 650 cm^{-1} at a spectral resolution of 8 cm^{-1} with 32 scans per spectrum and beam spot size of 400 μm \times 400 μm . The maps were processed as ratios between the areas of the isocyanate and the $-\text{CH}_2-$ peaks in the spectral regions described earlier, and displayed as color contour maps.

16.4.3 RESULTS AND DISCUSSION

16.4.3.1 Fluorescence Probes

Several homogenous coatings were created to evaluate the fluorescence probes as an approach to measure cure. As shown in Figure 16.19 for a Probe 3 containing topcoat, the λ_{em} mass for Probe 3 exhibited a blue shift and intensity increase with increasing level of cure (longer cure time). Similar behavior was observed for a Probe 1 and Probe 5 containing coatings. However, the amount of blue shift and intensity increase was less than observed for Probe 3.

Using the LSCM to measure cure appears as promising as the fluorescence spectra data discussed earlier. The bright red areas of the image from a 5 h cured topcoat are a result of Probe 5 fluorescing (Figure 16.20). This red light can only come from the probe as a 560 nm filter is used to prevent any incident light from the only other light source (a 488 nm laser). The benefits of the LSCM method are the ability to visually track cure, as the color and intensity will decrease at higher degrees of cure, the ability to identify, quantify, and measure microdomains of cure homogeneity, and the ability to perform these tests at 100 nm slices to develop a three-dimensional understanding of how cure changes as a function of sample depth.

Unfortunately, both the fluorescence spectrometer and LSCM suffer from the same drawback, the inability to repeat measurements at the same position. The samples tested in this study were gradient compositions. The fluorescence spectrometer gathered spectra at a single point on the plate; then the plate was moved to collect spectra at a different position of the plate, which had a different

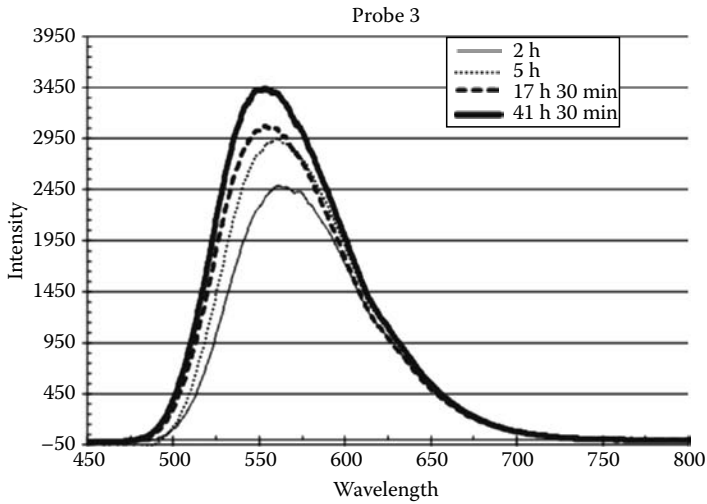


FIGURE 16.19 Fluorescence spectra of Probe 3 in topcoat as a function of room temperature cure time.

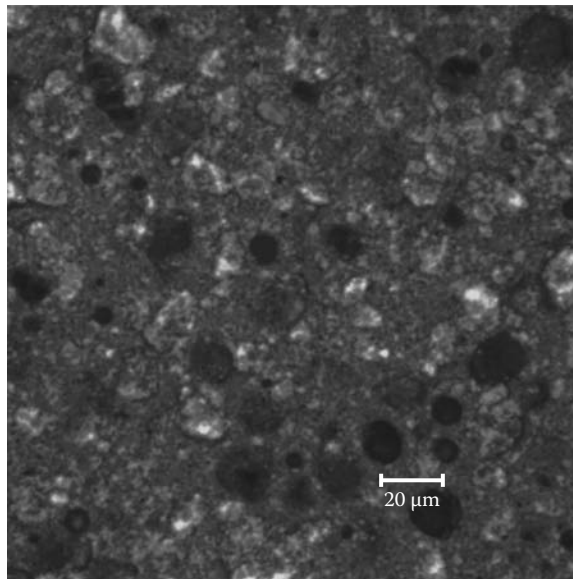


FIGURE 16.20 (See color insert following page 530.) Topcoat containing Probe 5. A LP 585 nm filter was used to remove incident light.

accelerator concentration. This tool was not equipped with a XY stage; therefore it was impossible to return to exactly the same positions to measure the degree of cure as a function of time. The experimental conditions, such as the detector gain, which could not be reproduced at every analysis time interval, further complicated the issue. The result of these complications was poor analysis reproducibility.

16.4.3.2 FTIR-RTM

After extensive baseline studies, FTIR-RTM was used for measuring the level of cure. The primary reasons for this decision was the high reproducibility of measuring cure by following isocyanate

absorption peak area, and the method was a quantitative measure of cure rather than an indirect measure, i.e., fluorescence probes.

The degree of cure is reported as a ratio of the isocyanate peak area (between 2251 and 2100 cm^{-1}) to the internal standard methylene peak area (between 3040 and 2700 cm^{-1}). Testing of control samples has determined this ratio to be 0.39 ± 0.05 (2σ) at 72 h for a conventional topcoat dry enough to fly. At 72 h there was still a significant amount of isocyanate, but the topcoat properties were sufficient to fly; therefore, the project goal was to obtain a 0.39 ratio at less than 72 h. Complete reaction of the isocyanate took 300 h using the conventional formulation.

A 50 cm long topcoat with a gradient composition of accelerator was prepared on the aluminum substrate. The gradient composition was created over the length of the coating where all testing indicated the composition was uniform through the topcoat and across the width. FTIR-RTM spectra of the gradient topcoat were collected at five positions at 4 h after spraying (Figure 16.21). The dependence of the isocyanate peak area on the testing position was an indirect indication of a gradient accelerator composition. The assumption was that the degree of cure was lower at 0 cm than at 45 cm, because there was a lesser amount of accelerator at 0 cm. This assumption is consistent with the relative amount of accelerator experimentally provided by the GCSC. The same topcoat panel was analyzed again at 152 h (Figure 16.22). A significant amount of cure took place over 148 h. At the low accelerator concentration measured end (5 cm) the isocyanate peak area decreased by 72% to a ratio value of 0.25. At the high accelerator concentration end (45 cm), the isocyanate peak area decreased by 95% to a value of 0.02, which is close to the instrument detection limit.

The series of the five FTIR-RTM mapping were obtained from a section of gradient #3 (spatial resolution of 1 mm by 1.6 mm, 125 by 16 spectra) are shown in Figure 16.23 as cure time versus accelerator concentration. The colorimetric scale on the right defines the relationship between the color and isocyanate/methylene peak ratios. Blue is the highest ratio (lowest cure) and red is the lowest ratio (highest cure). The project goal was to determine the concentrations where a ratio of 0.39 (yellow region of the map) can be achieved with a cure time less than 72 h. In this gradient, cure time was less than 72 h for the entire gradient (0.018–0.021 vol% accelerator). The average cure time was longer at the low concentration end (22 h), as compared with the high concentration end (12 h). Owing to the uncertainty in measuring small peak areas in this measurement, a ratio of 0.07 is considered complete isocyanate conversion. Complete reaction occurs much faster at the high concentration (55 h) as compared with the low concentration where at 165 h, the ratio was still higher than 0.07 (0.20).

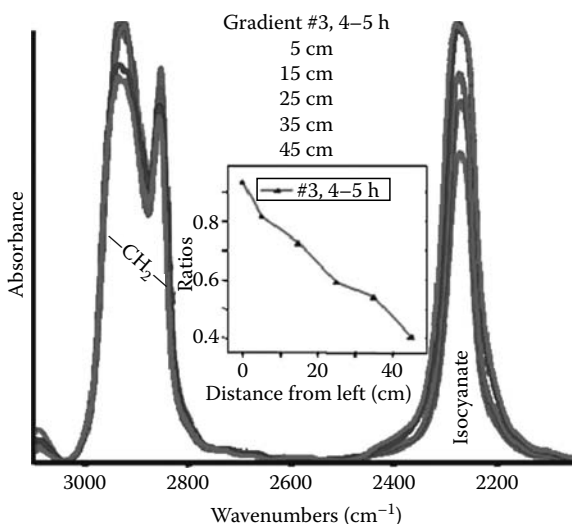


FIGURE 16.21 (See color insert following page 530.) FTIR of DBTDL lateral gradient topcoat sample taken between 4 and 5 h after spraying.

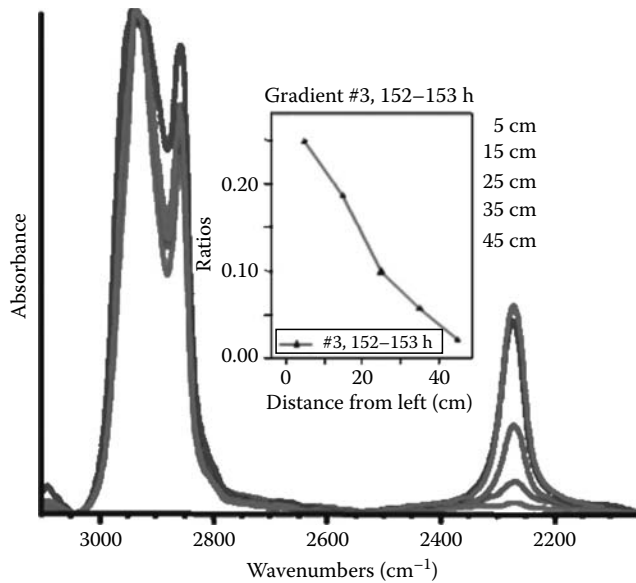


FIGURE 16.22 (See color insert following page 530.) FTIR of DBTDL lateral gradient topcoat sample taken between 152 and 153 h after spraying.

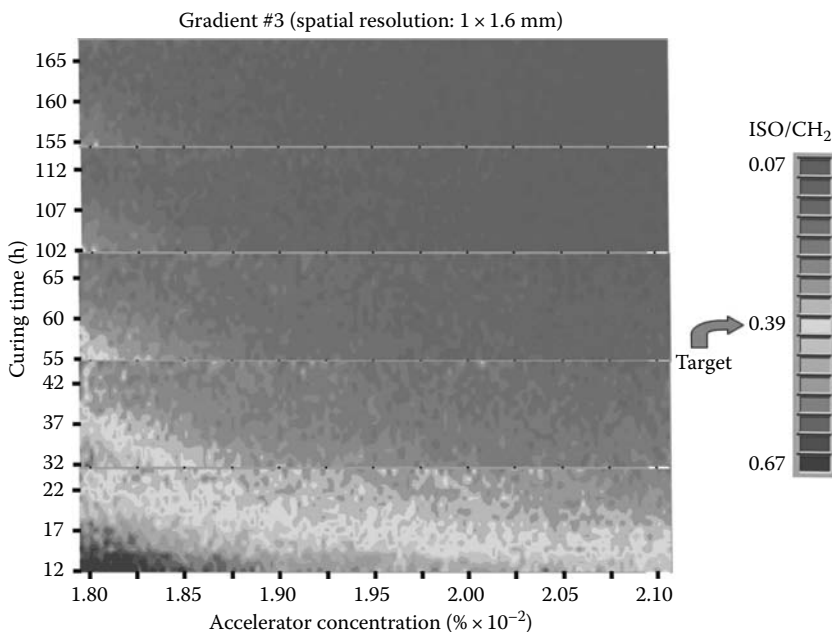


FIGURE 16.23 (See color insert following page 530.) FTIR-RTM mapping the same topcoat lateral gradient discussed in Figures 16.15 and 16.16.

16.4.3.3 Potential Application for Fire Testing

Creating gradient concentration coatings and subsequent analysis to measure degree of cure is a basic foundation for conducting a wide range of coating studies. Any number of other properties modifiers can be added to the formulation to evaluate coating performance as a function of additive type and concentration. In addition, multiadditive packages can be evaluated to identify possible

performance synergies similar to APP/PER and organoclay on PS flame spread and ignition (see Section 16.3). Another option is to create a coating with a gradient thickness rather than a gradient component concentration.

Intumescent fire resistive coatings are designed to provide an insulating barrier between flames and steel and are necessary to ensure the structural performance of the steel members at the temperatures anticipated during a fully developed fire. For coatings to be effective two characteristics are critical. One is the degree of intumescences (expansion) and the other is char layer physical strength. Both properties are highly dependent on applying the appropriate thickness and obtaining the appropriate degree of cure.

The tools and methods discussed in this section and other sections of this chapter are well aligned with the critical points of developing intumescent coatings, such as the ability to measure coating thickness, to measure degree of cure, to rapidly create compositional matrices, and test the fire performance of a coating. Specifically, the GCSC could be used to create gradient compositional coatings on steel plates. The gradients could be in additive package (multiadditives) types and concentrations (relative and total loading), and in coating thickness. The coating is cured and the degree of cure is measured using the FTIR-RTM. Ideally, the additives do not impact cure, but if they do impact this will be quickly realized and the coating could be reformulated to ensure the composition is appropriate to obtain a coating with uniform cure. After measuring the coating thickness the coating could be burned in the RPA (see Section 16.3). The RPA could be reconfigured to apply a constant flux environment over the gradient composition coating. This test could be performed at a variety of fluxes to obtain MFFS for a large range of compositions and heat fluxes.

16.4.4 CONCLUSION

The efforts described here focused on developing HT methods and tools to rapidly evaluate the cure rate of topcoats as a function of accelerator concentration. The development of this technology provides opportunities to extensively explore the impact other property modifying additives types and concentrations have on coating properties.

16.5 CHAPTER SUMMARY

The three case studies provided in this chapter describe how HT methods and tools were or could be used to accelerate our understanding of or more thoroughly explore the fire science of materials. The first case study discussed using HT synthesis and testing to develop novel, functional, transparent plastics from commodity starting materials that satisfy the stringent flammability requirements for use in aircraft cabin interiors. The second case study described the development and application of HT tools and methods to accelerate our understanding of polymer fire performance characteristics, such as MFFS. The third case study described the development of HT tools and methods to create and characterize coatings with gradient curing accelerator concentrations. Though fire performance testing was not applied in this study, the HT tools and methods discussed are the foundation required for HT-coating fire performance studies, such as evaluating FR type and concentration on the intumescent behavior of steel beam coatings.

As demonstrated in these studies a 10–100 times rate increase in information or volume of information can be achieved using HT. However, it is to be noted that these benefits are often not achieved until several years following tool installation. In fact, it took the authors nearly a year to appropriately configure these tools to generate the high-quality data discussed earlier. For companies it may be hard to justify investing thousands to millions of dollars without seeing a return on the investment for 5–10 years, especially since it is difficult to quantify and define the return. Immediate HT benefits are rarely obtained partly, because 70% or more of resources are spent in the insipient years learning how to best utilize the tools to obtain reproducible and meaningful information. Unfortunately, the versatility inherent to polymers often results in a frequent and

significant use of resources for methods development. Even after a decade of HT development and utilization, there is no hard and fast rule to what and how much of a benefit HT will have in research activities. However, it is safe to say with more in-house experience and less deviation from the original intent of the tool, the benefits should come faster. By in-house experience, we mean not only the personnel with the knowledge and the ability to repair, operate and build HT tools, but also the scientists with the knowledge and understanding of the science to ask the right questions, develop the right experiments, and have the ability to extract the knowledge from the data.

REFERENCES

1. Wikipedia, http://en.wikipedia.org/wiki/High-throughput_screening (accessed June 16, 2008).
2. Symyx, www.Symyx.com, San Jose, CA.
3. Instron, www.Instron.com, Norwood, MA.
4. ChemSpeed, <http://www.chemspeed.com/index.php> (accessed June 16, 2008).
5. Potyrailo, RA, Karim, A, Wang, Q, and Chikyow, T. 2004. *Combinatorial and Artificial Intelligence in Materials Science*. Warrendale, PA: Materials Research Society.
6. Davis, RD, Bur, AJ, and McBrearty, M et al. 2004. Dielectric spectroscopy during extrusion processing of polymer nanocomposites: A high throughput screening/characterization method to measure layered, silicate content and exfoliation, *Polymer*, 45, 6487–6493.
7. National Institute of Science and Technology, Building and Fire Research Laboratory website, <http://www.bfrl.nist.gov/861/obm.html> (accessed June 16, 2008).
8. ChemSpeed, http://www.chemspeed.com/index.php?path=markets_products/static&detailpage=26 (accessed June 16, 2008).
9. Symyx, <http://www.symyx.com/page.php?id=114> (accessed October 6, 2008).
10. Thermal Analysis Instruments, <http://www.tainstruments.com/product.aspx?id=9&n=1&siteid=11> (accessed June 16, 2008).
11. Instron, <http://www.instron.us/wa/resourcecenter/literature/usiminas.aspx> (accessed June 16, 2008).
12. Meredith, JC, Karim, A, and Amis, EJ. 2002. Combinatorial methods for investigations in polymer science, *MRS Bull.*, 27(4), 330–335.
13. Chigwada, G, Panchatapa, J, Jiang, DD, and Wilkie, C. 2005. Fire retardancy of vinyl ester nanocomposites: Synergy with phosphorous-based fire retardants, *Polym. Degradation Stab.*, 89(1), 85–100.
14. Chigwada, G and Wilkie, C. 2003. Synergy between conventional phosphorus fire retardants and organically-modified clays can lead to fire retardancy of styrenics, *Polym. Degradation Stab.*, 81(3), 551–557.
15. Wilkie, C, Chigwada, G, Gilman, JW, and Lyon, RE. 2006. High throughput techniques for the evaluation of fire retardancy, *J. Mater. Chem.*, 16, 2023–2030.
16. Zamarano, M. 2007. Thermoset fire retardant nanocomposites. In *Flame Retardant Polymer Nanocomposites*, Eds. A. Morgan and C. Wilkie, New York: John Wiley & Sons.
17. Conveney, PV, Evans, JR, and Whiting, A. Novel Clay-Polymer Nanocomposites Using Diversity-Discovery Methods: Synthesis, Processing, and Testing, Exclaim Poster, London, U.K. 2005. http://www.exclaim.org.uk/Posters/EPSCR_TD_10Jun05.pdf (accessed October 9, 2008).
18. Standard test method for determining flammability characteristics of plastics and other solid materials using microscale combustion calorimetry, ASTM D 7309-07, American Society for Testing and Materials (International), West Conshohocken, PA, 2007.
19. Van Krevelen, DW. 1997. *Properties of Polymers: Their Correlation with Chemical Structure; Their Numerical Estimation and Prediction from Additive Group Contributions*, 3rd edn. Amsterdam, The Netherlands: Elsevier.
20. Walters, RN and Lyon, RE. 2003. Molar group contributions to polymer flammability, *J. Appl. Polym. Sci.*, 87, 548–563.
21. United States Code of Federal Regulations. 2007. Title 14: *Aeronautics and Space*, Volume 1, Chapter I: Federal Aviation Administration, Parts 1–49.
22. Aircraft Material Fire Test Handbook. 2000. Federal Aviation Administration, Report DOT/FAA/AR-00/12, April.
23. RADEL R-700 TR, 2004. Product Data Sheet, Solvay Advanced Polymers, Alpharetta, GA.
24. Lyon, RE and Emerick, T. 2008. Non-halogen fire resistant plastics for aircraft interiors, *Polym. Adv. Technol.*, 19, 609–619.

25. Di, J, Davis, G, and Jackson, J et al. 2007. New transparent copolycarbonate compositions with low OSU heat release values, *Society of Plastics Engineers Annual Technical Conference, ANTEC 2007*, Cincinnati, OH.
26. Takemori, M, Sinha, M, and Jackson, K. 2007. Group contribution method to predict the flame resistance of polycarbonates, *5th Triennial International Aircraft Fire and Cabin Safety Research Conference*, Atlantic City, NJ.
27. Lyon, RE, Walters, RN, and Stoliarov, SI. 2007. Thermal analysis of flammability, *J. Therm. Anal. Calorimetry*, 89(2), 441–448.
28. Lyon, RE, Safronava, N, and Walters, RN. 2008. A statistical model for the flammability of plastics, *19th Annual BCC Research Conference on Recent Advances in Flame Retardancy of Polymeric Materials*, Stamford, CT, June 9–11.
29. Kroschwitz, JI. 1991. *High Performance Polymers and Composites*. New York: John Wiley & Sons.
30. Drysdale, DD. 1995. Fundamental fire properties of combustable materials. In *Improved Fire and Smoke Resistant Materials for Commercial Aircraft Interiors: A Proceedings*, Washington, DC: National Academy Press, pp. 37–44.
31. Lyon, RE. 2003. Ignition resistance of plastics, *SAMPE 2003 Proceedings*, Covina, CA, pp. 1452–1458.
32. Morgan, AB, Bundy, M, and Ohlemiller, T. 2007. Cone calorimetry analysis of UL-94 V-Rated plastics, *Fire Mater.*, 31, 257–283.
33. Panagiotou, J and Quintiere, JG. 2004. Generalizing flammability of materials. *Interflam 2004, 10th International Fire Science & Engineering Conference*, ed. S. Grayson. Greenwich, U.K.: Interscience Communications Ltd., pp. 895–905.
34. Cloisite 15A, Southern Clay Products, Gonzales, TX.
35. Babrauskas, V and Peacock, R. 1992. Heat release rate: The single most important variable in fire hazard, *Fire Saf. J.*, 18, 255.
36. Gilman, JW, Davis, RD, and Shields, JR et al. 2004. Development of high throughput methods for flammability property characterization, *SAMPE Proceedings*, Long Beach Convention Center Long Beach, CA, May 18–20.
37. Quintiere, JG. 1995. Chapter 14. Surface flame spread, *SFPE Handbook of Fire Protection Engineering*, 2nd edn. Boston, MA: NFPA.
38. ASTM E1321 08, *Standard Test Method for Determining Material Ignition and Flame Spread Properties*, Fire and Flammability Standards, 2008.
39. Brocchini, S, James, K, Tangpasuthadol, V, and Kohn, J. 1997. A combinatorial approach for polymer design, *J. Am. Chem. Soc.*, 119, 4553.
40. Meredith, JC, Karim, A, and Amis, E. 2000. High-throughput measurement of polymer blend phase behavior, *Macromol.*, 33(16), 5760–5762.
41. Smith, AP, Douglas, JF, and Meredith, C et al. 2001. High-throughput characterization of pattern formation in symmetric diblock copolymer films, *J. Polym. Sci.: Part B: Polym. Phys.*, 39, 2141.
42. Karim, A, Yurekli, K, and Meredith, C et al. 2002. Combinatorial methods for polymer materials science: Phase behavior of nanocomposite blend films, *Polym. Eng. Sci.*, 42, 1836.
43. Petro, M, Safir, A, and Nielsen, RB et al. 2001. U.S. Patent 6,260,407.
44. Meredith, JC, Karim, A, and Amis, E. 2002. Combinatorial methods for investigations in polymer materials science, *MRS Bull.*, 27, 330.
45. Eidelman, N and Simon, CG. 2004. Characterization of Combinatorial polymer blend composition gradients by FTIR microspectroscopy, *J. Res. Natl. Inst. Stand. Technol.*, 109(2), 219–231.
46. Gilman, J, Davis, R, and Montgomery, C. 2004. High throughput screening methods for military aircraft topcoat cure accelerator, *2004 Coatings Project Final Report*, <http://fire.nist.gov/bfrlpubs/>

17 Fire Toxicity and Its Assessment

Anna A. Stec and T. Richard Hull

CONTENTS

17.1	Introduction.....	453
17.2	Toxic Components of Fire Effluents	454
17.2.1	Asphyxiant Gases	455
17.2.1.1	Carbon Monoxide.....	455
17.2.1.2	Hydrogen Cyanide.....	455
17.2.2	Irritant Gases	455
17.2.2.1	Hydrogen Halides.....	456
17.2.2.2	Nitrogen Oxides	456
17.2.2.3	Organoirritants	457
17.2.2.4	Particulates	457
17.2.3	Effect of Toxicants on Different Species	459
17.2.4	Estimation of Fire Effluent Toxicity from Chemical Composition Data.....	460
17.2.5	Fire Conditions on Fire Toxicity.....	462
17.3	Assessment of Fire Toxicity.....	465
17.3.1	General Requirements for Bench-Scale Generation of Fire Effluents.....	466
17.3.2	Open Tests.....	466
17.3.3	Closed Chamber Tests	467
17.3.3.1	Tests Based on the NBS Smoke Chamber ISO 5659-2.....	467
17.3.4	Flow-Through Tests	468
17.3.4.1	Simple Tube Furnace Flow-Through Test	468
17.3.4.2	Steady-State Tube Furnace Methods.....	469
17.3.4.3	Fire Propagation Apparatus	470
17.3.5	Correlation of Different Bench-Scale Test Data.....	470
17.3.6	Correlation of Bench- and Large-Scale Test Data.....	472
17.4	Conclusions	473
	References.....	474

17.1 INTRODUCTION

The importance of the toxic effects of fire effluents has been rapidly increasing over the last 5 years. This chapter describes the types and effects of toxic effluents that fires produce, and the different methods that exist to assess fire toxicity, using animal exposure studies, laboratory scale, and large-scale generation of fire effluents, followed by a discussion on how different materials and fire conditions influence the generation of toxic products.

The majority of fire deaths result from the inhalation of toxic gases. The asphyxiant gases, carbon monoxide and hydrogen cyanide, have yields that vary considerably with fire conditions, and this has proved difficult to replicate on a laboratory scale. In addition, fire gases contain respiratory irritants, which inhibit breathing, causing flooding of the lungs. Coupled with the visual obscuration

of smoke, the effects of irritants on the eyes and lungs can prevent escape, although the cause of death is almost always ascribed to asphyxiant gases, usually to carbon monoxide.

Recently, two significant developments have raised the profile of fire toxicity. The first is the development of the steady-state tube furnace (SSTF) (ISO TS 19700:2006), which has been shown to replicate the toxic product yields corresponding to the individual stages of fires. The second is the acceptance of performance-based fire design as an alternative to prescriptive fire regulations, so that architects can specify the components within a building based on a safe escape time, within which toxic and irritant gas concentrations must not approach a lethal level (ISO 13571:2007).

17.2 TOXIC COMPONENTS OF FIRE EFFLUENTS

Fire gases contain a mixture of fully oxidized products, such as carbon dioxide (CO₂), partially oxidized products, such as carbon monoxide (CO) and aldehydes, fuel and fuel degradation products, such as aliphatic or aromatic hydrocarbons, and other stable gas molecules, such as hydrogen halides (HCl, HBr), and hydrogen cyanide (HCN).¹ The toxic hazards associated with fire and the inability of victims to escape from fire atmospheres is often considered in terms of major hazard factors: heat, smoke, and toxic combustion products.² Heat, smoke, and irritant gases may impair escape, and sometimes lung damage causes death in those managing to escape.

The main combustion products are divided into two classes: asphyxiant gases, which prevent oxygen uptake by cells, with loss of consciousness and ultimately death, and irritant gases, which cause immediate incapacitation, mainly by their effects on the eyes and upper respiratory tract, and longer-term damage deeper in the lung. The effect of asphyxiants and deep lung irritants depends on the accumulated doses, the sum of each of the concentrations multiplied by the exposure time, for each product; upper respiratory tract irritants are believed to depend on the concentration alone.³ The most common toxic components of fire effluent are presented in Table 17.1. The specification of gases to be determined in particular standard tests is somewhat arbitrary, and may not adequately define the effluent toxicity.⁴ There is also the potential for species to be present in the fire gas, which have not been well characterized in terms of chemical structure or toxicity and would be difficult to identify or to assess their toxic hazards, although the existence of important acute toxicants, which have yet to be characterized is less likely than for toxicants with longer-term or delayed effects.

Carbon dioxide content in fresh air varies 300–600 ppm, depending on location, and is almost always present at higher levels in fire gases. Inhalation of carbon dioxide stimulates respiration rate, tidal volume, and causes acidosis (an increase in the acidity of the blood). The result is an increase in inhalation of oxygen and toxic gases produced by the fire. It has moderate toxicity, in its own right, exposure to a 50,000 ppm (5%) concentration for 30-min produces signs of intoxication; above 70,000 ppm unconsciousness results in a few minutes.

Oxygen depletion, also a feature of fire gases, can be lethal once oxygen concentration has fallen below tenable levels (~6%). However, from a fire toxicity perspective it is generally assumed that

TABLE 17.1
List of Main Asphyxiant and Irritant Gases

Asphyxiant Gases	Irritant Gases	Other Components Which Should Be Monitored
Carbon monoxide (CO); hydrogen cyanide (HCN)	Hydrogen fluoride (HF); hydrogen chloride (HCl); hydrogen bromide (HBr); nitrogen dioxide (NO ₂); sulfur dioxide (SO ₂); organo-irritants	Oxygen (O ₂); carbon dioxide (CO ₂)

Source: ISO-TR 9122-1:1989, *Toxicity of Combustion Products-Part 1*.

heat and other gases will have already prevented survival, while other toxicants such as CO or HCN, will be present in lethal quantities further from the fire where oxygen depletion would not be considered harmful. However, oxygen depletion and high levels of CO₂ and CO would result from oxidative pyrolysis of biofuels in an enclosed storage facility, endangering people entering the enclosure.

17.2.1 ASPHYXIANT GASES

Narcotic gases or asphyxiants cause a decrease in oxygen supplied to body tissue, resulting in central nervous system depression, with loss of consciousness and ultimately death. The severity of the effects increases with increasing dose.² The main asphyxiants, carbon monoxide and hydrogen cyanide, have been widely studied and are the best understood.⁵

17.2.1.1 Carbon Monoxide

The toxic effect of carbon monoxide is characterized by a lowered oxygen-delivery capacity of the blood, even when a partial pressure of oxygen and the rate of blood flow rate are normal. Carbon monoxide binds to the hemoglobin in red blood cells resulting in the formation of carboxyhemoglobin (COHb), with stability constant 200 times greater than that of oxyhemoglobin, impeding the transport of oxygen from lungs to the body. This causes deterioration in mental and muscular performance. CO also combines with myoglobin in the muscle cells, impairing diffusion of oxygen to cardiac and skeletal muscles.⁶ Carbon monoxide has a cumulative effect, from which the body takes time to recover. About 50% of blood carbon monoxide is eliminated in the first hour, while complete elimination takes from several hours to a few days. When inhaled, CO impairs an individual's ability to escape by decreasing the amount of oxygen, causing different effects at different concentrations of carbon monoxide (COHb) in the blood. At CO levels of 10 ppm for short periods, impairment of judgment and visual perception occur; exposure to 100 ppm causes dizziness, headache, and weariness; loss of consciousness occurs at 250 ppm; inhalation of 1000 ppm results in rapid death. Chronic long-term exposures to low levels of carbon monoxide are suspected of causing disorders of the respiratory system and the heart.⁷

17.2.1.2 Hydrogen Cyanide

Hydrogen cyanide is approximately 25 times more toxic than carbon monoxide through the formation of the cyanide ion formed by hydrolysis in the blood.² Unlike carbon monoxide, which remains primarily in the blood, the cyanide ion is distributed throughout the extracellular fluid of tissues and organs.⁵ Two mechanisms have been identified for the toxic effects of cyanide. The first is by combination with the ferric ion in mitochondrial cytochrome oxidase, preventing electron transport in the cytochrome system and inhibiting the use of oxygen by the cells. The second results in a brief stimulation, followed by severe depression, of respiratory frequency, accompanied by convulsions, respiratory arrest, and death.⁸ HCN also causes rapid incapacitation, preventing escape, and then, with CO, contributes to death from asphyxiation. One analysis of fire death data showed a recent decline in COHb and a rise in blood cyanide levels,⁹ probably because of the increased use of nitrogen-containing synthetic polymers. The uptake, distribution, metabolism, and excretion of cyanide is much more complex than for CO, and thus there is no simple and robust method for quantifying CN⁻ in fire victims. Therefore, the contribution of HCN to fire deaths is difficult to assess, and sometimes analysis for CN⁻ takes place only when lethal concentrations of CO are absent.

17.2.2 IRRITANT GASES

In contrast to the well-defined effects of asphyxiant toxicants, the effects of exposure to irritants are much more complex. Incapacitating irritants and smoke can cause death indirectly by preventing escape from fire. Most irritant fire effluents produce signs and symptoms of both sensory and upper

respiratory tract irritation, and of pulmonary irritation. However, in postmortem analysis these are similar to the effects of heat exposure. Sensory and upper respiratory tract irritation stimulates the trigeminal and vagus nerve receptors in the eyes, nose, throat, and upper respiratory tract causing discomfort, then severe pain. The central nervous system's response to acidic and organic irritant gases in mice is to inhibit breathing, causing the respiration rate to fall to 10% of its normal value, while in primates and humans the same stimulus results in hyperventilation. The effects range from tears and reflex blinking of the eyes, pain in the nose, throat and chest, breath-holding, coughing, excessive secretion mucus, to bronchoconstriction, and laryngeal spasms.⁶ At sufficiently high concentrations, or when attached to submicron particles, such as soot, most irritants can penetrate deeper into the lungs, causing pulmonary irritation effects, which may cause postexposure respiratory distress and death, generally occurring from a few hours to several days after exposure, due to pulmonary edema (flooding of the lungs).⁵

17.2.2.1 Hydrogen Halides

Hydrogen chloride (HCl) and hydrogen bromide (HBr) are strong acids that dissociate entirely in water. Both may be present in fire gas, for example from polyvinyl chloride (PVC) or brominated flame retardants, and since the damage caused by the acidity is independent of the anion (Cl^- or Br^-). The current discussion focuses on HCl, it is also applicable to HBr.

Hydrogen chloride (HCl) is an acid gas, which causes severe irritant effects at low concentrations (around 100 ppm) but only results in death at very high concentrations (in mice 2600 ppm, and in rats 4700 ppm for 30 min exposures¹⁰). The difficulty in quantifying a threshold level for incapacitation, and the high levels of HCl evolved during decomposition of certain materials has led to a long-running controversy over the maximum atmospheric concentrations of HCl in fire gas, from which escape is still possible.

There is only one report of human exposure to HCl gas at concentrations relevant to fires,¹¹ which found that humans could tolerate exposure to 10 ppm HCl, while at 70 and 100 ppm humans had to leave the room because of intense irritation, coughing, and chest pains, indicating that 100 ppm is intolerably irritating to humans. That data has led to the guidelines¹² that the maximum concentration tolerable for 1 h is between 50 and 100 ppm, and that 1000–2000 ppm is dangerous for even short exposures. These guidelines were corroborated using an animal model that correctly predicted intolerable irritation levels for humans for other inorganic gases such as sulfur dioxide, ammonia, chlorine, and a wide variety of organic chemicals, including formaldehyde, acrolein, etc.,^{13,14} indicating that 300 ppm would be intolerable to humans.¹⁵

Table 17.2 summarizes the expected effects of HCl on humans¹⁶ showing that concentrations of 50–100 ppm are barely tolerable for exposures up to an hour, while exposure to concentrations of 1000 ppm of HCl are dangerous, causing pulmonary edema after just a few minutes of exposure.

The physical manifestations of the action of HCl in rats, based on the observations during one study,¹⁷ seems to be primarily that of the mechanical blockage of the upper airways caused by the extreme inflammatory and corrosive action of a strong mineral acid on these tissues. Postmortem examination indicated almost a total destruction from the nasal passage to the pharynx, but surprisingly a little damage to airways below the trachea. Amongst obligatory nose-breathers, the lower sensitivity of rats than mice to HCl has been ascribed to the differences in their nasal passages. When a tube was used to bypass these passages, the response of rats occurred at similar concentrations to those of mice.¹⁸ This has led to the suggestion that species that breathe through their mouth (such as humans, especially in the stressful situation of escaping from a fire) may be more sensitive to the effects of HCl than obligate nose-breathers, such as rodents.¹⁶ In summary, a small amount of HCl causes incapacitation, preventing escape, but a much larger quantity is required to cause death directly.

17.2.2.2 Nitrogen Oxides

Nitric oxide (NO) and nitrogen dioxide (NO_2) are nonflammable gases present in fire effluents. At high concentrations, nitric oxide is rapidly oxidized in air to form nitrogen dioxide; however, at

TABLE 17.2
Inhalation Exposure of Humans to Hydrogen Chloride

Approximate Concentration (ppm)	Exposure Time	Effect	Reference
1–5		Limit of detection by odor	
≥5	Unspecified	Immediately irritating	[75]
>10	Occupational	Highly irritating, although workers develop some tolerance	[75]
10	Prolonged	Maximum tolerable	[12]
10–50	A few hours	Maximum tolerable	[12]
35	Short	Throat irritation	[12]
50–100	1 h	Maximum tolerable	[12]
1000–2000	Short	Dangerous	[12]

Source: National Research Council of the National Academies, Hydrogen chloride: Acute exposure guideline levels, *Acute Exposure Guideline Levels for Selected Airborne Chemicals*, Vol. 4, The National Academies Press, Washington, DC, 2004, 79.

the concentrations found in fire gases, most of the nitric oxide remains unchanged. Nitrogen dioxide dissolves rapidly in water to form nitric and nitrous acid. At high concentrations these acids can cause pulmonary edema and death.^{19,20} However, low concentrations of nitric oxide gas have been used to aid breathing in the treatment of respiratory disorders.²¹ In the blood, it combines with oxy-hemoglobin to form methemoglobin, between 5 and 20 times faster than oxygen and the resulting compound breaks down slowly,¹⁹ giving effects similar to hypoxia; it forms nitrates; if the blood oxygen is low it can combine with hemoglobin to form nitrosohemoglobin. Excessive levels of nitric oxide in blood have been shown to cause low blood pressure. However, it has been reported that tobacco smoke can contain up to 1000 ppm of nitric oxide, but this does not cause death.^{19,22}

17.2.2.3 Organoirritants

Large numbers of known irritant chemicals have been found to occur in fire atmospheres.^{23,24} The irritant chemicals released in fires are formed during the pyrolysis and partial oxidation of materials, and the combinations of products from different materials are often remarkably similar.²⁴ However, for all organic materials and particularly for simple hydrocarbon polymers such as polypropylene or polyethylene, the main pyrolysis products, which consist of various hydrocarbon fragments, are innocuous.⁶ Thus when polypropylene is pyrolyzed in nitrogen the product such as ethylene, ethane, propene, cyclopropane, formaldehyde, butane, acetaldehyde, toluene, styrene, etc., are produced,⁶ and such an atmosphere was found to have no effect upon primates.^{23,25} However, when these products are oxidized during nonflaming decomposition in air, some are converted to highly irritant products, and such atmospheres were indeed found to be highly irritant to both mice and primates. In reports of mouse exposure experiments, some fire retardant materials, which could be induced to flame only intermittently, with considerable smoke production, were found to produce atmospheres up to 300 times more irritant than the same polymer in its nonfire retardant state, which burned cleanly.²⁶ Table 17.3 shows some of more toxic, commonly encountered organic species in fire gas, with the concentration considered Immediately Dangerous to Health or Life (IDLH) (NIOSH).²⁷

17.2.2.4 Particulates

Death in fire may be caused either by gases, which are directly toxic or, which cause such irritation that they impair vision and breathing, preventing escape, or by smoke, which not only impairs

TABLE 17.3
Common Organoirritants Found
in Fire Gas with IDLH Values

Substance	IDLH Value (ppm)
Acetaldehyde	2000
Acrolein	2
Carbon monoxide	1200
Benzene	500
Crotonaldehyde	50
Formaldehyde	20
Phenol	250
Toluene	500

Source: Blomqvist, P. et al., *Fire Mater.*, 31(8), 495, 2007.

escape ability by visible obscuration, but also contains particulate matter, which is sufficiently small to pose a respiratory hazard. In spite of large amounts of particulates generated in a fire, relatively few investigations have been made on the particles (size, distribution, and composition) from such fires.²⁸

The particle size distribution is dependent on the tested material, and temperature and fire conditions. The particle size of the spherical droplets from smoldering combustion is generally of the order of $1\ \mu\text{m}$, while the size of the irregular soot particulates from flaming combustion is often larger but much harder to determine and dependent on measuring technique and sampling position. The hazard areas for humans as a function of particle size are presented in Figure 17.1.

The general effect of particulates is to cause fluid release and inflammation, preventing gas exchange. Inflammation of the terminal bronchioles can result in complete blockage. Edema fluid

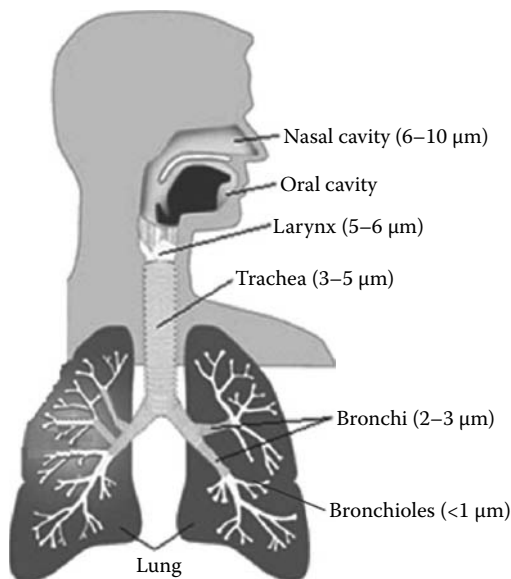


FIGURE 17.1 Particle deposition in the respiratory system.

disrupts the dispersion of the lung surfactant, causing collapse of the alveolae from higher surface tension of the fluid. The smallest particles ($<0.5\ \mu\text{m}$) penetrate into the lung interstitium (between the alveolar surface the blood capillaries), where they have been shown to be particularly dangerous, causing interstitial and luminal edema. They can also transcend the air/blood barrier and enter the blood stream, triggering dangerous immune responses from the white blood cells, including polymer fume fever and increased platelet stickiness leading to heart attacks. Particulates, and other irritants can change lung efficiency expressed as compliance (how easily the lung opens in response to pressure reduction or how much stiffer the lung tissue is becoming) and resistance (how easily air flows in and out of the lung or how much the airways are becoming blocked or flooded). Passage of oxygen through the blood/gas barrier can only occur in the absence of fluid in the lungs.²⁹

In addition, the particulates can act as vehicles for transport of noxious molecules deep into the lungs. Some work has been reported on HCl, estimating that over an exposure time of 1 h, about 2 mg of HCl would be deposited deep in the lungs by soot.⁶

17.2.3 EFFECT OF TOXICANTS ON DIFFERENT SPECIES

There are a number of published papers presenting an estimation of toxic products by using animals as indicators of the toxicity.^{1,20,30} Mice, rodents, or primates are exposed to pure gas mixtures or fire gases to determine an incapacitation or lethality. However, there is no direct relationship between these data and the limits for humans. Some data indicates that the mechanism of toxicity of some gases is the same in rodents and humans. For other gases, the response is known to be different.⁶ Some literature suggests that the use of mice may not be reliable because of their very fast respiration rate and narrow airways. Differences between species such as respiratory rate and volume may produce different relative results in toxicity tests. A paper by Hartzell et al.³⁰ suggest that when considering acute lethal effects, primates may resist about 1.3 times greater concentrations of HCl and HCN than rats, whereas rats resist about 1.6 times greater concentrations of CO. Nitric oxide also has different effects on different species. Exposure of rats to 1500 ppm for 15 min and to 1000 ppm for 30 min, and of lambs to 80 ppm for 60–180 min does not cause adverse effects, but the exposure of rabbits to 5 ppm for 14 days causes interstitial edema. It is necessary to understand the accuracy and uncertainties of animal testing methods for fire hazard assessment. Table 17.4 presents and compares lethal toxic potencies of the most common fire effluents for different animal species,³⁰ showing considerable variation between species.

The effect of fire effluents on human life cannot be measured directly for legal and ethical reasons. It may be estimated from the effect on animals either directly, using animal exposure, or indirectly from tables of concentrations leading to a particular effect (such as the limit below that causing irreparable damage, death, or incapacitation of 50% of the population, etc.). In each case, the data rely on the untested assumption that effects on animal subjects (usually rats) may be simply

TABLE 17.4
Comparison of LC₅₀ (30 min Exposure)
for Different Animals

Chemical Agent	Mice	Rats	Primates
CO (ppm)	3500	5300–6600	2500–4000
HCN (ppm)	165	110–200	170–230
HCl (ppm)	2600	3800	5000
Low oxygen (%)	6.7	7.5	6–7

Source: Esposito, F.M. and Alarie, Y., *J. Fire Sci.*, 6, 195, 1988.

extrapolated to humans. For example, it has been reported²⁰ that rat data cannot be extrapolated to baboon data when irritant gases are the principal toxicants.

17.2.4 ESTIMATION OF FIRE EFFLUENT TOXICITY FROM CHEMICAL COMPOSITION DATA

Exposure to toxic fire effluents can lead to a combination of physiological and behavioral effects of which physical incapacitation, loss of motor coordination, disorientation are only a few. Furthermore, survivors of a fire may experience postexposure effects, complications, and burn injuries, leading to death or long-term impairment. The major effects, such as incapacitation or death, may be predicted using existing rat lethality data, as described in ISO 13344³¹ or more recently, based on the best available estimates of human toxicity thresholds as described in ISO 13571,⁵ by quantifying the fire effluents in different fire conditions in small-scale tests, using only chemical analysis, without animal exposure.

The general approach in generating toxic potency data from chemical analysis is to assume additive behavior of individual toxicants, and to express the concentration of each toxicant as its fraction of the lethal concentration for 50% of the population for a 30 min exposure (LC_{50}). Thus an fractional effective dose (FED) equal to one indicates that the sum of concentrations of individual species will be lethal to 50% of the population over a 30 min exposure. Two equations have been developed for the estimation of the FED for lethality from the chemical composition of the environment in the physical fire model. Each begins with the precept that the fractional lethal doses of most gases are additive, as developed by Tsuchiya and Sumi.³²

$$FED = \frac{m[CO]}{[CO_2] - b} + \frac{21 - [O_2]}{21 - LC_{50,O_2}} + \frac{[HCN]}{LC_{50,HCN}} + \frac{[HCl]}{LC_{50,HCl}} + \frac{[HBr]}{LC_{50,HBr}} + \dots \quad (17.1)$$

Both equations have been taken from ISO 13344³¹ and use LC_{50} values for lethality to provide reference data for the individual gases to calculate toxic potency, based on rats exposed for 30 min. The N-Gas model in Equation 17.1 assumes that only the effect of the main toxicant CO is enhanced by the increase in respiration rate caused by high CO_2 concentrations (expressed as a step function with one value of m and b for CO_2 concentrations below and another for those above 5%).

The Purser model, presented in Equation 17.2, uses V_{CO_2} a multiplication factor for CO_2 driven by hyperventilation, therefore, increasing the FED contribution from all the toxic species, and incorporates an acidosis factor A to account for toxicity of CO_2 in its own right.³¹

$$FED = \left\{ \frac{[CO]}{LC_{50,CO}} + \frac{[HCN]}{LC_{50,HCN}} + \frac{[AGI]}{LC_{50,AGI}} + \frac{[OI]}{LC_{50,OI}} + \dots \right\} \times V_{CO_2} + A + \frac{21 - [O_2]}{21 - 5.4} \quad (17.2)$$

$$V_{CO_2} = 1 + \frac{\exp(0.14[CO_2]) - 1}{2}$$

where

[AGI] is the concentration of acid gas irritants

[OI] is the concentration of organic irritants

A is an acidosis factor equal to $[CO_2] \times 0.05$

Both of these equations only relate to lethality, or *cause of death*. However, many people fail to escape from fires because of the incapacitating effect of smoke (obscuring visibility) and its irritant components, which cause pain, preventing breathing, or *reason for death*. ISO 13571⁵ considers the four major hazards from fire, which may prevent escape (toxic gases, irritant gases, heat, and smoke obscuration). It includes a calculation for predicting the incapacitation of humans exposed to fire effluents, indicating, in a nonnormative appendix, that the effects of heat, smoke, and toxicants

may be estimated independently. Equations 17.2 and 17.3 have been taken from ISO 13571. They calculate the FED of asphyxiants, CO and HCN, and the fractional effective concentration (FEC) of sensory irritants in the fire effluent that limit escape. Equation 17.2 represents the generally accepted case that there are only two significant asphyxiant fire gases –CO and HCN. The FED value is calculated using the exposed dose relationship (concentration–time product, $C \cdot t$) for CO. The lethal $C \cdot t$ product corresponds to the incapacitating dose ($C \cdot t$) for CO of $35,000 \mu\text{L L}^{-1} \text{ min}$, equal to around 1170 ppm for 30 min exposure) and an exponential relationship for HCN (because asphyxiation by HCN exposure does not fit a linear relationship).

$$\text{FED} = \sum_{t_1}^{t_2} \frac{[\text{CO}]}{35,000} \Delta t + \sum_{t_1}^{t_2} \frac{\exp([\text{HCN}] / 43)}{220} \Delta t \quad (17.3)$$

$$\begin{aligned} \text{FEC} = & \frac{[\text{HCl}]}{\text{IC}_{50,\text{HCl}}} + \frac{[\text{HBr}]}{\text{IC}_{50,\text{HBr}}} + \frac{[\text{HF}]}{\text{IC}_{50,\text{HF}}} + \frac{[\text{SO}_2]}{\text{IC}_{50,\text{SO}_2}} + \frac{[\text{NO}_2]}{\text{IC}_{50,\text{NO}_2}} + \frac{[\text{acrolein}]}{\text{IC}_{50,\text{acrolein}}} \\ & + \frac{[\text{formaldehyde}]}{\text{IC}_{50,\text{formaldehyde}}} + \sum \frac{[\text{irritant}]}{\text{IC}_{50,\text{irritant}}} \end{aligned} \quad (17.4)$$

Equation 17.4 uses a similar principle to Equation 17.1 to estimate the combined effect of all irritant gases.

The additive model is almost certainly an over simplification, because the effects occur in different organs (lungs, muscles, brain, etc.), although it is as likely to be an overestimate as an underestimate. However, more controversy surrounds the toxic potency values used in these models (Tables 17.4 and 17.5). These range from direct application of rat lethality data for single gas exposures to humans, to estimates made by committees of experts.⁵ Data exist to show that both simplifications are unjustified.^{33,34} There are several gases where the additive methodology is known to be wrong. For example, at CO_2 concentrations of 5% (common in diluted fire effluents), the respiratory volume per minute (RMV) increases by a factor of 3 increasing the dose of fire gas inhaled. Purser's model addresses this by applying a correction factor (itself a function of CO_2 concentration) to all the individual toxicant ratios, not just CO.⁶ However, ~50 ppm nitric oxide (usually present in fire gas) opens up the airways, allows improved respiration, but also greater exposure to other toxicants. HCN initially increases the respiration rate, and then severely suppresses it; irritant gases such as HCl suppress it by a factor of around 10 in stationary rats and mice.³⁵ There is also growing evidence that other chemical species present in fire gas (such as particulates and isocyanates), which are not normally included in these predictions of fire gas toxicity, can be some of, or even the most toxicologically significant species. However, while the FED and FEC values are valid relative to one another, the dilution factor of 1 g/50 L (or whatever) is arbitrary.

TABLE 17.5
Toxic Gas Concentrations Leading to Death (ISO 13344)
and Incapacitation Impairing Escape (ISO 13571)

	Concentration Giving FED = 1 Using ISO 13344 (ppm)	Concentration Giving FEC/FED = 1 Using ISO 13571 (ppm)
CO	5700	1170
HCN	165	100
HCl	3800	1000
NO_2	170	250

17.2.5 FIRE CONDITIONS ON FIRE TOXICITY

Fire gases result from the pyrolysis, oxidative pyrolysis, and flaming combustion of organic materials, and can comprise a complex mixture of many different compounds. The temperature and oxygen concentration vary significantly during a fire and between different fires, and as a consequence the gases produced in different stages of a fire may vary significantly. ISO have identified a number of different fire stages. Whereas some real-life fires may be represented by a single fire stage, other fires may pass through several different stages.³⁶

The graph (Figure 17.2) illustrates a fire starting with a slow induction period, but once ignition is reached it grows very quickly until limited either by the access of oxygen or by the availability of the fuel.

The product yields are particularly dependent upon the composition of the polymeric material, the temperature, and the ventilation conditions. Once the temperature of the surface is raised sufficiently (generally to around 300°C), then a process of thermal decomposition by oxidative pyrolysis begins. The products of nonflaming decomposition tend to be rich in partly decomposed organic molecules (many of which are irritants), carbon monoxide, and smoke particulates. This scenario presents a particular hazard to a sleeping subject in a small enclosure such as a closed bedroom, which can reach a lethal dose over a number of hours.⁶

A useful concept in characterizing or predicting the gas-phase flaming combustion conditions, and the yields of products and hydrocarbons, is the equivalence ratio (ϕ), presented in Equation 17.5. If the amount of oxygen balances the amount of fuel exactly, then the conditions are said to be stoichiometric, and the equivalence ratio equal to 1. In the early stages of fire, the equivalence ratio may be lower, when there is more than the stoichiometric amount of air available, and the conditions are well-ventilated, whereas in the later stages of a fire, when there is not enough air available and the conditions are under-ventilated, the equivalence ratio will be greater than 1. Toxic product yields have been shown to be highly dependent upon the fuel/oxygen ratio,³⁷ and this approach has led to a better understanding of the factors affecting fire toxicity.

$$\phi = \frac{\text{Actual fuel / air ratio}}{\text{Stoichiometric fuel / air ratio}} \quad (17.5)$$

After ignition, fire development may occur in different ways, depending on the environmental conditions as well as on the arrangement of fuel. An early well-ventilated flaming fire is characterized

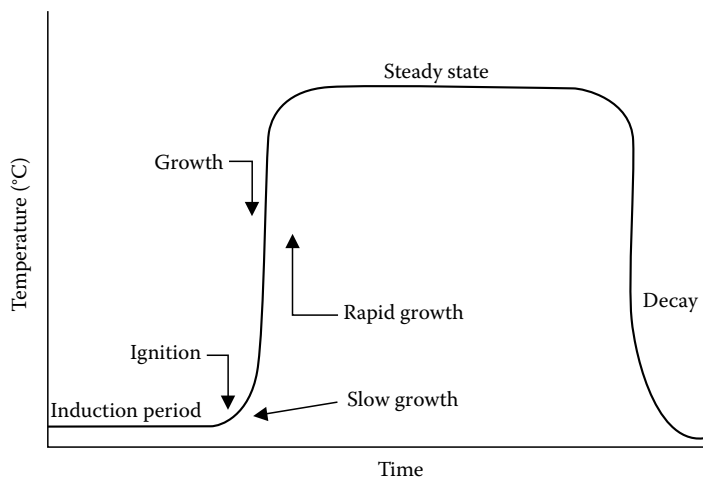


FIGURE 17.2 Schematic fire growth curve.

by an equivalence ratio less than unity, and during the early stages is likely to be less than 0.5. This means that there is always more than enough oxygen mixed with the fuel gases.

High yields of smoke, toxins, and irritants are generated at temperatures around 600°C as the fire stage changes to under-ventilated flaming in an enclosure fire. A room occupant is exposed to a highly toxic effluent mixture capable of causing incapacitation and death from asphyxiation within a few minutes. They will also suffer from exposure to heat, with a possibility of burns.

The final category of flaming fire scenario in enclosures is the postflashover under-ventilated flaming fire.⁶ Flashover can occur when the upper-layer temperature is sufficiently high (around 800°C or above) to cause ignition of combustible materials. The effluent plume is similar in composition to that of a preflashover under-ventilated fire, fuel-rich (ϕ between 1.5 and 5) combustion conditions, with very low oxygen concentrations, and high concentrations of asphyxiant gases (CO, HCN), organic irritants, and smoke particles. Since the temperatures are higher and the conditions somewhat more extreme, the yields of toxic products may be somewhat higher than for preflashover under-ventilated fires. The heat release rate, and therefore the rate of effluent production, is very high. Postflashover fires are therefore extremely hazardous, because a large amount of hot toxic effluent plume material can rapidly fill extensive building spaces remote from the seat of the fire.⁶ In the United Kingdom, and probably across Europe, where rooms and buildings tend to be smaller with less open layouts, most fire deaths (70% in 2006 in the United Kingdom) result from small fires when the victim is in the room of fire origin. Conversely, in the United States, only 21% of fire deaths occur in the room of origin of the fire, and 67% occur on another floor.³⁸ Thus, in the United Kingdom, flashover fires are not the major cause of fire fatalities, whereas in the United States it is believed that 80% of fire deaths could be avoided if flashover could be prevented.

The classification of different fire stages shows that fire hazards, and particularly the toxic hazards, depend upon the combustion conditions. In buildings, the majority of fires that are hazardous to life are likely to involve under-ventilated flaming, either pre- or postflashover. Since in the United Kingdom the majority of injuries and deaths from fire occur in domestic dwellings (77%), most deaths can be attributed to preflashover under-ventilated combustion. However, the greatest numbers of deaths from single fire disasters will almost always be attributable to post-flashover conditions.

Fire effluent toxic potency is a function of the material and the fire conditions, and also the fire environment (enclosure, geometry, and ventilation). To assess the fire hazard, toxic potency data must be relevant to the likelihood of particular end-use fire situations. Such fires will develop through stages that have been defined by ISO.³⁶ The ISO fire stages, from nonflaming to well-ventilated flaming to under-ventilated flaming, have been characterized in terms of heat flux, temperature, oxygen availability, CO/CO₂ ratio, equivalence ratio ϕ , and combustion efficiency. Details of this classification are given in Table 17.6.

To see how the predicted toxicity varies for different polymers and fire conditions,³⁹ the FED (calculated using ISO 13344³¹) is compared with the FED and FEC calculated using ISO 13571.⁵

Toxicities are expressed as the effluent generated from burning 1 g of material in 200 L of air, based on an established standard.⁴⁰ Organoirritants in the fire effluent (measured as the difference in CO₂ before and after passing over the secondary oxidizer) were considered collectively using an organic yield of 10 mg L⁻¹ to result in incapacitation, as described by Purser.⁶

The contribution to the FED and FEC from each of the principal fire gas toxicants was determined for different polymers, using the SSTF (described later). Figures 17.3 and 17.4 show a comparison of the fire hazard expressed as FED for lethality, estimated using the methodology presented in ISO 13344 (based on rat lethality data) compared with the FED for incapacitation from ISO 13571, which omits hypoxia, but includes a separate estimate of incapacitation (FEC) and lethality (FED), for low density of polyethylene (LDPE), polystyrene (PS), unplasticized PVC, and polyamide (PA) 6.6. For well-ventilated conditions, this shows a generally low toxicity of products, with the exception of unplasticized PVC, which has a high yield of HCl resulting from the chain stripping of PVC, and of CO resulting from the inhibition of the oxidation of CO by the HCl. This shows the greater

TABLE 17.6
ISO Classification of Fire Stages, Based on ISO TS 19706

Fire Stage	Heat (kW m ⁻²)	Max Temp (°C)		Oxygen (%)		Equivalence Ratio φ	$\frac{V_{CO}}{V_{CO_2}}$	Combustion Efficiency (%)
		Fuel	Smoke	In	Out			
Nonflaming								
1a. Self-sustained smoldering	n.a.	450–800	25–85	20	0–20	—	0.1–1	50–90
1b. Oxidative, external radiation	—	300–600		20	20	<1		
1c. Anaerobic external radiation	—	100–500		0	0	>>1		
Well-ventilated flaming								
2. Well-ventilated flaming	0–60	350–650	50–500	~20	0–20	<1	<0.05	>95
Under-ventilated flaming								
3a. Low vent. room fire	0–30	300–600	50–500	15–20	5–10	>1	0.2–0.4	70–80
3b. Postflashover	50–150	350–650	>600	<15	<5	>1	0.1–0.4	70–90

Source: Robinson, J.E. et al., in *Proceedings of the 11th International Conference, Interflam*, London, U.K., 2007.

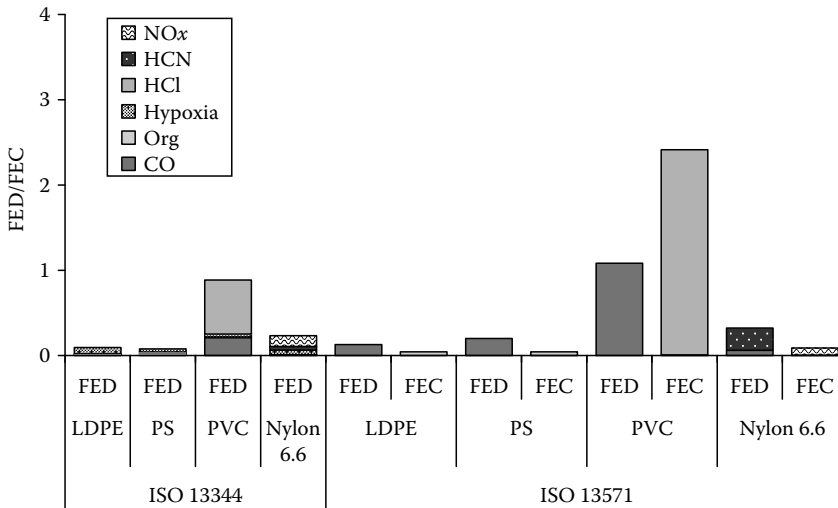


FIGURE 17.3 FED and FEC contribution for well-ventilated conditions from the principal fire gas toxicants determined in different polymers.

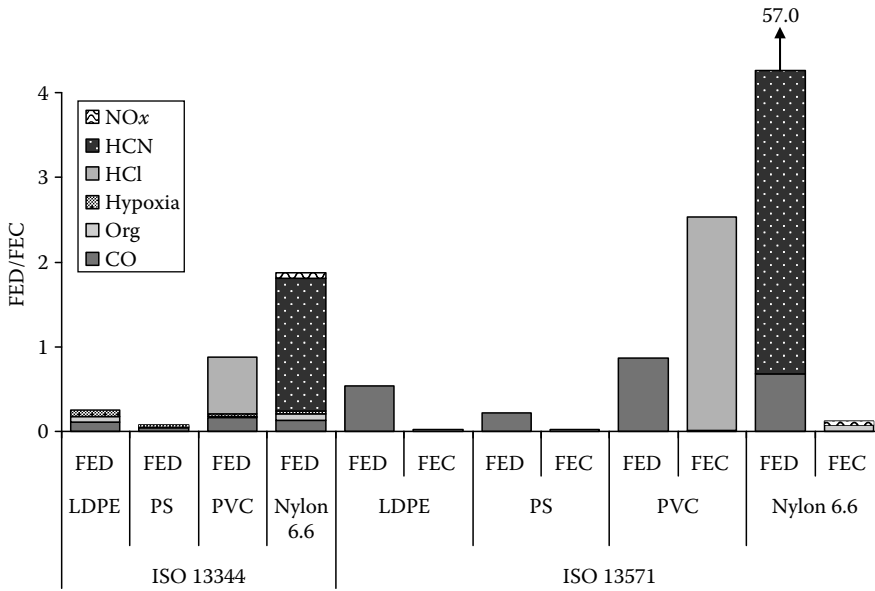


FIGURE 17.4 FED and FEC contribution for under-ventilated conditions from the principal fire gas toxicants determined in different polymers. (Adapted from Robinson, J.E. et al., *Proceedings of the 11th International Conference, Interflam*, London, U.K., 2007.)

toxicological significance of HCl over CO from unplasticized PVC, and the much greater effect of the HCl when incapacitation preventing escape, not actual death is used as the end point. It is notable that this large FEC is obtained even though the IC_{50} value of 1000 ppm HCl is rather higher than that considered intolerable.

In addition, when PA 6.6 is burned in under-ventilated conditions, there is a small but significant contribution from HCN, and its oxidation product NO_2 . The lower level for incapacitation rather than lethality of CO and HCN gives higher values for these two toxicants using ISO 13571.

Instead of normalizing the data to an arbitrary 1 g in 200 L, the fire toxicity of a material can be expressed as an LC_{50} , which in this case is the specimen mass M of a burning polymeric material, which would yield an FED equal to one within a volume of 1 m^3 . The relation to the FED from the N-Gas model is given in Equation 17.6.

$$LC_{50} = \frac{M}{FED \times V} \tag{17.6}$$

where V is the total volume of diluted fire effluent in m^3 at STP. The accuracy of LC_{50} values determined in this manner is quoted as $\pm 30\%$ if the concentrations of all the contributing toxicants are measured and included.^{41,42} Comparing the toxic potencies of different materials, the lower the LC_{50} (the smaller the amount of materials necessary to reach the toxic potency) the more toxic the material is. LC_{50} values should be referenced to the fire condition under which they were measured.

17.3 ASSESSMENT OF FIRE TOXICITY

Fire gas toxicity is an essential component of any fire hazard analysis. However, fire toxicity, like flammability, is both scenario and material dependent. Bench-scale assessment of fire gas toxicity either adopts an integrative approach, where the material is burnt in a fixed volume of air, allowing the initially well-ventilated fire condition to become under-ventilated to an unknown degree, or the ventilation is controlled, so that individual fire stages may be replicated.

The ideal small-scale method for assessing fire toxicity must allow the toxic product yields from each fire stage to be determined, allowing the assessment of each material under each fire condition. This appears to be the only way in which the complexities of full scale burning behavior can be realistically addressed on a bench scale.

17.3.1 GENERAL REQUIREMENTS FOR BENCH-SCALE GENERATION OF FIRE EFFLUENTS

Guidance on assessment of physical fire models has been published in ISO 16312-1,⁴³ and reviewed elsewhere.⁴⁴ In all fire smoke toxicity tests, specimens are decomposed by exposure to heat, resulting in “forced combustion” driven by an applied heat flux from a flame, radiant panel, etc. Some tests use a pilot flame or spark igniter to facilitate ignition, while others rely on self-ignition of the sample. When flaming combustion occurs, this will increase the radiant heat flux back to the sample, typically between 2 and 10 times. This will have two significant effects on the fire effluent. First, the existence of flames will help to drive the combustion process to completion, by increasing the temperature and hence the reaction rates, which will tend to reduce the toxicity of the fire effluent (favoring CO₂ over CO and organic molecules). Secondly, the higher heat flux will pyrolyze more material at a greater rate, increasing the amount of material in the vapor phase, and reducing the concentration of oxygen, both of which will increase the toxicity of the fire effluent. Unfortunately, these effects are so large that, rather than cancelling each other out they can result in very large differences in the toxic product yield between different fire toxicity tests. Clearly, the presence or absence of flaming combustion is critical to the interpretation of the results from combustion toxicity assessments. In some conditions, specimens will either pyrolyze or self-ignite, but the scatteredness of results will be very large if flaming combustion is inconsistent. Once flaming is established, combustion will drive itself to completion (and hence the toxicity will be reduced), provided there is sufficient oxygen, and the flame is not quenched. If the flame is cooled rapidly, e.g., by excessive ventilation or a cool surface, the yield of toxic products will increase. Ultimately the value of the bench-scale toxicity assessment is dependent on its ability to predict large-scale burning behavior, and therefore validation must involve a comparison with large-scale test data. Unfortunately most large-scale test data have been obtained under well-ventilated conditions, and when data from under-ventilated fire scenarios, such as the ISO 9705 Room test, are made available, the change of sample mass and the air flow to the fire during the test is not generally known. Of the standard methods used for toxicity assessment, there are three general types, well-ventilated or open methods, closed box tests, and tube furnaces.

17.3.2 OPEN TESTS

Most bench-scale fire tests, such as the cone calorimeter, are open, and run in well-ventilated conditions. They are generally unsuitable for the estimation of toxic product yields because the high degree of ventilation, coupled with the rapid quenching of fire gases, increased the yield of products of incomplete combustion through premature flame quenching, rather than through under-ventilation.⁴⁵ This cancellation of errors may, in some circumstances, give yields closer to those of real fires, but open tests are not a reliable means of assessing fire toxicity for anything other than well-ventilated conditions.

The fire zone of the standard cone calorimeter apparatus^{46,47} is well-ventilated but the apparatus has been modified for tests under oxygen-depleted conditions. Standardization of the controlled atmosphere cone calorimeter is currently under discussion within ISO. This uses an enclosure around the specimen and radiator, and a controlled input flow of nitrogen and air, but has met with limited success. In some tests, the effluent may continue to burn as it emerges from the chamber giving ultimately well-ventilated flaming. In others, under reduced oxygen concentrations, the fuel lifts from the surface, and ignition does not occur.⁴⁸ The CO yields in the open cone calorimeter have been found to correlate with an equivalence ratio of 0.7 for a range of cable sheathing materials.^{45,49} The relatively high dilution of fire gases in, and stainless steel construction of, the hood and duct, may lead to difficulties in detecting some effluent components. Fire gases pass through the center of conical heater, and then are quenched by the cold duct, which may affect their composition.

17.3.3 CLOSED CHAMBER TESTS

Closed cabinet tests and their operation may be likened to a small fire burning in a closed room. The specimen is decomposed by a heat source and the resulting effluent accumulates within the cabinet. The decomposition system is either mounted within the cabinet as in the aircraft⁵⁰ and maritime tests⁵¹ or may be outside, connected to the cabinet by a short duct, as in ASTM E 1678.⁵²

A direct consequence of the closed cabinet is that the fire effluent accumulates within the cabinet and the fire gas concentrations, therefore, increase as the specimen burns and the gases will change with oxygen depletion. For laminated or layered specimens, the effluent will also change as the flame burns through different layers. As the specimen decomposes, the hot effluent rises to the upper part of the chamber, where it may accumulate or circulate around the chamber due to natural convection. Thus, the product concentration will depend on where the gas samples are taken from, and the heat transfer from gas to the chamber walls altering the position of the smoke layer, which will recede away from cold walls. The smoke density values will be unaffected provided a vertical light path is used. Although mixing fans are used in some smoke density tests, they are rarely used in toxicity tests probably because of their influence on the burning behavior. Both the aircraft and maritime tests require the smoke to be sampled at specified times (although burning may have proceeded at different rates) from gas sampling probes in the geometric center of the cabinet.

If the effluent is stratified, the gas sample is obviously unrepresentative, but if it is uniformly distributed, then the gas flowing into the fire zone may be oxygen depleted and fire gases may be recycled through the fire zone. These latter effects will be greater with thicker specimens, which would be expected to generate more smoke, due to more complete consumption of oxygen and hence to under-ventilation.

Therefore, closed box tests give a complete product yield of burning from well-ventilated to under-ventilated conditions, but without giving any indication of how the yield varies with fire condition. They are not generally able to sustain flaming combustion in under-ventilated conditions, where the toxic hazard is usually the greatest. Another potential source of error may occur as the fire effluent is heated and excess pressure is released or stickier components within the effluent, such as hydrogen chloride are deposited onto the walls of the cabinet.

17.3.3.1 Tests Based on the NBS Smoke Chamber ISO 5659-2⁵³

The smoke chamber (Figure 17.5) is a well-established piece of equipment, designed to monitor only the smoke evolution from burning materials, to minimize visible obscuration of escape routes during a fire. Its widespread acceptance has led to its use in a number of industry-specific toxicity

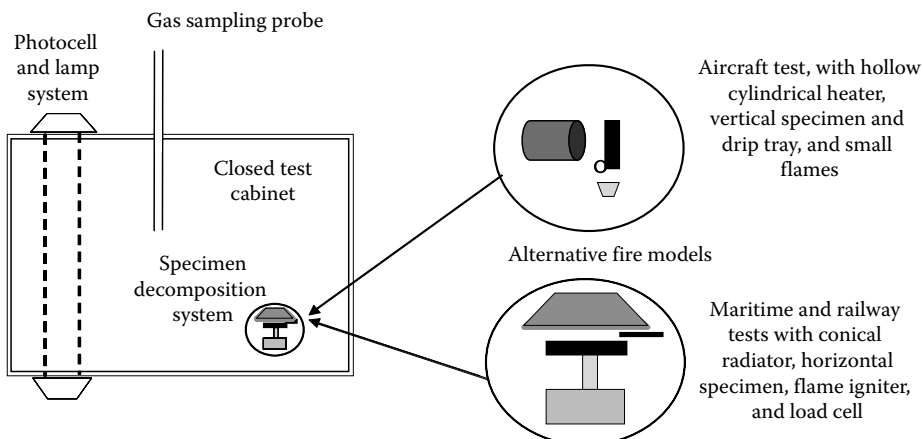


FIGURE 17.5 Diagram of fire smoke toxicity test based on NBS smoke chamber. (From Hull, T.R. and Paul, K.T., *Fire Saf. J.*, 42, 349, 2007. With permission.)

tests. The Aircraft test⁵⁰ (prEN 2824, 5 and 6) uses the vertical radiator and vertically mounted test specimen of ASTM E 662⁵⁴ and is specified for components for passenger aircraft cabins (Figure 17.5). Airbus ABD 3 and Boeing BSS 7239⁵⁰ use the same apparatus but specify different gas analysis methods. The IMO test⁵¹ is based on the ISO 5659-2 using a conical heater, with the sample mounted horizontally on a load cell, and is used to specify materials and products for large passenger ships and high speed surface craft. A reduced version of this test is used in the United Kingdom for railway vehicles⁵⁵ as BS 6853, B2. The European specification (EN TS 45545-2⁵⁶) uses the IMO toxicity test at 50 kW m⁻² without the pilot igniter and with FTIR analysis to determine the toxicity of railway vehicle components. In the aircraft test, flaming conditions are generated by a series of small flames along the base of the vertical specimen, but in other tests it occurs when specimens are ignited by a single pilot flame or self-ignite.

In all of these tests, the specimens, 75 mm square and up to 25 mm thick, are exposed to radiant heat with and without a pilot flame(s). Decomposition takes place inside a closed cabinet of 0.51 m³. There is no control of the air flow or oxygen concentration through the fire zone and the effluent is mixed by natural convection, as it accumulates within the closed cabinet. Gases are sampled using probes mounted in the center of the cabinet.

Flaming tests result in some oxygen depletion, which can vary with the thermal stability and thickness of the specimen and also decreases with increasing test duration. The flaming fire stage is difficult to assess but may be related to ISO stage 2, well-ventilated or stage 3a, small-ventilated. The IMO tests at 50 kW m⁻² could possibly represent stage 3b, postflashover flaming and may change from 2 to 3a or 3b during a test.

The advantages of these tests are that they use a widely available, standard smoke test apparatus, with the addition of simple gas sampling probes in the center of the cabinet and relatively simple gas analysis systems to determine the specified gases. The test specimen is heated from one side and the effects of surface protection layers can be determined. The principal limitations are that the air supply to the fire zone is not controlled, and testing can cause oxygen depletion, which will change the toxic product yield by an unknown amount, while effluent may be recycled through the fire zone. Alternatively, the effluent may stratify and gas samples may not be representative of the effluent generated. Specimens that drip in the aircraft test may give erroneous results, if the liquid falls to the tray or cabinet floor and is not burned.

17.3.4 FLOW-THROUGH TESTS

In these methods, the specimen is thermally decomposed with or without flaming in a furnace over flowing air, which drives the effluent to the gas determining or sampling systems.

17.3.4.1 Simple Tube Furnace Flow-Through Test

The NF X 70-100 method⁵⁷ (Figure 17.6) was developed to estimate the toxicity of materials and products used in railway vehicles, initially in France. This is a small-scale static tube furnace, in which the test specimen (typically 1 or 0.1 g for low density materials), is pushed, in a crucible, into the middle of the furnace tube and thermally decomposed, using furnace temperatures of 400°C, 600°C, and 800°C to represent smoldering, well-ventilated and under-ventilated conditions in flowing air at 2 L min⁻¹, where they may pyrolyze and autoignite. For most materials at a temperature of 400°C they will not ignite, so the condition is 1b, oxidative pyrolysis. At a temperature of 600°C, the rate of pyrolysis may be fairly slow, giving a well-ventilated fire condition, whereas at 800°C the fire condition may be closer to under-ventilated, as the rate of pyrolysis exceeds the stoichiometric air supply rate. The effluent is driven through gas detection systems, bags, or bubblers for subsequent analysis.

This method is easy to use, uses simple equipment with specified operating conditions of temperature and air flow. It is increasingly used for fire toxicity testing of materials used for railway vehicles and is also included in prEN45545-2. The lack of requirement for flaming to be observed

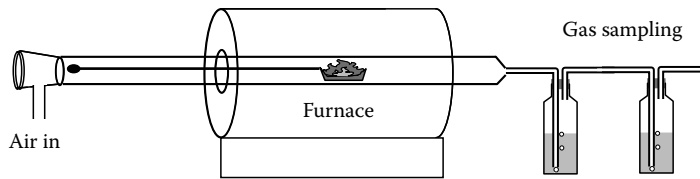


FIGURE 17.6 Schematic of NF X 70-100 test. (From Hull, T.R. and Paul, K.T., *Fire Saf. J.*, 42, 352, 2007. With permission.)

leaves the assignment of fire stage 2 to be assumed for most materials at 600°C and 3a or 3b for materials at 800°C. A practical limitation is the number of replicate test runs needed to obtain sufficient samples for complete gas analysis.

17.3.4.2 Steady-State Tube Furnace Methods

The SSTF ISO TS 19700⁵⁸ (also known as the Purser furnace) allows the possibility of controlling the fire conditions during burning. This forces combustion by feeding the sample into a furnace of increasing heat flux at a fixed rate, thus replicating each fire stage by steady-state burning. The results are intended to form part of the input to ISO 13344,³¹ ISO 13571,⁵ and fire risk assessments, which are specifically related to the ISO fire stages. The test uses the same apparatus as BS 7990⁵⁹ and IEC 60695-7-50 and -51⁶⁰ shown in Figure 17.7, with the air flow and temperature required to replicate each fire stage shown in Table 17.7. Alternatively, as a research tool, or to generate data for fire modeling, the yields can be determined at a fixed temperature as a function of the equivalence ratio ϕ .

Adjustment of temperature, air flow rate, or specimen introduction rate may be required to simulate a specified ISO fire stage. A strip specimen or pieces are spread in a silica boat over a length of 800 mm at a loading density of 25 mg mm⁻¹ and fed into a tube furnace at a rate of 1 g min⁻¹ with flowing air. Secondary air is added in a mixing chamber to give a total gas flow of 50 L min⁻¹ for analysis. The toxic potency of the effluent is assessed during the steady-state burn period.

This method enables the toxic potency of a material of unknown composition to be determined under known, steady-state fire conditions (temperature and equivalence ratio), which relate directly

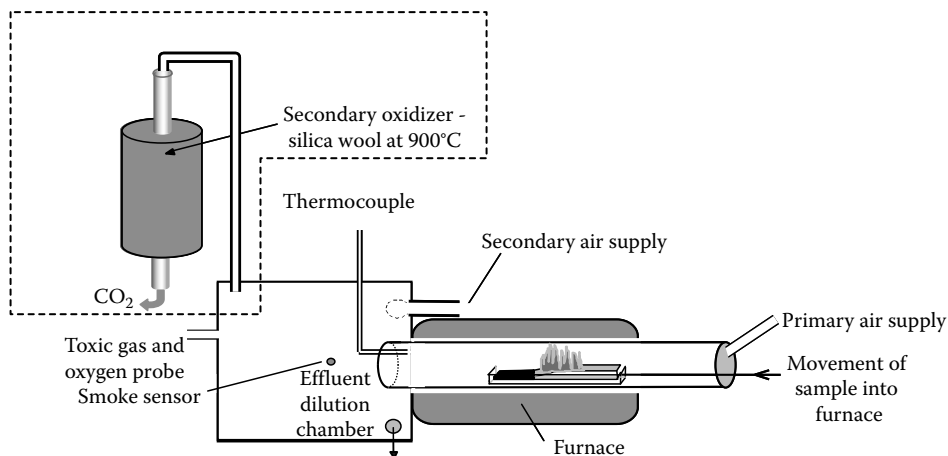


FIGURE 17.7 Diagram of apparatus of ISO TS 19700. The secondary oxidizer (inside dotted line) is for the determination of total hydrocarbons in the ISO standard. (From Hull, T.R. and Paul, K.T., *Fire Saf. J.*, 42, 353, 2007. With permission.)

TABLE 17.7
Furnace Conditions Corresponding to Characteristic Stages of Burning Behavior

Fire Type	Temperature (°C)	BS 7990 Primary Air Flow (L min ⁻¹)	ISO TS 19700 Primary Air Flow (L min ⁻¹)	IEC 60695-7-50 Primary Air Flow (L min ⁻¹)
1. Smoldering (nonflaming fires)	350	2	2	1.1
2. Well-ventilated flaming	650	10 ^a	10 ^a	22.6
3a. Small under-ventilated flaming fires	650	Twice stoichiometric fuel/air ratio	Twice stoichiometric fuel/air ratio	—
3b. Fully developed under-ventilated fires	825	Twice stoichiometric fuel/air ratio	Twice stoichiometric fuel/air ratio	2.7

^a Subject to verification of ventilation condition.

to the end use fire hazard. The use of a high secondary air flow usually ensures that all the required gas samples can be taken during a single run. Smoke obscuration may also be determined. Unlike the closed box methods that may give toxic product data for a continuum of fire stages, in this method a separate run is required for each fire stage. In addition to analysis of the gases specified in ISO 13344 (CO₂, CO, O₂, HCN, NO_x, HCl, HBr, HF, SO₂, acrolein, and formaldehyde), there is a requirement to determine the total hydrocarbons. This may be achieved by passing part of the air-diluted test effluent through a secondary combustion furnace to allow the determination of the products of incomplete combustion even for materials of unknown composition. The ISO TS 19700 protocol allows determination of the equivalence ratio required for different fire stages, even for materials of unknown composition and thus enables the toxic potency of a material to be determined under known, steady-state fire conditions (temperature and equivalence ratio), which relate directly to the end use fire hazard. Crucially, this method has been shown to replicate the toxic product yields from large-scale tests, see Section 17.3.6.

17.3.4.3 Fire Propagation Apparatus⁶¹

This method⁶¹ shown in Figure 17.8 is also suited to obtaining toxicity data since the ventilation condition is well controlled, and the heat flux can be varied to force burning in under-ventilated conditions. The yield data have been published as a function of equivalence ratio, and have been used to calculate FED and LC₅₀ values.^{62,63}

17.3.5 CORRELATION OF DIFFERENT BENCH-SCALE TEST DATA

The range of toxicity test methods is bound to produce different fire conditions, and hence different toxic product yields. Four test methods (NBS Smoke Chamber, NF X 70-100, Fire Propagation Apparatus [FPA], and SSTF) have been compared, primarily from published data^{64–66} using the carbon monoxide yields and hydrocarbon yields (not recorded in the NFX tests), which are both fairly good indicators of fire condition, for four materials (LDPE, PS, PVC, and Nylon 6.6), at two fire conditions, well-ventilated and under-ventilated. The CO and hydrocarbon yields are shown in Figures 17.9 and 17.10.

For LDPE, the FPA, and SSTF show significant differences between the low CO yields of well-ventilated burning and the higher yields of under-ventilated fires. The NBS smoke chamber shows only a slight difference between the well-ventilated and under-ventilated fire conditions, while the

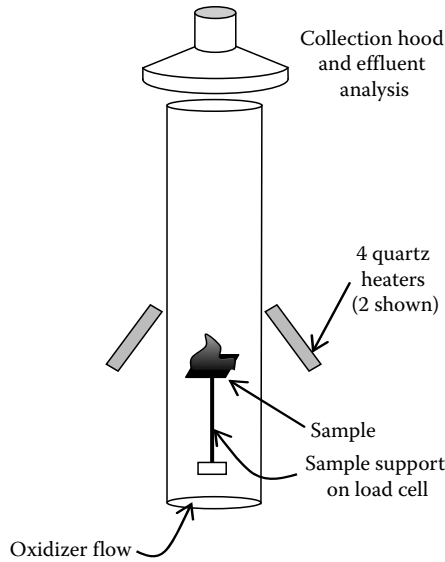


FIGURE 17.8 Fire propagation apparatus. (From Hull, T.R. and Paul, K.T., *Fire Saf. J.*, 42, 357, 2007. With permission.)

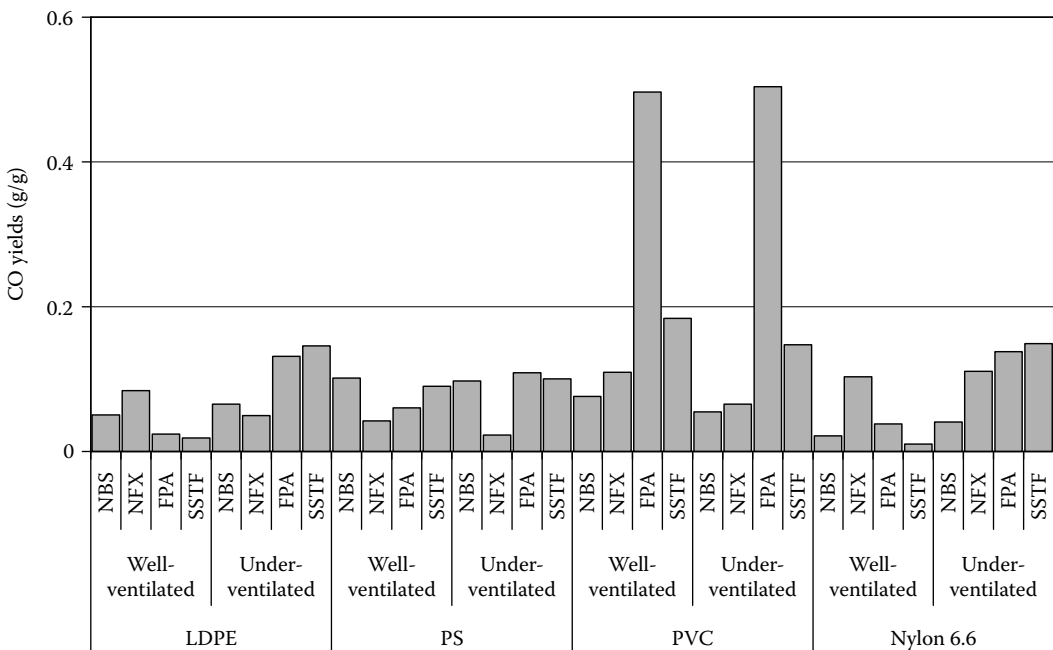


FIGURE 17.9 CO yields g/g for four polymers using four test methods at two fire conditions.

NFX 70-100 gives the anomalous result of a higher CO yield for well-ventilated flaming than for under-ventilated. Although hydrocarbons are not always included in a toxicity assessment, their presence is a good indicator of the fire condition. For LDPE, all the tests show a dramatic increase in hydrocarbon yields for under-ventilated combustion.

It has already been reported that the enhanced stability of the aromatic ring in the decomposition products of PS give higher CO yields in well-ventilated conditions and lower CO yields in

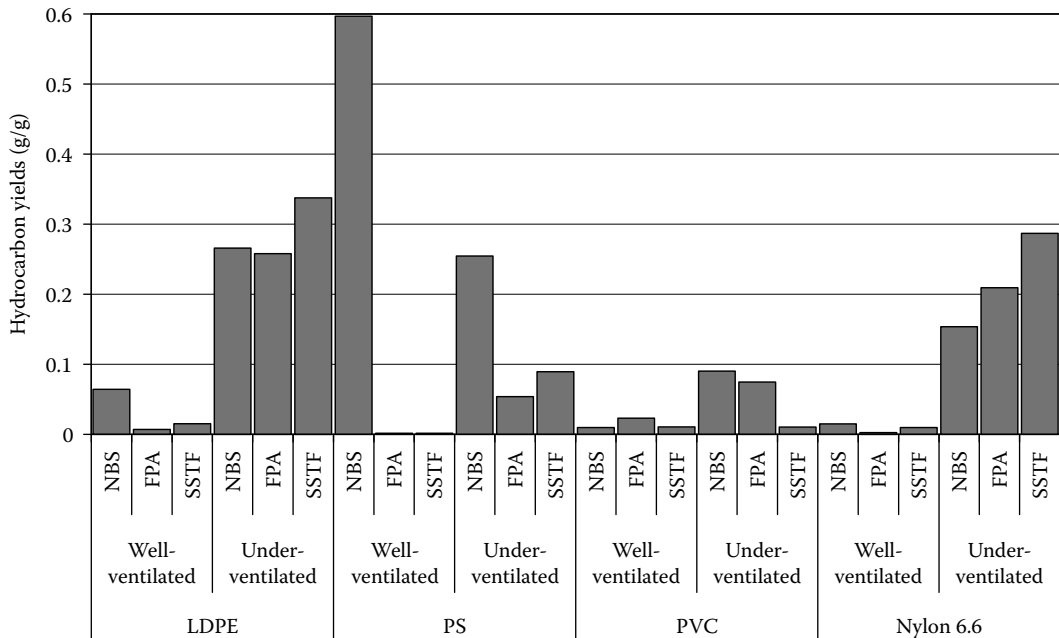


FIGURE 17.10 Hydrocarbon yields g/g for four polymers using four test methods at two fire conditions.

under-ventilated conditions than aliphatic polymers such as LDPE.⁶⁷ This trend is observed in the FPA, and in the SSTF, but the reverse trend is seen in the NBS smoke chamber, and more markedly in the NFX 70-100. The hydrocarbon yields show very large differences for PS, with over half of the polymer being pyrolyzed to hydrocarbons under well-ventilated conditions and about a quarter in under-ventilated conditions. Conversely, the FPA and SSTF show very low hydrocarbon yields under well-ventilated conditions, but high yields in under-ventilated conditions.

For PVC, there is little difference between the CO yields for the two fire conditions for most of the tests, although the FPA gives much higher, consistent yield, while the other three tests give a lower yield for under-ventilated flaming. For hydrocarbons, there are significant increases in yield between the well-ventilated and under-ventilated flaming conditions for the NBS and FPA methods, but not for the SSTF.

For PA 6.6 all the tests show an increase in CO yield from well-ventilated to under-ventilated, although the values vary from very low (NBS and SSTF) to fairly high (NFX 70-100) for well-ventilated conditions, while all tests except the NBS smoke chamber are able to replicate the higher CO yields of under-ventilated combustion consistently for PA 6.6. For hydrocarbons, a clear, consistent trend is observed between the low yields of well-ventilated combustion and the higher yields of under-ventilated combustion.

In summary, the FPA and the SSTF show consistent differentiation between well-ventilated and under-ventilated yields of CO and hydrocarbons for all materials (except for hydrocarbons from PVC in under-ventilated conditions). The NBS smoke chamber shows little differentiation between fire conditions, especially for CO yields, while the NF X 70-100 shows no consistency between fire conditions and yield for the materials reported here.

17.3.6 CORRELATION OF BENCH- AND LARGE-SCALE TEST DATA

The validity of a bench-scale study of fire behavior is dependent on how it translates to the real scale. In general, real scale fires (both laboratory tests and unwanted fires) are poorly defined, and exhibit high sensitivity to a number of uncontrolled variables.

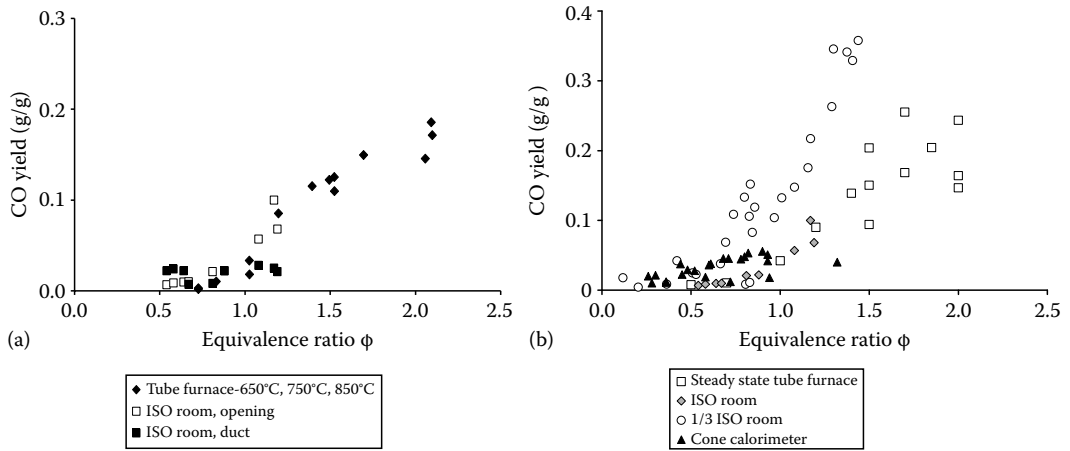


FIGURE 17.11 Comparison of CO yields as a function of equivalence ratio ϕ for polypropylene and PA 6.6 tested in the SSTF and the large-scale ISO room (a) and for nylon 6.6 tested in the $1/3$ ISO room and controlled atmosphere cone calorimeter (b).

Full- and large-scale tests have demonstrated that toxic product yields are highly dependent on the combustion conditions. Fire stages and types can be characterized either in terms of CO/CO₂ ratio, or preferably in terms of equivalence ratio, which provide reasonably good predictive metrics for product yields.

Few studies have reported correlations between bench- and large-scale test data, and most of these have used the SSTF.^{68–70}

Comparison of the yields of carbon monoxide from burning polypropylene (Figure 17.11a) and PA 6.6 (Figure 17.11b) show a strong dependence on equivalence ratio and consistency between bench- and large-scale.⁷¹ Figure 17.11b also includes data from the controlled atmosphere calorimeter, showing a failure to replicate the higher CO yields associated with under-ventilated fires. Both figures show much greater CO yields for under-ventilated burning, with a higher degree of scatter in those data points.

The large-scale test data (from the ISO room corner test) show very good agreement with the SSTF data. It is notable that the controlled atmosphere cone shows higher CO yields in well-ventilated conditions and, crucially, lower CO yields in under-ventilated conditions. It has been reported⁷² that correction can be applied to the calculation of equivalence ratio from the controlled atmosphere cone.

17.4 CONCLUSIONS

Fire toxicity, the largest cause of death in fires, is becoming better understood and tools now exist to assess those hazards. The effect of incapacitation on fire victims, rather than outright lethality, has generally been underplayed as the ultimate reason for the fire death, although witness accounts of fires frequently describe intolerable fumes. To a large extent, this is because of the reliability and simplicity of ascribing a COHb level >50% to death by carbon monoxide poisoning. While it is entirely appropriate that forensic fire investigations need to establish that a victim was breathing at the time of the fire, it is wrong to assume that CO is the only, or indeed the major hazard, in all fire effluent.

The methods for estimation of FED and FEC allow materials developers to assess their products, and if the fire toxicity is likely to be high, to see which species are to blame and take remedial action. Since incapacitation in a fire will result in a fire death in the same way as lethality (unless the incapacitated victim is fortunate enough to be rescued) it is more appropriate to use the incapacitation methodology of ISO 13571 than the rat lethality methodology of ISO 13344.

There are a large number of different methods used for bench-scale assessment of combustion toxicity, and the applicability of test data to fire hazard assessment is not always clear. Obviously, toxic potency data should not be used in isolation but should either be a part of a classification scheme or as part of the input to fire risk and fire safety engineering assessments. It is important that uncertainty or confidence limits should be used with toxic potency data, because they are often relatively large. Fire effluent toxic potency does not have a unique value but is a function of the material and the fire conditions, particularly temperature and oxygen availability in the fire zone, and also the fire environment (enclosure, geometry, and ventilation). To assess the fire hazard, toxic potency data must be relevant to the end use fire situation, and the fire condition, which can be defined using the ISO classification of fire stages.

Globalization of trade and relaxation of national barriers drive the need for international harmonization of toxicity testing. ISO specifications and standards provide a common basis on which the toxic potency has to be determined. A number of standard fire smoke toxicity tests are available and it is important to consider their relevance and limitations before selecting a method. Some of these tests do not appear to represent any fire stage; some represent several fire stages separately; others represent the progress of a fire through an indeterminate number of stages. Further, some test methods produce data, which is a function of both the flammability of the specimen and the yield of toxic products, while others provide toxic product yield data, which is independent of the burning behavior. Finally, chemical methods of assessment provide a breakdown of the concentrations of individual toxicants, from which toxic potencies can be calculated, while the earlier animal-based assays only give an overall estimate of the toxic potency of the fire smoke. Although it has been argued that animal-based methods are more likely to identify any new unusually high toxic potency products, provided the human and test animal responses are similar, it should be noted that there have only been two such instances^{23,73,74} in the last three decades, and neither would be expected to be significant in a real fire.

The general trend has shifted from standard tests, which includes precise details of apparatus, procedure, method of assessment, and specification of results, to more recent approaches, which define the apparatus and procedure necessary to obtain data relevant to end use fire situations. The later requires the involvement of suitably qualified personnel to define the necessary test conditions, effluent analyses, and to interpret results to ensure they are relevant to the end-use application.

The SSTF (Purser furnace) has shown itself to be an excellent tool for generation of reliable data for different materials and fire conditions, for use in robust fire hazard assessments.

REFERENCES

1. H.L. Kaplan, A.F. Grand, and G.E. Hartzell, Toxicity and the smoke problem, *Fire Safety Journal*, 7(1), 11–23, 1984.
2. G. Hartzell, Overview of combustion toxicology, *Toxicology*, 115(1), 7–23, 1996.
3. D. Purser, The application of exposure concentration and dose to evaluation of the effects of irritants as components of fire hazard, *Interflam Conference*, Interscience Publications, London, U.K., 2007.
4. ISO-TR 9122-1:1989, *Toxicity of Combustion Products: Part 1:General*.
5. ISO 13571:2007, *Life-threatening components of fire-Guidelines for the estimation of time available for escape using fire data*.
6. D.A. Purser, Toxicity assessment of combustion products, *SFPE Handbook of Fire Protection Engineering*, 3rd Edition, National Fire Protection Association, Quincy, MA, pp. 2–83, 2002.
7. S. Manahan, *Environmental Chemistry*, 6th Edition, CRC Press, Boca Raton, FL, 1994.
8. Y. Alarie, Toxicity of fire smoke, *Critical Reviews in Toxicology*, 32(4), 259, 2002.
9. R.A. Anderson, A.A. Watson, and W.A. Harland, Fire deaths in the Glasgow area. II. The role of carbon monoxide, *Medicine Science and the Law*, 21, 60–66, 1981; Fire deaths in the Glasgow area. III. The role of hydrogen cyanide, *Medicine Science and the Law*, 22, 35–40, 1982.
10. K.L. Darmer, E.R. Kinkead, and L.C. DiPasquale, Acute toxicity in rats and mice exposed to hydrogen chloride gas and aerosols, *American Industrial Hygiene Association Journal*, 35(10), 623–631, 1974.
11. L. Matt, *Beitrag Fur Lehre Von Der Entwicklung Giftiger Gase Auf Den Menschen*, Doctoral Dissertation, Universitat Wurzburg, 1889.

12. Y. Henderson and H.W. Haggard, *Noxious Gases and the Principles of Respiration Influencing Their Action*, Reinhold Publishing, New York, 1943.
13. L.E. Kane, C.S. Barrow, and Y. Alarie, A short-term test to predict acceptable levels of exposure to airborne sensory irritants, *American Industrial Hygiene Association Journal*, 40, 207–229, 1979.
14. Y. Alarie, G.D. Nielsen, and M. Schaper, Animal bioassays for evaluation of indoor air quality. In: *Indoor Air Quality Handbook*. Spengler, J.D., Samet, J.M., and McCarthy, J.F. Eds. McGraw-Hill, New York, p. 23.1, 2000.
15. C.S. Barrow, Y. Alarie, J.C. Warrick, and M.F. Stock, Comparison of the sensory irritant response in mice to chlorine and hydrogen chloride, *Archives of Environmental Health*, 32(2), 68–76, 1977.
16. National Research Council of the National Academies, Hydrogen Chloride: Acute Exposure Guideline Levels, *Acute Exposure Guideline Levels for Selected Airborne Chemicals*, Vol. 4, The National Academies Press, Washington, DC, p. 79, 2004.
17. C. Crane, D. Sanders, B. Endecott, and J. Abbott, *Times to Incapacitation and Death for Rats Exposed Continuously to Atmospheric Hydrogen Chloride Gas*, Inhalation Toxicology, part 4, Federal Aviation Administration, Civil Aeromedical Institute, Report Number FAA-AM-85-4, May 1985.
18. D.M. Stavert, D.C. Archuleta, M.J. Behr, and B.E. Lehnert, Relative acute toxicities of hydrogen fluoride, hydrogen chloride, and hydrogen bromide in nose- and pseudo-mouth-breathing rats, *Fundamental and Applied Toxicology*, 16, 636–655, 1991.
19. K.T. Paul, T.R. Hull, K. Lebek, and A.A. Stec, Fire smoke toxicity: The effect of nitrogen oxides, *Fire Safety Journal*, 43, 243–251, 2008.
20. H.L. Kaplan, Effects of irritant gases on avoidance/escape performance and respiratory response of the baboon, *Toxicology*, 47, 165–179, 1987.
21. B.P. Kavanagh and R.G. Pearl, Inhaled nitric oxide in anesthesia and critical care medicine, *International Anesthesiology Clinics*, 33(1), 181–210, 1995.
22. P. Blomqvist, Private Communication, SP Swedish National Testing and Research Institute, Boras, Sweden, 2008.
23. D.A. Purser and W.D. Woolley, Biological studies of combustion atmospheres, *Journal Fire Science*, 1, 118–144, 1983.
24. W.D. Woolley and P.J. Fardell, Basic aspects of combustion toxicology, *Fire Safety Journal*, 5, 29–48, 1982.
25. D.A. Purser and P. Buckley, Lung irritation and inflammation during and after exposures to thermal decomposition products from polymeric materials, *Medicine Science and the Law*, 23(2), 142–150, 1983.
26. D.A. Purser, Unpublished Data, 1984.
27. NTIS Publication No. PB-94-195047: *Documentation for Immediately Dangerous to Life or Health Concentrations (IDLH): NIOSH Chemical Listing and Documentation of Revised IDLH Values (as of 3/1/95)*, 1995.
28. P. Blomqvist, T. Hertzberg, H. Tuovinen, K. Arrhenius, and L. Rosell, Detailed determination of smoke gas contents using a small-scale controlled equivalence ratio tube furnace method, *Fire and Materials*, 31(8), 495–521, 2007.
29. T. Hertzberg and P. Blomqvist, Particles from fires—A screening of common materials found in buildings, *Fire and Materials*, 27, 295–314, 2003.
30. G.E. Hartzell, A.F. Grand, and W.G. Switzer, In: *Fire and Polymers Hazards, Identification and Prevention*, Nelson, G.L. (Ed.) ACS Symposium Series, American Chemical Society, Washington, DC, 1990.
31. ISO 13344:1996 *Estimation of lethal toxic potency of fire effluents*.
32. Y. Tsuchiya and K. Sumi, Evaluation of the toxicity of combustion products, *Journal of Fire and Flammability*, 3, 46–50, 1972.
33. F.M. Esposito and Y. Alarie, Inhalation toxicity of carbon monoxide and hydrogen cyanide gases released during the thermal decomposition of polymers, *Journal of Fire Sciences*, 6, 195–242, 1988.
34. B.C. Levin, New research avenues in toxicology: 7-gas N-gas model, toxicant suppressants, and genetic toxicology, *Toxicology*, 115, 89–106, 1996.
35. T.R. Hull, A.A. Stec, and K.T. Paul, Hydrogen chloride in fires, *Fire Safety Science—Proceedings of the 9th International Symposium*, held in Karlsruhe, Germany, International Association of Fire Safety Science, London, 2008, 665–676.
36. ISO TS 19706:2004 *Guidelines for assessing the fire threat to people*.
37. W.M. Pitts, The global equivalence ratio concept and the formation mechanisms of carbon monoxide in enclosure fires, *Progress in Energy and Combustion Science*, 21, 197–268, 1995.
38. *Fire Protection Handbook*, National Fire Protection Association, Quincy, MA, 1997.
39. J.E. Robinson, T.R. Hull, K. Lebek, A.A. Stec, E.R. Galea, A. Mahalingam, F. Jia, M.K. Patel, H. Persson, and T. Journeaux, *Proceedings of the 11th International Conference, Interflam*, London, U.K., 2007.

40. BS 6853:1999 *Code of Practice for Fire Precautions in the Design and Construction of Passenger Carrying Trains*.
41. BS 7899-1:1997 *Code of practice for assessment of hazard to life and health from fire. General guidance*.
42. BS 7899-2:1999 *Assessment of hazard to life and health from fire—Part 2*.
43. ISO 16312-1:2006 *Guidance for assessing the validity of physical fire models for obtaining fire effluent toxicity data for fire hazard and risk assessment—Part 1: Criteria*.
44. T.R. Hull and K.T. Paul, Bench-scale assessment of combustion toxicity—A critical analysis of current protocols, *Fire Safety Journal*, 42, 340–365, 2007.
45. B. Schartel and T.R. Hull, Development of fire-retarded materials: Interpretation of cone calorimeter data, *Fire and Materials*, 31, 327–354, 2007.
46. ISO 5660-1:1993 *Fire tests—Reaction to fire—Part 1: Rate of heat release from building products (cone calorimeter method)*.
47. ISO 5660-2: 2002 *Reaction-to-fire tests—Heat release, smoke production and mass loss rate—Part 2: Smoke production rate (dynamic measurement)*.
48. M.R. Christy, R.V. Petrella, and J.J. Penkala, *Controlled-Atmosphere Cone Calorimeter*, *Fire and Polymers II*, ACS Symposium Series 599, Washington, DC, 1995.
49. T.R. Hull, C.L. Wills, T. Artingstall, D. Price, and G.J. Milnes, In: *Fire Retardancy of Polymers New Application of Mineral Fillers*, Le Bras, M., Wilkie, C.A., Bourbigot, S., Duquesne, S., and Jama, C. (Eds.) Royal Society of Chemistry, Cambridge, U.K., 2005.
50. prEN 2824 (Aerospace Series) *Burning behaviour, determination of smoke density and gas components in the smoke of materials under the influence of radiating heat and flames—Test equipment apparatus and media*; prEN2825—*Determination of smoke density*; prEN 2826—*Determination of gas concentrations in the smoke*; ABD 0031 *Fire-Smoke-Toxicity (FST) Test Specification (Airbus Industries)*; Boeing BSS 7239 *Test method for toxic gas generation by materials on combustion*.
51. IMO MSC.41(64) *Interim standard for measuring smoke and toxic products of combustion*, *International Maritime Organisation*.
52. ASTM E1678 *Standard method for measuring smoke toxicity for use in fire hazard analysis*.
53. ISO 5659-2 *Plastics—Smoke Generation—Part 2, Determination of Specific Optical Density*.
54. ASTM E 662 *Test for Specific Optical Density of Smoke Generated by Solid Materials*.
55. BS 6853 *Code of Practice for fire precautions in the design and construction of passenger carrying trains, Annex B*.
56. EN TS 45545-2:2008 *Railway applications—Fire protection on railway vehicles—Part 2: Requirements for fire behaviour of materials and components—Annex D Testing procedure for analysis of toxic gases*.
57. NFX 70-100 *Analysis of pyrolysis and combustion gases. Tube furnace method. Part 1, Methods of analysis of gas generated by thermal degradation. Part 2, Method of thermal degradation using tube furnace*.
58. ISO TS 19700:2006 *Controlled Equivalence Ratio Method for the Determination of Hazardous Components of Fire Effluents*.
59. BS 7990 *Tube furnace method for the determination of toxic products yields in for effluents*.
60. IEC 60695 *Fire Hazard testing—Part 7-50: Toxicity of fire effluents—Estimation of toxic potency: Apparatus and test method*; IEC 60695 *Fire hazard testing—Part 7-51: Toxicity of fire effluent—Estimation of toxic potency: Calculation and interpretation of test results*; PD IEC 60695-7-3:1998 *Fire hazard testing, Part 7-3: Toxicity of fire effluent, use and interpretation of test results*.
61. ASTM E 2058-02a *Standard Test Methods for Measurement of Synthetic Polymer Material Flammability Using a Fire Propagation Apparatus (FPA) ASTM*, 2002.
62. A. Tewarson, Generation of heat and chemical compounds in fires, *SFPE Handbook of Fire Protection Engineering*, 3rd Edition, National Fire Protection Association, Quincy, MA, Chapters 3–4, 2002.
63. A. Tewarson, F.H. Jiang, and T. Morikawa, Ventilation-controlled combustion of polymers, *Combustion and Flame*, 95, 151–169, 1993.
64. A.A. Stec, K. Kaczorek, and T.R. Hull, *Fire Safety Journal* (in preparation).
65. T.R. Hull, A.A. Stec, K. Lebek, and D. Price, Factors affecting the combustion toxicity of polymeric materials, *Polymer Degradation and Stability*, 92, 2239–2246, 2007.
66. A.A. Stec, T.R. Hull, K. Lebek, J.A. Purser, and D.A. Purser, The effect of temperature and ventilation condition on the toxic product yields from burning polymers, *Fire and Materials*, 32, 49–60, 2008.
67. T.R. Hull, J.M. Carman, and D.A. Purser, Prediction of CO evolution from small-scale polymer fires, *Polymer International*, 49, 1259–1265, 2000.
68. P. Blomqvist, T. Hertzberg, and H. Tuovinen, A small-scale controlled equivalence ratio tube furnace method—Experiences of the method and the link to large scale fires, *Interflam Conference*, Interscience Publications, London, U.K., 2007.

69. B. Andersson, F. Markert, and G. Holmstedt, Combustion products generated by hetero-organic fuels on four different fire test scales, *Fire Safety Journal*, 40, 439–465, 2005.
70. T.R. Hull, K. Lebek, A.A. Stec, K.T. Paul, and D. Price, Bench scale assessment of fire toxicity, in *Advances in the Flame Retardancy of Polymeric Materials: Current Perspectives Presented at FRPM'05*, Scharfel, B. (Ed.), Herstellung and Verlag, Norderstedt, Germany, 235–248, 2007.
71. A.A. Stec, T.R. Hull, J.A. Purser, and D.A. Purser, Comparison of toxic product yields from bench-scale to ISO room, *Fire Safety Journal*, 44, 62–70, 2009.
72. J. Hietaniemi, R. Kallonen, and E. Mikkola, Burning characteristics of selected substances: Production of heat, smoke and chemical species, *Fire and Materials*, 23, 171–181, 1999.
73. E. Metcalfe, A.R. Thomas, and M.K. Patel, The thermo-oxidative degradation of PTFE in the NBS cup furnace toxicity test, *Fire and Materials*, 15, 53–58, 1991.
74. J. Rossi, A.E. Jung, D. Ritchie, J.W. Lindsey, A.E. Nordholm, Tissue distribution, metabolism, and clearance of the convulsant trimethylol propane phosphate in rats, *Drug Metabolism and Disposal*, 26, 1058–1062, 1998.
75. H.B. Elkins, *The Chemistry of Industrial Toxicology*, 2nd Edition. John Wiley & Sons, New York, p. 79, 1959.

18 Modeling Thermal Degradation of Polymers by Population Balance Methods

J. E. J. Staggs

CONTENTS

18.1 Introduction	479
18.2 General Concepts of Discrete Population Balance Methods.....	483
18.2.1 Introduction	483
18.2.2 Moments	483
18.2.3 The Linear Population Balance Model.....	483
18.2.4 Volatilization.....	484
18.3 The General Bond-Weighted Random Scission Model.....	485
18.3.1 Overview.....	485
18.3.2 Pure Random Scission.....	486
18.3.3 Symmetric Power Law Bond Weights.....	490
18.3.4 Other Scission Models within the Bond-Weighted Family	491
18.4 Depropagation.....	494
18.4.1 Simple End-Chain Scission	494
18.4.2 Combined End-Chain and Random Scission	495
18.4.3 Depropagation with Random Scission Initiation.....	497
18.4.4 Thermal Degradation of PMMA.....	499
18.5 Recombination.....	500
18.6 Chain Stripping.....	504
18.7 Conclusion	506
References.....	507

18.1 INTRODUCTION

There are four distinct mechanisms for the thermal degradation of polymers namely: random scission, end-chain scission, chain stripping, and cross-linking. Thermal degradation of a particular polymer will typically involve one or more of these processes in possibly complex combinations. Polymers such as polymethylmethacrylate (PMMA), polytetrafluoroethylene, and polyoxymethylene are thought to degrade primarily by end-chain scission, owing to the high fraction (greater than 91%) of monomer present in the volatile products. Polyethylene and polypropylene probably degrade mainly by random scission and produce less than 1% of monomer in the volatile products. Polystyrene is thought to undergo a mixture of random scission and end-chain scission and produces ~40% of the monomer. Polyvinylchloride (PVC) undergoes a chain-stripping step during the first stage of its degradation, where HCl is liberated from side groups along the main polymer chain, leaving the backbone of the molecule intact and polyacrylonitrile undergoes cross-linking during

degradation.¹ Other factors such as the physical structure, bond structure, and chemical composition of the polymer molecule also influence thermal stability. For example, chain branching and double bonds in the backbone of the molecule have a weakening effect on thermal stability, whereas cross-linking and the presence of an aromatic ring tend to have strengthening effects.

A critical component to any mathematical model of pyrolysis, ignition, or even flame spread is the modeling of small-scale thermal degradation. Traditionally, thermal degradation processes in solids are considered to be analogous to chemical reactions in gases and liquids and are modeled in terms of sets of kinetic rate equations, typically of the form

$$\frac{d\mathbf{m}}{dt} = \mathbf{K}\mathbf{m}, \quad (18.1)$$

where

\mathbf{m} is a vector of mass fractions of various species

\mathbf{K} is a matrix of Arrhenius coefficients of the form $A \exp(-T_A/T)$.^{2,3}

Sometimes individual reactions are generalized to include a reaction order as an additional parameter: $dm/dt = -km^n$. No distinction is made between the various degradation mechanisms in these models—the form of the equations does not depend on specific scission type. The activation temperature T_A is often written in terms of an activation energy E_A as $T_A = E_A/R$, where R is the gas constant—another hangover from statistical mechanics of gas particles. An example of this approach is the thermal degradation of PVC⁴ using a mechanism proposed by Anthony,⁵ involving essentially four steps, where \mathbf{K} is of the form

$$\mathbf{K} = \begin{pmatrix} -k_1 & 0 & 0 & 0 \\ r_1 k_1 & -k_2 - k_3 & 0 & 0 \\ 0 & k_2 & -k_4 & 0 \\ 0 & 0 & r_2 k_4 & -k_5 \end{pmatrix}. \quad (18.2)$$

Detailed kinetic schemes have also been proposed for many other polymers and the work of Bockhorn et al.^{6–8} is representative of this large area of the literature for schemes relating to polyamide 6, PP, PE, and other polymers. Other experimental approaches, mainly aimed at identifying Arrhenius parameters in similar schemes, are discussed by Howell,⁹ Lehrle et al.,¹⁰ Shyichuk,¹¹ Wilkie,¹² and Holland and Hay.^{13,14}

The application of a kinetic scheme to the degradation of a polymer usually involves a curve-fitting process, where solutions of the rate equations (or derived quantities) are adjusted so that they fit one or more thermogravimetric (TG) curves as closely as possible. The Arrhenius parameters giving the best fit are then taken as optimal and often assumed to give a unique set of values that characterize the degradation. To take a simple example, consider a one-step reaction modeled by the rate equation $dm/dt = -k(T)m^n$. The widely used approach of Freeman and Carroll for constant heating rate experiments (with heating rate H) involves plotting $y = dv/du$ vs. $x = (T^2 du/dT)^{-1}$, where $v = \ln(A/H) - T_A/T + nu$ and H is the heating rate. The reaction order n is estimated from the y -intercept of this plot and the gradient used to obtain T_A . Once these parameters have been found, the preexponential factor is estimated from the v -intercept of a plot of v vs. $z = -T_A/T + nu$ (the intercept being $\ln(A/H)$). Unfortunately, there are concerns over the efficacy of this method in determining the reaction order. Liu and Fan¹⁵ showed that there are potentially large errors involved in determining the intercept of the (x, y) plot that effectively render the estimate for n meaningless.

Many simpler alternatives exist when one can assume that the reaction order is unity. For example, when $n = 1$, the specific mass is given by $m = \exp(-E(T))$, where E may be approximated to a good degree, when T_A is large, by

$$E(T) \approx \left(\frac{T}{T_B}\right)^2 e^{-T_A/T}, \quad T_B = \sqrt{\frac{HT_A}{A}} \quad (18.3)$$

(see later in the chapter for a derivation of this result). Then it follows that if we set $u = -\ln(m)/T^2$, a plot of $y = \ln u$ vs. $x = -1/T$ will be linear with gradient T_A and y-intercept $-2 \ln T_B$. If nothing else, this approach gives a good initial set of parameters for more sophisticated techniques based on optimization strategies.*

Another method to obtain a quick approximation for A and T_A is given in Ref. 16. Here the characteristic temperature range of the degradation step, together with the temperature at which 50% of the mass is lost is used to estimate the Arrhenius parameters (Figure 18.1). If T_c is the characteristic temperature and ΔT_c the characteristic temperature range, then the Arrhenius parameters are estimated from

$$T_A \approx 2.89 \frac{T_c^2}{\Delta T_c}, \quad A \approx \frac{2He^{T_A/T_c}}{\Delta T_c}. \quad (18.4)$$

Sets of kinetic rate equations are relatively convenient to use and often reproduce experimental TG curves well, but a significant drawback is the lack of a firm theoretical justification in their application. There is no published evidence justifying why the theory of statistical physics, which underpins the kinetics of reactions in gases, should be applicable to the thermal degradation of solids. In recent years, there have been attempts to describe thermal degradation reactions using alternative, but scientifically justifiable, methods. The application of Monte Carlo methods^{17,18} is perhaps the most relevant approach to the present discussion. Here, computer simulations are conducted using random number generators to pick molecules or bonds at random for reaction and the evolution of

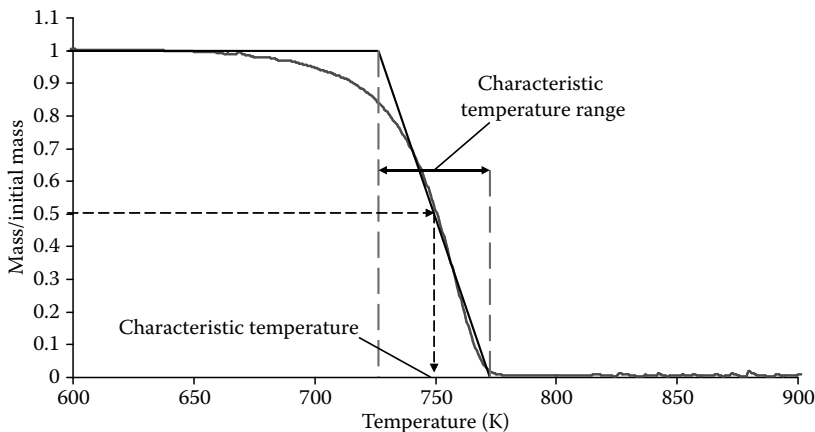


FIGURE 18.1 Characteristic temperature and temperature range of single step decomposition.

* Such methods solve the kinetic equation for the specific mass, which is then compared with the experimental value to obtain a residual. The kinetic parameters are then adjusted using a global optimization method to minimize the residual.

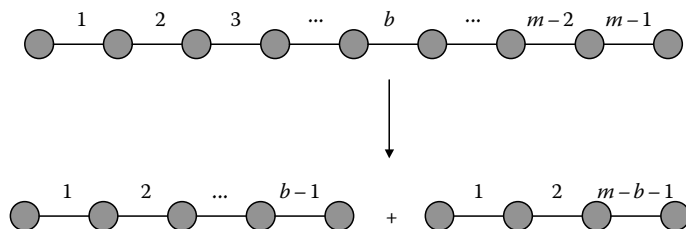


FIGURE 18.2 Illustration of random scission.

the frequency distribution of molecules is monitored. A good example of this approach is the case of pure random scission of linear polymers, where a polymer molecule is considered as a simple chain of repeat units. A molecule is chosen at random from the distribution and a bond within the molecule is randomly allocated for scission. Suppose that the molecule selected had m repeat units and bond b was selected for scission. The result of the scission process is to produce two new molecules with b and $m - b$ repeat units, respectively (Figure 18.2).

The effect of repeatedly applying this process to an initial unimolecular distribution is illustrated in Figure 18.3. Here, we see the frequency distribution of the molecular population, as progressively more bonds are broken: r denotes the ratio of broken bonds to the initial number of bonds in the population.

In this chapter, we shall look at a similar approach to modeling the evolution of distributions of polymer molecules undergoing specific scission processes. However, instead of Monte Carlo simulations, the processes will be defined in terms of population balances, which give rise to systems of ordinary differential equations. There are considerable advantages to be gained from this approach, the most obvious being the prediction of the evolution of the molecular weight distribution (MWD). Many important polymer properties, such as viscosity, are highly dependent on the molecular weight and knowledge of the way that the MWD changes overtime may well give new insights into the importance of such properties on degradation. Also, information about the composition of volatile species produced during degradation can improve ignition and heat release modeling. For example, if the volatile species consist only of simple hydrocarbons $V_m = C_m H_{2(m+1)}$ and the mole fraction of V_m in the evolved gas is ξ_m , then assuming complete combustion and that the oxygen consumption principle applies, the total heat released will be $209.6 \sum_m (3m + 1) \xi_m$ kJ per

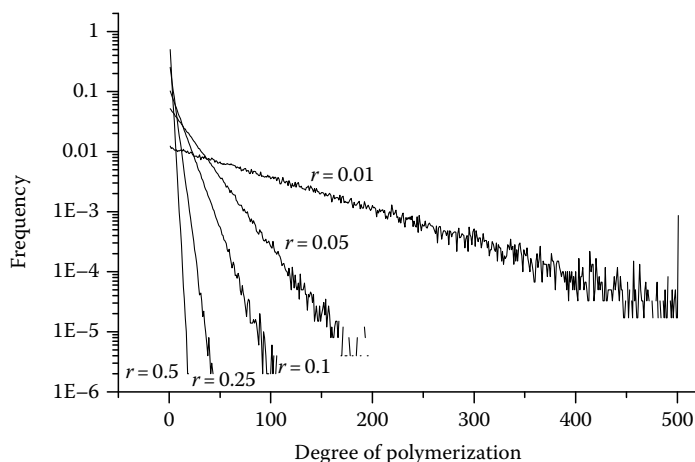


FIGURE 18.3 Evolution of population undergoing random scission.

mole of gas, where the summation is taken over all volatile species. Finally, the latent heat terms in energy conservation equations for thermal degradation may be significantly improved, since in the population balance approach, we know how many bonds are broken and what the products are. This then enables a correctly formulated thermodynamic calculation.

Although population balance methods are relatively undeveloped for interesting polymers, the author believes they have great potential. Each of the four distinct thermal degradation mechanisms mentioned earlier will be analyzed in detail and examples involving specific polymers will be discussed wherever possible. Furthermore, some relevant combinations of mechanisms (such as combined random scission and end-chain scission) will also be discussed.

18.2 GENERAL CONCEPTS OF DISCRETE POPULATION BALANCE METHODS

18.2.1 INTRODUCTION

Population balance models (PBMs) fall into two categories: discrete and continuous. In the continuous case, a polymer molecule is viewed as an infinitely divisible length of string. In the discrete case, the molecule is considered as a finite chain of repeat units linked together by bonds. The continuous model has certain technical advantages over the discrete model, but the discrete model remains as the more realistic approach. The general aim of a PBM is to implement one or more scission mechanisms and to arrive at a set of governing equations that describes the evolution of a distribution of molecules. The model can then be extended to include a mechanism for volatilization of light molecular weight species to predict the variation of total mass and hence enable comparison with an experimental thermal analysis technique.

In recent years, McCoy and coworkers have contributed greatly to the field of population balance modeling (mainly for the case of continuous models),^{19–23} but the first applications seem to have appeared in the literature in the 1950s and 1960s. Simha et al.²⁴ considered a degradation mechanism involving initiation, depropagation, inter- and intramolecular transfer and second-order termination. Boyd²⁵ later extended this solution for a different initial MWD and also considered different termination mechanisms. He also considered the effect of volume change during degradation in a short letter.²⁶

18.2.2 MOMENTS

For simplicity, the discussion will be restricted to linear molecules of homopolymers, although this simplification is by no means necessary for the theoretical framework. We consider a population of molecules where $P_i(t)$ denotes the number of molecules with i repeat units (mers), linked by $i - 1$ bonds, at time t . Thus, the total number of molecules in the population is $N(t) = \sum_{i=1}^{\infty} P_i(t)$.

The m th moment of the distribution μ_m is defined as $\mu_m = \sum_{i=1}^{\infty} i^m P_i$ and for a population of homopolymers, the total mass of the distribution is proportional to μ_1 . It is a necessary condition for any PBM without volatilization that the total mass is conserved, i.e., $d\mu_1/dt = 0$. The number-averaged and mass-averaged molecular masses of the distribution are proportional to μ_1/N and μ_2/μ_1 , respectively, and the polydispersity is defined as $\eta = N\mu_2/\mu_1^2$.

18.2.3 THE LINEAR POPULATION BALANCE MODEL

A PBM implements specific scission or recombination mechanisms that act on individual molecules within the population. The rates of individual scissions or recombinations are generally temperature dependent. For discrete models, this leads to a set of ordinary differential equations that describes

the evolution of the population. Thus if $\mathbf{P} = (P_1, P_2, \dots)^T$ is a vector whose components are the individual frequencies of the population, a general PBM may be written as

$$\frac{d\mathbf{P}}{dt} = \mathbf{f}(\mathbf{P}, T, t), \quad (18.5)$$

where

T is the temperature

\mathbf{f} is a vector-valued function that is determined by the specific scission and recombination mechanisms.

In practice, many scission mechanisms result in a set of linear differential equations, which simplifies matters somewhat if closed-form expressions are required for the individual frequencies. Also, in many practical situations of interest, it is possible to express the PBM in terms of a single scission frequency $k(T)$. Under these conditions the PBM reduces to

$$\frac{d\mathbf{P}}{dt} = k(T)\mathbf{A}\mathbf{P}, \quad (18.6)$$

where \mathbf{A} is a matrix of coefficients that do not depend on \mathbf{P} . The question of the functional form of the bond-breaking frequency is important and it is reasonable to assume that k is of Arrhenius form $k(T) = A\exp(-T_A/T)$.

It is convenient for this situation to define a dimensionless time τ by

$$\frac{d\tau}{dt} = k \quad (18.7)$$

that enables us to write the linear PBM as $d\mathbf{P}/d\tau = \mathbf{A}\mathbf{P}$. Now, if the initial distribution is given by $\mathbf{P}(0) = \mathbf{P}_0$, the general solution of the linear PBM may be written as

$$\mathbf{P}(t) = e^{\tau\mathbf{A}}\mathbf{P}_0. \quad (18.8)$$

Here $e^{\tau\mathbf{A}}$ is the *matrix exponential*, defined by $e^{\tau\mathbf{A}} = \sum_{j=0}^{\infty} (\tau^j/j!)\mathbf{A}^j$ and $\mathbf{A}^0 \equiv \mathbf{I}$, where \mathbf{I} is the identity matrix. Unfortunately, the general solution in this form is not very convenient—the calculation of matrix exponentials being a difficult process—and so it is necessary to look at individual cases in detail.

18.2.4 VOLATILIZATION

To predict a volatilization rate, it is necessary to quantify how rapidly the sufficiently light species in the distribution evaporate. Some authors²⁰ have employed relatively involved mass transfer processes in order to model evaporation in some detail. However, in the present case we shall take the view that as soon as sufficiently light species form, they immediately volatilize.^{27–30} For scission processes that do not involve recombination, this is tantamount to assuming that there is a characteristic number of repeat units m_v below which polymer molecules are classified as volatile. So, to define the remaining mass in the distribution, consisting of nonvolatile species, the concept of a *partial moment* is used. The m th partial moment $\mu_m^{(j)}$ of the distribution is defined as

$$\mu_m^{(j)} = \sum_{i=j}^n i^m P_i. \quad (18.9)$$

This corresponds to the restriction of the m th moment to species with at least j repeat units. Hence the fraction of nonvolatile mass to initial mass (referred as *specific mass*) is then approximated by $\mu_1^{(m)}/\mu_1$.

18.3 THE GENERAL BOND-WEIGHTED RANDOM SCISSION MODEL

18.3.1 OVERVIEW

The case of random scission where specific weights can be assigned to each bond in the molecule³⁰ is extremely useful and encompasses many scission mechanisms of practical interest, such as pure random scission and break-at-a-point. In this model, although the overall bond-breaking process is random, each bond within a molecule is assigned a relative probability of breaking so that one is able to specify weak locations in the molecule, such as at the ends. We shall consider only the case where molecules undergo scissions at present, i.e., there are no recombinations. Combined scission and recombination is dealt with later in the chapter.

When there are no recombinations, the degree of polymerization of the population can only decrease. Therefore, let the largest molecule in the initial population have n repeat units. Let the relative probability of bond j breaking within an i -mer be $w_j^{(i)}$, so that $\sum_{j=1}^{i-1} w_j^{(i)} = 1$. Taking the rate at which bonds break in a group of i -mers to be proportional to the number of bonds in the group then in time step Δt , the expected number of j -mers and $(i-j)$ -mers formed from the scission of bond j in a population of i -mers is $k(i-1)w_j^{(i)}P_i\Delta t$, where k is the temperature dependent bond-breaking rate. Now, i -mers are formed by the scission of bonds $(j-i)$ and i in any j -mer of greater degree of polymerization than the i -mer. Consequently, the expected number of i -mers formed from scissions in larger molecules in time step Δt is $\sum_{j=i+1}^n k(j-1)(w_{j-i}^{(j)} + w_i^{(j)})P_j\Delta t$. Since i -mers are removed from the population at rate $k(i-1)P_i$, the evolution of the population will be governed by the system of linear ordinary differential equations

$$\frac{dP_i}{d\tau} = \begin{cases} -(i-1)P_i + \sum_{j=i+1}^n (j-1)(w_{j-i}^{(j)} + w_i^{(j)})P_j, & i = 1, 2, \dots, n-1, \\ -(n-1)P_n, & i = n, \end{cases} \quad (18.10)$$

where as mentioned earlier, τ is defined as $d\tau/dt = k$. Note that since n -mers can only be removed from the population (these are the largest molecules in the initial population), then there is no production term in the equations for $i = n$. The initial conditions are $P_i(0)/N(0) = v_i$, where v_i is the fraction of i -mers in the initial population.

The model equations result in an upper-triangular form for the matrix \mathbf{A} of Equation 18.6, which may be consequently exploited to construct the general solution. Starting with the equation for $i = n$ and proceeding backwards, the general solution may be determined implicitly as

$$\frac{P_n(\tau)}{N(0)} = v_n e^{-(n-1)\tau}, \quad (18.11)$$

$$\frac{P_i(\tau)}{N(0)} = v_i e^{-(i-1)\tau} + \sum_{j=i+1}^n (j-1)(w_{j-i}^{(j)} + w_i^{(j)}) \int_0^\tau P_j(t')/N(0) dt', \quad i = 2, \dots, n-1, \quad (18.12)$$

$$\frac{P_1(\tau)}{N(0)} = v_1 + \sum_{j=2}^n (j-1)(w_{j-1}^{(j)} + w_1^{(j)}) \int_0^\tau P_j(t')/N(0) dt'. \quad (18.13)$$

It follows from Equation 18.10 that the moments of the distribution evolve according to

$$\frac{d\mu_m}{d\tau} = \sum_{j=1}^n S_{m,j} P_j, \quad (18.14)$$

where

$$S_{m,j} = (j-1) \sum_{i=1}^{j-1} (i^m + (j-i)^m - j^m) w_i^{(j)}. \quad (18.15)$$

Thus when $m = 1$ we see that $S_{m,j} = 0$ and so it follows that $d\mu_1/d\tau = 0$, confirming that the first moment is conserved. Also, when $m = 0$, $S_{m,j} = (j-1) \sum_{i=1}^{j-1} w_i^{(j)} = j-1$ (since the summation of individual bond weights must be unity) and so it follows that $dN/d\tau = \mu_1 - N$. Therefore, irrespective of the initial conditions and the bond weights, the number of molecules in the distribution N and the number-average degree of polymerization χ evolve according to

$$\frac{N(\tau)}{N(0)} = \chi_0 - (\chi_0 - 1)e^{-\tau}, \quad \chi(\tau) = \frac{1}{1 - (1 - 1/\chi_0)e^{-\tau}}, \quad (18.16)$$

respectively, where $\chi_0 = \mu_1/N(0)$ is the initial number-average degree of polymerization of the population. Having briefly considered the general bond-weighted model, we shall now go on to look at some specific examples in greater detail.

18.3.2 PURE RANDOM SCISSION

An important special case of the general bond-weighted model is when all bonds are equally likely to break and consequently all bond weights are equal, i.e., $w_i^{(j)} = 1/(j-1)$ for all i -mers. We shall look at this case in some detail for the simplified (but still relevant) case of a unimolecular initial distribution, where $v_n = 1$, $v_i = 0$, $i = 1, \dots, n-1$. Let $P_i(\tau) = N(\tau)e^{-(i-1)\tau}F(\tau)$. Then for large n , F satisfies the equation

$$\frac{dF}{d\tau} + \frac{F}{N} \frac{dN}{d\tau} = 2F \sum_{i=1}^{\infty} e^{-i\tau}. \quad (18.17)$$

The summation on the right of this equation is the infinite sum of a geometric progression and consequently is equal to $e^{-\tau}/(1 - e^{-\tau})$. Now noting from Equation 18.16 that when $\tau > 0$, $dN/d\tau \approx Ne^{-\tau}/(1 - e^{-\tau})$, it follows from Equation 18.17 that an approximate solution, valid when $\tau > 0$ and n is large, is $F \approx 1 - e^{-\tau}$. So, when the initial degree of polymerization is large, the relative frequencies are given approximately by

$$\frac{P_i(\tau)}{N(\tau)} \approx e^{-(i-1)\tau}(1 - e^{-\tau}). \quad (18.18)$$

Thus, we see that the population of molecules follows an exponential distribution, implying that a plot of the log of frequency vs. degree of polymerization at a fixed time should be linear. It is worth noting that this solution agrees well with the Monte Carlo simulations for pure random scission

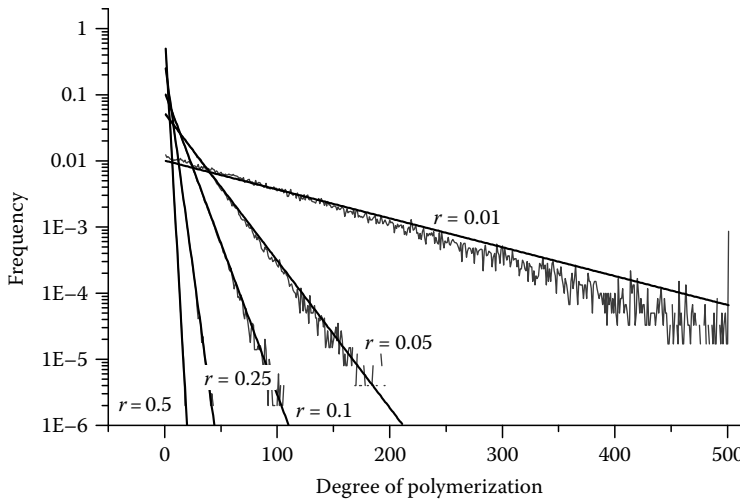


FIGURE 18.4 Comparison of population balance model with Monte Carlo model.

mentioned in Section 18.1, as Figure 18.4 confirms. The dark solid curves of this figure correspond to the PBM and the lighter lines correspond to the Monte Carlo simulation. As before, r denotes the fraction of bonds broken.

Also, if we define $E_j = \sum_{i=j}^{\infty} e^{-(i-1)\tau}$, it is a simple matter to show that

$$E_j = \frac{e^{-(j-1)\tau}}{1 - e^{-\tau}}, \quad (18.19)$$

$$\sum_{i=j}^{\infty} i e^{-(i-1)\tau} = E_j - \frac{dE_j}{d\tau}. \quad (18.20)$$

It then follows directly that the specific mass is given to a good degree of approximation by

$$\frac{\mu_1^{(m_v)}(\tau)}{\mu_1} \approx m_v e^{-(m_v-1)\tau} - (m_v - 1)e^{-m_v\tau}. \quad (18.21)$$

Furthermore, it may be shown (see Ref. 30 for details) that the polydispersity is given (when $\tau > 0$) by $\eta \approx 1 + e^{-\tau}$.

It transpires that this model represents TG data for polyethylene reasonably well, as Figures 18.5 and 18.6 confirm. The polyethylene sample used here was supplied by Polymer Laboratories (U.K.) inc. (part no. 2650-3001, batch no. 26503-1) with a molecular weight of 2015 g/mol and a polydispersity of 1.14. Although this polymer has a much lighter molecular weight than most commercial polymers, it is free of additives, and has few branch points along the molecule and relatively low polydispersity. The experiments were conducted in nitrogen (at a heating rate of 10 K/min for the first figure), using a Shimadzu TGA-50 machine with initial sample masses of ~ 8 mg.

The model may be conveniently fitted to experimental data using a straightforward spreadsheet. Suppose that we have a set of TG data in the form of three columns—time (s), temperature (K), and mass/initial mass. The basic idea is to assume values for the Arrhenius parameters $J = \ln A$ and T_A for some fixed value of m_v . We then calculate k and hence τ , using the fact that $\tau = \int_0^t k(T(t')) dt'$ (a suitable numerical rule such as the trapezium rule suffices for this). Having obtained τ , we may

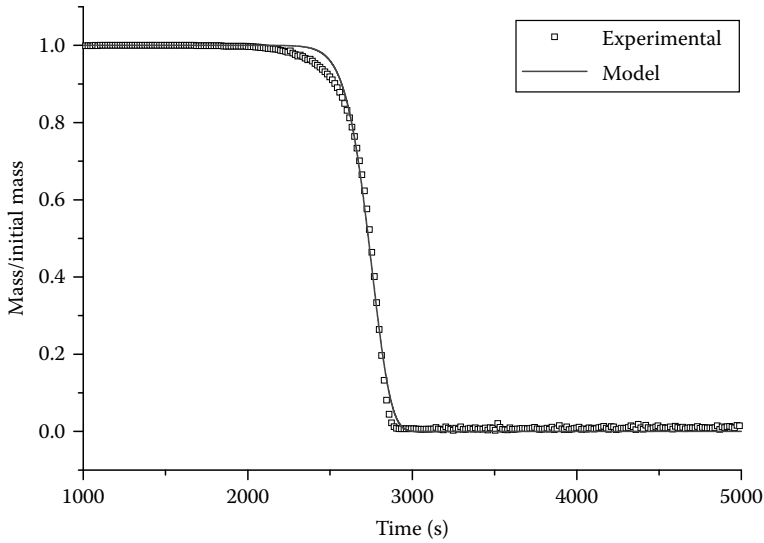


FIGURE 18.5 Comparison of model with constant heating rate TGA.

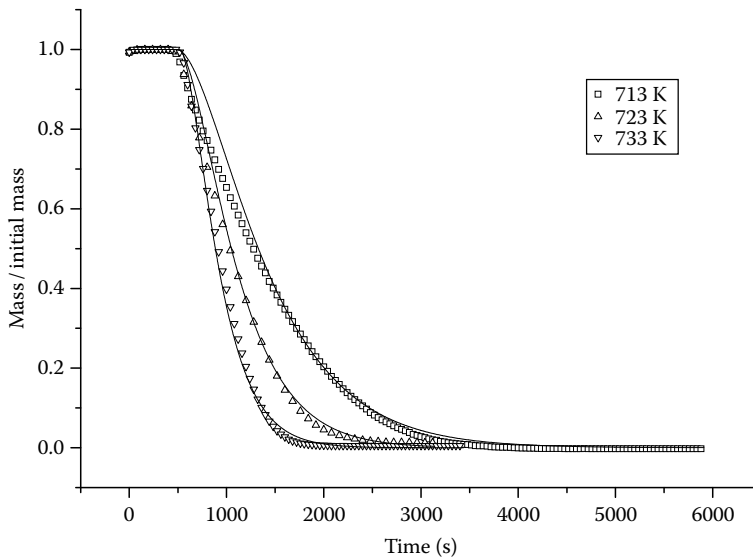


FIGURE 18.6 Isothermal TG comparison with model. Symbols correspond to experimental data and curves to model predictions.

then calculate the predicted specific mass using Equation 18.21. The square of the difference between the calculated specific mass and the experimental value is then calculated to obtain a total residual for the fit. The Arrhenius parameters are then adjusted using a global minimization procedure, such as the one implemented in the Solver add-in of MS-Excel, to minimize the total residual.

An example spreadsheet implementing this procedure is shown in Figure 18.7. The experimental data are in columns A–C. The calculated experimental specific mass is in column D. The Arrhenius parameters are shown highlighted in column J, together with the assumed value for m_v .

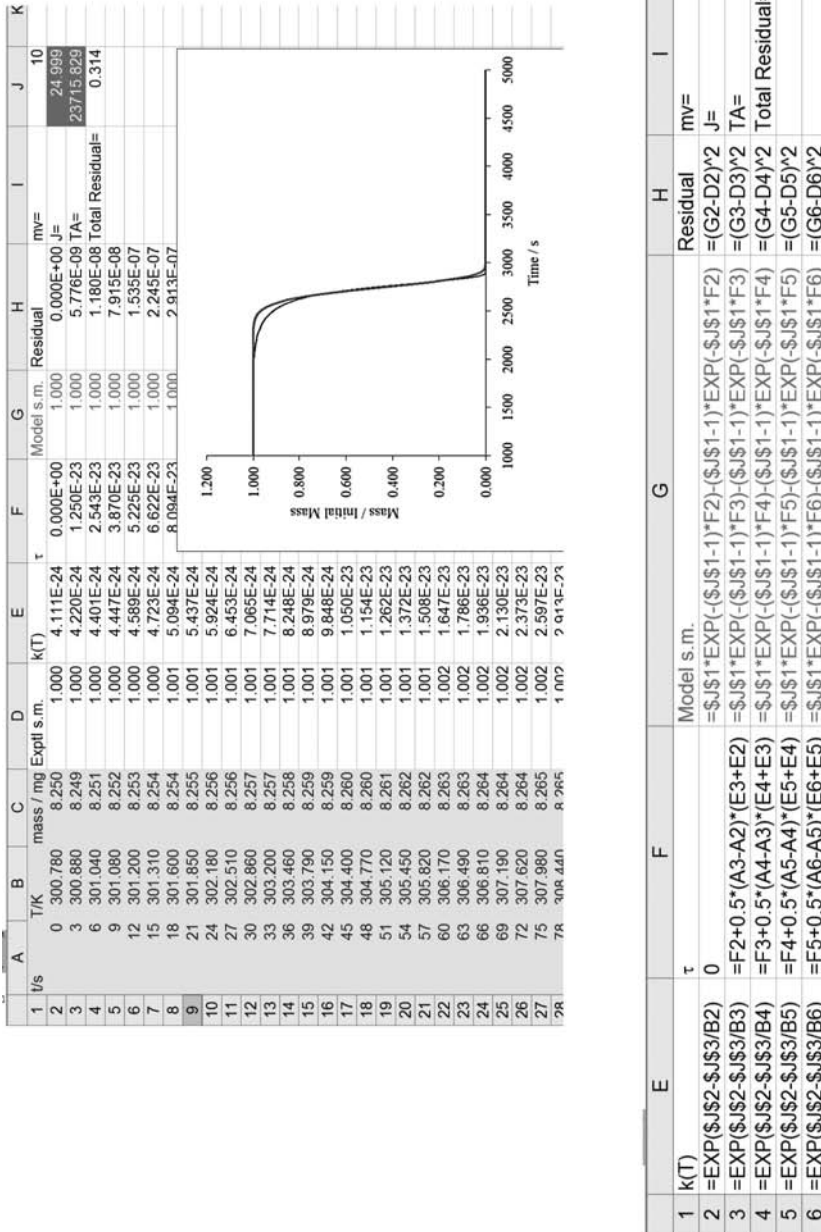


FIGURE 18.7 Microsoft Excel spreadsheet for random scission model and relevant formula.

When the TG experiment is conducted at a constant heating rate, the situation is simpler. If the heating rate is H , then

$$\tau = \frac{1}{H} \int_0^T k(T') dT'. \quad (18.22)$$

Note that we have taken the lower bound of the integral as 0 rather than the initial temperature T_a . For realistic parameter values, this introduces a negligible error into the expression for τ , as $\int_0^{T_a} k(T') dT'$ is very small. The reason for this modification is that we may then go on to find a convenient closed form expression for τ (shown subsequently). So, assuming an Arrhenius form for k , on integration of Equation 18.22 by parts it follows that

$$\tau = \frac{AT}{H} e^{-T_A/T} \left\{ 1 - \frac{T_A}{T} e^{T_A/T} E_1\left(\frac{T_A}{T}\right) \right\}, \quad (18.23)$$

where $E_1(z) = \int_z^\infty \frac{e^{-x}}{x} dx$ denotes the *exponential integral*. Now when z is large, $1 - ze^z E_1(z) \sim 1/z$ and so it follows that for large activation temperature

$$\tau \approx \frac{T^2}{T_B^2} e^{-T_A/T}, \quad (18.24)$$

where $T_B^2 = HT_A/A$. This last formula may then be used in place of the numerical integration rule to calculate τ .

18.3.3 SYMMETRIC POWER LAW BOND WEIGHTS

Another useful submodel of the general bond-weighted model is where weights are assigned to bonds symmetrically from the midpoint of the molecule and either reduce or increase as one proceeds to the ends of the molecule. An example of this is the symmetric power law distribution³⁰ where the individual weights are defined in terms of two parameters: λ and an exponent κ . The individual weights are given by

$$w_i^{(j)} = \frac{1 + (\lambda - 1) \left| (2i - j) / (j - 2) \right|^\kappa}{j - 1 + (\lambda - 1) \sigma_j^{(\kappa)}}, \quad j \geq 3, \quad 1 \leq i \leq j - 1, \quad (18.25)$$

with $w_1^{(2)} = 1$, $w_1^{(3)} = w_2^{(3)} = 1/2$ and

$$\sigma_j^{(\kappa)} = \sum_{i=1}^{j-1} \left| \frac{2i - j}{j - 2} \right|^\kappa, \quad j \geq 3. \quad (18.26)$$

Here λ is the ratio of the probability of an end bond breaking to the probability of a bond breaking in the middle of the molecule. Examples of the distribution of bond weights for an individual molecule is shown in Figure 18.8 for the case where the likelihood of bonds breaking increases with distance away from the molecule centre.

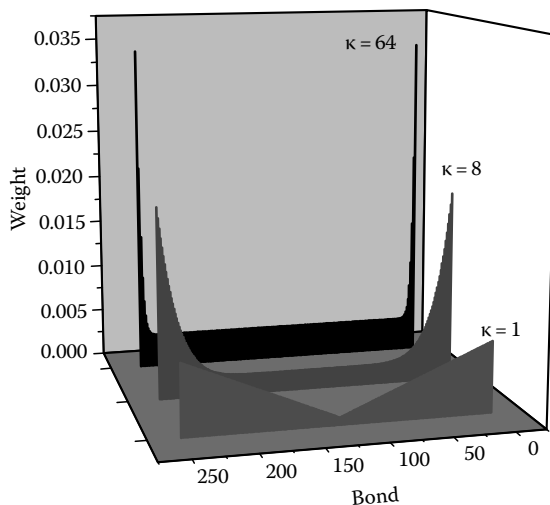


FIGURE 18.8 Power law bond weights.

When $\lambda = 1$, or $\kappa = 0$, the case of pure random scission is recovered. For $j \geq 3$, as $\kappa \rightarrow \infty$, an end-bond weighted case is recovered where

$$w_i^{(j)} = \begin{cases} \frac{\lambda}{2\lambda + j - 3}, & i = 1 \text{ or } j - 1, \\ \frac{1}{2\lambda + j - 3}, & i = 2, 3, \dots, j - 2. \end{cases} \quad (18.27)$$

This case may be thought of as a special case of random scission, where the probability of an internal bond breaking in the molecule is constant, but the probability of the two end bonds breaking is different. Such a case would be relevant where the molecule had different functional end groups that created local weak points. When λ is large, it may be shown that the frequency distribution is essentially binomial* and that the remaining mass for initially large degree of polymerization varies according to $\mu_1^{(m_v)}/\mu_1 \approx e^{-\tau}$.

We should expect therefore that, for large λ , the power-law specific masses should lie between two limits: the lower provided by pure random scission and the upper provided by the limit as $\kappa \rightarrow \infty$, i.e., $e^{-\tau}$. The graph in Figure 18.9 shows specific masses for $\kappa = 1, 8, 64$, and $\lambda = 10$ ($m_v = 11$) together with the two limits discussed earlier.

18.3.4 OTHER SCISSION MODELS WITHIN THE BOND-WEIGHTED FAMILY

There are many other types of scission mechanism that may be modeled within the bond-weighted framework. Perhaps the most obvious of these is break-at-a-point. Here, we suppose that there are specific locations within a molecule where bond breaking is more likely than anywhere else. Let θ represent the fractional position along the length of a molecule at which scission occurs, where $0 < \theta \leq 0.5$. Hence for a j -mer, this implies that the bond b closest to $\theta(j - 1)$ will break. In general, b will be given by the values in Table 18.1.

* Note that another binomial frequency distribution arises when considering chain stripping: see later in the chapter.

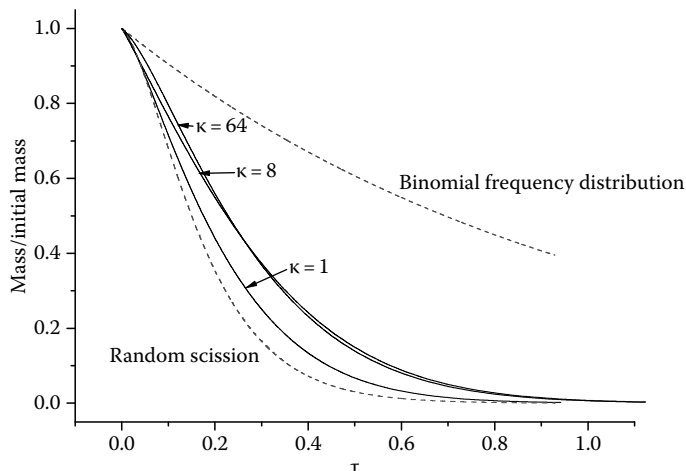


FIGURE 18.9 Specific masses for power law PBM.

Here $\text{int}(\)$ denotes the integer part of a real number. The bond weights are given in Table 18.2.

So for example, if the molecule has a weak location at its midpoint, application of this scission mechanism would result in a population of molecules of lengths $\frac{1}{2}$, $\frac{1}{4}$, etc., of the original molecule. The effect of the location of the weak bond on the mass remaining is illustrated in Figure 18.10.

Another relevant example is the alternating bond weight model. Here, we consider the repeat units as linked by two different bonds that alternate throughout the molecule. This case would apply to the thermal degradation of PVC after dehydrochlorination, where an alternating bond structure of the form $\text{C}-\text{C}=\text{C}-\text{C}=\dots$ exists along the polymer backbone.^{1,2,5} Let the ratio of the individual weights for the two bond types be λ . Then for an i -mer

$$w_i^{(1)} = \frac{2}{i + (i-2)\lambda}, \quad w_i^{(2)} = \frac{2\lambda}{i + (i-2)\lambda},$$

$$w_i^{(j)} = w_i^{(j-2)}, \quad j = 3, 4, \dots, i-1, \quad \text{if } i \text{ is even,} \quad (18.28)$$

$$w_i^{(1)} = \frac{2}{(i-1)(1+\lambda)}, \quad w_i^{(2)} = \frac{2\lambda}{(i-1)(1+\lambda)}, \quad w_i^{(j)} = w_i^{(j-2)}, \quad j = 3, 4, \dots, i-1, \quad \text{if } i \text{ is odd.} \quad (18.29)$$

The ratio of bond weights λ has a large effect on the population frequencies, as Figure 18.11 shows. The solid straight lines on the figure correspond to the frequencies for the pure random scission model discussed earlier. Interestingly, even though the bond weight ratio λ has a large effect on the frequency distributions, it has little effect on the remaining mass, as Figure 18.12 confirms.

TABLE 18.1
Bond Locations for Break-at-a-Point

Condition	Value of b
$\theta(j-1) < 1$	1
$\theta(j-1) - \text{int}(\theta(j-1)) < 0.5$	$\text{int}(\theta(j-1))$
$\theta(j-1) - \text{int}(\theta(j-1)) \geq 0.5$	$1 + \text{int}(\theta(j-1))$

TABLE 18.2
Bond Weights for Break-at-a-Point

Condition	Bond Weight $w_i^{(j)}$
$i \neq b$	0
$i = b$ and $b = j - b$	1
$i = b$ or $i = j - b$ and $b \neq j - b$	1/2

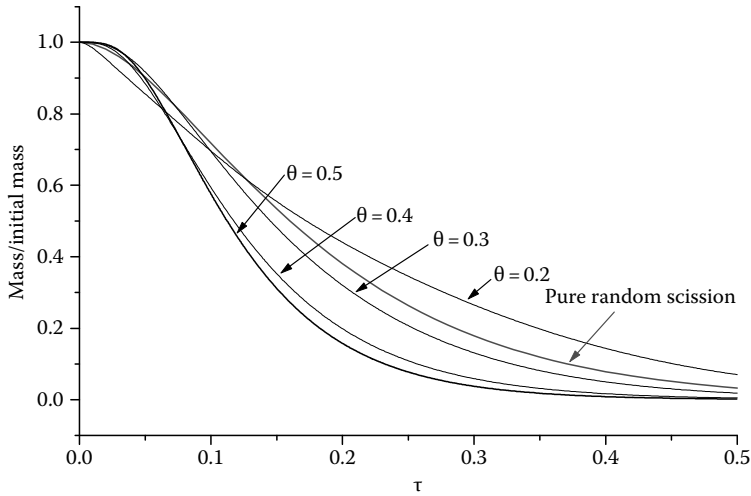


FIGURE 18.10 The effect of break-at-a-point scission on remaining mass.

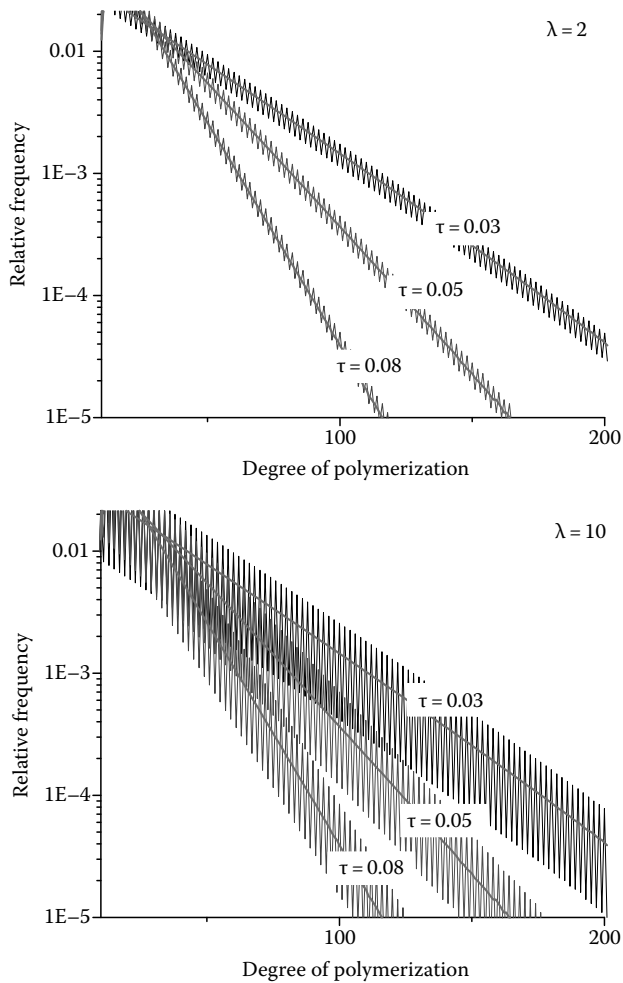


FIGURE 18.11 Frequency distributions for alternating bond weights. Bond weight ratio $\lambda = 2$ (top) and $\lambda = 10$ (bottom).

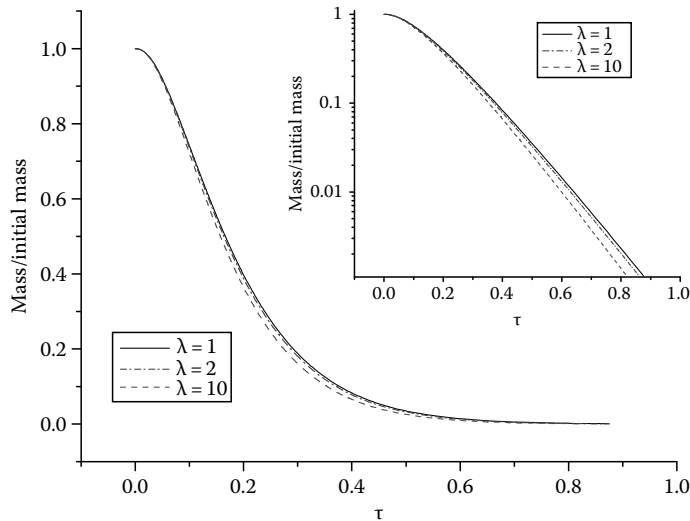


FIGURE 18.12 Specific mass for alternating bond model (inset is plotted on a log scale).

18.4 DEPROPAGATION

18.4.1 SIMPLE END-CHAIN SCISSION

An important step in the thermal degradation of many polymers such as PMMA involves depropagation. Here the polymer molecule or radical fragment rapidly unzips in such a way that produces mainly a monomer. This process may be modeled simply by a rapid reaction where an i -mer is converted to an $(i - 1)$ -mer plus a monomer: $P_i \rightarrow P_{i-1} + P_1$. In reality, this is a gross oversimplification of the process and a more sophisticated model will be discussed subsequently and also later in the chapter in relation to the thermal degradation of PMMA.

The basic equations governing the evolution of a population by depropagation (or end-chain scission) have been analyzed in detail by Kostoglou³¹ and later by Staggs²⁹, and we shall briefly review the model here. Now unlike the random scission model, where we consider the number of bonds breaking in the population, here only one bond per molecule breaks—an end bond—and so we consider the number of molecules at any particular instant that degrade. So in a population of i -mers, let $k^{(d)} P_i \Delta t$ molecules undergo end-chain scission in time step Δt per second. Here $k^{(d)}$ is the fractional end-chain scission rate, which is assumed to be independent of the molecule size. Kostoglou³¹ investigates the general case when $k^{(d)}$ depends on the degree of polymerization. Now if n is the maximum degree of polymerization of the population, and there are no recombinations, then it follows that for $2 \leq i \leq n - 1$, in time step Δt , the number of i -mers will decrease by an amount $k^{(d)} P_i \Delta t$ (these molecules forming $(i - 1)$ -mers and monomers) and will increase by $k^{(d)} P_{i+1} \Delta t$ from end-chain scission of $(i + 1)$ -mers. The largest molecules in the population can only be removed from the population and monomers can only be added from end-chain scission of larger molecules. Hence, defining τ as above by $d\tau/dt = k^{(d)}$, the following set of ordinary differential equations is obtained:

$$\left. \begin{aligned} \frac{dP_n}{d\tau} &= -P_n, \\ \frac{dP_i}{d\tau} &= P_{i+1} - P_i, \quad 2 \leq i \leq n-1, \\ \frac{dP_1}{d\tau} &= P_2 + \sum_{i=2}^n P_i. \end{aligned} \right\} \quad (18.30)$$

The general solution of this set of equations may be constructed and it may be confirmed by direct substitution into Equation 18.30 that if v_i is the initial fraction of i -mers in the population

$$\frac{P_i}{N(0)} = e^{-\tau} \sum_{j=i}^n \frac{\tau^{n-j}}{(n-j)!} v_{n+i-j}, \quad 2 \leq m \leq n. \quad (18.31)$$

For the particular case of a unimolecular initial distribution

$$\frac{P_i}{N(0)} = e^{-\tau} \frac{\tau^{n-i}}{(n-i)!}, \quad 2 \leq m \leq n. \quad (18.32)$$

Hence when n is large, it follows that $\sum_{i=2}^n P_i = e^{-\tau} \sum_{i=2}^n \frac{\tau^{n-i}}{(n-i)!} \approx e^{-\tau} e^{\tau} = 1$ and consequently from Equation 18.30 that $P_1/N(0) \approx \tau$. Therefore for large n , because monomers are the only volatile species formed until all molecules in the population have unzipped to sufficiently light species, if the end-chain scission is the only process, then the specific mass remaining in the population varies approximately according to $1 - \tau/n$ (see Ref. 29 for the details of this derivation). The dependence of specific mass on initial degree of polymerization is unsurprising given the fact that with end-chain scission, there is only one site per molecule (and end bond) that can produce a monomer. Therefore for fixed mass, as the initial degree of polymerization increases, there are proportionately fewer molecules in the population (and so fewer sites that can form monomers) and so the volatilization rate must decrease correspondingly.

18.4.2 COMBINED END-CHAIN AND RANDOM SCISSION

It has already been noted above that the thermal degradation of PS is thought to involve a mixture of end-chain and random scission mechanisms. Guaita et al. have investigated this case using a mixture of experimental and Monte Carlo methods³² and we now consider the corresponding PBM.

If random scission occurs together with end-chain scission (but at a different rate) then defining τ by $d\tau/dt = k^{(d)}$, the population balance equations (PBEs) for these combined processes are

$$\frac{dP_i}{d\tau} = \begin{cases} P_2 + (1 + 2\alpha^{(r)}) \sum_{j=2}^n P_j, & i = 1, \\ -\{1 + \alpha^{(r)}(i-1)\} P_i + P_{i+1} + 2\alpha^{(r)} \sum_{j=i+1}^n P_j, & 2 \leq i < n, \\ -\{1 + \alpha^{(r)}(n-1)\} P_n, & i = n. \end{cases} \quad (18.33)$$

Here $\alpha^{(r)} = k^{(r)}/k^{(d)}$ is the ratio of random scission rate to end-chain scission rate. Now, for a distribution with initially large degree of polymerization under isothermal conditions, it may be confirmed by direct substitution into Equation 18.33 that the solutions of these equations for $i > 1$ are

$$\frac{P_i(\tau)}{\mu_1} = \exp \left\{ - \left[1 + \alpha^{(r)}(i-1) \right] \tau + \frac{1}{\alpha^{(r)}} (1 - e^{-\alpha^{(r)}\tau}) \right\} (1 - e^{-\alpha^{(r)}\tau})^2, \quad (18.34)$$

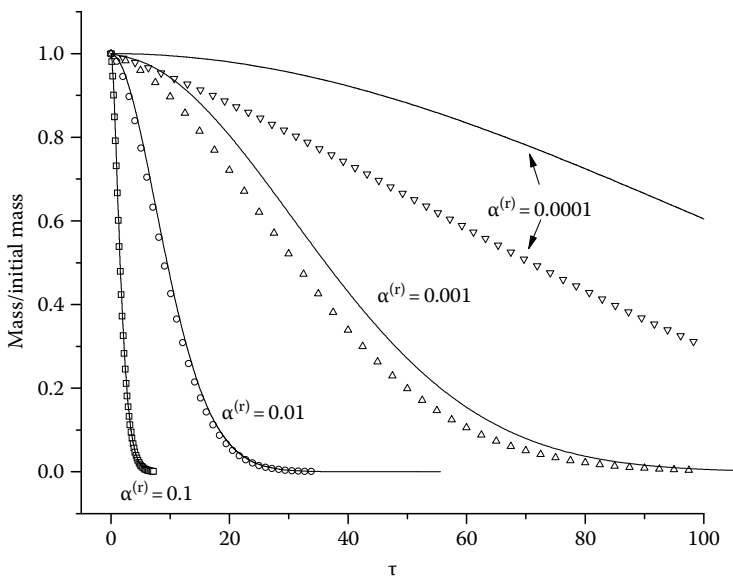


FIGURE 18.13 Comparison of approximation for specific mass (solid curves) with numerical calculation (symbols) for initially unimolecular distribution with $n = 200$.

These solutions are of the same overall form as those for the pure random scission case considered above and so it may be shown by a similar argument to that used to obtain Equation 18.21 that the specific mass is given by

$$\frac{\mu_1^{(m_v)}(\tau)}{\mu_1} = \exp \left\{ - \left[1 + \alpha^{(r)}(m_v - 1) \right] \tau + \frac{1}{\alpha^{(r)}} (1 - e^{-\alpha^{(r)}\tau}) \right\} \left\{ m_v - (m_v - 1)e^{-\alpha^{(r)}\tau} \right\}. \quad (18.35)$$

These approximations are reliable apart from when $\alpha^{(r)}$ is very small, as Figure 18.13 confirms. As $\alpha^{(r)} \rightarrow 0$, the remaining mass approaches 1, which is the correct (but practically useless) limit for end-chain scission of a population with initially infinite degree of polymerization. For a realistic population with initially finite degree of polymerization, this is unhelpful as the correct limit is $1 - \tau/n$. It may be shown that when $O(\alpha^{(r)}) > 1/n$, and n is large, the initial distribution of polymer molecules has little effect on the frequencies and the approximations remain valid.

The effect of the ratio of random scission rate to end-chain scission rate on mass remaining is shown in Figure 18.14 for $m_v = 11$. There is a slow qualitative change in the specific mass as $\alpha^{(r)}$ increases, although this is difficult to see in the figure. Generally speaking, for fixed end-chain scission rate, as the random scission rate increases we should expect the specific mass to decrease and this is confirmed in the figure. We should also expect the qualitative behavior of the specific mass to become more exponential with increasing $\alpha^{(r)}$.

The fraction of monomer in the volatile species should be a strong function of the relative random scission rate and this is often taken as an indicator of the balance between end-chain and random scission in experimental observations.¹ We should expect that when end-chain scission dominates, the fraction of monomer in the volatile species should be close to 1. As more random scissions occur, the fraction will reduce. When random scission dominates, the spectrum of volatile species should be approximately flat, implying that the fraction of monomers should approach $1/(m_v - 1)$ as $\alpha^{(r)} \rightarrow \infty$. Figure 18.15 shows the monomer fractions (from numerical solutions of the

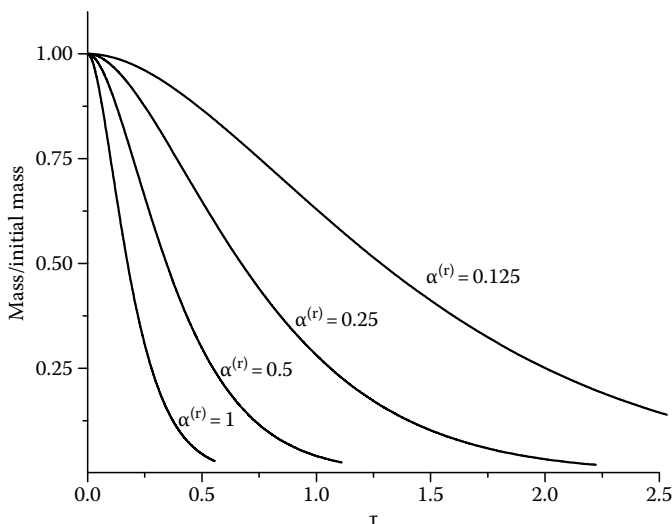


FIGURE 18.14 Effect of relative scission ratio on specific mass for combined end-chain and random scission.

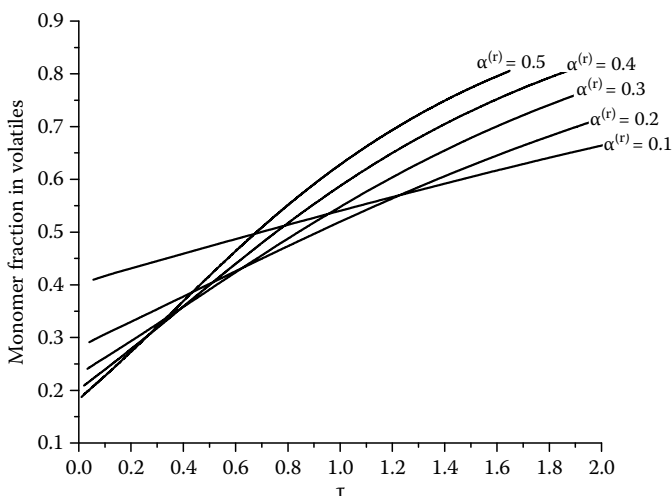


FIGURE 18.15 Fraction of monomer in volatile species for initially unimolecular distribution with $n = 200$.

PBEs for initially unimolecular distributions) as functions of τ for different random/end-chain scission ratios. Note that the general behavior discussed earlier is recovered, although the monomer fraction becomes a strong function of τ as $\alpha^{(r)}$ increases. The graph in Figure 18.16 shows the average monomer fraction over the first 50% of mass lost (again from numerical solutions of the PBEs for initially unimolecular distributions) as a function of $\alpha^{(r)}$.

18.4.3 DEPROPAGATION WITH RANDOM SCISSION INITIATION

A better model of thermal degradation by depropagation may be obtained if we distinguish between polymer molecules and radical fragments in the population. Here, we consider radical species R_i being formed from an initial random scission reaction. Once formed, the radical species then undergo

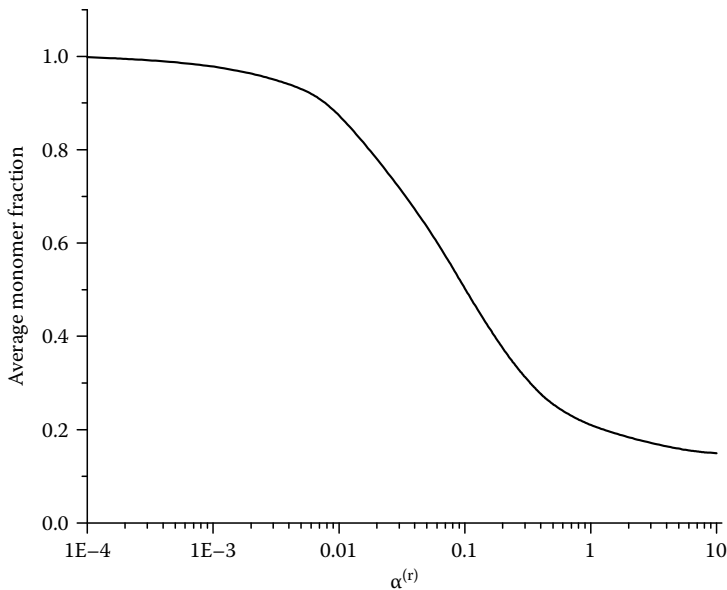


FIGURE 18.16 Average monomer fraction over first 50% of mass lost for initially unimolecular distribution with $n = 200$.

depropagation to form monomers and lower order radicals. Our modified degradation mechanism is therefore: $P_i \rightarrow R_{i-r} + R_r$ (initiation to form the radical species) and $R_i \rightarrow R_{i-1} + P_1$ (depropagation). The PBEs for this process are formed from a combination of the pure random scission and end-chain scission models and are given for $i \neq 1$ by

$$\frac{dP_i}{dt} = -(i-1)k^{(r)}P_i, \quad (18.36)$$

$$R_n = 0, \quad \frac{dR_i}{dt} = k^{(d)}(R_{i+1} - R_i) + 2k^{(r)} \sum_{j=i+1}^n P_j, \quad 2 \leq i \leq n. \quad (18.37)$$

when $k^{(d)} \gg (n-1)k^{(r)}$, radical species are converted into monomers as soon as they form and so the dynamics are dominated by the rate at which initiation takes place. Consequently, if v_i is the initial fraction of i -mers, when $k^{(d)} \gg (n-1)k^{(r)}$ it follows that the mass remaining will be given approximately by $\mu_1^{(2)}/\mu_1 \approx \sum_{i=2}^n i v_i e^{-(i-1)\tau} / \sum_{i=2}^n i v_i$. Here τ is defined by $d\tau/dt = k^{(r)}$. When the initial population is unimolecular, this simplifies to $\exp(-(n-1)\tau)$.

For the case when initiation does not control the dynamics, the situation is a little more complicated. However, for an initially unimolecular distribution, it is possible to show by successively solving the equations starting at $i = n$ and proceeding backwards, that for isothermal conditions, the solution to the PBEs is

$$\frac{P_n}{N(0)} = e^{(\lambda-1)\tau}, \quad (18.38)$$

$$\frac{R_i}{N(0)} = \frac{2(1-\lambda^{n-i})}{(n-1)\lambda^{n-i}} \{e^{(\lambda-1)\tau} - e^{-\tau}\} - \frac{2e^{-\tau}}{(n-1)\lambda^{n-i}} \sum_{j=1}^{n-i-1} (\lambda^j - \lambda^{n-i}) \frac{\tau^j}{j!}, \quad 2 \leq i \leq n-1, \quad (18.39)$$

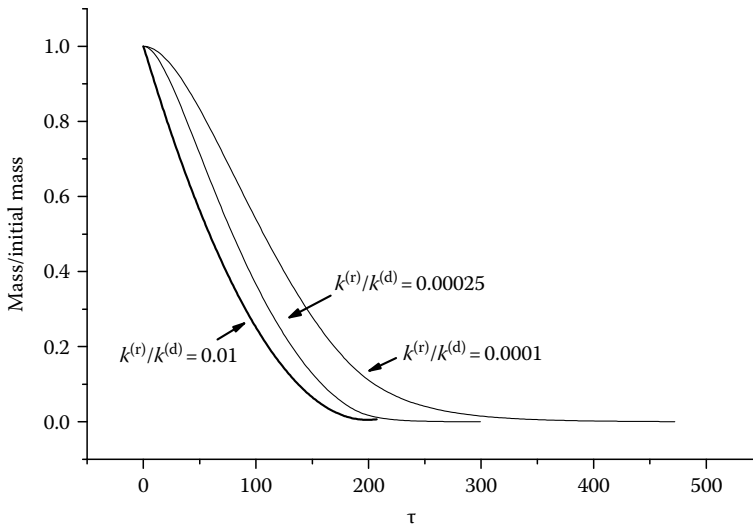


FIGURE 18.17 Specific mass for depropagation with random scission initiation.

$$\lambda = 1 - (n-1) \frac{k^{(r)}}{k^{(d)}}, \quad \tau = k^{(d)}t. \quad (18.40)$$

when $k^{(r)}/k^{(d)}$ is small, it may be shown³³ that the remaining mass is given to a good approximation by

$$\frac{\mu_1^{(2)}}{\mu_1} \approx \begin{cases} 1 - \beta \left(\tau - \frac{1 - e^{(\lambda-1)\tau}}{1-\lambda} \right) + \frac{\tau^2}{n(n-1)}, & \tau < \tau^*, \\ \frac{\beta}{1-\lambda} \left(e^{(\lambda-1)(\tau-\tau^*)} - e^{(\lambda-1)\tau} \right) - \frac{2\tau^* e^{(\lambda-1)(\tau-\tau^*)}}{n(n-1)(1-\lambda)}, & \tau \geq \tau^*, \end{cases} \quad (18.41)$$

$$\tau^* = n - n^{1/2}, \quad \beta = \frac{2}{n} \left(1 + \frac{1}{n-1} + \frac{1}{(n-1)(1-\lambda)} \right). \quad (18.42)$$

The variation of specific mass is illustrated in Figure 18.17 for various ratios of $k^{(r)}/k^{(d)}$.

18.4.4 THERMAL DEGRADATION OF PMMA

Of course, radical species may be converted back to polymer molecules by termination. Examples of specific termination reactions are first order, where $R_i \rightarrow P_i$ and second order, where $R_i + R_j \rightarrow P_{i+j}$. At present, there is an uncertainty in the literature over which of these candidates is the most suitable for specific degradation mechanisms.

The thermal degradation of PMMA has been considered in detail^{13,33-36} and the case of first order termination is analyzed in Ref. 33. If the rate of termination is $k^{(T)}$, the PBEs for this case are

$$\frac{dP_i}{d\tau} = \begin{cases} \alpha^{(T)} R_1 + \sum_{j=2}^n R_j, & i = 1, \\ \alpha^{(T)} R_i - \alpha^{(r)}(i-1)P_i, & 2 \leq i \leq n, \end{cases}$$

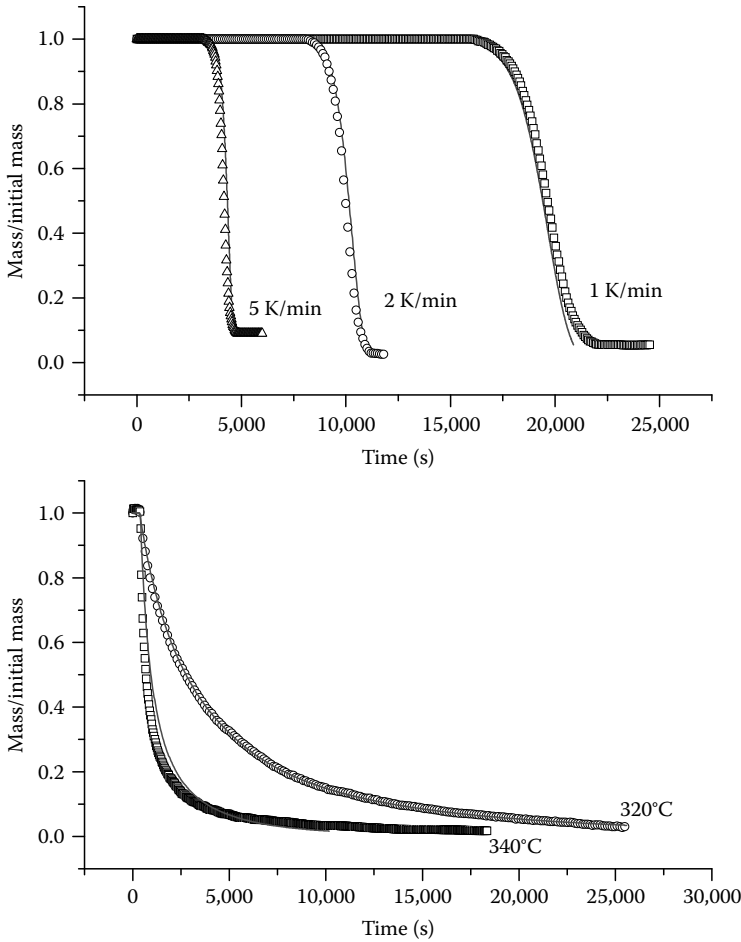


FIGURE 18.18 Comparison of TG experiments (constant heating rate: top, isothermal: bottom). Solid curves are model predictions and symbols are experimental results.

$$\frac{dR_i}{d\tau} = \begin{cases} -\alpha^{(T)}R_1 + R_2 + 2\alpha^{(r)}\sum_{j=2}^n P_j, & i = 1, \\ -(1 + \alpha^{(T)})R_i + R_{i+1} + 2\alpha^{(r)}\sum_{j=i+1}^n P_j, & 2 \leq i < n. \end{cases}$$

TABLE 18.3
Arrhenius Parameters
for PMMA Model

	A (s ⁻¹)	T _A (K)
k ^(r)	6.172 × 10 ¹¹	21,885
k ^(d)	1.789 × 10 ¹⁶	21,115
k ^(T)	2.850 × 10 ¹³	18,001

with $R_n = 0$ as above. Here $d\tau/dt = k^{(d)}$, $\alpha^{(T)} = k^{(T)}/k^{(d)}$, and $\alpha^{(r)} = k^{(r)}/k^{(d)}$. This model gives very good agreement with experimental TG results, as shown in Figure 18.18. The polymer samples for the TG experiments were obtained from Polymer Laboratories (U.K.) inc. (part no. 2023-3001, batch no. 20233-11). The Arrhenius parameters for the various reaction rates are shown in Table 18.3, where it is assumed that each k is of the form $k = A \exp(-T_A/T)$.

18.5 RECOMBINATION

Processes such as cross-linking, second-order termination of radical species, and polymerization are all examples of recombination. Here, we consider second-order recombination, where two molecules or radical fragments may join to form a new molecule of higher degree of polymerization.

This case has been dealt with for continuous (rather than discrete) probability distributions in an earlier paper.²⁷ Also, it is worth noting that the physics of this process are similar to the process of coagulation in atmospheric physics.³⁷

So, if P_i and P_j are the frequencies of i -mers and j -mers in the population, we consider the process where an i -mer and j -mer combine to form an $(i + j)$ -mer. Again, let the total number of molecules in the population be $N = \sum_{j=1}^{\infty} P_j$ and suppose that in time step Δt , $Nk^{(+)}\Delta t$ molecules recombine to form larger species. Thus, $Nk^{(+)}\Delta t$ molecules will be removed from the population and $Nk^{(+)}\Delta t/2$ new molecules will be created (since two molecules combine to form a new molecule). It therefore follows that the number of molecules in the distribution will evolve according to $dN/dt = -Nk^{(+)}/2$, implying that

$$\frac{N(\tau)}{N(0)} = \exp\left(-\frac{\tau}{2}\right), \quad (18.43)$$

where $d\tau/dt = k^{(+)}$. Now, if $f_i = P_i/N$ is the probability of selecting a j -mer at random from the population, it follows that the probability of generating a new i -mer is $\sum_{j=1}^{i-1} f_j f_{i-j}$. Since monomers can only be consumed and not generated, it follows that the evolution of the population is given by

$$\left. \begin{aligned} \frac{dP_1}{d\tau} &= -P_1, \\ \frac{dP_i}{d\tau} &= -P_i + \frac{1}{2N} \sum_{j=1}^{i-1} P_j P_{i-j}, \quad i > 1. \end{aligned} \right\} \quad (18.44)$$

It transpires that the general solution of the recombination equations may be found using a *discrete Laplace transform*. If \mathbf{a} is a vector with components a_j , $j = 1, 2, \dots$, then the discrete Laplace transform of \mathbf{a} is defined as

$$\langle \mathbf{a} \rangle = \sum_{j=1}^{\infty} e^{-js} a_j, \quad s > 0. \quad (18.45)$$

This transformation is analogous to the unilateral z -transform,³⁸ defined by $\widehat{\mathbf{a}}(z) = \sum_{j=1}^{\infty} a_j/z^j$, where $z = e^s$. Now, let $*$ denote the *discrete convolution operator*: if \mathbf{a} and \mathbf{b} are two vectors, then $\mathbf{a}*\mathbf{b}$ is itself a vector with j th component $(\mathbf{a}*\mathbf{b})_j = 0$ if $j = 1$ and $(\mathbf{a}*\mathbf{b})_j = \sum_{i=1}^{j-1} a_i b_{j-i}$ when $j > 1$. Then it may be shown that the convolution operator has the property that $\langle \mathbf{a}*\mathbf{b} \rangle = \langle \mathbf{a} \rangle \langle \mathbf{b} \rangle$.

Returning to the problem at hand, let $P_i = N^2 p_i/N(0)$ and $x = 1 - N/N(0)$. Now, in terms of the vector \mathbf{p} , the recombination equations may be written as

$$\frac{d\mathbf{p}}{dx} = \mathbf{p} * \mathbf{p}. \quad (18.46)$$

Taking the discrete Laplace transform of this equation and noting the relation mentioned in the preceding text regarding the convolution operator, gives $d\langle \mathbf{p} \rangle/dx = \langle \mathbf{p} \rangle^2$, which has solution

$$\langle \mathbf{p} \rangle = \frac{\langle \mathbf{p}_0 \rangle}{1 - x \langle \mathbf{p}_0 \rangle}. \quad (18.47)$$

Here $\mathbf{p}_0 = \mathbf{P}(0)/N(0)$ are the corresponding initial values for \mathbf{p} . Since $x < 1$, we may write this last equation as

$$\langle \mathbf{p} \rangle = \langle \mathbf{p}_0 \rangle \sum_{j=0}^{\infty} x^j \langle \mathbf{p}_0 \rangle^j, \quad (18.48)$$

and on taking inverse transforms, it follows that the general solution for \mathbf{P} may be written as

$$\frac{\mathbf{P}}{N(0)} = e^{-\tau} \sum_{j=1}^{\infty} \mathbf{p}_0^{*j} (1 - e^{-\tau/2})^{j-1}. \quad (18.49)$$

Here, \mathbf{p}_0^{*j} denotes the result of applying the discrete convolution operator $*$ to \mathbf{p}_0 a total of $j - 1$ times, i.e., $\mathbf{p}_0^{*2} = \mathbf{p}_0 * \mathbf{p}_0$, $\mathbf{p}_0^{*3} = \mathbf{p}_0 * \mathbf{p}_0 * \mathbf{p}_0$, etc.

For the special case of simple polymerization of an initial population consisting entirely of monomers, it follows that

$$\frac{P_i}{N(0)} = e^{-\tau} (1 - e^{-\tau/2})^{i-1}. \quad (18.50)$$

The graph in Figure 18.19 shows the development of an initially normal distribution of molecules by recombination. As τ increases, peaks appear in the distribution at locations corresponding to multiples of the initial average degree of polymerization.

When combined with other scission processes, the situation is more complicated and general solutions are harder to find. If we consider the case of pure random scission and recombination, the PBEs for $i > 1$ may be written as

$$\frac{dP_i}{d\tau} = -(i-1)P_i + 2 \sum_{j=i+1}^{\infty} P_j - \alpha P_i + \frac{\alpha}{2N} \sum_{j=1}^{i-1} P_j P_{i-j}, \quad (18.51)$$

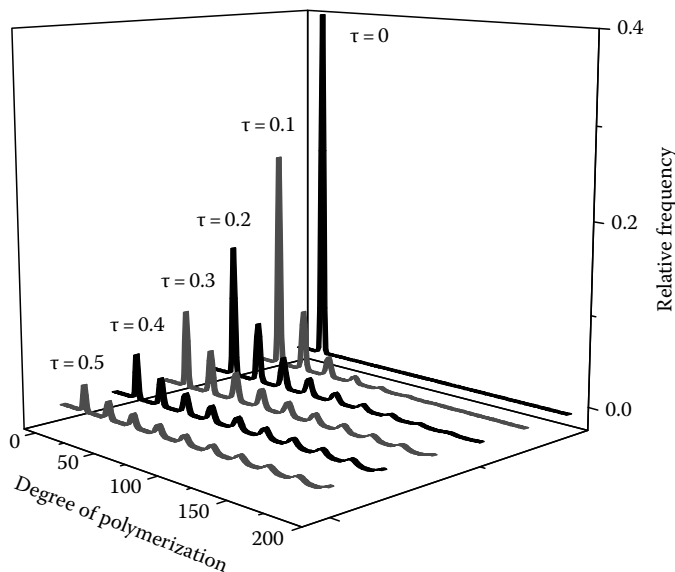


FIGURE 18.19 Evolution of an initially normal distribution by second-order recombination.

where $\alpha = k^{(+)}/k^{(r)}$ and $d\tau/dt = k^{(r)}$. Now, summing Equation 18.51 over i from $i = 1 \dots \infty$ gives a differential equation for the evolution of the total number of molecules in the population. This may readily be solved to give

$$\frac{N(\tau)}{N(0)} = \frac{\chi_0}{1 + \alpha/2} (1 - e^{-(1+\alpha/2)\tau}) + e^{-(1+\alpha/2)\tau}, \quad (18.52)$$

where χ_0 is the initial number-average degree of polymerization.

Returning to the case of the full model, comparison with the cases of pure random scission and recombination mentioned earlier suggests that seeking a solution of the form $P_i = \lambda^{i-1}(\tau)F(\tau)$ might be useful. Substitution into the model equations gives

$$\frac{d\lambda}{d\tau} = -\lambda + \frac{\alpha}{2N} F^2, \quad \frac{1}{F} \frac{dF}{d\tau} = \frac{2\lambda}{1-\lambda} - \alpha, \quad (18.53)$$

and when $\alpha N(0)/N$ is small, it may be shown that the solutions of these equations yields the approximate solution for the frequencies as

$$\frac{P_i}{N(0)} \approx \chi_0 e^{-(i-1+\alpha)\tau} (1 - e^{-\tau})^2, \quad \tau > 0. \quad (18.54)$$

The approximation is compared with numerical solutions for an initially unimolecular population with $\alpha = 2$, $\chi_0 = 100$, in Figure 18.20.

When considering volatilization, one must be careful. Simply calculating the first partial moment will give incorrect results since recombination of molecules with degrees of polymerization in the range 1 to $m_v - 1$ will introduce molecules into the population with degrees of polymerization greater than m_v (unlike the cases of scission-only mechanisms considered earlier). Therefore, we must stipulate that $P_i(0) = 0$ and $dP_i/d\tau = 0$ for $1 \leq i \leq m_v - 1$. In general, the effect of recombination is to slow down the rate of mass loss, as Figure 18.21 shows. Here, we see specific mass plotted as a

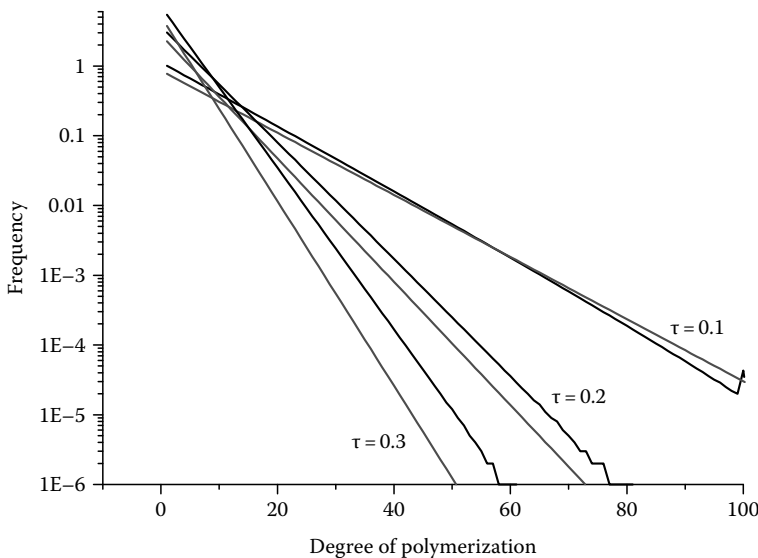


FIGURE 18.20 Approximate solution for simultaneous random scission and recombination.

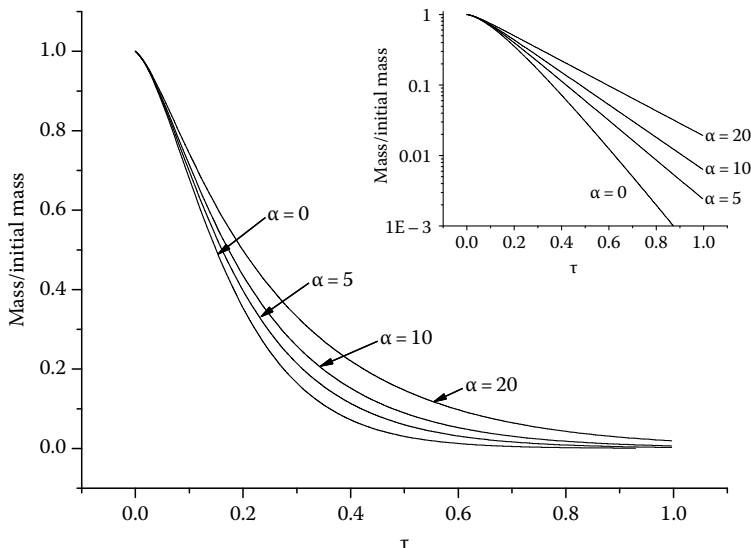


FIGURE 18.21 Random scission with recombination for different values of $\alpha = k^{(+)}/k^{(\tau)}$ (inset is plotted on a log scale).

function of τ for various values of α for random scission with recombination. The inset graph shows mass plotted on a logarithmic axis and confirms that apart from the initial period, mass loss remains exponential as α increases.

18.6 CHAIN STRIPPING

Chain stripping is a mechanism whereby side groups are lost from the main polymer chain, leaving the backbone intact. It is important in the thermal degradation of PVC, where the initial mass loss corresponds to dehydrochlorination: $[-\text{CH}_2\text{CHCl}-]_n \rightarrow [-\text{C}_2\text{H}_2-]_n + n\text{HCl}$. Let $P_i^{(j)}$ denote the number of i -mers with j side groups in the population. Initially, suppose that there are n_i side groups, so that $0 \leq j \leq n_i$. Thus, the total number of i -mers is $P_i = \sum_{j=0}^{n_i} P_i^{(j)}$. Now, if $k^{(s)}$ is the rate of bond breaking by chain stripping and since there are a total of $jP_i^{(j)}$ bonds available, the PBEs for chain stripping of i -mers are

$$\frac{dP_i^{(j)}}{d\tau} = \begin{cases} P_i^{(1)}, & j=0, \\ -jP_i^{(j)} + (j+1)P_i^{(j+1)}, & 1 \leq j < n_i, \\ -n_i P_i^{(n_i)}, & j = n_i. \end{cases} \quad (18.55)$$

Here $d\tau/dt = k^{(s)}$. It is a straightforward matter to show that the overall number of i -mers in the population is conserved, i.e., $dP_i/d\tau = 0$ and that the appropriate solution of these equations with initial conditions $P_i^{(j)}(0) = 0$, $0 \leq j < n_i$, $P_i^{(n_i)} = P_i$ is

$$\frac{P_i^{(0)}}{P_i} = (1 - e^{-\tau})^{n_i}, \quad (18.56)$$

$$\frac{P_i^{(j)}}{P_i} = e^{-j\tau} C_j^{n_i} (1 - e^{-\tau})^{n_i - j}, \quad 1 \leq j < n_i, \quad (18.57)$$

$$\frac{P_i^{(n_i)}}{P_i} = e^{-n_i\tau}. \quad (18.58)$$

Here, $C_j^{n_i}$ denotes the binomial coefficient $n_i!(j!(n_i - j)!)$. Now if $M^{(s)}$ denotes the mass of a side group that is eliminated and $M^{(l)}$ denotes the mass of a repeat unit in the chain-stripped molecule, then the total mass of i -mers M_i is given approximately by

$$M_i = \sum_{j=0}^{n_i} (iM^{(l)} + jM^{(s)})P_i^{(j)} = iM^{(l)}P_i + M^{(s)} \sum_{j=0}^{n_i} jP_i^{(j)}. \quad (18.59)$$

So, defining $\mu^{(i)} = \sum_{j=0}^{n_i} jP_i^{(j)}$, it is easy to show from the PBEs that $d\mu^{(i)}/d\tau = -\mu^{(i)}$, from which it follows that $\mu^{(i)} = n_i P_i e^{-\tau}$. Hence, the mass of i -mers is given by $M_i = (iM^{(l)} + n_i e^{-\tau} M^{(s)})P_i$ and the total mass M of a population of initial degree of polymerization n is $M = M^{(l)} \sum_{i=1}^n iP_i + e^{-\tau} M^{(s)} \sum_{i=1}^n n_i P_i$. If we let the initial mass be M_0 and the final mass be M_∞ , then the specific mass is given by

$$\frac{M}{M_0} = \frac{M_\infty}{M_0} + \left(1 - \frac{M_\infty}{M_0}\right) e^{-\tau}. \quad (18.60)$$

If we aim to compare specific mass with constant heating rate TG data, then we may make further simplifications. Using expression 18.23 mentioned earlier to approximate τ , and defining x and y by

$$x = -\frac{1}{T}, \quad y = \log \left\{ -\frac{1}{T^2} \log \left(\frac{M - M_\infty}{M_0 - M_\infty} \right) \right\}, \quad (18.61)$$

it follows that a plot of x vs. y should be linear with gradient T_A and y-intercept $\log(A/HT_A)$. Now for the particular case of PVC, we have that $M^{(l)} = M^{(C_2H_2)} = 26$ g/mol, $M^{(s)} = M^{(HCl)} \approx 37$ g/mol, and $n_i = i$, so that the specific mass for the chain-stripping model is $M/M_0 = 0.41 + 0.59e^{-\tau}$. Figure 18.22 shows

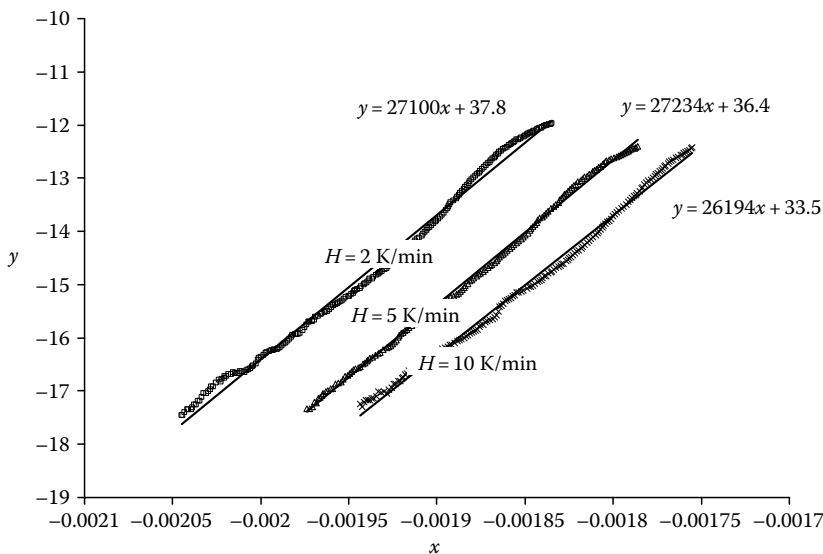


FIGURE 18.22 Analysis of constant heating rate TG data for the dehydrochlorination step of PVC.

TABLE 18.4
Arrhenius Parameters
for the Dehydrochlorination
of a PVC Sample

H (K/min)	T_A (K)	$J = \ln(A)$
2	27,100	44.6
5	27,234	44.1
10	26,194	41.9

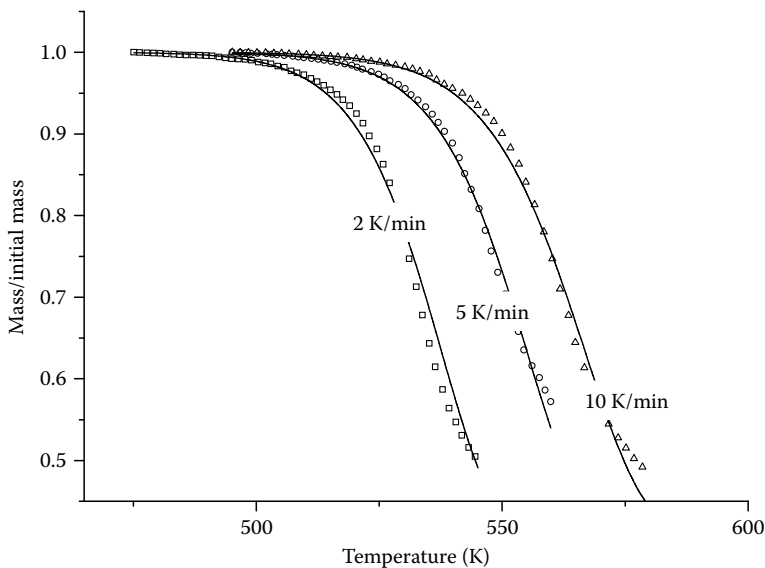


FIGURE 18.23 Comparison of the PBM for chain stripping with dehydrochlorination of PVC in constant heating rate TGA.

a plot of x vs. y for PVC samples (Sigma–Aldrich 189588) at three different heating rates (2 K/min, 5 K/min, and 10 K/min). The derived values of activation temperatures and $J = \ln(A)$ are convincingly similar (with the possible exception of J for the 10 K/min case) and are shown in Table 18.4. The graph in Figure 18.23 compares the specific mass as predicted by the chain-stripping model with the TG data using the Arrhenius parameters in Table 18.4. Note that the experimental curves do not lose all of the 59% of mass that is possible through chain stripping alone—presumably through the effect of char-forming cross-linking reactions.

18.7 CONCLUSION

Although the application of population balance methods to thermal degradation is not straightforward, it has the great benefit of being scientifically justifiable. All of the four main thermal degradation processes may be modeled using population balance methods and agreement with TG data for simple mechanisms appearing to be good. Furthermore, the insights gained from a detailed analysis of thermal degradation are of enormous practical help to those seeking to model combustion and ignition processes. The additional complexity of a PBM of thermal degradation presents

no significant computational challenges and is certainly no worse than a detailed kinetic model of gas phase oxidation processes (where perhaps a few hundred reactions are explicitly described). The population balance approach also has the potential advantage of providing detailed information about the composition of volatile species as they form—thereby giving better input data for gas phase oxidation models and so enabling more detailed descriptions of ignition. The challenge now, however, is twofold. PBMs must be formulated to model the complex decomposition behavior of interesting polymers. Also, it remains to incorporate population balance methods into detailed pyrolysis models so that realistic fire scenarios may be modeled.

REFERENCES

1. Cullis, C. F. and Hirschler, M. M. *The Combustion of Organic Polymers*, Clarendon Press, Oxford, U.K., 1981.
2. Madorsky, S. L. *Thermal Degradation of Organic Polymers*. Wiley, New York, 1964.
3. Hatakeyama, T. and Quinn, F. X. *Thermal Analysis: Fundamentals and Applications to Polymer Science*, 2nd Edn., Wiley, Chichester, U.K., 1999.
4. Staggs, J. E. J. Simple mathematical models of char-forming polymers. *Polymer International* 2000; 49: 1147.
5. Anthony, G. M. Kinetic and chemical studies of polymer cross-linking using thermal gravimetry and hyphenated methods. Degradation of polyvinylchloride. *Polymer Degradation and Stability* 1999; 64: 353.
6. Bockhorn, H., Hornung, A., Hornung, U., and Weichmann, J. Kinetic study on the non-catalysed and catalysed degradation of polyamide 6 with isothermal and dynamic methods. *Thermochimica Acta* 1999; 337: 14.
7. Bockhorn, H., Hornung, A., Hornung, U., and Schwaller, D. Kinetic study on the thermal degradation of polypropylene and polyethylene. *Journal of Analytical and Applied Pyrolysis* 1999; 48: 17.
8. Bockhorn, H., Hornung, A., and Hornung, U. Mechanisms and kinetics of thermal decomposition of plastics from isothermal and dynamic measurements. *Journal of Analytical and Applied Pyrolysis* 1999; 50: 25.
9. Howell, B. A. The application of thermogravimetry for the study of polymer degradation. *Thermochimica Acta* 1989; 148: 375.
10. Lehrle, R. S., Atkinson, D., Cook, S., Gardner, P., Groves, S., Hancox, R., and Lamb, G. Polymer degradation mechanisms: New approaches. *Polymer Degradation and Stability* 1993; 42: 281.
11. Shyichuk, A. V. Polymer degradation with simultaneous scission and crosslinking. Weight-average molecular weight changes in the case where crosslinking rate surpasses scission rate. *European Polymer Journal* 1998; 34: 113.
12. Wilkie, C. A. TGA/FTIR: An extremely useful technique for studying polymer degradation. *Polymer Degradation and Stability* 1999; 66: 301.
13. Holland, B. J. and Hay, J. N. The kinetics and mechanisms of the thermal degradation of poly(methyl methacrylate) studied by thermal analysis-Fourier transform infrared spectroscopy. *Polymer* 2001; 42: 4825.
14. Holland, B. J. and Hay, J. N. The value and limitations of non-isothermal kinetics in the study of polymer degradation. *Thermochimica Acta* 2002; 388: 253.
15. Liu, N. A. and Fan, W. C. Critical consideration on the Freeman and Carroll method for evaluating global mass loss kinetics of polymer thermal degradation. *Thermochemica Acta* 1999; 338: 85.
16. Staggs, J. E. J. Thermal degradation of solids using single-step first-order kinetics. *Fire Safety Journal* 1999; 32: 17.
17. Emsley, A. M. and Heywood, R. J. Computer modelling of the degradation of linear polymers. *Polymer Degradation and Stability* 1995; 49: 145.
18. Platowski, K. and Reichert, K. Application of Monte Carlo methods for modelling of polymerisation reactions. *Polymer* 1999; 40: 1057.
19. McCoy, B. J. and Madras, G. Evolution to similarity solutions for fragmentation and aggregation. *Journal of Colloid & Interface Science* 1998; 201: 200.
20. McCoy, B. Distribution kinetics for temperature-programmed pyrolysis. *Industrial and Engineering Chemistry Research* 1999; 38: 4531.

21. McCoy, B. J. and Madras, G. Discrete and continuous models for polymerization and depolymerization. *Chemical Engineering Science* 2001; 56: 2831.
22. McCoy, B. Polymer thermogravimetric analysis: Effects of chain-end and reversible random scission. *Chemical Engineering Science* 2001; 56: 1525.
23. Madras, G. and McCoy, B. Numerical and similarity solutions for reversible population balance equations with size-dependent rates. *Journal of Colloid and Interface Science* 2002; 246: 356.
24. Simha, R., Wall, L. A., and Blatz, J. Depolymerisation as a chain reaction. *Journal of Polymer Science* 1950; 5: 615.
25. Boyd, R. H. Theoretical depolymerization kinetics in polymers having an initial "most probable" molecular weight distribution. *Journal of Chemical Physics* 1959; 31: 321.
26. Boyd, R. H. The effect of changing volume in the kinetics of bulk polymer degradation. *Journal of Polymer Science* 1961; 49: S1.
27. Staggs, J. E. J. A continuous model for vaporization of linear polymers by random scission and recombination. *Fire Safety Journal* 2005; 40: 610.
28. Staggs, J. E. J. Modelling random scission of linear polymers. *Polymer Degradation and Stability* 2002; 76: 37.
29. Staggs, J. E. J. Modelling end-chain scission and recombination of linear polymers. *Polymer Degradation and Stability* 2004; 85: 759.
30. Staggs, J. E. J. Discrete bond-weighted random scission of linear polymers. *Polymer* 2006; 47: 897.
31. Kostoglou, M. Mathematical analysis of polymer degradation with end-chain scission. *Chemical Engineering Science* 2000; 55: 2507.
32. Guaita, M., Chiantore, O., and Costa, L. Changes in degree of polymerisation in the thermal degradation of polystyrene. *Polymer Degradation and Stability* 1985; 12: 315.
33. Staggs, J. E. J. Population balance models for the thermal degradation of PMMA. *Polymer* 2007; 48: 3868.
34. Inaba, A. and Kashiwagi, T. A calculation of thermal degradation initiated by random scission. I. Steady state radical concentration. *Macromolecules* 1986; 19: 2412.
35. Inaba, A. and Kashiwagi, T. A calculation of thermal degradation initiated by random scission. II. Unsteady state radical concentration. *European Polymer Journal* 1987; 23: 871.
36. Inaba, A., Kashiwagi, T., and Brown, J. E. Effects of initial molecular weight on thermal degradation of poly(methyl methacrylate): Part 1—Model 1. *Polymer Degradation and Stability* 1988; 21: 1.
37. Seinfeld, J. H. and Pandis, S. N. *Atmospheric Chemistry and Physics. From Air Pollution to Climate Change*. Wiley, New York, 1998; 12.
38. Jury, E. I., *Theory and Application of the Z-Transform Method*, Krieger Pub Co., Huntington, New York, 1973.

19 Micro- to Mesoscale Testing and Modeling for Nanocomposite Polymers in Fires

Michael A. Delichatsios and Jianping Zhang

CONTENTS

19.1	Introduction.....	510
19.2	Materials	512
19.3	Microscale Experiments and Measurements	512
19.3.1	Rheology–Viscosity (Affecting Dripping and Structure of the Char Layer).....	512
19.3.2	TGA/DSC and Modulated DSC	515
19.3.2.1	TGA/DSC for Heat of Melting and Heat of Pyrolysis	515
19.3.2.2	Modulated DSC for Specific Heat, Heat of Melting	515
19.3.3	TGA/FTIR/ATR	516
19.3.3.1	Degradation Behaviors in N ₂	516
19.3.3.2	Degradation Behaviors in Air	517
19.3.3.3	TG/FTIR for Gas Analysis.....	518
19.3.3.4	TG/ATR for Polybutylene Terephthalate for the Structure of Condensed Phase	521
19.4	Mesoscale Experiments and Measurements	523
19.4.1	Tube Furnace.....	523
19.4.1.1	Experimental Details.....	523
19.4.1.2	Results and Discussions	524
19.4.2	Cone Calorimeter.....	525
19.4.2.1	Experimental Details.....	525
19.4.2.2	Results and Discussions	525
19.4.3	Universal Flammability Apparatus	530
19.4.3.1	Experimental Details.....	530
19.4.3.2	Results and Discussions	531
19.5	Numerical Prediction of Polymer Behavior in the Cone Using TGA Measurements in Nitrogen	531
19.5.1	Kinetic Parameters in the TGA	531
19.5.1.1	Predicted Surface Temperature History in the Cone for TGA Obtained Pyrolysis Rate.....	532
19.5.1.2	Predicted Mass Loss in the Cone Calorimeter.....	533
19.6	Numerical Model for the Pyrolysis of Polymer Nanocomposites.....	533
19.6.1	Mathematical Formulations	534
19.6.2	Numerical Details	537
19.6.3	Deduced Effective Thermal Properties for the PA6 Nanocomposite	537

19.6.4	Results and Discussions	539
19.6.4.1	Derived Correlation between the Heat Flux Ratio and the Pyrolyzed Depth.....	539
19.6.4.2	Predicted Mass Loss Rates.....	540
19.7	Further Validation of the Model	541
19.7.1	Application to EVA and PBT Nanocomposites	541
19.7.1.1	Material and Experimental Details.....	541
19.7.1.2	Experimental Ignition Times	541
19.7.1.3	Deduced Effective Thermal Properties.....	542
19.7.1.4	Results and Discussions	542
19.7.2	Extension of the Model for Different Loadings of Nanoclay	544
19.8	Conclusions	547
	Acknowledgments.....	548
	References.....	548

19.1 INTRODUCTION

A challenge for fire safety is to reduce the fire hazards (i.e., heat fluxes and toxicity) by reducing the flammability of the source material through the design and modification of commonly used materials such as polymers to make them more fire resistant and less toxic than the base polymer materials. The modification of a polymer can be obtained by the addition of fire-retardant chemicals and nanoparticles. Because it is difficult to make new nanocomposite polymers in large quantities, it is essential to determine the fire behavior of new formulations (even hopefully in large scale) using microscale quantities (mg mass) and experimental methods such as thermogravimetric analyzer (TGA), differential scanning calorimeter (DSC), modulated DSC (MDSC), Fourier transform infrared radiometry (FTIR), attenuated total reflection (ATR), and rheometry that can provide information about the degradation of the solid phase and the composition of the gaseous products. Although these measurements have been available for a long time, it is only in the last decade (starting with a proposal to FAA) that a concerted effort is being made to quantitatively relate these microscale measurements with measurements in mesoscale apparatus (such as the tube furnace, cone, and Universal Flammability Apparatus (UFA)). This challenge, progress, and needs for further work are summarized in this chapter with the further step of relating the mesoscale measurements to large-scale fires (e.g., Single Burning Item test) left out. The present subject is focused on nanocomposite polymers, although some comparative data are included for nanocomposite polymers that are mixed with phosphorous-based intumescent fire retardants (e.g., Exolit). Rheometry and TGA/ATR for the solid residue can be used to characterize melting and consistency of char. TGA/DSC/MDSC provide information about the thermal and transport properties and heats of melting and pyrolysis. TGA /FTIR (or mass spectroscopy (MS), not discussed in this chapter) provide the composition of the pyrolysis gases. These measurements are consistent and can be used for the quantitative prediction of behavior in the mesoscale experiments (Tube furnace, cone, UFA). However, the tendency of nanoparticle additives to form a layer as soon as pyrolysis starts (in mesoscale or large-scale experiments) requires a new method and model to characterize the reduction of mass loss rates (MLRs) caused by the shielding effects of the layer.

This chapter presents a review of the progress relating flammability measurements and properties deduced from microscale experiments of milligram size samples with measurements obtained from mesoscale experiments of sample size about 100 g. We present a comprehensive and integrated approach based on sound scientific method, yet practical for assessing the flammability of nanocomposite polymers in the early stage of their formulations where only milligram order quantities are available. Our approach does not extend to quantum chemistry or molecular dynamics to

determine flammability properties *ab initio*, because their use is still not feasible even in simplified situations. We also do not include in this chapter how the properties determined from microscale and mesoscale experiments can be used to determine the fire behavior in large real fires, where the turbulent buoyancy flow can change the flammability impact for different materials concerning the generation of heat fluxes and production of toxicity gases such as CO and HCN; these studies will be included in other reports and papers.

The development of new materials and new fire retardants to replace brominated fire retardants makes it imperative to develop new methods to characterize their flammability performance in milligram quantities and also to design fire-safe materials *ab initio*. We envision to effect this assessment by developing a methodology that can lead to a material flammability certificate. Such a certificate will allow the prediction of the fire behavior of materials in real fires including fire growth and toxic (smoke and gases) production. This methodology has emerged from long experience in material flammability and fire dynamics by the authors and others, and is supported by recent work in the European PREFIRE NANO, FIRENET project, and EPSRC (United Kingdom) and other industrial grants. The contribution of participants in these projects is greatly appreciated.

A proposed list of measurements follows together with the appropriate measuring equipment:

Microscale experiments:

- Tendency to dripping (based on rheology)
- Solid degradation in milligram scale (using TG, DSC, and MDSC for heat of pyrolysis and specific heat)
- Solid residue analysis at different temperatures using TG /ATR
- Gaseous products in milligram scale (using TGA/FTIR/MS for toxicity and ignition kinetics)

Mesoscale experiments:

- Tube furnace (toxicity)
- Cone calorimeter in standard atmosphere (to assess the effectiveness of nanoparticles and intumescent fire retardants and also measure heat release rates (HRRs) and product yields)
- Special calorimeter (UFA to assess combustion in under-ventilated conditions and evaluate tendency for dripping and char strength by performing experiments in vertical orientation)

It is intended to use these properties for the assessment of alternative flame retardants (FRs) (including nanoparticles, phosphates, and inorganic metal oxides) in comparison with brominated fire retardants by quantitatively assessing:

- Tendency to dripping
- Low HRR
- Late ignition
- Strength of char (e.g., to avoid erosion)
- Low smoke including the smoke point of the material
- Low toxicity and possibly, corrosivity

Finally, based on these properties the global effect of these materials in fire can be addressed by quantifying:

- Their behavior in standard tests (UL94, LOI, SBI)
- Their behavior in large fires
- Impact on life and property safety and damage
- Recyclability

While these tasks are not included in this chapter, by understanding all the basic fire performances outlined in the chapter one can develop correlations and understandings on material behavior in standard and large fire tests as well as life/property safety and recyclability.

19.2 MATERIALS

The materials included in this chapter for illustration are nanocomposite polymers combined with intumescent commercial phosphorous fire retardants. In this chapter, different base polymers (e.g., PA6, PBT, PP, and EVA) are mentioned for illustrating the methodology but the focus will be on PA6. For the present purpose, the composition of a PA6 nanocomposite is described next to make the development of the present methodology more clear.

Polyamide 6 (PA6, by Rhodia) was modified with a nanoclay (NC) (Cloisite 30B by Southern Clay) and a FR chemical (OP1311 by Clariant). In total, combinations of the polymer (PA6), NC, and fire retardant (FR) provide four formulations, i.e., PA6, PA6/NC, PA6/FR, and PA6/NC/FR. In addition, commercially available PA6 nanocomposite with 2.5 wt % clay by UBE Chemical Co. was also used as a reference material. Compounds of all the materials were prepared at Centro di Cultura per l'Ingegneria delle Materie Plastiche (CDCMP) in Italy by melt blending in a Leistritz ZSE 27 co-rotating intermeshing twin screw (27 mm) extruder with length/diameter ratio of 40. The screw speed was set to 200 rpm, the mass flux at 10 kg/h and the processing temperature range from 210°C to 230°C. The polymer blend was loaded in the main feed and the fillers were added to the molten polymer by means of a gravimetric side feeder. The extruded materials were cooled in water and then pelletized. The compositions of all formulations are shown in Table 19.1.

The dispersion morphology of prepared materials was studied with a multitechnique approach, by means of rheology, scanning electron microscopy (SEM), x-ray diffraction (XRD), and nuclear magnetic resonance (NMR). The results of these tests showed that the so formulated PA6 nanocomposites used in the present study are fully exfoliated [1,2].

19.3 MICROSCALE EXPERIMENTS AND MEASUREMENTS

19.3.1 RHEOLOGY–VISCOSITY (AFFECTING DRIPPING AND STRUCTURE OF THE CHAR LAYER)

The dynamic viscosity and storage modulus of the melt polymer can characterize (1) the degree of dispersity (i.e., intercalation) of the nanocomposite polymer [1,2], (2) the dripping tendency in mesoscale or large-scale fires [3,4], and (3) the structure of the char layer formed during pyrolysis in mesoscale or large-scale fires [5–7].

Rheological measurements were carried out at a Dynamic Analyzer Rheometer RDA II from Rheometrics. Parallel plate geometry with a plate diameter of 25 mm was used to perform the tests where thin films of materials of 1 mm thickness were inserted. To ensure the viscoelastic

TABLE 19.1
Compositions of All PA6-Based Formulations

Material	Abbreviation	NC (wt %)	FR (wt %)
PA6	PA6	—	—
PA6 + OP1311	PA6 + FR	—	18
PA6 + Cloisite 30B	PA6 + NC	5	—
PA6 + OP1311 + Cloisite 30B	PA6 + FR + NC	5	18
PA6 + Clay (UBE)	PA6 + NC (UBE)	2.5	—

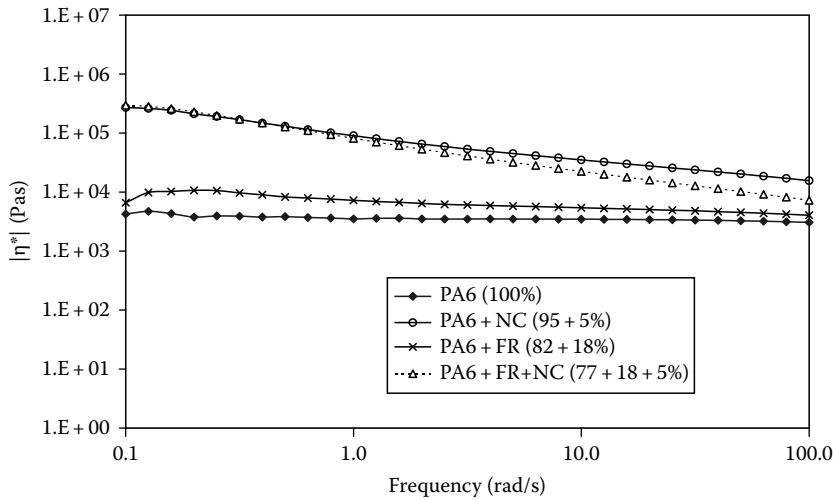


FIGURE 19.1 Complex viscosity curves for PA6, PA6 + NC, PA6 + FR, and PA6 + NC + FR.

region, linear rheological measurements were performed at a frequency range of 0.1–100 rad/s. Elastic complex viscosities (η^*) were obtained at 240°C. The temperature control was accurate to within $\pm 1^\circ\text{C}$. Experiments were conducted under a nitrogen atmosphere to avoid oxidative degradation of the specimen.

A comparison of the complex viscosities for PA6, PA6 + NC, PA6 + FR, and PA6 + NC + FR is shown in Figure 19.1. The steady-state viscosity behavior of PA6 shows perfect Newtonian behavior, whereas the absolute value of the melt viscosity of the PA6 + NC sample is significantly higher than that of neat PA6, particularly at low shear rates, indicating that the nanostructure of the nanocomposite consists of a percolated network superstructure of exfoliated platelets [1,2]. However, the complex viscosity of the PA6 + NC sample decreases sharply with increasing frequency, exhibiting pronounced shear thinning with a shear thinning component $\eta = -0.42$. This implies a higher extent of silicate exfoliation on the nanoscale with a macroscopic preferential orientation of clay layers [1,2]. This was also verified by XRD analysis of PA6 + NC, which shows complete disappearance of the clay peak, suggesting exfoliated nanodispersion within the polymer matrix.

The structural network formed in nanocomposites (PA6 + NC) is further emphasized by the behavior of the storage modulus (G'), which is extremely sensitive to morphological state. The storage (G') and loss (G'') moduli are plotted against frequency in Figure 19.2. Compared with PA6, the storage modulus of PA6 + NC is increased by a factor of 200. This behavior may be due to an elastic-dominant response of clay platelets on the rheological behavior at low frequencies. At low frequencies, the storage modulus is higher than the loss modulus, suggesting more solid-like behavior as compared with neat PA6. In contrast, at higher frequencies, the storage modulus is lower than the loss modulus indicating that the effect of clay particles on the rheological behavior is weak and that the segmental motion of polymer molecular chains is dominant. The frequency at which G'' crosses G' curve is called cross-over frequency and is characteristic of filler volume fraction.

With the addition of FR, the shear thinning component of PA6 + NC is further increased to $\eta = -0.56$. As shown in Figure 19.2c, the storage modulus for PA6 + NC + FR is slightly increased, whereas the loss modulus is in fact reduced. This type of rheological behavior may suggest that with increasing volume fraction the clay platelets or aggregates are more hindered in their rotation and movement, leading to a structure that can cause solid-like behavior. It can also be seen that with the

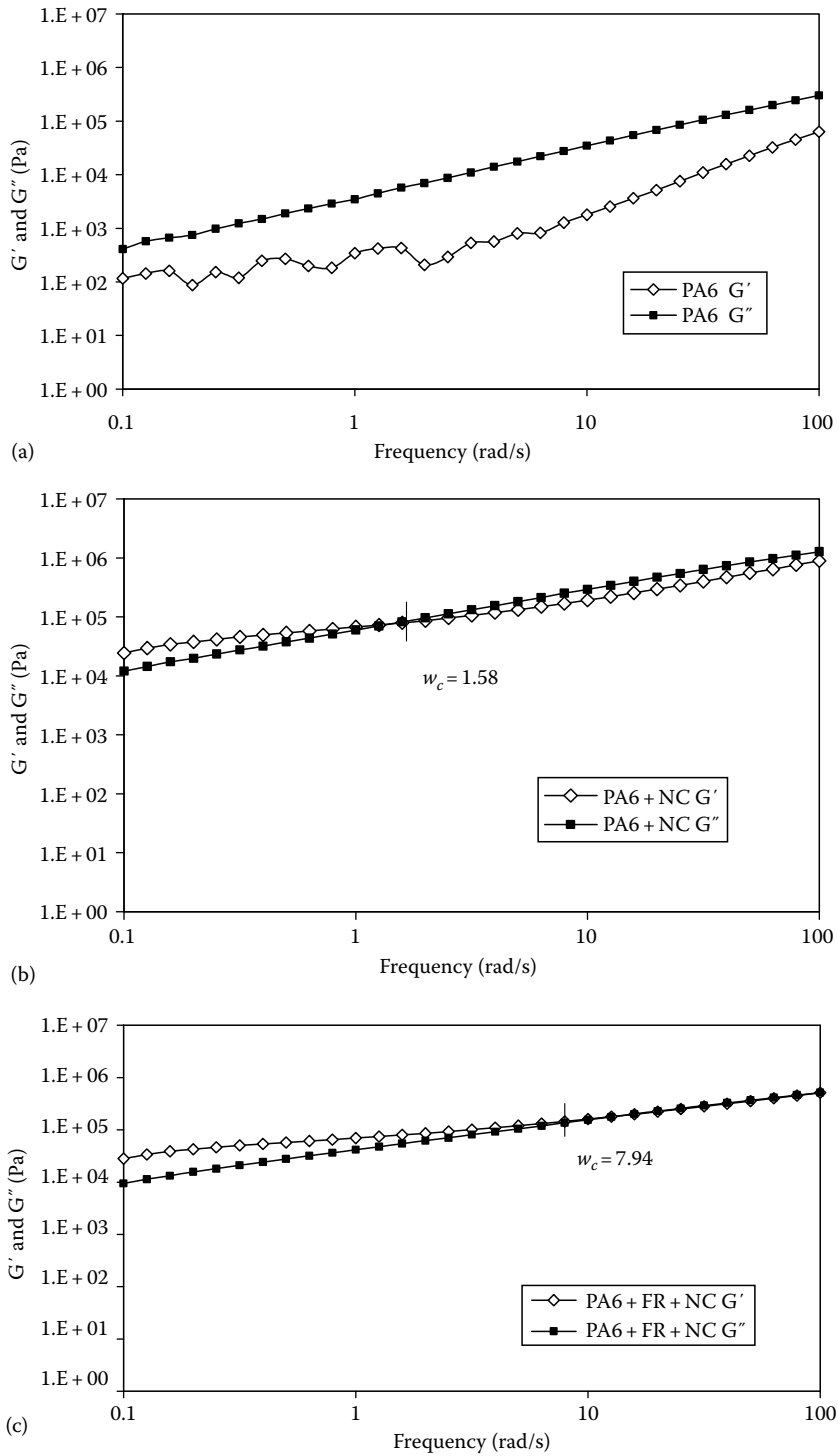


FIGURE 19.2 Storage modulus and loss modulus for (a) PA6, (b) PA6 + NC, and (c) PA6 + NC + FR.

formation of more solid-like network structure, the cross-over frequency for PA6 + NC + FR shifts toward a higher frequency 7.94 rad/s compared with 1.58 rad/s for PA6 + NC.

The melting behavior can be extracted from the dynamic viscosity [3,4]. The dynamic viscosity also affects the morphology of the char, which may improve the shielding efficiency from the fire by the nanoparticle layer formed on the polymer [5–7].

19.3.2 TGA/DSC AND MODULATED DSC

19.3.2.1 TGA/DSC for Heat of Melting and Heat of Pyrolysis

Table 19.2 summarizes properties measured by DSC (through heat flow measurements) for the materials in this illustration, including glass transition temperature, T_g , melting temperature, T_m , crystallization temperature, T_{crys} , heat of melting, ΔH_m , and heat of crystallization, ΔH_{crys} . The presence of clay in PA6 + NC(Cloisite 30 B) seems to have an effect merely on the phase (γ or α) formed and the temperature of crystallization, whereas PA6 + NC(UBE) does have a higher crystallization temperature, heat of melting, and heat of crystallization. Addition of FR seems to have no significant effects on these properties.

The heat of pyrolysis was measured at the University of Ulster using a Mettler Toledo TGA/SDTA851^e measuring module, with temperature accuracy $\pm 0.5^\circ\text{C}$ and temperature reproducibility of $\pm 0.3^\circ\text{C}$. All the samples weighted to a Mettler Toledo XS205 Dual Range Analytical Balance were approximately $20.0 \pm 0.10\text{ mg}$. The samples were placed in an alumina (Al_2O_3) pan (with no lid) of $70\mu\text{L}$ volume capacity and heated under a dynamic linear rate of $10^\circ\text{C}/\text{min}$, in $50\text{ mL}/\text{min}$ nitrogen (N_2) flow, from 25°C to 700°C . Measuring the heat of pyrolysis is challenging. The heats of pyrolysis obtained at Ulster are about half the value obtained in a recent paper, which we consider more reliable [8].

19.3.2.2 Modulated DSC for Specific Heat, Heat of Melting

MDSC, by varying the furnace temperature sinusoidally, has been used to determine the specific heat of PA6 materials (similar measurements have been performed for polypropylene nanocomposites). The materials were heated from -80°C to 250°C at $2^\circ\text{C}/\text{min}$. The reversible signal recorded during the experiment is related to the specific heat of the sample. The specific heat values versus temperature for the different PA6-based formulations are given in Figure 19.3, showing no significant differences between different formulations. The peaks noted on the specific heat curves correspond to the transition from the solid to the liquid states.

The measured values of specific heat and heat of melting (as listed in Table 19.2) have been used to predict the heating and pyrolysis behavior of 100 mg samples of the materials in the cone calorimeter in Section 19.6.

TABLE 19.2
Summary of Properties Measured by DSC at CDCMP
for Different Materials

Material	T_g ($^\circ\text{C}$)	T_m ($^\circ\text{C}$)			T_{crys} ($^\circ\text{C}$)	ΔH_m (J/g)	ΔH_{crys} (J/g)
		γ	α				
PA6	54	—	214	220	186	68	65
PA6 + NC	52	211	213	220	190	68	65
PA6 + NC (UBE)	53	208	217	220	193	79	70
PA6 + FR	54	—	214	219	186	63	62
PA6 + NC + FR	52	210	212	219	186	70	62

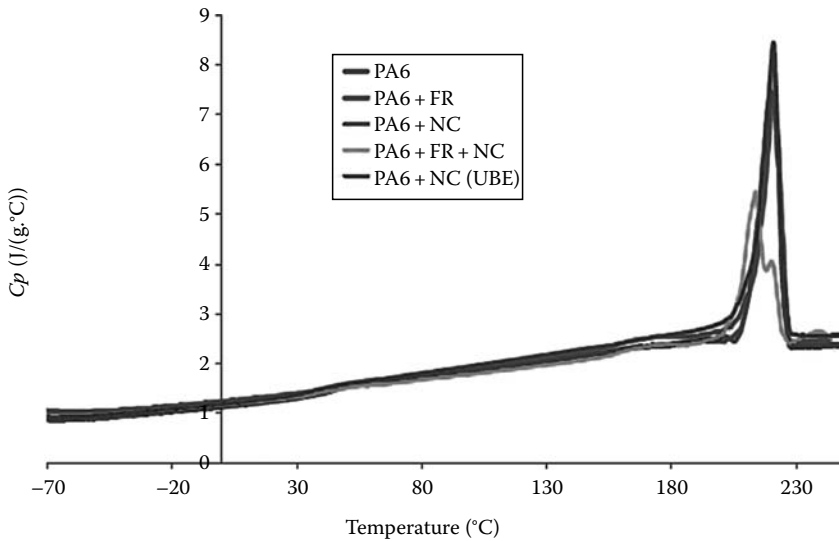


FIGURE 19.3 Measured specific heats of PA6 materials in the modulated DSC apparatus.

19.3.3 TGA/FTIR/ATR

Thermogravimetric analysis (TGA) experiments were carried out in nitrogen and air to evaluate the degradation of the polymers as a function of temperature. The TGA experiments were carried out in a Perkin Elmer Pyris 1 TGA apparatus, from 20°C–800°C with a heating rate of 20°C/min under a flow rate of 75 cm³/min of synthetic air or nitrogen. Each sample, in the form of powders weighing 10 ± 0.01 mg was placed in a platinum pan, vertically mounted in the TGA. In addition to the TGA measurements, the gaseous products of the degradation were measured by connecting an FTIR apparatus to the TGA. Finally, the condensed phase drawn from the TGA at different temperatures was analyzed by ATR. These results are described in the following.

19.3.3.1 Degradation Behaviors in N₂

Thermogravimetric analyses were first performed in nitrogen at different heating rates (1°C/min, 2°C/min, 5°C/min, 10°C/min, and 20°C/min). Figure 19.4 shows a comparison of the weight loss and weight loss rate for different formulations for the heating rate of 10°C/min. Note that similar results obtained for the other heating rates are not reported here for the sake of brevity. The curves for PA6 and PA6 + NC depict a one-stage degradation process. From the TGA curves, it seems that the inclusion of the NC alone does not alter the thermal degradation behavior of PA6 apart from its influence on increased char (residual mass) formation, as also observed by others [9,10]. The inclusion of FR chemical on the other hand (PA6 + FR and PA6 + FR + NC) changes the degradation behavior by lowering the degradation temperature (increased degradation rate) in an additional step around 300°C–350°C (15–20 min). This low temperature weight loss does not match the weight loss curve for OP1311 in Figure 19.5, which shows a single main degradation step with maximum weight loss rate at 460°C. This fact evidences for an interaction between PA6 matrix and OP 1311, leading to the low temperature weight loss stage.

It is likely that the presence of phosphorous or nitrogen in OP 1311 did catalyze the degradation of the PA6 polymer and thereby lowered the onset temperature. The mechanism is probably through electron capturing and transport by the more electropositive phosphorus or nitrogen (from the FR), from the hydrocarbons of the polymer monomer (ϵ -caprolactam) or to the competitive electron sharing with the amide group of the monomer. These more electropositive elements also promoted to some extent the char formation through network cross-linking.

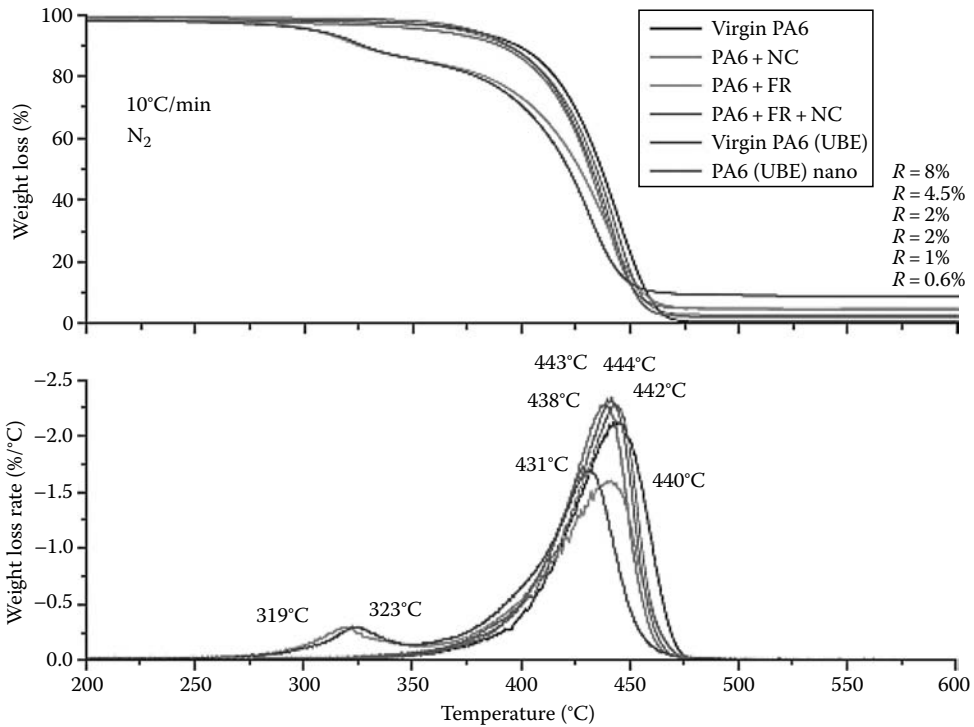


FIGURE 19.4 (See color insert following page 530.) TG/DTG curves of PA6, PA6 + NC, PA6 + FR, and PA6 + FR + NC in nitrogen.

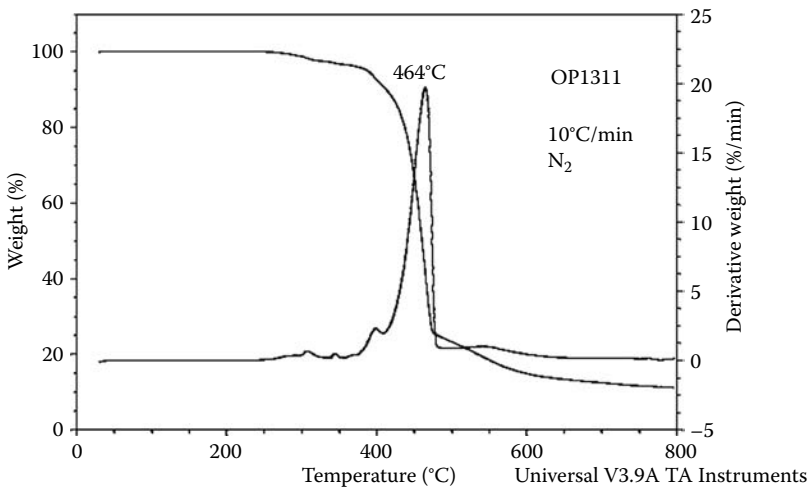


FIGURE 19.5 TG/DTG curves for OP1311 by Clariant.

19.3.3.2 Degradation Behaviors in Air

Figure 19.6 presents the TG differential thermo gravimetric (DTG) curves of the PA6 materials in air, again for a heating rate of 10°C/min. The thermal degradation of PA6 occurs in a two-step process. The first step between 300°C and 480°C corresponding to a weight loss of 89 wt% can be assigned to the release of NH₃, H₂O, CO₂, and caprolactam as main products [11]. The second step (480°C–600°C) corresponds to the decomposition in air of the char formed during the first step.

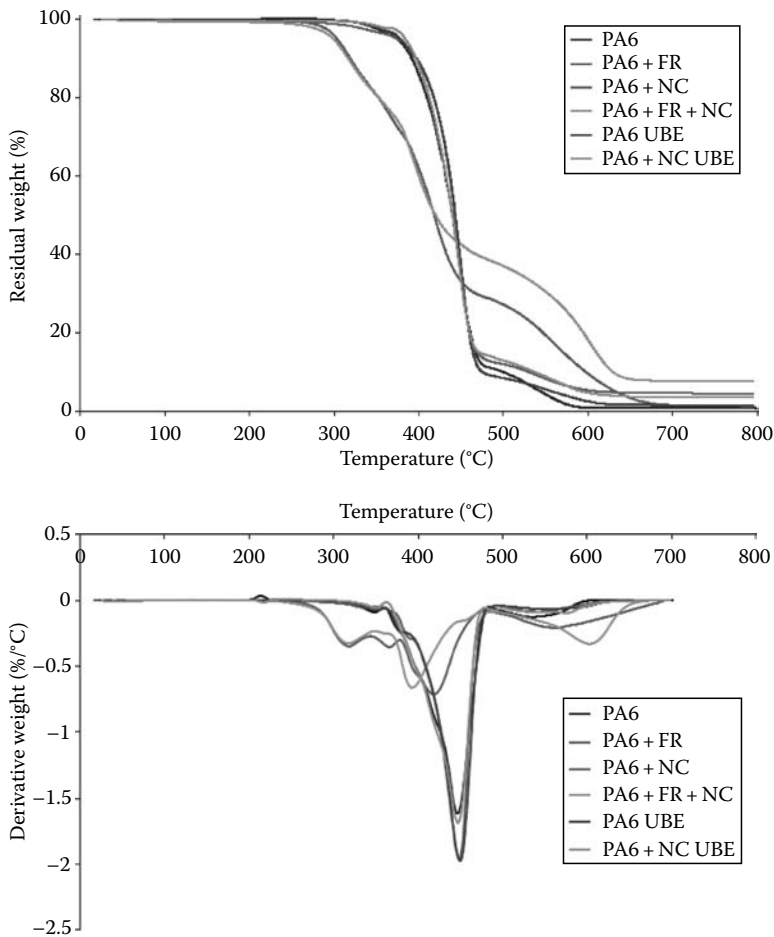


FIGURE 19.6 (See color insert following page 530.) TG/DTG curves of PA6, PA6 + NC, PA6 + FR, and PA6 + FR + NC in air.

The curves of PA6 and PA6 + NC are very similar, indicating again that the presence of nanoparticles does not modify the thermal stability of PA6. The fire-retarded formulations, in contrast, present three main steps of degradation. Between 250°C and 480°C (first two steps of degradation) the materials are less thermally stable than PA6, but then between 480°C and 670°C (third step), a much higher residue is maintained for both intumescent formulations with and without clay. It seems that more carbonaceous residue is formed during the earlier stage of degradation and that the decomposition of the formed residue in air is slower than for pure PA6. The incorporation of nanoparticles in the PA6 + OP1311 formulation improves the char strength.

19.3.3.3 TG/FTIR for Gas Analysis

The TG apparatus was coupled with a Thermo Nicolet NEXUS 470 FTIR using a custom made connection. The TG/FTIR setup involved a modification of the glassware, allowing the heated transfer line from FTIR to be extended through an open fitting in the enclosed glassware. This setup allowed sampling of gases just above the degrading sample. The gas cell had a volume of 49 cm³ and 17 cm optical path length. To limit the effect due to condensation, the 1.0 m long transfer line was heated to 200°C, while the TGA interface was heated to 240°C. FTIR measurements were carried out in a wavelength range of 400–4000 cm, with 16 scans and resolutions of 4 per cm.

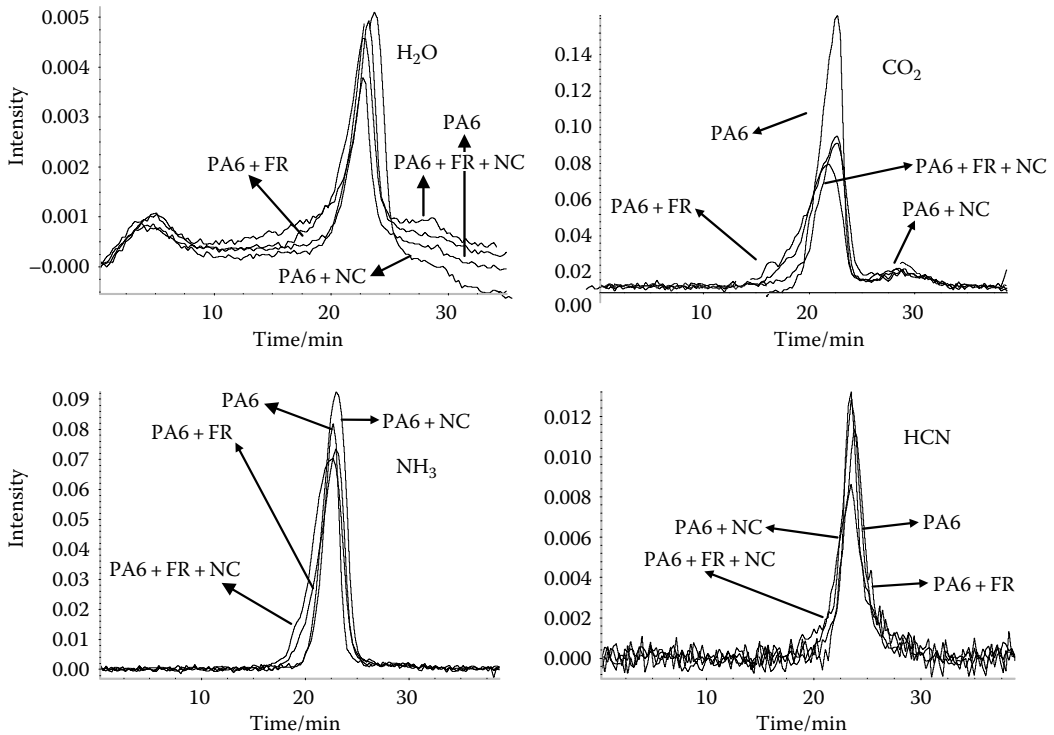


FIGURE 19.7 TG/FTIR: Specific evolved gas profiles of H_2O , CO_2 , NH_3 , and HCN in nitrogen.

The specific gas profiles were obtained by integrating over the wavelength as a function of time. The results of H_2O , CO_2 , ammonia (NH_3), and hydrogen cyanide (HCN) in nitrogen are shown in Figure 19.7, while those in air in Figure 19.8. For comparison purpose, all values were normalized by the total mass loss in the TGA. The specific evolved gas profiles of different gases in nitrogen are very similar for different materials, except that a much higher production of CO_2 is observed for PA6 and a decrease of HCN production is found for PA6 + FR + NC. On the other hand, the specific evolved gas profiles in air are quite different for different materials. Noticeably, the FR-contained materials yield less H_2O and HCN. For CO_2 , there appears a shift of the peak values for the FR-containing materials, indicating that in the second step the degradation of the FR produces a lot of carbon dioxide. This is consistent with the finding in Figure 19.7 that there is a drastic increase of production of CO_2 compared with H_2O . Another important observation is that the FR reduces the production of CO in the first step considerably, although it does promote CO in the second step. Finally, the FR-containing materials have slightly higher NH_3 production than non-FR materials.

In Table 19.3, the total gas evolved for different species was obtained by integrating the instantaneous values in time. In nitrogen, the amount of H_2O evolved increases with the inclusion of the NC when PA6 is compared with PA6 + NC and PA6 + FR with PA6 + FR + NC. This is likely caused by the liberation of water from clay. The same trend is observed for NH_3 while the opposite trend is apparent for CO_2 . In the case of PA6 + FR + NC, the increase in NH_3 might be partly caused by the evolution of water and consequent hydrolysis of the triazine ring, which in subsequent steps produces cyanuric acid and finally ammonia and carbon dioxide. The decreased levels of CO_2 might be related to a difference in the degradation pathways and possibly trapping of hydrocarbons and production of an aromatic char structure [12]. In the air, the fractions will depend on oxidation

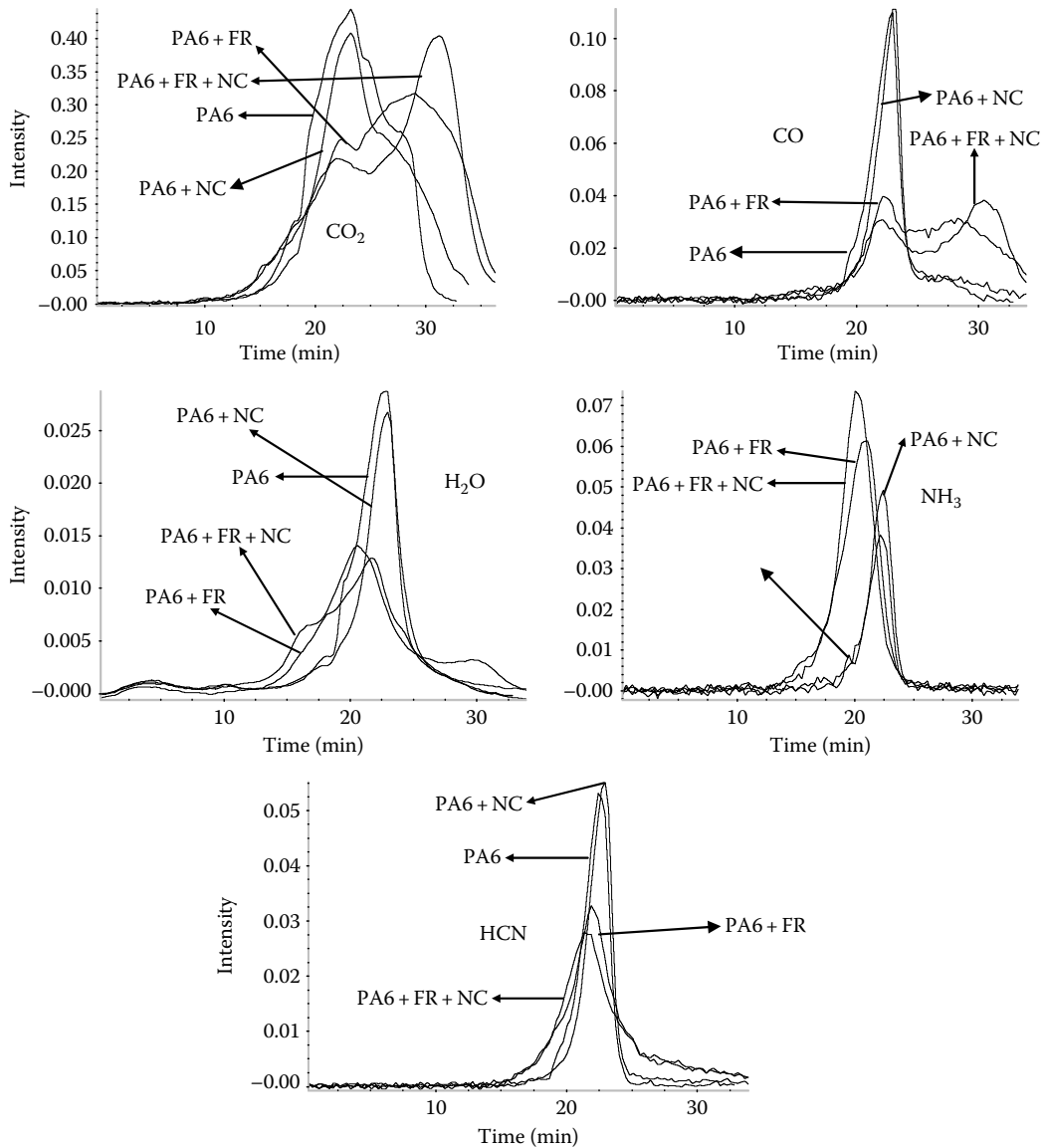


FIGURE 19.8 TG/FTIR: Specific evolved gas profile of CO_2 , CO , H_2O , NH_3 , and HCN in air.

reactions. The increased amounts of CO_2 produced by the FR samples are believed to be a function of degradation of the intermediate char at higher temperatures. Also the FR does not contribute to significant increase of HCN either in N_2 or air.

The main findings of the TG/FTIR study are:

1. The TGA results indicate that the curves for PA6 and PA6 + NC depict one-step degradation, whereas PA6 + FR and PA6 + FR + NC show two-stage decomposition process under nitrogen. The inclusion of NC alone does not alter the thermal degradation of PA6 apart from its influence on increased char (residual mass) formation. On the other hand, FR changes the degradation behavior by lowering the degradation temperature in PA6 + FR and PA6 + FR + NC composites. It is observed that a lot of FR goes to the gas phase as diethylphosphinic acid.

TABLE 19.3
TG/FTIR: Total Integrated (Absorption) Values of the Specific Gas Profiles in Nitrogen and Air Atmospheres

Atmosphere	Gas	Wave Number Range/Peak (cm ⁻¹)	Baseline (cm ⁻¹)	Integrated Values/Mass Loss			
				PA6	PA6 + NC	PA6 + FR	PA6 + FR + NC
N ₂	H ₂ O	1507	1500–1520	0.08	0.11	0.12	0.14
	CO ₂	661–675	661–675	2.55	1.71	2.21	1.81
	NH ₃	3315–3341	3315–3341	1.02	1.59	1.42	1.75
	HCN	710–715	710–715	0.11	0.12	0.11	0.12
Air	H ₂ O	1507	1500–1520	0.76	0.65	0.56	0.75
	CO ₂	661–675	661–675	23.5	22.2	29.0	29.0
	NH ₃	3315–3341	3315–3341	0.62	0.82	1.62	1.83
	HCN	710–715	710–715	0.84	0.89	1.06	1.04
	CO	2030–2142	2030–2142	2.07	2.05	2.44	2.50

- All the composites (PA6, PA6 + FR, PA6 + NC and PA6 + FR + NC) show a two-step decomposition process; the second step degradation step is due to transient char formation.
- The main gases evolved from PA6 and PA6 + NC in nitrogen are ϵ -caprolactam, hydrocarbons, carbon dioxide, water, and ammonia. Other composites namely PA6 + FR and PA6 + FR + NC evolve the same volatiles with an additional phosphorus containing species. PA6 + FR yields diethylphosphinic acid (from aluminum diethylphosphinate), and the water and carbon dioxide arise from the decomposition of melamine polyphosphate through condensation and hydrolytic decomposition.
- The products of thermo-oxidative are carbon monoxide, carbon dioxide, water, and HCN for all the composites. The second major degradation step, as observed by TGA in air, produces mainly carbon dioxide. In comparison with the results under nitrogen peaks due to ϵ -caprolactam and hydrocarbons are less in strength since the oxidation disrupts them by fragmenting them into carbon dioxide and water.
- The yield of toxic gas namely the HCN does not increase when phosphinate FR is used.

19.3.3.4 TG/ATR for Polybutylene Terephthalate for the Structure of Condensed Phase

While the condensed phase analysis of the residue (by FTIR-ATR) of PA6 is ongoing, we present the results of TG/ATR for polybutylene terephthalate (PBT)-modified by a phosphinate FR or nanoparticles (sepiolite) or the combination of phosphinate and nanoparticles.

The samples from the TGA tests were taken out at different temperatures, 25°C, 330°C, 360°C, 390°C, and 450°C, and analyzed by FTIR-ATR. The FTIR-ATR spectra of the sample at 25°C (virgin material) and its residue at 450°C are shown in Figure 19.9a–d for PA6, PA6 + NC, PA6 + FR, and PA6 + NC + FR, respectively.

Figure 19.9a–d shows that both the phosphinate FR and the nanoparticles change the structure of char compared with pure PBT. In contrast to the pure polymer, which leaves a char consisting of oligomeric components of PBT, the fire-retarded polymer (by phosphinate or nanoparticles) leaves a char consisting of polycyclic aromatic hydrocarbons (PAHs). The PAH structure of the char is expected to make the char stronger and capable to withstand erosion in full-scale fire tests. This observation is verified from the strength analysis of the char residue in intermediate scale

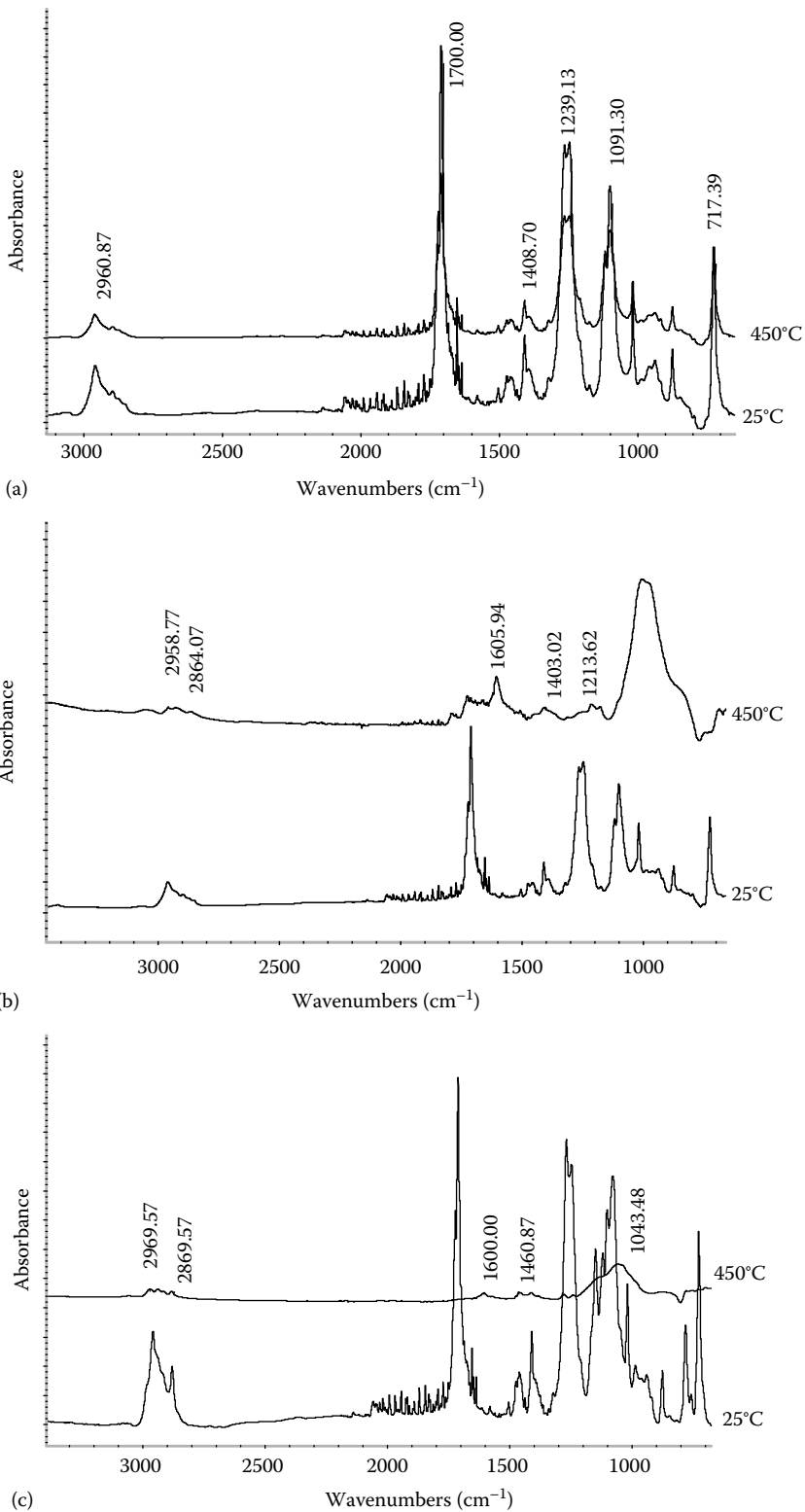


FIGURE 19.9 (a) FTIR (ATR) spectra of PBT at 25°C and its solid residue at 450°C; (b) TG/ATR: Spectra of PBT + NC at 25°C and its solid residue at 450°C; (c) TG/ATR: Spectra of PBT + FR at 25°C, and its solid residue at 450°C.

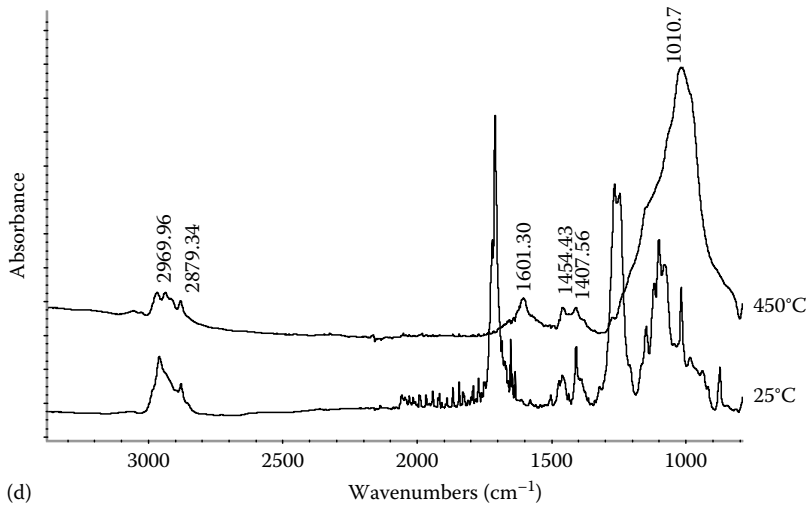


FIGURE 19.9 (continued) (d) TG/ATR: Spectra of PBT + NC + FR at 25°C, and its solid residue at 450°C.

flammability experiments such as those in the cone calorimeter, where char is formed behind the flames in the absence of oxygen. The main findings of the TG/ATR test are:

- The char at 450°C for PBT is an oligomeric component, whereas the char from PBT + FR and PBT + NC formulations comprise aluminum phosphinate and sepiolite, respectively along with PAHs. Specifically, the char from the formulation PBT + FR + NC consists of aluminum phosphinate, sepiolite and PAH with alkyl groups attached.
- During the degradation process, FR interacts chemically with PBT and degrades to ethylene and aluminum phosphinate. Above 390°C aluminum phosphinate reacts chemically with PBT. In contrast, the grafted organic molecule degrades from NC leaving behind the sepiolite network and the NC acting catalytically with PBT (See discussion in Sections 19.3 and 19.4).
- The char from PBT + FR + NC would be stronger than the char from pure PBT, because PBT upon degradation produces only the oligomers. The PAH structure of the char is expected to make the char stronger and capable of withstanding erosion in full-scale fire tests. This observation is verified from the strength analysis of the char residue in intermediate scale flammability experiments such as those in the cone calorimeter, where char is formed behind the flames in the absence of oxygen.

19.4 MESOSCALE EXPERIMENTS AND MEASUREMENTS

19.4.1 TUBE FURNACE

19.4.1.1 Experimental Details

The fire toxicity of each material has been measured under different fire conditions. The influence of polymer nanocomposite formation and fire retardants on the yields of toxic products from fire is studied using the ISO 19700 steady-state tube furnace, and it is found that under early stages of burning more carbon monoxide may be formed in the presence of nanofillers and fire retardants, but under the more toxic under-ventilated conditions, less toxic products are formed. Carbon monoxide yields were measured, together with HCN, nitric acid (NO), and nitrogen dioxide (NO₂) yields for PA6 materials, for a series of characteristic fire types from well-ventilated to large vitiated. The yields are all expressed on a mass loss basis.

19.4.1.2 Results and Discussions

Figure 19.10 shows the CO yields from the PA6-based materials under different fire conditions. This shows consistently lower CO yields for well-ventilated burning compared with small or large under-ventilated conditions [13]. Under well-ventilated conditions it shows increased CO yields for materials including NC or a fire retardant, but surprisingly the combined effect of both FR and NC result in lower CO yield. Under the more toxic under-ventilated conditions, overall the yields of CO are much higher, but there is little difference between small and large under-ventilated conditions, or on incorporation of either fire retardant or NC [13].

A similar trend to carbon monoxide is observed for PA6 for HCN. HCN yields increase with reduced ventilation, but is less sensitive to the furnace temperature. The NO_2 , NO, and HCN yields are presented in Figure 19.11.

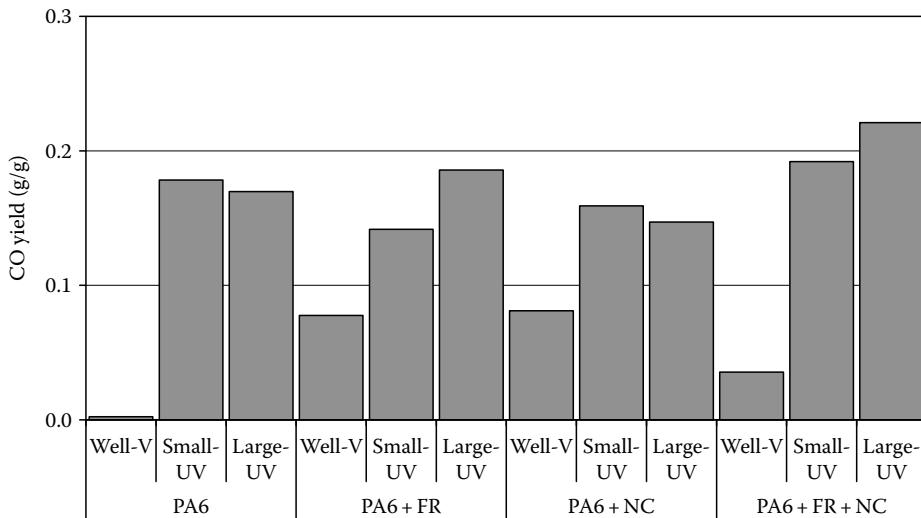


FIGURE 19.10 Carbon monoxide yields for PA6-based materials in tube furnace.

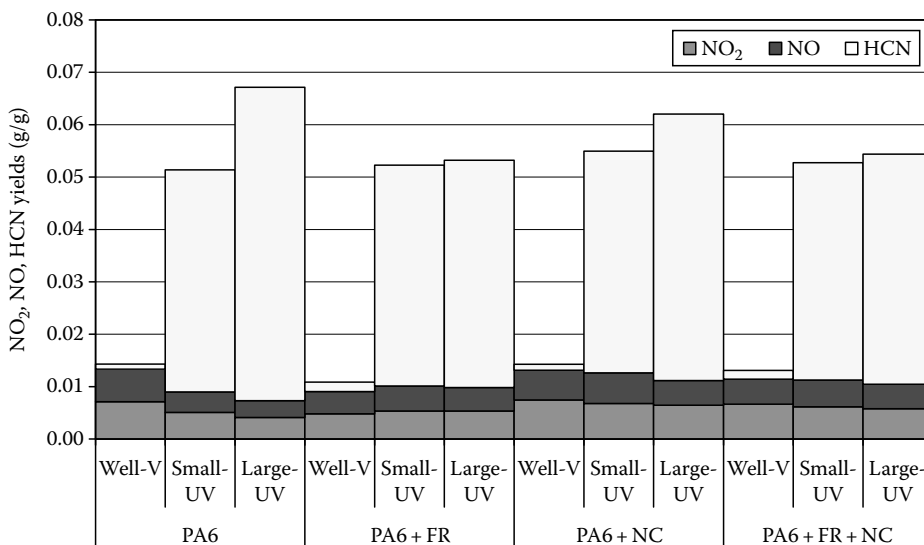


FIGURE 19.11 HCN, NO_2 , and NO yields for PA6-based materials in tube furnace.

The higher yield of HCN for PA6 + FR for well-ventilated flaming corresponds to a higher yield of CO for the same conditions. It is interesting to note that the HCN yield increases with the severity of the fire condition, whereas the CO yield levels off or even decreases. Results are consistent with the TGA/FTIR data presented in Table 19.3, Section 19.3.3.3.

19.4.2 CONE CALORIMETER

19.4.2.1 Experimental Details

Slab samples having dimensions of $100 \times 100 \times 6$ mm were manufactured by extrusion at CDCMP in Italy. A summary of the compositions and physical properties of the PA6-based materials for the Cone tests is listed in Table 19.4.

Prior to the tests, all the samples were dried in a vacuum oven at 80°C for at least 72 h to minimize the moisture effect and then transferred to a desiccator. Measurements were carried out on a cone calorimeter provided by the Dark Star Research Ltd., United Kingdom. To minimize the conduction heat losses to insulation and to provide well-defined boundary conditions for numerical analysis of these tests, a sample holder was constructed as reported in [14] with four layers (each layer is 3 mm thick) of Cotronic ceramic paper at the back of the sample and four layers at the sides. A schematic view of the sample holder is shown in Figure 19.12. Three external heat fluxes (40 , 50 , and 60 kW/m^2) were used with duplicated tests at each heat flux.

19.4.2.2 Results and Discussions

19.4.2.2.1 Ignition Times

The ignition time for each test, in which a constant heat flux was impinging on the sample, was obtained by examining the second derivate of the mass loss data or the first derivative of the HRR data. Both methods yield similar results after the time delay for transporting the hot gas to the HRR analyzer in the hood is accounted for. A summary of the ignition time for all the tests conducted is

TABLE 19.4
Composition and Physical Properties of PA6-Based Materials

	PA6	PA6/NC_UBE	PA6/NCloisite	PA6/FR	PA6/NC/FR
Mass (g)	65.3	66.5	66.8	69.2	69.0
ρ (kg/m^3)	1129	1137	1137	1185	1177
PA6 (%)	100	97.5	95	82	77
NP (%)	—	2.5	5	—	5
FR (%)	—	—	—	18	18

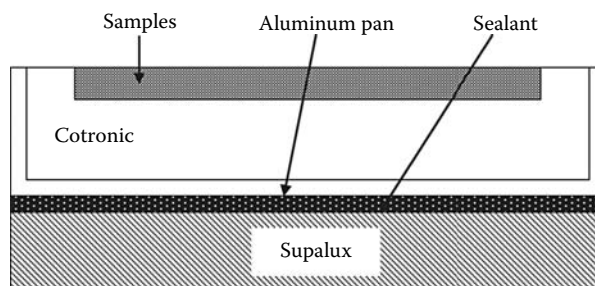


FIGURE 19.12 A schematic view of the sample holder used in cone calorimeter tests.

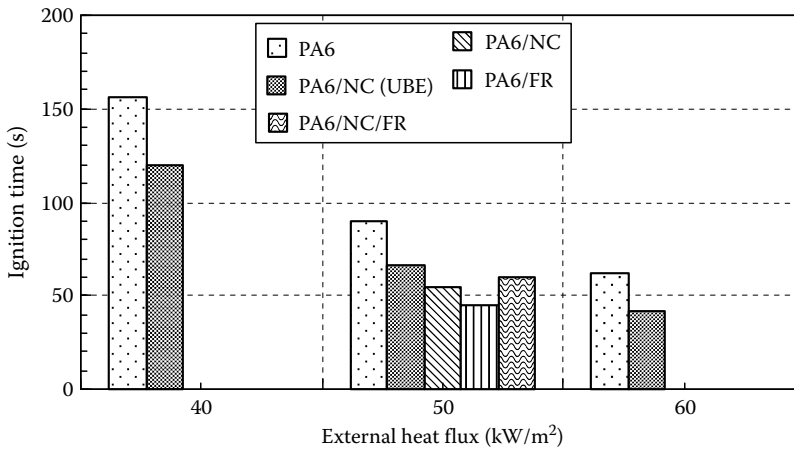


FIGURE 19.13 Experimental ignition time of PA6-based materials at different heat fluxes.

presented in Figure 19.13, where for duplicated tests the final ignition time is taken as the average of two tests. Ignition appears to occur earlier with NC with similar results reported in [15] for a different PA6 nanocomposite. It should however be pointed out that there is no general conclusion with regard to the effect of NC on ignition of polymers, because both delaying and accelerating ignition by NC have been noted in the literature as well as in the PredFIRE project.

19.4.2.2.2 Mass Loss Rate

The Savitzky–Golay (SG) smoothing algorithm developed in [16] was used in this work to smooth the mass loss data. The smoothed MLR for PA6/NC (UBE) at different heat fluxes are shown in Figure 19.14 together with those for pure PA6 obtained under the same test conditions. It is seen that nanoparticles have a negligible effect prior to the first peak MLRs and the reduction at the steady burning stage is also moderate about an average of 15%. However, the second peak MLRs observed for pure PA6 due to the back side effect, which occurs when the material throughout has a uniform temperature as a result of heat accumulation at the insulated back, is essentially removed by the addition of 2.5 wt % nanoparticles. These results seem to indicate that the fire retardancy effect of

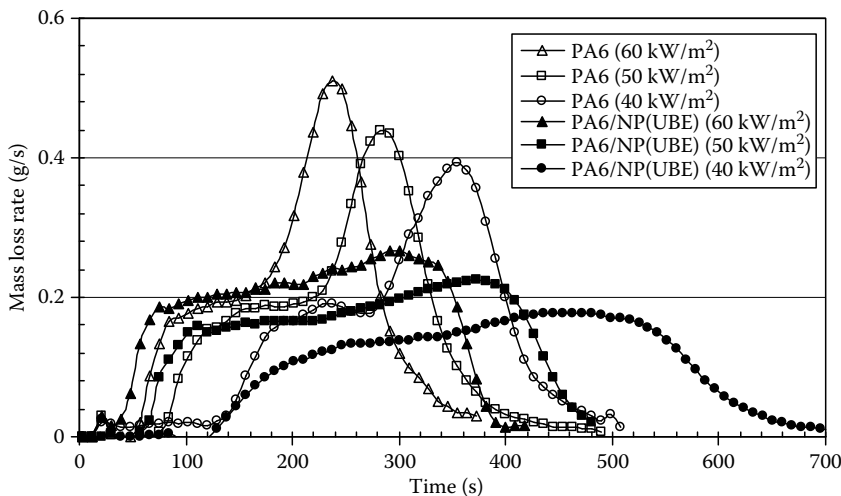


FIGURE 19.14 Comparison of the mass loss rate history of PA6 and PA6/NC (UBE) at different heat fluxes (sample thickness is 6 mm).

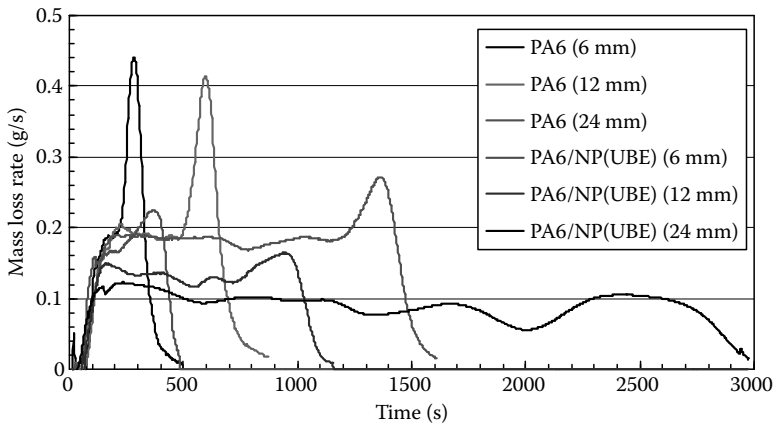


FIGURE 19.15 (See color insert following page 530.) Comparison of the mass loss rate for PA6-based materials at different sample thicknesses at 50 kW/m².

the surface layer increases as the pyrolysis process progresses because the depth of the surface layer increases with more nanoparticles accumulated on the surface.

To examine the effect of thickness, tests were carried out for 6, 12, and 24 mm samples at 50 kW/m², for which the results for PA6 and PA6/NC (UBE) are compared in Figure 19.15. For a 12 mm PA6 sample, the steady burning MLR is almost constant, about 0.19 g/s. A plateau shows typical behavior of thermally thick materials. Although there is a significant reduction of the second peak MLRs by PA6/NC (UBE), the reduction of the MLRs at the steady burning stage is, however, moderate, only about 25%.

19.4.2.2.3 Heat Release Rate

Figure 19.16 shows a comparison of the HRR of PA6 and PA6/NC (UBE) at different heat fluxes. As the HRR is proportional to the MLR, the proportional factor being the heat of combustion, the HRR results have similar trends to those in the MLR. Significant reduction of the second peak HRRs was achieved by the nanocomposite.

A comparison of the HRR of PA6, PA6-nano, PA6/FR, and PA6/NP/FR is presented in Figure 19.17. The FR reduces the HRR more substantially compared with the NC, but it is worth noting

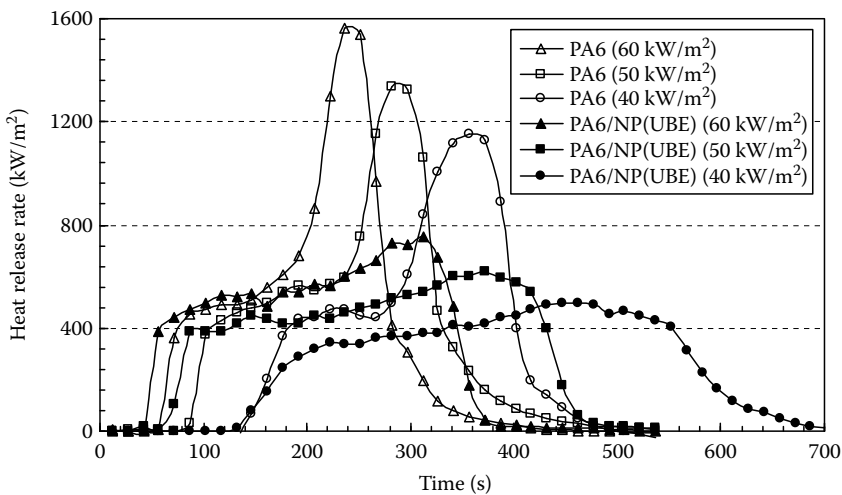


FIGURE 19.16 Comparison of the heat release rate of PA6 and PA6-nano at different heat fluxes (sample thickness is 6 mm).

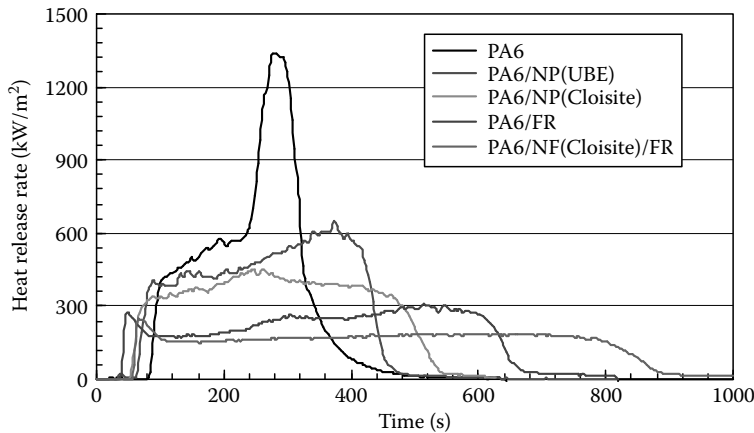


FIGURE 19.17 (See color insert following page 530.) Comparison of the HRR of PA6 and PA6/NC (UBE), PA6/NC, PA6/FR, and PA6/NC/FR at 50 kW/m² (sample thickness is 6 mm).

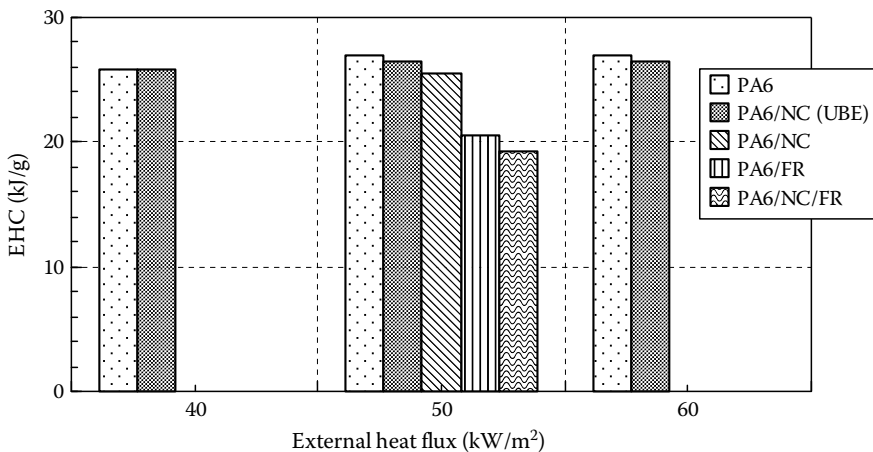


FIGURE 19.18 Comparison of effective heat of combustion (EHC) for PA6-based materials at different heat fluxes.

that the FR concentration 18 wt % compared with 2.5 and 5 wt % of NC. Although PA6/NC/FR has the lowest HRR, with a reduction of 70% in comparison with pure PA6, it shows only marginal improvement over PA6/NC.

19.4.2.2.4 Effective Heat of Combustion

Figure 19.18 presents a comparison of the effective heat of combustion (EHC), calculated as the ratio of the total heat release (THR) to the total mass lost (TML), for all the formulations. An average value of 26.5 ± 1 kJ/g was observed for all tests with PA6, PA6/NC, and PA6/NC (UBE). For PA6/FR and PA6/NC/FR, the EHC is significantly smaller—21 kJ/g for PA6/FR and 19 kJ/g for PA6/NC/FR. Like most phosphorus fire retardants, char formation is the main chemical (cross-linking) mechanism [17].

19.4.2.2.5 Smoke, Carbon Monoxide, and Carbon Dioxide Production

Figures 19.19 through 19.21 present smoke, carbon monoxide, and carbon dioxide yield for all the PA6-based materials, respectively. Pure PA6 generally produces the lowest smoke and carbon monoxide, while PA6/NC and PA6/NC (UBE) yield slightly higher values. This is one of the main advantages of nanocomposites, as they do not result in increasing the production of smoke and toxic gases in comparison with most fire retardants. It is important to note that adding FR (both PA6/NP

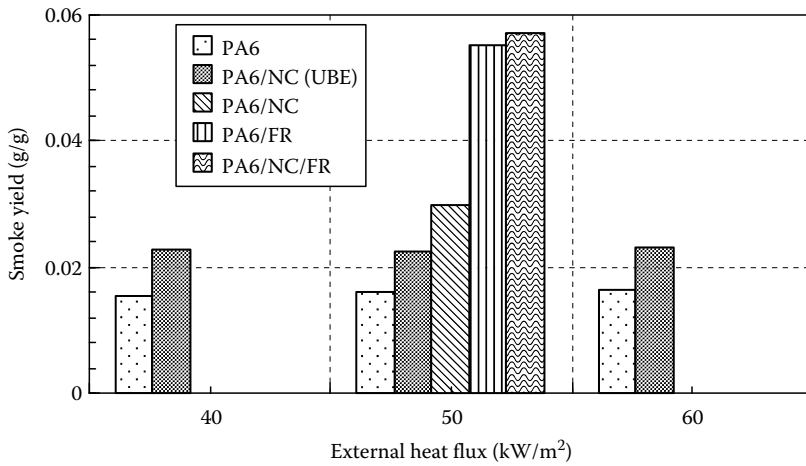


FIGURE 19.19 Comparison of smoke yield for PA6-based materials at different heat fluxes.

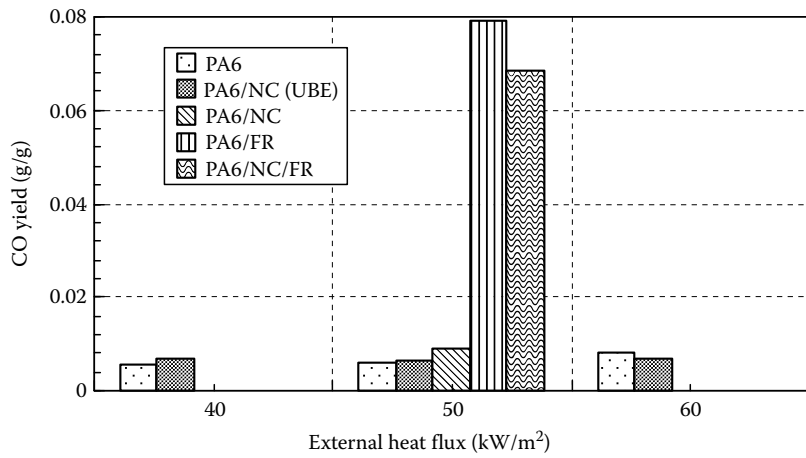


FIGURE 19.20 Comparison of carbon monoxide yield for PA6-based materials at different heat fluxes.

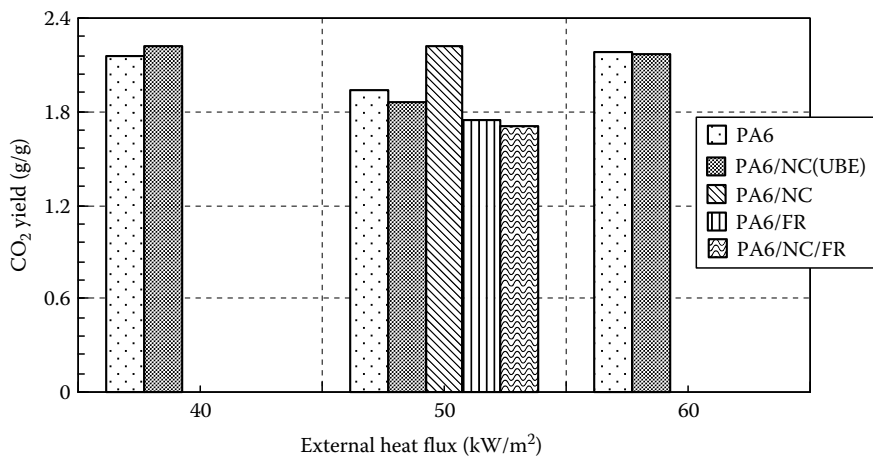


FIGURE 19.21 Comparison of carbon dioxide yield for PA6-based materials at different heat fluxes.

and PA6/NC/FR) results in much higher smoke and carbon monoxide production. For smoke and carbon monoxide, the increase is by a factor of 3 and 10, respectively. In terms of carbon dioxide production, there is no distinctive difference between all formulations, though FR-contained materials seem to have less production of CO_2 .

19.4.3 UNIVERSAL FLAMMABILITY APPARATUS

19.4.3.1 Experimental Details

The UFA shown in Figure 19.22 has a controlled oxidizer atmosphere and representing burning on a 100 mm diameter sample in horizontal orientation in a more realistic way than the standard cone calorimeter. Tests were conducted in over-ventilated fires but at reduced oxygen concentration (15%, 17.5%, and 21%) in the oxidizer stream. Because of in-depth absorption of the sample under infrared radiation, samples with and without a layer of carbon black coating were tested.

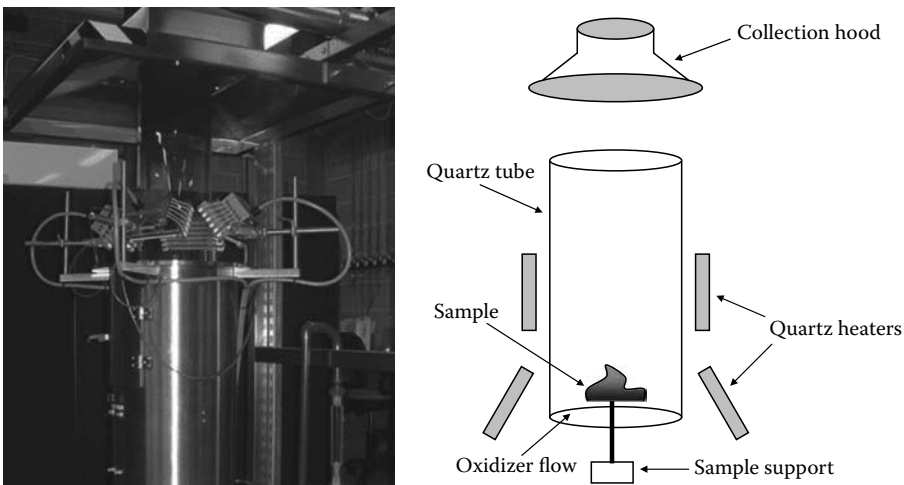


FIGURE 19.22 (See color insert following this page) The universal flammability apparatus (UFA) (left) and a schematic view of the UFA (right).

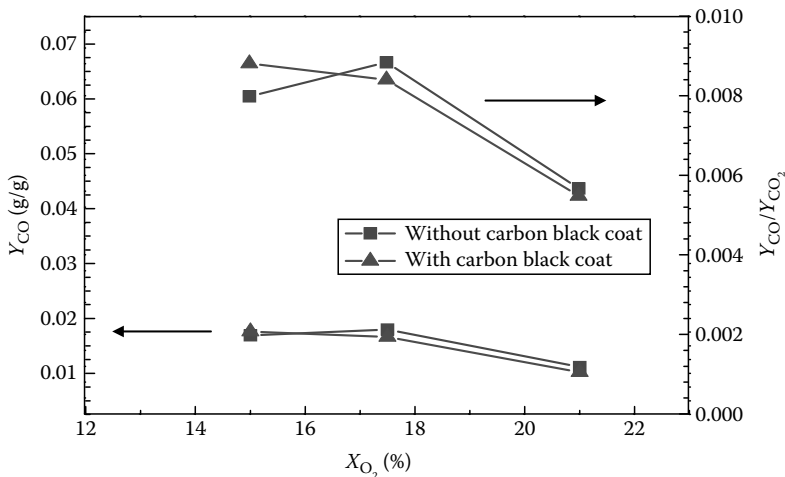


FIGURE 19.23 Carbon monoxide yield and CO/CO_2 ratio for PA6 in over-ventilated fires but at reduced oxygen concentration in the oxidizer stream in the UFA apparatus.

19.4.3.2 Results and Discussions

Figure 19.23 shows a comparison of the CO yield and CO/CO₂ ratio for PA6 samples w/wo carbon black coating. Both CO yield and CO/CO₂ ratio increases with reduced oxygen concentration. Results on under-ventilated conditions were not yet available during the preparation of this report.

19.5 NUMERICAL PREDICTION OF POLYMER BEHAVIOR IN THE CONE USING TGA MEASUREMENTS IN NITROGEN

This section shows how the kinetic parameters, namely the pre-exponential factor and activation energy that can be derived from the TGA measurements of a PA6 sample are used in a numerical model to predict the surface temperature history and mass loss of the sample with finite thickness in the cone calorimeter.

19.5.1 KINETIC PARAMETERS IN THE TGA

Figure 19.24 shows the TGA measurements of a PA6 sample in nitrogen (represented as symbols) at five heating rates, i.e., 1, 2, 5, 10 (also shown in Figure 19.4), and 20 K/min, along with the best fits (represented as lines) obtained using a first-order reaction mechanism, i.e.,

$$\frac{dX}{dt} = (1 - X)A_r e^{-\frac{E}{RT}} \quad (19.1)$$

where

X is the fraction of the mass lost

t is the time

A_r is the pre-exponential factor

E is the activation energy

R is the universal constant

T is the temperature of the solid

The derived optimal values for E and $\log(A_r)$ are 196.4 kJ/mol and 11.988/s, respectively.

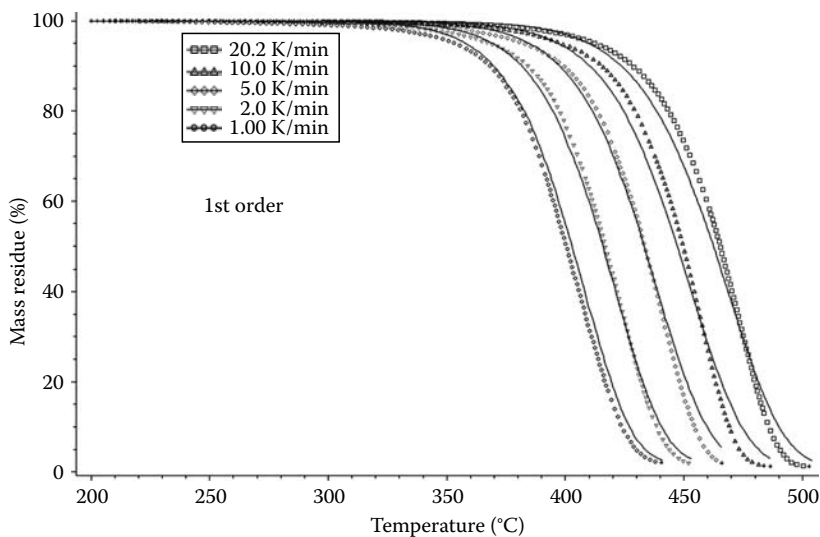


FIGURE 19.24 TGA degradation of PA6 in nitrogen at different heating rates. Symbols denote experimental data and lines are the best fits from the model using one-step reaction mechanism.

19.5.1.1 Predicted Surface Temperature History in the Cone for TGA Obtained Pyrolysis Rate

The Arrhenius expression (Equation 19.1) using the activation energy and pre-exponential factor derived from TGA measurements of a PA6 sample in N_2 was incorporated in a standard 1D pyrolysis model described in Section 19.6. The thermal properties used in the model are the ones from the ignition tests (Section 19.4.2.2) as described in Section 19.6 in conjunction with the MDSC experiments (Section 19.3.2.2). Figures 19.25a–c show the predicted surface temperature histories for

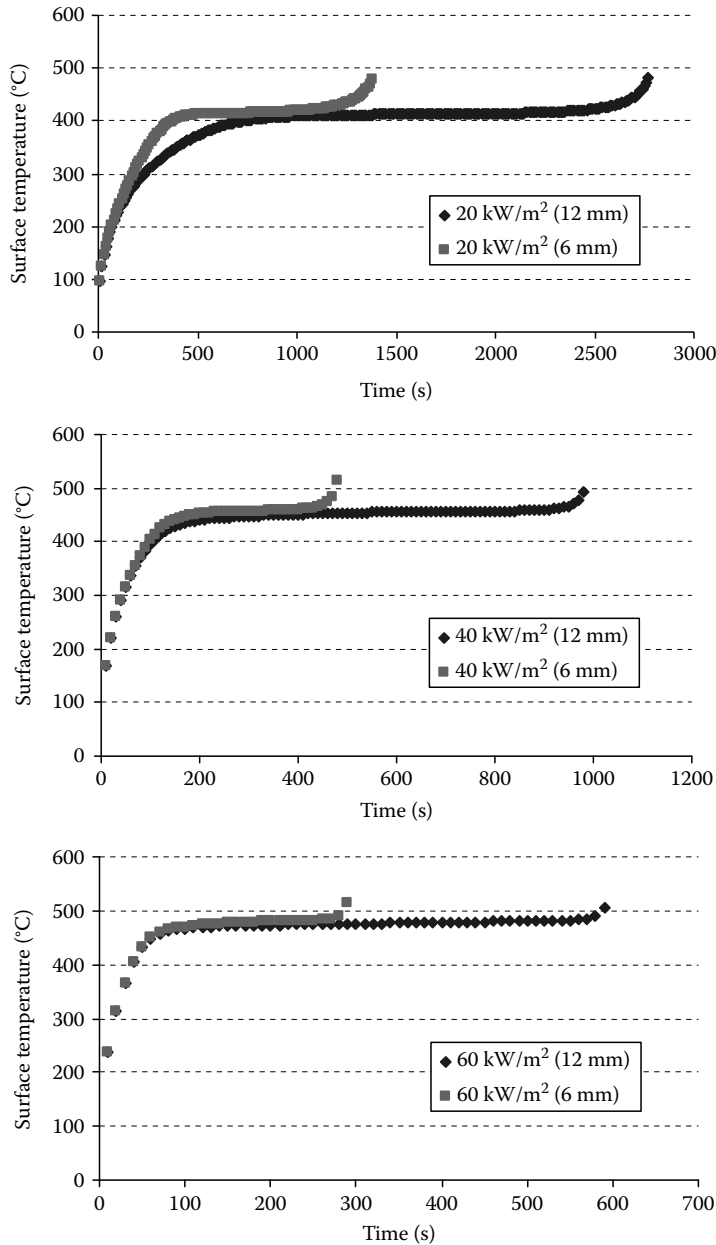


FIGURE 19.25 Predicted surface temperature histories for 6 and 12 mm PA6 samples in N_2 at (a) 20, (b) 40, and (c) 60 kW/m².

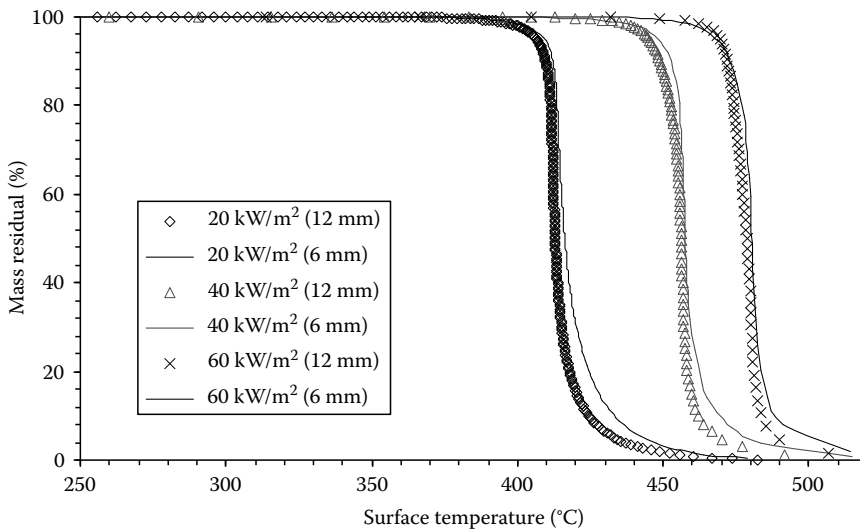


FIGURE 19.26 Predicted surface temperature using the kinetic energy and pre-exponential factor derived in the TGA against mass residue for 6 and 12 mm PA6 samples at different heat fluxes.

thermally intermediate (6 mm) and thick (12 mm) conditions at 20, 40, and 60 kW/m², respectively. It is shown that the main pyrolysis process occurs nearly at a constant temperature. However, the predicted steady-state surface temperature appears to be dependent on external heat flux, increasing from 415°C at 20 kW/m² to 450°C at 40 kW/m² and 480°C at 60 kW/m². The ignition temperature for pure PA6 derived from the ignition tests (described in Section 19.6) has a value of 715 K (442°C), well in the range of the results shown here. Thus the thermal model is a good accepted engineering approximation for this case.

19.5.1.2 Predicted Mass Loss in the Cone Calorimeter

In Figure 19.26, the TGA measurements are “related” to the predictions in the cone calorimeter by plotting the surface temperature history against the normalized residual mass (the residual mass normalized to the initial mass) for 6 and 12 mm samples at different heat fluxes using the 1D model as in the previous section. It is interesting to note that sample thickness has negligible effect on the predicted surface temperature, which is nearly constant except in the regions near the end of the pyrolysis process where the material becomes thermally thin. Because of the thin layer near the end of pyrolysis a similarity appears in the MLR between the TGA results in Figure 19.24 and cone results in Figure 19.26, indicating that the exposed surface in the cone calorimeter pyrolyzes in a similar way to the sample in the TGA. Another important observation from the present results is that the heating rates from 1–20 K/min in the TGA cover the behavior of the polymer for the heating fluxes in the cone for the range of 20–60 kW/m².

19.6 NUMERICAL MODEL FOR THE PYROLYSIS OF POLYMER NANOCOMPOSITES

The present numerical model was developed based on a standard noncharring model using the ignition temperature concept, i.e., the surface temperature remains constant after reaching the prescribed ignition temperature until the material pyrolyzes completely. The accuracy of the standard noncharring model was demonstrated by comparing model predictions with exact analytical solutions and the results generated by an integral model.

19.6.1 MATHEMATICAL FORMULATIONS

The development of the present methodology is inspired by an analytical study for the pyrolysis of charring materials [18], where it was shown that the heat flux at the char–virgin interface (with the assumption that surface absorptivity and emissivity are one) has the following form:

$$\dot{q}_{\text{net}}''(t) = \frac{d}{\delta_c + d} (\dot{q}_{\text{ext}}'' - \sigma T_{\text{ig}}^4) \quad (19.2)$$

where

δ_c is the char thickness

\dot{q}_{ext}'' is the external heat flux

d is a characteristic radiation length that also takes into account the change of conductivity, k_c , with temperature:

$$d = \frac{k_c(T_{\text{ig}})T_{\text{ig}}}{4\sigma T_{\text{ig}}^4} \quad (19.3)$$

Here T_{ig} denotes the ignition temperature that can be determined from the ignition tests and σ is the Stefan–Boltzmann radiation constant.

Note that convection heat losses were neglected in the analyses in [18] as radiation is the dominant mode of heat losses at high temperatures.

Rearranging Equation 19.2, we obtain

$$1 + \frac{\delta_c}{d} = \frac{(\dot{q}_{\text{ext}}'' - \sigma T_{\text{ig}}^4)}{\dot{q}_{\text{net}}''(t)} \quad (19.4)$$

Equation 19.4 implies that the heat flux at the char–virgin interface will decrease with increasing char depth or decreasing conductivity. Comparing Equations 19.2 and 19.4 and noting that d is a material constant, we obtain that the heat flux at the interface is a function only of the char depth δ_c .

Although burning of nanocomposites is different from that of charring materials, because for charring materials (such as wood) it can be usually assumed that the volume does not change before and after burning, whereas for nanocomposites the volume can change significantly because of the small amount of nanoparticles (typically less than 5%) used, the heat transfer mechanisms are similar for both cases. Both involve formation of a surface layer (a char layer for charring materials whereas a nano layer for nanocomposites), and the thickness of the surface layer increases as pyrolysis continues. Thus, we expect that Equation 19.4 also applies to nanocomposites as verified next in this section. In addition, we propose that the depth of the nano surface layer δ_c is proportional to the pyrolyzed depth δ_{pyro} (i.e., the depth of the material pyrolyzed) and this proposition will be verified in the numerical result.

Now a new parameter can be defined for nanocomposites to characterize the reduction of the heat flux on the unpyrolyzed material. This parameter (hereafter denoted by $\text{ratio}_{\text{flux}}$) can be expressed in Equation 19.5, as the ratio of the net incoming heat flux on the surface for the case when there is no surface ($\dot{q}_{\text{net}}''_0$) over the actual heat flux at the interface of the surface (nano) layer and virgin material in the presence of the surface layer ($\dot{q}_{\text{net}}''(t)$).

$$\text{ratio}_{\text{flux}}(t) = \frac{\dot{q}_{\text{net}}''_0}{\dot{q}_{\text{net}}''(t)} \quad (19.5)$$

By definition, $\text{ratio}_{\text{flux}}$ has a value of one prior to the formation of the surface layer, and increases as the fire retardancy of surface layer increases (e.g., the depth of the surface layer increases). The expressions of $\dot{q}_{\text{net}}''_0$ and $\dot{q}_{\text{net}}''(t)$ will be derived next.

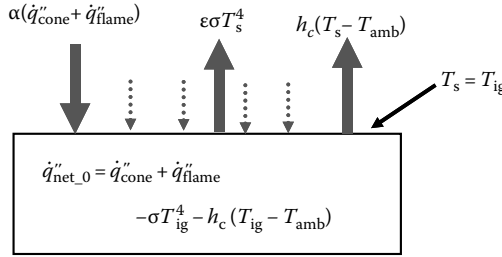


FIGURE 19.27 Schematic view of heat transfer for the case when there is no surface layer.

The net incoming heat flux on a pyrolyzing surface for the case when there is no surface layer, \dot{q}''_{net_0} , can be calculated using the energy balance on the surface with the surface temperature being the ignition temperature as shown in Figure 19.27:

$$\dot{q}''_{net_0} = \dot{q}''_{cone} + \dot{q}''_{flame} - \sigma T_{ig}^4 - h_c(T_{ig} - T_{amb}) \tag{19.6}$$

where

\dot{q}''_{cone} is the nominal heat flux from the cone

\dot{q}''_{flame} represents a sudden increase of the imposed heat flux after ignition due to the flame and a constant value of 10kW/m² is used following [19]

T_{ig} denotes the ignition temperature that is determined from the ignition tests

σ is the Stefan–Boltzmann constant

h_c is the convective heat transfer coefficient which takes a value of 7 kW/m-K based on the finding in a previous study using a steel plate in the cone calorimeter [20]

The ambient temperature $T_{amb} = 300$ K

The radiation from the ambient is negligible, whereas the absorption coefficient α and the emissivity ϵ shown in Figure 19.27 are taken equal to one. Note that for a given material exposed to a constant heat flux \dot{q}''_{net_0} remains constant during pyrolysis.

A schematic view of heat transfer during pyrolysis of nanocomposite with the surface layer is shown in Figure 19.28. We note that similar to charring materials the temperature at the interface of surface layer and virgin material is assumed to be at the ignition temperature while the surface temperature may increase far beyond the ignition temperature. The increased surface temperature has the primary effect on the reduced heat flux transfer to the virgin layer because of the increasing reradiation heat losses. However, because the surface temperature is unknown, the actual heat flux at the interface cannot be derived based on the energy balance of the surface layer, but fortunately it can be determined by

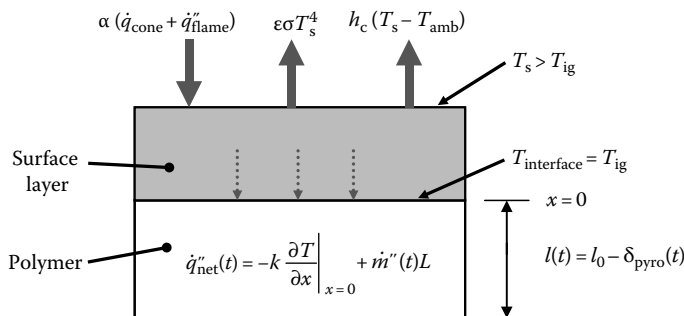


FIGURE 19.28 Schematic view of heat transfer during pyrolysis of nanocomposite with the surface layer.

considering the energy balance of the unpyrolyzed (virgin) layer based on the experimental mass loss data with the assistance of numerical calculations as following:

We consider here the 1D conduction equation governing the unpyrolyzed layer:

$$\rho c \frac{\partial T}{\partial t} = \frac{\partial}{\partial x} \left(k \frac{\partial T}{\partial x} \right) \quad (19.7)$$

where

k , ρ , and c are respectively the conductivity, density, and specific heat of the polymer

T is the temperature

t is the time

x is the distance from the surface toward inside the solid

For ease of numerical solutions, $x = 0$ is always located at the top surface as shown in Figure 19.28. The thickness of the unpyrolyzed material also changes as pyrolysis continues. The effective thermal properties (k and c) of the polymer are deduced from the ignition tests as detailed in Section 19.6.3.

The boundary conditions for the front ($x = 0$) and back ($x = l(t)$) surfaces are, respectively, Before ignition:

$$\begin{aligned} -k \frac{\partial T}{\partial x} \Big|_{x=0} &= \alpha \dot{q}_{\text{cone}}'' - \epsilon \sigma T_s^4 - h_c (T_s - T_{\text{amb}}) \\ -k \frac{\partial T}{\partial x} \Big|_{x=l} &= 0 \end{aligned} \quad (19.8)$$

After ignition:

$$\begin{aligned} T_s &= T_{\text{ig}} \\ -k \frac{\partial T}{\partial x} \Big|_{x=l(t)} &= 0 \end{aligned} \quad (19.9)$$

where the backside is designed to be adiabatic as the samples were insulated at the back with low conductivity Cotronic ceramic paper. The surface emissivity ϵ and the surface absorptivity α are assumed to be one as the exposed top surface of the samples in the experiments was painted with black paint. After ignition the sample thickness, $l(t)$, decreases with time due to mass loss and is therefore calculated dynamically by subtracting the pyrolyzed depth, δ_{pyro} , from the initial thickness, where δ_{pyro} is obtained by integrating the instantaneous experimental MLR, \dot{m}'' , as

$$\delta_{\text{pyro}} = \frac{\int_0^t \dot{m}''(\tau) d\tau}{\rho} \quad (19.10)$$

While solving Equation 19.2, one can construct numerically the conduction heat flux on the surface of the unpyrolyzed material (i.e., $-k\partial T/\partial x|_{x=0}$) and thus the actual heat flux transferred into the unpyrolyzed material can be found by considering the energy balance at the surface of the unpyrolyzed material as shown in Figure 19.28:

$$\dot{q}_{\text{net}}''(t) = -k \frac{\partial T}{\partial x} \Big|_{x=0} + \dot{m}''(t)L \quad (19.11)$$

where

$\dot{m}''(t)$ is the experimental MLR

L is the latent heat of pyrolysis, which can be determined from DSC tests or by considering the energy balance at the peak MLR in the cone calorimeter tests

Because of the difficulties in accurately measuring the heat of pyrolysis in DSC, manifested by the fact that the measurements at University of Ulster are only about half the values in another study in [8], the values determined in the cone calorimeter, which are also close to those reported in [8], are used in the present analysis.

19.6.2 NUMERICAL DETAILS

Equation 19.7 was discretized in space using the finite volume method and in time the fully implicit method to ensure numerical stability. The discretized equation was solved using a tri-diagonal matrix algorithm (TDMA) solver. A nonuniform grid system was used, with denser grids toward the pyrolysis front where large temperature gradients are expected. The smallest grid size is about 0.01 mm. Sensitivity tests showed that for 6 mm samples a grid number of 48 and a timestep of 0.05 s yield results, which are essentially independent of the grid size and timestep. As the sample thickness l changes with time due to mass loss, the mesh was regenerated at each new timestep, and the temperatures at the grid nodes on the new mesh were determined from the ones on the old mesh using a linear interpolation.

19.6.3 DEDUCED EFFECTIVE THERMAL PROPERTIES FOR THE PA6 NANOCOMPOSITE

For the thermally thick condition, effective thermal properties (i.e., thermal inertia, $k\rho c$, and ignition temperature, T_{ig}) can be deduced from time to ignition experiments, which follow a standard procedure in the cone calorimeter. Theory and experiments showed that ignition usually occurs at a constant temperature independent of the imposed heat flux. The effective thermal properties can thus be determined at a time which is inversely proportional to the square root of the external heat flux. However, if materials are thermally intermediate (i.e., neither thermally thick nor thermally thin) a modification of plotting ignition time data is required to obtain thermal properties and the critical heat flux [21]. The corrected ignition time for the PA6 nanocomposite is plotted in Figure 19.29, where F_1 and F_2 are given in [21] as functions of $X = \delta / (\alpha_2 \cdot \dot{q}''_{cone})$ and have a value of one for the thermally thick condition.

The diffusivity, α_2 , is subsequently determined under the condition that the intercepts of the linear fits for the thermally thick and thin conditions are equal. For the PA6 nanocomposite, when the diffusivity is equal to $0.9 \times 10^{-7} \text{ m}^2/\text{s}$, the intercepts are almost the same at about 11.5 kW/m^2 . These intercepts are equal to the 0.64 fraction of the critical heat flux (below which there is no ignition) for ignition [21], and thus the critical heat flux can be calculated equal to $11.5/0.64 = 17.9 \text{ kW/m}^2$. The ignition temperature can then be calculated by considering the critical heat flux equal to surface reradiation and convection losses:

$$\dot{q}''_{cr} = \sigma(T_{ig}^4 - T_{amb}^4) + h_c(T_{ig} - T_{amb}) \quad (19.12)$$

To determine the thermal inertia, we note that the ignition time for thermally thick materials can also be expressed as

$$t_{ig} = \frac{\pi}{4} k\rho c \frac{(T_{ig} - T_{amb})^2}{(\dot{q}''_{cone} - 0.64\dot{q}''_{cr})^2} \quad (19.13)$$

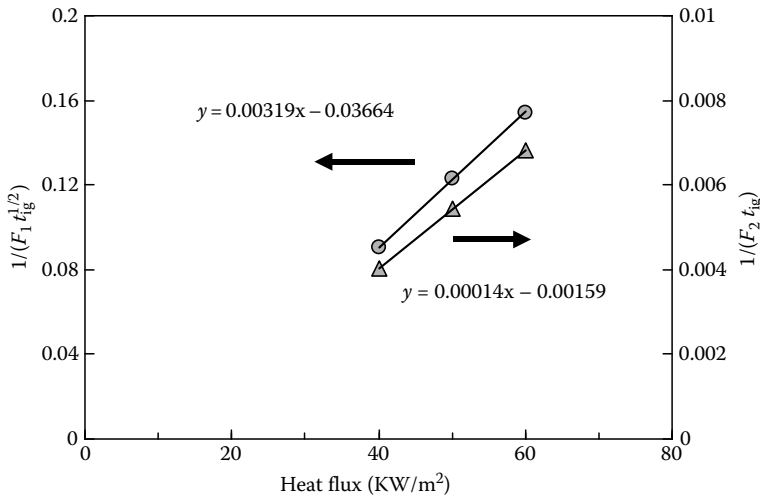


FIGURE 19.29 Corrected ignition time for the PA6 nanocomposite. Thermal diffusivity, α_2 , equals to 0.9×10^{-7} m²/s. F_1 and F_2 are derived analytically in [21] as functions of $X = \delta/(\alpha_2 \cdot \dot{q}_{cone}'')$, where δ is the initial sample thickness and \dot{q}_{cone}'' is the nominal heat flux from the cone.

From the slope of the plot for the thermal thick condition in Figure 19.29, the thermal inertia $k\rho c$ can be found using Equation 19.13 having a value of $0.62 \text{ kJ}^2/\text{m}^4 \text{ K}^2 \text{ s}$. With density and diffusivity known, the specific heat and conductivity can then be derived. A summary of the thermal properties and critical heat flux is presented in Table 19.5. For comparison purpose, the data reported in [22] for pure PA6 at the ambient temperature are also included. There is in general good consistency between the two sets of data. The fact that the deduced specific heat in this work is higher than the one reported in [22] can be explained by the dependence of the specific heat on temperature as noted by our DSC measurements showing that the specific heat increases from 1600 to 3000 J/kg K when temperature changes from ambient to around 490 K.

For the latent heat of pyrolysis, it is worthwhile to note that a wide range of values measured using DSC were reported in the literature. For example, in [8], a value of $1390 \pm 90 \text{ J/g}$ was reported for PA6, whereas 560 J/g was reported by Frederick and Mentzer [23]. In addition, the DSC tests by our group showed the average value for PA6 is around 500 J/g. The disagreement highlights the large uncertainties in measuring the heat of pyrolysis. As discussed earlier, an alternative method is to examine the energy balance at the second peak MLR/HRR in the cone for pure polymers. At the second peak MLR/HRR, the sample has a uniform temperature and thus the internal conduction can be neglected. After examining the data obtained at different heat fluxes, an average value

TABLE 19.5
Effective Thermal Properties of the PA6 Nanocomposites
Derived from the Ignition Tests, Along with the Literature Values Reported for Pure PA6

	α m ² /s	\dot{q}_{cri}'' kW/m ²	T_{ig} K	k W/m-K	c J/kg-K	$k\rho c$ (kJ ² /m ⁴ -k ² -s)	L J/g
PA6/NC(UBE)	0.9×10^{-7}	17.9	725	0.23	2300	0.62	—
PA6	1.37×10^{-7}	—	705	0.24	1550	—	1000

Source: Lyon, R.R. and Janssens, M.L., Polymer flammability, Office of Aviation Research Washington, DC, 20591, DOT/FAA/AR-05/14, 2005.

of 1000J/g was found. In the present study, we made the assumption that the PA6 nanocomposite has the same heat of pyrolysis as pure PA6, because the small amount of nanoparticles was used, and DSC and TGA data also showed little difference between the nanocomposite and pure PA6. This assumption is also justified by the fact that pure polymers and polymer nanocomposites have the same EHC from the cone calorimeter results indicating again that there is no chemical effect by nanoparticles.

19.6.4 RESULTS AND DISCUSSIONS

The key calculation results in the heat flux ratio, $\text{ratio}_{\text{flux}}(t) = \dot{q}''_{\text{net}_0} / \dot{q}''_{\text{net}}(t)$, which could be expressed as a function of time. But to examine the validity of Equation 19.4 for nanocomposites, the heat flux ratio is presented as a function of the pyrolyzed depth, i.e., the thickness of the pyrolyzed depth.

19.6.4.1 Derived Correlation between the Heat Flux Ratio and the Pyrolyzed Depth

The reduction of the external heat flux to the sample due to a surface layer formation, as $\text{ratio}_{\text{flux}}(t) = \dot{q}''_{\text{net}_0} / \dot{q}''_{\text{net}}(t)$, is plotted in Figure 19.30 against the pyrolyzed depth, δ_{pyro} , for one of the duplicated tests at 40kW/m² (6 mm sample). Three regions can be identified, namely (1) a relatively constant $\text{ratio}_{\text{flux}}$ in the first region, (2) a nearly linear increase in the second region, and (3) a sharp increase in the third region. In the first region, the relatively constant heat flux ratio indicates that nanoparticles are less effective at this stage of pyrolysis because the depth of the surface layer is small. Its value (about 1.15) is slightly higher than the ideal value (one), which could be due to the assumption in the calculations of a sudden increase of the imposed heat flux after ignition to represent the flame effect. The sudden increase in the third region is due to the fact that the MLR and the conduction heat flux term (the first term on the RHS of Equation 19.11) are small at the end of pyrolysis resulting in small values of \dot{q}''_{net} and thus large values of $\text{ratio}_{\text{flux}}$. It is however the second region representing the main pyrolysis process that is of most importance in the present analysis. This region is characterized by a nearly linear increase of $\text{ratio}_{\text{flux}}$ against δ_{pyro} .

The finding shown in Figure 19.30 verifies our early proposition that the thickness of the surface layer is proportional to the pyrolyzed depth. The thickness of the surface layer is assumed to be proportional to the amount of nanoparticles accumulated on the surface assuming that nanoparticles initially are uniformly distributed in the polymer and nanoparticles do not pyrolyze during burning

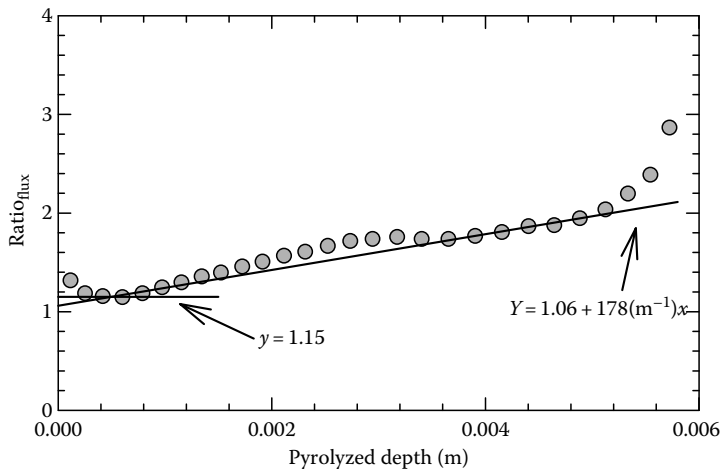


FIGURE 19.30 Calculated instantaneous heat flux ratio, $\text{ratio}_{\text{flux}}(t) = \dot{q}''_{\text{net}_0} / \dot{q}''_{\text{net}}(t)$, against the pyrolyzed depth, δ_{pyro} , for one of the duplicated tests at 40kW/m² (the sample thickness is 6 mm). Two lines represent the best fits of the calculated results.

(dehydroxylation of nanoparticles occurs upon heating but the total weight loss is only about 6% of the nanoparticles weight and thus negligible). The assumption of uniform distribution of nanoparticles in the PA6 nanocomposite is also supported by our results of SEM, XRD, rheological analyses, and NMR spectroscopy measurements, indicating that the PA6 nanocomposite used in this study is fully exfoliated [1,2]. By best fitting in Figure 19.30, one obtains the following approximate correlation:

$$\text{ratio}_{\text{flux}} = 1.15 \quad \text{for} \quad \delta_{\text{pyro}} < 5 \times 10^{-4} \text{ m} \quad (19.14a)$$

$$\text{ratio}_{\text{flux}} = 178(\text{m}^{-1})\delta_{\text{pyro}} + 1.06 \quad \text{for} \quad \delta_{\text{pyro}} \geq 5 \times 10^{-4} \text{ m} \quad (19.14b)$$

Here, the third region is ignored anticipating it has negligible influence on the main pyrolysis process because it is relatively short.

19.6.4.2 Predicted Mass Loss Rates

In this section, the correlation in the heat flux ratio versus the pyrolyzed depth given by Equation 19.14 is incorporated into the numerical model to predict the pyrolysis process of the PA6 nanocomposite at different heat fluxes and thicknesses. The boundary conditions remain as those given by Equations 19.8 and 19.9. However, the MLR is now calculated from the heat flux ratio correlation in Equation 19.14 as

$$\dot{m}''(t) = \frac{\dot{q}_{\text{cone}}'' + \dot{q}_{\text{flame}}'' - \sigma T_{\text{ig}}^4}{\text{ratio}_{\text{flux}} \cdot L} \quad (19.15)$$

where $\text{ratio}_{\text{flux}}(t)$ is dynamically determined from $\delta_{\text{pyro}}(t)$ using Equation 19.14 and δ_{pyro} is obtained by integrating the calculated instantaneous MLR in time using Equation 19.10.

Figure 19.31 compares the predicted MLRs with the experimental ones for the 6 mm sample at different heat fluxes. The predictions generally capture the trends of the experimental data and are in quantitative agreement with the measurements. This is an important finding of this work as the correlation in the heat flux ratio and pyrolyzed depth (Equation 19.14) was deduced for one heat flux (40 kW/m²), but our results demonstrate that the same correlation can also be applied to predict pyrolysis at other heat fluxes. In other words, the correlation is independent of the heat flux but depends only on the depth of pyrolyzed material, or equivalently the amount of nanoparticles accumulating on the surface. As we have adopted a simple correlation between $\text{ratio}_{\text{flux}}$ and δ_{pyro} , some discrepancies are noted at the end of the pyrolysis process, where the predictions fail to reproduce the drops of the experimental MLRs. This is, however, consistent with the treatment that the region corresponding to the end of the pyrolysis in Figure 19.30 was ignored.

To examine the validity of the present methodology to samples of different thicknesses, the same correlation given by Equation 19.14 is used to predict the burning rate for the 12 and 24 mm samples at 50 kW/m². For the calculation of the thicker samples, the same parameters were used except that 64 grids were used for the 12 mm sample and 96 grids for the 24 mm sample. A comparison of the predicted and experimental MLRs is shown in Figure 19.32. First, we note that there are some unexpected dips and peaks in the experimental results because the thicker samples were obtained by gluing of 6 mm sample (especially clear for the 24 mm sample). Apparently, the contact between different layers of the samples affects heat transfer mechanisms and thus the pyrolysis process. Nonetheless, the overall results are encouraging as the predictions reproduce the typical behaviors of charring materials with two peaks that also agree quantitatively with the experimental data. The average relative differences between the predictions and measurements are within 20%. For the 12 mm sample, the model seems to underestimate slightly the MLR under 600 s, after which the agreement between the prediction and experiment is reasonably good, whereas for

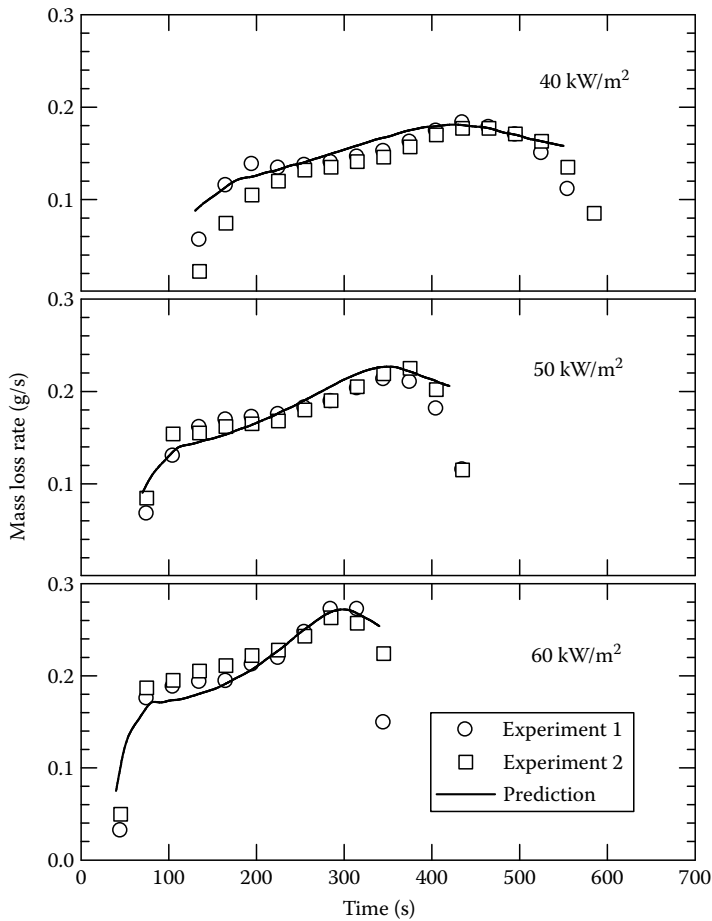


FIGURE 19.31 PA6 nanocomposite: Comparisons of experimental and predicted MLRs for 6 mm samples at three heat fluxes.

the 24 mm sample the model generally underpredicts the MLR; however, the experimental errors (fluctuations) are clear for this thickness preventing from further quantitative assessment of the accuracy of the model.

19.7 FURTHER VALIDATION OF THE MODEL

19.7.1 APPLICATION TO EVA AND PBT NANOCOMPOSITES

19.7.1.1 Material and Experimental Details

In this work, tests were also conducted for other polymers with different type or loading of nanoparticles. These materials are an ethylene-vinyl acetate (EVA) nanocomposite with 5 wt % organoclay by Kabelwerk EUPEN AG/Belgium, and a PBT nanocomposite with 5 wt % Sepiolite. The samples size is the same as the one for PA6 (i.e., 100 × 100 × 6 mm). Similar to the PA6 tests, three external heat fluxes (40, 50, and 60 kW/m²) were used with duplicated tests at each heat flux level.

19.7.1.2 Experimental Ignition Times

The duplicated tests, in general, show good repeatability, and the average ignition times of the duplicated tests for the EVA and PBT nanocomposites are summarized in Table 19.6.

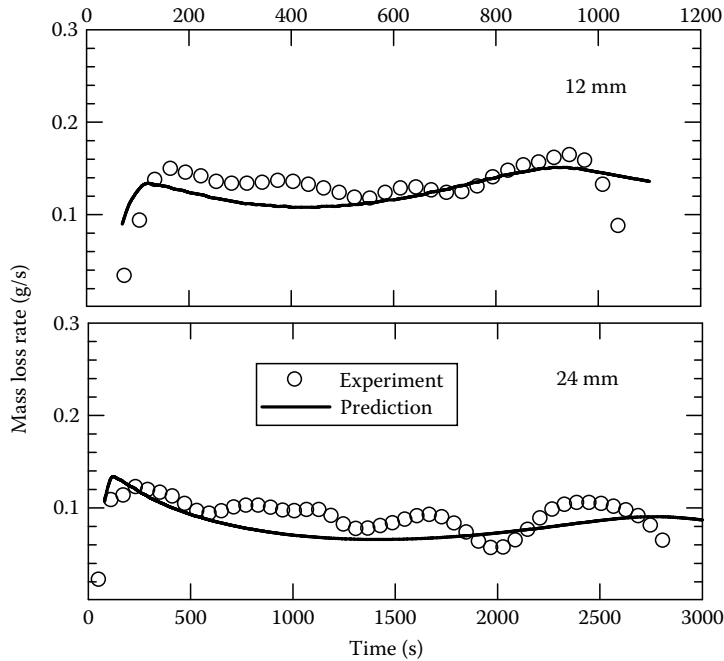


FIGURE 19.32 PA6 nanocomposite: Comparisons of experimental and predicted MLRs for 12 and 24 mm samples at 50 kW/m^2 .

TABLE 19.6
Average Experimental Ignition Times (in s)
for EVA and PBT Nanocomposites
at Different Heat Fluxes

	40 kW/m^2	50 kW/m^2	60 kW/m^2
EVA Nanocomposite	70	47.5	28
PBT Nanocomposite	73	39.5	27.5

19.7.1.3 Deduced Effective Thermal Properties

The methodology [21] that has been used to the PA6 nanocomposite to deduce the thermal properties and critical heat flux was applied to the EVA and PBT nanocomposites (Section 19.7.1.1). The corrected ignition times as a function of the external heat flux for both EVA and PBT nanocomposites are shown in Figure 19.33. The final deduced thermal properties and critical heat flux are summarized in Table 19.7, along with the values reported for pure EVA and PBT in [22].

19.7.1.4 Results and Discussions

In Figure 19.34a, the history of the calculated heat flux ratio, $\text{ratio}_{\text{flux}}$, is plotted against the pyrolyzed depth, δ_{pyro} , for the EVA nanocomposite for one of the duplicated tests at 50 kW/m^2 . As we noted previously for the PA6 nanocomposite, the heat flux ratio $\text{ratio}_{\text{flux}}$ increases linearly with δ_{pyro} during the main pyrolysis process. These results further support the validity of Equation 19.4 for nanocomposites. By neglecting the region near the end of pyrolysis and drawing two lines of best fit in Figure 19.34a, we obtain

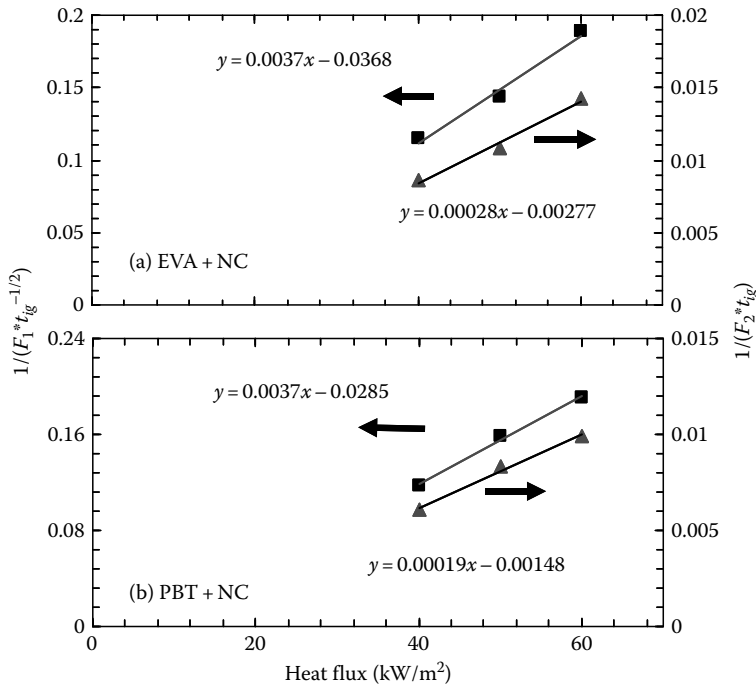


FIGURE 19.33 Corrected ignition time for (a) EVA and (b) PBT nanocomposites. Thermal diffusivity, α , equals to 2.6×10^{-7} and 1.25×10^{-7} m²/s for EVA and PBT nanocomposites, respectively.

TABLE 19.7
Effective Thermal Properties of PA6, EVA, and PBT Nanocomposites
Derived in This Work, Together with Those Reported for Pure Polymers

	α m ² /s	\dot{q}_{cri}'' kW/m ²	T_{ig} K	k W/m-K	c J/kg-K	$K\rho c$ (kJ ² /m ⁴ -k ² -s)	L J/g
PA6/NC	0.9×10^{-7}	17.9	725	0.23	2300	0.62	1000
PA6	1.37×10^{-7}	—	705	0.24	1550	—	—
EVA/NC	2.6×10^{-7}	11.3	668	0.44	1845	0.765	2000
EVA	2.67×10^{-7}	—	—	0.34	1370	—	—
PBT/NC	1.25×10^{-7}	12.1	680	0.28	1733	0.645	1000
PBT	1.01×10^{-7}	—	650	0.22	1610	—	—

Source: Lyon, R.R. and Janssens, M.L. Polymer flammability, Office of Aviation Research Washington, DC, 20591, DOT/FAA/AR-05/14, 2005.

$$\text{ratio}_{flux} = 1.2 \quad \text{for} \quad \delta_{pyro} < 4 \times 10^{-4} \text{ m} \quad (19.16a)$$

$$\text{ratio}_{flux} = 500(\text{m}^{-1})\delta_{pyro} + 1.0 \quad \text{for} \quad \delta_{pyro} \geq 4 \times 10^{-4} \text{ m} \quad (19.16b)$$

Figure 19.34b shows the calculated ratio_{flux} against δ_{pyro} for the PBT nanocomposite at 50kW/m². Similar to the result of the EVA nanocomposite, ratio_{flux} increases linearly with δ_{pyro} , but only up to about 4mm. The further decrease of ratio_{flux} with δ_{pyro} is consistent with the observation in the experimental data where slight increases of the MLR were noted. The different behavior of the PBT nanocomposite from the EVA nanocomposite or from the PA6 nanocomposite indicates that the

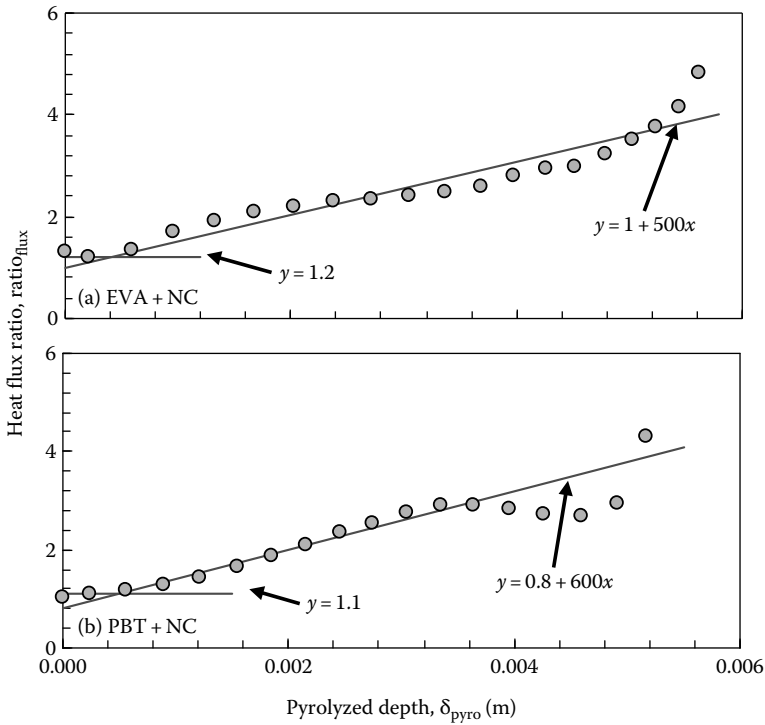


FIGURE 19.34 Calculated heat flux ratio, $ratio_{flux}$, against pyrolyzed depth, δ_{pyro} , for (a) EVA and (b) PBT nanocomposites at 50 kW/m^2 . Two lines represent the best fits of the calculation results, which are also used to predict the mass loss rate.

effect of the surface (nano) layer depends on the type of polymers as well as on the type and loading of nanofillers. Nonetheless, through best fitting we obtain

$$ratio_{flux} = 1.1 \quad \text{for} \quad \delta_{pyro} < 5 \times 10^{-4} \text{ m} \tag{19.17a}$$

$$ratio_{flux} = 800(\text{m}^{-1})\delta_{pyro} + 0.8 \quad \text{for} \quad \delta_{pyro} \geq 5 \times 10^{-4} \text{ m} \tag{19.17b}$$

The correlation given by Equations 19.16 and 19.17 are used to predict the MLRs at various heat flux, and the results are given in Figures 19.35 and 19.36 for the EVA and PBT nanocomposites, respectively. In general, the predictions are in good agreement with the measurements. The ignition times (indicated by sudden increases of the MLRs) and the first peak MLRs are correctly predicted. These results again demonstrate that the same correlations can also be applied to predict pyrolysis at other heat fluxes. In other words, for a given nanocomposite, proportionality factor (between the heat flux ratio and pyrolyzed depth) is independent of the heat flux and, as shown for the PA6 nanocomposite, of the initial sample thickness, but depends only on the amount of nanoparticles accumulating on the surface or equivalently the pyrolyzed depth.

19.7.2 EXTENSION OF THE MODEL FOR DIFFERENT LOADINGS OF NANOCCLAY

To examine the optimized loading for a PA6/MMT nanocomposite, a series of tests were conducted in the cone calorimeter [24] with various (2%, 5%, and 10%) loadings of nanofillers. The experimental HRR/MLR are reproduced in Figure 19.37, where it was found that the HRR/MLR decrease as the concentration of nanofillers increase up to 10%. The main objective of this section

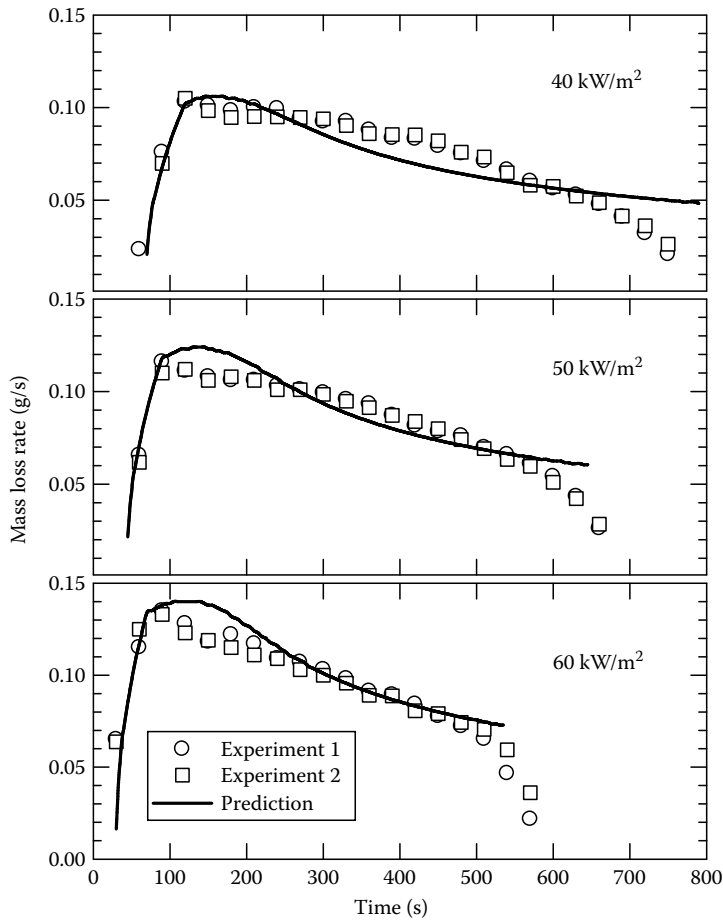


FIGURE 19.35 EVA nanocomposite—comparisons of experimental and predicted MLRs for 6 mm samples at three heat fluxes.

is to extend the model to account for the change in the nanofiller loading, or, in other words, to use the experimental data at one nanofiller loading to predict the burning behaviors of nanocomposite at other loadings.

As shown earlier, for a given nanocomposite (PA6, EVA, and PBT) the heat flux ratio is proportional to the pyrolyzed depth by a factor K , although the factor K may vary with the type of polymer and the type and loading of nanofillers. Furthermore, we assume implicitly that the density and conductivity of the surface layer do not change with different nanofiller loadings, thus the factor K would be proportional to the loading. With this assumption, the factor K for one of the three loadings is found by optimization or, more specifically, comparing the predictions with the experimental data, whereas that for other loadings can be determined proportionally. For example, for the 5% case K is found to be $142 \text{ (m}^{-1}\text{)}$. Thus, we have

$$\text{ratio}_{\text{flux}} = 1.15 \quad \text{for} \quad \delta_{\text{pyro}} < 5 \times 10^{-4} \text{ m} \tag{19.18a}$$

$$\text{ratio}_{\text{flux}} = 142(\text{m}^{-1})(\delta_{\text{pyro}} - 5 \times 10^{-4}) \times C_{\text{nano}}/5 + 1.15 \quad \text{for} \quad \delta_{\text{pyro}} \geq 5 \times 10^{-4} \text{ m} \tag{19.18b}$$

where C_{nano} denotes the nanofiller loading (%).

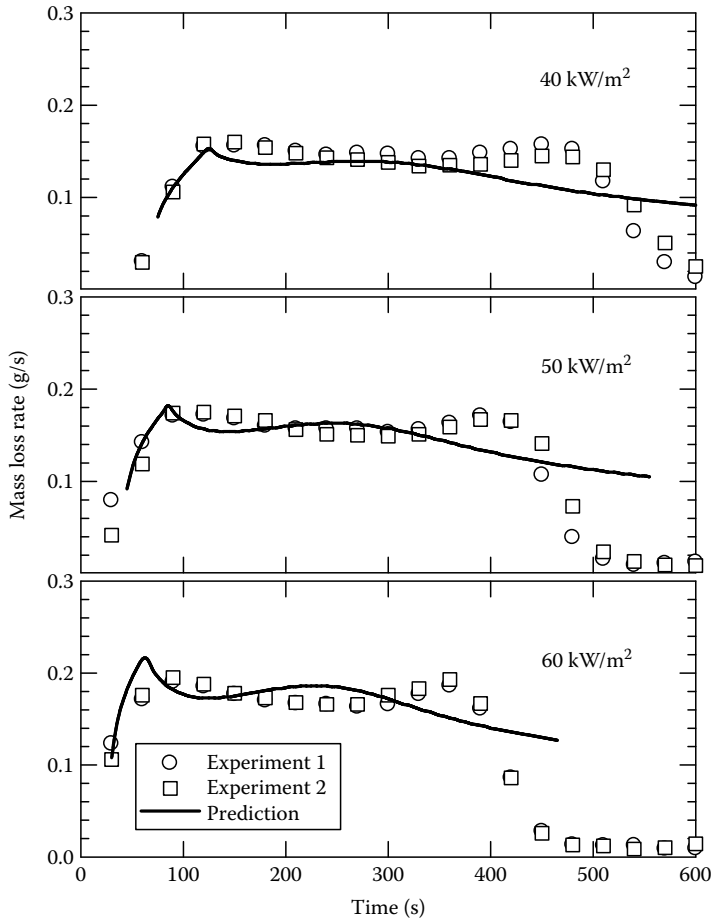


FIGURE 19.36 PBT nanocomposite—comparisons of experimental and predicted MLRs for 6 mm samples at three heat fluxes.

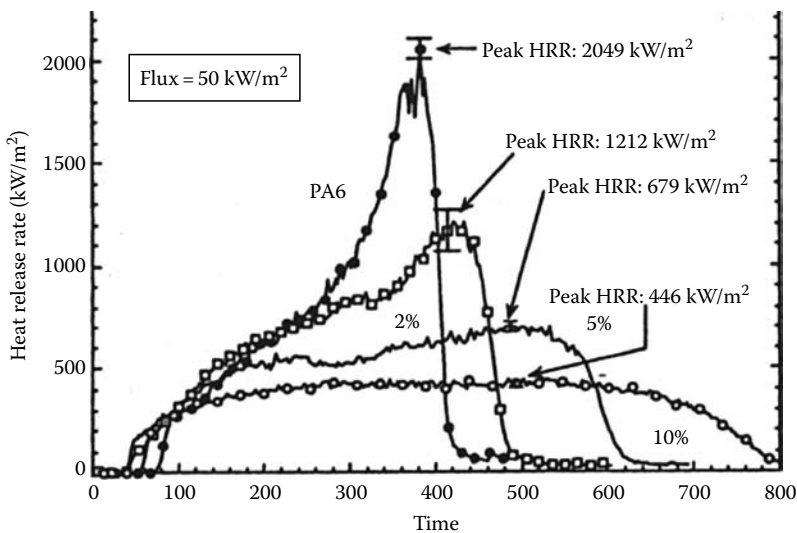


FIGURE 19.37 HRRs for pure PA6 and intercalated PA6/MMT nanocomposites (mass fraction 2%, 5%, and 10%). (Reproduced from Morgan, A.B. et al., *Fire Polym.*, ACS Sym. Ser., 797, 9, 2001.)

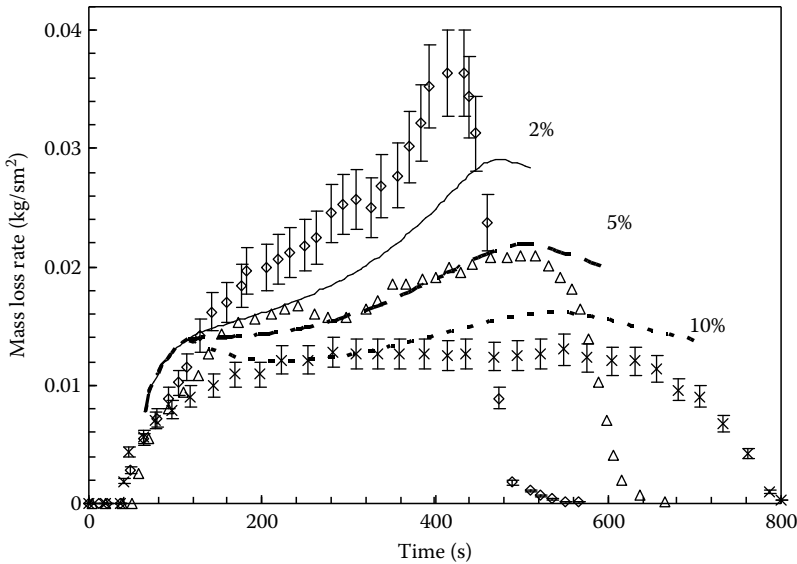


FIGURE 19.38 Comparisons of the predicted and experimental MLRs for different nanofiller loadings at 50 kW/m^2 . The MLRs for 2% and 10% cases were calculated from the reported HRRs for these cases and the effective heat of combustion (EHC) determined from the HRR and MLR data for the 5% case.

Figure 19.38 shows a comparison of the predicted and experimental MLRs at different nanofiller loadings. It is worthwhile to point out that the experimental MLRs for 2% and 10% nanocomposites were not reported, but calculated by dividing the HRRs in Figure 19.37 over the EHC. The EHC was determined from the HRR and MLR of 5% nanocomposite, having a value of $33 \pm 3 \text{ kJ/kg}$. The error bars in Figure 19.38 thus indicate uncertainties of $\pm 10\%$. It is noted that the model predicts that the MLR increases with increasing concentration of nanofillers. The prediction for the 10% case is good, whereas the model underestimates the MLR for the 2% case. This underestimation may be explained partly by the observation that the experimental HRR for the 2% case is essentially the same as pure PA6 up to 280 s [24], indicating that no surface layer was formed during this period because of the small amount of nanofillers and the PA6 nanocomposite being intercalated. In addition, the assumption that the pyrolyzed depth is proportional to the nanofiller loading is only approximate implying that the packing density of the nanofiller and the conductivity of the surface layer may change slightly with the nanofiller loading.

19.8 CONCLUSIONS

We have shown in this chapter that microscale measurements can provide a good screening method for the design of fire-resistant materials modified by nanoparticles (and fire retardants) and also, they can be used to quantitatively model and predict the behavior in mesoscale experiments even though an additional parameter is needed to predict the reduced MLR in the mesoscale experiments. The major breakthroughs and challenges are the following:

1. Rheometry of the nanocomposite polymer provides information about the viscosity and shear modulus that can be used to predict the melting behavior in mesoscale experiments.
2. Rheometry can also point to the consistency and strength of the char layer.
3. TGA/ATR for the structure of the condensed phase at different temperatures can also provide information about the strength and consistency of the char.
4. DSC/MDSC can be used to determine the thermal and transport properties as well as the heat of melting and pyrolysis. The measurement of heat of pyrolysis is very challenging and needs more investigation.

5. TGA/ FTIR provides the composition of the pyrolyzing gases but it needs simplifications in the calibration concerning the quantification of the product yields. These results are consistent with the tube furnace and cone results but more work is needed in this area.
6. The tube furnace is a practical method for assessing the production of toxic gases, but it needs more work to make the results applicable for modeling large-scale fires.
7. A methodology and a new parameter have been developed to quantify the effect of the nanoparticles in reducing the mass loss rate in the mesoscale experiments (i.e., cone) where all other properties have been determined from the microscale experiments.

ACKNOWLEDGMENTS

We thank all partners in the PREDFIRE project, Jeff Gilman for useful discussions, and Charlie Wilkie for inviting us to prepare this review. Finally, we thank Mary Delichatsios for a useful review of the final document.

REFERENCES

1. Samyn, F., Bourbigot, S., Jama, C., Bellayer, S., Nazare, S., Hull, R., Castrovinci, A., and Camino, G. (2008) Characterisation of the dispersion in polymer flame retarded nanocomposites, *European Polymer Journal* 44(6):1631–1641.
2. Samyn, F., Bourbigot, S., Jama, C., Bellayer, S., Nazare, S., Hull, R., Castrovinci, A., and Camino, G. (2008) Crossed characterisation of polymer-layered silicate (PLS) nanocomposite morphology: TEM, x-ray diffraction, rheology and solid-state nuclear magnetic resonance measurements, *European Polymer Journal* 44(6):1642–1653.
3. Ohlemiller, T. J. and Shields, J. R., Aspects of the Fire Behavior of Thermoplastic Materials, NIST TN 1493; NIST Technical Note 1493; p. 158, January 2008.
4. Ohlemiller, T. J. and Shields, J. R., Assessment of a Medium-Scale Polyurethane Foam Flammability Test. NIST TN 1495; NIST Technical Note 1495; p. 45, February 2008.
5. Cipriano, B. H., Kashiwagi, T., Raghavan, S. R., Yang, Y., Grulke, E. A., Yamamoto, K., Shields, J. R., and Douglas, J. F. (2007) Effects of aspect ratio of MWNT on the flammability properties of polymer nanocomposites, *Polymer* 48(20):6086–6096.
6. Kashiwagi, T., Flame Retardant Mechanism of the Nanotubes-Based Nanocomposites Final Report, NIST GCR 07–912; Final Report; p. 68, September 2007.
7. Kashiwagi, T., Fagan, J., Douglas, J. R., Yamamoto, K., Heckert, A. N., Leigh, S. D., Obrzut, J., Du, F., Lin-Gibson, S., Mu, M., Winey, K. I., and Hagenmueller, R. (2007) Relationship between dispersion metric and properties of PMMA/SWNT nanocomposites, *Polymer* 48(16):4855–4866.
8. Stoliarov, S. I. and Walters R. N. (2008) Determination of the heats of gasification of polymers using differential scanning calorimetry, *Polymer Degradation and Stability* 93(2):422–427.
9. Pramoda, K. P., Liu, T., Liu, Z., He, C., and Sue, H. J. (2003) Thermal degradation behaviour of polyamide 6/ clay nanocomposites, *Polymer Degradation and Stability* 81(1):47–56.
10. Jang, B. N. and Wilkie, C. A. (2005) The effect of clay on the thermal degradation of polyamide 6 in polyamide 6/clay nanocomposites, *Polymer* 46(10):3264–3274.
11. Herrera, M., Matuschek, G., and Kettrup, A. (2001) Main products and kinetics of the thermal degradation of polyamids, *Chemosphere* 42(5):601–607.
12. Bourbigot, S., Le Bras, M., Dabrowski, F., Gilman, J. W., and Kashiwagi, T. (2000) PA6-Clay nanocomposite hybrid as char forming agent in intumescent formulations, *Fire and Materials* 24:201–208.
13. Stec, A. A. and Hull, T. R. New Strategies and Mechanisms, Royal Society of Chemistry, (In press Mar 2008).
14. de Ris, J. L. and Khan, M. M. (2000) Sample holder for determining material properties, *Fire and Materials* 24:219–226.
15. Kashiwagi, T., Grulke, E., Hilding, J., Groth, K., Harris, R., Butler, K., Shields, J., Kharchenko, S., and Douglas, J. (2004) Thermal and flammability properties of polypropylene/carbon nanotube nanocomposites, *Polymer* 45(12):4227–4239.
16. Staggs, J. E. J. (2005) Savitzky–Golay smoothing and numerical differentiation of cone calorimeter mass data, *Fire Safety Journal* 40(6):493–505.

17. Green, J. Phosphorus-containing flame retardants, in *Fire Retardancy of Polymeric Materials*, Grand, A. F. and Wilkie, C. A. (Eds.), Marcel Dekker Inc., New York, 2000, Chap. 5, pp. 147–170.
18. Delichatsios, M. A. and de Ris, J. L., An analytical model for the pyrolysis of charring materials, Technical report, J.I. OK0J1.BU, Factory Mutual Research, 1983.
19. Delichatsios, M. A., Paroz, B., and Bhargava, A. (2003) Flammability properties for charring materials, *Fire Safety Journal* 38(3):219–228.
20. Zhang, J., Delichatsios, M. A., and Tofilo, P. Determination of the convective heat transfer coefficient in three-dimensional inverse heat conduction problems, *Fire Safety Journal* (In press Jan 2009).
21. Delichatsios, M. A. (2005) Piloted ignition times, critical heat fluxes and mass loss rates at reduced oxygen atmospheres, *Fire Safety Journal* 40(3):197–212.
22. Lyon, R. R. and Janssens, M. L., Polymer flammability, Office of Aviation Research Washington, DC, 20591, DOT/FAA/AR-05/14, 2005.
23. Frederick, W. J. and Mentzer, C. C. (1975) Determination of heats of volatilization for polymers by differential scanning calorimetry, *Journal of Applied Polymer Science* 19:1799–1804.
24. Morgan, A. B., Kashiwagi, T., Harris, R. H., Campbell, J. R., Shibayama, K., Iwasa, K., and Gilman, J. W. (2001) Flammability properties of polymer-clay nanocomposites: Polyamide-6 and polypropylene clay nanocomposites, *Fire and Polymers*, Nelson, G. L. and Wilkie, C. A. (Eds.), 2001, ACS Sym. Ser. 797:9–23.

20 Full-Scale Fire Modeling

Chris Lautenberger and Simo Hostikka

CONTENTS

20.1	Introduction.....	551
20.2	Gas-Phase Physics Required to Predict Fire Growth.....	552
20.2.1	Fluid Dynamics.....	552
20.2.1.1	Navier–Stokes Equations	552
20.2.1.2	Turbulence Modeling (LES/RANS).....	553
20.2.2	Combustion	555
20.2.2.1	Why Combustion Modeling?	555
20.2.2.2	Mixture Fraction Formulation.....	556
20.2.2.3	Computation of Reaction Rate	558
20.2.3	Heat Transfer.....	559
20.2.3.1	Radiation	559
20.2.3.2	Convection.....	561
20.3	Condensed-Phase Pyrolysis	562
20.3.1	Condensed-Phase Heat Conduction.....	562
20.3.2	Liquid Fuels	563
20.3.3	Solid Fuels: Empirical Models.....	564
20.3.4	Solid Fuels: Heat Transfer Limited Pyrolysis Models	565
20.3.5	Solid Fuels: Finite-Rate (Kinetically Limited) Pyrolysis Models	566
20.3.6	Material Property Estimation	567
20.4	CFD Simulation of Large-Scale Burning and Fire Growth.....	568
20.4.1	Burning Rate Prediction for Stationary (Nonspreading) Fires.....	569
20.4.2	Flame Spread on Flat Surfaces and Combustible Corners	570
20.4.3	Rail Cars	573
20.4.4	Dalmarnock Fire Tests.....	575
20.4.5	Forensic Fire Reconstruction	576
	List of Symbols.....	579
	Abbreviations.....	580
	Acknowledgments.....	580
	References.....	580

20.1 INTRODUCTION

Fire safety engineering is used to ensure that the risk of fire-induced losses for humans, property, environment, and the surrounding society associated with the target of the analysis is acceptable by the common standards of the society. Additional objectives may be imposed, for example, by economic goals and needs to protect cultural heritage. Fire safety engineering is typically used to design the fire safety measures of new buildings or transportation vehicles. Traditionally, the design is based on a set of prescriptive requirements for the physical characteristics, such as the dimensions of the fire compartments, classification of structures, and width and length of evacuation routes. These requirements are described in national (or state) building codes and are based mainly on

experimental findings and accumulated lessons learned from past fires. An alternative design methodology is a performance-based design, where the effectiveness of fire safety measures is assessed by considering the performance of an entire system, not as a fulfillment of individual prescriptive requirements given by the building code. An essential part of the design process is the analysis of the risks associated with fires and assessment of the efficiency of the proposed fire safety measures.

The increased size and complexity of new buildings creates new demands for simulation techniques. During the last few years, computational fluid dynamics (CFD) has become the most widely used technique for the simulation of smoke transport and fire spread. Simpler techniques, such as hand-calculation formulas and two-zone models, still have an important role in engineering because they are faster and easier to use than CFD, but the majority of fire simulations are currently performed using CFD. One application of CFD-based fire modeling that is becoming more routine in use is fire development modeling (sometimes called flame spread modeling or fire growth modeling). In this type of simulation, the overall heat release rate (HRR) and species production rates are actually calculated (predicted) as the fire develops, rather than specified beforehand.

This chapter reviews the aspects of physical and numerical modeling necessary to simulate fire development with present fire models, focusing in particular on CFD models. The emphasis is put on physical phenomena such as fluid dynamics, combustion, radiation, solid-phase heat transfer, and flame spread. The features of large eddy simulation (LES) and Reynolds-averaged Navier–Stokes (RANS) models and the challenges of radiation modeling are discussed in detail. The issues of numerical implementations and user interfaces are discussed briefly. Models designed for special applications, such as explosions or direct numerical simulation (DNS) of combustion processes, are not discussed. Several examples of CFD-based predictions of large-scale fire development are presented to give an idea about current capabilities and limitations.

20.2 GAS-PHASE PHYSICS REQUIRED TO PREDICT FIRE GROWTH

In the 2002 *Society of Fire Protection Engineers (SFPE) Handbook* chapter concerning CFD fire modeling, Cox and Kumar [1] presented the principles, practices, and instruction for the proper use of CFD in fire applications from the perspective of the RANS technique. When the chapter was written, it was widely accepted that the proper method for low-speed turbulent flow was RANS using an eddy viscosity turbulence model such as the k - ϵ model, SIMPLE pressure correction algorithm [2] or some of its variants, and the various submodels like eddy break-up (EBU) [3] for combustion. However, in recent years, owing to faster computers and specialized algorithms, LES is now considered by many to be the preferable technique to study fire-driven flows. LES is used in Fire Dynamics Simulator (FDS) [4,5], which was made publicly available in the year 2000. Although there is little fundamental difference between RANS and LES, other than the treatment of time dependence in the Navier–Stokes equations, the article of Cox and Kumar [1] provides little guidance for FDS users because it focuses on RANS. This example illustrates how rapidly a computational field of engineering may evolve.

CFD fire models can be classified based on many different criteria, with RANS vs. LES being probably the most widely used. Other possibilities would be the type of radiation model, availability, price, user interface, and hardware requirement. All these aspects have been discussed in the review paper of Olenick and Carpenter [6].

20.2.1 FLUID DYNAMICS

20.2.1.1 Navier–Stokes Equations

Most physical phenomena in fires can be described as the transfer of heat and mass and chemical reactions in either gas or condensed phases. The physics of the fluid flow are governed by the conservation equations of mass, momentum, and enthalpy:

$$\frac{\partial \rho}{\partial t} + \nabla \cdot \rho \mathbf{u} = \dot{m}''' \quad (20.1)$$

$$\frac{\partial}{\partial t} (\rho \mathbf{u}) + \nabla \cdot \rho \mathbf{u} \mathbf{u} = -\nabla p + \rho \mathbf{g} + \mathbf{f} + \nabla \cdot \boldsymbol{\tau} \quad (20.2)$$

$$\frac{\partial}{\partial t} (\rho h) + \nabla \cdot \rho h \mathbf{u} = \nabla \cdot \left[\frac{k}{c_p} \nabla h - \mathbf{q}_r \right] \quad (20.3)$$

These equations are called the Navier–Stokes equations, and when supplemented by the state equation for fluid pressure and species transport equations, they form the basis for any computational model describing the flows in fires. For simplicity, several approximations are inherent (see Equation 20.3) (no Soret/Dufour effects, no viscous dissipation, Fickian diffusion, equal diffusion coefficients of all species, unit Lewis number).

The core of any CFD model is its Navier–Stokes solver. The numerical solution of these equations is considered by many to be a “mature” field, because it has been practiced for over 30 years, but the nature of turbulence is still one of the unsolved problems of physics. All current solvers are based on the approximations that have their effects on the applicability of the solver and the accuracy of the results—also in the fire simulations. The aspects of turbulence modeling are discussed in the next section.

Virtually all CFD fire models assume low Mach number flow, which is adequate in typical fire application, but not for high velocity cases and explosions. Inclusion of the compressibility effects in fire simulations would increase the computational cost considerably. One of the few compressible fire models is the Uintah Computational Framework developed at C-SAFE project of the University of Utah [7].

20.2.1.2 Turbulence Modeling (LES/RANS)

Current practical CFD fire models fall into one of the two major categories: RANS or LES. The difference of these two categories is the nature of the starting equations: In RANS, the Navier–Stokes equations are *time* or *ensemble averaged* before the derivation of the discrete form suitable for programming as a solver algorithm. The solver then finds a *steady state* or *quasi steady state* solution for the equations. Time-dependent flows can be solved as long as the time scale of the mean flow is large compared with that of the turbulent fluctuations [7]. In LES, the time averaging is not performed, and the solutions can be considered “accurate” in time, meaning that the variations in the solution correspond to the motions resolvable by the numerical grid. The marching in time takes place using a short time step Δt , which is usually defined by the following stability criterion:

$$\Delta t < \min_{ijk} (\Delta x_{ijk} / u_{ijk}) \quad (20.4)$$

where Δx and u are the grid cell size and velocity, respectively, and the minimum is found over the entire computational domain. Equation 20.4 is called Courant–Friedrichs–Lewy (CFL) condition [8,9] after the German mathematicians who proposed it in 1928—well before modern computers. In explicit numerical solvers, the CFL condition must be met to ensure solution stability. For implicit solvers, the constraint for the time step is not caused by the stability criteria but the requirement of temporal accuracy, often leading to a time step of the same order as given by Equation 20.4.

In LES, the filtering is performed in space, although the actual filtering is usually limited to the length scales below the grid cell size. This may be confusing, since in the fluid dynamics literature, the derivation of LES algorithms usually involves the spatial filtering operation:

$$\bar{\phi}(\mathbf{x}, t) = \int_{\Omega} G(\mathbf{x} - \mathbf{x}') \phi(\mathbf{x}', t) d\mathbf{x}' \quad (20.5)$$

where $G(\mathbf{x} - \mathbf{x}')$ is a filtering window. In the actual models, the filtering volume Ω is usually set equal to the numerical grid cell, and the cell value simply represents a volumetric average in the cell.

The difference between RANS and LES is depicted in Figure 20.1, which shows the temperature fields of a pool fire flame. While the RANS result shows smooth variations and looks like a laminar flame, the LES result clearly illustrates the large-scale eddies. Both results are the correct solutions of the corresponding equations. However, the time accuracy of LES is also essential for the quantitative accuracy of the buoyancy-driven flows. As Rehm and Baum have shown [10], the dynamic motions or “eddies” are responsible for most of the air entrainment into the fire plumes. Because these motions cannot be captured by RANS, LES is usually better suited for fire-driven flow. LES typically requires a finer spatial resolution than RANS. Examples of RANS-based fire CFD models are JASMINE, KAMELEON [11], SMARTFIRE [12], SOFIE [13], ISIS [14], and ISIS-3D [15]. Examples of LES models are the FDS [4,5] and SMAFS [16], developed at Lund University. Fire simulations using LES have also been performed by Cheung et al. [17] and Gao et al. [18].

There are certain applications where RANS has a clear advantage over LES. RANS models can take advantage of any *a priori* knowledge of the mean flow direction by accepting high aspect ratio grid cells. An example of such an application is a flow in a tunnel, where the grid cells can be made long and thin, giving good accuracy in the direction normal to the tunnel walls but saving cells in the direction of the tunnel, where variations are slow. In LES, all the velocity components are present with a likelihood of the same order, and the cell aspect ratios being close to unity. For this reason, tunnel simulations using LES are computationally expensive. The second type of application where RANS is advantageous is the simulation of long, quasi-steady or steady-state fires. In such cases, RANS allows fast marching in time using long time steps, while LES is bound by the CFL condition.

Turbulence modeling and time accuracy are closely related. In RANS solvers, turbulence models are used to describe all the turbulent properties of the flow. A range of different models have been

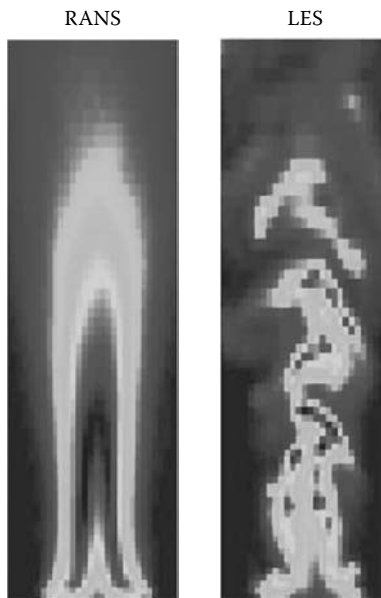


FIGURE 20.1 (See color insert following page 530.) A comparison of temperature fields in pool fire flame simulations using RANS and LES.

developed. The differences in the models have been mainly related to the assumption of homogenous ($k-\epsilon$, $k-\omega$) or inhomogeneous (Reynolds stress models) turbulence and the treatment of boundary layers (wall functions vs. small Reynolds number models). The inability of these models to accurately predict entrainment into buoyant plumes has been known for some time, and is more fundamental than just the turbulence closure problem. A review of the turbulence modeling in RANS is given by Kumar [19], and the effect of turbulence models on the CFD simulation of buoyant diffusion flames has been studied by Liu and Wen [20].

In LES, the role of turbulence models is only to describe the subgrid scale phenomena that cannot be resolved on the computational grid. In regions of high shear, the subgrid scale models have a stronger effect on the solution and additional research is still needed to find good solutions for handling these flows. Examples of high shear flows in fire simulations are the solid wall boundaries and the interface of the hot and cold flows in doors and windows.

Despite the relatively short history of LES fire modeling, the accuracy of LES technique in fire simulation has been studied extensively. Early validation of FDS predecessors was performed by comparing simulations against salt water experiments [21–23], fire plumes [24,25], and room fires [26]. More recently, the FDS model has been validated for fire plumes [27] and fires in enclosures in the context of the World Trade Center investigation [28,29] and the fire model validation project sponsored by the U.S. Nuclear Regulatory Commission [30]. Some of the above cases and numerous others have been collected to the Validation guide of FDS [4, Vol 3] (not yet published as a separate document).

In RANS simulations, boundary layers have traditionally been handled using wall functions that assume a logarithmic velocity profile on the wall. In simple applications, these functions work well, having the most serious problems in situations involving separation and reattachment. Similar “subgrid scale wall functions” can be derived for LES, or the effect of the wall can be taken into account in the subgrid scale model of viscosity [32]. Currently, FDS does not include any wall functions. Only an adjustment of the slip-velocity boundary condition and simple heat transfer coefficient correlations are used. In their comparison of measured and predicted turbulence statistics, Zhang et al. [33] showed that even with these simple boundary treatments, FDS was able to produce good flows at room scales. Naturally, new techniques must be studied to improve the accuracy of solid-phase heat transfer and flame spread predictions.

20.2.2 COMBUSTION

20.2.2.1 Why Combustion Modeling?

The most important difference between the majority of CFD applications and fire CFD is what drives the flow. In typical nonfire CFD, the boundary conditions such as inflow velocity drive the flow. Fire problems, in turn, are always driven by the combustion source terms. The accuracy of the combustion model is therefore essential for the quality of the whole simulation. Depending on the nature of the simulation, different aspects of combustion modeling become important: in the prediction of heat transfer from the flames to the nearby surfaces, the *spatial distribution* of the HRR is important because it determines the temperature field. Flame spread simulation is an important example where the fine details of the temperature field determine the heat fluxes and heating of the condensed-phase. For simulation of quantities that are far from the flame zone, such as smoke filling of a large building, it is important that the combustion model can accurately predict the *global* HRR, which acts as a source of buoyancy and energy. For the simulation of toxic hazards, the completeness of the chemical reactions and the production of gaseous species, such as CO, are important.

Fire science has always been a small field compared with combustion science, which is clearly the closest relative. Through the history of fire CFD, combustion models that have been developed for other combustion problems have been directly applied to fire problems. When doing that, the above-mentioned aspects of fire simulation should be kept in mind. In particular, the

requirement of an accurate global/integrated HRR value must be ensured (this is rarely found interesting in combustion science). The theoretical challenge for the modeling comes from the range of combustion phenomena relevant to large-scale fire development: lean premixed combustion, partially premixed combustion, nonpremixed combustion, and rich combustion during postflashover burning.

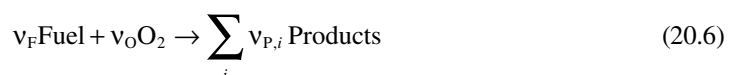
Over the last 30 years, considerable progress has been made in understanding elementary chemical reactions relevant to combustion and pollutant formation. Even for simple hydrocarbons, hundreds of reactions and intermediate species are involved in the oxidation process. For example, the GRI-Mech 3.0 mechanism (intended primarily for the combustion of methane, a relatively simple hydrocarbon) includes 325 elementary reactions and 53 species [34]. Additional reactions and intermediate species must be considered to describe the oxidation of higher hydrocarbons produced in fires. It is not yet possible to predict the chemical composition of these gases; even if this was possible, the combustion mechanism required to describe the oxidation of these gases would involve such a large number of species that computer power limitations would preclude the use of such a mechanism in practice except for highly simplified (i.e., one-dimensional (1D) steady state) calculations. In fire growth modeling, complex combustion processes are usually relegated to either a single “global” irreversible reaction with infinite (mixing limited) or finite (temperature limited) rate, single or two-step reactions with an empirical “mixing time” as a rate, or a flamelet library representing the numerous reactions that cannot be explicitly calculated.

In addition to the inherent complexity of microscale combustion processes, the range of length (and time) scales relevant to combustion and turbulence also presents significant computational challenges for fire growth modeling. The thickness of the reaction zone in a diffusion flame and the Kolmogorov microscale are of the order of 1 mm or finer, but currently available computer power limits grid sizes used in three-dimensional (3D) simulations of room-scale fire growth to ~25 mm. For these reasons, DNS of large-scale fire growth is not yet feasible. Consequently, CFD-based fire growth modeling requires the use of simplified descriptions of combustion and turbulence involving subgrid-scale or stochastic models [35,36]. The consequences of these turbulence and combustion modeling approaches on flame spread predictions have not been thoroughly explored.

20.2.2.2 Mixture Fraction Formulation

In the formulation of numerical models for combustion, a number of simplifying assumptions and approximations are typically made. In an Eulerian framework, combustion modeling requires solution of the gas-phase transport equation for some scalar representing the fuel concentration. Owing to the computational cost, the number of simultaneous gaseous fuels is often limited to one. In real fires, a range of different fuels are produced from different materials, but in gas-phase combustion modeling the different fuels are represented by a single fuel. The effect of this approximation has not been studied, but if we are mainly interested in far-field quantities it is reasonable to assume that the effect is small as long as the correct amount of energy is released by taking into account the differences in heat of combustion. Where errors may be introduced is when simulating combustion of fuels with disparate combustion characteristics in a single simulation, e.g., a compartment fire in which both methane (lightly sooting) and acetylene (highly sooting with luminous flames) are burned.

In full-scale fire modeling, a diffusion flame structure is usually assumed. However, in many fire situations, such as underventilated fires, premixed or partially premixed flame theory may be more appropriate. The Burke-Schumann description of the diffusion flames can be used to conveniently represent the transport of gaseous species by a single scalar quantity called *mixture fraction*. For a simple one-step reaction:



the mixture fraction is defined as a fraction of the mass that originated in the fuel stream:

$$Z = \frac{sY_F - (Y_O - Y_O^\infty)}{sY_F^f + Y_O^\infty}; \quad s = \frac{\nu_O M_O}{\nu_F M_F} \tag{20.7}$$

where

Y_O and Y_F are the mass fractions of oxygen and fuel, respectively

Y_F^f is the mass fraction of fuel in the fuel stream

Y_O^∞ is the ambient mass fraction of oxygen

s is the stoichiometric oxygen to fuel mass ratio

M_F and M_O are the quantities of the fuel and oxygen molecular weights, respectively

The benefits of using the mixture fraction are twofold: (1) instead of solving separate transport equations for fuel, oxygen, nitrogen, and their combustion products, it is sufficient to solve a single transport equation for mixture fraction and calculate individual species concentrations from the value of the mixture fraction using the so-called state relations [38], and (2) since the mixture fraction is a perfectly conserved scalar, it is not necessary to calculate species formation/destruction rate source terms, which can be expensive to evaluate and cannot be accurately evaluated on coarse grids. An example of state relations is shown in Figure 20.2 for ethanol. The transport equation for mixture fraction is

$$\rho \frac{DZ}{Dt} = \nabla \cdot \rho D \nabla Z \tag{20.8}$$

where

D is the diffusion coefficient

D/Dt is the material derivative

This equation shows that the mixture fraction is a conserved scalar—its transport equation has no source or sink terms.

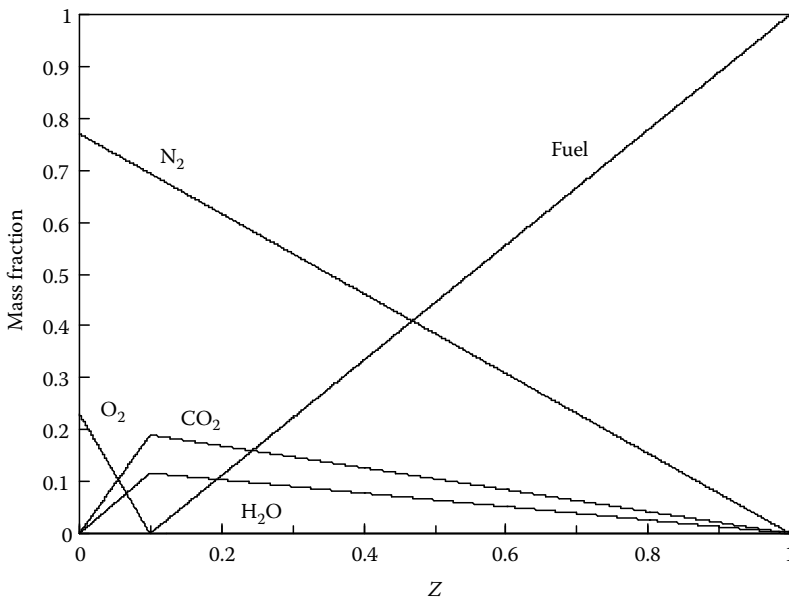


FIGURE 20.2 State relations for ethanol.

20.2.2.3 Computation of Reaction Rate

The combustion reaction rate is controlled both by the availability of fuel and oxygen kinetic effects (temperature). In full-scale fire modeling, the resolvable length and time scales are usually much larger than those associated with the scales of the chemical combustion reaction, and it is common to assume that the reactions are infinitely fast. The local reaction rate depends on the rate at which oxygen and fuel are transported toward the surface of stoichiometric mixture fraction, shown in Figure 20.2 as a point where both oxygen and fuel mass fractions go to zero. For almost 20 years, the EBU or eddy dissipation models were the standard models used by the combustion CFD community. With the EBU, in its simplest form, the local rate of fuel consumption is calculated as [3]:

$$R_{\text{FU}} = \bar{\rho} \frac{\varepsilon}{k} \min \left[C_R Y_F, \frac{C'_R Y_O}{s} \right] \quad (20.9)$$

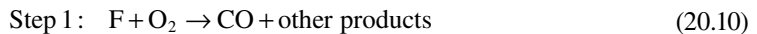
where

- k and ε are, respectively, the turbulent kinetic energy and its dissipation rate
- Y_F and Y_O are the time-averaged mass fractions of fuel and oxidant, respectively
- C_R and C'_R are empirical constants

The form of EBU expression is mainly based on dimensional arguments. The ratio k/ε is the turbulent time scale. If the turbulence intensity is high, so is the fuel consumption. For the prediction of secondary species, such as CO, HCl, and soot, more advanced models using flamelets [37] have been used. The flamelets (and state relations) can be determined either experimentally [39] or computationally, using detailed models for combustion chemistry [40] that incorporate strain rate effects.

In LES, the application of EBU-type combustion models is not straightforward, because the turbulence quantities ε and k are not explicitly calculated. The models developed by combustion scientists for LES are usually based on flamelets and rely on good spatial accuracy where both temperature and concentration fields are well captured in the vicinity of the reaction zone. The subgrid scale turbulence and combustion are related by assuming a statistical distribution of conditions inside a grid cell—instead of uniform conditions indicated by the averaged cell values. For simplicity, some presumed shape for the probability density function (pdf) representing the statistical distribution of conditions is assumed (i.e., beta function, clipped Gaussian, etc.). Then, the shape of the pdf is determined based on the mean, variance, and sometimes higher order moments of the pdf as determined from the filtered temperature/species fields. Unfortunately, in a typical fire simulation, neither the temperature nor the species concentrations are accurately captured and the necessary pdf parameters may be difficult to determine. Robustness can thus only be achieved by simplicity.

In FDS, a generalized mixture fraction formulation assuming two-step combustion is used:



The first step is infinitely fast, consuming all of either the fuel or the oxygen in the grid cell. On the basis of the empirical arguments, an upper limit is placed on the volumetric HRR. Typically, this limit is about 200 kW/m² of flame area [41]. Mixing-based constraints of the reaction rate are currently being investigated. The second step converts CO to CO₂ and is assumed to happen infinitely

fast in the regions where Step 1 is also taking place, and at finite rate elsewhere. In addition, a simple empirically based model for local extinction is used [41].

The use of laminar flamelet combustion models within FDS have been studied by Yang et al. [42] and Kang and Wen [43]. Unfortunately, the performance or advantage over the simple flame-sheet model in large-scale fire simulation was not demonstrated in these studies. In full-scale calculations, the mixture fraction and temperature fields close to the flame sheet have overshoots, caused by the second-order transport scheme. It is still unclear how the laminar flamelet models that require both second and first moments of the local mixture fraction field could work in this situation.

In computations of very fine spatial and temporal resolution, local chemical equilibrium cannot be assumed and the chemical reactions are described as *finite-rate reactions*. The temperature dependence of the reaction rate is presented as an Arrhenius reaction:

$$R_{\text{FU}} \propto e^{-E/RT} \quad (20.12)$$

The Arrhenius form of the reaction results from the Maxwell speed distribution and the rate at which molecular bonds in gas-phase species are broken [44]. In full-scale fire modeling, the finite reaction rates must be considered if one attempts to model things such as CO and soot production and oxidation, or ignition and extinction. However, then the simple mixture fraction formulation must be supplemented by additional variables keeping track of the reaction progress.

20.2.3 HEAT TRANSFER

20.2.3.1 Radiation

In enclosure fires, radiation may be the dominant mode of heat transfer. For flames burning in an open atmosphere, the radiative fraction of overall heat transfer ranges from less than 0.1 to 0.4, depending both on the fuel type and the fire diameter [45]. Owing to the important role that radiation plays in fires, all fire CFD models have a radiation model that solves the radiation transport equation (RTE) [46,48]:

$$\underbrace{\mathbf{s} \cdot \nabla I_{\lambda}(\mathbf{x}, \mathbf{s})}_{\text{rate of change}} = - \underbrace{[\kappa_{\lambda}(\mathbf{x}) + \sigma_{\lambda}(\mathbf{x})] I_{\lambda}(\mathbf{x}, \mathbf{s})}_{\text{rate of attenuation}} + \underbrace{\kappa_{\lambda}(\mathbf{x}) I_{\text{b}}(\mathbf{x}, \lambda)}_{\text{emission source}} + \underbrace{\frac{\sigma_{\lambda}(\mathbf{x})}{4\pi} \int_{4\pi} \Phi(\mathbf{s}, \mathbf{s}') I_{\lambda}(\mathbf{x}, \mathbf{s}') d\Omega'}_{\text{in-scattering}} \quad (20.13)$$

where

\mathbf{s} is the unit direction vector

I_{λ} is the intensity at wavelength λ

$\kappa_{\lambda}(\mathbf{x})$ and $\sigma_{\lambda}(\mathbf{x})$ are the local absorption and scattering coefficients at λ , respectively

I_{b} is the emissive power of the medium

$\Phi(\mathbf{s}, \mathbf{s}')$ is the scattering phase function giving the scattered intensity from direction \mathbf{s}' to \mathbf{s}

The terms of the RTE have the following interpretations: the left-hand side is the rate of change of the intensity in direction \mathbf{s} ; the first right-hand side (rhs) term describes the attenuation by absorption and scattering to other directions; the second rhs term is the emission source term; the last rhs term is the in-scattering integral, describing how much intensity is gained by scattering from all the other directions to the present direction. The intensity depends on location, direction, and wavelength. Typically, wavelength dependence is eliminated by first integrating the RTE over the frequency spectrum, and solving RTE for the integrated field.

Two physical aspects of thermal radiation make radiation modeling particularly challenging:

1. *Soot formation and oxidation*: In fires, soot is usually the dominant emitter and absorber of radiation. The modeling of soot formation and oxidation processes is therefore important for the accurate prediction of radiant emissions. Detailed models that solve for soot number density and mass fraction have been developed over the years, and implemented also in fire CFD models such as SOFIE [64], and more recently in [65] and [66]. In post-flame conditions, the problem is mostly following of the soot produced in the flame zone. Currently, FDS can only follow this passive soot, but “engineering” models for soot formation and oxidation that rely on the laminar smoke point height have been postulated [67–69]. Unfortunately, the soot formation and oxidation processes are sensitive to the temperature and the same problems appear as in detailed combustion modeling.
2. *T^4 dependency of radiation source term*: For the spectrally integrated RTE, the emission source term is

$$\kappa I_b = \kappa T^4 \quad (20.14)$$

where T is the local temperature. Owing to the T^4 -dependence, the emission source term is extremely sensitive to errors in temperature. For example, a 15% underestimation of temperature would lead to a source term that is too small (48%). In large-scale fire simulation, this kind of error in the flame region can rarely be avoided. The problem is typically solved by modeling the emission term either as a constant fraction of HRR (used in FDS) or using precomputed flamelet libraries (e.g., SOFIE).

As with combustion modeling, the development of radiation modeling in fire CFD has consisted mostly of adapting techniques developed for combustion simulations. However, fire radiation modeling may be even more challenging and its role is more pronounced than in the pure combustion problems. A wide range of different radiation models have been used for fire CFD over the years. The models mainly differ from each other in the way they solve the spatial and angular field of intensity. The simple models like P-1 and six flux models [46] were popular in the early years. In P-1, the diffusion approximation of RTE is adopted, and spherical harmonics are used to develop the intensity. It is best suited for optically thick cases where intensity fields have smooth variations. The six flux model in turn is related to the use of Cartesian grid system; the intensity is solved in the six coordinate directions. The ray tracing models such as discrete transfer (DT) [47] are theoretically good for fires but may become computationally expensive. In DT, the RTE is integrated along the imaginary lines of sight, or rays, starting from the boundaries of the domain.

The flux models such as discrete ordinates methods (DOM) [48] and finite volume method (FVM) [49] are currently the most popular in new models. In these models, the solid angle is first divided to small control angles or directions, and the flux of intensity for each direction is solved separately in space. DOM and FVM are very similar techniques. In DOM, the angular distributions are defined by generalized S_N and T_N quadratures. In FVM, the polar/azimuthal discretization is model-specific but the angular integration is performed exactly. The numerical accuracy of FVM depends on how the local propagation of intensity is solved [50,51]. The most general solution technique of radiation transport is the use of Monte Carlo (MC) where the radiative emission and absorption processes are modeled by sending large number of photons with random energy and direction. It is currently beyond the computational resources in most practical simulations, but an important validation tool for the other models. However, MC can be used if the spatial resolution of the simulation is very coarse, in which case the total number of photons does not become prohibitive. Various modeling approaches for radiative heat transfer in pool fires are compared in [52].

An important parameter in RTE that needs modeling is the calculation of the absorption coefficient $\kappa(\mathbf{x}, \lambda)$, which depends on the local gas and soot concentrations. In a typical fire CFD, a gray gas is assumed, which means that the spectral dependency of κ is not considered; instead κ_λ is replaced with an integrated value of κ that is obtained by integrating over the entire wavelength

spectrum. Some aspects of the spectral resolution can be captured by dividing the spectrum to a relatively small number of bands, determining “band mean” values of κ , and solving a separate RTE for each band. In the combustion literature, a large number of wide-band models have been developed to account for the band-structure of the emission spectra of the most important combustion gases. The most accurate results could be obtained by using a narrow-band model, where separate RTEs are solved for hundreds of wavelengths [53,54]. This is still too expensive for practical fire CFD. The use of correlated- k [55] and spectral narrow-band and global gas radiation models [56,57] have been studied at Kingston University.

The following properties of thermal radiation are challenges from the viewpoint of computational efficiency:

1. *Inhomogeneity*: The strong inhomogeneity of the optical properties and temperature field makes the simplest and fastest models (P-1 and six flux models) inaccurate. The presence of large optically thin areas aggravates the ray effect for all the models dealing with discrete directions, especially the ray tracing methods.
2. *Spectral dependence*: In most large-scale fire simulations, emission from soot dominates over gas and solid wall emissions. The gray gas assumption is a good approximation for sooty flames, because soot particles emit continuously over the entire wavelength spectrum. However, in lightly sooting fires, emission and absorption by CO_2 and H_2O are important. The emission/absorption spectra of these gases have sharp peaks that make the gray gas assumption inaccurate.
3. *Time dependence*: The inherent time dependence of fires sets strong requirements for computational efficiency. In RANS models, the radiation field must be updated within the internal iterations of the time step, but the computational cost can be relaxed by solving RTE only every N th iteration. In SOFIE, for example, it is typical to use $N = 10$. In FDS, the time accuracy of the radiation field has been relaxed by solving the FVM equations typically every third time step and only part of the directions at a time.
4. *Scattering*: When a beam of radiation meets soot or water droplets, it is scattered to all directions. The distribution of directions, given by the phase function, depends on the ratio of particle size to wavelength. The scattering has a tremendous effect on the radiation blocking ability of the fine water sprays and smoke. Owing to the computational complexity, scattering has often been neglected in fire CFD models. To accurately simulate water mist and sprinkler systems, this effect should be taken into account. There are actually two challenges related to the scattering: The first challenge is the computation of the radiative properties, i.e., absorption and scattering coefficients and the scattering phase function. For water droplets, Mie-theory can be used for the calculation of *single droplet* radiative properties. Free subroutines performing these Mie-calculations are available for use in the radiation solvers [58,59]. The integration over the spectrum and droplet size distribution must be performed in the model. The second challenge is the computation of the scattering integral. The first approximation is to use isotropic scattering, which considerably simplifies the computation. Full integrations using DOM and FVM have been performed in simplified scenarios [60–62], but not yet in practical fire CFD. In FDS, the scattering integral is approximated by a combination of functions describing isotropic and forward scattering [63].

20.2.3.2 Convection

Convective heat transfer takes place between the fluid phase and solid walls and obstructions, and the convective heat flux is calculated as a product of convective heat transfer coefficient and temperature difference between the solid and gas phases:

$$\dot{q}'' = h \cdot \Delta T \quad (20.15)$$

For simple boundary-layer flows, h can be determined analytically; more often, h is determined from empirical correlations that can be found in most heat transfer texts. This is a simple and practical way of computing convection in full-scale fire simulations.

The actual physical phenomena lumped behind the apparent simplicity of Equation 20.15 are heat conduction and mixing within the fluid flow boundary layer. With sufficient grid resolution, CFD models can solve the velocity and temperature profiles within near-wall boundary layers, and the convective heat transfer rate to the wall can be directly calculated from the temperature gradient at the wall, making specification of a convective heat transfer coefficient unnecessary. However, since the boundary layers appearing in fire-induced flows are typically only few centimeters thick, and grid cells are usually in the order of 10 cm or coarser in large-scale fire simulations, it is practically impossible to achieve sufficient spatial resolution to resolve near-wall boundary layers in full-scale fire simulations. Consequently, convective heat transfer rates must be calculated from Equation 20.15 using an appropriately determined value of h .

In RANS models, the solid wall boundary conditions have traditionally been modeled using wall functions. Wall functions use empirical profiles to replace the actual boundary conditions, such as no-slip (zero velocity) condition at solid surfaces. An example of an empirical law is the logarithmic velocity profile:

$$u^+ = \frac{1}{\kappa} \ln(y^+) + C \quad (20.16)$$

where

u^+ is dimensionless velocity

y^+ is dimensionless wall distance

κ is von Karman's constant (about 0.41)

C is a constant (about 5.1)

The form and complexity of the wall functions is closely related to the turbulence model closure used.

20.3 CONDENSED-PHASE PYROLYSIS

In a spreading fire, combustion occurs when gaseous fuel liberated from condensed-phase (solid or liquid) materials mixes with the surrounding oxidizer and reacts with oxygen, thereby releasing heat and combustion products. This heat supports further fuel heating and gasification. Therefore, condensed-phase processes are one of the primary factors controlling ignition, burning, and flame spread in fires. Accurate simulation of flame spread and fire growth requires accurate simulation of condensed-phase fuel generation processes.

Generically, a pyrolysis model is an algorithm that calculates the rate at which solid combustibles generate gaseous fuel (pyrolyzate, CO) or other gases (CO₂, H₂O) when thermally stimulated. Pyrolysis models range from simple empirical formulations that rely heavily on fire test data to complex models that simulate microscale physical and chemical processes in detail. In this chapter, we provide only a brief review of different pyrolysis modeling approaches that have been applied to simulate large-scale fire growth with CFD. The reader is referred to recent reviews of pyrolysis modeling strategies for fire simulation [71] and wood pyrolysis [72] for a detailed account.

20.3.1 CONDENSED-PHASE HEAT CONDUCTION

Solution of condensed-phase heat transfer equation is needed to analyze structural response to fires and simulate flame spread on solid surfaces. The solution of this conjugate heat transfer problem simulate is typical for fires, but rarely found in commercial CFD packages. Over the years, different techniques have been developed to tackle this problem. Since solid-phase heat transfer

is a completely separate problem from the fluid dynamics problem, the following techniques are model-specific, and can be applied to both RANS and LES.

1. The simplest technique is to use separate numerical solvers for the fluid and solid phases and to exchange information through the boundary conditions. The use of separate solvers allows a flexible gridding inside the solid phase, which is required because of the three orders of magnitude difference in thermal conductivities between the solid and gas. It is also easy to include various physical phenomena such as charring and moisture transfer. Quite often, 1D solution of the heat conduction equation on each wall cell is sufficiently accurate. This technique is implemented as an internal subroutine in FDS.
2. Separate solvers of 3D heat conduction can be linked to the CFD solver, either as an external model (e.g., KAMELEON) or internal subroutine (SOFIE). Specialized algorithms may be needed to model the connection between the gas and solid phases due to the disparity in length and time scales [70]. In the recent ECSC project concerning the CFD modeling of natural fires (*The development and validation of a CFD-based engineering methodology for evaluating thermal action on steel and composite structures, coordinated by BRE, U.K.*), a 3D heat conduction model was developed for SOFIE. The model allows the simulation of temperature profiles in structural metallic elements such as beams and columns. The information between the fluid and solid phases is passed through the boundary conditions, and fine structural gridding can be used. The solver requires a special user interface developed by BRE (U.K.) and is limited to I-shaped elements.
3. A full coupling of the solid and fluid phases can be achieved by solving a single enthalpy equation, common for both phases. Such an approach was used in SOFIE [13], but the use of a structured grid system usually prevented the necessary refinement inside the solids. A fully coupled system is being developed in the C-SAFE project at the University of Utah [31].

For practical simulations of large-scale fire development, the first of the above three techniques is typically used. The condensed-phase geometry is broken into multiple separate 1D calculations. Each solid surface (such as a door or the seat cushion on a chair) is broken up into multiple “patches,” each having a surface area corresponding to that of the gas-phase cell face to which it abuts. For each patch, a 1D calculation is performed to determine the internal condensed-phase temperature profile and gaseous fuel generation rate. Each condensed-phase patch serves as a boundary condition to the gas-phase CFD model. Coupling is achieved by passing the surface temperature and mass flux of gaseous species (primarily gaseous pyrolyzate) from the condensed-phase pyrolysis model to the gas-phase CFD model.

For the usual 1D approach, a particular condensed-phase patch knows nothing of its neighboring patches, i.e., no heat is transferred through the condensed-phase in a direction parallel to the solid surface. In some specialized flame spread calculations (primarily two-dimensional (2D) opposed flow flame spread), multidimensional heat transfer through the condensed-phase has been considered. Heat conduction through the condensed-phase is more important in opposed or lateral flame spread than in upward flame spread. Lateral and opposed flame spread are difficult to accurately model in large-scale fire simulations because (1) heat conduction through the condensed-phase in a direction parallel to the surface is usually not considered, and (2) the gas-phase preheat length scales associated with lateral or opposed flame spread are usually much smaller than the grid size.

20.3.2 LIQUID FUELS

In many situations involving liquid-fueled fires, the burning rate is specified, e.g., using correlations [73], rather than calculated. However, under some circumstances it may be desirable to actually predict the burning rate of liquid fuels. This is normally accomplished by applying the Clausius-Clapeyron

relations to determine the partial pressure of fuel vapor immediately above a liquid fuel pool. This does not provide the gaseous fuel mass flux, so an iterative procedure is required where the mass flux is adjusted according to the difference between the current first gas cell fuel concentration and Clausius-Clapeyron prediction.

Although predicting the burning rate of a liquid pool fire with CFD seems simple, there are several complicating factors. Calculated burning rates are sensitive to the rate of heat transfer back to the fuel surface calculated by the CFD model. Particularly in large-scale pool fires, radiation blockage by pyrolyzate gases, and possibly soot, can affect heat transfer rates back to the fuel surface. This phenomenon is not yet quantitatively understood. Furthermore, many liquid fuels are semitransparent to thermal radiation, so in-depth attenuation of thermal radiation must be accurately captured for an accurate prediction of burning rates. Other confounding effects include pool spreading, internal convection, and surface-tension-driven flows. Fire models do not account for these phenomena, e.g., FDS treats liquid fuels as solids that do not flow or migrate. Pool fire burning rates have been predicted with CFD fire modeling [74–76].

20.3.3 SOLID FUELS: EMPIRICAL MODELS

Of the several approaches that have been used to calculate fuel generation rates from solid materials in CFD-based fire growth calculations, the simplest are empirical models. Instead of attempting to model the physical processes that lead to gaseous fuel production inside decomposing solids, empirical data that can be measured (transient heat release or mass loss rate) or inferred (heat of gasification) from common bench-scale fire tests such as the Cone Calorimeter are used to characterize fuel generation processes.

With empirical pyrolysis models, a material's burning rate is zero until its surface is heated to its ignition temperature (T_{ig}), at which time ignition occurs. After ignition, the mass loss rate of a fuel element is estimated from the net heat flux to the fuel's surface (\dot{q}_{net}'') divided by the effective heat of gasification (ΔH_g):

$$\dot{m}''(t) = \frac{\dot{q}_{net}''(t)}{\Delta H_g} \quad (20.17)$$

The effective heat of gasification in Equation 20.17 is a material fire property that is the quantity of heat required to generate unit mass of volatiles at temperature T_{ig} from unit mass of solid initially at T_0 .

As an alternative to Equation 20.17, a solid material's HRR (or mass loss rate) after ignition is sometimes related directly to transient measurements obtained from small-scale fire tests. This is expressed in Equation 20.18:

$$\dot{m}''(t - t_{ig,mod}) = \dot{m}_{exp}''(t - t_{ig,mod} + t_{ig,exp}) \quad (20.18)$$

where a subscript “mod” denotes model, and a subscript “exp” denotes experiment. Essentially, the mass loss rate of a solid fuel element is zero until ignition occurs when its surface temperature reaches T_{ig} at time t_{ig} . After ignition, the fuel generation rate is the same as the fuel generation rate measured experimentally. Since the net heat flux to the fuel surface does not appear in Equation 20.18, fuel generation is decoupled from the radiative and convective environment that develops in the simulation.

The primary shortcoming of the approach in Equation 20.18 is that it is implicitly assumed that the net heat flux history to which the material in the model is exposed is identical to the experimental net heat flux history. Laboratory experiments usually involve instantaneous application of high heat flux levels (50 kW/m² or higher) that remain constant throughout the experiment. This type of heat flux history does not necessarily occur in spreading fires, where applied heat flux levels may change over time as the fire develops. Bench-scale laboratory experiments are conducted on small fuel samples burning

under well-ventilated conditions, and real fires are unlikely to have the same ventilation conditions. In actual fires, fuel packages interact with one another and the fire compartment, so different parts of the same material may burn differently because they are exposed to different thermal conditions. This effect cannot be captured by a model that directly applies bench-scale fire test data without considering the applied heat flux levels, so model results are sensitive to the irradiance level at which experimental data are collected. Internal gradients of temperature and species in materials burning in bench-scale fire tests can be much different than those that develop in real fires, so their fuel production characteristics may also be different. In an attempt to account for some of the deficiencies pointed out here, an acceleration function has been introduced [77,78] where the modeled HRR is essentially related to the total heat flux absorbed by the solid.

Empirical approaches are useful when macroscale HRR measurements are available but little or no information is available regarding the thermophysical properties, kinetic parameters, and heats of reaction that would be necessary to apply a more comprehensive pyrolysis model. Although these modeling approaches are crude in comparison with some of the more refined solid-phase treatments, one advantage is that all required input parameters can be obtained from widely used bench-scale fire tests using well-established data reduction techniques. As greater levels of complexity are added, establishing the required input parameters (or “material properties”) for different materials becomes an onerous task.

20.3.4 SOLID FUELS: HEAT TRANSFER LIMITED PYROLYSIS MODELS

Pyrolysis models can be classified in many ways (i.e., single-step, multistep, charring, noncharring, integral models, etc.). Owing to fundamental differences in the way that the gaseous fuel generation reaction is treated, it is useful to distinguish between heat transfer limited and kinetically limited pyrolysis models, and this differentiation is used here.

In heat transfer limited models, pyrolysis occurs at an infinitely thin front. For noncharring solids, this pyrolysis front coincides with the exposed surface (ablation models); for charring solids, the pyrolysis front separates a char region from a virgin fuel region, in a manner akin to the separation of the melt and condensed-phase in the classical Stefan problem. For both charring and noncharring solids, the pyrolysis rate is zero until a critical temperature is reached, usually called the pyrolysis temperature (T_p), and sometimes equated with the ignition temperature, T_{ig} . After T_p is reached, the pyrolysis front is maintained at this temperature and the pyrolysis rate is determined from a heat balance at the pyrolysis front. This heat balance takes into account the rate of heat transfer to and from the pyrolysis front and the reaction enthalpy. The latter, often called the heat of vaporization (ΔH_v) or heat of volatilization (ΔH_{vol}), is the quantity of heat required to generate unit mass of volatiles from the condensed-phase at T_p . It is not the same as the effective heat of gasification ΔH_g mentioned earlier. For noncharring fuels, the mass loss rate is proportional to the surface regression rate, and for charring fuels the mass loss rate is proportional to the propagation rate of the char/virgin interface.

Temperature profiles can be determined from the transient heat conduction equation or, in integral models, by assuming some functional form of the temperature profile *a priori*. With the former, numerical solution of partial differential equations is required. With the latter, the problem is reduced to a set of coupled ordinary differential equations, but numerical solution is still required. The following equations embody a simple heat transfer limited pyrolysis model for a noncharring polymer that is opaque to thermal radiation and has a density that does not depend on temperature. For simplicity, surface regression (which gives rise to convective terms) is not explicitly included.

$$\rho c \frac{\partial T}{\partial t} = \frac{\partial}{\partial z} \left(k \frac{\partial T}{\partial z} \right) \quad \text{for } 0 < z < \delta \quad \text{and} \quad t > 0 \quad (20.19a)$$

$$-k \left. \frac{\partial T}{\partial z} \right|_{z=0} = \dot{q}_{\text{net}}'' \quad \text{for } t < t_p \quad (20.19b)$$

$$T|_{z=0} = T_p \quad \text{for } t \geq t_p \quad (20.19c)$$

$$-k \left. \frac{\partial T}{\partial z} \right|_{z=0} = \dot{q}_{\text{net}}'' - \dot{m}'' \Delta H_{\text{vol}} \quad \text{for } t \geq t_p \quad (20.19d)$$

where

δ is the material thickness

t_p is the time at which the surface temperature reaches T_p

\dot{q}_{net}'' is the net rate of heat transfer to the surface

\dot{m}'' is the primary quantity of interest, the gaseous fuel generation rate

These equations take a slightly different form if surface regression is considered or a charring material is considered. A boundary condition at $z = \delta$ is also required to complete the problem specification.

The basic assumption inherent to heat transfer limited pyrolysis models is that heat transfer rates, rather than decomposition kinetics, control the pyrolysis rate. Consequently, thermal decomposition kinetics do not come into play, other than indirectly through specification of T_p . This approximation is often justified on the basis of high activation energies typical of condensed-phase pyrolysis reactions, i.e., the reaction rate is very small below T_p but then increases rapidly with temperature in the vicinity of T_p owing to the Arrhenius nature, and the high activation energy, of the pyrolysis reaction.

This type of model works well at high applied heat flux levels, where the pyrolysis front is thin. Simplicity is its advantage: it is not necessary to specify any parameters related to the decomposition kinetics. A large body of flame spread modeling work has applied this type of model, but there is a tendency to focus with great detail on gas-phase phenomena (i.e., full Navier–Stokes, detailed radiation models, multistep combustion reactions) and treat the condensed-phase fuel generation process in an approximate manner.

20.3.5 SOLID FUELS: FINITE-RATE (KINETICALLY LIMITED) PYROLYSIS MODELS

In kinetically limited models, the pyrolysis rate is no longer calculated solely from a heat balance at the pyrolysis front. Instead, the rate at which the condensed-phase is volatilized depends on its temperature. This gives a local volumetric reaction rate ($\text{kg}/\text{m}^3\text{-s}$); by assuming that all volatiles escape instantaneously to the exterior gas-phase with no internal resistance, the fuel mass flux is obtained by integrating this volumetric reaction rate in depth. One consequence is that the pyrolysis reaction is distributed spatially rather than confined to a thin front as with heat transfer limited models and the thickness of the pyrolysis front is controlled by decomposition kinetics and heat transfer rates. For a pyrolysis reaction with high activation energy or for very high heat transfer rates, the pyrolysis zone becomes thin, and kinetically limited models tend toward heat transfer limited models.

For a noncharring solid, a kinetically limited model is embodied by Equation 20.20:

$$\rho c \frac{\partial T}{\partial t} = \frac{\partial}{\partial z} \left(k \frac{\partial T}{\partial z} \right) - \dot{\omega}_{\text{fg}}''' \Delta H_{\text{vol}} \quad \text{for } 0 < z < \delta \quad (20.20a)$$

$$\dot{\omega}_{\text{fg}}''' = \rho A \exp \left(-\frac{E}{RT} \right) \quad \text{for } 0 < z < \delta \quad (20.20b)$$

$$\dot{m}'' = \int_0^{\delta} \dot{\omega}_{ig}''' d\zeta \quad (20.20c)$$

Boundary conditions at $z = 0$ and $z = \delta$ are also required to complete the problem. It has been assumed that the solid is opaque to thermal radiation, its density does not depend on temperature, surface regression is negligible, heat transfer from the condensed-phase to the gas-phase inside the decomposing solid is negligible, and the reaction is single-step and first order. These equations take a slightly different form if any of these assumptions change or if a charring solid is considered. Though surface regression may be an important phenomenon for predicting mass burning rates long after ignition, it does not usually have a large effect on the calculated flame spread rates (e.g., the surface regression velocity is at most 1% of the upward flame spread rate on a noncharring polymer [79]).

Despite the higher burden associated with determining the required material properties, this type of pyrolysis model offers greater flexibility than approaches that use the heat of gasification or measured burning rate approaches. The computational requirements of kinetically limited pyrolysis models are not much greater than those of heat transfer limited models, so there is little performance to be gained by using a heat transfer limited model in lieu of a finite-rate model. Since the CPU time required for the solid-phase pyrolysis routines is small in comparison with the CPU time required for the gas-phase routines in CFD-based simulations of large-scale flame spread, there is little computational advantage to using empirical or heat transfer limited pyrolysis models instead of a finite-rate pyrolysis model.

20.3.6 MATERIAL PROPERTY ESTIMATION

One of the most challenging aspects of fire growth modeling is characterizing solid materials, objects, or assemblies in terms of the material properties that control their overall reaction to fire. This is a difficult task for materials that exhibit charring, swelling/intumescence, shrinkage, multi-step decomposition kinetics, or for those that have a layered structure. To avoid the complexity associated with real-world fuels, most pyrolysis and flame spread modeling studies have used materials that can be described by a single-step decomposition reaction. Widely studied materials include noncharring polymers such as polymethylmethacrylate (PMMA) and wood.

The FDS5 pyrolysis model is used here to qualitatively illustrate the complexity associated with material property estimation. Each condensed-phase species (i.e., virgin wood, char, ash, etc.) must be characterized in terms of its bulk density, thermal properties (thermal conductivity and specific heat capacity, both of which are usually temperature-dependent), emissivity, and in-depth radiation absorption coefficient. Similarly, each condensed-phase reaction must be quantified through specification of its “kinetic triplet” (preexponential factor, activation energy, reaction order), heat of reaction, and the reactant/product species. For a simple charring material with temperature-invariant thermal properties that degrades by a single-step first order reaction, this amounts to ~11 parameters that must be specified (two kinetic parameters, one heat of reaction, two thermal conductivities, two specific heat capacities, two emissivities, and two in-depth radiation absorption coefficients).

This would not be problematic if standardized, reliable, reproducible, and inexpensive laboratory tests were available to estimate each of the required properties. Although several specialized laboratory tests are available to measure some properties (e.g., specific heat capacity can be determined by differential scanning calorimetry [DSC]), many of these tests are still research tools and standard procedures to develop material properties for fire modeling have not yet been developed. Even if standard procedures were available, it would likely be so expensive to conduct 5+ different specialized laboratory tests for each material so that practicing engineers would be unable to apply this approach to real-world projects in an economically viable way. Furthermore, there is no guarantee that properties measured independently from multiple laboratory tests will provide accurate predictions of pyrolysis behavior in a slab pyrolysis/combustion experiment such as the Cone Calorimeter or Fire Propagation Apparatus.

It seems that comparison of a pyrolysis model's predictions to Cone Calorimeter (or similar) experimental data has become the de facto standard for assessing "accuracy." Therefore, one approach to material property estimation involves working backward from Cone Calorimeter data. The basic idea (to use a pyrolysis model as a virtual representation of a Cone Calorimeter or similar experiment and adjust the material properties until the model calculations match the experimental data) is straightforward and has been independently proposed by several researchers. The challenge stems from the number of parameters that must be simultaneously optimized. For the simple charring material mentioned earlier, there are 11 adjustable parameters that must be simultaneously optimized, so manual optimization is impractical. Automated brute force search techniques suffer from the high dimensionality (large number of adjustable parameters) of the problem. Assuming each parameter could take on 10 different values (a much higher number is actually more reasonable), there are 10^{11} different combinations of model input parameters that must be explored to find the combination that best matches the experimental data. If 0.1 s of CPU time is required to evaluate each solution, it would take over 300 CPU-years to evaluate all possible combinations. The situation becomes more complicated when one considers temperature-dependent thermal properties, multi-step reactions, etc. It can be seen that while the basic idea seems simple, below the surface looms a considerable computer science challenge.

One method that has been proposed to estimate the material properties needed for pyrolysis modeling from Cone Calorimeter (or similar) experiments involves the application of a genetic algorithm (GA) [80–83]. GAs are a class of stochastic search and optimization tools that operate on the principles of Darwinian evolution or natural selection, sometimes called survival of the fittest. Although initial applications of the genetic algorithm-based optimization are promising, these techniques are not yet mature and further development is needed. Other optimization methods such as simulated annealing or hybrid combinations may be more appropriate. The feasibility of using differential thermogravimetric (DTG) data obtained at multiple oxygen concentrations to develop simplified condensed-phase reaction kinetics mechanisms that include the effect of oxygen on the decomposition process is being investigated recently. Similarly, DSC data obtained at multiple oxygen concentrations could be used to extract the associated heats of reaction and their dependence on oxygen concentration, but this has not yet been demonstrated.

20.4 CFD SIMULATION OF LARGE-SCALE BURNING AND FIRE GROWTH

Simulation of flame spread and fire growth is one of the most challenging modeling problems in fire CFD. The origin of the challenging nature of fire growth modeling is that it requires accurate simulation of several subprocesses:

1. Flame temperature and thermal radiation. In large fires, flame radiation dominates heat transfer to unburned and burning fuel.
2. Flame structure and heat transfer in the region close to the wall. In small fires, the near field flames are responsible for most of the heat transfer to the wall. In a typical fire simulation, this region is totally covered by one or two grid cells, making it impossible to capture the flame structure and temperature distribution. Some kind of subgrid scale model of this region is needed in fire CFD models to accurately model the flame spread. The subgrid scale model might use the ideas of wall functions and boundary-layer flame structures [84].
3. Heat transfer and pyrolysis inside the solid material.

In the context of fire CFD, it is sometimes appropriate to distinguish between *flame* and *fire* spread simulations. Flame spread simulation usually means the ability to predict the fire growth starting from a *small initial fire* or ignition point, where all the three subprocesses are important but the second subprocess dominates the heat transfer. Fire spread, in turn, means the ignition of solid surfaces in the presence of a relatively *large initial fire* dominating the heat transfer by radiation. In practice,

the small and large initial fires should be defined relative to the CFD mesh: a large initial fire spans from 10 to 20 grid cells, for example.

Solid-phase pyrolysis models have been coupled to CFD for simulating bench-scale fire tests, small-scale laminar flame spread in normal and microgravity, 2D upward flame spread, reduced-scale compartment fires, and building-scale compartment fires. This section reviews CFD-based large-scale fire growth modeling for scenarios where flame spread is dominated by upward or concurrent flame spread. Although only published papers or reports are discussed here, many private firms are now applying fire growth modeling on actual design projects and in support of fire litigation. However, this work often remains proprietary and is not published in the open literature, so it is likely that CFD-based flame spread modeling is now being applied more frequently than inspection of the current literature suggests.

Typically, a fire growth model is evaluated by comparing its calculations (predictions) of large-scale behavior to experimental HRR measurements, thermocouple temperatures, or pyrolysis front position. The overall predictive capabilities of fire growth models depend on the pyrolysis model, treatment of gas-phase fluid mechanics, turbulence, combustion chemistry, and convective/radiative heat transfer. Unless simulations are truly blind, some model “calibration” (adjusting various input parameters to improve agreement between model calculations and experimental data) is usually inherent in published results, so model calculations may not truly be predictions.

To rigorously assess a model’s predictive capabilities for flame spread modeling, or make suggestions as to how it could be enhanced by improving various subroutines, some level of deconstruction is necessary. This involves independently analyzing turbulence, combustion, flame heat transfer, and solid-phase phenomena before bringing them together to simulate large-scale flame spread. If a model reproduces well large-scale experimental flame spread data, it does not necessarily mean that all physics relevant to the flame spread process are accurately modeled. Instead, the good agreement between model calculations and experimental data may be due to the compensating effects. A model that overestimates flame heat fluxes may be able to reproduce experimental flame spread data if the pyrolysis model underestimates the mass loss rate. This should be kept in mind when viewing the large-scale flame spread modeling results presented subsequently, which are intended primarily to give the reader an idea of the level of agreement between model calculations and experimental data that has been obtained to date.

20.4.1 BURNING RATE PREDICTION FOR STATIONARY (NONSPREADING) FIRES

Before considering spreading fires, we first examine the simpler case of a stationary solid or liquid pool fire where the pyrolysis area does not change with time. Physically, the burning rate (more precisely, mass loss rate or HRR) of a stationary fire is controlled by condensed-phase fuel generation processes and the rate of heat feedback from the flames (or external heat sources) to the burning fuel. Accurate prediction of burning rates with CFD-based fire modeling requires accurate prediction of flame heat transfer and condensed-phase pyrolysis (or evaporation for liquid fuels). Since these processes drive fire growth rates in spreading fires, prediction of burning rates of stationary fires is of direct relevance to fire growth modeling.

Surprisingly, much less work has been conducted to predict burning rates of stationary fires (particularly on solid fuels) than spreading fires. The studies that have been conducted to date fall into two primary categories: (1) prediction of burning rates in small-scale flammability experiments such as the Cone Calorimeter [85,86], and (2) prediction of burning rates in liquid pool fires [74–76].

Hostikka et al. [74] used LES to predict the burning rate of methanol pool fires and found that for fires between 10 cm and 100 cm in diameter the calculated burning rates were overpredicted by ~35%–100%. Novozhilov and Koseki [75] simulated heptane, toluene, and ethanol pool fires up to 1 m in diameter and found that predicted burning rates matched experimental data within ~25%.

20.4.2 FLAME SPREAD ON FLAT SURFACES AND COMBUSTIBLE CORNERS

One of the simplest large-scale geometries relevant to real world fire growth modeling is vertical upward flame spread on a free-standing wall, meaning that the wall is not part of a compartment. Compartment effects, such as accumulation of a hot ceiling layer, do not come into play.

Vertical flame spread on a PMMA wall 5 m in height has been modeled by Liang [87] using FDS Version 2, which included a heat transfer limited pyrolysis model. Good agreement between the measured and calculated pyrolysis height was obtained. More recently, Kwon et al. [88] used FDS4, which includes a high heat flux form of the finite-rate pyrolysis model, to simulate the same experiment. In the FDS4 study, the calculated HRR initially increased at a rate that is slower than that observed experimentally, but then jumped to a higher HRR. This behavior was found to be sensitive to a feature of FDS4 gas-phase combustion model that automatically adjusted the stoichiometric value of mixture fraction on coarse grids; however, this adjustment is no longer used in FDS5 owing to a reformulated combustion model [41]. Zhang et al. [89] modeled the same configuration using SOFIE, and obtained good agreement between their model calculations and the experimental data. In Figure 20.3, the experimental flame spread data are compared with the model calculations of Liang [87], Kwon et al. [88], and Zhang et al. [89]. The differences in the calculations shown in Figure 20.3 are attributed to different solid-phase models, gas-phase solvers, user assumptions, and model input parameters; no conclusions should be drawn regarding the accuracy of one model compared with another on the basis of Figure 20.3.

Consalvi et al. [90] used a 2D RANS model with a heat transfer limited pyrolysis model to simulate upward flame spread on PMMA. The calculated position of the pyrolysis front brackets the available experimental data, i.e., when using a value of T_p toward the higher end of the range reported in the literature the spread rate is under-predicted, and when using a value of T_p toward the lower end of the range reported in the literature, the model overpredicts the spread rate. This highlights the importance of material properties for large-scale flame spread modeling.

Lowndes et al. [91] used the commercial CFD model Fluent to simulate flame spread along a conveyor belt. Fluent, at the time this modeling was conducted, did not contain a conventional pyrolysis model in the sense that is normally implied in the fire literature. Instead, the authors adapted a “discrete phase model,” which is intended to simulate the combustion of pulverized coal.

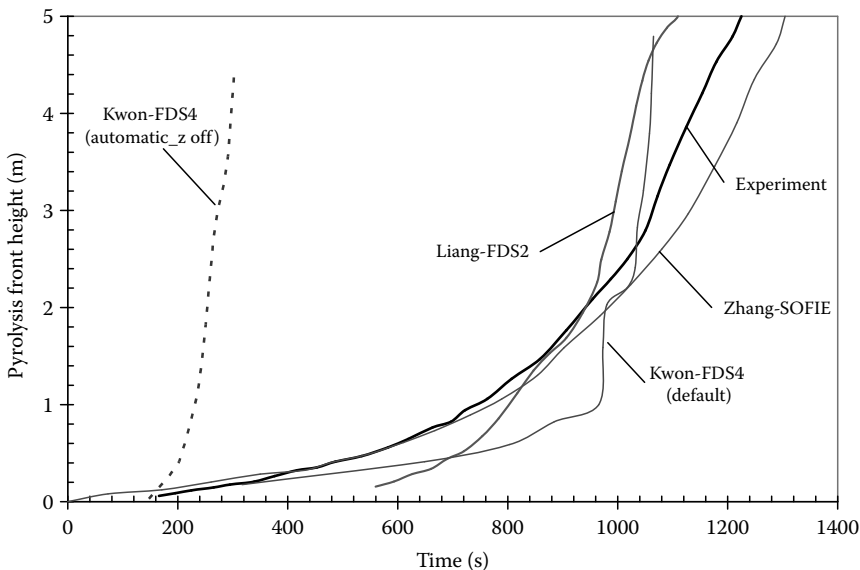


FIGURE 20.3 Comparison of measured and modeled pyrolysis front height for vertical flame spread on 5 m PMMA panel.

Essentially, the conveyor belt was approximated as an ensemble of combustible particles. This approach is similar to the treatment of natural fuels such as trees and shrubs in the experimental version of FDS known as Wildland Urban Interface FDS (WFDS) [92]. Lowndes et al. [91] found that the model qualitatively replicated the flame spread that was observed experimentally. However, no quantitative comparison between modeled pyrolysis front position or HRR and analogous experimental data was given. Modeling a single continuous surface, such as a conveyor belt, as an ensemble of combustible particles is a novel idea, but it is not clear in this particular case whether the relevant physics of condensed-phase pyrolysis were accurately represented.

Fire growth in a combustible corner (e.g., ISO 9705 or similar) has received considerable attention from modelers. One of the earliest 3D models of large-scale fire growth is due to Yan and Holmstedt [93] who used CFD to model fire growth on particle board. Generation of gaseous fuel was modeled in two different ways. In the first, the HRR of a solid fuel element was zero until its surface was raised to its ignition temperature. Then, the HRR per unit area of that fuel element was specified as that measured in the Cone Calorimeter. With the second method, a heat transfer limited pyrolysis model was used to calculate the pyrolysis rate. Interestingly, the results obtained from both methods were similar. The authors presented comparisons between model calculations and experimental data for HRR, gas-phase temperatures, wall and ceiling solid-phase temperatures, radiative heat flux, and mass flux through openings. The high level of agreement between model calculations and experimental data was remarkable considering this as one of the earliest 3D simulations of large-scale fire spread and that the grid spacing was coarse by today's standards. Yan and Holmstedt's [93] measured and modeled HRR (total HRR calculated using pyrolysis model) are shown in Figure 20.4. More recently, Theuns et al. [94] conducted similar simulations of the same experiments, with a focus on the effect of material properties.

Other workers have used CFD to model fire growth on wood in the room/corner test. Figure 20.5 shows the experimentally measured HRR from a room/corner test on spruce panels compared with the predictions of a prerelease version of FDS2 using a kinetically limited charring pyrolysis model at three different grid resolutions [95]. It can be seen that the predicted HRR is quite sensitive to the underlying grid spacing. Moghaddam et al. [96] used FDS (probably Version 3 or 4) to model flame

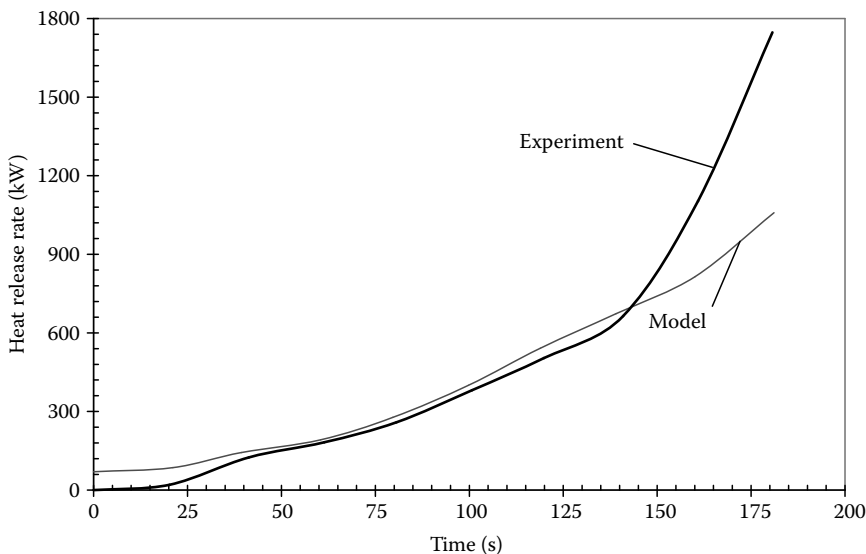


FIGURE 20.4 Comparison of measured and modeled HRR in room corner test on particle board. Model calculations are for total HRR calculated with heat transfer limited pyrolysis model. (Adapted from Yan, Z. and Holmstedt, G., *Fire Saf. J.*, 27, 201, 1996.)

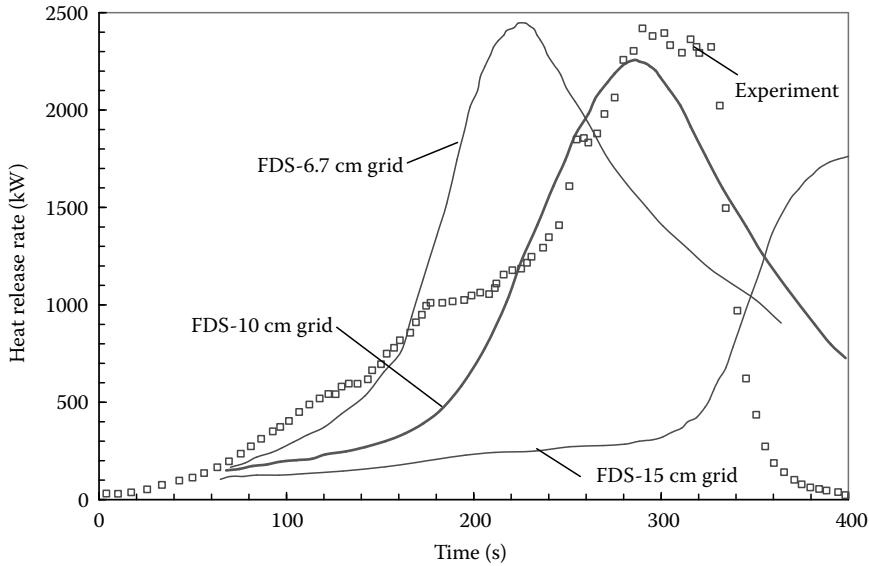


FIGURE 20.5 CFD-based prediction of spruce panel fire growth in room corner fire test at three different grid spacings compared with experimental data. (Adapted from Hostikka, S. and McGrattan, K.B., Large eddy simulation of wood combustion, in *Interflam*, Edinburgh, U.K., pp. 755–762, 2001.)

spread on plywood in a room/corner fire test. These authors noted sensitivity to grid size and selection of the fuel reaction. Results for their ethanol reaction case are shown in Figure 20.6.

Carlsson [97] used several different CFD models to simulate flame spread on wood both on a flat wall and in a room/corner experiment. Figure 20.7 gives a comparison of the measured HRR and

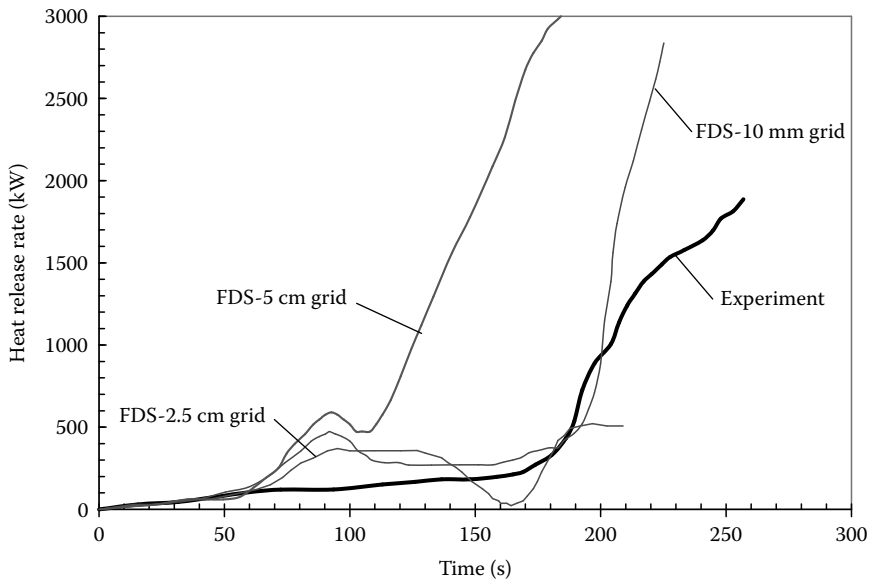


FIGURE 20.6 Comparison of measured and modeled HRR in room/corner test on plywood. From Moghaddam et al. [96] for ethanol reaction case. (Adapted from Moghaddam, A.Z. et al., Fire behavior studies of combustible wall linings applying fire dynamics simulator, in *Proceedings of the 15th Australasian Fluid Mechanics Conference*, Sydney, Australia, 2004.)

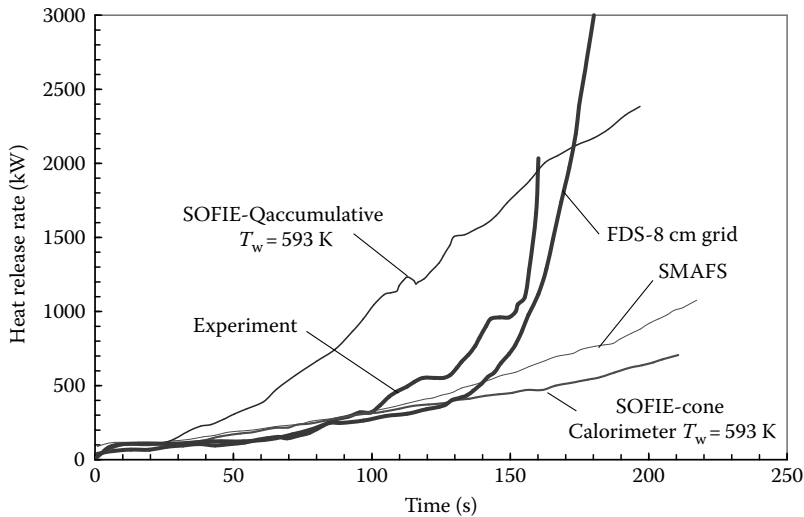


FIGURE 20.7 Comparison of measured and modeled HRR in room/corner test with wood lining materials. (Adapted from Carlsson, J., Computational strategies in flame-spread modelling involving wooden surfaces—An evaluation study, Lund University Department of Fire Safety Engineering, Lund, Sweden, Report 1028, 2003.)

that calculated with four different models: SMAFS (developed at Lund University), SOFIE (accumulative pyrolysis model), SOFIE (Cone Calorimeter pyrolysis model), and FDS (presumably using an early version of the FDS4 pyrolysis model). As mentioned earlier, differences in the calculations are attributed to different solid-phase models, gas-phase solvers, user assumptions, and model input parameters; no conclusions should be drawn regarding the accuracy of one model in comparison with another.

Hietaniemi et al. [76] used a prerelease version of FDS4 to model fire spread on several materials in several different configurations and compared the calculated results with experimental data. This is one of the most comprehensive (in terms of the number of materials and the number of different configurations simulated) large-scale flame spread modeling studies conducted to date. The materials simulated include spruce timber (SBI, room/corner, and 6 m cavity), medium density fiber board (SBI and room/corner), PVC wall carpet on gypsum board (SBI, room/corner), upholstered furniture (furniture calorimeter and ISO room), and polyethylene-sheathed cables in 6 m cavity.

In the study of Hietaniemi et al. [76], the model reproduced well most of the experiments conducted on spruce, but the calculated HRR was sensitive to the back-face boundary condition in the SBI test and the observed decay in the HRR in the cavity experiment was not captured by the model. Modeled HRR for medium density fiberboard closely matched room/corner test data, whereas HRR in the SBI test was not reproduced as closely. The HRR of the PVC wall carpet was reproduced reasonably well in the SBI test, but was overpredicted in the room corner test, probably owing to the discrepancy between the back-face boundary condition in reality and in the model. For the upholstered chair, FDS underestimated the time to ignition and the peak HRR compared with experimental data for both the furniture calorimeter and ISO room cases. Finally, for the polyethylene-sheathed cables in the 6 m cavity, the modeled HRR matched the experimental data fairly closely. In general, the results of Hietaniemi et al. [76] are encouraging.

20.4.3 RAIL CARS

An estimate of the HRR of rail cars is needed to design emergency egress and ventilation systems in underground stations and tunnels. However, rail cars are too large expensive to burn at full scale. Fire growth modeling, combined with bench-scale and reduced-scale/mockup fire testing, is currently the

best way to estimate HRRs of rail vehicles (at the time of writing, there is some discussion around conducting full-scale fire tests on rail cars).

Capote et al. [98] used FDS4 to model fire growth in a real-scale mockup of a train passenger compartment. The experiments were conducted as part of the European FIRESTARR program in a test compartment that was 2.3 m high, 1.9 m wide, and 2.0 m in length. The primary combustible materials were the wall and ceiling linings. In lieu of using the FDS4 pyrolysis model, the authors assumed that ignition occurred at a specified temperature, and then followed a predetermined HRR that was determined from Cone Calorimeter testing. Since materials may not be exposed to the same convective and radiative history in the simulation as in the laboratory, this approach should be applied with care (see Section 20.3.3).

The authors [98] note sensitivity to the ignition temperature and the Cone Calorimeter irradiance, at which the experimental data were obtained. Comparison of model calculations and experimental data are presented for five different tests. The model calculations matched the experimental HRR least closely for “Material B,” and most closely for “Material C.” Figure 20.8 shows the model calculations and experimental data for these two cases.

The thorough MS thesis of Chiam [99] describes many of the issues that the modeler must contemplate when conducting large-scale fire growth modeling. In this thesis, FDS4 was used to model fire growth in a rail vehicle using two different methods: (1) materials were assumed to ignite when the surface temperature reached a critical value, at which point they followed a predetermined HRR curve that was determined from Cone Calorimeter data; (2) the FDS4 thermoplastic pyrolysis model was used, with input parameters estimated from Cone Calorimeter data. Interestingly, the author reports similar results for both methods (similar to Yan and Holmstedt [93]). Chiam [99] suggests 10 MW as a peak HRR of a train in a tunnel. There is no comparison of model calculations to real-scale experimental data in Chiam’s work.

Coles et al. [100] used FDS5 to simulate fire development in a reduced-scale mockup of a rail vehicle in an ISO room (3.6 m deep, 2.4 m wide, 2.4 m high). The mockup included seats and seat shrouds, wall lining, ceiling linings, and carpet. The initiating fire was a propane burner placed between two seats. Measurements included HRR, thermocouple temperatures, and heat flux levels. For each material, material properties (preexponential factor, activation energy, heat of reaction and virgin and char thermal conductivity, specific heat capacity, and density) were estimated from Cone Calorimeter data via genetic algorithm optimization [80]. Simulations were conducted for a grid spacing of 5 cm and 2.5 cm, and it was found that the grid spacing did not have a significant effect on the calculated HRR curve. Figure 20.9 gives a comparison of the measured and modeled HRR for a grid spacing of 5 cm and 2.5 cm. The peak HRR is overestimated by ~10% and it occurs ~50 s later in the model than in experimentation.

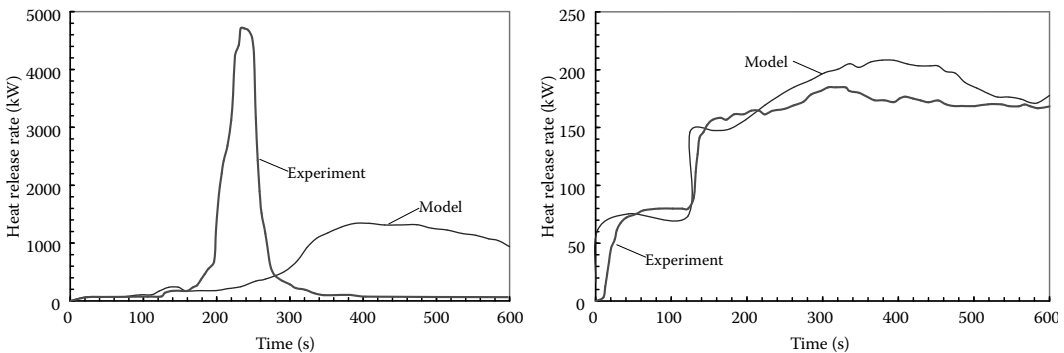


FIGURE 20.8 Comparison of FDS4 calculations and experimental data for fire growth in real-scale mockup of train passenger compartment. Left: Material A; Right: Material C. (Adapted from Capote, J.A. et al., *Fire Mater.*, 32, 213, 2008.)

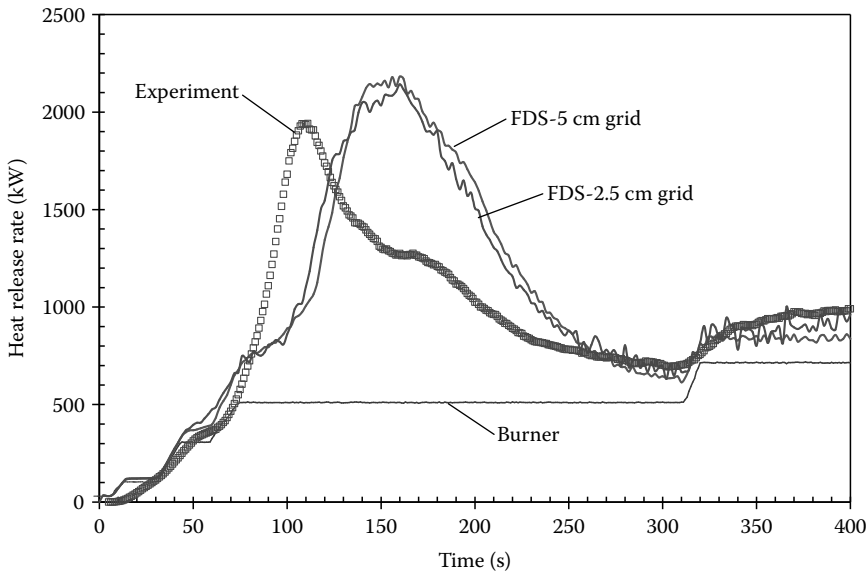


FIGURE 20.9 Comparison of measured and modeled (FDS5) HRR for rail car mockup. (Adapted from Coles, A. et al., Using computer fire modeling to reproduce and predict FRP composite fire performance, in *Composites & Polycon 2009*, American Composites Manufacturers Association, Tampa, FL, January 15–17, 2009.)

20.4.4 DALMARNOCK FIRE TESTS

The 2006 Dalmarnock Fire Tests, organized by the University of Edinburgh, have stimulated several studies of fire growth modeling. In Dalmarnock Test One, a two-bedroom apartment was outfitted with a large number of sensors (thermocouples, velocity probes, smoke detectors, heat flux sensors, light extinction sensors) and video cameras. A sofa was ignited, and the fire spread until flashover occurred after 5 min. HRR was estimated from vent flows and oxygen depletion measurements.

A round robin was organized wherein several teams modeled the fire spread before they were provided with the experimental results (*a priori* simulations) [101]. Participants were given basic information regarding the layout of the apartment and the types of combustibles present, but they were not provided with small-scale test data (i.e., Cone Calorimeter, thermogravimetric analysis, etc.) to characterize any of the combustibles present in the apartment. Most teams used FDS4, and two teams used CFAST.

Figure 20.10 shows several of the FDS4 HRR estimates from the round robin compared with the estimated experimental HRR for the first 10 min of the fire. There is a large variation in the modeled HRRs (and temperatures). This is not surprising given that participants presumably used literature data or ad hoc estimates, rather than small-scale laboratory test data on the actual contents, to determine the pyrolysis model input parameters. Accurate simulation of fire growth requires accurate specification of input parameters, particularly those related to solid-phase pyrolysis. Consequently, the variation in the HRRs shown in Figure 20.10 demonstrates a user effect, i.e., different input parameters specified by different users give different results even though the same model was used; no conclusions should be drawn from the *a priori* Dalmarnock modeling regarding the accuracy of FDS for simulating fire growth.

Dalmarnock Test One has also been the subject of *a posteriori* modeling studies [102,103], i.e., the modelers had full access to the experimental data. FDS4 was used to model the early stages of Dalmarnock Test One [103], and a brief parametric study was conducted to evaluate the effect

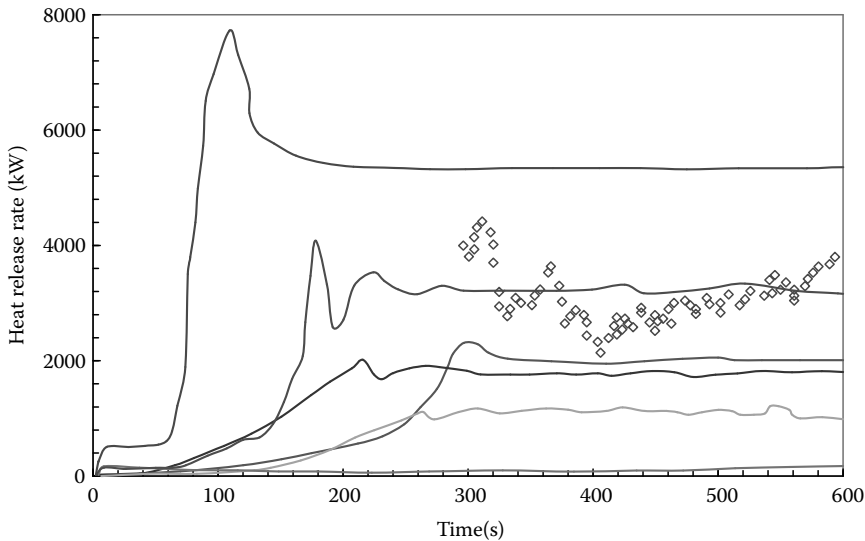


FIGURE 20.10 *A priori* FDS4 estimates of HRR in first 10 min of Dalmarnock Test One. Solid lines are FDS4 predictions of different round robin participants, and individual points are experimental data.

of model parameters, particularly those that affect the initial fire spread. The reason for this is that, it was found in the Round Robin study mentioned earlier that the time at which the second item ignited (bookshelf) was found to drive the overall fire growth. The results of the parametric study comply with one's expectation to a great extent.

Then, Lazaro et al. [104] used FDS5 to simulate the entire course of Dalmarnock Test One. Instead of using the FDS5 pyrolysis model, different materials (desks, bookcases, tables, computer monitors) were assumed to ignite at a user-specified ignition temperature at which point they burned according to predetermined HRR per unit area that was estimated on the basis of experimental burning rate data after reaching. Owing to the inherent assumption that materials are exposed to the same convective and radiative environment in the simulation as in the laboratory (discussed in Section 20.3.3), the approach used by Lazaro et al. [104] to simulate Dalmarnock Test One should be applied with caution.

20.4.5 FORENSIC FIRE RECONSTRUCTION

Fire growth modeling has been used as a tool to reconstruct several fires, including the fires in World Trade Center 1 and 2 [105], the Cook County Administrative Building [106], and the Station Nightclub Fire [107]. Predicting fire development in these complex geometries requires small-scale fire testing combined with intermediate-scale fire testing. Typically, Cone Calorimeter (or similar) data are used to develop initial estimates of pyrolysis model coefficients. Fire development in actual-scale fire tests is then predicted with computer modeling and the model is tuned (in a fairly ad hoc way) until its calculations are reasonably representative of the large-scale experimental data. The basic idea is that the "calibrated" model can then be used to predict fire development in other geometries or extrapolate to larger scales.

This basic approach was applied as part of NIST's technical investigation into the 2003 Station Nightclub fire. This investigation included fire testing on a full-scale mockup of the drummer's alcove (where polyurethane foam was ignited by pyrotechnic gerbs), a raised platform for the band, and part of the dance floor that was adjacent to the platform. The primary fuels in the mockup were convoluted polyurethane foam and plywood paneling. Gypsum board and carpet were also present. Tests were conducted with and without sprinklers.

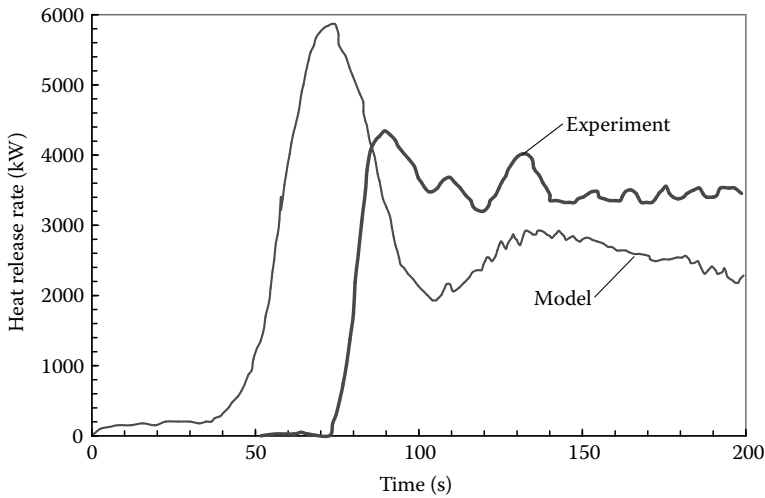


FIGURE 20.11 Comparison of measured and modeled HRR in unsprinklered mockup of drummers’ alcove/stage area in Station Nightclub Fire. (Adapted from Grosshandler, W. et al., Report of the Technical Investigation of the Station Nightclub Fire, NIST NCSTAR 2, Vol. I, Building and Fire Research Laboratory, National Institute of Standards and Technology, Gaithersburg, MD, 2005.)

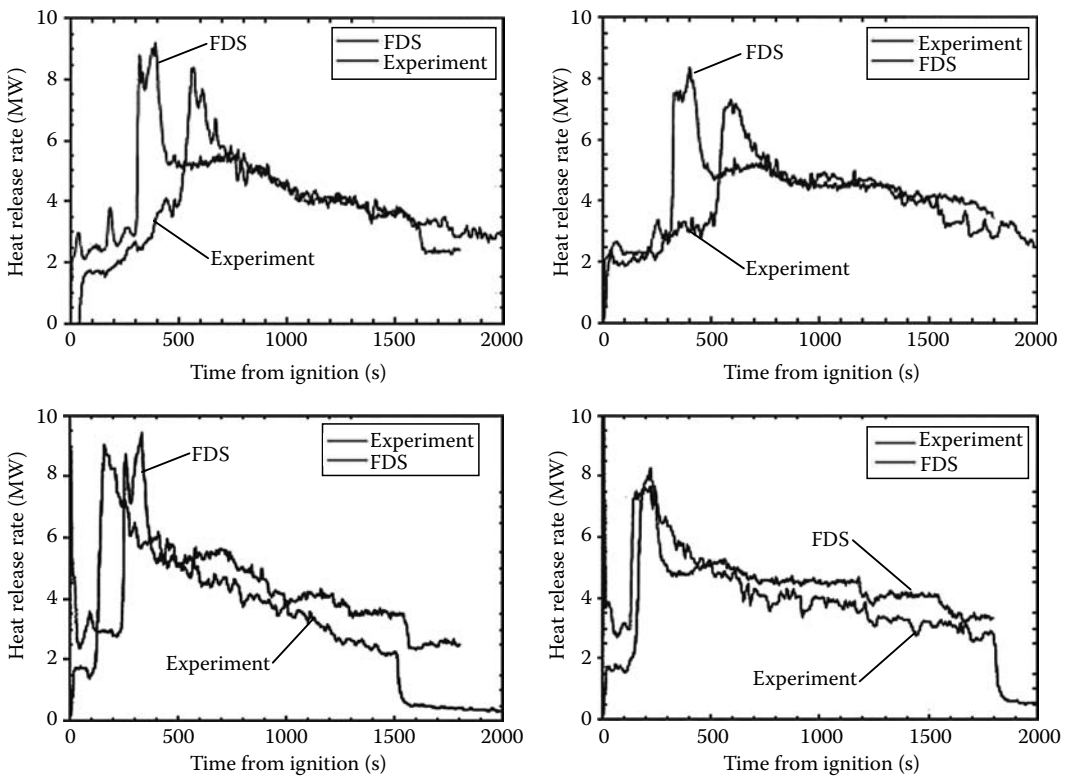


FIGURE 20.12 HRRs for single workstation fire experiments from NIST WTC investigation [105]. Clockwise from upper left: a single, undamaged workstation; a workstation with ceiling tiles added; a workstation with tiles and jet fuel applied; a workstation with just jet fuel applied. (From Gann, R.G. et al., Reconstruction of the Fires in the World Trade Center Towers, NIST NCSTAR 1-5, Federal Building and Fire Safety Investigation of the World Trade Center Disaster, Gaithersburg, MD: National Institute of Standards and Technology, 2005.)

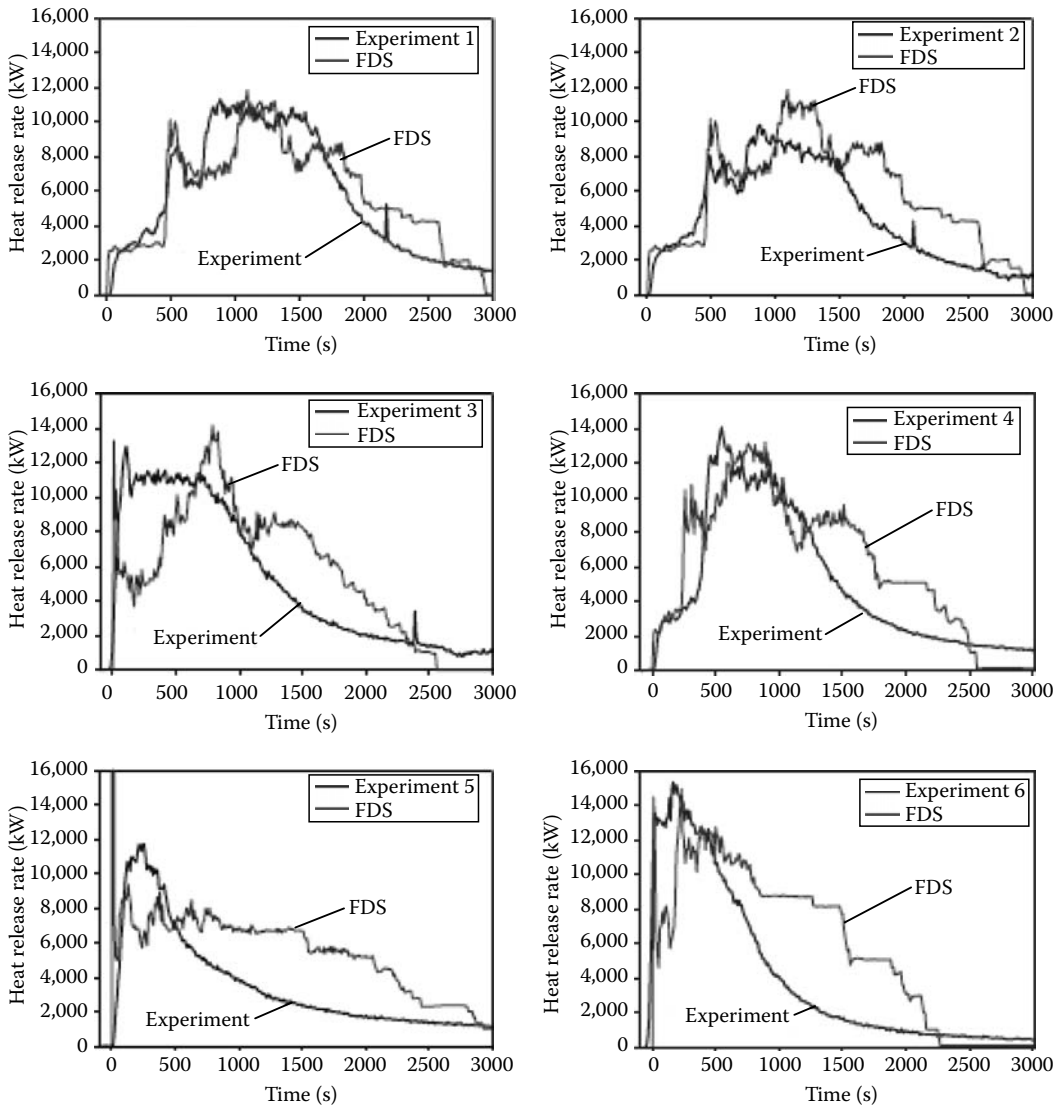


FIGURE 20.13 HRRs for multiple workstation experiments from NIST WTC investigation. (Adapted from Gann, R.G. et al., *Reconstruction of the Fires in the World Trade Center Towers*, NIST NCSTAR 1–5, *Federal Building and Fire Safety Investigation of the World Trade Center Disaster*, 2005.)

A prerelease version of FDS4 was used to simulate the mockup tests. Generation of gaseous fuel from the solid-phase was modeled with an ignition temperature/heat of gasification approach. Material properties were estimated from the literature and Cone Calorimeter testing. Figure 20.11 shows a comparison of the measured and modeled HRR for the unsprinklered mockup. In addition to simulating the laboratory mockup, fire growth in the as built Station Nightclub was simulated, and a peak HRR of approximately 55 MW was estimated.

FDS3 was used to model fire growth in the Cook County (Illinois) Administration Building Fire. After conducting full-scale HRR experiments on chairs and workstations, FDS3 was used to simulate the fire development (with an ignition temperature/heat of vaporization pyrolysis model). Material properties were adjusted to match the known sequence of events. No comparison of large-scale experimental data and model results was given.

As part of NIST's investigation into the September 11, 2001 fires in World Trade Center Towers 1 and 2, large-scale fire experiments were conducted to measure the HRR of single workstations and multiple (3) workstations in a compartment [105]. FDS4 was used to simulate these experiments, with material properties estimated from Cone Calorimeter data. Mass loss rates were estimated with an ignition temperature/heat of gasification pyrolysis model. The results of the single-workstation experiments/simulations are shown in Figure 20.12 and the multiworkstation experiments are shown in Figure 20.13.

LIST OF SYMBOLS

A	Cell face area
B	Radiative emission term
C	Cross sectional area (absorption or scattering)
C	Speed of light
F	Probability density function
F	Probability distribution function
I	Intensity
ijk	Cell indices
\mathbf{q}''	Heat flux vector
M	Cell index
N	Number of spectral bands or solid angles
S_e	Energy source
T	Temperature
t	Time
t_g	Growth time of the heat release rate
U	Total combined intensity
V_{ijk}	Cell volume
\mathbf{x}	Random vector, position vector

GREEKS

χ_r	Local radiative fraction
ϵ	Enthalpy dissipation rate, surface mean hemispherical emissivity
Φ	Scattering phase function
ϕ	Joint density function, azimuthal angle
κ	Absorption coefficient
λ	Wavelength
Ω	Random space, solid angle
θ	Polar angle
ρ	Density
σ	Scattering coefficient, Stefan-Boltzmann constant

SUPERSCRIPTS

D	Droplet
M	Mean droplet property
λ	Spectral value
N	Average over spectral band
R	Radiant
x,y,z	Coordinate directions
w	Water

ABBREVIATIONS

CFD	computational fluid dynamics
CFL	Courant–Friedrichs–Lewy
DNS	direct numerical simulation
FDS	fire dynamics simulator
EBU	eddy break-up
DOM	discrete ordinates methods
DT	discrete transfer
FVM	finite volume method
LES	large eddy simulation
RANS	Reynolds-averaged Navier–Stokes
RTE	radiation transport equation

ACKNOWLEDGMENTS

Chris Lautenberger would like to thank the National Science Foundation for its support under Award Number 0730556, “Tackling CFD Modeling of Flame Spread on Practical Solid Combustibles.”

REFERENCES

1. Cox, G. and Kumar, S. Modelling enclosure fires using CFD. In: *SFPE Handbook of Fire Protection Engineering*, 3rd Edition. Quincy, MA: Society of Fire Protection Engineers, 2002, pp. 3-194–3-218.
2. Patankar, S.V. and Spalding, D.B.A. Calculation procedure for heat, mass and momentum transfer in three-dimensional parabolic flows. *International Journal for Heat and Mass Transfer*, 1972. 15, 1787–1806.
3. Magnussen B. and Hjertager G.H. On mathematical modelling of turbulent combustion with special emphasis on soot formation and combustion. In: *Proceedings of 16th International Symposium on Combustion*. Pittsburgh, PA: The Combustion Institute, 1976, pp. 719–729.
4. McGrattan, K.B., Hostikka, S., Floyd, J.E., Baum, H., and Rehm, R. *Fire Dynamics Simulator (Version 5): Technical Reference Guide*. Gaithersburg, MD: National Institute of Standards and Technology, October 2007. NIST Special Publication 1018-5.
5. McGrattan, K.B., Klein, B., Hostikka, S., and Floyd, J.E. *Fire Dynamics Simulator (Version 5): User's Guide*. Gaithersburg, MD: National Institute of Standards and Technology, October 2007. NIST Special Publication 1019-5.
6. Olenick, S. and Carpenter, D. An updated International Survey of Computer Models for fire and smoke. *Journal of Fire Protection Engineering*, 2003. 13, 87–110.
7. Ferziger, J.H. and Perić, M. *Computational Methods for Fluid Dynamics*. Heidelberg, Germany: Springer, 1997, 364 p. Corrected 2nd printing.
8. Courant, R., Friedrichs, K.O., and Lewy, H. Über die partiellen Differentialgleichungen der mathematischen Physik. *Mathematische Annalen*, 1928. 100, 32–74.
9. Courant, R., Friedrichs, K., and Lewy, H. On the partial difference equations of mathematical physics. *IBM Journal*, 1967. 11(2), 215–234. English translation of the 1928 German original paper.
10. Baum, H.R. and Rehm, R.G. Calculations of three dimensional buoyant plumes in enclosures. *Combustion Science and Technology*, 1984. 40, 55–77.
11. Holen, J., Brostrom, M., and Magnussen, B.F. Finite difference calculation of pool fires. In: *Proceedings of the 23rd Symposium (International) on Combustion*. Pittsburgh, PA: Combustion Institute, 1990, pp. 1677–1683.
12. Taylor, S., Petridis, M., Knight, B., Ewer, J., Galea, E.R., and Patel, M. SMARTFIRE: An integrated computational fluid dynamics code and expert system for fire field modelling. In: Hasemi, Y. (ed.) *Proceedings of Fifth (5th) International Symposium on Fire Safety Science*. March 3–7, Melbourne, Australia. Boston, MA: International Association for Fire Safety Science, 1997, pp. 1285–1296.
13. Welch, S. and Rubini, P. Three-dimensional simulation of a fire-resistance furnace. In: Hasemi, Y. (ed.) *Proceedings of Fifth (5th) International Symposium on Fire Safety Science*. March 3–7, Melbourne, Australia. Boston, MA: International Association for Fire Safety Science, 1997, pp. 1009–1020.

14. Suard, S., Audouin, L., Babik, F., Rigollet, L., and Latche, J.C. Verification and validation of the ISIS CFD code for fire simulation. *Workshop on Assessment of Calculation Methods in Fire Safety Engineering*, San Antonio, TX, April 10, 2006. ISO/TC 92/SC4. 28 p.
15. Greiner, M. and Suo-Anttila, A. Radiation heat transfer and reaction chemistry models for risk assessment compatible fire simulations. *Journal of Fire Protection Engineering*, 2006. 16(2), 79–104.
16. Yan, Z. Large eddy simulation of soot formation in a turbulent diffusion flame. In: Gottuk, D.T. and Lattimer, B.Y. (eds.). *Proceedings of Eighth International Symposium on Fire Safety Science*, September 18–23. Beijing, China: International Association for Fire Safety Science, 2005. Poster abstract.
17. Cheung, A.L.K., Cheung, S.C.P., Yeoh, G.H., and Yuen, R.K.K. Investigation of pulsating behaviour of buoyant fires by using large eddy simulation (LES) approach with soot and radiation. In: Gottuk, D.T. and Lattimer, B.Y. (eds.) *Proceedings of Eighth International Symposium on Fire Safety Science*, September 18–23. Beijing, China: International Association for Fire Safety Science, 2005. Poster abstract.
18. Gao, P.Z., Liu, S.L., Chow, W.K., and Fong, N.K. Large eddy simulations for studying tunnel smoke ventilation. *Tunnelling and Underground Space Technology*, 2004. 19(6), 577–586.
19. Kumar, S. Mathematical modelling of natural convection in fire—A state of the art review of the field modelling of variable density turbulent flow. *Fire and Materials*, 1983. 7, 1–24.
20. Liu, F. and Wen, J.X. The effect of different turbulence models on the CFD simulation of buoyant diffusion flames. *Fire Safety Journal*, 2002. 37(2), 125–151.
21. McGrattan, K.B., Rehm, R.G., and Baum, H.R. Fire-driven flows in enclosures. *Journal of Computational Physics*, 1994. 110(2), 285–291.
22. Rehm, R.G., McGrattan, K.B., Baum, H.R., and Cassel, K.W. Transport by gravity currents in building fires. In: *Fire Safety Science—Proceedings of the Fifth International Symposium*. Boston, MA: International Association for Fire Safety Science, 1997, pp. 391–402.
23. Clement, J.M. and Fleischmann, C.M. Experimental verification of the fire dynamics simulator hydrodynamic model. In: *Fire Safety Science—Proceedings of the Seventh International Symposium*. Worcester, MA: International Association for Fire Safety Science, 2002, pp. 839–862.
24. Baum, H.R., McGrattan, K.B., and Rehm, R.G. Three dimensional simulations of fire plume dynamics. In: Hasemi, Y. (ed.). *Proceedings of Fifth (5th) International Symposium on Fire Safety Science*, March 3–7. Melbourne, Australia. Boston, MA: International Association for Fire Safety Science, 1997, pp. 511–522.
25. Baum, H.R. and McCaffrey, B.J. Fire induced flow field—Theory and experiment. In: *Proceedings of the Second International Symposium on Fire Safety Science*, New York: International Association for Fire Safety Science, 1989, pp. 129–148.
26. McGrattan, K.B., Baum, H.R., and Rehm, R.G. Large eddy simulations of smoke movement. *Fire Safety Journal*, 1998. 30, 161–178.
27. Ma, T.G. and Quintiere, J.G. Numerical simulation of axi-symmetric fire plumes: Accuracy and limitations. *Fire Safety Journal*, 2003. 38(5), 467–492.
28. Hamins, A., Maranghides, A., McGrattan, K.B., Johnsson, E., Ohlemiller, T., Donnelly, M., Yang, J., Mulholland, G., Prasad, K., Kukuck, S., Anleitner, R., and McAllister, T. Report on Experiments to Validate Fire Dynamic and Thermal-Structural Models for Use in the World Trade Center Investigation. Gaithersburg, MD: National Institute of Standards and Technology, 2004. NIST Special Publication 1000-B.
29. Hamins, A., Maranghides, A., McGrattan, K.B., Ohlemiller, T., and Anleitner, R. Experiments to Validate Models of Fire Growth and Spread for use in the World Trade Center Investigation. Gaithersburg, MD: National Institute of Standards and Technology, 2004. NIST Special Publication 1000-10E.
30. McGrattan, K.B. Verification and validation of selected fire models for nuclear power plant applications. *Fire Dynamics Simulator (FDS)*, Volume 7. Gaithersburg, MD: National Institute of Standards and Technology. Washington, DC: Nuclear Regulatory Commission. Palo Alto, CA: Electric Power Research Institute, 2007, Volume 7, 205 p. NUREG-1824, EPRI 1011999.
31. de St. Germain, J.D., McCorquodale, J., Parker, S.G., and Johnson, C.R. Uintah: A massively parallel problem solving environment. *Ninth IEEE International Symposium on High Performance and Distributed Computing*. Piscataway, NJ: IEEE, 2000, pp. 33–41.
32. Pope, S.B. Ten questions concerning the large-eddy simulation of turbulent flows. *New Journal of Physics*, 2004. 6, 1–24.
33. Zhang, W., Hamer, A., Klassen, M., Carpenter, D., and Roby, R. Turbulence statistics in a fire room model by large eddy simulation. *Fire Safety Journal*, 2002. 37(8), 721–752.

34. Smith, G.P., Golden, D.M., Frenklach, M., Moriarty, N.W., Eiteneer, B., Goldenberg, M., Bowman, C.T., Hanson, R.K., Song, S., Gardiner, W.C., Lissianski, V.V., and Qin, Z., GRI Mech 3.0, http://www.me.berkeley.edu/gri_mech/, accessed August 6, 2008.
35. Fox, R.O. *Computational Models for Turbulent Reacting Flows*. Cambridge, U.K.: Cambridge University Press, 2003.
36. Poinso, T. and Veynante, D. *Theoretical and Numerical Combustion*. Philadelphia, PA: Edwards, Inc., 2005.
37. Peters, N. Laminar diffusion flamelet model in non-premixed turbulent combustion. *Progress in Energy and Combustion Science*, 1984. 10, 319–339.
38. Bilger, R.W. Reaction rates in diffusion flames. *Combustion and Flame*, 1977. 30, 277–284.
39. Köylü, U.O. and Feath, G.M. Carbon monoxide and soot emissions from liquid-fueled buoyant turbulent diffusion flames. *Combustion and Flame*, 1991. 87, 61–76.
40. Tuovinen, H., Blomqvist, P., and Saric, F. Modelling of hydrogen cyanide formation in room fires. *Fire Safety Journal*, 2004. 39(8), 737–755.
41. Floyd, J.E. and McGrattan, K.B. Extending the mixture fraction concept to address under-ventilated fires. *Fire Safety Journal*, 2008. 44, 291–300.
42. Yang, R., Weng, W.G., Fan, W.C., and Wang, Y.S. Subgrid scale laminar flamelet model for partially premixed combustion and its application to backdraft simulation. *Fire Safety Journal*, 2005. 40(2), 81–98.
43. Kang, Y. and Wen, J.X. Large eddy simulation of a small pool fire. *Combustion Science and Technology*, 2004. 176(12), 2193–2223.
44. Williams, F.A. *Combustion Theory: The Fundamental Theory of Chemically Reacting Flow Systems*, 2nd Edition. Menlo Park, CA: Benjamin/Cummings, 1985, 680 p.
45. Beyler, C.L. Fire hazard calculations for large, open hydrocarbon fires. In: *SFPE Handbook of Fire Protection Engineering*, 3rd Edition. Quincy, MA: Society of Fire Protection Engineers, 2002, pp. 3-268–3-314.
46. Siegel, R. and Howell, J.R. *Thermal Radiation Heat Transfer*, 2nd Edition. New York: Hemisphere Publishing Corporation, 1981, 862 p.
47. Lockwood, F.C. and Shah, N.G. A new radiation solution method for incorporation in general combustion prediction procedures. In: *Proceedings of the 18th Symposium (International) on Combustion*. Pittsburgh, PA: The Combustion Institute, 1981, pp. 1405–1416.
48. Özisik, M.N. *Radiative Transfer and Interactions with Conduction and Convection*. New York: John Wiley & Sons Inc., 1973, 575 p.
49. Raithby, G.D. and Chui, E.H. A finite-volume method for predicting radiant heat transfer in enclosures with participating media. *Journal of Heat Transfer*, 1990. 112(2), 415–423.
50. Raithby, G.D. Discussion of the finite-volume method for radiation, and its application using 3D unstructured meshes. *Numerical Heat Transfer, Part B*, 1999. 35, 389–405.
51. Chai, J.C., Lee, H.S., and Patankar, S.V. Finite volume method for radiation heat transfer. *Journal of Thermophysics and Heat Transfer*, 1994. 8(3), 419–425.
52. Jensen, K.A., Ripoll, J.-F., Wray, A.A., Joseph, D., and El Hafi, M. On various modeling approaches to radiative heat transfer in pool fires. *Combustion and Flame*, 2007. 148(4), 263–279.
53. Grosshandler, W. RadCal: A Narrow Band Model for Radiation Calculations in a Combustion Environment. Gaithersburg, MD: National Institute of Standards and Technology, 1993. NIST Technical Note TN 1402.
54. Yan, Z. and Holmstedt, G. Fast, Narrow-band computer model for radiation calculations. *Numerical Heat Transfer, Part B*, 1997. 31, 61–71.
55. Demebele, S. and Wen, J.X. Evaluation of a fast correlated-k approach for radiation calculations in combustion systems. *Numerical Heat Transfer Part B*, 2003. 44(4), 365–385.
56. Demebele, S., Zhang, J., and Wen, J.X. Assessments of spectral narrow band and weighted-sum-of-gray-gases models for computational fluid dynamics simulations of pool fires. *Numerical Heat Transfer Part B*, 2005. 48(3), 257–276.
57. Zhang, J., Demebele, S., Karwatzki, J., and Wen, J.X. Effect of radiation models on CFD simulations of upward flame spread. In: Gottuk, D.T. and Lattimer, B.Y. (eds.) *Proceedings of Eighth International Symposium on Fire Safety Science*, September 18–23. Beijing, China: International Association for Fire Safety Science, 2005, pp. 421–432.
58. Wiscombe, W. Mie scattering calculations: Advances in technique and fast, vector-speed computer codes. Boulder, CO: National Center for Atmospheric Research, 1979 (revised 1996). NCAR Technical Note NCAR/TN-140+STR.

59. Bohren, C.F. and Huffman, D.R. *Absorption and Scattering of Light by Small Particles*. New York: John Wiley & Sons, 1983, 530 p.
60. Berour, N., Lacroix, D., Boulet, P., and Jeandel, G. Radiative and conductive heat transfer in a nongrey semitransparent medium. Application to fire protection curtains. *Journal of Quantitative Spectroscopy & Radiative Transfer*, 2004. 86, 9–30.
61. Trivic, D.N., O'Brien, T.J., and Amon, C.H. Modeling the radiation of anisotropically scattering media by coupling Mie theory with Finite volume method. *International Journal of Heat and Mass Transfer*, 2004. 47, 5765–5780.
62. Collin, A., Boulet, P., Lacroix, D., and Jeandel, G. On radiative transfer in water spray curtains using the discrete ordinates method. *Journal of Quantitative Spectroscopy & Radiative Transfer*, 2005. 92, 85–110.
63. Hostikka, S. and McGrattan, K. Numerical modeling of radiative heat transfer in water sprays. *Fire Safety Journal*, 2006. 41(1), 76–86.
64. Moss, J.B. and Stewart, C.D. Flamelet-based smoke properties for the field modelling of fires. *Fire Safety Journal*, 1998. 30, 229–250.
65. Yeoh, G.H., Yuen, R.K.K., Chueng, S.C.P., and Kwok, W.K. On modelling combustion, radiation and soot processes in compartment fires. *Building and Environment*, 2003. 38(6), 771–785.
66. Wen, J.X., Huang, L.Y., and Roberts, J. The effect of microscopic and global radiative heat exchange on the field predictions of compartment fires. *Fire Safety Journal*, 2001. 36(3), 205–223.
67. Lautenberger, C.W., de Ris, J.L., Dembsey, N.A., Barnett, J.R., and Baum, H.R. A simplified model for soot formation and oxidation in CFD simulation of non premixed hydrocarbon flames. *Fire Safety Journal*, 2005. 40(2), 141–176.
68. Beji, T., Zhang, J.P., and Delichatsios, M. Determination of soot formation rate from laminar smoke point measurements. *Combustion Science and Technology*, 2008. 180, 927–940.
69. Beji, T., Zhang, J., and Delichatsios, M. Soot formation and oxidation in fires from laminar smoke point measurements. *Fire Safety Science—Proceedings of the Ninth International Symposium*, 2008 (in press).
70. Prasad, K.R. and Baum, H.R. Coupled fire dynamics and thermal response of complex building structures. In: Chen, J.H., Colket, M.D., Barlow, R.S., and Yetter, R.A. (eds.). *Proceedings of the 30th Symposium (International) on Combustion*, Volume 30. July 25–30, 2004, Chicago, IL. Pittsburgh, PA: Combustion Institute, 2005. Part 2, pp. 2255–2262.
71. Lautenberger, C. and Fernandez-Pello, C. Pyrolysis modeling, thermal decomposition, and transport processes in combustible solids. In: Faghri, M. and Sundén, B. (eds.). *Transport Phenomena in Fires*. Boston, MA: WIT Press, 2008, pp. 209–259.
72. Di Blasi, C. Modeling chemical and physical processes of wood and biomass pyrolysis. *Progress in Energy and Combustion Science*, 2008. 34, 47–90.
73. Babrauskas, V. Heat release rates. In: *The SFPE Handbook of Fire Protection Engineering*. 3rd Edition. Quincy, MA: National Fire Protection Association, 2002, pp. 3–26.
74. Hostikka, S., McGrattan, K.B., and Hamins, A. Numerical modeling of pool fires using LES and finite volume method for radiation. *Fire Safety Science—Proceedings of the Seventh International Symposium*, Worcester, MA, 2003, pp. 383–394.
75. Novozhilov, V. and Koseki, H. CFD prediction of pool fire burning rates and flame feedback. *Combustion Science and Technology*, 2004. 176, 1283–1307.
76. Hietaniemi, J., Hostikka, S., and Vaari, J. FDS Simulation of Fire Spread—Comparison of Model Results with Experimental Data. VTT Building and Transport, Technical Report VTT Working Paper 4, Espoo, Finland: 2004.
77. Mitler, H.E. Predicting the spread rates of fires on vertical surfaces. *Proceedings of the Combustion Institute*, 1990. 23, 1715–1721.
78. Mitler, H.E. and Steckler, K.D. SPREAD—A Model of Flame Spread on Vertical Surfaces. NISTIR 5619, Gaithersburg, MD: National Institute of Standards and Technology, 1995.
79. Tewarson, A. and Ogden, S.D. Fire behavior of polymethylmethacrylate. *Combustion and Flame*, 1992. 89, 237–259.
80. Lautenberger, C., Rein, G., and Fernandez-Pello, A.C. The application of a genetic algorithm to estimate material properties for fire modeling from bench-scale fire test data. *Fire Safety Journal*, 2006. 41, 204–214.
81. Rein, G., Lautenberger, C., Fernandez-Pello, A.C., Torero, J.L., and Urban, D.L. Application of genetic algorithms and thermogravimetry to determine the kinetics of polyurethane foam in smoldering combustion. *Combustion and Flame*, 2006. 146, 95–108.

82. Saha, B., Karthik Reddy, P., and Ghosal, A.K. Hybrid genetic algorithm to find the best model and the globally optimized overall kinetics parameters for thermal decomposition of plastics. *Chemical Engineering Journal*, 2008. 138, 20–29.
83. Matala, A., Hostikka, S., and Mangs, J. Estimation of pyrolysis model parameters for solid materials using thermogravimetric data. *Fire Safety Science—Proceedings of the Ninth International Symposium*, Karlsruhe, Germany, 2008.
84. Atreya, A. and Baum, H.R. Model of opposed-flow flame spread over charring materials. In: Chen, J.H. and Colket, M.D. (eds.). *Proceedings of the 29th Symposium (International) on Combustion*, Volume 29, July 21–25, Sapporo, Japan. Pittsburgh, PA: Combustion Institute, 2002, Part 1, pp. 227–236.
85. Linteris, G., Gewuerz, L., McGrattan, K., and Forney, G. Modeling solid sample burning. *Fire Safety Science—Proceedings of the Eighth International Symposium*, Beijing, China, 2005, pp. 625–636.
86. Jiang, Y. Decomposition, ignition, and flame spread on furnishing materials. PhD Dissertation, Melbourne, Australia: Victoria University Center for Environment Safety and Risk Engineering, 2006.
87. Liang, M. Evaluation Studies of the Flame Spread and Burning Rate Predictions by the Fire Dynamics Simulator. MS thesis, College park, MA: University of Maryland, 2002.
88. Kwon, J.-W., Dembsey, N.A., and Lautenberger, C.W. Evaluation of FDS V.4: Upward flame spread. *Fire Technology*, 2007. 43, 255–284.
89. Zhang, J., Dembele, S., Karwatzki, J., and Wen, J.X. Effect of radiation models on CFD simulations of upward flame spread. *Fire Safety Science—Proceedings of the Eighth International Symposium*, Vista, FL, 2005, pp. 421–432.
90. Consalvi, J.L., Pizzo, and Porterie, B. Numerical analysis of the heating process in upward flame spread over thick PMMA slabs. *Fire Safety Journal*, 2008. 43, 351–362.
91. Lowndes, I.S., Silvester, S.A., Giddings, D., Pickering, S., Hassan, A., and Lester, E. The computational modeling of flame spread along a conveyor belt. *Fire Safety Journal*, 2007. 42, 51–67.
92. Mell, W.E., Jenkins, M.A., Gould, J., and Cheney, P. A physics-based approach to modelling grassland fires. *International Journal of Wildland Fire*, 2007. 16, 1–22, doi:10.1071/WF06002.
93. Yan, Z. and Holmstedt, G. CFD and experimental studies of room fire growth on wall lining materials. *Fire Safety Journal*, 1996. 27, 201–238.
94. Theuns, E., Merci, B., Vierendeels, J., and Vandevelde, P. Influence of solid material properties on numerical large scale flame spread calculations. *Interflam*, Edinburgh, U.K., 2004, pp. 1245–1256.
95. Hostikka, S. and McGrattan, K.B. Large eddy simulation of wood combustion. *Interflam*, Edinburgh, U.K., 2001, pp. 755–762.
96. Moghaddam, A.Z., Moinuddin, K., Thomas, I.R., Bennets, I.D., and Culton, M. Fire behavior studies of combustible wall linings applying fire dynamics simulator. *Proceedings of the 15th Australasian Fluid Mechanics Conference*, Sydney, Australia, 2004.
97. Carlsson, J. Computational strategies in flame-spread modelling involving wooden surfaces—An evaluation study. Lund, Sweden: Lund University Department of Fire Safety Engineering, Report 1028, 2003.
98. Capote, J.A., Alvear, D., Mariano, L., and Espina, P. Heat release rate and computer fire modeling vs. real-scale fire tests in passenger trains. *Fire and Materials*, 2008. 32, 213–229.
99. Chiam, B.H. Numerical Simulation of a Metro Train. Christchurch, New Zealand: University of Canterbury, Department of Civil Engineering, Fire Engineering Research Report 05/1, 2005.
100. Coles, A., Lautenberger, C., Wolski, A., Smits, B., and Wong, K. Using computer fire modeling to reproduce and predict FRP composite fire performance. *Composites & Polycon*, Tampa, FL: American Composites Manufacturers Association, January 15–17, 2009.
101. Rein, G., Torero, J.L., Jahn, W., Stern-Gottfried, J., Ryder, N.L., Desanghere, S., Lazaro, M., Mowrer, F., Coles, A., Joyeux, D., Alvear, D., Capote, J.A., Jowsey, A., and Reszka, P. A priori modeling of fire test one. In: Rein, G., Abecassis-Empis, C., and Carvel, R. (eds.), Chapter 10 in *The Dalmarnock Fire Tests: Experiments and Modeling*. Edinburgh, U.K.: University of Edinburgh, 2007, pp. 173–192.
102. Jahn, W., Rein, G., and Torero, J.L. A posteriori modeling of fire test one. In: Rein, G., Abecassis-Empis, C., and Carvel, R. (eds.), Chapter 11 in *The Dalmarnock Fire Tests: Experiments and Modeling*. Edinburgh, U.K.: University of Edinburgh, 2007, pp. 193–210.
103. Jahn, W., Rein, G., and Torero, J.L. The effect of model parameters on the simulation of fire dynamics. *Fire Safety Science—Proceedings of the Ninth International Symposium*, Karlsruhe, Germany, 2008.
104. Lazaro, M., Boehmer, H., Alvear, D., Capote, J.A., and Trouve, A. Numerical simulation of fire growth, transition to flashover, and post-flashover dynamics in the dalmarnock fire test. *Fire Safety Science—Proceedings of the Ninth International Symposium*, Karlsruhe, Germany, 2008.

105. Gann, R.G., Hamins, A., McGrattan, K.B., Mulholland, G.W., Nelson, H., Ohlemiller, T.J., Pitts, W.M., and Prasad, K.R. Reconstruction of the fires in the World Trade Center Towers, NIST NCSTAR 1-5, Federal Building and Fire Safety Investigation of the World Trade Center Disaster, Gaithersburg, MD: National Institute of Standards and Technology, 2005.
106. Grosshandler, W., Bryner, N., Madrzykowski, D., and Kuntz, K. Report of the Technical Investigation of the Station Nightclub Fire, NIST NCSTAR 2: Vol. I. Gaithersburg, MD: Building and Fire Research Laboratory, National Institute of Standards and Technology, 2005.
107. Madrzykowski, D. and Walton, W.D. Cook County Administration Building Fire, 69 West Washington, DC, Chicago, IL, October 17, 2003: Heat Release Rate Experiments and FDS Simulations. NIST Special Publication SP-1021, Building and Fire Research Laboratory, 2004.

21 Regulations, Codes, and Standards Relevant to Fire Issues in the United States

Marcelo M. Hirschler

CONTENTS

21.1	Background: Regulations, Codes, and Standards.....	588
21.2	Regulations	589
21.2.1	How Does Regulation for Fire Safety Work in the United States?.....	589
21.2.2	Federal Regulations	591
21.2.3	State Regulations	592
21.2.4	Local Regulations	593
21.2.5	Regulations of Specific Items	594
21.2.5.1	Aircraft	598
21.2.5.2	Ships.....	600
21.2.5.3	Trains and Underground Rail Vehicles.....	601
21.2.5.4	Motor Vehicles	606
21.2.5.5	School Buses	608
21.2.5.6	Cigarettes	608
21.2.5.7	Flammable Fabrics.....	609
21.2.6	Comparison with International Regulations.....	615
21.3	Codes	621
21.3.1	International Code Council Codes	621
21.3.1.1	International Building Code	622
21.3.1.2	International Fire Code.....	625
21.3.1.3	International Residential Code	626
21.3.1.4	International Mechanical Code.....	627
21.3.1.5	International Existing Building Code.....	627
21.3.1.6	International Wildland Urban Interface Code	627
21.3.1.7	International Performance Code.....	628
21.3.2	National Fire Protection Association Codes and Standards.....	628
21.3.2.1	National Electrical Code.....	628
21.3.2.2	National Life Safety Code	632
21.3.2.3	Uniform Fire Code.....	633
21.3.2.4	NFPA Building Code.....	634
21.3.2.5	Buildings of Historic or Cultural Interest.....	635
21.3.2.6	Ships.....	636
21.3.2.7	Manufactured Housing	637

21.3.2.8	Air Conditioning Standard	637
21.3.2.9	Other NFPA Codes and Standards	638
21.3.3	International Association of Plumbing and Mechanical Officials Codes	639
21.3.3.1	Uniform Mechanical Code	639
21.4	Standards	639
21.4.1	Organizations and Committees Issuing Fire Standards or Standards with Fire Tests.....	639
21.4.2	Standard Test Methods	640
21.4.2.1	Ignitability.....	640
21.4.2.2	Ease of Extinction.....	644
21.4.2.3	Flammability.....	644
21.4.2.4	Flame Spread	644
21.4.2.5	Heat Release.....	646
21.4.2.6	Smoke Obscuration	648
21.4.2.7	Smoke Toxicity	649
21.4.2.8	Microcalorimetry.....	651
21.4.2.9	Cigarette Ignition	652
21.4.3	Tests for Specific Products or Materials	652
21.5	Product Liability	653
21.6	Conclusions.....	654
	Abbreviations	654
	Appendix A Key Fire Standards from ASTM, NFPA, and UL.....	656
	References.....	661

21.1 BACKGROUND: REGULATIONS, CODES, AND STANDARDS

North American fire safety requirements are based on an assortment of regulations, codes and standards and are not and probably will never be, uniform. It is important, therefore, to start by defining the terms to be used and then discussing the various organizations involved.

- a. Regulations are documents with the force of law which list the general objectives and act as a framework for more detailed requirements. One example could be a national law requiring sprinkler protection of a certain type of occupancy.
- b. Codes are documents connected with regulations, but which comprise more specific requirements and are valid for particular cases such as hospitals or schools. If they also offer practical solutions, they may be called codes of practice. An example associated with the national law mentioned earlier would be a building code detailing the layout of the sprinklers in each type of building.
- c. Standards are documents referred to either in regulations or codes, and which put forward special techniques to quantify the results. Typical examples of standards are the test methods and specifications. Examples associated with the national law mentioned earlier would be specifications describing sprinkler construction test methods assessing their effectiveness.
- d. Specifications are documents that describe the requirements for a particular material or product for use by a specific purchaser. This is a document that is often a part of an open solicitation or an agreement, and can be between two parties or a generic request. An example associated with the scheme mentioned earlier could involve requirements for the type of sprinkler pipe and/or the discharge density.
- e. Guides are documents that explain the concepts associated with particular issues, such as test methods or properties. An associated example would be a guide explaining why sprinklers help in fires and what the effect of discharge density could be.

These definitions are generic enough that they can be applied worldwide. In the European Union (EU), for example, the European Commission (EC) issued the Construction Products Directive (CPD) that all the member states are required to comply with and which contains “essential requirements” associated with fire safety. The governments of the individual member states (countries) issue regulations adopting certain requirements and incorporating them into their own local codes. These codes can then reference national or international standards. It is important to point out, however, that the codes and standards are issued by organizations associated with the governments of the individual countries.

In the United States, the Federal Government is entitled to regulate the fire safety of the consumer products and transportation vehicles, but it rarely does. In fact, there are very few consumer products for which the fire safety is being regulated (via the Consumer Product Safety Commission [CPSC]). CPSC is an organization governed by a set of commissioners appointed by the U.S. President, with congressional approval, which regulates the following: wearing apparel fabrics, children’s sleepwear, carpets and rugs, and mattress sets. CPSC has also published a notice of its intent to regulate upholstered furniture (more details presented later). In fact, CPSC is required to regulate all consumer products that contain “flammable fabrics” and is not permitted to regulate cigarettes. CPSC also regulates, indirectly, the use of hazardous materials, which include flammable solids (this indirectly affects toys, as will be discussed later). Various agencies are required to regulate the fire safety of the transportation vehicles. All other materials and products are regulated via the adoption of one of the various codes (issued by private organizations) by a state or local government, or (rarely) by their issuance of their own special regulations.

Canada has a system that is intermediate between the EU regulatory system (which is intended to be, at least ultimately, based on directives and/or regulations from the EC) and the U.S. system (where codes and standards are both developed by private companies and can be adopted, or not, by the various state and local governments). The National Building Code (NBC) of Canada can be different from provincial building codes, and standards are issued by private companies.

In the United States, there are two primary companies that develop codes: International Code Council (ICC) and National Fire Protection Association (NFPA). ICC develops a full family of codes, including the following: International Building Code (IBC),¹ International Fire Code (IFC),² International Mechanical Code (IMC),³ International Wildland Urban Interface Code (IWUIC),⁴ International Residential Code (IRC),⁵ and International Existing Building Code (IEBC),⁶ which have been adopted widely throughout the country. NFPA also develops a full family of codes, with equivalent codes to most ICC codes. However, two NFPA codes (National Electrical Code, or NEC or NFPA 70⁷ and Life Safety Code or NFPA 101⁸) are unique and have no ICC equivalent. NFPA is also one of the premier developers of fire safety standards, including a few key ones: NFPA 90A (air conditioning standard),⁹ NFPA 13 (sprinkler standard),¹⁰ and NFPA 130 (rail standard).¹¹ Fire tests (standards) are developed primarily by the American Society for Testing and Materials (ASTM) International and by NFPA, although FM Global (formerly, Factory Mutual) and Underwriters Laboratories (UL) have also developed some widely used tests.

The individual U.S. states have always been entitled to issue their own regulation, as long as there is no contradiction with the federal legislation, which is normally nonexistent. Thus, California has long had regulation for the fire performance of upholstered furniture and mattresses, based on the requirements developed at the California Bureau of Home Furnishings and Thermal Insulation (CBHF), and this has occasionally been emulated by some other states.

21.2 REGULATIONS

21.2.1 HOW DOES REGULATION FOR FIRE SAFETY WORK IN THE UNITED STATES?

As explained earlier, the U.S. system works primarily on the basis of individuals who are not employees of codes and standards organizations, but are codes and standards “volunteers,” working within the private codes and standards organizations, to develop new standards as well as revise existing

standards, which are then incorporated into new codes (or into revisions of existing codes). These people are called “volunteers” because their participation in the process is neither funded by the codes and standards organizations within which they are active, nor by the U.S. government (unless they are government employees). Each code development organization has a unique consensus process by which public proposals and comments are being processed into new or revised documents. A successful process always consists of two stages before new documents or substantial revisions are approved.

The process of adoption of codes and standards is tightly controlled by each organization, so that no unfair advantage is provided to any individual interest and all concerns are addressed. For example, the ICC requires that the “Final Action” on all code changes be completed at a public meeting where the voting is restricted to public officials. In the case of organizations like ASTM International (formerly the American Society for Testing and Materials [ASTM]) and the NFPA voting, membership in the committees is strictly balanced by having representatives from producers or manufacturers and representatives from any other interests or stakeholders.

In some cases, the standards developed by the trade associations, instead of the standards-making bodies, are included within the codes. However, such types of standards are frowned upon in recent years and it is rare that they are newly included. They are, however, often “grandfathered” (i.e., allowed to remain because they have been in the relevant code or in its predecessor for years). Such standards must still comply with some consensus rules, and many of them tend to be eventually replaced by standards issued by the major standards development organizations.

There are very few products for which the fire safety is actually mandated by the federal government. The fire safety of the following products is covered by the federal regulation:

1. Wearing apparel is regulated by CPSC and is covered since the promulgation of the Flammable Fabrics Act (FFA) in 1953, by a 45° angle flammability test for apparel fabrics (CS 191-53), which became effective in 1954, and is still valid, as 16 CFR 1610.¹² The FFA later started covering other products.
2. Ignitability of carpets and rugs is regulated by CPSC and is also covered as a result of the FFA, since the development of the requirements in 1970 and 1971, by regulations based on the methenamine pill test, as 16 CFR 1630¹³ and 16 CFR 1631.¹⁴
3. Flammability of children’s sleepwear is regulated by CPSC and is also covered as a result of the FFA, since a small-scale vertical open flame ignition test was developed in 1971, as 16 CFR 1615.¹⁵ This was expanded to older children in 1974, as 16 CFR 1616.¹⁶
4. Smoldering ignition of mattresses is regulated by CPSC and is also covered by the FFA, since the smoldering test in 16 CFR 1632¹⁷ was introduced in 1972.
5. Flammable solids, products which are considered as “dangerous goods” for transportation purposes, and “hazardous materials” for storage and display purposes, have been regulated under the Federal Hazardous Substances Act (FHSA), by means of rules governing their amounts for storage and transport based on a candle test in 16 CFR 1500.44.¹⁸ Hazardous materials (including flammable solids) are regulated by both CPSC and the Department of Transport. A flammable solid is often defined as follows: flammable solid—a solid, other than a blasting agent or explosive, that is liable to cause fire through friction, absorption or moisture, spontaneous chemical change, or which retains heat from manufacturing or processing or which can be ignited readily, and when ignited burns so vigorously and persistently to create a serious hazard.
6. Open flame ignition of mattresses is regulated by CPSC and is covered, once again, by the FFA, since the fairly severe open flame test for mattress sets in 16 CFR 1633¹⁹ came into effect in 2007.
7. Flammability of toys is regulated by CPSC and is covered since 2008 by the application of ASTM F 963,²⁰ a standard specification for toys which includes the requirements that: (a) “materials other than textiles (excluding paper) used in toys shall not be flammable, as defined under 16 CFR 1500.3 (c) (6) (vi)” under the FHSA and (b) any textile fabrics used in toys must comply with 16 CFR 1610 (see above).

8. Proposed fire safety regulations for upholstered furniture have existed since the CPSC issued various advanced notices of the proposed rulemaking in the 1990s and early 2000s, and a notice of the proposed rulemaking (NPRM) in 2007.²¹ However, no regulation exists in 2008.
9. Fire safety of a variety of transportation vehicles (but not all) is covered by other federal government agencies, mostly subsidiary to the Department of Transportation, including National Highway Traffic Safety Administration (NHTSA, for highway vehicles), Federal Aviation Administration (FAA, for aircraft), Federal Railroad Administration (FRA, for interstate and intercity trains), and U.S. Coast Guard (USCG, for ships). The Federal Transit Administration (FTA) has jurisdiction over U.S. buses and underground fixed guideway vehicles, but it has never issued requirements and still simply recommends “guidelines” issued in the 1970s.
10. Fire safety of mine conveyor belts is covered by the Mine Safety and Health Administration (MSHA), subsidiary to the Department of Labor (responsible for the safety of miners). It has instituted some requirements, in accordance with a 1969 Act, which then became the 1977 Federal Mine Safety and Health Act. This regulation mandates the use of “flame-resistant conveyor belts.” The follow-up legislation was introduced in 2007.

With regard to state and local authorities having jurisdiction, they are not permitted to issue regulation that conflicts with federal regulation, because of the issue of “preemption.” In other words, it is not legal for a state or local authority to require that a particular product be less safe than is required by the federal regulations. On the other hand, it is normally acceptable for a state or local jurisdiction to impose requirements that exceed those issued by the federal government. Therefore, as the information mentioned earlier demonstrate that there are very few examples of federal fire safety regulation, state and local authorities have wide opportunities for taking necessary action.

21.2.2 FEDERAL REGULATIONS

For the federal (national) government to introduce a new regulatory requirement, it must show the need for it. Once the need has been demonstrated to the satisfaction of the government agency that is going to issue the regulation, an NPRM is published in the *Federal Register*. An NPRM must be issued by law when a regulatory agency of the U.S. Federal Government wishes to add, remove, or change a rule (or regulation) as a part of the rulemaking process. The NPRM procedure is required and defined by the Administrative Procedure Act and not the Constitution. It was created by the U.S. Congress to force agencies to listen to the comments and concerns of people who are likely to be affected by the regulation. Examples of agencies subject to these procedures are: CPSC, FAA, FRA, NHTSA, USCG, MSHA, and Environmental Protection Agency (EPA). The NPRM is published in the Federal Register and typically gives 60 days for public comment from any interested party, and an additional 30 days for reply comments. The original comments may still be filed in the reply comments “window.” In fact, complex regulation often winds up being preceded by an Advance Notice of Proposed Rulemaking (ANPRM). Each notice includes:

- A statement of the time, place, and nature of the proposed rulemaking proceeding;
- A reference to the authority under which it is issued;
- A description of the subjects and issues involved, or the substance and terms of the proposed regulation;
- A statement of the time within which written comments must be submitted; and
- A statement of how and to what extent interested persons may participate in the proceeding.

At least in theory, the relevant authority having jurisdiction (AHJ) must start by making a cost-benefit analysis that investigates the history of losses and assesses the benefits to result from the regulation. In fact, to some extent at least, local and state authorities must go through a similar process.

This complex set of rules, which can be derailed at many stages of the process, explains why federal regulations are rare in the area of fire safety, where the “push” to introduce regulation is rarely front-page news. Typically, changes in regulations follow flashy headlines, associated with a specific large fire loss.

21.2.3 STATE REGULATIONS

It is rare for individual states to issue specific regulations associated with fire safety, but some states have done so. In particular, the California Bureau of Home Furnishings and Thermal Insulation (CBHF) has issued a number of Technical Bulletins addressing various furnishings fire issues (Table 21.1). No other state has been as proactive as California. However, some activities have taken

TABLE 21.1
California: Technical Bulletins and Some Other Fire Safety Regulations

Number	Last Issued	Withdrawn	Title
26	1987		Requirements for record keeping and prototype testing of mattresses for compliance with State and Federal Flammability Laws. Questions and Answers about the Amended Mattress Flammability Standard 16 CFR 1632 (FF 4-72)
106	1986	2007	Requirements, test procedures, and apparatus for testing the resistance of a mattress or mattress pad to combustion which may result from a smoldering cigarette
116	1980		Requirements, test procedure, and apparatus for testing the flame retardance of upholstered furniture
117	2000		Requirements, test procedures, and apparatus for testing the flame retardance of resilient filling materials used in upholstered furniture
121	1980		Flammability test procedure for mattresses for use in high-risk occupancies
129	1992		Flammability test procedure for mattresses for use in public buildings
133	1991		Flammability test procedure for seating furniture for use in public occupancies
603	2003	2007	Requirements and test procedure for resistance of a mattress/box spring set to a large open flame
16 CFR 1632	2007		Standard for the flammability (cigarette ignition resistance) of mattresses and mattress pads (replaces CA TB 106)
16 CFR 1633	2007		Standard for the flammability (open flame) of mattress sets (replaces CA TB 603)
Draft TB 604	2007		Test procedure and apparatus for the open-flame resistance of filled bedclothing
Draft TB 117 Plus	2002		Requirements, test procedure, and apparatus for testing the flame and smolder resistance of upholstered furniture
Title 19 Ch 2 Art 4	2007		Tents, awnings, and other fabric enclosures—flame resistance and labeling
Title 19 Ch 7 Art 1	2007		Standards of flammability: wearing apparel—prohibition of tris(2,3-dibromopropyl) phosphate
Title 19 Ch 7 Art 2/3	2007		Standards of flammability: hospital fabrics, sheets, and pillowcases, sleepwear

TABLE 21.2
Massachusetts: Some Fire Safety Regulations

Number	Title
527 CMR 19.00	Tentage
527 CMR 21.00	Decorations, curtains, draperies, blinds, and other window treatments
527 CMR 29.00	Upholstered furniture, molded seating, and reupholstered furniture

place in Massachusetts, where the Board of Fire Prevention Regulations also has issued a number of fire safety requirements (Table 21.2).

In recent years, many U.S. states have issued regulations governing the sale of the so-called “fire-safe cigarettes.” These are cigarettes with lower ignition propensity, which are assessed by the virtue of their performance in ASTM E 2187 (Standard Test Method for Measuring the Ignition Strength of Cigarettes).²² This regulation was first adopted by New York, in 2003, and was then followed by many other states. New York passed the legislation in 2003 and implemented the law in 2004. The regulations became effective by August 1, 2008, in 15 other states; 19 states have regulations with effective dates between 2008 and 2010, and the laws were passed in 13 other states and in Washington, DC, in 2008, making a total of 35 states (with over 80% of the U.S. population) having passed the legislation requiring that cigarettes sold there be fire-safe. Several other states are currently considering the legislation. The Coalition for Fire-Safe Cigarettes, headed by the president of NFPA, has been spearheading the effort to have this legislation adopted. The objective is, of course, to make people safer from fire by encouraging states to require that all cigarettes be designed so that they are less likely to start a fire. Between 700 and 900 people die each year in the United States as a result of fires caused by cigarettes, according to NFPA. Figure 21.1 (issued by NFPA) shows the status of the regulation in the early 2008.

However, the most typical (and important) way for individual states to apply fire safety regulations is by adoption of codes. Table 21.3 (developed by ICC) shows the adoption of the ICC codes (or International Codes, issued by the ICC). Table 21.4 (also from ICC) presents the notes for Table 21.3.

As far as NFPA codes are concerned, as stated earlier, there are two key codes of relevance to fire safety that have no ICC equivalent. They are the National Electrical Code (NEC, NFPA 70), which has been adopted by virtually every state in the United States, and the National Life Safety Code (NFPA 101), which has been adopted by the majority of the states, as shown in Figure 21.2 (issued by NFPA).

In the 1980s, New York incorporated into its code (New York State Uniform Fire Prevention and Building Code), in Article 15, Part 1120, a requirement for “Combustion Toxicity Testing,”²³ based on a smoke toxicity test developed at the University of Pittsburgh.²⁴ The test method was never standardized by either ASTM or NFPA because of the several concerns about its scientific validity.^{25–28} The New York State regulation did not include pass/fail criteria and has since been rescinded.

21.2.4 LOCAL REGULATIONS

It is even less common in the United States for the local jurisdictions to adopt specific regulations that differ from the federal (or state) requirements. A fairly unique set of stringent upholstered furniture fire-safety requirements were managed by the Boston Fire Department for the city, based on the recommendations from the fire department’s Chemistry Department in the 1970s and 1980s. Another unusual requirement was put in place by the Department of Buildings in the city of New York, for smoke toxicity testing, also based on the University of Pittsburgh test. This requirement, as opposed to the one in New York, did have pass/fail criteria.

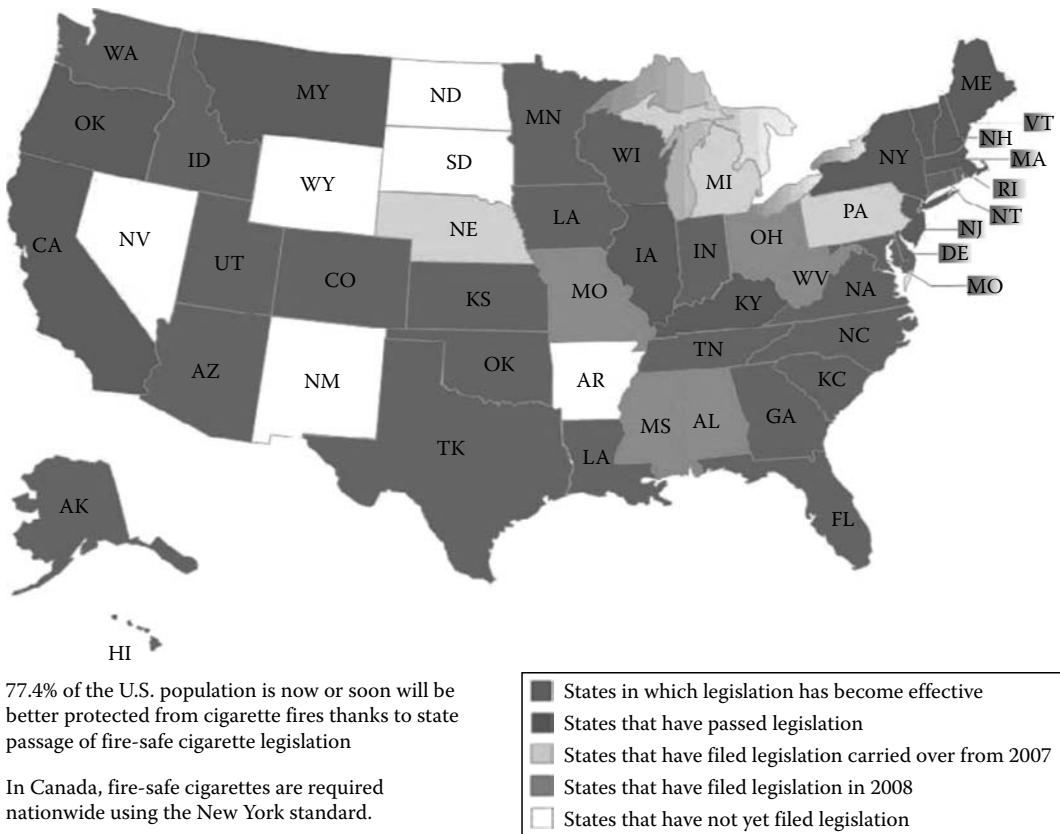


FIGURE 21.1 (See color insert following page 530.) Legislation for fire-safe cigarettes in the United States—early 2008.

It is not unusual for the cities, especially the larger ones, such as Chicago or Los Angeles, to adopt a citywide code or set of codes. This can take place in different ways. The city of Los Angeles, CA, for example, has generally adopted its own building and fire codes, which are modifications of the applicable California code. On the other hand, the city of Chicago, IL, has issued its own independent building code. It is also not unusual for specific events or personalities to influence local bans on certain products. One example is a requirement in Chicago that all cables in plenums be enclosed in metal raceways, while most codes and standards (including the NEC) require that cables be listed and fire tested for plenum use.

21.2.5 REGULATIONS OF SPECIFIC ITEMS

The key items regulated are components in vehicles and items covered under the FFA. NFPA has developed statistics that show average annual U.S. vehicular losses (1980–1998): 433,000 fires, with 679 civilian fire fatalities, 2990 civilian fire injuries, and \$959.0 millions in total fire losses.²⁹ In structures, the numbers, from 1980 to 1998, are 682,200 fires, with 4440 civilian fire fatalities, 23,014 civilian fire injuries, and \$6438.3 millions in total fire losses.³⁰ In fact, the data show that the number of vehicular fires is almost two-thirds of the number of structure fires. The heat release rate obtained from a burning automobile has been shown to be in the range of 1.5–8.0 MW, roughly the same order as heat released from a fully involved room in a home.³¹

**TABLE 21.3
ICC Codes-Adoption by State (Early 2008)**

ST	Jurisdiction	IBC	IRC	IFC	IMC	IPC	IPSDC	IFGC	IECC	IPMC	IEBC	ICCP	IUWIC	IZC
AL	Alabama	X06	X06	X06, L	X06, L	X06, L	L	X06, L	L	L	L	L	L	L
AK	Alaska	X03	L06	X03	X03	L		X03						
AZ	Arizona	X00	L	X03	L	L		L	X00	X00	L	L	L	L
AR	Arkansas	X00	X00	X00	X00	X06	L	X06	X03	L	L			
CA	California	X06		X06										
CO	Colorado	L	L	L	L	L	L	L	L	L	L	L	L	L
CT	Connecticut	X03	X03	X03	X03	X03		X03	X03	L	X03			
DE	Delaware	L	L	L	L	X03	L	L	L	L	L			
DC	District of Columbia	X00	X00	X00	X00	X00		X00	X00	X00				
FL	Florida	X03	X03		X03	X03		X03	X06		X03			
GA	Georgia	X06	X06	X06	X06	X06		X06	X06		L			
HI	Hawaii	X06	X03											
ID	Idaho	X03	X06	X03	X03			X03	X03		L			L
IL	Illinois	L	L	L	L	L	L	L	X06	L	L	L	L	L
IN	Indiana	X06	X03	X06	X06			X06	X06	L				L
IA	Iowa	X06	X06	X06	X06	L	L	L	X06	L	X06			L
KS	Kansas	X03	X03	X03	L03	L03	L	L03	X06	L	L			
KY	Kentucky	X06	X06	L	X06			X06	X06	L				
LA	Louisiana	X06	X06		X06			X06	L	L	X06			
ME	Maine	X03,L	X03	L	X06	L	L	L	X03	L	X03			L
MD	Maryland	X06	X06		X06	X06,L	L	L	X06		X06			
MA	Massachusetts	A03	X03		A03					L	X03	L		
MI	Michigan	X03	X03	L	X03	X03	L	X03		L				
MN	Minnesota	X06	X06	X06	X06			X06		L				
MS	Mississippi	L	L	L	L	L	L	L	L	L	L	L	L	L
MO	Missouri	X00	X00	L	X00	X00, X03	L	X00	L	L	L	L	L	L
MT	Montana	X06	X06	L	X06			X06	X03		X06			L
NE	Nebraska	X00	X00	L	L	L	L	L	X03	L	L		L	L
NV	Nevada	X03	X03	X03	L	L	L	L	X03	L	X03	L	L	L

(continued)

**TABLE 21.3 (continued)
ICC Codes-Adoption by State (Early 2008)**

ST	Jurisdiction	IBC	IRC	IFC	IMC	IPC	IPSDC	IFGC	IECC	IPMC	IEBC	ICCP	IUWIC	IZC
NH	New Hampshire	X06	X06	L	X06	X06			X06	L				
NJ	New Jersey	X06	X06		X06			X06	X06	L				
NM	New Mexico	X03	X03	L	L	L		L	X03	L	X03	L		
NY	New York	X03	X03	X03	X03	X03		X03	X03	X03				
NC	North Carolina	X03	X00	X03	X03	X03		X03	X03					
ND	North Dakota	X	X	L	X	L		X		L				
OH	Ohio	X06	X03	X06	X06	X06		X06	X06	L				L
OK	Oklahoma	X06	X03	X06	X06	X06		X06	X03	X06	X06	X06	L	L
OR	Oregon	X06	X06	X06	X06	X06		X06						
PA	Pennsylvania	X06	X06	X06	X06	X06		X06	X06	L	X06	X06	X06	
RI	Rhode Island	X06	X06		X06	X06		X06	X06	L06				
SC	South Carolina	X06	X03	X06	X06	X06		X06	X06	L06	L06	L06		
SD	South Dakota	X00	L	X00	X00	L	L	L	L	L	L	L	L	
TN	Tennessee	L	L	L	L	L		L	L	L	L	L	L	L
TX	Texas	X03	X00	L	L	L	L	L	X00	L	L	L	L	L
UT	Utah	X06	X06	X03	X06	X06		X06	X06					
VT	Vermont	X03	L03			X03			X04					
VA	Virginia	X06	X06	X06	X06	X06		X06	X06	X06	X06			
WA	Washington	X06	X06	X06	X06	X06		X06	L	L	L	L	L	
WV	West Virginia	X03	X03	X03	X03	X03		X03	X03	L00	X03	L		
WI	Wisconsin	X06		L	X06	X06		X06	X06	X06	X06			
WY	Wyoming	X	L	X	X	L	L	X	L	L	L	L		
TY	U.S. Territories													
PR	Puerto Rico					X								
VI	U.S. Virgin Islands	X03	X03		X03				X03					

X, effective statewide; A, adopted, but may not yet be effective; L, adopted by local governments; S, supplement; 06, 2006 edition; 04, 2004 edition; 03, 2003 edition; 00, 2000 edition.

TABLE 21.4
ICC Codes-Notes by State Presented in Table 21.3

ST	Jurisdiction	Chart Comments
AL	Alabama	IBC, IFC, IMC, IPC, IFGC—AL Building Commission: state-owned, schools, hotels, movie theaters
AZ	Arizona	AZ-Department of Health Services, health care institutions
CO	Colorado	IBC, IFC: Colorado Division of Fire Safety
CT	Connecticut	IFC: Portions used in the CT State Fire Code; ICC/ANSI A117.1
IL	Illinois	IECC: Commercial only; as modified by the 2001 Supplement; IBC, IFC, IMC, IFGC, IPMC, IECC: State Board of Education Facilities other than vehicular. Does not apply to Chicago; IBC: IL Department of Health
IN	Indiana	2006 building, fire, mechanical, and fuel gas codes went into effect 06/16/2008
IA	Iowa	IBC, IRC, IMC, IEBC, IECC: State-owned and rented structures
KS	Kansas	Applies to state-owned facilities
KY	Kentucky	IECC: Buildings other than 1&2 family regulated by the KRC
MD	Maryland	IPC: Industrialized housing. Other codes: edition shown may not be in use locally; check with local jurisdiction
MO	Missouri	State Office Space—03 IPC; Modular Construction—00 IBC, IRC, IMC, IPC, IFGC
NV	Nevada	IBC, IFC: SFM, schools, health care, state buildings, commercial buildings for counties over 100k. IBC, IRC, IFC, IECC, IEBC NV Public Works Board, state buildings
NM	New Mexico	NM Construction Industries Division; state-wide minimum code for all buildings
OH	Ohio	Residential Code is the 2003 IRC with amendments
OK	Oklahoma	IRC is 2003 but IMC, IPC, and IFGC portions of the IRC are 2006
SD	South Dakota	IBC, IFC: Approved for local adoption; IMC for state school construction
TN	Tennessee	IBC repealed re: SFM Rules 11/19/07
TX	Texas	Jurisdictions authorized by state law to adopt later editions of IBC, IRC, IPC, IMC, IFGC, and IECC

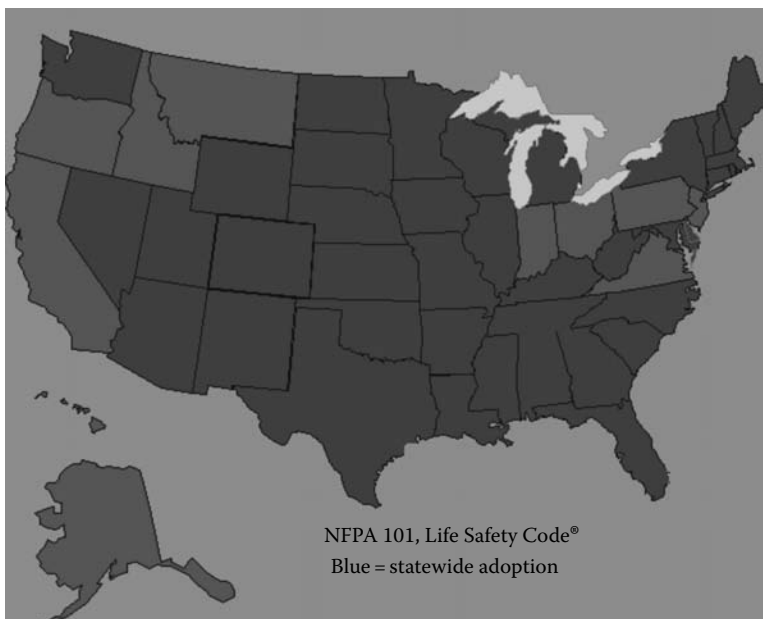


FIGURE 21.2 (See color insert following page 530.) Adoption of the life safety code in the United States—Early 2008.

In view of the concern that insufficient attention was being placed on the problem of transportation vehicle fire safety, the NFPA Fire Protection Research Foundation (FPRF) created, in late 2002, a Research Advisory Council on Fire and Transportation Vehicles, with Marcelo Hirschler as the Technical Coordinator. The Transportation Council addressed vehicle fire safety in five modes of transportation (road, rail, water, air, and underground fixed guideway) and investigated the requirements (or guidelines) in the areas of fire safety. The Transportation Council decided that, although there are some unique characteristics depending on the type of vehicle, all modes of transportation require adequate fire safety and have some commonality. It also decided that private cars (including, and perhaps especially, minivans and sports utility vehicles) represent the mode of transportation with the highest fire losses. The issues studied were: reaction-to-fire (furnishings and contents), fire resistance (structural fire protection), detection and suppression, egress, ignition sources (including wiring and arson), propulsion systems (fuels and fuel tanks), and ventilation. Although the Transportation Council focused primarily on the U.S. fire problem, it became apparent that: (a) most of the fire issues will be the same irrespective of where the vehicle operates and (b) many vehicles cross international borders continually, so that the fire problem is “exported” from one country to another. In some areas, this is already being addressed by the international organizations or by “de facto” arrangements, whereby a certain organization is known to develop rules that are followed by many (or most countries). Transportation Council research found fire safety regulation only for: trains traveling between cities and across state lines (FRA), ships (USCG), aircraft (FAA), and road vehicles (NHTSA). The only mandatory fire safety regulation for road vehicles is a requirement that materials within 13 mm of the passenger compartment have a flame spread rate of less than 11 mm/min when tested according to FMVSS 302,³² something that applies to cars, lorries or trucks, buses, and school buses (see also Section 21.2.5.4). Cars usually have to meet the same requirements throughout the world, although the standard called out has different designations (including ISO 3795 in Europe),³³ and the test is often not mandatory for cars (but only for road vehicles used to transport multiple passengers). A comprehensive white paper was published in 2004 by the FPRF council.³⁴

21.2.5.1 Aircraft

The FAA has developed a series of requirements for many of the materials and products contained in airplanes. Its regulations, contained in FA 25.853, cover four categories of aircraft: transport-category airplanes (Federal Aviation Regulation [FAR] Part 25), small airplanes (FAR Part 23), rotorcraft of all categories (FAR Parts 27 and 29), and engines and propellers (FAR Part 33 and 35). All the relevant fire tests are contained in the *Aircraft Materials Fire Test Handbook*,³⁵ for which periodic updates are issued. The FAA has also published a notice³⁶ that advises the public that the FAA considers the material flammability tests described in the latest version of that document to be the preferred acceptable test methods for showing compliance with the relevant regulations. The required test methods (nonpropulsion) are described in Chapters 1 through 10 and 15, and they are acceptable methods for showing compliance with, or provide an equivalent level of safety to, the required regulations as outlined in the chapter. Although these test methods cannot—and do not—supersede any method specified by and described in the regulations, they represent an acceptable means of compliance with the relevant regulation and, in some cases, a preferred option over the specified method. However, the FAA will consider other alternative methods that demonstrate an equivalent level of safety on a case-by-case basis, along with the necessary supportive data. Chapters 11 through 14 contain the required test methods (propulsion) and they remain as the name indicates. The test methods described in Chapters 18 through 22 are nonrequired test methods; they are included in the Handbook for use as test methods applications, where, currently, there are no requirements, and no process is required for their modification.

The principal fire tests in the Aircraft Materials Fire Test Handbook are the following:

1. Chapter 5: Heat release rate test. The test is based on the Ohio State University (OSU) rate of heat release (RHR) calorimeter³⁷, which has also been standardized as ASTM E 906³⁸ (see also Section 4.1.1). The test exposes a vertical test specimen ca. 150 mm × 150 mm (6 in. × 6 in.) to an incident radiant heat flux of 35 kW/m² from four horizontal glow bars for 5 min, in the presence of an open-flame pilot burner. The test applies to the vast majority of nonmetallic materials contained inside the aircraft, typically vertical panels (which are often laminated and have multiple layers), ceiling and wall linings, luggage compartment racks, carts, and so on. It does not cover foams and fabrics for seats and draperies, windows, floor coverings (carpets), electrical wiring, insulation, or firewalls. The acceptance criteria are an average maximum heat release rate during the 5 min test that does not exceed 65 kW/m² and an average total heat released during the first 2 min of the test that does not exceed 65 kW min/m².
2. Chapter 6: Smoke test. The test is based on the National Bureau of Standards (NBS, now NIST, National Institute of Standards and Technology) smoke density chamber, which has also been standardized as ASTM E 662³⁹ (see also Section 4.1.1). The test exposes a vertical test specimen ca. 75 mm × 75 mm (3 in. × 3 in.) to an incident radiant heat flux of 25 kW/m², from a radiant heat burner for 4 min, in the presence of an open-flame pilot burner. The test applies to the same materials as the heat release rate test. The acceptance criterion is an average maximum specific optical density of smoke that does not exceed 200 (no units).
3. Chapter 7: Oil burner test for seat cushions. The test exposes a seat cushion to an oil burner (kerosene or fuel oil) at a rate of 126 mL/min (2 gal/h) gas flow for 2 min. The acceptance criteria are: a burn length not exceeding 432 mm (17 in.) and a weight loss not exceeding 10%.
4. Chapters 1 through 3: Bunsen burner tests for miscellaneous materials. The tests are all conducted in cabinets and they include vertical test (Chapter 1: 12 or 60 s), horizontal test (Chapter 2: 30 s), and 45° angle test (Chapter 3: 15 s). These tests apply mostly to materials and products in smaller noncommercial aircraft.
5. Chapter 4: 60° angle Bunsen burner test for electric wire insulation. The test is also conducted in a cabinet and the flame is applied for 30 s. Manufacturers of commercial aircraft tend to require higher fire performance than that which this test provides, but many of the electrical services incorporated into the aircraft by the airlines use this test.
6. Chapter 18: Horizontal Bunsen burner test for blankets. This is similar to the test in Chapter 2, but is applied for 12 s.
7. Chapter 23: Ignitability test for thermal/acoustic insulation. This test is based on the flooring radiant panel test for carpets and other floor coverings, which has also been standardized as ASTM E 648⁴⁰ (see also Section 21.4.1.1). The test exposes a bag of insulation material to a radiant panel at an angle of 30°, so that the incident radiant heat gradually decreases further away, and is measured from the exposure point. The test assesses whether the bag of insulation ignites and spreads the flame for ca. 50 mm (2 in.).
8. Chapter 24: Burn through test for thermal/acoustic insulation blankets used in the fuselage. This test uses the same type of oil burner as the one for seat cushions (Chapter 7), but the fuel flow rate is 378 mL/min (6 gal/h) of gas flow for 4 min. The acceptance criteria are: no flame penetration through the insulation blanket and a heat released by the insulation not exceeding 22.7 kW/m².

The requirements were obtained as a result of full-scale aircraft tests conducted by the FAA and by airframe manufacturers, which showed the key importance of heat release criteria for proper fire safety. The criteria were based on the concept of ensuring that, in a survivable postcrash scenario,

aircraft evacuation can be completed in 5 min. Moreover, fires should not happen or self-extinguish in hidden areas. The FAA was asked by the aircraft industry to add the smoke obscuration test, because that had been a test required by the manufacturers in the past. The FAA does not have any regulatory smoke toxicity or material composition tests (because the research conducted showed that they were not needed), but some aircraft manufacturers and airlines do have such requirements.

21.2.5.2 Ships

The USCG regulates all ships that moor in the U.S. ports (both on the exterior coasts and on rivers or lakes). The United States is a signatory to the International Convention for the Safety of Life at Sea (SOLAS)⁴¹ and the USCG will enforce the corresponding regulations, which are issued by the International Maritime Organization (IMO)⁴².

All ships that engage in the international trade and fly the flag of a country that has signed the SOLAS convention must comply with the regulations of IMO, detailed in the SOLAS book, periodically amended by “Resolutions” of the IMO committees, and ratification by the signatory states. Details of the fire issues are given in the IMO Fire Test Procedures Code (FTP),⁴³ which is also reissued regularly. Some special vessels are regulated separately: high-speed craft that is never too far from shore is regulated by the IMO High Speed Craft Code (HSC).⁴⁴ The HSC code applies to small vessels, within certain parameters, which operate at a minimum specified high speed and carry a maximum number of passengers and make no overnight trips. However, in the United States, many ships never leave the inland waters, or simply hug coastal areas and often choose not to be covered by SOLAS. The USCG regulates all ships that use the U.S. ports and enforces SOLAS or HSC requirements for those ships that need to meet those rules. All ships that sail in the U.S. waters must comply with the requirements specified by the USCG, laid out by the U.S. Federal Government—Coast Guard: Title 46, Shipping, Code of Federal Regulations, Parts 1–199,⁴⁵ and in a NVIC (USCG Guide to Structural Fire Protection).⁴⁶ The Coast Guard is also the AHJ over ships engaging in international trade and sailing into the U.S. waters or U.S. ports; such ships must comply with IMO regulations and need not comply with separate Coast Guard requirements. With the instructions from the U.S. Federal Government that standards should, whenever possible, be delegated to private organizations, the Coast Guard and NFPA agreed to develop a consensus code, NFPA 301, Code for Safety to Life from Fire on Merchant Vessels,⁴⁷ for ships that do not sail in the international waters. NFPA 301 references both SOLAS and HSC for the corresponding types of ships. The USCG has a policy of permitting ships to comply with NFPA 301 instead of its requirements, but this code is rarely used, because it contains very onerous sprinkler requirements that exceed those of the USCG.

The IMO regulations, via the FTP code, cover reaction-to-fire requirements for: cables (electric wires and cables), carpeting (floor coverings), deck coverings, fabrics, interior finish, mattresses and bedding, piping, and upholstered furniture. They also cover fire-resistance requirements for bulkheads, dampers, doors, windows, and other divisions. The fire resistance requirements are based on testing to the time–temperature curve in ISO 834,⁴⁸ instead of the one used in the United States, from ASTM E 119.⁴⁹ Although the differences are of minor relevance technically, they do mean that testing must be accomplished with the correct standard. The fire-safety philosophy used by SOLAS for materials and products in ships is the limitation on the amounts of combustible materials, while trying to build the ships as much as possible out of noncombustible materials (often stated as “steel or equivalent”). The HSC code has deviated considerably from this concept by developing heat release and smoke release criteria for “fire restrictive materials,” which are combustible but have excellent fire performance, as assessed by a very severe room-corner heat release fire test, ISO 9705.⁵⁰ The rationale for this change in philosophy has been the fact that composites and other materials with excellent fire performance are much lighter than steel and can permit the ships to travel much faster.

The USCG regulations include reaction-to-fire requirements for the same products as the FTP code, but the tests required tend to be more realistic or severe. In particular, upholstered furniture and mattresses need to meet open-flame tests and not just smoldering tests, for example. Smaller

boats are usually intended to comply with NFPA 302, Fire Protection Standard for Pleasure and Commercial Motor Craft,⁵¹ but are not actually regulated.

Finally, the U.S. Navy also has its own set of requirements for military ships and submarines. It has, for some time now, been pursuing a similar type of approach to the HSC code approach.⁵² In this case, there is an additional advantage in moving away from the steel products: the alternative materials are much less detectable by the enemy radar.

NFPA 301 has much more restrictive reaction-to-fire test requirements for furnishings and contents than SOLAS. However, its latest edition (dated 2008) permits the omission of many, if not most, of the reaction-to-fire requirements if the vessel is sprinklered or has a water-mist system installed. This means that the requirements can be omitted for passenger ships, as all Group I passenger vessels (i.e., those with either over 3000-day passengers or over 300-overnight passengers) and Group II passenger vessels (i.e., those with either over 1000- and under 3000-day passengers or over 150- and under 300-overnight passengers) and all passenger vessels with overnight accommodations for passengers must have a sprinkler or water-mist system, to protect “all accommodation, service, and storage spaces.” This makes the reaction-to-fire requirements for passenger ships mostly optional.

21.2.5.3 Trains and Underground Rail Vehicles

As a result of the 1973 Urban Mass Transportation Administration (UMTA) program to improve fire safety of public transport, “Guidelines for Flammability and Smoke Emission Specifications” for materials used in transportation vehicles were generated. Although these guidelines have developed somewhat over the years, they are still based on the fire-testing technology available in the 1970s, but the FRA has made them mandatory regulations for trains connecting cities or crossing state lines,^{53,54} while the FTA still uses them as guidelines for urban trains (including underground fixed guideway vehicles) and buses. Table 21.5 shows the most recent FRA rulemaking to that effect. The table is the basis of the regulations for reaction-to-fire of materials and products. The two principle fire tests used are a radiant panel test for flame spread (ASTM E 162)⁵⁵ and a static smoke obscuration test (ASTM E 662). The table contains detailed instructions and pass/fail criteria for all types of materials and products in trains (except for wire and cable products, which were eliminated between the 1999 and 2002 editions). These rules have ensured that the seating materials used no longer lead to dramatic fires, but some of the tests are less than fully adequate, so that their results may have random ability to predict real fire behavior.⁵⁶ FRA has realized that heat release rate is particularly critical as it is the single property that indicates the intensity of the fire, and controls whether a fire in a particular product will become large enough to ignite the next item. In fact, it has been shown that the heat release rate is much more important than smoke toxicity or ignitability in determining the time remaining for occupants to escape. In view of this, FRA now permits approvals to be based on the use of alternative approaches to the prescriptive table, using heat release for hazard assessment. Both ASTM and NFPA have developed standard documents that address the way to do this: ASTM E 2061⁵⁷ and NFPA 130; a review of these standards has been published recently.⁵⁸ Both considered the reaction-to-fire properties of wire and cable products as critical, and the use of these documents is prevalent whenever a specifier (usually a local transportation authority) wants to exceed FRA regulations or is not bound by them (e.g., outside the United States). ASTM E 2061 is a guide on how to assess fire hazard in rail transportation vehicles, which gives detailed instructions, and can be followed in two ways: by complying with a version of “the table” or by analyzing the fire hazard of the rail car with modern fire modeling technology. NFPA 130 is a standard with broader applicability, because it includes the entire rail system, and also has both a version of “the table” and a section on a performance-based approach. Table 21.6 contains the rail vehicle materials requirements from NFPA 130-2007. This standard also requires that all cables meet the flame-spread (with a vertical cable tray test, UL 1581-1160,⁵⁹ being the minimum acceptable) and smoke-obscuration criteria. The standard requires all wires and cables to meet one of the acceptable NEC cable tests (except for the small-scale vertical wire or VW-1 test),⁶⁰ namely UL 1581-1160 (UL test), UL 1581-1164 (CSA test,⁶¹ equivalent to CSA FT4⁶² and to IEEE 1202⁶³), UL 1666 (riser),⁶⁴ or NFPA 262 (plenum).⁶⁵

TABLE 21.5
FRA Requirements for Passenger Rail Materials (2002)

Category	Function of Material	Flammability		Smoke Emission	
		Test Procedure	Performance Criteria	Test Procedure	Performance Criteria
Cushions, mattresses	All ^{a-h}	ASTM D 3675	Is ≤ 25	ASTM E 662	D _s (1.5) ≤ 100 D _s (4.0) ≤ 175
Fabrics	Seat upholstery, mattress ticking and covers, curtains, draperies, wall coverings, and window shades ^{a-c,f,h}	14 CFR 25 Appendix F, Part I (vertical test)	Flame time ≤ 10 s; burn length ≤ 6 in.	ASTM E 662	D _s (4.0) ≤ 200
Other vehicle components ^{a-i}	Seat and mattress frames, wall and ceiling panels, seat and toilet shrouds, tray and other tables, partitions, shelves, opaque windscreens, end caps, roof housings, and component boxes and covers ^{ab} Flexible cellular foams used in armrests and seat padding ^{a,b,d,f}	ASTM E 162	Is ≤ 35	ASTM E 662	D _s (1.5) ≤ 100 D _s (4.0) ≤ 200
	Thermal and acoustic insulation ^{a,b}	ASTM D 3675	Is ≤ 25	ASTM E 662	D _s (1.5) ≤ 100 D _s (4.0) ≤ 175
	HVAC ducting ^{a,b}	ASTM E 162	Is ≤ 25	ASTM E 662	D _s (4.0) ≤ 100
	Floor covering ^{a,m}	ASTM E 162 ASTM E 648	Is ≤ 25 CRF ≥ 5 kW/m ²	ASTM E 662	D _s (4.0) ≤ 100 D _s (1.5) ≤ 100
	Light diffusers, windows and transparent plastic windscreens ^{bn}	ASTM E 162	Is ≤ 100	ASTM E 662	D _s (4.0) ≤ 200 D _s (1.5) ≤ 100
Elastomers ^{a,j,k}	Window gaskets, door nosings, intercar diaphragms, roof mats, and seat springs	ASTM C 1166	Average flame propagation ≤ 4 in.	ASTM E 662	D _s (4.0) ≤ 200 D _s (1.5) ≤ 100
Structural components ^o	Flooring ^p , other ^r	ASTM E 119	Pass	ASTM E 662	D _s (4.0) ≤ 200

^a Materials tested for surface flammability shall not exhibit any flaming running or dripping.
^b The ASTM E 662 maximum test limits for smoke emission (specific optical density) shall be measured in either the flaming or nonflaming mode, utilizing the mode that generates the most smoke.
^c Testing of a complete seat assembly (including cushions, fabric layers, upholstery) according to ASTM E 1537 using the pass/fail criteria of Cal TB 133, and testing of a complete mattress assembly (including foam and ticking) according to ASTM E 1590 using the pass/fail criteria of Cal TB 129 shall be permitted in lieu of the test methods prescribed herein, provided the assembly component units remain unchanged or new (replacement) assembly components possess equivalent fire performance properties to the original components tested. A fire-hazard analysis must also be conducted which considers the operating environment within which the seat or mattress assembly will be used in relation to the risk of vandalism, puncture, cutting, or other acts which may expose the individual components of the assemblies to an ignition source. Footnotes e, f, g, and h apply.

- ^d Testing is performed without upholstery.
- ^e The surface flammability and smoke-emission characteristics shall be demonstrated to be permanent after dynamic testing according to ASTM D 3574, Test I2 (Dynamic Fatigue Test by the Roller Shear at Constant Force) or Test I3 (Dynamic Fatigue Test by Constant Force Pounding) both using Procedure B, except that the test samples shall be a minimum of 6 in. (154 mm) by 18 in. (457 mm) by the thickness of the material in its end-use configuration or multiples thereof. If Test I3 is used, the size of the indenter described in Paragraph 96.2 shall be modified to accommodate the specified test specimen.
- ^f The surface flammability and smoke-emission characteristics shall be demonstrated to be permanent by washing, if appropriate, according to FED-STD-191A Textile Test Method 5830.
- ^g The surface flammability and smoke-emission characteristics shall be demonstrated to be permanent by dry-cleaning, if appropriate, according to ASTM D 2724.
- ^h Materials that cannot be washed or dry-cleaned shall be so labeled and shall meet the applicable performance criteria after being cleaned as recommended by the manufacturer.
- ⁱ Signage is not required to meet any flammability or smoke-emission performance criteria specified in this Appendix.
- ^j Materials used to fabricate miscellaneous, discontinuous small parts (such as knobs, rollers, fasteners, clips, grommets, and small electrical parts) that will not contribute materially to fire growth in end-use configuration are exempt from flammability and smoke emission performance requirements, provided that the surface area of any individual small part is less than 16 in.² (100 cm²) in end-use configuration and an appropriate fire hazard analysis is conducted which addresses the location and quantity of the materials used, and the vulnerability of the materials to ignition and contribution to flame spread.
- ^k If the surface area of any individual small part is less than 16 in.² (100 cm²) in end-use configuration, materials used to fabricate such a part may be tested in accordance with ASTM E 1354 as an alternative to both (a) the ASTM E 162 flammability test procedure, or the appropriate flammability test procedure otherwise specified in the table, and (b) the ASTM E 662 smoke generation test procedure. Testing shall be at 50 kW/m² applied heat flux with a retainer frame. Materials tested in accordance with ASTM E 1354 shall meet the following performance criteria: average heat release rate (\dot{q} = 180) less than or equal to 100 kW/m², and average specific extinction area (σ_s) less than or equal to 500 m²/kg over the same 180-s period.
- ^l Carpeting used as a wall or ceiling covering shall be tested according to ASTM E 162 and ASTM E 662 and meet the respective criteria of I_s less than or equal to 35 and D_s (1.5) less than or equal to 100, and D_s (4.0) less than or equal to 200. Footnotes a and b apply.
- ^m Floor covering shall be tested with padding in accordance with ASTM E 648, if the padding is used in the actual installation.
- ⁿ For double window glazing, only the interior glazing is required to meet the requirements specified herein. (The exterior glazing is not required to meet these requirements.)
- ^o Penetrations (ducts, etc.) shall be designed against acting as passageways for fire and smoke, and representative penetrations shall be included as part of test assemblies.
- ^p A structural flooring assembly separating the interior of a vehicle from its undercarriage shall meet the performance criteria during a nominal test period as determined by the railroad. The nominal test period must be twice the maximum expected time period under normal circumstances for a vehicle to stop completely and safely from its maximum operating speed, plus the time necessary to evacuate all the vehicle's occupants to a safe area. The nominal test period must not be less than 15 min. Only one specimen need be tested. A proportional reduction may be made in the dimensions of the specimen, provided it serves to truly test the ability of the structural flooring assembly to perform as a barrier against under-vehicle fires. The fire resistance period required shall be consistent with the safe evacuation of a full load of passengers from the vehicle under worst-case conditions.
- ^q Portions of the vehicle body which separate major ignition sources, energy sources, or sources of fuel-load from vehicle interiors, shall have sufficient fire endurance as determined by a fire-hazard analysis acceptable to the railroad which addresses the location and quantity of the materials used, as well as the vulnerability of the materials to ignition, flame spread, and smoke generation. These portions include equipment-carrying portions of a vehicle's roof and the interior structure separating the levels of a bi-level car, but do not include a flooring assembly subject to Footnote p. A railroad is not required to use the ASTM E 119 test method.

TABLE 21.6
NFPA 130-2007 Requirements for Passenger Vehicle Rail Materials

Category	Function of Material	Flammability		Smoke Emission	
		Test Procedure	Performance Criteria	Test Procedure	Performance Criteria
Cushioning	All individual flexible cushioning materials used in seat cushions, mattresses, mattress pads, armrests, crash pads, and grab rail padding ^{g-e}	ASTM D 3675	Is ≤ 25	ASTM E 662	D _s (1.5) ≤ 100 D _s (4.0) ≤ 175
Fabrics	Seat upholstery, mattress ticking and covers, curtains, draperies, window shades, and woven seat cushion suspensions ^{g-e,f-h}	14 CFR 25 Appendix F, Part I (vertical test)	Flame time ≤ 10 s; Burn length ≤ 6 in.	ASTM E 662	D _s (4.0) ≤ 200
Other vehicle components	Seat and mattress frames, wall and ceiling lining and panels, seat and toilet shrouds, toilet seats, trays and other tables, partitions, shelves, opaque windcreens, combustible signage, end caps, roof housings, articulation bellows, exterior shells, nonmetallic skirts, and component boxes and covers ^{ab,j-k}	ASTM E 162	Is ≤ 35	ASTM E 662	D _s (1.5) ≤ 100 D _s (4.0) ≤ 200
	Thermal and acoustical insulation ^{ab}	ASTM E 162	Is ≤ 25	ASTM E 662	D _s (4.0) ≤ 100
	HVAC ducting ^{ab}	ASTM E 162	Is ≤ 25	ASTM E 662	D _s (4.0) ≤ 100
	Floor covering ^{bl}	ASTM E 648	CRF ≥ 5 kW/m ²	ASTM E 662	D _s (1.5) ≤ 100 D _s (4.0) ≤ 200
	Light diffusers, windows and transparent plastic windcreens ^{bi}	ASTM E 162	Is ≤ 100	ASTM E 662	D _s (1.5) ≤ 100 D _s (4.0) ≤ 200
Elastomers ^{aj}	Window gaskets, door nosings, intercar diaphragms, seat cushion suspension diaphragms, and roof mats	ASTM C 1166	Pass (15)	ASTM E 662	D _s (1.5) ≤ 100 D _s (4.0) ≤ 200
Structural components ^m	Flooring ⁿ , other ^o	ASTM E 119	Pass		D _s (4.0) ≤ 200

Requirements not included by FRA—see description following notes

^a Materials tested for surface flammability shall not exhibit any flaming running or dripping.

^b The ASTM E 662 maximum test limits for smoke emission (specific optical density) shall be based on both the flaming and nonflaming modes.

^c Testing of a complete seat assembly (including cushions, fabric layers, upholstery) according to ASTM E 1537 using the pass/fail criteria of Cal TB 133, and testing of a complete mattress assembly (including foam and ticking) according to ASTM E 1590 using the pass/fail criteria of Cal TB 129 shall be permitted in lieu of the test methods prescribed herein, provided the assembly component units remain unchanged or new (replacement) assembly components possess equivalent fire performance properties to the original components tested. A fire-hazard

analysis shall also be conducted that considers the operating environment within which the seat or mattress assembly will be used in relation to the risk of vandalism, puncture, cutting, or other acts which may expose the individual components of the assemblies to an ignition source. The requirements of footnotes e, f, g, and h shall be met.

- d Testing shall be performed without upholstery.
- e The surface flammability and smoke-emission characteristics shall be demonstrated to be permanent after dynamic testing according to ASTM D 3574, Test 12 or Test 13, both using Procedure B, except that the test samples shall be a minimum of 150mm (6 in.) \times 450mm (18 in.) \times the thickness used in end-use configuration, or multiples thereof. If Test 13 is used, the size of the indenter described in Section 96.2 of ASTM D 3574 shall be modified to accommodate the specified test specimen.
- f The surface flammability and smoke-emission characteristics shall be demonstrated to be permanent by washing, if appropriate.
- g The surface flammability and smoke-emission characteristics shall be demonstrated to be permanent by dry-cleaning, if appropriate, according to ASTM D 2724.
- h Materials that cannot be washed or dry-cleaned shall be so labeled and shall meet the applicable performance criteria after being cleaned as recommended by the manufacturer.
- i Combustible operational and safety signage shall not be required to meet flame spread or smoke-emission requirements, if the combustible mass of a single sign does not exceed 500g (1.1 lb) and the aggregate area of combustible signage does not exceed one square foot per foot of car length.
- j Materials used to fabricate miscellaneous, discontinuous small parts (such as knobs, rollers, fasteners, clips, grommets, and small electrical parts) that will not contribute materially to fire growth in end-use configuration are exempt from flammability and smoke-emission performance requirements, provided that the surface area of any individual small part is less than 100cm² (16in.²) in end-use configuration, and an appropriate fire-hazard analysis is conducted that addresses the location and quantity of the materials used and the vulnerability of the materials to ignition and contribution to flame spread.
- k Carpeting used as a wall or ceiling covering shall be tested according to ASTM E 162 and ASTM E 662 and shall meet the respective criteria of I_s less than or equal to 35, D_s (1.5) less than or equal to 100, and D_s (4.0) less than or equal to 200 (see footnotes a and b).
- l Floor covering shall be tested with padding in accordance with ASTM E 648, if the padding is used in the actual installation.
- m Penetrations (ducts, etc.) shall be designed against acting as passageways for fire and smoke, and representative penetrations of each type shall be included as a part of the test assemblies. Fire-resistance testing on assemblies shall be conducted in general accordance with ASTM E 119. See corresponding section in NFPA 130.
- n See section on ASTM E 119 testing in NFPA 130.
- o Portions of the vehicle body that separate the major ignition source, energy sources, or sources of fuel load from vehicle interiors shall have fire resistance as determined by a fire-hazard analysis, acceptable to the AHJ, that addresses the location and quantity of the materials used, as well as vulnerability of the materials to ignition, flame spread, and smoke generation. These portions include equipment-carrying portions of a vehicle's roof and the interior structure separating the levels of a bi-level car, but do not include a flooring assembly subject to the NFPA 130 section on fire resistance testing. In those cases, the use of the ASTM E 119 test procedure shall not be required.
- p Wires and cables are permitted if they have been listed by any of the following methods:
1. Tray cable, listed via UL 1581-1160 (UL tray), plus low specific optical density of smoke via ASTM E 662 (specific optical density of smoke at 4-min into the test that does not exceed 200 in the flaming mode and 75 in the nonflaming mode).
 2. Tray test, listed via UL 1581-1164 (CSA tray), plus CSA ST1 low smoke.
 3. Tray cable, listed via UL 1685, with limited smoke.
 4. Riser cable, listed via UL 1666, plus low specific optical density of smoke via ASTM E 662 specific optical density of smoke at 4 min into the test that does not exceed 200 in the flaming mode and 75 in the nonflaming mode).
 5. Plenum cable, listed via NFPA 262.
- Wires and cables used for fire-alarm systems and smoke alarms must comply with the above and one of the following:
1. Be capable of having 15 min circuit integrity when tested in accordance with IEC 60331-11.
 2. Demonstrate that, if circuit integrity is tested during the vertical flame test, a current continues operating for at least 5 min during the test.
 3. Have fire-alarm circuit integrity cable in accordance with NFPA 70.

21.2.5.4 Motor Vehicles

The statistics of fire losses show that over two-thirds of all fires in vehicles occur in road vehicles, and over 95% of those occur in automobiles (a category that includes, of course, the popular private minivans and sports utility vehicles).²⁹ Moreover, the very mild fire safety requirements for cars, namely FMVSS 302,³² were set by NHTSA in 1969 to address the problem of people discarding lit cigarettes in cars. This means that the requirements have not changed in some 40 years, when there were many fewer than the current 130 million cars in the United States, and when cars had much more steel and much less plastic. The increased use of plastics has made cars much more fuel-efficient (lower weight) and allowed more flexibility in design and esthetics, but at the expense of increasing the potential for fire losses. Significant amount of recent work has highlighted some critical fire-safety deficiencies of the materials used in this area.^{66–69} In particular, such work showed problems in terms of the reaction-to-fire properties of automobile materials (from the passenger and engine compartments) in private cars (many of which are highly combustible and have poor fire performance) and in terms of the fire resistance properties of the so-called barrier materials used. For example, real-scale tests on actual cars showed that small fires in the engine compartment (not even involving liquid fuels) would penetrate into the passenger compartment through the “engine cover” in less than 2 min, and that the “engine cover” would actually burn at low heat fluxes, and not offer any type of real barrier.⁶⁷ Figure 21.3 shows the temperature reached in the front and rear seats, headliner, duct, vent, and carpet following ignition with a small ignition source in the engine compartment: temperatures exceeding 700°C were reached quickly in all cases.⁶⁷ It was also shown that materials used for the headliner, the foam padding and especially, the duct, were of particularly poor fire performance, with high heat release rates. Furthermore, the NHTSA website contains extensive information on research conducted on fire safety of private cars as a result of the agreement between the U.S. Federal Government and General Motors.⁷⁰ NHTSA has recognized that there is a serious fire-safety problem and has undertaken research programs, in conjunction with Southwest Research Institute, to investigate alternative tests for material regulation, probably the

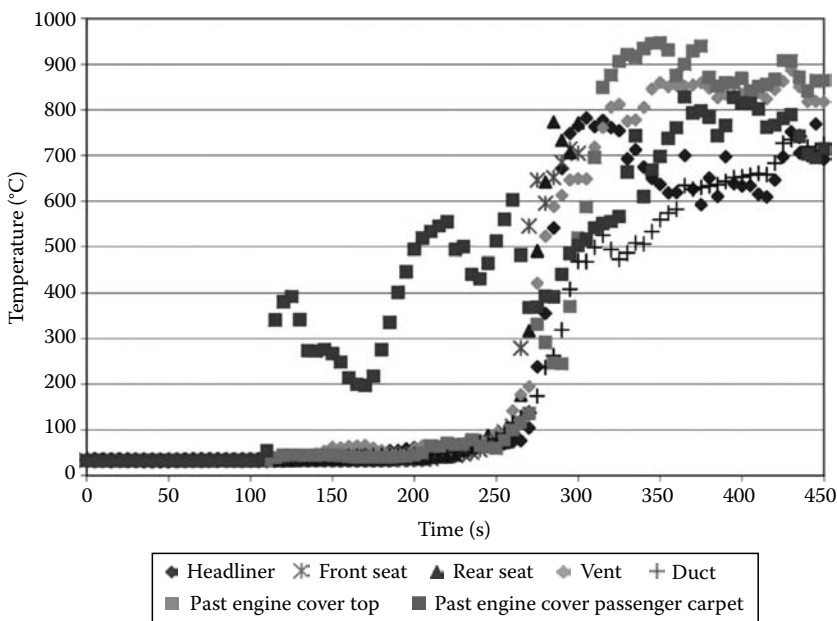


FIGURE 21.3 (See color insert following page 530.) Temperatures in tests of real vans. (From Hirschler, M.M. et al., Fire hazard associated with passenger cars and vans, *Fire and Materials Conference*, San Francisco, CA, January 27–28, Interscience Communications, London, U.K., 2003, 307–319.)

cone calorimeter (ASTM E 1354),⁷¹ a source of heat release information. However, no regulatory action ensued and none appeared to be imminent.

One of the NFPA technical committees, entitled “Hazard and Risk of Contents and Furnishings,” is responsible for providing guidance to other NFPA technical committees on areas associated with fire hazard and fire risk of contents and furnishings. In 1996, the committee developed NFPA 555, “Guide on Methods for Evaluating Potential for Room Flashover.” Separately, the committee is also working on the development of a document for vehicles (especially highway vehicles) intended to be parallel to NFPA 555, which would focus on ways to lower fire hazard for occupants of such vehicles. The document has been assigned to the Annual 2010 cycle, after the committee has addressed the input from the automotive industry and other public sources. The latest draft of NFPA 556 is entitled “Guide on Methods for Evaluating Fire Hazard to Occupants of Passenger Road Vehicles.” It consists of various chapters, including administrative ones. The key concept is that the guide would include a discussion on the types of vehicles, a general description of passenger road vehicle fires and background information, an approach to evaluating vehicle fire hazard, how to develop objectives and design criteria for vehicle designs and an investigation of individual typical fire scenarios, evaluation methods and tools (including test methods and fire models), and further guidance. This will include recommended types of mitigation strategies, such as decreasing the ignition propensity of materials, decreasing heat release of materials, and designing improvements in vehicle engineering, while ensuring that the changes do not affect the vehicle safety or performance in terms of issues other than fire. In terms of fire properties, clearly, it is principally important to reduce ignitability, heat release, and the potential for flame spread, which is why the test most widely considered for assessing the materials’ and products’ fire properties is the cone calorimeter, ASTM E 1354. The document is likely to recommend the use of tests based on heat release, at various levels: full-scale, fuel package scale, and individual material scale, so as to obtain data that are quantitative enough for fire-hazard assessment. Guidance stresses the performance-based approach and contrasts it with the continued use of FMVSS 302 as the sole fire safety tool, as the exclusive use of FMVSS 302 is unlikely to be consistent with significant decreases in fire losses associated with road vehicles. Particularly, with the growing use of combustible materials in road vehicles, a mild ignition test such as FMVSS 302 is clearly insufficiently severe to ensure that materials meeting it would provide passengers and drivers with enough time to escape in the case of a fire. It is important to recognize that, although full-scale tests are the most accurate way of understanding both deficiencies in road vehicle fire safety and to develop mitigation strategies, their high cost means that other strategies should also be used. For example, testing of sections, such as individual road vehicle compartments or fuel packages in a furniture calorimeter (i.e., under a hood, above a load cell), will allow an understanding of the interactions between the materials and products contained in the various sections of the road vehicle. Testing the fire properties of materials or products searching for an individual fire property should always be accompanied by an overall analysis that indicates that a resulting improvement, or apparent improvement, in the fire property assessed will be accompanied by an actual improvement in fire safety in the road vehicle. Battipaglia et al.⁷² used the ASTM fire-hazard assessment framework for assessing the fire hazard of automotive materials in the engine compartment of a passenger road vehicle following a collision. It is to be expected that NHTSA will consider work such as this and NFPA 556 (if and when it is issued), to develop considerations for highway vehicle fire safety that is adequately predictive of real-scale fire performance.

Note that the ASTM committee on plastics (ASTM D20) has developed a standard, ASTM D 5132,⁷³ which is a consensus standard version of the FMVSS 302 requirement. The development of such consensus standards resembling regulation is not uncommon; the consensus standard cannot be used for approval of a material or product, but is often easier for a lab to follow and can be helpful for incorporating improvements, even if they cannot be recognized by the AHJ. In other words, such standards are basically intended for use by regulatory authorities outside the United States, by AHJs, or codes that go beyond federal regulations. Of course, this is important principally when the test is of use for improving fire safety.

21.2.5.5 School Buses

The AHJ is NHTSA and the fire-safety requirements are included, together with all other NHTSA vehicle safety requirements in FMVSS 301⁷⁴ and FMVSS 302.³² FMVSS 301 deals with the structural integrity of the school bus and with the needed exits.

With regard to FMVSS 302, the same concerns expressed earlier about the validity of the fire tests on materials included in FMVSS 302 have also been expressed by the NIST about school buses.⁷⁵ In fact, the report showed that school bus seat materials complying with FMVSS 302 would easily cause flashover on the bus with a small ignition source. In the case of school buses, the report was the result of an investigation on a horrific school bus accident. May 14, 2008 marked the 20-year anniversary of the worst drunk driving crash in the U.S. history, the Carrollton KY school bus fire. Drunk driver, Larry Mahoney, was northbound in the southbound lanes of Highway I-71 when he hit a school bus carrying 67 people. The bus caught fire trapping and killing 27 people, 24 of them children, and injuring 34 others.

Fortunately, for school children, in spite of the inactivity of the federal government, local education authorities in many U.S. states and Canadian provinces have decided to adopt a very simplistic but effective fire test, namely the National Safety Council Standard “School bus seat upholstery fire block test,” which was approved by the National Conference on School Transportation as part of the National Standards for School Buses and National Standards for School Bus Operations.⁷⁶ The test involves putting a few sheets of newspaper in a paper bag, placing the bag on a school bus seat and igniting it with a match. If the seat is made of adequate materials, most of it will not burn and if the materials are unsafe, the seat padding and cover will be completely destroyed. Unfortunately, this test has not been adopted by all the local education authorities and it is being applied in different ways. The ASTM subcommittee E05.17, on fire safety and transportation, is working on the development of a paper bag seat test method based on the National Safety Council Standard.

21.2.5.6 Cigarettes

A key new development throughout North America is the requirements for cigarettes to comply with ASTM E 2187,²² so that they are less likely to cause ignition of upholstery fabrics. These cigarettes are often designated as “fire-safe cigarettes,” an incorrect designation, as they are still capable of igniting cellulosic fabrics, in some 25% of the cases. The test assesses whether a cigarette is capable of igniting filter paper, by burning past a certain mark, with multiple replicates. A cigarette complies with the regulation if it does not cause ignition more than 25% of the time. This level of ignition power represents a dramatic decrease when compared with “normal” cigarettes, which ignite almost all cellulosic fabrics, unless the fabric has been specially treated. The cigarettes should more properly be designated as reduced ignition propensity cigarettes.

The key factor in determining smoldering combustion of cigarettes is their paper. The paper-modification approach most commonly used for manufacturing reduced ignition propensity cigarettes is the use of “banded” paper. This is roughly equivalent to increasing the weight of the paper or decreasing its porosity, but instead of changing these properties across the entire length of the cigarette, the paper is designed to have intermittent bands with altered properties. The intent is for the cigarette to self-extinguish when the ignited end hits a band and the cigarette is not being smoked, but to retain its normal smoking properties when it is not burning through a band.

On October 1, 2005, Canada became the first country to adopt the requirement for reduced ignition propensity cigarettes nationwide. In the United States, as of August 1, 2008, reduced ignition propensity cigarettes were adopted in 16 states: Alaska, California, Connecticut, Illinois, Kentucky, Maine, Maryland, Massachusetts, Montana, New Hampshire, New Jersey, New York, Oregon, Rhode Island, Utah, and Vermont. The following 20 states have effective dates for the legislation between 2008 and 2010: Arizona, Colorado, Delaware, Florida, Georgia, Hawaii, Idaho, Indiana, Iowa, Kansas, Louisiana, Minnesota, North Carolina, Oklahoma, Pennsylvania, Tennessee, Texas, Virginia, Washington, and Wisconsin. Laws passed in the following states in 2008: Arizona, Colorado, Florida, Georgia, Hawaii, Idaho, Indiana, Kansas, Oklahoma, Tennessee, Virginia,

Washington, and Wisconsin, as well as Washington, D.C. This indicates that 36 states (with over 80% of the U.S. population) have passed legislation requiring that cigarettes sold there be fire-safe. Several other states are currently considering the legislation. Seven states have bills under discussion at the state assembly or senate level (Alabama, Michigan, Mississippi, Missouri, Nebraska, Ohio, and West Virginia) and only a few states are yet to file any legislation.

Besides North America, “reduced ignition propensity cigarette” regulation has been in effect in Australia and is on its way in the EU. On August 5, 2008, the EC announced that all cigarettes sold throughout the EU should be self-extinguishing “fire-safe” brands within the next 3 years. It has been reported that Switzerland, not a member of the EU, may follow the suit. In 2007, the 27 EU member states approved a commission proposal that would require the tobacco industry to manufacture cigarettes with special paper that will cause a cigarette to self-extinguish after 60 s, if left unattended. Data from 14 EU member states (along with Iceland and Norway) show that cigarette-related fires account for some 11,000 fires each year, with 520 deaths and 1600 injuries; the elderly are disproportionately affected.

Requirements for the sale of reduced ignition propensity cigarettes indicate that the probability of cigarette (smoldering) ignition of upholstery fabrics is decreased, even if the upholstery fabrics do not “pass” the smoldering ignition tests. As a result of the success of the campaign for “fire-safe” cigarettes, a discussion has started as to whether smoldering ignition (and even flaming ignition) tests should be eliminated. This would be a serious fire-safety mistake. There are three reasons for the need for smoldering ignition tests in North America: (1) “fire-safe” cigarettes can still ignite fabrics, (2) traditional cigarettes are still commercially available (e.g., from the areas where there is no regulation, including the autonomous American-Indian nations), and (3) the treatments used for improving the flaming performance of fabrics are usually ineffective in improving the smoldering ignition performance.

21.2.5.7 Flammable Fabrics

21.2.5.7.1 Wearing Apparel

As discussed earlier, since the 1950s, wearing apparel (or clothing) is regulated via the flammability test for apparel fabrics in 16 CFR 1610.¹² In the test, samples tested are placed in a sample holder at a 45° angle, and the igniter flame is imposed on the upper surface of the sample. The test method requires that replicate, preconditioned samples of fabrics used in clothing apparel comply with one of the following criteria:

- a. No ignition when subjected to a small gas diffusion flame emitted from a burner based on a hypodermic needle during an exposure of 1.0 s, or
- b. If the fabric sample ignites, the flames shall not spread 127 mm (5 in.) in less than 3.5 s.

The regulation addresses the sensitivity of this test method to fabric weight (or areal density) by providing that fabrics with an areal density exceeding 88.3 g/m² (2.6 oz/yd²) are permitted to be excluded from testing. These are considered too heavy to ignite under the test conditions.*

A typical criticism of this test method, for example, is that ordinary newsprint, and even tissue paper, will meet its requirements. That is a valid criticism. However, there seems to be general agreement that, in spite of its lack of sophistication, this test method has been successful in eliminating the fabrics with the poorest fire performance from the general population of fabrics in use for apparel in the United States. Thus, fabric types such as the fibrous “torch” sweaters with raised surface fibers that ignite readily and spread flame quickly are no longer legally sold in the United States due to the test requirements. The test has also been able to screen out the use of very sheer

* 16 CFR 1610 states: 1610.62 (4) Note 2—Some textiles never exhibit unusual burning characteristics and need not be tested. 16 CFR 1610.37 (d). Such textiles include plain surface fabrics, regardless of the fiber content, weighing 2.6 oz. or more per sq. yd., and plain and raised surface fabrics made of acrylic, modacrylic, nylon, olefin, polyester, wool, or any combination of these fibers, regardless of weight.

(i.e., light weight) fabrics and cotton garments that are ultralight. Thus, it has effectively removed extremely flammable fabrics from the market place. However, significant numbers of children and older adults are burned when their lightweight, loose fitting clothing made from 100% cellulosic or polyester cellulosic blend fabrics catch fire.

Some forensic experts ignore the added frequency of fire injuries or fire fatalities among the very young and the very old, when defending the 16 CFR 1610 test as sufficient, suggesting that additional requirements are unnecessary. Note that the ASTM committee on textiles (ASTM D13) has developed a standard, ASTM D 1230,⁷⁷ which is a consensus standard version of the 16 CFR 1610 requirement. A recent set of studies^{78,79} has shown that changes in the regulation would be helpful. Testing was conducted to search for possible correlations between the fabric test modes, fabric composition, and fire-related properties. The general trend found demonstrated that as areal density (weight) of the fabrics increase, both their times to forced ignition and their times to spread flame across their surface to the top of a vertical sample also increase, leading to improved fire performance. The most important consequence of this observation is that better fire performance in heavier fabrics is largely, *but not fully*, independent of fabric composition. Consequently, the hazard to an individual wearing a garment composed of a specific fabric type is a far more complex issue than that which can be simply assessed based on whether the fabric is composed of a thermoplastic material, a charring material, or a blend. Moreover, in terms of the regulatory implications, it appears that the regulation of very lightweight fabrics should be an important consideration and that the U.S. regulatory cut-off value, set at 88.3 g/m² (2.6 oz/yd²), is relatively arbitrary.

21.2.5.7.2 *Carpets and Rugs*

The ignitability of carpets and rugs is regulated by requiring compliance with the methenamine pill test, included in 16 CFR 1630¹³ and 16 CFR 1631.¹⁴ As is often the case with the U.S. regulatory tests, the test is more properly described by an ASTM consensus standard, in this case ASTM D 2859,⁸⁰ under the jurisdiction of the ASTM committee on fire standards (ASTM E05). It is important to point out that: (a) some imported small carpets and rugs (usually, those made of cotton and other cellulose) are often not tested and may not comply with the requirement and (b) codes in the United States have not normally been requiring methenamine pill results, but have focused on critical radiant flux requirements, based on ASTM E 648.⁴⁰

21.2.5.7.3 *Children's Sleepwear*

The flammability of children's sleepwear is regulated via the small-scale vertical open-flame ignition tests in 16 CFR 1615¹⁵ and 16 CFR 1616.¹⁶ In addition, an ASTM D13 standard exists as an alternative, namely ASTM D 6545.⁸¹ The critical part of the regulation is that children's sleepwear must be tight-fitting (and the regulation contains strict measurements) or must pass the test. The regulation has exceptions for sleepwear used by very young children (babies). A key concern associated with the regulation is the fact that garments that do not meet the requirements are offered for sale as "active wear" and are sold at lower prices than sleepwear, even though they are clearly designed to be used as sleepwear. Outside the United States, regulation on the surface-burning characteristics of children's pajamas and their snug fit has also been implemented in New Zealand.

21.2.5.7.4 *Mattresses, Mattress Sets, and Sleep Products (Bedding)*

Smoldering ignition of mattresses is regulated via the smoldering test in 16 CFR 1632.¹⁷ Since 2007, open-flame ignition of the mattresses and mattress sets is regulated via the fairly severe open-flame test for mattress sets in 16 CFR 1633.¹⁹ On March 28, 2000, attorney Whitney Davis, director of the Children's Coalition for Fire-Safe Mattresses submitted four petitions to CPSC concerning mattress flammability. The petitions proposed four options: (1) an open-flame standard similar to the full-scale test set forth in California Technical Bulletin 129 (CA TB 129)⁸²; (2) an open-flame standard similar to the component test set forth in British Standard BS 5852, using a fairly severe crib 5 ignition source⁸³ (see ignition sources described in BS 5852 in Table 21.7); (3) a warning label

TABLE 21.7
Ignition Sources Described in BS 5852

Ignition source 0	Smoldering cigarette
Tubular sources	<p>A burner tube consisting of a length of stainless steel tube, with 8.0 ± 0.1 mm ($5/16 \pm 0.004$ in.) outside diameter and 6.5 ± 0.1 mm (0.26 ± 0.004 in.) internal diameter and 200 ± 5 mm (7.9 ± 0.2 in.), connected by a flexible tube via a flow meter, fine control valve, an optional on–off valve and a cylinder regulator providing a nominal outlet pressure of 2.8 kPa containing butane. The flow meter shall be calibrated to supply butane gas flow rates as required in 6.5.1 through 6.5.3. The flexible tube connecting the output of the flow meter to the burner tube shall be 2.5–3.0 m (8–10 ft) in length with an internal diameter of 7.0 ± 1.0 mm (0.28 ± 0.004 in.).</p> <p>Gas: Butane gas, with a known net heat of combustion of 49.6 ± 0.5 MJ/kg, is the fuel for this ignition source. Meter the flow rate of butane and keep it constant throughout the test. Measure the gas flow rate at a pressure of 101 ± 5 kPa (standard atmospheric pressure, measured at the flow gage) and a temperature of $20^\circ\text{C} \pm 5^\circ\text{C}$.</p>
Ignition source 1	45 mL/min at 25°C (77°F), corresponding to a flame height of 35 mm (1.4 in.), measured from the top of the burner tube, when held vertically upward and when the flames are burning freely in air.
Ignition source 2	160 mL/min at 25°C (77°F), corresponding to a flame height of 145 mm (5.7 in.), measured from the top of the burner tube, when held vertically upward and when the flames are burning freely in air.
Ignition source 3	350 mL/min at 25°C (77°F), corresponding to a flame height of 240 mm (9.4 in.), measured from the top of the burner tube, when held vertically upward and when the flames are burning freely in air.
Wood crib sources	The wood crib is constructed using wood (pine lumber conditioned to constant humidity) and cotton (long-fiber, pure, dry, untreated, surgical grade cotton not more than 6 mm [0.25 in.] and not less than 4 mm [0.16 in.] thick). The wood cribs are constructed so that the sticks in each layer are parallel to one another and at right angles to the sticks in the adjacent layer. The sticks in each layer are placed as far away from each other as possible (except for the two main cribs forming the base of crib 6), without overlap at the ends, forming a square-sectioned crib. The sticks are glued together with wood adhesive. Cotton is placed at the bottom of the cribs, with the “fluffy” side up. The cotton is glued to the sticks at the bottom of the crib with minimal amounts of wood adhesive.
Ignition source 4	The crib is constructed with 10 sticks, each of which is 40 ± 2 mm (1.6 ± 0.08 in.) long and has a square section of 6.5 ± 0.5 mm ($1/4 \pm 0.02$ in.). There are 5 layers of 2 sticks each. The total mass of sticks is 8.5 ± 0.5 g. The bottom of the crib is covered by a flat horizontal layer of cotton approximately 40×40 mm (1.6×1.6 in.) in area.
Ignition source 5	The crib is constructed with 20 sticks, each of which is 40 ± 2 mm (1.6 ± 0.08 in.) long and has a square section of 6.5 ± 0.5 mm ($1/4 \pm 0.02$ in.). There are 10 layers of 2 sticks each. The total mass of the sticks is 17.0 ± 1.0 g. The bottom of the crib is covered by a flat horizontal layer of cotton approximately 40×40 mm (1.6×1.6 in.) in area.
Ignition source 6	The crib consists of an outside crib and an inside crib. The outside crib is constructed with eight sticks, each of which is 80 ± 2 mm (3.2 ± 0.08 in.) long and has a square section of 12.5 ± 0.5 mm ($1/2 \pm 0.02$ in.). There are 4 layers of 2 sticks each. The inside crib is constructed with 10 sticks, each of which is 40 ± 2 mm (1.6 ± 0.08 in.) long and has a square section of 6.5 ± 0.5 mm ($1/4 \pm 0.02$ in.). There are 5 layers of 2 sticks each. The total mass of the sticks is 60.0 ± 2.0 g. The bottom of the inside crib is covered by a flat horizontal layer of cotton approximately 40×40 mm (1.6×1.6 in.) in area.
Ignition source 7	The crib consists of an outside crib and an inside crib. The outside crib is constructed with 18 sticks, each of which is 80 ± 2 mm (3.2 ± 0.08 in.) long and has a square section of 12.5 ± 0.5 mm ($1/2 \pm 0.02$ in.). There are 9 layers of 2 sticks each. The inside crib is constructed with eight sticks, each of which is 40 ± 2 mm (1.6 ± 0.08 in.) long and has a square section of 6.5 ± 0.5 mm ($1/4 \pm 0.02$ in.). There are 5 layers of 2 sticks each. The total mass of the sticks is 126.0 ± 4.0 g. The bottom of the inside crib is covered by a flat horizontal layer of cotton approximately 40×40 mm (1.6×1.6 in.) in area.

Source: BS 5852, *Methods of Test for Assessment of the Ignitability of Upholstered Seating by Smoldering and Flaming Ignition Sources*, British Standards Institution, London, U.K.

for mattresses warning of polyurethane foam fire hazards, and (4) a permanent, fire-proof mattress identification tag. Whitney Davis had previously been working with California Assemblyman John Dutra, as a result of which the California legislature passed a law, Assembly Bill AB 603, in 2001. AB 603 required that all mattresses manufactured or sold in California be “fire retardant,” without details. Before AB 603 was issued, the state of California required all foam used for mattresses to comply with California Technical Bulletin 117 (CA TB 117).⁸⁴ CA TB 117 includes a vertical fire test for foam that could not be “passed” unless the polyurethane foam used contained some level of flame retardants. There is no consensus as to whether foam complying with CA TB 117 resulted in mattresses with highly increased fire safety. It is clear, however, that such foam would delay ignition of the mattress from small open flames and would even inhibit ignition from very small open flames. California also has a voluntary standard for high-risk occupancies, known as CA TB 129. The gas burner used as the ignition source in CA TB 129 is a T-shaped burner that applies propane gas for 180 s at a flow rate of 12 L/min. The test is severe enough that it can usually not be met unless the foam contained in the mattress is flame-retarded. This also became a consensus standard as ASTM E 1590⁸⁵ through the ASTM E05 committee, which does not have its own pass/fail criteria.

AB 603 was initially expected to require that mattresses comply with CA TB 129. After a research project was conducted at the NIST on behalf of the mattress industry, a new test was developed, based on using a new dual burner.^{86–87} This resulted in the issuance of California Technical Bulletin 603 (CA TB 603),⁸⁸ which went into effect for all mattresses sold in the state of California since January 1, 2005. It is important to point out that CA TB 603 is a significantly less severe test than CA TB 129, and mattresses sold as complying with the test often use barriers without adding flame retardants into the foam. In fact, if the barrier is pierced or damaged (by the effect of vandalism and/or of children playing with sharp objects), experience indicates that mattresses can comply with CA TB 603 but release large amounts of heat. However, in the absence of vandalism, clearly mattresses complying with CA TB 603 offer a significant improvement in fire safety. Eventually, CPSC issued their rulemaking (law) and developed 16 CFR 1633,¹⁹ which is technically equivalent to CA TB 603, but has some added requirements, in terms of labeling and record keeping. 16 CFR 1633 went into effect throughout the United States on July 1, 2007. 16 CFR 1633 requires that all mattresses, mattress/foundation sets, and futons sold in the United States meet the following pass/fail criteria: (a) the peak heat release rate does not exceed 200 kW during the 30 min test and (b) the total heat release does not exceed 25 MJ in the first 10 min of the test. The propane gas flames from the dual burner are applied for 70 s (top burner, at a flow rate of 12.9 L/min) and 50 s (side burner, at a flow rate of 6.6 L/min), giving a total applied heat release of 27 kW. The total observation period from the start of the test is 30 min.

The codes in the United States have long interpreted this regulation applies only to residential mattresses, and that higher fire safety requirements should apply to high-risk environments, such as jails or prisons, hospitals, and university dormitories. NFPA 101 contains requirements that mattresses in health care occupancies as well as detention and correctional occupancies that are not sprinklered, must comply with a peak heat release rate of 250 kW and a total heat release of no more than 40 MJ in the first 5 min of the test when tested to ASTM E 1590 (or CA TB 129). The IFC² had the same requirements up to 2006, but revised the requirement in 2007, so that the peak heat release rate is 100 kW and the total heat release is not more than 25 MJ in the first 10 min of the test. It also revised the requirements for detention occupancies, so that they no longer have a sprinkler exception: the mattresses must comply with the requirements irrespective of the presence of sprinklers. The 2009 edition of NFPA 101⁸ has similar requirements to those in the 2007 edition of the IFC. However, the IFC also requires, since 2007, that mattresses in college and university dormitories meet the same criteria as those in hospitals.

As a result of the same petition that led to CA TB 603 and 16 CFR 1633, California AB 603 also mandated that filled bed products, such as comforters, pillows, and bed spreads, should also exhibit

improved fire performance. CBHF studied the flammability of filled bed products and found that these products significantly contribute to mattress fires. In collaboration with the federal government, industry, and commercial laboratories, CBHF is working on California Technical Bulletin 604 (CA TB 604) to address this hazard. CBHF intends CA TB 604 to be a performance-based standard that would not prescribe the use of any specific additives or flame retardants, but would encourage the use of innovative methods and products to increase fire performance without affecting the environment. In effect, the draft of CA TB 604 issued in 2007 consists of three tests, all to be conducted in a small test chamber (or a small hood). They include: a flat filled/bed clothing products test, a pillow/cushion and loose-fill materials test, and a mattress pad test. The pass/fail criteria are based on weight loss (mass loss) for the first two tests and/or the generation of a hole for the flame to penetrate through (as seen by visual observation) in the third test. The ignition source is a propane gas burner tube (a 250–300 mm long stainless steel tube, 8 mm in outside diameter, 6.5 mm internal diameter). In the first test, multiple layers of flat filling materials are inserted in a case made of standard sheeting fabric or the product's actual cover fabric. The test specimen is placed on a horizontal cement board on a weighing device and ignited at one corner. In the second test, the filling materials are encased in a case made of the standard sheeting fabric or the ticking/fabric used in the actual bed product to encase the loose-filling materials. The test specimen is placed on a horizontal cement board on a weighing device and ignited at one corner. In the last test, a specimen of the mattress pad or its filling material is sandwiched between the layers of standard sheeting fabrics. The specimen is subjected to a small open flame applied to the center point of the top surface and observations of the burning behavior and burn patterns are used to assess fire performance. The regulatory timeline has been started and is expected to result in California regulation, sometime in 2010. This regulation is likely to result in changes in the requirements for all residential filled bed products and significantly increase fire safety. CPSC has issued an ANPRM, but this process has been stagnant in the recent years.

21.2.5.7.5 Upholstered Furniture

In 1994, the National Association for State Fire Marshals (NASFM) submitted a petition to CPSC to enact mandatory regulation for the flammability of upholstered furniture. The recommendation by NASFM was that the requirements for upholstered furniture flammability used in California or those used in the United Kingdom be implemented. CPSC has been studying this issue since then. Initially, in 2001, CPSC recommended an ignition test for the upholstery fabrics similar to the small gas burner sources in BS 5852.⁸³ This was widely derided as inappropriate, as it did not (and could not) address the issue of the heat release from the padding materials. Following other concerns expressed by the interested parties, CPSC conducted studies of effectiveness of flame retardants, toxicity of flame retardants, and many others. In the meantime, CBHF developed a draft revision of CA TB 117 (often known as CA TB 117 plus), which was made public in February 2002. This draft regulation addressed most of the concerns that had been expressed about CA TB 117, particularly regarding the fabric test and the lack of substantive foam and composite tests. However, it has not yet been implemented. In 2005, CPSC staff proposed a fire test scheme of 14 options, including smoldering and open-flame tests as well as individual component and composite tests; however, this was never approved. This was also never implemented, for both technical and political reasons (CPSC has spent long periods without a quorum of commissioners, political appointees). At a briefing of commissioners on December 6, 2007, a series of four options was presented to the commissioners: (a) the adoption of CA TB 117 plus, (b) the adoption of the 2001 recommendation by CPSC staff, (c) the adoption of the 2005 recommendation by CPSC staff, or (d) the adoption of a recommendation addressing only smoldering combustion for cover fabrics. In an NPRM, dated March 4, 2008, the commissioners chose to go with a smoldering combustion test for cover fabrics and a barrier test for fabrics failing the smoldering test, which would become 16 CFR 1634. Comments on this NPRM were due in May 2008, and will be acted upon in the near future.

In fact, CPSC never implemented mandatory smoldering requirements for upholstered furniture fire safety, but there has been widespread voluntary use of smoldering tests for components (ASTM E 1353,⁸⁹ from ASTM committee E05) by the trade association for residential furniture manufacturers (Upholstered Furniture Action Council [UFAC]) and for composites (ASTM E 1352,⁹⁰ from ASTM committee E05) by the trade association for contract furniture (Business and Institutional Furniture Manufacturers Association [BIFMA]). In summary, what CPSC staff has proposed is continued inaction, as the smoldering tests are applied to the vast majority of upholstered furniture items by the trade associations since the late 1970s. The proposed test contained in the draft 16 CFR 1634 is different from the one in ASTM E 1353, but will have very similar outcome for the applicable fabrics: cellulosic cover fabrics will fail and thermoplastic fabrics will pass. It is of interest, however, that the draft 16 CFR 1634 applies only to cover fabrics and not to any other upholstered furniture components, while ASTM E 1353 applies to all components and ASTM E 1352 applies to mock-ups also containing all components. This means that, if the new regulation comes into effect, not only foams (or any other fillings), but also welt cords and all other interior fabrics will be unregulated.

Requirements for upholstered furniture flammability exist in various states, including California, based on California Technical Bulletin 133 (CA TB 133),⁹¹ which was also made into a consensus standard by ASTM committee E05 as ASTM E 1537.⁹² The gas burner used as the ignition source in CA TB 133 is a square-shaped burner that applies propane gas for 80 s at a flow rate of 13 L/min. The test is severe enough that it can usually not be met, unless the foam contained in the upholstered furniture item is flame-retarded. The pass/fail criteria are a peak heat release rate of 80 kW and a total heat released that does not exceed 25 MJ over the first 10 min of the test. In California, moreover, all foam contained within upholstered furniture must be flame-retarded to comply with CA TB 117. Moreover, the IFC and NFPA 101 both have parallel requirements to those discussed earlier for mattresses. In other words, the 2006 editions of both the codes contain requirements that upholstered furniture items in health care occupancies as well as detention and correctional occupancies that are not sprinklered must comply with a peak heat release rate of 250 kW and a total heat release of no more than 40 MJ in the first 5 min of the test, when tested to ASTM E 1537 (or CA TB 133). However, the 2007 edition of the IFC and the 2009 edition of NFPA 101 lowered these values to 80 kW and 25 MJ over 10 min. Finally, the IFC 2007 added college and university dormitories to the list and eliminated the sprinkler exception for detention occupancies.

21.2.5.7.6 *Mine Conveyor Belts*

The fire safety of mine conveyor belts is covered by the MSHA. The convoluted history of requirements is described by Verakis.⁹³ The regulation mandates the exclusive use of “flame-resistant conveyor belts,” without details. The actual test used is a Bunsen burner-type test, based on ASTM D 635 (UL 94HB),⁹⁴ which has been shown to be inappropriate for the associated fire hazard. Originally, large-scale tunnels were used to classify the flammability of the conveyor belts, but those tunnels have since been destroyed. There have been fire-testing research projects addressing the correlation of the various proposed tests with standard tests, but nothing has been implemented till date.

The Technical Study Panel on the Utilization of Belt Air and the Composition and Fire Retardant Properties of Belt Materials in Underground Coal Mining was created under Section 11 of the Mine Improvement and New Emergency Response Act of 2006 (MINER Act) (Public Law 109–236), and was chartered under the provisions of the Federal Advisory Committee Act (FACA). The Panel’s charge was to prepare and submit this report concerning the utilization of the belt air and the composition and fire retardant properties of the belt materials in underground coal mining to the Secretary of Labor, the Secretary of Health and Human Services, the Committee on Health, Education, Labor, and Pensions of the Senate, and the Committee on Education and the Workforce of the House of Representatives. Its final report was published in December 2007.⁹⁵ The recommendations of the panel regarding a fire test for conveyor mine belts was the use of the BELT test for regulatory

purposes, replacing the Bunsen burner test currently in 30 CFR §18.65, which was based on ASTM D 635 (or UL 94HB). The BELT test was developed by the U.S. Bureau of Mines, and is conducted in a 1.7 m (5.5 ft) long and 0.2 m² (1.5 ft²) ventilated tunnel. The belt material sample size is 1.5 m (5 ft) long and 230 mm (9 in.) wide. The sample is ignited by applying a gas burner to the front edge of the belt sample with the flames distributed equally on the top and bottom surfaces of the sample. After 5 min, the burner is removed, and the belt sample is allowed to burn until the flames are out. A belt passes the BELT if, in three separate trials, there remains a portion of the conveyor mine belt sample that is undamaged across its entire width. If, in any of the three trials, fire damage extends to the end of the sample, the conveyor belt formulation fails the test. Comparison testing showed excellent agreement for 19 of the belts between the pass/fail results of the large-scale fire gallery test and the BELT. Agreement has been reached to implement this, but the regulation still needs to consider the public input.

On June 19, 2008, the MSHA published in the Federal Register, a Request for Information (<http://www.msha.gov/REGS/FEDREG/RFI/E8-13633.pdf>), with comments due by early September, as to whether tests exist that can be used for assessing conveyor-belt combustion toxicity and smoke density. Comments had to be identified with “RIN 1219-AB60” and sent to MSHA. The information collected will potentially result in developing additional requirements for conveyor mine belts.

21.2.5.7.7 *Other Materials and Products*

Flammable solids are regulated under the FHSA in terms of storage and transport. That is picked up by fire codes, like the IFC, which lay out the maximum allowable quantities of hazardous materials permitted in various occupancies, depending on the type of construction. The amount of flammable solids that can be stored is very limited, unless the storage location has been constructed as a “hazardous location,” which means that it is built to extreme safety. An unusual added wrinkle is presented by the fact that CPSC defines what constitutes a flammable solid as “a material that exhibits a flame spread rate exceeding 2.5 mm/s when exposed to the flame in the test contained within 16 CFR 1500.44.”¹⁸ It has been found that nonflame-retarded polyurethane foam is a flammable solid.⁹⁶ The consequence of this finding may be that upholstered furniture that is not flame-retarded cannot be stored (or kept) in showrooms or storage facilities that are not built as hazardous locations. This concept is still being developed, but it may lead to a voluntary requirement by major retailers of upholstered furniture, that all furniture shipped to them must have flame-retarded foam.

ASTM F 963²⁰ is a standard specification for toys which includes the requirements that: (a) “materials other than textiles (excluding paper) used in toys shall not be flammable, as defined under 16 CFR 1500.3 (c) (6) (vi)” under the FHSA and (b) any textile fabrics used in toys must comply with 16 CFR 1610 (see above). Recent legislation, intended to prevent the use of lead in toys, has mandated that all toys comply with ASTM F 963. This leads to the unusual fact that children’s toys must be safer than their upholstered furniture.

21.2.6 COMPARISON WITH INTERNATIONAL REGULATIONS

It is important to point out that the abovementioned regulations do not include any requirements in the United States for construction products (building products) or electrical wires and cables (or their optical fiber equivalents), other than in some transportation vehicles. As explained earlier, these requirements are contained in codes, which may be adopted into regulation. Most other developed countries have government-mandated regulation for such products.

In the case of the EU, the EC has developed “directives” including one requiring “safety in case of fire.”⁹⁷ The consequence of this is the development of a scheme for the classification of products,⁹⁸ starting with construction products other than “floorings” and “floorings” (Tables 21.8 through 21.10). Basically, four tests are used: a noncombustibility test (EN ISO 1182),⁹⁹ an oxygen bomb calorimeter (EN ISO 1716),¹⁰⁰ an intermediate-scale heat release apparatus (the SBI, EN 13823),¹⁰¹ and a small ignitability apparatus (EN ISO 11925-2).¹⁰² Every country (or member state)

is entitled to choose the limits that apply to each application, but they should all, eventually, adopt the overall scheme. To help with the development and implementation of this scheme, the European Community has developed a “reference scenario” fire test, namely the ISO 9705 room-corner test,⁵⁰ and uses other tests as surrogates. Table 21.8 shows the concept of what each class is intended to represent in the European Community standard testing approach. The specific classification schemes for construction products (excluding floorings) and floorings are in presented Tables 21.9 and 21.10. Subsequently, the EC addressed fire testing of linear pipe thermal insulation products,¹⁰³ and, later, of electric cables.¹⁰⁴ The details are shown in Tables 21.11 and 21.12, respectively. The scheme for electric cables is based on the EC FIPEC project¹⁰⁵ and the test is a proposed EN standard.¹⁰⁶ The information on these requirements can be found as part of the EU directives. These requirements are included as regulation by all European member states, with various implementation dates. The individual European countries have had different regulatory approaches to fire safety regulation, but most of them are in the process of being withdrawn.

On the other hand, in the EU, there are no regulatory requirements for upholstered furniture or mattresses, but the United Kingdom and Ireland have adopted regulations as far back as 1988 (for furniture) and 1989 (for mattresses).^{107,108} These regulations, based on the use of BS 5852,⁸³ have proved to be very effective in improving fire safety, as shown by a research project commissioned by the U.K. Department of Trade and Industry, after over 10 years.¹⁰⁹ The EC also undertook a

TABLE 21.8
European Community Concept for Classes

Fire Class	Tests Simulations		Time to Flashover	Contribution to Fire Growth
A1	Fully developed fire in a room	Single burning item in a room	No flashover	None
A2	Fully developed fire in a room	Single burning item in a room	No flashover	None
B	Small fire attack on limited area	Single burning item in a room	No flashover	Extra small
C	Small fire attack on limited area	Single burning item in a room	After 10 min	Small
D	Small fire attack on limited area	Single burning item in a room	2–10 min	Medium
E	Small fire attack on limited area		Before 2 min	Large
F	No A1 through E			

Essential definitions for European Community regulations:

“Material”: a single basic substance or uniformly dispersed mixture of substances, for example, metal, stone, timber, concrete, mineral wool with uniformly dispersed binder, polymers.

“Homogeneous product”: a product consisting of a single material, having uniform density and composition throughout the product.

“Nonhomogeneous product”: a product that does not satisfy the requirements of a homogeneous product. It is a product composed of one or more components, substantial and/or nonsubstantial.

“Substantial component”: a material that constitutes a significant part of a nonhomogeneous product. A layer with a mass per unit area $\geq 1.0 \text{ kg/m}^2$ or a thickness $\geq 1.0 \text{ mm}$ is considered to be a substantial component.

“Nonsubstantial component”: a material that does not constitute a significant part of a nonhomogeneous product. A layer with a mass per unit area $< 1.0 \text{ kg/m}^2$ and a thickness $< 1.0 \text{ mm}$ is considered to be a nonsubstantial component.

Two or more nonsubstantial layers that are adjacent to each other (i.e., with no substantial component(s) in-between the layers) are regarded as one nonsubstantial component and, therefore, must altogether comply with the requirements for a layer being a nonsubstantial component.

For nonsubstantial components, distinction is made between internal nonsubstantial components and external nonsubstantial components, as follows.

“Internal nonsubstantial component”: a nonsubstantial component that is covered on both sides by at least one substantial component.

“External nonsubstantial component”: a nonsubstantial component that is not covered on one side by a substantial component.

TABLE 21.9
European Community Classes of Reaction to Fire Performance for Construction Products Excluding Floorings, Linear Pipe Thermal Insulation Products, and Electrical Cables

Class	Test Method(s)	Classification Criteria	Additional Classification
A1	EN ISO 1182 ^a and	$\Delta T \leq 30^\circ\text{C}$ and $\Delta m \leq 50\%$ and $t_f = 0$ (i.e., no sustained flaming)	—
	EN ISO 1716	$\text{PCS} \leq 2.0\text{MJ/kg}^{\text{a}}$ and $\text{PCS} \leq 2.0\text{MJ/kg}^{\text{b,c}}$ and $\text{PCS} \leq 1.4\text{MJ/m}^2^{\text{d}}$ and $\text{PCS} \leq 2.0\text{MJ/kg}^{\text{e}}$	—
A2	EN ISO 1182 ^a or	$\Delta T \leq 50^\circ\text{C}$ and $\Delta m \leq 50\%$ and $t_f \leq 20\text{ s}$	—
	EN ISO 1716 and	$\text{PCS} \leq 3.0\text{MJ/kg}^{\text{a}}$ and $\text{PCS} \leq 4.0\text{MJ/kg}^{\text{b}}$ and $\text{PCS} \leq 4.0\text{MJ/m}^2^{\text{d}}$ and $\text{PCS} \leq 3.0\text{MJ/kg}^{\text{e}}$	—
	EN 13823 (SBI)	$\text{FIGRA} \leq 120\text{ W/s}$ and LFS < edge of specimen and $\text{THR}_{600\text{s}} \leq 7.5\text{ MJ}$	Smoke production ^f and flaming droplets/particles ^g
B	EN 13823 (SBI) and	$\text{FIGRA} \leq 120\text{ W/s}$ and LFS < edge of specimen and $\text{THR}_{600\text{s}} \leq 7.5\text{ MJ}$	Smoke production ^f and flaming droplets/particles ^g
	EN ISO 11925-2 ^h exposure = 30 s	$F_s \leq 150\text{ mm}$ within 60 s	
C	EN 13823 (SBI) and	$\text{FIGRA} \leq 250\text{ W/s}$ and LFS < edge of specimen and $\text{THR}_{600\text{s}} \leq \text{MJ}$	Smoke production ^f and flaming droplets/particles ^g
	EN ISO 11925-2 ^h exposure = 30 s	$F_s \leq 150\text{ mm}$ within 60 s	
D	EN 13823 (SBI) and EN ISO 11925-2 ^h exposure = 30 s	$\text{FIGRA} \leq 750\text{ W/s}$ and $F_s \leq 150\text{ mm}$ within 60 s	Smoke production ^f and flaming droplets/particles ^g
E	EN ISO 11925-2 ^h exposure = 15 s	$F_s \leq 150\text{ mm}$ within 20 s	Flaming droplets/particles ⁱ
F	No performance determined		

Abbreviations: ΔT , temperature rise; Δm , mass loss; t_f , duration of flaming; PCS, gross calorific potential; FIGRA, fire growth rate; $\text{THR}_{600\text{s}}$, total heat release; LFS, lateral flame spread; SMOGRA, smoke growth rate; $\text{TSP}_{600\text{s}}$, total smoke production; F_s , flame spread.

^a For homogeneous products and substantial components of nonhomogeneous products.

^b For any external nonsubstantial component of nonhomogeneous products.

^c Alternatively, any external nonsubstantial component having a $\text{PCS} \leq 2.0\text{MJ/m}^2$, provided that the product satisfies the following criteria of EN 13823 (SBI): $\text{FIGRA} \leq 20\text{ W/s}$; and LFS < edge of specimen, and $\text{THR}_{600\text{s}} \leq 4.0\text{ MJ}$ and s1 and d0.

^d For any internal nonsubstantial component of nonhomogeneous products.

^e For the product as a whole.

^f In the last phase of the development of the test procedure, modifications of the smoke measurement system have been introduced, the effect of which needs further investigation. This may result in a modification of the limit values and/or parameters for the evaluation of smoke production.

s1 = $\text{SMOGRA} \leq 30\text{ m}^2/\text{s}^2$ and $\text{TSP}_{600\text{s}} \leq 50\text{ m}^2$; s2 = $\text{SMOGRA} \leq 180\text{ m}^2/\text{s}^2$ and $\text{TSP}_{600\text{s}} \leq 200\text{ m}^2$; s3 = not s1 or s2.

^g d0 = No flaming droplets/particles in EN 13283 (SBI) within 600 s; d1 = No flaming droplets/particles persisting longer than 10 s in EN 13823 (SBI) within 600 s; d2 = not d0 or d1. Ignition of the paper in EN ISO 11925-2 results in a d2 classification.

^h Under conditions of surface flame attack and, if appropriate to the end-use application of the product, edge flame attack.

ⁱ Pass = no ignition of the paper (no classification). Fail = ignition of the paper (d2 classification).

TABLE 21.10
European Community Classes of Reaction to Fire Performance for Floorings

Class	Test Method(s)	Classification Criteria	Additional Classification
A1fl	EN ISO 1182 ^a and	$\Delta T \leq 30^\circ\text{C}$ and $\Delta m \leq 50\%$ and $t_f = 0$ (i.e., no sustained flaming)	—
	EN ISO 1716	$\text{PCS} \leq 2.0 \text{ MJ/kg}^{\text{a}}$ and $\text{PCS} \leq 2.0 \text{ MJ/kg}^{\text{b}}$ and $\text{PCS} \leq 1.4 \text{ MJ/m}^2^{\text{c}}$ and $\text{PCS} \leq 2.0 \text{ MJ/kg}^{\text{d}}$	—
A2fl	EN ISO 1182 ^a or	$\Delta T \leq 50^\circ\text{C}$ and $\Delta m \leq 50\%$ and $t_f \leq 20 \text{ s}$	—
	EN ISO 1716	$\text{PCS} \leq 3.0 \text{ MJ/kg}^{\text{a}}$ and $\text{PCS} \leq 4.0 \text{ MJ/m}^2^{\text{b}}$ and $\text{PCS} \leq 4.0 \text{ MJ/m}^2^{\text{c}}$ and $\text{PCS} \leq 3.0 \text{ MJ/kg}^{\text{d}}$	—
	And		
Bfl	EN ISO 9239-1 ^e	Critical flux ^f $\geq 8.0 \text{ kW/m}^2$	Smoke production ^g
	EN ISO 9239-1 ^e and EN ISO 11925-2 ^h Exposure = 15 s	Critical flux ^f $\geq 8.0 \text{ kW/m}^2$ $F_s \leq 150 \text{ mm}$ within 20 s	Smoke production ^g —
Cfl	EN ISO 9239-1 ^e and EN ISO 11925-2 ^h Exposure = 15 s	Critical flux ^f $\geq 4.5 \text{ kW/m}^2$ $F_s \leq 150 \text{ mm}$ within 20 s	Smoke production ^g —
	Dfl	EN ISO 9239-1 ^e and EN ISO 11925-2 ^h Exposure = 15 s	Critical flux ^f $\geq 3.0 \text{ kW/m}^2$ $F_s \leq 150 \text{ mm}$ within 20 s —
Efl	EN ISO 11925-2 ^h Exposure = 15 s	$F_s \leq 150 \text{ mm}$ within 20 s	—
Ffl	No performance determined		

Abbreviations: ΔT , temperature rise; Δm , mass loss; t_f , duration of flaming; PCS, gross calorific potential; F_s , flame spread.

^a For homogeneous products and substantial components of nonhomogeneous products.

^b For any external nonsubstantial component of nonhomogeneous products.

^c For any internal nonsubstantial component of nonhomogeneous products.

^d For the product as a whole.

^e Test duration = 30 min.

^f Critical flux is defined as the radiant flux at which the flame extinguishes or the radiant flux after a test period of 30 min, whichever is the lower (i.e., the flux corresponding with the furthest extent of spread of flame).

^g s1 = Smoke $\leq 750\%$ min; s2 = not s1.

^h Under conditions of surface flame attack and, if appropriate to the end-use application of the product, edge flame attack.

TABLE 21.11
European Community Classes of Reaction-to-Fire Performance for Linear Pipe Thermal Insulation Products

Class	Test Method(s)	Classification Criteria	Additional Classification
A _{1L}	EN ISO 1182 ^a and	$\Delta T \leq 30^\circ\text{C}$ and $\Delta m \leq 50\%$ and $t_f = 0$ (i.e., no sustained flaming)	—
	EN ISO 1716	PCS ≤ 2.0 MJ/kg ^a and PCS ≤ 2.0 MJ/kg ^b and PCS ≤ 1.4 MJ/m ² ^c and PCS ≤ 2.0 MJ/kg ^d	—
A _{2L}	EN ISO 1182 ^a or	$\Delta T \leq 50^\circ\text{C}$ and $\Delta m \leq 50\%$ and $t_f \leq 20$ s	—
	EN ISO 1716 and	PCS ≤ 3.0 MJ/kg ^a and PCS ≤ 4.0 MJ/kg ^b and PCS ≤ 4.0 MJ/m ² ^c and PCS ≤ 3.0 MJ/kg ^d	—
	EN 13823 (SBI)	FIGRA ≤ 270 W/s and LFS < edge of specimen and THR _{600s} ≤ 7.5 MJ	Smoke production ^e , and flaming droplets/particles ^f
B _L	EN 13823 (SBI) and	FIGRA ≤ 270 W/s and LFS < edge of specimen and THR _{600s} ≤ 7.5 MJ	Smoke production ^e , and Flaming droplets/particles ^f
C _L	EN ISO 11925-2 ^h exposure = 30 s	$F_s \leq 150$ mm within 60 s	Smoke production ^e , and Flaming droplets/particles ^f
	EN 13823 (SBI) and	FIGRA ≤ 460 W/s and LFS < edge of specimen and THR _{600s} ≤ 15 MJ	
D _L	EN ISO 11925-2 ^h exposure = 30 s	$F_s \leq 150$ mm within 60 s	Smoke production ^e , and Flaming droplets/particles ^f
	EN 13823 (SBI)	FIGRA $\leq 2,100$ W/s and THR _{600s} ≤ 100 MJ	
E _L	EN ISO 11925-2 ^h exposure = 30 s	$F_s \leq 150$ mm within 60 s	Flaming droplets/particles ^g
F _L	EN ISO 11925-2 ^h exposure = 15 s	$F_s \leq 150$ mm within 20 s	
F _L	No performance determined		

Abbreviations: ΔT , temperature rise; Δm , mass loss; t_f , duration of flaming; PCS, gross calorific potential; FIGRA, fire growth rate; THR_{600s}, total heat release; LFS, lateral flame spread; SMOGRA, smoke growth rate; TSP_{600s}, total smoke production; F_s , flame spread.

^a For homogeneous products and substantial components of nonhomogeneous products.

^b For any external nonsubstantial component of nonhomogeneous products.

^c For any internal nonsubstantial component of nonhomogeneous products.

^d For the product as a whole.

^e s1 = SMOGRA ≤ 105 m²/s² and TSP_{600s} ≤ 250 m²; s2 = SMOGRA ≤ 580 m²/s² and TSP_{600s} ≤ 1600 m²; s3 = not s1 or s2.

^f d0 = No flaming droplets/particles in EN13823 (SBI) within 600 s; d1 = No flaming droplets/particles persisting longer than 10 s in EN 13283 (SBI) within 600 s; d2 = not d0 or d1. Ignition of the paper in EN ISO 11925-2 results in a d2 classification.

^g Pass = No ignition of the paper (no classification); fail = ignition of the paper (d2 classification). Fail = ignition of the paper (d2 classification).

^h Under conditions of surface flame attack and, if appropriate to end-use application of product, edge flame attack.

TABLE 21.12
European Community Classes of Reaction to Fire Performance
for Electric Cables

Class	Test Method(s)	Classification Criteria	Additional Classification
A _{ca}	EN ISO 1716	PCS ≤ 2.0 MJ/kg ^a	
B1 _{ca}	FIPEC ₂₀ Scenario 2 ^e	$F_s \leq 1.75$ m and THR _{1200s} ≤ 10 MJ and Peak HRR ≤ 20 kW and FIGRA ≤ 120 W/s	Smoke production ^{b,f} and flaming droplets/ particles ^c and acidity ^{d,h}
	And		
	EN 60332-1-2	$H \leq 425$ mm	
B2 _{ca}	FIPEC ₂₀ Scenario 1 ^e	$F_s \leq 1.5$ m; and THR _{1200s} ≤ 15 MJ; and Peak HRR ≤ 30 kW; and FIGRA ≤ 150 W/s	Smoke production ^{b,f} and flaming droplets/ particles ^c and acidity ^{d,g,h}
	And		
	EN 60332-1-2	$H \leq 425$ mm	
C _{ca}	FIPEC ₂₀ Scenario 1 ^e	$F_s \leq 2.0$ m; and THR _{1200s} ≤ 30 MJ; and Peak HRR ≤ 60 kW; and FIGRA ≤ 300 W/s	Smoke production ^{b,f} and flaming droplets/ particles ^c and acidity ^{d,g,h}
	And		
	EN 60332-1-2	$H \leq 425$ mm	
D _{ca}	FIPEC ₂₀ Scenario 1 ^e	THR _{1200s} ≤ 70 MJ; and Peak HRR ≤ 400 kW; and FIGRA ≤ 1300 W/s	Smoke production ^{b,f} and flaming droplets/ particles ^c and acidity ^{d,g,h}
	And		
	EN 60332-1-2	$H \leq 425$ mm	
E _{ca}	EN 60332-1-2	$H \leq 425$ mm	
F _{ca}	No performance determined		

Abbreviations: ΔT , temperature rise; Δm , mass loss; t_p , duration of flaming; PCS, gross calorific potential; FIGRA, fire growth rate; THR_{600s}, total heat release; LFS, lateral flame spread; SMOGRA, smoke growth rate; TSP_{600s}, total smoke production; F_s , flame spread; FIPEC, Fire Performance of Electric Cables (Reference 105).

^a For the product as a whole, excluding metallic materials, and for any external component (i.e., sheath) of the product.

^b $s_1 = TSP_{1200} \leq 50$ m² and Peak SPR ≤ 0.25 m²/s. $s_{1a} = s_1$ and transmittance in accordance with EN 61034-2 ≥ 80%; $s_{1b} = s_1$ and transmittance in accordance with EN 61034-2 ≥ 60% < 80%; $s_2 = TSP_{1200} \leq 400$ m² and Peak SPR ≤ 1.5 m²/s; $s_3 =$ not s_1 or s_2 .

^c For FIPEC₂₀ Scenarios 1 and 2: $d_0 =$ No flaming droplets/particles within 1200 s; $d_1 =$ No flaming droplets/particles persisting longer than 10 s within 1200 s; $d_2 =$ not d_0 or d_1 .

^d EN 50267-2-3: $a_1 =$ conductivity < 2.5 μS/mm and pH > 4.3; $a_2 =$ conductivity < 10 μS/mm and pH > 4.3; $a_3 =$ not a_1 or a_2 . No declaration = no performance determined.

^e Air flow into chamber shall be set to 8000 ± 800 L/min. FIPEC₂₀ Scenario 1 = EN 50399-2-1:2007 with mounting and fixing as below. FIPEC₂₀ Scenario 2 = EN 50399-2-1:2007 with mounting and fixing as below.

^f The smoke class declared for class B1_{ca} cables must originate from the FIPEC₂₀ Scen 2 test.

^g The smoke class declared for class B2_{ca}, C_{ca}, D_{ca} cables must originate from the FIPEC₂₀ Scen 1 test.

^h Measuring the hazardous properties of gases developed in the event of fire, which compromise the ability of the persons exposed to them to take effective action to accomplish escape, and not describing the toxicity of these gases.

research project (known as CBUF) to investigate how such a scheme could be used in Europe,¹¹⁰ but the successful research has not yet been implemented. The CBUF project recommended the use of full-scale heat release tests, similar to those used in the United States for upholstered furniture and mattresses in codes (such as ASTM E 1537⁹² and ASTM E 1590⁸⁵), and recommended the use of the small-scale heat release test, the cone calorimeter (ASTM E 1354⁷¹), for predicting full-scale test results. In fact, CBUF developed small-scale tests with both individual component materials and with composites and models for using the small-scale test data.

In Canada, the system is somewhat similar to the United States, in the development of building codes and an electrical code, but the organization developing them is a part of the National Research Council, and not a separate standards developing organization, as in the United States.

21.3 CODES

21.3.1 INTERNATIONAL CODE COUNCIL CODES

As explained earlier, in the United States, there are two primary organizations that develop codes: ICC and NFPA; they are both private companies. ICC develops a full family of codes, including the following: IBC,¹ IFC,² IMC,³ IWUIC,⁴ IRC,⁵ and IEBC,⁶ which have been adopted widely throughout the country.

Until the mid-1990s, the United States had three regional code development companies: (1) International Conference of Building Officials (ICBO),¹¹¹ which issued the Uniform Building Code (UBC), primarily used in the 25 states west of the Mississippi, (2) Building Officials and Code Administrators (BOCA),¹¹² which issued the NBC, primarily used in the Northeast and Midwest, and (3) Southern Building Code Conference International (SBCCI),¹¹³ which issued the Standard Building Code (SBC), primarily used in the Southeast. The three organizations chose to join up to form ICC, to develop the ICC set of codes in a uniform fashion and to discontinue the old codes (also called the legacy codes). At least some of the legacy codes also had parallel documents dealing with the other issues that needed codification, but not all of them had complete sets.

For all ICC codes, the first edition was developed by a series of committees who worked to combine the best aspects of all legacy codes. Those drafts were then made available to the public for submission of code development proposals. ICC then set up a series of code development committees dealing with each one of the codes [in the case of the IBC and the IRC, more than one committee was set up]. Proposals submitted by the public (and not by ICC staff) are considered by each committee at a code development hearing meeting. The committees vote on their decisions following opportunities for proponents and opponents to explain the pros and cons of each proposal. Once the committees have voted (and their options are to accept a proposal as submitted, make modifications to any proposal, or disapprove it), there is the option for debate and voting by the attendees on the committee action. The results of the committee actions and the public debate/vote are published and comments from the public are sought. These comments are discussed at "Final Action Hearings" where proponents and opponents of the comments discuss the pros and cons. The final decision on these comments is reached by a vote of officials present. At the conclusion of this process, a revised code is published. Since the year 2000, a new set of ICC codes has been published every 3 years. After 18 months of the publication of a set of codes, an interim set of code supplements is published. From that moment on, new proposals have been dealing with the wording in the supplements and not with that in the full published code, unless there has been no approved change to the wording of specific sections. Jurisdictions are entitled to adopt the full codes or the codes with the supplements. This allows proposed improvements to be incorporated into the codes with a fairly short window between the innovation and the new code. For example, the 2009 ICC codes incorporated proposals made as late as August 2007, with the corresponding comments made as late as June 2008. The issuance of intermediate ICC codes via supplements after 18 months has been discontinued, and the ICC codes following the 2009 editions will be directly the 2012 editions.

All the documents (mostly standards) referenced in an ICC code must comply with the ICC policy on the referenced documents. This policy has been applied strictly to new referenced documents, but not as strictly to “grandfathered” documents that originate in the legacy codes. The two key provisions of this policy are the following:

1. All documents referenced by ICC must be fully written in mandatory language (including the fact that they cannot contain the words “may” or “should” other than in nonenforceable sections) to be permitted to be referenced. This has been a key reason for the fact that many standards issued by ISO or International Electrotechnical Commission (IEC) have not been able to be referenced, as they are often written in nonmandatory language. This has also resulted in extensive changes in the way consensus standards (by ASTM, NFPA, and others) have been written and revised. In fact, NFPA demands that all its documents (other than guides or recommended practices) are written in mandatory language, and so does the ASTM committee on fire standards (ASTM E05), but other ASTM committees and other organizations have not yet adopted this policy.
2. All the referenced documents must have been issued as a result of a full consensus process. This has been the reason that many documents newly issued by trade associations and similar organizations have not been adopted by the codes.

21.3.1.1 International Building Code

The IBC applies to the “construction, alteration, movement, enlargement, replacement, repair, equipment, use and occupancy, location, maintenance, removal, and demolition of every building or structure or any appurtenances connected or attached to such buildings or structures.” However, the IBC does not apply to “detached one- and two-family dwellings and multiple single-family dwellings (townhouses) not more than three stories above grade plane in height with a separate means of egress and their accessory structures,” to which the IRC applies.

The 2009 edition of the IBC consists of 34 chapters, plus a chapter on the referenced standards and a few appendices, which are not a mandatory portion of the code and can be adopted (or not) separately by individual AHJs. The key chapters associated with fire safety are the following:

- Chapter 2: Definitions of terms.
- Chapter 3: Use and occupancy classification of buildings. Requirements are usually based on what the type of use is for a building (or portion of a building).
- Chapter 4: Detailed requirements for some special occupancy buildings.
- Chapter 5: General building heights and areas.
- Chapter 6: Types of construction. The permission to use combustible materials or the type of fire resistance ratings are a function of whether the building is constructed completely, or primarily, of noncombustible materials.
- Chapter 7: Fire resistant-rated construction. This chapter addresses the separation requirements between rooms/compartments in buildings and between buildings, and also deals with insulation.
- Chapter 8: Interior finish and trim.
- Chapter 9: Fire protection systems: suppression and detection systems (including sprinklers and smoke detectors).
- Chapter 14: Exterior walls: dealing with wall coverings and siding.
- Chapter 15: Roof assemblies and roof structures.
- Chapter 23: Wood (including fire retardant-treated wood).
- Chapter 26: Plastics: this includes foam plastic insulation, plastic veneer, and light transmitting plastics.
- Chapter 27: Electrical: this contains a reference to the NEC [7] and some provisions that are specific to the IBC and different from the NEC.

In Chapter 8, wall and ceiling interior-finish materials must be tested for flame spread and smoke, in accordance with the traditional Steiner tunnel test (ASTM E 84,¹¹⁴ a 7.3 m [25 ft] tunnel with the test specimen on the underside of the ceiling). The Steiner tunnel provides results as a flame-spread index (FSI) and a smoke-developed index (SDI). As an alternative, all materials are permitted to be tested using a room-corner test for heat and smoke release (NFPA 286).¹¹⁵ There is clear evidence that the Steiner tunnel test is appropriate for some materials but not for all of them, and that NFPA 286 is a suitable test for any wall or ceiling interior finish material. Some materials (textile and expanded vinyl wall coverings) are permitted to be tested by using a less severe room-corner test (NFPA 265),¹¹⁶ but the room must also be sprinklered. Some other materials (foam plastics, solid high-density polyethylene [HDPE]) are only allowed to be fire tested for interior finish use via the NFPA 286 test and not via ASTM E 84, because of evidence that the results from the Steiner tunnel test are misleading. They can also be covered by a thermal barrier (such as gypsum board). Very thin (<0.9 mm thick) materials coated onto the wall surfaces are exempted from testing, because they are believed to produce insufficient heat or flames to cause serious problems. Very thick structural members are exempted from testing, because they are believed to be of low enough ignitability such that they do not provide a serious hazard. Interior trim (which occupies less than 10% of a wall or ceiling surface) is tested by the same means as other interior finish, but is allowed greater leniency (and is often also tested using thin strips of material rather than full thickness test specimens). Recent trends have started incorporating specific mounting practices for the use of ASTM E 84 with a variety of materials, such as wall coverings, to ensure adequate testing results. Table 21.13 contains many of the needed details. The IBC also has a table that describes

TABLE 21.13
IBC Fire Test Requirements for Interior Wall and Ceiling Finish Materials

Material	Test Method	Acceptance Criterion
Interior wall and ceiling finish materials, except as shown below in this table		
	ASTM E 84	Class A: FSI \leq 25 – SDI \leq 450
	ASTM E 84	Class B: 75 \leq FSI < 25 – SDI \leq 450
	ASTM E 84	Class C: 200 \leq FSI < 75 – SDI \leq 450
	NFPA 286	No flashover; no flames to extremities of samples; Pk HRR \leq 800 kW; TSR \leq 1,000 m ² —permitted where Class A, B, or C is required
Materials having a thickness less than 0.036 in. (0.9 mm) applied directly to the surface of walls or ceilings		
		No testing required
Exposed portions of structural members		
		No testing required
Foam plastics (exposed foam plastics and foam plastics used in conjunction with a textile or vinyl facing or cover)		
	NFPA 286	No flashover; no flames to extremities of samples; Pk HRR \leq 800 kW; TSR \leq 1000 m ²
	FM 4880	Pass (also required to meet ASTM E 84, Class A, B, or C, depending on application)
	UL 1040	Pass (also required to meet ASTM E 84, Class A, B, or C, depending on application)
	UL 1715	Pass (also required to meet ASTM E 84, Class A, B, or C, depending on application)
		Alternatively: cover foam with thermal barrier—foam must also meet ASTM E 84, Class B
Textile wall coverings		
	NFPA 286	No flashover; no flames to extremities of samples; Pk HRR \leq 800 kW; TSR \leq 1000 m ²
	NFPA 265, Method B	No flashover; no flames to extremities of samples; TSR \leq 1000 m ²
	ASTM E 84	ASTM E 84, Class A, but also requires sprinklers—must use ASTM E 2404

(continued)

TABLE 21.13 (continued)
IBC Fire Test Requirements for Interior Wall and Ceiling Finish Materials

Material	Test Method	Acceptance Criterion
Textile ceiling coverings		
	NFPA 286	No flashover; no flames to extremities of samples; Pk HRR \leq 800kW; TSR \leq 1000m ²
	ASTM E 84	ASTM E 84, Class A, but also requires sprinklers—must use ASTM E 2404
Expanded vinyl wall coverings		
	NFPA 286	No flashover; no flames to extremities of samples; Pk HRR \leq 800kW; TSR \leq 1000m ²
	NFPA 265 Method B	No flashover; no flames to extremities of samples; TSR \leq 1000m ²
	ASTM E 84	ASTM E 84, Class A, but also requires sprinklers—must use ASTM E 2404
Expanded vinyl ceiling coverings		
	NFPA 286	No flashover; no flames to extremities of samples; Pk HRR \leq 800kW; TSR \leq 1000m ²
	ASTM E 84	ASTM E 84, Class A, but also requires sprinklers—Must use ASTM E 2404
Site-fabricated stretch systems		
	NFPA 286	No flashover; no flames to extremities of samples; Pk HRR \leq 800kW; TSR \leq 1000m ²
	ASTM E 84	ASTM E 84, Class A—must use ASTM E 2573
HDPE		
	NFPA 286	No flashover; no flames to extremities of samples; Pk HRR \leq 800kW; TSR \leq 1000m ²
Interior trim, other than foam plastic		
		Combustible trim, excluding handrails and guardrails, cannot exceed 10% of the wall or ceiling area in which it is located
	ASTM E 84	Class C
	NFPA 286	No flashover; no flames to extremities of samples; Pk HRR \leq 800kW; TSR \leq 1000m ² —permitted where Class A, B, or C is required
Foam plastic used as interior trim		
		1. The minimum density of the interior trim must be 320kg/m ³ (20lb/ft ³)
		2. The maximum thickness of the interior trim must be 12.7 mm (0.5 in.) and the maximum width must be 204 mm (8 in.).
		3. The interior trim cannot constitute more than 10% of the aggregate wall and ceiling area of a room or space.
	ASTM E 84	FSI \leq 75
	NFPA 286	No flashover; no flames to extremities of samples; Pk HRR \leq 800kW; TSR \leq 1000m ² —permitted where Class A, B, or C is required
Wood used for ornamental purposes, trusses, paneling, or chancel furnishing in assembly occupancy places of religious worship		
		No testing required

which applications, for each occupancy, must have materials that meet the requirements of Class A, B, or C. Interior floor finish materials must meet the requirements based on critical radiant flux in the ASTM E 648⁴⁰ test.

This section cannot describe all the provisions in the code, but the code contains specific requirements for a variety of materials, both based on the type of material and its application. For example requirements exist for insulation materials (loose-fill, foamed, and others), kiosks and children's playground structures in malls, siding, combustible materials in exterior walls, roofs and decks, and glazing materials, among the others. It also specifies that all materials contained within plenums must meet the requirements of the IMC.³

21.3.1.2 International Fire Code

The IFC code establishes regulations affecting or relating to structures, processes, premises, and safeguards regarding:

1. The hazard of fire and explosion arising from the storage, handling or use of structures, materials, or devices;
2. Conditions hazardous to life, property, or public welfare in the occupancy of structures or premises;
3. Fire hazards in the structure or on the premises from occupancy or operation;
4. Matters related to the construction, extension, repair, alteration or removal of fire suppression, or alarm systems.

The IFC applies to:

1. Structures, facilities, and conditions arising after the adoption of the relevant IFC edition.
2. Existing structures, facilities, and conditions not legally in existence at the time of adoption of the relevant IFC edition.
3. Existing structures, facilities, and conditions when identified in specific sections of the IFC.
4. Existing structures, facilities, and conditions which, in the opinion of the fire-code official, constitute a distinct hazard to life or property.

The IFC also applies to:

1. Conditions and operations arising after the adoption of the relevant IFC edition.
2. Existing conditions and operations.

The IFC does not allow any change to be made in the use or occupancy of any structure which would place the structure in a different division of the same group or occupancy or in a different group of occupancies, unless such structure is made to comply with the requirements of both the IFC and the IBC. Subjected to the approval of the fire-code official, the use or occupancy of any existing structure can be changed and the structure can be occupied for purposes in other groups, without conforming to all the requirements of both the IFC and IBC for those groups, provided the new or proposed use is less hazardous, based on life and fire risk, than the existing use.

The design and construction of new structures must comply with the IBC, and any alterations, additions, changes in use, or changes in structures required by the IFC, which are within the scope of the IBC, must be made in accordance with the IBC.

With regard to historic buildings, the provisions of the IFC relating to the construction, alteration, repair, enlargement, restoration, relocation or moving of buildings, or structures is not mandatory for existing buildings or structures identified and classified by the state or local jurisdiction as historic buildings, when such buildings or structures do not constitute a distinct hazard to life or property. Fire protection in designated historic buildings and structures is provided in accordance with an approved fire protection plan.

The 2009 edition of the IFC consists of 44 chapters, along with a chapter on referenced standards and a few appendices, which are not a mandatory portion of the code and can be adopted (or not) separately by individual AHJs. The key chapters associated with fire safety are the following:

- Chapter 2: Definitions of the terms
- Chapter 8: Interior finish, decorative materials, and furnishings
- Chapter 9: Fire protection systems: suppression and detection systems (including sprinklers and smoke detectors)
- Chapter 27: Hazardous materials

- Chapter 34: Flammable and combustible liquids
- Chapter 35: Flammable gases
- Chapter 36: Flammable solids

The requirements for interior finish and trim materials in Chapter 8 of the IFC are coordinated with those in the IBC, with some exceptions. As the IFC applies to new and existing buildings, some requirements in Chapter 8 apply only to “newly introduced” interior finish materials, and some requirements are simply missing. The IFC also contains, in Chapter 8, requirements for upholstered furniture and mattresses in some regulated occupancies, principally hospitals, nursing homes, board and care facilities, college and university dormitories, prisons, and jails. The requirements are based on the tests in ASTM E 1537⁹² and ASTM E 1590,⁸⁵ with the pass/fail criteria developed by CBHF and incorporated into CA TB 133⁹¹ and CA TB 129⁸² (equivalent to the ASTM standards). The materials must also meet smoldering test requirements. Additional requirements exist for curtains and drapes, decorations (including combustible vegetation), and some waste baskets.

21.3.1.3 International Residential Code

The provisions of the IRC⁵ apply to the construction, alteration, movement, enlargement, replacement, repair, equipment, use and occupancy, location, removal, and demolition of the detached one- and two-family dwellings and townhouses not more than three storeys above-grade in height, with a separate means of egress and their accessory structures. The IRC is intended to provide minimum requirements to safeguard the public safety, health and general welfare through affordability, structural strength, means of egress facilities, stability, sanitation, light and ventilation, energy conservation, and safety to life and property from fire and other hazards attributed to the built environment.

The legal occupancy of any structure existing on the date of adoption of a particular edition of the IRC will be allowed to continue without change, except if it is deemed necessary by the building official for the general safety and welfare of the occupants and the public. Additions, alterations, or repairs to any structure must conform to the requirements for a new structure, without requiring the existing structure to comply with all of the requirements of the code, unless otherwise stated. Additions, alterations, or repairs should not cause an existing structure to become unsafe or adversely affect the performance of the building.

The 2009 edition of the IRC consists of 42 chapters, along with a chapter on referenced standards and a few appendices, which are not a mandatory portion of the code, and can be adopted (or not) separately by individual AHJs. The key chapters associated with fire safety are the following:

- Chapter 2: Definitions of the terms
- Chapter 3: Building planning. This chapter contains virtually all the requirements associated with fire safety, including those for interior finish, foam plastics, insulation, and siding
- Chapter 7: Wall covering
- Chapter 8: Roof-ceiling construction
- Chapter 9: Roof assemblies
- Chapter 16: Duct systems

General requirements for residential construction tend to use, when they exist, the same tests as those used in the IBC, but with milder requirements.

The 2009 edition of the IFC contains requirements for installation of residential sprinklers in all new one- and two-family dwellings and townhouses, effective from January 2011. This is a brand new requirement and is parallel to what is also required (see below) in NFPA 101 and NFPA 5000. It also contains requirements for installation of carbon monoxide detectors.

21.3.1.4 International Mechanical Code

The IMC regulates the design, installation, maintenance, alteration, and inspection of mechanical systems that are permanently installed and utilized to provide control of environmental conditions and related processes within the buildings. It does not regulate the installation of fuel gas distribution piping and equipment, fuel gas-fired appliances, and fuel gas-fired appliance venting systems. Also, mechanical systems in detached one- and two-family dwellings and multiple single-family dwellings (townhouses), not more than three storeys high with separate means of egress and their accessory structures, are regulated by the IRC. Other exclusions are historical buildings and existing buildings.

The key provisions covered by this code are those for materials in the ducts and plenums as well as the piping systems. Plenums are enclosed portions of the building structure, which are not occupiable and have been designed to allow air movement and serve as part of an air distribution system. These concealed spaces can move air (and smoke) easily between the building compartments without the occupants being aware of it. Therefore, typically, fairly severe requirements govern all materials permitted in plenums. The only materials permitted are: wires and cables that meet criteria based on the NFPA 262⁶⁵ plenum cable fire test or that are enclosed in noncombustible raceways, pneumatic tubing, based on UL 1820,¹¹⁷ sprinkler pipes, based on UL 1887,¹¹⁸ fiber optic raceway systems, based on UL 2024,¹¹⁹ and combustible electrical equipment, based on UL 2043,¹²⁰ so that each one is covered by a special test for that product. Foam plastic wall and ceiling insulation must meet the NFPA 286 room-corner test or be covered by a thermal barrier or a steel skin. All other materials, including pipe and duct insulation, must meet the requirements of a FSI of 25 and a SDI of 50 in the ASTM E 84 Steiner tunnel test (a much more severe smoke criterion than that for nonplenum areas, where the SDI is allowed to reach 450).

21.3.1.5 International Existing Building Code

The provisions of the IEBC apply to the repair, alteration, change of occupancy, addition, and relocation of the existing buildings. The intent is to provide flexibility to permit the use of alternative approaches to achieve compliance with minimum requirements to safeguard the public health, safety, and welfare insofar as they are affected by the repair, alteration, change of occupancy, addition, and relocation of the existing buildings. A building or portion of a building that has not been previously occupied or used for its intended purpose in accordance with the laws in existence at the time of its completion must comply with the provisions of the IBC or the IEBC, as applicable, for new construction or with any current permit for such occupancy.

This code contains relatively few fire safety provisions, unless a problem has been found, and such provisions are deemed necessary by the code official for the general safety and welfare of the occupants and the public. However, when buildings are being renovated, the IEBC often requires that the provisions of either the IBC or the IFC apply.

21.3.1.6 International Wildland Urban Interface Code

The objective of the IWUIC is to establish minimum regulations consistent with the nationally recognized good practice for the safeguarding of life and property, so as to mitigate the risk to life and structures from intrusion of fire from wildland fire exposures and fire exposures from adjacent structures, and to mitigate structure fires from spreading to wildland fuels. The extent of the regulation is intended to be tiered, commensurating with the relative level of hazard present, as the unrestricted use of property in wildland–urban interface areas is a potential threat to life and property from fire and resulting erosion. The IWUIC code is intended to supplement the jurisdiction’s building and fire codes, if such codes have been adopted, to provide for special regulations to mitigate the fire- and life safety hazards of the wildland–urban interface areas.

Traditionally, the IWUIC code contained requirements for fire resistance-rated construction, but the 2009 edition also contains alternate requirements based on “ignition-resistant materials,” which

is required to meet one of the number of reaction-to-fire tests, principally, the 30 min version of the ASTM E 84 test that is used for defining fire-retardant treated wood, for example, in Chapter 23 of the IBC or in NFPA 703.¹²¹ Such materials can be made out of fire-retardant-treated wood as well as out of wood-plastic composites or plastic lumber, as long as they all meet the same fire test, as well as mechanical and aging requirements. This is a brand new concept: using materials without a fire resistance rating in wildland areas.

21.3.1.7 International Performance Code

This code was developed to provide a performance-based alternative to the use of the prescriptive IBC and IFC. It requires adequate fire safety, but is not explicit in the way that this is obtained. For example, the chapter on fire prevention has a language such as the following.

“The objective of the code is to limit or control the likelihood that a fire will start because of the design, operation, or maintenance of a facility or its systems so as to minimize impacts on people, property, processes, and the environment. Facility services, systems and activities that represent a potential source of ignition or can contribute fuel to an incipient fire must be designed, operated, managed, and maintained to reduce the likelihood of a fire starting. Electrical, mechanical, and chemical systems or processes and facility services capable of supplying sufficient heat under normal operating conditions or anticipated failure modes to ignite combustible system components, facility elements or nearby materials must be designed, operated, managed, and maintained to prevent the occurrence of fire. The quantities, configurations, characteristics, or locations of combustible materials, including components or facility systems, facility elements, facility contents and accumulations of readily ignitable waste or debris must be managed or maintained to prevent ignition by facility service equipment and other ignition sources associated with processes normally present or expected to be present within the facility. Ignition and fuel source interactions must be designed, operated, and maintained so as to prevent the occurrence of ignition or to control the extent of atmospheres likely to pose an ignition hazard.”

This code is still relatively rarely used.

21.3.2 NATIONAL FIRE PROTECTION ASSOCIATION CODES AND STANDARDS

NFPA is the other major developer of codes in the United States. Table 21.14 shows all the NFPA codes and a number of documents that are of key regulatory importance even though they are not codes. This includes the NFPA 13 series of sprinkler standards (NFPA 13, 13D, and 13R), which form the bases for all the requirements for sprinkler installations in the United States (and probably worldwide), NFPA 130 (for trains and underground systems), NFPA 99 (which govern all health care occupancies, in conjunction with the Life Safety Code), and NFPA 90A (for air conditioning, which regulates materials in ducts and plenums). NFPA documents are revised every 3–5 years, with the period being 3 years for all codes. With regard to the major codes, the NFPA codes are at a disadvantage over the competing ICC codes, which are revised twice in the same period.

21.3.2.1 National Electrical Code

The National Electrical Code (NFPA 70, NEC⁷) regulates all the electrical installations and also all the electrical and optical fiber cables. Chapter 2 describes the overall wiring requirements (including, in particular, grounding in Article 250). Chapter 3 describes the wiring methods and materials, which includes Article 300, which is a type of general guide through the code with the requirements for many applications and materials (including plenums, ducts, and other spaces used for environmental air, in section 300.22). Article 310 (Conductors for General Wiring) contains a table that describes the materials to be used and the standard that addresses the material composition and the fire performance of the material, usually based on a small-scale UL fire test. Other articles in Chapter 3 address the different types of cables and raceways. Thus, in Article 334, NM cables (or nonmetallic sheathed cables) are described, and they are one example of cables that need to have flame-retarded

TABLE 21.14
NFPA Codes and Other NFPA Key Documents

NFPA 1	Uniform Fire Code
NFPA 30	Flammable and Combustible Liquids Code
NFPA 30A	Code for Motor Fuel Dispensing Facilities and Repair Garages
NFPA 42	Code for the Storage of Pyroxylin Plastic
NFPA 52	Vehicular Fuel Systems Code
NFPA 54	National Fuel Gas Code
NFPA 58	Liquefied Petroleum Gas Code
NFPA 59	Utility LP Gas Plant Code
NFPA 70	National Electrical Code
NFPA 72	National Fire Alarm Code
NFPA 85	Boiler and Combustion Systems Hazard Code
NFPA 101	Life Safety Code
NFPA 301	Code for Safety to Life from Fire on Merchant Vessels
NFPA 400	Hazardous Materials Code
NFPA 430	Code for the Storage of Liquid and Solid Oxidizers
NFPA 432	Code for the Storage of Organic Peroxide Formulations
NFPA 434	Code for the Storage of Pesticides
NFPA 490	Code for the Storage of Ammonium Nitrate
NFPA 495	Explosive Materials Code
NFPA 900	Building Energy Code
NFPA 909	Code for the Protection of Cultural Resources Properties—Museums, Libraries, and Places of Worship
NFPA 914	Code for Fire Protection of Historic Structures
NFPA 1122	Code for Model Rocketry
NFPA 1123	Code for Fireworks Display
NFPA 1124	Code for the Manufacture, Transportation, Storage, and Retail Sales of Fireworks and Pyrotechnic Articles
NFPA 1125	Code for the Manufacture of Model Rocket and High Power Rocket Motors
NFPA 1127	Code for High Power Rocketry
NFPA 5000	Building Construction and Safety Code
Other key NFPA Standards	
NFPA 13	Standard for the Installation of Sprinkler Systems
NFPA 13D	Standard for the Installation of Sprinkler Systems in One- and Two-Family Dwellings and Manufactured Homes
NFPA 13R	Standard for the Installation of Sprinkler Systems in Residential Occupancies up to and Including Four Stories in Height
NFPA 80	Standard for Fire Doors and Other Opening Protectives
NFPA 90A	Standard for the Installation of Air-Conditioning and Ventilating Systems
NFPA 99	Standard for Health Care Facilities
NFPA 130	Standard for Fixed Guideway Transit and Passenger Rail Systems
NFPA 220	Standard on Types of Building Construction
NFPA 221	Standard for High Challenge Fire Walls, Fire Walls, and Fire Barrier Walls
NFPA 225	Model Manufactured Home Installation Standard
NFPA 318	Standard for the Protection of Semiconductor Fabrication Facilities
NFPA 501	Standard on Manufactured Housing

outer sheaths (or jackets). Other examples include Power and Control Tray Cables (Article 336) and Service Entrance Cables (Article 338, unless they are used underground). Similarly, conduits and raceways (enclosed channels designed expressly for holding wires, cables, or busbars) have specific Articles, with additional functions as permitted in this Code, and many of those require the materials (or the final products) to meet some type of fire test (generally not included in the NEC, but in the specific product standard). Thus, for example, HDPE conduit (Article 353) has no fire performance requirements, but is intended for underground installations, while reinforced thermosetting resin conduit (RTRC, Article 355) does have fire-performance requirements and can be used exposed and concealed in a variety of locations (but not in plenums). Polyvinyl chloride (PVC) conduit is made into various types of products, including rigid PVC conduit (RNC, Article 352), liquidtight nonmetallic conduit (LFNC, Article 356), and electrical nonmetallic tubing (ENT, Article 362). PVC has inherently improved fire performance and its conduits can generally be used in a variety of locations, but again, usually not in plenums, unless specifically formulated for that use. Chapter 4 of the NEC addresses flexible cords and cables, and many of them are also required to meet some fire tests, at least in terms of the materials of composition. Chapter 5 includes a variety of special occupancies and is similar to a building code, in that it describes the materials and products permitted in those applications. Special occupancies include hazardous locations, health care facilities (including hospitals, Article 517), and places of assembly (Article 518), which have very restrictive requirements. Other occupancies with much more lenient requirements include carnivals, circuses, fairs, and similar events (Article 525). Article 550 addresses wiring in manufactured homes and is coordinated with NFPA 501 (Ref. [122], see Section 3.2.7). Chapter 6 addresses special equipment, and the key article important to fire safety is Article 645, on Information Technology Equipment, which regulates wiring in computer rooms. Of particular interest is the fact that it requires cables in “under raised floors” to meet a vertical cable tray test and not the more severe plenum cable test, in spite of the fact that such locations are often deemed to be plenums.

Chapter 7 is the chapter dealing with “Special Conditions” and it addresses most of the cables with highly improved fire performance. Thus, Articles 725 (Class 1, Class 2, and Class 3 Remote-Control, Signaling, and Power-Limited Circuits), 760 (Fire Alarm Systems), and 770 (Optical Fiber Cables and Raceways) all use the same two schemes for fire performance of cables, as shown in Figures 21.4 and 21.5. The figures show that the best is NFPA 262,⁶⁵ a cable fire test for flame spread and smoke, conducted in a modified Steiner tunnel (86 kW or 294,000 BTU/h), for which the requirements in the NEC are that the maximum peak optical density should not exceed 0.5, the maximum average optical density should not exceed 0.15, and the maximum allowable flame travel distance should not exceed 1.52 m (5 ft). The next test, in the order of decreasing severity is UL 1666,⁶⁴ known

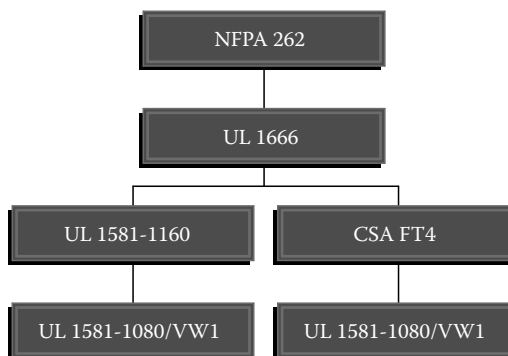


FIGURE 21.4 Flame-spread requirements for cables in the NEC, in order of decreasing flame-spread severity.

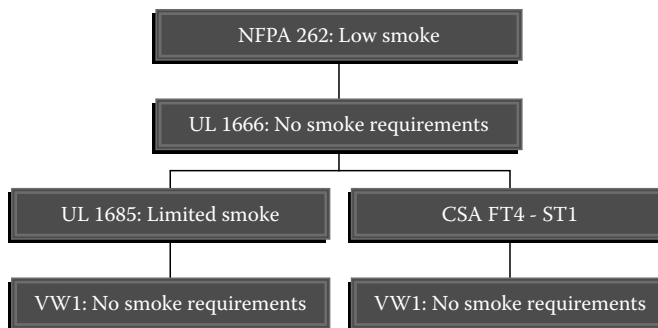


FIGURE 21.5 Smoke-release requirements for cables in the NEC, with corresponding hierarchy (in order of decreasing flame-spread severity).

as the “riser cable test,” which requires that, when exposed to a 155-kW (530,000 BTU/h) flame, the cable must be capable of preventing the carrying of fire vertically from floor to floor. The next rung in the severity scale is the vertical cable tray test, and there are two parallel tests, both of which allows the cable to be used in the same application, even though the tests are not of equal severity: UL 1581-1160⁵⁹ and UL 1581-1164,⁶⁰ which is equivalent to the CSA FT4 test⁶² and the IEEE 1202 test.⁶³ Both these tests are now contained with the UL 1685.¹²³ The concept in these cable tray tests is that the cable does not spread flame vertically far enough. The specimen is roughly 2.4 m high and the requirement is that the char length (cable destruction) does not go all the way to the top (UL 1581-1160) or does not reach 1.5 m (UL 1581-1164). The flame is ~20 kW (70,000 BTU/h), applied for 10 min, with the burner perpendicular to the cable tray (in the UL 1581-1160) and at a 20° angle (in the UL 1581-1164). The NEC does not require smoke measurements for these tests, but UL 1685 (as well as IEEE 1202 and CSA FT4) does have smoke pass/fail requirements. The fourth and minimal test in the NEC hierarchy is the small-scale Bunsen burner UL VW-1 test, vertical wire test,⁶⁰ with only 500 W, and which simply requires the wire not to burn all the way basically. Chapter 8, on communications systems, has the same scheme for the articles mentioned earlier, and it applies to Articles 800 (communications circuits), 820 (Community Antenna Television and Radio Distribution Systems), and 830 (Network-Powered Broadband Communications Systems). Of interest is the fact that Chapter 8 is not subject to the requirements of Chapters 1 through 7, except where the requirements are specifically referenced in Chapter 8.

The independence of Chapter 8 is particularly important when dealing with plenum cables, for which the charging section is 300.22, which reads as follows:

“300.22 Wiring in Ducts, Plenums, and Other Air-Handling Spaces.”

The provisions of this section apply to the installation and uses of electrical wiring and equipment in ducts, plenums, and other air-handling spaces.

FPN: See Article 424, Part VI, for duct heaters.

- A. Ducts for Dust, Loose Stock, or Vapor Removal. No wiring systems of any type shall be installed in ducts used to transport dust, loose stock, or flammable vapors. No wiring system of any type shall be installed in any duct or shaft containing only such ducts, used for vapor removal or ventilation of commercial-type cooking equipment.
- B. Ducts or Plenums Used for Environmental Air. Only wiring methods consisting of Type MI cable, Type MC cable employing a smooth or corrugated impervious metal sheath without an overall nonmetallic covering, electrical metallic tubing, flexible metallic tubing, intermediate metal conduit, or rigid metal conduit without an overall nonmetallic covering shall be installed in ducts or plenums specifically fabricated to transport environmental air. Flexible metal conduit shall be permitted, in lengths not exceeding 1.2 m (4 ft),

to connect physically adjustable equipment and devices permitted in these ducts and plenum chambers. The connectors used with flexible metal conduit shall effectively close any openings in the connection. Equipment and devices shall be permitted within such ducts or plenum chambers, only if they are necessary for their direct action upon, or sensing of, the contained air. In cases where equipments or devices are installed, and illumination is necessary to facilitate maintenance and repair, enclosed gasketed-type luminaires shall be permitted.

- C. Other Space Used for Environmental Air. This section applies to space used for environmental air-handling purposes other than ducts and plenums as specified in 300.22 (A) and (B). It does not include habitable rooms or areas of buildings, the prime purpose of which is not air handling.

FPN: The space over a hung ceiling used for environmental air-handling purposes is an example of the type of other space to which this section applies.

Exception: This section cannot be applied to the joist or stud spaces of dwelling units where the wiring passes through such spaces perpendicular to the long dimension of such spaces.

1. Wiring Methods. The wiring methods for such space shall be limited to totally enclosed, nonventilated, insulated busway having no provisions for plug-in connections, Type MI cable, Type MC cable without an overall nonmetallic covering, Type AC cable, or other factory-assembled multiconductor control or power cable that is specifically listed for the use, or listed prefabricated cable assemblies of metallic manufactured wiring systems without nonmetallic sheath. Other types of cables, conductors, and raceways shall be permitted to be installed in electrical metallic tubing, flexible metallic tubing, intermediate metal conduit, rigid metal conduit without an overall nonmetallic covering, flexible metal conduit, or, where accessible, surface metal raceway or metal wireway with metal covers or solid bottom metal cable tray with solid metal covers.
 2. Equipment. Electrical equipment with a metal enclosure or with a nonmetallic enclosure listed for the use and having adequate fire-resistant and low-smoke-producing characteristics, and associated wiring material suitable for the ambient temperature shall be permitted to be installed in such space unless prohibited elsewhere in this code.
 3. Exception: Integral fan systems shall be permitted where their use is specifically identified.
- D. Information Technology Equipment. Electrical wiring in air-handling areas beneath the raised floors for Information Technology Equipment shall be permitted in accordance with Article 645.

The NFPA Standards Council has stated that NFPA 90A⁹ is responsible for requirements for all materials and products in ducts and plenums, but this has been very controversial, because it indicates that the committee responsible for NFPA 90A (a small committee called Technical Committee on Air Conditioning) mandates requirements for ducts and plenums in all the major NFPA codes (NFPA 70, NFPA 101, and NFPA 5000).

21.3.2.2 National Life Safety Code

The 2009 edition of the Life Safety Code (NFPA 101) consists of 43 chapters, along with a few appendices, which are not a mandatory portion of the code and can be adopted (or not) separately by individual AHJs. The key chapters are the following:

- Chapter 2: Mandatory references
- Chapter 3: Definitions of the terms
- Chapter 4: General
- Chapter 5: Performance-based code alternative
- Chapter 6: Classification of occupancy and hazard of contents

- Chapter 7: Means of egress
- Chapter 8: Features of fire protection (such as compartmentation, barriers, and partitions)
- Chapter 9: Building service and fire protection equipment (such as sprinklers, alarms, and detectors)
- Chapter 10: Interior finish, contents, and furnishings (key chapter on reaction to fire requirements)
- Chapters 11 through 43: New and existing occupancy chapters

The requirements for interior finish are very similar to those in the IBC and IFC, except that it is less comprehensive, does not address some materials such as HDPE or site fabricated stretch systems, and does not include the requirement to apply any of the standard practices for use of the Steiner tunnel, ASTM E 84. This is partially owing to the longer period between the proposals and issuance of a new code.

Each of the occupancy chapters makes their independent decision as to whether the corresponding committee wants to incorporate requirements for interior finish, upholstered furniture, mattresses, or decorations. One consequence of this is that several occupancy chapters have decided that upholstered furniture and mattress requirements (for both smoldering and flaming ignition) should not be applied to their occupancies. Chapter 10 of Appendix A contains a table with a summary of the generic requirements for interior finish for each type of material.

21.3.2.3 Uniform Fire Code

The new Uniform Fire Code (NFPA 1)²⁴ is a blend of two documents, the NFPA Fire Prevention Code (also known as NFPA 1) and the Uniform Fire Code previously issued by the Western Fire Chiefs, which was a partner of ICBO, when ICBO issued the UBC. The 2009 edition consists of 73 chapters, although several of them are “reserved” for future use.

The purpose of the Uniform Fire Code is to prescribe minimum requirements necessary to establish a reasonable level of fire and life safety, and property protection from the hazards created by fire, explosion, and dangerous conditions. It applies to both new and existing conditions. If there is a conflict between a general requirement and a specific requirement for a particular occupancy or situation, the specific requirement applies. If two or more classes of occupancy occur in the same building or structure, and are so intermingled that separate safeguards are impracticable, means of egress facilities, construction, protection, and other safeguards must comply with the most restrictive fire-safety requirements of the occupancies involved. The code also applies to vehicles and vessels when they are in a fixed location and are occupied as buildings. The code applies to buildings permitted for construction after the adoption of a particular edition of NFPA 1, but only with the provisions for new buildings. Buildings in existence or permitted for construction prior to the adoption of a particular edition of NFPA 1 must comply with the provisions for the existing buildings. Repairs, renovations, alterations, reconstruction, change of occupancy, and additions to buildings must comply with both NFPA 101 and the building code. Newly introduced equipment, materials, and operations regulated by NFPA 1 need to comply with the requirements for new construction or processes.

The scope of the Uniform Fire Code includes the following:

1. Inspection of permanent and temporary buildings, processes, equipment, systems, and other fire and related life safety situations
2. Investigation of fires, explosions, hazardous materials incidents, and other related emergency incidents
3. Review of design and construction plans, drawings, and specifications for life safety systems, fire protection systems, access, water supplies, processes, and hazardous materials and other fire and life safety issues

4. Fire and life safety education of fire brigades, employees, responsible parties, and the general public
5. Existing occupancies and conditions, the design and construction of new buildings, remodeling of existing buildings, and additions to existing buildings
6. Design, alteration, modification, construction, maintenance, and testing of fire protection systems and equipment
7. Access requirements for fire department operations
8. Hazards from outside fires in vegetation, trash, building debris, and other materials
9. Regulation and control of special events, including, but not limited to, assemblage of people, exhibits, trade shows, amusement parks, haunted houses, outdoor events, and other similar special temporary and permanent occupancies
10. Interior finish, decorations, furnishings, and other combustibles that contribute to fire spread, fire load, and smoke production
11. Storage, use, processing, handling, and on-site transportation of flammable and combustible gases, liquids, and solids
12. Storage, use, processing, handling, and on-site transportation of hazardous materials
13. Control of emergency operations and scenes
14. Conditions affecting fire-fighter safety

Chapter 10 addresses the various fire safety concerns, including combustible vegetation (which is usually not permitted in most of the occupancies) and other combustible contents. In particular, Section 10.20 in Chapter 10, addresses indoor children's playground structures, which exceed 3.1 m (10 ft) in height and 14.9 m² (160 ft²) in area. The materials of construction of these playgrounds must be among the following: fire retardant-treated wood, light-transmitting plastics, foam plastics, and balls with a maximum heat release rate of less than or equal to 100 kW when tested in accordance with UL 1975, aluminum composite materials that are Class A in ASTM E 84 or via NFPA 286, textiles and films complying with the flame propagation performance criteria of NFPA 701, and rigid plastic materials with a peak RHR less than or equal to 400 kW/m² when tested in accordance with ASTM E1354 at an incident heat flux of 50 kW/m² in the horizontal orientation at a thickness of 6 mm. The floor covering under the children's playground structure must meet a Class I interior floor finish classification in accordance with ASTM E 648 (flooring radiant panel).

Chapter 20 addresses the occupancy fire safety and this is where most requirements for reaction-to-fire testing are included, usually by "extraction" of the requirements from the Life Safety Code (NFPA 101), for interior finish, furnishings, and decorations.

Chapter 19 addresses the combustible waste and refuse, and includes the specific requirement that nonmetallic rubbish containers exceeding a capacity of 0.15 m³ (5 ft³ or 40 gal) should meet a peak RHR not exceeding 300 kW/m² at a flux of 50 kW/m² when tested in the horizontal orientation, at a thickness as used in the container but not less than 6 mm (0.25 in., 6 mm), in accordance with ASTM E 1354 (cone calorimeter).

Chapters 21 through 34 address individual occupancies. Chapter 60 addresses hazardous materials, and all subsequent chapters address some specific hazardous materials, including aerosols, compressed gases, corrosives, explosives, fireworks, flammable and combustible liquids, flammable solids, and toxics. Much of the old misleading information about some of these hazardous materials has been taken out of recent editions.

21.3.2.4 NFPA Building Code

The NFPA Building Construction and Safety Code or NFPA 5000¹²⁵ is the alternate building code to the IBC. In structure, it is similar to the Life Safety Code (NFPA 101), in that it starts with general requirements and then includes chapters on occupancies. It is also similar to the NFPA 1 and the UBC in that, after Chapter 40, it has specific chapters on individual materials, such as plastics, wood, glass, and gypsum board. It also contains a performance option alternative in Chapter 5.

NFPA 5000 addresses those construction, protection, and occupancy features necessary to minimize danger to life and property. The purpose of NFPA 5000 is to provide minimum design regulations to safeguard life, health, property, and public welfare, and to minimize injuries by regulating and controlling the permitting, design, construction, quality of materials, use and occupancy, location, and maintenance of all buildings and structures within the jurisdiction and certain equipment specifically regulated herein. The provisions of the code apply to the construction, alteration, repair, equipment, use and occupancy, maintenance, relocation, and demolition of every building or structure, or any appurtenances connected or attached to such buildings or structures within the jurisdiction. The provisions of the code also apply to existing buildings and structures if any one of the following conditions applies:

1. A change of use or occupancy classification occurs.
2. A repair, renovation, modification, reconstruction, or addition is made.
3. The building or structure is relocated.
4. The building is considered damaged, unsafe, or a fire hazard.
5. A property line that affects compliance with any provision of this code is created or relocated.

The key chapters are the following:

- Chapter 2: Mandatory references
- Chapter 3: Definitions of the terms
- Chapter 4: General
- Chapter 5: Performance-based code alternative
- Chapter 6: Classification of occupancy and hazard of contents
- Chapter 7: Construction types and heights and areas
- Chapter 8: Fire resistive construction
- Chapter 10: Interior finish, contents, and furnishings (key chapter on reaction to fire requirements)
- Chapter 11: Means of egress
- Chapters 16 through 33: New occupancy chapters
- Chapters 41 through 48: Materials (concrete, aluminum, masonry, steel, glass and glazing, gypsum board, and plastics)
- Chapter 55: Fire protection systems and equipment

Chapter 10 of NFPA 5000 is virtually identical to the corresponding chapter of NFPA 101, except that it does not address, of course, furniture, mattresses, or decorations. It also has a similar table in the appendix describing the requirements for each type of interior finish. In fact, the same technical committee is responsible for the Life Safety Code and Building Code chapters.

21.3.2.5 Buildings of Historic or Cultural Interest

There are two codes addressing buildings of particular interest: NFPA 909 Code for the Protection of Cultural Resource Properties—Museums, Libraries, and Places of Worship¹²⁶ and NFPA 914 (Code for Fire Protection of Historic Structures).¹²⁷ NFPA 909 and NFPA 914 include definitions for various terms, which are important to understand what the codes intend:

Cultural Resource Properties. Buildings, structures, sites, or portions thereof that are culturally significant or that house culturally significant collections for museums, libraries, and places of worship.

Historic Building. A building that is designated or deemed eligible for such designation, by a local, regional, or national jurisdiction as having historical, architectural, or cultural significance.

Historic Fabric. Original or added building or construction materials, features, and finishes that existed during the period that is deemed to be most architecturally or historically significant, or both.

Historic Preservation. A generic term that encompasses all aspects of the professional and public concern related to the maintenance of a historic structure, site, or element in its current condition, as originally constructed, or with the additions and alterations determined to have acquired significance over time.

Historic Site. A place, often with associated structures, having historic significance.

Historic Structure. A building, bridge, lighthouse, monument, pier, vessel, or other construction that is designated or that is deemed eligible for such designation by a local, regional, or national jurisdiction as having historical, architectural, or cultural significance.

Therefore, the intent is for NFPA 909 to address buildings, new or old, that have cultural significance, either because of their contents (museums, libraries, and the like) or because they are used for religious ceremonies. On the other hand, NFPA 914 deals with older buildings (or structures) that have some historic significance, because of some particular historic association with the building. In many countries, buildings or structures are entitled to be declared as having historic significance if they are more than 100 years old. However, not every structure that has survived for 100 years may be of historic significance. Usually, there is a need for the AHJ to make a determination that the building or structure is associated with some historic event or represents some very unusual characteristic that makes it worth preserving (and often expending the necessary funds to update it for fire safety). Libraries, museums, and places of worship that are housed in historic structures need to comply with the requirements of both NFPA 909 and NFPA 914. In the NFPA system, the three key codes: the building code, the life safety code, and the fire code, all incorporate special considerations for historic buildings, which comply with NFPA 914. On the other hand, only NFPA 5000 (the building code) and NFPA 1 (Uniform Fire Code) incorporate requirements for NFPA 909; they say that buildings, structures, or spaces that are or contain cultural resource properties must be constructed in accordance with NFPA 909. In the ICC set of codes, there are no references to either of these codes, because the concept of buildings of particular significance is not considered.

The requirements contained in both of these codes tend to represent a lower level of passive fire protection than in other buildings (especially for NFPA 914), because of the interest in preserving the historic “look.”

21.3.2.6 Ships

NFPA has issued NFPA 301⁴⁷ to allow regulation of merchant vessels (ships) to be based on a consensus document. The code covers three types of vessels: passenger, cargo, and tank vessels and it is intended to apply to ocean-going towing vessels in future editions, in anticipation of an expected U.S. law mandating fire-protection upgrades. Future editions may also add other types of vessels. Chapter 8 contains general fire-safety requirements for any vessel, but they will only apply if referenced in the specific vessel or occupancy chapter. This chapter includes requirements for interior finish, upholstered furniture, mattresses, case furniture, draperies, stacking chairs, nonmetallic rubbish containers, and contains the overall requirements for electrical and optical fiber wires and cables. Interior wall and ceiling finish must comply with the FSI and the SDI of 20 and 10, respectively, based on ASTM E 84¹⁴ or they must meet the same requirements as in building codes, when tested based on the room-corner test (NFPA 286¹⁵). They are also allowed to comply with the requirements of the IMO FTP code,⁴³ which involves testing for smoke obscuration (based on ASTM E 1995¹²⁸ or NFPA 270¹²⁹ or ISO 5659-2¹³⁰), flame spread (based on the apparatus also used for the Lateral Ignition and Flame Spread Test [LIFT] test, per ASTM E 1317),¹³¹ and heat content (based on ISO 1716).¹³² Upholstered furniture must meet the requirements of the ASTM E 1537 full-scale heat release test,⁹² with the requirements of CA TB 133.⁹¹ Mattresses must meet the requirements of the ASTM E 1590 full-scale heat release test,⁸⁵ with the requirements of CA TB 129.⁸² The

requirements for furnishings in this chapter would result in better fire safety than those associated with the IMO SOLAS fire tests,⁴¹⁻⁴³ but unfortunately, the code includes statements that exclude requirements if the space is fully protected by a sprinkler or water mist system. Stacking chairs must meet the requirements that ensure that each chair cannot cause flashover in the small compartments. Nonmetallic rubbish containers must meet a cone calorimeter pass/fail criterion. The requirements for wire and cable are based on those of the National Electrical Code,⁷ except that the minimum requirements are that cables meet the UL 1581 vertical cable tray fire test⁵⁹ and they need not be grounded (a logical requirement in ships).

Chapters 10 through 17 address the individual spaces within each type of vessel; the key chapters associated with fire safety are the ones for accommodation spaces (Chapter 10) and medical spaces (Chapter 11). Chapter 21 is the overall chapter for passenger vessels and it is here that the requirements from earlier chapters are called for or not. A key requirement in this chapter is the one that requires that an automatic sprinkler system or a water mist system be installed on Group I and Group II passenger vessels and on all passenger vessels with overnight accommodations for passengers, to protect all accommodation, service, and storage spaces. Group I passenger vessels are those with either over 3000-day passengers or over 300-overnight passengers and Group II passenger vessels are those with either over 1000- and under 3000-day passengers or over 150- and under 300-overnight passengers.

Neither cargo vessels nor tank vessels have too many requirements associated with fire safety, and the key issues covered in their chapter (Chapter 20) are construction specifications and active fire protection. However, the code also states that interior finish and furnishings in exits and exit accesses must meet the requirements of Chapter 8 and that accommodation spaces must meet the requirements of Chapter 10 (and these vessels are rarely sprinklered).

21.3.2.7 Manufactured Housing

Manufactured homes are built and installed according to the U.S. Department of Housing and Urban Development's (HUD) Manufactured Home Construction and Safety Standards (MHCSS). The standards address structural, fire safety, and energy-efficiency issues and require adequate ventilation. This regulation supersedes local and state building codes and is the current minimum standard that all HUD-code homes are required to meet. The NFPA periodically updates NFPA 501, Standard on Manufactured Housing.¹²² NFPA 501 is the standard currently approved by the industry and other stakeholders, but has yet to be officially adopted by HUD. The NFPA standard does not have authority over the older MHCSS regulation, but rather provides recommendations to HUD. Research conducted in 2004 by the U.S. Department of Energy (DOE) authors has contributed to NFPA 501's improved stringency of thermal efficiency. NFPA 501 has also incorporated improvements over the current HUD-code based on the experiences of energy-efficient manufactured home programs and fire safety, an area in which improvements continue, as it has happened with all consensus standards.

In terms of fire safety, there are no fire resistance requirements and all interior surfaces must comply with the FSI of 200 in the Steiner tunnel test, ASTM E 84,¹¹⁴ or a radiant panel index of 200 in the radiant panel test, ASTM E 162.⁵⁵ Thermal insulation materials, other than foam plastics, must meet an ASTM E 84 Class A requirement (i.e., FSI \leq 25 and SDI \leq 450) and loose-fill insulation must meet the same requirements as the building codes, which are mostly based on smoldering tests (as the materials tend to be cellulosic). Foam plastic insulation must be treated as in the building codes as well (see Table 21.13): it cannot be used exposed (expensive foam that meets the NFPA 286 test is not used in manufactured housing) and must meet an ASTM E 84 Class B requirement behind the thermal barrier.

21.3.2.8 Air Conditioning Standard

NFPA 90A⁹ is a key document, because it controls all the fire-safety requirements for ducts and plenums in the NFPA system. The requirements are basically very similar to those in the IMC.

The only materials permitted in plenums are: wires and cables that meet the criteria based on the NFPA 262⁶⁵ plenum cable fire test or that are enclosed in noncombustible raceways, pneumatic tubing, based on UL 1820,¹¹⁷ nonmetallic sprinkler pipes, based on UL 1887,¹¹⁸ fiber optic raceway systems, based on UL 2024,¹¹⁹ and combustible electrical equipment, based on UL 2043,¹²⁰ so that each one is covered by a special test for that product. Foam plastic wall and ceiling insulation must meet the NFPA 286 room-corner test or be covered by a thermal barrier or a steel skin. All other materials, including pipe and duct insulation, must meet the requirements of the FSI of 25 and the SDI of 50 in the ASTM E 84 Steiner tunnel test (a much more severe smoke criterion than that for nonplenum areas, where the SDI is allowed to reach 450). The standard also notes that electrical wires and cables listed to a more severe requirement, UL 2424¹³³ can be used without further testing; this is very important, because the UL 2424 requirement is based on “limited combustible” cables, that have a very low heat content (when tested to NFPA 259)¹³⁴ and a very low smoke release (when tested to ASTM E 84); they are almost invariably constructed of fluoropolymer materials, while other plenum cables tend to be constructed of fire retarded materials. It also notes that electrical wires and cables as well as optical fiber cables installed in the metal raceways or metal-sheathed cable are not considered to be exposed to the airflow, and need not meet the requirements of NFPA 262. Plenum cables are permitted to be installed in three of the types of plenums covered by the standard: ceiling cavity plenums, raised floor plenums, and air-handling room plenums, but not in apparatus casing plenums or in ducts. The materials of construction of the plenums themselves, and all other plenum or duct contents, must be made of “limited combustible” materials. Finally, ducts and plenums are not permitted to be used for storage.

It is of interest to point out that there has been much debate regarding the use of plenum cables, owing to various attempts to replace them by cables complying with UL 2424. These efforts were unsuccessful, because they have been seen by committee members, NFPA members and public officials as an attempt by certain manufacturers to gain market share without a justification based on fire safety or fire losses.

21.3.2.9 Other NFPA Codes and Standards

As discussed earlier, NFPA 130¹¹ is another important document, because it is used for the regulation of train and underground system, by authorities having jurisdiction over local rail systems in some U.S. systems, some Canadian ones, and some Asian ones. Table 21.6 shows the reaction-to-fire requirements for rail cars. NFPA 130 also includes requirements for stations and trainways as well as rail vehicles. The key issues to be considered in stations are the same as in other assembly occupancies, namely electrical, interior finish, upholstered furniture, decorations, and trash disposal. With regard to trainways, the standard looks at the effect of areas that are potentially concealed spaces and considers that factor.

The NFPA 13 series of sprinkler standards (NFPA 13,¹⁰ 13D,¹³⁵ and 13R¹³⁶) form the bases for all the requirements for sprinkler installations in the United States (and probably worldwide). These standards do not contain any requirements for passive fire protection, but explain how to install sprinklers and in what spaces the sprinkler protection is needed. The recent adoption of requirements for sprinklers in residences and townhouses in the IRC is based on NFPA 13D systems, but most nonresidential occupancies are sprinklered based on the more stringent NFPA 13 systems.

NFPA 99¹³⁷ governs all health care occupancies, in conjunction with the Life Safety Code and the National Electrical Code. In fact virtually all hospitals, and the Joint Commission for the Accreditation of Healthcare Organizations (JCAHO), which regulates hospitals, use the combination mentioned earlier almost without any other consideration.

Other NFPA documents that are important for specific applications are NFPA 30 (Flammable and Combustible Liquids Code), NFPA 54 (National Fuel Gas Code), NFPA 75 (Standard for the Protection of Information Technology Equipment), and NFPA 318 (Standard for the Protection of Semiconductor Fabrication Facilities).

21.3.3 INTERNATIONAL ASSOCIATION OF PLUMBING AND MECHANICAL OFFICIALS CODES

Beyond the Western Fire Chiefs Association issuing the Uniform Fire Code, now NFPA 1, another organization was a partner to ICBO, namely the International Association of Plumbing and Mechanical Officials (IAPMO) who issued the Uniform Mechanical Code (UMC)¹³⁸ and the Uniform Plumbing Code (UPC). They continue to do so, but now have an agreement with NFPA so that the UMC and the UPC are NFPA's equivalents to the ICC codes. The UPC has little, if any, importance with regard to fire issues.

21.3.3.1 Uniform Mechanical Code

The UMC applies to the addition to or erection, installation, alteration, repair, relocation, replacement, use or maintenance of heating, ventilating, cooling, refrigeration systems, incineration, or other miscellaneous heat-producing appliances. It also covers design. In effect, there is a considerable amount of overlap with NFPA 90A.⁹

The key provisions covered by this code are those for materials in ducts and plenums and for hydronic piping systems. Just like in the IMC and in NFPA 90A, the only materials permitted in plenums are: wires and cables that meet criteria based on the NFPA 262⁶⁵ plenum cable fire test or that are enclosed in noncombustible raceways, pneumatic tubing, based on UL 1820,¹¹⁷ sprinkler pipes, based on UL 1887,¹¹⁸ fiber optic raceway systems, based on UL 2024,¹¹⁹ and loudspeakers and recessed lighting fixtures, based on UL 2043,¹²⁰ so that each one is covered by a special test for that product. Foam plastic wall and ceiling insulation must meet the NFPA 286 room-corner test or be covered by a thermal barrier or by a steel skin. All other materials, including pipe and duct insulation, must meet the requirements of the FSI of 25 and the SDI of 50 in the ASTM E 84 Steiner tunnel test (a much more severe smoke criterion than that for nonplenum areas, where the SDI is allowed to reach 450). However, insulation of hydronic pipe systems is allowed to be tested by NFPA 274,¹³⁹ instead of using ASTM E 84 (with the 25/50 pass/fail criteria). NFPA 274 is a heat release test in which a set of pipes is insulated in a vertical chase, exposed to a gas burner and the heat and smoke release are measured. The pass/fail criteria used by the UMC are: a maximum peak heat release rate of 300 kW, a maximum total heat release of 50 MJ, a maximum total smoke release of 500 m², and the flames cannot extend 305 mm or more above the top of the vertical portion of the apparatus at any time during the test. The UMC also explicitly permits (if listed) a series of specific piping materials permitted for use in these systems.

21.4 STANDARDS

21.4.1 ORGANIZATIONS AND COMMITTEES ISSUING FIRE STANDARDS OR STANDARDS WITH FIRE TESTS

As discussed earlier, fire test standards are developed primarily in the United States by the ASTM International and NFPA, although FM Global (formerly, Factory Mutual) and ULs have also developed some widely used tests. Within ASTM, the following committees have developed fire tests:

- ASTM E05: fire standards (primary fire standards development committee, with subcommittees on smoke and combustion products (which includes heat release), surface burning, combustibility, external fire exposures, furnishings and contents, transportation, large-scale tests, and fire resistance)
- ASTM C16: thermal insulation
- ASTM D07: wood (primarily subcommittee D07.07)
- ASTM D09: electrical and electronic insulating materials (primarily subcommittee D09.21)
- ASTM D13: textiles (primarily subcommittee D13.52)

- ASTM D20: plastics (primarily subcommittee D20.30)
- ASTM F15: consumer products
- ASTM F23: personal protective clothing and equipment (primarily subcommittee F23.80)
- ASTM F25: ships and marine technology (primarily subcommittee F25.03)
- ASTM F33: detention and correctional facilities (primarily subcommittee F33.05)

These same committees have also developed some specifications and practices which reference fire tests (and pass/fail criteria), and also occasionally contain some new fire tests. The NFPA Technical Committee on Fire Tests is the developer of all fire tests for NFPA. Two other international organizations are systematic developers of fire tests, most of which are primarily used in Europe: International Organization for Standardization (ISO) and IEC. Within ISO and IEC, the key technical committees are:

- ISO TC92: fire safety (with subcommittees on fire initiation and growth, fire containment (or fire resistance), fire threat to people and the environment (or smoke toxicity), and fire-safety engineering)
- ISO TC61: plastics (primarily subcommittee SC4)
- IEC TC20: Electric cables
- IEC TC89: Fire-hazard testing

There is an agreement between ASTM Committee E05, the NFPA Fire Tests Committee, and UL that duplication of fire-test standards between those organizations must be minimized.

21.4.2 STANDARD TEST METHODS

21.4.2.1 Ignitability

Unless a material ignites, there is no fire. Therefore, low ignitability is a key property. All combustible materials ignite, but, from the point of view of ignitability, the higher the temperature that a material has to reach before it ignites (or the longer time until it reaches that temperature), the safer it is. Therefore, measures of ignition are of three types:

1. The minimum temperature for ignition (in the absence or presence of a pilot source of ignition),
2. The time to ignition under a certain applied thermal insult (typically, a heat flux or a flame of a particular size), and
3. The minimum (or critical) heat flux required to reach ignition (because temperature and heat flux can be correlated with the Stefan–Boltzmann constant and black-body radiation).

The traditional method of assessing ignition temperatures is done with a test, such as the Setchkin chamber (ASTM D 1929),¹⁴⁰ which has been used for many years to determine self-ignition temperatures and flash-ignition temperatures (with an applied pilot flame) of many materials. ASTM D 1929 uses small pieces (typically pellets) as specimens, exposed inside a vertical furnace tube, heated electrically, under a slow air flow. Its results are no longer considered very indicative of fire hazard, because the exposure is not truly representative of real fires. However, results from this test are frequently required in specifications and quoted in data sheets, and the test is referenced in building codes to determine the suitability of some plastics for use in construction, because it represents an easily understandable single number. The time to ignition at a certain incident heat flux is an excellent way of comparing material properties, but it will give a numerical result only, of course, if the heat flux is high enough to cause ignition. The advantage of the critical heat flux for ignition is

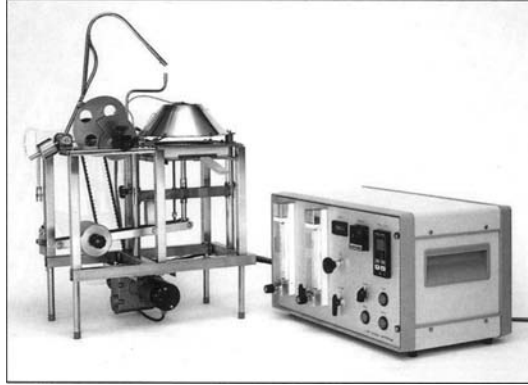


FIGURE 21.6 ISO 5657 ignitability apparatus.



FIGURE 21.7 Cone calorimeter.



FIGURE 21.8 OSU heat release rate calorimeter.

that it can always be assessed; it results from extrapolation after measurements made at a variety of heat fluxes.

There are three other standard test methods used purely for assessing ignitability: a radiant cone heater with an intermittent gas-flame igniter (ISO 5657,¹⁴¹ Figure 21.6, sometimes called the dipping duck test because of the shape of the igniter) and two tests for electrical materials coated onto wires: ASTM D 3874¹⁴² or IEC 60695-2-2¹⁴³ (needle flame test) and ASTM D 6194¹⁴⁴ or IEC 60695-2-10¹⁴⁵ (glow wire test). The glow wire test involves bringing an electrically heated wire in contact with the material and simulating the thermal stresses resulting from faults or overload conditions during cable use. The needle flame test simulates the flame that can result from a fault or overload condition. The needle flame test can also be used to obtain information on flame spread. In the case of the glow wire ignition test (ASTM D 6194 or IEC 60695-2-10), the information obtained is the temperature (in °C) at which the coated wire ignites, and the thickness of the coating required for ignition. In the case of the needle flame ignition test (ASTM D 3874 or IEC 60695-2-2), the information obtained is whether ignition occurred and whether it happened with edge flames (E) or with facing flames (F), as well as the thickness of the coating required for ignition. Edge flames are a more severe ignition source than the facing flames, so that if there is no ignition with edge flames, ignition will not occur with the facing flames. Similarly, ignition becomes more likely with the sample becoming thinner, and hence, if ignition does not occur at 1 mm, it will not occur at 3 mm thickness, but the reverse is not the case.

Other test methods can also be used to assess ignitability, together with other properties. Some important ones are: the cone calorimeter (ASTM E 1354,⁷¹ Figure 21.7, which has the assessment of heat and smoke release as its primary purpose); the OSU calorimeter (ASTM E 906,³⁸ Figure 21.8, which also

has the assessment of heat and smoke release as its primary purpose, and which is used by the FAA for regulatory purposes, as discussed earlier), and the Lateral Ignition and Flame Spread Test (LIFT, ASTM E 1321,¹⁴⁶ Figure 21.9, which has the assessment of flame spread as its primary purpose).

A study demonstrated the time-to-ignition (at three incident heat fluxes) in the cone calorimeter for a set of 35 materials (all plastics and Douglas fir wood) (Table 21.15).¹⁴⁷ Materials that do not ignite under the heat flux to which they have been exposed are shown as having the (arbitrary) time to ignition of 10,000s. Table 21.15 also shows the minimum ignition flux to cause ignition within 100s or 600s, from the same test method. While a higher time to ignition represents better ignitability performance, the opposite is true for the critical ignition flux: the higher, the better. It should be noted that the value presented for the extrapolation of the critical flux for ignition is not reliable under 15 kW/m^2 , and hence, all such data are shown as " $\leq 15 \text{ kW/m}^2$."

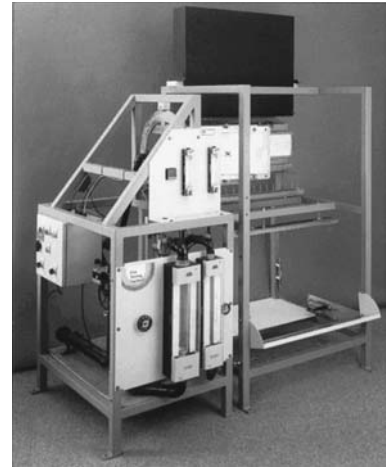


FIGURE 21.9 Lateral ignition and flame spread test.

TABLE 21.15
Ignitability of Materials in the Cone Calorimeter

	Time to Ignition (in s) at Heat Flux			Heat Flux (in kW/m^2) for a Time to Ignition of	
	20 kW/m^2	40 kW/m^2	70 kW/m^2	600s	100s
PTFE NV	10,000	10,000	252	63	83
VTE 3 V	10,000	1,212	17	45	64
VTE 2 V	10,000	1,253	424	60	110
VTE 4 V	10,000	10,000	1583	86	115
PCARB NV	10,000	182	75	34	43
VTE 1 V	10,000	1,271	60	47	65
CPVC V	10,000	621	372	42	90
PVC CIM V	5,159	73	45	30	39
PVC WC FR V	236	47	12	≤ 15	31
PVC LS V	5,171	187	43	33	44
XLPE NV	750	105	35	22	40
PVC WC SM V	176	36	14	≤ 15	27
PVC EXT V	3,591	85	48	30	39
PVC WC V	117	27	11	≤ 15	22
ACR FR NV	200	38	12	≤ 15	28
PCARB B NV	6,400	144	45	32	42
PPO GLAS NV	465	45	35	18	33
PPO/PS NV	479	87	39	17	38
ABS FV NV	5,198	61	39	30	38
ABS FR NV	212	66	39	≤ 15	33
FL PVC V	102	21	15	≤ 15	20
DFIR NV	254	34	12	≤ 15	29
PS FR NV	244	90	51	≤ 15	38

TABLE 21.15 (continued)
Ignitability of Materials in the Cone Calorimeter

	Time to Ignition (in s) at Heat Flux			Heat Flux (in kW/m ²) for a Time to Ignition of	
	20kW/m ²	40kW/m ²	70kW/m ²	600s	100s
ACET NV	259	74	24	≤15	35
PU NV	12	1	1	≤15	≤15
PMMA NV	176	36	11	≤15	27
THM PU NV	302	60	38	≤15	34
NYLON NV	1,923	65	31	27	37
ABS NV	236	69	48	≤15	34
PS NV	417	97	50	15	40
EPDM/SAN NV	486	68	36	18	36
PBT NV	609	113	59	20	41
PET NV	718	116	42	22	42
PE NV	403	159	47	≤15	50
PP NV	218	86	41	≤15	37

Abbreviation: PTFE, polytetrafluoroethylene sheet (samples were two sheets with 3 mm thickness each, Du Pont); VTE 3, flexible vinyl thermoplastic elastomer alloy wire and cable jacket experimental compound, example of the third of several families of VTE alloys; VTE 2, flexible vinyl thermoplastic elastomer alloy wire and cable jacket experimental compound, example of the second of several families of VTE alloys; VTE 4, semiflexible vinyl thermoplastic elastomer alloy wire and cable jacket experimental compound, example of a family of VTE alloys containing CPVC; PCARB, polycarbonate sheeting (Lexan 141–111, General Electric); VTE 1, flexible vinyl thermoplastic elastomer alloy wire and cable jacket experimental compound, example of the first of several families of VTE alloys; CPVC, chlorinated poly(vinyl chloride) sheet compound (BFGoodrich); PVC CIM, poly(vinyl chloride) general purpose rigid custom injection molding compound with impact modifier additives (BFGoodrich); PVC WC FR, flexible wire and cable poly(vinyl chloride) compound (containing fire retardants) (BFGoodrich); PVC LS, poly(vinyl chloride) rigid experimental sheet extrusion compound with smoke suppressant additives (BFGoodrich); XLPE, black nonhalogen flame retardant, irradiation crosslinkable, polyethylene copolymer cable jacket compound (DEQD-1388, Union Carbide); PVC WC SM, flexible wire and cable poly(vinyl chloride) compound (containing minimal amounts of fire retardants) (BFGoodrich); PVC EXT, poly(vinyl chloride) rigid weatherable extrusion compound with minimal additives (BFGoodrich); PVC WC, flexible wire and cable poly(vinyl chloride) compound (nonfire retarded) (BFGoodrich); ACR FR, Kydex: fire retarded acrylic paneling, blue (samples were 4 sheets at 1.5 mm thickness each, Kleerdex); PCARB B, commercial polycarbonate sheeting (Commercial Plastics); PPO GLAS, blend of polyphenylene oxide and polystyrene containing 30% fiberglass (Noryl GFN-3-70, General Electric); PPO/PS, blend of polyphenylene oxide and polystyrene (Noryl N190, General Electric); ABS FV, polymeric system containing acrylonitrile butadiene styrene and some poly(vinyl chloride) as additive; ABS FR, Cyclocac KJT acrylonitrile butadiene styrene terpolymer fire retarded with bromine compounds (Borg Warner); FL PVC, standard flexible poly(vinyl chloride) compound (noncommercial; similar to a wire and cable compound) used for various sets of testing (including Cone Calorimeter RHR ASTM round robin; it contains PVC resin 100phr; diisodecyl phthalate 65phr; tribasic lead sulphate 5phr; calcium carbonate 40phr; stearic acid 0.25phr); DFIR, Douglas fir wood board; PS FR, fire retarded polystyrene, Huntsman 351 (Huntsman); ACET, polyacetal: polyformaldehyde (Delrin, Commercial Plastics); PU, polyurethane flexible foam, nonfire retarded (Jo-Ann Fabrics); PMMA, poly(methyl methacrylate) (25 mm thick, lined with cardboard, standard RHR sample); THM PU, thermoplastic polyurethane containing fire retardants (estane, BFGoodrich); NYLON, nylon 6,6 compound (Zytel 103 HSL, Du Pont); ABS, Cyclocac CTB acrylonitrile butadiene styrene terpolymer (Borg Warner); PS, polystyrene, Huntsman 333 (Huntsman); EPDM, copolymer of ethylene propylene diene rubber (EPDM) and styrene acrylonitrile (SAN) (Rovel 701); PBT, polybutylene terephthalate sheet (Celanex 2000-2 polyester, Hoechst Celanese); PET, polyethylene terephthalate soft drink bottle compound; PE, polyethylene (Marlex HXM 50100); PP, polypropylene (Dypro 8938).

21.4.2.2 Ease of Extinction

Once ignited, if it is easier to extinguish a material, then the resulting fire hazard is lower. ASTM D 2863¹⁴⁸ is used to determine the limiting oxygen index (or LOI, Figure 21.10), which is the minimum oxygen concentration (in a flowing mixture of oxygen and nitrogen) required to support candle-like downward flaming combustion. This means that, in principle, a material with LOI values above 25–27 should only burn under extreme conditions. In reality, the test serves principally as a measure of the ease of extinction of the material. The small specimen is placed vertically inside a glass column and ignited at the top with a small gas flame. This test method has excellent repeatability and reproducibility, and can generate numerical data covering a very broad range of fire performance. However, once more, the test method is inappropriate as a predictor of real-scale fire performance, mainly because of the low heat input and the artificiality of the high oxygen environments used. It is widely required in specifications and quoted in data sheets, and is suitable as a quantitative quality control tool during manufacturing, and as a semiquantitative indicator of the effectiveness of additives, during research and development, for low incident energy situations.

An application of this test method is ISO 4589-3,¹⁴⁹ a method which assesses the LOI at a variety of temperatures (Figure 21.11). The combination of these results allows a prediction of the flammability temperature, at which the LOI has a predicted value of 21, and the percentage of ash remaining after the test.

21.4.2.3 Flammability

Once ignited, the greater the flammability of a material, the greater will be the hazard associated with it. A small-scale flammability test which is very extensively used for plastic materials is the family of UL 94 tests¹⁵⁰ also standardized in ASTM, ISO, and IEC, but most widely known by the UL standard designation).

In this test, a small sample of material (127 mm × 13 mm, or 5 in. × 0.5 in.) is exposed vertically to a small Bunsen burner-type flame from underneath (in the UL 94 V test) and the results show a rating, ranging from V-0 (best), through V-1, V-2 to “B” (for Burn). Materials with a “B” rating on the UL 94 Vertical test can also be tested in the less severe UL 94 HB (for horizontal burning), where the assessment is whether a flame spread rate of 4 in./min is achieved. It is the most widely used fire-test specification for plastic materials, especially fire-retarded ones, and forms the basis of the famous “Yellow Card” used by ULs to list the plastic materials. The results from these tests are almost invariably found in a variety of specifications and data sheets.

21.4.2.4 Flame Spread

The tendency of a material to spread a flame away from the fire source is critical to understand the potential fire hazard. Flame-spread tests may refer to organic polymers themselves or to materials in diverse applications (such as textiles or electrical insulation sleeving), or to whole structures



FIGURE 21.10 Oxygen index fire test apparatus.



FIGURE 21.11 Temperature index apparatus.

(such as furniture or building components). Most of the tests can be classified in terms of the angle between the exposed surface and the horizontal. Thus, this angle may vary between 0° , for a horizontal material burning on its upper surface, through 180° , for a horizontal material burning on its lower surface, and 240° , for a material burning on its lower surface but rotated a further 60° from the horizontal, up to 270° , for a material burning vertically downward.¹⁵¹ This surface angle is closely related both to the extent to which the gaseous products of combustion heat the surface before the flame front reaches it, and to the extent to which the hot gases penetrate into the polymer. Sample sizes can range very widely, from very small to quite large (7.3 m \times 0.56 m, or 24 ft \times 22 in., ASTM E 84).¹¹⁴

Two other test apparatuses are also suitable to assess flame spread of materials: those in ASTM E 162,⁵⁵ radiant panel (which is also used for cellular plastics, as ASTM D 3675¹⁵²) and the one in ASTM E 1321,¹⁴⁶ also known as the LIFT test. A variation of the latter is used by the marine industry (ASTM E 1317).¹³¹

The Steiner tunnel test method (ASTM E 84)¹¹⁴ was developed by Al Steiner for building materials,¹⁵³ such as wood or gypsum board. It has been adopted by every building and fire code in the United States. It is perhaps the most widely accepted test for surface flammability in North America, and there are a large number of application tests developed from it. The most famous is the one used for electrical cables needed for plenum use (NFPA 262,⁶⁵ formerly also known as UL 910, now withdrawn), and there are also application tests for pneumatic tubing, sprinkler piping, and optical fiber raceways. The specimen in ASTM E 84 is a building material (normally up to 0.15 m thick), either in one unbroken length or in separate sections joined end-to-end, which is mounted face downward, so as to form the roof of a horizontal tunnel 305-mm high. The fire source, two gas burners, ignites the sample from below with an 89 kW fire source. When plastics were started to being used in construction, this test was applied to them, in spite of the fact that it is not always appropriate. For example, samples that cannot be retained in place above the tunnel floor, or which melt and continue burning on the tunnel floor (typical behavior for most thermoplastics) are still being tested with this equipment, in spite of the results being misleading. It can also produce wrong results for thin materials.¹⁵⁴ The normal output is the FSI, calculated based on the area under the flame-spread distance vs. time curve. The FSI index is a relative number based on an FSI = 0 for cement board and FSI = 100 for red oak flooring. The results are used in the codes as classes, with Class A being an FSI of up to 25, Class B being an FSI of 26 up to 75, and Class C being an FSI of 76 up to 200. The test method also assesses smoke obscuration, and assigns the SDI, based on a similar concept to the FSI. To be classified as Class A, B, or C, a material must have an SDI not exceeding 450.

ASTM Test Method E 162⁵⁵ (Figure 21.12) is also used to determine the FSI, albeit different from the one assessed by the Steiner tunnel, and it is normally known as the radiant panel index. The radiant panel index is calculated as the product of a “flame spread factor” and a “heat evolution factor,” using techniques described in the standard. The test apparatus consists of a gas-fed radiant panel, in front of which an inclined (at a 30° angle) specimen (150 \times 460 mm) is exposed to a radiant flux equivalent to a black body temperature of 670°C (943°K), namely approximately 45 kW/m^2 , in the presence of a small gas pilot flame. The maximum thickness that can be tested in the normal specimen holder is 25 mm, but alternative specimen holders can accommodate thicker specimens. The ignition is forced near the upper edge of the specimen and the flame front progresses downward. The radiant panel index (I_s) (formerly, FSI) is calculated as



FIGURE 21.12 ASTM E 162 radiant panel test.

the product of a flame-spread factor, which results from the measurements of flame-front position and time, and a heat evolution factor, which is proportional to the maximum temperature measured in the exhaust stack. This test has also not been shown to be an adequate predictor of real-scale fire performance. If the specimen melts or causes flaming drips, this is likely to affect the flame spread in a way that is uneven. The test method simply requires that such events be reported. Moreover, if flame spread is very rapid, the flame-spread value is potentially lost unless recording is continuous. This apparatus is often referred to as the radiant panel, and results from this test are frequently required in regulations, particularly, for the transportation environments (both foamed and rigid materials) and detention environment specifications (foamed materials), and are quoted in the data sheets.

The LIFT apparatus (ASTM E 1321)¹⁴⁶ was developed as an improvement on the apparatus in ASTM E 162.⁵⁵ The specimen size for flame spread studies is 155 × 800 mm, with a maximum thickness of 50 mm (and a smaller specimen is used for ignition studies). The test method determines the critical flux for flame spread, the surface temperature needed for flame spread, and the thermal inertia or thermal heating property (product of the thermal conductivity, density, and specific heat) of the material under test. These properties are mainly used for assessment of fire hazard and input into fire models. A flame-spread parameter is also determined, and this can be used as a direct way of comparing the responses of the specimens. This test method appears well-suited for materials (or composites), which are nonmelting and which can be ignited without raising the incident flux to potentially dangerous limits. It has been used successfully for the predictions of full-scale flame-spread performance.¹⁵⁵

21.4.2.5 Heat Release

The key question to ask in a fire accident is: “How big is the fire?” The critical fire property that presents the answer to that question is the maximum RHR. A burning product will spread a fire to the nearby products, only if it gives off enough heat to ignite them. Moreover, the heat has to be released fast enough not to be dissipated or lost while traveling through the cold air surrounding any product that is not on fire. Therefore, fire hazard is dominated by the RHR.^{110,156–161} In fact, the RHR has been shown to be much more important than either ease of ignition, smoke toxicity, or flame spread in controlling the time available for potential victims of a fire to escape.¹⁶² In the late 1960s, Edwin Smith, at the OSU, developed the first bench-scale test instrument, the OSU RHR calorimeter (ASTM E 906),³⁸ to measure RHR.¹⁶³

In the early 1980s, Vytenis Babrauskas, at the NIST (then NBS), developed a more advanced test method to measure RHR: the cone calorimeter (ASTM E 1354).^{71,164} This fire test instrument can also be used to assess other fire properties, the most important of which are the ignitability (as discussed earlier), mass loss, and smoke released. Moreover, results from this instrument correlate with those from full-scale fires.^{165–170} To obtain the best overall understanding of the fire performance of the materials, it is important to test the materials under a variety of conditions. Therefore, tests are often conducted at a variety of incident heat fluxes. The peak rates of heat release (and total heat released) of the same materials shown in Table 21.15 at each incident flux, are shown in Table 21.16.¹⁴⁷

A number of modern full-scale fire test methods have been developed for products, relying on heat release rate measurements, such as those involving testing of upholstered furniture (ASTM E 1537⁹² and CA TB 133⁹¹), mattresses (ASTM E 1590,⁸⁵ CA TB 129,⁸² CA TB 603,⁸⁸ 16 CFR 1633,¹⁹ and ASTM F 1085 [Annexes A1 and A3]¹⁷¹), stacking chairs (ASTM E 1822¹⁷²), electrical cables (ASTM D 5424,¹⁷³ ASTM D 5537,¹⁷⁴ and UL 1685¹²³), plastic display stands (UL 1975),¹⁷⁵ other decorative items (NFPA 289,¹⁷⁶ a generic furniture calorimeter test), electrical equipment (UL 2043),¹²⁰ or wall-lining products (NFPA 265,¹¹⁶ NFPA 286,¹¹⁵ ASTM E 2257,¹⁷⁷ and ISO 9705¹⁷⁸). In fact, room-corner tests are now being used in the codes, as alternatives to replace the

TABLE 21.16
Heat Release (of the Materials listed in Table 21.15) in the Cone
Calorimeter (ASTM E 1354) at Three Incident Heat Fluxes

Material	Flux 20kW/m ²		Flux 40kW/m ²		Flux 70kW/m ²	
	Pk RHR (kW/m ²)	THR (MJ/m ²)	Pk RHR (kW/m ²)	THR (MJ/m ²)	Pk RHR (kW/m ²)	THR (MJ/m ²)
PTFE	3	0.3	13	11.7	161	69.1
VTE 3	4	5.1	43	31.5	70	48.8
VTE 2	9	5.7	64	66.1	100	39.0
VTE 4	14	13.2	87	25.9	66	57.4
PCARB	16	0.1	429	119.2	342	121.7
VTE 1	19	12.2	77	48.1	120	63.4
CPVC	25	14.7	84	37.4	93	44.9
PVC CIM	40	3.0	175	24.3	191	93.0
PVC WC FR	72	36.5	92	51.7	134	65.5
PVC LS	75	6.6	111	73.6	126	75.5
XLPE	88	87.6	192	126.2	268	129.2
PVC WC SM	90	49.0	142	75.4	186	73.4
PVC EXT	102	2.9	183	90.8	190	96.5
PVC WC	116	47.3	167	95.7	232	94.4
ACR FR	117	20.5	176	86.7	242	77.2
PCARB B	144	35.4	420	134.7	535	143.5
PPO GLAS	154	111.0	276	125.8	386	125.7
PPO/PS	219	103.6	265	128.5	301	134.3
ABS FV	224	80.7	291	108.5	409	114.1
ABS FR	224	38.3	402	70.3	419	61.0
FL PVC	233	116.4	237	98.2	252	86.3
DFIR	237	46.5	221	64.1	196	50.0
PS FR	277	93.0	334	94.5	445	82.0
ACET	290	143.9	360	141.3	566	167.1
PU	290	9.4	710	13.2	1221	13.3
PMMA	409	691.5	665	827.9	988	757.1
THM PU	424	110.0	221	119.3	319	120.1
NYLON	517	188.0	1313	226.3	2019	233.8
ABS	614	160.0	944	162.5	1311	162.5
PS	723	202.6	1101	210.1	1555	197.8
EPDM	737	213.1	956	199.8	1215	215.7
PBT	850	96.7	1313	169.9	1984	197.4
PET	881	93.3	534	113.7	616	125.5
E	913	161.9	1408	221.0	2735	227.5
PP	1170	231.3	1509	206.9	2421	231.1

ASTM E 84 Steiner tunnel test, thus generating more useful results. Figure 21.13 shows a room-corner test layout. The cone calorimeter fire-performance index (with tests conducted at 50kW/m²)¹⁷⁹ was shown to be a good predictor of time to flashover in FAA full aircraft fires^{170,180} and in the ISO 9705 room-corner test.¹⁸¹ In addition, the same cone calorimeter tests, but using only heat release criteria, have been shown to have almost perfect predictability of ISO 9705 room-corner test rankings.¹⁸¹

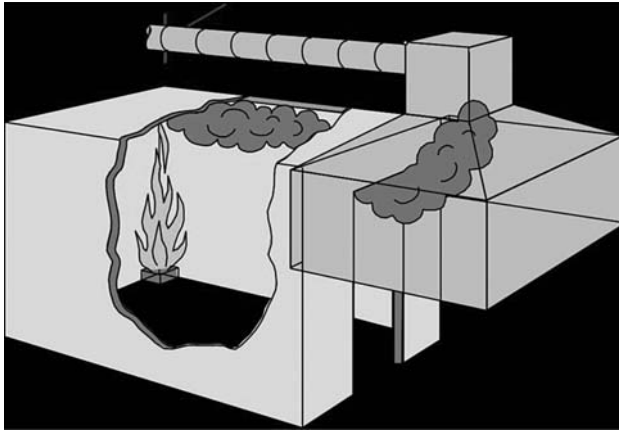


FIGURE 21.13 Schematic of room-corner test.

21.4.2.6 Smoke Obscuration

Smoke obscuration (reduction in light transmitted) is a serious concern in a fire, because a decrease in visibility reduces the light available, thus hindering both escape from the fire and rescue by safety personnel. The main way in which a fire causes visibility decreases is through smoke emission. This decrease in visibility is the result of a combination of two factors: how much material is burnt in the real fire (which will be less if the material has better fire performance) and how much smoke is released per unit material burnt.

Despite the understanding that smoke obscuration ought to be measured in a large scale, or by a method which can predict large-scale smoke release, the most common small-scale test method for measuring smoke from burning products is the traditional smoke chamber in the vertical mode (ASTM E 662)³⁹ (Figure 21.14). The test results are expressed in terms of a quantity called “specific optical density,” which is defined in the test standard. This test has now been shown to have some serious deficiencies. The most important problem is misrepresentation of the smoke



FIGURE 21.14 ASTM E 662 smoke chamber.



FIGURE 21.15 ASTM E 1995 smoke chamber conical heater.

obscuration found in real fires and found for melting materials, such as thermoplastics.^{182–185} When materials that melt or drip when exposed to flame, are exposed vertically in the smoke chamber test, the molten portions may have escaped the effect of the radiant heat source.¹⁸⁶ This means that some of the material does not burn during the test (and does not give off smoke), suggesting a low test result. In a real fire, all the molten material will burn and generate smoke. If these dripping products are exposed horizontally, the entire sample will be consumed and much more smoke will be released. The problem associated with the spread of fire from the flaming melt that occurs when thermoplastic materials have not been properly fire retarded, has recently been highlighted by NIST work.¹⁸⁷ An alternate fire test also exists, which assesses smoke obscuration in a closed chamber, ASTM E 1995¹²⁸ or NFPA 270¹²⁹ or ISO 5659-2¹³⁰; it uses a conical heater instead of the traditional ASTM E 662 heater (Figure 21.15).

The cone calorimeter,⁷¹ which is a dynamic flow-through fire test, can also be used to assess smoke obscuration. The rankings tend to be quite different from those found with the static smoke chamber and are much more realistic. Several empirical parameters have been proposed to make this compensation for incomplete sample consumption, including one called the smoke factor (SmkFct), determined in small-scale RHR calorimeters.¹⁸⁸ It combines the two aspects mentioned earlier: the light obscuration (as the total smoke released) and the peak RHR.

The majority of the materials with low flame spread (or low heat release) also exhibit low smoke release. However, it has been shown in several series of room-corner test projects (with the tested material lining either the walls or the walls and the ceiling), that ~10% of the materials tested (8 out of 84) exhibited adequate heat-release (or fire growth) characteristics, but have very high smoke release (Table 21.17 and Figure 21.16).^{189,190} These materials would cause severe obscuration problems if used in buildings. A combination of this work, and the concept that a visibility of 4 m is reasonable for people familiar with their environment,¹⁹¹ has led all the U.S. codes to include smoke pass/fail criteria when room-corner tests are used as alternatives to the ASTM E 84 Steiner tunnel test.

21.4.2.7 Smoke Toxicity

Toxic potency values are most often assessed from the most suitable small-scale smoke toxicity test (NIST radiant test, using rats as the animal model, but only for confirmatory purposes, standardized in ASTM E 1678¹⁹² and NFPA 269¹⁹³). The results from this test have been well validated with regard to toxicity in full-scale fires. However, such validation cannot be done to a better approximation than a factor of 3. This is illustrated by the fact that the range of the toxic potency of the smoke of almost all materials is so small that it pales in comparison with the ranges of toxic potencies of

TABLE 21.17
Results of Five Series of Tests Using Room-Corner Fire Tests

Series of Room-Corner Tests Conducted by	Materials Reaching Early Flashover	Materials with Adequate Heat and Low Smoke	Materials with Adequate Heat and High Smoke	Number of Materials Tested
Southwest Research Institute (SwRI)	1	8	1	10
Eurefic	14	12	2	28
SBI	12	15	3	30
USCG	3	5	1	9
BFGoodrich	1	5	1	7
Overall	31	45	8	84

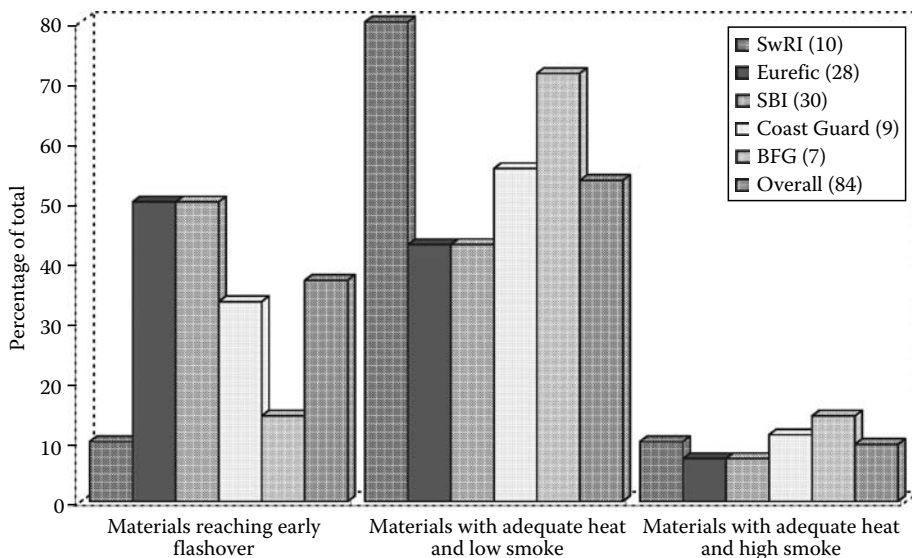


FIGURE 21.16 (See color insert following page 530.) Smoke and heat release in room-corner tests.

typical poisons.¹⁹⁴ Consequently, all smoke is extremely toxic, virtually irrespective of the material that is burning. The majority of fire fatalities are a result of inhalation of smoke and combustion products, rather than being the consequence of burns. Various organizations have been trying for many years to develop test methods and guidance documents on smoke toxicity, but emotional responses arise from discussions on interpretation of results or requirements for the use of animals as test surrogates. The following is now accepted by many fire scientists,^{26,158,161,195–200} and is critical to understanding how to assess fire hazard:

- Most fire fatalities occur in fires that become very large. In fact, the U.S. statistics indicate that such fires account for over six times more fatalities than all other fires. This is illustrated by NFPA statistics of the U.S. fires in the 1986–1990 time period.^{201,202} Similar information can be obtained from other time periods.
- Carbon monoxide concentrations in the atmospheres of flashover fires (the fires most likely to produce fatalities) are determined by geometric variables and oxygen availability, but are virtually unaffected by the chemical composition of the fuels.

TABLE 21.18
Yields of Carbon Monoxide in Fires, as Reported in the Literature

Material	Yield	Reference	Organization
Plywood walls, wood fiberboard ceiling	0.35	Budnick ²⁰⁴	HUD
FR plywood walls, wood fiberboard ceiling	0.42	Budnick ²⁰⁴	HUD
Plywood walls, no ceiling	0.10	Budnick ²⁰⁴	HUD
Upholstered chair, bed FR plywood walls	0.36	Budnick et al. ²⁰⁵	HUD
Plywood walls, bed	0.31	Budnick et al. ²⁰⁵	HUD
Plywood walls, wood cribs, cellulosic ceiling tile	0.29	Levine and Nelson ²⁰⁶	NIST
Non-FR chair, TV cabinets, cables, etc.	0.22	Babrauskas et al. ¹⁹⁵	FRCA
FR chair, TV cabinets, cables, etc.	0.23	Babrauskas et al. ¹⁹⁵	FRCA
PMMA walls	0.28	NIST unpublished	NIST
Wood cribs	0.15	Gottuk et al. ²⁰⁷	VPI
Flexible PU foam	0.25	Gottuk et al. ²⁰⁷	VPI
PMMA	0.30	Gottuk et al. ²⁰⁷	VPI
Hexane	0.23	Gottuk et al. ²⁰⁷	VPI
Propane	0.23	Beyler ²⁰⁸	Harvard
Propene	0.20	Beyler ²⁰⁸	Harvard
Hexanes	0.20	Beyler ²⁰⁸	Harvard
Toluene	0.11	Beyler ²⁰⁸	Harvard
Methanol	0.24	Beyler ²⁰⁸	Harvard
Ethanol	0.22	Beyler ²⁰⁸	Harvard
Isopropanol	0.17	Beyler ²⁰⁸	Harvard
Acetone	0.30	Beyler ²⁰⁸	Harvard
Polyethylene	0.18	Beyler ²⁰⁸	Harvard
PMMA	0.19	Beyler ²⁰⁸	Harvard
Pine	0.14	Beyler ²⁰⁸	Harvard
Average CO yield	0.236	24 cases	5 studies

- Carbon monoxide yields in full-scale flashover fires are ~0.2 g/g, which can be calculated to correspond to a toxicity of 25 mg/L.^{158,200} This consistent yield of carbon monoxide is illustrated by a set of 24 studies, and such results are shown in Table 21.18.^{203–208}
- The consequence of this is that any toxic potency (LC_{50}) higher than 8 mg/L will be subsumed within the toxicity of the atmosphere, and is of no consequence. Thus, values 8 or greater should be converted to 8 mg/L for reporting purposes. Moreover, almost all common materials have virtually the same smoke toxicity; their associated fire hazard will not be a function of smoke toxic potency.
- A comprehensive study of fire (and nonfire) fatalities associated with carbon monoxide showed that carbon monoxide inhalation statistically tracks fire fatalities.^{199,200,203}

Consequently, smoke toxicity measurements are often of minimal consequence to fire-hazard assessment.

21.4.2.8 Microcalorimetry

In recent years, a new fire-test instrument was developed: the pyrolysis combustion flow calorimeter (PCFC) or microcalorimeter.^{209,210} This instrument (Figure 21.17) was developed by Richard Lyon and his coworkers at the FAA laboratories. It enables the determination of parameters such as specific heat release rate (W/g), heat of combustion (J/g), and ignition temperature (°K), to be quickly determined from very small (1–50 mg) test specimens. The technique has been standardized by ASTM as ASTM D 7309. Data from the PCFC has been shown to be capable of being correlated

with data from standard heat release instrument fire tests (such as the cone calorimeter or the OSU calorimeter) and with other flammability results (such as the LOI or the UL 94). The data is also consistent with the data obtained from an oxygen bomb calorimeter, so as to assess and predict flammability properties.

The PCFC technique utilizes traditional oxygen depletion calorimetry. The specimen is first heated at a constant rate of temperature rise (typically 1–5 K/s) in a pyrolyzer. The thermal decomposition products are swept from the pyrolyzer by an inert gas. The gas stream is mixed with oxygen and enters a combustor at 900°C, where the decomposition products are completely oxidized. Oxygen concentrations and flow rates of the combustion gases are used to determine the oxygen depletion involved in the combustion process, and the heat release, as well as the heat release capacity (HRC), is determined from these measurements. Subsequently, the ignition temperature and the HRC parameter can be determined and used to compare PCFC data with data from other test methods. The HRC is defined as the ratio of the heat release rate and the heating rate. The peak heat release rates determined in cone calorimeter experiments correlate well with peak HRC data from PCFC experiments. In terms of other tests, results from the LOI (ASTM D 2863) test method exhibit a reciprocal correlation with HRC values, while HRC can also be a rough indicator for UL 94 ratings. In approximate terms, it has been said that HRC results can classify materials into three ranges of material flammability, as follows:

- Materials with $HRC > 400 \text{ J/g-K}$: poor fire performance
- Materials with $400 \text{ J/g-K} < HRC < 200 \text{ J/g-K}$: average fire performance
- Materials with $200 \text{ J/g-K} > HRC$: superior fire performance

The advantage that this instrument offers over traditional calorimeters is the very small sample size and the ease of performing tests, so that up to 50–60 tests can be conducted in a single day.

21.4.2.9 Cigarette Ignition

All the tests discussed earlier are basically flaming ignition tests. However, the test methods also exist for assessing the ignitability from cigarette ignition and the capability of cigarettes to ignite fabrics. Thus, ASTM E 1353⁸⁹ assesses the capability of individual fabrics and foams from being ignited by cigarettes, with the intent of using them for controlling smoldering ignition of upholstered furniture and mattress components. As discussed earlier, this test is very similar to the UFAC test that is used voluntarily by many (or most) manufacturers of the U.S. residential upholstered furniture. ASTM E 1352⁹⁰ is similar to ASTM E 1353, but it addresses the smoldering ignition of composites and it is similar to the voluntary test from BIFMA for the U.S. contract upholstered furniture. The test in 16 CFR 1632¹⁷ is a federally mandated approach to smoldering ignition of mattresses. In all these tests, a standard cigarette is used and applied on fabrics, foams, or composites.

In contrast, ASTM E 2187²² is a test for assessing the ignition power of cigarettes. In the test, the cigarettes are assessed for their capability of igniting the filter paper (as a surrogate for a cellulosic fabric). In this case, the cigarette is the item to be assessed and not the fabric or the foam.

21.4.3 TESTS FOR SPECIFIC PRODUCTS OR MATERIALS

As discussed earlier, a number of organizations and technical committees develop fire-test methods or specifications that are specific to some particular material or product. It is not possible to cover all of them in this work and they are usually publicly available from the responsible organization via their website.



FIGURE 21.17 Microcalorimeter.

Within ASTM, technical committees associated with plastics, electrical materials, textiles, protective clothing, thermal insulation, consumer products, detention and correctional facilities, and ships have developed tests that are often application tests that are of specific interest to the products involved. One fire test has spawned more application standards than any other, primarily because of its vast use in the United States: ASTM E 84 (Steiner tunnel). Thus, NFPA 262, UL 1820, UL 1887, ASTM E 2231, ASTM E 2404, ASTM E 2573, ASTM E 2579, and ASTM E 2599 are all test methods and practices based on the Steiner tunnel test. In some cases, the base apparatus is being modified (although usually it is permissible to conduct the ASTM E 84 test in the apparatus of the other test, but it is often not permissible to conduct the other test in any apparatus complying with the ASTM E 84 apparatus). The other test method that has resulted in many application standards is the cone calorimeter; the standards are ASTM D 5485, ASTM D 6113, ASTM E 1474, ASTM E 1740, and ASTM F 1550.

Organizations such as FM Global and ULs compete with the broader-based standards development organizations (ASTM and NFPA) in developing some fire tests. However, in many cases, these tests are being replaced by those from ASTM and/or NFPA. A number of trade associations also develop test methods, but these are being replaced. Appendix A contains the key fire test standards from ASTM, NFPA, and UL.

21.5 PRODUCT LIABILITY

In the United States, there is an added factor that is an alternate to the regulations: product liability. A number of specifications require materials suppliers to ensure that their materials meet certain criteria with regard to flammability (and sometimes, smoke) performance, often exceeding regulatory requirements. Those are the markets into which manufacturers of improved fire-safety materials and products supply their materials or products. Therefore, any responsible company will naturally strive to meet the appropriate requirements with the materials that it supplies.

In the present situation in the United States, where some manufacturers meet the letter (and not always the spirit) of the law, product liability is a critical component of safety (including fire safety). Product liability represents an added line of defense for the consumer over and above the regulation, but only when regulation is flawed. Attorneys representing potential plaintiffs are very sophisticated, and can hire consultants with extensive experience in fire investigation and flammability testing. It is not unusual for a consultant (or the lawyer who uses the said consultant) to be able to use complex fire models and to understand the fundamental implications of test results from a broader perspective than the technical personnel in some manufacturing companies.

Once product liability “kicks in,” in a particular incident, the situation facing a manufacturer involves the financial aspect of minimizing expenses, and technical issues start playing a minor role, although all arguments are presented in technical language. Furthermore, at this stage, compliance with all regulations and specifications is no longer considered as an issue: failure to comply is an automatic admission of “guilt,” but compliance does not bring automatic “acquittal.” The issue that will be considered by the legal counsel (on each side) will be whether “due diligence” was used by defendant, and whether state-of-the-art concepts were employed when the product that was involved in the fire was manufactured. The history of decision making by the manufacturer will be brought into the open, and the methods relied upon to make recommendations and reach conclusions will be analyzed.

A manufacturer who can show that the materials (or products) made cannot be faulted because nothing better is available to meet the usage guidelines put forward by the final customer (and not necessarily the specifications), using the most modern experimental techniques and mathematical models is most likely to be successful in preventing product liability concerns, and may even not face many lawsuits of this kind.

The best defense for a manufacturer is to ensure that the precautions taken at every stage were such that a manufacturer has “gone the extra mile,” and investigated the materials or products being sold beyond the specifications. In particular, when deficiencies of certain techniques (e.g., fire tests)

are known, it is still essential for a manufacturer to conduct all the needed testing to meet the specifications. However, additional testing or modeling must also be conducted to ensure that the safety of the user of the product is not compromised.

If this is not possible, for either practical or theoretical reasons, document trails are needed to show what course of action was considered, and the rationale for the decisions made. A good basic rule is always that the manufacturers should be more aware of the shortcomings of their materials or products than their customers, and should share the knowledge with the public. Product liability lawyers make it their business to care how manufacturers test for flammability to ensure that the public is adequately protected.

21.6 CONCLUSIONS

This paper describes the regulatory (and semiregulatory) situation in North America, in the area of fire safety. In recent years, there are considerable improvements in fire safety, but they are often relatively difficult to notice because of the slow adoption of codes and standards by local and state governments. Examples of positive developments for fire safety have occurred in the areas of rail transportation vehicles (underground and above the ground) and children's playgrounds. Similarly, changes are occurring in the areas of regulated upholstered furniture and mattresses in high-risk environments as well as residential mattresses. The potential exists for positive developments in the area of fire safety for polypropylene siding and filled bed products. However, the prognosis for positive developments of any kind in the area of residential upholstered furniture looks very bleak. Finally, there is an area which is likely to lead to tremendous improvements in fire safety: the requirements for cigarettes to have reduced ignition propensity.

In conclusion, the promotion of improved fire safety should continue to be a key societal goal, and it can be achieved, in the United States, through further work in the codes and standards arena.

ABBREVIATIONS

REGULATIONS, CODES, STANDARDS, AND ORGANIZATIONS

AFSC	American Fire Safety Council (US)
AHJ	Authority Having Jurisdiction (US)
ANPRM	Advance Notice of Proposed Rulemaking (US)
ASTM	American Society for Testing and Materials (now ASTM International)
BIFMA	Business and Institutional Furniture Manufacturers Association (US)
BOCA	Building Officials and Code Administrators (US)
BRE	Building Research Establishment (U.K.)
BSEF	Bromine Science and Environmental Forum
BSI	British Standards Institution
CA TB	California Technical Bulletin
CBHF	California Bureau of Home Furnishings and Thermal Insulation
CBUF	Combustion Behavior of Upholstered Furniture EC Research Project
CEN	European Committee for Standardization
CO	Carbon monoxide
CPD	European Commission Construction Products Directive
CPSC	Consumer Product Safety Commission (US)
CSA	Canadian Standards Association
EC	European Commission
EN	Euro Norm (European Standard)
EPA	Environmental Protection Agency (US)
EU	European Union
FAA	Federal Aviation Administration (US)

FAR	Federal Aviation Regulation (US)
FFA	Flammable Fabrics Act (US)
FHSA	Federal Hazardous Substances Act (US)
FIPEC	Fire Performance of Electrical Cables EC Research Project
FM	FM Global (formerly, Factory Mutual)
FMVSS	Federal Motor Vehicle Safety Standard (US)
FPRF	NFPA Fire Protection Research Foundation (US)
FRA	Federal Railroad Administration (US)
FTA	Federal Transit Administration (US)
FTP	IMO Fire Test Procedures Code
FSC	Coalition for Fire Safe Cigarettes
FSI	Flame Spread Index (ASTM E 84)
HRC	Heat Release Capacity (from Microcalorimeter)
HSC	IMO High Speed Craft Code
HUD	Department of Housing and Urban Development (US)
IAFC	International Association of Fire Chiefs
IAPMO	International Association of Plumbing and Mechanical Officials (US)
IBC	International Building Code (US)
ICBO	International Conference of Building Officials (US)
ICC	International Code Council (US)
IEC	International Electrotechnical Commission
IEBC	International Existing Building Code (US)
IEEE	Institute of Electrical and Electronics Engineers (US)
IFC	International Fire Code (US)
IMC	International Mechanical Code (US)
IMO	International Maritime Organization
IRC	International Residential Code (US)
ISO	International Organization for Standardization
ISPA	International Sleep Products Association (US)
IWUIC	International Wildland Urban Interface Code (US)
LIFT	Lateral Ignition and Flame Spread Test, ASTM E 1321
LOI	Limiting oxygen index
LPCB	Loss Prevention Control Board (U.K.)
LPS	Loss Prevention Standard (U.K.)
MSHA	Mine Safety and Health Administration (US)
NASFM	National Association of State Fire Marshals (US)
NBS	National Bureau of Standards (US)
NEC	National Electrical Code, NFPA 70 (US)
NEMA	National Electrical Manufacturers Association (US)
NFPA	National Fire Protection Association
NFPA 101	National Life Safety Code (US)
NFPA 5000	National Building Construction and Safety Code (US)
NHTSA	National Highway Traffic Safety Administration (US)
NIST	National Institute of Standards and Technology (US)
NPRM	Notice of Proposed Rulemaking (US)
NVIC	Navigation and Vessel Inspection Circular (US)
ODPM	Office of the Deputy Prime Minister (U.K.)
OSU	Ohio State University
PCFC	Pyrolysis Combustion Flow Calorimeter (Microcalorimeter)
RoHS	EC Directive on Restriction of Hazardous Substances
RHR	Rate of heat release
SBCCI	Southern Building Code Conference International (US)

SBI	Single Burning Item (European Norm EN 13823)
SDI	Smoke Developed Index (ASTM E 84)
SFPE	Society of Fire Protection Engineers (US)
SOLAS	International Convention for the Safety of Life at Sea (from IMO)
SP	Swedish National Testing and Research Institute
SRM	Standard Reference Material
THR	Total heat released
UFAC	Upholstered Furniture Action Council (US)
UFC	Uniform Fire Code (also known as NFPA 1)
UL	Underwriters Laboratories
UKAS	United Kingdom Accreditation Service
UMC	Uniform Mechanical Code (US)
UMTA	Urban Mass Transportation Administration (US)
UPC	Uniform Plumbing Code (US)
USFA	United States Fire Administration
USCG	United States Coast Guard
VW-1	UL Small-Scale Vertical Wire Fire Test in UL 1581
WEEE	EC Directive on Waste Electrical and Electronic Equipment

APPENDIX A KEY FIRE STANDARDS FROM ASTM, NFPA, AND UL

Key ASTM Fire Standards (ASTM International, 100 Bar Harbor Drive, West Conshohocken, PA, 19428-2959)

ASTM C 1485: Standard Test Method for Critical Radiant Flux of Exposed Attic Floor Insulation Using an Electric Radiant Heat Energy Source

ASTM D 568: Standard Test Method for Rate of Burning and/or Extent and Time of Burning of Flexible Plastics in a Vertical Position

ASTM D 635: Standard Test Method for Rate of Burning and/or Extent and Time of Burning of Self-Supporting Plastics in a Horizontal Position

ASTM D 777: Standard Test Method for Flammability of Treated Paper and Paperboard

ASTM D 1230: Standard Test Method for Flammability of Apparel Textiles

ASTM D 1360: Standard Test Method for Fire Retardancy of Paints (Cabinet Method)

ASTM D 1929: Standard Test Method for Determining Ignition Temperature of Plastics

ASTM D 2843: Standard Test Method for Density of Smoke from the Burning or Decomposition of Plastics

ASTM D 2859: Standard Test Method for Flammability of Finished Textile Floor Covering Materials

ASTM D 2863: Standard Test Method for Measuring the Minimum Oxygen Concentration to Support Candle-Like Combustion of Plastics (Oxygen Index)

ASTM D 3014: Standard Test Method for Flame Height, Time of Burning, and Loss of Weight of Rigid Cellular Plastics in a Vertical Position

ASTM D 3659: Standard Test Method for Flammability of Apparel Fabrics by Semirestraint Method

ASTM D 3675: Standard Test Method for Surface Flammability of Flexible Cellular Materials Using a Radiant Heat Energy Source

ASTM D 3801: Standard Test Method for Measuring the Comparative Extinguishing Characteristics of Solid Plastics in a Vertical Position

ASTM D 3874: Standard Test Method for Ignition of Materials by Hot Wire Sources

ASTM D 4151: Standard Test Method for Flammability of Blankets

ASTM D 4804: Standard Test Methods for Determining the Flammability Characteristics of Nonrigid Solid Plastics

ASTM D 4986: Standard Test Method for Horizontal Burning Characteristics of Cellular Polymeric Materials

ASTM D 5048: Standard Test Method for Measuring the Comparative Burning Characteristics and Resistance to Burn-through of Solid Plastics Using a 125-mm Flame

ASTM D 5132: Standard Test Method for Horizontal Burning Rate of Flexible Cellular and Rubber Materials Used in Occupant Compartments of Motor Vehicles

ASTM D 5424: Standard Test Method for Smoke Obscuration of Insulating Materials Contained in Electrical or Optical Fiber Cables When Burning in a Vertical Cable Tray Configuration

ASTM D 5485: Standard Test Method for Determining the Corrosive Effect of Combustion Products Using the Cone Corrosimeter

ASTM D 5537: Standard Test Method for Heat Release, Flame Spread, Smoke Obscuration, and Mass Loss Testing of Insulating Materials Contained in Electrical or Optical Fiber Cables When Burning in a Vertical Cable Tray Configuration

ASTM D 6113: Standard Test Method for Using a Cone Calorimeter to Determine Fire-Test-Response Characteristics of Insulating Materials Contained in Electrical or Optical Fiber Cables

ASTM D 6194: Standard Test Method for Glow Wire Ignition of Materials

ASTM D 6413: Standard Test Method for Flame Resistance of Textiles (Vertical Test)

ASTM D 6545: Standard Test Method for Flammability of Textiles Used in Children's Sleepwear

ASTM D 7016: Standard Test Method to Evaluate Edge Binding Components Used in Mattresses after Exposure to an Open Flame

ASTM D 7140: Standard Test Method to Measure Heat Transfer through Textile Thermal Barrier Materials

ASTM D 7309: Standard Test Method for Determining Flammability Characteristics of Plastics and Other Solid Materials Using Microscale Combustion Calorimetry

ASTM E 69: Standard Test Method for Combustible Properties of Treated Wood by the Fire-Tube Apparatus

ASTM E 84: Standard Test Method for Surface Burning Characteristics of Building Materials

ASTM E 108: Standard Test Methods for Fire Tests of Roof Coverings

ASTM E 119: Standard Test Methods for Fire Tests of Building Construction and Materials

ASTM E 136: Standard Test Method for Behavior of Materials in a Vertical Tube Furnace at 750°C

ASTM E 162: Standard Test Method for Surface Flammability of Materials Using a Radiant Heat Energy Source

ASTM E 648: Standard Test Method for Critical Radiant Flux of Floor-Covering Systems Using a Radiant Heat Energy Source

ASTM E 662: Standard Test Method for Specific Optical Density of Smoke Generated by Solid Materials

ASTM E 814: Standard Test Method for Fire Tests of Through-Penetration Fire Stops

ASTM E 906: Standard Test Method for Heat and Visible Smoke Release Rates for Materials and Products

ASTM E 970: Standard Test Method for Critical Radiant Flux of Exposed Attic Floor Insulation Using a Radiant Heat Energy Source

ASTM E 1317: Standard Test Method for Flammability of Marine Surface Finishes

ASTM E 1321: Standard Test Method for Determining Material Ignition and Flame Spread Properties

ASTM E 1352: Standard Test Method for Cigarette Ignition Resistance of Mock-Upholstered Furniture Assemblies

ASTM E 1353: Standard Test Methods for Cigarette Ignition Resistance of Components of Upholstered Furniture

ASTM E 1354: Standard Test Method for Heat and Visible Smoke Release Rates for Materials and Products Using an Oxygen Consumption Calorimeter

ASTM E 1474: Standard Test Method for Determining the Heat Release Rate of Upholstered Furniture and Mattress Components or Composites Using a Bench Scale Oxygen Consumption Calorimeter

ASTM E 1529: Standard Test Methods for Determining Effects of Large Hydrocarbon Pool Fires on Structural Members and Assemblies

ASTM E 1537: Standard Test Method for Fire Testing of Upholstered Furniture

ASTM E 1590: Standard Test Method for Fire Testing of Mattresses

ASTM E 1623: Standard Test Method for Determination of Fire and Thermal Parameters of Materials, Products, and Systems Using an Intermediate-Scale Calorimeter (ICAL)

ASTM E 1678: Standard Test Method for Measuring Smoke Toxicity for Use in Fire Hazard Analysis

ASTM E 1822: Standard Test Method for Fire Testing of Stacked Chairs

ASTM E 1966: Standard Test Method for Fire-Resistive Joint Systems

ASTM E 1995: Standard Test Method for Measurement of Smoke Obscuration Using a Conical Radiant Source in a Single Closed Chamber, With the Test Specimen Oriented Horizontally

ASTM E 2010: Standard Test Method for Positive Pressure Fire Tests of Window Assemblies (withdrawn)

ASTM E 2032: Standard Guide for Extension of Data from Fire Resistance Tests Conducted in Accordance with ASTM E 119

ASTM E 2058: Standard Test Methods for Measurement of Synthetic Polymer Material Flammability Using a Fire Propagation Apparatus (FPA)

ASTM E 2074: Standard Test Method for Positive Pressure Fire Tests of Window Assemblies (withdrawn)

ASTM E 2187: Standard Test Method for Measuring the Ignition Strength of Cigarettes

ASTM E 2231: Standard Practice for Specimen Preparation and Mounting of Pipe and Duct Insulation Materials to Assess Surface Burning Characteristics

ASTM E 2257: Standard Test Method for Room Fire Test of Wall and Ceiling Materials and Assemblies

ASTM E 2404: Standard Practice for Specimen Preparation and Mounting of Textile, Paper or Vinyl Wall or Ceiling Coverings to Assess Surface Burning Characteristics

ASTM E 2405: Standard Test Method for Determination of Fire and Thermal Parameters of Materials Using an Intermediate Scale Test with Vertically Oriented Specimen

ASTM E 2573: Standard Practice for Specimen Preparation and Mounting of Site-Fabricated Stretch Systems to Assess Surface Burning Characteristics

ASTM E 2579: Standard Practice for Specimen Preparation and Mounting of Wood Products to assess Surface burning Characteristics

ASTME 2599: Standard Practice for Specimen Preparation and Mounting of Reflective Insulation and Sheet Radiant Barriers for Building Applications

ASTM F 955: Standard Test Method for Evaluating Heat Transfer through Materials for Protective Clothing upon Contact with Molten Substances

ASTM F 1002: Standard Performance Specification for Protective Clothing for Use by Workers Exposed to Specific Molten Substances and Related Thermal Hazards

ASTM F 1060: Standard Test Method for Thermal Protective Performance of Materials for Protective Clothing for Hot Surface Contact

ASTM F 1085: Standard Specification for Mattress and Box Springs for Use in Berths in Marine Vessels (Annexes A1 and A3)

ASTM F 1358: Standard Test Method for Effects of Flame Impingement on Materials Used in Protective Clothing Not Designated primarily for Flame Resistance

ASTM F 1449: Standard Guide for Industrial Laundering of Flame, Thermal, and Arc Resistant Clothing

ASTM F 1534: Standard Test Method for Determining Changes in Fire-Test-Response Characteristics of Cushioning Materials after Water Leaching

ASTM F 1550: Standard Test Method for Determination of Fire-Test-Response Characteristics of Components or Composites of Mattresses or Furniture for Use in Correctional Facilities after Exposure to Vandalism, by Employing a Bench-Scale Oxygen Consumption Calorimeter

ASTM F 1930: Standard Test Method for Evaluation of Flame Resistant Clothing for Protection against Flash Fire Simulations Using an Instrumented Manikin

ASTM F 1939: Standard Test Method for Radiant Heat Resistance of Flame Resistant Clothing Materials with Continuous Heating

ASTM F 2302: Standard Performance Specification for Labeling Protective Clothing as Heat and Flame Resistant

ASTM F 2700: Standard Test Method for Unsteady-State Heat Transfer Evaluation of Flame Resistant Materials for Clothing with Continuous Heating

ASTM F 2701: Standard Test Method for Evaluating Heat Transfer through Materials for Protective Clothing upon Contact with a Hot Liquid Splash

ASTM F 2702: Standard Test Method for Radiant Heat Performance of Flame Resistant Clothing Materials with Burn Injury Prediction

ASTM F 2703: Standard Test Method for Unsteady-State Heat Transfer Evaluation of Flame Resistant Materials for Clothing with Burn Injury Prediction

NFPA Fire Test Standards (National Fire Protection Association, 1 Battery March park, Quincy, MA, 02269).

NFPA 251: Standard Methods of Tests of Fire Endurance of Building Construction and Materials

NFPA 252: Standard Methods of Fire Tests of Door Assemblies

NFPA 253: Standard Method of Test for Critical Radiant Flux of Floor Covering Systems Using a Radiant Heat Energy Source

NFPA 255: Standard Method of Test of Surface Burning Characteristics of Building Materials

NFPA 256: Standard Methods of Fire Tests of Roof Coverings (withdrawn)

NFPA 257: Standard on Fire Test for Window and Glass Block Assemblies

NFPA 258: Recommended Practice for Determining Smoke Generation of Solid Materials (withdrawn)

NFPA 259: Standard Test Method for Potential Heat of Building Materials

NFPA 260: Standard Methods of Tests and Classification System for Cigarette Ignition Resistance of Components of Upholstered Furniture

NFPA 261: Standard Method of Test for Determining Resistance of Mock-Up Upholstered Furniture Material Assemblies to Ignition by Smoldering Cigarettes

NFPA 262: Standard Method of Test for Flame Travel and Smoke of Wires and Cables for Use in Air-Handling Spaces

NFPA 263: Standard Method of Test for Heat and Visible Smoke Release Rates for Materials and Products (withdrawn)

NFPA 265: Standard Methods of Fire Tests for Evaluating Room Fire Growth Contribution of Textile Coverings on Full Height Panels and Walls

NFPA 266: Standard Method of Test for Fire Characteristics of Upholstered Furniture Exposed to Flaming Ignition Source (withdrawn)

NFPA 267: Standard Method of Test for Fire Characteristics of Mattresses and Bedding Assemblies Exposed to Flaming Ignition Source (withdrawn)

NFPA 268: Standard Test Method for Determining Ignitability of Exterior Wall Assemblies Using a Radiant Heat Energy Source

NFPA 269: Standard Test Method for Developing Toxic Potency Data for Use in Fire Hazard Modeling

NFPA 270: Standard Test Method for Measurement of Smoke Obscuration Using a Conical Radiant Source in a Single Closed Chamber

NFPA 271: Standard Method of Test for Heat and Visible Smoke Release Rates for Materials and Products Using an Oxygen Consumption Calorimeter

NFPA 272: Standard Method of Test for Heat and Visible Smoke Release Rates for Upholstered Furniture Components or Composites and Mattresses Using an Oxygen Consumption Calorimeter (withdrawn)

NFPA 274: Standard Test Method to Evaluate Fire Performance Characteristics of Pipe Insulation

NFPA 275: Standard Method of Fire Tests for the Evaluation of Thermal Barriers Used Over Foam Plastic Insulation

NFPA 285: Standard Method of Test for the Evaluation of Flammability Characteristics of Exterior Nonload-Bearing Wall Assemblies Containing Combustible Components Using the Intermediate-Scale, Multistory Test Apparatus

NFPA 286: Standard Methods of Fire Tests for Evaluating Contribution of Wall and Ceiling Interior Finish to Room Fire Growth

NFPA 287: Standard Test Methods for Measurement of Flammability of Materials in Cleanrooms Using FPA

NFPA 288: Standard Methods of Fire Tests of Floor Fire Door Assemblies Installed Horizontally in Fire Resistance-Rated Floor Systems

NFPA 289: Standard Method of Fire Test for Individual Fuel Packages

NFPA 290: Standard for Fire Testing of Passive Protection Materials for Use on LP-Gas Containers

NFPA 701: Standard Methods of Fire Tests for Flame Propagation of Textiles and Films

NFPA 703: Standard for Fire Retardant Impregnated Wood and Fire Retardant Coatings for Building Materials

NFPA 705: Recommended Practice for a Field Flame Test for Textiles and Films

Key UL Fire Test Standards (Underwriters Laboratories Inc., 333 Pfingsten Road, Northbrook, IL 60062-2096):

UL 9: Standard for Fire Tests of Window Assemblies

UL 10B: Standard for Fire Tests of Door Assemblies

UL 214: Standard for Safety Tests for Flame-Propagation of Fabrics and Films (withdrawn)

UL 263: Standard for Fire Tests of Building Construction and Materials

UL 555: Standard for Fire Dampers

UL 555C: Standard for Ceiling Dampers

UL 555S: Standard for Leakage Rated Dampers for Use in Smoke Control Systems

UL 723: Standard for Test for Surface Burning Characteristics of Building Materials

UL 790: Standard for Standard Test Methods for Fire Tests of Roof Coverings (2004)

UL 910: Standard for Safety Test for Flame-Propagation and Smoke-Density Values for Electrical and Optical-Fiber Cables Used in Spaces Transporting Environmental Air (withdrawn)

UL 1040: Standard for Fire Test of Insulated Wall Construction

UL 1479: Standard for Fire Tests of Through-Penetration Firestops

UL 1056: Standard for Safety Fire Test of Upholstered Furniture (withdrawn)

UL 1581: Reference Standard for Electrical Wires, Cables, and Flexible Cords, Section 1080, VW-1 (Vertical Wire) Flame Test

UL 1581: Reference Standard for Electrical Wires, Cables, and Flexible Cords, Section 1160. UL Vertical-Tray Flame Test

UL 1581: Reference Standard for Electrical Wires, Cables, and Flexible Cords, Section 1164. CSA Vertical-Tray Flame Test

UL 1666: Test for Flame Propagation Height of Electrical and Optical-Fiber Cables Installed Vertically in Shafts

UL 1685: Standard Vertical-Tray Fire-Propagation and Smoke-Release Test for Electrical and Optical-Fiber Cables

UL 1715: Standard for Fire Test of Interior Finish Material

UL 1820: Standard for Safety Fire Test of Pneumatic Tubing for Flame and Smoke Characteristics

UL 1887: Standard for Safety Fire Test of Plastic Sprinkler Pipe for Visible Flame and Smoke Characteristics

UL 1895: Standard for Safety Fire Test of Mattresses (withdrawn)

UL 1975: Standard for Fire Tests for Foamed Plastics Used for Decorative Purposes

UL 2024: Standard for Optical-Fiber and Communications Cable Raceway

UL 2043: Standard for Safety Fire Test for Heat and Visible Smoke Release for Discrete Products and Their Accessories Installed in Air-Handling Spaces

UL 2079: Standard for Tests for Fire Resistance of Building Joint Systems

REFERENCES

1. International Building Code (IBC), International Code Council, Washington, DC.
2. International Fire Code (IFC), International Code Council, Washington, DC.
3. International Mechanical Code (IMC), International Code Council, Washington, DC.
4. International Wildland Urban Interface Code (IWUIC), International Code Council, Washington, DC.
5. International Residential Code for One- and Two-family Dwellings (IRC), International Code Council, Washington, DC.
6. International Existing Building Code (IEBC), International Code Council, Washington, DC.
7. NFPA 70, National Electrical Code (NEC), National Fire Protection Association, Quincy, MA.
8. NFPA 101, National Life Safety Code, National Fire Protection Association, Quincy, MA.
9. NFPA 90A, Standard for the Installation of Air-Conditioning and Ventilating Systems, National Fire Protection Association, Quincy, MA.
10. NFPA 13, Standard for the Installation of Sprinkler Systems, National Fire Protection Association, Quincy, MA.
11. NFPA 130, Standard for Fixed Guideway Transit and Passenger Rail Systems, National Fire Protection Association, Quincy, MA.
12. 16 CFR 1610, Title 16, Commercial Practices, Chapter II, Consumer Product Safety Commission, Part 1610, Standard for the Flammability of Clothing Textiles, Flammable Fabrics Act Regulations, U.S. Federal Government, Washington, DC.
13. 16 CFR Part 1630, Title 16, Commercial Practices, Chapter II, Consumer Product Safety Commission, Part 1630, Standard for the Surface Flammability of Carpets and Rugs (FF 1-70), Flammable Fabrics Act Regulations, U.S. Federal Government, Washington, DC.
14. 16 CFR Part 1631, Title 16, Commercial Practices, Chapter II, Consumer Product Safety Commission, Part 1631, Standard for the Surface Flammability of Small Carpets and Rugs (FF 2-70), Flammable Fabrics Act Regulations, U.S. Federal Government, Washington, DC.
15. 16 CFR 1615, Title 16, Commercial Practices, Chapter II, Consumer Product Safety Commission, Part 1615, Standard for the Flammability of Children's Sleepwear: Sizes 0 through 6X (FF 3-71), Flammable Fabrics Act Regulations, U.S. Federal Government, Washington, DC.
16. 16 CFR 1616, Title 16, Commercial Practices, Chapter II, Consumer Product Safety Commission, Part 1616, Standard for the Flammability of Children's Sleepwear: Sizes 7 through 14 (FF 5-74), Flammable Fabrics Act Regulations, U.S. Federal Government, Washington, DC.
17. 16 CFR 1632, Title 16, Commercial Practices, Chapter II, Consumer Product Safety Commission, Part 1632, Standard for the Flammability of Mattresses (FF 4-72), Flammable Fabrics Act Regulations, U.S. Federal Government, Washington, DC.
18. 16 CFR 1500.44, Title 16, Commercial Practices, Chapter II, Consumer Product Safety Commission, Part 1500, Hazardous Substances and Articles; Administration and Enforcement Regulations: Method for determining extremely flammable and flammable solids, U.S. Federal Government, Washington, DC.
19. 16 CFR 1633, Title 16, Commercial Practices, Chapter II, Consumer Product Safety Commission, Part 1633, Standard for the Flammability (Open Flame) of Mattress Sets, Flammable Fabrics Act Regulations, U.S. Federal Government, Washington, DC.

20. ASTM F 963, Standard Consumer Safety Specification for Toy Safety, Annual Book ASTM Standards, American Society for Testing and Materials, West Conshohocken, PA.
21. Proposed 16 CFR part 1634 Standard for the Flammability of Residential Upholstered Furniture, Bethesda, MD, March 4, 2008. <http://www.cpsc.gov/businfo/frnotices/fr08/cpscf08.html>.
22. ASTM E 2187, Standard Test Method for Measuring the Ignition Strength of Cigarettes, Annual Book ASTM Standards, American Society for Testing and Materials, West Conshohocken, PA.
23. New York State Combustion Toxicity Regulations: Combustion Toxicity Testing, Article 15, Part 1120 (9 NYCRR 1120)—Effective December 16, 1986.
24. Alarie, Y.C. and Anderson, R.C., Toxicologic and acute lethal hazard evaluation of thermal decomposition products of synthetic and natural polymers, *Toxicol. Appl. Pharmacol.*, 51, 341 (1979).
25. Norris, J.C., Investigation of the dual LC₅₀ values in woods using the University of Pittsburgh combustion toxicity apparatus, in *Characterization and Toxicity of Smoke*, Ed. H.J. Hasegawa, ASTM STP 1082, American Society for Testing and Materials, Philadelphia, PA, pp. 57–71, 1990.
26. Hirschler, M.M., General principles of fire hazard and the role of smoke toxicity, in *Fire and Polymers: Hazards Identification and Prevention*, Ed. G.L. Nelson, ACS Symposium Series 425, American Chemical Society, Washington, DC, Chapter 28, pp. 462–478, 1990.
27. Hirschler, M.M., Smoke toxicity measurements made so that the results can be used for improved fire safety, *J. Fire Sci.* 9, 330–47 (1991).
28. Hirschler, M.M., Toxicity of the smoke from PVC materials: New concepts, *Prog. Rubber Plast. Technol.*, 10(2), 154–69 (1994).
29. Ahrens, M., *U.S. Vehicle Fire Trends and Patterns*, NFPA, Quincy, MA, August 2001.
30. Ahrens, M., *The U.S. Fire Problem Overview Report: Leading Causes and Other Patterns and Trends*, NFPA, Quincy, MA, June 2001.
31. Janssens, M.L., Database on full-scale calorimeter tests on motor vehicles, *HAR-AAA TC Meeting*, Detroit, MI, October 23–24, 2006.
32. FMVSS 302, Motor Vehicle Safety Standard No. 302, Flammability of Materials—Passenger Cars, Multipurpose Passenger Vehicles, Trucks and Buses, National Highway Traffic Safety Administration, Washington, DC. [Code of Federal Regulations § 571.302, originally Federal Register 34, No. 229, pp. 20434–20436 (December 31, 1969)].
33. ISO 3795, Road Vehicles, and Tractors and Machinery for Agriculture and Forestry—Determination of Burning Behaviour of Interior Materials, International Organization for Standardization (ISO), Geneva, Switzerland.
34. M.M. Hirschler (Technical Coordinator) et al., *Fire and Transportation Vehicles—State of the Art: Regulatory Requirements and Guidelines—A White Paper*, Fire Protection Research Foundation Research Advisory Council on Transportation Vehicles, Quincy, MA, October, 2004.
35. U.S. Department of Transportation, *Aircraft Materials Fire Test Handbook*, Federal Aviation Administration, Washington, DC. <http://www.fire.tc.faa.gov/>
36. Federal Register, Vol. 66, No. 36/Thursday, February 22, 2001, FAA Policy on Use of the *Aircraft Materials Fire Test Handbook*, pp. 11197–11199, 2001.
37. Smith, E.E., in *Ignition, Heat Release and Noncombustibility of Materials*, Ed. A.F. Robertson, ASTM STP 502, American Society for Testing and Materials, Philadelphia, p. 119, 1972.
38. ASTM E 906, Standard Test Method for Heat and Visible Smoke Release Rates for Materials and Products, Annual Book ASTM Standards, American Society for Testing and Materials, West Conshohocken, PA.
39. ASTM E 662, Standard Test Method for Specific Optical Density of Smoke Generated by Solid Materials, Annual Book ASTM Standards, American Society for Testing and Materials, West Conshohocken, PA.
40. ASTM E 648, Standard Test Method for Critical Radiant Flux of Floor-Covering Systems Using a Radiant Heat Energy Source, Annual Book ASTM Standards, American Society for Testing and Materials, West Conshohocken, PA.
41. International Convention for the Safety of Life at Sea (SOLAS), With Periodic Amendments, Consolidated Edition, International Maritime Organization, London, U.K., 1974.
42. International Maritime Organization (IMO), London, U.K.
43. *International Code for Application of Fire Test Procedures (FTP Code)*, International Maritime Organization, London, U.K.
44. *International Code of Safety for High-Speed Craft (HSC Code)*, International Maritime Organization, London, U.K.
45. Code of Federal Regulations, U.S. Federal Government—Coast Guard: Title 46, Shipping, CFR, Parts 1–199, Subchapter J: Electrical Engineering (Parts 110–113).

46. U.S. Coast Guard, NVIC (Navigation and Vessel Inspection Circular), U.S. Coast Guard Guide to Structural Fire Protection.
47. NFPA 301, Code for Safety to Life from Fire on Merchant Vessels, National Fire Protection Association, Quincy, MA.
48. ISO 834-1, Fire-Resistance Tests—Elements of Building Construction—Part 1: General Requirements, International Organization for Standardization (ISO), Geneva, Switzerland.
49. ASTM E 119, Standard Test Methods for Fire Tests of Building Construction and Materials, Annual Book ASTM Standards, American Society for Testing and Materials, West Conshohocken, PA.
50. ISO 9705, International Standard Fire Tests—Full Scale Room Test for Surface Products, International Organization for Standardization (ISO), Geneva, Switzerland.
51. NFPA 302, Fire Protection Standard for Pleasure and Commercial Motor Craft, National Fire Protection Association, Quincy, MA.
52. Sorathia, U., Materials in military applications, in *Business Communications Company Fourteenth Ann. Conference on Recent Advances in Flame Retardancy of Polymeric Materials*, June 2–4, 2003, Stamford, CT, Business Communications Co., Ed. M. Lewin, Norwalk, CT, 2003.
53. Federal Register, Vol. 64, No. 91/Wednesday May 12, 1999, Department of Transportation, Federal Railroad Administration, 49 CFR Part 216 et al., Passenger Equipment Safety Standards; Final Rule, pp. 25539–25705, 1999.
54. Federal Register, Vol. 67, No. 122/Tuesday, June 25, 2002, Department of Transportation, Federal Railroad Administration, 49 CFR Part 238, [FRA Docket No. PCSS–1, Notice No. 8] RIN 2130–AB48, Passenger Equipment Safety Standards, pp. 42892–42912, 2002.
55. ASTM E 162, Standard Test Method for Surface Flammability of Materials Using a Radiant Heat Energy Source, Annual Book ASTM Standards, American Society for Testing and Materials, West Conshohocken, PA.
56. Peacock, R.D., Bukowski, R.W., Jones, W.J., Reneke, P.A., Babrauskas, V., and Brown, J.E., Fire safety of passenger trains: A review of U.S. and foreign approaches, National Institute of Standards and Technology (under contract to U.S. Dept. of Transportation, John A. Volpe National Transportation Systems Center, Cambridge, MA), Gaithersburg, MD, 20899, (NIST Technical Note 1406), 1994.
57. ASTM E 2061, Guide for Fire Hazard Assessment of Rail Transportation Vehicles, Annual Book ASTM Standards, American Society for Testing and Materials, West Conshohocken, PA.
58. Hirschler, M.M., Fire safety in rail transportation vehicles: Special focus on recent activities at the Federal Railroad Administration, NFPA 130 and ASTM E 2061, *Fire Protection Research Foundation Fire Risk and Hazard Assessment Research Application Symposium*, July 9–11, Baltimore, MD, 2003.
59. UL 1581, Reference Standard for Electrical Wires, Cables, and Flexible Cords, Section 1160, UL Vertical-Tray Flame Test, Underwriters Laboratories, Northbrook, IL.
60. UL 1581, Reference Standard for Electrical Wires, Cables, and Flexible Cords, Section 1080, VW-1 (Vertical Wire) Flame Test, Underwriters Laboratories, Northbrook, IL.
61. UL 1581, Reference Standard for Electrical Wires, Cables, and Flexible Cords, Section 1164, CSA Vertical-Tray Flame Test, Underwriters Laboratories, Northbrook, IL.
62. CSA FT4, Vertical Cable Tray Test in CSA 22.2, Test Methods for Electrical Wires and Cables (C22.2 No. 0.3), Canadian Standards Association, Rexdale, Ont., Canada.
63. IEEE 1202, Standard for Flame Testing of Cables for Use in Cable Tray in Industrial and Commercial Occupancies, Institute of Electrical and Electronics Engineers, Piscataway, NJ.
64. UL 1666, Test for Flame Propagation Height of Electrical and Optical-Fiber Cables Installed Vertically in Shafts, Underwriters Laboratories, Northbrook, IL.
65. NFPA 262, Standard Method of Test for Fire and Smoke Characteristics of Wires and Cables, National Fire Protection Assn., NFPA, Quincy, MA.
66. Grayson, S.J. and Hirschler, M.M., Fire performance of plastics in car interiors, *Flame Retardants*, February 5–6, London, pp. 197–207, Interscience Communications, London, U.K., 2002.
67. Hirschler, M.M., Hoffmann, D.J., Hoffmann, J.M., and Kroll, E.C., Fire hazard associated with passenger cars and vans, *Fire and Materials Conference*, San Francisco, CA, January 27–28, Interscience Communications, London, U.K., pp. 307–319, 2003.
68. Janssens, M.L. and Huczek, J.P., Comparison of fire properties of automotive materials, in *Business Communications Company Fourteenth Ann. Conference on Recent Advances in Flame Retardancy of Polymeric Materials*, June 2–4, Ed. M. Lewin, Stamford, CT, Norwalk, CT, 2003.
69. Hirschler, M.M., Improving the fire safety of road vehicles, Chapter 17 in *Advances in Fire Retardant Materials*, Eds. R. Horrocks and D. Price, Woodhead Publishing Ltd., London, U.K., 2008.

70. National Highway Traffic Safety Administration (NHTSA), Car and Van Fire Research Work Conducted under the General Motors Corporation—Settlement Agreement—Section B. Fire Safety Research at the web site: <http://dms.dot.gov/>, Docket #3588
71. ASTM E 1354, Standard Test Method for Heat and Visible Smoke Release Rates for Materials and Products Using an Oxygen Consumption Calorimeter (cone calorimeter), Annual Book ASTM Standards, American Society for Testing and Materials, West Conshohocken, PA.
72. Battipaglia, K., Huczek, J., Janssens, M., and Miller, M., Development of a method to assess the fire hazard of automotive materials, in *Proceedings of the Interflam'04, 10th International Fire Safety Conference*, July 5–7, Edinburgh, U.K., Interscience Communications, U.K., pp. 1587–1596, 2004.
73. ASTM D 5132, Standard Test Method for Horizontal Burning Rate of Polymeric Materials Used in Occupant Compartments of Motor Vehicles, Annual Book ASTM Standards, American Society for Testing and Materials, West Conshohocken, PA.
74. Code of Federal Regulations, Title 49, Transportation, Chapter V, National Highway Traffic Safety Administration, Department of Transportation, Part 571, Federal Motor Vehicle Safety Standards, 571.301 Standard No. 301; Fuel system integrity.
75. Braun, E., Davis, S., Klote, J., Levin, B., and Paabo, M., Assessment of the fire performance of school bus interior components, NISTIR 4347, National Institute of Standards and Technology, Gaithersburg, MD, 1990.
76. School bus seat upholstery fire block test, approved by the National Conference on School Transportation as part of the National Standards for School Buses and National Standards for School Bus Operations (available from National Safety Council, 444 North Michigan Avenue, Chicago, IL, 60611), 1990.
77. ASTM D 1230, Standard Test Method for Flammability of Apparel Textiles, Annual Book ASTM Standards, American Society for Testing and Materials, West Conshohocken, PA.
78. Hirschler, M.M. and Piansay, T., Survey of small scale flame spread test results of modern fabrics, *Fire Mater.*, 31, 373–386 (2007).
79. Hirschler, M.M., Zicherman, J.B., and Umino, P.Y., Forensic evaluation of clothing flammability, *Fire Mater.* (DOI:10.1002/fam.997-US: <http://dx.doi.org/10.1002/fam.997>) 2009.
80. ASTM D 2859, Standard Test Method for Flammability of Finished Textile Floor Covering Materials, Annual Book ASTM Standards, American Society for Testing and Materials, West Conshohocken, PA.
81. ASTM D 6545, Standard Test Method for Flammability of Textiles Used in Children's Sleepwear, Annual Book ASTM Standards, American Society for Testing and Materials, West Conshohocken, PA.
82. CA TB 129, California Technical Bulletin 129, Flammability Test Procedure for Mattresses for Use in Public Buildings, California Bulletin of Home Furnishings and Thermal Insulation, North Highlands, CA.
83. BS 5852, Methods of Test for Assessment of the Ignitability of Upholstered Seating by Smoldering and Flaming Ignition Sources, British Standards Institution, London, U.K.
84. CA TB 117, California Technical Bulletin 117, Requirements, Test Procedures and Apparatus for Testing the Flame Retardance of Resilient Filling Materials Used in Upholstered Furniture, California Bulletin of Home Furnishings and Thermal Insulation, North Highlands, CA.
85. ASTM E 1590, Standard Method for Fire Testing of Mattresses, Annual Book ASTM Standards, American Society for Testing and Materials, West Conshohocken, PA.
86. Ohlemiller, T., Shields, J., McLane, R., and Gann, R., Flammability assessment methodology for mattresses, National Institute of Standards and Technology NISTIR 6497, Gaithersburg, MD, June, 2000.
87. Ohlemiller, T. and Gann, R., Estimating Reduced Fire Risk Resulting from an Improved Mattress Flammability Standard, National Institute of Standards and Technology Technical Note 1446, Boulder, CO, August, 2002.
88. CA TB 603, California Technical Bulletin 603, Requirements and Test Procedure for Resistance of a Mattress/Box Spring Set to a Large Open Flame, California Bureau of Home Furnishings and Thermal Insulation, North Highlands, CA.
89. ASTM E 1353, Standard Test Methods for Cigarette Ignition Resistance of Components of Upholstered Furniture, Annual Book ASTM Standards, American Society for Testing and Materials, West Conshohocken, PA.
90. ASTM E 1352, Standard Method of Test for Cigarette Ignition Resistance of Mock-Up Upholstered Furniture Assemblies, Annual Book ASTM Standards, American Society for Testing and Materials, West Conshohocken, PA.
91. CA TB 133, California Technical Bulletin 133, Flammability Test Procedure for Seating Furniture for Use in Public Occupancies, California Bulletin of Home Furnishings and Thermal Insulation, North Highlands, CA.
92. ASTM E 1537, Standard Method for Fire Testing of Upholstered Furniture, Annual Book ASTM Standards, American Society for Testing and Materials, West Conshohocken, PA.

93. Verakis, H., Conveyor Belt Flammability, Mine Safety & Health Administration, Triadelphia, WV. <http://www.msha.gov/beltair/msha/january/verakis2007presentation.ppt>, 2007.
94. ASTM D 635, Standard Test Method for Rate of Burning and/or Extent and Time of Burning of Self-Supporting Plastics in a Horizontal Position, Annual Book ASTM Standards, American Society for Testing and Materials, West Conshohocken, PA.
95. Mutmansky, J.M., Brune, J.F., Calizaya, F., Mucho, T.P., Tien, J.C., and Weeks, J.L., The final report of the Technical Study Panel on the utilization of belt air and the composition and fire retardant properties of belt materials in underground coal mining, 2007. <http://www.cdc.gov/niosh/mining/mineract/pdfs/BeltAirFinalReport122007.pdf>
96. Hirschler, M.M. and Earl, T., Is upholstered furniture a flammable solid?, *Business Communications Company Seventeenth Annual Conference on Recent Advances in Flame Retardancy of Polymeric Materials*, June 9–11, Ed. M. Lewin, Stamford, CT, Norwalk, CT, 2008.
97. The Construction Products Directive as regards the classification of the reaction-to-fire performance of construction products, Council Directive 89/106/EEC, 21 December 1988, Brussels, Belgium, 1988, European Commission, Enterprise and Industry Directorate-General, Construction.
98. EN 13501-1, Fire Classification of Construction Products and Building Elements—Part 1: Classification Using Test Data from Reaction to Fire Tests, CEN (European Committee for Standardization), Brussels, Belgium.
99. EN ISO 1182, Reaction to Fire Tests for Building Products—Non-Combustibility Test, CEN (European Committee for Standardization), Brussels, Belgium.
100. EN ISO 1716, Reaction to Fire Tests for Building Products—Determination of the Heat of Combustion, CEN (European Committee for Standardization), Brussels, Belgium.
101. EN 13823, Reaction to Fire Tests for Building Products. Building Products Excluding Floorings Exposed to the Thermal Attack by a Single Burning Item, CEN (European Committee for Standardization), Brussels, Belgium.
102. EN ISO 11925-2, Reaction to Fire Tests—Ignitability of Building Products Subjected to Direct Impingement of Flame—Part 2: Single-Flame Source Test, CEN (European Committee for Standardization), Brussels, Belgium.
103. Pipe insulation: Commission decision of 26 August 2003 amending Decision 2000/147/EC implementing Council Directive 89/106/EEC as regards the classification of the reaction-to-fire performance of construction products (2003/632/EC), 2003.
104. Cables: Commission decision of 27 October 2006 amending Decision 2000/147/EC implementing Council Directive 89/106/EEC as regards the classification of the reaction-to-fire performance of construction products (2006/751/EC), 2006.
105. Grayson, S., Van Hees, P., Vercellotti, U., Breulet, H., and Green, A., Fire performance of electrical cables—New test methods and measurement techniques. Final report of EU SMT project SMT4-CT96-2059, Interscience Communications, London, U.K., 2000.
106. EN 50399, Common test methods for cables under fire conditions—Heat release and smoke production measurement on cables during flame spread test—Test apparatus, procedures, results, European Committee for Standardization, Brussels, Belgium.
107. United Kingdom Furniture Regulations, The Furniture and Furnishings (Fire) (Safety) Regulations 1988, Statutory Instrument 1988 No. 1324—Amended 1993 by Statutory Instrument 1993 No. 207.
108. United Kingdom Mattress Regulations, The Furniture and Furnishings (Fire) (Safety) Regulations 1988, Statutory Instrument 1988 No. 1324—Amended 1989 by Statutory Instrument 1989 No. 2358.
109. U.K. Government Consumer Safety Research, Effectiveness of the Furniture and Furnishings (Fire) (Safety) Regulations 1988, Consumer Affairs Directorate, Dept. Trade and Industry, London, U.K., June 2000. [Research conducted by Professor Gary Stevens, Univ. of Surrey, Guildford, U.K.].
110. CBUF Report, Fire safety of upholstered furniture—The final report on the CBUF research programme, Ed. B. Sundstrom, EUR 16477 EN, European Commission, Measurements and Testing Report, Contract No. 3478/1/0/196/11-BCR-DK(30), Interscience Communications, London, U.K.
111. ICBO (International Conference of Building Officials), Whittier, CA.
112. BOCA (Building Officials and Code Administrators), Country Club Hills, IL.
113. SBCCI (Southern Building Code Conference International), Birmingham, AL.
114. ASTM E 84, Standard Test Method for Surface Burning Characteristics of Building Materials, Annual Book ASTM Standards, American Society for Testing and Materials, West Conshohocken, PA.
115. NFPA 286, Standard Methods of Fire Tests for Evaluating Contribution of Wall and Ceiling Interior Finish to Room Fire Growth, National Fire Protection Association, Quincy, MA.
116. NFPA 265, Standard Methods of Fire Tests for Evaluating Room Fire Growth Contribution of Textile Coverings on Full Height Panels and Walls, National Fire Protection Association, Quincy, MA.

117. UL 1820, Standard for Safety Fire Test of Pneumatic Tubing for Flame and Smoke Characteristics, Underwriters Laboratories, Northbrook, IL.
118. UL 1887, Standard for Safety Fire Test of Plastic Sprinkler Pipe for Visible Flame and Smoke Characteristics, Underwriters Laboratories, Northbrook, IL.
119. UL 2024, Standard for Optical-Fiber and Communications Cable Raceway, Underwriters Laboratories, Northbrook, IL.
120. UL 2043, Standard for Safety Fire Test for Heat and Visible Smoke Release for Discrete Products and Their Accessories Installed in Air-Handling Spaces, Underwriters Laboratories, Northbrook, IL.
121. NFPA 703, Standard for Fire Retardant Impregnated Wood and Fire Retardant Coatings for Building Materials, National Fire Protection Association, Quincy, MA.
122. NFPA 501, Standard on Manufactured Housing, National Fire Protection Association, Quincy, MA.
123. UL 1685, Standard Vertical-Tray Fire-Propagation and Smoke-Release Test for Electrical and Optical-Fiber Cables, Underwriters Laboratories, Northbrook, IL.
124. NFPA 1, Uniform Fire Code, National Fire Protection Association, Quincy, MA.
125. NFPA 5000, Building Construction and Safety Code, National Fire Protection Association, Quincy, MA.
126. NFPA 909, Code for the Protection of Cultural Resource Properties—Museums, Libraries, and Places of Worship, National Fire Protection Association, Quincy, MA.
127. NFPA 914, Code for Fire Protection of Historic Structures, National Fire Protection Association, Quincy, MA.
128. ASTM E 1995, Standard Test Method for Measurement of Smoke Obscuration Using a Conical Radiant Source in a Single Closed Chamber, with the Test Specimen Oriented Horizontally, Annual Book ASTM Standards, American Society for Testing and Materials, West Conshohocken, PA.
129. NFPA 270, Standard Test Method for Measurement of Smoke Obscuration Using a Conical Radiant Source in a Single Closed Chamber, National Fire Protection Association, Quincy, MA.
130. ISO 5659-2, Plastics—Smoke Generation—Part 2: Determination of Optical Density by a Single-Chamber Test, International Organization for Standardization (ISO), Geneva, Switzerland.
131. ASTM 1317, Standard Test Method for Flammability of Marine Surface Finishes, Annual Book ASTM Standards, American Society for Testing and Materials, West Conshohocken, PA.
132. ISO 1716, Reaction to Fire Tests for Building Products—Determination of the Heat of Combustion, International Organization for Standardization (ISO), Geneva, Switzerland.
133. UL Subject 2424, Outline of Investigation for Cable Marked Limited Combustible, Underwriters Laboratories, Northbrook, IL.
134. NFPA 259, Standard Test Method for Potential Heat of Building Materials, National Fire Protection Association, Quincy, MA.
135. NFPA 13D, Standard for the Installation of Sprinkler Systems in One- and Two-Family Dwellings and Manufactured Homes, National Fire Protection Association, Quincy, MA.
136. NFPA 13R, Standard for the Installation of Sprinkler Systems in Residential Occupancies up to and Including Four Stories in Height, National Fire Protection Association, Quincy, MA.
137. NFPA 99, Standard for Health Care Facilities, National Fire Protection Association, Quincy, MA.
138. UMC, Uniform Mechanical Code, International Association of Plumbing and Mechanical Officials (IAPMO), Ontario, CA.
139. NFPA 274, Standard Test Method to Evaluate Fire Performance Characteristics of Pipe Insulation, National Fire Protection Association, Quincy, MA.
140. ASTM D 1929, Standard Test Method for Determining Ignition Temperature of Plastics, Annual Book ASTM Standards, American Society for Testing and Materials, West Conshohocken, PA.
141. ISO 5657, Reaction to Fire Tests—Ignitability of Building Products Using a Radiant Heat Source, International Organization for Standardization, Geneva, Switzerland.
142. ASTM D 3874, Standard Test Method for Ignition of Materials by Hot Wire Sources, Annual Book ASTM Standards, American Society for Testing and Materials, West Conshohocken, PA.
143. IEC 60695-2-2, Fire Hazard Testing—Part 2: Test Methods—Section 2: Needle-Flame Test, International Electrotechnical Commission, Geneva, Switzerland.
144. ASTM D 6194, Standard Test Method for Glow Wire Ignition of Materials, Annual Book ASTM Standards, American Society for Testing and Materials, West Conshohocken, PA.
145. IEC 60695-2-10, Fire Hazard Testing—Part 2-10: Glowing/Hot-Wire Based Test Methods—Glow-Wire Apparatus and Common Test Procedure, International Electrotechnical Commission, Geneva, Switzerland.
146. ASTM E 1321, Standard Test Method for Determining Material Ignition and Flame Spread Properties, Annual Book ASTM Standards, American Society for Testing and Materials, West Conshohocken, PA.
147. Hirschler, M.M., Heat release from plastic materials, Chapter 12a, in *Heat Release in Fires*, Elsevier, London, U.K., Eds. V. Babrauskas and S.J. Grayson, pp. 375–422, 1992.

148. ASTM D 2863, Standard Test Method for Measuring the Minimum Oxygen Concentration to Support Candle-Like Combustion of Plastics (Oxygen Index), Annual Book ASTM Standards, American Society for Testing and Materials, West Conshohocken, PA.
149. ISO 4589-3, Plastics—Determination of Burning Behaviour by Oxygen Index—Part 3: Elevated-Temperature Test, International Organization for Standardization, Geneva, Switzerland.
150. UL 94, Standard for Test for Flammability of Plastic Materials for Parts in Devices and Appliances, Underwriters Laboratories, Northbrook, IL.
151. Cullis, C.F. and Hirschler, M.M., *The Combustion of Organic Polymers*, Oxford University Press, Oxford, U.K., 1981.
152. ASTM D 3675, Standard Test Method for Surface Flammability of Flexible Cellular Materials Using a Radiant Heat Energy Source, Annual Book ASTM Standards, American Society for Testing and Materials, West Conshohocken, PA.
153. Steiner, A.J., Underwriters Laboratories, *Res. Bull.* No. 32, 1944.
154. Belles, D.W., Fisher, F.L., and Williamson, R.B., How well does the ASTM E84 predict fire performance of textile wallcoverings? *Fire J.*, 82(1), 24–30, 74 (1988).
155. Quintiere, J.G. and Harkleroad, M., *New Concepts for Measuring Flame Spread Properties*, U.S. National Bureau Standards, Gaithersburg, MD, NBSIR 84-2943, 1984.
156. Babrauskas, V., Effective measurement techniques for heat, smoke and toxic fire gases, *International Conference FIRE: Control the Heat-Reduce the Hazard*, Fire Research Station, October 24–25, London, U.K., #4, 1988.
157. Babrauskas, V. and Grayson, S.J., *Heat Release in Fires*, Elsevier, London, U.K., 1992.
158. Hirschler, M.M., Fire retardance, smoke toxicity and fire hazard, in *Proceedings of the Flame Retardants '94*, British Plastics Federation Editor, Interscience Communications, London, U.K., January 26–27, pp. 225–237, 1994.
159. Hirschler, M.M., Analysis of and potential correlations between fire tests for electrical cables, and how to use this information for fire hazard assessment, *Fire Technol.*, 33, 291–315 (1997).
160. Hirschler, M.M., How to decide if a material is suitable for an application where fire safety is required, *Flame Retardants 2002*, February 5–6, London, pp. 45–56, Interscience Communications, London, U.K., 2002.
161. Hirschler, M.M., Fire safety, smoke toxicity and acidity, *Flame Retardants 2006*, February 14–15, London, pp. 47–58, Interscience Communications, London, U.K., 2006.
162. Babrauskas, V. and Peacock, R.D., Heat release rate: The single most important variable in fire hazard, *Fire Saf. J.*, 18, 255–72 (1992).
163. Smith, E.E., Heat release rate of building materials, in *Ignition, Heat Release and Noncombustibility of Materials*, ASTM STP 502, (A.F. Robertson, editor), p. 119, American Society for Testing and Materials, Philadelphia, 1972.
164. Babrauskas, V., Development of the Cone Calorimeter. A Bench-Scale Heat Release Rate Apparatus Based on Oxygen Consumption, National Bureau of Standards, NBSIR 82-2611 (1982).
165. Hirschler, M.M., The measurement of smoke in rate of heat release equipment in a manner related to fire hazard, *Fire Saf. J.*, 17, 239–258 (1991).
166. Babrauskas, V., *Bench-scale methods for prediction of full-scale fire behavior of furnishings and wall linings*, Technology Report 84-10, Society of Fire Protection Engineers, Boston, MA, 1984.
167. Babrauskas, V., Upholstered furniture room fires—Measurements, comparison with furniture calorimeter data, and flashover predictions, *J. Fire Sci.*, 2, 5–19 (1984).
168. Babrauskas, V. and Krasny, J.F., Prediction of upholstered chair heat release rates from bench-scale measurements, in *Fire Safety. Science and Engineering*, ASTM STP 882, Ed. T.Z. Harmathy, p. 268, American Society for Testing and Materials, Philadelphia, PA, 1985.
169. Hirschler, M.M., Tools available to predict full scale fire performance of furniture, in *Fire and Polymers. II. Materials and Tests for Hazard Prevention*, Ed. G.L. Nelson, ACS Symposium Series 599, Developed from ACS Symposium in 208th ACS National Meeting, August 21–25, 1994, Washington, DC, Chapter 36, pp. 593–608, American Chemical Society, Washington, DC, 1995.
170. Lyon, R.E., Fire-safe aircraft cabin materials, in *Fire and Polymers. II. Materials and Tests for Hazard Prevention*, Ed. G.L. Nelson, ACS Symposium Series 599, Developed from ACS Symposium in 208th ACS National Meeting, August 21–25, 1994, Washington, DC, Chapter 38, pp. 618–638, American Chemical Society, Washington, DC, 1995.
171. ASTM F 1085, Standard Specification for Mattress and Box Springs for Use in Berths in Marine Vessels (Annexes A1 and A3), Annual Book ASTM Standards, American Society for Testing and Materials, West Conshohocken, PA.
172. ASTM E 1822, Standard Method for Fire Testing of Stacked Chairs, Annual Book ASTM Standards, American Society for Testing and Materials, West Conshohocken, PA.

173. ASTM D 5424, Standard Test Method for Smoke Obscuration of Insulating Materials Contained in Electrical or Optical Fiber Cables When Burning in a Vertical Cable Tray Configuration, Annual Book ASTM Standards, American Society for Testing and Materials, West Conshohocken, PA.
174. ASTM D 5537, Standard Test Method for Heat Release, Flame Spread, Smoke Obscuration, and Mass Loss Testing of Insulating Materials Contained in Electrical or Optical Fiber Cables When Burning in a Vertical Cable Tray Configuration, Annual Book ASTM Standards, American Society for Testing and Materials, West Conshohocken, PA.
175. UL 1975, Standard for Fire Tests for Foamed Plastics Used for Decorative Purposes, Underwriters Laboratories, Northbrook, IL.
176. NFPA 289, Standard Method of Fire Test for Individual Fuel Packages, National Fire Protection Association, Quincy, MA.
177. ASTM E 2257, Standard Test Method for Room Fire Test of Wall and Ceiling Materials and Assemblies, Annual Book ASTM Standards, American Society for Testing and Materials, West Conshohocken, PA.
178. ISO 9705, Room Fire Test in Full Scale for Surface Products, ISO 9705, International Organization for Standardization, Geneva, Switzerland.
179. Hirschler, M.M., Use of heat release rate to predict whether individual furnishings would cause self propagating fires, *Fire Saf. J.*, 32, 273–296 (1999).
180. Sarkos, C.P. and Hill, R.G., Evaluation of aircraft interior panels under full-scale cabin fire test conditions, AIAA-85-0393, *AIAA 23rd Aerospace Sciences Meeting*, Reno, NV, 1985.
181. Wickstrom, U. (Programme Manager), *Proceedings of the International EUREFIC Seminar*, September 11–12, Copenhagen, Denmark, Interscience Commun., London, U.K., 1991.
182. Babrauskas, V., Applications of predictive smoke measurements, *J. Fire Flamm.*, 12, 51 (1981).
183. Quintiere, J.G., Smoke measurements: An assessment of correlations between laboratory and full-scale experiments, *Fire Mater.*, 6, 145 (1982).
184. Babrauskas, V., Use of the cone calorimeter for smoke prediction measurements, in *SPE RETEC Conference on PVC: The Issues*, Atlantic City, NJ, p. 41, 1987.
185. Hirschler, M.M., Smoke in fires: Obscuration and toxicity, Plenary Lecture, *Business Communications Company Conference on Recent Advances in Flame Retardancy of Polymeric Materials*, May 15–17, Stamford, CT, Eds. G.S. Kirshenbaum and M. Lewin, pp. 70–82, Norwalk, CT, 1990; Hirschler, M.M., How to measure smoke obscuration in a manner relevant to fire hazard assessment: Use of heat release calorimetry test equipment, *J. Fire Sci.*, 9, 183–222 (1991).
186. Breden, L.H. and M. Meisters, M., The effect of sample orientation in the smoke density chamber, *J. Fire Flamm.*, 7, 234 (1976).
187. Ohlemiller, T.J. and Shields, J.R., Aspects of the fire behavior of thermoplastic materials, NIST Technical Note 1493, National Institute of Standards and Technology, Gaithersburg, MD 20899, January 2008.
188. Hirschler, M.M., Smoke and heat release and ignitability as measures of fire hazard from burning of carpet tiles, *Fire Saf. J.*, 18, 305–324 (1992).
189. Hirschler, M.M. and Janssens, M.L., Smoke obscuration measurements in the NFPA 265 Room-Corner Test, *Proceedings of the 6th Fire and Materials Conference*, February 22–23, Ed. S.J. Grayson, San Antonio, TX; Interscience Commun., London, U.K., pp. 179–198, 1999.
190. Hirschler, M.M., Fire Performance of Organic Polymers, Thermal Decomposition, and Chemical Composition, American Chemical Society, *Fire and Polymers—Materials and Solutions for Hazard Prevention*, ACS Symposium Series 797, Eds. G.L. Nelson and C.A. Wilkie, Washington, DC, pp. 293–306, 2001.
191. Jin, T., Studies of emotional instability in smoke from fires, *J. Fire Flamm.*, 12, 130–142 (1981).
192. ASTM E 1678, Standard Test Method for Measuring Smoke Toxicity for Use in Fire Hazard Analysis, Annual Book ASTM Standards, American Society for Testing and Materials, West Conshohocken, PA.
193. NFPA 269, Standard Test Method for Developing Toxic Potency Data for Use in Fire Hazard Modeling, National Fire Protection Association, Quincy, MA.
194. Hirschler, M.M., Fire hazard and toxic potency of the smoke from burning materials, *J. Fire Sci.*, 5, 289–307 (1987).
195. Babrauskas, V., Harris, R.H., Gann, R.G., Levin, B.C., Lee, B.T., Peacock, R.D., Paabo, M., Twilley, W., Yoklavich, M.F., and Clark, H.M., *Fire Hazard Comparison of Fire-Retarded and Non-Fire-Retarded Products*, NBS Special Publ. 749, National Bureau of Standards, Gaithersburg, MD, 1988.
196. Mulholland, G.W., in W.M. Pitts, Executive summary for the workshop on developing a predictive capability for CO formation in fires, NISTIR 89-4093, National Institute of Standards and Technology, Gaithersburg, MD, p. 25, 1989.

197. Babrauskas, V., Harris, R.H., Braun, E., Levin, B.C., Paabo, M., and Gann, R.G., The Role of Bench-Scale Data in Assessing Real-Scale Fire Toxicity, NIST Tech. Note # 1284, National Institute of Standards and Technology, Gaithersburg, MD, 1991.
198. Babrauskas, V., Levin, B.C., Gann, R.G., Paabo, M., Harris, R.H., Peacock, R.D., and Yusa, S., *Toxic Potency Measurement for Fire Hazard Analysis*, NIST Special Publication # 827, National Institute of Standards and Technology, Gaithersburg, MD, 1991.
199. Debanne, S.M., Hirschler, M.M., and Nelson, G.L., The importance of carbon monoxide in the toxicity of fire atmospheres, in *Fire Hazard and Fire Risk Assessment*, Ed. M.M. Hirschler, ASTM STP 1150, American Society for Testing and Materials, Philadelphia, PA, pp. 9–23, 1992.
200. Hirschler, M.M. (Editor-in-chief), and Debanne, S.M., Larsen, J.B., and Nelson, G.L., *Carbon Monoxide and Human Lethality—Fire and Non-Fire Studies*, Elsevier, London, U.K., 1993.
201. Gann, R.G., Babrauskas, V., Peacock, R.D., and Hall, J.R., Fire conditions for smoke toxicity measurement, *Fire Mater.*, 18, 193–99 (1994).
202. Hall, J.R., The U.S. Fire Problem Overview Report—Leading Causes and Other Patterns and Trends, National Fire Protection Association, Quincy, MA, March 1998.
203. Hirschler, M.M., The role of carbon monoxide in the toxicity of fire atmospheres, in *Proceedings of the 19th International Conference on Fire Safety*, Ed. C.J. Hilado, Product Safety Corp., San Francisco, CA, January 10–14, pp. 163–84, 1994.
204. Budnick, E.K., *Mobile Home Living Room Fire Studies*, NBSIR 78-1530, National Bureau of Standards, Gaithersburg, MD, 1978.
205. Budnick, E.K., Klein, D.P., and O’Laughlin, R.J., Mobile Home Bedroom Fire Studies: The Role of Interior Finish, NBSIR 78-1531, National Bureau of Standards, Gaithersburg, MD, 1978.
206. Levine, R.S. and Nelson, H.E., Full Scale Simulation of a Fatal Fire and Comparison of Results with two Multiroom Models, NISTIR 90-4268, National Institute of Standards and Technology, Gaithersburg, MD, 1990.
207. Gottuk, D.T., Roby, R.J., Peatross, M.J., and Beyler, C.L., CO production in compartment fires, *J. Fire Protect. Eng.*, 4, 133–50 (1992).
208. Beyler, C.L., Major species production by diffusion flames in a two-layer compartment fire environment, *Fire Saf. J.*, 10, 47–56 (1986).
209. Lyon, R.E. and Walters, R.N., Pyrolysis combustion flow calorimetry, *J. Anal. Appl. Pyrolysis*, 71(1), 27–46 (2004).
210. ASTM D 7309, Standard Test Method for Determining Flammability Characteristics of Plastics and Other Solid Materials Using Microscale Combustion Calorimetry, Annual Book ASTM Standards, American Society for Testing and Materials, West Conshohocken, PA.

22 Changing Chemical Regulations and Demands

Susan D. Landry

CONTENTS

22.1	Introduction.....	672
22.2	Regulatory Drivers and Demands.....	672
22.2.1	The Precautionary Principle.....	672
22.2.2	Science-Based Drivers.....	673
22.2.2.1	Chemical Inventories.....	673
22.2.2.2	TSCA.....	675
22.2.2.3	Hazard × Exposure = Risk.....	676
22.2.2.4	Risk Assessment.....	677
22.2.2.5	REACH.....	681
22.3	Current Flame-Retardant Regulatory Activity.....	687
22.3.1	European Union.....	687
22.3.1.1	RoHS Directive.....	687
22.3.1.2	WEEE Directive.....	688
22.3.1.3	REACH.....	688
22.3.1.4	Other European Activity.....	689
22.3.2	Asia and Japan.....	689
22.3.2.1	China.....	689
22.3.2.2	Korea.....	689
22.3.2.3	Japan.....	690
22.3.3	North America.....	691
22.3.3.1	Risk Assessments.....	691
22.3.3.2	EPA Activity.....	692
22.3.3.3	CPSC.....	693
22.3.3.4	State Legislation.....	693
22.3.3.5	Canada.....	694
22.3.3.6	Other Activity.....	695
22.4	Development of Sustainable Solutions.....	696
22.4.1	Selection Criteria for “Green” Solutions.....	696
22.4.1.1	Green Chemistry.....	697
22.4.1.2	Flame-Retardants and “Green Solutions”.....	697
22.4.2	Incorporation of Life-Cycle Thinking.....	698
22.4.3	Product Stewardship.....	698
22.5	Conclusions.....	699
	References.....	700

22.1 INTRODUCTION

The use of flame-retardants has played a significant role in making homes, hotels, hospitals, nursing homes, offices, automobiles, and public transportation safer. They have no doubt helped to save countless lives.¹ While fire continues to be an ever-present threat to society and improvements in fire safety standards appear to be stalled, flame-retardants, and generally all chemicals, have been coming under tremendous environmental attack.^{2,3} The attacks stem from the fact that low levels of particular flame-retardants have been detected in the environment and, in some cases, in animals and humans.^{4,5}

Improvements in analytical techniques and the ability to accurately and readily detect chemicals to extremely low levels (parts per trillion) have sparked fear at the mention of detection of any chemical, regardless of the risk associated with it.^{6,7} Governmental, environmental group, and consumer concerns have led to a considerable amount of pressure being placed on regulators to prohibit the use of chemicals that are detected in the environment, including particular flame-retardants or classes of flame-retardants.

The pressure to eliminate particular chemicals or classes of chemicals comes in the form of considerable media misinformation and the singling out of certain companies as low scorers in overall environmental rankings. As a result, manufacturers of electronic equipment and other consumer and industrial goods have become more conscience of public perception and have started to restrict certain materials even without legislation to restrict these materials being in place.

The pressure that chemicals have come under has led to a patchwork of worldwide chemical regulations. Regulations in one part of the world have an almost immediate impact throughout the globe, with regulations in each country having their own distinct differences. Evaluation of the risks of chemicals is the current focus of many regulatory programs. This approach takes into account the hazard of a substance, plus the exposure to the substance to determine the risk. One such program that entered into effect on July 1, 2007 in the European Union (EU) is the Registration, Evaluation, and Restriction of Chemicals (REACH). The principle of REACH is “no data, no market.” This approach is welcomed, as the importance to ensure that all flame-retardants are safe for use, now and in the future is well recognized. To do this, regulatory decisions need to be based on sound science. The regulation system in place also needs to be adhered to and accepted by everyone. If society is to operate effectively and efficiently, then acceptance of good regulatory programs is of utmost importance.

As the title of this chapter indicates, chemical regulations and demands are in a state of constant change. The drive to attain environmentally preferable products is a dynamic process. There is constant movement and trade-offs with the ultimate goal being to obtain “green” products. This chapter reflects the state of activity as of October 2008.

22.2 REGULATORY DRIVERS AND DEMANDS

Various regulatory drivers and demands from governmental organizations, environmental groups, and consumers all help to shape the worldwide landscape of chemical use. This section will focus on the precaution and science that impact the use of flame-retardants.

22.2.1 THE PRECAUTIONARY PRINCIPLE

The basic premise of the *Precautionary Principle* is that decision makers should implement regulatory measures to prevent or restrict actions that may harm humans or the environment, even though there is incomplete scientific evidence to assess the significance of the potential harm. It has been used as an underlying rationale in several international treaties and declarations. There are various definitions of the *Precautionary Principle* that are represented as “better safe than sorry.” The U.S. Environmental Protection Agency (EPA) defines it as, “When information about potential risks

is incomplete, basing decisions about the best ways to manage or reduce risks on a preference for avoiding unnecessary health risks instead of on unnecessary economic expenditures.”⁸

The *Precautionary Principle* focuses on the possibility that technologies or actions could pose unique, extreme, or unmanageable risks, even if considerable testing has already been conducted. The *Precautionary Principle* has been criticized for a variety of reasons. Some of these reasons include

- It makes a case for controlling or eliminating chemical substances that *might* cause harm
- It does not weigh the benefits of products
- It fails to acknowledge that even when technologies introduce new risks, other hazards are most often reduced, resulting in net benefits⁹
- It is a threat to technological progress, which is itself a threat to public health and environmental protection¹⁰

The *Precautionary Principle* differs from the current regulatory approach in the United States. Most regulatory decisions in the United States are based on scientific evidence and evaluation of the risks. This system allows for improvements in the quality of products or life, while identifying and minimizing any short-term or long-term potential hazard. U.S. federal regulatory bodies do incorporate conservative assumptions and factors of safety when determining if a product is safe or should be restricted. On the other hand, the EU has incorporated the *Precautionary Principle* into its environmental and health regulations. Two flame-retardants, pentabromodiphenyl ether (penta-BDE) and octabromodiphenyl ether (octa-BDE), were banned in the EU as of August 2004 based upon the *Precautionary Principle*. Each material was going through the EU Risk Assessment process [under Council Regulation (EEC) No 793/93 on the Control and Evaluation of the Risks of Existing Substances],^{11,12} and with data gaps and some risks identified, the *Precautionary Principle* was invoked. Several U.S. State prohibitions on penta- and octa-BDE have also followed the precautionary approach.¹³

The U.S. EPA and many other organizations point out that, when information about potential risks is incomplete, basing decisions to avoid unnecessary health risks is potentially the best option.⁸ When a good set of scientific data is available on a material, then the *Precautionary Principle* is not appropriate. Scientific data generated in the EU Risk Assessments or under risk assessment programs, such as REACH, that deem materials safe for continued use should effectively rule out the use of *Precautionary Principle*.

22.2.2 SCIENCE-BASED DRIVERS

This section contains information on several of the various science-based drivers that provide a platform to facilitate the use of science in decision making. The drivers included in this section are: Chemical Inventories, TSCA, Hazard \times Exposure = Risk, Risk Assessments, and Risk vs. Benefit.

22.2.2.1 Chemical Inventories

A chemical inventory is a listing of industrial chemicals manufactured in, or imported by, a country and is used primarily to distinguish between new and existing chemicals.¹⁴ It is basically a database created from information submitted to government authorities by manufacturers, processors, users, or importers. Depending on the country, the content of an inventory can range from the Chemical Abstracts Services (CAS) numbers or names of chemicals in commerce, to the amount produced and imported by specific location, to the amounts being used for different purposes.

The purpose of an inventory is to consolidate basic knowledge about chemicals imported, used, and manufactured in a country and serve as an important basis for informed chemical management. Inventories are the usual instrument for identifying chemicals that are already in commerce in a particular country and serve as the trigger for new chemical review programs.

An inventory is typically based on an act, directive, decree, or other legal instrument. The initial inventory includes a definition of the chemicals that exist in commerce in the jurisdiction. As chemicals are introduced into commerce, they are generally added and identified as new chemicals. This introduction of new chemicals results in most inventories being continuously updated.

Most countries with chemical inventories have excluded by-products, small product tests and laboratory quantities, and naturally occurring substances from their reporting schemes. One of the issues associated with inventories is the definition of a chemical. The definition of polymers is a complex issue that will vary depending upon the nature of the chemicals from which they are formed, their relative proportions, the order of reaction, and reaction conditions (duration, temperature, catalysts, etc.).¹⁴ Most inventories include polymers and treat all different polymeric substances and monomers as individual chemicals. Some countries, including the United States, have decided not to require updated reporting on the production of such polymers. None of the national chemical inventories include formulated mixtures, or preparations, such as paints and household cleaners, or articles such as automobiles, computers, and paper.

In most existing inventories, chemical identities are standardized through the use of CAS numbers, molecular formulas (chemicals with discrete structures), and IUPAC (International Union of Pure and Applied Chemistry) systematic nomenclature. Chemicals of unknown or variable composition, complex reaction products, and biological materials (UVCB), are usually listed alphabetically under subheadings or by definition.¹⁴ Some of the countries that have compiled various inventories include Australia, Canada, EU, Japan, Philippines, South Korea, and United States.

22.2.2.1.1 *Australia*

The Australia inventory is the Australian Inventory of Chemical Substances (AICS).^{15,16} It was established for the purpose of implementing the Industrial Chemicals (Notification and Assessment) Act 1989. The National Industrial Chemicals Notification and Assessment Scheme (NICNAS) operates under the Act for the notification and assessment of industrial chemicals and is administered by the National Occupational Health and Safety Commission (NOHSC). The list contains over 40,000 substances which gets added to regularly.

22.2.2.1.2 *Canada*

The Canadian new chemicals program uses two chemical inventories, the Domestic Substances List (DSL) and the Non-Domestic Substances List (NDSL). The DSL includes substances that were, between January 1, 1984, and December 31, 1986, in Canadian commerce, used for manufacturing purposes, or manufactured in or imported into Canada.¹⁷ It contains about 23,000 substances. One of the initiatives in the *Canadian Environmental Protection Act, 1999* (CEPA, 1999) requires the Minister of the Environment and the Minister of Health to “categorize” (Section 73, CEPA 1999) and then if necessary, conduct screening assessments (Section 74, CEPA 1999) of substances listed on the DSL to determine whether they are “toxic” or capable of becoming “toxic” as defined in the Act. The NDSL is a list of substances not on DSL but in commerce elsewhere in the world.¹⁸ The NDSL contains more than 58,000 entries.

22.2.2.1.3 *Europe*

The European Inventory of Existing Commercial Chemical Substances (EINECS) consists of substances on the market in the European Community between 1971 and 1981.¹⁹ These substances may be imported or manufactured without further notification. The list of 100,106 substances was published in 1990, and the contents are fixed. All chemicals that will be marketed after the September 18, 1981 are not placed on the EINECS. These chemicals have to be notified before they will be placed on the market according to the sixth Amendment of Directive 67/548/EEC, Directive 79/831/EEC. Once assessed, these new chemicals are listed on the European List of New Chemical Substances (ELINCS).²⁰ These substances must be notified by each new importer/manufacturer (although sometimes reduced notification packages may be accepted if the substance has already

been assessed once). The former European Chemicals Bureau (ECB) coordinated scientific and technical work of the EU notification scheme and risk assessment for new chemical substances (Directive 67/548/EEC including Annexes VII and VIII, Directive 93/67/EEC). On June 1, 2008, this notification scheme was revoked and replaced by the Regulation (EC) No 1907/2006 concerning the Registration, Evaluation, Authorization, and Restriction of Chemicals (REACH).^{21,22}

22.2.2.1.4 Japan

The Existing and New Chemical Substances (ENCS) regulates chemical substances that are either manufactured or imported in Japan.²³ It was initiated by the Kashin Act of Japan, which designated the Ministry of International Trade and Industry (MITI) as the responsible agency for compiling and publishing the list, as well as being the recipient for notifications regarding changes and new substances. The list is also referred to as the “MITI List” or “MITI Inventory.”

22.2.2.1.5 Philippines

The Philippines Inventory of Chemicals and Chemical Substances (PICCS) was published in April 1996. It contains approximately 24,000 chemicals and chemical substances. Chemicals manufactured, imported, distributed, or used in the Philippines in the 5 years prior to December 31, 1993 were nominated for inclusion in the Inventory.^{24,25}

22.2.2.1.6 South Korea

The Korean Existing Chemicals List (ECL) was established in 1991 under the Toxic Chemicals Control Law (TCCL).²⁶ The ECL, published by the Minister of Environment, is current through 1994 and contains approximately 30,000 substances. Newly manufactured or imported chemicals are subject to a toxicity examination by the Ministry of Environment (MOE).

22.2.2.1.7 United States

In the United States, the Toxic Substances Control Act (TSCA) Chemical Substances Inventory (derived from the *Initial Inventory* of the *TSCA Chemical Substance Inventory*) is a listing of chemical substances manufactured, imported, or in commercial use in the United States.²⁷ It is not a list of toxic chemicals, since toxicity is not a criterion for inclusion in the list. It was developed in response to Section 8 (d) of the TSCA, public law 94-469, and was prepared by the U.S. EPA.

The primary objective of the TSCA Inventory is to define what chemical exist in U.S. commerce for purposes of implementing the Toxic Chemicals Control Act. Specifically, chemicals not included on the Inventory are considered to be “new” chemicals under TSCA and are subject to the premanufacture notification (PMN) requirements stipulated under section 5 (a) of TSCA. The purpose of the TSCA Inventory is to identify those chemicals that exist in U.S. commerce, which have commercial applications that are not specifically addressed under other existing environmental legislation.

The initial Inventory covers chemicals that were manufactured in or imported into the United States for the period of January 1, 1975 through December 31, 1977. New chemicals that have completed PMN review are added to the Inventory after commercial manufacture of the chemical has commenced. In addition, the TSCA Inventory provides a basis for chemical screening, chemical risk assessment, and chemical management. Many new chemicals are submitted as confidential materials, which mean that information on structure, use, etc. is not available to the public.²⁸ The premise is that the release of this information would be detrimental to the financial interests of the submitting company.

22.2.2.2 TSCA

The TSCA became law on October 11, 1976 and came into effect on January 1, 1977, except Section 4 (f) which took effect 2 years later.²⁹ A major objective of TSCA is to characterize and evaluate the risks posed by a chemical to humans and the environment before the chemical is introduced into commerce. The Act authorized the U.S. EPA to secure information on all new and existing chemical substances. The Act also gave the EPA the authority to control any of the substances that were

determined to cause unreasonable risk to public health or the environment. The EPA has the authority to ban the manufacture or distribution in commerce, limit the use, require labeling, or place other restrictions on chemicals that pose unreasonable risks.

Originally, TSCA only encompassed the control of hazardous substances. The U.S. Congress later added additional titles to the Act, with the original part designated at “Title I—Control of Hazardous Substances.” This original section includes provisions for the testing of existing chemical substances and mixtures, regulation of hazardous chemical substances and mixtures, manufacture and processing notices, and requirements for managing imminent hazards and reporting and recordkeeping. All manufacturers (importers), processors, distributors, and users of chemical substances in the United States may be subject to TSCA reporting, recordkeeping, and testing requirements. TSCA primarily falls under SIC Codes 20–39 (Manufacturing). Typical types of Industry and sectors covered under TSCA include companies that are engaged in chemical production and importation, petroleum refining, paper production, and microelectronics manufacturing. Sectors include organics, inorganics, plastics, and chemical preparations.

The EPA may issue a civil administrative complaint to any person or company who violates the TSCA.³⁰ This complaint may impose a civil penalty, including recovery of any economic benefit of noncompliance, and may also require correction of the violation. The penalties for violations of TSCA may be up to \$27,500 per violation (per day).

TSCA was first enacted in 1976 and has been amended significantly three times. It is a federally managed law and is not delegated to states.³⁰ TSCA gives EPA broad authority to regulate the manufacture, use, distribution in commerce, and disposal of chemical substances. The law is overseen by the EPA Office of Pollution Prevention and Toxics (OPPT).³¹

TSCA places requirement that manufacturers perform various kinds of health and environmental testing, use quality control in their production processes, and notify EPA of information they gain on possible adverse health effects from use of their products. Under TSCA, “manufacturing” is defined to include “importing,” and thus all requirements applicable to manufacturers apply to importers as well. Under TSCA, EPA classifies chemical substances as either “existing” chemicals or “new” chemicals. Searches of the nonconfidential, public Inventory, are available.

Section 4 of TSCA requires manufacturers, importers, and processors of certain chemical substances and mixtures to conduct testing on the health and environmental effects of chemical substances and mixtures, unless they qualify for an exemption.³² Testing requirements cover existing chemicals that are both individual substances and mixtures. New chemicals are not covered, since they are addressed in the PMN process. EPA has established a “Master Testing List” that lays out testing priorities, based on risk and exposure potential.

On July 24, 2008, the EPA published a proposed test rule under Section 4 of TSCA for 19 chemical substances.³³ The proposed testing for each chemical under the proposed rule is deemed necessary by EPA to inform various data needs that will provide critical information about the environmental fate and potential hazards associated with these chemicals. The data will be used in conjunction with data on exposure and uses to evaluate potential health and environmental risks.

Section 5 of TSCA regulates the manufacture or import a “new” chemical substance for commercial purposes. Under this section, EPA requires notice before manufacture or importation of nonexempt substances. They then evaluate whether the chemical substance poses a threat to human health or the environment. This notice is called a PMN and must be submitted at least 90 days prior to the activity.³⁴ Manufacturers must also submit information on “significant new uses” of existing chemicals to EPA for its review. After its review of the PMN or Significant New Use information, EPA may limit, restrict, or prohibit the manufacture, use, distribution, or disposal of the chemical substance.

22.2.2.3 Hazard × Exposure = Risk

With the concern for risks associated with various chemicals, it is important to understand what defines risk. Risk is the chance that harm will actually occur, and it involves both hazard and

exposure.^{35,36} To determine the risk of a substance, both hazard and exposure must be taken into consideration, as expressed in this simple equation: Hazard \times Exposure = Risk.

Hazard is the potential to cause harm. A chemical hazard exists where a substance has a built-in ability to cause an adverse effect. Risk is the likelihood of harm. It is distinctly different from hazard, in that exposure is a key factor. If either hazard or exposure is missing, there is no risk.

Exposure is the extent to which the likely recipient of the harm is exposed, or can be influenced by, the hazard. The degree of exposure is a very important determinant of risk.³⁷ "All substances are poisons, there is none which is not a poison. The right dose differentiates a poison from remedy."³⁸ A low exposure to something that is highly hazardous may result in a low risk. Conversely, a high exposure to something of low hazard may result in a moderate or even high risk. With this in mind, every reasonable attempt must be made to attempt quantification and exposure to then proceed to attribute a measure at risk to it.

To assess risk, both hazard and exposure must be considered. Risk assessment is a management tool to determine whether, how, and in what circumstances, harm might be caused.³⁵ A good risk assessment will determine the human health and environmental characteristics of an individual chemical, not a class of chemicals and base conclusions on actual scientific data. The process should examine critical aspects of the chemical, including mammalian and environmental toxicology, environmental fate and releases (to water, soil, air, and from all operations throughout the lifecycle), and risk (exposures versus limits). After all this information is generated, a hazard assessment, exposure assessment, risk identification, and risk management should be generated. These results will determine if there is a need for more testing or whether there is a need for risk reduction.

Risks should always be justified by the anticipated benefits to society. A benefit is a valued or desired outcome. Risk management is the logical process of weighing the potential costs of risks against the possible benefits of allowing those risks to stand uncontrolled. Benefits of flame-retardants are not limited to saving lives, but also include reduction of injuries, reduction in loss of property, and reduction in local pollutants that result from fires. Clearly, the benefits of using flame-retardants are great and must be weighed against risks assessed in scientific risk assessments.

22.2.2.4 Risk Assessment

The EU Risk Assessment ("Council Regulation [EEC] 793/93 of 23 March 1993")³⁹ is well recognized as being the leading independent, transparent, and science-based system for assessing chemicals and substances in everyday use.⁴⁰ The Consumer Products Safety & Quality (CPS&Q) Unit, formerly known as European Chemicals Bureau (ECB), is part of the Institute for Health and Consumer Protection (IHCP), which is one of the seven scientific institutes in the European Commission's Joint Research Center (JRC).⁴¹ The CPS&Q is responsible for managing the risk assessment process. As will be discussed in further detail in Section 22.2.2.4.4, the EU Risk Assessment process was revoked on June 1, 2008 and replaced by the REACH Directive.

22.2.2.4.1 Background

The EU Risk Assessment process has been in place since the mid 1990s, and is used to evaluate the characteristics of a variety of high production volume chemicals.⁴² It is the most comprehensive assessment of these substances' environmental and health impacts throughout their entire life cycle. Each substance is assessed individually, not as a class. This process examines critical aspects of a chemical, including mammalian and environmental toxicology, environmental fate and releases (to water, soil, air, and from all operations throughout the lifecycle), and risk (exposures versus limits). After all this information is generated, a hazard assessment, exposure assessment, risk identification, and risk management is generated. This will determine whether there is a need for more testing or to reduce risks.

The responsibility for carrying out the Risk Assessment of a particular substance is entrusted to an individual EU Member State, known as a rapporteur.⁴⁰ The rapporteur is responsible for gathering relevant information and for making recommendations to the European Commission on any

control measures deemed necessary to be implemented to limit any significant risk that may exist. The Risk Assessment is separate to any risk management that may take place. The rapporteur uses all relevant information that is available and may, if necessary, ask for additional information and tests.

The substances evaluated for risk assessment were selected on the basis of potential concerns, areas of use, and volumes sold. Four priority lists were established.⁴² The risk assessments looked at the environmental and human health aspects of a chemical's use under a variety of scenarios. For each scenario, one of the following three conclusions was drawn:⁴³

- Conclusion I—There is a need for further information or testing
- Conclusion II—There is at present no need for further information or testing and no need for risk reduction measures beyond those which are being applied already
- Conclusion III—There is a need for limiting the risks; risk reduction measures, which are already being applied, shall be taken into account.

If a need for risk reduction was identified, a risk reduction strategy was developed under the guidance of a risk management committee.⁴⁰ In the ultimate case, the banning of the use of a substance could be implemented. The regulation also allowed for a regular review of new science, and if appropriate, the original conclusions could be changed. This process facilitates the conclusions reflecting the best, most up-to-date science.

22.2.2.4.2 *Flame-Retardant Risk Assessments*

Under this regulation, a number of flame-retardants have undergone this risk assessment process. In the first and second priority lists, the commercial polybrominated diphenyl ethers (PBDEs) (decabromodiphenyl ether [deca-BDE], octa-BDE, and penta-BDE) were evaluated. The conclusions of the EU Risk Assessments on octa-BDE and penta-BDE resulted in the elimination of their use in the EU as of August 2004.^{11,12,44,45} The 10 year EU Risk Assessment on deca-BDE resulted in both the environment and human risk assessment reports concluding that there are no significant risks in these areas.⁴⁶ On that basis, the EU Competent Authorities agreed on May 26, 2004 to finalize the risk assessment with no restrictions in the use of deca-BDE.^{47,48} Additional testing (neurotoxicity study), an independent biomonitoring program, an independent environmental sampling program, and a voluntary industry-monitoring program were put in place for deca-BDE. Since the initial publication of the risk assessments for deca-BDE, there have been a number of reviews of emerging science, and any need for further risk reduction measures has not been identified.

Other flame-retardants selected as priority chemicals for the EU Risk Assessment process included tetrabromobisphenol A (TBBPA), hexabromocyclododecane (HBCD), tris(2-chloroethyl) phosphate (TCEP), tris (2-chloropropyl) phosphate (TCPP), tris(2-chloro-1-(chloromethyl)ethyl) phosphate (TDCEP), and 2,2-bis(chloromethyl) trimethylene bis (bis(2-chloroethyl)phosphate) (V6). The flame-retardant synergist, antimony trioxide (Sb_2O_3), was also identified as a priority substance. Table 22.1 contains information on the EU Risk Assessments on the nine flame-retardants and one synergist.

The EU Risk Assessment on TBBPA was recently completed with the conclusions of no restrictions for use in any applications.^{49,50} Risk was identified at one specific additive user plant, so an active emissions control program has been put into place to help ensure that emissions do not occur.

The EU Risk Assessment on HBCD was also recently concluded.⁵¹ In the risk assessment, the results indicated that in the aquatic environment, HBCD would not fulfill the formal EU criterion for being regarded as persistent. The results of monitoring data in the environment and the food chain seemed to reveal increasing levels with time; hence the EU expert working group on persistent, bioaccumulative, toxic (PBT) substances and the risk assessment group (TCNES technical committee on new and existing substances) regarded HBCD as a PBT substance based on expert

TABLE 22.1
EU Risk Assessment Summary on Flame Retardants as of October 2008

Flame-Retardant	Status	Next Steps	Risks Identified	Conclusions	Classification	SCHER Report
Penta-BDE CAS# 32534-81-9	Concluded ^{11,44}	—	Data gaps, some risks identified	Banned in EU as of August 2004	—	
Octa-BDE CAS# 32536-52-0	Concluded ^{12,45}	—	Some risks identified	Banned in EU as of August 2004	—	
Deca-BDE CAS# 1163-19-5	Concluded ⁴⁶⁻⁴⁸	Additional tests, monitoring, and emissions control in progress	None	Safe for continued use Emissions control program active	None	Yes ⁵⁹
TBBPA CAS# 79-94-7	ENV and HH finalized ^{49,52}	None	ENV: risk identified at one additive user plant only HH: None	Not restricted for any applications Authorities have emission requirements Emissions control program active	R50/53	Yes ^{61,62}
HBCD CAS#s 25637-99-4 & 3194-55-6	ENV and HH finalized ⁵¹	Risk reduction strategy ongoing New Science— Current debate of PBT status	Currently classified a PBT— Risks identified	PBT Status Debate Will be transferred to the REACH Regulation Proposed to be on the SVHC list ⁵³	R50/53	Yes ⁵²
TCPP CAS# 13674-84-5	ENV and HH finalized ⁵⁴ Submitted to ECHA on May 30, 2008	Risk reduction strategy (RRS) C&L proposal in preparation (reprotox cat. 3 R62/63 discussed borderline), Submission by December 1, 2008	Reprotox, dermal, production	TCPP will be sold with the same existing labels until a final decision on classification is made	Xn, R22	Not complete
TDCP	ENV and HH finalized ⁵⁵	RRS in preparation	RDT, Carc, dermal, few scenarios	TDCP will be sold with the same existing labels	R51/53, R40	Not complete

(continued)

TABLE 22.1 (continued)
EU Risk Assessment Summary on Flame Retardants as of October 2008

Flame-Retardant	Status	Next Steps	Risks Identified	Conclusions	Classification	SCHER Report
CAS# 13674-87-8	Submitted to ECHA on May 30, 2008	Submission by December 2008	Reprotox, RDT, Carc	Mandatory label change when formally adapted	R51/53, T R60, Xn R22, R40	Not complete
TCEP CAS# 115-96-8	ENV and HH finalized ⁵⁶	Risk reduction strategy (RRS)				
V-6 CAS# 38051-10-4	ENV and HH finalized ⁵⁷ Submitted to ECHA on May 30, 2008	—	None	TL-10ST will have no labels required	None	Not complete
Sb₂O₃ CAS# 1309-64-4	ENV and HH ongoing	Further discussions in April 2008, Risk Assessment might be transferred to REACH if not finalized	ENV: risks identified for sediments at a few plants HH: no risks identified at this stage—discussions in progress	Will be transferred to the REACH	R38, R40	—

Notes: ENV = Environmental Sections; HH = Human Health Sections; PBT = Persistent, Bioaccumulative, and Toxic; C&L = Classification and Labeling; R22 = Harmful if swallowed; R38 = irritating to skin; R40 = Carcinogenic category 3, limited evidence of a carcinogenic effect; R50/53 = Very toxic to aquatic organisms, may cause long-term adverse effects in the aquatic environment; R51/53 = Toxic for aquatic environment, may cause long-term adverse effects in the aquatic environment; R60 = Toxic to reproduction category 2 (CMR category 2); R62/63 (reprotox category 3); T = Toxic, Xn = Harmful.

judgment. New monitoring information has become available, but not published, that indicates a reverse in the trend in the environment.⁵² This science puts into question the persistence of HBCD, and hence whether or not it is truly a PBT substance, as it is presently thought. This information has not yet been published, but should hopefully be soon. HBCD will be transferred over to the EU REACH Regulation. The European Chemicals Agency (ECHA) Member State Committee has identified HBCD as one of the 15 substances of very high concern (SVHC).⁵³ Later in October 2008 ECHA will, following a formal decision, include the 15 identified as SVHC in the candidate list and publish the list on its Web site.

The EU Risk Assessments on the four chlorophosphate flame-retardants—TCPP, TDCP, TCEP, and V-6—were recently finalized.^{54–57} For TCPP, TDCP, and TCEP all had some risks identified, so risk reduction strategy for each is in progress. The classification and labeling proposal is in preparation for TCPP. No risks were identified for V-6, hence this material will have no risk phrases associated with it.

22.2.2.4.3 SCHER Opinion

After the finalization of EU Risk Assessments, The European Commission Scientific Committee on Health and Environmental Risks (SCHER) is consulted for their opinion. SCHER is a scientific

expert panel reporting to the European Commission and performs an independent science review on the Risk Assessment results. It deals with questions relating to examinations of toxicity and ecotoxicity of chemicals, biochemicals, and biological compounds for human health and the environment.⁵⁸ For deca-BDE, the SCHER Opinion stated that the risk assessment had been “well done.”⁵⁹ Both the European Commission and the U.K. government, which led the environmental risk assessment, have made clear that the SCHER Opinion provided no new evidence demonstrating a risk from deca-BDE, and that the calls made in the Opinion for risk reduction measures to address the low levels of deca-BDE found in some environmental studies are already being addressed by the industry’s monitoring and emissions control programs developed in conjunction with the EU authorities.⁶⁰

The SCHER Opinion for TBBPA considered that the human health and environmental parts of the risk assessment of TBBPA to be of acceptable and of good quality.^{61,62} The EU Commission used the SCHER Opinion in the conclusion of no restrictions for use in any applications.

For HBCD, the SCHER Opinion expressed doubts on the Persistence of HBCD and recommended to reconsider the evaluation after the publication of the new data.⁵²

SCHER supports most of the conclusions of this risk assessment. A possible exception is the PBT classification as new data seems to indicate a rapid decrease in HBCD in porpoises along the UK coast after the production was ended in that country.

The SCHER Opinion was considered, but the risk assessment was not changed and finalized under the old existing chemicals regulation before June 1, 2008, when this regulation was superseded by REACH. For TCPP, TDCP, TCEP, and V-6, SCHER is not finished.

22.2.2.4.4 *The Future for Risk Assessments in the EU*

With the launch of ECHA on June 1, 2008, the EU Risk Assessment process, or Council Regulation (EEC) 793/93 on Existing Substances, was revoked.⁶³ It was replaced by the Regulation (EC) No 1907/2006 of the European Parliament and of the Council of December 18, 2006 concerning REACH. It established a ECHA, which will manage the registration, evaluation, authorization, and restriction process for chemical substances across the EU. These REACH processes were designed to provide additional information on chemicals, to ensure their safe use, and to ensure competitiveness of the European industry. The goal of the Agency will be to take the best available scientific and technical data and socioeconomic information into account in decision making.

22.2.2.5 REACH

The REACH Regulation is a new European Community Regulation on chemicals and their safe use (Regulation EC No 1907/2006).⁶⁴ It is the central act of the new European chemicals policy. The Directive 2006/121/EC contains technical adaptations of Directive 67/548/EEC that concern the classification, packaging, and labeling of dangerous substances and applies in parallel with REACH. REACH entered into force on June 1, 2007.⁶⁴ The operational launch of ECHA was on June 1, 2008. At this time, Council Regulation (EEC) 793/93 on Existing Substances was revoked and replaced by the REACH establishing a European Chemicals Agency, amending Directive 1999/45/EC and repealing Council Regulation (EEC) No 793/93 and Commission Regulation (EC) No 1488/94 as well as Council Directive 76/769/EEC and Commission Directives 91/155/EEC, 93/67/EEC, 93/105/EC, and 2000/21/EC.²² A review of Annexes I, IV, V, XI, and XIII of the REACH regulation will be carried out within 18 months after entry into force.⁶⁵ The provisions of this regulation will be phased-in over 11 years. Background and explanations of REACH can be found in a number of Web sites.⁶⁶⁻⁷¹

Prior to the REACH Regulation, the EU had a patchwork of many different Directives and Regulations that were developed for chemical substances. There were different rules for “existing” and “new” chemicals. Although some information existed on the properties and uses of existing substances, there was a concern that there was a lack of sufficient information publicly available to

assess and control these substances effectively. Concerns included the limited substances that had undergone the EU Risk Assessment process (Regulation (EC) 793/93) since 1993. This process included 141 high-volume chemicals that were identified as priority substances for risk assessment. Recommendations for risk reduction were not available for all these substances when this process was completed. REACH simplifies EU level regulation by replacing 40 existing pieces of legislation and creating a single system for all chemicals. It will help to provide more information on ~30,000 existing substances.

The REACH Regulation creates a single system for both “existing” and “new” substances. All substances are covered by this Regulation, unless explicitly exempted from its scope. The strategy of REACH is to ensure a high level of chemicals safety and a competitiveness of the EU chemicals industry.⁶⁵ The benefits of the REACH system will come over time, as more and more substances are phased in. The objectives that were balanced within the overall framework of this sustainable development were

- Protection of human health and the environment
- Maintenance and enhancement of the competitiveness of the EU chemical industry
- Prevention of fragmentation of the internal market
- Increased transparency
- Integration with international efforts
- Promotion of nonanimal testing
- Conformity with EU international obligations under the World Trade Organization (WTO)⁶⁴

The REACH Regulation gives greater responsibility and obligations to industry for the management of the risks from chemicals and providing safety information on the substances. Manufacturers and importers will be required to gather information on the properties of their chemical substances and to register the information in a central database run in Helsinki by ECHA.⁶⁴ This Agency will coordinate the REACH system by

- Managing the databases necessary to operate the system
- Co-coordinating the in-depth evaluation of suspicious chemicals
- Running a public database in which consumers and professionals can find hazard information

In addition, ECHA manages the registration process, carries out dossier evaluations, and coordinates the substance evaluation process and generally takes decisions resulting from evaluations, except in cases of disagreement among Member States representatives when the Commission would decide. It provides expert opinions to the Commission in the authorization and restriction procedures and has duties with regard to confidentiality and access to information. It also handles requests for exemptions from the registration requirement for product and process-oriented research and development, and facilitates the sharing of animal test data at the preregistration stage by enabling the formation of the Substance Information Exchange Forums (SIEFs).

Registration requires manufacturers and importers of chemicals to obtain relevant information on their substances and to use that data to manage them safely. To reduce testing on vertebrate animals, data sharing is required for studies on such animals. For other tests, data sharing is required on request by other registrants. Better information on hazards and risks and how to manage them safely will be passed up and down the supply chain. Downstream users will be brought into the system.

During the development of REACH the EU Commission held extensive dialog with stakeholders before and after the proposal was presented. Stakeholders sent over 6000 responses during the REACH Internet consultation and contributed to the REACH Impact Assessment both before and after the launch of the Commission REACH proposal in 2003.⁷⁵ One of the purposes of the collaboration was to help the EU Commission improve the design and cost effectiveness of the system.

The scope of the REACH Regulation is very wide and covers all substances manufactured, imported, used as intermediates or placed on the market, on their own, in preparations, or in papers.⁷³ Some exceptions to this are substances that are radioactive, subject to customs supervision, or are nonisolated intermediates. Waste is specifically exempted. Food that meets the definition of a substance, on its own or in a preparation, will be subject to REACH; however, such substances are largely exempted from Registration, Evaluation, and Authorization. Member States may exempt substances used in the interests of defense. Other substances are exempted from parts of REACH, where other equivalent legislation applies. The Commission will review the scope of the Regulation 5 years after entry into force.

REACH also calls for the progressive substitution of the most dangerous chemicals when suitable alternatives have been identified. The basic elements are described as follows:

- ECHA evaluates testing proposals made by industry and checks compliance with the registration requirements
- ECHA coordinates substance evaluations by the authorities to investigate chemicals with perceived risks. This assessment may be used later to prepare proposals for restrictions or authorization
- SVHC will be made subject to authorization
 - ECHA will publish a list containing such candidate substances
 - Applicants will have to demonstrate that risks associated with uses of these substances are adequately controlled or that the socioeconomic benefits of their use outweigh the risks
 - Applicants must also analyze whether there are safer suitable alternative substances or technologies
 - If suitable substances or technologies exist, applicants must prepare substitution plans
 - If suitable substances or technologies do not exist, information on research and development activities, if appropriate, should be provided
- The Commission may amend or withdraw any authorization on review if suitable substitutes become available
- ECHA will manage the technical, scientific, and administrative aspects of the REACH system at the community level, aiming to ensure that the legislation can be properly implemented and has credibility with all stakeholders
- A classification and labeling inventory of dangerous substances will help promote agreement within industry on the classification of a substance
- For some substances of high concern there may be a Community wide harmonization of classification by the authorities
- Rules on the access to information combine a system of publicly available information over the Internet, the current system of requests for access to information, and REACH-specific rules on the protection of confidential business information

22.2.2.5.1 *Registration*

Manufacturers and importers of substances must register each substance manufactured or imported in quantities of 1 t or above per year to be allowed to continue to manufacture or import this substance.⁷³ Registration involves the manufacturer or importer providing a completed registration dossier to the Agency. The technical dossier contains information on the properties, uses, and on the classification of a substance as well as guidance on safe use. The Regulation exempts certain substances that are adequately regulated under other legislation. Also, polymers are currently exempted from the requirement to register. Registration neither means that the dossier is in compliance with the legislation nor does it mean all the properties of the registered substance have been identified. Registration requires manufacturers and importers to submit the following:

The communication requirements of REACH ensure that manufacturers, importers, and their customers (i.e., downstream users and distributors) have the information they need to use chemicals safely. Information relating to health, safety and environmental properties, and risks and risk management measures is required to be passed both up and down the supply chain. The primary tool for information is the familiar safety data sheet (SDS) for all dangerous substances.

22.2.2.5.2 *Evaluation*

There are two types of evaluation with different aims, the dossier and substance evaluations. In the dossier evaluation, the Agency will do a quality check of the registration dossiers: The Agency may check the compliance of registration dossiers with the requirements laid down for registration in the Regulation. The Agency will check the testing proposal submitted as part of the registrations before testing is performed. This is to prevent unnecessary animal testing, repetition of existing tests, and poor quality tests. Third parties will also be invited to submit information that would avoid the need for vertebrate testing.

In the substance evaluation, further information from industry may be requested to clarify suspicions of risks to human health or the environment, at the request of the Agency in coordination with the Competent Authorities of Member States. The Agency will develop guidance on the prioritization of substances for further evaluation. The Agency will publish information on its Web site to identify which Member States will carry out the evaluation on each priority substance.

22.2.2.5.3 *Authorization*

For SVHC, to be used or placed on the market, authorization is required. Substances required to undergo authorization are as follows:

- CMR categories 1 and 2
- PBT
- vPvBs
- Identified from scientific evidence as causing probable serious effects to humans or the environment equivalent to those above on a case-by-case basis, such as endocrine disrupters

The European Commission will develop guidance to clarify the criteria for determining substances of equivalent concern. Substances that fall into these categories will be fed into the authorization system as resources allow. Their uses will not necessarily be banned. The Agency will publish a list of substances meeting the criteria above and reflecting its multiannual work plan, taking into consideration comments from interested parties.

The authorization procedure consists of two steps: The first step consists of the following decisions:

- Determine which substances on the candidate list will be included in the system (Annex XIV)
- Which uses of these substances will be exempted from the authorization requirement (sufficient controls established by other legislation currently in place)
- Which deadlines will have to be met and prioritize substances to focus resources

In the second step, manufacturers or users of substances included in Annex XIV will need to apply for an authorization for each use of the substance within the deadlines. This will include an analysis of possible substitutes, including information on relevant research and development activities, if appropriate. If this analysis shows that suitable alternatives are available, then the application must also include a substitution plan. An authorization will be granted if the applicant can demonstrate one of the following:

- Risk from the use of the substance is adequately controlled
- Socioeconomic benefits outweigh the risks
- No suitable alternative substances or processes

The PBT, vPvB, and CMR substances, for which a safe level cannot be defined, cannot be authorized based on adequate control of risk. Six years after the entry into force of the Regulation, the Commission will review whether endocrine disrupters should also be excluded from the adequate control route. The Agency will provide expert opinions on the application and the applicant has an opportunity to comment on draft opinions. The Commission will grant an authorization for each use meeting the above conditions. All authorizations will be reviewed after a certain time, which will be set on a case-by-case basis. In setting the length of this review period, the Commission will take into account relevant information, including the risks of the substance and of alternatives, socioeconomic benefits, analysis of alternatives and any substitution plan. If suitable substitutes have become available by the time of the review, the Commission may amend or withdraw the authorization, even one given for adequate control. Downstream users may apply for their own authorizations or may use a substance for an authorized use provided they obtain the substance from a company to whom an authorization has been granted and that they keep within the conditions of that authorization. Such downstream users will need to notify the Agency that they are using an authorized substance.

22.2.2.5.4 Restrictions

The Restrictions place conditions for the manufacture, placing on the market, or use of certain substances in the EU that are deemed to have unacceptable risks. Proposals for restrictions will be prepared by Member States or by the Agency on behalf of the Commission in the form of a structured Dossier. This Dossier is required to demonstrate that there is a risk to human health or the environment that needs to be addressed at Community level and to identify the most appropriate set of risk reduction measures. Deadlines for the procedure to prepare a Commission decision are set out in the Regulation. Interested parties will have an opportunity to comment and the Agency will provide opinions on any proposed restriction.

22.2.2.5.5 Classification and Labeling Inventory

A requirement for industry to classify and label dangerous substances and preparations according to standard criteria has long been a feature of the European chemicals legislation. REACH builds on this existing legislation. The classification and labeling inventory ensures that hazard classifications (and consequent labeling) of all dangerous substances manufactured in, or imported into, the EU are available to all with the aim of promoting agreement on the classifications. Industry will be required to submit all its classifications to the Agency, to be included in the inventory by December 1, 2010. To complement REACH, the Commission adopted on June 27, 2007 a new proposal for a Regulation on classification, labeling, and packaging of substances and mixtures.⁷⁴ The new proposal incorporates the classification criteria and labeling rules agreed at UN level, the so-called Globally Harmonized System of classification and labeling of chemicals (GHS). If agreement with the European Parliament and Council can be reached at first reading, the phasing-in of the new provisions could be made consistent with the relevant provisions of REACH, in particular the classification and labeling inventory.

22.2.2.5.6 Access to Information

Nonconfidential information on chemicals will be made available to help the public make decisions on the acceptability of the related risks of substances. Some information will be made public on the Agency's Web site, some information will generally be always kept confidential, and some may be made available on request in accordance with the Commission's normal rules on access to information.

22.2.2.5.7 REACH and Flame-Retardants

It is anticipated that substances that have completed risk assessments under regulation (EEC) 793/93 will be considered, in large part, as having met the requirements for technical dossier and chemical safety report submission, and to have had their registration evaluated. The conclusions of these risk assessments will be key to the determination of the necessity for restrictions or authorizations for use of the substance. So, for substances such as deca-BDE and TBBPA, that are not categorized as dangerous, or as PBT substances, or as vPvB substances, or as CMR categories 1 or 2, no restrictions should be expected. However, given the political debates that continue over the use of flame-retardants, it may be the case that proposals to include these substances as candidates for restrictions could be made.

Emerging chemical regulation, such as REACH, is focusing on the need for characterizing all chemical substances in use in terms of their environmental and human health impacts. This basic tenet of “no data—no market” will set the trend for regulations to be implemented in other parts of the world. The development of such information should allow sound, science-based decisions to be made about chemicals, their use, and, where necessary, substitution strategies. For the producers and down stream users of chemicals, there will be new opportunities for innovation, but within a more stable business environment than we have had in the recent past. This has to be positive for flame-retardants as well as for other chemicals.

22.3 CURRENT FLAME-RETARDANT REGULATORY ACTIVITY

Europe has been one of the focal points of regulatory activity on chemicals, including flame-retardants. Many other regions of the globe have followed in Europe’s regulatory footsteps with minor nuances in their regulations. Regulations in the major global regions are discussed below.

22.3.1 EUROPEAN UNION

The predominant regulations in the EU impacting flame-retardants have been the Restriction of the Use of certain Hazardous Substances in Electrical and Electronic Equipment (RoHS) Directive, Waste of Electrical and Electronic Equipment (WEEE) Directive, and more recently the REACH Regulation. While RoHS and WEEE only deal with electrical and electronic equipment as defined in the directives, REACH impacts all substances manufactured and used in the EU.

22.3.1.1 RoHS Directive

The Directive of the European Parliament and of the Council 2002/95/EC on the Restriction of the Use of certain Hazardous Substances in Electrical and Electronic Equipment (RoHS) was put into effect on July 1, 2006.^{75,76} It states that Member States shall ensure that new electrical and electronic equipment (EEE) put on the market shall not contain more than 0.1% of Pb, Hg, Cd, Cr(VI), polybrominated biphenyls (PBBs), PBDEs, or 0.01% Cr(VI). All other flame-retardants are compliant with the provisions of the RoHS Directive and can be used in EEE.

Discussions and debate related to the inclusion of deca-BDE in the RoHS Directive have been going on for years. It was originally planned that the inclusion of deca-BDE in the RoHS Directive was to be addressed upon completion of the results of the EU Risk Assessment. With a conclusion that there was no need for restrictions, eca-BDE was exempted from the provisions of the RoHS Directive for polymer applications on October 15, 2005. Confusion centering on what was meant by deca-BDE (commercial product with minor impurities or pure congener) came up in the summer of 2006. Since the commercial deca-BDE was the material evaluated in the EU Risk Assessment, major parts of the chemical, polymer, and electronics industries and significant elements within the EU shared this view.

On April 1, 2008, the European Court of Justice ruled that the European Commission used improper procedures to exempt deca-BDE from RoHS Directive. The ruling did not question positive EU Risk Assessment outcome of deca-BDE. The outcome of this April 1 ruling was that deca-BDE was banned in the use of electronic and electrical equipment after June 30, 2008.

There is now discussion as to whether more substances, including other flame-retardants, should be added to the RoHS Directive. The history of the RoHS Directive and potential additions raises some very real concerns over the fundamental relationship between results of risk assessments under regulation 793/93, REACH registrations and evaluations, and the RoHS Directive. Consistency is needed between the REACH Regulation and the other EU directives. REACH evaluations will determine whether restrictions are necessary in all applications including electronic applications, and where authorization for use is necessary.

22.3.1.2 WEEE Directive

The recycling of electronic waste foreseen in the EU Directive 2002/96/EC on the Waste of Electrical and Electronic Equipment (WEEE Directive) is based on the experience of a few European countries, where organizations managing voluntary take back systems on behalf of the EEE producers have been responsible for the collection and recycling of the WEEE. This directive calls for selective treatment of plastics containing brominated flame-retardants, as stated in Annex II.⁷⁷ Also required within the directive is the separation of printed wiring boards (PWB) of mobile phones (regardless of size) and of other devices if the surface of the PWB is greater than 10 cm², regardless of what flame-retardant is contained. The reason is to recover the valuable extractable metals (Ag, Au, Cu, Zn, Al, Ni) from the PWB.

The selective treatments of flame-retardant plastics are fulfilled when the WEEE plastics are treated (recovered, recycled, thermally disposed) together with other wastes, as is the case with energy recovery processes that are currently practiced in Europe.^{78,79} In this scenario, the joint recovery of plastics containing brominated flame-retardants with other materials complies with the purpose of the WEEE Directive without the removal requirement of Annex II. Recent technical studies and legal reviews demonstrate that WEEE plastics containing brominated flame-retardants are compatible with the EU WEEE Directive without separation and removal prior to the waste treatment. This has been confirmed by the 2006 EU Member States' guidance on the separation requirements of the WEEE Directive.⁸⁰

22.3.1.3 REACH

As mentioned in Section 22.1, REACH is the acronym for Registration, Evaluation and Authorization of Chemicals. The REACH regulation will affect all of the chemical industry, including flame-retardants, by requiring industry to register all existing and future new substances with a new European Chemicals Agency. The REACH regulation was published in the European Official Journal on December 30, 2006, under the number Regulation (EC) Number 1907/2006.⁸¹ Also, on December 18, the corresponding modification of the Dangerous Substances Directive 67/548 was published as EU Directive 2006/121/EC. Deadlines are in place for preregistration and registration of substances of >1 t. The deadlines are only applicable to substances that have been preregistered.⁸¹ Otherwise, a substance may not be sold or used in the EU until it has been registered (Art. 5).

New substances will have to be registered before they can be placed on the market, with registration possible on or after June 1, 2008. Voluntary registration before the mandatory deadlines is possible on or after June 1, 2008. There are no fixed deadlines for Authorization (starting at Art. 55, list Annex XIV, based on criteria in Annex XIII). Specific deadlines will be fixed for each "candidate substance," after a prioritization process. All SVHC will be subject to Authorization. These include chemicals that are level 1 or 2 CMR substances; PBT substances; vPvB substances or of equivalent concern (in particular having endocrine disruptive properties). Each Member State can also propose that other substances on the market be added to the candidate lists, via a complex process.

Flame-retardants that have gone through a EU Risk Assessment under Regulation 793/93/EC should be some of the first substances registered under the REACH. Several flame-retardants have already been tested by the EU and found to be compatible with the strict safety criteria of REACH, such as PBT and CMR criteria.

22.3.1.4 Other European Activity

Over the last several years, some regulatory activity related to flame-retardants has been seen in a limited number of European countries, particularly Norway and Sweden. Norway adopted a regulation banning deca-BDE in all sectors except transport (vehicles, ships, railway rolling material) to go into effect on April 1, 2008.⁸² This action is contradictory to EU legislation, and although Norway is not formally a part of the EU, it is bound by treaty obligations to follow many of the EU regulations. The European Commission, WTO, and Norwegian and European industries have all opposed this regulation and have requested Norway to follow EU procedures and decisions rather than taking a unilateral national measure. Industry objects to this dismissal of EU science, such as the EU Risk Assessment and the principles of the REACH Regulation, which base decisions on sound science, and has called on the European Commission and WTO to take urgent action to ensure that Norwegian law respects EU and international legal obligations.⁸³

Sweden, a part of the EU, when faced with a legal challenge from the EU, decided on May 8, 2008 to lift its national ban on the use of deca-BDE in textiles, furniture, and some electronic cable applications that was in place since January 1, 2007.⁸⁴ In doing so, the Swedish government eliminated the inconsistency between its restriction and a positive 10 year EU risk assessment of deca-BDE, which did not identify any significant risks that would justify restrictions on the flame-retardant. The Swedish government's limited ban of deca-BDE in late 2006 had no scientific basis and was subjected to a legal challenge by the EU authorities.

22.3.2 ASIA AND JAPAN

22.3.2.1 China

The "Administrative Measure on the Control of Pollution Caused by Electronic Information Products" (China-RoHS) entered into force in March 2007.⁸⁵ The legislation is applicable to import, manufacture, and sale of products in China. Products for export are specifically excluded. Many product types that are not within the scope of the EU RoHS are within the scope of the China RoHS and vice versa. In addition, the initial disclosure, declaration, and exemption requirements for a RoHS certificate in China are different from the EU RoHS. The same six hazardous substances are regulated (lead, cadmium, chromium(VI), mercury, PBBs, and PBDEs, with the exception of deca-BDE). The China RoHS is likely to be upgraded to national regulation and to be amended in the future to potentially cover more products. More detailed materials' testing is required in the China RoHS and is accepted only if performed by certified Chinese laboratories. A table in the product documentation must identify which hazardous substances are contained and which components are present.

22.3.2.2 Korea

The MOE manages chemicals in Korea. The Toxic Chemicals Control Act (revised in 2004) is the basic law regarding chemicals management in Korea.⁸⁶ The objective to this act is "To prevent risk caused by chemicals to human health or the environment" and "to control hazardous chemicals so that everyone can live in a healthy environment." The major tasks of the Toxic Chemicals Control Act include the following:

- Strengthening the basis for safe management of hazardous chemicals
- Risk management of chemicals from a standpoint of human health protection
- Establishing a focused control system on specific hazardous chemicals
- Enhancing risk communication
- Introducing a new chemical registration and evaluation system

The five chapters of this act include a framework plan for hazardous chemicals control, TRI, etc.; new chemical notification, risk assessment, etc.; safe control of toxic chemicals, banned or restricted chemicals, responses to chemical accidents, etc.; supplementary provisions; penalty provisions.

There are approximately 400 kinds of new chemicals produced or introduced per year in Korea. From 1991 to 2006, 4679 chemical evaluations were completed. For existing chemicals, 983 chemicals were evaluated by 2006. Basic data is collected on new and existing chemicals. For new chemicals, this includes hazard assessment, expected amount of use, and chemicals used. For existing chemicals, this includes safety testing, environmental monitoring, survey of distribution or release. The next phase for both new and existing chemicals is risk assessment, followed by risk management/communication. Flame-retardants currently produced are not regulated by this act.

The New Chemicals Evaluation System is a new system that will be put into place by 2010 to address global flow, including the following:

- Expansion of the assessment items to meet OECD recommendation
- Enhancing the role of industry in chemicals data production
- Strengthening information sharing on chemicals through supply chain

This system is the risk management of chemicals based on public health that includes the following:

- Establishment of receptor-oriented risk assessment system
- Life cycle management of living goods containing hazardous substances
 - Chemical exposure monitoring on a daily basis
- Protection of vulnerable people (e.g., children) from hazardous substances
 - Periodic monitoring of exposure to hazardous substances contained in children's goods and establishment of management system

22.3.2.3 Japan

Japan's Ministry of International Trade and Industry (MITI) was formed in 1949 and reorganized as the Ministry of Economy, Trade and Industry (METI) in 2001. METI is responsible for The Chemical Substances Control Law. It focuses on properties of chemical substances such as "persistence," "bioaccumulation," "long-term toxicity to humans," and "toxicity to plants and animals" (hazards) and the likelihood of the chemical substance causing damage by remaining in the environment (risk).⁸⁷ The law stipulates regulatory classifications and the measures to be taken for each classification. The classifications include the following:

- Class I Specified Chemical Substances
- Class II Specified Chemical Substances
- Type I Monitoring Chemical Substances
- Type II Monitoring Chemical Substances
- Type III Monitoring Chemical Substances

After the 2003 amendment to the law, it became mandatory for manufacturers and importers to report hazard information that they gathered on the properties of chemical substances they handle. Several schemes were also introduced to this law at that time. They include the following:

- Evaluation and regulation scheme with the objective of preventing adverse effect on the environment
- Monitoring scheme for persistent and highly bioaccumulative existing chemical substances
- Evaluation system focused on the likelihood of discharge into the environment

HBCD is classified in the “Type I Monitoring Chemical Substances” category. The criteria in this category include the following:

- Notification of quantity manufactured or imported, intended use of the chemical substance
- Publication of the name and notified volume of substances whose total manufacturing and import volume is 1 t or more
- Guidance and advice (when necessary to prevent environmental pollution)
- If necessary from the perspective of risk, the government directs the manufacturer or importer to conduct a hazard (long-term toxicity to humans or top predators) survey.⁸⁷

In an effort to reduce or eliminate emissions of HBCD to the environment, the Voluntary Emissions Control Action Program (VECAP™) was introduced in Japan.

Concerns exist in Japan over the use of phosphorus flame-retardants. The concern with the use of red phosphorus is the potential generation of phosphine gas during burning. There are also concerns with the use of phosphate esters. There is also dust concern over the use of antimony trioxide.

22.3.3 NORTH AMERICA

The primary focus of flame-retardant activity in North America has been on the PBDE family of flame-retardants. Much of the information generated on various flame-retardants for EU Risk Assessments has been utilized in the different U.S. government agency programs discussed here. As far as chemical legislation is concerned, the United States has a patchwork of regulatory activity that is confusing and far too fragmented and inefficient. Even with the best of intentions, the plethora of proposed regulations has led to the creation of new problems as substitution of one substance by another is implemented, and has added significant red tape, costs, and uncertainty for business. The information in the subsequent text covers the major areas of activity on flame-retardants in North America.

22.3.3.1 Risk Assessments

Quantitative risk assessments have been performed on a variety of flame-retardants used both in upholstered furniture fabric and foam. The National Research Council performed a quantitative risk assessment on 16 chemicals (or chemical classes) identified by the U.S. Consumer Product Safety Commission (CPSC). The results were published in 2000.⁸⁸ The 16 flame-retardants included in this NRC study were HBCD, deca-BDE, alumina trihydrate, magnesium hydroxide, zinc borate, calcium and zinc molybdates, antimony trioxide, antimony pentoxide and sodium antimonate, ammonium polyphosphates, phosphonic acid, (3-[[hydroxymethyl]amino]-3-oxopropyl)-dimethyl ester, organic phosphonates, tris (monochloropropyl) phosphate, tris (1,3-dichloropropyl-2) phosphate, aromatic phosphate plasticisers, tetrakis (hydroxymethyl) hydronium salts, and chlorinated paraffins. The conclusions of the assessment was that the following flame-retardants can be used on residential furniture with minimal risk, even under worst-case assumptions:

- HBCD
- deca-BDE
- Alumina trihydrate
- Magnesium hydroxide
- Zinc borate
- Ammonium polyphosphates
- Phosphonic acid (3-[[hydroxymethyl]amino]-3-oxopropyl)-dimethyl ester
- Tetrakis hydroxymethyl phosphonium salts (chloride salt)

The CPSC staff performed quantitative risk assessments on various flame-retardants for both upholstered residential furniture fabrics and foam.⁸⁹ CPSC addresses chemical hazards under the Federal Hazardous Substances Act (FHSA), which is risk based. For fabrics, five flame-retardants were evaluated, that include antimony trioxide, deca-BDE, HBCD, phosphonic acid, (3-[[hydroxymethyl]amino]-3-oxopropyl)-, dimethyl ester (PA), and tetrakis (hydroxymethyl) phosphonium chloride (THPC). These flame-retardants were selected for study because they are used to comply with the U.K. upholstered furniture flammability standard (except THPC) and fabric samples were available for testing. The staff concluded in 2006 that deca-BDE, HBCD, and PA would not present a hazard to consumers and that additional data would be needed to assess antimony trioxide and THPC.

CPSC staff performed a preliminary assessment of the potential health risks associated with the use of selected FR chemicals in upholstered furniture foam. FR-treated foam samples that could be used to meet the draft standard and were available to the CPSC staff for testing included melamine; tris(1,3-dichloro-2-propyl)phosphate (TDCP); a mixture containing triphenyl phosphate (TPP), phenol isopropylated phosphate (PIP), and octyl tetrabromobenzoate (OTB). Other flame-retardants that could be used in foam have been discussed by the U.S. EPA Design for the Environment Program. Based on limited exposure or toxicity data, the following preliminary conclusions were published in 2006:

- Melamine-treated foam is not expected to present a hazard to consumers
- Inhalation studies are lacking for TDCP, TPP, PIP, and OTB
- Empirical data on vapor phase emissions or indoor concentrations are needed on TDCP, TPP, PIP, and OTB
- Chemical-specific migration and release data are needed on TPP and PIP
- Additional toxicity data are needed on TPP and PIP
- Basic toxicity and physicochemical data is needed for OTB

The EU Risk Assessment on TDCP, which was recently finalized, should help address concerns regarding vapor phase emissions or indoor concentrations.

22.3.3.2 EPA Activity

The U.S. EPA issued the “Polybrominated Diphenyl Ethers (PBDEs) Project Plan” report in May 2006.⁹⁰ It identified a number of activities that the EPA was conducting regarding PBDEs, as well as activities it intended to initiate or consider. In March 2008, the second progress report, “Tracking Progress on U.S. EPA’s Polybrominated Diphenyl Ethers (PBDEs) Project Plan: Status Report on Key Activities,” was issued.⁹¹ Updates were reported to the assessment of substitutes for penta-BDE and octa-BDE, assessment and evaluation of deca-BDE, assessment of the risks of penta-BDE and octa-BDE, and tracking of developments concerning other brominated flame-retardants of interest.

The U.S. EPA Design for Environment (DfE) program is in place to work in partnership with a broad range of stakeholders to better understand the environmental health and safety aspects of materials.⁹² One potential outcome of this is to reduce risk to people and the environment by preventing pollution. Three of the EPA’s DfE programs include or are focused on flame-retardants. They include the following:

- Furniture Flame Retardancy Partnership
 - The focus of this program was to evaluate the environmental profiles of chemical flame-retardant alternatives for use in low-density polyurethane foam.⁹³ The program was a joint venture between the Furniture Industry, Chemical Manufacturers, Environmental Groups, and the EPA to better understand fire safety options for the furniture industry. It assessed 14 formulations of flame-retardant products most likely to be used in this application. The project began in December 2003 and the report was issued in September 2005.⁹⁴

- Wire and Cable Partnership
 - The focus of this program was to evaluate the environmental impacts of the current standard material formulations and alternative formulations.⁹⁵ The partnership used a life-cycle assessment (LCA) approach to examine the impacts of heat stabilizers, polymer systems, and flame-retardants used in insulation and jacketing for selected wire and cable products. The project began in March 2004 and the report was issued in May 2008.⁹⁶
- Flame-Retardants in Printed Circuit Boards Partnership
 - The focus of this program is to identify and characterize commercially available flame-retardants used in FR-4 printed circuit boards and their environmental, health, safety and environmental fate aspects.⁹⁷ The project began in February 2006 and the program is currently in progress

22.3.3.3 CPSC

Flame-retardants can and are used to protect the polyurethane foam as well as the covering fabric used in upholstered furniture from both small open flames and smoldering ignition. While flame-retardants do not put out fires, they do provide crucial added time for the occupants to leave the residence, thus saving lives. Where flame-retardants have been used in upholstered furniture for many years, such as the United Kingdom, the reduction in fire deaths over the years has been attributed to the use of approved and studied flame-retardants. In 1991, the National Association of State Fire Marshals petitioned the Consumer Product Safety Commission to develop a standard to deal with flammability issues related to residential upholstered furniture. This was in response to the high incidence of deaths due to fires caused by small open flames and smoldering cigarettes. Since that time, the Commission has made several proposals dealing with one element or another of the problem but has failed to come up with a comprehensive standard that has the support of the furniture industry while allowing for the highest levels of fire safety. The most recent activity was that the CPSC issued a Notice of Proposed Rulemaking on their latest proposal and accepted comments until May 19, 2008. There were 86 comments received.⁹⁸ It is unclear if and when flammability standard for residential upholstered furniture will be finalized.

22.3.3.4 State Legislation

In the United States, a patchwork of state legislative activity that is not necessarily based on science is a chronic problem. Legislation enacted on flame-retardants has focused on PBDEs. Legislation has been enacted by several U.S. states prohibiting the use of the former penta- and octa-BDE products and articles containing them. These states include California, Hawaii, Illinois, Maryland, Minnesota, New York, and Oregon. Use-specific restrictions on deca-BDE have been enacted in Maine and Washington State.

22.3.3.4.1 Maine

In Maine, LD 1658 prohibits the use of deca-BDE in mattresses, mattress pads, and textiles used in residential furniture beginning in 2008, and in the casings of televisions and computers beginning in 2010.⁹⁹ The law further authorizes the Department of Environmental Protection (DEP) to engage in discretionary rulemaking to prohibit the use of other flame-retardants in Maine. Specifically, rulemaking can prohibit the use of a flame-retardant in mattresses, mattress pads, or upholstered furniture intended “for indoor use in a home or other residential occupancy that has plastic fibers containing that flame retardant” or “a television or computer that has a plastic housing containing that flame retardant,” provided an alternative flame-retardant that is deemed “safer” by the Maine DEP and Maine Center for Disease Control, acceptable to the State Fire Marshal from a fire safety perspective, and is nationally available. The law does not contain any definitions, does not require the use of flame-retardants in any specific products, and does not identify an alternative to deca-BDE. The uses of deca-BDE that are exempted from the law are

- Transportation vehicles or products or parts for use in transportation vehicles or transportation equipment
- Products or equipment used in industrial or manufacturing processes
- Electronic wiring and cable used for power transmission

22.3.3.4.2 *Washington State*

In Washington State, HB 1024 provides definitions and establishes a process under which the State of Washington can identify, analyze, and approve “alternative” flame-retardants that could come into use in Washington to replace the use of deca-BDE.¹⁰⁰ The Departments of Ecology and Health, as well as a newly created fire safety committee, will have to determine that any proposed alternative flame-retardant is “safer and technically feasible and meets applicable fire safety standards” as a replacement for deca-BDE in televisions, computers, and domestic upholstered furniture. No prohibition on the use of deca-BDE in these applications can go into effect prior to January 1, 2011, provided suitable alternative flame-retardants are available. The bill places a prohibition on the use of deca-BDE in mattresses beginning January 1, 2008; however, this has no practical impact, since deca-BDE is not actually used in residential mattresses. All uses of deca-BDE not specifically mentioned in the legislation are exempt.

Under the recently passed bill, the Departments of Ecology and Health, as well as a newly created fire safety committee, will have to determine that any proposed alternative flame-retardant is “safer and technically feasible and meets applicable fire safety standards” as a replacement for deca-BDE in televisions, computers, and domestic upholstered furniture. No prohibition on the use of deca in these applications can go into effect prior to January 1, 2011, provided suitable alternative flame-retardants are available. The bill places a prohibition on the use of deca-BDE in mattresses beginning January 1, 2008; however, this has no practical impact, since deca-BDE is not used to any significant extent in residential mattresses. All uses of deca-BDE not specifically mentioned in the legislation are exempt.

22.3.3.4.3 *California “Green Chemistry Initiative”*

The “Green Chemistry Initiative” was signed into law in California in October 2008 to examine the regulatory process, under which chemicals should be evaluated and regulated.¹⁰¹ This includes two bills, AB 1879 and SB 509. As the name suggests the plan is to develop a regulatory framework, which will encourage the development of “green chemistry” solutions to environmental and human health issues arising from currently used chemicals. Ideas for how this initiative might best be structured have been explored with a wide range of stakeholders under the “*Conversation with California*” banner. This has included brainstorming sessions, symposia, a Web log, the creation of a Science Advisory Panel, and publication of a comprehensive report. The results of this initiative should be seen in the near future, as the goals are ambitious, as stated below:

A California Green Chemistry Initiative would chart a new course to a better world. It would engage academia, business, and government in partnership to stimulate economic growth using clean new technologies. It would cut toxic waste while increasing markets and global competitiveness working together with Nations. It could replace the current piecemeal approach with a market-driven strategy that favors innovation. Green Chemistry is an opportunity to get it right, a chance to reinvent invention and lead the nation in the 21st century.¹⁰²

22.3.3.5 **Canada**

In December 2006, the Canadian federal government announced a new *Chemical Substances Plan* to prioritize chemicals targeted for risk assessment and risk management.¹⁰³ The aim of this new Plan is to use “science-based” information to protect our health and the environment by

- Taking immediate action on chemical substances of high concern, based on their potential to cause harm
- Taking action over the next 3 years on consumer products, food, pharmaceuticals, personal care products, and some older pesticides so as to reassess their risk profile in the light of new science
- Taking action on research, including biomonitoring, to learn more and to measure success

The first step of the Chemical Substances approach in Canada is categorization, followed by risk assessment and risk management. By 2006 some 23,000 chemical substances had been categorized to identify those that were

- *Inherently toxic* to humans or to the environment and that might be
 - *Persistent* (take a very long time to break down)
 - *Bioaccumulative* (collect in living organisms and end up in the food chain)
- Substances to which people might have *greatest potential for exposure*¹⁰³

For all those chemical substances so categorized as needing further attention, a screening risk assessment is required. There can be three results at this stage: no further action is required, the chemical substance is determined to be toxic and measures may be needed for control, or it is placed on the Priority Substances List (PSL) and subjected to an in-depth assessment.

In July 2008, Environment Canada published a final regulation allowing the continued use, sale, and import of deca-BDE in Canada.¹⁰⁴ The rule also prohibits the use, sale, offer for sale, and import of penta and octa-BDE. In addition, the manufacture of all PBDEs in Canada, which does not currently occur, is prohibited. The rule states that additional measures and activities are being developed, including the following:

- A regulation to control PBDEs in manufactured items
- Voluntary approach to minimize releases to the environment from the use of the deca-BDE commercial mixture in the manufacturing of semifinished and finished products
- A detailed review of newly published science on deca-BDE to determine whether further controls are warranted
- Development of a management strategy for PBDE-containing products at end-of-life
- Monitoring of Canadians' exposure to PBDEs and concentrations in the environment

Screening risk assessments are also underway for TBBPA and HBCD. It is not clear as to when these will be completed, but we anticipate sometime in 2008.

22.3.3.6 Other Activity

Several organizations have initiated projects to investigate and compare the choices of flame-retardant laminates for PWB. These projects include the predominant flame-retardant used in FR-4 PWB, tetrabromobisphenol A (TBBPA). Some of these projects also address all brominated flame-retardants and polyvinylchloride (PVC) usage in all components of electronics. Projects include the following:

- iNEMI Technical Feasibility Study
 - The National Electronics Manufacturers Initiative (iNEMI) has a technical feasibility study in progress on flame-retardants used in PWB.¹⁰⁵
- High Density Packaging User Group
 - The High Density Packaging User Group (HDPUG) has four projects in progress in various stages of completion that address halogen-free electronics in different ways.¹⁰⁶

- IPC Low-Halogen Electronics Standard
 - The Association Connecting Electronics Industries (IPC) has organized a task group (4-33A) to review the industry standard for definitions and data-supported threshold limits associated with halogen-free electronics.¹⁰⁷ This includes printed circuit boards, components, electronics assemblies, cables, and mechanical plastics.

All three of these organizations have international members and participation on various committees and task groups.

22.4 DEVELOPMENT OF SUSTAINABLE SOLUTIONS

Sustainability has become the goal for many companies and industries. The three aspects of sustainability (environmental, society, and economic concerns) must be reconciled for sustainable development to be achieved. Sustainable solutions meet the needs of the present without compromising the ability of future generations to meet their own needs.¹⁰⁸ Sustainable chemicals should be functional, cost effective, and safe. Risks associated with the life cycle (manufacture, use, and final disposal) should be understood, properly managed, and acceptable. An understanding of the life-cycle implications for alternative chemistries or technologies is an important aspect of sustainability that often gets overlooked. In substituting one flame-retardant or technology for another, unforeseen consequences could arise that would impact society or the ecosystem.

Some of the areas that chemical manufacturers aspire to in terms of sustainability are as follows:

- Minimizing industry's environmental footprint
 - Through advances in technology and operating practices
 - Reduce total emissions of chemicals to air and water
- Improving safety performance
 - At facilities and during transportation
 - Establish goals for further improvement injuries, releases, and process safety incidents
- Providing essential products and economic benefits
 - Flame-retardants are valuable products to society
 - Save lives
 - Reduce injury
 - Reduce destruction of property
 - Reduce local pollutants that are a result of fires

The chemical industry views sustainability as a challenge put before all parts of society. Advances made in industrial operations, improved performance, and improvements to society (by the use of flame-retardants) all help to improve living standards and the environment. Reducing or eliminating emissions of chemicals to air and water can further minimize exposure to humans. The flame-retardant industry is firmly committed to providing needed resources and leadership to help provide safe and sustainable products that provide a valuable service to society.

22.4.1 SELECTION CRITERIA FOR "GREEN" SOLUTIONS

The idea of "green" solutions includes the sustainable management of resources and stewardship of the environment. The definition of green chemicals is difficult because the concept comprises a variety of factors: perception, empirical values, geographical area of use, the application that they are used, available alternatives, and knowledge of the total manufacturing process.¹⁰⁹ A combination of green chemistry, incorporation of life cycle thinking, and excellent product stewardship can work together to provide a sustainable future for flame-retardants.

22.4.1.1 Green Chemistry

The 12 principles of green chemistry were developed by Paul Anastas and John C. Warner to help explain what the definition means in practice.¹¹⁰ The principles cover such concepts as

- The design of processes to maximize the amount of raw material that ends up in the product
- The use of safe, environment-benign substances, including solvents, whenever possible
- The design of energy efficient processes
- The best form of waste disposal: do not create it in the first place

The 12 principles are

1. *Prevent waste*—Design chemical syntheses to prevent waste, no waste to treat or clean up
2. *Design safer chemicals and products*—Design chemical products to be fully effective, yet have little or no toxicity
3. *Design less hazardous chemical syntheses*—Design syntheses to use and generate substances with little or no toxicity to humans and the environment
4. *Use renewable feedstock*—Use raw materials and feedstock that are renewable
5. *Use catalysts, not stoichiometric reagents*—Minimize waste by using catalytic reactions
6. *Avoid chemical derivatives*—Avoid using blocking or protecting groups or any temporary modifications if possible. Derivatives use additional reagents and generate waste
7. *Maximize atom economy*—Design syntheses so that the final product contains the maximum proportion of the starting materials—few, if any, wasted atoms
8. *Use safer solvents and reaction conditions*—Avoid using solvents, separation agents, or other auxiliary chemicals (if necessary, use innocuous chemicals)
9. *Increase energy efficiency*—Run chemical reactions at ambient temperature and pressure whenever possible
10. *Design chemicals and products to degrade after use*—Design chemical products to break down to innocuous substances after use so that they do not accumulate in the environment
11. *Analyze in real time to prevent pollution*—Include in-process real-time monitoring and control during syntheses to minimize or eliminate the formation of by-products
12. *Minimize the potential for accidents*—Design chemicals and their forms (solid, liquid, or gas) to minimize the potential for chemical accidents (explosions, fires, and releases to the environment)

The use of “Green Chemistry” can result in products that are more environmentally preferable and sustainable.

22.4.1.2 Flame-Retardants and “Green Solutions”

For the selection of alternative flame-retardants for a specific application, aspects that must be considered include

- Physical/chemical properties of alternatives during manufacturing
- Physical/chemical properties of alternatives during use (including reliability of end products)
- Need for alternate polymer systems and associated impacts
- Environmental and health risk of alternatives during manufacturing, use, and end-of-life
- Necessary qualification testing (including testing in use)
- Price of alternatives
- Expenses of changes in tools and machinery

Flame-retardants that are preferable would have been evaluated in risk assessments to ensure acceptable environmental profiles, human health profiles, and risk management in place. The use of excellent product stewardship to keep flame-retardants out of the environment is a key to sustainability of the products and an important attribute of “Green Solutions.”

22.4.2 INCORPORATION OF LIFE-CYCLE THINKING

The concept of life-cycle thinking and the use of LCA can help provide a thorough picture of the environmental footprint for given decisions. Life-cycle thinking considers the cradle-to-grave implication of an action, and some of the benefits include the following:

- Develop a systematic evaluation of the environmental consequences and identify the impacts of a specific product or process throughout its entire life cycle or selected stages of the life cycle
- Quantify environmental releases to air, water, and land for each life-cycle stage and major contributing process
- Analyze environmental trade-offs among alternative products or processes
- Determine the impacts of product substitution
- Understand the relative environmental burdens resulting from evolutionary changes in given processes or products over time¹¹

LCA is a systematic process for identifying, quantifying, and assessing environmental impacts throughout the life cycle of a product, process, or activity. It considers energy and material uses and releases to the environment from “cradle to grave.”¹¹ This includes raw material extraction through manufacturing, transportation, use, and disposal. LCA is often used in conjunction with other environmental management tools, such as risk assessment and environmental impact assessment. A life-cycle approach does not necessarily embody every methodological aspect called for in a traditional LCA, but it does use a cradle-to-grave systems perspective to evaluate the full life-cycle impacts of a product or process. Various industries, the military, and governments have been using life-cycle approaches, and often LCA, to increase the role of science in decisions on product and process designs.

22.4.3 PRODUCT STEWARDSHIP

Concerns have been raised about the findings of chemicals, including some flame-retardants, in humans or the environment.^{4,5} Even though the levels found are extremely low and have not been shown to pose a risk to the environment or to human health,^{6,7} every effort should be made to minimize the release of chemicals from manufacture and use, where the largest potential for emissions exists.

To address emissions of flame-retardants, a Voluntary Emissions Control Action Program (VECAP™) was initiated by the Bromine Science and Environmental Forum (BSEF).¹² The VECAP Pilot program was initiated in the U.K. textiles industries in 2004 to reduce emissions of deca-BDE in line with the Code of Good Practice. After 1 year of implementation, the U.K. Pilot Program achieved a 75% reduction in emissions to water.¹³ The second year, a total of 90% reduction in emissions was then realized.

VECAP has seen significant successes and was subsequently implemented in five other European Member States, North America, Japan, and other parts of Asia. It has expanded to reduce release potential of other flame-retardants to the environment, including phosphorus flame-retardants. This program is not only a flame-retardant program; it is a model program for all polymer additives. Companies participating in VECAP follow a cycle of continuous improvement. This starts with a commitment to the Code of Good Practice and verification of the actual

working procedures with those required according to the Code of Good Practice. Then the company will critically analyze its product flow and processes to identify the potential for emissions. Measuring and recording the relevant data will identify the actual emissions baseline throughout the entire production process. Once this emissions balance is known, an emissions report can be drawn up which will enable closure of the mass balance. The methodology and discipline of the VECAP mass balance assumes that material not accounted for during this process is an “emission.” This has led to an exhaustive examination of the process and has resulted in the discovery of new potential emission sources. An improvement plan is implemented; operational results are evaluated; potential for further emission reductions investigated to ensuring effective continuous improvement.

By committing to applying proactive product stewardship practices, the safe and environmentally friendly use of flame-retardants can continue. VECAP provides both a practical and cost-effective means of controlling emissions of flame-retardants. This program is a potential model for chemical management that could be applied to other chemicals. Users and producers applying the principles of VECAP have demonstrated that by undertaking a series of simple and low cost measures at the production level, significant levels of emissions can be reduced. As global producers of chemicals, the flame-retardant manufacturers that initiated the VECAP program are deeply committed to protecting the environment, ensuring the safety and security of our operations, and safeguarding the health and safety of employees and of the communities in which we live and work. In addition to reducing emissions of flame-retardants from all stages of all processes, VECAP results in cost savings via recovered product and demonstrates leadership in a self-regulated stewardship program. This program will help to ensure a sustainable future for flame-retardants.

22.5 CONCLUSIONS

Emerging chemical regulations are focusing on the need for characterizing all chemical substances in use in terms of their environmental and human health impacts. This tendency will set the trend for similar regulations to be implemented in other parts of the world. A basic tenet is that without supporting data, then substances will not be allowed on the market. This development should allow sound, science-based decisions to be made about existing chemicals, their use, and, where necessary, substitution strategies. For the producers and down stream users of chemicals, there will be new opportunities for innovation, but within a more stable business environment than in the recent past. This has to be positive for flame-retardants as well as for other chemicals. The regulation system in place also needs to be adhered to and accepted by everyone. If society is to operate effectively and efficiently, then acceptance of good regulatory programs is of the utmost importance.

The use of flame-retardants provides a valuable service to society. While the use of these materials is necessary to achieve an acceptable level of flame retardancy in many applications, minimizing or eliminating environment emissions is of the utmost importance. Product Stewardship is becoming increasingly recognized as the responsible and ethical management of the health, safety, and environmental aspects of a product throughout its total life cycle. When common goals throughout the supply chain are defined and pursued, benefits for all the businesses involved are achieved. Everyone involved in the production, handling, use, and disposal of flame-retardants has a shared responsibility to ensure safe management and use. The adoption of excellent product stewardship, such as VECAP can result in every member of the supply chain playing its part in protecting humans and the environment from potential harm.

Chemical regulations and demands are in a state of constant change. The drive to attain environmentally preferable products is a dynamic process. There is constant movement and trade-offs with the ultimate goal being to obtain “green” products. This chapter reflects the state of activity as of October 2008.

REFERENCES

1. Proven simple actions could save up to 850 lives each year from fires in Europe, June 1, 2005, http://portal.surrey.ac.uk/portal/page?_pageid=799,434945&_dad=portal&_schema=PORTAL
2. Karter, M.J., Jr., Fire loss in the United States during 2007, August 2008, <http://www.nfpa.org/assets/files/PDF/OS.fireloss.pdf>
3. Why do we worry about brominated flame retardants?, November 15, 2007, <http://www.rsc.org/ScienceAndTechnology/Policy/EHSC/Brominated.asp>
4. Sjödin, A., Wong, L., Jones, R.S., Park, A., Zhang, Y., Hodge, C., DiPietro, E., McClure, C., Turner, W., Needham, L.L., Patterson, Jr., D.G., Serum concentrations of polybrominated diphenyl ethers (PBDEs) and polybrominated biphenyl (PBB) in the United States population: 2003–2004, *Environmental Science and Technology*, 2008, 42(4), 1377–1384.
5. Bogdal, C., Schmid, P., Kohler, M., Muller, C.E., Iozza, S., Buchell, T.D., Scheringer, M., Hungerbühler, K., Sediment record and atmospheric deposition of brominated flame retardants and organochlorine compounds in Lake Thun, Switzerland: Lessons from the past and evaluation of the present, *Environmental Science and Technology*, 2008, 42, 6817–6822.
6. Making sense of chemical stories, <http://www.senseaboutscience.org.uk/index.php/site/project/13/>
7. Kucewicz, W.P., Brominated flame retardants: A burning issue, American Council on Science and Health, August 2006, www.acsh.org/publications/pubID.1374/pub_detail.asp
8. EPA definition of precautionary principle, <http://www.epa.gov/OCEPAterms/pterm.html>
9. Guldberg, H., Challenging the precautionary principle, July 1, 2003, <http://www.spiked-online.com/Articles/00000006DE2F.htm>
10. Adler, J.H., Dangerous precaution, September 13, 2002, <http://www.nationalreview.com/adler/adler091302.asp>
11. http://ecb.jrc.it/DOCUMENTS/Existing-Chemicals/RISK_ASSESSMENT/EURATS/CONCLUSIONS/eurats_concl_015.pdf
12. http://ecb.jrc.it/DOCUMENTS/Existing-Chemicals/RISK_ASSESSMENT/EURATS/CONCLUSIONS/eurats_concl_014.pdf
13. http://info.sen.ca.gov/pub/03-04/bill/asm/ab_0301-0350/ab_302_bill_20030724_enrolled.html
14. <http://www.chem.unep.ch/irptc/Publications/toolbk/mod1.pdf>
15. http://www.nicnas.gov.au/Industry/Existing_Chemicals.asp
16. <http://stneasy.cas.org/dbss/chemlist/aics.html>
17. <http://www.ec.gc.ca/substances/ese/eng/dsl/dslprog.cfm>
18. http://www.ec.gc.ca/CEPARRegistry/subs_list/NonDomestic.cfm
19. http://ec.europa.eu/environment/chemicals/exist_subst/index.htm
20. <http://ecb.jrc.it/new-chemicals/>
21. <http://www.chemicalspolicy.org/downloads/swedish%20non-haz%20prod.pdf>
22. <http://eur-lex.europa.eu/JOHtml.do?uri=OJ:L:2006:396:SOM:EN:HTML>
23. <http://stneasy.cas.org/dbss/chemlist/encs.html>
24. <http://www.emb.gov.ph/eeid/PICCS.htm>
25. <http://www.safepharmlabs.com/downloads/registration%20documents/HO53.pdf>
26. <http://stneasy.cas.org/dbss/chemlist/ecl.html>
27. <http://library.dialog.com/bluesheets/html/bl0052.html>
28. <http://www.scils.rutgers.edu/~creegank/TSCA/International%20Inventories.htm>
29. <http://www.epa.gov/compliance/civil/tsca/tscaenfstatreq.html>
30. <http://www.chemalliance.org/Tools/background/back-tsca.asp>
31. <http://www.chemalliance.org/Tools/background/back-tsca-links.asp>
32. <http://www.epa.gov/opptintr/chemtest/index.htm>
33. http://federalregister.gov/OFRUpload/OFRData/2008-16992_PI.pdf
34. <http://www.epa.gov/oppt/newchems/index.htm>
35. <http://www.cefic.org/Files/Publications/Risk%20&%20Hazard2.pdf>
36. <http://www.agius.com/hew/resource/hazard.htm>
37. http://www.stopcancer.org/default2.asp?active_page_id=133
38. Kane, A.S., Dose response concepts, Applied Toxicology NURS 735—Module 1, <http://aquaticpath.umd.edu/appliedtox/dose-response.pdf>
39. COUNCIL REGULATION (EEC) No 793/93 of March 23, 1993 on the evaluation and control of the risks of existing substances, March 5, 1993, http://www.bsef.com/regulation/overview_ra/DOC%201%20%20%20Council%20Regulation%20793-93.pdf

40. Overview Risk Assessment Procedure, http://www.bsef.com/regulation/overview_ra/index.php?/regulation/overview_ra/overview_ra.php
41. <http://ecb.jrc.it/>
42. <http://ecb.jrc.it/existing-chemicals/>
43. http://ecb.jrc.ec.europa.eu/documents/TECHNICAL_GUIDANCE_DOCUMENT/EDITION_2/tgdpart1_2ed.pdf
44. http://ecb.jrc.it/documents/Existing-Chemicals/RISK_ASSESSMENT/REPORT/penta_bdpereport015.pdf
45. http://ecb.jrc.it/documents/Existing-Chemicals/RISK_ASSESSMENT/REPORT/octareport014.pdf
46. <http://eur-lex.europa.eu/LexUriServ/LexUriServ.do?uri=OJ:C:2008:131:0007:0012:EN:PDF>
47. http://ecb.jrc.it/documents/Existing-Chemicals/RISK_ASSESSMENT/REPORT/decabromodiphenyletherreport013.pdf
48. http://ecb.jrc.it/DOCUMENTS/Existing-Chemicals/RISK_ASSESSMENT/EURATS/CONCLUSIONS/eurats_concl_013.pdf
49. http://ecb.jrc.it/documents/Existing-Chemicals/RISK_ASSESSMENT/REPORT/tbbpaHHreport402.pdf
50. http://ecb.jrc.it/DOCUMENTS/Existing-Chemicals/RISK_ASSESSMENT/EURATS/CONCLUSIONS/eurats_concl_402.pdf
51. http://ecb.jrc.it/DOCUMENTS/Existing-Chemicals/RISK_ASSESSMENT/EURATS/CONCLUSIONS/eurats_concl_044.pdf
52. http://ec.europa.eu/health/ph_risk/committees/04_scher/docs/scher_o_093.pdf
53. http://echa.europa.eu/chem_data_en.asp
54. http://ecb.jrc.it/DOCUMENTS/Existing-Chemicals/RISK_ASSESSMENT/EURATS/CONCLUSIONS/eurats_concl_425.pdf
55. http://ecb.jrc.it/DOCUMENTS/Existing-Chemicals/RISK_ASSESSMENT/EURATS/CONCLUSIONS/eurats_concl_426.pdf
56. http://ecb.jrc.it/DOCUMENTS/Existing-Chemicals/RISK_ASSESSMENT/EURATS/CONCLUSIONS/eurats_concl_068.pdf
57. http://ecb.jrc.it/DOCUMENTS/Existing-Chemicals/RISK_ASSESSMENT/EURATS/CONCLUSIONS/eurats_concl_428.pdf
58. http://ec.europa.eu/health/ph_risk/committees/04_scher/04_scher_en.htm
59. http://www.bsef.com/env_health/hhr_decabde/Final%20SCHER%20Opinion%20March%202005.pdf
60. http://www.bsef.com/env_health/hhr_decabde
61. http://ec.europa.eu/health/ph_risk/committees/04_scher/docs/scher_o_020.pdf
62. http://ec.europa.eu/health/ph_risk/committees/04_scher/docs/scher_o_071.pdf
63. http://echa.europa.eu/reach_en.asp
64. http://ec.europa.eu/environment/chemicals/reach/reach_intro.htm
65. http://ec.europa.eu/environment/chemicals/reach/reviews_en.htm
66. http://reach.jrc.it/guidance_en.htm
67. <http://echa.europa.eu/>
68. http://ec.europa.eu/environment/chemicals/reach/background/i_a_en.htm
69. http://echa.europa.eu/doc/reach/echa_08_gf_04_data_sharing_en_20080721.pdf
70. http://echa.europa.eu/doc/reach/echa_08_gf_05_registration_en_20080721.pdf
71. http://echa.europa.eu/doc/reach/echa_08_gf_06_infreq_csr_part_a_en_20080721.pdf
72. http://echa.europa.eu/doc/reach/echa_08_gf_07_infreq_csr_part_d_en_20080721.pdf
73. http://ec.europa.eu/environment/chemicals/reach/pdf/2007_02_reach_in_brief.pdf
74. http://ec.europa.eu/enterprise/reach/ghs_more_on_com_proposal_en.htm
75. <http://www.rohs.eu/english/index.html>
76. http://eur-lex.europa.eu/LexUriServ/site/en/oj/2003/l_037/l_03720030213en00190023.pdf
77. <http://eur-lex.europa.eu/LexUriServ/LexUriServ.do?uri=CELEX:32002L0096:EN:HTML>
78. http://www.bsef.com/recycling/thermal_processes/index.php
79. http://www.bsef.com/regulation/eu_legislation/
80. <http://international.vrom.nl/docs/internationaal/Guidance.pdf>
81. <http://eurlex.europa.eu/LexUriServ/LexUriServ.do?uri=OJ:L:2006:396:0001:0849:EN:PDF>
82. http://www.regjeringen.no/Upload/MD/Vedlegg/Forskrifter/Regulation_decabromodiphenylether_091207.pdf
83. http://www.bsef.com/newsmanager/uploads/norwegian_governemnt_moves_-_ebfrip_press_release_18012008_%282%29.pdf
84. <http://www.regeringen.se/sb/d/10626/a/104665>

85. <http://www.aeanet.org/chinarohs>
86. <http://www.env.go.jp/chemi/reach/second/lee.pdf>
87. http://www.meti.go.jp/english/policy/mono_info_service/kagaku/chemical_substances/chemical_substances03_2.html
88. http://books.nap.edu/openbook.php?record_id=9841&page=11
89. <http://www.cpsc.gov/LIBRARY/FOIA/FOIA07/brief/UFurn2.pdf>
90. <http://www.epa.gov/oppt/pbde/pubs/proj-plan32906a.pdf>
91. <http://www.epa.gov/oppt/pbde/pubs/pbdestatusreport.pdf>
92. <http://www.epa.gov/dfe/index.htm>
93. <http://www.epa.gov/dfe/pubs/projects/flameret/index.htm>
94. <http://www.epa.gov/dfe/pubs/index.htm#ffr>
95. <http://www.epa.gov/dfe/pubs/projects/wire-cable/index.htm>
96. <http://www.epa.gov/dfe/pubs/wirecable/lca.htm>
97. <http://www.epa.gov/dfe/pubs/projects/pcb/index.htm>
98. <http://www.cpsc.gov/library/foia/foia08/pubcom/pubcom.html>
99. <http://janus.state.me.us/legis/LawMakerWeb/summary.asp?ID=280024506>
100. www.leg.wa.gov/pub/billinfo/2007-08/Pdf/Bills/House%20Passed%20Legislature/1024-S.PL.pdf
101. California solidifies Green Chemistry Initiative, Oct 7, 2008, <http://www.eponline.com/articles/68230/>
102. http://www.dtsc.ca.gov/PollutionPrevention/GreenChemistryInitiative/upload/Executive_Summary.pdf
103. <http://www.chemicalsubstances.gc.ca>
104. http://www.chemicalsubstanceschimiques.gc.ca/interest-interet/pbde_e.html
105. http://www.inemi.org/cms/projects/ese/halogen_free.html
106. www.hdpug.org
107. <http://www.ipc.org/committeedetail.aspx?Committee=4-33a>
108. Report of the World Commission on Environment and Development: Our Common Future, August 4, 1987, http://www.channelingreality.com/Documents/Brundtland_Searchable.pdf
109. <http://www.prnewswire.com/cgi-bin/stories.pl?ACCT=109&STORY=/www/story/03-10-2005/0003161414&EDATE>
110. <http://www.epa.gov/greenchemistry/pubs/principles.html>
111. http://www.ead.anl.gov/pub/doc/LCA_final_report.pdf
112. www.vecap.info
113. VECAP™ Annual Progress Report 2006, www.bsef.com/newsmanager/uploads/2006_vecap_annual_progress_report.pdf

23 Flame Retardant Design for Fiber-Reinforced Materials

Michael G. Stevens and Alexander B. Morgan

CONTENTS

23.1	Introduction to Fiber-Reinforced Materials	703
23.2	Typical Resins and FR Additives Used in FRP Applications	704
23.3	Typical Fiber Reinforcements	706
23.4	Fabrication Processes	707
23.5	Effect of Fiber Content and Composite Thickness on FR Performance.....	709
23.6	Applications for FRP Materials	716
23.6.1	Mass Transit.....	716
23.6.2	Industrial Applications.....	718
23.6.3	Architectural Applications.....	718
23.6.4	Aerospace Applications	720
23.6.5	Marine Applications	721
23.7	Conclusions	722
	References.....	722

23.1 INTRODUCTION TO FIBER-REINFORCED MATERIALS

Most polymers are used in applications by themselves, especially thermoplastic polymers. For thermoset materials though, the pure polymer does not have enough strength or stiffness to be used by themselves in many applications. In these cases, the mechanical properties can be increased by incorporating fibers into the resin. These materials are commonly referred to as composites or fiber-reinforced polymers (FRP). If the fibers are glass, then sometimes they are referred to as fiberglass or glass-reinforced polymers (GRP) or fiberglass-reinforced polymers (FRP). It should be noted that for common practice is to use FRP generically for all composites, regardless of fiber reinforcement. Of course, these composites can be reinforced with a variety of other fibers, including carbon fiber, aramid (Nomex, Kevlar), and even natural plant fibers (jute, sisal). Even the glass fibers can be of different compositions, with glasses such as E-glass and S-2 glass being the most common. These FRP composites are used in many applications where light weight, good corrosion resistance, and high strength to weight ratio are desired. Many applications use these advantages to replace other materials of construction such as steel, aluminum, and wood. Indeed, these enhanced properties has led to the widespread use of polymer composites in aerospace, maritime, chemical industry, and mass transport applications. The heightened increase and sensitivity to fuel costs has led to a huge push to put composites into as many vehicle applications as possible to save weight, and therefore improve fuel efficiency. Some recent examples of this trend are military naval vessels built entirely out of FRP composite, as well as new aircraft such as the Boeing 787, which has an all composite fuselage as well as major composite parts, its wings.

FRP materials are made up of the polymer and reinforcing fibers. The polymer is typically a thermoset polymer; thermoplastics can be used as well. Some typical thermoset polymers used are epoxy resins, unsaturated polyester resins, epoxy vinyl ester resins, phenolic resins, and high performance aerospace resins such as cyanate esters, polyimides, and bismaleimides. These resins

will be discussed later in this chapter. Since the resin in the composite holds the fiber form together, it dominates the toughness, corrosion resistance, and fire performance of the composite. The fibers provide the strength and stiffness to the composite. So while these are different components, the resin and fibers have to be looked at together in the application. Varying the resin type and content or varying the type, orientation, and amount of fibers will vary the performance greatly. There are many guidelines for FRP design, but these are always set by the performance requirements of the application. This will determine the type of resin to use, the type of reinforcements to use, and the amount of reinforcing fibers.

The different methods of obtaining the fire resistance of the polymers have been discussed in previous chapters (Chapters 4 through 13). Fire codes and fire tests relevant to FRPs have also been discussed in previous chapters (Chapters 14 through 16 and 20 through 22), but there will be some discussions of tests solely relevant to composites in this chapter. This chapter will focus primarily on some methods for preparing FRPs, some of the factors that have to be considered when designing an FRP part and typical applications where fire retardant FRP materials are used.

23.2 TYPICAL RESINS AND FR ADDITIVES USED IN FRP APPLICATIONS

As described earlier, there are many resin types that can be used in making an FRP laminate. The choice of resin will depend on many factors, including

- Mechanical performance requirements
- Chemical/corrosion resistance requirements
- Composite manufacture process (resin viscosity requirements)
- Coadditives needed for material performance (UV, oxidation resistance)
- Fire performance

This chapter will mainly focus on designing thermoset resin FRP materials for fire performance. Many of the chemical and additive methods for making these resins fire retardant have been discussed previously in Chapters 4 through 13 and the details will not be included in this chapter except where appropriate to describe the designing of the FRP material for fire performance.

For commodity applications, there are four major classes of resins that are used in FRP applications. They are phenolic resin, epoxy resin, unsaturated polyester resin, and epoxy vinyl ester resins. A more complete description of these types of resins and their many variations can be found in *Handbook of Thermoset Plastics*.¹ This is not a comprehensive list of resins used in composite manufacture, as commodity materials like polyurethanes and isocyanurate resins are sometimes used as well to make FRP parts. However, these materials are not covered in this chapter owing to their limited use, but, the principals of fire safety that apply for the resins described subsequently apply to these materials as well.

Phenolic resins were the first thermoset resin used commercially. These resins have some unique properties for fire performance in that the phenol–formaldehyde resin and resorcinol–formaldehyde resins are naturally char forming materials. This char forming nature of the resin gives them some inherent fire resistance. They also tend to generate low levels of smoke when they burn. Where high levels of fire performance are required, these phenolic resins are used because of these properties. The drawback of these resins is that they are harder to process, since they give off water as they react and they tend to have low toughness. This will affect the impact resistance of the final part. More importantly, the way in which the phenolic composite part is processed will affect its fire performance. Excess voids from water formation in the phenolic part will lead to spalling and forceful delamination of the composite during burning of the material, leading to potentially catastrophic mechanical failure of these materials when aflame.² Therefore, autoclave processes or careful design of cure cycles is required to get all the water out of the curing phenolic and ensure a void-free part.

Epoxy resins are another class of resin that can be used when fire retardant properties are required. The most common fire retardant used with epoxy resin is tetrabromobisphenol A, which is used in place of bisphenol A to synthesize the epoxy resin. This will have the bromine reacted onto the back bone of the polymer. Other cocuring additives can also be used with the brominated epoxy resin to enhance the FR performance of the cured laminate such as antimony oxide (a synergist only for brominated compounds) or phosphorus compounds. Even some intumescent additives can be used to effectively flame retard epoxy resin, as well as mineral fillers, but these nonsoluble additives have their limits on loading as too much material will yield excellent fire performance, but poor mechanical properties. Epoxy resins are composed of the epoxy resin and a hardener, which initiates the polymerization of the epoxy groups. The hardener could have a variety of chemical structures, could also be something that flame retards the epoxy, could be from 5% to 50% of the total formulation, and not surprisingly could have an impact on the fire performance of the cured resin. Aliphatic diamine curing agents obviously will add some fuel to the epoxy, while aromatic diamines and anhydride curing agents provide some additional potential for char formation.

Unsaturated polyester resins are the most widely used resins in the composites market. They are used in many applications including boat hulls, vehicle shells, fuel/pressure tanks, light-weight shelters, building components, and wind turbine blades, for example. Typically, these unsaturated polyesters are flame retarded with halogenated FR additives, the most common being the tetrabromophthalic anhydride. This incorporates the bromine in the backbone of the polymer during the polymerization of the resin. Other brominated and chlorinated materials such as dibromoneopentyl glycol or chlorendic anhydride can also be used to incorporate halogens into the backbone of the polymer. Having the halogen incorporated in the backbone of the polymer is more efficient and more stable than using brominated additives such as decabromodiphenyl oxide, which is often abbreviated or referred to in industry as “decabrom.” Some fabricators do use decabrom in unsaturated polyesters to obtain the fire retardancy. This can be done, but care needs to be taken to guarantee the proper level of additive in the resin, since it is added in as solid filler and can settle out of the resin. Antimony compounds such as antimony trioxide and antimony pentoxide can be used as a synergist with the halogens to reduce the total amount of halogen required to reach the desired fire performance. The main disadvantage to the use of halogenated resin is that they generate a high level of smoke during a fire since they inhibit vapor phase combustion (see Chapter 4 for more details). The other common approach that is used with unsaturated polyester resins is to use aluminum trihydrate (ATH) in the resin. With the proper loading of this inexpensive mineral filler, good flame spreads, and low smoke values can be obtained. However, the high loading levels of ATH required for good fire performance could have an adverse effect on the processing (high viscosity) and mechanical properties of the composite. Resins have been developed that are designed to be used with the high filler loadings and still able to be processed and have reasonable balance of mechanical properties, but even these resins have trade-offs compared with systems utilizing halogenated FR additives. Further, the level of ATH required to be used is dependent on the fire test required for the material. For example, flame spread and smoke requirements of the application as required by building code dictate flame spread and smoke release as determined by ASTM E-84. Composites on maritime vessels may require very strict flame and smoke requirements thus dictating very high loading of ATH.

Epoxy vinyl ester resins are a special class of unsaturated resin. This resin is made by capping an epoxy resin with methacrylic acid and then dissolving in styrene monomer to the desired viscosity. This gives mechanical properties similar to epoxy resins, but the processibility (low viscosity allowing for resin infusion processes) of an unsaturated polyester resin. As with unsaturated vinyl esters, the most common fire retardant vinyl ester resin is based on a resin made from a halogenated system, tetrabromobisphenol A. The level of bromine in the resin and the presence of antimony will determine the fire performance of the resin. These resins are normally used for corrosion resistant equipment or when fire performance and high mechanical properties are required. It is very difficult to get a low smoke value with a brominated vinyl ester resin again due to the fact that bromine

inhibits vapor phase combustion, which in turn prevents clean burning. In some cases, the resin can be filled with ATH to meet the desired flame spread and smoke requirement, as well as intumescent FR packages, but again, the more filler used, the harder it becomes to process the resin and maintain a good balance of properties. Further, since epoxy vinyl esters are so often used in resin infusion processes, many additives insoluble in styrene or other vinyl monomer (such as methyl methacrylate) may filter out onto the fiber reinforcement as the resin flows into the composite mold. If the material filters out it will not be uniform in the part for fire protection, and more likely, the filtered material will block up the infusion points and prevent the part from being successfully made. The particle size to be allowed through the fiber reinforcement really depends upon the fineness and mesh size of the fiber reinforcement, and in this case the engineer or material scientist designing the part will have to consider these things if the typical halogenated FR additives cannot be used. To date there are very few commercial nonhalogenated FR additives that have been found to work well with epoxy vinyl esters, hence the continued use of brominated FR additives.

High performance aerospace resins such as cyanate esters,^{3,4} bismaleimides, phthalonitriles,⁵⁻⁷ and polyimides⁸ typically have much lower levels of flammability due to their chemical structures and a propensity for these materials to char upon exposure to heat and flame. However, these resins can burn just as easily as the other commodity materials depending upon their chemical structures. When thinking about flame retardancy of any thermoset material, like with thermoplastics, it helps to look at the chemical structure of the polymer itself, as its chemical structure will directly impact the fire performance of the material.⁹ This is very true for the high performance thermosets, and is true of commodity resins as well. Since the high performance resins are primarily aromatic structures, they tend to start with lower heat release potential to start with, and therefore are much easier to flame retard. Typically though, these materials, especially bismaleimides and polyimides, are not flame retarded currently, they are being pushed into higher heat flux exposure applications (engine components, wings/components exposed to engine wash), which may begin to require flame retardants to be added even into these low heat release materials.

23.3 TYPICAL FIBER REINFORCEMENTS

The most common reinforcement used in FRP applications is glass fibers. The type of glass used is based on the process being used and the desired mechanical properties of the final composites. E-glass is very common for most FRP applications, with stronger (and more expensive) S-2 glass being used for very strict composite applications such as blast/ballistic protection (military), and large structures (wind turbine blades, aerospace composites). The glass reinforcement can be in many forms including chopped glass mat, continuous strand mat, strands of roving that is chopped as it is applied to a preform shape, woven roving, filament winding roving, and knitted roving. In general, the chopped glass fibers provide the lowest mechanical properties in the FRP, followed by continuous strand mat, which provides a little higher performance and then woven roving with highest performance. The highest strength values will be obtained when using either knitted roving or filament wound roving. The choice of fiber lay-up and type really depends upon the manufacturing chosen for the FRP part, as some processes lend themselves to making large structures (chopped), while woven roving tends to be more appropriate to high performance smaller dimension parts. Obviously, the reinforcing fibers give the FRP its strength and stiffness once the resin is cured, so the choice of fiber is the most important for the structural integrity of the composite. With regards to fiber loading levels for the FRP, in general, the higher the fiber content the higher the mechanical properties.

Other fibers can also be used for reinforcement as mentioned in Section 23.1, including carbon, aramid (Kevlar), and natural fibers. In general, carbon fibers will give the highest strength and modulus values in the laminate while keeping the weight of the composite the lightest. Also, carbon fibers can bring some other benefits to the composite including thermal and electrical conductivity through the fibers depending upon fiber chemical composition. Kevlar fibers bring strength and weight benefits between those of glass and carbon fibers, whereas natural fibers tend to bring some

of the lowest enhancements in mechanical durability. However, natural fibers bring strong advantages in cost (very inexpensive), light weight (fibers of low density), and sustainability areas that cannot be obtained with other fiber types. All of these fiber types come in the same geometries and rovings typically seen with glass fibers mentioned in the previous paragraph.

The amount, type, and to some extent the geometry, of fiber reinforcement can have an effect on the fire performance of the composite. Some work demonstrating this will be discussed later in this chapter. Most of the fire performance of an FRP comes from the resin. Glass fibers are non-combustible so they do not contribute to the burning of the material and the higher volume fraction in the composite will give better fire performance in the composite. Carbon fibers are sometimes considered to be noncombustible, but, they can be burned with enough heat exposure.¹⁰ The same is considered of aramid fibers,¹⁰ but these definitely can combust in a fire along with the natural fibers, where the type of fiber can play an important role in the flammability of the composite.¹¹

23.4 FABRICATION PROCESSES

There are many fabrication processes that can be used to fabricate FRP parts. The fabrication process used will depend on the shape of the part being made, the properties required, and the number of parts being made. The most common processes are hand lay-up, spray-up, filament winding, compression molding (including autoclave processing), pultrusion, resin transfer molding (RTM), vacuum-assisted resin transfer molding (VARTM), infusion process, and continuous panel process. It should be noted that all of these processes will work with any type of fiber (glass, carbon, aramid, natural, etc.) provided that the fiber in question has the durability to survive that process, or, comes in a form needed for that process. When a particular process is incompatible with a fiber type, it will be mentioned; for all practical purposes it is safe to assume otherwise, i.e., these other fiber types can be used with the processes mentioned subsequently. Further, it must be pointed out that many fibers are coated to be compatible with a particular process or resin type. This coating or “sizing” is not in high enough concentration to affect flammability performance, but, it is very important when considering processing or composite mechanical strength.

Hand lay-up and spray-up processes are used for low-volume custom parts. In this process, the fiber in the hand lay-up process is manually wet out. Most of the time, this process uses chopped strand glass mat, but it will work with other fibers. Higher properties can be obtained by using woven roving or knitted mats in combination with the chopped strand mat for additional strength properties. The spray up process applies the resin and fiber through a chopper gun, which sprays a set amount of resin and chopped fiber onto the mold (or tool) shape. This process is typically limited to resin systems that have up to about 1000 cps viscosity, but, the use of solvents is sometimes utilized to lower the viscosity of a resin to allow it to be compatible with this process. However, the use of solvents is under increasing scrutiny due to emission and environmental issues that come when the solvent evaporates off in this process. There are no particle size restrictions in the hand-lay up/spray-up processes, which mean that one does not have to worry about particles filtering out and not being available for fire protection on the resulting composite part. This allows for the use of very large particle size flame retardants such as intumescent packages, mineral fillers, and expandable graphite. This process is the least expensive with regard to equipment to start making parts; hence it is continuously and widely used despite a heavy reliance upon manual labor to produce the part. However, the popularity of this technique is that this method can also accommodate the most complex part shapes of all of the processes outlined in this section.

Filament winding is normally used when the equipment is cylindrical like a tank, pipe, or duct work. This gives much higher mechanical properties than those provided by the hand lay-up/spray-up processes, which can also produce these geometries. This process has continuous fibers that are wet out in a bath containing the resin and placed on a rotating mandrel. The fibers can be wound at different angles to vary the properties of the laminates with fiber content in this process falling typically in the range of 50%–70%. The resin viscosity requirement for this process ranges

from about 200 cps to 1000 cps. Not surprisingly, the process is limited to cylindrical shapes or shapes that will work with a spinning mandrel. For fire applications though, this process makes good sense for conduit designed to protect cables, power lines, or water lines. This process is fairly insensitive to FR particle size and solubility of the FR additive in the resin, but, large particle sizes can and will give a rough surface finish to the product if they are too large.

Compression molding is used for higher volume parts that are not very complex in geometry. The cost of the tooling required and the presses for this process limits its use to applications where high volumes of the same part are required. The fiber and resin is made into either a “prepreg” (pre-impregnated fiber form) or sheet molding compound (SMC). These are thickened before molding. The prepreg or SMC are then molded under high pressure and temperature. The cycle times in this process are normally short. The SMC compound is typically made with fillers with a typical viscosity of 10,000–30,000 cps. This compound is mixed with chopped fibers and then run through a set of heated rollers to help wet out the fibers. For compression molding, there is no limit to the particle size of the filler used in this process provided prepreg or SMC is being used; for autoclave processes and film + fabric compression molding process, particle size is very important. Autoclave processes are very similar to compression molding in that a resin and fiber form and compressed against a tool shape under heat and pressure. Instead of a heated press though, a pressurized vessel (an autoclave) is used to produce high-quality void-free parts. This process is typically used for aerospace and military components, but has not expanded further because of the size limitations and capital costs of autoclave equipment. In the autoclave process, layers of prepreg or resin film (viscosity similar to SMC) and dry fabric and stacked and then vacuum bagged (multiple layers to help force the part to consolidate) against the tool to produce the part. During the autoclave process, the heat and pressure cause the resin to move and flow and fully wet out the fibers, and in this process, particles in the resin can move about. If they are too large, they can consolidate on the fabric surface, leaving resin- and additive-rich domains in the part. This in turn can lead to poor mechanical and flammability performance. Besides the particle size, compression molding/autoclave molding has a pronounced effect on phenolic resin flammability. Specifically, phenolic resins that are autoclaved or compression mold processed tend to be void free, and do not suffer from the spalling typically seen in hand-layup, infusion, RTM, or VARTM type panels.²

RTM is normally used for medium volume parts. The tooling cost for RTM process is much less than compression molding, but more expensive compared with hand lay-up process. This process has the fibers placed in the tool and closed with pressure. The resin is then injected with pressure to fill the part. This can be done at room temperature or at elevated temperatures depending on the desired cycle time. A modified version of the process uses vacuum to assist in the filling of the mold. This is referred to as VARTM or RTM Light. The ideal viscosity range for a formulated resin system for RTM and VARTM processes is 200–600 cps. VARTM is similar to the RTM process except that it uses vacuum to pull the resin into the mold. This process gives higher fiber content and lower voids compared with other processes. This is normally used when high strength properties are required, as the presence of voids will weaken the mechanical strength of the part. VARTM is also used when the autoclave process is not practical (very large parts needed) or not economical. The types of FR additives that can be used in this process are limited because of the very real possibility of the fiber reinforcement filtering the FR additive out of the resin and concentrating it at the fiber surface. Typically, a maximum particle size of 4 μm is recommended for most fiber reinforcements, but the particle size will be determined by the fiber diameters and fabric weaves. Anything larger than this will most likely be filtered out of the resin, which will lead to nonuniform flammability performance in the part, and in some cases prevent the part from being made, as the FR additive has dammed the resin at the entry ports into the mold. The viscosity range that can be used in this process is generally low. The ideal viscosity range is 100–200 cps viscosity. A viscosity of up to 500 cps can be used if a slower fill time is acceptable. It is very hard to wet out the glass fibers and fill the part if the viscosity is over 500 cps. If soluble flame retardant additives are used with this process, care must be taken to ensure that the FR additives do not increase the viscosity, especially if they are coreactive FR additives.

The pultrusion process is used for making structural parts in a continuous process. The fibers are pulled through resin bath to wet out the fibers with resin. These wet fibers are then pulled through a heated die to shape and cure the resin. When the part comes out of the die it is a cured finished part. The typical viscosity range for resin systems used in pultrusion process is 500–3000 cps. For FR additive particle size, pultrusion is fairly tolerant of large particles provided the particles do not prevent the tight packing of the fibers being pulled through the die. Related to pultrusion is the continuous panel process, which is used for high volumes of mostly flat panels or corrugated panels. This process has the fibers placed on a continuously moving belt that goes through a forming area and then through a heated oven area. This process typically uses viscosities in the 250–600 cps range, as it is hard to get good fiber wet out at higher viscosities. The additive particle size range for this process can go up to 22 μm .

When considering composite fabrication, generally the type of part to be made dictates the fabrication process, not the fire performance. If the part cannot be made to specification, and at reasonable cost, then no amount of good fire performance will sell the part. In general, the composite fabrication processes listed here do not directly affect flammability performance other than dictating what types of additives (particle size) can be used. However, there are exceptions to this, including the presence of voids in phenolics² and uneven fiber/resin concentrations in composites. Where there are resin-rich pockets there exists the possibility for uneven flame spread and smoke release performance. Further, these pockets that may heat and expand at different rates can lead to composite delamination during a fire. The delamination of a composite can lead to premature structural failure of the part under fire, or worse, expose additional surface area to fire exposure, which in turn accelerates the burning of the composite.¹² This is particularly true for composite sandwich structures.^{13,14} Therefore, care must be taken to produce a quality composite by the process method that is chosen, and to study the composite structure for defects before submitting it for fire testing.

23.5 EFFECT OF FIBER CONTENT AND COMPOSITE THICKNESS ON FR PERFORMANCE

When designing FRP parts that have fire retardant requirements, there are several critical items that have to be considered. First, the fire performance and smoke requirements for the application are to be considered. Next will be the mechanical property requirements and the manufacturing process that will be used to make the parts. This will help in determining which resin, which FR additives, and fiber construction to be used for the part. The first issue, fire and smoke performance, are set by the end-use application for the FR part. For building and construction applications, this is typically ASTM E-84 in the United States or Single Burning Item (SBI) in the European Union (EU), but for aerospace and ship hulls, Federal Aviation Regulations (FAR) and International Maritime Organization (IMO) codes apply. The reader should look to Chapters 14, 15, and 21 to get a better understanding of the specific fire tests involved, as those fire tests and the measurements help determine the flame retardant/fire protection approach. In this section, we will focus primarily on flame spread/smoke release from ASTM E-84, as the effects of laminate construction have been well studied for this test.

The laminate construction in FRP parts can have an effect on flame spread and smoke test results. A study was conducted by Stevens¹⁵ and published in the proceedings of Composites 2007 conference. This study looked at how glass fiber content and panel thickness affected the ASTM E-84 flame spread index (FSI) and smoke developed index (SDI). The effects of fiber content and thickness on cone calorimeter results were also evaluated. Another study was conducted by Dempsey¹⁶ looking at the effect of glass content in several fire tests, and in this paper, he also found a correlation between the FR performance and glass content.

The ASTM E-84 test is currently listed as the standard test used for the qualifying materials for interior and exterior finish materials in the U.S. building codes. The FSI considers both the ignition

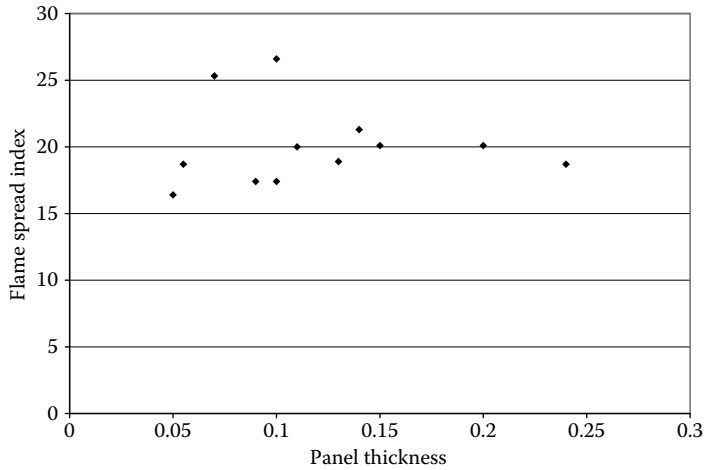


FIGURE 23.1 Effect of thickness on FSI.

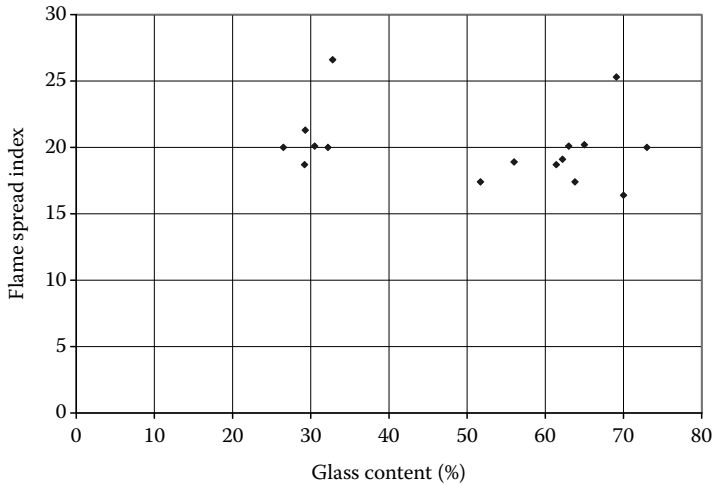


FIGURE 23.2 Effect of glass content on FSI.

time and the distance that the flame front travels during the 10-min test. The FSI is a relative number to an FSI of 0 for cement board, and an FSI equal to 100 for select grade red oak. The FSI number is always rounded to the nearest multiple of 5. A Class I or Class A FSI refers to an FSI of ≤ 25 . Class II or Class B refers to a laminate with a FSI of 30–75. Class III or Class C refers to a FSI of 80–200. Anything with a FSI over 200 is not classified. Some interior applications require a SDI rating as well. This is also based on red oak being a SDI of 100. The SDI rating for interior finish materials in the building codes is ≤ 450 . Some applications, for example, exterior of buildings or industrial equipment, use the ASTM E-84 FSI, but they do not always have a smoke requirement.

Two resins were used to do the first study on laminate construction. The first was a brominated epoxy vinyl ester resin with antimony pentoxide and the second was a brominated unsaturated polyester resin. They were both promoted to cure at room temperature with methyl ethyl ketone peroxide catalyst. The panels were then postcured at 250°F (121°C) for 8 h. Panels were prepared that varied in glass content from 25% to 70% and panel thickness varying from 0.05 in. to 0.25 in. and were tested at the same testing facility. A summary of the FSI test data for the first set of panels tested are shown in Figures 23.1 and 23.2. This graph in Figure 23.1 plots the FSI value versus the panel thickness. This data would indicate that the thickness of the test panel has no effect on the measured

FSI. All of the FSI values were within the standard deviation of the test. It should also be noted that the different types of glass and the various glass contents did not affect the FSI as shown in Figure 23.2. The first set of laminates tested had an FSI value between 15 and 25.

It was expected that the higher glass content laminates should have had a lower FSI. To determine if this is the case, a second set of panels were prepared that have typical FSI values in a laminate with 25% glass ranging from 20 to 50. Panels were made at 25% glass and 60% glass. The test results are shown in Figure 23.3. This does show that when the FSI of the laminate is greater than 30 on a 25% glass panel, going to 60% glass significantly reduces the FSI. When the FSI of the laminate is <25, the reduction seen by going to 60% glass is within the standard error of the test. That is why in the first experiment, it did not show up as reducing the FSI.

The data for the SDI are shown in the graphs labeled Figures 23.4, 23.5, and 23.6. The graphs of the SDI versus panel thickness (Figure 23.4) show that the laminate construction can have a large effect on the SDI value. It appears that the glass content of the panel and the thickness of the panel can affect the SDI value. This was seen in both sets of experiments that were run. Looking at the flame spread distance and smoke curves that are recorded during the test gives some insight into the reason

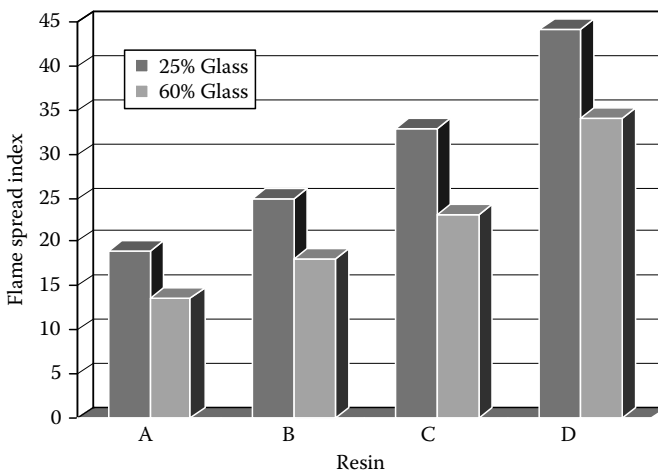


FIGURE 23.3 Effect of panel thickness on SDI.

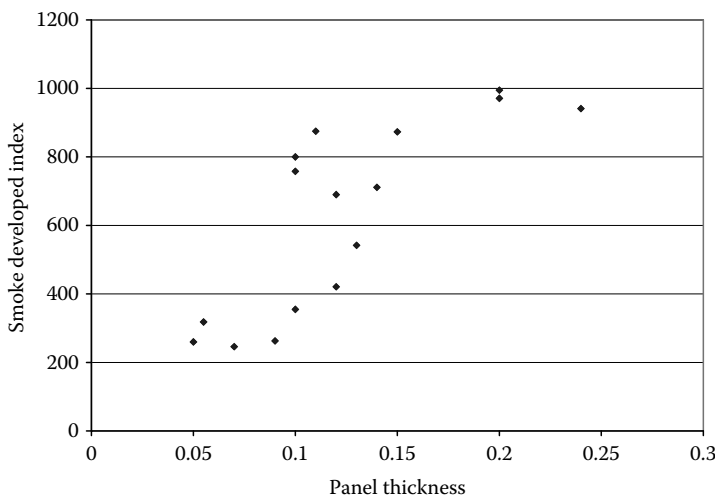


FIGURE 23.4 Effect of glass content on SDI.

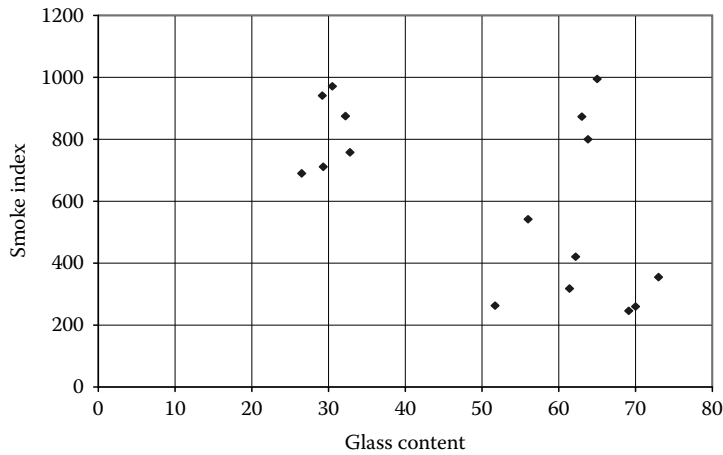


FIGURE 23.5 Effect of glass content on FSI for second set of experiments.

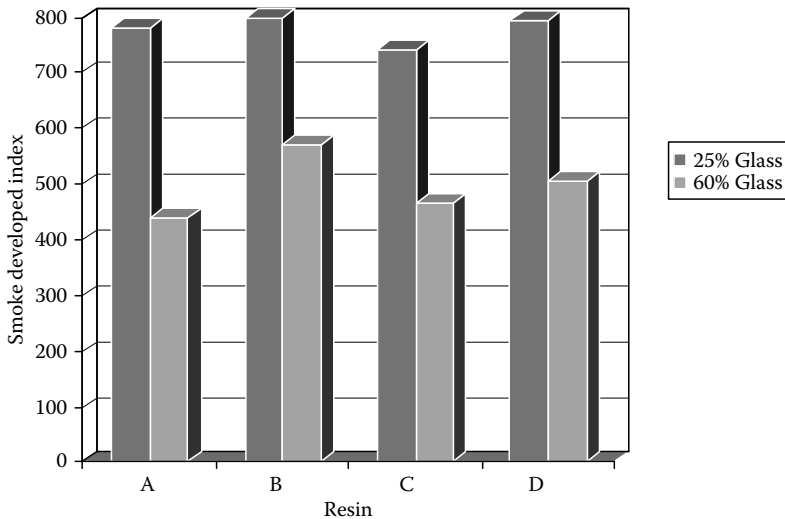


FIGURE 23.6 Effect of glass content on ASTM SDI for second set of experiments.

why these two parameters affect the SDI value. The curves for the light obscuration and flame spread distance overtime during the test for a thin and thick panel are shown in Figures 23.7 and 23.8. On the thinner panels it shows the flame front traveling along the panel for the certain time period and then the front starts receding (Figure 23.7). When the flame front starts receding, the percent light obscuration starts to decrease, which means less smoke is being given off. The total amount of resin in the panel seems to be the controlling factor on the SDI value. The SDI will probably maximize at different thicknesses depending on the resin content of the panel. As seen in Figure 23.8, higher glass content in the panel will give a lower smoke value for the same thickness of the panel.

Cone calorimeter testing was also conducted on the second set of panels at both 50 kW/m^2 and 100 kW/m^2 heat fluxes. This data is in Table 23.1. The only value that showed any significant difference between the 25% and 60% glass content laminates was the total heat release rate (HRR) and the specific extinction area (SEA). By going from 25% glass to 60% glass, the total HRR was reduced by 30%–50%. The higher glass content also showed a reduction in the smoke as measured by SEA.

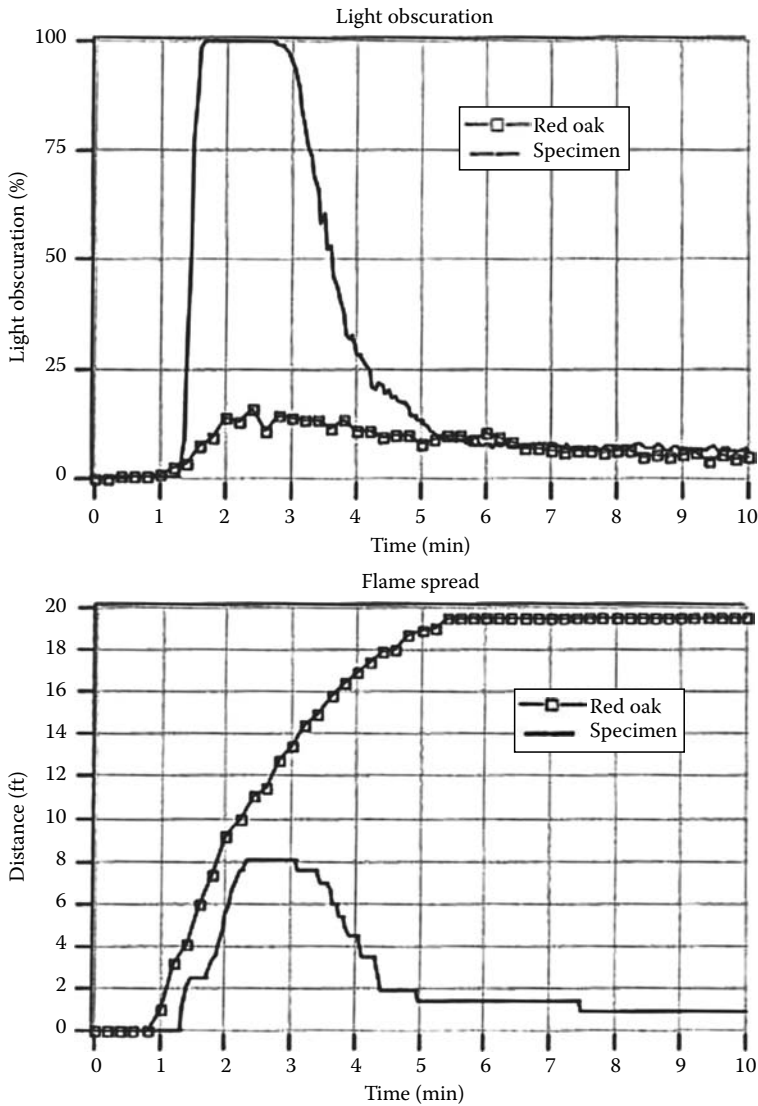


FIGURE 23.7 ASTM E-84 test curves for 0.1 in. thick panel with 73% glass.

The results from these tests shows that when comparing resins used in FRP laminates the glass content and the thickness needs to be the same. The laminate need to be tested in the qualifying test with the same fiber construction, fiber content, and thickness, as it will be used to have a true measurer of its performance. Another factor that needs to be taken into account is the fire test being run. A resin system may do well in one test, but not in another test. The method of obtaining the fire performance is the reason for this. One example of these was reported by Stevens.¹⁷ This study compared FRP laminates made from two resins that both met the ASTM E-84 FSI and SDI for a Class 1 material. One of the materials was a halogenated polyester resin and the other material was a modified acrylic resin filled with 150 parts of ATH to 100 parts of resin. The results of the two materials are shown in Table 23.2. Even though the halogenated resin and a lower FSI rating in the ASTM E-84 test, it failed the room corner burn test. The modified acrylic resin filled with ATH easily passed the room corner burn test.

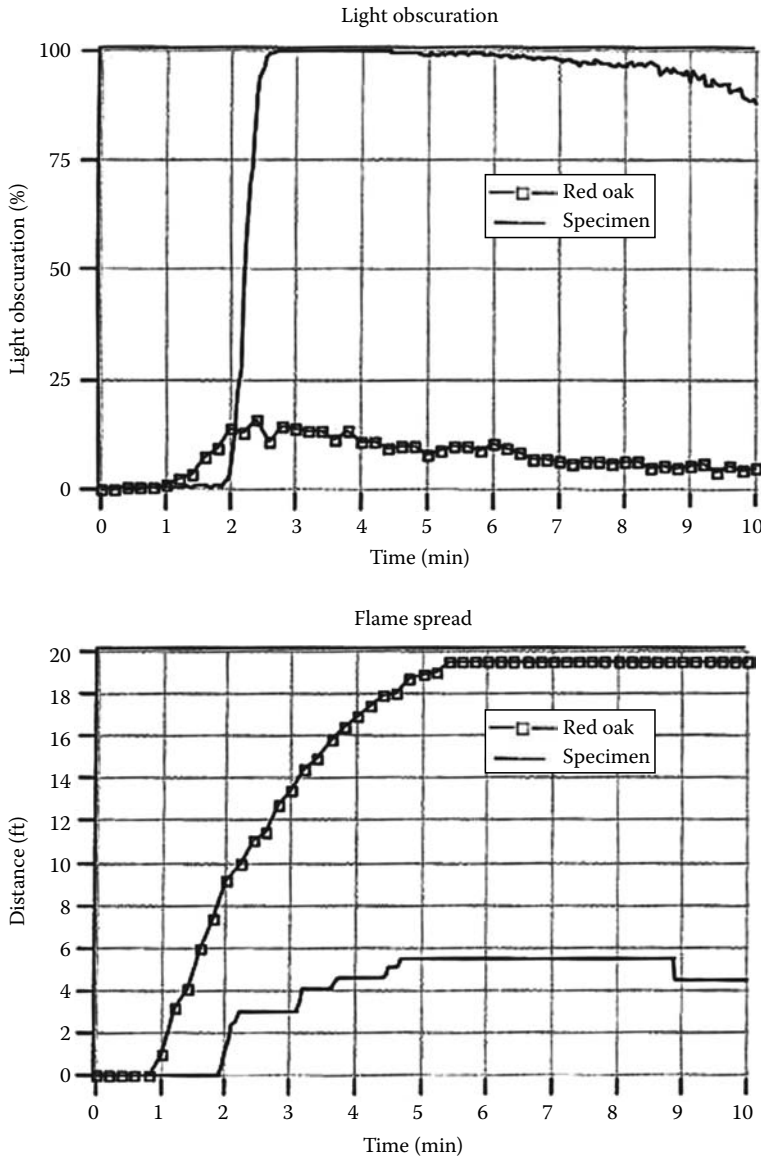


FIGURE 23.8 ASTM E-84 test curves for 0.2 in. thick panel with 65% glass.

This has been seen with other fire tests as well. Because so many fire tests are used to mimic specific fire risk scenarios, and therefore measure flammability in very different ways, there tends to be little correlation between the different fire tests used around the world (see Chapters 14 and 15 for more details). The FRP system has to be studied in the regulatory tests that it will be used in to verify that it will meet the requirements. Some work has been done by several people developing predictive models to use as screening tests for larger tests. This is used mostly in research and development to screen new systems before running the full scale test that takes a lot of material and costs much more. Dempsey et al.¹⁸ have published a work showing that glass content can affect the fire performance behavior in other flame spread tests. This study also showed that higher glass contents will give better performance in flame spread and smoke tests.

TABLE 23.1
Effect of Glass Content on Test Results

Resin	A	A	B	B	C	C	D	D
Glass content (%)	28	64	25.8	61.8	29	60	23	61
FSI	19	13.5	25	18	33	23	44	34
SDI	779	439	800	569	740	465	795	503
E1354 @ 50kW/m ²								
T_{ig} (s)	46	51	49	51	48	45	47	51
Peak HRR (kW/m ²)	163	234	217	249	249	255	299	355
Total HRR (MJ/m ²)	33.4	17.9	41.2	24.7	42.4	27.6	47.6	26.9
EHC (MJ/kg)	9.2	9.5	10.3	11.6	13.3	12.8	13.4	14.5
SEA (m ² /kg)	1510	1329	1553	1300	1724	1439	1619	1457
E1354 @ 100 (kW/m ²)								
T_{ig} (s)	15	18	16	18	15	19	16	19
Peak HRR (kW/m ²)	281	316	294	358	361	400	406	427
Total HRR (MJ/m ²)	33.9	17.8	40.7	26.1	43.7	29.5	51.9	31.9
EHC (MJ/kg)	9.1	10.4	10.1	11.8	11.4	12.8	12.9	13.6
SEA (m ² /kg)	1813	1505	1626	1580	1812	1720	1847	1649

TABLE 23.2
ASTM E-84 and NFPA 286 Room Corner Burn Test Results

Resin	Class A Requirement	Halogenated Polyester Resin	Modified Acrylic Resin
ATH level (phr)		0	150
ASTM E-84 FSI	≤25	20	25
ASTM E-84 smoke index	≤450	400	75
NFPA 286—peak net HRR, MW	<1	3.9	0.38
NFPA 286—peak heat flux at the floor (kW/m ²)	<20	26.4	5.8
NFPA 286—average upper layer temperature (°C)	600	891	533
NFPA 286—flame existing door	None	Yes	No
NFPA 286—auto-ignition of paper target	No	Yes	No
NFPA 286—total smoke released (m ²)	<1000	2072	76

For tests other than E-84, there have been some studies on the effects of fiber loading and fiber layout on composite flammability. This has primarily been work done by the U.S. Navy on the flammability of composites used in naval vessel flammability,^{19,20} or work by Kandola et al.^{10,21,22} on the effect of fiber type and content on polymer composites studied by cone calorimeter. More work is being conducted in studying the effects of fiber orientation and lay-up not on overall flammability performance, but flammability performance under structural load. This is the most important for aircraft, vehicles, and buildings where the composites are structural members. The concern here is

that when these composites are heated by flame, the polymer will soften above the glass transition temperature and the composite will fail. However, concerns also exist that some composites may also have problems with the fiber laminates breaking apart or falling apart during a fire, which contribute negatively to the flammability performance. There have only been some preliminary studies looking at this to date, and so far only by cone calorimeter.²³ More work is needed in this area to better understand how fiber loading, chemistry, and structure (weave, unitape, etc.) affect material flammability, and a good summary of the work to date can be found in a book by Mourtiz and Gibson published in 2006.²⁴

23.6 APPLICATIONS FOR FRP MATERIALS

As with any real world application, the material scientist must look to the end-use properties and performance of the application when selecting a material to use. One of the reasons to use FRP is the improved strength to weight ratio. The typical density of an FRP is about 1.5 g/mL while steel is about 8.9 g/mL and aluminum is about 2.8 g/mL. FRP materials also can have better fatigue resistance compared with stainless steel. For example, an FRP material made from an epoxy vinyl ester resin went >1,000,000 cycles when tested at 10% of ultimate stress and 5000 cycles when tested at 30% of ultimate stress.²⁵ Stainless steel only went 4000 cycles at 10% of ultimate stress and only 200 cycles when tested at 30% of ultimate stress. Not surprisingly, different applications can have widely different requirements and therefore, it is important to consider all of the requirements (mechanical, cost, manufacture technique, solvent/heat/cold resistance, fire performance) for the application when choosing the resin to use and the fiber reinforcement. As indicated earlier in the chapter, resin choice will strongly dictate fire performance, but it will also play a strong role in the other properties required in an FRP. For fire performance, which is the focus of this chapter, applications of FRP composites will be discussed in this section. Again, fire performance requirements are set by codes and standards (reviewed in Chapter 21), but it is important for the material scientist to collect their own data on this and make sure that they are very familiar with the fire tests before trying to design an FRP system.

23.6.1 MASS TRANSIT

The mass transit industry is growing rapidly on a global basis due to increasing population in urban centers, or due to increasing fuel costs. The test requirements vary widely around the world. The United States, for instance, has fire regulations for passenger trains traveling between cities described in Code of Federal Regulations title 49 CFR part 216, Federal Railroad Administration. There is a second voluntary standard for intercity trains referred to as Docket 90. The National Fire Protection Association (NFPA) also has a fire code for mass transit vehicles called NFPA 130. Also, most South American countries follow the requirements of NFPA 130 for their mass transport (rail) systems. Finally, there are European standards for subway cars and trains, which can be very strict on fire safety of materials used in mass transit construction. These standards are a mix of local (national) standards and attempted EU “harmonized” standards, which will be discussed later in this section. All of these standards have flame spread and smoke requirements to protect passengers from fire hazards and give them enough time to evacuate cars safely. In the United States, the flame spread requirement is based on the ASTM E162 radiant panel test and the smoke requirement is based on ASTM E662 smoke density test. Under this U.S. standard, the requirement for all vehicle walls and ceilings is a maximum flame spread of 35 and maximum smoke density at 90 s of 100 and a maximum smoke density at 4 min of 200. Some of the train car manufactures have more stringent requirements and include a smoke toxicity test requirement as well. Because of the smoke and smoke toxicity requirements in this application, halogen flame retardants are not generally used (see Chapter 4 for why halogenated FR induces more smoke). Most of these parts are made using unsaturated polyester resins, epoxy vinyl ester resins, or modified acrylic resins

that are filled with ATH or intumescent FR packages (such as ammonium polyphosphate). These resins are chosen because of their ease of manufacture and relatively low cost given the large size of the applications in question. These applications include seats, interior and exterior wall panels, lavatories, engineer's consoles, etc. Some parts such as flooring are made out of phenolic resin to meet the ASTM E119 requirement of 15 min without the temperature exceeding 200°F on the back side of the panel for floors in passenger trains. Depending upon the size and dimensions of the part in question, particular processes will be favored, which will dictate resin choice, which will in turn dictate base fire performance. To date, most of the parts in mass transport are made using a hand lay-up or spray-up process, but some manufactures are switching to closed mold processes such as RTM or vacuum infusion processes (Figures 23.9, 23.10).

Currently in Europe each country has its own fire standard for mass transit vehicles. These tests do not correlate well with each other or with the U.S. test requirements. This makes it difficult for suppliers, since they may have to use different systems to meet the requirement for each country. The EU is in the process of developing a unified standard EN 45545 that will be accepted all over



FIGURE 23.9 Innovia people mover at DFW airport built by Bombardier.



FIGURE 23.10 Front end of TGV high-speed train in France.

Europe. This will make it easier for qualifying materials because the classifications will be the same all over Europe. The flame spread test is based on the IMO radiant panel test ISO 5658-2. The heat release is measured using ISO 5660-2 cone calorimeter. Smoke opacity is measured by EN ISO 5659-2 and smoke toxicity is measured by EN ISO 5659-2 with FT-IR used to measure toxic smoke components. All of these lead to giving the product a rating of HL1, HL2, or HL3. Each country can specify the rating level required for the applications in their country. Research is ongoing at this time to determine how to best meet these standards through resin choice, composite manufacture process, and the use of FR additives. The HL3 rating is the rating with the most stringent requirements, which would probably require a phenolic resin or a highly filled modified acrylic resin to meet the requirements. The standard filled polyester resins in commercial use today likely can meet the HL1 and HL2 ratings. It will be difficult to meet even the HL1 rating with an unfilled halogenated polyester resin owing to the smoke release from the halogenated FR.

It becomes even harder to develop a global resin when one realizes that the Asian countries have been using the requirements of either Europe or the United States depending on who is designing the equipment. They are looking at implementing their own codes in the future but until this is done, the material scientist will have to consider these local regulations in designing a fire safe FRP for mass transport applications.

23.6.2 INDUSTRIAL APPLICATIONS

The use of FRP in industrial applications has been around for over 50 years. Some typical applications where these are used include chemical storage tanks, scrubbers, carbon absorbers, stacks, stack liners, duct work, fan housings, fan blades, etc. They were first used in 1953 when a chlorinated polyester resin was used to make the cell covers and headers at a chlorine plant. The acceptance and use of these materials have only grown since then. The main reason that FRP is used in these applications is for their improved corrosion and chemical resistance in many environments. In some cases, there is also a fire retardant requirement when FRP materials are used in chemical operations. The most common test for fire retardancy used in these applications is the ASTM E-84 Steiner Tunnel test. Most of the time regulators are looking for a FSI of <25 in these applications. The resin selection for these applications is first done on the environments it will be exposed to and at the exposure temperatures. A brominated epoxy vinyl ester resin is typically the main resin used when both corrosion resistance and fire retardancy is required. These systems give very good chemical resistance to both acids and bases and can achieve the desired flame spread rating of <25. The laminate will have a corrosion barrier that consists of a veil layer that is 90% resin and 10 fiber followed by chopped strand glass layer that is 70% resin and 30% glass fibers. The corrosion liner is not included in the structural wall calculations. The structural portion of the equipment is normally made by filament winding to obtain high strength and modulus in the structural wall. The normal resin content of these tanks is 30% with 70% glass. Fillers are not used in the corrosion liner, because it can reduce the corrosion resistance of the resin. Fillers are also not generally used in the structural layer except for when antimony trioxide or antimony pentoxide is used to get improved flame spread results with the halogenated vinyl ester resin.

The use of these resins will continue to grow as they replace metals in many applications because of longer life, lower maintenance, and in many cases, lower initial costs. FRP gives the engineer more design flexibility on the shape of the equipment and design the strength and stiffness where it is needed the most. The use of finite element analysis has helped to put more science into designing the strength and stiffness of the equipment instead of empirically experimenting and running tests to see what is obtained.

23.6.3 ARCHITECTURAL APPLICATIONS

The use of FRP in architectural applications has been going for many years. They are used to produce exterior decorative items such as cornices, facades, sky lights, etc. (Figure 23.11) and have also



FIGURE 23.11 The cap at Union Station in Columbus, OH.

been used to make interior finish wall panels. The requirements for these applications are governed by the building codes. The current building code is applied to FRP the way it is applied to any material. The International Building Code that will come out in 2009 will have a new section for FRP. This section describes how the code should be applied to FRP parts in interior and exterior applications. Some changes were also implemented in this code change. If the part is above 40 feet in height, then it will have a major effect on the use of FRP materials in exterior applications. The previous code requirement was for anything over 40 feet to be noncombustible. This would eliminate the use of any FRP material on buildings above 40 feet. An exemption was approved at the IBC code hearings that will be in the 2009 building code. The exemption is that if the FRP material has an ASTM E-84 FSI of <25 and it does not cover more than 20% of the exterior area of the building, then it can be used at any height. This will now allow the use of FRP made from halogenated polyester resins to be used on decorative trim pieces such as cornices and domes without getting a variance from the code official. This should increase the use of FRP in these applications.

The use of FRP is desired to replace older materials of construction such as concrete, stucco, etc. They have been used in many historical preservation projects. The reason they are desired is because of light weight, durability ease of installation, and low maintenance (no dry rot, attack by insects, mold, etc.). These are typically nonstructural parts made by spray-up process or continuous panel process. An example are shown in Figure 23.11. This market is expected to continue to grow. The main resin used for exterior architectural applications are halogenated polyester resins. Since there is not a smoke requirement, resins that meet the ASTM E-84 flame spread requirement of <25 can be used for this application. The other common material used for these applications is polyester resin or modified acrylic resins that are filled with ATH. The ATH filled resins can also be used in interior applications since they will typically also have low smoke values.

The EU has also implemented a new unified standard for building materials in EN 13501-2. This uses the SBI test EN 13823. (See Chapter 21 for more details on these fire codes.) The classifications in this standard are shown in Table 23.3. These classifications do not correlate to the U.S. classifications based on ASTM E-84 test. Testing has been done that shows that a halogenated resin that can give a Class A classification by ASTM E-84 gave a Euroclass D flame spread rating and a S3 smoke rating; rather poor performance in the Euroclass rating system but considered very good by ASTM E-84. The level of halogen required to obtain a Euroclass B is much higher than what it takes to make a Class A flame spread in ASTM E-84 test. It has also been found that the introduction of mineral fillers such as ATH will help give a better Euroclass rating. An all ATH filled modified acrylic resin system with 150 phr of ATH has been able to meet the Euroclass B,S1,d0 classification. Halogenated resin systems normally give an S3 smoke rating, even when ATH is included in the formulation. It is much easier to meet the S1 smoke rating with a halogen-free resin system.

TABLE 23.3
European Classifications from EN 13501
for Construction Products

Euroclass	Typical Products Examples	Previous National Classifications		
		France	Germany	U.K.
A1	Stone, concrete	NC	A1	NC
A2	Gypsum boards	M0	A2	0/NC
B	Wood (treated)	M1		0
C	Wall covering on gypsum board	M2	B1	1
D	Wood (untreated)	M3		2
E	Low-density wood fiberboard	M4	B2	
E	Some plastics		B3	

A continuous FRP panel manufacturer has been able to formulate a translucent panel that can meet the Euroclass B,S1,d0 requirements and have had the panels certified in Europe for building applications.

A draft review paper titled *Plastics-Guidance* in the assessment of fire characteristics of fire performance of fiber-reinforced composites is available in ISO document number ISO/DIS 25762. This gives a review of how several common FRP materials perform in the new Euroclass tests that will be used in classifying building products and transit vehicles in Europe. The materials tested included standard unsaturated polyester resin, FR polyester resin, pultruded-modified acrylic resin with ATH, two phenolic resins, and an automotive polypropylene FRP material. This shows how the products will perform in the new tests that will be used in Europe. The results outlined in this document show that a wide range of performance can be obtained from the different materials. This paper does go into the reaction to fire tests that are going to be used and makes recommendations on how to apply these to determine fire hazards in an application. This is a very good review paper and one that should be read by the fire safety engineer or materials scientist pursuing work in this area. The new unified standard for Europe should make it easier to get FRP systems approved for use in Europe, since it only has to be tested once, instead of being tested in every country where the product needs to be used.

23.6.4 AEROSPACE APPLICATIONS

For some of the same reasons that composite use has grown in mass transport (ease of manufacture, fuel savings) the use of composites in the aerospace industry continues to grow. The requirements for these applications are in the Federal Aviation Administration codes. Most of the fire code requirements for FRP materials are for interior applications. These requirements can be found in FAR Section 25.855. One area that has used FRP for many years is the cargo area. All cargo areas must contain a liner that is not part of the aircraft wall. The most common material of construction for the cargo liners is halogenated unsaturated polyester resins. These can be formulated to meet the requirements of this application. The requirement for this application is the 60 s Bunsen Burner test. There is no smoke or smoke toxicity requirement for the cargo liners. The requirement for lining the inside of the passenger compartment is much more stringent if the plane is designed to carry more than 20 passengers. The passenger cabin requires that HRR, smoke, and smoke toxicity all be measured. Halogenated resins cannot be used in these applications owing to high heat release and nuisance gases such as HCl and HBr being generated during burning. For FRP materials to pass these stricter requirements in interior applications, more inherently fire retardant resin systems

such as phenolic resins have to be used. For interior applications, The Ohio State University (OSU) rate of heat release test and the ASTM E662 smoke density test are used for qualifying materials for these interior applications. The OSU test is similar to the cone calorimeter but has significant differences that must be considered when comparing the two techniques.²⁶ The Federal Aviation Administration has funded work on trying to develop more inherently fire retardant resins for use in aircraft interiors and has made great progress in this area, with several recent crashes allowing the passengers ample time to escape from the aircraft before the fuel and fire penetrated the fuselage. The new area of concern for aerospace composites is not for interior, but is for exterior applications. With new large aircraft (Boeing 787, Airbus A380) having major amounts of the aircraft composed of carbon-fiber-reinforced composite (wings, fuselage), external tests such as the FAA oil-fueled burner test for measuring time to fuselage burn-through become important tests to consider. Flammability of aerospace composites for exterior applications is just now being studied, and no new standards other than the existing FAA ones have been set.

23.6.5 MARINE APPLICATIONS

Most of the applications of FRP in the marine industry do not require fire retardant resins. This is primarily for the pleasure boat industry with the exception of the fuel tanks. The fire code for fuel tanks is governed by the U.S. coast guard in the United States. The requirements are given in 33CFR183 Subpart J. The fire performance requirement is only part of what needs to be considered for this application. The most important part is to use a resin that can hold up to the fuel in the tank. This has become even more of an issue in recent years when 10% ethanol was added into gasoline. This made the gasoline a much more aggressive solvent. Many resins that had been used for 15 years could no longer be used, because the ethanol containing gasoline was causing the resin on the inside of the tank to swell and break apart. Resins has been developed that can be used in this application and is still a good application for FRP.

For larger vessels, the IMO has codes that are used for any ocean going vessels or vessels traveling in international waters. The requirement for wall ceiling and bulkhead linings is very difficult to pass. This requires a resin with a very low flame spread, low smoke, and smoke toxicity. The applications are mostly for lavatories and passenger compartment walls.

The U.S. Navy has sponsored research at Virginia Tech to look at structural performance of FRP for the previously mentioned deck applications. This included work on determining the postfire structural properties. This work was reported in detail in the doctorate dissertation of Steven Boyd in 1996.²⁷ Gibson et al.²⁸ did work on modeling the residual mechanical properties of composites after fire. There have been recent studies on the mechanical properties of composites after fire,²⁹⁻³¹ some of which have been cited previously in this chapter.^{13,14} The requirements for the Navy applications have been described by Sorathia.^{19,20,32}

When structural properties need to be maintained in maritime applications, a high char yield material will normally do better in fire resistance tests like ASTM E119. The other way to meet the longer fire resistance times is by using a core material that can help insulate the back side of the composite. The core materials that have been used successfully are balsa wood and polyisocyanurate foam. There are nonmaritime commercial applications, which also use this approach. One example is the Fire Safe House that is designed to protect miners in case of a fire or collapse inside of a mine. This incorporates a composite made from a fire retardant vinyl ester resin with a core that allows this composite wall to obtain greater than a 1 h fire rating on the ASTM E119 fire resistance test.

Another example of a structural FRP maritime application is grating for offshore oil platforms. The U.S. Coast Guard and IMO have set up a test for qualifying composite grating for this application. The test requires the grating to be exposed to the hydrocarbon fire temperature profile in the ASTM E119 test apparatus. A weight is placed on the grating and it cannot deflect more than a steel

grating under the conditions. The system currently used is a composite grating that is pultruded from a phenolic resin. Phenolic resins are char forming and this is the reason for its good performance in this application.

23.7 CONCLUSIONS

The use of FRP is growing in many areas where fire resistance is required. The proper choice of resin and reinforcement is very important and must be carefully considered by looking at the final part performance requirement and the fire codes/standards that govern this application. Most of the fire performance comes from the resin part of the composite. Higher fiber volume content will reduce the total amount of organic material in the system and will typically give a little better fire performance in the part, but this may not always be practical depending upon other product requirements such as part weight and density. There continues to be difficulty in correlating regulatory tests between nations, but more importantly, in testing methods for developing new resins as the final regulatory tests can be quite large in scale. As discussed in Chapter 16 of this book, work is still being done to try and use small-scale tests to predict the performance of large-scale tests. This will be very helpful in the future development work to enable screening systems for various applications.

Many of the applications that use composites only require a surface burning test or a reaction to fire test. Even though some of these tests can be passed with a fire protection coating on the surface (intumescent or other type of fire barrier), it is recommended that the whole composite be made with a fire retardant resin system. This is to ensure that if the surface coating is damaged the part still has protection against fire. This is important as any gaps in the coating will allow the flame to quickly overwhelm nonflame retarded resin, which in turn leads to increased flame spread and in some cases composite structural failure. Structural applications normally require a fire resistance test as well. To obtain good performance against this type of test, the use of a charring resin or a sandwich composite with a core material that will char and insulate the back side of the composite is preferred.

To conclude, there are many applications where fire retardant FRP can be used and demand for FRP materials is likely to continue to increase due to the superior properties that FRP materials can have. Again, many factors need to be evaluated when determining whether FRP can be used and what resin and reinforcement system needs to be used to meet the requirements. When a flame retardant FRP is designed, the following factors must be considered:

- What reaction to fire test will be used?
- What performance is required?
- What are the required structural properties?
- What process will be used to fabricate the parts?

With this information the correct resin and reinforcing fibers can be chosen to obtain a successful FRP material.

REFERENCES

1. Goodman, S. H., *Handbook of Thermoset Plastics*, Noyes Publication, Westwood, NJ, 1998.
2. Feih, S., Mathys, Z., Mathys, G., Gibson, A. G., Robinson, M., and Mouritz, A. P. Influence of water content on failure of phenolic composites in fire, *Polym. Degrad. Stabil.* 2008, 93, 376–382.
3. Ramirez, M. L., Walters, R., Lyon, R. E., and Savitski, E. P. Thermal decomposition of cyanate ester resins, *Polym. Degrad. Stabil.* 2002, 78, 73–82.
4. Lyon, R. E., Walters, R. N., and Gandhi, S. Combustibility of cyanate ester resins, *Fire Mater.* 2006, 30, 89–106.

5. Sumner, M. J., Sankarapandian, M., McGrath, J. E., Riffle, J. S., and Sorathia, U. Flame retardant novolac-bisphthalonitrile structural thermosets, *Polymer* 2002, 43, 5069.
6. Laskoski, M., Domingues, D. D., and Keller, T. M. Processable phthalonitrile resins with high-thermal and oxidative stability, *Fire and Polymers IV: Materials and Concepts for Hazard Prevention ACS Symposium Series #922*, Ed. Wilkie, C. A. and Nelson, G. L., American Chemical Society, Washington, DC, 2005, pp. 378–390.
7. Dominguez, D. D. and Keller, T. M. Phthalonitrile-epoxy blends: Cure behavior and copolymer properties, *J. Appl. Polym. Sci.* 2008, 110, 2504–2515.
8. Williams, M. K., Holland, D. B., Melendez, O., Weiser, E. S., Brenner, J. R., and Nelson, G. L. Aromatic polyimide foams: Factors that lead to high fire performance, *Polym. Degrad. Stabil.* 2005, 88, 20–27.
9. Walters, R. N. and Lyon, R. E. Molar group contributions to polymer flammability, *J. Appl. Polym. Sci.* 2002, 87, 548–563.
10. Kandola, B. K., Horrocks, A. R., and Rashid, M. R. Effect of reinforcing element on burning behaviour of fibre—Reinforced epoxy composites, *Proceedings of 17th Annual BCC Conference on Flame Retardancy*, Stamford, CT, May 22–24, 2006.
11. Manfredi, L. B., Rodriguez, E. S., Wladyka-Przybylak, M., and Vazquez, A. Thermal degradation and fire resistance of unsaturated polyester, modified acrylic resins and their composites with natural fibres, *Polym. Degrad. Stabil.* 2006, 91, 255–261.
12. Elmughrabi, A. E., Robinson, M., and Gibson, A. G. Effect of stress on the fire reaction properties of polymer composite laminates, *Polym. Degrad. Stabil.* 2008, 93, 1877–1883.
13. Ulven, C. A. and Vaidya, U. K. Post-fire low velocity impact response of marine grade sandwich composites, *Composites: Part A* 2006, 37, 997–1004.
14. Ulven, C. A. and Vaidya, U. K. Impact response of fire damaged polymer-based composite materials, *Composites: Part B* 2008, 39, 92–107.
15. Stevens, M., How does laminate construction affect fire performance of FRP composites, *Proceedings of Composites and Polycon*, Tampa, FL, October, 2007.
16. Dempsey, N., *Proceedings of Composites and Polycon*, Tampa, FL, October, 2007.
17. Stevens, M., NFPA 286 room corner burn test an alternative test for interior finish materials of construction, *Proceedings of Fire and Materials Conference*, San Francisco, CA, 2003.
18. Dempsey, N., Avila, K., Mihyun, K., Lautenberger, C., and Dore, C. Fire characteristics of polyester FRP composites with different glass contents, *Proceedings of Composites and Polycon 2007 Conference*, Tampa, FL, October, 2007.
19. Sorathia, U., Long, G., Gracik, T., Blum, M., and Ness, J. Screening tests for fire safety of composites for marine applications, *Fire Mater.* 2001, 25, 215–222.
20. Sorathia, U. and Perez, I. Navy R&D programs for improving the fire safety of composite materials, *Fire and Polymers IV: Materials and Concepts for Hazard Prevention*, ACS Symposium Series #922, Ed. Wilkie, C. A. and Nelson, G. L. American Chemical Society, Washington, DC, 2005, pp. 185–199.
21. Kandola, B. K., Myler, P., Horrocks, A. R., El-Hadidi, M., and Blair, D. Empirical and numerical approach for optimization of fire and mechanical performance in fire-retardant glass-reinforced epoxy composites, *Fire Safety J.* 2008, 43, 11–23.
22. Kandola, B. K., Akonda, M. H., and Horrocks, A. R. Use of high-performance fibres and intumescent as char promoters in glass-reinforced polyester composites, *Polym. Degrad. Stabil.* 2005, 88, 123–129.
23. Morgan, A. B. Fire performance of polymer + fiberglass reinforced composites with and without polymer nanocomposite technology, *Proceedings of 19th Annual BCC Conference on Flame Retardancy*, Stamford, CT, June 9–11, 2008.
24. Ed. Mouritz, A. P. and Gibson, A. G. *Fire Properties of Polymer Composite Materials*, Springer, AA Dordrecht, the Netherlands, 2006, ISBN 978-1-4020-5355-9.
25. Michael, G. S., Bugnicourt, E., and Coutelen, P. Comparison of fiber reinforced polymers in global fire performance tests, *Proceedings of Fire and Materials*, San Francisco, CA, January, 2009.
26. Filipczak, R., Crowley, S., and Lyon, R. E. Heat release rate measurements of thin samples in the OSU apparatus and the cone calorimeter, *Fire Safety J.* 2005, 40, 628–645.
27. Boyd, S., *Compression Creep Rupture of an E-Glass/Vinyl Ester Composite Subjected to Combined Mechanical and Fire Loading Conditions*, Dissertation for Doctor of Philosophy in Engineering Mechanics, 2006.
28. Gibson, A. G., Wright, P. N. H., Wu, Y. S., Mouritz, A. P., Mathys, Z., and Gardiner, C. P. Modelling residual mechanical properties of polymer composites after fire. *Plast. Rubber Compos.* 2003, 32(2), 81.
29. Lattimer, B. Y., Ouellette, J., and Sorathia, U. Large-scale fire resistance tests on sandwich composites. In: *Proceedings of the 60th SAMPE*, Long Beach, CA, May, 2004.

30. Gibson, A. G., Wright, P. N. H., Wu, Y. S., Mouritz, A. P., Mathys, Z., and Gardiner C. P. Fire integrity of polymer composites using the two layer model. In: *Proceedings of the 60th SAMPE*, Long Beach, CA, May, 2004.
31. Mouritz, A. P. and Mathys, Z., Post-fire mechanical properties of glass-reinforced polyester composites. *Compos. Sci. Technol.* 2001, *61*, 475.
32. Sorathia, U., Ness, J., and Blum, M. Fire safety of composites in the US Navy. *Composites, Part A: Appl. Sci. Manufact.* 1999, *30*, 707–713.

24 Flame Retardancy Design for Textiles

Baljinder K. Kandola

CONTENTS

24.1	Introduction.....	725
24.2	Measurement of Fabric Flammability and Testing Standards.....	726
24.2.1	Simple Ignition Tests.....	727
24.2.2	Flame Spread.....	727
24.2.3	Heat Release Tests.....	728
24.2.4	Mannequin Tests.....	730
24.2.5	Full Product Tests.....	730
24.3	Flammability of Different Fiber and Textile Types.....	731
24.4	Application-Based Hazards and Performance Requirements.....	732
24.4.1	Apparel Fabrics.....	733
24.4.2	Protective Clothing.....	734
24.4.3	Curtains and Drapes.....	735
24.4.4	Upholstery and Bedding Fabrics.....	735
24.4.5	Floor Coverings.....	735
24.4.6	Tents and Marquees.....	736
24.4.7	Transportation.....	736
24.4.8	Fiber-Reinforced Polymeric Composites.....	737
24.5	Fire-Retardant Strategies (or Approaches).....	738
24.5.1	Surface Treatments.....	739
24.5.1.1	Flame-Retardant Finishes.....	739
24.5.1.2	Coatings.....	742
24.5.1.3	Plasma Coating.....	743
24.5.2	Fire-Retardant Additives/Copolymers in Synthetic Fibers.....	744
24.5.3	Nanocomposite-Based Flame Retardants in Textiles.....	745
24.5.4	Heat Resistant and Inherently Fire-Retardant Fibers.....	754
24.5.5	Fiber Blending.....	756
24.5.6	Composite Assemblies: Design Issues.....	757
24.6	Future Trends.....	757
	References.....	757

24.1 INTRODUCTION

The term textile, more commonly used for fibers, yarns, and fabrics for apparel clothing and furnishing, has expanded in meaning and applications since last century after the development of synthetic and high performance fiber-forming polymers. Until the 1940s, natural fibers like cotton, wool, silk, have been used as apparel, curtains, and furnishing fabrics; and flax, jute, sisal etc., as technical (e.g., ropes, tents) and geotextiles. The first commercially available synthetic fiber, viscose rayon, a regenerated cellulosic fiber was developed around 1910. In 1939, the first synthetic thermoplastic

fiber forming polymer, nylon 6,6 (polyamide) was synthesized, followed by polyester in 1950s and polyolefins in 1960s. These developments revolutionized the textile world with new fibers offering several advantages over natural fibers and often at a competitive price. Their general popularity derives from improved durability, easy-care properties, and attack by biological agents such as insects and mildew. The application areas expanded from the traditional textiles areas like apparel, upholstery, furnishing, towels, curtains, carpets, etc., to technical (ropes, parachute fabrics), transport (reinforcement of tires, seat belts, brakes, interior furnishing fabrics), industrial products (packaging, filters in chemical plants), buildings (roof liners), geotextiles, and medical textiles. However, thermoplasticity of these fibers limits their applications in certain areas where high temperatures are achieved, e.g., protective clothing for firefighters and workers for oil and gas industry and molten metal workers. The real breakthrough came in 1970s with the development of aramid fibers and other high performance fibers in 1980s, which could be used as protective and safety clothing. The development of inorganic fibers like glass and carbon expanded their use in fiber-reinforced composites for load-bearing structures in transportation and construction industry.

The hazard posed by burning textiles has also been realized for centuries and salts like alum have been used since those times to reduce their flammability and so confer flame retardancy. With new fiber developments and application areas, fire hazards have also grown over the years. Synthetic fibers being thermoplastic, on ignition melt and drip, moving away from ignition source and hence, do not burn further and in some cases pass certain flammability standards. However, synthetic fibers/fabrics are not heat resistant and pose problem of melt dripping, the molten drips being very hot can cause severe burns to the wearer's feet. These can also be burning drips, which although take the flame away from the burning material, can fall on other combustible materials and hence, become the source of ignition. The development of inherently fire-retardant aramid fibers has been a real breakthrough in the area of fire retardancy, establishing them as protective and safety clothing materials.

In different applications while some materials must be fireproof, others can be fire resistant. The terms "resist," "retard," and "proof" have different meanings. While the words "resist" and "retard" imply a late ignition or low flame spread, "proof" is an absolute term not to be affected from the fire.¹ This chapter reviews the flammability of different fiber/fabric types used for different applications and fire-retardant strategies involved to make them fire retardant. This chapter is not exhaustive but is complementary to other chapters written in the past.²⁻⁶

24.2 MEASUREMENT OF FABRIC FLAMMABILITY AND TESTING STANDARDS

Textile materials have high fiber surface to mass ratio and hence, tend to ignite easily. As for most applications the textiles are exposed to environment and hence, due to ease of accessibility of oxygen, burn faster than other bulk polymers. In general, flammable fabrics are those fabrics, which ignite when subjected to a small flame for durations of up to 12 s and continue to burn after the source has been removed. Most of the work on flammable fabrics is therefore concerned and directed toward the observation and measurement of ease of ignition, the rate and extent of flame spread, the duration of flaming, measurement of heat release and heat of combustion, and quantitative description of burning debris, such as melt dripping. Rarely if ever does a single test method enable all these parameters to be measured. For self-extinguishing fabrics, such as flame-retarded fabrics, test methods include measurement of time of afterflame and afterglow and extent of fire damage in terms of char length, hole size, or weakened sample length.

No single laboratory test can determine the complete burning character of a particular textile.⁷ There are two types of tests, scientific or research test methods and the standard test methods. The research test methods help in understanding the burning behavior and are used to develop new products or fire-retardant finishes.

Amongst the research methods, most popular is the limiting oxygen index (LOI), also called oxygen index (OI) and defined as the minimum concentration of oxygen, expressed as volume

percent, in a mixture of oxygen and nitrogen that will just support flaming combustion of a material.⁸ Generally, textiles having LOI values of 21 vol% or less burn rapidly, those having values in the range 21–25 vol% burn slowly, and those with LOI \geq 26 vol% exhibit some level of flame retardancy⁷ and usually pass most small flame ignition tests in the horizontal and vertical orientations.³ LOI tests are mainly used in determining the flammability of different fibers and effect of different flame-retardant treatments and finishes. However, LOI value may be influenced by many fabric structural variables for the same fiber type,⁷ hence is a relative rather than absolute value. Moreover, because the sample ignition occurs at the top and the sample burns vertically downward, this is not true representative of the burning of freely hanging material in the real world.

In the past, different countries had their own textile standard testing methods.^{7,9} Since 1990 within EU, there has been an attempt to normalize these standards. In the United Kingdom, for example, most new British Standards are prefixed by BS EN or BS EN ISO. Most of the test methods are based on the principle that test should be straightforward and easy to apply, and are application specific. The standard test methods usually involve “pass-fail” or performance rating criteria¹⁰ and are mostly product application specific. Some selective and more relevant test methods are discussed here in brief, and for detailed information the reader is referred to a recent review by Nazare and Horrocks.¹¹

24.2.1 SIMPLE IGNITION TESTS

A simple ignition test includes a vertically oriented fabric subjected to a standard gas flame applied to the face or lower edge of the fabric specimen. Ignition is monitored by visual observations and the time taken to ignite the specimen is recorded. This test is used in many standards including BS 5438, EN ISO 6941, FAR (Federal Aviation Regulation) Part 25, etc. Many flammability standards like BS 5722 require simple vertical strip test, measured by BS5438 Test 2. This involves subjecting a vertically oriented fabric to a standard igniting flame source either at the edge or on the face of the fabric for specified time (10 s). If after the removal of ignition source, the flame reaches either end of the fabric, it fails the test. If the flame is extinguished, the char length, size of hole if present, afterglow, and nature of any debris (molten drip, etc.) are noted.

24.2.2 FLAME SPREAD

Rate of flame spread is usually calculated by measuring the distance and recording the time taken of the advancing flame front to reach defined distances. The upward fire spread is far more rapid than downward and horizontal flame spread and hence, adopted as a better means of measuring the fire hazard of a fabric. Therefore, most standards including BS 5438:1989,¹² standards for curtains and drapes, BS EN ISO 15025:2002 use this type of bench-scale test method for measuring vertical flame spread properties of fabrics in particular. In BS 5438 Test 3, for example a sample size of 560 mm \times 170 mm is used across which cotton trip threads connected to timers are placed and the time taken to cut through each thread is used to measure the burning rate. For research purposes, sometimes samples of limited sizes are available, for which the test can be modified for indicative burning rate results. For example, in our laboratory we developed a number of synthetic fibers containing polymer-layered silicate nanoclays and reactive flame-retardants (FRs) (discussed in detail in a later section). Owing to limited sample sizes, sample holder, 190 \times 70 mm, used in Test 1 of BS 5438 standard was used. Samples were marked at 60, 120, and 180 mm intervals. The first 10 mm of sample burning was not taken into account and so times of burning were recorded once the flame had reached a line drawn 10 mm from the bottom edge, against which the standard flame was applied for 10 s as specified in the test. A video film was taken of the burning of each sample from which times to reach 60, 120, and 180 mm marks or to achieve flameout were noted and from this, burning behavior of each sample was observed and rate of flame spread calculated.¹³

Measurement of flame spread under external heat flux is necessary where the thermal radiation is likely to impinge on the textile materials, for example, the flooring material of the building or transport vehicles whose upper surfaces are heated by flames or hot gases, or both. The French test method, NF P 92-503 Brûleur Electrique or "M" test involves radiant panel for testing flame spread of flexible textile materials. This test method (flame spread under external heat flux) is the basis of that used by the FAA (Federal Aviation Administration) for assessing flammability of textile composites used in thermal/acoustic insulation materials (FAR 25.856 (a)) used in aircraft and has also been included by the EU for fire test approval of floorings such as prEN ISO 9239 and BS ISO 4589-1.

For textile materials used as interior wall-coverings in U.K. buildings including railway carriages, where the fabric could be in a vertical orientation attached to the wall panel, measurement of rate of flame spread under external heat flux is one of the requirements. For such applications, the test method (BS 476 Part 7) essentially requires a vertically oriented specimen exposed to gas-fired radiant panel with incident heat flux of 32.5 kW/m^2 for 10 min. In addition, a pilot flame is applied at the bottom corner of the specimen for 1 min 30 s and rate of flame spread is measured. The same principle is used in the French test for carpets, NF P 92-506.

24.2.3 HEAT RELEASE TESTS

When textiles comprise part of a building or transport structure, heat release rate (HRR) measurement becomes an important criterion. One of the original, successful small-scale calorimeter was developed at Ohio State University (OSU), defined in the aviation standard FAR 25.853 Part IV Appendix F and ASTM E906-1983 for determining the heat release of internal structural materials in commercial aircraft originally in the United States and now worldwide. In this calorimeter, a vertically oriented composite is exposed to a heat flux of 35 kW/m^2 . A maximum peak HRR (PHRR) of $\leq 65 \text{ kW/m}^2$ and average HRR over the first 2 min of the test not exceeding 65 kW/m^2 are required for a textile composite to achieve a pass. In most cases, the interiors are made of glass fiber-reinforced phenolic composites, which are inherently FR. The textile material (wool, silk, or wool/silk blend) if used, is usually glued on an aramid board. The textile materials used although are inherently FR, need flame-retardant back-coating to pass the composite test discussed earlier.¹⁴ The OSU calorimeter is difficult to access outside of accredited testing laboratories and consequently expensive to use. The greater availability and more scientific data output from the cone calorimeter has led a number of researchers including ourselves¹⁴ to compare heat release from cone and OSU calorimeters, so that cone calorimeter can be used to assess the flammability parameters of materials for aerospace. It was concluded that the cone and OSU calorimeters, used according to ISO 5660 and FAR 25.853 Part IV, respectively, do not give similar results at a particular heat flux. The main reasons for this are the different ignition sources and methods for measuring HRR in these two instruments. For samples that are difficult to ignite, it was observed that results at 35 kW/m^2 in the OSU correlate with those from cone calorimeter at 50 kW/m^2 for PHRR values. However, the PHRR was delayed in the latter because of the spark ignition source used. Owing to delayed ignition in the cone, THR for 2 min values were also different than in OSU calorimeter; however, all the values after 5 min exposure were similar.¹⁴

More sophisticated bench-scale equipment, which measures HRR by oxygen consumption is the cone calorimeter. In this test, the fabric or composite specimen mounted over an insulating ceramic blanket is exposed to an external heat flux ($0\text{--}75 \text{ kW/m}^2$). The volatiles released from the heated specimen are ignited using spark igniter and the time taken to ignite the gases is recorded as time-to-ignition (TTI) of the specimen tested. Originally designed to study the fire characteristics of building materials that are physically and hence thermally thick, the cone calorimeter can now be used for thermally thin materials such as fabrics¹⁵ although not as a standard test, as yet. It has also been used for characterizing furnishing fires, which incorporates the samples in a composite fabric/filling form (for example, an upholstery fabric on top of a polyurethane (PU) foam).¹⁶

Work in our laboratory^{10,15} has shown that when single layer of fabrics are tested with a cone calorimeter, fabrics curl, melt, and some char, thus changing the specimen configuration under the incident heat flux. Intumescent fiber-containing samples such as silk and wool, in particular, formed a large dome-like char over the entire surface when heated prior to ignition. This dome structure sometimes reached a maximum height of 25 mm at the centre, which resulted in a variation of distance between the sample surface and the cone heater. The specimen even sometimes touched the pilot ignition system, resulting in ignition by impingement, or fouling of the igniter. In case of acrylic and polyester:cotton, specimens shrank away rapidly from the radiant source, posing the problem of change in specimen configuration factor due to reduction in thickness and reduction in flux intensity imposed upon the surface. To stabilize fabrics and improve reproducibility, a cross wire grid as shown in Figure 24.1a was used across the surface of the fabric specimens. The design of grid has also an effect on time to ignition values and the PHRR values.¹⁷ With the grid shown in Figure 24.1a we tested light-weight cotton (87 g/m²), heavy-weight cotton (180 g/m²), polyester:cotton (65:35,105 g/m²), acrylic (118 g/m²), light-weight silk (71 g/m²), heavy-weight silk (174 g/m²), and wool (173 g/m²) under 35 kW/m² external heat flux. In general and apart from silk and wool, single layer specimen results showed acceptable reproducibility in that CV ≤ 13%.¹⁵ We also studied the effect of fabric layering (1–10 layers) on cone parameters. With increasing number of fabric layers, TTI values increased as expected. The effect on peak heat release values plotted in Figure 24.1b

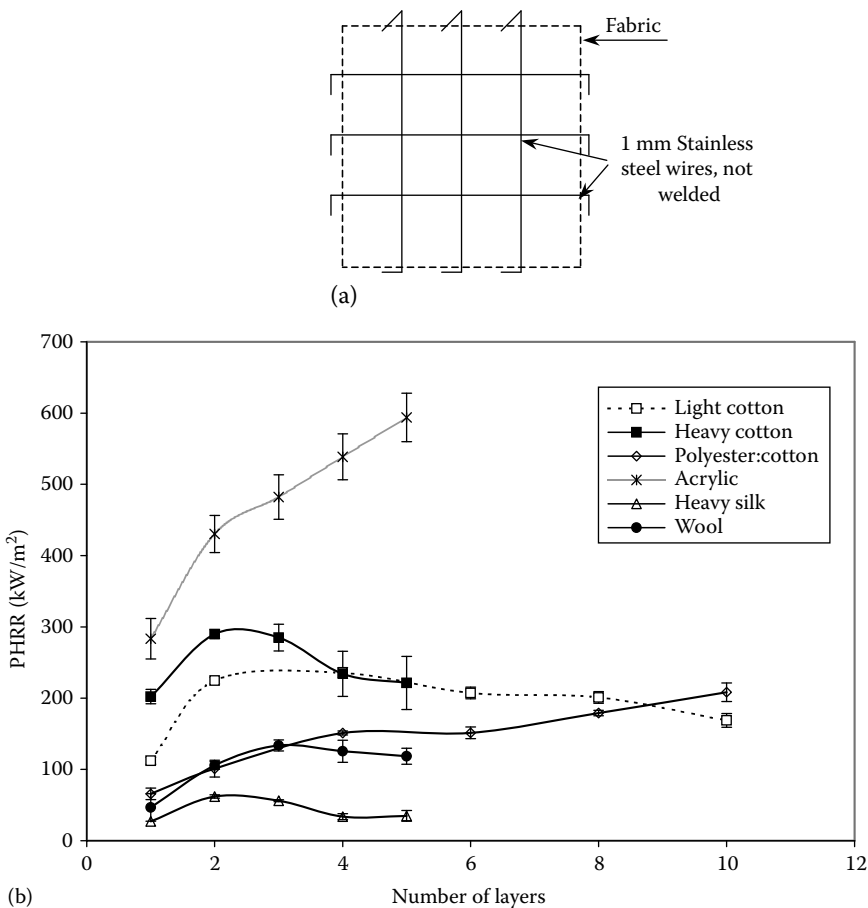


FIGURE 24.1 (a) Textile sample-retaining grid for the cone calorimeter and (b) effect of layers on PHRR values of all fabric samples. (From Nazaré S. et al., *Fire Mater.*, 26, 191, 2002. With permission.)

shows that the increase in PHRR is significant when the number of layers increase from a single layer to 2–3 layers, stabilized or even decreases with a further increase in number of layers. The probable reason for this effect may be because the specimen becomes physically and thermally thick and that the diffusion of volatiles from beneath the surface is impeded by char formation in adjacent layers, which then reduces burning rates and respective PHRR values. This approach to thermally thick behavior is seen only for the char-forming fabrics such as cotton, silk, and wool (see Figure 24.1b). However, the total heat released (THR), which reflects the total specimen mass and fuel content, was higher for the multilayer specimen than the single-layer specimens.

24.2.4 MANNEQUIN TESTS

The major means of determining the fabric burn hazard of textiles and more particularly, clothing assemblies, has been in the use of sensor-equipped mannequins. A typical mannequin is equipped with 100–122 individual heat-flux sensors distributed over the surface of the body. The test garment is placed on the mannequin at ambient temperature conditions and exposed to intense fire or flash fire simulation sources with controlled heat flux, duration, and flame distribution. The sensors measure incident heat flux upon the underlying mannequin surface during and after exposure. The changing temperature of the mannequin surface temperature simulates damage to human tissue at two skin thicknesses, one representing a second degree burn injury point and the other a third degree burn injury point is calculated. The computerized data acquisition system also calculates surface heat fluxes, skin temperature distribution histories, and predicts the skin burn damage for each sensor location. These tests offer a more analytical means of assessing apparel-burning hazards and predict potential skin burn hazards of garments. They are useful in research but are very expensive and complex to be used in standard test procedures¹⁸, although a new draft standard ISO/DIN 13506.3 is currently being assessed. A major problem with this test is poor reproducibility because of fitting of the clothing assembly over the mannequin torso, even when garment sizes are identical. This is particularly the case in firefighter's clothing, where the overlap between topcoat and trousers may present a thermal weakness during flame exposure. Overall mannequins are considered to be important in simulating the burn injury severity in real life accidents. More details about mannequin tests can be found in a review by Camenzind et al.¹⁹

24.2.5 FULL PRODUCT TESTS

Products mostly comprise different materials. For example, upholstered furniture consists of textile material covering PU foam on the supporting metal or wooden frame. Flammability tests for upholstered furniture using various ignition sources were first developed in 1979 as a British Standard BS 5852: Parts 1 and 2 in the United Kingdom. Source 0 is a smoldering cigarette and Source 1 a small butane flame, which simulates a lighted match. Sources 2 and 3 are more intense flame sources. The test specimen is a composite specimen consisting of fabric and filling material. A similar composite specimen assembly is used in the U.S. standard Cal TB 116 for testing flame retrace of upholstered furniture. In addition to the smoldering cigarette ignition source, BS 5852:1979 and its subsequent variants define use of a variety of pinewood cribs (Source 4–7), which match the calorific outputs of increasing numbers of full size newspaper sheets. Development of BS 5852 as small-scale composite test was a breakthrough in realistic model testing that cheaply and accurately indicated the ignition behavior of full-scale products of complex nature.²⁰ Good reproducibility, cost-effectiveness, and easy-to-use features of BS 5852 have led to the establishment of the concept, which was further employed for flammability testing of bedding and mattresses.³ For full product as a chair or mattress, furniture calorimeter is used.

Other textile products that require composite flammability testing are protective clothing assemblies for fire fighters' suits, military flight suits, etc. Flammability standards and test methods for textile components in protective clothing have been discussed by Bajaj²¹ and Horrocks.²²

Their reviews suggest that standard bench-scale tests for separate determination of flame resistance, thermal insulation/protection, and heat resistance may be undertaken on a single fabric or a composite form in a manner that reflects a real application or product requirement.

24.3 FLAMMABILITY OF DIFFERENT FIBER AND TEXTILE TYPES

The burning behavior of fibers depends upon their physical and chemical properties. All natural and synthetic fibers are organic polymers and no organic material can withstand intense and prolonged heat without degradation, even in the absence of oxygen. Given sufficient oxygen and energy input, these materials will burn. The burning of polymer/fiber is essentially a three-phase process—heating, thermo-pyrolytic or decomposition, and finally ignition. The behavior of a polymer/fiber during the initial or primary heating phase depends to a considerable extent on the nature of its composition. Thermoplastic fibers, because of their linear molecular chains will generally melt in the temperature range of 100°C–250°C and start to flow. Because of loss of rigidity, they move away from ignition source, hence further pyrolysis and ignition in some cases is prevented. Natural fibers like cellulose, wool, and silk on the other hand remain unchanged during this stage. Their three-dimensional cross-linked molecular structure prevents softening or melting. Their decomposition or pyrolysis occurs between 250°C and 500°C, depending upon the chemical composition of the fiber. Pyrolysis or decomposition involves unzipping of the polymer chains to yield flammable monomers or the random elimination of small chemical fragments. Both types of products can sustain gas-phase flame reactions. The flammable gases formed by pyrolysis mix with atmospheric oxygen, reach the lower flash on limit and are either ignited by external flame, or if temperature is sufficiently high, self-ignite. In some cases, however, recombination of some of these fragments also occur and leads to the formation of aromatic condensed ring system, called char which is stable under the pyrolytic conditions.

The major difference between fibers and bulk polymers is the small thickness of individual fibers, typically being 15–30 μm in diameter, yielding yarns of 50–100 μm diameter and fabrics having thicknesses varying from as low as 100 μm to several millimeters. Owing to very high fiber surface-to-mass ratios the temperature gradient through the thickness of the fiber is very low, hence above-mentioned reactions occur very fast, leading to easy ignition. Melting, pyrolysis, and combustion temperatures and flammability behavior of different fiber types taken from literature are given in Table 24.1.

The burning behavior of fabrics depends upon many factors such as fiber type or fiber blend ratio, fabric area density, fabric structure (woven, knitted, or nonwoven, open structure or closely woven etc.), finishes, and garment design, point of ignition and the intensity of ignition source, orientation of fabric (vertical or horizontal), etc. Owing to their thermally thin character and the open structure of the textiles, it is easy for air to circulate between the burning fibers. In case of thermoplastics some fabrics may cause shrinkage in one or more directions, curl (see Section 24.2.3), and hence, change geometry. With thermoplastics or blends with higher ratio of thermoplastic fibers, melting occurs, giving rise to often flaming molten drips.

As discussed in Section 24.2, from burning hazard point of view the important parameters are TTI, rate of flame spread, and rate of heat release. In our laboratory, we have studied these parameters for selective fabrics, most commonly used as apparels and the results are given in Table 24.2.^{10,15,23} Although the LOI values given in Table 24.1 are different for different fiber types, all fabrics ignited within 1–3 s, when studied by BS 5438 Test 1. Auto ignition temperatures for all fabrics were determined by placing the fabrics in a pre-heated tube furnace at different temperatures. Flame spread results under different orientations show that the fire hazard is maximum when the fabrics are free hanging in the vertical direction. Light cotton as expected has higher rate of flame spread than others. Acrylic has lower flame spread rate than other fabrics, whereas has the highest peak and total HRR amongst all fabrics. These results show that the flame spread rate is inversely proportional to the fabric area density. Similar conclusion that “for a particular fiber type, the heavier the fabric

TABLE 24.1
Thermal and Flammability Properties of Some Commonly Used Fibers

Fiber	Melting Temp. (°C)	Pyrolysis Temp. (°C)	Ignition Temp. (°C)	LOI (%)
Natural fibers				
Cotton	—	350	350	18.4
Wool	—	245	600	25
Silk	—	320	600	23
Synthetic–thermoplastic				
Nylon 6	215	431	450	20–21.5
Nylon 6,6	265	403	530	20–21
Polyester	255	420–477	480	20–21.5
Polypropylene	165	469	550	18/6
Poly vinyl chloride	>180	>180	450	37–39
Synthetic–char formers				
Viscose	—	350	420	18.9
Acrylic	>320	290	>250	18.2
Modacrylic	>240	273	690	29–30
High performance fibers				
Meta-aramid (e.g., Nomex)	375	310	500	28.5–30
Para-aramid (e.g., Kevlar)	560	590	>550	29
Oxidized acrylic	—	>640	—	55
Polybenzylimidazole (PBI)	—	>500	>500	40–42
Polytetrafluorethylene (PTFE)	>327	400	560	95

Sources: Bajaj, P., *Handbook of Technical Textiles*, Woodhead Publishing Ltd., Cambridge, U.K., 2000; Horrocks, A.R., *Textiles for Protection*, Woodhead Publishing Ltd., Cambridge, U.K., 2005.

the better it behaves in a fire” could also be drawn from a recent study by Hirschler and Piansay,²⁴ where they conducted a flammability study of 50 fabrics with different fiber types and different area densities using the NFPA 701 small-scale test.²⁵

24.4 APPLICATION-BASED HAZARDS AND PERFORMANCE REQUIREMENTS

Designing FR textiles for required level of performance for specific end uses requires an understanding of the end-use conditions and specific flammability performance standards. Textiles in different applications are used either as a single component (e.g., apparel, curtains, bedsheets, etc.) or a component of the composite structure (e.g., furniture). In the latter, components other than textile material and their lay-up will also influence the burning behavior of the whole structure. This section discusses different fiber and fabric types used for different applications, associated fire hazards, and most relevant flammability performance standards. In Section 24.2, testing standards were discussed, which are used for testing materials to comply with performance standards discussed briefly in this section and in detail elsewhere.¹¹

TABLE 24.2
Ignition, Flame Spread, and Heat Release Properties of Some Commonly Used
Fabrics as Apparel

Fabric	Ignition Time Using BS 5438, Test 1 (s)		Auto-Ignition		Flame Spread Rate Using Modified BS 5438 Test 3 (m/s)			Cone Results at 35 kW/m ² Heat Flux		
	Face Ign.	Edge Ign.	Ign. Temp. (°C)	Ign. Time (s)	45°			TTI (s)	PHRR (kW/m ²)	THR (MJ/m ²)
	Vertical	Angle	Horizontal							
Light-weight cotton (87 g/m ²)	2	1	480	16	57	37	6	9	94	1.0
Heavy-weight cotton (180 g/m ²)	4	1	480	35	27	18	3	14	128	3.2
Polyester: cotton (65:35, 105 g/m ²)	2	1	574	20	37	24	9	10	154	1.9
Acrylic (118 g/m ²)	a		—	—	23	13	6	17	292	4.5
Light-weight silk (71 g/m ²)	2	2	909	3	c	c	c	c	c	c
Heavy-weight silk (174 g/m ²)	b	3	655	4	c	c	c	28	45	1.0
Wool (173 g/m ²)	3	3	746	3	23	12	14	16	171	2.9

Sources: Gawande (Nazaré), S., Investigation and prediction of factors influencing flammability of nightwear fabrics, PhD thesis, University of Bolton, Bolton, U.K., 2002; Nazaré, S. et al., *Fire Mater.*, 26, 191, 2002; Horrocks, A.R. et al., *Recent Advances of Flame Retardancy of Polymeric Materials*, Vol. XI, Lewin, M. (Ed.), *Proceedings of the 2000 Conference*, Business Communication Company, Stamford, CT.

^a Flames extinguished when the flame was moved away.

^b Fabric melted away from the flame.

^c Test not performed.

24.4.1 APPAREL FABRICS

Apparel fabrics for normal use generally include cotton, viscose, polyester, nylon, wool, silk fibers, and their blends. Adult apparel fabrics are generally not flame retarded because of lack of both consumer demand and stringent mandatory standards. The flammability behavior of some fabrics commonly used for apparels has been discussed in Section 24.3. In normal use apparel fabrics usually do not catch fire, but if they do, the risks of death/injury per incident are high (almost one in four accidents²⁶), this is especially the case with loose clothing, e.g., ladies nightwear²⁷ and saris worn by Indian women. The U.K. Nightwear (Safety) Regulations, 1985 requires the testing of all nightwear, including pajamas, and dressing gowns and demands that adult and children's nightwear carry a permanent label showing whether or not each item meets the requirements of BS 5722:1984²⁸ (which uses Test 3 of BS 5438: 1976, discussed in Section 24.2.2). This latter

performance standard defines a maximum permissible burning rate of a vertically oriented fabric. European standard EN 1103 requires that all types of apparel exhibit a flame propagation rate (FPR) of at most 90 mm/s.²⁹ Both of these tests are good in predicting the potential hazard of fabrics made of natural fibers but do not take into account the thermoplasticity of synthetics, hence cannot relate the hazard to actual skin burns. There is no relationship between FPR and actual skin burns.³⁰ Fabrics made of blends with high percentages (>50%) of synthetic fibers usually pass these tests, but can present an increased burn risk due to the combined flame spread and melting effects of thermoplastics.¹⁰

24.4.2 PROTECTIVE CLOTHING

Protective textiles often have to protect the wearer from more than one condition, hence need multifunctional properties. With regard to fire hazard, in addition to FR properties they should also be thermally resistant. Thermal protection relates to the ability of textile to resist conductive, convective, radiant thermal energy or a combination of two or more. Typical flame temperatures may range from 600°C to 1000°C, hence the textile structure should be able to withstand these temperatures without undergoing melting or degradation and thus losing geometrical coherence. Hence, synthetic thermoplastic fibers cannot be used for applications where very high performance is required. In most applications, multilayered clothing assemblies are used. The most important aspect of protective clothing testing is the evaluation of burn injury protection and thermal characteristics of clothing systems, which can be undertaken using an instrumented mannequin as discussed in Section 2.4. Resistance to heat transfer by convective flame, radiant energy, or plasma energy sources is quantified in terms of thermal protective index (TPI) often related to the time taken for an underlying skin sample with or without an insulating air gap to achieve a minimum temperature or energy condition sufficient to generate a second degree burn. This can be done by measuring the time for a thermocouple placed behind a fabric or assembly to reach a critical temperature equivalent to that causing a radiant energy source. Although this area is very vast and includes many applications, only selected examples are discussed here and for detailed information referred to other reviews.²²

Firefighters' clothing: Common firefighter's protective clothings consist of a flame-resistant outer layer made from Nomex, Kevlar, or Zylon, and two inner layers.³¹ The second layer is a moisture barrier and usually consists of aramid fiber. It increases firefighters' comfort and protection by preventing moisture, liquid, or vapor from reaching the skin when performing a task in a fire. Owing to its insulation value and ability to block the passage of hot gas and steam, it can promote some burn protection. The inner layer is the thermal barrier that blocks the transfer of heat from the firefighting environment to the body of the wearer. The felt or batting is made from Nomex, Kevlar, a mixture of these two fibers, or polybenzimidazole (PBI).³¹ Gloves are made from heavy-duty leather and Nomex liner. Relevant test methods for their performance testing include BS EN 469:1995, US NFPA 2112 standard for protection of personnel against flash fires.

Military personnel battlefield clothing: Fireproof garments currently used in many armed forces are made of single-layer aramid material (e.g., Nomex, DuPont), which is inherently fire retardant. However, owing to the high cost of these and similar materials they are used only for specialized applications such as coveralls for tank crewmen or to protect service personnel involved in military operations with potential for catastrophic fires. The low cost, lower performance FR treatments applied to more conventional fibers as finishes, FR-modified synthetic (polyester and nylon) and regenerated fibers, use of fiber blends, and alteration of fabric construction or garment configuration are often preferred. For U.S. army, outer garments are made from 50% nylon/50% cotton, whereas T-shirts are 100% cotton. Flammability standards for military textiles are not clearly defined and different commercial suppliers to different armies across the globe use different standards and test methods to specify their products. For detailed information, see other reviews written specifically on military clothing.^{32,33}

Police protective garments or systems: Only for first response operations, the armed police forces need protective clothing for protection against chemical, biological, radiological, and nuclear threats, termed as CBRN personal protective equipment. In a hostile situation the clothing may also be expected to protect against flame and the radiant heat caused by fire, ballistic impact as well as resistance to shrapnel and slashing. The clothing is a multilayered assembly,³⁴ FR part of which is normally Proban-treated cotton, Kevlar aramid (DuPont), or Twaron (AKZO). The whole fabric assembly is very heavy. Work is going in our laboratory to reduce the number of layers with fabric structures of multifunctional properties. There are no specific standard for their testing, but other methods for protective clothing, e.g., BS EN 469:1995 are used.

24.4.3 CURTAINS AND DRAPES

Curtains and drapes are vertically oriented fabrics used in interior furnishings and hence can ignite easily. The fibers involved are usually cotton, wool, silk, polyester, and nylon. The flammability testing of fabrics is often carried out by mounting the specimen vertically on the testing rig. The principal U.K. flammability test uses Test Method 3 described in BS 5438:1976 for curtains and drapes, which measures the rate of flame spread of a vertically oriented fabric specimen. For curtains and drapes used for domestic usage, the flame application time is typically 10 s, whereas for contract furnishing, the test is more severe with longer flame application time of 15 s. The test is even more stringent for the more hazardous applications such as hospitals, prison, etc. For these applications, the fabric has to be tested with four flame application times of 5, 15, 20, and 30 s. Other relevant standards are BS 5867: Part 2:1980, BS EN 13772:2003, NFPA 701 (United States) and NBC (National Building Code of Canada)—ULC-S 109.

24.4.4 UPHOLSTERY AND BEDDING FABRICS

In upholstered seating and mattresses and bedding, the textile material is component of a composite structure, and is the exposed part. The statistics show that most domestic fires start by smoking in beds or upholstered furniture.^{35,36} Some of the notorious fires caused by furniture in United Kingdom are Woolworths fire in 1979 (12 fatalities, 15 injuries), and Stardust in 1981 (10 fatalities, 53 injuries).³ For upholstered furniture, fabrics (usually polypropylene, cotton, wool, and blends) are used on a PU foam and the whole assembly is on a wooden or metallic frame. BS 5852 test method tests the whole piece of furniture and uses different ignition sources ranging from cigarette (Source 0) to a butane gas flame (Source 1) and to pinewood cribs of different sizes (Sources 3–7). The sources are selected based on application areas, e.g., for domestic furniture, Source 1 and for military and certain sleeping wards in hospital, Source 7 is used. In California, the Cal TB 133 test method uses oxygen depletion calorimetry for testing flammability of seating used in public occupancies such as public auditoriums, hotels, hospitals, etc. This test method uses a 250 m² tube burner with heat generating capacity of 18 kW. The burner is placed on the seating area for 80 s. This full-scale furniture item is tested in a room and the pass/fail criterion depends on the measurements used i.e., temperature increase at the ceiling thermocouple or PHRR.

Bedding materials have traditionally been combustible materials. In the United States, the California Test Bulletin CAL TB 106 and Cal TB 603 test methods are used for testing ignition resistance of mattresses uses a burning cigarette and large open flames from a gas burner, respectively. In the United Kingdom, the standard BS 6807:1996 is used to assess ignitability of mattresses and uses ignition sources specified in BS 5852.

24.4.5 FLOOR COVERINGS

Cotton, viscose, nylon, polypropylene, acrylic, polyester, or wool are generally used in carpets as the face or pile fabric over Neoprene latex. Carpets are usually flame retarded by back-coating with antimony-halogen system. The primary U.K. tests for carpet are BS 6307:1982³⁷ and BS 4790:1987,³⁸

which uses a methenamine tablet and hot metal nut, respectively, as ignition sources placed in the center of the specimen. The damaged zone is measured and the flaming or afterglow time is also recorded. In the United States ASTM E648³⁹ and NFPA 253⁴⁰ standards for floor covering textile materials are mainly applicable in the construction industry. These standards use the radiant panel test to evaluate the tendency of a flooring system to spread flame when exposed to the radiant heat flux. For transportation applications, carpets are tested according to the requirements of respective transportation departments. For floor coverings in motor vehicles, the BS ISO 3795:1989 and FMVSS 302 (U.S. Office of Vehicle Safety Compliance of the National Highway Traffic Safety Administration) are used, which measure horizontal rate of flame spread. For aerospace applications, the FAR 14CFR25 (Airworthiness Standards: Transport Category Airplanes) uses a radiant panel and a vertical flame test with carpet sample suspended vertically in a chamber. For naval applications the IMO (International Maritime Organization) Fire Test Procedures (FTP) for testing flammability of carpets (46CFR72.05-55) uses the radiant panel test method.¹¹

24.4.6 TENTS AND MARQUEES

Tents, marquees, etc., which use textile materials as single layer of fabrics (mostly cotton, cotton-synthetic blends, etc.), can be ignited easily as happened in Saudi Arabia where 10,000 tents caught fire during Hajj in 2002 and 360 pilgrims died.³ Hence, the fabrics used for such purposes should either be inherently FR or have a durable FR treatment. Testing standards for tented structures involve the British standard BS 7837:1996, where fabric is tested in vertical orientation with bottom edge-ignition, BS 7157:1989 using the range of pinewood cribs of various dimensions as ignition sources and BS EN 14115:2002⁴¹ with exposure of specimen to radiative heat. Other relevant tests are Swedish SIS 65 00 82, American NFPA-701,⁴² ASTM E84⁴³ tunnel test, and Australian standard AS 1530.2.

24.4.7 TRANSPORTATION

Textiles in transportation are used as seat coverings, carpets, wall coverings, battery separators, tires, belts, clutch lining, etc. Especially the seats, and sometimes, other interior materials, foam materials are used beneath the covering fabric for more comfort. Although, flame-retarded foams are used, fireblocker materials are used between the face fabric and the foam.⁴⁴ Fireblockers, made from inherently fire-retardant fibers like oxidized acrylics and aramids, were first used for aircraft seats and now being increasingly used on trains, buses, and coaches. The performance requirements for textiles in transportation are more demanding compared with domestic applications as their use in the former is more rigorous and they have to withstand daylight and UV radiations. From flammability point of view, the performance requirements are application specific, e.g., requirements for aerospace are more stringent than those for motor vehicles.

Motor vehicles: Most of the passenger car interiors including car seats are made of polyester fiber (90% of the world market), and in some cases polypropylene fiber. The flammability testing of fabrics used in motor vehicles, in particular, cars are not mandatory due to the fact that fire incidents in motor vehicles are rare and, moreover, fire spreads relatively slowly. Most manufacturers test seating covers and carpets conform to the U.S. FMVSS (Federal Motor Vehicle Safety Standard) 302 test, which is a simple horizontal flame spread test. Other similar standards are German DIN 75 200, British, Australian BS AU 169, and Japanese JIS D 1201 automotive standards. The curtains and blinds are tested according to tests specific to them discussed earlier.

Rail vehicles: Textile flammability standards are extremely severe, because fires in railways can spread very quickly and can result in significant losses. Furnishing fabrics used in railway seatings, mainly 85% wool/15% nylon or polyester of FR grade (e.g., Trevira CS),⁴⁴ are tested in European countries as a complete assembly with UIC (Union Internationale des Chemins de Fer.) 564.2. In the United States, ASTM E 1537-98 and in the United Kingdom, ceiling lining materials are tested according to BS 476.

Aircraft: Seats in the aeroplane need to conform to highest standards of fire safety hence are usually made from wool (Zirpo treated), wool/nylon blends, or leather. Flammability testing of all textile materials is regulated by the U.S. FAA under FAR and these latter extend to all commercial airliners operating across the world internationally. All textiles present in an aircraft have to pass the test requirements defined in FAR 25.253(b) in which a Bunsen burner flame impinges upon the bottom edge of a vertically oriented sample. For seats, the complete seat assembly is tested. For textiles attached to internal wall and ceiling panels or partitions, they are tested as a composite for heat release using the OSU calorimeters as discussed in Section 24.2.3.

Ships: Cruise ships use a large amount of furnishing fabrics, e.g., bedding, curtains, carpets, etc., hence need to have durable high standards of flame retardancy. Standards required are DIN 4102 class B and BS476.⁴⁴ Flammability standards and test for furnishing fabrics, bedding, and draperies used in ships and submarine have been developed by the IMO and the National Fire Protection Association (NFPA) which include Safety of Life at Sea (SOLAS), High Speed Craft (HSC), and FTP codes. The FTP code describes the flammability tests and performance criteria for combustible materials and Sorathia has recently reviewed this area.⁴⁵ Bedding components including mattresses, pillows, blankets, quilts, and bedspreads used in ships are tested in accordance with IMO Resolution A.688 (17) according to SOLAS and HSC Code, whereas NFPA 301 requires mattresses and mattress pads to comply with NFPA 267, ASTM E1590, and 16 CFR 1632 test methods. When tested according to the IMO Resolution A.688 (17), the bedding should not ignite readily or exhibit progressive smoldering when subjected to smoldering or flaming ignition.

24.4.8 FIBER-REINFORCED POLYMERIC COMPOSITES

High performance fibers like glass, carbon, and aramid are being increasingly used as reinforcing element in polymeric resins to form structural composites. Composites' application is increasing in all transport applications, in particular aerospace, trains, ships, and motor vehicles. The fiber-reinforced composites are generally less flammable than cast neat resins of similar thicknesses due to lower resin contents in the former and also the fibers present act as fillers and thermal insulators.⁴⁶ Thick laminates with more fabric layers burn slowly giving lower heat release than thin laminates with less fabric layers.⁴⁷ Amongst different composite types, there are different factors that can affect the flammability of the laminate and its residual mechanical property, namely, (1) fiber type (glass, carbon, aramid etc.), (2) volume content of fiber, and (3) reinforcement type (weave type, fiber/yarn arrangement, etc.). While glass fibers are noncombustible, exposure to high temperatures can result in softening and finally, melting, which effectively lowers their mechanical properties. On the other hand, other commonly used fibers such as carbon and aramid are nonthermoplastic but because they are organic in nature, will decompose or oxidize at elevated temperatures.

In our recent work, we have studied the effect of different fiber types on the burning behavior of epoxy composites.^{48,49} Thermal decomposition behavior of glass, carbon, and aramid fibers in air is shown in Figure 24.2a where glass shows inert behavior with no major mass loss up to 800°C, whereas, carbon fibers start losing mass at 280°C probably by physical desorption of volatiles and are fully oxidized at 800°C, leaving 5% charred residue. The aramid fiber starts losing mass earlier than carbon fiber. The thermogravimetric (TGA) curves for all fibers/resin combinations in 1:1 mass ratio shown in Figure 24.2b indicate that apart from glass fiber, both resin and fiber decompose or lose mass. This shows that carbon and aramid fibers may add to the fuel content, which in case of carbon is due to solid-state oxidation. However, the TGA technique is not truly representative of actual fire conditions. The burning behavior of the laminates prepared from these fibers was studied by cone calorimetry at 50kW/m² heat flux. Heat release curves in Figure 24.3a show that the aramid-containing laminate has the lowest peak, although the heat release curves are broader than other samples and it burns for longer times. The aramid-containing composite had the highest THR value, which is a consequence of its decomposition and fuel-generating property as shown by the TGA results. However, contrary to the TGA results, the carbon fiber did not show any significant degradation (see Figure 24.3b),

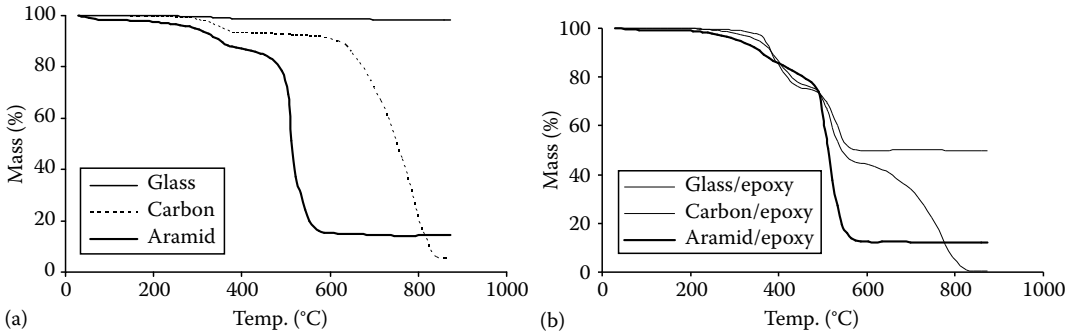


FIGURE 24.2 TGA curves in air of (a) glass, carbon, and aramid fibers and (b) fiber/epoxy mixtures in 1:1 mass ratio. (From Kandola, B.K. et al., Recent advances of flame retardancy of polymeric materials, in *Proceedings of the 17th Conference*, Lewin, M. (Ed.), BCC, Stamford, CT, 2006. With permission.)

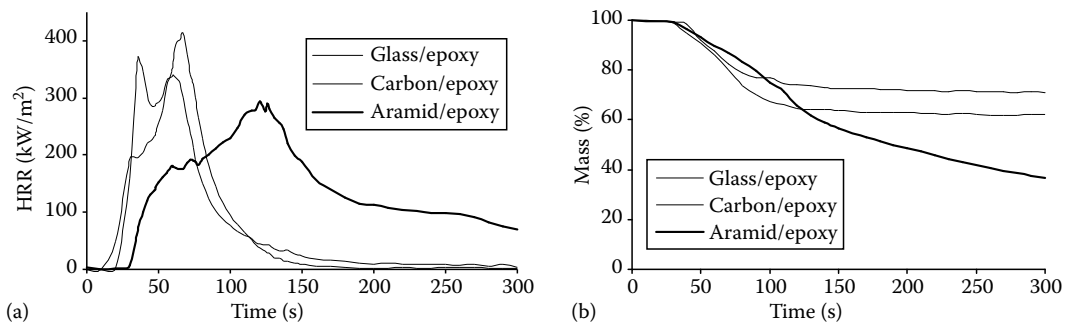


FIGURE 24.3 (a) Heat release rate and (b) mass loss versus time curves for different fiber/epoxy composites at 50 kW/m² heat flux. (From Kandola, B.K. et al., Effect of fibre type on fire and mechanical behaviour of hybrid composite laminates, *Proceedings of the 2006 SAMPE Fall Technical Conference*, Dallas, TX, November 6–9, 2006.)

which is not surprising since carbon does not decompose and the mass loss in TGA is due to solid-state oxidation. For detailed information about this work, the reader is referred to our other publications, where these results are also analyzed in terms of effect of resin content and fabric area density.^{48,49}

Flammability standards for composites are beyond the scope of this chapter, but are discussed elsewhere.⁴⁶

24.5 FIRE-RETARDANT STRATEGIES (OR APPROACHES)

Similar to bulk polymers, textile fibers/fabrics also need certain elements such as phosphorus, nitrogen, halogen, sulfur, boron, metals, etc., to render them FR. The FR elements containing chemicals can be either applied to existing fibers/fabrics on their surface as finishes, introduced as additives in polymer before fiber production (in synthetic fibers), or introduced into the polymer backbone (inherently FR fibers). FRs functioning by physical means only, such as alumina trihydrate, magnesium hydroxide etc., are not usually used for textiles, because for them to be effective as FRs large quantities (>40 wt % of the polymer) are required, which is not possible to be introduced within the fiber or on the surface. The most effective FRs are those that function in condensed phase and promote char formation by converting the organic fiber structure to carbonaceous char and

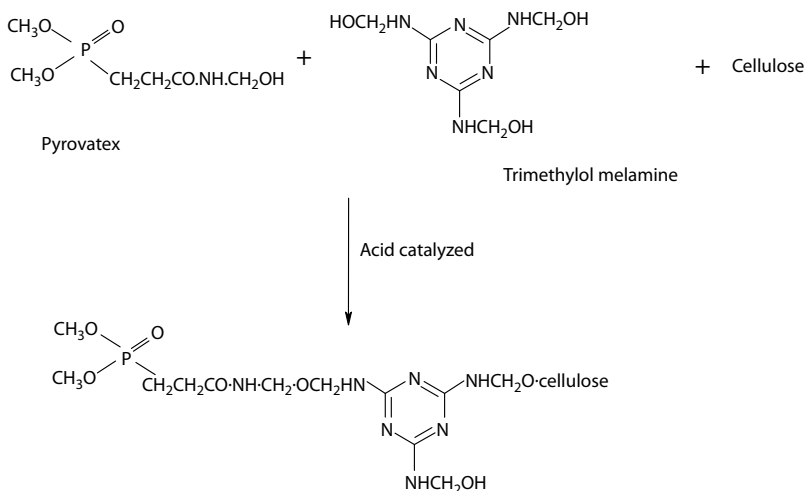
hence reduce volatile fuel formation.⁵⁰ Most often these FRs functioning mainly by chemical means require absorption of heat to operate, and release nonflammable gases like CO₂, NH₃, and H₂O during chemical action, hence also function by physical means by cooling the substrate below the combustion temperature and diluting the flaming zone with nonflammable gases. These condensed phase active FRs are more effective in natural fibers such as cotton and wool with polymer backbone having reactive side-groups, which on removal lead to unsaturated carbon bond formations and eventually a carbonaceous char following elimination of most of the noncarbon atoms present.⁵⁰ Synthetic fibers like polyester, polyamides, and polypropylene on the other hand tend to pyrolyze by chain scission or unzipping reactions and lack reactive groups and are not char-forming polymers and hence, cannot be effectively flame retarded with these chemicals.³ Vapor phase active halogenated FRs, however, will work with any fiber type, since they interfere with the flame chemistry by generating free radicals. The detailed mechanisms of action of these FRs on textiles are similar to the ones in bulk polymers and are beyond the scope of this chapter, for which readers are referred to other chapters in this book and other such reviews.⁵¹ The main issues with flame-retarding textiles, however, are the method of application/introduction of these FRs on/in textiles, their wash durability, and effect on other textile properties such as tensile and tear strength, handle, drape, appearance, etc. This section therefore reviews different fire retardant strategies based on the methods of application. Natural fibers/fabrics are generally treated with FR finishes in the finished fabric form. In synthetics usually additives are added to the molten polymer/polymer dope before fiber extrusion or FR copolymers/homopolymers are used. However, a coating with the help of resin binder can be applied to any fiber/fabric types. This section also reviews inherently fire-retardant fibers, blends, and some other novel approaches to flame retard fibers.

24.5.1 SURFACE TREATMENTS

Surface treatment is the oldest method of flame retarding the textiles, dating back to 1735 when borax, vitreol (a metal sulfate), and some other mineral substances were patented in England for flame retarding canvas and linen.⁵² There are two types of surface treatments, finishes and coatings. Finish is applied by impregnating the fabrics in the aqueous solution of the chemical as a textile finishing process. Coating on the other hand is application of a continuous or discontinuous layer on the surface of the fabric generating heterogeneous fabric/polymer composite.⁵³ These are discussed in detail in this section. In textiles, the main issue with any treatment is the durability to laundering. Some treatments are nondurable to laundering, others may be semidurable and withstand a single water soak or dry cleaning process and durable ones withstand 50 wash cycles. Durability requirements are usually determined by the application and specified by associated regulation.

24.5.1.1 Flame-Retardant Finishes

Most of the treatments and formulations were developed in 1950–1970 period^{3,4,6} and in terms of new chemistry nothing much has changed since then. Several interesting reviews have been published in this area.^{3,4,6,18,26} Finishes are usually applied by pad-dry method where fabric is passed through the chemical formulation (mostly in aqueous form), passed through rollers to squeeze out the excess and then dried in oven at 120°C. This gives a nondurable finish. To get a semidurable or durable finish, fabric is passed through another oven set at higher temperature (usually 160°C) where a curing stage allows a degree of interaction between the finish and the fiber. In some cases, curing stage might also involve chemical treatment; the best example is Proban process (discussed subsequently), which requires ammonia gas curing process to polymerize the applied finish into the internal fiber voids. As discussed earlier, finishes are applied to fabrics from natural fiber types, although there are some available commercially for synthetic fibers as well. Some generic types of finishes are discussed subsequently; for more information and their commercial grades details, the reader is referred to other reviews.^{3,6,26}



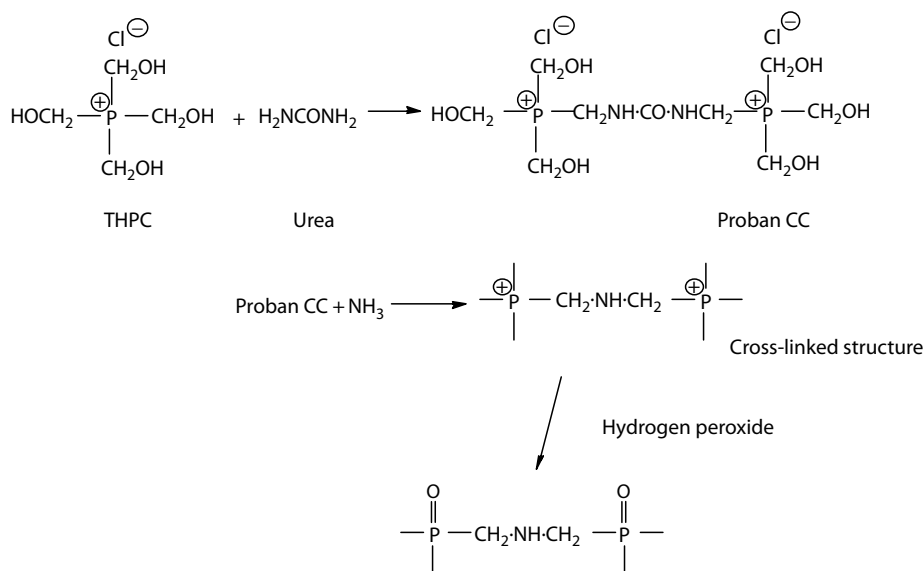
SCHEME 24.1

Cotton: Ammonium phosphates are the most effective FRs for cotton as first identified by Gay-Lussac in 1821 and still widely used. All phosphates on heating release phosphoric acid, which catalyses dehydration reactions of cellulose to yield char at the expense of volatiles formation reactions.⁵⁰ However, ammonium phosphates like mono- or diammonium phosphates are water soluble, hence applicable as nondurable treatments only. Ammonium bromide can be used in combination with ammonium phosphates to provide some vapor-phase FR action. Other examples include borax and boric acid, ammonium sulfamate, and sulfates. These nondurable finishes are useful for disposable fabrics, insulation, wall boards, theatrical scenery, packaging material, paper, etc. Ammonium polyphosphates (APPs) are used in combination with urea to provide semidurable finishes and by curing at 160°C, when some phosphorylation can occur. Semidurable finishes are very useful for materials that may not need frequent washings, e.g., mattresses, drapes, upholstery, carpets, etc. Some commercial examples of semidurable finishes include Flammentin FMB (Thor Specialities), Pyrovatim PBS (Ciba, now marketed by Huntsman), etc.²⁶

Amongst the commercially successful durable finishes, one type is based on *N*-methylol dialkyl phosphonopropionamides, from which well-known product, Pyrovatex CP (Ciba) is derived. Pyrovatex CP (*N*-methylol dimethyl phosphonopropionamide) is applied with a methylolated melamine resin in the presence of phosphoric acid, which catalyses the formation of pyrovatex-resin-cellulose moieties via the C(6) OH group, represented by the reactions in Scheme 24.1. Research at Bolton to lower the formaldehyde release during the finishing process⁵⁴ helped Ciba to introduce a low formaldehyde grade of Pyrovatex CP. Another commercial product based on similar chemistry is Thor's Aflammit KWB.

Other most successful durable treatment is based on tetrakis (hydroxymethyl) phosphonium derivatives. Very well-known brand marketed as Proban CC (Rhodia, previously Albright & Wilson) involves padding of tetrakis (hydroxymethyl) phosphonium chloride (THPC) urea solution onto the cotton fabric, curing with ammonia in a specially designed reactor to generate a highly cross-linked three-dimensional polymer network. The fabric is then treated with hydrogen peroxide, which converts P³⁺ to the P⁵⁺ state. The reactions are shown in Scheme 24.2. Other similar commercial product is Thor's Aflammit P. In literature many combinations of tetrakis (hydroxymethyl) phosphonium derivatives with other salts have been reported,⁵⁰ but the most successful so far has been the THPC-urea-NH₃ system discussed earlier.

Pyrovatex CP type treatments have more dye affinity, and hence, are used for curtains, apparels (nightwears), etc., whereas Proban CC, which retains greater strength, is used for hospital bed sheets, military applications, hotels, nursing homes, etc.⁴ Some other durable treatments for cotton



SCHEME 24.2

include Akzo Nobel's Fyrol 51, now called Fyroltex HP, Firestop's Noflan (a phosphorus-chlorine based product), discussed in detail by Weil and Levchik in their review.²⁶

Viscose: In principle all the treatments effective on cotton should be effective on viscose as well. However, the delicate viscose fibers cannot withstand the harsh finishing processes, and are rarely treated with a finish. However, Lyocell (Coutaulds) can be treated with Pyrovatex CP (Ciba) to produce FR Lyocell.⁵⁵ The work at Bolton has shown that this fiber being more reactive than cotton needed only half the normal amount of this FR treatment applied to cotton cellulose to produce an equivalent degree of flame resistance.

Polyester: Tris(2,3-dibromopropyl) phosphate was the successful finish developed in the 1970s for polyester fabrics, but was withdrawn from the market after a short time owing to carcinogenicity. Since then, the major product used in the thermosol dyeing treatment of polyester fabric has been Rhodia's Antiblaze 19 or Amgard CU, or Special Materials' SMC 688.²⁶ Some other commercial products include Thor's Afflamit PE, Zschimmer & Scharz Mohsdorf's (Germany) Flammex DS, and Chemtura's CD-75PM[®] (hexabromocyclododecane, HBCD).²⁶

Cotton-polyester blends: For blends sometimes finishes, which are successful on one type of fiber, may prove to have antagonistic effect on blends.³ The general rule is to apply finish suitable to the majority fiber present or apply halogen-based coating (see Section 24.5.1.2). Most nondurable finishes for cotton will function on cotton-rich blends with polyester, but not for the polyester rich blend unless some bromine is present.³ Durable treatments such as Proban and Pyrovatex type finishes can be applied on higher cotton content fabrics, e.g., 80:20 cotton/polyester.

Wool: Wool, though not as flammable as cotton, still needs flame retardation for specific applications, e.g., carpets, upholstered furniture in transport, etc. Ammonium phosphates and polyphosphate, boric acid-borax, and ammonium bromide can be successfully used in nondurable FR finishes for wool. Various commercial products have been reviewed by Horrocks.³ The most successful durable treatment for wool is Zirpro, developed by Benisek, which involves exhaustion of negatively charged complexes of zirconium or titanium onto positively charged wool fibers under acidic conditions at 60°C. The treatment can be applied to wool at any processing stage from loose fiber to fabric using exhaustion techniques.

Silk: Silk although is not very flammable (LOI 23%), needs FR treatment for certain applications, e.g., nightwear garments, curtains, interior decoration of executive jet aeroplanes, etc. Nondurable finishes containing mixture of borax and boric acid,⁵⁶ inorganic salts and quaternary ammonium salts, urea-phosphoric acid salt⁵⁷ have been reported to be effective on silk. Semidurable finishes like organophosphorus FR and trimethylolmelamine (TMM),⁵⁶ Pyrovatex CP (Ciba)⁵⁸ are also reported to be effective on silk.

24.5.1.2 Coatings

As mentioned earlier, FR coatings can be applied on the surface of the fabric (including on the back) to confer flame retardancy to the overall fabric. Typical textile coating polymers include natural and synthetic rubbers (polyisobutylene, styrene butadiene, poly(butadiene-acrylonitrile), poly(chloroprene), etc.), poly(vinyl chloride) or PVC plastisols and emulsions, poly(vinyl alcohols), formaldehyde-based resins, acrylic copolymers, PUs, silicones, and fluorocarbons, used for different applications such as water resistance, flexibility, moisture permeability, and flame retardancy. Some coatings have varying levels of inherent flame retardancy (e.g., PVC and other chlorine- and fluorine-containing polymers), although the more commonly used polymers and copolymers are quite flammable and so presence of FR additives is necessary to flame retard both the coating matrix polymer and the underlying textile substrate. FRs used for coatings include different phosphates and phosphonates, e.g., triaryl phosphate, cresyl diphenyl phosphate, oligomeric phosphate-phosphonate, etc. The commercial products of these chemicals are discussed by Horrocks in a recent review.⁵³

Back-coating: Back-coating of textiles is a well-established application method where the FR formulation containing brominated organic species and antimony trioxide is applied in a bonding resin to the reverse surface of the fabric. Application methods include doctor blade or the knife-coating methods and the formulation is as a paste or foam. Most typical brominated derivatives are decabromodiphenyl oxide (DBDPO) and hexabromocyclododecane (HBCD). Such back-coatings are effective on a wide range of fabrics, including nylon, polypropylene, polyester-nylon blends, acrylics, and many blends. Important applications are in domestic, industrial, and automotive upholstered furniture, and draperies for hotels and other public buildings. However, there are environmental issues about the use antimony and bromine-containing chemicals and risk analysis based debate continues in organizations such as the U.S. National Academy of Sciences, U.S. Consumer Product Safety Commission (CPSC), the European Flame Retardants Association (EFRA), and the Bromine Science and Environmental Forum (BSEF). All halogen and more specifically, bromine-containing FRs have come under scrutiny, and while some like penta- and octabromodiphenyl ether have been banned, others like decabromodiphenyl ether (DBDE) and tetrabromobisphenol A have been subjected to risk assessments and have been found to be safe. However, in spite of the scientific evidence, there is a pressure to replace bromine-containing FRs. Attempts to reduce the use of brominated FRs in textile back-coatings have met with varying degrees of success.^{59,60} In our laboratory phosphorus-based intumescent FRs have been tried in back-coating formulations on 100% cotton and 35% cotton-65% polyester blend fabrics. Out of many FRs, only APP-based formulations yielded simulated match passes but failed after the required 40°C water soak treatment.⁶¹ To sensitize the decomposition or flame-retarding efficiency of APP, metal ions as synergists for APP have also been used.⁶¹ Metal ions promote thermal degradation of APP at lower temperatures than in their absence, and this enables FR activity to commence at lower temperatures in the polymer matrix thereby enhancing FR efficiency; however, the problem of durability to water soaking still remains.

At Bolton, we also have attempted to introduce volatile and possible vapor phase-active, phosphorus-based FR components in back-coating formulations.^{60,62} The selected FRs included tributyl phosphate (TBP), a monomeric cyclic phosphate Antiblaze CU (Rhodia Specialties) and the oligomeric phosphate-phosphonate Fyrol 51 (Akzo). When combined with an intumescent char-forming pentaerythritol (PER) derivative (NH1197, Chemtura) and applied as a back-coating on to cotton and polypropylene substrates, significant improvements in overall flame retardancy were observed.

In a recently published work by Bourbigot et al.,^{63–65} microencapsulation of ammonium phosphate with PU and polyurea shells has been carried out to make an intrinsic intumescent system compatible in normal PU coating for textiles. Microencapsulation of ammonium phosphate helps in reducing the water solubility of the phosphate and hence, increases the durability of the textile back-coating.

The inclusion of nanoparticles in coating formulations has been investigated by Devaux et al.,⁶⁶ where nanoclay and polyhedral oligomeric silsesquioxanes (POSS) in PU coatings applied to polyester and cotton fabrics were found to reduce peak heat release values of back-coated fabrics as determined by cone calorimetry. However, neither nano-species increased ignition times nor reduced extinction times in fact the reverse happened. Thus it was evident that the presence of nanoparticles alone could not impart a flame-retarding effect. A similar study at Bolton by Horrocks et al.⁶⁰ has shown that the introduction of nanoparticulate clays has no beneficial effect to a back-coating polymeric film and the introduction of fumed silica to a flame-retarded back-coating formulation reduces its effectiveness.

Intumescent coatings: Intumescent coatings have been around for nearly 70 years, normally used as surface treatments for structural materials and metals to protect them from heat and fire. On heating, they form a foamed char, which thermally insulates the underlying structure. In textiles although they can be used a surface coating on the fabric,⁶⁷ usually they are applied in between different fabric layers, which are then needlebonded to consolidate the whole structure.⁶⁸ Horrocks et al. have patented such a structure where nonwoven web of FR cellulosic fibers treated with intumescent could produce high flame- and heat-resistant fabric structures and in some instances could withstand air exposure temperatures up to 1200°C for about 10 min.⁶⁹ In a published work, it has been shown that ammonium and melamine phosphate-containing intumescent applied in a resin binder can raise the fire and heat barrier properties of flame-retarded viscose and cotton fabrics to levels similar to that for similarly structured commercially available nonwoven fabrics comprising aramid and carbonized acrylic fibers. The thermal insulative properties of these fabrics were observed by embedding thermocouples between layers of fabrics and measuring their temperatures as function of time during exposure to 50 kW/m² heat flux in a mass loss calorimeter.⁷⁰ Residual mass of coherent fabric chars and thermal resistance values obtained from this data are shown in Figure 24.4, which illustrates the superior barrier properties afforded by the char formed, which are comparable with commercial barrier fabrics, namely Panotex and Dufelt.⁷⁰ This study was also extended to wool and wool-containing blended fabrics.⁷¹ The intumescent chemicals, however, are water soluble, and hence these fabric structures can be used only in application where washing is not required, e.g., flexible barrier and fire blanket materials.

In carpets, the intumescent layer can be applied between the tufting and the backing, or on the upper surface of the backing. The intumescent material also closes up the interstices of the fire-exposed fabric. Nylon carpets made with this backing are fire retardant and are said to meet airline standards for fire safety.²⁶

24.5.1.3 Plasma Coating

Plasma technology can be used for surface modification (etching) of fibers and fabrics, functionalization of surface or surface coating by deposition of a thin layer on the surface followed by grafting. Cold plasma technology can simultaneously graft and polymerize monomers onto the surface of the textile substrate. In the so-called plasma-induced-graft-polymerization process, the plasma is used to activate the surface and the plasma of an inert gas is used to initiate polymerization of the non-volatile or solid monomer on the surface of the substrate. One of the pioneering works on FR treatment of fabrics using cold plasma was reported in the 1980s by Simonescu et al.,⁷² where surface grafting of rayon fabrics was carried out with phosphorus-containing polymers and improvement in fire-retardant properties was observed. The more recent studies of low pressure argon plasma graft polymerization by Tsafack and Levalois-Grützmaier⁷³ reports the successful grafting of phosphorus-containing acrylate monomers (diethyl(acryloyloxyethyl)phosphate (DEAEP), diethyl-2-(methacryloyloxyethyl)phosphate (DEMEP), diethyl(acryloyloxyethyl)phosphonate (DEAMP),

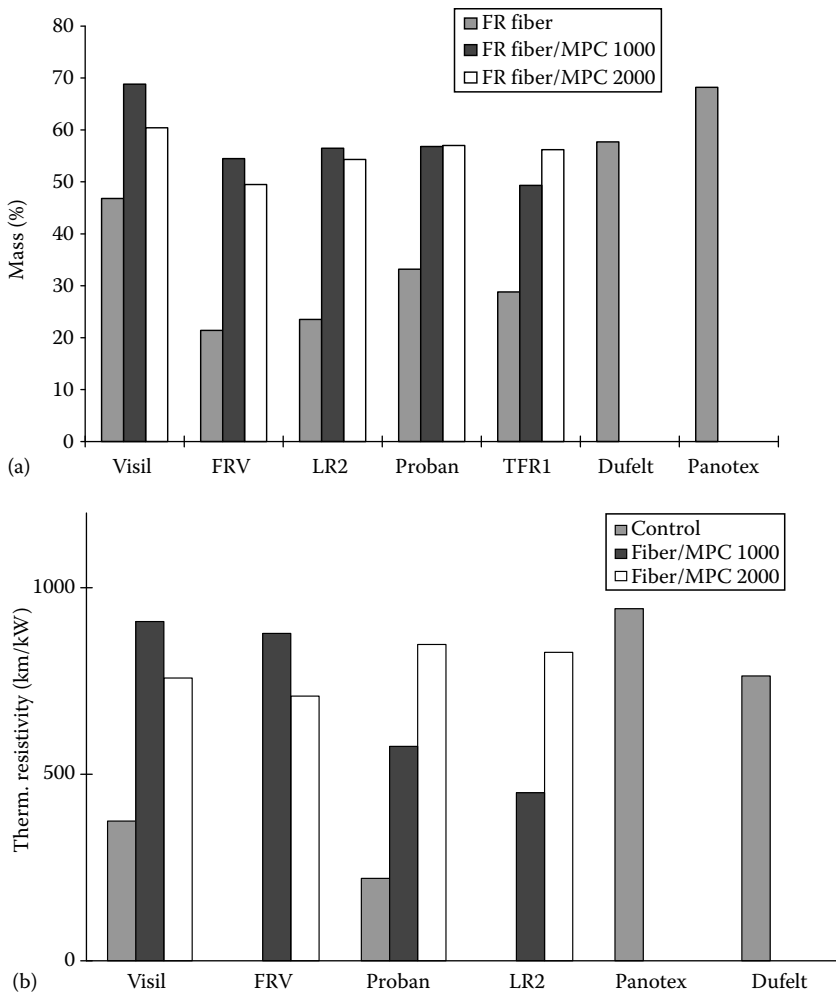


FIGURE 24.4 (a) Residual mass of coherent fabric chars following exposures to heat fluxes of 50 kW/m² for 5 min and (b) thermal resistivities for different fabrics obtained by embedding thermocouples through the thickness of the fabric structure during mass loss calorimeter experiment⁷⁰ (Key: Vis, Visil; FRV, Lenzing Viscose FR; LR2, APP-treated cotton; Proban, Proban-treated cotton; TFR1, phosphonamide-treated cotton; Panotex, carbonized acrylic fabric; Dufelt, aramid fabric. MPC 1000 = APP/melamine/pentaerythritol intumescent and MPC 2000 = Antiblaze NW (Rhodia) intumescent). (From Kandola, B.K. and Horrocks, A.R., *Fire Mater.*, 24, 265, 2000. With permission.)

and dimethyl(acryloyloxymethyl)phosphonate (DMAMP) onto polyacrylonitrile fabrics. In a more recent work by Vannier et al. at Lille using Plasma Induced Graft-Polymerization (PIGP),⁷⁴ polyethylene methacrylate phosphate was grafted on the cotton fabric. The LOI values rose from 21 vol % for the pure cotton to 32 vol % for the FR cotton. The treated fabric could achieve M2 rating, compared with M3 rating by pure cotton.

Nanoparticles with homogeneous size can be embedded on textile substrates by plasma polymerization/etching process or by plasma polymerization/co-sputtering process. To this effect, work is in progress in our laboratory.

24.5.2 FIRE-RETARDANT ADDITIVES/COPOLYMERS IN SYNTHETIC FIBERS

As the title suggests, this approach is applicable to synthetic fibers only where either one of the monomer/homopolymer can be flame retarded or the FR molecules can be attached to the polymer chain during

polymerization, or FR additives can be introduced in the polymer melt or in solution prior to extrusion. Synthetic fibers thus produced are also called inherently FR. Some exemplar fibers are discussed here.

Viscose or rayon: A well-known inherently FR viscose fiber is Viscose FR, marketed by Lenzing. The fiber is produced by adding Sandoz 5060 (Clariant 5060)-bis(2-thio-5,5-dimethyl-1,3,2-dioxaphosphorinyl)oxide in the spinning dope before extrusion. As this additive is phosphorus based, it is similar to other phosphorus-based FRs in terms of mode of action (condensed phase).

The second example is Visil fiber, developed in Finland by Säteri Fibers (formerly Kemira) by adding polysilicic acid (Visil) and aluminum (Visil AP). Visil on heating releases polysilicic acid, which being a Lewis acid acts in condensed phase by catalyzing dehydration reactions of cellulose resulting in the formation of carbon monoxide, carbon dioxide, and ultimately highly cross-linked char. The silica residue in this char acts as a thermal insulator. At Bolton we have extensively used this fiber in preparing thermal barrier fabrics using interactive intumescent and surface treatments as already discussed in Section 24.5.1.2.

Polyester: One of the most successful commercially available FR polyester fiber is Trevira CS, which is produced by incorporating a comonomeric phosphinic acid unit into the PET polymeric chain. Examples of FR additives used in polyester are bisphenol-S-oligomer derivatives (Toyobo GH), cyclic phosphonates (Antiblaze CU and 1010, Rhodia), and phosphinate salts (Clariant). All these FRs do not promote char formation.³

Polypropylene: Zhang and Horrocks have recently reviewed different FRs used for polypropylene fibers.⁷⁵ Although in principle, phosphorus-containing, halogen-containing, silicon-containing, metal hydrate and oxide are effective in rendering PP FR, invariably these FRs are required in high levels, typically >20% w/w, to achieve specified level of flame retardancy. However, such high levels render the processing of compounded polymer into fibers difficult and the resulting fiber properties unsuitable for textile applications. Apart from antimony-halogen or in some cases, tin-halogen formulations only one single FR system, tris(tribromoneopentyl) phosphate (FR 372, ICL) is presently effective in polypropylene when required for fiber end-uses. PP is very sensitive to UV radiations and normally requires UV-stabilizer for outdoor use. NOR 116 (Ciba), a thermally stable hindered amine (an oligomer-linked *N*-alkoxy-2,2,6,6-tetramethyl-4-substituted-morpholine) used for UV-stability, is also reported to have some FR properties. Latest development for flame-retarding PP is by nanocomposite-based FRs, which is discussed in detail in a separate section.

Polyamides: It is very difficult to incorporate additives in polyamides because of their melt reactivities. The recent developments for the flame retardancy of polyamides concern mainly the inclusion of nanoparticles, discussed in Section 24.5.3.

24.5.3 NANOCOMPOSITE-BASED FLAME RETARDANTS IN TEXTILES

Although there has been considerable amount of research going on in area of polymer nanocomposites as discussed in Chapters 11 and 12, there has been a limited success in developing textile structures out of them. The major difference between fibers and bulk polymers is the small thickness of individual fibers, typically 15–30 μm in diameter, yielding yarns of 50–100 μm diameter and fabrics having thicknesses varying from as low as 100 μm to several millimeters. For fire-retardant properties, it is believed that the presence of clay in a polymer promotes carbonaceous-silicate build-up on the surface during burning, which insulates the underlying material.^{76,77} The accumulation of silicate layers on the surface is due to gradual degradation and gasification of the polymer. Or according to other theory the migration of silicates to the surface is due to the lower surface free energy of the clays and by convection forces, arising from the temperature gradients, perhaps aided by movement of gas bubbles present during melting of the thermoplastic polymers.⁷⁸ This mechanism works fine for thick polymer plaques. However, for physically and thermally thin samples like textiles, there is not enough time to make thermal barrier and hence the nanoclays in textiles are not as effective as

seen in bulk polymers. The other important issue is that although nanoclays reduce PHRR during cone calorimetric testing, they have no effect on TTI. Most often simple techniques such as LOI show that the addition of nanoclays and other nanoparticles do not significantly increase LOI values unless their presence modifies the burning behavior by reducing melt dripping character of the polymer.⁷⁹ They, however, do promote char formation in otherwise noncharring polymers, which is an advantageous effect. To the best of author's knowledge there are no commercially available inherently fire-retardant polymer-nanocomposite fibers. Most of the work is still on the lab scale, which is reviewed in this section.

In case of cotton, the use of nanocomposites in coatings has already been mentioned under Section 24.5.1.2. The only reported cotton-clay nanocomposites work is by White⁸⁰ where cotton with MMT clay in a 50% solution of 4-methylmorpholine *N*-oxide (MMNO) was produced in the form of large plaques. However, no fiber or textile structures could be obtained.

Solarski et al. have developed polylactic acid (PLA)-clay nanocomposites fibers⁸¹ by melt blending organomodified (OM)-MMT (1–4 wt %) with PLA and then melt spinning into multifilament yarns. The dispersion of the clay in the yarns was reported to be quite good. The multifilaments were knitted and the flammability was studied using cone calorimetry at an external heat flux of 35 kW/m². Depending on the clay loading, the PHRR value decreased by up to 38% demonstrating improved fire performance of these PLA fibers.

For polyester, the reported work⁸² done in Sichuan University of China, involves adding MMT clay in a copolymer of poly(ethyleneterephthalate), which with a phosphorus-containing monomer could produce PET with higher thermal stability and char-forming tendency. However, fibers were not produced from this PET-nanocomposite polymers.

Polypropylene: There is a considerable research done on polypropylene–nanocomposites as bulk polymers, which is outside the scope of this chapter; however, the major work in the textile area has been in our laboratories at Bolton.^{13,83,84} One of the difficulties of incorporating nanoclays into polypropylene is the lack of polar groups in the polymer chain, which makes direct intercalation or exfoliation almost impossible. Most often maleic anhydride-grafted polypropylene is used as a compatibilizer, which enhances the interaction between the clay and polymer with strong hydrogen bonding between –OH or –COOH and the oxygen groups of clay. However, presence of such compatibilizers usually has adverse effects on fiber properties.⁷⁵ While this effect is concentration dependent, to keep the rheological properties necessary for extrusion into fiber, lower levels are preferred. Levels between 1% and 3% w/w of grafted PP along with sufficient compounding have been shown to improve the dispersion of the clay platelets in the PP matrix.^{13,84} Table 24.3 (Samples 1–7) shows the effect of nanoclay and compatibilizer levels on the fiber and fabric properties, where compatibilizer used is maleic-anhydride grafted polypropylene (Pb–Polybond 3200, Crompton Corporation) and clay is Bentone 107, Elementis (E), a MMT clay modified with dimethyl, dehydrogenated tallo quaternary ammonium ion. The effect of different clays (Cloisite 20A and 30B (Southern Clay Products, United States) and MMT modified with vinyltriphenyl phosphonium bromide (PCI)) and compatibilizers (polypropylene grafted with diethyl-*p*-vinylbenzyl phosphonate (DEP)) was also studied and shown by samples 8–12 in Table 24.3. All PP polymers were compounded in a twin screw extruder (Thermoelectron) with a temperature profile over six heating zones between 179°C and 190°C. Filaments were extruded from compounded pellets using a laboratory-sized Labline Mk 1 single screw melt extruder, with the temperature profile of 180°C–230°C of different zones and extruding through a 40 hole spinneret. Tapes (40 mm width, 0.6 mm thickness) were also extruded using a tape die in place of the spinneret, primarily to provide samples more convenient for microscopic investigation and LOI studies, while having experienced both compounding and extrusion cycles similar to that for filaments. Filaments were knitted into fabric strips with a small, hand, circular knitting machine, gauge E7.

The presence of compatibilizer helped in improving dispersion of clay in PP as shown in Figure 24.5 and the dispersion improved with the increase in compatibilizer level (Figure 24.5b–d).¹³ However, the clays were not exfoliated or intercalated, but dispersed at nanolevel as shown by TEM

TABLE 24.3
Effect of Clay and Compatibilizer Type and Levels on Physical and Flammability Properties of Polypropylene Fibers/Fabrics

S No	Sample	Sample Composition			Fiber Properties		Fabric Area Density, (g/m ²)	Flame Spread, Time to Mark (s)		
		Graft, Level (wt %)	Clay, Level (wt %)	Film LOI (vol %)	Modulus (N)	Tenacity (cN/tex)		60 mm, <i>t</i> ₁	120 mm, <i>t</i> ₂	Flame out
Effect of compatibilizer and clay levels										
1	PP	—	—	20.1	3.9	32.6	430	3.0	37	59
2	PP-3%E	—	E, 3%	^a	4.4	36.8	345	3.1	29	37
3	PP-1% Pb-3%E	Pb, 1%	E, 3%	20.3	4.4	28.3	207	4.6	45	76
4	PP-2% Pb-3%E	Pb, 2%	E, 3%	20.2	5.9	31.6	214	3.6	22	40
5	PP-5% Pb-3%E	Pb, 5%	E, 3%	20.3	3.7	25.0	282	3.8	—	29
6	PP-5%E	—	E, 5%	20.6	2.6	20.5	247	3.8	17	28
7	PP-1% Pb-5%E	Pb, 1%	E, 5%	20.5	2.8	17.5	194	3.0	14	22
Effect of different compatibilizers and clays										
8	PP-Pb-E	Pb, 1%	30B, 3%	20.0	2.6	9.9	288	4	—	33
9	PP-Pb- 30B	Pb, 1%	30B, 3%	20.0	2.7	14.8	333	7.8	—	27
10	PP-DEP- 30B	DEP, 1%	30B, 3%	^a	2.8	17.5	302	4.0	—	22
11	PP-DEP- PCI	DEP, 1%	PCI, 3%	^a	2.4	30.9	258	7.0	—	15
12	PP-Pb- 20A	Pb, 1%	20A, 3%	20.2	3.3	22.6	253	5.4	36	44

Source: Smart, G. et al., *Polym. Adv. Technol.*, 19, 658, 2008. With permission.

Note: Samples 3 and 8 although have same composition, were extruded with different draw ratios and hence show different properties.

^a Test not performed.

image of sample containing 20A clay⁸³ in Figure 24.6. Although higher levels of compatibilizer help in improving the dispersion of nanoclay, the physical properties of the fibers deteriorate as is shown in Table 24.3. The addition of 1% Polybond has no effect on the modulus of sample 2, but increasing the level to 2% increases the modulus from 4.4 to 5.9 N/tex. A further increase in the Polybond level to 5% shows a decrease in modulus to 3.7 N/tex. Out of different clays, fibers with clay 20A (sample 20A) show better physical properties. Owing to different fiber properties, fabrics produced were of different area densities (Table 24.3). The clays had minimal effect on LOI of the extruded tapes (Table 24.3), which is not surprising as the clays reduce the ignition time. The clays also change the burning behaviors of thermoplastics by holding them together rather than letting them melt away. In some cases, they reduce the LOI as observed for polyamide (discussed later in this section).

In our earlier study, we studied the flammability of these knitted fabrics by cone calorimetry,⁸³ but could not get reproducible results. This was due to samples being very thin and there was considerable bubbling and flowing of the polymer during burning which caused anomalies in the balance

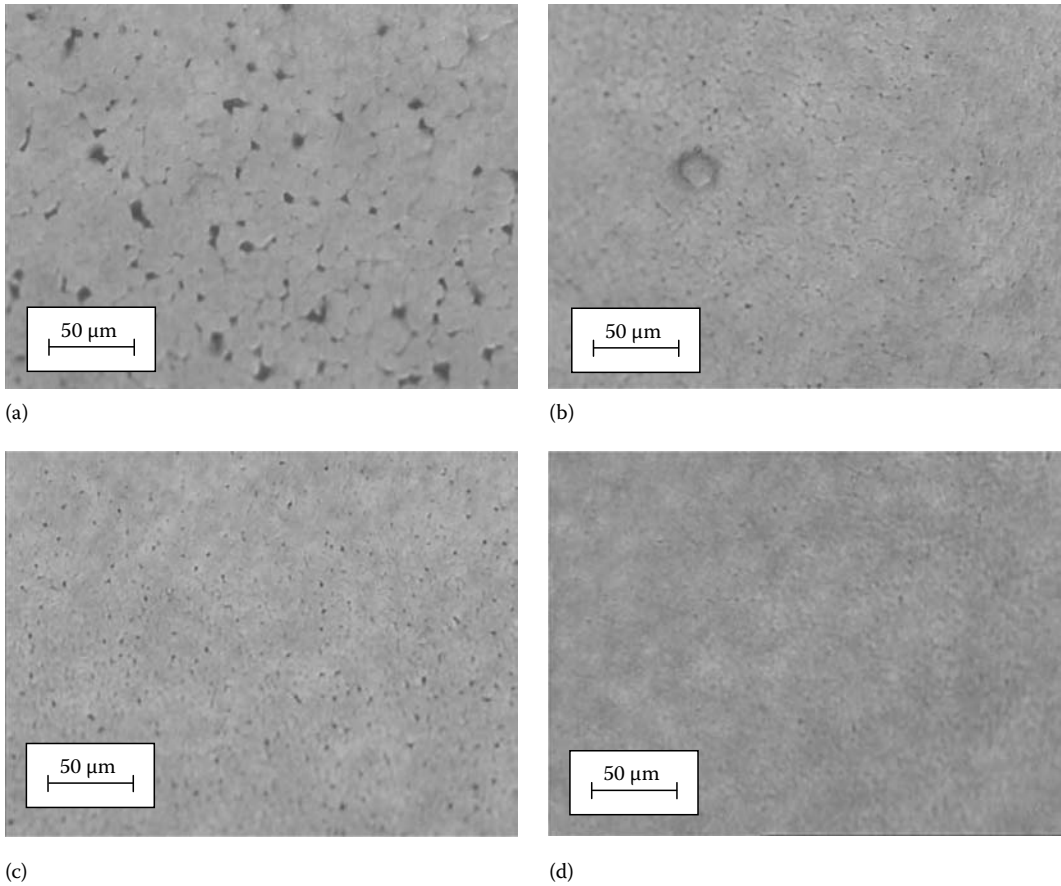


FIGURE 24.5 Optical micrographs (200 \times) of PP-nanoclay and PP-graft-PP-nanoclay tape samples showing the effects of graft-PP and graft levels on dispersion of clay. (a) Sample 1; PP-3%E (b) Sample 2; PP-1%PB-3%E (c) Sample 3; PP-2%PB-3%E (d) Sample 4; PP-5%PB-3%E (From Smart, G. et al., *Polym. Adv. Technol.*, 19, 658, 2008. With permission.)

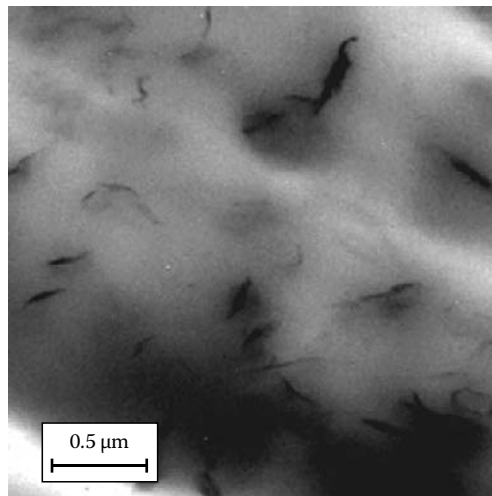


FIGURE 24.6 TEM of polypropylene containing 3% compatibilizer (Pb) and 2.5% Cloisite 20A clay.

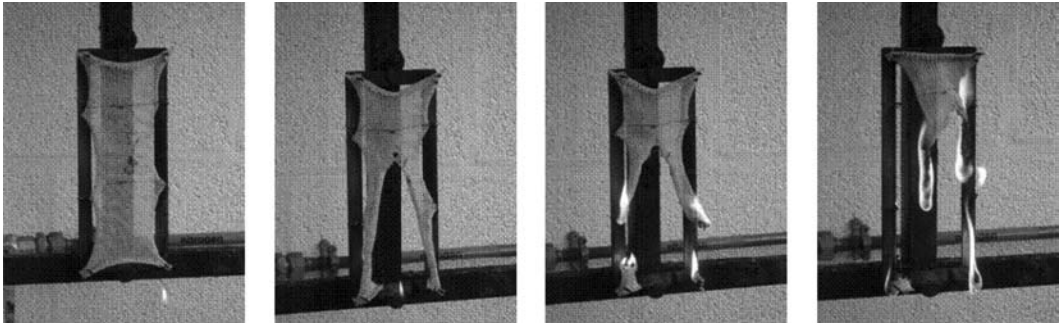


FIGURE 24.7 (See color insert following page 530.) Flame spread test of PP using BS 5438 Test 1 rig.

recording weight loss. Nevertheless it was observed that the clay presence had no effect on TTI, but the PHRR decreased as the dispersion improved. The main conclusion from this study was that the clay presence leads to the char formation in an otherwise nonchar forming polypropylene.

To make a more realistic flammability study of fabrics, we tested them for flame spread test on BS 5438 rig¹² used for flammability of textile materials, using sample holder used in Test 1 of this standard. The details have already been given in Section 24.2.2. Sample size was 190 mm × 70 mm. Samples were marked at 60, 120, and 180 mm. First 10 mm of sample burning was not taken into account. Flame was applied on the edge as specified in the test. Time to reach 60 mm (t_1), 120 mm (t_2), and 180 mm (t_3) or flameout were noted and shown here in Table 24.3. Samples 1–7, where effects of clay and compatibilizer levels are assessed, show little difference in the time taken to reach the 60 mm mark with values ranging from 3.0 to 4.6 s. It can be seen that fabric containing highest level (5%) of compatibilizer and 3% clay (sample 5) self-extinguished, whereas the fabric with 1% compatibilizer and 3% clay (Sample 3) took an average time of 45 s to reach the 120 mm mark. Although many samples reached this mark, a few went on to burn up completely. The 100% PP sample burns completely in approximately 59 s with much dripping and the remaining fabric twisting back on itself, spreading the flame further up the fabric strip (See Figure 24.7). By conversion to rates of burning and plotting against burning length as in Figure 24.8, a better distinction between the individual performances may be gained. It can be seen that fabric samples, 100% polypropylene and PP-1%Pb-3%E fabrics burn faster than the others followed by PP-3%E sample. The flame spread rates for samples containing compatibilizer are relatively slower with the slowest behavior shown by PP-5%Pb-3%E sample. However, between 60 and 120 mm, PP-1%Pb-3%E burns slower than others.

Samples containing different types of clays burned differently depending upon the clay type, as can be seen from Table 24.3 and Figure 24.8b. All samples containing only clay and compatibilizer except PP-Pb-20A (sample 12), namely PP-Pb-30B (sample 9), PP-DEP-30B (sample 10), PP-Pb-E (sample 8), and PP-DEP-PCl (sample 11) self-extinguished beyond 60 mm but before 120 mm. The best results in terms of lowest burning rates are shown by samples PP-Pb-30B and PP-DEP-PCl, which had burning times to 60 mm of 7.8 and 7.0 s, respectively. This study indicated that with the proper choice of compatibilizer and the nanoclay, flammability of a polymer could be reduced.

A subsequent study investigated the effect of introducing conventional FRs to PP-nanocomposites. The FRs were both phosphorus- and halogen-containing. Phosphorus-containing FRs included APP (Amgard MCM, Rhodia Specialities, United Kingdom), melamine phosphate, NH (Antiblaze NH, Rhodia Specialities Ltd., United Kingdom), and PER phosphate (NH1197, Chemtura), and the bromine-containing tris (tribromopentyl) phosphate (FR 372, DSBG, Israel) and tris(tribromophenyl)cyanurate, FR 245 (DSBG, Israel) species (see Table 24.4). Hindered amine stabilizer NOR 116 (Ciba) was also used as a UV-stabilizer. The clay used for this set of samples was Elementis E. Extrusion into filaments proved to be challenging because of problems with optimizing clay and FR dispersion and this was especially the case when APP was present

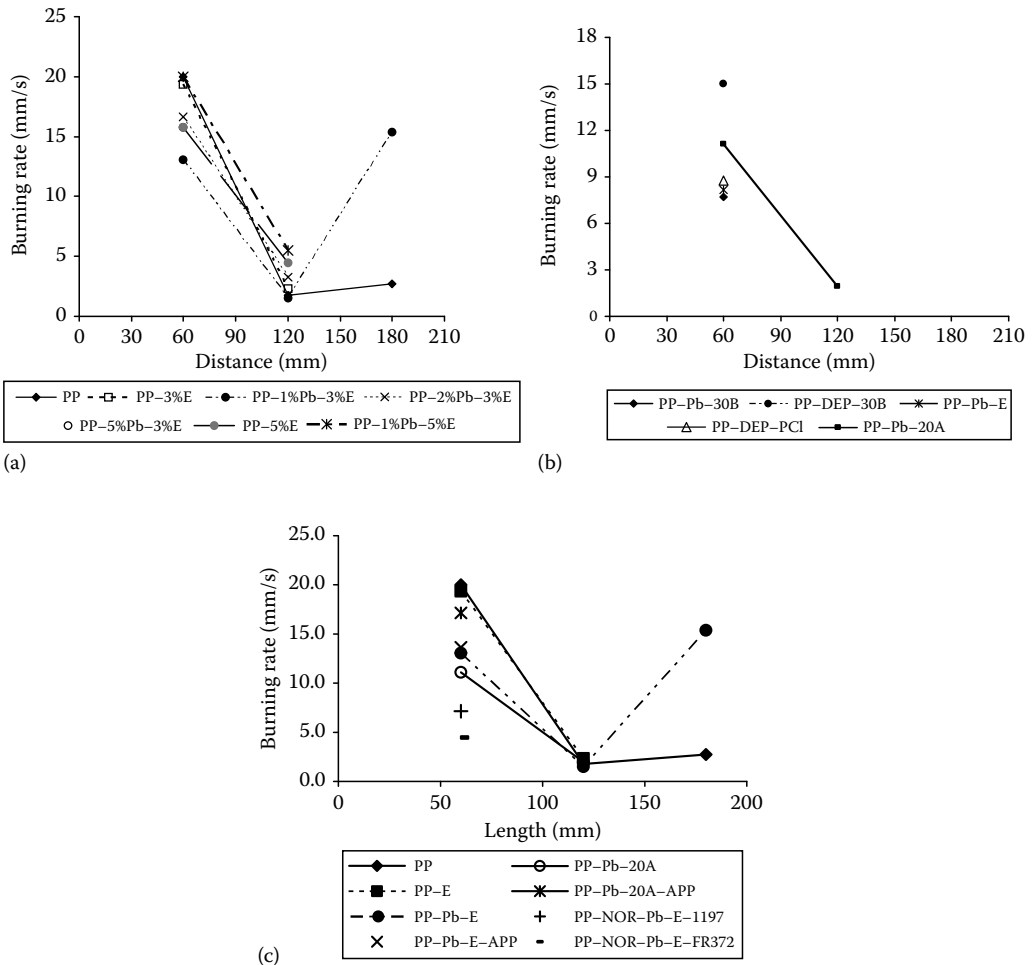


FIGURE 24.8 Burning rates for PP fabrics corresponding to samples given in (a) and (b) Table 24.3, and (c) Table 24.4. (From Smart, G. et al., *Polym. Adv. Technol.*, 19, 658, 2008. With permission.)

because of its very poor dispersion and relatively large particle size (25–30µm). Hence, fabrics produced were of different area densities. In some cases, fabrics could not be knitted. LOI values of strings were unaffected by either the presence of clays or FR but then the low concentrations of FRs present (5 wt %) would not be expected to raise the LOI values significantly when present alone.⁷⁶ TGA results show that PP decomposes completely leaving no char. In the presence of clay, ~2% char is left behind, which may be due to silica content of the clay. All FRs except FR 245 helped in increasing char formation.

Burning behavior in terms of timing to reach 60 (t_1) and 120 mm (t_2) marks and to extinguish (flame out) is given in Table 24.4. The effect of clay and compatibilizer (Pb) in the time taken to reach the 60mm mark is minimal with values ranging from 3 to 5 s. The PP control sample melts, drips, and does not burn steadily due to its thermoplastic nature, hence longer time (59 s) to reach the 120 mm mark. PP sample burns completely in approximately 71 s with much dripping, remaining fabric twisting back on itself spreading the flame further up the fabric strip. Rate of flame spread was very slow for samples containing NH1197 and FR372 and they self-extinguished after 34 and 45 s, respectively. This is more clearly seen by flame spread rate in Figure 24.8c, where results for

TABLE 24.4
Sample Composition, TGA, and LOI Results of Compounded Polymer Chips, Tapes and Strings, and Effect of Additives on the Fiber and Fabric Properties

Sample	Char Yield at 800°C from TGA (%)	LOI of Strings (%)	Fiber Properties			Flame Spread (s)		
			Mod (N)	Ten (cN/tex)	Fabric Area Density (g/m ²)	60 mm, t ₁	120 mm, t ₂	Flame out
PP	0	19.2 ^a	3.8	34.9	345	3	59	71
PP-NOR- Pb-E	2.0	17.5	3.9	22.6	—	—	—	—
PP-NOR- Pb-E-APP ^b	3.2	17.8	—	—	—	—	—	—
PP-NOR- Pb-E-NH ^c	2.9	17.9	2.5	11.2	—	—	—	—
PP-NOR- Pb-E-1197	2.2	17.8	3.8	23.9	290	8	—	34
PP-NOR-Pb- E-FR245 ^b	2.5	17.2	—	—	—	—	—	—
PP-NOR-Pb- E-FR372	2.0	18.7	3.2	21.7	360	14	—	45

Note: PP, polypropylene; E (E 107) = Clays, 3% w/w; Pb, polybond (maleic anhydride grafted PP), 1% w/w; NOR = UV stabilizer, 1% w/w; APP, NH, 1197, FR245, FR372 = Flame retardants, 5% w/w.

^a LOI value for tape.

^b Could not extrude compounded polymer into filaments.

^c Could not knit filaments into fabric.

samples given in Table 24.4 and also some additional samples reported elsewhere¹³ are included. Samples containing APP (PP-Pb-20A-APP, PP-PbB-E-APP) burned up to the 60 mm mark quickly, for 4 s and when observed burnt quite readily and vigorously, although the flame did flicker quite significantly, which was not observed in other samples. This phenomenon was probably due to the poor dispersion and low level of APP. Poor dispersion would mean the flame would stutter when it reached a particle of APP but the level was not high enough to extinguish the flame.¹³

This work has demonstrated that we have been successful in extruding fibers from these polymer nanocomposites, knit them into textiles, and test their flammability. These prototype nanocomposite FR fiber-forming polymers and textile materials based upon them could be taken forward by interested parties for scale-up and commercial development.

Bourbigot et al.⁸⁵ at Lille have used poly(vinylsilsesquioxane) (POSS) in PP (110 wt%) to melt spin filaments, which were then knitted into fabrics. POSS was thermally stable and no degradation was detected in the processing conditions. They have tested the flammability of the fabrics using cone calorimetry. POSS presence had minimal effect on peak heat and total heat release values of PP fabric, but delayed the TTI. This behavior of POSS is opposite to that of layered silicates, which have minimal effect on TTI, but reduce PHRR. Authors claim that POSS does not act as a FR but only as a heat stabilizer via a decrease of the ignitability.

Researchers in the Lille group have also been successful in preparing yarns from polypropylene/multiwalled carbon nanotubes (MWNT) (1% and 2% by mass) nanocomposites.^{6,86} Fabrics knitted from these yarns were tested by cone calorimetry. PHRR reduced by 50% for a fraction of nanotubes of only 1 wt % but the TTI of the nanocomposite was shorter. This is shown in Figure 24.9.

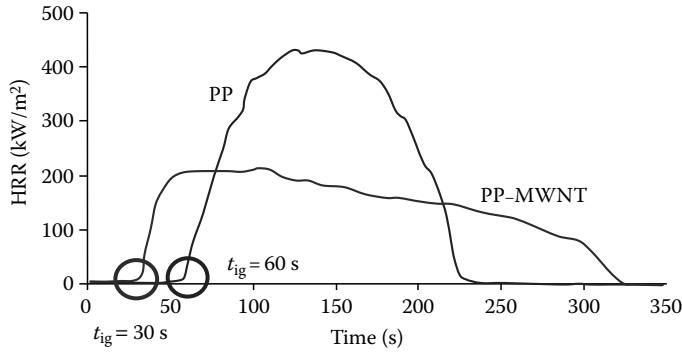


FIGURE 24.9 HRR values versus time of PP and PP/MWNT fabrics at 35 kW/m². (From Bourbigot, S., *Advances in Fire Retardant Materials*, Woodhead Publishing Ltd., Cambridge, U.K., 2008. With permission.)

Polyamides: Bourbigot et al. in 2001 reported the fire performance of nylon 6 or PA-6/clay hybrid fibers made by melt blending and by melt spinning.⁸⁷ PA-6 nanocomposite exhibited an exfoliated structure and no degradation of the clay was observed after processing. However, the yarns were not very uniform owing to reagglomeration of the MMT platelets, resulting in poor mechanic properties.⁶ The fabrics prepared from these yarns were of 1020 g/m² area density and 2.5 mm thickness. These were tested by a cone calorimeter at 35 kW/m² heat flux, where ignition times of 70 and 20 s and PHRR values of 375 and 250 kW/m², respectively, for the normal and nanocomposite polyamide 6 fabrics were recorded. While the latter represents a significant 33.3% reduction in PHRR, ignition resistance was significantly reduced and total heat release was little affected. It must be noted that these fabrics have very high area density; hence this reduction in peak heat release might not be reflected by fabrics of area densities normally used as apparel fabrics, i.e., 100–200 g/m².

Using nylon 6 and 6.6 cast films as models for eventual fiber geometries, earlier work in our own laboratories^{53,79,88,89} suggested that nanoclays on their own will not be able to fulfill all the required features of an ideal FR such as conferring ignition resistance, self-extinguishability, and char-forming propensity. However, they may increase the effectiveness of more normal FRs and thus enable lower quantities to be used, an especially important requirement in synthetic fiber production and processing. The effect of FRs APP, melamine phosphate, PER, PER phosphate, cyclic phosphate, intumescent mixtures of APP, PER, and melamine, and ammonia cross-linked polymer of a tetrakis(hydroxyl phosphonium salt-urea condensate (as Proban CC polymer (Rhodia)) etc., in the presence and absence of nanoclay was studied. Using LOI as a means of measuring increased FR properties, it was shown that the addition of low levels (2% w/w) of nanoclay does increase the overall FR behavior of films in the presence of defined concentrations (11%–27% w/w) of FR thus enabling lower concentrations of the latter to be used. However, melamine phosphate showed antagonistic behavior with nanoclay resulting in agglomeration of the clay.

Recently, we have extended this work to melt blend nanoclays with nylon 6, using the same methodology as for polypropylene discussed earlier, with the temperature profile over six heating zones in the compounder between 240°C and 260°C.⁹⁰ Nylon 6 was compounded with Cloisite 15A and 25A nanoclays at different levels (see Table 24.5). Commercially available nylon 6 containing 2% nanoclay (UBE Industries Ltd.) was also used. The dispersion of nanoclays was much easier for nylon 6 and filaments could be extruded without problem. Owing to high processing temperature of nylon 6, all FRs mentioned earlier and also used for polypropylene could not be used here as many of them start degrading at 260°C. Only melamine phosphate, NH (Antiblaze NH, Rhodia Specialities Ltd., UK), and tris (tribromopentyl) phosphate (FR 372, DSBG, Israel) could be compounded with nylon 6 (Table 24.5). In Table 24.5, the LOI values and the burning behavior of strands of the compounded polymers (length = 110 mm, diameter = 1.8 ± 0.2 mm) are given. Flame spread tests were

TABLE 24.5
Sample Composition, TGA, LOI, and Flame Spread Results of Compounded Polymer Chips and Strings of Nylon 6 with/without Clays and Flame Retardants

No	Sample	Sample Composition			Horizontal Flame Spread (s)		Vertical Flame Spread (s)	
		Clay, Level (wt %)	FR, Level (wt %)	LOI of Strings (vol %)	Time to Reach 50 mm	Time to Reach 100 mm	Time to Reach 50 mm	Time to Reach 100 mm
1	N6	—	—	22.4	28 (30 mm)	—	31	55
Effect of nanoclays								
2	UBE	^a , 2%	—	18.2	31 (40 mm)	—	26	43
3	N6–15A 3%	15A, 3%	—	19.5	38	65 (90 mm)	29	50
4	N6–15A 5%	15A, 5%	—	19.7	36	70	23	40
5	N6–15A 8%	15A, 8%	—	19.8	28	69	19	41
6	N6–25A 3%	25A, 3%	—	19.1	54	95	22	35
7	N6–25A 5%	25A, 5%	—	19.8	40	67	23	37
8	N6–25A 8%	25A, 8%	—	20.3	24	59	17	31
9	N6–25A 4%–15A 4%	15A, 4%; 25A, 4%	—	20.1	69	145	20 (25 mm)	—
Effect of flame retardants								
10	N6–NH 5%	—	NH, 5%	20.1	33	40 (60 mm)	30	59
11	N6–NH 10%	—	NH, 10%	20.5	56	—	26	—
Effect of nanoclays and flame retardants								
12	UBE–NH 5%	^a , 3%	NH, 5%	19.8	24 (25 mm)	—	16 (10 mm)	—
13	UBE + FR 372 5%	^a , 3%	FR 372, 5%	19.4	50	63 (75 mm)	20 (25 mm)	—
14	N6–15A 3%–NH 5%	15A, 3%	NH, 5%	19.9	25 (35 mm)	—	16	30
15	N6–25A 3%–NH 5%	25A, 3%	NH, 5%	20.3	27	55	12 (3 m)	—
16	N6–25A 3%–NH 10%	25A, 3%	NH, 10%	19.4	43	56 (70 mm)	20	28
17	N6–25A 5%–NH 5%	25A, 5%	NH, 5%	19.3	42 (45 mm)	—	29	46

Source: Ratnayaka, A., High performance fire retardant synthetic fibres incorporating nanocomposites, MSc thesis, University of Bolton, Bolton, U.K., May 2007.

^a Nanoclay type not known.

^b Values in the brackets denote maximum burning length.

done by a modified UL-94 test to observe their burning behavior in both horizontal and vertical orientations. The first 10 mm of sample burning was not taken into account and so times of burning were recorded once the flame had reached a line drawn 10 mm from the edge against which flame of 30 mm was applied for 10 s as specified in the test. A video film was taken of the burning of each sample from which times to reach 50 (t_1) and 100 mm (t_2) marks or to achieve flameout were noted. It was observed that nylon melt and drips and hence does not burn for a longer time. With clay presence, the melting and dripping reduced but as the clay was able to hold the polymer there, it burnt more than pure polymer. With very high clay levels, the char formation tendency increased as can

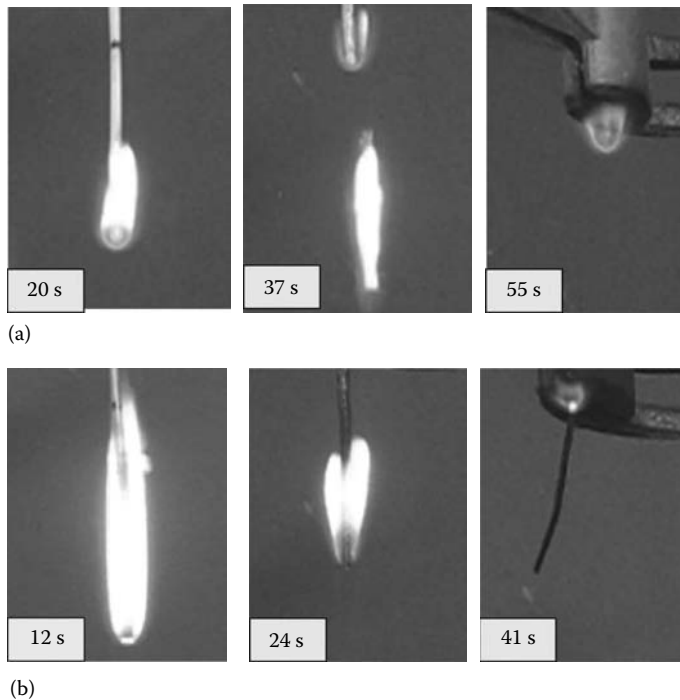


FIGURE 24.10 (See color insert following page 530.) Vertical burning behavior of (a) nylon 6 and (b) nylon 6 strings containing 8% 15A nanoclay. (From Ratnayaka, A., High performance fire retardant synthetic fibres incorporating nanocomposites, MSc thesis, University of Bolton, Bolton, U.K., May 2007.)

be seen from Figure 24.10 where a strand of nylon 6 is burning with flaming drips. In contrast, the sample containing clay burns steadily and after burning the char remains intact. FR 372 reduced the burning of commercial nylon 6 product containing nanoclay (UBE). Melamine phosphate, however, showed once again antagonistic effect as observed for film samples mentioned earlier and reported elsewhere.^{79,88,89}

All samples discussed in Table 24.5 could not be extruded into fibers, only containing nanoclays could be processed and are reported in Table 24.6.⁹⁰ The fiber properties results show that modulus and tenacity increases by increasing clay level up to 5%, after that the fiber properties deteriorate. Nylon 6 normally forms an extensible fiber with a low draw ratio and these fibers had very high elongation at break values. The burning behavior was similar to that observed with strands, that the nanoclays reduce the thermoplasticity, hence change the burning behavior of nylon. Work is still in progress to obtain nylon 6–nanocomposite fibers with better physical and thermal properties.

24.5.4 HEAT RESISTANT AND INHERENTLY FIRE-RETARDANT FIBERS

Inherently flame and heat resistant fibers are either all-aromatic polymeric structures or inorganic and mineral based. The aromatic fibers are mostly used for apparel applications as protective clothing. Some commonly used fiber types are given in Table 24.1 and discussed subsequently. These are nonthermoplastic, combustion-resistant with decomposition temperatures above 375°C³ and with LOI values 30 vol % or more. Moreover, they have char-forming tendency. For detailed information about their chemical structures and mode of decomposition, the reader is referred to a review by Bourbigot et al.⁹¹

TABLE 24.6
Effect of Clays on Physical and Flammability Properties of Nylon 6 Fibers/Fabrics
Prepared from Samples Given in Table 24.5

Sample	Fiber Properties		Fabric Area Density (g/m ²)	Flame Spread, Time to Mark (s)			Comments
	Modulus (N)	Tenacity (cN/tex)		60 mm, t ₁	120 mm, t ₂	Flame Out	
N6	60.7	16.5	254	12	—	12	Burnt very slowly, melting and dripping occurred, extinguished in a very short time due to dripping.
UBE	118.2	9.7	220	8	—	21	Small flame and dripping observed, self-extinguished
N6-15A 3%	72.5	9.1	214	5	—	18	Medium flame, dripping observed.
N6-15A 8%	67.7	7.2	118	3	7	21	Burnt very fast with big flame, no dripping.
N6-25A 3%	52.6	7.2	190	5	—	19	Burnt slowly with small flame, dripping occurred
N6-25A 5%	83.5	10.5	270	7	—	39	Burnt with medium flame, dripping occurred
N6-25A 8%	74.9	6.4	220	3	6	28	Burnt very fast with medium flame, no dripping.

Source: Ratnayaka, A., High performance fire retardant synthetic fibres incorporating nanocomposites, MSc thesis, University of Bolton, Bolton, U.K., May 2007.

First example of this type is aramids, which are most well known and exploited for protective clothing. They have aromatic repeat units bonded together by strong amide—CO.NH—, imide—CO.NN< or both in alternating manner. The most commonly used aramids are meta-aramids (Nomex, DuPont and Conex, Teijin), para-aramid (Kevlar, DuPont and Technora, Teijin), poly-*m*-phenylenediamine isophthalamide (Twaron, DSM), and poly(aramid-aramid) fiber (Kermel, Rhone-Poulenc). Nomex is used in fire fighters and military protective apparel and accessories, as well as electrical insulation paper. Kevlar, the most fire-resistant of the aramids, has been much used in military protective garments and protective fabrics in vehicles. However, aramid fibers have poor UV stability. The problem appears as discoloration or fading, cracking and sometimes, total product disintegration if cracking has proceeded far enough. This affects the fire performance of the product as well. Kevlar and Kermel have poor UV stability. Twaron HM (High modulus) has similar tensile strength as Kevlar 49, but better UV resistance. Technora fiber's lower UV resistance can be enhanced by dyeing the naturally gold fiber black.

Polybenzazole group of fibers include PBI (Celanese) and polybenzoxazole (Zylon, Toyobo). These are wholly aromatic structures. The applications for PBI include fire-blocking fabrics for aircraft seats, firefighters suits, racing-car driver suit, etc. However, these fibers have poor resistance to both UV and visible light, and so must be protected from intense radiation source.

Phenolic or novoloid fibers, produced by spinning and postcuring of phenol formaldehyde precondensate are noncombustible and char formers. However, owing to poor fiber strength and abrasion properties, they are not suited for making apparel. Common example is Kynol, which can be blended with Nomex or FR viscose to produce protective clothing. Melamine fibers are other examples, which are produced by condensation reaction of formaldehyde with melamine or substituted melamines. Basofil (BASF) is an example used in commercial aircraft seating, fire fighter turnout gear, industrial protective clothing, friction parts, and automotive insulation.

Halogen-containing fibers namely modacrylics fibers are typically copolymers of vinyl chloride or vinylidene dichloride and acrylonitrile. Although these fibers do not melt-flow or drip, they shrink rapidly when exposed to the fire. Because of this, the best use of modacrylic fibers is in blends.

Polyphenylene sulfide fibers are other group of inherently FR fibers. Example is Diofort (Diolen Industrial Fibers, the Netherlands).

Semicarbon or oxidized polyacrylonitrile fibers, produced by thermo-oxidative stabilization of either viscose or acrylic fibers, have excellent heat resistance, do not melt or burn, and have excellent resistance to molten metal splashes. Panox (RK Textiles), Panotex (Universal Carbon Fibers), and Pyron (Zoltek Corp) are some examples, produced from acrylic fibers.

Inorganic fibers: This group of fibers includes glass, carbon, and ceramic fibers. Glass and carbon fibers have already been mentioned in the Section 24.4.8. Glass fiber is nonflammable but melts at temperatures above 600°C. Carbon fibers are extremely resistant to high temperatures: Their melting temperature is 4000°C.⁶ They can also be considered as flame resistant since they will burn only at very high temperatures or in high oxygen-containing atmospheres. They hence are ideal choice for applications requiring extremely high temperatures, for example, in the filtration of molten iron. A number of ceramic fibers, SiC, silicon or boron nitride, polycarbosilicones, alumina etc., have been developed. Another example is Basalt, produced from relatively low-melting natural aluminosilicate rock. These ceramic fibers can withstand temperatures between 1000°C and 1400°C. The fibers, however, are very abrasive and may cause problems during processing. Their main application is in fire barriers and insulation materials.

24.5.5 FIBER BLENDING

Fiber blending is a very common method of reducing the flammability of flammable fibers. Polyester is usually blended with cotton and this polycotton, if has lower than 50% polyester content can pass the simple vertical strip flammability test. With higher polyester content, sometimes the blended fiber is more flammable than the individual components. This is called wicking effect where the cotton acts like a wick, holding the polyester component together, which burns. Cotton–nylon blend are also quite commonly used to reduce flammability of cotton.

Wool and Visil fiber are blended to improve latter's fiber properties, but the flammability of the blend is also reduced. Cotton–wool blends are quite common as well. Aramids are blended with many fibers for different applications. Nomex can be blended with FR viscose and FR wool to produce fire-blocking fabric, e.g., for aircraft seats.⁴ Nomex blended with Kevlar shows better performance than 100% Nomex in fire fighters' outer protective garments.²⁶ Various blends of glass fibers with aramids, melamine fibers, PVC fibers, and polyester have been reported for use in fire-protective nonwoven veils for upholstery and mattresses.⁹²

24.5.6 COMPOSITE ASSEMBLIES: DESIGN ISSUES

In Sections 24.3 and 24.5 the flammability and fire resistance of individual fiber/fabric type are discussed. However, as also discussed before, the fire resistance of a fabric not only depends upon the nature of components and the FR treatments applied, but also on fabric area density, construction, air permeability, and moisture content. Nonwovens, for example, will have superior properties to woven or knitted structure, even if all other variables are kept the same.⁹³ The air entrapped within the interstices of any fabric structure and between layers of fabrics within a garment assembly provides the real thermal insulation. For effective thermal and fire resistance in a fabric structure, these insulating air domains need to be maintained.²² In general, for protective clothing and fire-block materials, for best performance multilayered fabric structures are employed. The assembly structures can be engineered to maximize their performance. It is beyond the scope of this chapter to go into details of these composite structures; hence the reader is referred to the literature on specified applications and products available.

24.6 FUTURE TRENDS

It is evident that the demand for fire and heat resistant textiles at affordable price will sustain the research and development in this area. Development of high-performance fibers with inherently high levels of fire and heat resistance is a major breakthrough in this area, but invariably these are expensive and used only when performance requirements justify cost. There is still need to flame retard conventional textiles such as cotton, wool, etc. For cotton there are well-established phosphorus- and nitrogen-containing commercial FR finishes (e.g., Pyrovatex, Ciba and Proban, Rhodia), which act in condensed phase and presently are not under threat from environmental point of view. However, for many applications using different fiber types including cotton, antimony–halogen-based back-coatings are used, which are under pressure to be replaced by other environmentally friendly chemicals. The way forward is to introduce other volatile species, such as phosphorus-containing, in these coatings.

New trends involve the use of nanoparticles in synthetic fibers. Polymer-layered silicates, nanotubes, and POSS have been successfully introduced in a number of textile fibers, mainly polyamide-6, polypropylene, and polyester. Although they reduce the flammability of these fibers, but on their own are not effective enough to confer flame retardancy to a specified level. However, in presence of small amounts of selected conventional FRs (5–10 wt %), synergistic effect can be achieved. With this approach fibers having multifunctional properties can also be obtained, e.g., water repellency or antistatic properties along with fire retardancy. Most of the work in this area at present is on the lab scale and there is a potential to take this forward to a commercial scale.

Plasma technology involving modification of fiber and textile surface has a history spanning about 40 years and although it has gained commercial significance within other sectors such as in improving paint/coating adhesion to plastics for automotive and other applications, its adoption by the textile industry has been slow. Plasma technology offers a possible means of achieving novel nanocoatings having the desired thermal shielding effects. Nanoparticles with homogeneous size can be embedded on textile substrates by plasma polymerization/etching process or by plasma polymerization/co-sputtering process, offering opportunities for investigations.

REFERENCES

1. Lyons, J.W. 1970. Introduction: An Overview. In *The Chemistry and Uses of Fire Retardancy*, Wiley Interscience, New York, 1970, p. 2.
2. Hauser, P.J. and Schindler, W.D. 2004. Flame retardant finishes. In *Chemical Finishing of Textiles*, Schindler, W.D. and Hauser P.J. (Eds.), Woodhead Publishing/CRC, Cambridge, U.K./Boca Raton, FL, pp. 98–116.

3. Horrocks, A.R. 2001. Textiles. In *Fire Retardant Materials*, Horrocks, A.R. and Price, D. (Eds.), Woodhead Publishing Ltd./CRC, Cambridge, U.K./Boca Raton, FL, pp. 128–181.
4. Bajaj, P. 2000. Heat and flame protection. In *Handbook of Technical Textiles*, Horrocks, A.R. and Anand, S.C. (Eds.), Woodhead Publishing Ltd., Cambridge, U.K., pp. 223–263.
5. Horrocks, A.R., Kandola, B.K., Davies, P.J., Zhang, S., and Padbury, S.A. 2005. Developments in flame retardant textiles: A review, *Polym. Deg. Stab.*, 88: 3–12.
6. Bourbigot, S. 2008. Flame retardancy of textiles: New approaches. Chapter 2 in *Advances in Fire Retardant Materials*, Horrocks, A.R. and Price, D. (Eds.), Woodhead Publishing Ltd., Cambridge, U.K., pp. 9–40.
7. Horrocks A.R., Tunc, M., and Price, D. 1989. The burning behaviour of textiles and its assessment by oxygen-index methods, *Textile Progress*, 18(1/2/3): 1–186.
8. ASTM D2863-00: Standard method for measuring the minimum oxygen concentration to support candle-like combustion of plastics (oxygen index).
9. Standards for Testing of Interior Textiles, Frankfurt, Trevira (formerly Hoechst) GmbH, 1997.
10. Gawande (Nazaré), S. 2002. Investigation and prediction of factors influencing flammability of night-wear fabrics. Ph.D. Thesis, University of Bolton, Bolton, U.K.
11. Nazare, S. and Horrocks, A.R. 2008. Flammability testing of fabrics. In *Fabric Testing*, Hu, J. (Ed.), Woodhead Publishing Ltd., Cambridge, U.K., Chapter 12, pp. 339–388.
12. BS 5438:1989 British Standard Methods of test for flammability of textile fabrics when subjected to a small igniting flame applied to the face or bottom edge of vertically oriented specimens.
13. Smart, G., Kandola, B.K., Horrocks, A.R., and Marney, D. 2008. Polypropylene fibers containing dispersed clays having improved fire performance Part II: Characterization of fibers and fabrics from PP—nanoclay blends, *Polym. Adv. Technol.*, 19: 658–670.
14. Kandola, B.K., Horrocks, A.R., Padmore, K., Dalton, J., and Owen, T. 2006. Comparison of cone and OSU calorimetric techniques to assess the flammability behavior of fabrics used for aircraft interiors, *Fire Mater.*, 30(4): 241–255.
15. Nazaré S., Kandola, B.K., and Horrocks, A.R. 2002. Use of cone calorimetry to quantify the burning hazard of apparel fabrics, *Fire Mater.*, 26: 191–199.
16. Fire Safety of Upholstered Furniture—the final report on the CBUF research programme, EUR 16477EN, Sundstrom, B. (Eds.), 1994. Interscience Communications Ltd., London, U.K.
17. Mikkola, E. 1993. Communication: Raised grid for ignitability and RHR testing. *Fire Mater.*, 17(1): 47–48.
18. Horrocks, A.R. 1986. Flame-retardant finishing of textiles. *Rev. Prog. Coloration*, 16: 62–101.
19. Camenzind, M.A., Dale, D.J., and Rossi, R.M. 2007. Manikin test for flame engulfment evaluation of protective clothing: Historical review and development of a new ISO standard. *Fire Mater.*, 31(5): 285–296.
20. Horrocks, A.R. and Kandola, B.K. 2004. Flammability testing of textiles. In *Plastics Flammability Handbook*, Troitzsch, J. (Eds.), Hanser Publication, Munich, Germany, Chapter 6, pp. 173–188.
21. Bajaj, P. 2000. Finishing of technical textiles. In *Handbook of Technical Textiles*, Horrocks, A.R. and Anand, S.C. (Eds.), Woodhead Publishing, Cambridge, U.K., pp. 152–172.
22. Horrocks, A.R. 2005. Thermal (heat and fire) protection. In *Textiles for Protection*, Scott, R.A. (Ed.), Woodhead Publishing, Cambridge, U.K., Chapter 15, pp. 398–440.
23. Horrocks, A.R., Gawande, S., and Kandola, B.K. 2000. The burning hazard of clothing—The effect of textile structures and burn severity. In *Recent Advances of Flame Retardancy of Polymeric Materials*, Volume XI, M. Lewin; *Proceedings of the 2000 Conference*, Business Communication Company, Stamford, CT.
24. Hirschler, M.M. and Piansay, T. 2007. Survey of small-scale flame spread results of modern fabrics. *Fire Mater.*, 31(6): 373–386.
25. Davis, S. and Villa, K.M. 1989. Development of a multiple layer test procedure for inclusion in NFPA 701: Initial experiments, NISTIR 89-4138. National Institute of Standards and Technology: Gaithersburg, MD, August 1989.
26. Weil, E.D. and Levchik, S. 2008. Flame retardants in commercial use or development for textiles. *J. Fire Sci.*, 26: 243–281.
27. Horrocks, A.R., Nazare, S., and Kandola, B.K. 2004. The particular flammability hazards of nightwear. *Fire Safety J.*, 39(4): 259–276.
28. BS 5722:1984 British Standard specification for flammability performance of fabrics and fabric assemblies used in sleepwear and dressing gowns.
29. EN 1103. Textiles Burning Behaviour Fabrics for Apparel Detailed Procedure to Determine the Burning Behaviour of Fabrics for Apparel. European Committee for Standardization: Brussels, Belgium, 1995.

30. Rossi, R.M., Bruggmann, G., and Stämpfli, R. 2005. Comparison of flame spread of textiles and burn injury prediction with a manikin. *Fire Mater.*, 29(6): 395–406.
31. Holmes, D.A. 2000. Textiles for survival. In *Handbook of Technical Textiles*, Horrocks, A.R. and Anand, S.C. (Eds.), Woodhead Publishing, Cambridge, U.K., pp. 461–489.
32. Scott, R.A. 2005. Flight suits for military aviators. In *Textiles for Protection*, Scott, R.A. (Ed.), Woodhead Publishing, Cambridge, U.K., Chapter 24, pp. 678–698.
33. Nazare, S. 2008. Fire protection in military textiles. In *Advances in Fire Retardant Materials*, Horrocks, A.R. and Price, D. (Eds.), Woodhead Publishing Ltd., Cambridge, U.K., Chapter 19.
34. Seed, M., Anand, S.C., Kandola, B.K., and Fulford, F. 2008. Chemical, biological, radiological and nuclear protection. *Tech. Textil. Int.*, 39–46.
35. Bajaj, P. and Sengupta, A.K. 1992. Protective clothing. *Textile Process*, The Textile Institute, 22 (2-3-4): 2–5.
36. Fung, W. 2002. Flame retardancy. In *Coated and Laminated Textiles*, Woodhead Publishing, Cambridge, U.K., pp. 71–77.
37. BS 6307:1982, ISO 6925-1982 Method for determination of the effects of a small source of ignition on textile floor coverings (methenamine tablet test).
38. BS 4790:1987-Method for determination of the effects of a small source of ignition on textile floor coverings (hot metal nut method).
39. ASTM E648-00:2000 Standard test method for critical radiant flux of floor-covering systems using a radiant heat energy source.
40. NFPA 253:2006 Standard method of test for critical radiant flux for floor covering systems using a radiant heat energy source.
41. BS EN 14115:2002, British Standard for burning behavior of materials for marquees, large tents and related products.
42. NFPA 701:2004 Standard Methods of fire tests for flame propagation of textiles and films.
43. ASTM E84-07a:2007 Standard Test Method for surface burning characteristics of building materials.
44. Fung, W. 2000. Textiles in transportation. In *Handbook of Technical Textiles*, Horrocks, A.R. and Anand, S.C. (Eds.), Woodhead Publishing, Cambridge, U.K., Chapter 18, pp. 490–528.
45. Sorathia, U. 2008. Flame retardant materials for maritime and naval applications. In *Advances in Flame Retardant Materials*, Horrocks, A.R. and Price, D. (Eds.), Woodhead Publishing, Cambridge, U.K., Chapter 19.
46. Kandola, B.K. and Kandare, E. 2008. Composites having improved fire performance. In *Advances in Fire Retardant Materials*, Horrocks, A.R. and Price, D. (Eds.), Woodhead Publishing Ltd., U.K., Chapter 16.
47. Kandola, B.K., Horrocks, A.R., Myler, P., and Blair, D. 2002. The effect of intumescent on the burning behavior of polyester-resin-containing composite. *Composites: Part A*, 33: 805–817.
48. Kandola, B.K., Horrocks, A.R., and Rashid, M.R. 2006. Effect of reinforcing element on burning behavior of fiber-reinforced epoxy composites. In *Recent Advances of Flame Retardancy of Polymeric Materials*, Lewin, M. (Ed.), *Proceedings of the 17th Conference*, BCC, Stamford, CT.
49. Kandola, B.K., Myler, P., Horrocks, A.R., Herbert, K., and Rashid, M.R. 2006. Effect of fibre type on fire and mechanical behaviour of hybrid composite laminates. In *Proceedings of the 2006 SAMPE Fall Technical Conference*, November 6–9, Dallas, TX.
50. Kandola, B.K., Horrocks, A.R., Price, D., and Coleman, G.V. 1996. Flame retardant treatments of cellulose and their influence on the mechanism of cellulose pyrolysis. *J. Macromol. Sci. –Rev. Macromol. Chem. Phys.*, C36(4): 721–794.
51. Lewin, M. and Weil, E.D. 2001. Mechanism and modes of action in flame retardancy of polymers. In *Fire Retardant Materials*, Horrocks, A.R. and Price, D. (Eds.), Woodhead Publishing Ltd./CRC, Cambridge, U.K./Boca Raton FL, pp. 31–68.
52. Wyld, O. 1735. British Patent 551.
53. Horrocks, A.R. 2008. Flame retardant textile coatings and laminates. In *Advances in Fire Retardant Materials*, Horrocks, A.R. and Price, D. (Eds.), Woodhead Publishing Ltd., Cambridge, U.K., Chapter 7.
54. Horrocks, A.R. and Roberts, D. 1998. Minimization of formaldehyde emission. In *Proc. Conf. Ecotextile'98: Sustainable Develop.*, Bolton, U.K., Woodhead Publishing Ltd., Cambridge, U.K., 1999.
55. Hall, M.E., Horrocks, A.R., and Seddon, H. 1999. The flammability of Lyocell. *Polym. Deg. Stab.*, 64: 505–510.
56. Zhou, H. 1995. Now and future of flame retardancy of fabrics, *Guangxi Textile Sci. Technol.*, 24(2): 35–39.
57. Achwal, W.B. 1987. Flame retardant finishing of cotton and silk fabrics. *Colourage*, 6: 16–30.
58. Guan, J.P. and Chen, G.Q. 2006. Flame retardancy finish with an organophosphorus retardant on silk fabrics. *Fire Mater.*, 30(6): 415–424.

59. Davies, P.J., Horrocks, A.R., and Alderson, A. 2005. The sensitization of thermal decomposition of APP by selected metal ions and their potential for improved cotton fabric flame retardancy. *Polym. Deg. Stab.*, 88: 114–122.
60. Horrocks, A.R., Davies, P.J., Alderson, A., and Kandola, B.K. 2005. The challenge of replacing halogen flame retardants in textile applications: Phosphorus mobility in back-coating formulations'. In *Proceedings of 10th European Meeting of Fire Retardant Polymers, FRMP'05*, Berlin, September 6–9, 2005; *Advances in the Flame Retardancy of Polymeric Materials: Current perspectives*, Scharrel, B. (Ed.), Norderstedt, Germany, 2007, pp. 141–158.
61. Horrocks, A.R., Wang, M.Y., Hall, M.E., Sunmonu, F., and Pearson, J.S. 2000. Flame retardant textile back-coatings. Part 2. Effectiveness of phosphorus-containing flame retardants in textile back-coating formulations. *Polym. Int.*, 49: 1079–1091.
62. Horrocks, A.R., Davies, P., Alderson, A., and Kandola, B.K. 2007. The potential for volatile phosphorus-containing flame retardants in textile back-coatings. *J. Fire Sci.*, 25(6): 523–540.
63. Giraud, S., Bourbigot, S., Rochery, M., Vroman, I., Tighzert, L., Delobel, R., and Poutch, F. 2005. Flame retarded polyurea with microencapsulated ammonium phosphate for textile coating. *Polym. Deg. Stab.*, 88: 106–113.
64. Saihi, D., Vroman, I., Giraud, S., and Bourbigot, S. 2005. Microencapsulation of ammonium phosphate with a polyurethane shell part I: Coacervation technique. *React. Funct. Polym.*, 64: 127–138; 66(2006): 1118–1125.
65. Bourbigot, S., Le Bras, M., Duquesne, S., and Rochery, M. 2004. Recent advances for intumescent polymers. *Macromol. Mater. Eng.*, 289(6): 499–511.
66. Devaux, E., Rochery, M., and Bourbigot, S. 2002. Polyurethane/clay and polyurethane/POSS nanocomposites as flame retarded coating for polyester and cotton fabrics. *Fire Mater.*, 26(4–5): 149–154.
67. Tolbert, T.W., Dugan, J.S., Jaco, P.J., and Hendrix, J.E., Spring Industries Inc., U.S. Patent 333174, 4 April 1989.
68. Von Bonin, W. and Von Gizycki, U., Bayer, A.G., Europ. Patent 91121065.6, 9 December 1991.
69. Horrocks, A.R., Anand, S.C., and Hill, B.J., U.K. Patent GB 2279084 B, 20 June 1995.
70. Kandola, B.K. and Horrocks, A.R. 2000. Complex char formation in flame-retarded fibre intumescent combinations—IV. Mass loss calorimetric and thermal barrier properties. *Fire Mater.*, 24: 265–275.
71. Horrocks, A.R. and Davies, P.J. 2000. Char formation in flame-retarded wool fibres, Part 1. Effect of intumescent on thermogravimetric behaviour. *Fire Mater.*, 24(3): 151–157.
72. Simionescu, C.I., Dénes, F., Macoveanu, M.M., Cazacu, G., Totolin, M., Percec, S., and Balaur, D. 1980. Grafting of rayon fabrics with phosphorus containing polymers in cold plasma in order to obtain flame-retardant materials. *Cell. Chem. Technol.*, 14: 869–883.
73. Tsafack, M.J. and Levalois-Grützmaier, J. 2006. Plasma-induced graft-polymerisation of flame retardant monomers onto PAN fabrics. *Surf Coat Tech.*, 200: 3503–3501.
74. Vannier, A., Duquesne, S., Bourbigot, S., Delobel, R., Magniez, C., and Vouters, M. 2006. The use of plasma induced polymerization technology to develop fire retardant textiles. *Proceeding of International Conference on Textile Coating & Laminating*, November 2006, 8–29, Barcelona, Spain.
75. Zhang, S., and Horrocks, A.R. 2003. A review of flame retardant polypropylene fibers. *Prog. Polym. Sci.*, 28: 1517–1538.
76. Bourbigot, S., Gilman, J.W., and Wilkie, C.A. 2004. Kinetic analysis of the thermal degradation of polystyrene–montmorillonite nanocomposite. *Polym. Deg. Stab.*, 84(3): 483–492.
77. Gong, F., Feng, M., Zhao, C., Zhang, S., and Yang, M. 2004. Thermal properties of poly(vinyl chloride)/montmorillonite nanocomposites. *Polym. Deg. Stab.*, 84(2): 289–294.
78. Lewin, M. 2003. Some comments on the modes of action of nanocomposites in the flame retardancy of polymers. *Fire Mater.*, 27(1): 1–7.
79. Horrocks, A.R. and Kandola, B.K. 2007. Potential applications of nanocomposites for flame retardancy. In *Flame Retardant Polymer Nanocomposites*, Morgan, A.B. and Wilkie, C.A. (Eds.), Wiley-VCH, Verlag GmbH & Co, KGaA, Hoboken, NJ, Chapter 11.
80. White, L.A. 2004. Preparation and thermal analysis of cotton-clay nanocomposites. *J. Appl. Polym. Sci.*, 92(4): 2125–2131.
81. SolarSKI, S., Mahjoubi, F., Ferreira, M., Devaux, E., Bachelet, P., Bourbigot, S., Delobel, R., Murariu, M., Da Silva Ferreira, A., Alexandre, M., Degée, P., and Dubois, P. 2007. (Plasticized) Polylactide/clay nanocomposite textile: Thermal, mechanical, shrinkage and fire properties. *J. Mater. Sci.*, 42(13): 5105–5117.
82. Wang, D.-Y., Wang, Y.-Z., Wang, J.-S., Chen, D.-Q., Zhou, Q., Yang, B., and Li, W.-Y. 2005. Thermal oxidative degradation behaviours of flame-retardant copolyesters containing phosphorous linked pendent group/montmorillonite nanocomposites. *Polym. Deg. Stab.*, 87: 171–176.

83. Horrocks, A.R., Kandola, B.K., Smart, G., Zhang, S., and Hull, T.R. 2007. Polypropylene fibers containing dispersed clays having improved fire performance. I. Effect of nanoclays on processing parameters and fiber properties. *J. Appl. Polym. Sci.*, 106(3): 1707–1717.
84. Kandola, B.K., Smart, G., Horrocks, A.R., Joseph, P., Zhang, S., Hull, T.R., Ebdon, J., Hunt, B., and Cook, A. 2008. Effect of different compatibilizers on nanoclay dispersion, thermal stability and burning behavior of polypropylene–nanoclay blends. *J. Appl. Polym. Sci.*, 108(2): 816–824.
85. Bourbigot, S., Le Bras, M., Flambard, X., Rochery, M., Devaux, E., and Lichtenhan, J. 2005. Polyhedral oligomeric silsesquioxanes: Application to flame retardant textiles. *Fire Retardancy of Polymers: New Applications of Mineral Fillers*, Le Bras, M., Bourbigot, S., Duquesne, S., Jama, C., and Wilkie, C.A. (Eds.), Royal Society of Chemistry (Pub), U.K., pp. 189–201.
86. Bellayer, S., Bourbigot, S., Flambard, X., Rochery, M., Gilman, J.W., and Devaux, E. 2004. Polymer/MWNTs nanocomposite yarns and fabrics: Processing, characterization and flammability and thermal properties. *Proceedings of the 4th Autex Conference*, ENSAIT, Roubaix 2004, O-3W1.
87. Bourbigot, S., Devaux, E., and Flambard, X. 2001. Flammability of polyamide-6/clay hybrid nanocomposite textiles. *Polym. Deg. Stab.*, 75(2): 397–402.
88. Padbury, S.A., Horrocks, A.R., and Kandola, B.K. 2003. The effect of phosphorus-containing flame retardants and nanoclay on the burning behaviour of polyamides 6 and 6.6. *Proceedings of the 14th Conference 'Advances in Flame Retardant Polymers*, Stamford, Norwalk, CT: Business Communications; 2003.
89. Horrocks, A.R., Kandola, B.K., and Padbury, S.A. 2005. The effect of functional nanoclays in enhancing the fire performance of fibre-forming polymers. *J. Text. Inst.*, 94: 46–66.
90. Ratnayaka, A. High performance fire retardant synthetic fibres incorporating nanocomposites, M.Sc. Thesis, University of Bolton, U.K., May 2007.
91. Bourbigot, S. and Flambard, X. 2002. Heat resistance and flammability of high performance fibres: A review. *Fire Mater.*, 26(4–5): 155–168.
92. Weller, D.E. 2007. (to Owens Corning), European Patent Appl. 1,771,615.
93. Lee, Y.M. and Barker, R. 1987. Thermal protective performance of heat-resistance fabrics in various high intensity heat exposures. *Text. Res. J.*, 57(3): 123–132.

25 FR Design for Foam Materials

Michele Modesti and Alessandra Lorenzetti

CONTENTS

25.1	Introduction.....	763
25.2	Polyurethane Foams.....	765
25.2.1	Reactive Flame-Retardants.....	765
25.2.2	Additive Flame-Retardants.....	766
25.2.2.1	Halogen Flame-Retardants.....	767
25.2.2.2	Phosphorus Flame-Retardants.....	767
25.2.2.3	Expandable Graphite.....	770
25.2.2.4	Melamine and Its Derivative.....	771
25.2.2.5	Inorganic Flame-Retardants.....	772
25.3	Polystyrene Foams.....	773
25.4	Other Foams.....	775
25.4.1	Polyolefin Foams.....	775
25.4.2	Polyvinyl Chloride Foams.....	775
25.4.3	Phenolic Foams.....	776
25.5	Polymer Nanocomposites Foams.....	776
	References.....	777

25.1 INTRODUCTION

Polymeric foams are cellular materials and, like all organic materials are combustible but their burning behavior differs from that of the bulk polymer. Foamed materials are a two-phase system built-up by many cells comprising solid walls and struts and filled with a gaseous phase (mainly blowing agent or air). This particular structure is responsible of typical features of foams like low thermal conductivity and high surface area, which confers to such materials also high flammability. Differences occur also between closed or open cell foams. In closed cell foams, the foams cells are isolated from each other and cavities are surrounded by complete cell walls and filled with the blowing agent, which may be flammable. Open cell foams are instead made up of broken cell walls and therefore cells contain air.

Fire involving polymeric cellular materials develops in extremely rapid way when compared with solid polymer, giving rise to high temperatures and producing large amount of smoke in a short period of time. This is not due to their chemical nature but to their morphological structure and then, even if the fuel contribution per unit volume may be low (due to their low density), the rate of heat release (HRR) is high. Owing to their cellular structure, foams possess a high surface area per unit mass and this results in almost complete pyrolysis of combustible matter nearby the radiation and flame, while the material is in immediate contact with atmospheric oxygen. Consequently, foams have a greater tendency to burn than solid material. In the case of closed cell rigid foams (e.g., foams used for thermal insulation), the low thermal conductivity causes a slow heat transfer, therefore bringing to a fast heat buildup on the surface, thus decreasing the time for reaching the ignition temperature; this, obviously, contributes significantly to pyrolysis and burning.¹ Moreover, during pyrolysis of closed cell foams, an increased amount of flammable compounds may be released due

to the potential presence of flammable blowing agent inside the foam cells. Otherwise, in open cell foam the pyrolysis and burning may be accelerated because the oxygen, which feeds the fire, is readily available within the foam, and this can lead to smoldering; also a chimney effect can occur that speeds up the propagation.^{2,3}

For common thermally thick combustible materials (greater than a few millimeters) the time to ignition is proportional to the product $k \cdot \rho \cdot c$ (where k is the thermal conductivity, ρ is the density, and c is the heat capacity), which represents the thermal inertia of the sample. Thermal inertia characterizes the rate of surface temperature rise of the material when exposed to heat. Low values of thermal inertia lead to a rapid temperature rise for a given applied heat flux and hence, to a rapid ignition.⁴ Polymeric foams have much lower thermal conductivity and density than the corresponding solid materials, thus the surface temperature of the first heats up more rapidly than that of the latter. Foam surface may reach the ignition temperature 10 times faster than the solid polymer.⁵

Several studies have been carried on the effect of foam density, mean cell size, surface area on thermal stability, and flammability properties of polymeric foams. Stone et al.⁶ studied the effect of density over a wide range on the combustion characteristics of flexible polyurethane (PU) foams; density was varied over a wide range by thermally compressing foams to varying degree. The authors reported evidences that the thin molten film coming from hot pressing of the foam is not a factor in determining OSU (Ohio State University) calorimeter⁴ performance. Three kinds of foams were analyzed: char-forming inorganic filled foams, melamine-filled melting foams, and unfilled foams. They showed that peak of heat release rate (PHRR) is fairly constant with density for char-forming foams, while it increases for melting and unfilled foams. Considering the PHRR/density ratio, all foams showed similar behavior: the ratio showed an extraordinary drop as the density was raised to approximate the density of an unfoamed polymer. Similar studies were reported by Schrock et al.,⁷ where they compared the flammability of polyurethane flexible foam with different densities, also considering the variation in chemical structure because they changed the polyurea amounts and melamine content as well. They reported that the results of OSU calorimeter test indicated that density dominates trends in combustion over polymer morphology. Bian et al.⁸ studied the effect of foam density of cast molded PU rigid foams filled with expandable graphite (EG) on flammability properties through the use of limiting oxygen index and horizontal and vertical burning tests, and achieved the same results: the fire behavior is better at higher densities because of a more compact burned layer. Lefebvre et al.⁹ reported statistical studies on correlation between some physical properties and FMVSS 302 (Federal Motor Vehicle Safety System); physical properties analyzed include density and porosity, measured as foam resistance to the passage of a constant flow of air. They showed a lower flame spread for higher density polyurethanerigid foams in FMVSS 302 test, but they did not reveal any correlation between FMVSS 302 results and foam porosity measured as airflow. Also, Zammarano et al.¹⁰ studied the effect of foam density and airflow on PHRR using a modified cone calorimeter that measures HRR while taking into account dripping effect and heat feedback due to the formation of a pool-fire.¹¹ The density was changed increasing talc concentration (0–20 wt%). For all talc samples the PHRR increases with the corrected density (density calculated by subtracting the mass of talc from the total mass of the specimen and keeping the volume unchanged), as it can be expected, because the amount of combustible volatiles produced during thermal degradation is proportional to the corrected density of the foams. Thus, high density leads to higher PHRR but also to lower flame spread rate, as already reported by Lefebvre et al.⁹ The same authors reported that there is no evident correlation between PHRR and airflow in their test configuration.

Similar studies on foam morphology were reported by Williams et al.^{12,13} for polyimide foams with different densities or surface area; also two different chemical formulations were used. Comparing foams with the same chemical composition, it was shown that no consistent correlation could be found between PHRR and foam density or open cell content while greater correlation is proved between the surface area and PHRR because they showed the same trend. Foams having the same density but different surface area and chemical composition show great variation of PHRR (up to 50%) both at 75 and 50 kW/m².

Burning behavior differs also according to the foam type. Thermoplastic foams such as polystyrene and polyolefin foam, when exposed to heat, soft and melt without forming char and hence they tend to burn with flaming droplets.⁴ A similar behavior is observed also for PUF. In these systems, the produced melt promotes severe dripping that increases the fire hazard. In fact, this downward flow of flaming liquid often results in a pool-fire that boosts HRR due to a significant increase in the burning area and to feed back between the flame on the pool-fire and the residual foam.¹⁴ Otherwise, that is not the case for flame-retarded grades, which withdraw rapidly from the flame zone due to the melting and shrinking so that ignition does not occur frequently. Thermosetting foams do not withdraw from the flames on account of their three-dimensional cross-linked structure but are not easy to ignite. Rapid charring occurs and the carbonized layer protected the underlying foam from further attack by flames and causes extinction.¹

Many polymer foams are available, but the foam market is mainly based on polyurethane, polystyrene, polyolefin, and polyvinylchloride foams and this market is still increasing owing to environmental concerns related to energy saving. Therefore, in the following sections, flame retardancy of such foams will be reported; moreover, owing to their particular fire behavior some details for phenolic foams will also be shown.

25.2 POLYURETHANE FOAMS

Polyurethane foams, both rigid and flexible, are one of the most widely used polymeric foams. Rigid foam are used in general purpose as well as high-tech applications such as aeronautics, sports, leisure, railway and road transport, cooled transport, nautical structural components, blades of wind turbines, thermal and acoustic insulation in construction as well; flexible PU foams are used in upholstery and bedding and very often they are covered by other materials, which influence the fire behavior of the underneath foam. For practical use of these foams, fire-retardant properties are required to fulfill different requirements depending on national or international standard and end-use application. Several reviews on flame-retardants for polyurethane foams have been recently reported (e.g., by Levchik and Weil^{15–17} and by Wang¹⁸). Flame-retardancy of PU foam is achieved through use of reactive or additive flame-retardants: the first are chemically linked to the polymer backbone while the latter are added to foam formulations as separate compounds.

25.2.1 REACTIVE FLAME-RETARDANTS

With regard to reactive flame-retardants, two routes can be followed to improve thermal stability and fire behavior of PU foams: use of brominated or phosphorus-containing polyol or, for rigid foams, the introduction inside polymer backbone of more thermally stable structure than urethane, mainly isocyanurate, but also uretidione rings or carbodiimide.¹⁹

Several brominated polyols are commercially available, such as tetrabromophthalic anhydride based ester, dibromoneopentyl glycol, and tribromoneopentyl alcohol;¹⁸ generally they are used in conjunction with polyether or polyester polyols for the development of formulations having high fire performance²⁰; for example, suitably formulated PU foam may be classified as “B” according to the new European standard based on the single burning item (SBI) test.²¹ There are also blend of reactive bromine polyol and liquid phosphate ester, which results in a lower viscosity liquid for improving processing and storage characteristics.²² It was reported that aliphatic bromine, aromatic bromine, phosphorus, and also aliphatic chlorine caused synergistic effects in fire-extinguishing of pentane-blown foams containing 2,3-dibromo-2-butene-1,4-diol.²³

Also phosphorus- and nitrogen-containing polyols are shown to be effective in flame retardancy of PU foams²⁴; such as polyols based on phosphonic acid ester or obtained by partial or full substitution of methylol groups of tetrakis(hydroxymethyl)phosphonium chloride with amine; several examples of such polyols were reported by Levchik and Weil.¹⁵ Rigid PU foam modified with these polyols showed improved oxygen index values; moreover better results were achieved with higher functionality polyols.

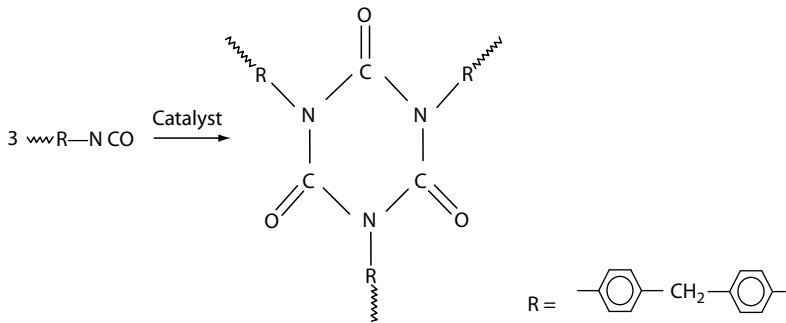


FIGURE 25.1 Formation of PIR.

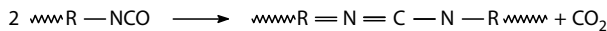


FIGURE 25.2 Formation of carbodiimide linkages.

Other polyols modifications include the use of other cyclic compounds of phosphorus and nitrogen, e.g., polyphosphazene, which are both incorporated for making a prepolymer²⁵ and partly substituting them to polyols.²⁶ Both studies showed the effectiveness of polyphosphazenes in enhancing charring of polymer and thus preventing further combustion. When using suitable formulation, the limiting oxygen index is higher than 30%, comparable with that of highly flame-retarded PUR foams, although a drawback is represented by poor mechanical properties.

Another way of improving flame retardancy through a reactive approach is based on reactions involving isocyanate. For achieving high thermal stability and better fire behavior, often isocyanurate groups were introduced in PU rigid foam. Isocyanurate (or trimer) were obtained by cyclotrimerization of the isocyanate to polyisocyanurate rings (PIR) in the presence of a suitable catalyst (Figure 25.1):

Under the conditions of reaction, the carbodiimide linkage obtained by the condensation of two isocyanate groups cannot be excluded (Figure 25.2). Some polyisocyanurate foams have very high thermal stability and may require no or very low flame-retardants addition to pass fire tests¹⁵ but their physical properties are unsatisfactory. Hence, the presence of urethane bonds is essential, as it lowers the cross-linking density of the matrix and therefore the friability characteristics²⁷ to obtain foams with suitable mechanical properties. The content of isocyanurate groups is characterized by the NCO index,²⁸ which represents the excess of NCO groups with respect to hydrogen-active compounds: the higher the NCO index the higher the isocyanurate content in the foams. Further improvements of fire behavior of PU foams were tried by modifying MDI (4,4'-diphenylmethane diisocyanate) isocyanate with dicarboxylic acid or anhydride (such as adipic acid or trimellitic anhydride) to produce a modified isocyanate, containing amide or imide groups, which in the following cyclotrimerization reaction, leads to amide- or amide-imide modified polyisocyanurate-polyurethane (PIR-PUR) foams. It was shown that such materials have greater thermal stability than PURs or unmodified PIRs, but they do not exhibit improved fire behavior in cone calorimeter test.²⁹

25.2.2 ADDITIVE FLAME-RETARDANTS

Additive flame-retardants may be more easily incorporated in polyurethane formulation. Several class of compounds have been used to improve flame retardancy of PU foams; such compounds are halogen- (very often chloroalkyl-phosphate) or phosphorous-based compounds, although also other substances, like as EG, melamine, aluminum trihydrate and magnesium hydroxide, may be used.

25.2.2.1 Halogen Flame-Retardants

While reactive halogen compounds are mainly based on bromine, additive halogen containing flame-retardants are based on chlorine. Several kind of chlorophosphate are reported in literature as flame-retardants for both rigid and flexible polyurethane foams: tris(chloro-ethyl)-phosphate (TCEP), tris(chloro-isopropyl)-phosphate (TCPP), tris(1,3-dichloro-isopropyl)-phosphate (TDCP), tetrakis(chloro-ethyl)ethylene diphosphate (TCED), dichloroethyl methylphosphate.³⁰ All these compounds are very effective and versatile, but they show some negative effects, due to chlorine, since they give rise to toxic and dense smoke,³¹ which chokes the people in the toxic and acidic fumes and causes costly damage to equipment; moreover, materials which contain halogenated compounds may be recycled with greater difficulty.

Feske and Brown³² used TCPP and TCEP in conjunction with brominated polyol and showed that these are more effective than other nonhalogenated phosphorous-based flame-retardants and that TCPP performed better than TCEP. One of the most widely used commercial phosphor-halogen flame-retardant for polyurethane foam is TDCP, which has been studied by Ravey et al.^{33,34} TDCP has a greatly reduced volatility, much lower water solubility, and high stability toward the amine catalysts used in foam manufacture.³⁵ Ravey et al. showed that, even if about 80% of TDCP volatilizes at 200°C, it acts both in condensed and vapor phase. The extent of activity in each phase depends on the way of specimen ignition: when top-down burning takes place, the action is mainly in condensed phase through the development of a compact char layer, while for bottom-up ignition large amount of TDCP enters the flame and hence the flame-retardant action is mainly in vapor phase. Najafi-Mohajeri et al.³⁶ found out that it may reduce the PHRR by 21%, even if better results were obtained for nonfoamed PU polymer such as thermoplastic polyurethane (TPU); moreover, the presence of halogen causes a significant increase in smoke and CO production. Use of TCCP and TDCP in flexible PU foam were reported by Bastian and Lefebvre^{9,37} in conjunction with melamine. Both are effective in flame retardancy as they lower the first PHRR but due to their different degradation temperatures (TCCP degrades earlier than TDCP), TDCP shows synergism with melamine while TCCP does not.

International flammability standards, which can be achieved by the use of halogenated phosphate esters include

- For flexible PU foam: BS4735, UL94 HF1, Italian CSE RF4, Consumer Protection Act 1988, BS5852 schedule 1, Crib 5, California Bulletin 117, Federal Motor Vehicles Safety Standard No. 302
- For rigid PU foam: Standards of performance to BS 476 parts 6 and 7, French Epiradiateur NFP92-501, German DIN 4102³⁸

25.2.2.2 Phosphorus Flame-Retardants

Extensively used flame-retardants for PU foams are phosphorous compounds which bring the formation of a protective char layer, even if a partial gas phase action is deemed since long.³⁹ According to recent research of Modesti and Lorenzetti (unpublished results) for polyurethane foams, it seems that the extent of gas phase action with respect to condensed phase may depend on the oxidation state of phosphorus, as already reported by Schartel et al.⁴⁰ for epoxy resins. Phosphorus flame-retardants for PU are based on phosphate and phosphonate, which have hydroxyl groups to bind to the polyurethane matrix but also phosphinate may be successfully used.⁴¹ Dealing with phosphate, the more extensively used compounds are triethyl phosphate (TEP) and ammonium polyphosphate (APP), which are used since long in flame-retarded PU foams; also aromatic phosphates, such as triphenylphosphate and biphenyltolylol phosphate⁴² are used. The use of sodium dihydrogenphosphate in mixture with sodium hydrogen sulfate, trisodium pyrophosphate is also proposed in literature for PU rigid foams.⁴³ When dealing with water blown flexible PU foams, there are suitable phosphorus compounds that have to be used to avoid scorch and to reduce VOC (volatile organic compound)

emission, as, for example, triarylphosphates, such as isopropyl phenyl diphenyl phosphate, sometimes in combination with bromine-containing additive, other than the now-discontinued pentabromodiphenyl ether.⁴⁴ Aromatic phosphates are preferred because it is highly probable that the appearance of scorch is related to the interaction of aliphatic phosphates and aromatic amines. Scorch is, in fact, a kinetically controlled phenomenon and scorching foams are those foams, which are able to develop color in the timescale of the industrial foaming process, whereas nonscorching foams are those which need more time for yellowing. Some fire retardants, such as aliphatic phosphates, tend to accelerate scorching by interaction with aromatic amines structures, deriving from hydrolysis of isocyanates, in timescale and temperature compatible with the industrial foaming process, thus leading to the formation of easily oxidizable structures.⁴⁵ Aryl phosphate cannot alkylate amino groups and hence do not aggravate scorch.

Phosphates typically act leading to the formation of a compact char layer owing to the formation of polyphosphoric acids that catalyze the carbonization of the host polymer⁴⁶; otherwise, also a radical mechanism in the gas phase is believed to occur for some phosphorus compounds. Since most of the phosphorus-containing flame-retardants act via the same reaction mechanism, it can be assumed that the flame-retarding effect increases with increasing phosphorus content in the polymer. However, nonreactive liquid phosphorus flame-retardants have the disadvantage that they soften the polymer and hence only limited amounts of such compounds may be used (about 10–15 phr based on polyol); reactive phosphorus compounds do not show this plasticizing effect but they are more expensive. However, the plasticizing effect of nonreactive phosphorus FR are often used to decrease the viscosity of raw materials (polyols or isocyanate), particularly when high amount of filler are employed.

APP is solid filler and hence has no plasticizing effect; even if it is believed that it acts only in solid phase, it is quite effective. APP may be used also in intumescent systems, which bring the formation of very porous char structures. Intumescent systems require an acid source, a charring agent, and a blowing agent. The acid source may be APP that during its degradation catalyzes the dehydration reaction, favoring the char formation. The charring agent, i.e., the carbon source, is generally a polyhydric compound (e.g., pentaerythritol, polyvinylalcohol, melamine-formaldehyde resins) but in case of polyurethane foams, the charring agent is the polymer itself. Finally, the blowing agent may be APP itself or, better, APP may be used in conjunction with melamine or its derivatives (melamine cyanurate, melamine phosphate, melamine pyrophosphate) in suitable ratio (e.g., 3:1), giving synergistic effect. It is assumed that blowing function arises from the evolution of volatile products formed by thermal treatment, but a blowing effect may also arise from the product evolved in the charring step. Intumescence occurs only if the chemical reactions and physical process take place in the appropriate sequence as the temperature increases: the blowing gases must evolve at a suitable stage of the gelation process. The use of APP or APP and cyanurate melamine (MC) in PIR-PUR and polyurethane foams were reported by Modesti and Lorenzetti.^{47,48} The results obtained for PIR-PUR foams showed that the PHRR is not affected by APP content while in case of APP-MC filled foams, the PHRR decreases when the filler quantity is increased, owing probably to the endothermic decomposition reaction of MC, the sublimation of melaminic compound, and the formation of a more stable intumescent char layer. When a compact char layer is formed (i.e., when APP is used alone) the CO production increases because the continuous char developed decreases the amount of oxygen reaching the underlying polymer thus promoting CO formation. The presence of melamine enables a reduction of CO production, probably because of the formation of N-C-P-moieties⁴⁹ in the char, which reduces the amount of C in the gas phase. Otherwise, dealing with PUR foams, it was shown that the mixed APP-MC system is not better than APP alone, even if it is fairly better than MC alone. This difference may be due to the different polymeric matrix, which constitutes the carbon source of the intumescent system: while PIR-PUR foams are characterized by the formation of a very compact char layer when exposed to high temperature, even in the absence of filler, PUR foams are not. Then, in the first polymer, the carbon source is suitable for the development of the intumescent system while in the second it is not.

Other phosphorus compounds used in flame retardancy of PU foams, mainly for rigid ones, are dimethyl methylphosphonate (DMMP), diethyl ethylphosphonate (DEEP), and more recently dimethyl propylphosphonate (DMPP). DMMP is the most effective, because it contains P amount near the maximum possible for a phosphorus ester (25 wt%), and therefore on a weight basis is highly efficient as a flame-retardant; DEEP, which is claimed to be less susceptible to undesirable interactions with haloaliphatic components, such as blowing agents or with amine catalysts, and DMPP have lower phosphorus content (i.e., 18.6 and 20.3 wt%, respectively) and hence are slightly less effective but they have the advantage that they are not classified as toxic or harmful. It shall also be highlighted that some phosphonates are controlled by the UN as dual-purpose chemicals. This means that they are considered as potential precursors to chemical weapons manufacture and consequently there is a control placed on their sale and distribution. The regulation does not consider the practicality or feasibility of the synthesis, it is applied generally to any phosphonate where there is a methyl, ethyl, or propyl group attached directly to a phosphorus atom. This classification has no relevance to the toxicity profile of the flame-retardant itself.⁵⁰

Other phosphorus compounds, which can be successfully employed in PU foams are hypophosphites (or phosphinate) based on sodium, calcium, magnesium, or zinc. The use of these compounds is widely reported in scientific literature for polyamide, poly(1,4-butylene terephthalate) and epoxy resin by Braun et al.^{51,52} for PU foam the use is proposed by Modesti and Lorenzetti^{41,53} and in some patents.⁵⁴ Also synergism between hypophosphites and some nitrogen-containing compounds (such as cyanurate melamine, melamine phosphate, or polyphosphate) are reported.⁵² Improvements on thermal stability and limiting oxygen index were achieved when 20 wt% of hypophosphite is used in PU rigid foam⁴¹; better results were obtained using aluminum-based hypophosphite, probably because of the lower decomposition temperature of these compounds with respect to the other ones (calcium- and magnesium-based hypophosphites). Cone calorimeter tests of PU rigid foams filled with aluminum hypophosphite showed that such a compound is an effective flame-retardant for polyurethane foams as it lowers the PHRR and the total heat evolved (THE) (Figure 25.3); otherwise a slight increase of smoke density was also observed. The results obtained showed that the flame retardancy action takes place both in condensed and gas phases.

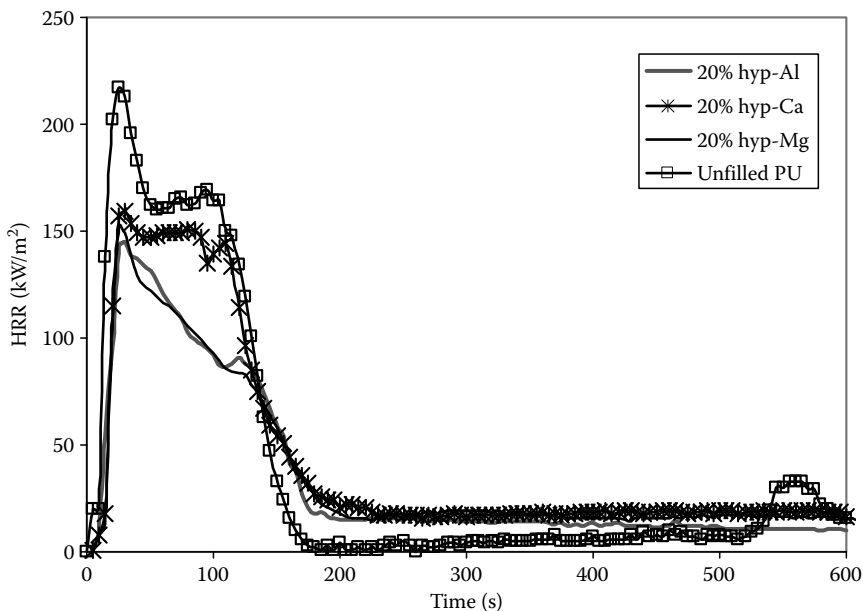


FIGURE 25.3 HRR for unfilled PU foam and aluminum (hyp-Al), calcium(hyp-Ca), and magnesium (hyp-Mg) hypophosphite-filled PU foams.

Also red phosphorus (RP) has been proposed for flame retardancy of polyurethane and polyisocyanurate-polyurethane foams.^{55,56} To avoid the risk of handling powdered RP (i.e., to overcome phosphorus flammability and phosphine generation during storage and processing) RP dispersed in polyol may be used. RP is the more concentrate source of phosphorus; therefore, it is an effective flame-retardant at low concentration (2–10 wt%). It was reported⁵⁵ that the presence of RP improves the fire reaction of the PIR-PUR foams filled with EG: in fact, foams containing both EG and RP, are rated as DIN 4102-B2 in the presence of 10 wt.% of EG, while in the presence of EG only 57.15 wt.% of filler is needed to obtain a B2 pentane blown PIR-PUR foam; moreover, the use of RP increases also oxygen index (O.I.).

25.2.2.3 Expandable Graphite

The use of EG in flexible PU foams was firstly patented by Dunlop limited in 1987⁵⁸; since then, the use of EG was increased, both in flexible and rigid foam, because of its effectiveness and since it is a halogen-free flame-retardant. Several authors dealt with EG for flame retardancy of flexible and rigid PU foams.^{57,59–61} EG may be considered simultaneously as the catalyst, the char-forming agent, and the blowing agent, owing to its chemical structure. The EG is, in fact, based on natural graphite flakes with intercalated acids. Depending on the raw material and the acid treatment, the expansion rate is up to 250 times its original volume. Several grades of EG, characterized by different expansion temperature (from 150°C to 220°C), are available depending on acid used in intercalation: grades treated with sulfuric acids begin to expand to 160°C or 220°C; with nitric or acetic acid the expansion starts at about 150°C. The right choice is based on the onset temperature of the decomposition of the polymer: the flame-retardant has to be active as soon as the polymer begins to decompose. If it acts too soon, the action will be completely finished when the polymer starts to decompose and release volatile flammable products; if it acts too late, obviously, the degradation has already involved the whole polymer. For polyurethane foams, considering their own decomposition onset, the suitable EG grades are those modified by sulfuric acid; moreover, in this way a catalyst for dehydration reaction is readily available, in spite of nitric or acetic acid, which are not effective as catalysts for this reaction. According to Camino et al.,⁶² the expansion of EG is due to a redox process between H₂SO₄, intercalated between graphite layers and the graphite itself that originates the blowing gases according to the reaction:



Several authors showed that EG does not increase the thermal stability of filled PU foams, while leads to sensible improvements of fire behavior. Shi et al.⁶⁰ studied the effect of particle sizes EG on the fire-retardant properties of high-density rigid polyurethane foam. Samples of EG with different particle sizes were obtained by pulverization in an ultra-high-speed mixer for 4 and 13 min, respectively. It was shown that the received (EG0) and 4 min pulverized EG (EG4) efficiently improved the fire-retardant properties of PU rigid foams, whereas 13 min pulverized EG (EG13) did not. The char of the burned composites filled with EG0 and EG4 covered the whole surface of the samples and formed a complete physical barrier. This barrier material prevented combustible gases from feeding the flame and also isolated oxygen efficiently from the burning material. EG13 did not produce enough char to cover the whole surface of the burning sample, resulting in poor fire-retardant property of the RPUF composites. Modesti and Lorenzetti⁶³ showed that *n*-pentane blown foams containing at least 15 wt% of EG can be classified as DIN 4102-B2 materials. Moreover, in presence of 25 wt% of EG, the PHRR lowers itself by about 60% and the mean HRR value by about 80%. Otherwise, the use of EG leads to an increase in the CO/CO₂ weight ratio, probably because in the presence of EG the equilibrium between CO and CO₂ moves toward right owing to the higher carbon concentration, thus favoring CO development:



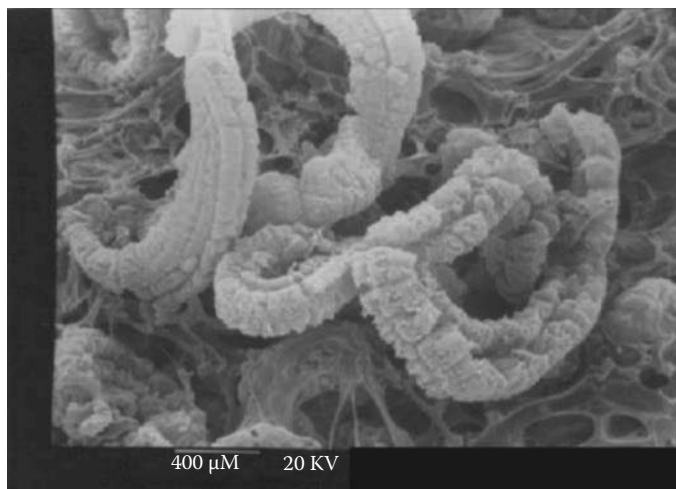


FIGURE 25.4 Superficial char layer of EG-filled PU foam after oxygen index test. (From Modesti, M. and Lorenzetti, A., *Eur. Polym. J.* 2, 263, 2003. With permission.)

Also a hindering effect toward oxygen diffusion, owing to the intumescent char layer formed, may be responsible for CO increase: when oxygen concentration is low, incomplete combustion is favored over a complete one. The char morphology in presence of EG is particular: the char has the so-called worm like structure (Figure 25.4) due to the expansion of EG.

Synergism between EG and phosphorus compounds (such as triethyl phosphate, TEP, and RP) were proven by the same authors.⁵⁷ In general, it can be seen that the combination of those fire retardants leads to a synergic effect: in the presence of constant amount of TEP (3 wt%) and increasing quantity of EG (0 up to 15 wt%) the LOI rises more than in the case of an additive effect. It is believed that a synergic effect could take place owing to a possible complementary way of fire retardancy of TEP and EG: in fact, it is well known that the first, being a phosphorous compound, acts in solid phase but probably to a certain extent in gas phase while EG acts in the solid phase, forming an intumescent char layer that prevents further decomposition. Also when RP was used in conjunction with EG, improvement of oxygen index was observed, although the increase is more limited than for EG-TEP filled foams. This may be due to the different fire retardant action of TEP and RP: TEP acts mainly in vapor phase,⁶⁴ while RP acts mainly in condensed phase and hence TEP flame retardancy is complementary to EG while RP acts in quite similar way to EG.

25.2.2.4 Melamine and Its Derivative

Melamine and some of its derivative, such as melamine cyanurate, melamine borate, melamine phosphate, are also used in flame retardancy of PU foams, both flexible and rigid ones although in rigid foams other flame-retardants have to be used in conjunction.⁴² Batt and Appleyard⁶⁵ stated that melamine is more effective than alumina trihydrate, magnesium hydroxide, APP, and ammonium borates, although the combination of melamine and a phosphorus-halogen fire retardant is superior to that of either additive used singly. Melamine acts through endothermic decomposition, which withdraws energy to the system, evolution of ammonia, which dilutes gas phase, and formation of condensation polymers such as melam, melom, melom, which constitute the superficial char layer.⁶⁶ While Batt and Appleyard⁶⁵ found no evidence for stable char formation at temperature above 450°C, Dick et al.⁶⁷ showed by in situ (HNMR)-H-1 definitive evidence that melamine, in flexible PU foams, acts in the condensed phase in terms of promoting the formation of rigid

char, which forms in more significant quantity by 450°C. Two schemes of condensation process have been proposed by Costa and Camino⁶⁸: the first states that condensation process leads to the fused-ring structure of cyameluric triamide, which reacts as a trifunctional monomer to give the final condensate; the second states that the melamine is the trifunctional monomer, which progressively condenses to give a product in which triazine rings are linked by –NH– bridges. Melamine derivative also have additional flame retardancy action: for example, melamine phosphate also releases water at 280°C–320°C with simultaneous condensation of phosphoric acid to pyro- and poly-phosphates.⁴²

Since melamine is not soluble in the polyol or MDI, it should be very fine dispersed so that it does not interfere with the foaming process. The effect of melamine particle size on properties of flexible PU foams was studied by Kageoka et al.⁶⁹ They reported that the foam with the finer particles showed higher hardness, better tensile properties, and less flammability than that with the larger ones. A flame-retarded foam with better physical properties can be manufactured by a polyol including melamine particles smaller than the strut thickness of the resultant foam.

Price et al.⁷⁰ showed that the addition of melamine into polyurethane flexible foam was very effective at reducing HRRs and suppressing smoke and CO production during the initial combustion stage. Owing to the interaction that occurs between melamine and the evolved toluene isocyanate fraction arising from the decomposition of polyurethane foam, the resulting polymeric structures so formed will reduce the amount of aromatic smoke precursors evolved thus suppressing smoke in the event of a fire. This polymeric structure will also degrade to a char, reducing the amount of combustibles volatilized and hence the HRR, and also the char would form a protective layer on the surface of the polyurethane foam. The same authors compared the behavior of cotton covered PU flexible foams filled with melamine or melamine and chlorinated phosphate.⁷¹ Considering non-flame retarded cotton fibers, they showed that there is no significant variation in PHRR while the total heat release (THR) is generally lower for foams containing melamine only. Melamine filled foams gave a lower peak of rate of smoke release (RSR) value, but a higher rate of smoke production after the peak time compared with the melamine-phosphate filled foams.

25.2.2.5 Inorganic Flame-Retardants

Alumina trihydrate (ATH) is reported since long in flame retardancy of PU foams by Bonsignore.⁷² Its use is nowadays mainly for rigid foams since, as reported by Nahafi-Mohajeri et al.³⁶ it is less effective than melamine in PU flexible foams. The main limitation arises from its thermal stability in applications where processing temperatures exceed 220°C, at which ATH starts to decompose. Generally, high amount of ATH (about 20 wt% or more) has to be used to be effective; this lead to high viscosity of raw materials that may be overcome using liquid flame-retardants, such as TEP, DMMP, or TCPP, in conjunction.⁷³ To also improve processability, surface-modified grades (mainly with silane) of ATH are now available which give better dispersion with increased compatibility with the resin matrix, resulting in lower viscosity or increased loading, for improved processing and properties. Another inorganic flame-retardant that may be used in PU foam is magnesium hydroxide that decomposes at higher temperatures than ATH (340°C in spite of 220°C). Also magnesium hydroxide is available in silane-treated grade for improving rheological properties. Such compounds may be used in conjunction because the decomposition of magnesium hydroxide begins when the decomposition of ATH is almost complete; however, no significant improvements are achieved in thermal stability (Figure 25.5). Both compounds act through an endothermic release of water (i.e., as heat sink), which dilutes gas phase and by the formation of a metal oxide coating on polymer surface; however, this layer is less effective in improving thermal stability than for example APP (Figure 25.5). Magnesium oxide is a stabilizer for the layer formed by ATH, as it modifies the char network making it more compact but also more stiff.⁷⁴ When the char is very stiff, its delamination from polymer surface may occur. To avoid the delamination, it may be useful to employ zinc borate (ZB) that promotes the formation of a low melting glass, hence avoiding an excessive increase of char stiffness. Zinc borate aids in developing a more glassy protective residual layer, because it

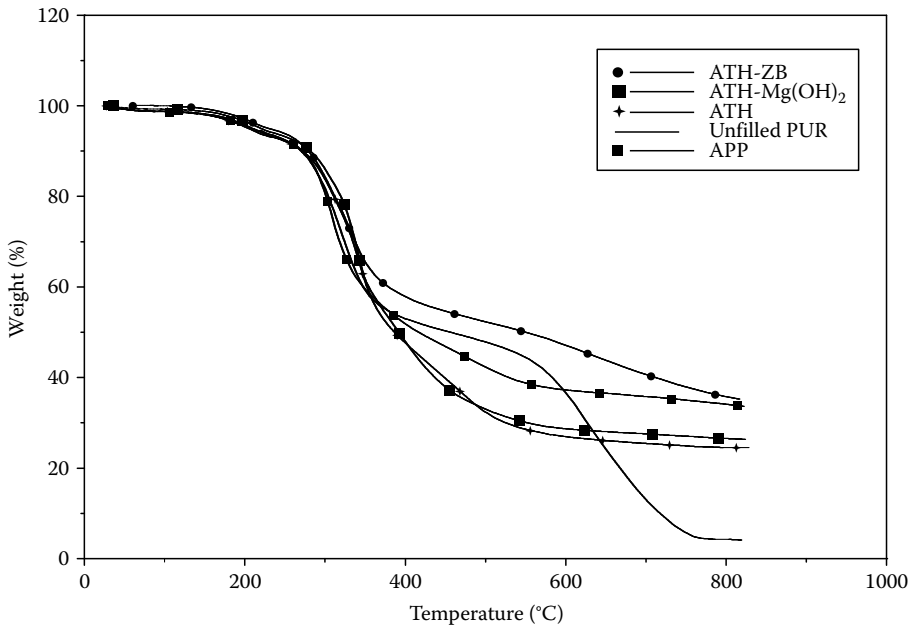


FIGURE 25.5 TGA curves in nitrogen of PU foams filled with ATH, Mg(OH)₂, ZB, and APP.

affects the structure, the expansion, and the mechanical resistance of the ceramic-like protective layer,⁷⁵ thus reducing the degradation rate and increasing the thermal stability (Figure 25.5).

In general, borates (ammonium borate, zinc borate) may be used as flame-retardants for PU foams: they release water/ammonia, which dilutes the gas phase, and boric acid that catalyzes the formation of protective char layer. It has already been pointed out that its action takes place as smoke suppressants, afterglow suppressants, corrosion inhibitors, and synergistic agent. Zinc borate is used mainly in conjunction with traditional fire retardant additives (halogen-containing and halogen-free systems including alumina trihydrate, magnesium hydroxide, RP or APP).⁷⁶

Other inorganic compounds that have been proposed as flame-retardants for PU foam are silicon-based compounds, both reactive and additives ones.³⁶ Several silicon-based additive fire retardants were used by Modesti and Lorenzetti in PU rigid foams.⁴¹ In particular, it was shown that the use of ATH, APP, and kaolin (i.e., aluminosilicate) is effective in lowering the PHRR, which may also be further reduced using Mg(OH)₂ and ZB (Figure 25.6). The reduced flammability in ATH-APP-kaolin filled foams may be due to the reaction between ATH, aluminosilicate, and APP which leads to the formation of aluminophosphate and silicophosphate, which are catalysts active for the synthesis of a protective carbon-based material.⁷⁷ Further improvement on fire behavior, evaluated through cone calorimeter, is observed when ZB is also used: the PHRR and the THE further decrease (although only slightly). This may be due to the formation of borophosphates and zinc phosphates, which stabilize phosphorous species.⁷⁵

25.3 POLYSTYRENE FOAMS

Polystyrene foam is the most widely produced expanded polymeric material after polyurethane foams.⁷⁸ There are two main types of PS foam: extruded polystyrene (XPS) and expanded polystyrene (EPS). XPS is obtained through one-step process, feeding PS granules into an extruder where they are melted and critical additives are mixed with the viscous fluid that is formed. Then, a blowing agent is injected to make the mixture foamable. Under carefully controlled heat and pressure conditions, the foamable mixture is forced through a die, at which time foaming and shaping occurs.

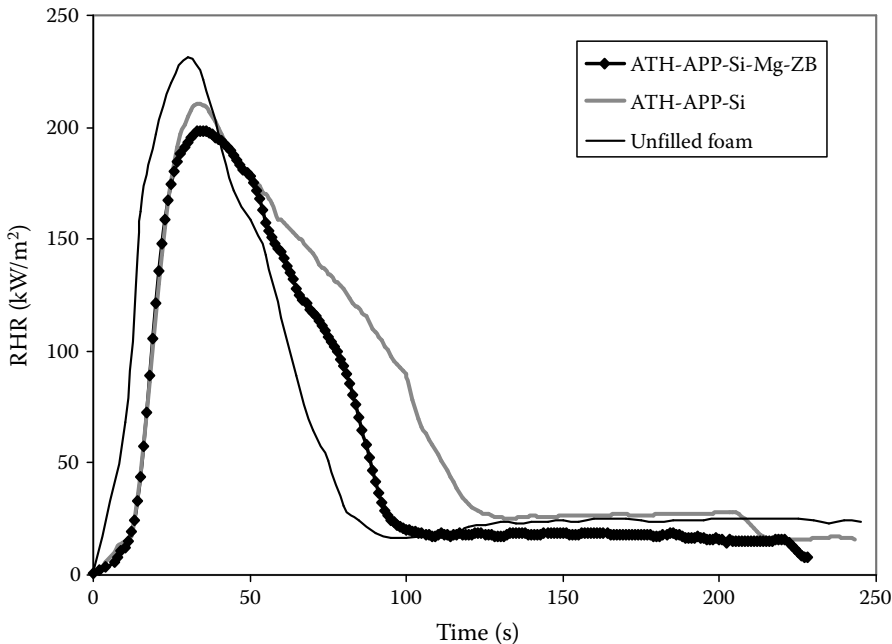


FIGURE 25.6 Heat release rate for PU foams filled with ATH, APP, kaolin, $\text{Mg}(\text{OH})_2$, and ZB.

In this process flame-retardants are fed in the extrusion process. EPS is obtained in a two-step process: in the first step beads containing blowing agent are prepared by suspension polymerization of styrene; in the second step the beads are expanded in the mold. In this case, flame-retardants are added during polymerization.

Several compounds may be used as flame-retardants for PS foams but generally halogen flame-retardants are the most used even if, due to environmental and human health concerns, a continuous search for halogen-free FR is going on. A very recent detailed review on FR for PS foams is reported by Levchik and Weil,⁷⁹ other useful data may be found in patent literature.

The most widely used flame-retardant for PS foams is hexabromocyclododecane (HBCD) although other bromine compounds, such as tetrabromobisphenol A bis (allyl ether) and tribromophenyl allyl ether are still proposed.^{22,80} Morose⁸¹ reported the use of flame-retardants containing tetrabromo-cyclooctane or dibromoethyl dibromo-cyclohexane as alternatives to HBCD for EPS foam. Both unstabilized and stabilized HBCD are commercially available, the first being used for EPS and the latter for XPS. It is known that HBCD offers unique performance in polystyrene foams, because it is effective at low level, that is around 0.7% in EPS, and 2.5% in XPS,⁸² but due to actual concerns on some bromine compounds, many researches are devoted to finding alternative halogen-free FR for PS foam or synergistic agent with HBCD, to reduce bromine FR content needed for fulfill several fire regulations. A well-known synergist for halogen FR, i.e., antimony trioxide, is not used in PS foam because it interferes with the foaming process. It is reported⁸³ that liquid peroxide, hydroperoxide or a peroxide solution (e.g., di-*tert*-butyl peroxide, *tert*-butyl hydroperoxide, a solution of dicumyl peroxide in pentane) may be used as flame-retardant synergist with HBCD. Generally speaking, compounds such as azo compounds, thiazole compounds, dimethyldiphenylbutane, dioctyl tin maleate and dibutyl tin maleate, quinone imines, benzothiazole sulfenamides, disulfides, and bibenzyl compounds, which are able to generate radicals at temperature lower than HBCD, may be used as synergists since they are able to promote the degradation of the HBCD, because they abstract protons off the aliphatic portion of HBCD with the release of the bromine radical. In addition, the reactive radicals are capable of breaking

down the styrene polymer chain during a fire, hence allowing the foam to melt away from the fire source.^{84,85} In the same reference, the authors reported that when using phosphate compounds, such as triphenylphosphate, the amount of HBCD may be reduced less than about 2.5 wt%. Also nitrogen-phosphorus compounds (e.g., APP, melamine polyphosphate), tetrazole compounds (e.g., 5,5'-bistetrazole diguanidine salt), isocyanuric acid, metal borates (e.g., zinc borate) and boron oxide (e.g., diboron trioxide, diboron trioxide surface-treated with the melamine resin),⁸⁶ tetraalkyl piperidine hydroxylamine ester⁸⁷ are reported as synergists with HBCD.

Patent literature reports also on halogen-free composition for PS foams, using phosphorus compound, such as RP, triphenyl phosphate, diphenyl cresyl phosphate, APP or diphenyl phosphate, and metal hydroxide such as magnesium or aluminum hydroxide.⁸⁸ It is reported that PS foams containing a mixture of EG (6–10 wt%), inorganic compound (5–10 wt%) and RP, triphenyl phosphate (TPP) or 9,10-dihydro-9-oxa-10-phosphaphenanthrene 10-oxide (DOP)), and chalk compounds (5–10 wt%)⁸⁹ or containing EG and phosphorus compounds such as RP, triphenylphosphate diphenyl cresyl phosphate, APP, melamine phosphate, resorcinol diphenyl phosphate, and dimethyl methylphosphonate in suitable amounts⁹⁰ fulfills DIN 4102-B2 requirements.

25.4 OTHER FOAMS

25.4.1 POLYOLEFIN FOAMS

Polyolefin (PO) foams are tough, flexible, and resistant to chemical and abrasion; however, they are characterized by a low inherent fire resistance and hence quite high amounts of flame-retardants are needed to fulfill fire safety requirements. Therefore, when fire requirements are stringent, generally styrene and engineered plastics are used in spite of polyolefin foams because, for example, for complying UL 94 V-0 rating, 30%–40% fire retardant is normally required for PO foams while only 10%–20% FR additives are required for styrenic foams.⁹¹

Halogenated compounds such as bis(alkyl ether)tetrabromobisphenol A or decabromodiphenyl oxide (DECA) may be used as flame-retardants for polyolefin foams, eventually using antimony oxide, metal oxides, boric acid salts, and metal hydroxides as synergist.⁹² For example Weil and Levchik⁹³ reported that using suitable amounts of DECA and Sb_2O_3 , polyethylene foams rated UL94 HF-1 are obtained.

Also inorganic compounds such as aluminum and magnesium hydroxide are used as FR for PO foams. To improve processability, surface-modified grades (with silane or fatty-acid) of aluminum and magnesium hydroxide are also now available, which give better dispersion with increased compatibility with the resin matrix, resulting in lower viscosity or increased loading, for improved processing and properties. Sterically hindered amine ether, which is generally used as stabilizer for organic materials such as polyolefins, is reported as FR for PO foams.⁹⁴ In the same patent, references to other suitable FR for PO foams are reported, as for example, APP and bromine-phosphorus based compound.

A polyethylene flexible closed cell polymeric foam containing 22 wt% of EG as fire retardant is capable of pass the test of FAR 25 Appendix F of U.S. Federal Aviation Authority; similar results were obtained using 18 wt% of EG and 5 wt% of Saytex 102E (Albemarle, decabromodiphenyl oxide) and 3 wt% of antimony oxide.⁹⁵

25.4.2 POLYVINYL CHLORIDE FOAMS

Depending on the content of plasticizers, polymer processing aids, and thermosetting binders, polyvinyl chloride (PVC) foams can be flexible, semirigid, or even rigid. Because of their range of properties, PVC foams have numerous uses. Frequently, they form part of structurally complex, multicomponent articles such as floor coverings or window frames. PVC rigid foams are inherently

flame-retarded materials because of the high chlorine content and hence the literature on flame retardancy of such foams is limited. When organic plasticizer is added to PVC to obtain flexible foams, the chlorine content is decreased and hence the fire behavior becomes worse. Replacing the organic plasticizer, in part or in whole, with nonflammable phosphate ester plasticizer gives product of varying degree of flame retardancy. For example, tricresyl phosphate, diphenyl cresyl phosphate, tris(2-ethylhexyl)phosphate, and 2-ethylhexyl diphenyl phosphate may be used. Green reported that the phosphate ester does not improve the flame retardancy, but simply replaces the flammable organic plasticizer.⁹⁶ Other flame-retardants widely used are antimony oxide and chlorinated paraffins; moreover, alumina trihydrate and zinc borate are also used.⁹⁷ The zinc borate functions as a flame-retardant, smoke suppressant, afterglow suppressant, and antitracking agent and it is a synergist of chlorine and bromine-containing flame-retardants or polymers. In a recent cone calorimeter study, it was shown that, in flexible PVC, partial replacement of antimony oxide with the zinc borate can reduce not only the PHRR, but also carbon monoxide production drastically at a heat flux of 35 kW/m.^{2,98} It is believed that zinc borate reacts with hydrogen chloride released from thermal decomposition of PVC; then zinc chloride catalyzes dehydrohalogenation and promotes cross-linking. This leads to an increase in char yield, and, even more important, a significant decrease in smoke formation.⁹⁹ Reduction in PVC flammability and smoke development were achieved also when using a combination of aluminum oxide trihydrate and zinc oxide¹⁰⁰ or using zinc hydroxystannate and zinc stannate compounds, which may exert their action in both the condensed and vapor phases, but mainly in the condensed phase as Lewis acids.¹⁰¹

25.4.3 PHENOLIC FOAMS

Like other thermosets, the material does not melt and when ignited a carbon skeleton is formed. Unlike most structural foams, phenolic foams exhibit excellent FST (flame, smoke, toxicity) properties because of its low flammability, low smoke density, and low production cost. As a result, phenolic foams are particularly attractive for aircraft, civil construction, and electronic applications, where FST performance is critical. Phenolic foam can, in an appropriate form, achieve all the following European fire certifications: UK Class O, Dutch NEN 6065/6066 Class 1, German B1, Belgian A1, French M1, and Scandinavian NT 036 Class 1.¹⁰² However, phenolic foams are brittle and friable and these properties have severely limited most structural applications, and presently limit the use of phenolic foams to insulating applications. It was shown that PF showed very low PHRR when tested by cone calorimeter; worsening of their fire behavior may arise by modification of PF with other polymers, e.g., epoxy resins, in order to improve mechanical properties of PF.¹⁰³ The foams containing brominated epoxy in the main chains displayed far greater flame retardance than those containing conventional epoxy resin and thus, lower PHRRs were observed.

The afterglow of open-cell foams (pinking) can be suppressed by the addition of flame-retardants such as boron trioxide or aluminum hydroxide. Hybrid foams with good mechanical properties and low combustibility can be produced from PF resins and polyisocyanates.¹⁰⁴

25.5 POLYMER NANOCOMPOSITES FOAMS

Recently, new approaches on flame retardancy deal often with nanofillers and in this section some examples of improvements of fire behavior of polymeric foams obtained by use of nanoclays or nanofibers will be shown. Much more details on flame retardancy of polymeric nanocomposite may be found elsewhere as for example in the book edited by A. B. Morgan and C. A. Wilkie¹⁰⁵ or in scientific review.¹⁰⁶ Polymer nanocomposites have enhanced char formation and showed significant decrease of PHRR and peak of mass loss rate (PMLR). In most cases the carbonaceous char yield was limited to few weight %, due to the low level of clays addition, and consequently the total HRR was not affected significantly. Hence, for polymer nanocomposites alone, where no additional flame-retardant is used, once the nanocomposite ignites, it burns slowly but does not self-extinguish

until most of the fuel has been combusted.¹⁰⁷ During combustion, the clay collapses down to form a clay-rich barrier and it is likely that the clay induces some chemical cross-linking of decomposing polymer due to the long residence times for polymeric radicals and some catalytic capability of clays to aromatize hydrocarbons.¹⁰⁵ However, it shall be underlined that generally these nanocomposites materials by themselves are unable to pass regulatory fire safety tests such as UL-94 V.¹⁰⁶

Recently, the use of nanoclays was reported for improving fire behavior of PS foams since these fillers, employed by 3–5 wt% give drip-free materials.¹⁰⁸ Han et al.¹⁰⁹ performed a simple test where a piece of soft paper soaked with ethanol was placed on the table and the rod foam samples were ignited and burned above it. For the pure PS foam the burning sample dripped down quickly and ignited the paper. On the contrary, the nanocomposite PS foam sample containing 5 wt% of Cloisite® 20A (montmorillonite-based clay with a surface modifier, dimethyl dihydrogenated tal-low quaternary ammonium chloride, by Southern Clay Products Inc.) forms a char during burning without dripping, preventing fire spreading. The same test with the same results was reported also by Guo et al.¹¹⁰ for metallocene polyethylene/wood fibers composite foam containing 5 wt% of Cloisite 20A; the same authors stated that the burning rate, according to ASTM D 635-03 (Standard test method for rate of burning or extent and time of burning of plastics in a horizontal position) for the nanocomposites was lower than that of unfilled composites. Nanoclays act in similar way also in PU foams, i.e., forming a char layer on polymer foams but Zammarano et al.¹¹ showed that the use of carbon nanofibers (CNFs) instead of organomodified layered silicates (OMLS) is more useful in PU flexible foams in preventing dripping behavior. They reported that there are no significant differences in PHRR for PU flexible foams containing a brominated-phosphorus flame-retardant filled with talc or OMLS and that both foams drip under cone calorimeter test, while when CNFs are used the PHRR is much lower and the sample does not exhibit any melt flow to the catch pan; in addition the sample retained its shape while only shrinking slightly. The thermally stable entangled fiber network formed during combustion and the absorption of the liquefied polymer are believed to be the key elements that prevent melt dripping of CNF foams. When dealing with organomodified montmorillonite, the fire behavior of PU foams may be further improved through using phosphonium-modified montmorillonite, as reported by Modesti et al.⁵³ They studied the fire behavior by cone calorimeter test of PU rigid foams filled with aluminum hypophosphites and unmodified or OMLS and they showed that while the presence of commercial OMLS did not affect the THR, phosphonium intercalated in the clay galleries leads instead to its decrease. Seo et al.¹¹¹ reported that using increasing amount of MDI modified clay, in PU foams containing 10 wt% of TCPP, the extinguishing time after flame removal and the burning zone, measured according ASTM D 4986, decrease.

REFERENCES

1. Troitzsch, J. How do foams perform under fire conditions?. In *Fire and Cellular Polymers*, Buist, J.M., Grayson, S.J., Woolley, W.D., Eds.; Elsevier Applied Science: London, U.K., 1986; pp. 77–91.
2. Dobbs, J.; Daems, D. Product stewardship. In *The Polyurethanes Book*, Randall, D., Lee, S., Eds.; Wiley: New York, 2003; pp. 39–62.
3. Hilado, C.J. Flammability characteristics of cellular plastics. *Ind. Eng. Chem. Prod. Res. Dev.* 1967, 6, 154–166.
4. Madrzykowski, D.; Stroup, D.W. Flammability hazard of materials. In *Fire Protection Handbook*, 20th edn, Cote, A.E., Grant, C.C., Hall, C.C. et al., Eds; National Fire Protection Association: Quincy, MA, 2008; vol. 1, pp. 31–48.
5. Drysdale, D.D. Fundamentals of the fire behaviour of cellular polymers. In *Fire and Cellular Polymers*, Buist, J.M., Grayson, S.J., Woolley, W.D., Eds.; Elsevier Applied Science: London, U.K., 1986; pp. 61–75.
6. Stone, H.; Pcolinsky, M.; Parrish, D.B.; Beal, G.E. Effect of foam density on combustion characteristics of flexible polyurethane foam. *Books of Abstract*, Polyurethanes World Congress, Nice, France, September 24–26, 1991.
7. Schrock, A.K.; Solis, R.; Beal, G.E.; Shorpenske, R.G.; Parrish, D.P. The influence of polymer morphology on the combustion of melamine filled flexible foams. *J. Fire Sci.* 1990, 8, 174–193.

8. Bian, X.C.; Tang, J.H.; Li, Z.M.; Lu, Z.Y.; Lu, A. Dependence of flame-retardant properties on density of expandable graphite filled rigid polyurethane foams. *J. Appl. Polym. Sci.* 2007, 104, 3347–3355.
9. Lefebvre, J.; Bastin, B.; Le Bras, M.; Duquesne, S.; Ritter, C.; Paleja, R.; Poutch, F. Flame spread of flexible polyurethane foam: Comprehensive study. *Polym. Test* 2004, 23, 281–290.
10. Zammarano, M.; Gilman, J.W.; Kramer, R.H. et al. Effect of nanoparticles on flammability of flexible polyurethane foams. Proceedings of 19th Annual BCC Conference on Flame Retardancy—Recent Advances in Flame Retardancy of Polymeric Materials, Stamford, CT, 2008.
11. Zammarano, M.; Kramer, R.H.; Harris, R. et al. Flammability reduction of flexible polyurethane foams via carbon nanofiber network formation. *Polym. Adv. Technol.* 2008, 19, 588–595.
12. Williams, M.K.; Weiser, E.S.; Fesmire, J.E. et al. *Book of Abstracts*, 41st Space Congress, Cape Canaveral, FL, April 27–30, 2004.
13. Williams, M.K.; Holland, D.B.; Melendez, O. et al. Aromatic polyimide foams: Factors that lead to high fire performance. *Polym. Degr. Stab.* 2005, 88, 20–27.
14. Ohlemiller, T.; Shields, J. Aspects of the fire behavior of thermoplastic materials, NIST Technical Note 1493, 2008.
15. Levchik, S.V.; Weil, E.D. Thermal decomposition, combustion and fire-retardancy of polyurethanes—A review of the recent literature. *Polym. Int.* 2004, 53, 1585–1610.
16. Weil, E.D.; Levchik, S.V. Commercial flame retardancy of polyurethanes. *J. Fire Sci.* 2004, 22, 183–209.
17. Levchik, S.V.; Weil, E.D. A review of recent progress in phosphorus-based flame retardants. *J. Fire Sci.* 2006, 24, 345–364.
18. Wang, J.Q.; Chow, W.K. A brief review on fire retardants for polymeric foams. *J. Appl. Polym. Sci.* 2005, 97, 366–376.
19. Saiki, K.; Sasaki, K. Carbodiimide-modified polyisocyanurate foams: Preparation and flame resistance. *J. Cell. Plastics* 1994, 30, 470–484.
20. Fallon, S.; Roark, R. Novel flame retardants for hydrocarbon blown polyisocyanurate foams. *Book of Abstracts, Polyurethanes Expo*, Orlando, September 30–October 3, 2003; American Plastics Council: Washington, pp. 42–46.
21. http://www.solvay-fluor.com/chemicals/IXOL_B_251 (accessed June 2008).
22. http://www.albemarle.com/Products_and_services/Polymer_additives/Flame_retardants/Flame_retardants_application_selector/Foams/ (accessed June 2008).
23. Brzozowski, Z.K.; Kijenska, D.; Zatorski, W. New achievements in fire-safe polyurethane foams. *Des. Monomers Polym.* 2002, 2–3, 183–193.
24. Sivriev, C.; Zabski, L. Flame retarded rigid polyurethane foams by chemical modification with phosphorus- and nitrogen-containing polyols. *Eur. Polym. J.* 1994, 30, 509–514.
25. Reed, C.S.; Taylor, J.P.; Guigley, K.S. et al. Polyurethane/poly[bis(carboxylatophenoxy)phosphazene] blends and their potential as flame-retardant materials. *Polym. Eng. Sci.* 2000, 40, 465–472.
26. Modesti, M.; Zanella, L.; Lorenzetti, A.; Bertani, R.; Gleria, M. Thermally stable hybrid foams based on cyclophosphazenes and polyurethanes. *Polym. Degrad. Stab.* 2005, 87, 287.
27. Modesti, M.; Simioni, F.; Checchin, M.; Pielichowski, J.; Prociak, A. Thermal stability and fire performance of modified polyisocyanurate foams. *Cell. Polym.* 1999, 18, 329–342.
28. Randall, D.; Lee, S. Appendix 1. In *The Polyurethanes Book*, Randall, D, Lee, S., Eds; Wiley: New York, 2003; pp. 447–452.
29. Modesti, M.; Lorenzetti, A.; Simioni, F.; Checchin, M. Influence of different flame retardant on fire behaviour of modified PIR/PUR polymers. *Polym. Degr. Stab.* 2001, 74, 475–479.
30. McGovern, M. High resiliency polyurethane foams with improved static fatigue properties, PCT US Patent 5157056, assigned to ARCO Chemical Technology, 1992.
31. Camino, G.; Luda, M.P.; Costa, L. *Proceedings of Chemical Industry and Environment 1993*; Barcelona, 1993; Girona, C.J. Ed.; p. 221.
32. Feske, E.F.; Brown, W.R. Flame retardant pentane blown polyisocyanurate foams for roofing. *Book of Abstracts, Proceedings of Polyurethanes Expo 2002*, Salt Lake City, UT, October 13–16, 2002; American Plastics Council: Washington, 2002; pp. 32–40.
33. Ravey, M.; Keidar, I.; Weil, E.D.; Pearce, E.M. Flexible polyurethane foam. II. Fire retardation by tris(1,3-dichloro-2-propyl) phosphate. Part A. Examination of the vapor phase (the flame). *J. Appl. Polym. Sci.* 1998, 68, 217–229.
34. Ravey, M.; Weil, E.D.; Keidar, I.; Pearce, E.M. Flexible polyurethane foam. II. Fire retardation by tris(1,3-dichloro-2-propyl) phosphate. Part B. Examination of the condensed phase (the pyrolysis zone). *J. Appl. Polym. Sci.* 1998, 68, 231–254.

35. Weil E.D. Phosphorus flame retardants. In *Kirk-Othmer Encyclopedia of Chemical Technology*, 4th edn.; Wiley: New York, 2001; vol. 10, pp. 976–998.
36. Najafi-Mohajeri, N.; Jayakody, C.; Nelson, G.L. Cone calorimetric analysis of modified polyurethane elastomers and foams with flame-retardant additives. In *Fire and Polymers. Materials and Solutions for Hazard Prevention*, Nelson, G.L., Wilkie, C.A., Eds.; ACS Symposium Series 797; American Chemical Society: Washington, 2001; pp. 79–89.
37. Bastin, B.; Lefebvre, J.; Paleja, R. Fire behaviour of polyurethane foams. *Book of Abstracts, Proceedings of Polyurethanes Expo 2002*, Salt Lake City, UT, October 13–16, 2002; American Plastics Council: Washington, 2002; pp. 244–254.
38. <http://www.flameretardants.eu> (accessed June 2008).
39. Peters E.N. Flame-retardant thermoplastics. I. Polyethylene-red phosphorus. *J. Appl. Polym. Sci.* 1979, 24, 1457–1464.
40. Schartel, B.; Braun, U.; Balabanovich, A.I. et al. Influence of the oxidation state of phosphorus on the decomposition and fire behaviour of flame-retarded epoxy resin composites. *Polymer* 2006, 47, 8495–508.
41. Modesti, M.; Lorenzetti, A. Recent trends in flame retardancy of polyurethane foams. In *Progress in Polymer Degradation and Stability Research*, Moeller, H.W., Ed.; Nova Science Publisher: New York, 2008; pp. 115–148.
42. Bleuel, E.; Boehme, P.; Rotermund, U. et al. 2002. Fundamentals of flame retardation: The burning process and the mode of action of flame retardants. *Book of Abstracts, Proceedings of Polyurethanes Expo 2002*, Salt Lake City, UT, October 13–16, 2002; American Plastics Council: Washington, 2002; pp. 234–243.
43. Kulesza, K.; Pieliowski, K. Thermal decomposition of bisphenol A-based polyetherurethanes blown with pentane Part II—Influence of the novel NaH₂PO₄/NaHSO₄ flame retardant system. *J. Anal. Appl. Pyrolysis* 2006, 76, 249–253.
44. Levchik, S.V.; Weil, E.D. 2005. A review of recent progress in phosphorus-based flame retardants. *J. Fire Sci.* 2006, 24, 345–364.
45. Luda, M.P.; Costa, L.; Bracco, P.; Levchik, S.V. Relevant factors in scorch generation in fire retarded flexible polyurethane foams: II Reactivity of isocyanate, urea and urethane groups. *Polym. Degrad. Stab.* 2004, 86, 43–50.
46. Kishore, K.; Mohandas K. Mechanistic studies on the action of ammonium phosphate on polymer fire retardancy *Combust. Flame* 1981, 43, 145–153.
47. Modesti, M.; Lorenzetti, A.; Simioni, F.; Checchin, M. Influence of different flame retardants on fire behaviour of modified PIR/PUR polymers. *Polym. Degrad. Stab.* 2001, 74, 475–479.
48. Lorenzetti, A. Synthesis of modified cellular polymers: Study on alternative blowing agents in relation to thermal insulating properties and fire behaviour. PhD Dissertation, Padova University, Padova, Italy, 2002.
49. Kuryla, W.C.; Papa, A.J. *Flame Retardancy of Polymeric Materials*, vol. 3; Marcel Dekker: New York, 1975; p. 31.
50. <http://www.flameretardants.eu/content/Default.asp?PageID=168> (accessed June 2008).
51. Braun, U.; Schartel, B.; Fichera, M.A.; Jager, C. Flame retardancy mechanisms of aluminium phosphinate in combination with melamine polyphosphate and zinc borate in glass-fibre reinforced polyamide 6,6. *Polym. Degrad. Stab.* 2007, 92, 1528–1545.
52. Braun U.; Schartel B. Flame retardancy mechanisms of aluminium phosphinate in combination with melamine cyanurate in glass-fibre-reinforced poly(1,4-butylene terephthalate) *Macromol. Mater. Eng.* 2008, 293, 206–217.
53. Modesti, M.; Lorenzetti, A.; Besco, S.; Hrelja, D.; Semenzato, S.; Bertani, R.; Michelin, R.A.. Synergism between flame retardant and modified layered silicate on thermal stability and fire behaviour of polyurethane nanocomposite foams. *Polym. Degrad. Stab.* 2008, 93, 2166–2171.
54. Knop, S.; Sicken, M.; Hoerold, S. Flame retardant formulation. PCT US Patent 7,332,534 assigned to Clariant Produkte GmbH, 2008.
55. Modesti, M.; Lorenzetti, A. Halogen-free flame retardants for polymeric foams *Polym. Degrad. Stab.* 2002, 78, 167–173.
56. Zatorski, W.; Brzozowski, Z.K.; Lebek, K. Production of PUR and PUR-PIR foams with red phosphorus as a flame retardant. *Polimery* 2005, 50, 686–689.
57. Modesti, M.; Lorenzetti, A.; Simioni, F.; Camino G. Expandable graphite as an intumescent flame retardant in polyisocyanurate-polyurethane foams. *Polym. Degrad. Stab.* 2002, 77, 195–202.
58. Bell, R.W.H. Flexible, flame-retardant polyurethane foams. PCT US Patent 4698369 assigned to Dunlop Limited, 1987.

59. Modesti, M.; Lorenzetti, A. Improvement on fire behaviour of water blown PIR-PUR foams: Use of an halogen-free flame retardant. *Eur. Polym. J.* 2003, 2, 263–268.
60. Shi, L.; Li, ZM; Xie, BH. et al. Flame retardancy of different-sized expandable graphite particles for high-density rigid polyurethane foams. *Polym. Int.* 2006, 8, 862–871.
61. Bian, XC; Tang, JH; Li, ZM. et al. Dependence of flame-retardant properties on density of expandable graphite filled rigid polyurethane foam. *J. Appl. Polym. Sci.* 2007, 104, 3347–3355.
62. Camino, G.; Duquesne, S.; Delobel, R. et al. 2001. Mechanism of expandable graphite fire retardant action in polyurethanes. In *Fire and Polymers. Materials and Solutions for Hazard Prevention*, Nelson, G.L., Wilkie, C.A., Eds.; ACS Symposium Series 797; American Chemical Society: Washington, 2001; pp. 90–109.
63. Modesti, M.; Lorenzetti, A. Flame retardancy of polyisocyanurate–polyurethane foams: Use of different charring agents. *Polym. Degrad. Stab.* 2002, 78, 341–347.
64. Weil, E.D.; Levchik, S.V.; Ravey, M.; Zhu, W.M. A survey of recent progress in phosphorus-based flame retardants and some mode of action studies. *Phosphorus, Sulfur Silicon Relat. Elem.* 1999, 144, 17–20.
65. Batt, A.M.; Appleyard, P. The mechanism and performance of combustion modified flexible foams in small scale fire tests. *J. Fire Sci.* 1989, 7, 338–363.
66. Bann, B.; Miller, S.A. Melamine and derivatives of melamine. *Chem. Rev.* 1958, 58, 131–172.
67. Dick, C.M.; Denecker, C.; Liggat, J.J. et al. Solid state C-13 and in situ H-1 NMR study on the effect of melamine on the thermal degradation of a flexible polyurethane foam. *Polym. Int.* 2000, 49, 1177–1182.
68. Costa L., Camino G. Thermal behaviour of melamine *J. Therm. Anal.* 1988, 34, 423–429.
69. Kageoka, M.; Tairaka, Y.; Kodama, K. Effects of melamine particle size on flexible polyurethane foam properties. *J. Cell. Plastics* 1997, 33, 219–237.
70. Price, D.; Liu, Y.; Milnes, G.J. et al. An investigation into the mechanism of flame retardancy and smoke suppression by melamine in flexible polyurethane foam. *Fire Mater.* 2002, 26, 201–206.
71. Price, D.; Liu, Y.; Milnes, G.J. et al. Burning behaviour of foam/cotton fabric combinations in the cone calorimeter. *Polym. Degrad. Stab.* 2002, 77, 213–220.
72. Bonsignore, P.V. Alumina trihydrate as a flame retardant for polyurethane foams. *J. Cell. Polym.* 1981, 17, 220–225.
73. Bonsignore, P.V.; Levendusky, T.L. Alumina trihydrate as a flame retardant and smoke suppressive filler in rigid high density polyurethane foams. *J. Fire Flammability* 1977, 8, 95–114.
74. Zarzycki, J. *Glasses and the Vitreous State*. Cambridge University Press: Cambridge, U.K., 1991; Chapter 8, pp. 227–239.
75. Samyn, F.; Bourbigot, S.; Duquesne, S.; Delobel R. Effect of zinc borate on the thermal degradation of ammonium polyphosphate. *Thermochim. Acta* 2007, 456,134–144.
76. <http://www.boraxfr.com/> (accessed June 2008).
77. Bourbigot, S.; Le Bras, M.; Bréant, P. et al. Zeolites: New synergistic agents for intumescent fire retardant thermoplastic formulations—criteria for the choice of the zeolite. *Fire Mater.* 1996, 20, 145–154.
78. <http://www.azom.com/details.asp?ArticleID=1557> (accessed June 2008).
79. Levchik, S.V.; Weil, E.D. New developments in flame retardancy of styrene thermoplastics and foams. *Polym. Int.* 2008, 57, 431–448.
80. http://www.e1.greatlakes.com/fr/products/jsp/all_fr_prod.jsp (accessed June 2008).
81. Morose, G. An overview of alternatives to tetrabromobishenol A (TBBPA) and hexabromocyclododecane (HBCD), <http://www.sustainableproduction.org/downloads/AternativestoTBBPAandHBCD.pdf> (accessed June 2008).
82. <http://www.flameretardants.eu/Content/Default.asp?PageID=156> (accessed June 2008).
83. Hahn, K.; Ehrmann, G.; Ruch, J. et al. Synergistic flame-proof mixtures for polystyrene foams, PCT Patent Application, to Basf AG, WO/2006/007996, 2006.
84. Eichhorn, J. Synergism of free radical initiators with self-extinguishing additives in vinyl aromatic polymers. *J. Appl. Polym. Sci.* 1964, 8, 2497–2524.
85. Vo, C.V.; Boukami, S. Fire resistant styrene polymer foams with reduced brominated fire retardant, US Patent 6579911, assigned to The Dow Chemical Company, 2003.
86. Oohara, Y.; Hirose, F.; Sato, T. et al. Extruded styrene resin foam and process for producing the same, US Patent 6,762,212 to Kaneka Corporation, 2004.
87. Roth, M.; Simon, D.; Leslie, G. et al. Flame retardant polymer compositions containing hydroxylamine esters, US Patent 7,230,042 to Ciba Specialty Chemicals Corp, 2007.
88. Scherzer, D.; Hahn, K.; Lorenz, M. et al. Expandable styrene polymers containing halogen-free flame retardants, European Patent EP0834529, assigned to BASF AG, 1998.

89. Hahn, K.; Ehrmann, G.; Ruch, J. et al. Expandable styrol polymers rendered flame-proof without using halogen, PCT Patent Application WO/2006/058734, assigned to BASF AG, 2008.
90. Dietzen, F.J.; Gluck, G.; Ehrmann, G. et al. Flame-proofed polystyrene foamed materials, PCT US Patent 6420442 assigned to Basf AG, 2002.
91. Wang, J.Q.; Chow, W.K. A brief review on fire retardants for polymeric foams. *J. Appl. Polym. Sci.* 2005, 97, 366–376.
92. Tokoro, H.; Tsurugai, K.; Shioya, S.; Oikawa, M. Flame-retardant foamed particles of polyolefin resin. PCT US Patent 5,569,681 assigned to JSP Corporation, 1996.
93. Weil, E.D.; Levchik, S.V. Flame retardants in commercial use or development for polyolefins. *J. Fire Sci.* 2008, 26, 5–43.
94. Stuart, J.B.; Skarke, S.C.; Ogita, T. et al. Flame retardant polyolefin resin pre-expanded particles and in-mold foamed articles prepared therefrom, PCT US Patent 6,822,023 assigned to Kaneka Corporation, 2001.
95. Wallace, W.R.; Baumforth, R.J. Flame retardant flexible foam, PCT US Patent 5719199 assigned to Kay-Metzeler Limited, 1998.
96. Green, J. Phosphorus containing flame retardant. In *Fire Retardancy of Polymeric Materials*, Grand, A.F., Wilkie, C.A., Eds; Marcel Dekker Ltd: New York, 2000; pp. 147–170.
97. Bunten, M.J.; Newman, M.W.; Smallwood, P.V.; Stephenson, R.C.. Vinyl chloride polymers. In *Encyclopedia of Polymer Science and Engineering*, 2nd edn., Kroschwitz, J.I., Ed; Wiley: New York, 1989; vol. 17, pp. 241–327.
98. Shen, K.K.; Kochesfahani, S.; Jouffret, F. Zinc borates as multifunctional polymer additives. *Polym. Adv. Technol.* 2008, 19, 469–474.
99. Yang, Y.; Shi, X.; Zhao, R. Flame retardancy behaviour of zinc borate. *J. Fire Sci.* 1999, 17, 355–361.
100. Lawson, D.F.; Kay, E.L. Flame and smoke retardants for polyvinyl chloride. PCT US Patent 3,957,723, assigned to The Firestone Tire & Rubber Company, 1976.
101. Qu, H.; Wu, W.; Wie, H.; Xu, J. Metal hydroxystannates as flame retardants and smoke suppressants for semirigid poly(vinyl chloride). *J. Vinyl Addit. Technol.* 2008, 14, 84–90.
102. <http://www.epfa.org.uk/properties.htm> (accessed June 2008).
103. Auad, M.L.; Zhao, L.H.; Shen, H.B. Flammability properties and mechanical performance of epoxy modified phenolic foams. *J. Appl. Polym. Sci.* 2007, 104, 1399–1407.
104. Smith, S.B. Flame-retardant benzylic-ether phenolic modified foam and method of preparing same, PCT US Patent 4,390,641 assigned to Thermocell Development, Ltd, 1983.
105. Morgan, A.B.; Wilkie, C.A. *Flame Retardant Polymer Nanocomposites*; Wiley: Hoboken, NJ, 2007.
106. Morgan, A.B. Flame retarded polymer layered silicate nanocomposites: A review of commercial and open literature systems. *Polym. Adv. Technol.* 2006, 17, 206–217.
107. Bartholmai, M.; Schartel, B. Layered silicate polymer nanocomposites: New approach or illusion for fire retardancy? Investigations of the potentials and the tasks using a model system. *Polym. Adv. Technol.* 2004, 15, 355–364.
108. Loh, R.R.; Polasky, M.E.; Delaviz, Y. et al. Polystyrene foam containing a modifier-free nanoclay and having improved fire protection performance, PCT Patent Application WO/2007/030719, assigned to Owens Corning Intellectual Capital, 2007.
109. Han, X.; Zeng, C.; Lee, L.J. et al. Extrusion of polystyrene nanocomposite foams with supercritical CO₂. *Polym. Eng. Sci.* 2004, 43, 1261–1275.
110. Guo, G.; Wang, K.H.; Park, C.B. et al. Effects of nanoparticles on the density reduction and cell morphology of extruded metallocene polyethylene/wood fiber nanocomposites. *J. Appl. Polym. Sci.* 2007, 104, 1058–1063.
111. Seo, W.J.; Sung, Y.T.; Kim, S.B. et al. Effects of ultrasound on the synthesis and properties of polyurethane foam/clay nanocomposites. *J. Appl. Polym. Sci.* 2006, 102, 3764–3773.

26 Material Design for Fire Safety in Wire and Cable Applications

Jeffrey M. Cogen, Thomas S. Lin, and Paul D. Whaley

CONTENTS

26.1	Introduction.....	783
26.2	Flame Test Standards for Fabricated Wire and Cable	785
26.3	Polymer and Flame-Retardant Material Selection.....	788
26.3.1	Poly(Vinyl Chloride).....	788
26.3.2	Polyolefins: Polyethylene and Polypropylene Copolymers	789
26.3.3	Fluoropolymers	793
26.3.4	Silicone Polymers	794
26.3.5	Other Polymers	794
26.4	Laboratory Flammability Tests for Wire and Cable Materials.....	794
26.5	Correlations among Flammability Tests	795
26.6	Industry Trends and Issues.....	800
26.6.1	Geographical Fragmentation	800
26.6.2	Environmental Concerns	800
26.6.3	Other Industry Trends and Issues	801
26.7	Summary.....	801
	References.....	802

26.1 INTRODUCTION

In the United States alone, fire departments respond to approximately 1.8 million fire calls per year; tens of thousands of people are injured or killed in fires, and fire-related property loss is in the billions of dollars.¹ It is further estimated that approximately 6812 fires were caused in the United States in 2004 from electrical distribution systems, which includes electrical wiring.¹ Although much progress has been made in recent years with respect to fire safety, internationally, loss to life and property due to fires are still at levels that underscore the need for further improvements.² In analyzing the cable industry standards in Europe, it has been pointed out that although cables make up only about 0.5% of the cost of a new building, they nevertheless play a critical role in safety, as exemplified by the Düsseldorf airport fire in 1996, which was caused by a cable catching fire during a welding operation, killing 17 and injuring 62.³

On account of their proximity to electrical systems and the accompanying potential heat and spark sources, wires and cables utilized in enclosed spaces are usually required to have fire safety characteristics as described in various codes and standards.

Applications requiring flame retardant (FR) wire and cable include

- Building wire, including low voltage power and communication networks
- Control cables, including chemical plants and nuclear power plants
- Portable power cables, including elevator cables, mining cables, and welding cables

- Industrial power distribution cable
- Robotic cables, including welding, automotive fabrication, body painting, and semiconductor manufacturing
- Factory automation cable, including food and beverage packaging, automotive, and materials handling
- Marine/transit cable, including military, commercial vessels, small boats, railroad, rapid transit, aircraft, and automobiles
- Cables for tunnels

Both by application and by geography, fire safety standards are highly diverse and complex. Some standards tend to focus primarily on preventing ignition and flame spread, while others put additional emphasis on reducing smoke generation and toxic/corrosive by-products from burning wires and cables.

Wire and cable constructions are also quite diverse. All wires and cables have an electrical or optical signal transmission conductor. The most common electrical conductor is copper, which is commonly seen in everything from low voltage communications cables to extra-high voltage electrical power cables. Aluminum conductors are used to reduce the weight, particularly in electrical power transmission. In the case of fiber optics, the optical signal transmission conductor is predominantly a glass fiber with niche applications using plastic optical fiber (POF). Other than having a secondary impact on fire behavior of wires and cables via their impact on thermal conductivity and heat capacity of the overall construction, conductors clearly are not flammable or combustible materials (with the exception of POF).

Conductors are generally encapsulated with a polymeric insulating layer except for some power applications where oil-impregnated paper is still used as insulation. These single conductor entities can be incorporated into larger designs enclosed in an outer jacketing material. The internal cable design can optionally include metallic layers, FR tapes, water-blocking tapes, semiconductive tapes or layers, inner polymeric tubes called buffer tubes to protect optical fibers, and structural strength members.

In some cases, there are also options for installation that can provide the needed flame retardancy instead of relying on the wire and cable materials. For example, a non-FR cable can be installed within a metal duct to provide the required level of flame resistance. Reliance on a FR or incombustible protective duct or other component that is functionally or mechanically distinct from the wire or cable is considered to be outside the scope of the present discussion, and is generally not a cost-effective approach to cable system design.

In principle, material selection, cable design, and installation method can work together to produce the solution for meeting performance requirements within standards. However, in many cases the standards have evolved based upon certain materials and constructions, thus limiting material selection options unless one is willing to propose changes to standards, which is a lengthy proposition.

A conceptual framework for approaching material selection for FR wire and cable is shown in Figure 26.1.

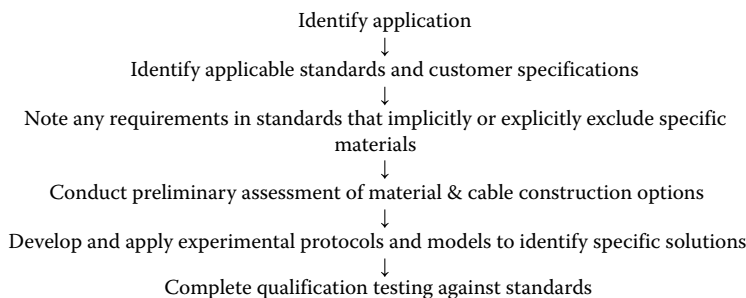


FIGURE 26.1 Conceptual framework for material selection and wire and cable product development.

Within that framework, the most effective constructions to meet existing requirements have been developed based on a variety of polymers including poly(vinyl chloride) (PVC), polyolefins, silicones, and fluoropolymers. Researchers are continually striving to develop more cost-effective compositions and cable constructions to enable replacement of more expensive materials with less expensive ones. In some cases, OEMs, cable manufacturers, and material suppliers are working to pass new standards that allow for substitution of new classes of materials or designs.

A number of trends are also having a significant influence on the direction of material selection. These include a slow but steady increase in the drive for green chemistry and sustainability, end-of-life issues such as disposal and recycling, reduction in reliance on toxic or hazardous chemicals, and adoption of the lowest cost technology and manufacturing while still demanding high quality and longevity of installed wires and cables.

This chapter starts with an overview of how the standards drive FR material selection within the wire and cable industry. Although the standards in the wire and cable industry are varied and complex, they provide the critical framework for approaching wire and cable product development and commercialization. Criteria for material selection will then be reviewed, including considerations for the selection of polymers, FRs, and achieving the critical balance of properties required in today's wire and cable materials. This is followed by an overview of the important area of flammability testing for wire and cable applications, including not only fabricated wires and cables, but also materials. The discussion also focuses on the important question of efficient laboratory screening of materials. The chapter concludes with a brief discussion of key geographical and environmental trends in the FR wire and cable industry.

26.2 FLAME TEST STANDARDS FOR FABRICATED WIRE AND CABLE

Flammability tests for fabricated wires and cables are generally specified in the applicable wire and cable testing standards and can involve assessment of flame spread, heat release characteristics, smoke generation, and corrosivity of combustion gases. Flame spread measures the time to reach certain height or distance in the wire or cable as well as the length damaged by the flame. Additionally, some tests assess whether or not the insulation or jacketing material drips during the test.

In the wire and cable industry, the cable standards or specifications play a critical role in determining selection and formulation of insulations or jacketing materials.⁴⁻⁶ In general, wire and cable standards define fire performance requirements for reducing flame propagation of cables, smoke generation, corrosivity of combustion gases, and maintaining circuit integrity. Here, we give a brief discussion of representative FR wire and cable standards. A comprehensive discussion is beyond the scope of this chapter. It is recommended that prior to beginning formulation or product development one carefully reviews any standards that may apply. A general discussion of representative standards is provided in this section of the chapter. Some material-specific aspects of the standards are also discussed later in the chapter.

There are several standards organizations in different countries that regulate fire performances of cables⁷⁻¹⁰. Table 26.1 shows some examples of flame propagation tests for single wires or cable bundles from different countries.

International Electrotechnical Commission (IEC) is an international standards body established in the United Kingdom to prepare and publish international standards for all electrical, electronic, and related technologies. IEC technical committee TC 20 (working group 18) is responsible for defining the standards for "burning characteristics of electric cables." Underwriters Laboratories Inc. (UL) and Canadian Standards Associations (CSA) are two major organizations that define wire and cable flame testing standards in the United States and Canada, respectively. In the United States, the National Electrical Code (NEC) also establishes a set of standards and requirements for flame spread and smoke generation of wires and cables installed in office building, residences, and factories. These codes are prepared by National Fire Protection Association (NFPA) and provide installation guidelines for flame-resistant cables. For example, communication cables can have

TABLE 26.1
Examples of Flame Propagation Tests

Country	Horizontal, Single Wire	Vertical, Single Wire	Vertical Tray, Bundled Cables	Riser, Bundled Cables	Plenum, Horizontal Bundled Cables
International		IEC 60332-1, 2	IEC 60332-3 IEEE 383 IEEE 1202		
United Kingdom		BS 4066-1	BS 4066-3		
United States	UL 1581 HB	UL 1581 VW-1	UL 1685	UL 1666	NFPA 262 (UL 910)
Canada		CSA FT-1	CSA FT-4		CSA FT-6
Japan	JIS C-3005	JIS C-3005	JIS C-3521		

different flame-resistance ratings from the lowest fire-resistance level to the highest fire-resistance level according to the 2008 NEC (NFPA 70)¹¹: UL 1581¹² VW-1, UL 1685¹³ Vertical Tray (or CSA FT-4¹⁴), UL 1666,¹⁵ and NFPA 262 (formerly UL-910).¹⁶ These standards specify flame application angle and time, flame energy input, airflow rate, cable mounting, and quantity of cable tested. IEC 60332-1,¹⁷ IEC 60332-2,¹⁸ UL 1581 VW-1, and CSA FT-1¹⁹ are single vertical wire flame test protocols. IEC 60332-3,²⁰ UL 1685, CSA FT-4, IEEE 383,²¹ and IEEE 1202²² define flame propagation for vertically bundled cables attached to a tray. NFPA 262 (UL 910) defines flame propagation and smoke characteristics in a Steiner Tunnel for a bundle of electrical or optical fiber cables used in the horizontal air-handling spaces (plenums) of buildings. The flame energy input used in the test is 88kW. A cable that passes this test is considered to be a low-smoke cable. The UL 1666 riser cable burn test simulates a cable installation in a building riser shaft with exposure to a large fire source (154kW flame energy input) and requires cables pass both flame spread and heat generation (measured via temperature rise) requirements. UL 1685 is a tray cable test for electrical or optical fiber cables similar to the IEEE 383 cable test originally developed to evaluate cables used in the nuclear power generation industry.^{23,24} UL 1685 also measures total smoke release and the peak smoke release rate during the 20 min flaming test with 20kW flame energy input. A cable that meets both the flame and smoke requirements of UL 1685 is permitted to carry a limited-smoke (LS) marking.

Benchmarking material smoke generation helps cable designers select appropriate materials for cables designed to be used in enclosed spaces where low levels of smoke generation are necessary for improved fire safety. Smoke generation tests are specified in IEC 61034-1,²⁵ IEC 61034-2,²⁶ NES 711,²⁷ BS 7622-1,²⁸ and EN 50268-1.²⁹ In Europe, IEC 61034 is also known as 3 m cube test, which uses 1 L of burning alcohol as the fire source to burn a 1 m horizontal cable and measures the light transmittance in a 3 × 3 × 3 m (27 m³ volume) chamber. This test has been used by the London Underground to distinguish low-smoke materials from other cable materials. Reduced smoke generation is generally achieved by the use of halogen-free FR materials in the cable construction but fluoropolymers can also provide low smoke performance.

Corrosivity of combustion gases can be detrimental to electronic devices as well as communication equipment. Acidity tests are used to measure the corrosivity of combustion gases. The acidity tests are specified in the IEC 60754-1,³⁰ EN 50267-1,³¹ and BS 6425-1³² standards. These tests are conducted on the cable insulation or jacketing materials instead of finished cables and are useful to distinguish between halogen and halogen-free materials. In these tests, the sample is heated to 800°C for 20 min and the amount of halogen acid gas (except hydrofluoric acid) is measured with an upper allowed limit of 0.5 wt %. Alternatively, IEC-60754-2,³³ EN 50267-2,³⁴ and

BS-6425-2³⁵ quantifies the degree of acidity by measuring pH and conductivity of combustion gases with the sample heated up to 935°C for 30 min. To pass the test, the pH has to be above 4.3 and the conductivity has to be less than 10 μS/mm. The NES 713³⁶ toxicity index test is a Naval Engineering Standard designed to analyze a specified set of gaseous species (e.g., CO, CO₂, SO₂, HCl, NH₃, HF, etc.) generated from burning a test sample. Collectively, the measured gas concentrations are used to calculate the toxicity index of the cable material based on individual toxicity factors for each specified gas where a higher calculated toxicity index indicates a potentially more toxic combustion gas.

Maintaining circuit integrity under fire condition is critical to continued operation of fire safety equipment (i.e., sprinklers, water pumps, etc.), which in turn improves safety for building occupants. IEC 60331,³⁷ BS 6387,³⁸ UL 2196³⁹ test standards define the requirements for circuit integrity under fire, water spray, and mechanical shock environments.⁴⁰ BS 6387 also classifies the cable material according to performance under different test conditions (fire, water spray, and mechanical shock). For example, when the cable is tested under a specified flame temperature with electrical current passing at its rated voltage, the cable material can be classified into four categories: Class A (650°C for 180 min), Class B (750°C for 180 min), Class C (950°C for 180 min), and Class S (950°C for 20 min). BS EN 50200 is another important test that provides fire-resistance classifications based on the cable performance under an 850°C fire plus mechanical shock. (British standard EN 50200 “Method of test for resistance to fire of unprotected small cables for use in emergency circuits.”)

The choice of FR polymers for insulation or jacketing can affect how cables perform in the flame tests. There are also cable flame testing standards developed for specific wire and cable applications. For example, the U.S. Navy, a major user of reduced emissions cables, has published MIL-DTL-24640B⁴¹ and MIL-DTL-24643B⁴² standards that set shipboard cable requirements on cable flame spread, smoke generation, and acidity of combustion gases, in addition to mechanical properties, heat resistance, and oil resistance. Different coupling agents and metal hydroxide FRs were developed and evaluated for a halogen-free FR compound meeting the shipboard cable requirements.⁴³ In the automotive industry, single wire flame tests are specified for automotive wires in SAE J1128,⁴⁴ SAE J1678,⁴⁵ ISO 6722,⁴⁶ and JASO D 608⁴⁷ standards in addition to heat aging, mechanical properties, and oil resistance requirements. In some cases, automotive OEMs specify specific flame performance requirements different from the general standard. A study has shown the challenge involved in balancing the various property requirements to meet the SAE J1128 and Chrysler MS 8288⁴⁸ standards.⁴⁹ For control cable and appliance wire applications, UL 44,⁵⁰ UL 83,⁵¹ and UL 758⁵² specify horizontal or vertical flame test requirements as well as mechanical property and long-term electrical property requirements under wet and dry environments. Overviews are available on the importance of proper selection of FR materials to meet control cable and appliance wire requirements.⁵³

In Europe, classification of cables according to reaction-to-fire performance is being developed under the Construction Products Directive (CPD).^{54,55} The cables are grouped into seven classes, A_{ca}, B1_{ca}, B2_{ca}, C_{ca}, D_{ca}, E_{ca}, and F_{ca}, according to their contribution to fire measured by gross calorific potential, flame spread, total heat release, peak heat release rate (PHRR), and fire growth rate index (FIGRA). Additional classifications are made based on smoke production, flaming droplets/particles, and acidity. The above properties are measured according to a number of specifications, including EN ISO 1716, FIPEC₂₀, EN 60332-1-2, and EN 50267-2-3. Products complying with the requirements of the CPD will be able to carry a CE mark, which is expected to facilitate free trade of cables used in building construction.

Selection of polymer type and FR additive technology can have significant impact on meeting flame resistance requirements as specified by the above standards.⁵⁶ Therefore, material selection and standards are directly interrelated. A summary of key material options for FR wire and cable applications follows.

26.3 POLYMER AND FLAME-RETARDANT MATERIAL SELECTION

As mentioned earlier, polymer material selection for wire and cable is driven by market requirements to meet a balance of mechanical, thermal, chemical, and electrical properties. When the application requires FR polymer materials, the selection of the appropriate FR system requires balancing the relevant FR characteristics (ignition, flame spread, smoke, acid-gas, and toxicity) with these market requirements. In general, the FRs used in wire and cable applications parallel selections made for those same polymers in other application areas. However, specific wire and cable market requirements for fluid resistance, wet insulation resistance, high frequency communications, and long-term heat aging performance typically result in more limited approaches for FR materials. In many cases, technology approaches for improving filler dispersion, modifying filler surface properties, and compatibilization of the polymer–filler interface are necessary to meet market requirements. As previously mentioned, cable constructions are diverse and often the wire or cable system (not just an individual material component) is required to pass the relevant wire and cable standard. Thus material and construction approaches are relevant to achieving acceptable flame retardancy. The construction approach is sometimes used to address trade-offs in flame retardancy performance with other market requirements. Fire performance testing is often required by customers and standards agencies when any material of construction is altered or when cable design is modified.

The most common polymers used in FR wire and cable applications are PVC, polyolefins, fluoropolymers, and silicone polymers. Thermoplastic polyurethanes (TPUs) and other specialty polymers such as chlorosulfonated polyethylene also serve niche applications in wire and cable. The approaches to achieve flame retardancy in each of these polymer systems along with issues unique to wire and cable application are discussed in the following sections.

26.3.1 POLY(VINYL CHLORIDE)

PVC, introduced over 70 years ago as a wire insulation material,^{57,58} is a ubiquitous material in wire and cable because of its dielectric strength, volume resistivity, mechanical strength, chemical resistance, water resistance, good processability, and flame retardancy. This combination of properties is achieved in a very cost-effective manner and thus PVC is the material of choice in applications where PVC meets the market requirements.⁵⁹ PVC finds application as an insulation material in building and automotive primary wire. Specifications for PVC building wire are found in UL-83 “Thermoplastic-Insulated Wires and Cables” for temperature ratings of 60°C, 75°C, and 90°C, in wet and dry environments⁵¹. Eligible markings for flame performance include HB (UL-1581), VW-1 (UL-1581), and UL-1685/FT-4/IEEE 1202 (without smoke measurements). For automotive primary wire, thermoplastic PVC serves the following thermal ratings: SAE J-1128 (80°C)⁴⁴ and ISO-6722 (85°C–Class A and 100°C–Class B).⁴⁶ PVC jacketing compounds are used in tray (UL-1685)¹³, riser (UL-1666)¹⁵, and plenum cables (UL-910).¹⁶ Jacketing compounds used in plenum are generally referred to as low-smoke PVC owing to the specialty formulation required to pass UL-910 testing metrics for flame spread, instantaneous smoke, and total smoke released.¹⁶

PVC has a limiting oxygen index (LOI) of 47 (rigid)⁶⁰ and, for a commodity polymer, has a low total heat release (11.3 kJ/g) that is more typical of engineering polymers such as polyetherimides (PEI), polyetherketones (PEK), and polyetheretherketones (PEEK).⁶¹ In addition to the high chlorine content in PVC, flame retardancy is thought to be aided by char formation as a result of the degradation mechanism where dechlorination upon heating forms a conjugated polyene structure followed by benzene formation and then subsequently by polyaromatic structures that either form crosslinked char or generate smoke.⁶²

Flexible PVC is used in both insulating and jacketing materials where formulations include plasticizers, stabilizers, lubricants, and fillers, which are carefully selected to meet application requirements. Plasticizer type and addition level in PVC allows rigid PVC (T_g of $\sim 80^\circ\text{C}$)⁶³ to have

brittleness temperatures as low as -60°C .^{64,65} The most common plasticizers are phthalate esters while for applications requiring low plasticizer volatility, trimellitates and polymeric plasticizers are utilized.^{65,66} With conventional phthalates, flexible PVC has an LOI in the 25–32 range⁶⁰ while achieving brittleness temperatures required in wire and cable applications of -20°C to as low as -60°C .⁶⁴ Phosphate esters, chlorinated paraffins, and tetrabromophthalate ester-based plasticizers can be incorporated to offset reductions in the inherent flame retardancy of PVC due to common plasticizers.^{62,65,67} In all wire and cable applications, plasticizer volatility is matched with the temperature rating resulting in, generally, the use of phthalates at lower temperatures and trimellitates at higher temperatures.⁶⁶ PVC stabilizer selection is critical to meeting heat aging requirements and electrical property performance. PVC stabilization was dominated by several Pb-based stabilizers, each tailored for performance for a specific wire temperature rating.^{68,69} Owing to regulatory pressure (RoHS), Pb and other heavy metal-based stabilizer systems like cadmium, are being replaced by other metal soap systems (Ca/Zn, Ca/Al/Zn), which has required significant industry activity to requalify PVC insulation materials.^{70,71}

The role of fillers in PVC for wire and cable applications can range from extenders to functional additives. Calcium carbonate and kaolin are the two most common fillers in PVC applications.⁷² For insulation compounds, electrical grade kaolin is partially calcined to offer improved resistivity while also improving tear strength with no effect on tensile strength but some reduction in elongation.⁷² For enhanced flame retardancy, antimony trioxide (Sb_2O_3) filler is used due to the significant synergy with halogens.^{73,74} Either antimony trioxide or aluminum trihydroxide (ATH), or their mixtures, significantly increase LOI of phthalate plasticized PVC.⁷⁵ Aluminum trihydroxide, magnesium hydroxide, and zinc borate and their mixtures are used for low-level smoke production and operate by endothermic dehydration and char formation.^{62,76} Even more effective smoke suppressants are molybdenum trioxide (MoO_3), ammonium octamolybdate (AOM), and zinc hydroxystannate (ZHS).⁶² As molybdenum is reported to work in the solid phase to reduce benzene formation^{62,77} molybdates are precipitated on minerals with moderate surface area to enhance the smoke suppression effectiveness on a molybdenum weight basis.⁷⁸ Similarly, ZHS coated on metal hydrates suppresses smoke generation over metal hydrate alone.⁷⁶ Hydrotalcite, an acid absorber used as a PVC costabilizer,⁷⁹ is also reported to reduce smoke generated during PVC combustion.^{80,81}

Significant effort has been expended on toxicity,^{82,83} smoke irritancy,⁸⁴ and smoke corrosivity^{85,86} testing of PVC materials. There is a significant impact of combustion conditions (temperature and ventilation)⁸⁷ and experimental scale⁸⁸ on toxic product yields. However, smoke corrosivity has been a big concern of the communications industry as equipment damage is related more to smoke than heat.⁸⁹ Increased corrosion rates were correlated with increased smoke production⁸⁹ where damage to electronic components must be dealt with immediately or be subject to premature failure.⁹⁰ Smoke corrosivity issues with PVC have resulted in a trend toward nonhalogen materials based on polyolefins.

26.3.2 POLYOLEFINS: POLYETHYLENE AND POLYPROPYLENE COPOLYMERS

After PVC, polyolefin copolymers, predominantly polyethylene copolymers, are the next most widely used material for FR applications in wire and cable. Polyethylenes have very good dielectric strength, volume resistivity, mechanical strength, low temperature flexibility, and water resistance. In contrast to PVC, polyolefins are not inherently FR and thus are more highly formulated, requiring the addition of FRs to meet market requirements for flame retardancy. For this reason, and because of the steady global trend toward halogen-free materials for wire and cable applications, more space will be devoted to this section on FR polyolefins compared with the above discussion of PVC.

FR polyolefins find application in building wires, industrial control cables, automotive primary wire, and data cables. Specifications for thermoplastic building wire are found in UL-83 “Thermoplastic-Insulated Wires and Cables” for temperature ratings of 75°C and 90°C in wet and dry environments.⁵¹ Specification for industrial control cables are found in UL-44

“Thermoset-Insulated Wires and Cables” for temperature ratings of 75°C and 90°C in wet and dry environments.⁵⁰ Crosslinked polymers, either polyethylene or its copolymers, crosslinked ethylene–propylene rubbers, and their mixtures, are the commonly used materials. Eligible markings for flame performance include horizontal burn, VW-1, and UL-1685/FT-4/IEEE 1202 with optional marking for limited smoke (LS). For automotive primary wire, crosslinked polyethylene serves the following thermal ratings: SAE J-1128 (125°C)⁴⁴ and ISO-6722 (125°C–Class C).⁴⁶ Polyethylene insulation compounds are used for twisted copper pairs used in data cables where FR selection is focused on the preservation of electrical property performance at high frequencies. The individual twisted pairs are not subjected to flame retardancy requirements, but reductions in insulation material fuel load aid the capability of the jacketed system to pass relevant fire performance testing. Polyethylene jacketing compounds are used in tray (UL 1685)¹³ and riser (UL 1666)¹⁵ applications and nonhalogenated jacketing compounds with inherent low smoke characteristics are excellent choices for transit/shipboard/military cables and in other areas where public safety is a concern.

Polyethylene has an LOI of 17.0⁶⁰ with a total heat release of 41.6 kJ/g⁶¹ and it has no tendency for char formation. The heat release capacity (1676 J/(g K)) is the highest among all polymers tested and requires an extensive amount of FR additive to meet wire and cable industry requirements for flame retardancy. Polar copolymers of ethylene with vinyl acetate (EVA), ethyl acrylate (EEA), and butyl acrylate (EBA) are commonly used in FR compounds. These copolymers are made in high pressure tubular or autoclave reactors and have excellent extrusion characteristics. The level of comonomer can be varied with higher comonomer addition resulting in a material with higher LOI and lower heat release but still no inherent robust char formation tendency (see subsequent text). Developments in single site catalysis have resulted in plastomers based on ethylene with higher α -olefins (butane, hexane, and octene) with densities ranging from 0.86 to 0.91 g/cc.^{91,92} Ethylene–propylene–diene monomer (EPDM) rubbers, typically based on ethylidene norbornene, find application in crosslinked materials.⁹² In each polyethylene copolymer, the comonomer role is to suppress crystallinity allowing sufficient FR filler incorporation while maintaining acceptable compound physical properties and flexibility, particularly at low temperatures. Polypropylene (PP) has an LOI of 17.1⁶⁰ with a total heat release of 41.4 kJ/g.⁶¹ It has no tendency to form char and has the second highest heat release capacity of those tested (1571 J/(g K))⁶¹ after polyethylene. PP is generally considered a rigid polymer but with advances in catalyst and process technology, there are PP copolymers suitable for wire and cable applications.⁹³ Higher melting temperatures of advanced PP copolymers offer higher melting temperatures and therefore, the possibility to replace crosslinked polyethylene with thermoplastic PP in selected applications. In wire and cable applications, polymer selection is influenced by the final material state, either crosslinked or thermoplastic. Crosslinking of the various polyethylenes can be achieved by, at a minimum, one curing technology (peroxide, irradiation, or moisture).⁴⁹ PP, owing to the presence of a tertiary carbon at every repeat unit and its tendency to undergo chain scission under free radical conditions, is not as readily crosslinkable as polyethylene and ethylene copolymers.

FR selection is generally the same for the various polyethylene copolymers and PPs but the overall levels need to be adjusted for changes in total heat release capacity (for polar copolymers) and due to different decomposition mechanisms. Thermal decomposition of nonpolar polyethylene copolymers, in inert atmospheres, initially proceeds through crosslinking followed by random-chain scissions where branch points, owing to introduction of α -olefins, lower the thermal stability.⁹⁴ PP has lower thermal stability than nonpolar polyethylene copolymers due to the tertiary carbon within every repeat unit that results in rapid random-chain scission.⁹⁴ Thermal decomposition of the polar ethylene copolymers proceeds in two steps. EVA copolymers initially degrade by deacetylation forming acetic acid and an unsaturation in the polymer backbone.⁹⁵ Similar to PVC, these unsaturations can participate in crosslinking reactions but are less effective because the maximum unsaturation level is limited by the vinyl acetate level (18–40 wt % is typical commercially) and a structure composed of unsaturations connected by long aliphatic sequences further decomposes by

random chain scission with no residual char.⁹⁵ Acrylate copolymers also have an initial decomposition where a carboxylic acid side group and the corresponding alkene, ethylene, or butene for EEA or EBA copolymers, respectively, is formed followed by rapid chain scission yielding no char in inert or oxidative atmospheres.⁹⁶

The selection of FRs in polyethylene copolymers are generally based on the application type: insulating or jacketing. For insulation materials where there is a significant emphasis on maintaining the excellent electrical properties, particularly dielectric loss, of the polyethylene material, halogenated FR additives are the preferred choices.⁹⁷ In polyethylene copolymers, aromatic brominated FRs are the most common along with some use of a chlorinated FR. Decabromodiphenyl oxide is a highly effective FR for polyethylene copolymers primarily due to its cost effectiveness, high bromine content, excellent thermal stability, low solubility, and a solid physical form.^{98,99} Minor issues with bloom (additive migration) in polyethylene copolymers are noted¹⁰⁰ but good dielectric constant and dissipation factor and lack of interference with crosslinking reactions promoted by peroxides make this FR an excellent choice for wire and cable insulation materials. Decabromodiphenyl ethane is comparable in its performance with decabromodiphenyl oxide because of the chemical similarity and temperature evolution of bromine and has a lower tendency to bloom.¹⁰⁰ The slightly better UV performance of the ethane as compared with the oxide does not justify the difference in cost but regulatory issues might motivate this change (*vide infra*). In thin-wall communication cable insulation materials, the larger particle size of commercial decabromodiphenyl ethane products as compared with decabromodiphenyl oxide products is a concern. Ethylene bistetrabromophthalimide is also used and despite its lower bromine content is nearly as effective as decabromodiphenyl oxide with the advantage of significantly better UV stability, good wet electrical performance, and nonblooming characteristics.^{98,99} The lone chlorinated FR is dodecachloro-dodecahydromethanodibenzocyclooctene and is used in wire and cable applications using polyethylene copolymers, particularly EPDM, because of its lower smoke tendency than the brominated FRs particularly when formulated with low levels of an iron compound.⁹⁸ Polyethylenes, with either brominated or chlorinated FR additives, typically utilize the known antimony-halogen synergism^{73,74} and also incorporate significant amounts of surface treated fillers which serve as anti-drip additives.⁹⁸ Synergism between brominated and chlorinated FR additives is reported.¹⁰¹ Smoke suppression technologies based on metal hydrates, zinc borate, molybdates, and ZHS can be used in conjunction with halogenated FR additives.

The dominant use of nonhalogenated FRs is in polyethylene copolymer systems. Metal hydrates, typically ATH and magnesium hydroxide, are often used at levels of 60+ wt % to meet flame retardancy requirements for wire and cable applications. An important contribution to the FR mechanism of metal hydrates is the endothermic release of water, which removes heat from the system. On a weight basis, magnesium hydroxide provides a higher endothermic heat sink than ATH.⁷⁵ Dehydration temperature is another factor in FR selection where peak dehydration temperatures for ATH are slightly above 300°C and for magnesium hydroxide is slightly above 400°C.⁷⁵ In formulated metal hydrate systems, true processing temperatures are lower in accordance with the initial stages of dehydration, which can cause voids and reduction of physical properties. For most polyethylene copolymers, ATH offers a sufficient processing coupled with its low cost to be the leading hydrate technology utilized in wire and cable applications. Magnesium hydroxide finds application for PPs where higher processing temperatures might be required or in polyethylene copolymer systems where there can be subtle differences in flame and smoke characteristics between magnesium hydroxide and aluminum trihydroxide.¹⁰²

Natural sources of ATH (Gibbsite extracted from Bauxite) and magnesium hydroxide (Brucite) are available but generally have large particle size as a result of grinding operations and contain significant amounts of impurities. In wire and cable applications, finer particles sizes are utilized for higher LOI values, improved mechanical properties, lower brittleness temperatures, and smoother surface characteristics despite the drawback of increased mixture viscosity.⁷⁵

Impurities in natural sources can result in poor color, lower retention of physical properties on long-term heat aging, and reduction in electrical properties with the presence of electrolytes. Therefore, fine precipitated ATH and magnesium hydroxide are favored as particle size can be controlled to a nominal 1 μm size with low surface area and they contain very low impurity levels. Magnesium hydroxide production processes, by manufacturer, have considerably more variation than ATH but both metal hydrates are considered products by process, which in many cases results in the need to qualify alternate sources or in some cases to reformulate around filler selection.

For electrical applications, the particle size of ATH has a significant effect on dielectric constant.¹⁰³ EPDM with 50 wt % ATH with particle sizes ranging from 0.7–20 μm was evaluated, which clearly shows that dielectric constant increases from 3.05 to 3.35 as particle size is lowered from 20 to 0.7 μm . When exposed to water at 90°C, finer particles had a higher absorption rate resulting in even greater changes in dielectric constant where after 6 months the dielectric constant increased from 4.3 to 8, as the particle size was decreased from 20 to 0.7 μm . Therefore, surface treatments of metal hydrates are critical to obtaining high volume resistivity in water. In one study, untreated ATH in EVA copolymers had volume resistivity of $1 \times 10^8 \Omega \text{ cm}$ while aminosilane treated ATH had volume resistivity of $1.6 \times 10^{12} \Omega \text{ cm}$ after 28 days in 50°C water.¹⁰⁰ In another study, surface treatment of magnesium hydroxide with fatty acids (stearic) shows reduction in dielectric constant and dissipation factor compared with untreated filler.¹⁰⁴ In wet applications, silane treated surfaces are believed to be very hydrolytically stable¹⁰⁵ but it is unclear that there is sufficient hydrolytic stability of the acid–base reaction of fatty acids with metal hydrates. UL specifications on insulation resistance in water at the temperature ratings of 75°C or 90°C are amongst the most difficult requirements.⁵³ With systems at or near 40 wt % by volume of filler, it is clear that wet electrical performance remains extremely challenging for metal hydrates.

In addition to electrical property performance, obtaining acceptable physical property performance of metal hydrate systems requires formulation approaches including surface treatments and coupling agents. For proper dispersion of fillers with hydroxyl surfaces, fatty acids are commonly used due to their low cost while surface treatment with organosilanes provides more hydrolytically stable systems. Reactive polymers can also be used to couple the filler-resin interface with the most common reactive polymers being polyolefins modified with maleic anhydride produced by a melt grafting process or as reactor grades, which are typically terpolymers of ethylene, polar comonomer, and maleic anhydride. In EVA–magnesium hydroxide systems, stearic acid has been shown to lower tensile strength and improve elongation.^{43,104} In EVA–ATH systems, aminosilane surface treatments have been shown to boost both tensile strength and elongation.¹⁰⁰ The tensile strength increase is postulated to occur from interaction of the amine with the carboxyl group in vinyl acetate and this is achieved without substantial changes to processing characteristics. Additionally, LOI improvement is achieved with aminosilane treated ATH (43.5) as compared with untreated ATH (41). In crosslinked polyolefin applications, vinylsilanes are commonly used surface treatments as the reactive vinyl group can participate in crosslinking and improve tensile strength and modulus¹⁰⁶ but generally at the cost of elongation performance.⁴³ Maleic anhydride grafted polyethylenes (MAH-g-PE) generally improve tensile strength while changes in elongation can depend on the specific selection of maleic anhydride grafted polymer and level.¹⁰⁷ With proper selection of the polyethylene base resin, the MAH-g-PE can help provide formulation latitude to achieve the overall balance of properties. Interestingly, MAH-g-PE systems exhibited improved cone calorimetry characteristics (time to ignition (TTI), time to peak heat release rate (TTPHRR), and total smoke released).¹⁰⁷ Coupling of filler with polymeric resins such as MAH-g-PE does significantly increase the viscosity and this has to be carefully balanced in the application.¹⁰⁸

Owing to the high loadings of metal hydrates, synergists for metal hydrate systems that would allow reductions in FR loading are actively being researched. Talc is found to be an LOI synergist at relatively low levels (3 wt %) in EVA–magnesium hydroxide systems¹⁰⁹ and subsequent research concluded that as talc surface area was increased the PHRR in cone calorimetry was significantly

reduced.¹¹⁰ Although smoke suppressants are generally not required in halogen-free systems, it has been reported that talc and zinc borate suppress smoke density in a magnesium hydroxide system.¹¹¹ Initial work on layered silicates (organically modified Montmorillonite) in several polymers (nylon, polystyrene, and PP) concluded that low-level addition (2–5 wt %) of layered silicates resulted in significant reductions in PHRR as measured by cone calorimetry and was as effective as 30 wt % decabromodiphenyloxide/Sb₂O₃ loadings in polystyrene.¹¹² A reasonable degree of exfoliation of the layered silicate in the resin system is required to achieve reductions in PHRR.¹¹³ EVA is one resin system in which exfoliation appears to be reasonably achieved and EVA-metal hydrate-layered silicate systems have been evaluated where the metal hydrate reduces total fuel load and layered silicates improve char formation.^{114–116} One study on coaxial cable jacketed with and without layered silicate in an EVA/ATH system showed that UL-1666 burn performance could only be achieved with addition of a layered silicate material.¹¹⁴ Additional studies show that LOI is significantly reduced while cone calorimetry measures are improved with addition of organically modified montmorillonites.¹¹⁶ For wire and cable applications where long-term heat aging performance is required, impurities within the lattice of the layered silicate are a concern,¹¹⁷ and thus research on synthetic nanocomposites with improved purity has been initiated^{118,119}. Additional nanomaterials, polyhedral oligomeric silsesquioxanes (POSS), and carbon nanotubes, single wall (SWNT) and multi-wall (MWNT)), have been evaluated as FRs and have shown significant effectiveness.¹¹³ Cable production using a blend of ATH, organoclay, and MWNT has been reported.¹²⁰ Evaluations have ascribed reductions in heat release rate to the ability of the filler to form a gel-like structure as measured by rheological measurements.¹²¹ More recently, sub-micron sized Boehmite has shown synergy in EVA–ATH systems.¹²²

Another technology for low voltage insulation is based on ethylene-acrylate copolymers with high levels of silicone fluids or gums and calcium carbonate.^{123,124} A system based on 65 wt % ethylene-butyl acrylate (EBA), 5 wt % silicone, and 35 wt % CaCO₃ has an LOI value ~34¹²³ and as a result of the high polymer loading, good volume resistivity is expected for use in insulation applications in addition to its use in jacketing. Significant research into the mechanism indicates the formation of carboxylic acid side groups from the ethylene-acrylate copolymer, which react with the CaCO₃ to form a calcium salt with release of CO₂ and H₂O.¹²⁴ Analysis of residue generated at 500°C in this system indicates CaCO₃ and SiO₂ (from silicone oxidation) are present while at 1000°C, residue analysis indicates the presence of calcium oxide (CaO), calcium silicate (Ca₂SiO₄), and calcium hydroxide (Ca(OH)₂) along with the presence of silicon oxycarbide.¹²⁴ An attempt to benchmark the ethylene acrylate copolymer–CaCO₃–silicone system against an EVA–metal hydrate system with a similar LOI using cone calorimetry indicated the ethylene acrylate copolymer–CaCO₃–silicone system has a lower TTI, a PHRR more than double, and a TTPHRR of half the EVA-metal hydrate system.¹²⁵

26.3.3 FLUOROPOLYMERS

Fluoropolymers are another class of material that finds utility in wire and cable constructions due to high service temperatures, chemical resistance, dielectric performance, and inherent flame retardancy. The first fluoropolymer used in wire and cable was polytetrafluoroethylene (PTFE), which has a continuous service temperature of ~260°C and thus is used as an insulation material in military/aerospace applications. PTFE has an LOI of 95,⁶⁰ an LOI of 49 at 300°C,⁶⁰ and a total heat release of 3.7 kJ/g.⁶¹ The drawback for this highly FR material is the inability to melt process the material, which limits larger scale wire and cable applications. Analogous to polyethylene copolymers, the industry developed copolymers of tetrafluoroethylene and hexafluoropropylene, also known as fluorinated ethylene–propylene (FEP) copolymers. The perfluorinated structure maintains the high thermal stability and inherent flame retardance. FEP, similar to PTFE, has a LOI of 95 and even at 300°C has a LOI of 50.⁶⁰ Copolymerization provides a melting point suppression which allows FEP to be melt processed with an upper service temperature of ~200°C allowing FEP to serve similar specialty markets as PTFE. Amongst FR materials useful as insulating materials, the electrical

properties of FEP are excellent. A dielectric constant of ~ 2 and very low dissipation factors (0.0003 at 100kHz and 0.0007 at 1 MHz)¹²⁶ allow use in high-speed communication cables (Category 5) rated at 100MHz. With inherent flame retardancy and electrical properties, FEP insulated copper is used in plenum cables, which must pass the most stringent cable test protocol, UL-910. Owing to its application in plenum cables, FEP is the market leader in the fluoropolymer family. Polyvinylidene fluoride (PVDF), a homopolymer of vinylidene fluoride, is the second most common fluoropolymer in the market. The methylene-fluoromethylene repeat unit combines the properties of polyethylene and PTFE with a service temperature of 150°C and an LOI of 43.7.⁶⁰ The dielectric constant and dissipation factor for PVDF are not at the performance level of FEP. Poly(ethylene-*co*-tetrafluoroethylene), poly(ethylene-*co*-chlorofluoroethylene), and poly(chlorotrifluoroethylene) are additional fluoropolymers, which find niche applications in wire and cable.

26.3.4 SILICONE POLYMERS

Silicone elastomers are the preferred materials when high temperature resistance and high flexibility are required. Silicone elastomers are formulated with reinforcing fillers to give acceptable mechanical properties and are generally heat-cured. High temperature performance results in use for under-the-hood automotive applications such as spark plug wires. Siloxane networks can form substantial char during combustion where the polymer backbone forms silica. Silicones formulated with kaolin, magnesium hydroxide, zinc borate, and their mixtures show significant char formation (67 wt %) in 28 wt % filler systems and excellent cone calorimetry measures.¹²⁷ With proper formulation of the system and cable design, the char can form an electrically insulating layer making this material suitable for circuit integrity applications (UL-2196).³⁹ Silicone compounds are commercially available that can be converted to a ceramic during the fire test and can be used for security cables with integrity requirements according to international norms.

26.3.5 OTHER POLYMERS

Small amounts of other polymers are used in certain niche applications, including chlorinated polyethylene (CPE), neoprene, chlorosulfonated polyethylene, nylon, and TPU.

26.4 LABORATORY FLAMMABILITY TESTS FOR WIRE AND CABLE MATERIALS

As discussed earlier, many FR qualification tests for wires and cables, according to applicable standards, require testing on a fully fabricated article. However, to conduct research toward new materials for use in wire and cable applications, it is often desirable to obtain directional information in the early stages by conducting laboratory-scale tests that are capable of discerning improvements in FR characteristics of materials. Later in the product development process, optimization, validation, and qualification must nevertheless be conducted on full-scale articles and equipment.

LOI based on ASTM D 2863¹²⁸ and temperature index based on NES 715¹²⁹ (or ISO 4589¹³⁰) have been used in the laboratory to assess the ease of extinction of cable compounds.⁴ The LOI determines the minimum concentration of oxygen in nitrogen that will support candle-like burning for at least 3 min. This test method has been widely used to measure flammability of plastics as well as cable compounds and is often reported in cable compound datasheets as a measure of material flammability. Since this is a simple, low-cost, and reliable test, it is sometimes used for material specification and quality control for certain wire and cable applications. The temperature index is the critical temperature at which the material sustains candle-like burning at an oxygen index of 21%. In general, the temperature index of fire-retardant cable compounds exceeds 250°C. UL 94¹³¹ is used to measure the propensity of a material to extinguish once it becomes ignited in a horizontal or vertical position. Though it is not a cable test, some material suppliers use UL 94 as a laboratory FR screening test in the early stages of development of FR formulations for wire and

cable applications. ASTM E 662¹³² is used to measure the smoke emission characteristics in a NBS (National Bureau of Standards) smoke chamber (914 × 610 × 914 mm) using a sheet of materials or small section cables. The light transmittance as a result of smoke accumulated within the chamber is then measured under a nonflaming (smoldering) and flaming mode. Both UL 94 and ASTM E 662 are being used by researchers for screening and developing wire and cable FR compounds before the formulations are scaled up to fabricated cable for flame and smoke generation tests.^{133–135}

A fire propagation apparatus (FPA) according to the ASTM E 2058¹³⁶ test standard is used to measure heat release characteristics of a material in a horizontal or vertical orientation under different conditions of external heat flux, ventilation, and oxygen concentration. For cable test specimens, this test method measures flame heat flux under 40% oxygen concentration to simulate the radiant heat flux from real-scale flames. The measured flame heat flux and the TTI of the material under different incident heat fluxes are used to derive a fire propagation index, which was found to have good correlation with large-scale fires according to the Factory Mutual Global parallel panel test that simulates the fire propagation of two facing vertical layers of electrical cables ignited by a 60 kW fire source. It has been found that the fire propagation test can be used to screen UL 910 (or NFPA 262) cables.¹³⁷

Cone calorimetry according to the ASTM E 1354¹³⁸ or ISO 5660¹³⁹ standards are commonly used in the laboratory to screen flammability of materials by measuring heat release characteristics of the compound.^{116,140} This device is similar to FPA but does not have the versatility of FPA. The cone calorimeter can determine the ignitability, heat release rates, effective heat of combustion, visible smoke, and CO₂ and CO development of cable materials. This test has been used extensively for wire and cable material evaluation. The microscale combustion calorimeter (MCC), also known as pyrolysis combustion flow calorimeter (PCFC), was recently introduced to the industry for screening heat release characteristics of FR materials.^{141,142} This device only requires milligram quantities of test specimen to measure the heat release capacity (maximum heat release potential). Cone calorimetry and MCC have been used in product development for flammability screening of wire and cable compounds.¹¹⁸

26.5 CORRELATIONS AMONG FLAMMABILITY TESTS

There have been attempts to establish correlations between laboratory screening tests, material tests, and cable tests discussed earlier.⁶ Although there are some successes in this effort, it is generally very difficult to correlate material flammability properties to actual cable performance under fire conditions. The flame propagation of a cable will depend on the cable conductor size, conductor type, cable mounting (single cable vs. bundled cables), insulation thickness, and materials used for insulation and jacketing. One certainly would not expect that a single material flammability property could predict the burning phenomena of a full cable construction. Following is a brief discussion of some examples of correlations established in the literature. The examples are illustrative of some of the published correlation studies, which have enjoyed varying levels of success.

Researchers have tried to correlate LOI with other flammability tests such as UL 94, ASTM E 84¹⁴³ Steiner tunnel test, cable tests, and cone calorimeter.¹⁴⁴ However, there has been limited success due to the downward burning of the test specimen and unrealistically high oxygen concentrations that do not mimic real fire scenarios. One study has found that there is a good hyperbolic correlation between LOI of the cable material and PHRR in the cone calorimeter test on cable samples, in particular, at a heat flux of 20 kW/m².¹⁴⁵ Cone calorimetry on cable samples was found to have relatively good correlation with full-scale cable tray burn tests according to the CSA FT-4 test protocol in terms of heat and smoke release.¹⁴⁶ The FIPEC study attempted to correlate cone calorimetry on materials and cables to full-scale (i.e., modified IEC 60332-3) and real-scale fire tests.¹⁴⁷ It showed some success in correlations of heat release characteristics and smoke generation using cone calorimetry on cable samples, full-scale, and real-scale testing. However, cone calorimetry on the materials had no correlation with cone calorimetry on the cable samples, full-scale, and real-scale

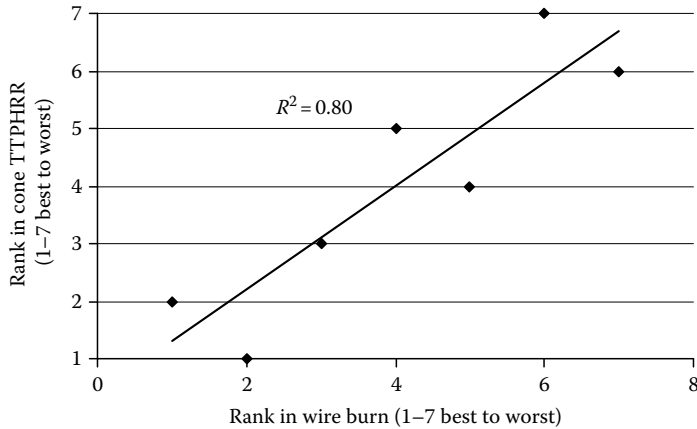


FIGURE 26.2 Spearman ranking order correlation between time to peak heat release rate (TTPHRR) and single wire burn. (From Cogen, J.M. et al., Assessment of flame retardancy in polyolefin-based non-halogen FR compounds, In *Proceedings of the 53rd IWCS/Focus International Wire and Cable Symposium*, 2004, pp. 185–190.)

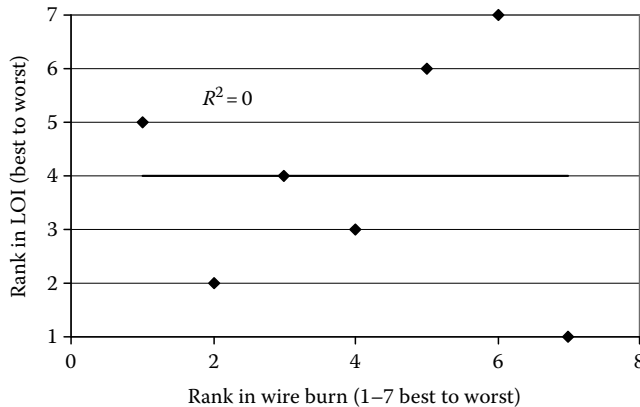


FIGURE 26.3 Spearman ranking order correlation between LOI and single wire burn. (From Cogen, J.M. et al., Assessment of flame retardancy in polyolefin-based non-halogen FR compounds, In *Proceedings of the 53rd IWCS/Focus International Wire and Cable Symposium*, 2004, pp. 185–190.)

testing. Single horizontal wire burn tests based on the Chrysler MS 8288 standard were found to have a good correlation with cone calorimetry in terms of TTPHRR, as shown in Figure 26.2.¹²⁵ Other cone calorimetry parameters such as TTI and PHRR had poor correlations with single wire burns in the same study. LOI was also found to be a poor predictor of the single wire burn test, as shown in Figure 26.3.

A probability function was proposed to screen the single wire burn flame spread using heat release capacity measured by PCFC on halogen-free FR compounds.¹⁴⁸ Figure 26.4 shows the probability of flame spread for a single wire burn as a function of heat release capacities of wire insulation compounds. It was suggested that the probability of flame spread for an insulated wire is less than 5% when the heat release capacity is less than ca. 320 J/g K.

Correlations were also established between UL 94, LOI, MCC, and cone calorimetry for both halogenated and nonhalogenated FR wire and cable compounds.¹⁴⁹ The study (Figure 26.5) indicated that LOI has poor correlation with MCC parameters due to different flame combustion mechanisms in the LOI (incomplete combustion) and the MCC (forced complete combustion) tests. This correlation was improved by taking into account the burning efficiencies (i.e., combustion and heat transfer efficiencies) of the polymer compounds.¹⁵⁰

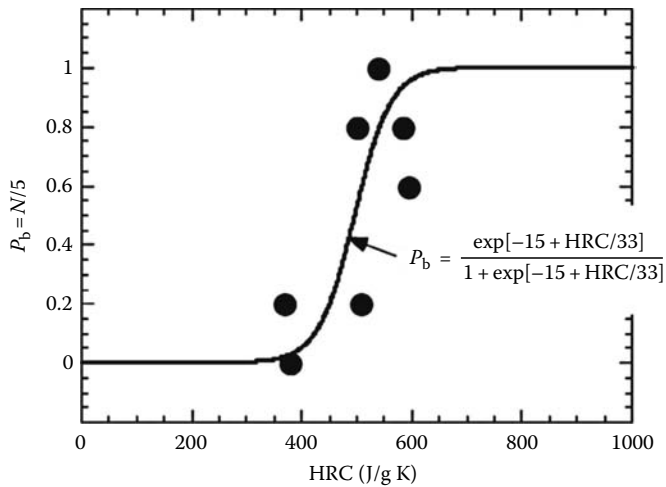


FIGURE 26.4 Probability for flame spread versus heat release capacity of compounds. (Cogen, J.M. et al., Correlations between pyrolysis combustion flow calorimetry and conventional flammability tests with halogen free flame retardant polyolefin compounds, *Fire Mater.*, 2009, 33, 33–50.)

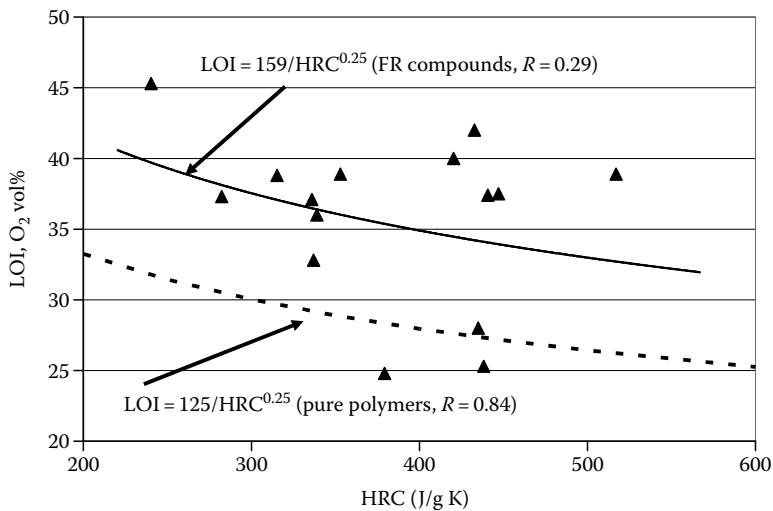


FIGURE 26.5 Relationships between LOI and HRC for pure polymers and FR compounds. (From Lin, T.S. et al., Correlations between microscale combustion calorimetry and conventional flammability tests for flame retardant wire and cable compounds, in *Proceedings of 56th International Wire and Cable Symposium*, 2007, pp. 176–185.) The LOI–HRC relationship for pure polymers is obtained from the literature. (From Lyon, R.E. and Janssens, M.L., Polymer flammability, Final Report DOT/FAA/AR-05/14 May, 2005.)

It was found that both cone calorimetry and MCC parameters could serve as screens for UL 94 ratings although there are certain ranges of parameters where UL 94 ratings cannot be clearly differentiated.¹⁴⁹ In the same study, FIGRA and fire performance index (FPI) had strong correlations with total heat released (THR) measured in MCC as indicated in Figures 26.6 and 26.7. It is interesting to note that halogenated FR tends to have a higher THR with higher FIGRA and lower FPI, while vice versa is reported for nonhalogenated FR trends.

The UL 1685 tray cable burn test was conducted on a cable construction with three different jacketing materials consisting of EVA polymer with 60 wt % $\text{Mg}(\text{OH})_2$ (EVA–MH), EVA polymer with 58 wt % $\text{Mg}(\text{OH})_2$ and 2 wt % nanoclay (EVA–MH–NanoM), and 1:1 EVA:PE with 58 wt %

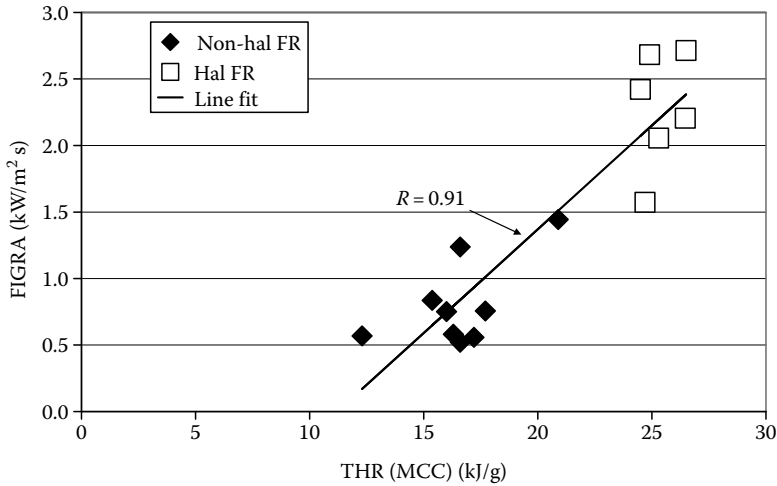


FIGURE 26.6 Relationship between FIGRA and THR measured in MCC (i.e., PCFC). FIGRA = PHRR/TTPHRR, FPI = TTI/PHRR, where PHRR is peak heat release rate, TTPHRR is time to peak heat release rate, and TTI is time to ignition. (Based on Lin, T.S. et al., Correlations between microscale combustion calorimetry and conventional flammability tests for flame retardant wire and cable compounds, in *Proceedings of 56th International Wire and Cable Symposium*, 2007, pp. 176–185.)

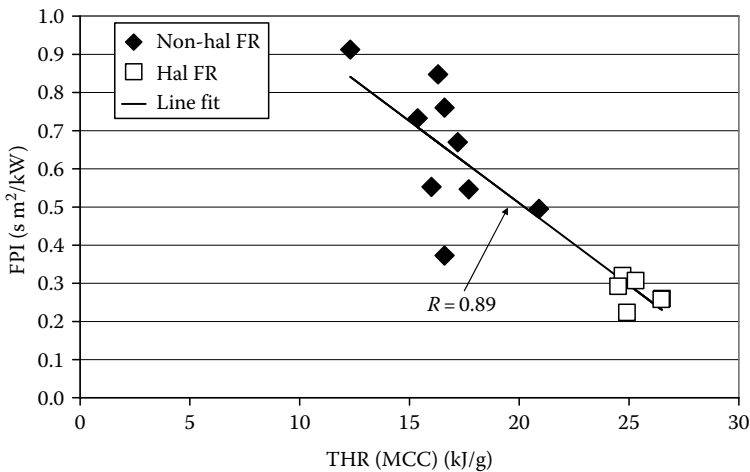


FIGURE 26.7 Relationship between FPI and THR measured in MCC (i.e., PCFC)-based on Reference 149. (From Lin, T.S. et al., Correlations between microscale combustion calorimetry and conventional flammability tests for flame retardant wire and cable compounds, in *Proceedings of 56th International Wire and Cable Symposium*, 2007, pp. 176–185.)

Mg(OH)₂ and 2 wt % nanoclay (EVA–PE–MH–NanoM).¹¹⁶ Figure 26.8 shows the flame propagation height as a function of testing time in the UL 1685 tray cable burn test. The result shows that the EVA–MH–NanoM sample had the shortest time to flameout and the least damage height. The EVA–MH sample had a higher damage height and took 1 ½ min longer to extinguish than EVA–MH–NanoM. The EVA–PE–MH–NanoM sample failed the UL 1685 test with flame height exceeding 8 ft after 20 min of flame application time.

The UL 94, LOI, and cone calorimetry were also conducted on the jacketing materials (see Table 26.2). The results show that EVA–MH–NanoM sample had the lowest PHRR, longest TTPHRR,

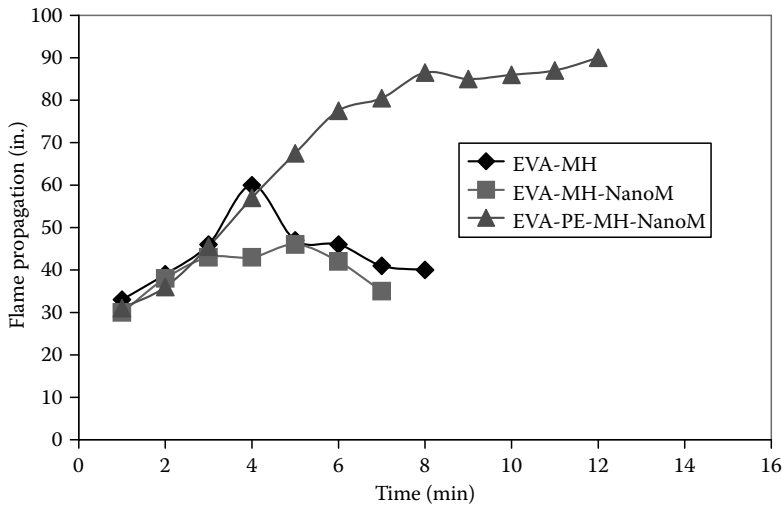


FIGURE 26.8 Flame propagation height versus time in UL 1685 tray cable burn test. (Whaley, P.D. et al., Nanocomposite flame retardant performance: Laboratory testing methodology, in *Proceedings of the 53rd IWCS/Focus International Wire & Cable Symposium*, 2004, pp. 605–611.)

TABLE 26.2
Flammability Comparison for Three Different
Flame-Retardant Formulations

	EVA-MH	EVA-MH-NanoM	EVA-PE-MH-NanoM
LOI (%)	44	37	33
UL 94	NR	V-0	V-0
PHRR (kW/m ²)	227	187	274
TTPHRR (s)	333	425	335
TTI (s)	113	184	128

Source: Whaley, P.D. et al., Nanocomposite flame retardant performance: Laboratory testing methodology, in *Proceedings of the 53rd IWCS/Focus International Wire & Cable Symposium*, 2004, pp. 605–611.

and longest TTI compared with the other two samples. It can be seen that the ranking of UL 1685 performance correlated very well with the performance ranking by PHRR. On the other hand, LOI and UL 94 ranking did not reveal the high flame resistance of EVA-MH-NanoM in the UL 1685 test.

Recent efforts have focused on the combination of high throughput (HT) FR compound preparation coupled with HT screening of FR properties.¹⁵¹ Work at Marquette University using a parallel flame device has resulted in a promising method that can be readily parallelized to provide HT capability to screen gram-scale materials based on the time of burning. This technique has been applied to study FR compositions in polystyrene¹⁵¹ and vinyl esters.¹⁵² Average burn times measured using the Marquette method correlated with PHRR and THR measured with cone calorimetry.¹⁵⁰ Work at NIST has resulted in a HT compound preparation method using a twin-screw extruder.¹⁵³ Various gradient heating methods are utilized to provide HT analysis of FR properties.^{154,155} Critical heat flux measured by the gradient heating method correlated well with the critical heat flux for burning calculated from PCFC.¹⁵¹ Some valuable correlations with traditional tests were obtained,

suggesting that such approaches offer longer-term potential for accelerating FR product development applied to wire and cable applications.

As one can see from the above discussion, establishing correlation between bench-scale flammability and cable flame tests is a difficult task because of complicated chemical and physical processes involved in the burning and combustion of polymer materials and cables. Much research is still needed to understand fundamental processes governing the flaming combustion of wire and cable compounds in actual cable designs and cable bundles in a given environment.

26.6 INDUSTRY TRENDS AND ISSUES

26.6.1 GEOGRAPHICAL FRAGMENTATION

As previously mentioned, the FR wire and cable market is complicated by the fact that standards and leading technologies to meet them are highly fragmented on a geographical basis. Although there is not a significant global trend toward harmonization of standards, there is a major effort under way toward harmonization of wire and cable standards for the building industry in the European Union. As discussed earlier, this effort is called the CPD.^{3,54,55} The CPD was initiated in 1988 and is now finally close to implementation. The CPD aims to create a single European market by removing the technical barriers to trade between Member States through the use of harmonized standards and approvals. It applies to all construction products, including cables that are produced for, or incorporated within building and civil engineering construction works. It harmonizes all construction products subject to regulatory controls for CE marking purposes. To put the fragmentation issue in perspective, in the domain of reaction of construction products to fire, member states of the EU use 30 different tests for cables.³ As the categories and requirements for cable ratings within the CPD are finalized and adopted by member countries, there is likely to be some impact on selection and de-selection of certain FR additives, polymers, and polymer compounds based on their ability to competitively meet the new standards. It is important to note that it is up to each member state to decide which classes will be used in specific applications. The CPD is predicted to impact 40% of products in the low voltage segment, 60% of products in the data and optical fiber segment, and 100% of products in the FR cable segment.³

The issue of geographical fragmentation poses significant challenges for the material suppliers and cable manufacturers. For the suppliers of FR additives, this means that there will continue to be a need for a broad range of choices in the industry, ranging from low-cost natural minerals to high performance intumescent additive blends, and many materials in between. For the cable compound formulator this means there will continue to be a need for materials with a broad array of property/performance/cost trade-offs, with each compound occupying an optimal “sweet spot” for a particular application.

26.6.2 ENVIRONMENTAL CONCERNS

Over a period of many years, there has been a steady trend in the global FR wire and cable market toward increased sustainability and environmentally sound wire and cable materials. This is manifest in terms of “green” solutions, sustainability, end-of-life issues (such as recycling), and increasing scrutiny of hazardous substances. Because these are not unique to the wire and cable industry, a detailed discussion of these various initiatives is beyond the scope of this document.

The European Union has been quite visible in recent years with such directives. RoHS (Restriction in the use of Hazardous Substances), WEEE (Waste of Electrical and Electronic Equipment), and REACH (Registration, Evaluation, Authorization, and Restriction of Chemical substances). RoHS places restrictions on use of lead, mercury, cadmium, hexavalent chromium, polybrominated biphenyls, and some polybrominated diphenylethers. WEEE targets responsible recycling of electronic equipment. REACH is a new European Community Regulation on chemicals and their safe use

(EC 1907/2006). As the name implies, it deals with the registration, evaluation, authorization, and restriction of chemical substances. The new law entered into force on 1 June 2007. The aim of REACH is to improve the protection of human health and the environment through the better and earlier identification of the intrinsic properties of chemical substances.¹⁵⁶ The ELV (End of Life Vehicles) directive aims to reduce the amount of environmentally unfriendly waste from ELVs. Similar initiatives are well developed in Japan and are evolving in China¹⁵⁷ and many other countries. In the United States, at the state level, some states (for example, Maine and California) are adopting material restrictions on PVC plasticizers and certain brominated FRs.

Some highly visible public statements have been made by several consumer electronic companies that can be inferred to have a direct impact on their FR material selection. Specific examples include Apple Computer's pledge to "completely eliminate the use of PVC and BFRs in its products by the end of 2008."¹⁵⁸ Dell¹⁵⁹ and Lenovo¹⁶⁰ have publicly stated their intentions to eliminate the use of PVC and BFRs in their products.

Another global trend in this general direction is the drive toward PVC wire and cable reformulation to remove lead stabilizers. Among the replacements are stabilizers based on zinc or calcium.¹⁶¹ In addition to lead, concern about certain phthalate plasticizers is increasingly being encountered, such as California's proposition 65, which may continue the pressure on certain PVC-based materials.

26.6.3 OTHER INDUSTRY TRENDS AND ISSUES

A number of other trends are listed briefly as follows, many of which were touched upon in other contexts earlier in this chapter:

- PVC plastic conduit being replaced by halogen-free materials to achieve low acidity/low smoke burn properties
- Strong push by some fluoropolymer suppliers and fluoropolymer cable manufacturers for adoption of specific standards that promote use of fluoropolymers (e.g., proposed limited combustible Plenum rating in the United States)
- Higher temperature requirements for automotive applications shifting from PVC to crosslinked polyolefin
- Increased amount of electronics in automobiles driving more auto wire usage and driving a need for thin-wall/down gauged wire to maintain or reduce space and weight requirements
- Potential move to higher voltage in automobiles (may drive changes in material requirements)
- Production of commodity cables migrating to low-cost regions, particularly Asia
- Shift to halogen-free low smoke FR compounds being lead by Asia and Europe

26.7 SUMMARY

Wires and cables that are utilized in enclosed spaces are usually required to have fire safety characteristics as described in various codes and standards. The codes and standards governing fire safety of wires and cables are highly complex and diverse, both by application and by geography, and play a critical role in determining selection and formulation of insulation and jacketing materials. Thus, careful review of applicable standards is essential prior to beginning formulation or product development.

PVC is a ubiquitous material in wire and cable due to its dielectric strength, volume resistivity, mechanical strength, chemical resistance, water resistance, good processability, and flame retardancy. This combination of properties is achieved in a very cost-effective manner and thus PVC is the material of choice in applications where PVC meets market requirements.

After PVC, polyolefins are the next most widely used material for FR applications in wire and cable. They have very good dielectric strength, volume resistivity, mechanical strength, low temperature flexibility, and water resistance. In contrast to PVC, polyolefins are not inherently FR and thus are more highly formulated, requiring the addition of FRs to meet market requirements for flame retardancy. Polyolefins are experiencing extensive interest as the trend toward halogen-free materials continues to build.

Fluoropolymers are another class of material that finds utility in wire and cable constructions due to high service temperatures, chemical resistance, dielectric performance, and inherent flame retardancy.

Although many FR qualification tests for wires and cables, according to applicable standards, must be conducted on a fully fabricated article, it is often desirable to obtain directional information in the early stages of product development by conducting laboratory-scale tests that are capable of discerning improvements in FR characteristics of materials. Therefore, there have been many attempts to establish correlations between laboratory screening tests, material tests, and cable tests. Although there are some successes in this effort, it is generally difficult to rigorously correlate material flammability properties to actual cable performance under fire conditions because of complicated chemical and physical processes involved in the burning and combustion of polymer materials and cables.

A number of trends are having a significant influence on the direction of material selection. These include a slow but steady increase in the drive for green chemistry and sustainability, end-of-life issues such as disposal and recycling, reduction in reliability on toxic or hazardous chemicals, and adoption of the lowest cost technology and manufacturing while still demanding high quality and longevity of installed wires and cables.

REFERENCES

1. *Fire in the United States 1995–2004*, 14th edn., FA-311/August 2007, U.S. Fire Administration/National Fire Data Center, Emmitsburg, MD.
2. World Fire Statistics, Geneva Association Information Newsletter, October, 2007.
3. White paper: Construction Products Directive (CPD), A European Directive to Ensure the Safety of Tomorrow's Buildings, Nexans, 2004.
4. Barnes, M.A., Briggs, P.J., Hirschler, M.M., Martheson, A.F., and O'Neill, J.T., A comparative study of the fire performance of halogenated and non-halogenated materials, for cable applications. Part II tests on cables, *Fire Mater.*, 1996, 20, 17–37.
5. Hirschler, M.M., Fire testing of electrical materials, *Electrical Insulating Materials: International Issues*, ASTM STP 1376, Hirschler, M.M. (Ed.), American Society for Testing and Materials, West Conshohocken, PA, 2000.
6. Hirschler, M.M., Survey of fire testing of electrical cables, *Fire Mater.*, 1992, 16, 107–118.
7. Troitzsch, J., *Plastic Flammability Handbook*, 3rd edn., Hanser Publishers, Munich/Hanser Gardner Publications, Inc., Cincinnati, OH, 2004.
8. Richter, S. and Schmidt, R., Testing of cables designed for fire resistance, A comparison of U.S. and European standards, *Proceedings of 46th International Wire and Cable Symposium*, Philadelphia, PA, 1997, pp. 752–760.
9. Nakagawa, Y. and Komai, T., Current Japanese standards for flammability tests on electric cables, *Fire Mater.*, 1993, 17(6), 265–270.
10. Buch, R., Fire test methods for electrical and dielectric materials, *IEEE Electrical Insulation Magazine*, 1990, 6(3), 12–19.
11. NFPA 70: National Electrical Code, National Fire Protection Association, Quincy, MA, 2008.
12. UL 1581: Reference Standard for Electrical Wires, Cables, and Flexible Cords, Section 1080, VW-1 (Vertical Specimen) Flame Test, UL, Northbrook, IL, 2006.
13. UL 1685: Standard for Safety Vertical-Tray Fire-Propagation and Smoke-Release Test for Electrical and Optical-Fiber Cables, UL, Northbrook, IL, 2007.
14. CSA FT-4: Canadian Standards Association, C22.2 No. 0.3-01, Section 4.11.4, Vertical Flame Test-Cables in Cable Trays/FT4, CSA, Toronto, Canada, 2001.

15. UL 1666: Standard for Test for Flame Propagation Height of Electrical and Optical-Fiber Cables Installed Vertically in Shafts, UL, Northbrook, IL, 2007.
16. (a) NFPA 262: Standard Method of Test for Flame Travel and Smoke of Wires and Cables for Use in Air-Handling Spaces, National Fire Protection Agency, Quincy, MA, 2007; (b) UL 910 Standard for Safety Test for Flame-Propagation and Smoke-Density Values for Electrical and Optical-Fiber Cables Used in Spaces Transporting Environmental Air, UL, Northbrook, IL, 1998.
17. IEC 60332-1: Tests on electric and optical fibre cables under fire conditions: Test for vertical flame propagation for a single insulated wire or cable, IEC, Geneva, Switzerland, 2004.
18. IEC 60332-2: Tests on electric and optical fibre cables under fire conditions: Test for vertical flame propagation for a single small insulated wire or cable, IEC, Geneva, Switzerland, 2004.
19. CSA FT-1 Canadian Standards Association, C22.2 No. 0.3-01, Section 4.11.1, Vertical Test/FT1, CSA, Toronto, Canada, 2001.
20. IEC 60332-3: Tests on electric cables under fire conditions: Test for vertical flame spread of vertically-mounted bunched wires or cables, IEC, Geneva, Switzerland, 2004.
21. IEEE 383-2003: Standard for qualifying class 1E electric cables and field splices for nuclear power generating stations, IEEE: Institute Of Electrical & Electronics Engineers, Piscataway, NJ, 2004.
22. IEEE 1202-2006: Standard for Flame-Propagation Testing of Wire and Cable, Institute of Electrical and Electronics Engineers, Piscataway, NJ, 2006.
23. Guida, T.J., Riser, cable tray and bench-type flame tests, *FRCA Fall Conference*, Newport, RI, 1998, pp. 63–70.
24. Przybyla, L.J., Guida, T.J., Williams, J.L., and Kaufman, S., Fire testing of riser cables, *J Fire Sci.*, 1984, 3, 9–25.
25. IEC 61034-1: Measurement Of Smoke Density Of Cables Burning Under Defined Conditions—Part 1: Test Apparatus, IEC, Geneva, Switzerland, 2005.
26. IEC 61034-2: Measurement Of Smoke Density Of Cables Burning Under Defined Conditions—Part 2: Test Procedure And Requirements, IEC, Geneva, Switzerland, 2006.
27. NES 711: Determination of the Smoke Index of The Products of Combustion From Small Specimens of Materials, U.K. Ministry Of Defence Naval Engineering Standards, Foxhill Bath, U.K., 1981.
28. BS 7622-1: Measurement Of Smoke Density Of Electric Cables Burning Under Defined Conditions—Test Apparatus, BSI: British Standards Institution, London, U.K., 1993.
29. EN 50268-1: Common Test Methods For Cables Under Fire Conditions—Measurement Of Smoke Density Of Cables Burning Under Defined Conditions, European Committee for Standardization, Brussels, Belgium, 2000.
30. IEC 60754-1: Test on Gases Evolved During Combustion of Materials from Cables—Part 1: Determination of the Amount of Halogen Acid Gas, IEC, Geneva, Switzerland, 1994.
31. EN 50267-1: Common Test Methods For Cables Under Fire Conditions. Tests On Gases Evolved During Combustion Of Materials From Cables. Apparatus, European Committee for Standardization, Brussels, Belgium, 1999.
32. BS 6425-1: Test On Gases Evolved During The Combustion Of Materials From Cables. Method For Determination Of Amount Of Halogen Acid Gas Evolved During Combustion Of Polymeric Materials Taken From Cables, BSI: British Standards Institution, London, U.K., 1990.
33. IEC 60754-2: Test Of Gases Evolved During Combustion Of Electric Cables—Determination Of Degree Of Acidity Of Gases Evolved During The Combustion Of Materials Taken From Electric Cables By Measuring pH And Conductivity, IEC, Geneva, Switzerland, 1997.
34. EN 50267-2: Common Test Methods For Cables Under Fire Conditions—Test On Gases Evolved During Combustion Of Materials From Cables—Procedures—Determination Of The Amount Of Halogen Acid Gas, Brussels, Belgium, 1999.
35. BS 6425-2: Test On Gases Evolved During The Combustion Of Materials From Cables—Determination Of Degree Of Acidity (Corrosivity) Of Gases By Measuring Ph And Conductivity, BSI: British Standards Institution, London, U.K., 1993.
36. NES 713: Determination Of The Toxicity Index Of The Products Of Combustion From Small Specimens Of Materials, U.K. Ministry Of Defence Naval Engineering Standards, Foxhill Bath, U.K., 1985.
37. IEC 60331: Tests For Electric Cables Under Fire Conditions—Circuit Integrity, IEC: Geneva, Switzerland, 1999.
38. BS 6387: Specification For Performance Requirements For Cables Required To Maintain Circuit Integrity Under Fire Conditions, BSI, London, U.K., 1994.
39. UL 2196: Standard for Tests for Fire Resistive Cables, UL, Northbrook, IL, 2006.

40. Grayson, S., Van Hess, P., Vercellotti, U., Breulet, H., and Green, A., Fire Performance of Electrical Cables—New Test methods and Measurement Techniques, Final Report of EU SMT Project SMT4-CT96-2056. Interscience Communications London, U.K., 2000.
41. MIL-DTL-24640B: Detail Specifications for Cables, Light-Weight, Electric, For Shipboard Use, Defense Standardization Program Office, Fort Belvoir, VA, 2002.
42. MIL-DTL-24643B: Detail Specifications for Cables and Cords, Electric, Low Smoke For Shipboard Use, Defense Standardization Program Office, Fort Belvoir, VA, 2002.
43. Lin, T.S., Bunker, S.P., Whaley, P.D., Cogen, J.M., and Bolz, K.A. Evaluation of metal hydroxides and coupling agents for flame resistant industrial cable applications, *54th IWCS/Focus International Wire and Cable Symposium*, Providence, RI, 2005, pp. 229–236.
44. J1128: Low Voltage Primary Cable, SAE: Warrendale, PA, 2005.
45. J1678: Low-Voltage Ultrathin Wall Primary Cable, SAE: Warrendale, PA, 2004.
46. ISO 6722: Road Vehicles—60V And 600V Single-Core Cables—Dimensions, Test Methods And Requirements, ISO, Geneva, Switzerland, 2006.
47. JASO D 608: Electrical Equipment—Heat-Resistant Low-Tension Cables For Automobiles, Jsaе, Gobancho Chiyoda-Ku, Tokyo, Japan, 1992.
48. Chrysler MS 8288: Cable Primary, Thin wall cross-linked polyethylene insulated, Chrysler Corporation Engineering Standard No. MS-8288, 2004.
49. Lin, T.S., Whaley, P.D., Cogen, J.M., and Wasserman, S.H., Advances in crosslinking technologies for high temperature under-the-hood automotive cable applications, *Proceedings of 52nd International Wire and Cable Symposium/Focus*, Philadelphia, PA, 2003, pp. 92–97.
50. UL 44: Thermoset-Insulated Wires and Cables, UL, Northbrook, IL, 2005.
51. UL 83: Thermoplastic-Insulated Wires and Cables, UL, Northbrook, IL, 2008.
52. UL 758: Standard for Appliance Wiring Material, UL, Northbrook, IL, 2008.
53. Claus, W.D., Keogh, M.J., and Ramachadran, S., Overview of electrical requirements in the selection of flame retarded wire and cable materials, *FRCA Fall Conference*, Rancho Minage, CA, 1995, pp. 47–62.
54. Journeaux, T.L., Development in regulatory classification methods that will affect the European cable industry and its suppliers, *Proceedings of Flame Retardants 2008*, London, England, 2008.
55. Robinson, J. and Loyens, W., Progress in the implementation of the European regulations for the reaction to fire properties of cables, *Proceedings of 56th International Wire and Cable Symposium*, Lake Buena Vista, FL 2007, pp. 340–346.
56. Kiddoo, D.B., Cable component material innovations for stringent fire safety and environmental compliance requirements, *Proceedings of 56th International Wire and Cable Symposium*, Lake Buena Vista, FL 2007, pp. 204–211.
57. Kotak, J., PVC Wire and cable compounds: An overview, *J. Vinyl Addit. Tech.*, 1983, 5(2), 77–78.
58. Vinyl Institute—Electrical Materials Council, Note: Vinyl—An enlightening look at the 50-year history of the world’s leading electrical material, *J. Vinyl Addit. Tech.*, 1991, 13(4), 223–225.
59. Babrauskas, V., Mechanisms and modes for ignition of low-voltage, PVC-insulated electrotechnical products, *Fire Mater.*, 2006, 30(2), 151–174.
60. Hirschler, M., Flammability and fire performance, in *PVC Handbook*, 1st edn., Wilkes, C.E., Summers, J.W., and Daniels, C.A. (Eds.), Hanser Publishers, Munich, Cincinnati, OH, 2005, Chapter 13, pp. 419–481.
61. Lyon, R.E. and Walters, R.N., Pyrolysis combustion flow calorimetry, *J. Anal. Appl. Pyrolysis*, 2004, 71, 27–46.
62. Levchik, S.V. and Weil, E.D., Review: Overview of the recent literature on flame retardancy and smoke suppression in PVC, *Polym. Adv. Technol.*, 2005, 16, 707–716.
63. Summers, J.W., A review of vinyl technology, *J. Vinyl Addit. Tech.*, 1997, 3(2), 130–139.
64. Kaufman, S., PVC in communications cable, *J. Vinyl Addit. Tech.*, 1985, 7(3), 107–111.
65. Allsop, M.W. and Vianello, G., Vinyl chloride polymers, in *Encyclopedia of Polymer Science & Technology*, John Wiley & Sons, New York, 2002.
66. Krauskopf, L.G. and Godwin, A., Plasticizers, in *PVC Handbook*, 1st edn., Wilkes, C.E., Summers, J.W., and Daniels, C.A. (Eds.), Hanser Publishers, Munich, Cincinnati, OH, 2005, Chapter 5, pp. 173–199.
67. Moy, P., Aryl phosphate ester fire-retardant additive for low-smoke vinyl applications, *J. Vinyl Addit. Tech.*, 2004, 10(4), 187–192.
68. Jennings, T.C. and Fletcher, C.W., Actions and characteristics of stabilizers, in *Encyclopedia of PVC*, 2nd edn., Volume 2, Nass, L.I. and Heiberger, C.A. (Eds.), Marcel Dekker, New York, 1988, Chapter 2, pp. 45–141.

69. Jennings, T.C. and Starnes, Jr., W.H., PVC Stabilizers and lubricants, in *PVC Handbook*, 1st edn., Wilkes, C.E., Summers, J.W., and Daniels, C.A. (Eds.), Hanser Publishers, Munich, 2005, Cincinnati, OH, Chapter 4, pp. 95–171.
70. Reddy, J.E. and Hackett, J.A., Advances in the stabilization of flexible PVC by using a liquid calcium zinc technology, *J. Vinyl Addit. Tech.*, 2002, 8(3), 171–175.
71. Kaseler, T.G., Non-lead stabilizer systems for PVC wire and cable extrusion (An Update), *J. Vinyl Addit. Tech.*, 1993, 15(4), 196–201.
72. Zazyczny, J.M. and Matuana, L.M., Fillers and reinforcing agents, in *PVC Handbook*, 1st edn., Wilkes, C.E., Summers, J.W., and Daniels, C.A. (Eds.), Hanser Publishers, Munich, Cincinnati, OH, 2005, Chapter 7, pp. 235–275.
73. Lewin, M., Synergism and catalysis in flame retardancy of polymers, *Polym. Adv. Technol.*, 2001, 12, 215–222.
74. Weil, E.D., Synergists, adjuvants, and antagonists in flame-retardant Systems, in *Fire Retardancy of Polymeric Materials*, Grand, A. and Wilkie, C. (Eds.), Marcel Dekker, New York, 2000, Chapter 4, pp. 115–145.
75. Horn, W.E., Inorganic hydroxides and hydroxycarbonates: Their function and use as flame-retardant additives, in *Fire Retardancy of Polymeric Materials*, Grand, A. and Wilkie, C. (Eds.), Marcel Dekker, New York, 2000, Chapter 9, pp. 285–352.
76. Cusack, P.A. and Hornsby, P.R., Zinc stannate-coated fillers: Novel flame retardants and smoke suppressants for polymeric materials, *J. Vinyl Addit. Tech.*, 1999, 5(1), 21–30.
77. Starns, W.M. Jr. and Edelson, D., Review—Mechanistic aspects of the behavior of molybdenum(VI) oxide as a fire-retardant additive for poly(vinyl chloride). An interpretive review, *Macromolecules*, 1979, 12(5), 797–802.
78. Walker, J.K. and Ho, W., New molybdate smoke suppressant for PVC, in *Proceedings of the 55th IWCS/Focus International Wire & Cable Symposium*, Providence, RI, 2006, pp. 404–409.
79. Grossman, R.F., Acid absorbers as PVC costabilizers, *J. Vinyl Addit. Tech.*, 2000, 6(1), 4–6.
80. Wang, X. and Zhang, Q., Effect of hydrotalcite on the thermal stability, mechanical properties, rheology and flame retardance of poly(vinyl chloride), *Polym. Int.*, 2004, 53, 698–707.
81. Yong-zhong, B., Zhi-ming, H., Shen-xing, L., and Zhi-xue, W., Thermal stability, smoke emission, and mechanical properties of poly(vinyl chloride)/hydrotalcite nanocomposites, *Polym. Deg. Stab.*, 2008, 93, 448–455.
82. Huggett, C. and Levin, B.C., Toxicity of the pyrolysis and combustion products of poly(vinyl chlorides): A literature assessment, *Fire Mater.*, 1987, 11, 131–142.
83. Hirschler, M.M. and Grand, A.F., Comparison of the smoke toxicity of four vinyl wire and cable compounds using different test methods *Fire Mater.*, 1993, 17, 79–90.
84. Hirschler, M.M. and Purser, D.A., Irritancy of the smoke (non-flaming mode) from materials used for coating wire and cable products, both in the presence and absence of halogens in their chemical composition, *Fire Mater.*, 1993, 17, 7–20.
85. Hirschler, M.M. and Smith, G.F., Corrosive effects of smoke on metal surfaces, *Fire Safety J.*, 1989, 15, 57–93.
86. Hirschler, M.M., Discussion of smoke corrosivity test methods: Analysis of existing tests and of their results, *Fire Mater.*, 1993, 17, 231–247.
87. Stec, A.A., Hull, T.R., Lebek, K., Purser, J.A., and Purser, D.A., The effect of temperature and ventilation condition on the toxic product yields from burning polymers, *Fire Mater.*, 2008, 32, 49–60.
88. Hull, T.R., Lebek, K., Pezzani, M., and Messa, S., Comparison of toxic product yields of burning cables in bench and large-scale experiments, *Fire Safety J.*, 2008, 43, 140–150.
89. Tewarson, A., Characterization of the fire environments in central offices of the telecommunications industry, *Fire Mater.*, 2003, 27, 131–149.
90. Gibbons, J.A.M. and Stevens, G.C., Limiting the corrosion hazard from electrical cables involved in fires, *Fire Safety J.*, 1989, 15, 183–190.
91. Chum, P.S., Kao, C.I., and Knight, G.W., Structure/property relationships in polyolefins made by constrained geometry catalyst technology, *Plast. Eng.*, June 1995, 21–23.
92. Lee, D.C., Laakso, R., Gross, L., Muskopf, J., Olefinic elastomers for wire and cable applications, in *Proceedings of the 55th IWCS/Focus International Wire & Cable Symposium*, Providence, RI, 2006, pp. 158–163.
93. Chen, T., Hendrix, A., Glogovski, T., and Butala, R., The characteristics of a non-halogen flame retardant compound using advanced thermoplastic elastomer, in *Proceedings of the 51st IWCS/Focus International Wire & Cable Symposium*, Lake Buena Vista, FL, 2002, pp. 589–593.

94. Beyler, C.L. and Hirschler, M., Thermal decomposition of polymers in *Handbook of Fire Protection Engineering*, 3rd edn., Dinunno, P.J. (Ed.), NFPA, Quincy, MA, 2001, Chapter 7, Section 1, pp. 110–131.
95. Camino, G., Sgobbi, R., Zaopo, A., Colombier, S., and Scelza, C., Investigation of flame retardancy in EVA, *Fire Mater.*, 2000, 24, 85–90.
96. McNeill, I.C. and Mohammed, M.H., A comparison of the thermal degradation behaviour of ethylene-ethyl acrylate copolymer, low density polyethylene and poly(ethyl acrylate), *Polym. Deg. Stab.*, 1995, 48, 175–187.
97. Watanabe, T., Watanabe, R., Kondou, T., and Ogasawara, T., Dielectric properties of flame retardants insulation material in the GHz frequency range, in *Proceedings of the 53rd IWCS/Focus International Wire & Cable Symposium*, Philadelphia, PA, 2004, pp. 88–92.
98. Weil, E.D. and Levchik, S.V., Flame retardants in commercial use or development for polyolefins, *J. Fire Sci.*, 2008, 26, 5–43.
99. Green, J., The flame retardation of polyolefins, in *Flame-Retardant Polymeric Materials*, Volume 3, Lewin, M., Atlas, S.M., and Pearce, E.M. (Eds.), Plenum Press, New York, 1982, Chapter 1, pp. 1–37.
100. Herbiet, R., Luther, D.W., and Thomas, S.G. Jr., Benefits of brominated & mineral based flame retardants for wire & cable in *Proceedings of the 50th IWCS/Focus International Wire & Cable Symposium*, Lake Buena Vista, FL, 2001, pp. 807–815.
101. Markezich, R.L., Flame retardants: Synergisms involving halogens, in *Plastics Additives – An A-Z Reference*, Pritchard, G. (Ed.), Chapman & Hall, London, U.K., 1998, pp. 327–338.
102. Rotheron, R.N., Effects of particulate fillers on flame-retardant properties of composites, in *Particulate-Filled Polymer Composites*, Rotheron, R. (Ed.), John Wiley & Sons, New York, 1995, Chapter 6, pp. 207–234.
103. Lee, C.H., Kim, S.W., Nam, J.H., Oh, W.J., Yoon, H.K., and Suh, K.S., Effect of particle size of alumina trihydrate on electrical properties of EPDM, *Conference on Electrical Insulation and Dielectric Phenomena*, Atlanta, GA, 1998, 1, pp. 112–115.
104. Shen, K.K., Olson, E., Amigouet, P., and Chen, T., Recent advances on the use of metal hydroxide and borates as fire retardants in halogen-free polyolefins, *17th Annual Conference on Flame Retardancy*, May 2006.
105. Plueddemann, E.P., Reminiscing on silane coupling agents, in *Silanes and Other Coupling Agents*, Mittal K.L. (Ed.), VSP, the Netherlands, 1992, pp. 3–19.
106. Weissenbach, K. and Mack, H., Silane coupling agents, in *Functional Fillers for Plastics*, Xanthos, M. (Ed.), Wiley-VCH, Weinheim, Germany, 2005, Chapter 4, 59–83.
107. Kim, O.Y., Yoon, S.H., Nam, G.J., and Lim, H.J., The effect of compatibilizers on the mechanical and flame retardant properties in HFFR compounds for automotive wire insulation, in *Proceedings of the 52nd IWCS/Focus International Wire & Cable Symposium*, Philadelphia, PA, 2003, pp. 352–356.
108. Whaley, P.D. and Han, S.J., Rheology of highly filled compounds for wire and cable applications, in *Proceedings of the 54th IWCS/Focus International Wire & Cable Symposium*, Providence, RI, 2005, pp. 285–289.
109. Durin-France, A., Ferry, L., Lopez Cuesta, J.M., and Crespy, A., Magnesium hydroxide/zinc borate/talc compositions as flame-retardants in EVA copolymer, *Polym. Int.*, 2000, 49, 1101–1105.
110. Clerc, L., Ferry, L., Leroy, E., and Lopez-Cuesta, J.M., Influence of talc physical properties on the fire retarding behaviour of (ethylene-vinyl acetate copolymer/magnesium hydroxide/talc) composites, *Polym. Deg. Stab.*, 2005, 88, 504–511.
111. Park, D.H., Kim, S., and Lee, G.J., Halogen-free flame retardant cable materials: Improvement of flame retardancy and suppression of smoke density, in *Proceedings of the 49th IWCS/Focus International Wire & Cable Symposium*, Atlantic City, NJ, 2000, pp. 422–426.
112. Gilman, J.W., Kashiwagi, T., Nyden, M., Brown, J.E.T., Jackson, C.L., Lomakin, S., Giannelis, E.P., and Manias, E., Flammability studies of polymer layered silicate nanocomposites: Polyolefin, epoxy, and vinyl ester resins, in *Chemistry and Technology of Polymer Additives*, Al-Malaika, S., Golovoy, A., and Wilkie, C.A., (Eds.), Blackwell Science, Oxford, U.K., 1999, Chapter 14, pp. 249–265.
113. Bourbigot, S., Duquesne, S., and Jama, C., Polymer nanocomposites: How to reach low flammability? *Macromol. Symp.*, 2006, 233, 180–190.
114. (a) Beyer, G., Nanocomposites as a new class of flame retardants, in *Proceedings of the 51st IWCS/Focus International Wire & Cable Symposium*, Lake Buena Vista, FL, 2002, pp. 584–588. (b) Beyer, G., Flame retardancy of nanocomposites based on organo clays and carbon nanotubes with aluminum trihydrate *Polym. Adv. Technol.*, 2006, 17(4), 218–225. (c) Beyer, G., Flame retardancy of nanocomposites—from research to technical products, Nanopolymers 2007, International Conference, Berlin, Germany, June 12–13, 2007 (2007), Publisher: Rapra Technology Ltd., Shrewsbury, U.K.

115. Cogen, J.M., Jow, J., Lin, T.S., and Whaley, P.D., New approaches to halogen free polyolefin flame retardant wire and cable compounds, in *Proceedings of the 52nd IWCS/Focus International Wire & Cable Symposium*, Philadelphia, PA, 2003, pp. 102–107.
116. Whaley, P.D., Cogen, J.M., Lin, T.S., and Bolz, K.A., Nanocomposite flame retardant performance: Laboratory testing methodology, in *Proceedings of the 53rd IWCS/Focus International Wire & Cable Symposium*, Philadelphia, PA, 2004, 605–611.
117. Beyer, G., Presentation at the *16th Annual BCC Conference Recent advances in flame retardancy of polymeric materials*, Stamford, CT, 2005.
118. Cogen, J.M., Lin, T.S., Morgan, A.B., and Garces, J.M., Novel synthetic nanocomposite materials and their application in polyolefin-based wire and cable compounds, in *Proceedings of the 52nd IWCS/Focus International Wire & Cable Symposium*, Philadelphia, PA, 2003, pp. 638–643.
119. Morgan, A.B., Whaley, P.D., Lin, T.S., and Cogen, J.M., The effects of inorganic-organic cations on EVA-magadiite nanocomposite flammability in *ACS Symposium Series 922, Fire and Polymers IV – Materials and Concepts for Hazard Prevention*, Wilkie, C.A. and Nelson, G., (Eds.), American Chemical Society, Washington D.C., 2006, Chapter 5, 48–60.
120. Beyer, G. Filler blend of carbon nanotubes and organoclays with improved char as a new flame retardant system for polymers and cable applications, *Fire Mater.*, 2005, 29, 61–69.
121. Kashiwagi, T., Du, F., Douglas, J.F., Winey, K.I., Harris, R.H. Jr., and Shields, J.R., Nanoparticle networks reduce the flammability of polymer nanocomposites, *Nature Mater.*, 2005, 4, 928–933.
122. Sauerwein, R., Application of submicron metal hydrate fillers in flame retardant cables, in *Proceedings of the 55th IWCS/Focus International Wire & Cable Symposium*, Providence, RI, 2006, pp. 399–403.
123. Davidson, N.S. and Wilkinson, K., U.S. Patent #5,091,453, 1992.
124. Hermansson, A., Hjertberg, T., and Sultan, B., The flame retardant mechanism of polyolefins modified with chalk and silicone elastomer, *Fire Mater.*, 2003, 27, 51–70.
125. Cogen, J.M., Whaley, P.D., Lin, T.S., and Bolz, K., Assessment of flame retardancy in polyolefin-based non-halogen FR compounds, in *Proceedings of the 53rd IWCS/Focus International Wire & Cable Symposium*, Philadelphia, PA, 2004, pp. 185–190.
126. Gangal, S.V., Perfluorinated polymers, FEP in *Encyclopedia of Polymer Science & Technology*, John Wiley & Sons, New York, 2002.
127. Genovese, A. and Shanks, R.A., Fire performance of poly(dimethyl siloxane) composites evaluated by cone calorimetry, *Composites: Part A*, 2008, 39, 398–405.
128. ASTM D 2863: Test Method For Measuring The Minimum Oxygen Concentration To Support Candle-Like Combustion Of Plastics (Oxygen Index), ASTM, West Conshohocken, PA 2006.
129. NES 715: Determination of The Temperature Index of Small Specimens of Materials NES: U.K. Ministry of Defense Naval Engineering Standards, Foxhill Bath, U.K., 1981.
130. ISO 4589-3: Plastics—Determination of Burning Behavior by Oxygen Index-Elevated-Temperature Test, ISO, Geneva, Switzerland, 1996.
131. UL 94: Standard for Tests for Flammability of Plastic Materials for Parts in Devices and Appliances, UL, Northbrook, IL 2006.
132. ASTM E 662: Test Method For Specific Optical Density Of Smoke Generated By Solid Materials, ASTM, West Conshohocken, PA, 2006.
133. Wang, Z., Shen, X., Fan, W., Hu, Y., Qu, B., and Zou, G., Effects of poly(ethylene-co-propylene) elastomer on mechanical properties and combustion behaviour of flame retarded polyethylene/magnesium hydroxide composites, *Polym. Int.*, 2002, 51(7), 653–657.
134. Fu, M. and Qu, B., Synergistic flame retardant mechanism of fumed silica in ethylene-vinyl acetate/magnesium hydroxide blends, *Polym. Deg. Stab.*, 2004, 85(1), 633–639.
135. Chen, T. and Isarov, A., New magnesium hydroxides enabling low-smoke cable compounds, *Proceedings of 56th International Wire and Cable Symposium*, Lake Buena Vista, FL 2007, pp. 191–196.
136. ASTM E 2058: Standard Test Methods for Measurement of Synthetic Polymer Material Flammability Using a Fire Propagation Apparatus (FPA), American Society for Testing and Materials: West Conshohocken, PA, 2002.
137. Khan, M.M., Bill, R.G. Jr., and Alpert, R.L., Screening of plenum cables using a small-scale fire test protocol, *Fire Mater.*, 2006, 30, 65–76.
138. ASTM E 1354: Test Method For Heat And Visible Smoke Release Rates For Materials And Products Using An Oxygen Consumption Calorimeter, West Conshohocken, PA 2008.
139. ISO 5660: Reaction-To-Fire Tests—Heat Release, Smoke Production And Mass Loss Rate—Part 1: Heat Release Rate (Cone Calorimeter Method), ISO, Geneva, Switzerland, 2002.

140. Barnes, M.A., Briggs, P.J., Hirschler, M.M., Matheson, A.F., and O'Neill, T.J., A comparative study of the fire performance of halogenated and non-halogenated materials for cable applications. Part I tests on materials and insulated wires, *Fire Mater.*, 1995, 20, 1–16.
141. Standard Test Method for Determining Flammability Characteristics of Plastics and Other Solid Materials Using Microscale Combustion Calorimetry, ASTM D 7309-07, American Society for Testing and Materials (International), West Conshohocken, PA, April 1, 2007.
142. Lyon, R.E., Walters, R.N., and Stoliarov, S.I., Screening flame retardants for plastics using microscale combustion calorimetry, *Polym. Eng. Sci.*, 2007, 47(10), 1501–1510.
143. ASTM E 84: Test Method For Surface Burning Characteristics Of Building Materials, UL, Northbrook, IL, 2008.
144. Weil, E.D., Hirschler, M.M., Patel, N.G., Said, M.M., and Shakir, S., Oxygen index: Correlations to other fire tests, *Fire Mater.*, 1992, 10, 159–167.
145. Nakagawa, Y., A comparative study of bench-scale flammability properties of electric cables with different covering materials, *J. Fire Sci.*, 1998, 16, 179–205.
146. Hirschler, M.M. and Shakir, S., Measurements of cable fire properties by using heat release equipment, *Proceedings of Flame Retardants 1992*, London, England, 1992.
147. The FIPEC Report, Fire Performance of Electric Cables-New Test Methods and Measurement Technique. Final Report of the European Commission. Interscience Communications, London, U.K., 2000.
148. Cogen, J.M., Lin, T.S., and Lyon, R.E., Correlations between pyrolysis combustion flow calorimetry and conventional flammability tests with halogen free flame retardant polyolefin compounds, *Fire Mater.*, 2009, 33, 33–50.
149. Lin, T.S., Cogen, J.M., and Lyon, R.E., Correlations between microscale combustion calorimetry and conventional flammability tests for flame retardant wire and cable compounds, *Proceedings of 56th International Wire and Cable Symposium*, Lake Buena Vista, FL, 2007, pp. 176–185.
150. Lyon, R.E., A molecular basis for polymer flammability, *Proceedings of Flame Retardant 2008*, London, England, 2008.
151. Wilkie, C.A., Chigwada, G., Gilman, J., and Lyon, R.E., High-throughput techniques for the evaluation of fire retardancy, *J. Mater. Chem.*, 2006, 16, 2023–2030.
152. Chigwada, G. and Wilkie, C.A., Synergy between conventional phosphorus fine retardants and organically-modified clays lead to fine retardancy of styrenics. *Polym. Degrad. Stab.*, 2003, 80, 551–557.
153. Chigwada, G., Jash, P., Jiang D.D., and Wilkie, C.A. Fire retardancy of vinyl ester nano composites: Synergy with phosphorus-based fire retardants, *Polym. Degrad. Stab.*, 2005, 89, 85–100.
154. Gilman, J.W., Bourbigot, S., Shields, J.R., Nyden, M., Kashiwagi, T., Davis, R.D., VanderHart, D.L., Demory, W., Wilkie, C.A., Morgan, A.B., Harris, J., and Lyon, R.E., High throughput methods for polymer nanocomposites research: Extrusion, NMR characterization and flammability property screening, *J. Mater. Sci.*, 2003, 38, 4451.
155. Gilman, J.W., Davis, R.D., Nyden, M., Kashiwagi, T., Shields, J.R., and Demory, W., in *High Throughput Analysis A Tool for Combinatorial Materials Science*, Potyrailo, R.A. and Amis, E.J. (Eds.), Kluwer Academic/Plenum Publishers, New York, 2004, p. 415.
156. Nyden, M., Gilman, J.W., Davis, R., and Shields, J.R., High throughput methods for flammability screening of multicomponent polymer blends and nanocomposites, *The Society for the Advancement of Materials and Process Engineering, 47th International Symposium, SAMPE 2002*, Long Beach, CA, May 12–16, 2002.
157. http://ec.europa.eu/environment/chemicals/reach/reach_intro.htm. <http://ec.europa.eu>
158. Are You Ready for RoHS and REACH? *China Plastic & Rubber Journal*, April 2008 (http://plastics.2456.com/eng/epub/n_details.asp?epubiid=3&id=2493).
159. Open letter from Steve Jobs <http://www.apple.com/hotnews/agreenerapple/>
160. http://www.dell.com/downloads/global/corporate/environ/Dell_BFR_Position.pdf
161. http://www.pc.ibm.com/ww/lenovo/procurement/Guidelines/BFR_PVC_Phase-out_Supplier_Letter_August_2007.pdf
162. Mizuno, K.M., Hirukawa, H., Kawasaki, O., Noguchi, H., and Suzuki, O., Development of Non-Lead Stabilized PVC Compounds for Insulated Wires and Cables, *Furukawa Review*, 1999, 18, 111–118.

Index

A

- AFM, *see* Atomic force microscopy
- Alkali metal borates
 - anhydrous borax, *see* Dehybor®
 - borax decahydrate
 - cellulosic fabrics, 209
 - WPCs, 210
 - borax pentahydrate, *see* Neobor®
 - disodium octaborate tetrahydrate, *see* Polybor®
 - miscellaneous alkali metal borate, 210
- Alkaline earth metal borates
 - barium metaborate, 215
 - calcium and magnesium borates, 214
- Alumina trihydrate (ATH)
 - decomposition enthalpy, 314
 - flame retardant, 165
 - high loadings, 219
 - melt-blending, 318
 - micron-sized particles, 181
 - red phosphorus, 176
 - thermal stability, 167
- Aluminum borate, 223
- Ammonium pentaborate (APB), 223–224
- Ammonium phosphates, 110
- Anhydrous boric acid, *see* Boric oxide
- Apparel fabrics, 733–734
- Aromatic polyesters, 88
- Arrhenius coefficients, 480
- Arrhenius law, 18
- ASTM E-84 test, 709–710, 715–716
- ATH, *see* Alumina trihydrate
- Atomic force microscopy (AFM), 276
- ATR, *see* Attenuated total reflection
- Attenuated total reflection (ATR)
 - PBT spectra, 521–523
 - TGA, 516
- Average mass loss rate (AMLR), 196, 308, 310

B

- Barium metaborate, 215
- Bench-scale reaction-to-fire test
 - concepts, 358–359
 - heat release rate
 - measurements, 364–367
 - pertinent material properties, 363–364
 - ignition
 - ASTM D 1929, 360
 - LIFT, 361–363
 - measurements, 359–360
 - pertinent material properties, 359
 - smoke and toxicity
 - cone calorimeter, 376–377
 - measurements, 371–374
 - NBS smoke chamber, 374–376
 - pertinent material properties, 370

- surface flame spread
 - LIFT, 369–370
 - measurements, 368
 - pertinent material properties, 367–368
 - Steiner tunnel test, 368–369
- Bis(2-ethylhexyl)hydrogen phosphate (BEHHP), 267
- Bolland and Gee reaction scheme, 19
- Bond-weighted random scission model
 - break-at-a-point
 - bond location and weight, 492
 - frequency distribution, 493
 - description, 485–486
 - pure random scission
 - experimental data, 488–489
 - exponential integral, 490
 - frequency vs. degree of polymerization, 486–487
 - isothermal TG comparison, 488
 - PBMs vs. Monte Carlo model, 487
 - symmetric power law, 490–491
- Borazine, 225
- Borester, boron–carbon compound and
 - boric acid esters, 225–226
 - boron carbide, 227
 - boronic acids, 226–227
- Boric acid
 - cellulose insulation, 211
 - cotton-batting, 211–212
 - fabrics and paper products, 212
 - plastics and coatings, 214
 - wood products
 - guanylurea phosphate (GUP) and WPC, 213
 - vacuum/pressure impregnation, 212
- Boric oxide, 214
- Boron-based FR, flame retardancy
 - mechanism
 - plastics and elastomers, 231–232
 - wood/cellulose, borates, 230–231
 - minerals, 208
 - products and applications
 - alkali metal borates, 209–210
 - alkaline earth metal borates, 214–215
 - borester and boron–carbon compounds, 225–227
 - boric acid and oxide, 211–214
 - miscellaneous, 229
 - nitrogen-containing compounds and, 223–225
 - phosphorus-containing compounds and, 227–228
 - silicon-containing compounds and, 228–229
 - transition and miscellaneous metal borates, 215–223
 - properties and applications, 209
- Boron phosphate, 227–228
- Borosilicate, borosilicate glass, and frits, 228
- Borosiloxane, 228–229
- Burning and fire growth, CFD simulation
 - Dalmarnock fire test, 575–576
 - flat surface and combustible corner
 - back-face boundary condition, 573
 - gaseous fuel generation, 571

- measured and modeled pyrolysis, 570
 - room/corner experiment, 572–573
 - forensic fire reconstruction, 576–579
 - rail cars
 - emergency egress and ventilation systems, 573–574
 - FDS4 calculations vs. experimental data, 574–575
 - small and large initial fire, 568
 - stationary fires, 569
- C**
- Carbonization process, chemical characterization
 - Raman spectroscopy, 244–245
 - ssNMR, *see* Solid-state nuclear magnetic resonance
 - XPS, *see* X-ray photoelectron spectroscopy
 - Carbon nanotubes (CNTs)
 - char reinforcing influence, 323
 - FR properties, 317
 - lower loading, 284
 - mechanical and electrical properties, 181
 - morphology/dispersion, 279
 - polymers, 266
 - stack alignment, 265
 - surface treatment, 272
 - CCA, *see* Cone calorimetric analysis
 - Cellulose degradation process, 28–29
 - CFD, *see* Computational fluid dynamics
 - Chain-reaction polymer
 - acrylics, 115–116
 - polystyrene and polyolefins, 116
 - Char formation and characterization
 - carbonaceous structures
 - graphite and diamond, 241
 - microscopy, 255–257
 - XRD, *see* X-ray diffraction
 - carbonization process, chemical characterization
 - Raman studies, 244–245
 - ssNMR, 241–244
 - XPS, 245–246
 - combustion residues, 240
 - description, 65
 - dynamic
 - char strength, 252–254
 - expansion degree, 250–251
 - foamed residue structure control, 247
 - intumescent systems, 246–247
 - viscoelastic properties, 247
 - viscosity, 248–249
 - expander, 239
 - islands formation, 240
 - reinforcer, 239
 - Chlorinated diphenyls, *see* Polychlorobiphenyls (PCBs)
 - CIL, *see* Compatibilizer interlayers
 - CNTs, *see* Carbon nanotubes
 - Codes, fire issue
 - ICC
 - building, 622–624, 627
 - description, 621
 - fire, 625–626
 - mechanical, 627
 - performance, 628
 - residential, 626
 - wildland urban interface, 627–628
 - NFPA
 - air conditions, 637–638
 - building code, 634–635
 - electrical code, 628–632
 - housing, 637
 - life safety code, 632–633
 - ships, 636–637
 - uniform fire code, 633–634
 - plumbing and mechanical official, 639
 - Comonomers structure, 34
 - Compatibilizer interlayers (CIL)
 - anionic surfactant, 332
 - composites, 331
 - cone calorimetric data, 336
 - Diels–Alder adduct, 331–332
 - HRR and THR, 333
 - NMM and OMM, 333–334
 - phase separation and structure, 335–336
 - shear-thinning coefficient, 335
 - Compression molding, 708
 - Computational fluid dynamics (CFD)
 - advantage, 50
 - buoyant diffusion flames, 555
 - heat release rate (HRR) evolution, 50–51
 - models, 552
 - Navier–Stokes solver, 553
 - packages, 562
 - Condensed phase mechanism, halogen
 - chloroparaffins
 - dehydrochlorination, 85
 - polymers destabilization, 85–86
 - thermal degradation, 82–83
 - volatile product, 83–85
 - metal compounds, synergistic systems
 - oxygen vs. nitrous oxide index, 86–87
 - polypropylene pyrolysis rate, 87
 - oxygen index, 82–83
 - Condensed-phase pyrolysis
 - heat conduction, 562–563
 - liquid fuels, 563–564
 - solid fuels
 - empirical models, 564–565
 - finite-rate, 566–567
 - heat transfer limited, 565–566
 - material property estimation, 567–568
 - Cone calorimeter
 - data
 - PET/OP950/OMPOSS formulation, 196
 - polymers and pre-ceramic polymer–polymer blends, 193
 - silica gel and potassium carbonate, 198
 - flammability tests, 397
 - structure, 364–365
 - test
 - heat release rate curves, 313
 - larch wood, boric acid, 213
 - LDPE/EVA filled samples, 315
 - sample holder, 525
 - Cone calorimetric analysis (CCA)
 - PNs flammability analysis, 283
 - polystyrene, 280
 - Construction products directive (CPD)
 - cable ratings, 800
 - reaction-to-fire performance, 787

Consumer Product Safety Commission (CPSC)
 apparel wearing, 590
 definition, 615
 FR, 693
 mattress flammability, 610
 preliminary assessment, 692
 Courant–Friedrichs–Lewy (CFL) condition, 553, 554
 Crib V test, 4

D

Dalmarnock fire test, 575–576
 Decabrom, 705
 Degradation
 flame retardance
 behavior and polymer, 36–38
 combustion, 32–33
 description, 32
 mechanism, PMMA and PS copolymers, 34
 polymer classification, 33
 and polymer stabilization, 34–36
 oxidative, 19
 polymers
 combustion cycle, 32
 fire, 31
 foams, 23–25
 high temperature-resistant, 30–31
 natural, 28–30
 thermoplastics, 20–23
 thermosets, 25–28
 thermal
 chemical structure, 16
 impurities, 18
 mechanism, decomposition products, 16
 process, 15–16
 in pure and stabilized state, 18–19
 stability, 17
 Dehybor®, 210
 Demands, chemical regulations and
 precautionary principle
 definitions, 672–673
 environmental and health regulations, 673
 product stewardship, 698–699
 regulatory activities, FR
 China, 689
 European Union (EU), 687–689
 Japan, 690–691
 Korea, 689–690
 North America, 691–696
 science-based drivers
 chemical inventory, 673–675
 REACH regulation, 681–687
 risks, 676–681
 TSCA, 675–676
 sustainable solutions
 green solution, 696–698
 life-cycle thinking, 698
 Diethyl ethylphosphonate (DEEP), 769
 Differential scanning calorimetry (DSC)
 analysis, 226
 apparatus, 516
 measurements, 538
 TGA, 515
 thermal decomposition, 169

Dimethyl methylphosphonate (DMMP), 769, 772
 Dimethyl propylphosphonate (DMPP), 769
 Dipping duck test, 641
 Discrete ordinates methods (DOM), 560, 561
 DSC, *see* Differential scanning calorimetry
 Dynamic characterization, char material
 expansion degree
 fire resistance properties, 251
 vs. temperature, 250–251
 intumescent systems, 246–247
 mechanical destruction, 247
 strength
 compression force vs. gap, 252–253
 heat release rate vs. time, 253–254
 measurement, 252
 viscoelastic properties, 248
 viscosity, carbonization
 data vs. temperature, 248
 heat treated material behavior, 249
 time vs. temperature, 248–249

E

Ethylene-butyl acrylate (EBA) formulation
 calcium salt formation, 140
 FR properties, 140–141
 Ethylene-vinyl acetate (EVA)
 HRR curves, 221
 nanocomposite application
 heat flux ratio, 542, 544
 ignition times, 541–542
 material and experiments, 541
 thermal properties, 542
 zinc borate and ATH, 220
 European Commission Scientific Committee on Health
 and Environmental Risks (SCHER), 680–681
 EVA, *see* Ethylene-vinyl acetate
 Expandable graphite, 141

F

FDS, *see* Fire dynamics simulator
 FEC, *see* Fractional effective concentration
 Federal Hazardous Substances Act (FHSA), 590, 615
 Federal Railroad Administration (FRA)
 fire safety regulation, 598
 passenger rail materials, 601–603
 FFA, *see* Flammable Fabrics Act
 FHSA, *see* Federal Hazardous Substances Act
 Fiber-reinforced materials, FR design
 carbon, aramid (Kevlar) and natural, 706–707
 fabrication processes
 compression molding and RTM, 708
 filament winding, 707–708
 hand lay-up and spray-up, 707
 pultrusion, 709
 fiber content and composite thickness
 fire tests, 713–716
 FSI test data, 709–711
 laminate construction, 709
 smoke-developed index (SDI), 711–712
 FRP materials application
 aerospace, 720–721
 architectural, 718–720

- industrial, 717
 - marine, 721–722
 - mass transit, 716–718
- mechanical properties, 703
- resins and additives, FRP applications
 - aerospace, 706
 - epoxy and unsaturated polyester, 705
 - epoxy vinyl ester, 705–706
 - phenolic, 704
- Fiber-reinforced polymers (FRP); *see also* Fiber-reinforced materials, FR design
 - fabrication processes
 - compression molding and RTM, 708
 - filament winding, 707–708
 - hand lay-up and spray-up, 707
 - pultrusion, 709
 - laminated construction, 709
 - materials application
 - aerospace, 720–721
 - architectural, 718–720
 - industrial, 717
 - marine, 721–722
 - mass transit, 716–718
 - reinforcements
 - aramid (Kevlar), 706–707
 - carbon, 706
 - e-glass, 706
 - natural fibers, 707
 - resins and FR additives
 - aerospace, 706
 - epoxy and unsaturated polyester, 705
 - epoxy vinyl ester, 705–706
 - phenolic, 704
- Fire
 - behavior and retardancy mechanism
 - bomb calorimeter, 408
 - combustion efficiency, 407
 - cone calorimeter, 406–407
 - flame retardancy effects, 410
 - intumescent coating, 412
 - material properties, 409–410
 - PA 66-GF, 414
 - Petrella approach, 413
 - P_{red} flame inhibition effect, 405
 - surface temperature, 411–412
 - TG-FTIR experiment, 406
 - vanishing flame retardancy, 411
 - dynamics
 - compartment, 49
 - modeling, 49–51
 - open, 48–49
 - risk scenario, 2
 - safety
 - description, 44
 - designing, 45
 - fire growth definition, 45–46
 - schematic presentation, 44
 - and society, 1–2
- Fire dynamics simulator (FDS)
 - internal subroutine, 563
 - LES, 552
 - validation, 555
- Fire effluents, toxic component
 - asphyxiant gases, 455
- conditions, fire
 - FED and FEC contribution, 463–465
 - growth curve, 462
 - hazards, 463
- estimation, chemical composition data
 - hazards, 460–461
 - physiological and behavioral effects, 460
 - potency values, 461
- irritant gases
 - hydrogen halides, 456
 - nitrogen oxides, 456–457
 - organoirritants, 457
 - particulates, 457–459
- Fire growth
 - combustion fundamentals
 - condensed fuel burning, 47–48
 - premixed and diffusion flames, 47
 - reactive gaseous mixtures, 46–47
 - dynamic fundamentals
 - compartment fires, 49
 - modeling, 49–51
 - open fires, 48–49
 - extinction control, 70–71
 - flame spread control, material parameters
 - classification, 58–59
 - co-current, 62
 - definition, 57–58
 - opposed-flow, 59–62
 - smoldering front propagation, 62–67
 - mass burning and energy release rate
 - definition, 67
 - energy balance, material surface, 68–69
 - heat release rate (HRRs), 67–68
 - mass transfer number, 69–70
- safety
 - definition, 45–46
 - objectives, 44–45
- solid fuel ignition
 - induced, 52–57
 - spontaneous, 51–52
- Fire growth prediction
 - combustion
 - description, 555–556
 - mixture fraction formulation, 556–557
 - reaction rate computation, 558–559
 - fluid dynamics
 - Navier–Stokes equations, 552–553
 - turbulence modeling, 553–555
 - heat transfer
 - convection, 561–562
 - radiation, 559–561
- Fire propagation apparatus (FPA), 363, 367, 470, 471, 795
- Fire resistance, intumescent coating
 - developments
 - acrylic, nanoclay, 156–157
 - char layer, 156, 157
 - heat radiator test, 157–158
 - synergists use, 155–156
 - test, 155
 - evaluation
 - cellulosic fire curve, 149–150
 - hydrocarbon test curve, 150
 - passive fireproofing materials, 148

- protection levels, 148–149
 - thick and thin film materials, 151
- small-scale test
 - cone calorimeter, 153
 - heat gradients, 153–154
 - heat radiator vs. UL-1709, 152–153
 - industrial furnace, 151–152
 - presentation, 152
 - swelling, image analysis, 153, 154
 - temperature, 155
- Fire-retardant fillers
 - application, 167–168
 - efficiency
 - multicomponent structures, 178
 - nanosize, 179–181
 - synergism, 175–178
 - magnesium hydroxide, 168
 - and polymer interactions
 - drip, 173
 - EVA copolymer, 171–173
 - thermal degradation, 171
 - smoke suppression
 - hydroxide decomposition and additives, 174
 - polymers, 173
 - thermal effects
 - combustion, 170–171
 - decomposition, 169–170
 - heat capacity, 170
 - types
 - aluminum hydroxide (Al(OH)₃), 164–166
 - boehmite and hydrotalcite, 167
 - calcium sulfate dihydrate, *see* Gypsum
 - magnesium carbonates, 166–167
 - magnesium hydroxide, 166
 - vapor-phase action, 173
- Fire safe transparent plastics
 - deterministic model, flammability
 - HRC, 429
 - thermal and combustion properties, 428
 - fire testing, 425
 - flammability, high throughput screening, 424–425
 - molar group contribution
 - polymer flammability, 432
 - thermal combustion properties, 425
 - values, 426–428
 - optimized formulations, flammability results, 432–433
 - statistical model, flammability
 - flame-spread theory, 431
 - thermal combustion properties, 430
- Fire test methods
 - cigarette ignition, 652
 - compartment
 - initiation, 350
 - post-flashover stage, 351–352
 - pre-flashover and flashover stage, 351
 - flame spread
 - ASTM test method, 645–646
 - LIFT apparatus, 646
 - organic polymers, 644–645
 - flammability
 - bench-scale reaction-to-fire, 354–355
 - large-scale reaction-to-fire, 355
 - small heat source ignition, 354
- heat release
 - burning products, 646
 - incident flux, 646–647
 - room-corner test, 647–648
- ignitability
 - cone calorimeter, 641–643
 - glow wire test, 641
 - measurement types, 640
- material reaction
 - heat release, 353
 - ignition, 352
 - smoke and toxic production, 353–354
 - surface flame spread, 353
- microcalorimetry, 651–652
- NFPA 550 fire concepts tree, 352
- products/materials, 652–653
- smoke obscuration
 - ASTM E 662 smoke chamber, 648
 - ASTM E 1995 smoke chamber, 649
- smoke toxicity
 - carbon monoxide yields, 651
 - potency values, 649
 - room-corner fire tests, 650
- Fire toxicity
 - assessment
 - bench-and large-scale test data, 472–473
 - closed chamber test, 467–468
 - data correlation, bench-scale test, 470–472
 - flow-through test, 468–470
 - generation, bench-scale, 466
 - open test, 466
 - effluent, components
 - asphyxiant gases, 455
 - estimation, chemical composition data, 460–461
 - fire conditions, 462–465
 - irritant gases, 455–459
 - toxicants effect, species, 459–460
- Flame retardance
 - combustion, 32–33
 - comonomer structure, 33–34
 - description, 32
 - mechanism, 34
 - polymer degradation processes
 - carbonization and volatilization, 37
 - chain scission and cross-linking, 37–38
 - pathways, 36
 - surface graft copolymerization, 38
 - stabilization, polymer
 - antioxidants, 35–36
 - character and behavior, 34–35
 - synthetic polymers, 33
- Flame retardancy
 - combustibility and thermal degradation/
 - decomposition, 3
 - definition, 2
 - fire, protection
 - additives use, 3
 - automobiles, 4
 - electronic, 5–6
 - insurance companies, 3–4
 - polyurethane foam flammability, 4–5
 - regulators and consumers, 6
 - fire-safety requirement, 8
 - materials, 2–3

- plastics, 7–8
 - research, 9–10
 - societal changes, 6
 - society and fire, 1–2
 - waste disposal and chemical use, 6–7
 - WEEE, 7
 - Flame-retardant (FR); *see also* Flame retardance; Flame retardancy
 - additives
 - expandable graphite, 770–771
 - halogen, 767
 - inorganic, 772–773
 - melamine and derivatives, 771–772
 - phosphorus, 767–770
 - chemistry, 8–9
 - research, 9–10
 - science and polymeric material fire safety
 - additives, 11
 - codes and standards, 11–12
 - multifunctional, 10–11
 - regulation changes, 12
 - test and prediction tools, 12–13
 - Flame spread
 - control
 - characteristics, 57–58
 - classification, 58–59
 - co-current, 62
 - concurrent flow and opposed, 58
 - opposed flame, 59–62
 - smoldering front propagation, 62–67
 - definition, 46
 - test, 749
 - Flammable Fabrics Act (FFA), 590, 597
 - Fluorinated ethylene–propylene (FEP) copolymer, 793–794
 - Fluoroborates, 229
 - Fluoropolymers
 - FEP, 793–794
 - PTFE, 793
 - Foam materials, FR design
 - phenolic, 776
 - polymer nanocomposites, 776–777
 - polyolefin, 775
 - polystyrene
 - expanded polystyrene (EPS), 774
 - extruded polystyrene (XPS), 773–774
 - hexabromocyclododecane (HBCD), 774–775
 - polyurethane
 - additive flame retardant, 766–773
 - reactive flame retardant, 765–766
 - polyvinyl chloride, 775–776
 - Fourier transform infrared radiometry (FTIR)
 - measurements, 518
 - PBT spectra, 522
 - phase analysis, 521
 - TGA, 516
 - Fourier transform infrared-reflectance transmission microscopy (FTIR-RTM)
 - mapping, 447–448
 - measurement, 446–447
 - Fourier transmission infrared (FTIR) spectroscopy, 276
 - FR, *see* Flame-retardant
 - FRA, *see* Federal Railroad Administration
 - Fractional effective concentration (FEC), 461, 463–465, 473
 - Fractional effective dose (FED), 373, 460, 461, 463–465, 470
 - French test method, 728
 - FTIR, *see* Fourier transmission infrared
 - FTIR-RTM, *see* Fourier transform infrared-reflectance transmission microscopy
 - Full product tests, 730–731
 - Full-scale fire modeling
 - burning and fire growth, CFD simulation
 - Dalmarnock fire test, 575–576
 - flat surfaces and combustible corners, 570–573
 - forensic fire reconstruction, 576–579
 - rail cars, 573–575
 - stationary fires, 569
 - condensed-phase pyrolysis
 - empirical models, 564–565
 - finite-rate models, 566–567
 - heat conduction, 562–563
 - heat transfer limited models, 565–566
 - liquid fuels, 563–564
 - material property estimation, 567–568
 - gas-phase physics
 - combustion, 555–559
 - fluid dynamics, 552–555
 - heat transfer, 559–562
 - Furniture calorimeter, 378
- ## G
- GA, *see* Genetic algorithm
 - Gas-phase mechanism, halogen
 - antimony compounds, synergistic effect
 - cellulose, 79–80
 - FR properties, 79
 - halides role, 82
 - oxygen and nitrous oxide index, 80–81
 - Sb₂O₃ chemical halogenation, 81
 - molecular-level, 77
 - physical theory, 78–79
 - styrene–oxygen mixtures, 78
 - thermal oxidation process, 77–78
 - Genetic algorithm (GA), 568
 - Guanidinium borate, 224
 - Gypsum, 167
- ## H
- Halogen-containing FR
 - application, polymers families
 - aromatic polyesters, 88
 - poly(vinyl chloride) and thermosetting resins, 90
 - polycarbonate and polyamides, 89
 - polyolefins, 89–90
 - polyurethanes, 90–91
 - styrenic homopolymer and copolymers, 88
 - textiles, 91
 - carbon–halogen bonds, 76
 - condensed phase action mechanism
 - dehydrochlorination, 85
 - destabilization, polymers, 85–86
 - hydrocarbons ratio, 83–84

- oxygen index, 82–83
 - synergistic systems, halogen–metal compounds, 86–87
 - thermal degradation, 84–85
 - environmental concerns
 - gas phase, radical trapping, 91–92
 - PBDPEs, 92–93
 - PCBs and PBBs, 92
 - REACH regulation, 94–95
 - risk assessment, 93–94
 - toxicity and, 93
 - gas-phase action mechanism
 - fire-extinguishing agents, 77
 - halocarbon–fuel mixture flammability, 78–79
 - low-pressure explosive combustion, 78
 - synergistic effect, antimony compounds, 79–82
 - vapor phase, 77–78
 - properties and use, 96–101
 - self-sustained polymer combustion cycle, 75–77
 - Hand lay-up/spray-up processes, 707
 - Heat of combustion, 47
 - Heat release rate (HRR)
 - clay charring activity, 341
 - curves, 441
 - flaming combustion, 430
 - vs. heat flux curve, 434
 - successive bins, 431
 - Heat release tests, 728–730
 - High-resolution transmission electron microscopy (HRTEM), 265
 - High throughput (HT) technique
 - description, 422–434
 - fire safe transparent plastics
 - deterministic model, 428–430
 - empirical molar group contributions, 425
 - fire testing, 425–428
 - flammability, 424–425
 - optimized formulations, 432–433
 - statistical model, 430–432
 - polymer flammability characterization
 - description, 434–435
 - flammability properties, 436–438
 - minimum flux, 438–441
 - RCC, 441–442
 - sample preparation, 435–436
 - screening intumescence coating
 - characterization, 444–445
 - description, 442–443
 - fire testing application, 448–449
 - fluorescence probes, 445–446
 - FTIR-RTM, 446–448
 - sample preparation, 443
 - HRR, *see* Heat release rate
 - HRTEM, *see* High-resolution transmission electron microscopy
- I**
- ICAL, *see* Intermediate-scale calorimeter
 - ICC, *see* International Code Council
 - Induced ignition
 - gas-phase, mechanism, 52–53
 - pyrolysis time, 53–57
 - Industrial furnace test, 151–152
 - Innovia people mover, 717
 - Inorganic FR
 - ATH, 772
 - silicon-based compounds, 773
 - zinc borate (ZB), 772–773
 - Intermediate-scale calorimeter (ICAL), 380
 - International Code Council (ICC)
 - building, 622–624, 627
 - description, 621
 - fire, 625–626
 - mechanical, 627
 - performance, 628
 - residential, 626
 - wildland urban interface, 627–628
 - International Electrotechnical Commission (IEC), 785–786
 - Intumescence coating, screening
 - characterization, 444–445
 - description, 442–443
 - fire testing potential application, 448–449
 - fluorescent probes, 444–446
 - FTIR-RTM
 - mapping, 447–448
 - measurement, 446–447
 - sample preparation, 443
 - thickness measurements, 444
 - Intumescence-based FR
 - coating, fire resistance
 - developments, 155–158
 - evaluation, 148–151
 - small-scale test and measurement, 151–155
 - description, 129
 - fire reaction
 - inorganic polymer, 144
 - organic polymer, 135–141
 - synergy, 144–147
 - textile, 141–144
 - fundamentals
 - charred layer, 130–131
 - coating, mode of action, 132
 - components, 131
 - development, 131–132
 - market, 133–134
 - references, 129–130
 - Intumescent organic polymer
 - inorganic-based systems
 - chalk filler and silicone, 140–141
 - mineral intumescent systems, 140
 - POSS, 141
 - organic-based systems
 - char former, 137–138
 - HB classification, 139–140
 - Melabis and b-MAP synthesis, 136
 - melamine salts of pentaerythritol phosphate (MPP)
 - preparation, 136–137
 - PA-6/OPI311 combustion residue, 139
 - phosphorus-containing char former, 138
 - phosphorus–nitrogen preparation, 137
 - polyols use, 135
 - zinc phosphinate salt (OP950), 140
 - Intumescent synergy
 - burnt barrels, LOI condition, 147
 - cone calorimeter data, 146–147

- definition, 144
- nano filler, 145
- polyvinylester (PVE) preparation, 145–146
- POSS and phosphate, 146
- Intumescent textile
 - cellulose fiber treatment, 142
 - FR PET fabrics, 143
 - mechanism via charring enhancement, 141–142
 - polyamides, 143–144
 - polyester fibers, 142–143
 - polypropylene fibers, 144
- K**
- Kevlar fibers, 706–707
- L**
- Lambert–Beer law, 371
- Large eddy simulation (LES)
 - algorithms, 553
 - FDS, 552
 - fire modeling, 555
 - vs. RANS, 554
- Large-scale reaction-to-fire test
 - furniture calorimeter, 378
 - ICAL, 380
 - room/corner test
 - apparatus and instrumentation, 378–379
 - combustion products, 379–380
 - protocols, 378
- Laser pyrolysis (LP), 337, 338
- Lateral ignition and flame spread test (LIFT)
 - apparatus, 646
 - flame spread properties, 369
 - material properties, 370
 - piloted ignition experiment, 362–363
 - radiant heat flux profile, 361
 - structure, 642
- Layered double hydroxides (LDHs)
 - clay, 264–265
 - decomposition products, 307
 - intercalation, 311
 - magnesium–aluminum, 180
 - SiO₂-coated, 180–181
 - structure, 308
 - synergistic effects, 309
- Layered silicate FR compound
 - ammonium polyphosphate
 - anionic clays, 307–308
 - montmorillonite and cationic clays, 303–307
 - brominated, 315–316
 - metal hydroxide
 - characteristic combustion parameter, 314–315
 - drawbacks and objectives, 313
 - hydroxide/MMT combination, 314
 - LDPE/EVA filled sample, 315
 - phosphorus and nitrogen compound
 - application, 310
 - chemical structures, 308
 - drawback, 308–309
 - heat release rate curves, 312–313
 - HTC60 and HTP60 sample, 311–312
 - LOI synergistic effects, 309
 - MCA roles, 311
 - in situ polymerization, 312
- LDHs, *see* Layered double hydroxides
- LDPE, *see* Low-density polyethylene
- LES, *see* Large eddy simulation
- LIFT, *see* Lateral ignition and flame spread test
- Limiting oxygen index (LOI)
 - flammability behavior, 391
 - and HRC pure polymers, 797
 - polyethylene, 790
 - PTFE, 793–794
 - PVC, 788–789
 - single wire burn test, 796
 - talca, 792
 - test, 356–357
 - and UL 94, 392, 395
 - values, 394
- Low-density polyethylene (LDPE), 19, 463, 464, 470–472
- M**
- Magnesium hydroxide sulfate hydrate (MHS) whiskers, 181
- Magnesium metaborate, 214
- Mannequin tests, 730
- Mass loss rates (MLRs)
 - energy balance, 537
 - experimental vs. predicted, 541
 - heat fluxes, 540
 - PA6 and PA6/NC, 526–527
 - PMMA nanocomposites, 284–285
- Material design, wire and cable
 - conceptual framework, 784–785
 - constructions, 784
 - flame test standards
 - circuit integrity, 787
 - combustion gases, 786–787
 - examples, 786
 - IEC, 785–786
 - flammability test correlations
 - high throughput (HT), FR and screening, 799–800
 - jacketing materials, 798–799
 - LOI, 795–796
 - probability function, 796–797
 - UL 1685 tray cable burn test, 797–798
 - industry trends
 - environmental concerns, 800–801
 - geographical fragmentation, 800
 - laboratory flammability tests
 - fire propagation apparatus and cone calorimetry, 795
 - LOI and temperature index, 794–795
 - polymer and FR material
 - fluoropolymers, 793–794
 - poly(vinyl chloride) (PVC), 788–789
 - polyolefins, 789–793
 - silicone polymer, 794
- Materials flammability development, fire test
 - behavioral stages, 388–389
 - behavior and retardancy mechanisms
 - bomb calorimeter, 408
 - combustion efficiency, 407
 - cone calorimeter, 406–407
 - flame retardancy effects, 410

- intumescent coating, 412
 - material properties, 409–410
 - PA 66-GF, 414
 - Petrella approach, 413
 - P_{red} flame inhibition effect, 405
 - surface temperature, 411–412
 - TG-FTIR experiment, 406
 - vanishing flame retardancy, 411
 - components, 388
 - developed fire, 403–404
 - forced flaming combustion
 - barrier properties, 401
 - bench-scale, 396
 - cone calorimeter, 399
 - fire residues., 403
 - flame-retarded materials, 400–401
 - HRR characteristic curves, 398
 - PP-g-MA/LS nanocomposite, 402
 - thermal properties, 397
 - THR and HRR, 398–399, 402
 - FR mechanisms, 387–388
 - hazards
 - fire protection, 405
 - ignition and subsequent fire growth, 404
 - ventilation condition, 404–405
 - ignition
 - fire properties, 389
 - flame retardancy mechanism, 393
 - LOI, 391–392
 - materials, LOI performance, 393–394
 - polymer, flame-retarded, 391
 - PP-g-MA and PP-g-MA/LS nanocomposite, 394–395
 - specimen thickness influence, 392
 - UL 94 and LOI, 395–396
 - LOI values, 390–391
 - properties, 389–390
 - protection goal, 390
 - Melamine cyanurate (MCA), 311, 315
 - Melamine–isocyanate interaction, 25
 - Mesoscale experiment
 - cone calorimeter
 - combustion effective heat, 528
 - HRR, 527–528
 - ignition times, 525–526
 - mass loss rate, 526–527
 - PA6-based materials, 525
 - smoke, carbon monoxide, 528–530
 - tube furnace
 - fire conditions, 523
 - ventilation, 524
 - UFA, 530–531
 - Metal hydroxides synergists, 175–176
 - Metallic interlayer (MIL)
 - characteristic integral values, 338–339
 - chemical-physical structure, 335–336
 - degradation progress, 339
 - FTIR spectrum, 337–338
 - MMT-Fe characteristics, 338
 - Metal–POSS, 194
 - Methyl methacrylate (MMA)
 - copolymers, 115
 - monomer, 34
 - polyester resin, 306
 - Minimum flux for flame spread (MFFS), 439–440
 - MLRs, *see* Mass loss rates
 - MMA, *see* Methyl methacrylate
 - MMT, *see* Montmorillonite
 - Molecular weight distribution (MWD), 482
 - Monte Carlo methods, 481
 - Montmorillonite (MMT)
 - combustion residues, 240
 - nanocomposites, 254
 - nanoparticles, 244–245
 - “M” test, 728
 - Multiwall CNTs (MWCNT), 181, 262, 265, 281, 317
 - MWD, *see* Molecular weight distribution
- ## N
- Nanoadditives
 - carbon nanotube, surface treatment, 272
 - clay structure and properties
 - LDH, 264–265
 - silicate, 263–264
 - structure and properties, carbon nanotube, 265–266
 - surface treatment, clay
 - compatibility/miscibility and, 269–272
 - modified structure, 267–268
 - organo-modifiers, 268
 - orientations/arrangements, 269
 - polymer matrix interface, 266–267
 - Nanocomposite polymers, fire
 - description, 511–512
 - EVA and PBT applications
 - ignition time, 541–542
 - material and experimental, 541
 - thermal properties, 542
 - flammability properties, 510–511
 - materials, 512
 - mesoscale experiments
 - cone calorimeter, 525–530
 - tube furnace, 523–525
 - UFA, 530–531
 - microscale experiments
 - rheology–viscosity, 512–515
 - TGA/DSC and, 515–516
 - TGA/FTIR/ATR, 516–523
 - nanoclay loading models
 - HRR/MLR, 544–546
 - predicted vs. experimental MLRs, 547
 - pyrolysis, numerical models
 - heat flux ratio and pyrolyzed depth, 539–540
 - mathematical formulations, 534–537
 - PA6, deduced effective thermal properties, 537–539
 - predicted mass loss rate, 540–541
 - TGA measurements, 531–533
 - Nanoparticles, flame retardants
 - carbon nanotubes, 316–317
 - nano-hydroxides
 - advantages and drawback, 318
 - condensed-phase action, 320
 - polyamide 6/CPA and, 318–319
 - nano-oxides, 320–321
 - POSS and PVE, 321–322
 - Nanosize fire-retardant fillers
 - boehmite and MSH whiskers, 181
 - magnesium–aluminum LDH, 180

magnesium hydroxide nanoparticles, 179–180
 SiO₂-coated nano-LDH, 180–181
 National fire protection association (NFPA)
 codes and standards
 air conditions, 637–638
 building, 634–635
 housing, 637
 life safety, 632–633
 ships, 636–637
 uniform fire, 633–634
 electrical code
 flame-spread requirements, 631
 flexible cords and cables, 630
 key documents, 628–629
 methods and equipment, wiring, 632
 wiring requirements, 628
 Navier–Stokes equations, 552–553
 NBS Smoke Chamber ISO 5659-2³³, 467–468
 Neobor[®], 210
 NFPA, *see* National Fire Protection Association
 NFPA 550 fire concepts tree, 352
 NF P 92–503 Brûleur Electrique, *see* “M” test
 NMM, *see* Nonmodified montmorillonite
 Nonmodified montmorillonite (NMM), 334
 Numerical integration rule, 490

O

Octamethyl POSS, 194
 Open fires, 48–49
 Optibor[®], *see* Boric acid
 Organophilic montmorillonite (OMM), 334, 340, 341
 Organophosphorus additive FR
 phosphine oxides, 113
 phosphonates
 dimeric, oligomeric, and cyclic phosphates, 111–112
 halogenated phosphates and, 111
 phosphates and, 110–111
 Orthoboric acid, *see* Boric acid

P

PBEs, *see* Population balance equations
 PBMs, *see* Population balance models
 PBT, *see* Polybutylene terephthalate
 Petrella approach, 413
 Phenolic foams, 776
 Phosphine–borane polymer, 228
 Phosphine oxides, 113
 Phosphonates
 cyclic oligomeric, 112
 halogenated phosphates and, 111
 phosphate and
 amine and esters, 110
 aryl, 110–111
 dimeric, 111–113
 dimethyl methylphosphonate, 111
 pentaerythritol, 112
 Phosphorus-based FR
 chain-reaction polymers
 acrylics, 115–116
 polystyrene and polyolefins, 116
 char layer and APP, 768
 DMMP, DEEP and DMPP, 769

elemental and compounds
 and nitrogen, 109
 solid forms, 108
 hypophosphites, 769–770
 inorganic additives
 ammonium phosphate, 110
 red phosphorus, 109
 mechanisms
 base polymers structural features, 119–120
 char formation, 121–122
 condensed-phase, 120–121
 physical effects, 123
 synergism, phosphorus-halogen, 122
 thermal degradation and flame retardance, 121
 vapor-phase, 120
 organophosphorus additive, phosphonates
 dimeric, oligomeric, and cyclic phosphates,
 111–112
 halogenated phosphates and, 111
 phosphates and, 110–111
 phosphine oxides, 113
 polyurethane foams, 767–768
 reactive flame retardants, 113
 step-reaction polymers
 polyamides, 114–115
 polyesters and polycarbonates, 114
 structure–toxicity relationships, 108
 surface grafting, 118
 thermoset
 epoxy resins, 117
 polyurethanes, 117–118
 unsaturated polyesters, 118
 PIL, *see* Polymer interlayer
 PMMA, *see* Polymethylmethacrylate
 PNs, *see* Polymer nanocomposites
 Police protective garments/systems, 735
 Polyamides–nanocomposite, nylon 6
 blend nanoclays, 752–754
 fiber properties, 754, 755
 vertical burning behavior, 754
 Polybor[®], 210
 Polybrominated biphenyls (PBBs)
 chemical structure, 92
 dibenzofurans and dibenzodioxins formation, 93
 Polybromo diphenyl (or biphenyl) ethers (or oxides)
 (PBDPEs), 92–94
 Polybutylene terephthalate (PBT)
 heat flux ratio, 542, 544
 ignition times, 541–542
 material and experiments, 541
 thermal properties, 542
 Polycarbonate, 89
 Polychlorobiphenyls (PCBs)
 chemical structure, 92
 dibenzofurans and dibenzodioxins formation, 93
 Polycyclic aromatic hydrocarbons (PAHs), 521, 523
 Polydimethylsilicone (PDMS), 187–189, 280–281
 Polyester chain scissions, 26
 Polyhedral oligomeric silsesquioxanes (POSS)
 degradation and combustion behavior, 197
 description, 141
 macromers and siloxane copolymers, 191–192
 molecules, 190–191
 and phosphates, 146

- polypropylene
 - combustion behavior, 194–196
 - fire behavior, multi filament yarn, 194, 195
- polyvinylester (PVE) preparation, 145–146
- preceramic materials, 192–193
- properties
 - flammability and mechanical, 193–194
 - FR, 197–198
- structure, 190
- synergistic effects, 196–197
- thermal and thermo-oxidative degradation, 192
- Polymer degradation; *see also* Flame retardance
 - natural
 - cellulose, 28, 29
 - protein, 28–30
 - thermoplastics
 - aliphatic polyamides, 20–21
 - polyacrylonitrile, 21–22
 - polyesters, 21
 - polyolefins, 20
 - polystyrene (PS), 22
 - PVC and EVA, 23
 - thermosets
 - epoxy resins, 26–27
 - maleimide and polyimide resins, 28
 - phenolic resins, 27–28
 - polyester resins, 25–26
 - vinyl ester resins, 26
- Polymer flammability characterization
 - description, 434–435
 - flammability properties
 - heat flux profile, 437
 - homogenous composition samples, 436
 - RCC, 437–438
 - minimum flux
 - heat flux field map, 438–439
 - MFFS experiments, 439–440
 - PS flame retarded formulations, 440–441
 - sample preparation, 435–436
- Polymeric system, fire retarded
 - CIL
 - anionic surfactant, 332
 - composites, 331
 - cone calorimetric data, 336
 - Diels–Alder adduct, 331–332
 - HRR and THR, 333
 - NMM and OMM, 333–334
 - phase separation and structure, 335–336
 - shear-thinning coefficient, 335
 - fire-induced degradation, 330–331
 - interfacial requirements, 330
 - interlayer types, 329
 - MIL
 - characteristic integral values, 338–339
 - chemical–physical structure, 335–336
 - degradation progress, 339
 - FTIR spectrum, 337–338
 - MMT-Fe characteristics, 338
 - PIL
 - expandable interlayer, 343
 - insulating interlayer, 340–341
 - mass loss curves, 341
 - protecting interlayer, 342
 - transporter and polyorganosiloxane interlayers, 342–343
 - RIL, 343–345
- Polymer interlayer (PIL)
 - expandable, 343
 - insulating interlayers, 340–341
 - mass loss curves, 341
 - protecting, 342
 - transporter and polyorganosiloxane, 342–343
- Polymer nanocomposites (PNs)
 - characterization
 - clay distribution and dispersion, 279
 - scattering/diffraction mode, 277
 - structure/morphology, 276
 - TEM micrograph, 277–279
 - XRD and TEM technique, 276–277
 - description, 262–263
 - fabrication, 261–262
 - FR compound, layered silicate
 - ammonium polyphosphate, 303–308
 - brominated compounds, 315–316
 - metal hydroxide, 313–315
 - phosphorus and nitrogen compounds, 308–313
 - mechanism, nanoadditive effect
 - char residue, 289–290
 - clay barrier forms, 288–289
 - paramagnetic radical trapping, 288
 - polymer matrix, 290
 - thermal degradation pathways, 289
 - nanoadditives
 - structure and properties, 263–266
 - surface treatment, 266–272
 - nanoparticles, flame retardants
 - carbon nanotube, 316–317
 - nano-hydroxide, 318–320
 - nano-oxides, 320–321
 - POSS and polyvinylester, 321–322
 - preparation
 - mechanical and thermal properties, 272
 - melt compounding, 274–275
 - in situ polymerization, 273
 - solvent blending, 273–274
 - structure
 - description, 274–275
 - polymer/clay nanocomposites (PCNs), 275
 - technology, 10–11
 - thermal and fire performance
 - CCA tool, 283
 - CNTs, 284–285
 - MCC technique, 287
 - nanoadditive nanodispersion, 279–280
 - parameters, 279
 - PSCNs, 282–283
 - single wall carbon nanotube (SWNT) dispersion, 286
 - TGA curves, 280–282
- Polymers
 - halogen-containing, 231
 - halogen-free, 231–232
 - relative thermal stability, 17
 - step-reaction
 - polyamides, 114–115
 - polyesters and polycarbonates, 114

- Polymethylmethacrylate (PMMA)
 fire-retardant mechanisms, 34
 thermal degradation, 494, 499
 thermogravimetric (TG) experiments, 500
- Polyolefins
 application, 789–790
 ATH and magnesium hydroxide, 791–792
 electrical applications, 792
 fire-retarded application, 89–90
 foams, 775
 FRs selection, 791
 LOI, 790
 low voltage insulation, 793
 metal hydrates, 792–793
 thermal decomposition, 790–791
- Polypropylene/clay nanocomposites (PPCNs), 286, 289
- Polypropylene-nanocomposite
 burning behavior, 750–751
 knitted fabrics flammability, 747, 749
 maleic anhydride-grafted, 746
 nanoclay and compatibilizer levels, 746–748
 phosphorus and halogen, FR, 749–750
 polypropylene/multiwalled carbon nanotubes (MWNT), 751–752
- Polystyrene/clay nanocomposite (PSCN)
 cross-linked, 270
 thermal stability, 282
 WAXS patterns, 277
- Polystyrene foams, 773–775
- Polytetrafluoroethylene (PTFE), 793–794
- Polyurethane (PU), foam thermal degradation, 24
- Polyurethanes, 90–91
- Polyvinyl chloride (PVC)
 Bolland and Gee reaction scheme, 19
 fillers role, 789
 flame inhibitors, 33
 flexible, 788–789
 foams, 775–776
 LOI, 788
 use, 23
- Population balance equations (PBEs)
 chain stripping, 504
 degradation mechanism, 498
 end-chain scission, 495
- Population balance models (PBM)s
 description, 483
 linear differential equations, 484
 volatilization, 484–485
- POSS, *see* Polyhedral oligomeric silsesquioxanes
- Protective clothing
 firefighters and military personnel battlefield, 734
 police protective garments, 735
- PTFE, *see* Polytetrafluoroethylene
- Purser's model, 461
- Pyrolysis
 definition, 48
 time, 53–57
- R**
- Radiation transport equation (RTE), 559–561
- Rapid cone calorimetry (RCC)
 MFFS and pHRR, 442
 screening tool, 441
- Reactive FR
 brominated polyols, 765–766
 carbodiimide linkage, 766
- Reactive gaseous mixtures, combustion
 exothermic reaction, 46
 heat of combustion, 47
 upper flammability limit, 46–47
- Red phosphorus (RP), 109, 770, 771, 773, 775
- Registration, Evaluation and Authorization of Chemicals (REACH); *see also* Science-based drivers
 and FR, 687
 halogenated flame retardants, 95
 reduction of hazardous substances (RoHS)
 and WEEE, 7
- Regulation, fire issues
 aircraft
 evacuation, 599–600
 principal fire tests, 599
 types, 598
 cigarettes, 608–609
 federal, 591–592
 flammable fabrics
 carpets and rugs, 610
 upholstered furniture, 613–614
 wearing apparel, 609–610
 vs. international regulations
 CBUF project, 621
 construction products, 615–616
 European community concept, 616–619
 local
 furniture fire-safety, 593
 life safety code, 594
 motor vehicles
 safety products, 590–591
 school buses, 608
 ships, 600–601
 state
 fire safety, 593
 furnishings fire issues, 592
 ICC code-notes, 595–597
 trains and underground rail vehicles
 fire-testing technology, 601
 FRA requirements, 602–603
 NFPA 130–2007 requirements, 604–605
 volunteers, 589–590
- Regulatory activity, flame-retardant (FR)
 Asia
 China, 689
 Korea, 689–690
 European Union, 687–689
 Japan, 690–691
 North America
 Canada, 694–695
 CPSC, 693
 Environmental Protection Agency (EPA) activity,
 692–693
 projects, 695–696
 risk assessments, 691–692
 state legislation, 693–694
 Norway and Sweden, 689
 REACH, 688–689
 reduction of hazardous substances (RoHS), 687–688
 WEEE, 688
- Reinforced-char-forming, interlayer (RIL), 343–345

- Reynolds-averaged Navier–Stokes (RANS) equations
 CFD fire models, 553
 vs. LES, 554
 technique, 552
 turbulence modeling, 555
- Rheometer, 250, 251
- Richtlinien für die Ausstattung und den Betrieb von
 strassen Tunnels (RABT) curves, 150
- Rijks Water Staat (RWS) curve, 150
- RIL, *see* Reinforced-char-forming, interlayer
- Room/corner test
 apparatus and instrumentation, 378–379
 combustion products, 379–380
 protocols, 378
- RTE, *see* Radiation transport equation
- S**
- Savitzky–Golay (SG) smoothing algorithm, 526
- SBI, *see* Single burning item test
- Scanning electronic microscopy (SEM)
 characterization, 142
 images, 156
 intumescent chars, 256
 phase-separation, 335
- Science-based drivers
 assessment, risk
 EU, 681
 FR, 678–680
 rapporteur, 677–678
 SCHER opinion, 680–681
 chemical inventory
 Australia and Canada, 674
 description, 673
 Europe, 674–675
 Japan, Philippines, South Korea
 and United States, 675
- REACH
 authorization, 685–686
 benefits, 682
 dangerous chemicals substitution, 683
 description, 681
 evaluation, 685
 and FR, 687
 registration, 683–685
 restriction, classification labeling inventory and
 information, 686
 risk, 676–677
 Toxic Substances Control Act (TSCA), 675–676
- SDBS, *see* Sodium dodecylbenzenesulfonate
- SEM, *see* Scanning electronic microscopy
- Seveso disaster, *see* Polybromo diphenyl (or biphenyl)
 ethers (or oxides) (PBDEs)
- Shear-thinning exponent, 335
- Sheet molding compound (SMC), 708, 741
- Silicon-based FR
 POSS, *see* Polyhedral oligomeric silsesquioxanes
 and silanes
 flammability properties, 188
 gasification modes, 187–188
 heat release, 187
 intumescent process, 189
 polyurethane (PU)/PDMS, 188–189
 silylation, polystyrene, 189–190
 silica and silicate
 burning behavior, 201–202
 flammability properties, 200
 gel and potassium carbonate, 198
 material properties, 199
 polypropylene heat release rate and mass loss,
 199–200
 synergistic effect, 202
 talc, 203
 zeolite, 202–203
- Silicone polymer, 794
- Simple ignition test, 727
- Single burning item test (SBI), 380, 403, 511, 573, 709,
 719, 765
- Single-wall CNTs (SWCNT)
 PMMA, 286
 structure, 265
- Small angle x-ray scattering (SAXS), 277
- Small heat source ignition test
 concepts, 355
 description, 354
 LOI, 356–357
 UL 94 20-mm vertical burning, 355–356
 use and limitation, 357–358
- Smoke suppression, 173–174
- Smoldering
 characterization, 62
 degradation process, 63–65
 forward, 66
 opposed, 65–66
 physical parameters control, 66–67
 smolder vs. combustion processes, 62–63
 virgin foam and smoldered char, 63
- Sodium dodecylbenzenesulfonate
 (SDBS), 267
- Solid-state nuclear magnetic resonance (ssNMR)
 APP/PER system, 243–244
 borophosphate formation, 242
 polymeric material, 241–242
 Raman spectroscopy, 244
 XPS, 245
- Spontaneous ignition, 51–52
- SSTF, *see* Steady-state tube furnace
- Standards, fire issues
 organizations and committees, 639–640
 test method
 cigarette ignition, 652
 flame spread, 644–646
 flammability, 644
 heat release, 646–648
 ignitability, 640–643
 microcalorimetry, 651–652
 products/materials, 652–653
 smoke obscuration, 648–649
 toxicity, smoke, 649–650
- Steady-state tube furnace (SSTF), 454, 463,
 469–474
- Steiner tunnel test, 368–369, 645
- Surface flame spread
 LIFT, 369–370
 measurements, 368
 modes, 353–354
 pertinent material properties, 367–368
 Steiner tunnel test, 368–369

- Sustainable solution development
 green solutions
 definition, 696
 FR and, 697–698
 green chemistry, 697
 life-cycle thinking, 698
 product stewardship, 698–699
- SWCNTs, *see* Single-wall CNTs
- Synergism, fire-retardant fillers
 flammability properties, 176
 metal hydroxides synergists, 175–176
 phosphorus-halogen, 122
 zinc borate and metal hydroxides, 178
 zinc hydroxystannate (ZHS)/zinc stannate (ZS) coated fillers, 177
- T**
- TEM, *see* Transmission electron microscopy
- Textiles, flame retardancy design
 additives/copolymers, synthetic fibers, 744–745
 coatings
 back-coating, 742–743
 intumescent, 743
 plasma, 743–744
 composite assemblies, 757
 condensed phase, 738–739
 fabric flammability and testing standards
 description, 726
 flame spread, 727–728
 full product test, 730–731
 heat release test, 728–730
 limiting oxygen index (LOI), 726–727
 mannequin test, 730
 simple ignition test, 727
 fiber blending, 756
 FR finishes
 cotton, 740–741
 nondurable and semidurable, 739
 silk, 742
 viscose, polyester, cotton-polyester blend and wool, 741
 halogenated, polymer family, 91
 hazards, application-based
 apparel fabrics, 733–734
 curtains, drapes, upholstery and bedding fabrics, 735
 fiber-reinforced polymeric composites, 737–738
 floor coverings, 735–736
 protective clothing, 734–735
 tents and marquees, 736
 testing standards, 732–733
 transportation, 736–737
 heat resistant and inherently fire-retardant fibers
 aromatic, 754–755
 inorganic fibers, 755
 nanocomposite-based
 cotton and polyester, 746
 fibers vs. bulk polymers, 745–746
 polyamides, 752–754
 polypropylene, 746–752
 surface treatment, 739
 types and fibre flammability, 731–732
- TGA, *see* Thermogravimetric analyzer
- TGV high-speed train, 717
- Thermal degradation modeling
 Arrhenius parameters, 481
 bond-weighted random scission model
 break-at-a-point, 491–494
 description, 485–486
 pure random scission, 486–490
 symmetric power law bond weights, 490–491
 chain stripping
 Arrhenius parameters, 506
 constant heating rate, 505–506
 mechanism, 504
 steps, 479–480
 depropagation
 combined end-chain and random scission, 495–497
 PMMA, 499–500
 random scission initiation, 497–499
 simple end-chain scission, 494–495
 description, 479–480
 energy conservation equations, 482–483
 kinetic rate equations, 480
 PBMs
 linear differential equations, 483–484
 moments and description, 483
 volatilization, 484–485
 recombination
 discrete convolution operator, 501–502
 Laplace transform, 501
 molecules, normal distribution, 502
 radical species and polymerization, 500–501
 random scission, 503–504
 simultaneous random scission, 503
 scission process, 482
 stability factors, 17
- Thermogravimetric analyzer (TGA)
 cone calorimeter, 533
 curve, 262, 279–283
 degradation behaviors
 in air, 517–518
 in N₂, 516–517
 DSC properties measurement, 515
 gas analysis, TG/FTIR
 degradation pathways, 519–520
 measurements, 518
 total integrated values, 520–521
 total mass loss, 519
 heat measurements, 515–516
 kinetic parameters, 531
 PBT, TG/ATR
 PBT spectra, 522–523
 test samples, 521
 surface temperature history, 532–533
- Thermoplastic polyurethane (TPU) coating systems, 137, 141, 194, 195, 224, 767, 788, 794
- Thermosetting system
 epoxy resins, 117
 polyurethanes, 117–118
 unsaturated polyesters, 118
- Thornton's rule, 364
- Time to ignition (TTI)
 calorimetry characteristics, 792
 clay nanofillers, 336
 mass loss curves, 341
- Toluene diisocyanate (TDI), 23, 24, 188, 307

Total heat release (THR)
 aramid-containing composite, 737
 CCA, 290
 HRR and, 400–402
 reduction, 320–321
 synergies, 310
Toxic Substances Control Act (TSCA), 675–676
Transmission electron microscopy (TEM), 276–279
Transportation, textile
 aircraft and ships, 737
 motor and rail, 736
TTI, *see* Time to ignition

U

UL 94 20-mm vertical burning test, 355–356
Universal flammability apparatus (UFA), 511, 530–531

V

Voluntary Emissions Control Action Program (VECAP),
 698–699

W

Waste of electrical and electronic equipment (WEEE)
 directive, 688
 environmental concerns, 800
 on flame retardants, 7
Wide angle x-ray scattering (WAXS), 277
Wien's displacement law, 358
Wood/cellulose, 230–231
Wood plastic composites (WPCs), 210, 222

X

X-ray diffraction (XRD)
 intercalated structure, 307
 measurements, 254–255
 organoclays, 277–278
 ternary composition, 309
 uses, 277
X-ray photoelectron spectroscopy (XPS)
 analysis, 337
 EG, 245–247
 vs. ssNMR, 245

Z

Zinc borates
 vs. barium metaborate, 218
 elastomer, 221
 Firebrake
 Firebrake 415, 223
 Firebrake 500, 222–223
 function, 216–217
 molecular structure, 216
 TGA, 215
 host, 215
 polyamides, 218–219
 polyolefins
 afterglow suppression, polypropylene, 220
 halogen-based flame retardant, 219
 polyvinyl chloride (PVC), 217–218
 thermosets/coating and WPC, 222

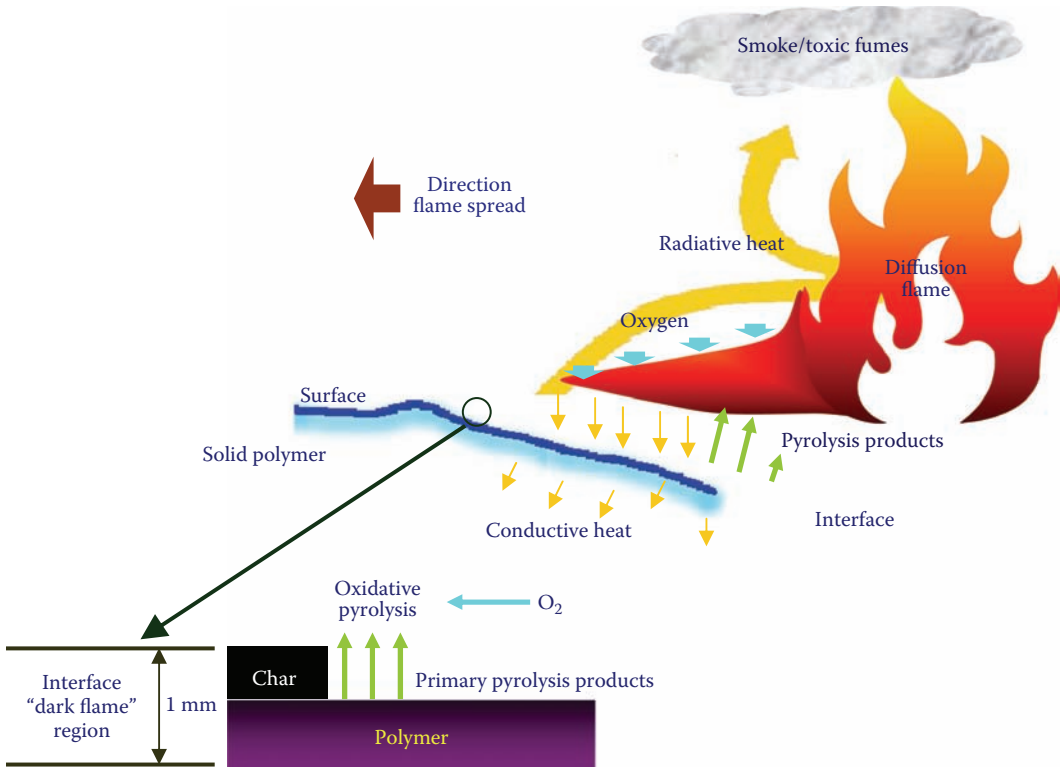


FIGURE 2.1 Schematic representation of a burning polymer.

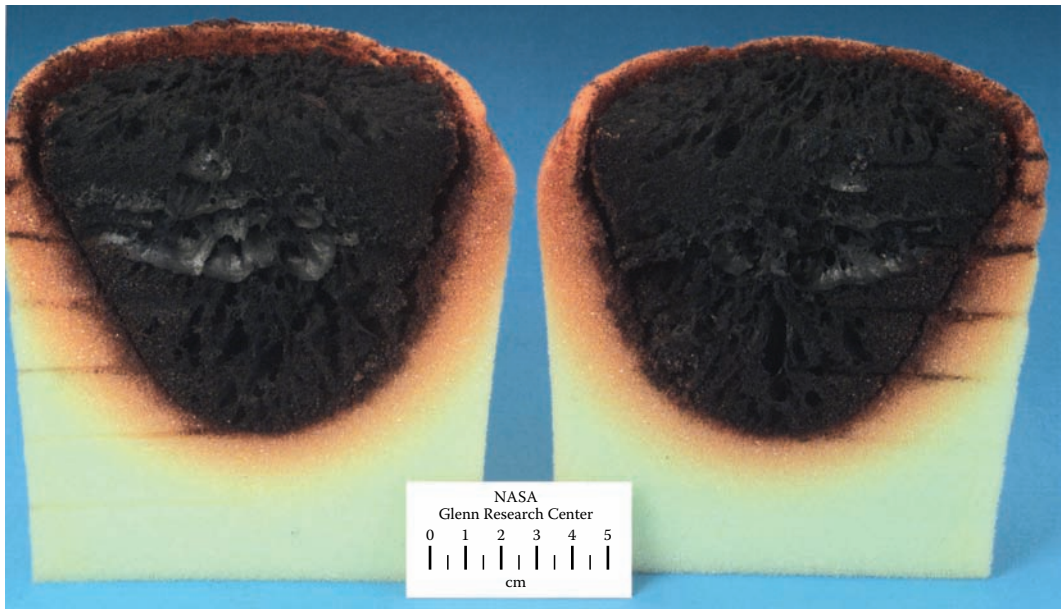


FIGURE 3.11 Photograph of a polyurethane foam sample through which a smolder reaction has propagated. (Photo courtesy of NASA.)

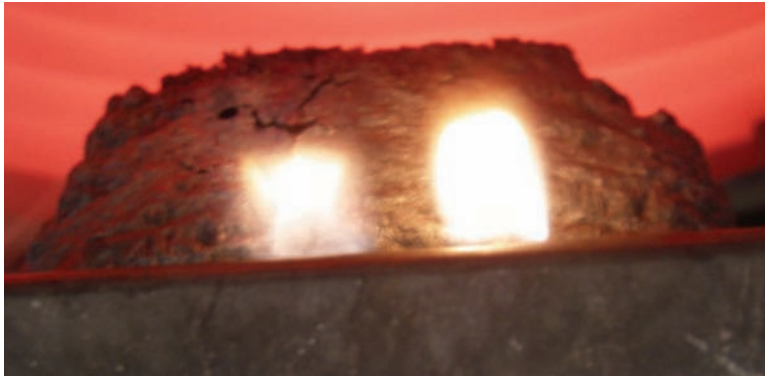
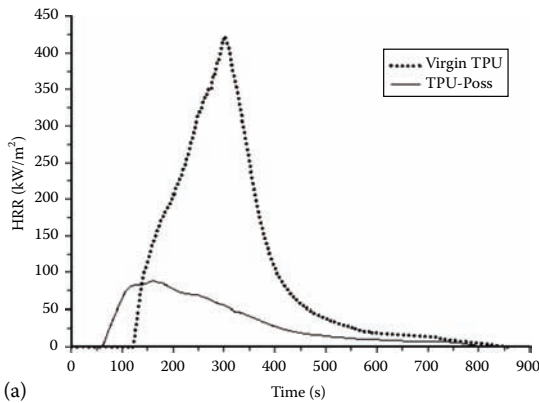


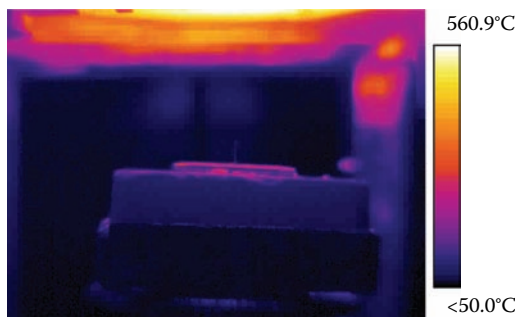
FIGURE 6.2 Intumescent poly(lactide) (PLA) during a cone calorimeter experiment. Note the small flames on the side of the intumescent “cake” showing how the intumescent coating smothers the fire.



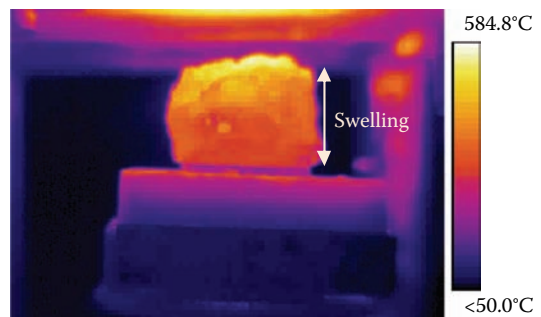
(a)

(b)

FIGURE 6.12 HRR as a function of time of pure TPU and TPU/FQ-POSS composite (external heat flux = 35 kW/m^2) (a) and intumescent char residue at the end of the cone experiment (b).



(a)



(b)

FIGURE 6.23 IR images of an intumescent coating on steel plate upon heating at $t = 0 \text{ s}$ (a) and at the maximum of expansion (b).

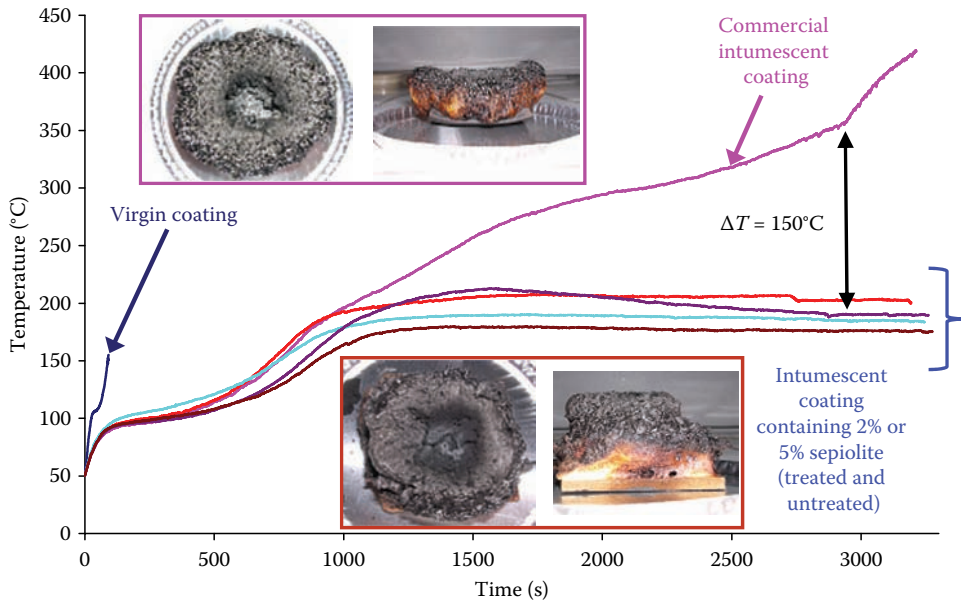


FIGURE 6.29 Temperature as a function of time of the backside of wooden plate protected by an intumescent coating containing sepiolite or not.

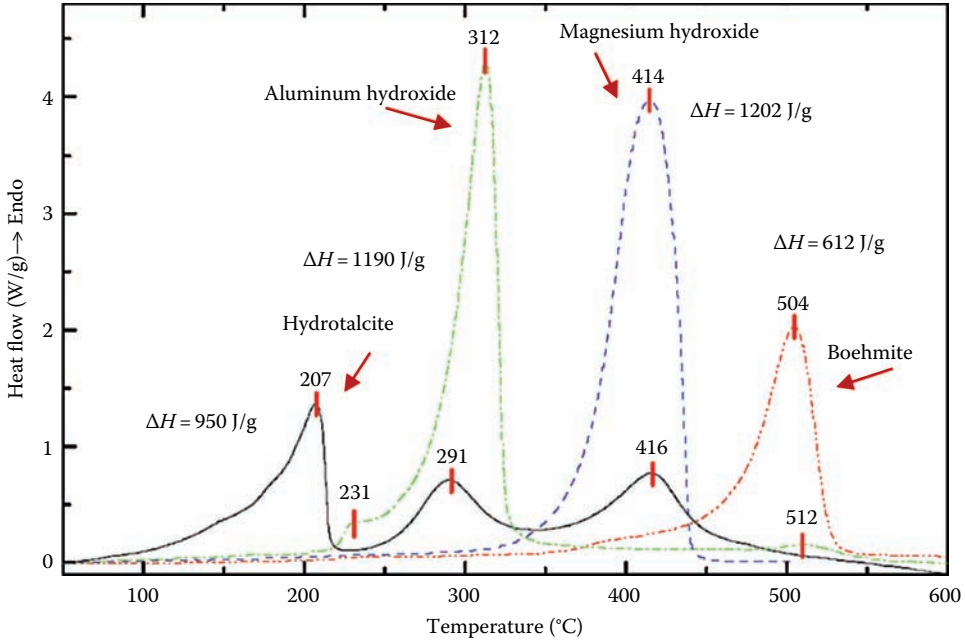


FIGURE 7.2 Endothermic decomposition of hydrated fillers. (From Camino, G. et al., *Polym. Deg. Stab.*, 74, 457, 2001. With permission.)

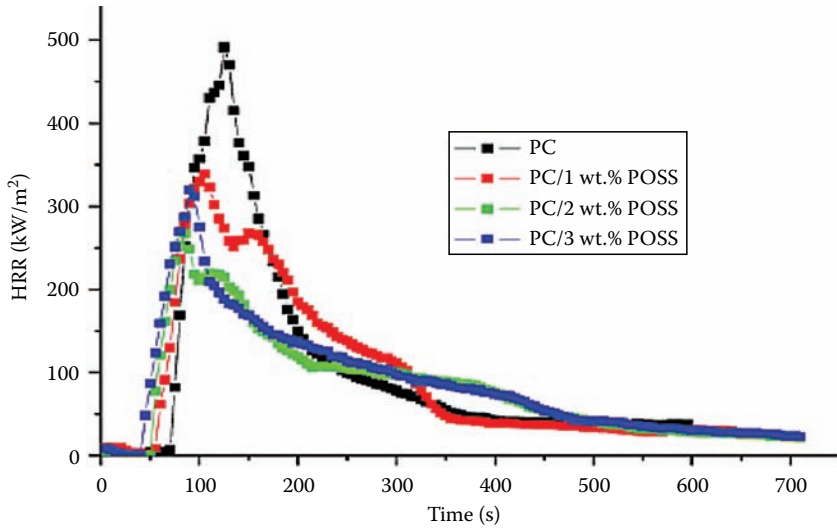


FIGURE 8.12 Rate of heat release curves of PC, PC/1 wt.% TPOSS, PC/2 wt.% TPOSS, and PC/3 wt.% TPOSS. (From Song, L. et al., *Polym. Degrad. Stab.*, 93, 627, 2008. With permission.)

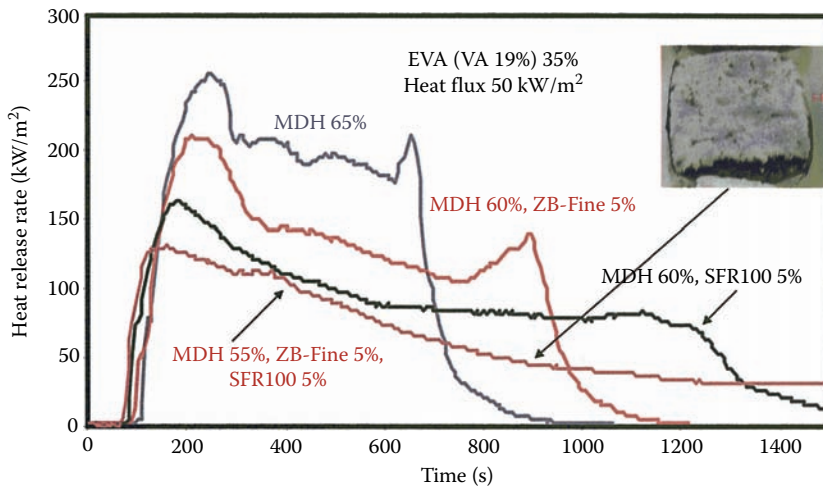


FIGURE 9.9 HRR curves of MDH/Firebrake ZB-Fine/silicone-SFR100 (total loading 65%) in EVA.

PA6/OP1311



(a)



(b)

PA6/OP1311/MMT



(a')



(b')

FIGURE 10.1 Combustion residues of PA6/OP1311 and PA6/OP1311/MMT from the cone calorimeter obtained at different characteristic times ((a) and (a') after ignition and (b) and (b') at maximum PHRR). (From Samyn, F., Compréhension des procédés d'ignifugation du polyamide 6, Apport des nanocomposites aux systèmes retardateurs de flamme phosphorés, PhD dissertation, University of Lille, Lille, France, 2007.)

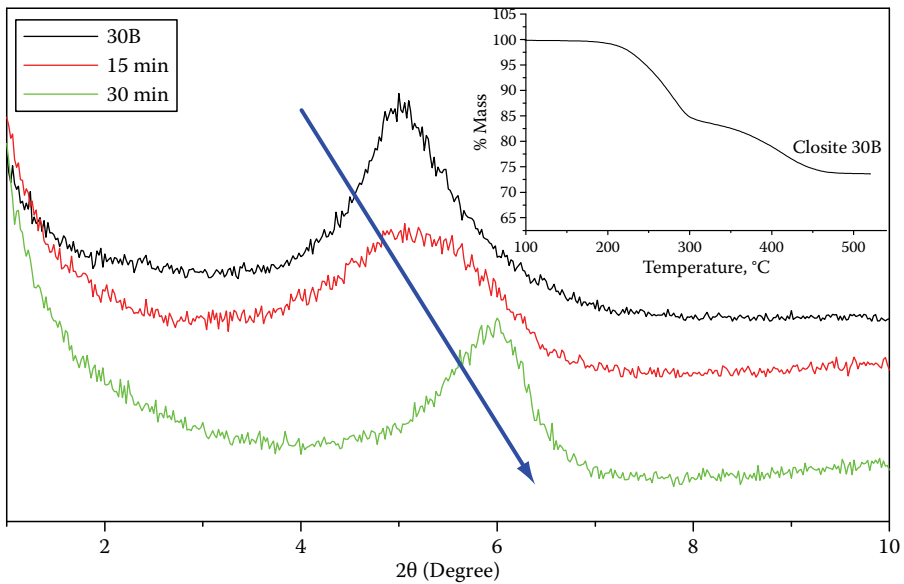


FIGURE 11.11 Thermal stability of Cloisite 30B seen in XRD patterns before and after heating at 190°C under air for 15 and 30 min; (inset) TGA result under N₂ at 20°C/min.

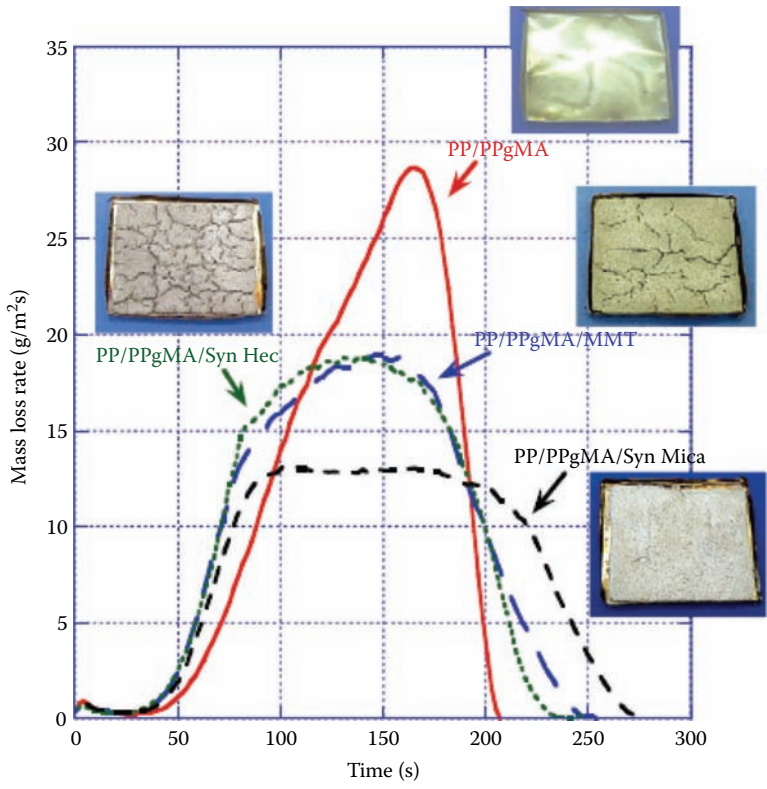


FIGURE 11.32 Effect of clay type on MLR of PP (84.6%)/PPgMA (7.7%)/clay (7.7%) at 50kW/m² in N₂. (From Cipiriano, B.H. et al., *Polymer*, 48, 6086, 2007. With permission.)

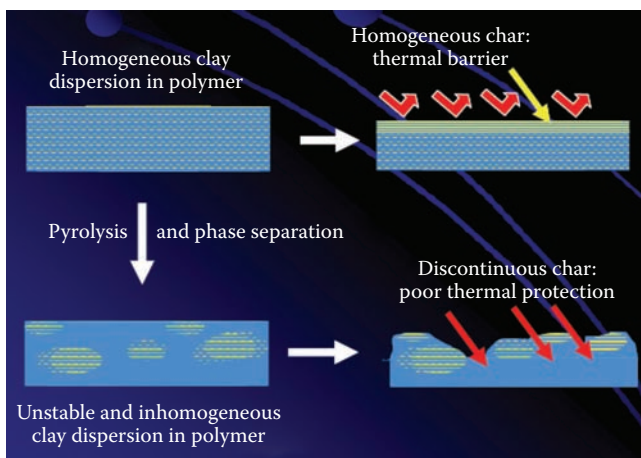


FIGURE 11.36 Mechanism of how crack-free and networked char barrier affects the thermal stability of polymer matrix. (From Gilman, J.F., Flame retardant polymer nanocomposite, http://www.epa.gov/oppt/nano/p2docs/casestudy2_gilman.pdf)

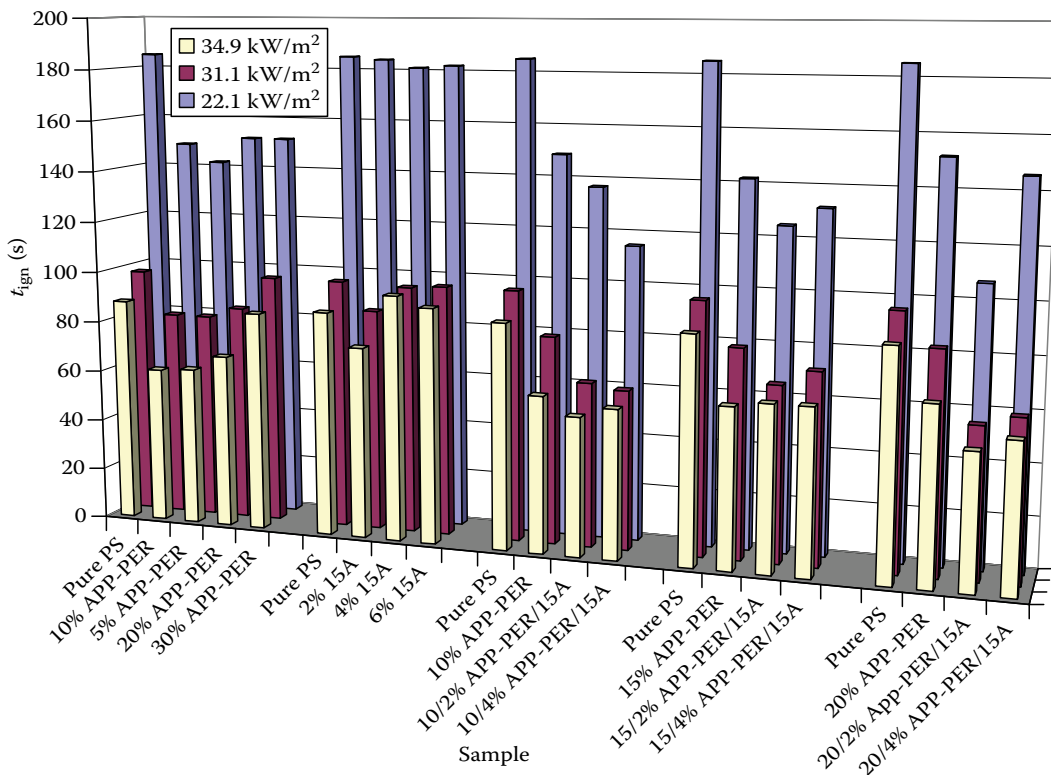


FIGURE 16.15 t_{ign} data for PS flame retarded formulations measured in the RPA. The ignition time of each formulation was measured at three different heat fluxes simultaneously. The heat fluxes are provided in the insert in units of kW/m² and are color matched with the data bars in the graph. The t_{ign} standard uncertainty, averaged over all fluxes where t_{ign} was measured, is $\pm 10\%$ (2σ).

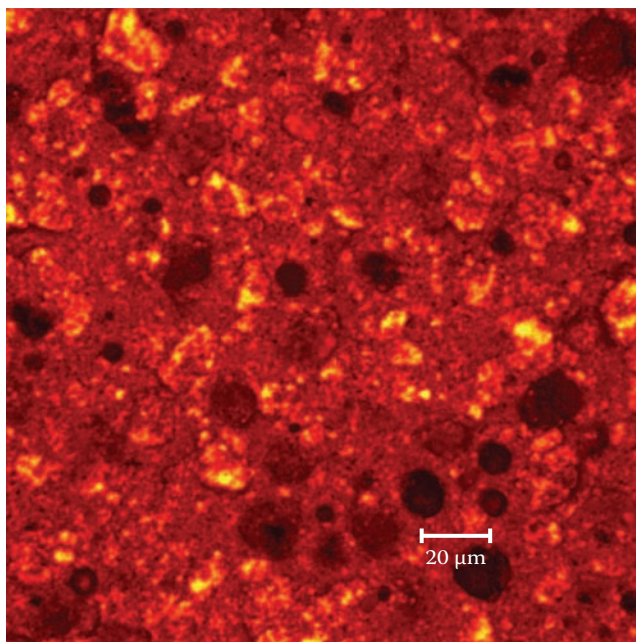


FIGURE 16.20 Topcoat containing Probe 5. A LP 585 nm filter was used to remove incident light.

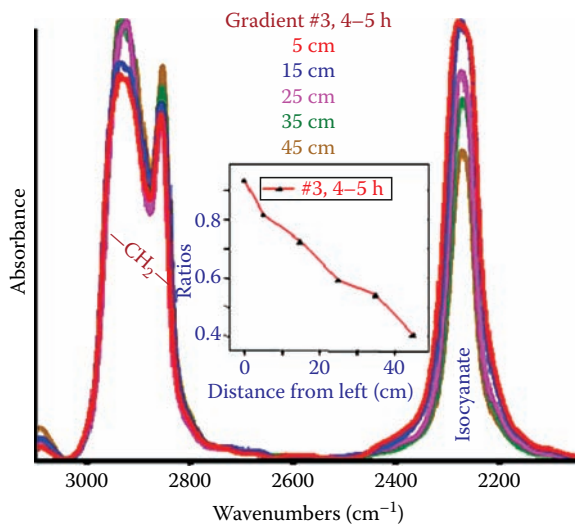


FIGURE 16.21 FTIR of DBTDL lateral gradient topcoat sample taken between 4 and 5 h after spraying.

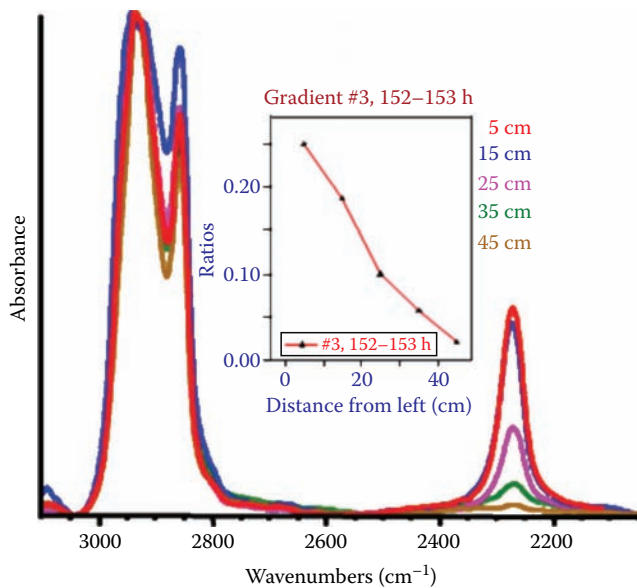


FIGURE 16.22 FTIR of DBTDL lateral gradient topcoat sample taken between 152 and 153 h after spraying.

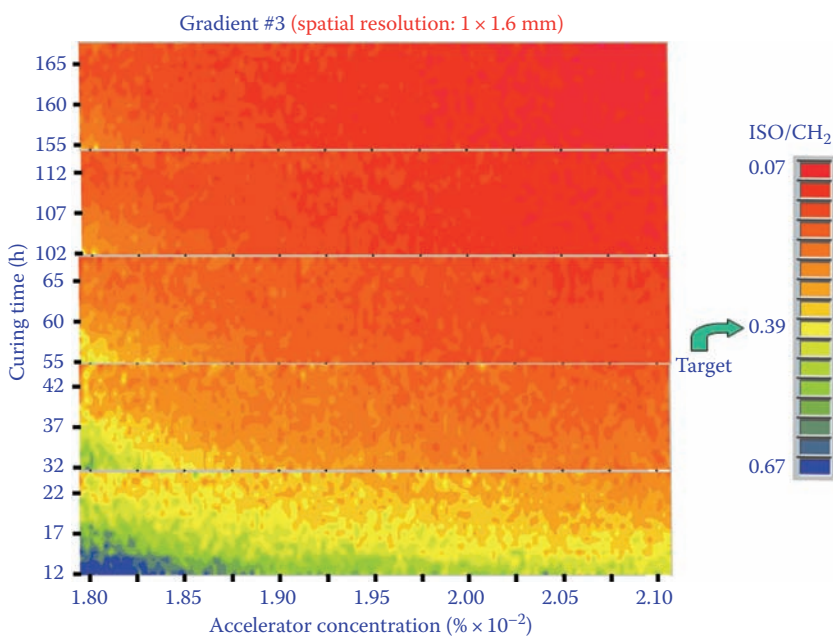


FIGURE 16.23 FTIR-RTM mapping the same topcoat lateral gradient discussed in Figures 16.15 and 16.16.

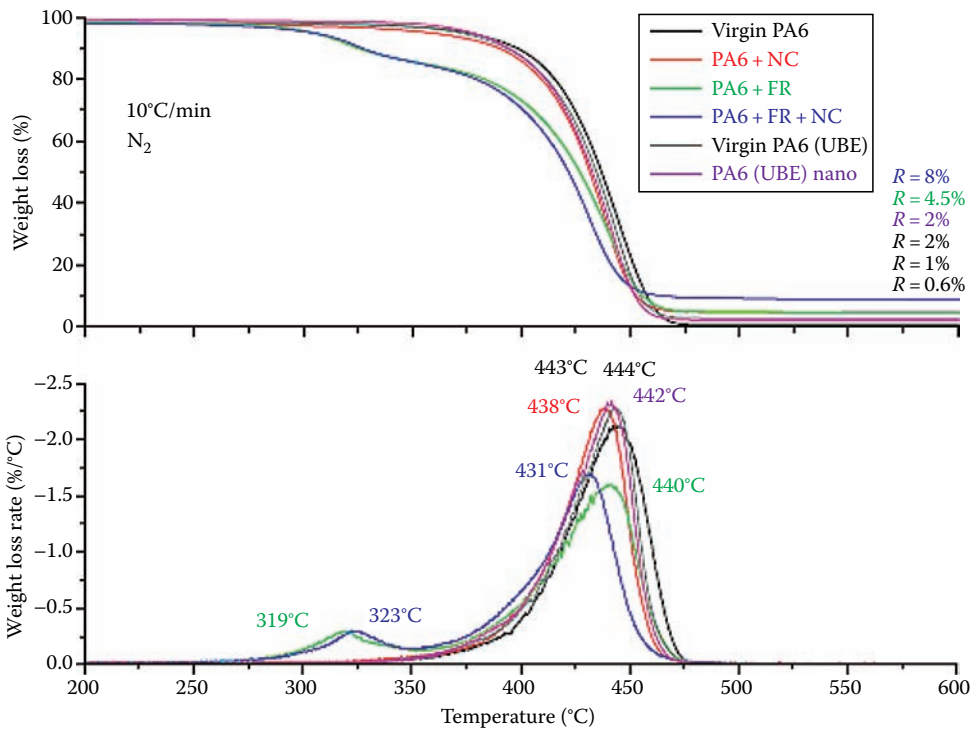


FIGURE 19.4 TG/DTG curves of PA6, PA6 + NC, PA6 + FR, and PA6 + FR + NC in nitrogen.

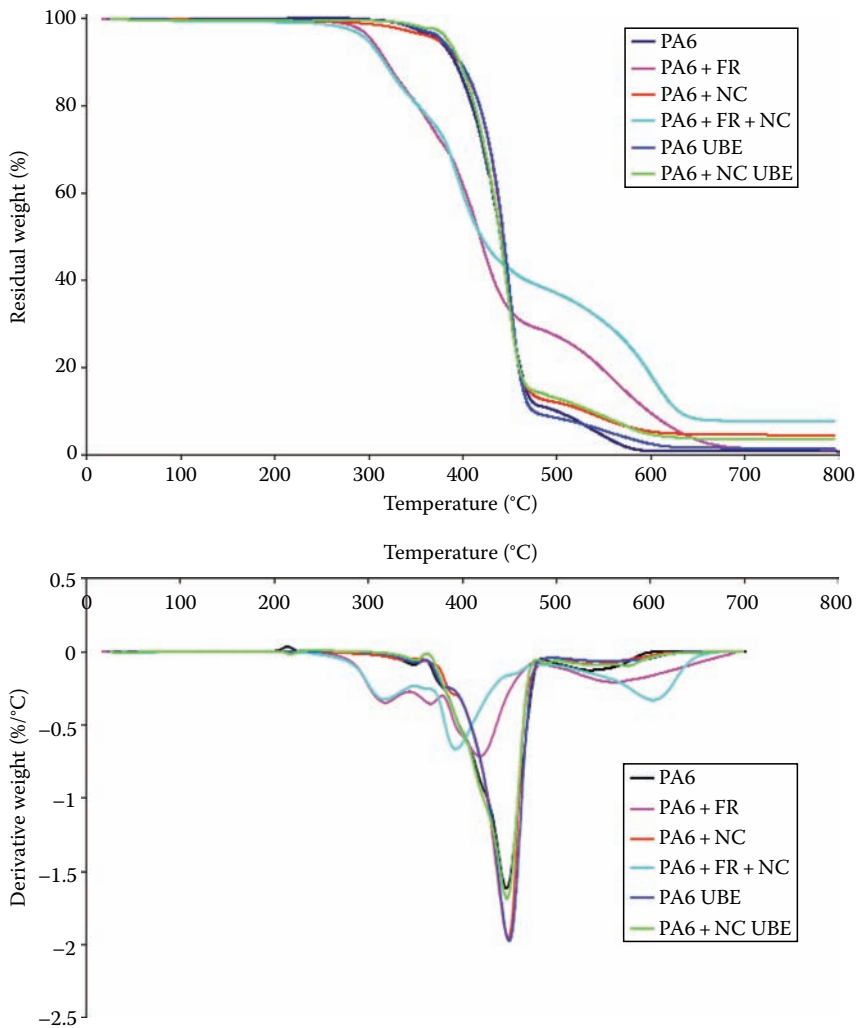


FIGURE 19.6 TG/DTG curves of PA6, PA6 + NC, PA6 + FR, and PA6 + FR + NC in air.

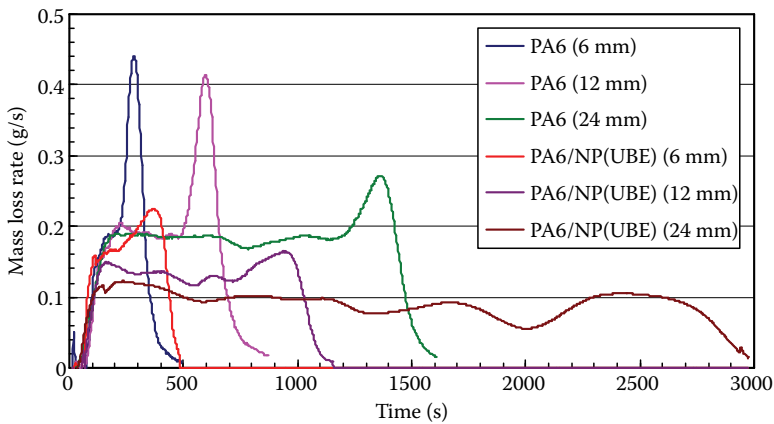


FIGURE 19.15 Comparison of the mass loss rate for PA6-based materials at different sample thicknesses at 50 kW/m².

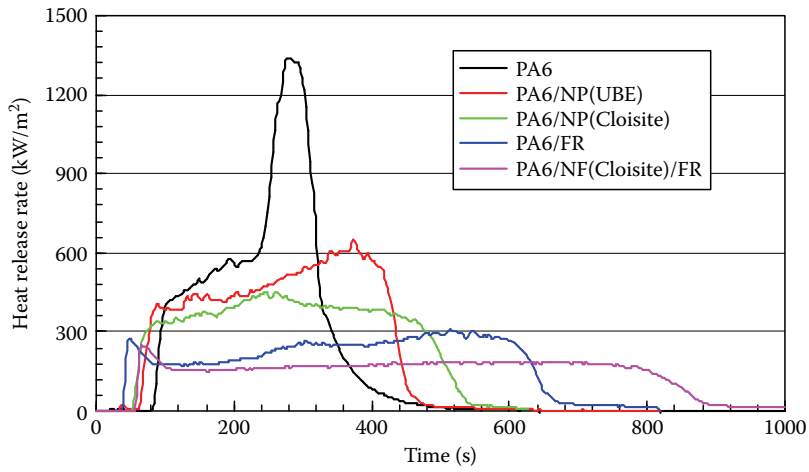


FIGURE 19.17 Comparison of the HRR of PA6 and PA6/NC (UBE), PA6/NC, PA6/FR, and PA6/NC/FR at 50kW/m² (sample thickness is 6 mm).

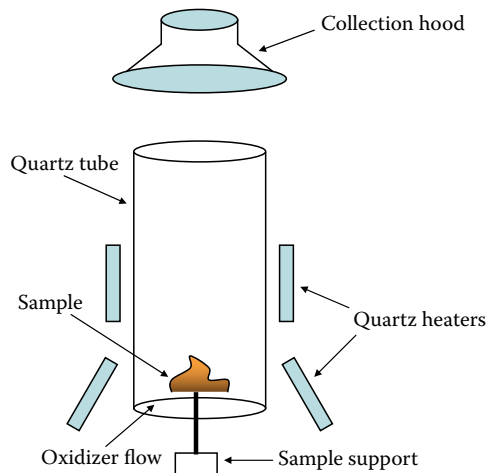
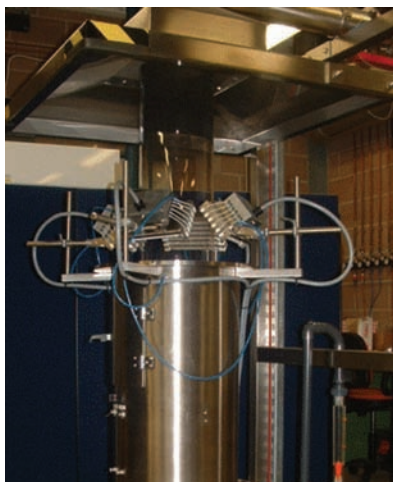


FIGURE 19.22 The universal flammability apparatus (UFA) (left) and a schematic view of the UFA (right).

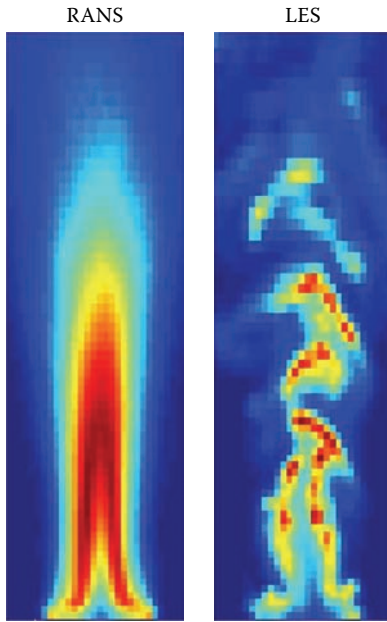


FIGURE 20.1 A comparison of temperature fields in pool fire flame simulations using RANS and LES.

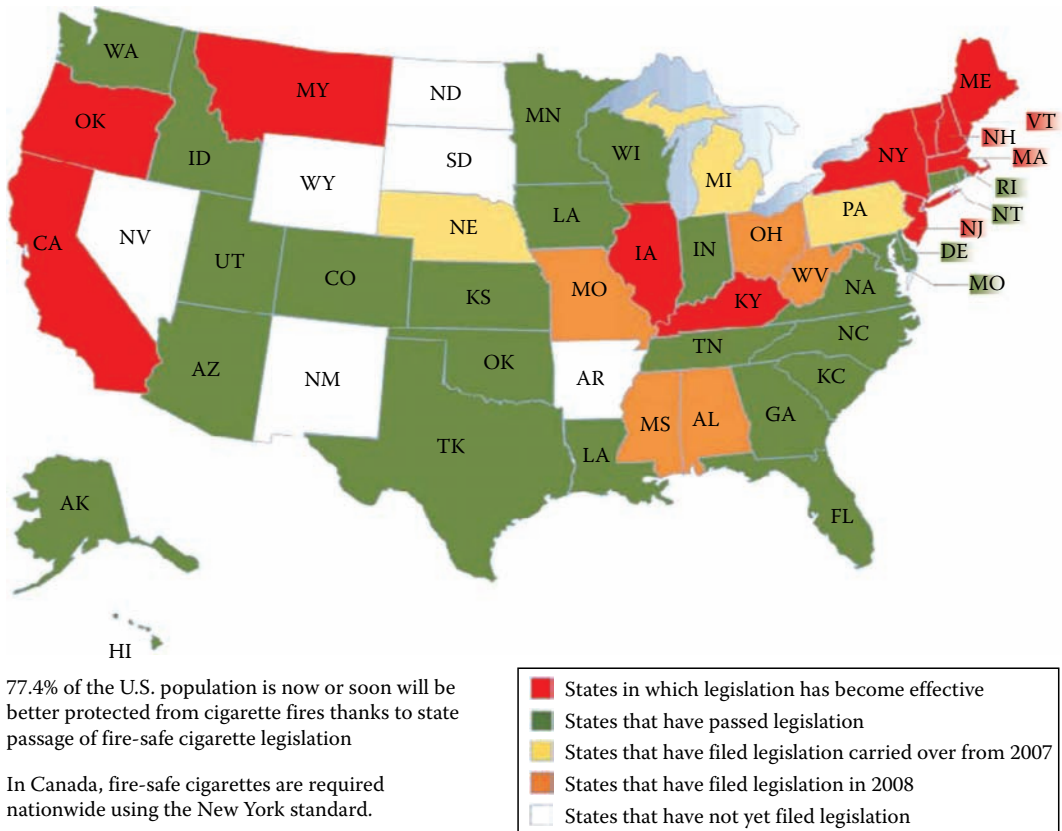


FIGURE 21.1 Legislation for fire-safe cigarettes in the United States—early 2008.

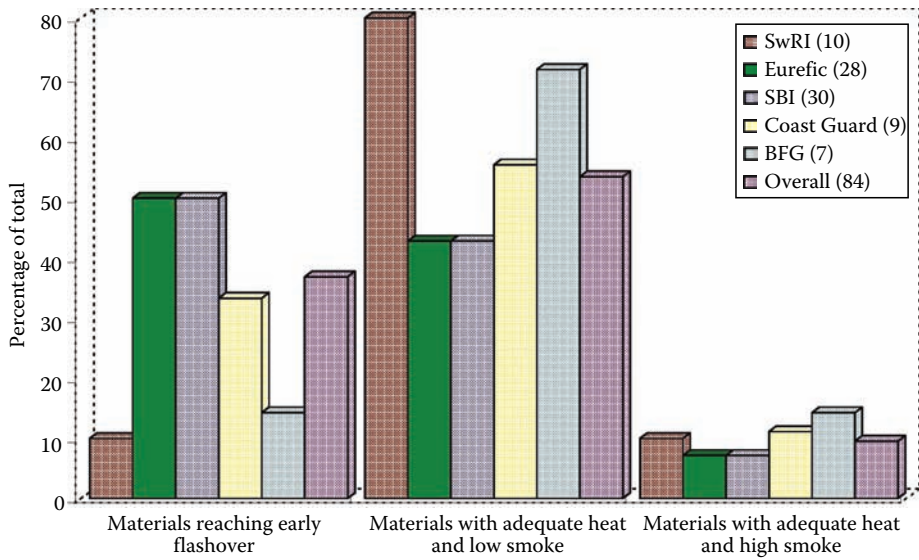


FIGURE 21.16 Smoke and heat release in room-corner tests.

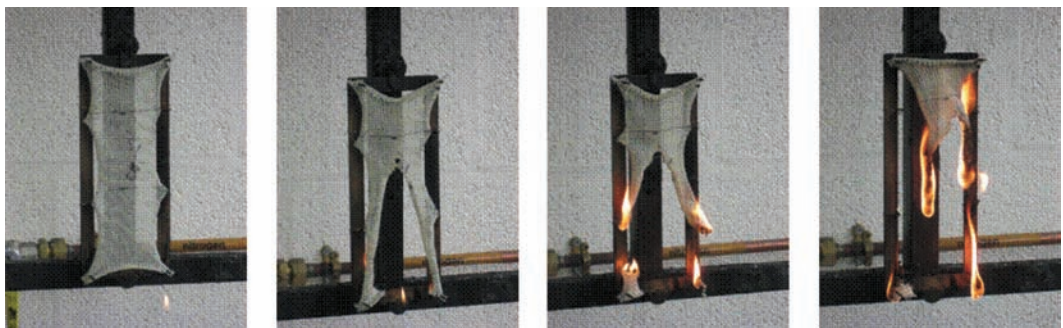


FIGURE 24.7 Flame spread test of PP using BS 5438 Test 1 rig.

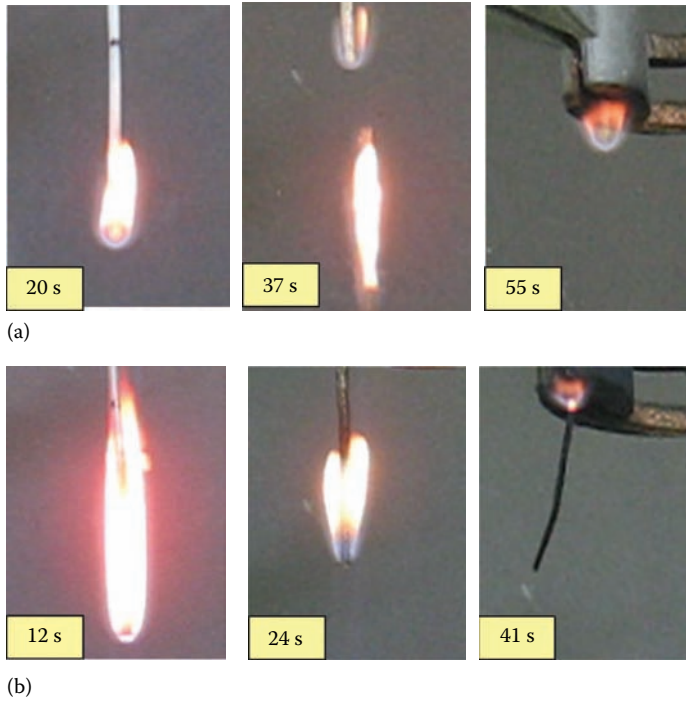









FIGURE 24.10 Vertical burning behavior of (a) nylon 6 and (b) nylon 6 strings containing 8% 15A nano-clay. (From Ratnayaka, A., High performance fire retardant synthetic fibres incorporating nanocomposites, MSc thesis, University of Bolton, Bolton, U.K., May 2007.)

TABLE 6.3
Combustion Residues of PA-6/OP1311 from the Cone Calorimeter Obtained at Different Characteristic Times

Before Ignition	After Ignition	At PkHRR	Final Residue
			
			—

Second Edition

Fire Retardancy of Polymeric Materials

When dealing with challenges such as providing protection while considering cost, mechanical and thermal performance, and simultaneously addressing increasing regulations that deal with composition of matter and life cycle issues, there are no quick, one-size-fits-all answers. Packed with comprehensive coverage, a scientific approach, step-by-step directions, and a distillation of technical knowledge, the first edition of *Fire Retardancy of Polymeric Materials* broke new ground. It supplied a one-stop resource for the development of new fire-safe materials.

The editors have expanded the second edition to echo the multidisciplinary approach inherent in current flame retardancy technology and put it in a revised, more user-friendly format. More than just an update of previously covered topics, this edition discusses:

- additional fire retardant chemistry
- developments in regulations and standards
- new flame retardant approaches
- fire safety engineering
- modeling and fire growth phenomena

The book introduces flame retardants polymer by polymer, supplemented by a brief overview of mode of action and interaction, and all the other ancillary issues involved in this applied field of materials science. The book delineates what, why, and how to do it, covering the fundamentals of polymer burning/combustion and how to apply these systems and chemistries to specific materials classes. It also provides suggested formulations, discusses why certain materials are preferred for particular uses or applications, and offers a starting point from which to develop fire-safe materials.

 **CRC Press**
Taylor & Francis Group
an **informa** business
www.crcpress.com

6000 Broken Sound Parkway, NW
Suite 300, Boca Raton, FL 33487
270 Madison Avenue
New York, NY 10016
2 Park Square, Milton Park
Abingdon, Oxon OX14 4RN, UK

83996



www.crcpress.com